The use of diatom transfer functions in estimating sea-surface temperature and sea-ice in cores from the southeast Indian Ocean

Leanne Kay Armand

A thesis submitted for the degree of Doctor of Philosophy of
The Australian National University.

December, 1997.

Australian Marine Quaternary Program
Department of Geology
Canberra.

Except where acknowledged in the text, this thesis represents original research by the author.

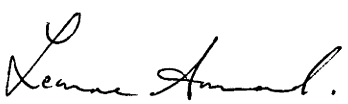

Leanne Armand

Dédié à mon Stéphane.

TABLE OF CONTENTS.

CHAPTER 1. INTRODUCTION AND METHODS.

1.1 BASIS OF THE STUDY 1
1.1.1. Significance of the study 1
1.1.2. Aims of the study 2
1.1.3. Format of the thesis 3
1.2. PREVIOUS DIATOM STUDIES - STATISTICAL AND REGIONAL 3
1.3. DIATOM ECOLOGICAL RESPONSES 6
1.3.1. Temperature 6
1.3.2. Sea-ice 7
1.4. SEDIMENTOLOGY 9
1.5. REGIONAL OCEANOGRAPHY 12
1.5.1. The Southern Ocean, its basins and the Antarctic Circumpolar Current 12
1.5.2. Oceanographic Fronts of the ACC 14
Polar Front 16
Subantarctic Front 16
Subtropical Convergence 16
1.5.3. Water masses 17
Surface water 17
Subsurface and Intermediate waters 19
Deep Water 20
Bottom water 21
1.5.4. Terminology of oceanic realms 23
1.6 SEA-ICE IN THE SOUTHERN OCEAN 24
1.6.1. Antarctic annual sea-ice cycle 24
Minimum 26
Growth 26
Maximum 26
Retreat 26
1.6.2. Sea-ice in region of study 28
1.6.3. Sea-ice formation and heat flux 29
1.6.4. Factors affecting sea-ice 31
Atmospheric winds, temperature, and pressure 31
Snow 32
Solar Radiation 33
Ocean Currents 33
1.6.5. Effect of sea-ice on global climate 33
Heat Flux 34
Oceanic circulation 34
Weather 35
Assessing Change 36
1.7 BASIC METHODOLOGY 36
1.7.1 Sampling and extraction 36
Core Material 36
Surface samples 37
1.7.2 Processing 37
1.7.3.Counting procedures 37

CHAPTER 2. ANALYSIS AND REVIEW OF THE DIATOM SURFACE SAMPLE DATABASE.

2.1 INTRODUCTION 41
2.1.1. The Pichon *et al.* (1992a) original 166 database 41
2.1.2. Pichon's additional data set 41
2.1.3. Armand's new data set 41
2.1.4. Abbott's southeast Indian Ocean sediment surface data set 43
2.2 TAXONOMIC REFORM 45
2.2.1. *Achnanthes brevipes* 45
2.2.2. *Actinocyclus actinochilus* 45
2.2.3. *Actinocyclus curvatulus* 45
2.2.4. Genus *Asteromphalus* 46
2.2.5. *Azpeitia tabularis* 47
2.2.6. *Cocconeis* species 48
2.2.7. *Coscinodiscus decrescens* 50
2.2.8. *Fragilaria striatula* 50
2.2.9. Genera *Fragilariopsis - Nitzschia - Pseudonitzschia* 50
2.2.10. *Fragilariopsis oceanica* 52
2.2.11. *Fragilariopsis ritscheri* 52
2.2.12.*Fragilariopsis* Cool taxa 56
2.2.13. *Fragilariopsis* Cylindriform Group 57
2.2.14. *Nitzschia sicula* 58
2.2.15. *Navicula gelida var. parvula* 59
2.2.16. Genera *Paralia* and *Melosira* 59
2.2.17. *Porosira* group 59
2.2.18. Genera *Rhizosolenia* and *Proboscia* 60
2.2.19. *Rhizosolenia hebetata* forma *semispina* 66
2.2.20. *Rhizosolenia styliformis* 70
2.2.21. Genus *Stellarima* 73
2.2.22. *Thalassionema nitzschioides* 74
2.2.23.*Thalassiosira antarctica/scotia* Group 78
2.2.24. *Thalassiosira* Eccentric group 79
2.2.25. *Thalassiosira frenguellii* 82
2.2.26. *Thalassiosira gracilis* taxa 82
2.2.27.*Thalassiosira* Lineati Group 82
2.2.28. *Thalassiosira maculata* 84
2.2.29. *Thalassiosira oestrupii* 85
2.2.30.*Thalassiosira oliverana* 85
2.3. REMOVAL OF SPECIES/TAXA FROM ANALYSIS 86
2.3.1.*Chaetoceros* vegetative and resting cells 86
2.3.2.*Thalassiothrix longissima, Thalassiothrix antarctica* and *Trichotoxon reinboldii* 89
2.3.3. *Dactyliosolen antarcticus* 90
2.3.4. *Silicoflagellate* species 91
2.3.5. *Eucampia antarctica* 94
2.4. SUMMARY 97

CHAPTER 3 NATURAL AND DISSOLUTION DATA SETS

CHAPTER 3. SECTION A. NATURAL DATABASE 101
3A.0. INTRODUCTION 101
3A.1. SAMPLE SELECTION CRITERIA 101
3A.1.1 Total number of specimens counted 101
3A.1.2. Old species 102
3A.1.3. Other information 105
3A.1.4. Communality levels 105

3A.2. RARE SPECIES 106
3A.3. SPECIES DISTRIBUTIONS 108
3A.3.1. *Achnanthes brevipes* 111
3A.3.2 *Actinocyclus actinochilus* 111
3A.3.3 *Actinocyclus curvatulus* 112
3A.3.4 *Asteromphalus hookeri* 115
3A.3.5 *Asteromphalus parvulus* 118
3A.3.6 *Azpeitia tabularis* 118
3A.3.7 *Cocconeis* spp. 120
3A.3.8 *Coscinodiscus marginatus* 122
3A.3.9 *Eucampia antarctica* 122
3A.3.10 *Fragilariopsis* Cool Taxa 124
3A.3.11 *Fragilariopsis curta* 127
3A.3.12 *Fragilariopsis* Cylindriform Group 129
3A.3.13 *Fragilariopsis doliolus* 132
3A.3.14 *Fragilariopsis kerguelensis* 132
3A.3.15 *Fragilariopsis pseudonana* 137
3A.3.16 *Fragilariopsis rhombica* 139
3A.3.17 *Fragilariopsis separanda* 139
3A.3.18 *Grammatophora arcuata* 141
3A.3.19 *Hemidiscus cuneiformis* 143
3A.3.20 *Navicula directa* 143
3A.3.21 *Odontella weissflogii* 146
3A.3.22 *Paralia* Taxa 148
3A.3.23 *Porosira* Group 150
3A.3.24 *Proboscia alata* 154
3A.3.25 *Rhizosolenia bergonii* 154
3A.3.26 *Rhizosolenia* otaria absent group 155
3A.3.27 *Rhizosolenia* otaria present group 155
3A.3.28 *Roperia tesselata* 158
3A.3.29 *Stellarima microtrias* 160
3A.3.30 *Stellarima stellaris* 162
3A.3.31 *Thalassionema* Taxa 162
3A.3.32 *Thalassiosira antarctica/scotia* Group 166
3A.3.33 *Thalassiosira decipiens* 168
3A.3.34 *Thalassiosira* Eccentric Group 168
3A.3.35 *Thalassiosira gracilis* Group 170
3A.3.36 *Thalassiosira lentiginosa* 173
3A.3.37 *Thalassiosira* Lineati Group 175
3A.3.38 *Thalassiosira oestrupii* Group 177
3A.3.39 *Thalassiosira oliverana* 179
3A.3.40 *Thalassiosira perpusilla* 181
3A.3.41 *Thalassiosira poroseriata* 183
3A.3.42 *Thalassiosira tumida* 186
3A.4. SPECIES WITH KNOWN BENTHIC-NERITIC HABITATS 186
3A.5. REGIONAL SAMPLE CONSIDERATIONS - ANTARCTIC PENINSULA AND ROSS SEA SAMPLES 187
3A.5.1 Antarctic Peninsula samples 187
3A.5.2 Ross Sea samples 189
CHAPTER 3. SECTION B. DISSOLUTION DATABASE 191
3B.1. DISSOLUTION DATA SET - INTRODUCTION 191
3B.2. DEGREE OF DISSOLUTION 193
3B.3 LOCATION OF SAMPLES 195
CHAPTER 3. SECTION C. THE MINIMISED DATABASE AND APPLIED RANKING METHODOLOGY. 198

CHAPTER 3. SECTION D. SUMMARY 201

CHAPTER 4 SEA-SURFACE TEMPERATURE TRANSFER FUNCTION.

4.1. INTRODUCTION, METHODOLOGY, ASSUMPTIONS 203
4.2 THE CURRENT PICHON *ET AL.* (1992) DTF166/34/4 206
4.2.1 Diagnostics of DTF166/34/4 206
4.3. TF WITH NEW DATABASE WITHOUT DISSOLVED SAMPLES 215
4.3.1 Choosing the appropriate number of factors to resolve and a communality cut-off value 215
4.3.2. Species relations to the number of factors resolved 217
4.3.3. Geographical distribution versus the number of factors resolved 223
The 6 factor model 223
The 4 factor model 229
4.3.4. Diagnostics of the DTF 115/24/6 model 234
4.3.5. Modified DTF109/24/6 and response 237
4.3.6 Comparison with original 166/34/4 DTF 245
Differences in species and factor associations 246
Differences in model output 249
4.4. SUMMARY 251

CHAPTER 5 SEA-ICE MODEL.

5.1 INTRODUCTION 255
5.1.1. Satellite sea-ice monitoring 256
5.1.2. Analysis of extent and concentration 256
Introduction and primary derivations 256
Concentration 257
Extent 257
Validation studies 258
5.1.3. Other problems associated with determining sea-ice concentration and the sea-ice edge 259
5.1.4. Sea-ice data used in this study 260
5.2 METHODOLOGY AND ASSUMPTIONS 262
5.3. SUMMARY 268

CHAPTER 6 SOUTHEAST INDIAN OCEAN CORE RECORDS.

6.1 INTRODUCTION AND LOCATION 269
6.2. CORE STRATIGRAPHY 269
6.2.1.Core E53-10 271
6.2.2. Diatom biostratigraphy 271
6.2.3. Isotope Stratigraphy and preliminary age model 272
6.2.4. Sedimentation rate 275
6.2.5. Absolute Diatom Abundance 280
6.2.6. The relative abundance record of *Cycladophora davisiana* 282
6.3. Cores MD88-779 285
6.3.1 Diatom recovery 285
6.3.2. Silicoflagellate recovery 288
6.3.3. Phytolith recovery 290
6.3.4. Summary 290
6.4 CORES MD88-784 AND MD88-787 293
6.4.1 Diatom recovery and factor analysis 293
Core MD88-784 296

DTF 109/24/6 Model....296
DTF 166/34/4 Model....298
MD88-787....299
DTF 109/24/6 Model....299
DTF 166/34/4 Model....301
Thalassiothrix/Trichotoxon spp. 304
Distephanus spp....304
Azpeitia tabularis....304
Thalassiosira trifulta....305
Fragilariopsis kerguelensis....305
Fragilariopsis separanda....305
6.4.2 SST estimation....306
MD88-784....306
The SST record from DTF 109/24/6....306
The SST record from DTF 166/34/4....308
Model Differences....308
MD88-787....308
The SST record from DTF 109/24/6....308
The SST record from DTF 166/34/4....310
Model Differences....310
Comparison of SST estimates between the two cores....312
6.4.3 Sea-ice estimation....313
6.5. A CLIMATIC HISTORY FOR CORE MD88-787....317
6.5.1. SST and sea-ice histories versus the oxygen-isotope record....318
6.5.2. Compatibility between sea-ice and SST records....321
6.5.3. Sea-ice and *Cycladophora davisiana* records....322
6.5.4. Movement of the Polar Front....323
6.5.5. Comparison of diatom derived SST results in the Southern Ocean....326
6.5.6 A comparison of past sea-ice reports in the Southern Ocean...328
6.6. PALAEOCEANOGRAPHIC TIME SLICES AND HYPOTHESES....329
6.6.1. Isotope-stage 7....331
6.6.2. Isotope-stage 6....331
6.6.3. Isotope-stage 5....333
6.6.4. Isotope-stage 4....336
6.6.5 Isotope-stage 3....336
6.6.6 Isotope-stage 2....337
6.6.7 Isotope-stage 1....339
6.7. THE ROLE OF BOTTOM WATER....340
6.8. THE ROLE OF SEA-ICE, MIXING DEPTH AND A MELT WATER LID 342
6.9. SUMMARY....343

CHAPTER 7 CONCLUSIONS AND FUTURE WORK

7.1 DIATOM DATABASE ANALYSIS RESULTS....351
7.2. MODEL CONSTRUCTION....352
7.3. LIMITATIONS AND APPLICABILITY OF THE PICHON ET AL. (1992A) TRANSFER FUNCTION....353
7.4 DEVELOPMENT OF THE SEA-ICE ESTIMATION MODEL....354
7.5. HISTORY OF OCEANOGRAPHIC CHANGE IN THE SOUTHEAST INDIAN OCEAN....355
7.6. FUTURE RESEARCH....356

REFERENCES.... 359

APPENDICES

A1. Floral list. ..... A1-1 - A1-17
A2. Plates ..... Plates 1- 18
1.1. Silica-selective methodology. 1.1-1
2.1. Original ranked 166 surface sample database. ..... 2.1-1 - 2.1-3
2.2. Raw data of 166 database. ..... 2.2-1 - 2.2-14
2.3. All new French raw data. ..... 2.3-1 - 2.3-6
2.4. Authors new surface samples - all species raw data ..... 2.4-1 - 2.4-2
2.5. Abbott's diatom counts - all data ..... 2.5-1 - 2.5-6
2.6. Citations of *Rhizosolenia* in the Southern Ocean ..... 2.6-1 - 2.6-2
3.1. Dissolved data set - raw data (Pichon *et al.* 1992b). ..... 3.1-1 - 3.1-3
3.2. Antarctic Diatom Database (ADB) - raw data. ..... 3.2-1 - 3.2-5
4.1. ADB parameters. ..... 4.1-1 - 4.1-2
4.2. Results of DTF 166/34/4. ..... 4.2-1 - 4.2-5
4.3. Varimax factor score matrices of factor models 3, 4, 6, 8, & 10 ..... 4.3-1 - 4.3-2
4.4. Results of DTF 115/24/6. ..... 4.4-1 - 4.4-4
4.5. Results of DTF 109/24/6. ..... 4.5-1 - 4.5-4
5.1. Sea-ice statistical models ..... 5.1-1 - 5.1-3
6.1. Core E53-10 - survey data 6.1-1
6.2. Core MD88-787 - Age model and other data. ..... 6.2-1 - 6.2-3
6.3. Core MD88-784 - Age model and other data. 6.3-1
6.4. Core MD88-779 - Age model and other data. 6.4-1
6.5. Core MD88-779 - raw data 6.5-1
6.6. Core MD88-787 - raw data ..... 6.6-1 - 6.6-4
6.7. Core MD88-784 - raw data ..... 6.7-1 - 6.7-3
6.8. Core MD88-787 SST and sea-ice estimates ..... 6.8-1 -6.8-3
6.9. Core MD88-784 SST estimates 6.9-1
6.10. Core MD88-787 August SST estimates using DTF 109/24/6 ..... 6.10-1-3

List of Figures.

CHAPTER 1.

1.1. Abbott's distribution of diatom assemblages in the southeast Indian Ocean 5
1.2. Representation of sedimentary accumulation patterns in the basins of the southeast Indian Ocean 10
1.3. Distribution of opaline silica in the sediments of the southeast Indian Ocean 11
1.4. Bottom Topography of the southeast Indian Ocean 13
1.5. Distribution of Fronts in the southeast Indian Ocean 15
1.6. Diagrammatic circulation of the transect through ~135°E in the southeast Indian Ocean 18
1.7. Distribution map of bottom potential temperature and pathways of the AABW in the southeast Indian Ocean 22
1.8. Biological zonation of Southern Ocean 25
1.9. Surface circulation patterns of ice and water in the Southern Ocean 27
1.10. Maximum sea-ice distribution around Antarctica for February and September 30
1.11. Summarised method of silica-selective extraction used in this study 38
1.12. Counting guide to diatom frustules 39

CHAPTER 2.

2.1. Distribution of data sets available to this study 42
2.2. Relative abundance distribution of *Azpeitia tabularis* and *A. tabularis* var *egregius* 49
2.3. Original distribution of species identified as *Fragilariopsis ritscheri* 54
2.4. Diagrammatic and illustrated variation of *Rhizosolenia* species in the Southern Ocean 64-65
2.5.a. Distribution of species identified as *Rhizosolenia hebetata f. semispina* 69
2.5.b. Relative abundance against February SST of *Rhizosolenia hebetata f. semispina* 69
2.6.a. Same as 2.5.a. for *Rhizosolenia styliformis* 71
2.6.b. Same as 2.5.b. for *Rhizosolenia styliformis* 71

2.7.a. Initial identification and distribution of species now identified under *Stellarima* genus 75
2.7.b. Combined *Stellarima* spp. relative abundance against February SST 75
2.8. Distribution of *Thalassiosira eccentric* group 81
2.9. Distribution of *Chaetoceros* vegetative cell relative abundances 87
2.10. *Chaetoceros* resting cell relative abundance 87
2.11.a. Distribution of *Dactyliosolen antarcticus* relative abundances as observed in the sediments 92
2.11.b. Same as 2.5.b. for *Dactyliosolen antarcticus* 92
2.12.a. Same as 2.11.a. for *Distephanus* spp 95
2.12.b. Same as 2.5.b. for *Distephanus* spp. 95
2.13.a. Same as 2.11.a. for *Dictyocha* spp. 96

2.13.b. Same as 2.5.b. for *Dictyocha* spp. 96

CHAPTER 3.

3.0. Samples removed from this study using selection criteria..... 104
3.1. Previous studies detailing diatom distributions in surface sediments 109
3.2.a.b. *Achnanthes brevipes* relative abundance distribution versus geography, SST, sea-ice cover and concentration 110
3.3.a.b. *Actinocyclus actinochilus* relative abundance distribution versus geography, SST, sea-ice cover and concentration 113
3.4.a.b. *Actinocyclus curvatulus* and *Coscinodiscus curvatulus* relative abundance distribution versus geography, SST, sea-ice cover and concentration..... 114
3.5.a.b. *Asteromphalus hookeri* relative abundance distribution versus geography, SST, sea-ice cover and concentration 116
3.6.a.b. *Asteromphalus parvulus* relative abundance distribution versus geography, SST, sea-ice cover and concentration 117
3.7.a.b. *Azpeitia tabularis* relative abundance distribution versus geography, SST, sea-ice cover and concentration 119
3.8.a.b. *Cocconeis* spp. relative abundance distribution versus geography, SST, sea-ice cover and concentration 121
3.9.a.b. *Coscinodiscus marginatus* relative abundance distribution versus geography, SST, sea-ice cover and concentration 123
3.10.a.b. *Eucampia antarctica* relative abundance distribution versus geography, SST, sea-ice cover and concentration 125
3.11.a.b. *Fragilariopsis cool taxa* relative abundance distribution versus geography, SST, sea-ice cover and concentration 126
3.12.a.b. *Fragilariopsis curta* relative abundance distribution versus geography, SST, sea-ice cover and concentration 128
3.13.a.b. *Fragilariopsis cylindriform* relative abundance distribution versus geography, SST, sea-ice cover and concentration 131
3.14.a.b. *Fragilariopsis doliolus* relative abundance distribution versus geography, SST, sea-ice cover and concentration 133
3.15.a.b. *Fragilariopsis kerguelensis* relative abundance distribution versus geography, SST, sea-ice cover and concentration 134
3.16.a.b. *Fragilariopsis pseudonana* relative abundance distribution versus geography, SST, sea-ice cover and concentration 136
3.17.a.b. *Fragilariopsis rhombica* relative abundance distribution versus geography, SST, sea-ice cover and concentration 138
3.18.a.b. *Fragilariopsis separanda* relative abundance distribution versus geography, SST, sea-ice cover and concentration 140
3.19.a.b. *Grammatophora arcuata* relative abundance distribution versus geography, SST, sea-ice cover and concentration 142
3.20.a.b. *Hemidiscus cuneiformis* relative abundance distribution versus geography, SST, sea-ice cover and concentration 144
3.21.a.b. *Navicula directa* relative abundance distribution versus geography, SST, sea-ice cover and concentration..... 145
3.22.a.b. *Odontella weissflogii* relative abundance distribution versus geography, SST, sea-ice cover and concentration 147
3.23.a.b. *Paralia* taxa relative abundance distribution versus geography, SST, sea-ice cover and concentration..... 149
3.24.a.b. *Porosira* group relative abundance distribution versus geography, SST, sea-ice cover and concentration..... 151
3.25.a.b. *Proboscia alata* relative abundance distribution versus geography, SST, sea-ice cover and concentration..... 153

3.26.a.b. *Rhizosolenia* otaria absent relative abundance distribution versus geography, SST, sea-ice cover and concentration.....156
3.27.a.b. *Rhizosolenia* otaria relative abundance distribution versus geography, SST, sea-ice cover and concentration.....157
3.28.a.b. *Roperia tesselata* relative abundance distribution versus geography, SST, sea-ice cover and concentration.....159
3.29.a.b. *Stellarima microtrias* relative abundance distribution versus geography, SST, sea-ice cover and concentration.....161
3.30.a.b. *Stellarima stellaris* relative abundance distribution versus geography, SST, sea-ice cover and concentration.....163
3.31.a.b. *Thalassionema* taxa relative abundance distribution versus geography, SST, sea-ice cover and concentration.....164
3.32.a.b. *Thalassiosira antarctica / scotia* group relative abundance distribution versus geography, SST, sea-ice cover and concentration.....167
3.33.a.b. *Thalassiosira decipiens* relative abundance distribution versus geography, SST, sea-ice cover and concentration.....169
3.34.a.b. *Thalassiosira* Eccentric group relative abundance distribution versus geography, SST, sea-ice cover and concentration.....171
3.35.a.b. *Thalassiosira gracilis* group relative abundance distribution versus geography, SST, sea-ice cover and concentration.....172
3.36.a.b. *Thalassiosira lentiginosa* relative abundance distribution versus geography, SST, sea-ice cover and concentration.....174
3.37.a.b. *Thalassiosira* Lineati group relative abundance distribution versus geography, SST, sea-ice cover and concentration.....176
3.38.a.b. *Thalassiosira* oestrupii group relative abundance distribution versus. geography, SST, sea-ice cover and concentration.....178
3.39.a.b. *Thalassiosira oliverana* relative abundance distribution versus geography, SST, sea-ice cover and concentration.....180
3.40.a.b. *Thalassiosira perpusilla* relative abundance distribution versus geography, SST, sea-ice cover and concentration.....182
3.41.a.b. *Thalassiosira poroseriata* relative abundance distribution versus geography, SST, sea-ice cover and concentration.....184
3.42.a.b. *Thalassiosira tumida* relative abundance distribution versus geography, SST, sea-ice cover and concentration.....185
3.43. Location of the five dissolved samples with bathymetry and maximum sea-ice extents.....192
3.44. Comparison of natural and dissolution data set relative abundance of the 3 most dissolution resistant diatom species against February SST.....192
3.45. Relative abundance distribution of major species against February SST.....194
3.46. Preliminary Diagnostic features of SST transfer function LKA 151/23/4.....196

CHAPTER 4.

4.1. Flow chart of the diatom transfer function.....205
4.2.a. Factor of distribution of DTF 166/34/4.....207
4.2.b. Factor analysis of DTF 166/34/4, Residual and communality excursions.....207
4.3. Summary diagnostic plot for February SST analysis for DTF 166/34/4.....211
4.4. Factor loading plots of the 4 resolved factors against

original observed SST data and estimated SST 213
4.5.a.b.c.d. Opal dissolution relationship of Factor 4 216
4.6. Response of increasing cumulative variance of the 115 ADB 218
4.7. Number of samples in the 115 ADB requiring removal. 218
4.8. Communality values of 115 samples of ADB as a function of increasing number of resolved factors 218
4.9. Factor analysis of 115/24/6, Factor 1 distribution 222
4.10. Factor analysis of 115/24/6, Factor 2 distribution 222
4.11. Factor analysis of 115/24/6, Factor 3 distribution 224
4.12. Factor analysis of 115/24/6, Factor 4 distribution 224
4.13. Factor analysis of 115/24/6, Factor 5 distribution 226
4.14. Factor analysis of 115/24/6, Factor 6 distribution 226
4.15. Factor dominance regions of DTF 115/24/6 228
4.16. Factor analysis of DTF 115/24/6, residual and communality excursions 228
4.17. Factor analysis of 115/24/4, Factor 1 distribution 230
4.18. Factor analysis of 115/24/4, Factor 2 distribution 230
4.19. Factor analysis of 115/24/4, Factor 3 distribution 231
4.20. Factor analysis of 115/24/4, Factor 4 distribution 231
4.21. Factor dominance regions of DTF 115/24/4 233
4.22. Factor analysis of DTF 115/24/4, residual and communality excursions 233
4.23. Summary diagnostic plots of February SST analysis of DTF 115/24/6 235
4.24.a. Factor dominance regions from factor analysis of DTF 109/24/6 238
4.24.b. Factor analysis of 109/24/6, residual and communality excursions 238
4.25. Summary diagnostic plots of February SST analysis of DTF 109/24/6 242
4.26. Factor loading plots of the 6 resolved factors against February SST 243
4.27. Distribution of Factor 5 factor-loadings against August SST values 245
4.28a.b. Summary curves of factor loading influences provided by DTF 166/34/4 and DTF 109/24/6 250

CHAPTER 5.

5.1. Relation between 3 sea-ice parameters:
a. February concentration versus monthly sea-ice cover 263
b. September concentration versus monthly sea-ice cover 263
c. February versus September sea-ice concentration 263
5.2. Factor loading relations to sea-ice concentrations and sea-ice cover :
a. February sea-ice concentration 264
b. September sea-ice concentration 264
c. sea-ice cover in months per year 265
5.3. Preliminary diagnostic plots for estimation of maximum and minimum sea-ice concentration and degree of monthly cover using Imbrie and Kipp methodology 266

CHAPTER 6.

6.1. Location of the 4 cores analysed in this thesis 270
6.2.a.b.c.d. Diatom biostratigraphy of 3 French MD88 cores 273

6.3.a.b.c. Derivation of preliminary age/depth model for core MD88-787 276
6.4.a.b.c. Derivation of preliminary age/depth model for core MD88-784 277
6.5.a.b.c. Derivation of preliminary age/depth model for core MD88-779 278
6.6. Presentation of linear sedimentation rates of 3 French cores against the SPECMAP age scale 279
6.7. Absolute diatom abundance (ADA) against the SPECMAP age scale 279
6.8. Relative abundance of the radiolarian *C. davisiana* against the SPECMAP age scale 283
6.9.a.b. Diatom relative abundance over the SPECMAP time in core MD88-779 287
6.10.a.b.c. SST estimation from *Dictyocha* and *Distephanus* silicoflagellate species in core MD88-779 289
6.11. Location of recently studied cores adjacent to MD88-779 291
6.12.a.b. Summary of the diatom data used in DTF used to derive SST estimates : MD88-784, MD88-787 295
6.13.a.b.c. Factor analysis results of core MD88-784 using DTF 109/24/6 297
6.14.a.b.c. Factor analysis of core MD88-787 300
6.15.a.b.c. SST estimates and communality, core MD88-784 307
6.16.a.b.c. SST estimates and communality, core MD88-787 309
6.17.a.b. Comparison of SST estimates on cores MD88-787 and MD88-784 using DTF 109/24/6 314
6.18.a.b.c. Sea-ice estimates from core MD88-787 315
6.19.a.b.c. Standard error estimates for sea-ice models 316
6.20.a.b.c.d.e. Climatic proxies for core MD88-787 319
6.21. Southern Ocean core locations using diatom transfer function 320
6.22. Polar Front movement analysis 325
6.23.a.b. Comparative SST estimates between core MD88-784, -787 and MD84-551, -527 327
6.24. Surface currents surrounding Australia 330
6.25. Schematic present day oceanographic setting 334
6.26. Schematic glacial oceanographic setting 335

List of Tables.

CHAPTER 1.

1.1. Recent literature on diatom analysis 4
1.2. Summary table of water mass characteristics 17

CHAPTER 2.

2.1. Comparative counts (Abbott and this study) on core top sample E36-6 44
2.2. List of extant *Fragilariopsis* and *Pseudonitzschia* living species relevant to this study 51
2.3. Species remaining in *Nitzschia* genus, which require generic reform 52
2.4. Occurrences of the species *F. ritscheri* in the literature 55
2.5. Observations of *Fragilariopsis* species to summer

SST in the South Atlantic sector 57
2.6. List of *Rhizosolenia* species in this study and their revised classification 66
2.7. Additional studies providing illustrations of *R. styliformis* 72
2.8. Incidences of species considered under the *Stellarima* genus 76-77
2.9. Samples containing "*Coscinodiscus bullatus*" or *Thalassiosira* cf. *maculata* 84
2.10. Summary of taxonomic revisions made through the three data sets available to the thesis 99-100

CHAPTER 3.

3.1. Samples with less than 270 specimens counted 103
3.2. Samples with greater than 1% reworked species 105
3.3. List of species in the Natural Database with relative abundances under 0.4% 107
3.4. Maximum abundances of diatoms >0.4% in the 129 natural sample database 107
3.5. Benthic/neritic species removed from consideration in thesis transfer function 187
3.6. Antarctic Peninsula region samples. *Chaetoceros* species and benthic/neritic components 189
3.7. Ross Sea region samples. *Chaetoceros* species and benthic-neritic components 190
3.8. Comparative maximum relative abundances of species in Diatom Databases of this study and Pichon *et al.* (1992a) 198
3.9. Specimens per species required for ranking inclusion 199
3.10. Ranking categories employed for each species used in the ADB 200

CHAPTER 4.

4.1. Vector Score Matrix (VFSM) for the DTF166/34/4 208
4.2. Summary table of highest factor scores/species under factor models (3, 4, 6, 8, and 10) 215
4.3. Samples with residual SST values >±2°C removed from further DTF analysis 237
4.4. Vector Factor Scores Matrix (VFSM) for the DTF109/24/6 239
4.5. Species and dominant factor alliances between the two DTF models 247

CHAPTER 6.

6.1. Core location details 269
6.2. No analogue samples in core MD88-784 under both DTF models 299
6.3. No analogue samples in core MD88-787 under both DTF models 301-302

ACKNOWLEDGMENTS

Concomitant with any Ph D thesis are the acknowledgments and gratitude one needs to extend to those who have offered scientific advice, moral support, financial assistance and encouragement during the moments of glory or disaster.

One person who deserves the biggest accolade is my supervisor, Patrick De Deckker. He showed courage in placing faith in an Australian mega-faunal fanatic who decide to turn a hand towards an unstudied group of oceanographic microfossils in the Australian scientific community (diatoms). There have been many moments, mostly via the phone or e-mail, that he has shown unfaltering confidence, offered advice and guidance, and risen above the normal expectations of a supervisor. His belief in my abilities has seen this thesis to its completion. For his late hours of corrections and un-ending help behind the scenes (and sharing of gourmand recipes) I thank him.

Full thanks must also be extended to my advisers Jean-Jacques Pichon and Rick Nunes-Vaz. They both assisted in getting this thesis on the road and bringing to my attention aspects of my thesis which were within their own research expertise. I thank Jean-Jacques for his patience with my French, explaining the in's and out's of transfer function application on the IBM, for access to his database and samples, and for lively discussions on diatom taxonomy and the implications they hold for transfer function analysis. Thank you also to Rick for being around to chat with and discuss oceanographic concepts.

There have been many diatom workers around the world who gave freely of their references and time in answering my questions. They include Lloyd Burckle, Uli Zielinski, Greta Fryxell, Ric Jordan, John Barron, Rainer Gersonde, Richard Crawford, Amy Leventer, David Harwood, Gustaaf Hallegraeff, Greta Hasle, Woody Wise and Xavier Crosta, among many. Both Uli and Lloyd have been invaluable as my diatom support team through the term of my thesis. Without their unfailing assistance, willingness to discuss many diatom and palaeo topics, and supplying me with many a good reference, this thesis and my own introduction to diatom studies would not have been so successful. I have, and continue to, value their friendship and our scientific relationships.

I have benefited from working with, meeting or receiving reference material from Ian Allison, Vicki Lytle, Tony Worby, Ian Simmonds, Gilles Bareille, Monique Labracherie, Laurent Labeyrie, Josette Duprat, Brad Opdyke, John Chappell, Steve Rintoul, Will Howard, Liz Sikes, Dan Mc Corkle, Harvey Marchant and many other palaeo workers world-wide. In particular, thanks must be extended to all the researchers and staff at the Université Bordeaux I, who welcomed my yearly visits.

On a statistical level, much thanks is extended to the statistical consulting unit at ANU, especially Simon Barry and Christine Donnelly who encouraged me to explore the world of statistics beyond computer programs, and who searched for alternative methods in predictive analyses. Without their help there would be no new sea-ice model. Dr Jean Braun at RSES, ANU, generously spent time developing and then checking programs which extracted the WOA data.

Peter Schweitzer (US Geological Survey) kindly supplied the CD on monthly average polar sea-ice concentration and pointed me in the best directions for gaining an insight into the derivations of satellite data. This help is gratefully acknowledged. The curators (Jonathan Bryan and Matthew Curren) and staff of the Antarctic Marine Geology Research Facility, Florida State University, are thanked for their assistance on many occasions in assisting with extraction or sending core material.

The opportunity to participate on the French PACIMA cruise is appreciated. I would like to thank IFRTP and TAAF for their financial and logistical support, but furthermore like to thank both Monique Labracherie and Jean-Louis Turon for their role in making the opportunity possible. The Australian French funds of IASOS (University of Tasmania) also provided financial assistance that made this scientific venture possible. Other financial assistance made available to me during my thesis term made very successful trips to both Japan and Germany possible. To Rainer Gersonde and Dr I. Koizumi, I extend much gratitude.

A small group of very important people also saw me through this thesis. Their help, but more importantly their friendship is deeply appreciated. Thank you Brian Harrold for all your hours of computer assistance, translations between machines, programs, and languages, but more importantly for indulgent chocolates, cappuccinos, and many a good late-night laugh. To my German buddy Stefan Nees, may we find jobs, continue in our merry madness of palaeoceanography and consume too much spicy Asian food. Thank you for being around when I needed an "English ear" in Europe. To Lynda Taylor, thanks for being a wonderful office mate and good friend. Lots of good memories and laughs will always remain. To Vicki Drappala and Angela Davis, thanks for being wonderful friends, we have survived Ph D's and the Geology Department, motherhood ought to be less stressful.

Special thanks also go to staff members of the Geology Department in particularly Maree Coldrick, Dick Barwick, Judith Shelley, Henry Zapasnik and Tim Munson who all assisted in many behind the scene, day to day or specific tasks that are a part and parcel of thesis life and progression.

To many friends or colleagues who passed through Geology, your help and friendship is appreciated (Mike Ayress, Ignatio Martinez, Helen Neil, Tony Rathburn, Chikara Hiramatsu, Ian, Elaine, Anne, Tim, Steve, Dan). To my friends who have been my lunch pals, weekend adventurers and fellow student sufferers during these four years: Chris, Leah (a million thanks for putting it together), Phil, Liz, Tim, Kendi, Kieran, Julie, Bill, Helen, Brett, Lindi, James, Karl, Paul, Mick, and Dave, I apologise for all the times I didn't turn up or left early because I was working, and thank you for being the very special group of people you are. Pour les amis Français (Sylvie, Claude, Gilles, Lara, Cécile, Santiago, Olivier, Cathy, J-Y, Eric le rude, Pascale, Christophe Eric et Carole,) un gros merci pour me supporter et pour bien garder mon mari.

To my Families Australian and Français - Thank you for your love, understanding, encouragement and financial assistance during the last 4 years,. May your pride in my achievements always be well placed. It will be wonderful to lead a normal life again and even more special to bring a grandchild into such special caring families. -Pour mes familles australienne et française, merci pour votre amour, aide, compréhension encouragement et soutien financier pendant ces 4 dernières années. Faites que votre fierté pour mon aboutissement soit toujours bien considérée. Il va être fantastique de pouvoir vivre de nouveau une vie normale mais surtout de pouvoir mettre au monde un bébé dans de telles familles bienveillantes.

Lastly but, of course more importantly, I thank Stéphane. You made me laugh when things went bad, composed the best gourmet meals to the envy of French Chefs and friends alike, dragged me away from the computer to enjoy our lives in snowy mountains and scrubby bush, and have shared all my trials and tribulations with unending love, encouragement and support. The end of this thesis is a celebration and achievement for us both.

ABSTRACT

This thesis examines in great detail, while employing strict statistical methods, the use of diatom transfer function models for estimation of sea-surface temperature and sea-ice in the southeast Indian Ocean. The examination of model applications is undertaken in three stages: species taxonomy and database compilation, model construction and robustness, and derivation of palaeoceanographic changes in down-core material. The southeast Indian Ocean sector is chosen for study to advance a Southern Ocean perspective on recent palaeoceanographic studies within the Tasman Sea. The study region also expands the applicability of the Southern Ocean diatom transfer method to a poorly known sector of the Southern Ocean.

Major taxonomic revision of diatom species observed in core-top material from three available diatom data sets is conducted. Twenty-nine species or taxa groupings are discussed in detail and require revision. Four additional diatom and silicoflagellate taxa are found incompatible between databases or unwarranted for transfer function analysis and therefore, are removed from further study.

A core-top diatom database is compiled using sample-selection criteria and through the removal of samples representing unique environmental regimes (ie. Antarctic Peninsula region). A total of 115 samples from an original 194 remain available for use, and are identified as the Antarctic Diatom Database (ADB). Species sedimentary distributions and relationships to several sea-surface parameters [viz. (1) February/August sea-surface temperature, (2) February/September sea-ice concentration, and (3) annual sea-ice cover] are analysed for the major species/taxa groups with relative abundances over 1%. Benthic/neritic species are removed from consideration as they are considered allochthonous in the derivation of open-ocean core parameter analysis. A total of 24 species with relative abundances over 2% are considered appropriate for further statistical analysis. The innovative dissolution data set of Pichon *et al.* (1992b) is found inappropriate for inclusion in the thesis database. The rejection is determined through the varied degree of dissolution, small sample size, and biogeographical coverage combined with over- and under-estimation of natural variability in the northern and southern samples respectively, which results in erroneous sea-surface temperature estimation.

Sea-surface temperature modelling using the Imbrie and Kipp method (1971; Pichon *et al.* 1987, 1992a) is emulated because it is currently the most appropriate model for diatom sea-surface temperature estimation. The ADB is factor analysed and comprehensively examined for a factor solution amenable to biogeographic and species partitioning. An over-simplified model misrepresents the range of relationships acting on the diatom distributions. Consequently, a 6-factor model is chosen, which is then compared and discussed against the original transfer function of Pichon *et al.* (1992a). Model robustness and variations in the databases are discussed substantially. Although both models have similar large multiple correlation coefficients and low standard error estimates, the actual residual analysis and inclusion of dissolution data witnesses greater departures in the Pichon *et al.* (1992) model in comparison to the 6-factor model compiled from the ADB.

A new method of sea-ice estimation is developed in the thesis. The method accounts for non-constant variance and the overwhelming number of zero data contained within the parameter data set. Three models are proposed which estimate sea-ice concentration in February and September, and annual sea-ice cover.

The two sea-surface temperature and three sea-ice models are then applied where possible to the four late Quaternary cores chosen for study in the southeast Indian Ocean sector, along a transect following the 146°E meridian. Oxygen-isotope analyses available for the cores allow age models to be developed. Sea-surface temperature estimates vary between the two SST models. The elevated number of non-analogue events and low communality values of the Pichon *et al.* (1992a) model diminish the confidence of the remaining sea-surface temperature estimates. This response is in direct contrast to the low number of non-analogues and high communalities of the sea-surface temperature model developed here in the thesis. The latter model is adopted for sea-surface temperature estimates of the core material conceding that warm sea-surface temperature estimates are under-estimated by up to 2°C. Sea-ice estimates are considered relevant and equitable with the sea-surface temperature estimates during cool intervals and provide open-ocean conditions during warm intervals. Sea-ice is also formally linked to the presence, but not amplitude, of the radiolarian *Cycladophora davisiana* abundances in the core samples.

Climatic interpretation of one core (MD88-787, 56°22.72'S, 145°17.56'E, 3020 mbsl) and isotopic time-slices for the region of study are proposed. The main conclusion determined from the integrated palaeontological and palaeoceanographic approaches derived from the core material propose a unique palaeoceanographic scenario south of the Tasman Sea during glacial isotopic-stages 2 and 6. The glacial scenario implies specific restructuring and stratification of the surface waters between the northward, advanced sea-ice edge and the Subtropical Convergence. Such restructuring is proposed to have affected Subantarctic Mode Water development and vertical mixing, consequently dampening diatom productivity at the surface and related abundances in the sediments. Allochthonous diatoms, observed as non-analogue events after transfer function analysis, point to enhanced Antarctic Bottom Water activity from the Ross Sea during these glacial episodes. In contrast, winnowing and changes in Central Deep Water velocity probably influence the sediment record of subantarctic core MD88-779 (47°50.69S, 146°32.75' E, 2260 mbsl) during the same glacial stages.

This page left intentionally blank.

and diverse, that is, in waters warmer than about 5°C. (Howard and Prell 1992). Antarctic radiolaria are reported living between 200-300m down to 4000m (Casey 1977, Morley and Stepien 1985), and so do not reflect sea-surface conditions in their variations.

Siliceous diatom frustules, the remains of the unicellular algae that are the major primary producers in the ocean, are the major component of the sediments in the Southern Ocean south of the Subtropical Convergence (Lisitzin 1972, Burckle 1984a). Diatoms are ideal for analysis of past sea-surface conditions, as algae they are restricted to the illuminated surface layer of the sea and survive within and under the sea-ice surrounding Antarctica. Work on obtaining SST estimates from diatoms, has shown promising results with standard errors of approx. ±1.3°C (Pichon *et al.* 1987, Pichon *et al.*1992a, Zielinski 1993). Although the temperature estimates are biased outside the main silica ooze belt by opal dissolution, this bias can be accounted for (Pichon *et al.* 1992b). The few available results from this method appear to be in agreement with results from other methods of evaluating temperature change (eg. oxygen-isotope ratios and foraminiferal estimates: Labeyrie *et al.* 1996; Vostok ice core records: Pichon *et al.* 1992a, Sowers *et al.*1993).

As Barrows *et al.* (1996) illustrate, so far there are no reliable palaeoceanographic data available in the Southern Ocean between Tasmania and Antarctica. A single core used in CLIMAP reconstructions was noted to have inconsistent sea-surface temperature (SST) estimates (CLIMAP Project Members 1984). Most recent palaeoceanographic studies in the Australian region have been confined to studies north of the South Tasman Rise to the Coral Sea and north of the Naturalist Plateau on the western coast of Australia. Many of such studies are compiled in a recent joint issue edited and summarised by De Deckker (1997). Thus, the study of diatoms in elucidating SST and sea-ice records in the late Quaternary was a direct attempt to rectify the current dearth of modern palaeoceanographical data relevant to Australian palaeoceanography. The results of this study are the first polar SST and sea-ice records available to assist in defining Australian past climate conditions.

1.1.2. Aims of the study.

As detailed above the primary aim of the thesis was to provide a considerably modernised interpretation of the southeast Indian Ocean sector during the late Quaternary. To reach this aim, the use of diatoms in the sediments was employed and focused on using the established diatom transfer method of Pichon *et al.* (1987, 1992a) to reconstruct the first SST history of the Southern Ocean south of Australia. Sea-ice estimation was to abridge the initial findings of Pichon *et al.* (1987).

Other aims of the thesis include:
- the construction of biogeographic and physical parameter relationships of diatom species observed in the sediments,
- the identification of past water-mass movement associated with frontal displacement,
- to advance a climatic interpretation of the study region drawing upon previous Southern Hemisphere studies of relevance.

1.1.3. Format of the thesis.

The format of the thesis in essence follows the derivation of minor aims to arrive at the major aim of the study. The thesis structure is presented through the following chapters:

Chapter 1 provides an introduction to the thesis, background information relevant to previous diatom studies and sea-ice and oceanography of the study region, and the basic methodology used to extract diatoms from sediment samples. Chapters 2 and 3 cover taxonomic issues and the database reorganisation, resulting in the database used in this thesis. Chapters 4 and 5 cover the statistical methodology and construction of the transfer functions for sea-surface temperature and sea-ice estimation respectively. Implementation of the two transfer functions on cores located in the southeast Indian Ocean and interpretation of the results are covered in Chapter 6. The conclusions and future directions are presented in Chapter 7.

1.2. PREVIOUS DIATOM STUDIES - STATISTICAL AND REGIONAL.

This work expands upon the methodology proposed by Pichon (1985) and Pichon *et al.* (1987, 1992a) for the diatom transfer function. The original transfer function was established for foraminifera in the equatorial regions by Imbrie and Kipp (1971). A history of use of both factor analysis and transfer function for marine diatoms was presented in Zielinski (table 1, 1993) and is up-dated by the works listed in Table 1.1.

Diatom research in the southeast Indian Ocean sector of the Southern Ocean is relatively sparse. The most comprehensive account of the surface and vertical distribution of marine diatoms was produced by Abbott (1971, 1973, 1974) who worked on *Eltanin* core top material and nine piston cores. His work distinguished the surface sediment occurrence of the diatoms into two assemblages (Figure 1.1). In addition, his climatic assessment derived from a ratio of the two assemblages applied to the cores, indicated that up to 10 warm and 9 cold climate peaks occurred during the Brunhes chron. Aside from Abbott's work, other reports of diatoms in the research region emanate from DSDP cruises (Mc Cullom 1975, Hajòs and Stradner 1974, Kennett *et al.* 1974, Burns 1977) but remain

Author	Region	Method	Result
Sancetta (1981)	Bering Sea	IKM, FA	4-factor model
DeVries and Schrader (1981)	Eastern Pacific, Peru Coast	none	Assemblage analysis, cold/warm water mass scenarios.
Krebs *et al.* (1987)	Arthur Harbour, Antarctica	IKM, FA	4 factor model, sea-ice type distribution
Burckle *et al.* (1987)	New Zealand to Ross Ice Shelf	IKM, FA	6-factor model, surface water diatoms distribution
Burckle (1987)	Weddell Gyre	IKM, FA	3-factor model water samples, 4 factor model sea-ice samples
Burckle (1989)	Northern Indian Ocean	IKM, FA	3-factor model, factor distribution maps, LGM analysis
Estrada and Delgado (1990)	Weddell Sea	PCA	3-PCA's resolved (35.6%)
Schrader and Sorknes (1991)	Eastern Pacific, Peru Coast	IKM, FA, R	7-factor model, 4 factors mapped, palaeoproductivity curve.
Schrader *et al.* (1993)	Eastern Equatorial Pacific	IKM, FA, R	4-factor model, Palaeoproductivity curve
van Iperen *et al.* (1993)	Indonesian Archipelago	IKM, FA	3-factors (87.7%), factor & taxa distribution maps.
Zielinski (1993)	South Atlantic sector of Southern Ocean	IKM, FA, R	3-factor model. Palaeotemp, Palaeosalinity, Palaeophosphate curves.
Schloss and Estrada (1994)	Weddell-Scotia confluence region	PCA, CA	3 PCA's, 2 clusters. Distribution of phytoplankton
Lapointe (1995)	Gulf of St. Lawrence, Canada	IKM, FA	7-factor model
Knaack *et al.* (1995)	Equatorial Atlantic Ocean	SIMMAX	Palaeoproductivity curves
Labeyrie *et al.* (1996)	southeast Indian Ocean	IKM, R	4-factor model, Palaeotemp. curve, comparison with Foraminifera Palaeotemp. curve.
Whitehead & McMinn (1997)	Fjords of Vestfold Hills, Antarctica	PCA, CA	5 clusters, 2 PCA's (58%) Palaeodepth estimation

Table 1.1. Recent literature on oceanic diatom analysis. Appended to Zielinski's (1993) Table 1. Abbreviations. LGM = Last Glacial Maximum; IKM = Imbrie and Kipp Method; FA = Factor analysis, PCA = Principal components analysis, R = Regression, CA = Cluster analysis, SIMMAX = an acronym for modern analogue technique using a similarity index.

little more than observational lists. Other diatom studies on both phytoplankton and sediment distributions in the vicinity of the research region have been covered by works including those of Hart (1937), Jousé *et al.* (1962a,b), Cassie (1963), Zernova (1970), Hasle (1976), Kozlova (1961, 1962, 1966, 1970, 1971), Burckle (1984a), Burckle *et al.* (1987), Leventer (1992), and Harwood and Maruyama (1992).

Since Abbott's preliminary division of two diatom assemblages, other workers have shown that the third zone, Antarctic, does have a stronger presence in the southeast Indian sector which Abbott could not observe (Burckle 1984, Pichon *et al.* 1992a).

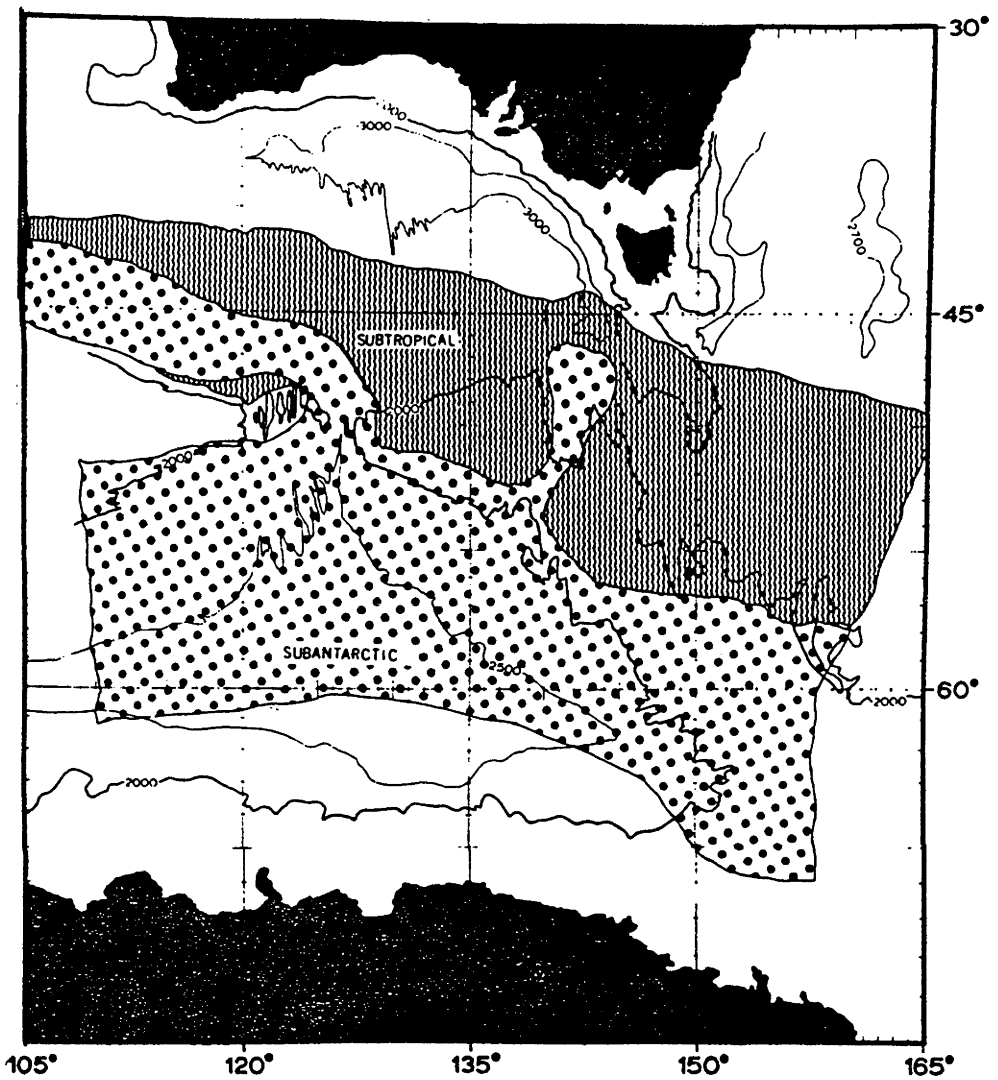

Figure 1.1. Abbott's distribution of diatom assemblages in the southeast Indian Ocean derived from his study of 154 *Eltanin* core tops. A third assemblage for the Antarctic region was found masked by the subantarctic assemblage and therefore, not defined. Excursions of the subantarctic assemblage to the north were related to the movement of bottom water currents through the Australian-Antarctic Discordance. (figure. 5, Abbott 1974).

Furthermore, diatom distributions (assemblage differences) have been observed to be variable on either side of oceanographic frontal positions (eg. Kozlova 1966, Hasle 1969, Burckle 1984a, Burckle *et al.* 1987, Gersonde 1990b).

1.3. DIATOM ECOLOGICAL RESPONSES

Diatom distributions in the polar regions have been attributed to physical and biological processes (Priddle *et al.* 1986, Smith and Sakshaug 1990). Physical processes acting on distribution include fronts, eddies, and sea-ice cover (eg. Bianchi *et al.* 1992, Kang *et al.* 1993, Dieckmann 1994, Yoder *et al.* 1994, Granata *et al.* 1995, Hibler and Zhang 1995, Ackley *et al.* 1996, Leventer and Dunbar 1996), each of which are characterised by variations in surface water structure, chemistry and temperature, and the atmosphere interface. Biological processes affecting distribution include sinking, grazing stress, and species physiology (eg. Krause 1981, Smetacek 1985, Palmisano *et al.*, 1987, El-Sayed 1988, Holm-Hansen and Mitchell 1991, Fisher *et al.* 1996, Fisher and Harrison 1996, Takahashi 1994). Furthermore, distributions in the sediments appear related to particle flux, dissolution, currents and preservation (eg. Jousé *et al.* 1971a,b, Lisitzin 1971, Frankes 1975, Kolla *et al.* 1978, Edmond *et al.* 1979, Nelson and Gordon 1982, Gersonde 1986, Leventer and Dunbar 1987, Wefer *et al.* 1988, Arrhenius 1988, Kamatani *et al.* 1988, Shemesh *et al.* 1989, Abelmann and Gersonde 1991, González 1992). Both physical and biological processes at the surface produce the primary distribution patterns of diatoms and yet, on a secondary level, influence the distributions in productivity due to a regulation of surface water stratification and nutrient/energy utilisation (Smith and Sakshaug 1990).

Brief discussions on both the documented physical and biological effects on diatoms of the two parameters dealt with in this work - temperature and sea-ice - are summarised below.

1.3.1. TEMPERATURE.

El-Sayed (1970, 1984) dispelled the myth of high productivity in the Southern Ocean as a function of high nutrient availability which continued to be observed between the Polar Front and the Antarctic Continent (Holm-Hansen *et al.* 1977). Distribution of diatoms was thus considered regulated in part by sea-surface temperature, water mass characters and mixing (Hasle 1969). Diatoms have been found to show growth response particular to the temperature range in which they survive (Suzuki and Takahashi 1995). Since this early concept, statistical studies have identified sea-surface temperature as one of the highest correlative physical characters that define Southern Ocean diatom distributions (eg. Burckle *et al.* 1987, Pichon 1985, Pichon *et al.*1987, 1992a). The role of temperature in distribution also reflects on the diatoms biological ability to survive and

grow in environments that are effected by varying light regimes and surface mixing as noted below.

Specific studies into the role of temperature on certain species of diatoms have revealed that diatoms regulate the rate of photosynthesis as a function of the temperature range in which they live (Neori and Holm-Hansen 1982, Smith *et al.* 1994) rather than by the limits of light and nutrient availability. Studies and models of photosynthetic rate and long daylight conditions with decreases in temperature allowed Antarctic diatoms to flourish, but with decreased daylight and increased surface mixing the respiration and growth rates of diatoms were found to decrease (Tilzer and Dubinsky 1987, Fiala and Oriol 1990). The hypothesis proposed being that, south of the PF, diatoms have slowed metabolisms (eg. as a function of temperature dependent photosynthesis (Davison 1991)) which reduces the use of nutrients and light energy (Tilzer *et al.* 1986, Jacques 1983). However, in contrast, many Antarctic diatoms are reported as unable to survive temperatures greater than 10-12°C making them psychrophilic (adapted to low temperatures) (Jacques 1983).

The uptake of nutrients, particularly silica, as a function of the environmental temperature in which a diatom lives, has also been shown to affect the morphology of that species. Studies on Antarctic diatoms by Syvertsen (1977), Villareal and Fryxell (1983), Fryxell (1986) and Fryxell (1991) have shown that a single species can vary in morphology due to such changes in silica and/or temperature variations.

Temperature does not appear to play a role in distribution or morphological change in species in the subtropical region (ie south of the STC) (Fryxell and Hasle 1972, Fenner *et al.* 1992). Whereas at the opposite end of habitat choice, diatoms in sea-ice and very low SST are found to be retarded in growth more by the level of salinity or light irradiation than temperature (Palmisano and Sullivan 1982, Palmisano *et al.* 1987, Aletsee and Jahnke 1992).

1.3.2. SEA-ICE

Diatoms are found existing both within and under sea-ice (eg. Clarke and Ackley 1984, Horner 1985, Garrison *et al.* 1983a, 1986, 1987, Garrison and Buck 1989, Ackley and Sullivan 1994). Distribution within the sea-ice environment has been linked with the availability of light, snow cover on sea-ice, and degree of salinity (Palmisano and Sullivan 1983, Palmisano *et al.* 1987, Eiken 1992). Additionally, sea-ice type (ie. frazil or congelation ice) could determine variations of diatom communities or their presence within or below the surface of the ice (Clarke and Ackley 1984, Garrison and Buck 1991). The role of an ice active substance which produces pitting on the sea-ice

(Raymond *et al.* 1994, Amsler and Raymond 1995) may be related to this variation in sea-ice diatom community types, but is otherwise hypothesised for a multitude of functions including ice growth inhibition, attachment site formation, or refraction of light through the sea-ice.

A review of sea-ice diatom ecophysiology is presented by Kirst and Wiencke (1995). They concluded that many stresses are a part of the sea-ice habitat diatoms are subject to. Such factors are low temperatures, freezing, high and low irradiance levels, high and low salinities, grazing pressure, nutrient depletion and deep mixing. The ability of Antarctic diatoms to decrease metabolic functions (respiration and photosynthesis) as mentioned above is linked to temperature control and adaptation, is a feature which permits their survival in such a variable environment.

An important facet of sea-ice is the pseudo-neritic environment it presents to phytoplankton (Hart 1934, 1942, Kozlova 1966). High levels of productivity have been linked to the marginal sea-ice zone in spring/summer from in situ studies (Smith and Nelson 1985, 1986, Wilson *et al.* 1986, Nelson *et al.* 1987, Sullivan *et al.* 1988, Fryxell and Kendrick 1988, Fryxell 1989, Smetacek *et al.* 1992) and by satellite means (Sullivan *et al.* 1988, Comiso *et al.* 1990). In the Marginal Ice Zone (MIZ) productivity is enhanced by several factors : apparent seeding from the sea-ice populations, increased light penetration, shallowing of the mixed layer a result of freshwater input, and reduced wind mixing (Ekman transport) due to the proximal location of the sea-ice (Smith 1987, Eiken 1992). The MIZ is a dynamic, seasonal one following the retreat and decay of sea-ice through spring and summer. The MIZ is comparable to the SIZ of Tréguer and Jacques (1992, Section 1.4.4). Diatoms are later concentrated into the sea-ice by frazil ice formation in the autumn (Garrison *et al.* 1983b, 1989).

A climatic effect derived from sea-ice diatoms in the MIZ, which is taking on increased importance, is the role they may play in producing particulate dimethyl-sulphide (DMSP) which can affect cloud condensation nuclei levels (Levasseur *et al.* 1994). Both Antarctic and Arctic studies have shown that sea-ice diatoms produce (DMSP) (Levasseur *et al.* 1994, Kirst *et al.* 1991). DMS levels inferred from atmospheric methane-sulphonate values at Vostok indicate late glacial periods with increased emissions of DMS (Legrand *et al.* 1991). Such increased emissions at the end of glacials are in line with an increase of evaporation and consequently precipitation in through interglacial periods (Yiou *et al.* 1985). The fact that sea-ice cover is considered greatly enhanced during at least the last glacial maximum (CLIMAP Project Members 1976, 1981) suggests that DMSP build-up within the ice, and subsequent release during the interglacial periods, are linked to the

presumably slow accumulation of DSMP from sea-ice diatom productivity extended over glacial periods.

1.4. SEDIMENTOLOGY.

The sedimentary patterns of the southeast Indian Ocean were summarised by Conolly and Payne (1972) (Figure 1.2). Moriarty (1977) looked at the clay minerals and silica content of the southeast Indian sector basin sediments and illustrated the distribution of opaline silica (Figure 1.3). His study concurs with others, which report polar sediments dominated by diatom remains that form a belt of diatom ooze between approximately 50° and 60°S (Lisitzin 1972, Goodell 1973, Burckle *et al.* 1984a).

In general, the basin sediment surfaces covering the Tasmania-Antarctic transect studied in this thesis have already been described. Core traverses made by Watkins and Kennett (1972) on *Eltanin* material corresponding to this study area indicate that the sediment tops occur within the Brunhes time frame, although in a mid-section between 50°S and 62°S in the 147-150°E traverse, bottom water erosion has exposed Gauss and Gilbert-aged sediments at the surface (2.6 My and 3.58 My respectively). The traverse along 140°E completed by Conolly and Payne (1972) suggests that calcareous ooze covers the ridge and to the north of 52°S, calcareous and siliceous oozes exist together between 52 and 55°S and siliceous ooze is dominant to the south of 55°S. The Brunhes period is associated with sediments up to 6m thick. Their traverse at 142-148°E shows essentially the same sediment facies as in the 140°E traverse, however, in the earlier Matuyama chron more siliceous ooze has been observed. A manganese pavement identified by Watkins and Kennett (1972) is also recognised by Conolly and Payne (1972) between 50-57°S at a transect 151°E. The sediments at the surface of the manganese pavements are much younger (Matuyama to Gauss aged) suggesting that bottom water has removed the recent sediments.

Recent work by Bareille (1991) in the southeast Indian Ocean suggests that cores located in the Subantarctic Zone have a mean recent sedimentation rate between 2-7.5 cm/Ka and cores in the Polar Front Zone have a mean recent sedimentation rate around 10-20 cm/Ka.

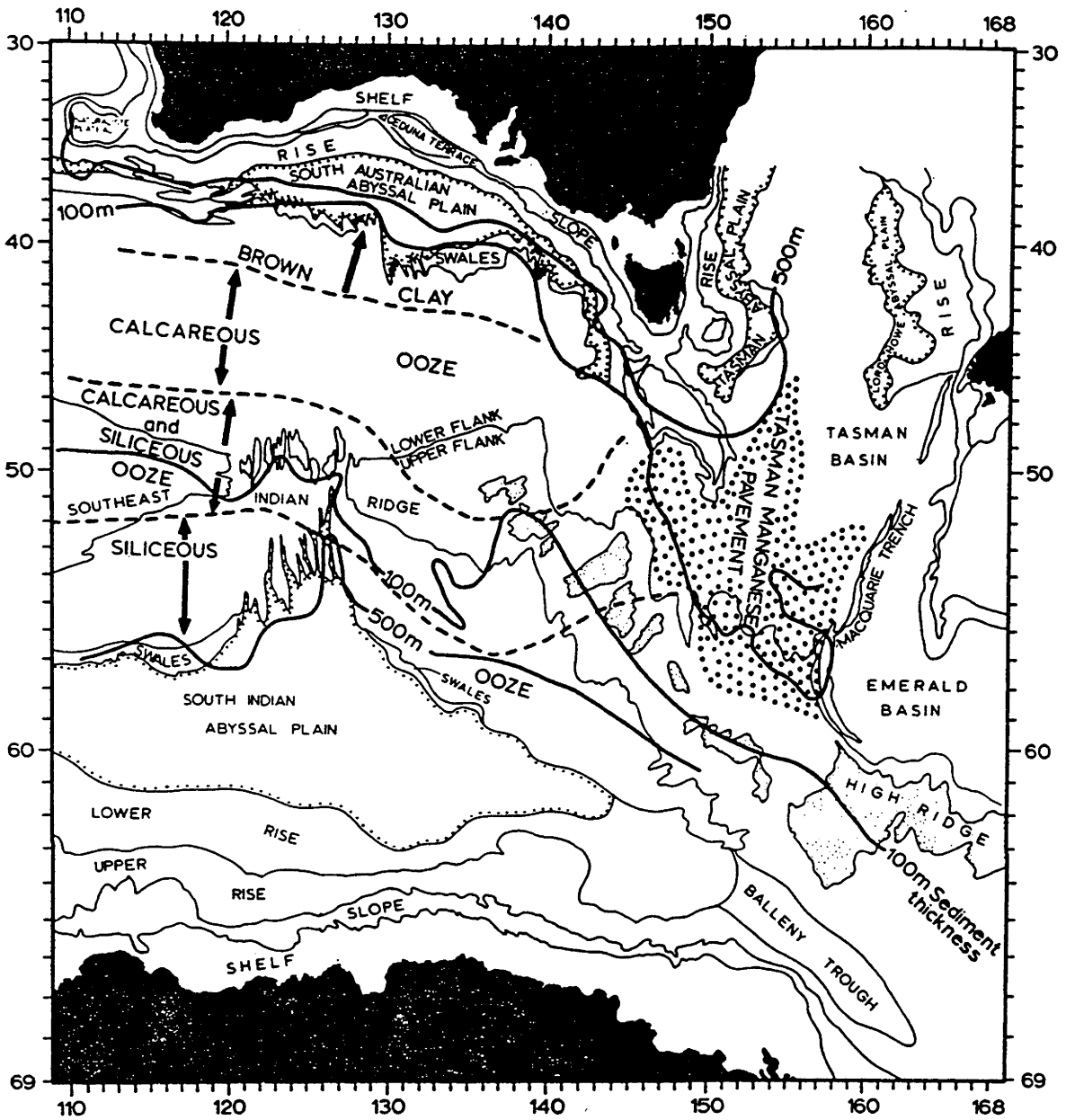

Figure 1.2. Representation of sedimentary accumulation patterns in the basins of the southeast Indian Ocean. The study transect of this thesis (140-150°E) traverses, from north to south, a manganese pavement, a mixed calcareous and siliceous ooze belt and a siliceous ooze belt. (from figure 1, Connolly and Payne 1972).

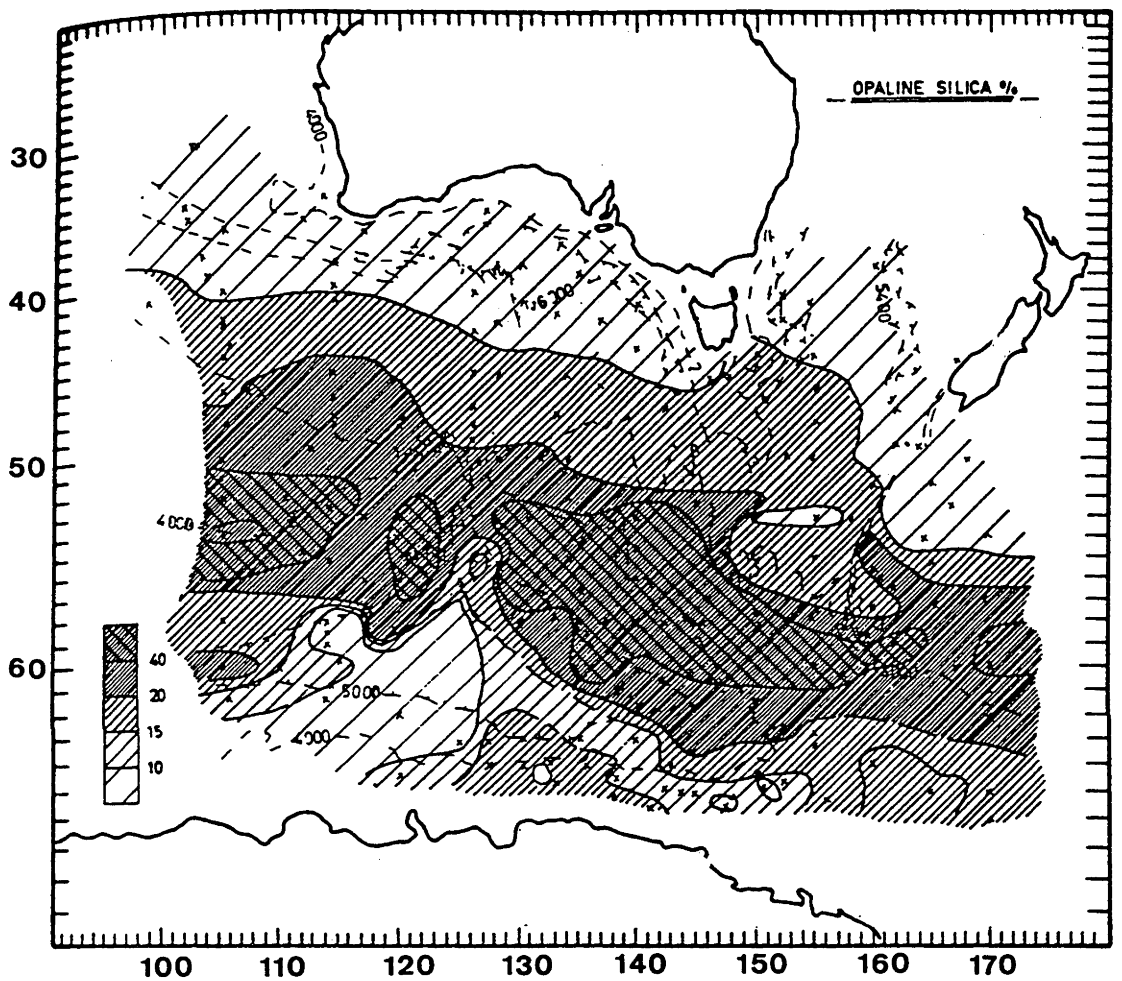

Figure 1.3. Distribution of opaline silica in the sediments of the southeast Indian Ocean. Sediments in the study transect (140-150°S) contain between 15-50% opaline silica. (from figure 13, Moriarty 1977).

1.5. REGIONAL OCEANOGRAPHY

1.5.1. THE SOUTHERN OCEAN, ITS BASINS AND THE ANTARCTIC CIRCUMPOLAR CURRENT.

The area of research is contained within the more frequently labelled Southern Ocean, the oceanic region from the coast of Antarctica (~70°S) to the Subtropical Convergence (~40°S) which acts as a connective pool to the world's oceans (Gordon 1971a, Tchernia 1980, Tomczak and Godfrey 1994). More accurately, the research region is contained in the south east area of the Indian Ocean, the Indian Ocean being defined from 20°E - 146.55°E (Tomczak and Godfrey 1994).

The bottom topography of the Australian Sector of the Indian Ocean (Figure 1.4) is dominated by the Mid-Ocean Ridge which traverses E-W at ~50°S, symmetrically splitting the distance between South Australia and Antarctica and then trends southward from 140°E (Hayes and Conolly 1972, Rodman and Gordon 1982). This ridge separates three basins; the South Australian Basin and the Tasman Basin to the north, and the South Indian Basin to the south (Rodman and Gordon, 1982).

The Australian-Antarctic Discordance is a series of fractures in the Mid-Ocean-Ridge between 120-125°E that form a deep passage between the South Australian and South Indian Basins (Figure 1.4). Another series of fractures occurs to the east where the Mid-Ocean-Ridge is displaced in blocks south-eastwards from 138°E to its junction with the Macquarie Ridge (Hayes and Conolly 1972, Conolly and Payne 1972). Known as the Tasman Fracture zone, it is important for the flow of bottom water to the north into the Tasman Sea across the Mid-Oceanic Ridge (Conolly and Payne 1972). The Tasman Basin is located between Australia and New Zealand, the Mid-Ocean-Ridge and the Macquarie Ridge. This basin is characterised by two regimes of sedimentation, those being north of 48°S are thick while those to the south are thin because of low or non-deposition (Hayes and Conolly 1972, Conolly, 1972).

The Southern Ocean is driven mostly to the east by prevailing westerly winds which occur between 35°S and 60°S, whereas south of 60°S to the Antarctic Continent a narrow band of slower westward-flowing water is driven by easterly winds (Lozano and Hays 1976, Tchernia 1980). The Antarctic Divergence is found between these two directions of water flow, and it is the region where upwelling occurs through the Ekman divergence produced by the wind fields (Gordon 1988).

As a result of the strong westerly winds, the eastward Antarctic Circumpolar Current (ACC) is formed in the northern Southern Ocean between ~40°S and 60°S (ie. it is bounded by the Subtropical Convergence to the north and by the Polar Front to the

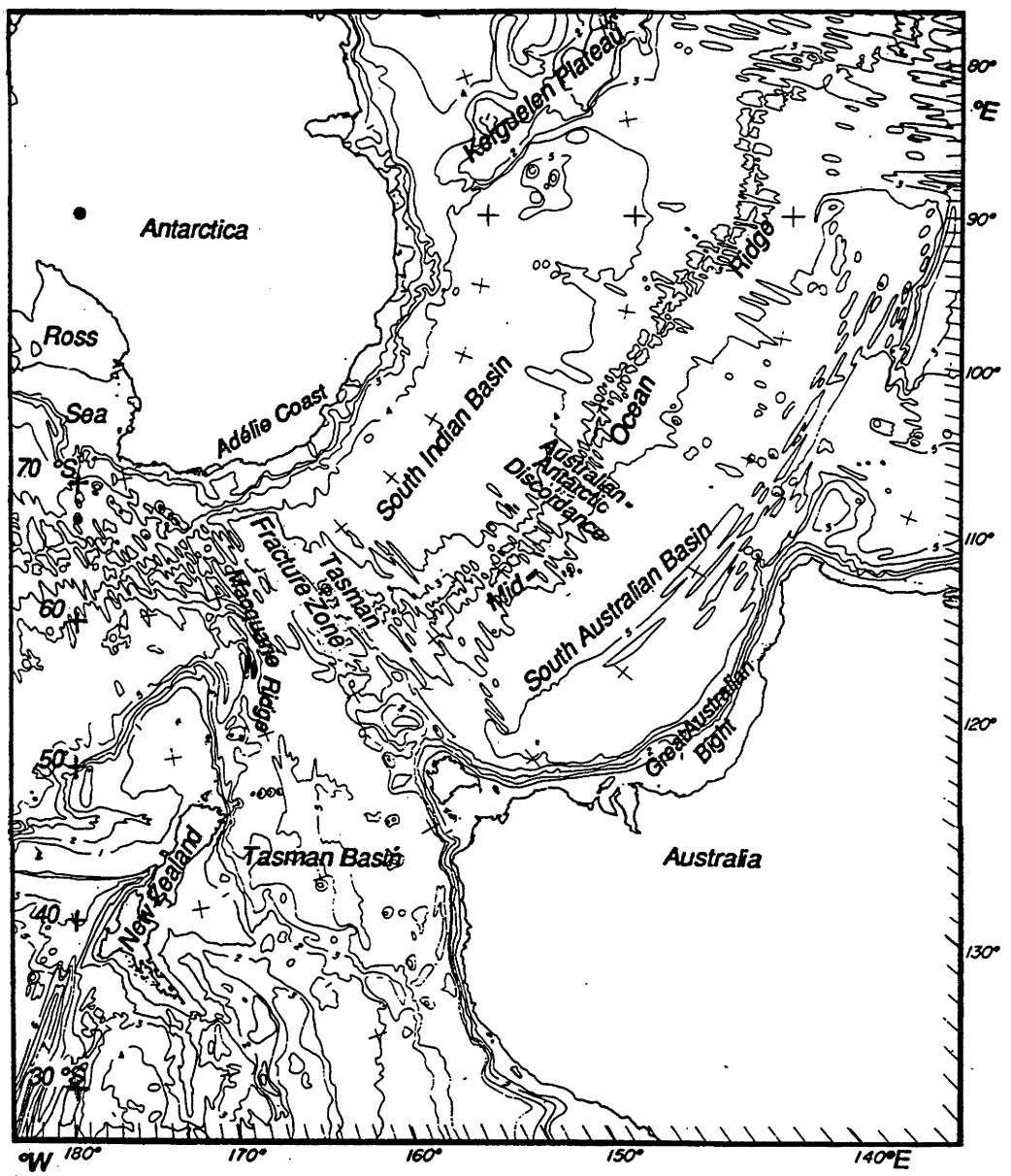

Figure 1.4. Bottom Topography of the southeast Indian Ocean, illustrating basins and other topographical and oceanographical features as described in the text. Contours in kilometres (Adapted from Gordon and Molinelli, 1986, plate 1).

south). The ACC has an estimated net transport between 100 and 158 x 10^6 m^3/s (100-158 Sv) with 80% of this total transport occurring between the Subantarctic Front and the Polar Front at ~50°S (Gordon 1972a, Rintoul and Church 1993, Orsi *et al.* 1995).

Bottom topography influences the latitudinal position of the ACC (Lozano and Hays 1976) in an effect known as the conservation of potential vorticity. Thus, where the ACC encounters troughs in the bottom topography, the current spreads itself vertically and moves southward. Under the alternative condition where the bottom topography forms a rise, such as near the south of New Zealand, the vertically squashed ACC conserves its angular momentum by diverting north (Gordon 1988, Whitworth III 1988, Dr R. Nunes-Vaz, pers. comm. 1994). South of Australia, in the region of research, the ACC follows the Mid-Ocean-Ridge south of the Tasman Sea, and then further south to the Macquarie Ridge (60°S) below New Zealand where it passes through to the Pacific Ocean (Gordon 1972a, 1972b, 1988, Whitworth III 1988, Tomczak and Godfrey 1994). Surface eddies in the ACC, particularly south of the Tasman Sea (Rochford 1981, Grieg 1982, Gordon 1988, 1991), are also influenced by the bottom topography. Morrow *et al.* (1992) suggest the surface eddies accelerate the mean flow of the ACC. Bottom topography is considered to steer the currents in the southeast Indian sector (Rintoul *et al.* 1997).

Deacon (1937) noted that the surface water flow of the ACC was meridional due to strong eastward surface winds throughout the Southern Ocean. However, as illustrated through his comprehensive research of surface temperature and salinity relationships, the ACC was observed to be zonally banded. Originally, three surface/sub-surface bands (fronts) were identified in the ACC; the Polar Front, the Subantarctic Front and the Subtropical Convergence. Since that time many other frontal divisions have been elucidated, these are summarised by Orsi *et al.* (1995), Belkin and Gordon (1996), and Rintoul *et al.* (1997). South of Australia (115-150°E) the three main fronts are observed (ie Polar Front, Subantarctic Front and the Subtropical Convergence, Figure 1.5) (Edwards and Emery 1982, Orsi *et al.* 1995, Belkin and Gordon 1996, Rintoul *et al.* 1997). Both the Polar Front and the Subantarctic Front have been observed as confluent in sections of the Indian Ocean and the southeast Indian Ocean contrary to the historical definitions (Park *et al.* 1993, Belkin and Gordon 1996).

1.5.2. Oceanographic Fronts of the ACC.

The circumpolar position for each of the fronts illustrated in this work are taken from Orsi *et al.* (1995) and are presented in Figure 1.5. Slight differences in the regional placement of the fronts are possible and, particular to this study, the variations since detected by Rintoul *et al.* (1997) indicate that such variation exists.

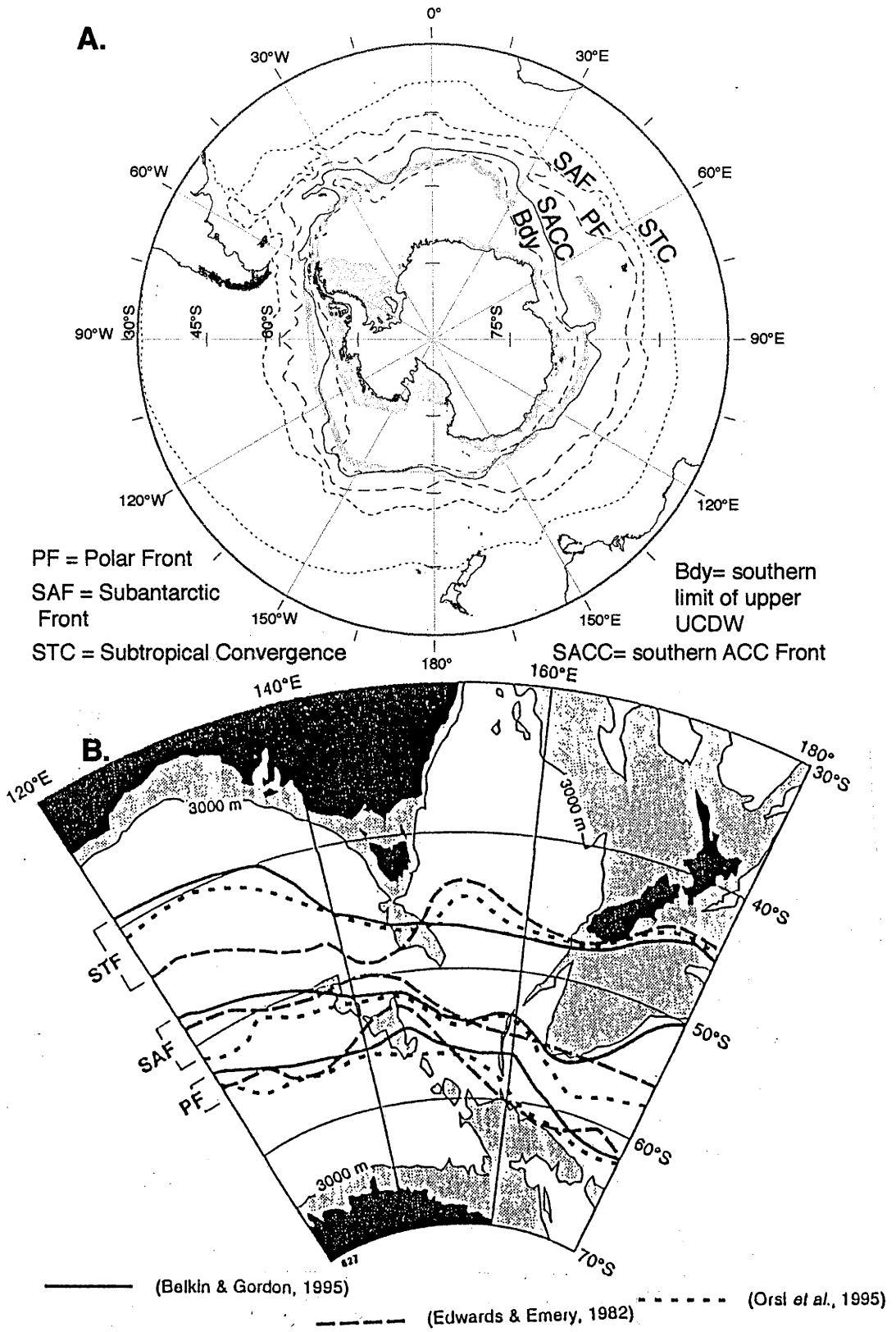

Figure 1.5. Distribution of Oceanographic Fronts. **A**) Oceanic Fronts of Orsi *et al.* (1995). Note that their southern limit of Upper Central Deep Water (Bdy) corresponds to the maximum Sept.sea-ice edge (grey line). The Kerguelen Plateau obstructs the Bdy front disturbing this relation. **B**) Regional Fronts of the southeast Indian Ocean. Variation in the placement of Fronts by the three main works available (from Rintoul *et al.* 1997, fig.10).

Polar Front

The Polar Front (PF) has been given several names (Meinardus line, Oceanic Polar Front, Antarctic Convergence, Antarctic Polar Front and Antarctic Front) because its characteristics suggest convergence, divergence or a combination of the two (Gordon 1971a, Peterson and Stramma 1991). The PF separates the Antarctic waters from the Subantarctic and was understood to be at the position of the northern most extent of the winter Antarctic Surface Water (or temperature minimum) (Park *et al.* 1993). Confusion of its actual position at the surface towards the north and at the sub-surface to the south (Deacon 1937, Gordon 1971a, 1971b), lead to the discovery of the northern surface expression of the front being named the Subantarctic Front (Burling, 1961). Most workers define the PF on a 2°C temperature minimum at between 100-300 m (refer to Belkin and Gordon (1996) for a comprehensive summary). The PF in the study transect is identified by a (200 m) temperature minimum of 2°C which is appears constantly near 53°S in the study region (Edwards and Emery 1982, Rintoul *et al.* 1997). Rintoul and Church (1993) recently identified the northern-most winter extent of the PF at 54°S between 146°E and 136°E. At the PF, the Antarctic Surface Water sinks under the Subantarctic Surface Water and contributes in the formation of Antarctic Intermediate Water (Tchernia, 1980).

Subantarctic Front

Identified by Burling (1961) south of New Zealand, and north of the PF, the Subantarctic Front (SAF) was characterised predominantly by a decrease in surface salinity of the order <34.5‰ at 100 - 400 m, where temperature was below 8°C. In the region south of Australia, Edwards and Emery (1982) identified the summer position of the SAF occurring between 49-54 °S from decreases in temperature and salinity gradients, while more recently Rintoul and Church (1993) identified the winter SAF at 50°S, 4° from the PF, between 146-136°E. The importance of the SAF lies in its climatic ability to define the origin of Subantarctic Mode Water that is the deep winter convective layers which sink to ventilate the tropical thermoclines (Mc Cartney 1977, Belkin and Gordon 1996). The SAF boundary has also been used by Heath (1985) to define two subantarctic water masses, the northern Australian Subantarctic Water and the southern Circumpolar Subantarctic Water.

Subtropical Convergence

Deacon (1937) defined the position of the Subtropical Convergence (or Subtropical Front) from his study of the Southern Ocean. South of Tasmania, he found surface waters exhibited a sharp increase in salinity between 34.6 to 35.1‰, and a concomitant increase of temperature from 11 to 13.5 °C, between 42-44°S. Gordon (1972), in the region south of Australia, noted the same salinity gradients at a depth of 20 m between

42-45°S; however, Edwards and Emery (1982) observed the gradient increase between 44-48°S. Rintoul *et al.* (1997) consistently located the STC between the South Tasman Rise and Tasmania in all transects of their study.

The STC is formed as a balance between warm saline subtropical waters driven to the southeast by south-easterly trade winds and cold, weakly saline subantarctic surface waters driven northeast by the westerly winds (Deacon, 1937, Prell *et al.*,1979, Tchernia, 1980). Due to the influence of the convergent wind fields, the STC is not stationary and is more often considered a zone with seasonal shifts as observed with the seasonal temperature variation. Thus, meanders, convolutions and eddies are an integral part of the STC structure (Cresswell *et al.*, 1978, Tchernia, 1980, Tomczak and Godfrey, 1994). Belkin and Gordon (1996) redefine the STC (Subtropical Front in their terminology) into various northern and southern expressions that are in line with the zonal observations of the past. They consider the STC in the western Australian region a continuation and amalgamation of the Agulhas Front and southern Subtropical Front.

1.5.3. WATER MASSES.

In general, water masses are conveniently defined by their particular relation between temperature and salinity, and transitions observed between such bodies refer to transitional waters that are caused by their mixing.

A regional transect from Tasmania to Antarctica (along ~135°S), diagrammatically illustrated in Figure 1.6, is used to depict the position of the water masses occurring in the study region. A summary of the characteristic of the water masses described below is shown in Table 1.2.

Water Mass	Temp. (°C)	Salinity (‰)	Diss. O2 ml/l (*m mol/l)	Density (Ót)	Depth (m)
STSW	12	>35.1	<6.0	<26.4	0-200
SASW	<9	<34.0	>6.5	<26.9	0-100 or 150
AASW	<5	33.8	>7.0	<27.4	0-100 or 250
SAMW	7.5-9	34.4-34.6	5.60-6 (260-280*)	26.8-26.9	500-750
AAIW	4-5	<34.4	4.40-5.40	27.2-27.3	800-1000
CDW	0.8-1.2	34.72-34.74	4.4-4.8	27.7	1000-4000
UCDW	2.7	34.4-34.7	4.15	-	1600-1800
AABW	-0.5-0.4	34.68-34.70	5.0-5.6	27.8	>4000

Table 1.2. Summary table of water mass characteristics as described in the text and additional information derived from Gordon and Molinelli (1986).

Surface water

From north to south there are three main surface waters. The first of these is the Subtropical Surface Water (STSW) travelling eastward interspersed by eddies in the

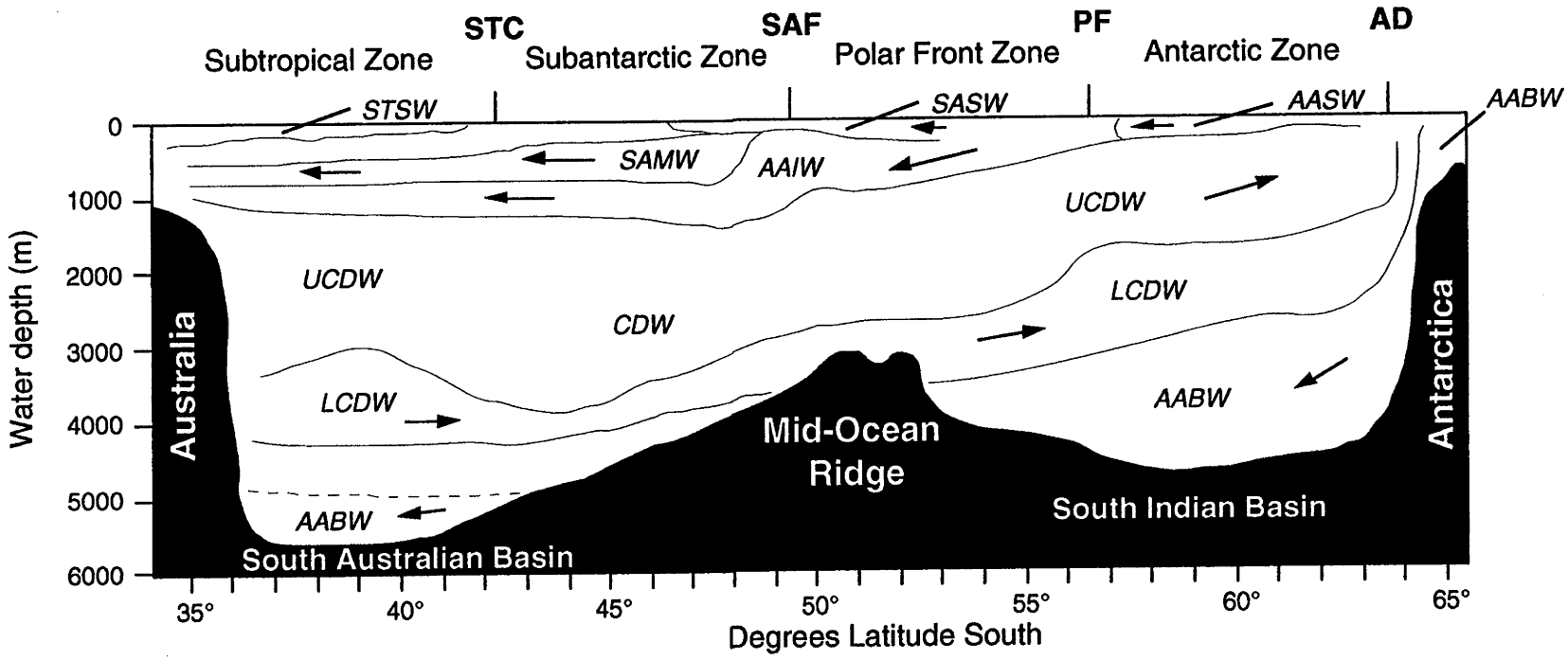

Water-mass:

AABW	Antarctic Bottom Water
AAIW	Antarctic Intermediate Water
AASW	Antarctic Surface Water
CDW	Central Deep Water
LCDW	Lower CDW
UCDW	Upper CDW
SAMW	Subantarctic Mode Water
SASW	Subantarctic Surface Water
STSW	Subtropical Surface Water

Oceanographic Fronts:

AD	Antarctic Divergence
PF	Polar Front
SAF	Subantarctic Front
STC	Subtropical Convergence

Figure 1.6. Diagrammatic circulation of the transect through ~135°E in the southeast Indian Ocean. The position of the Fronts, zones and water-masses are derived from reference in the text and modelled on the plates 141-144 in Gordon and Molinelli (1986). Note that the AABW in the South Australian Basin is divided by a dashed line. This indicates the difference between a water-mass that contains mixed CDW and AABW waters (Braatz and Corliss, 1984).

Subtropical Zone (defined in the subsequent sub-section). Flow of the STSW in the Great Australian Bight is found only to a depth of 200 m and dissipates to very small eddies by 400 m (Wyrtki, 1962a). In the western Indian Ocean, Park *et al.* (1993) defined its characteristics as temperature of less than 12°C, salinity >35.1‰ and oxygen content <6.0 ml/l. A current peculiar to the South Australian Sector STSW, is the Zeehan Current. This is a surface current which flows poleward in a 40 km wide mass along the western coasts of Victoria and Tasmania, to the tip of Tasmania as a result of Westerly winds during the winter in the Great Australian Bight (Baines *et al.*, 1983, Thompson and Veronis, 1983). Another autumn-winter seasonal surface current is the warm and relatively low saline Leeuwin Current. It passage passes from the Equatorial region along the West Australian Coast and into the Great Australian Bight region (Thompson and Veronis 1983, Rochford 1986).

Subantarctic Surface Water (SASW) is a shallow surface layer with salinity and oxygen content increasing with depth until at 100 - 150 m near 49-51°E a shallow oxygen maximum >7.0 ml/l appears. The characteristics known from the western Indian Ocean are: temperature < 9°C, salinity <34.0‰, and oxygen content >6.5 ml/l (Park *et al.* 1993). The SASW is derived in part from the Antarctic Surface Water (Gordon 1971a).

Antarctic Surface Water (AASW) spreads northwards from the Antarctic continent to the PF in a shallow, low salinity, low temperature and high-oxygen content mass in the top 100 - 250m (Deacon 1937, Gordon 1971a, Tomczak and Godfrey 1994). Characteristics for this water mass are; temperatures <5°C, salinity 33.8‰ and oxygen content >7.0 ml/l (Park *et al.*, 1993, Tchernia, 1980). A surface temperature minimum of ~2°C indicates the boundary between the new AASW and its previous winter mixed layer (Park *et al.* 1993). The AASW descends to form mostly Antarctic Intermediate Water when the temperature minimum is deeper than 200 - 300 m (Gordon 1971a).

Subsurface and Intermediate waters

The Antarctic Intermediate Water (AAIW) was initially thought to be derived from low salinity AASW subducted at the PF on its northward flow, and which was found beneath SASW (Rochford 1961, Bye 1968, Gordon 1971a, Tomczak and Godfrey 1994). This characteristic sub-surface salinity minimum is 34.3-34.4‰ which is observed at continued depth of 700 - 900 m south of Tasmania (Rochford 1963) and 700 m at the STC and 1000 m south of New Zealand (Heath 1985). The path of AAIW in the South-eastern Indian Ocean has been noted to travel northwest along the coast of Australia into the Indian Ocean at increasing depths below 1000 m (Rochford 1961, 1963).

More recently, a new method of AAIW formation has been proposed by Mc Cartney (1977), where advection and convection during winter overturn subantarctic waters to renew intermediate water near or north of the SAF, the water mass has been named Subantarctic Mode Water (SAMW) and is essentially identified by a sub-surface isothermal layer in the Indian Ocean of 10-12°C (Mc Cartney 1977, Heath 1985, Gordon 1991, England *et al.* 1993, Park *et al.* 1993, Rintoul and Church 1993, Belkin and Gordon 1996). Discussion is unresolved regarding the connection between AAIW and SAMW. Without doubt the SAMW in the Pacific, initially identified by Mc Cartney (1977), does not pass through the Drake passage (Peterson and Stramma, 1991) and thus the SAMW bodies observed in the Indian Ocean are derived locally. This has led to reports indicating that the SAMW in the South East Indian Ocean is a separate entity to AAIW and may still incorporate AASW (Rintoul and Church, 1993). Gordon (1991) and Belkin and Gordon (1996) suggested the SAMW south of Australia was a less dense variety of AAIW observed north of the PFZ around 30°S. Sloyan (1993) from a N-S transect at 155°E, described SAMW with a temperature range of 7.5-9°C, salinity of 34.4-34.6‰, density of 26.8-26.9 and an oxygen concentration of 260-280 m mol/l, overlying AAIW at a greater depth of 800 m with salinity <34.4‰ and density 27.2-27.3. It will be seen in Figure 1.6 that where possible, both intermediate water masses have been illustrated using the characteristics of Sloyan (1993).

Deep Water

Circumpolar Deep Water (CDW) is described as the most voluminous water mass of the Southern Ocean and is principally composed of North Atlantic Deep Water (NADW) from the Norwegian Greenland Sea (Whitworth III 1988, Sarnthein *et al.* 1994). In most of the sectors of the Southern Ocean, it is divided into two components, the Upper CDW and the Lower CDW. In the Indian Ocean in the Crozet-Amsterdam Region, Park *et al.* (1993) described the LCDW as a salinity maximum and nutrient minimum water located around 2900 m depth north of the SAF-SAF frontal zone shallowing to 2000 m to the south of it. It is composed of mixed NADW. The UCDW was recognised by its oxygen content minimum of 4.15 ml/l at a temperature of 2.7°C at a depth of 1600 - 1800 m north of the frontal zone, again shallowing to the south at 1000 m. Here, the UCDW is not derived from NADW, but alternatively from North Indian Deep Water (NIDW), as initially assumed by (Deacon 1937) and then identified as seasonally by Rochford (1965), and recently defined as entering the CDW to the west of Amsterdam Island by Park *et al.* (1993). However, Tomczak and Godfrey (1994) suggest that CDW in the South East Indian Ocean is not derived from NIDW but is derived from Western Pacific Circumpolar Deep Water in an westward current. Both Deacon (1937) and Gordon (1972) suggested flow of CDW was to the east and then south of the Tasman Rise. The CDW decreases with depth to the south where it is found to underlie the AASW south of the PF. As

mentioned earlier, it then releases its heat and nutrients, becomes aerated and diluted in respect to salinity, and is transformed into AAIW and SASW (Peterson and Stramma 1991). CDW measured in the South Australian Basin has properties of 0.8-1.2°C potential temperature, salinities of 34.72-34.74 ‰ and an oxygen content of 4.4 - 4.8 ml/l (Braatz and Corliss 1984).

Bottom water

The Antarctic Bottom Water (AABW) is characterised by high oxygen content and low salinity and temperature, and is found below the CDW (Park *et al.*, 1993). It originates through convection at or near the continental shelf through the freezing of sea-ice. Newly formed AABW is confined to where temperature is <0°C (Gordon 1991). AABW which migrates northwards, is a mixture of high-salinity shelf waters and the CDW (Braatz and Corliss 1984, Gordon 1991). Study of bottom water in the southeastern Indian Ocean has resulted in a well-documented origin and pathway. Wyrtki (1962b) indicated that the flow of AABW, at a depth of 3500 m, was strongly directed to the west from the South Australian Basin. Gordon (1971a) suggested that the AABW for the region was produced from the Ross Sea and later expanded this along with other workers (Gordon 1972, Gordon and Tchernia 1972, Conolly and Payne 1972) to include fresher AABW from the Adélie Coast. From these works, a AABW transport scenario was produced: high salinity AABW is produced in the Ross Sea, sinking and travelling westward along the continental rise of Wilkes Land where it mixes with a low salinity AABW originating from the Adélie Coast. This mixed AABW sinks and continues in a westward flow in the South Indian Ocean until it hits the Kerguelen Plateau which forces it northward. This flow continues northward where upon it reaches the Mid-Ocean Ridge and is then directed east. A northward flow from the South Indian Basin was then assumed to have occurred through the Tasman Fracture Zone into the Tasman Basin and eventually into the South-west Pacific Basin.

It was Kolla *et al.* (1976) who later described the northward path via the Australian-Antarctic Discordance between the South Indian Basin into the South Australian Basin. This flow they concluded, continued north and then west to the Wharton Basin as earlier suggested by Wyrtki (1962a). Confirmation of the route has been made with sediment transport studies (Eittreim *et al.*1972, Moriarty 1977, Kolla *et al.* 1978) and microfossil faunal assemblages (Braatz and Corliss 1984, Abbott 1973).

Finally, Rodman and Gordon (1982), separated the northward flows of the AABW, such that AABW produced from the Ross Sea was the main source of AABW transported through the Tasman Fracture Zone to the Tasman Basin, whereas the mixed AABW from the Ross Sea and Adélie Coast was the source of AABW to the South Indian and South

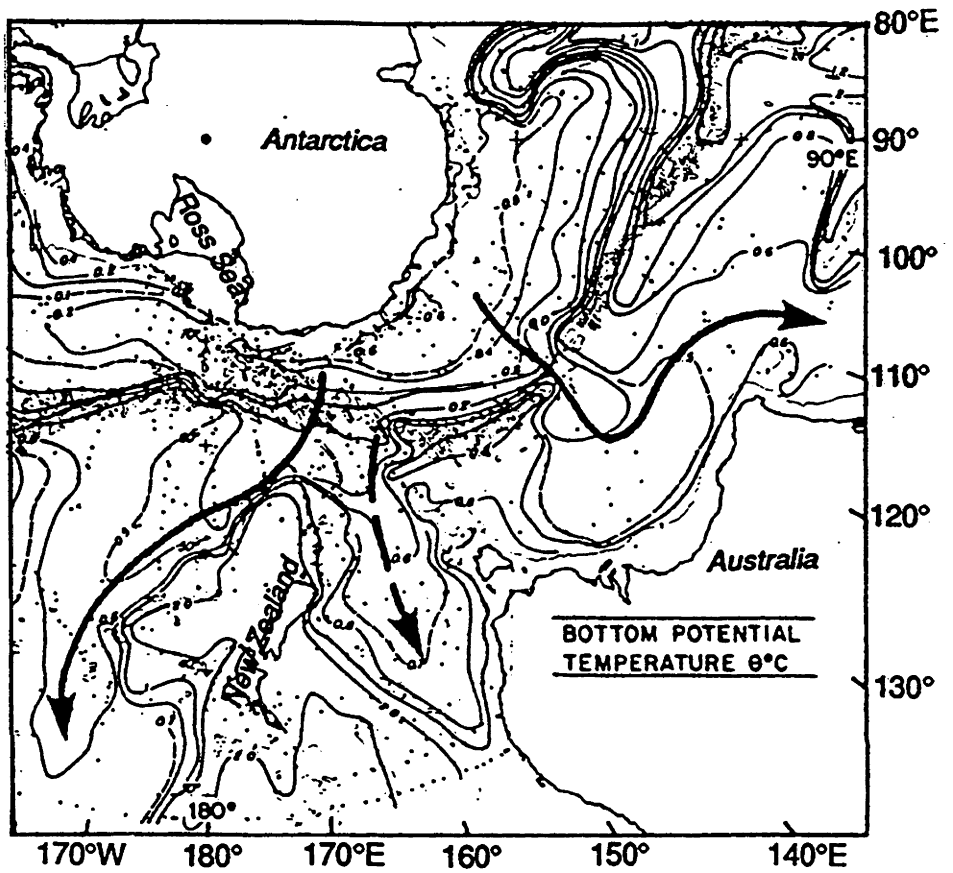

Figure 1.7. A bottom potential temperature distribution map of the southeast Indian Ocean with the pathways of the AABW indicated. Mixed AABW from the Ross Sea and Adélie Coast passes northward through the Australian-Antarctic Discordance and then westward in to the east Indian Ocean. The cooler and more saline AABW from the Ross Sea passes directly northward in to the Tasman Basin (dashed line) and the west Pacific Ocean. (from figure 2 in Gordon 1991).

Australian Basins (Figure 1.7). This particular warmer and less saline AABW is not believed to continue eastward to the Tasman Basin.

Characteristics of the mixed AABW found in the study region include potential temperatures of -0.5 to 0.4°C, a salinity of 34.68-34.70‰ and dissolved oxygen content of 5.0 - 5.6 ml/l (Braatz and Corliss 1984). This AABW is also reported to have a higher CFC signature than the AABW from the Ross Sea (Rintoul and Church 1993).

1.5.4. Terminology of oceanic realms.

Zonation of the Southern Ocean has occurred on two levels. Originally, zones were attributed to the regions occurring between the oceanographic fronts. These zones between the fronts are identified in Figure 1.6. The Antarctic Zone is the region between the Antarctic continent and the PF (Tomczak and Godfrey, 1994). North of this is the Antarctic Polar Front Zone or Polar Frontal Zone bounded sharply by the SAF and gradationally by the PF. It is mostly a 2-4° latitudinal width transitional zone between isotherms of 3-5°C (Gordon 1971a, Whitworth III 1988, Westall and Fenner 1990, Rintoul and Church 1993). In the Eastern Indian Ocean, the Polar Frontal Zone lies south of 50°S, but its widest expression occurs in the waters Southwest of Australia where the SAF and STC are located in a more northerly position (Edwards and Emery 1982, Howard and Prell, 1992). The region between the SAF and the STC is known as the Subantarctic Zone (Deacon 1937, Tomczak and Godfrey 1994). This Subantarctic Zone was defined more precisely by Rochford (1962) with the characteristics of isohalines south of 35‰, inorganic phosphate content between 0.30-0.6 µg-atom/l and temperatures less than 15.5°C. Gordon (1971a) suggested that this definition for the Subantarctic Zone was best applied to the surface waters as lower layers were meridionally continuous. Finally, located north of the prevailing westerly winds and the STC, is the Subtropical Zone. Here the water is characterised by high salinity between 35.8 - 35.5‰, and low inorganic phosphate content between 0.10 -015 µg-atom/l (Rochford, 1962).

On a second level, the biologically related zonation of the Southern Ocean was also defined on physical properties (Deacon 1982). In terms of diatom distributions, Hasle (1969) drew upon past observations by Hendey (1937), Hart (1942), Beklemishev (1964), and Cassie (1963) amongst others, and her own study in the Pacific to conclude all hydrographic boundaries were also floristic. These boundaries were also considered circumpolar. Later works (exemplified by Burckle *et al.* 1987, and Fenner *et al.* 1976) maintained the differentiation of diatom species in the surface waters linked to certain hydrographic boundaries and features.

The development of greater biological, chemical and physical understanding of the Southern Ocean has reached a culminative point in application of zonation terminology. The Southern Ocean was reviewed in terms of variations of physical parameters, nutrients and primary production and consequently divided into several sub-systems (Tréguer and Jacques 1992, Jacques and Fukushi 1994) which are illustrated in Figure 1.8. From the Antarctic coast the subsystems are as follows: the Permanent ice-zone (PIZ) observed in the embayments of the Ross and Weddell Sea and in Prydz Bay; encircled by the Coastal and Continental Shelf Zone (CCSZ), where ice free conditions occur between 2-3 months per year, nutrients are limited, and diatom blooms are intense; the Seasonal Ice Zone (SIZ), affected by seasonal sea-ice cover, varies in surface water mixing and stratification and is host to mobile moderate productivity levels as a function of sea-ice melting; exterior to the SIZ is the Permanently Open Ocean Zone (POOZ) that is characterised by ice free conditions, a well mixed surface layer, low productivity levels, and high nutrient levels including a silicate gradient that increases northward across the POOZ subsystem; and, finally, the Polar Front Zone (PFZ) that covers the region between the SAF and the STC, where primary productivity is considered high, silicate is limited, silicate deposits at the sea-floor are enhanced, and surface eddying and mixing occurs.

No subsystem was defined for the region between the PFZ and the STC by Tréguer and Jacques (1992), however, studies on phytoplankton biomass in this Subtropical Convergence Zone (STZ) indicate lower phytoplankton biomass and nutrients (Holm-Hansen *et al.* 1977, Plancke 1977, Zernova 1990, Sullivan *et al.* 1993, Comiso *et al.* 1993).

1.6 SEA-ICE IN THE SOUTHERN OCEAN.

1.6.1. ANTARCTIC ANNUAL SEA-ICE CYCLE.

The annual cycle of ice growth and decay with the associated maxima and minima around Antarctica, derived from results of satellite instruments, is briefly described here and later in Chapter 5. For detailed analysis on this topic refer to Zwally *et al.* (1983b) and Gloersen *et al.* (1992). Interannual variation of Antarctic sea-ice, although known historically, was first fully appreciated with the use of satellite imagery. In addition, the interannual variation was shown to differ considerably from one region to another (Zwally *et al.* 1983b). Although, the hypothesis for sea-ice cover being compensative between the Ross and Weddell Seas (Lemke *et al.* 1981, Ackley 1981) was not observed after a four year satellite study by Zwally *et al.* (1983b). Interannual differences in sea-ice

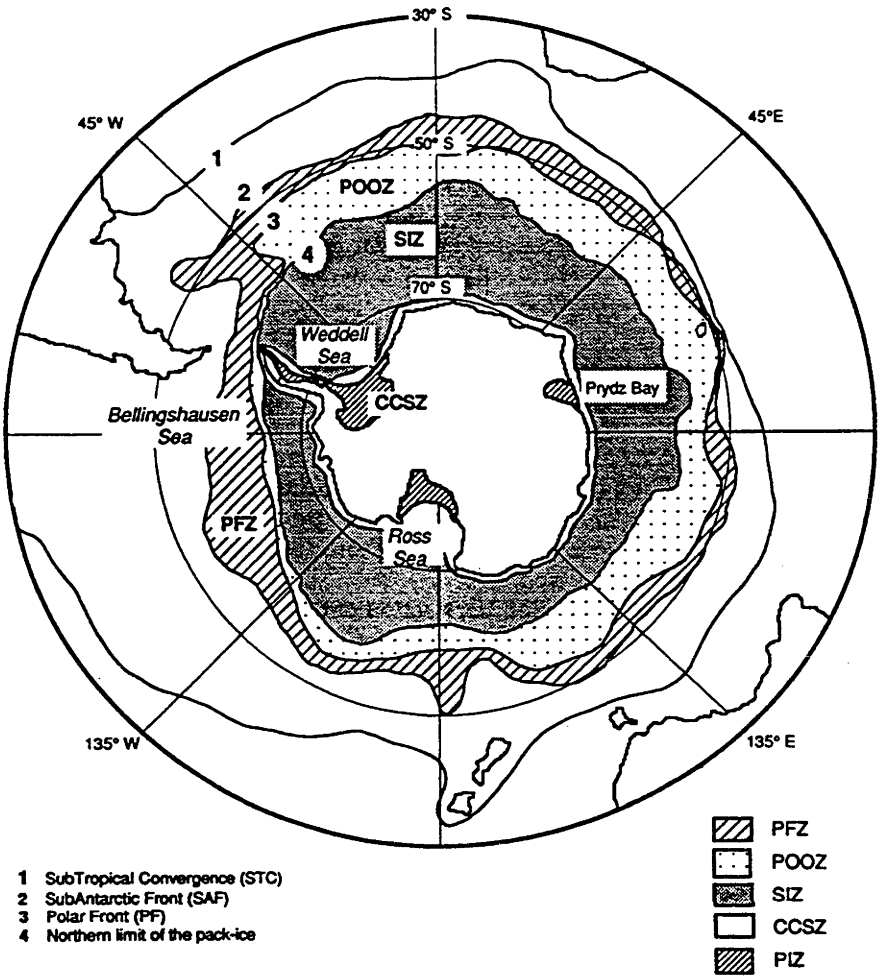

Figure 1.8. Zonation of Southern Ocean referred to in this thesis. (from figure 1 in Tréguer and Jacques 1992).

cover are produced from factors which influence all sea-ice but which have varying regional degrees of effect. The major cycle of sea-ice cover and retreat in the Southern Ocean is described below.

Minimum

February is identified as the month when minimum ice extent occurs. It is when most of the Antarctic coast is free of sea-ice. Of the 2.6×10^6 km^2 of summer sea-ice present, over half of this amount is located in the Weddell Sea (Zwally *et al.* 1983b).

Growth

March through May are the months of maximum sea-ice growth. Comiso and Zwally (1984) suggest from satellite data, that the growth is around 3 km per day. A strong correlation between the regions of ice growth and the westerly location of the cyclonic centres to the ice growth have been noted (Cavalieri and Parkinson 1981). The sea-ice is thus, formed by the advection of winds from the south and dispersed, once formed, to the north. Lemke *et al* (1981) believe the advection pattern of sea-ice follows that of the surface winds. There is a zonal atmospheric circulation pattern north of 60° latitude through the winter and this serves to extend the sea-ice in a corresponding zonal manner (Ackley 1996) (Figure 1.9).

Maximum

Maximum sea-ice extent is generally achieved in September (Cavalieri and Parkinson 1981). The maximum ice extent latitudes are between 65°S at 105°W to 55°S at 10°E. In general the ice extent is circular and this is likely to be a reflection of the zonal air temperature and pressure fields (Zwally *et al.* 1983b). Perturbations from the zonal atmospheric pattern come from high pressure systems which move poleward and can influence the dynamics of the sea-ice distribution by either moving ice or creating new ice in a westerly direction (Cavalieri and Parkinson 1981) or by retarding cooling and decaying ice cover (Parkinson and Cavalieri 1982).

Retreat

Estimated from ESMR satellite data (Parkinson and Cavalieri 1992) decay takes place over 4 months (October-January), initially at around 20 km per day (Comiso and Zwally 1984). The work of Zwally *et al.* (1983b) showed for the first time that the Antarctic spring-summer decay was considerably faster than the growth of ice in the autumn-winter period. Several factors influence the decay of sea-ice. Unlike in the growth period, the correspondence between the pattern of cyclonic centres and the retreat of the ice edge in December and January was not established (Cavalieri and Parkinson 1981).

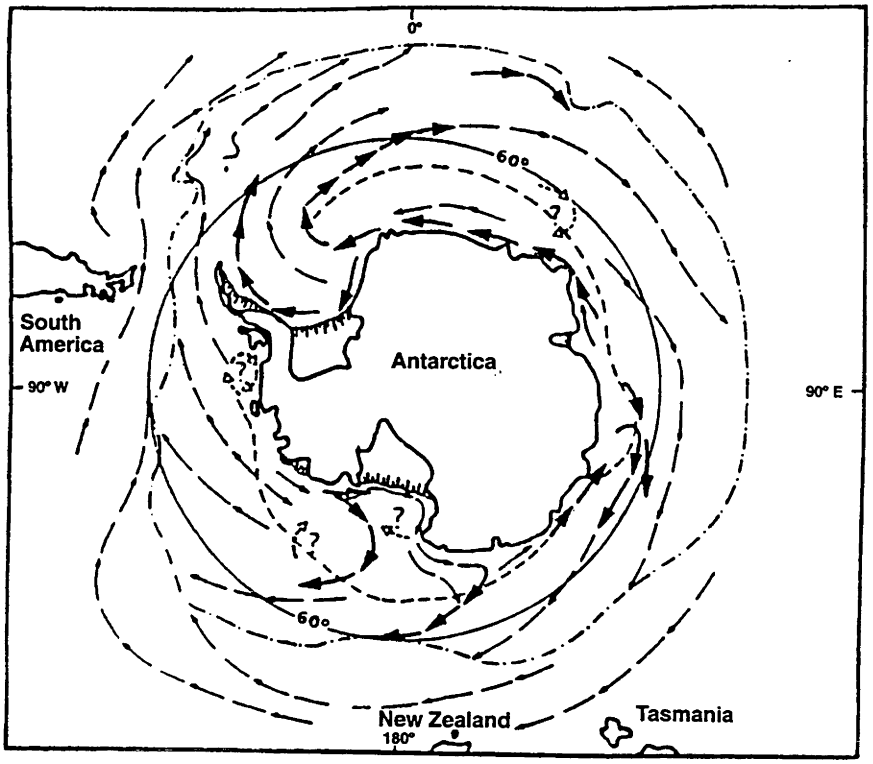

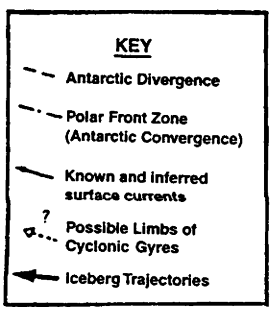

Figure 1.9. Surface circulation patterns of ice and water in the Southern Ocean. Including iceberg pathways. (Ackley 1996; fig. 23, modified from Gow and Tucker 1991.)

1.6.2. SEA-ICE IN REGION OF STUDY.

In this thesis, the region of particular interest for sea-ice is that between Australia and Antarctica (100°E to 160°E). In reference to sea-ice satellite work this region falls within the Pacific Ocean sector of Zwally *et al.* (90°E-160°E, (1983b), the West Pacific sector of Gloersen *et al.* (1992), and the East Indian Ocean sector of Parkinson (1992). In this region the Antarctic continent is at is furtherest north, and results from the satellite data observe the coast as generally ice free in the summer period (Ackley 1981, Zwally *et al.* 1983b, Parkinson 1992, Gloersen *et al.* 1992). With the fact that the ocean is farther north than other sections of the Southern Ocean, it experiences warmer ocean temperatures and therefore diminishes the summer presence of sea-ice (Parkinson 1992), and most likely retards the amount of sea-ice growth in the region, as has been observed by satellite. In general, the region has three times more ice in winter than summer, but this is in comparison to a seasonal variation of 6 times more in the Weddell Sea (Comiso and Zwally 1984). SMMR satellite data observed an ice extent ranging from ~0.3×10^6 km^2 in summer to a maximum of ~2.6×10^6 km^2 in winter (Gloersen *et al.* 1992).

Lemke *et al.* (1981) related the prevailing winds and/or ocean currents to the eastward drift of sea-ice anomalies (growth phase of sea-ice) in most of East Antarctica including the region of the South Indian Basin (130°). This was not supported by Ackley (1981) who suggested from early satellite data that East Antarctica has ice growth consistently to the north. Ackley (1981) notes the least interannual variation of sea-ice extent occurs in the East Antarctic sector, where by a constant lower rate of ice advance from March to September, culminates in a maximum sea-ice extent in October rather than in September as in other Antarctic sectors. He further suggested that, in this region, extreme temperature fluctuations may be necessary to significantly affect the sea-ice response. From Zwally et al (1983b) and Comiso and Zwally (1984), the annual cycle of sea-ice for the region of interest was given as :

Feb.- March	ice advance slow .
March-July	slow growth.
July-August	greatest rate of advance.
Sept.	continued slow advance or stasis.
Sept. -Oct .	slight advance in part of the Ross sea and off Wilkes Land (100°E-140°E).
Oct.-Nov.	decay widespread, retreat most dominant in this period.
Nov. -Dec.	in general for all Antarctic sea-ice, close to 40% of November ice cover is eliminated, and several coastal polynyas are observed to occur in the same place around East Antarctica.
Dec.- Jan.	slower decay.
Jan. - Feb.	reduced rate of decay.

The largest coastal polynya in the region appears to occur during April, off the Shackleton Ice Shelf (100°E) (Zwally *et al.* 1983b).

The sea-ice maximum February and September sea-ice extents provided by the 13 year compilation of satellite data are presented in Figure 1.10.

1.6.3. SEA-ICE FORMATION AND HEAT FLUX.

Antarctic sea-ice initiates with the formation of ice crystals (frazil) in the upper mixed layer, the water here being super cooled to at least -1.8°C (Ackley 1996). This frazil ice then coalesces at the surface into various forms depending on calm (nilas or grease ice) or disruptive water conditions (pancake ice) (Ackley 1991, Tucker *et al.* 1992, Ackley 1996). The thickness of the Antarctic sea-ice was estimated to be from several centimetres to several meters, and the width from 20 cm to several km (Zwally *et al.* 1983b). The thickness of sea-ice around East Antarctica (120-150°E) was observed to be in the order of 30 cm near the ice edge to 2 m in the interior (Allison and Worby 1994). In addition, snow cover was also noted to increase in cover from 7 cm at ice edge to 13 cm at the interior (Allison and Worby 1994). Sea-ice thickness increases predominantly by rafting of the pancakes, rather than through accretion of new ice to the base (Ackley 1991, Allison and Worby 1994).

The growth of Antarctic sea-ice is related to the cycle of heat flux. The ocean is cooled by two types of heat transfer - sensible and latent. Sensible heat is created as the ocean cools to the freezing point, whereas latent heat is released through ice formation (Zwally *et al.* 1985). The heat flux to the atmosphere from the ocean occurs through the formation of ice and is assisted by the displacement of the newly formed ice by winds. The sensible heat of the water is then also lost as the exposed region is further cooled by transfer of heat to the cooler atmosphere, this provides conditions for new ice formation. This increase in heat flux is also a result of the thermohaline convection of salt rejected by the formation of ice, which drives the dense, saline cooled water down (AABW) and brings in warm Circumpolar Deep Water to the surface.

The greatest heat flux to the atmosphere occurs during the maximum growth of sea-ice (eg early autumn) (Allison, 1981). Later in the winter season, reduction of sea-ice formation and increased thickness of the ice is thus transferred to reductions in heat flux, salt formation and convection. As a result of sea-ice formation, the transfer of ocean heat to the atmosphere is obscured and largely reduced because of this sea-ice boundary. Thus, sea-ice provides a boundary to mass and momentum (Parkinson 1992, Allison *et al.* 1993). The role of both katabatic, and particularly synoptic winds, is estimated to

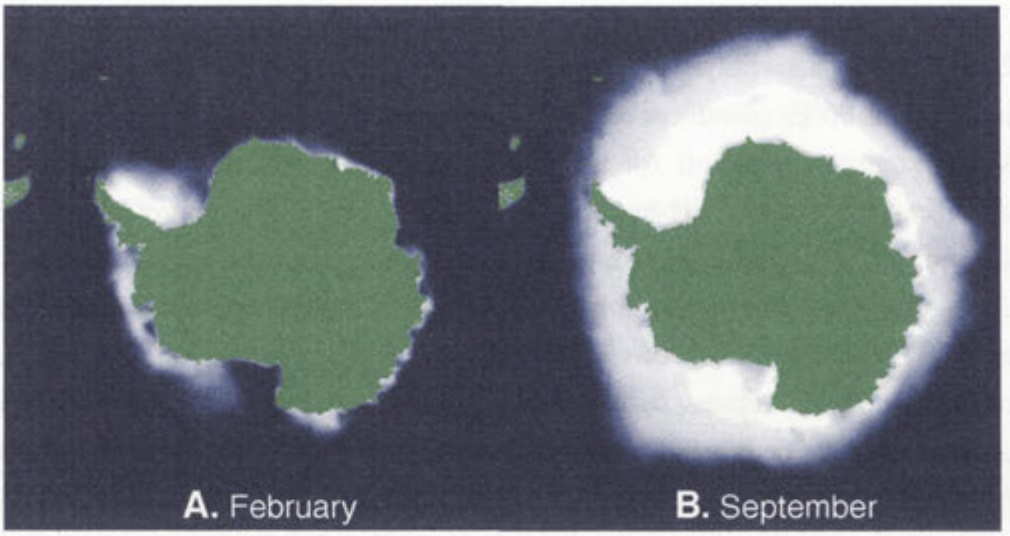

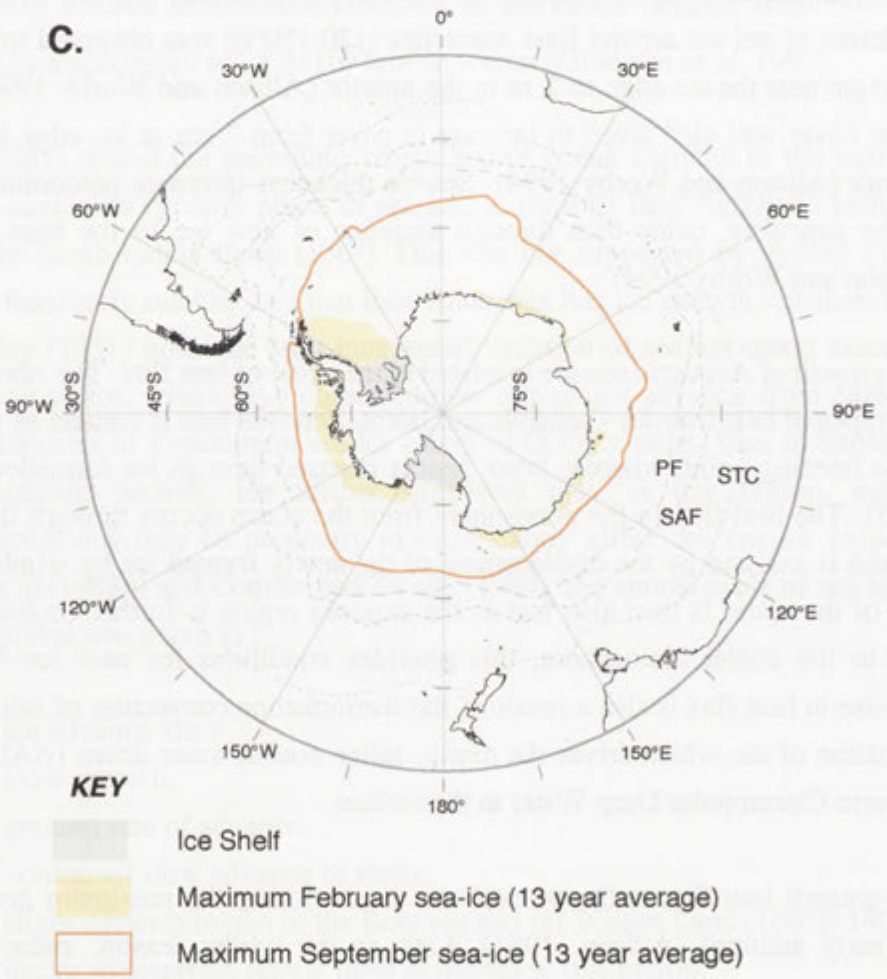

Figure 1.10. Maximum sea-ice distributions around Antarctica during February and September from 13-year averaged satellite data of Schweitzer (1995). **A**) Concentration image of maximum 13 year average February sea-ice , and **B**) September sea-ice. **C**) Plotted maximum extents in comparison with the Polar Front (PF), Subantarctic Front (SAF) and Subtropical Convergence (STC) of Orsi *et al.* (1995).

increase the rate of ice production in coastal polynyas (regions of open water around Antarctica) by 10 times the case of wind absence, hence resulting in a higher production of sea-ice, and subsequent high salinity shelf water (Cavalieri and Martin 1985). The large amounts of ice formed and salt ejected in the polynyas and leads around the coast initiate bottom water formation as indicated previously (Zwally *et al.* 1985).

1.6.4. FACTORS AFFECTING SEA-ICE.

The following factors affect the annual cycle of the sea-ice. The relationship with each factor and between factors provide us with some information on the interactive role which these factors play on sea-ice and likewise, in the subsequent subsection (1.5.5.), the role sea-ice plays on the factors. Although this is not a comprehensive list of items that can affect sea-ice in formation, presence, or decay, they include those elements which are known to have a significant modulating role.

Atmospheric winds, temperature, and pressure

Both the atmospheric temperature and the winds affect the freezing of the water and the melting and transport of ice (Parkinson 1992). Early satellite observations (Lemke *et al.* 1981) suggested the influence of the winds and atmosphere already cooled by regions with large sea-ice extents, would move into neighbouring sectors thus, enhancing further sea-ice formation, and advecting sea-ice into the neighbouring region as a function of wind type. Continuous satellite records from the western Weddell Sea region indicated this process occurred moving sea-ice and initiating sea-ice formation (Cavalieri and Parkinson 1981, Zwally *et al.* 1983b). Godfred-Spenning and Simmonds (in press) found that in general advances in the ice transport and thus the ice edge, were associated with greater cyclonic activity. They found that sea-ice was enhanced by the westerly winds mostly in winter and marginally in autumn.

The flow of katabatic winds from off the Antarctic continent influence the opening and closing of the coastal polynyas and leads (Zwally *et al.* 1983b). Wind stress provides energy to the Ekman divergence which generates open water regions with the ice pack. During winter this helps in expanding the ice extent and also provides further surface water for freezing, whereas in summer, the opening of the ice field assists in the reduction of ice concentration and disintegration of the sea-ice with increasing heat transfer (Ackley 1981). Regional differences, however, exist as to the influence of either synoptic winds or katabatic winds in maintaining or providing areas of open water. Along the Wilkes coastline, synoptic wind patterns are considered to have the greater influence (Cavalieri and Martin 1985), with seasonal associations strengthened between the

cyclones and the ice, from a lack in the winter, through to increasing positive associations in autumn (Godfred-Spenning and Simmonds in press).

Research by Enomoto and Ohmura (1990), on the half annual mean position of the wind field and the position of the ice extent concluded that the turning point in the growth and decay cycles of the sea-ice were related to crossovers between the sea-ice maximal extent and the atmospheric convergence line (ACL, the path of cyclones around Antarctica). During spring and autumn, the ACL contracts poleward, and in doing so change the wind fields at that boundary such that the westerly winds now act on regions previously subject to easterly winds south of the ACL. The wind change then places new stresses on the sea-ice and appears to assist in the break up of the sea-ice in the spring period. Other work which adds support to the role of the variation of the ACL associates increased cyclogenesis at the mean sea-ice edge during spring. Yet, during sea-ice advance in winter, the connection between sea-ice edge and the baroclinic zone is northerly of the mean sea-ice edge by 5 to 10° latitude (Godfred-Spenning and Simmonds in press).

Relating sea-ice extent to the air temperature was studied by Zwally *et al* (1983b). They followed the atmospheric 271.2K (~2°C) freezing isotherm in contrast to the ice edge during the 4 years of ESMR satellite data. The authors were able to propose that, as sea-ice extent in winter was south of the freezing isotherm, all variation of the extent was due to either oceanic dynamics, solar radiation or a movement of the isotherm from its mean position. This links with the observation made by Cavalieri and Parkinson (1981), and Parkinson and Cavalieri (1982), where air temperature maxima and minima were found to lead, by 1 to 1.5 months, the sea-ice minima and maxima extents respectively. Air temperature is also observed to have a far more interannual variability than sea-ice extent. The monthly-averaged air temperatures are found to be stable during the growth phase of sea-ice between May and October, and the coldest air temperatures have been located in the western Weddell Sea and the Ross sea, where the greatest sea-ice formation occurs (Zwally *et al.* 1983b).

Snow

Snow acts as an insulator between sea-ice surface temperature and air temperature (Allison 1981) such that the snow-ice interface remains generally constant at -4°C even though the air temperature can vary between -20° to 5°C (Comiso and Sullivan 1986). Snow cover has been observed to occur only on sea-ice that is at least 15 cm thick (identified as first-year ice and multi-year ice), rather than the thinner young and new ice. (Zwally *et al.* 1983b, Allison *et al.* 1993). The presence of snow reduces the growth of further ice, especially that of congelation ice which builds to the base of ice floes (Eiken *et al.* 1995). There are other roles which snow cover plays, but these are in relation to

radiation emitted from the sea-ice and the snow itself to satellite instruments and will be dealt with in Chapter 5. Overall, the most important role of snow cover is in modulating and restricting the heat flux between the ice and the atmosphere.

Solar Radiation

Solar radiation is associated both indirectly and directly with the annual cycle of the sea-ice. Despite direct radiative heat during spring and summer, the sea-ice decay is indirectly dominated by the indirect heat from the ocean and atmosphere (Zwally *et al.* 1983b, Crowley and Parkinson 1988a). This means that increases in open water during this decay phase from other processes, will enhance melt back, whereas in reduced open water conditions more sea-ice remains and hinders heat flux to the atmosphere. Sea-ice maxima at various longitudes were estimated to lag the solar radiation minimum by 2 to 3.5 months (Lemke *et al.* 1981) although, in the Australian region, this was as low as by 1 month.

Ocean Currents

Lemke *et al* (1981) alluded to the natural variability of the ocean as an important contributor to the lateral extent of the sea-ice. The varying position of the Antarctic Circumpolar Current (ACC) has been identified as a possible modulator to the amount of sea-ice accumulated against open ocean (Parkinson 1992). Ackley (1981) believed that the annual sea-ice cycle oscillated between the position of the northern extent of the ACC (ie. the PF) and the continent. Yet, in some cases, the sea floor topography deflecting the ACC has been found to be more important (Zwally *et al.* 1983b). From the correlation analysis between sea-ice edge and cyclone parameters, Godfred-Spenning and Simmonds (in press) suggested that in several cases where the correlations did not occur at the sea-ice edge but at 5 to 10° latitude to the north, oceanic fronts were the probable cause to variation. Work on associating the position of oceanic fronts to sea-ice extent, have not been investigated and due, to the nature of defining and estimating oceanic fronts on a time/seasonal basis, is probably some time away from being analysed.

The factors described above influence the amount of ice cover, its growth and decay, yet the role of sea-ice also affects the regional, hemisphere and global response to climate and possibly the controls on these modulating factors.

1.6.5. Effect of sea-ice on global climate.

The relationship between climate and sea-ice is a complex and a growing research area. The major difficulties in assessing global climate change from sea-ice records or extents are, primarily, that the records of sea-ice change are not long and are variable. In some cases, it is difficult to assess between data sets in trying to establish trends. Secondarily,

the real trends in sea-ice, be it annual, seasonal or local, are variable through time and so change due to affects from other physical/climatic phenomena. The role of sea-ice in climatic modelling is continually being assessed and several scenarios are presented in an edited volume by Peltier (1993).

Heat Flux

Sea-ice presence and the retardation of heat flux to the atmosphere are linked, as mentioned in preceding sections. The areas of open water at the poles balance the input of heat at mid and lower latitudes. Rate of heat flux is seasonal (Allison 1981) and does show some daily variation due to atmospheric air temperature input and strength of katabatic winds (Allison and Akerman 1980). During winter, leads and polynyas are found to release 100 times more heat to the atmosphere than the ice (Zwally *et al.* 1983b). It follows then that when sea-ice occurs during spring and summer, aside from increasing the albedo (diffused reflection) preventing absorption of the solar radiation - which in turn heats the surface water to assist in melting the ice - it also affects the rate of heat flux to the atmosphere (Zwally *et al.* 1983b) and cooling of the ocean (Ackley 1981).

Several general circulation models have already assessed various changes in the heat flux as a result of sea-ice presence and absence. As mentioned previously, the role of leads in the sea-ice during winter are crucial to the movement of heat from the ocean to the atmosphere. Simmonds and Budd (1990), with a prescribed 100% versus 50% winter sea-ice model, indicated the production of leads (50% condition) resulted in an atmospheric temperature increase of 6°C, a weakening of westerlies between 40-60°S and reductions in surface pressure over the sea-ice. Most of the heat produced was associated with sensible heat loss from ocean cooling. Removal of all the winter sea-ice in modelling runs expectedly responded with increases in surface pressures, fluxes of latent and sensible heat and an air temperature warming (Simmonds, 1981). This resulted in a change of the atmospheric circulation at 500 mb and slight strengthening of the zonal circulation and reduced upper westerlies by 3 ms^{-1}. Thus, increasing cyclonic activity. In a dynamic sea-ice-ocean model, a five year cooling-warming oscillation was simulated (Hibler and Zhang 1995). Here increased sea-ice presence increased ocean warming, which in turn lead to a diminished sea-ice content, and then subsequent ocean cooling.

Understanding the role sea-ice plays in heat-flux and associated feedbacks, are continuing areas of research both in situ studies and modelling experiments.

Oceanic Circulation

Sea-ice growth and associated salt rejection, induces bottom water formation. Regions of mass bottom-water formation have been linked to coastal polynyas off Antarctica such as

along the Wilkes Land region (Zwally *et al.* 1985). Again, when sea-ice production is decreased due to one of several other factors, the result is less bottom-water formation. The implications of such decreases mean the ocean lessens the thermohaline circulation pattern. Another important oceanic input that sea-ice performs is freshwater transport to the mid latitudes (Zwally *et al.* 1983b). This freshwater input has biological importance in providing a shallow medium of lower salinity, stability, and increased solar radiance believed important to the cycle of growth in phytoplankton (Sullivan *et al.* 1993).

Weather

Intrinsic to the presence of sea-ice is the role it plays as an important modulator of the seasonal and inter-annual variability of the weather (Ackley 1981). Thus, resulting in changes in wind patterns, precipitation, air pressure and temperature both over the ocean and land.

The biggest difficulties in assessing the connections between the sea-ice and the atmosphere are resultant of technological development in assessing circum-Antarctic synoptic patterns (eg cyclogenesis, cyclone pathways and persistence, reliable pressure readings) and the computing time associated in providing accurate data. To bring understanding to the weather and sea-ice relationships, General Circulation Models (GCM) are proposed. Simmonds and Budd (1991), as mentioned above, suggest that surface pressure is decreased with decreasing presence of sea-ice. They further suggested that these decreases would positively influence cyclogenesis. Later work (Simmonds and Wu 1993), utilising several levels of sea-ice concentration, concluded that cyclogenesis was generally decreased north of 65°S, with decreasing sea-ice concentration. The authors found that where the number of cyclones had increased principally around the Antarctic coast, the cyclones were progressively lower in strength as a result of decreasing sea-ice concentration. Thus, the results of increased open water is to increase heat flux, which heats air temperature and induces an immediate effect on surface pressure (Watkins and Simmonds 1995). Data from SSM/I satellite derived sea-ice concentrations used in conjunction with synoptic models indicated that the responses portrayed by prescribed slab sea-ice concentrations are considerably different, and thus strongly support the use of "real" sea-ice concentration data when modelling the atmospheric-sea-ocean system (Watkins and Simmonds 1995).

In the end, studying the variability of sea-ice and atmospheric responses will elucidate probable trends in Southern Hemisphere climate and global weather. Yet, as Godfred-Spenning and Simmonds (in press) point out, atmospheric effects on sea-ice, have yet to be assessed and included in GCM's.

Assessing Change

In assessing regional sectors for evaluation of sea-ice change or a climate signal, Parkinson (1992) suggested the winter Ross Sea and west Indian Ocean would be reasonable choices because of their consistent ice coverage and minimal variability during that season. It is perhaps in this region that the study of sea-ice extent in the past, as presented in this thesis, should be pursued. In addition to these ideas, Simmonds (in press) argues strongly that in estimating sea-ice extent there are dangers in further extrapolating their changes in time to the position of storm tracks. These stem from the current studies on cyclonic processes and sea-ice extent which are complex, involve other factors such as heat flux and air temperature and are, thus, limited in interpretation. However, he also mentions that connections in sea-ice 'concentrations' and these synoptic features may in the future help in elucidating the relationships and provide past cyclonic structure.

1.7 BASIC METHODOLOGY

The methodology and application of transfer function analysis adopted in this thesis follows procedures documented in the literature (Imbrie and Kipp 1971, Pichon *et al.* 1987, Pichon *et al.* 1992a, Zielinski 1993). Discussion of the basic sampling, processing and counting methodologies applied to all samples handled in the thesis are documented below. The statistical methodologies of both the SST and sea-ice transfer function methods are covered respectively in Chapters 4 and 5. The sea-ice method invokes no new sampling, processing or counting methodologies.

1.7.1 SAMPLING AND EXTRACTION.

Core Material.

Three cores [MD88-787 (56°22.72'S, 145°17.56'E), MD88-784 (54°11.48'S, 144°47.65'E), MD88-779 (47°00.0'S, 148°06.7'E) refer to Chapter 6 for further descriptions and map] were made available for study by the University of Bordeaux 1, through the courtesy of Dr J.-J. Pichon and Dr M. Labracherie. Sampling was completed by the French CNRS technical staff in 1988 in Bordeaux. No sedimentological log was made at this time. The samples received were boxed $1cm^3$ samples of sediment, marked with the core name and depth from the top of the core. All samples were taken at 10cm intervals.

Core E53-10 (49°00.0'S, 148°06.0'E) was sampled by the author in April 1993 while visiting the Antarctic Research Facility at Florida State University. The samples were taken following the standard practice at ANU. The approximate sample size was $1cm^3$.

Each sample was contained within a sealed plastic bag. Further sampling of both *Eltanin* piston and trigger core material was made by staff at the Antarctic Research Facility. These samples were contained in $1cm^3$ plastic boxes. All material was sampled at 10cm intervals, while trigger core material was taken at 5cm intervals.

Surface samples.

Thirteen box core samples taken during the French PACIMA cruise were taken directly from the water/sediment interface and stored in $1cm^3$ sample boxes (Dansie, 1994). A further 25 samples from the Antarctic CRC cruise (Exon *et al.* 1995, Armand 1995) off the South Tasman Rise were taken from both piston and box cores. These were sampled by cruise members and contained in $1cm^3$ boxes. Four trigger cores from *Eltanin* material were included and sampled as previously noted above.

Abbott's (1973) original count data was considered for inclusion to the surface data set. Of the original 154 samples covered by Abbott, only 60 of these samples were counted. In addition, only 41 of the 60 samples were considered modern surface samples (see section 2.1.4 and Appendix 2.5). The samples were prepared by taking a drop of un-processed sediment in suspension and placing this drop on a cover slip (Abbott 1973, p.26).

1.7.2 Processing.

The method used to clean, concentrate and mount diatom material for this work is described by Pichon *et al.* (1987). The method differs principally from Schrader and Gersonde (1978) and Zielinski (1993) in that the pipetting method or the 8 times repeated sedimentation and decanting of suspended diatom material over 12-48 hr periods was replaced with centrifugation. Furthermore, the initial freeze drying of the material to retain porosity was not utilised. Pichon (1985) found that centrifugation reduced the time required for sedimentation and retained the smaller diatoms (<15µm) which were often still in suspension under the Schrader and Gersonde (1978) method. It was found in this study that a second run for 3 minutes at 1500 revolutions per minute was required to ensure that the smaller diatoms were retained. This later requirement was a problem inherent in using an aged centrifuge. A summary of the method is presented in Figure 1.11 and a detailed account of the procedure is contained in Appendix 1.1.

1.7.3.Counting procedures.

Quantitative counting procedures emulate those described by Pichon (1985) and Pichon *et al.* (1987), whereby the three replicate slides representing one sample are counted until

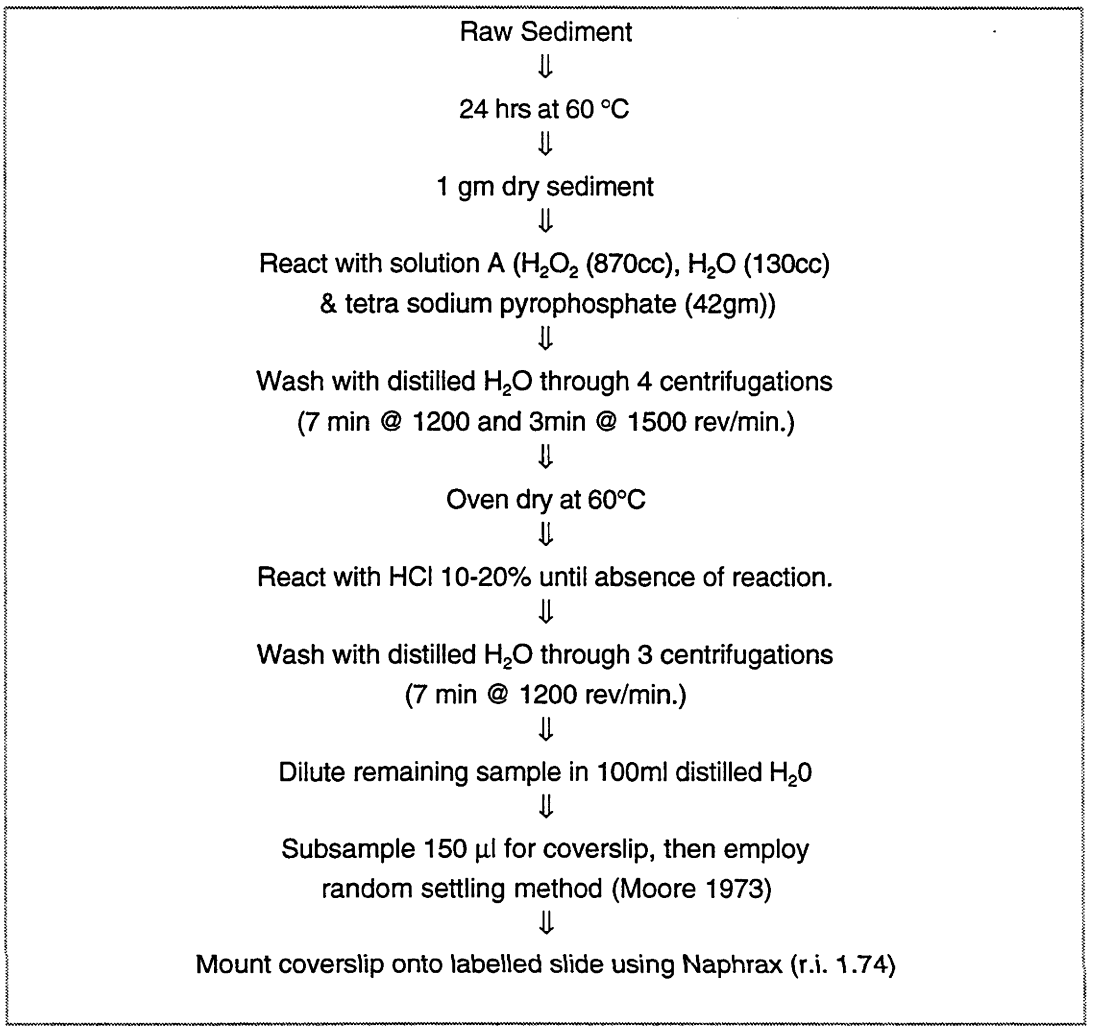

Figure 1.11. Summarised method of silica-selective extraction used in this study. For details refer to Appendix 1.1. (r.i. = refractive index).

a minimum of 300 diatom valves are examined. The procedure for counting involves the use of high power microscopy (x100 oil immersion objective and x10 eye pieces). This follows the recommended procedure detailed by Schrader and Gersonde (1978) and modified by Laws (1983), where every whole diatom frustule observed in each microscopic field of view along a transect, is recorded. The definition of a whole diatom frustule follows the approach described by Pichon (1985) and is as illustrated in Figure 1.12. A description of each of the categories is provided below:

1) Centric Diatoms (eg. *Thalassiosira*, *Coscinodiscus*) whole or two thirds refers to a count of 1.

2) Pennate Diatoms (eg. *Fragilariopsis*, *Nitzschia*, *Pseudonitzschia*) diatom valves with more than two thirds present are counted, this varies from Pichon (1985) where two ends

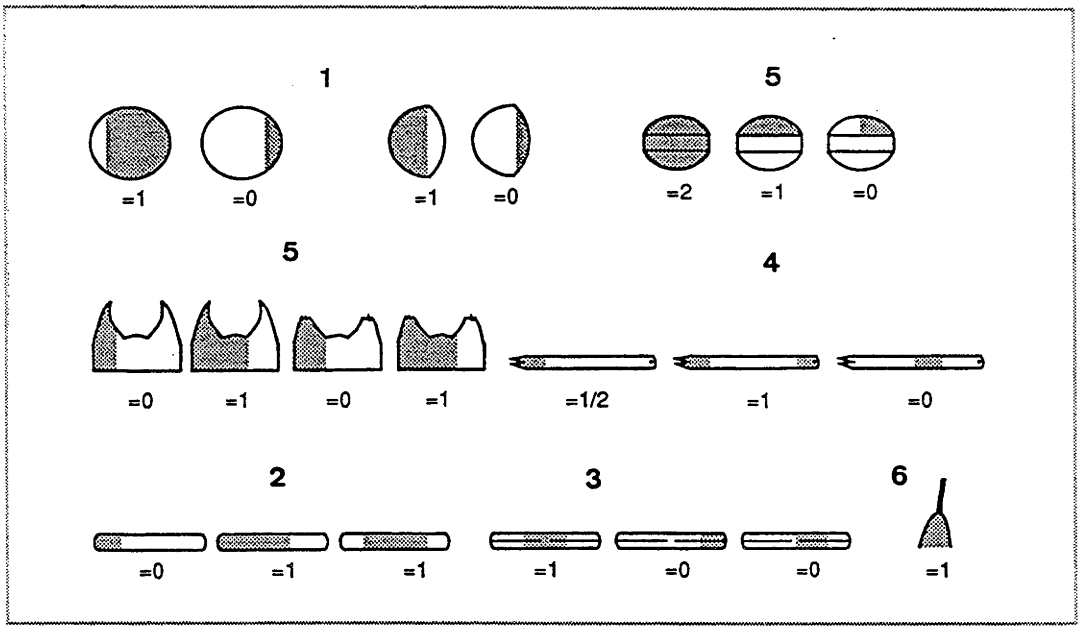

Figure 1.12 Counting guide to diatom frustules. Major numbers refer to the categories explained in the text and key below. Numbers below each illustration refer to the count equivalence determined from the shaded portion of each frustule illustrated. Modified from Zielinski (1993, figure 10.)

Key. 1 = centric diatoms (eg *Thalassiosira, Coscinodiscus*), 2 = Pennate diatoms (eg. *Fragilariopsis, Nitzschia*), 3 = Pennates with raphe (eg. *Navicula*), 4 = Pennates without raphe (eg. *Thalassiothrix, Trichotoxon*) 5 = Apically elevated diatoms (eg. *Chaetoceros* (5 upper right) and *Eucampia* (5 middle left)), 6 = Cylindrical diatoms (eg. *Rhizosolenia, Proboscia*).

are counted as representing presence of 1. Zielinski (1993) observed that by counting two valve ends as a whole along with those valves which were complete, the relative abundance of the species were over-estimated when only those valves that were two-thirds or complete were counted in the same transect.

3) Pennates with raphe (eg. *Navicula*) diatom valves that contain the middle portion illustrating the raphe are counted as 1, as are those that are two thirds or more.

4) Pennates with no raphe (eg. *Thalassiothrix, Trichotoxon, Thalassionema*) all pole ends are counted, the total counted is then divided by two as outlined by Schrader and Gersonde (1978), with exception to *Thalassionema* which was treated as in category 2.

5) Apically elevated diatoms (eg. *Eucampia, Chaetoceros*) valves that constitute more than two thirds of the total are counted as 1. In the case of a complete *Chaetoceros* diatom frustule with two joining valves the count is recorded as 2.

6) Cylindrical diatoms (eg. *Rhizosolenia, Proboscia*) only complete proboscoids, or those with accompanying otaria but missing the distal part of the proboscis are counted as 1.

The occurrence of two silicoflagellate genera, *Distephanus* and *Dictyocha*, were also recorded but excluded from the total number of diatoms observed (refer Chapters 2 and 6). These silicoflagellates provided information on cool or warm water regions, but are not necessary in the diatom analysis (Zielinski 1993). Only whole skeletons of each genus were counted.

Chapter 2
Analysis and review of the diatom surface sample database.

2.1 INTRODUCTION

The currently published diatom database (Pichon *et al.* 1992a, Sowers *et al.* 1993, Labeyrie *et al.* 1996) consists of 166 surface samples that includes 42 artificially dissolved samples. This original 166 database was provided in ranked format for use in this thesis (Appendix 2.1). When the addition of new surface samples to this 166 database was made and required ranking, differences between the original raw data and the ranked data were observed. These differences were investigated by obtaining the original raw count sheets (Pichon pers. comm. 1994) and re-entering these data. In completing this task several other inconsistencies were noted and instigated a thorough investigation of the diatom surface sample database. The following sections cover each of the problems encountered, the evolution of the database through these stages, and provide at the end of the following chapter the rigorously analysed diatom surface sample database used in this thesis.

All the available data sets containing diatom counts were compiled. These data sets were the 166 database used by Pichon, new data gathered separately by Dr Pichon and the author, and Abbott's southeast Indian Ocean surface sample data set. Each of these data sets are identified on Figure 2.1.

2.1.1. THE PICHON *ET AL.* (1992A) ORIGINAL 166 DATABASE.

All the original data from the count sheets was re-entered. This data is located in Appendix 2.2, and contains all the species initially identified. The primary species identifications are deemed crucial for the way data are handled when updating taxonomic affinity (section 2.2). The 166 surface sample database is henceforth referred to as the 166DB.

2.1.2. PICHON'S ADDITIONAL DATA SET.

New samples counts from Dr Pichon (pers. comm. 1994) have been added to the 166DB. There are 52 samples which originate from the Antarctic Peninsula, Ross Sea, Prydz Bay and Indian Ocean. All original identifications are used and the data are contained in Appendix 2.3.

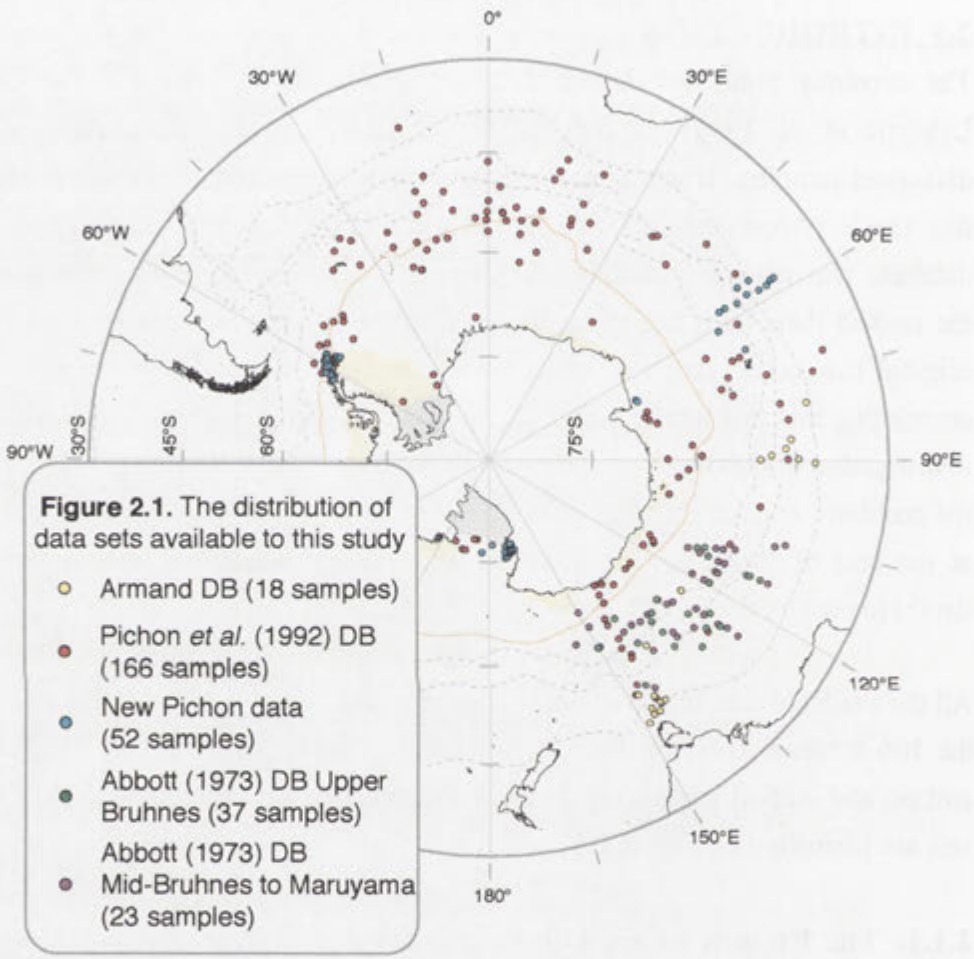

Figure 2.1. The distribution of data sets available to this study

- Armand DB (18 samples)
- Pichon *et al.* (1992) DB (166 samples)
- New Pichon data (52 samples)
- Abbott (1973) DB Upper Bruhnes (37 samples)
- Abbott (1973) DB Mid-Bruhnes to Maruyama (23 samples)

2.1.3. ARMAND'S NEW DATA SET.

New samples from PACIMA and South Tasman Rise cruise missions were prepared and counted during this thesis. The raw data of these 18 new samples are located in Appendix 2.4 and illustrated in Figure 2.1.

2.1.4. ABBOTT'S SOUTHEAST INDIAN OCEAN SEDIMENT SURFACE DATA SET.

The data previously collected by Abbott for his thesis on the distribution of diatoms in sediments of the southeast Indian Ocean (Abbott 1973) are located in a region of interest to this thesis which was sparsely covered by the previous work of Pichon *et al.*(1992). The Abbott samples were considered for inclusion to the surface sample data set and were kindly provided by Dr L. Burckle (Burckle pers. comm. 1994).

Of the 154 samples that Abbott surveyed in his thesis only 60 of these were actually documented in terms of floral counts. The 60 samples are recorded in Appendix 2.5. On inspection of the counts it became apparent that several common species were never identified (eg. *Thalassiosira antarctica*, *Fragilariopsis sublinearis*, *Thalassiosira lineata*, *Porosira glacialis*, *Odontella weissflogii*, *Cocconeis* spp., *Thalassiosira gracilis var expecta*, *Dactyliosolen antarcticus*, several *Rhizosolenia* species and the silicoflagellate genus *Dictyocha*). Furthermore, Abbott distinguished species that were not documented any further than a category species (eg. *Nitzschia* sp. 200) or split more common species into several presumably sub-species not currently recognised (eg *Nitzschia lanceolata*, *Nitzschia kerguelensis ovalis*). Abbott's thesis floral list contains considerably more species than are noted on the 60 count sheets available to this study. In terms of equating the counts made by Abbott to those routinely made today, several species would be presumed mis-identified or neglected in his observations.

To remedy this situation Abbott's thesis samples were sought. Unfortunately the samples could not be located within Abbott's collection contained within the Hanna chair diatom collection (University of California, P. Kocioleck, pers. comm. 1996), nor at the University of South Carolina where he completed his thesis (Thunell, pers. comm. 1996). Thus, the original slides could not be recounted. One sample was re-sampled from the Antarctic Marine Geology Research Facility at Florida State University (E36-6) to assist in establishing the taxonomic affinity of several species and to determine the thoroughness of his observations. The floral counts compiled by Abbott and those of the author are documented in Table 2.1.

The differences between the two observations are generally small and overall the dominant species show very similar presence. Yet there are several species which this author finds in some number that were either not noted by Abbott or observed in varying

abundances and vice-versa (eg. *Dactyliosolen antarcticus*, *Fragilariopsis rhombica*, *F. ritscheri*, *F. separanda*, *Melosira sol*, *Navicula directa*, *Thalassionema nitzschioides*, *Thalassiosira gracilis* and *Thalassiothrix* spp.) Although this example suggests that Abbott's data may be of some use combined with the diatom database compiled in this work there are other differences to keep in mind. Processing of Abbott's samples was not performed beyond suspending the sample in water and mounting a drop on a cover slip (p26, 1973), this is in distinct contrast to the silica-selective processing made with all other material used in the diatom database. Samples also integrate 2 cm of sediment which may not be representative of the sediment surface. Because of these differences and the loss of the original samples on which an updated counts could be made it was decided to abandon integration of Abbott's data set to the diatom database compiled in this study. The Abbott data set, however, provides insight in some instances to the distribution of several species in the Australian region when examined geographically (as refered to in subsections with section 2.2).

ABBOTT			ARMAND		
Species	**Raw**	**%**	**Raw**	**%**	**Species**
Asteromphalus hookeri	1	0.32	3	0.94	*Asteromphalus hookeri*
Coscinodiscus tabularis	7	2.27	10	3.13	*Azpeitia. tabularis*
Coscinodiscus marginatus	1	0.32	1	0.31	*Coscinodiscus marginatus*
Coscinodiscus occuloides	present				*Coscinodiscus occuloides*
-			12	-	*Dactyliosolen antarcticus* #
Distephanus speculum	9	2.92	7	2.19	*Distephanus* spp.
Eucampia balaustium	4	1.30	5	1.56	*Eucampia antarctica*
*Nitzschia kerguelensis**	132	65.58*	209	65.31	*Fragilariopsis kerguelensis*
*Nitzschia kerguelensis ovalis**	56	*	-		*Fragilariopsis kerguelensis*
*Nitzschia lanceolata**	14	*	-		*Fragilariopsis kerguelensis*
Nitzschia rhombica	1	0.32			*Fragilariopsis rhombica*
Nitzschia ritscherii	3	0.97			*Fragilariopsis ritscheri*
Nitzschia separanda	4	1.30	1	0.31	*Fragilariopsis separanda*
Melosira sol	3	0.97			*Melosira sol*
Navicula cf. *directa*			2	0.63	*Navicula directa*
Nitzschia sicula var. *rostrata*	2	0.65			*Nitzschia sicula* var. *rostrata*
Thalassionema nitzschioides			8	2.50	*Thalassionema nitzschioides*
-			1	0.31	*Thalassiosira antarctica*
Thalassiosira gracilis	4	1.30	11	3.44	*Thalassiosira gracilis*
Coscinodiscus lentiginous	19	6.17	23	7.19	*Thalassiosira lentiginosa*
Thalassiosira cf. *oestrupii*	1	0.32			*Thalassiosira oestrupii*
Shrimperiella antarctica	1	0.32	3	0.94	*Thalassiosira oliverana*
Thalassiothrix spp.	45	14.61	30	9.38	*Thalassiothrix* spp.
unknown	1	0.32	6	1.88	unknowns
TOTAL COUNT	308		320		

Table 2.1. Comparative counts on core top sample E36-6. Raw counts and percentage abundance of diatom species observed as provided by Abbott and the author. In general the differences are not large between the species and proportions observed. Clarification of Abbott's species taxonomic affinity requires further investigation, in particularly *Fragilariopsis kerguelensis* is considered to contain the species identified by Abbott as *Nitzschia kerguelensis, N. kerguelensis ovalis* and *N. lanceolata* as indicated by asterisks (*). # = counts not included in the total specimens observed.

2.2 TAXONOMIC REFORM.

The use of several diatom data sets and the evolution of the French database over the last 10 years has generated the need to confirm and update taxonomic identification. Such analysis allows use of all data available, reduces confusion and permits cross-correlation between the data sets.

Diatom taxonomy conforms with the main works of Van Landingham (1967-1979), Johansen and Fryxell (1985), Round *et al.* (1990), Simonsen (1992), and Hasle (1993). A taxonomic floral list has been compiled with supporting plates of the species encountered in the core material and surface samples prepared by the author (Appendices A1 and A2). Other relevant publications used in identifying the flora are also recorded in these appendices.

The following section comments on previous species identification and documents species changes or taxa groupings made specifically to the original data counts available for this work. Species distinguished by quotation marks are deemed no longer valid.

2.2.1. *ACHNANTHES BREVIPES*

"*ACHNANTHES BREVIPES* VAR. *ANGUSTATA*" (GREVILLE) CLEVE

ACHNANTHES BREVIPES AGARDH

Achnanthes brevipes var. *angustata* was identified by Pichon in his 166DB, and minus the variation in his newer sample set. Simonsen (1992) considers the variation of this species as a synonym of *Achnanthes parvula.* All observations are interpreted in the 166DB as belonging to the species and not the variation, as there are no illustrations or comments in any of the Pichon works which would enable conclusive identification of either *A. brevipes* or *A. parvula.*

2.2.2. *ACTINOCYCLUS ACTINOCHILUS*

"*CHARCOTIA ACTINOCHILUS*"(EHRENBERG) HUSTEDT

ACTINOCYCLUS ACTINOCHILUS (EHRENBERG) SIMONSEN

All previous records of *Charcotia actinochilus* were transferred by Simonsen (1982) to *Actinocyclus actinochilus.* The transfer of data from one species to the other was made over the life of the Pichon *et al.* (1992) database and is formally acknowledged here.

2.2.3. *ACTINOCYCLUS CURVATULUS*

COSCINODISCUS CURVATULUS GRUNOW IN SCHMIDT

ACTINOCYCLUS CURVATULUS JANISCH IN SCHMIDT

Taxonomic work by the author had, until recently, divided *Coscinodiscus curvatulus* and *Actinocyclus curvatulus* almost exclusively by the distinction of size, because the

pseudonodulus of the latter species could not be resolved under the light microscope. *A. curvatulus* is cited by Hustedt (1930) as ranging between 96 -106 µm in diameter which is generally larger than *C. curvatulus* which is cited as ranging in diameter from 40 - 100 µm and 20 - 40 µm for the variation *minor.*

Priddle and Fryxell (1985) first raised doubts over the separation of these two species suggesting that *C. curvatulus* may be an *Actinocyclus* species. Tomas (1996) have since synonymised *C. curvatulus* as *A. curvatulus* and expanded the definition of *A. curvatulus* to cover a much wider range of size and variation in areolation pattern. The observations of *A. curvatulus* and *C. curvatulus* in this study have been combined under *A. curvatulus* for further statistical analysis.

2.2.4. GENUS *ASTEROMPHALUS*

ASTEROMPHALUS HEPTACIS (BRÉBISSON) RALPHS

ASTEROMPHALUS HOOKERI EHRENBERG

ASTEROMPHALUS PARVULUS KARSTEN

ASTEROMPHALUS ROBUSTUS CASTRACANE

Reviewing the original count data of the 166DB has revealed the observations of five *Asteromphalus* species in the sediment samples: *A. heptacis, A. hookeri, A. hyalinus, A. robustus* and *A. parvulus*. With exception to *A. hyalinus*, the other four species are likely to have been confused between each other and synonyms mis-applied.

A. robustus was initially counted in early samples of the 166DB, alongside *A. parvulus, A. hookeri* and *A. heptacis*. Pichon (1985) probably derived *A. robustus* from the work of DeFelice and Wise (1981) and/or Burckle (1984a) when initially constructing his database, however, in later sample analysis *A. robustus* is no longer listed or observed. The probable reason being that Fenner *et al.* (1976) have placed *A. robustus* into synonymy with *A. hookeri*, which Pichon had used to describe this latter species.

It is important to note that *A. robustus* Castracane is a valid species but has been confused with *A. hookeri* and *A. brookeri* in the past (Van Landingham 1967, part 1, pg 341). Fenner *et al.* (1976) have without reference, synonymised *A. robustus* Castracane, as illustrated by Hustedt (1930), with *A. hookeri* Ehrenberg, even though the description provided by Hustedt remains a valid description for *A. robustus*. It is assumed then that all previous species identified originally as *A. robustus* were transferred to *A. hookeri* in the 166DB. As Pichon identified both *A. hookeri* and *A. robustus* in the same samples, although *A. robustus* was rarer, conservation of the two species and their data are maintained separately in this work.

Further taxonomic discrepancies were revealed between *A. hookeri* and *A. heptacis* during the Bremerhaven workshop (December 1996). The confusion in part appears to have been derived from the use of incorrectly labelled figures on plate 4 of Fenner *et al.* (1976). Here their figure 23 is identified as *A. heptacis*, when it should in fact be *A. hookeri*, and in figure 24 *A. heptacis* is labelled as *A. hookeri*. These same illustrations aided this author in identifying an "*A. heptacis*" species which was a larger species of *A. hookeri* with straight spokes. Since this error was detected all *A. heptacis* observations made by the author have been transferred to *A. hookeri*.

This error aside, more recent literature (Priddle and Fryxell 1985, Tomas 1996) suggest that the two jaggered spoked species *A. heptacis* and *A. parvulus* are conspecific. The species identified in the original database (Pichon 1985) as *A. parvulus* are indeed jaggered spoked *Asteromphalus* species (Pichon 1985, pl 1, fig. 6). This species is considerably larger than the similarly jaggered spoked form illustrated as *A. heptacis* and which are noted as rare in the sediments. Because Pichon also used the incorrectly labelled figures supplied by Fenner *et al.* (1976) to determine his species, the question is now raised as to which category specimens noted as *A. heptacis* in the 166DB were attributed to : a large variety of *A. hookeri* or *A. heptacis* ?

Although the solution here is to recount the samples in which these species have been observed, the fact that they occur in the sediment samples with a relative abundance generally less than 2%, means temporarily that the effect of incorrect identification is within the normal counting error and can be considered a minor concern to the role of the transfer function. Under this consideration and falling in line with the view that *A. heptacis* and *A. parvulus* are conspecific (Tomas 1996), all previous observations of *A. heptacis* made by Pichon are transferred to *A. parvulus*. This is also in line with the correctly illustrated forms he depicted in his thesis (Pichon 1985 pl. 1, figs 6, 7, 9).

2.2.5. *AZPEITIA TABULARIS*

"*COSCINODISCUS TABULARIS*" GRUNOW 1884

"*COSCINODISCUS TABULARIS* VAR. EGREGIUS" (RATTRAY) HUSTEDT 1928

AZPEITIA TABULARIS (GRUNOW) FRYXELL AND SIMS 1986

The genus *Azpeitia* was reviewed by Fryxell *et al.* (1986) where they transferred *Coscinodiscus tabularis* to *Azpeitia tabularis*. No formal transferring of the species variation *egregius* identified by Hustedt (1930) was made. It is here informally transferred to the genus *Azpeitia*. Fenner *et al.*(1976) and Zielinski (1993) appear to be the only workers having identified this variation. Fenner *et al.* (l.c.) found it rarely in their sediment samples and within the same range as the major species form. The variate form is distinguished by its lack of a central hyaline ring, denser areolation more

commonly with eccentric form and reduced marginal hyaline ring (Hustedt 1930, Fenner *et al.* 1976).

Fryxell *et al.* (1986) noted that species of *A. tabularis* have a large variety of morphological forms including cold and warm water forms but did not indicate if the loss of the central hyaline ring was considered within this range. Furthermore, Fryxell *et al.* (1986) consider *A. tabularis* as the only Antarctic species of *Azpeitia*. The recent distribution maps of *A. tabularis* in the South Atlantic (Zielinski and Gersonde 1997, fig. 7) contain a mixture of the two forms because of the lack of distributional differentiation cited by Fenner *et al.* (l.c.). This does not seem unreasonable considering Hustedt (1930) noted transitional forms between the higher species and the variate were possible. In Zielinski and Gersonde's (1997) South Atlantic sector distribution, abundances of *A. tabularis* are most pronounced in the subantarctic zone where summer SST range from 10-20°C, this is consistent with sediment occurrences reported by DeFelice and Wise (1981) and Abbott (1974). The species most southern expression was linked to the winter sea-ice edge (Zielinski and Gersonde 1997). Other occurrences of *A. tabularis* in sediments along the Antarctic coast could be linked to open ocean currents penetrating beneath the coastal fast ice (Tanimura, 1992).

Identifications of *A. tabularis* (*C. tabularis*) and *A. tabularis* var *egregius* were originally counted separately in the 166DB, but have only recently been re-counted separately again after a period of lumping. Distribution of these two forms are illustrated in Figure 2.2. Since there does not seem to be any further information on a separation of cold and warm water forms, or distributional detail on the rarer variate form, all data in this thesis will pool the *A. tabularis* and *A. tabularis* var *egregius* counts for further analysis. There is a need, however, to note the distribution of the two species to ascertain the truth of this lack of distribution differentiation.

2.2.6. *Cocconeis* species

Several *Cocconeis* species have been previously recorded in the Pichon 166DB. They are *Cocconeis fasciolata, C. costata, C. costata* var. *kerguelensis* and *C. californica. C. costata* appears to be the most dominate of these benthic species. Both *C. costata, C. fasciolata* and other benthic *Cocconeis* species have been used as palaeo-depth indicators (Whitehead and McMinn, 1997) in Antarctic coastal waters.

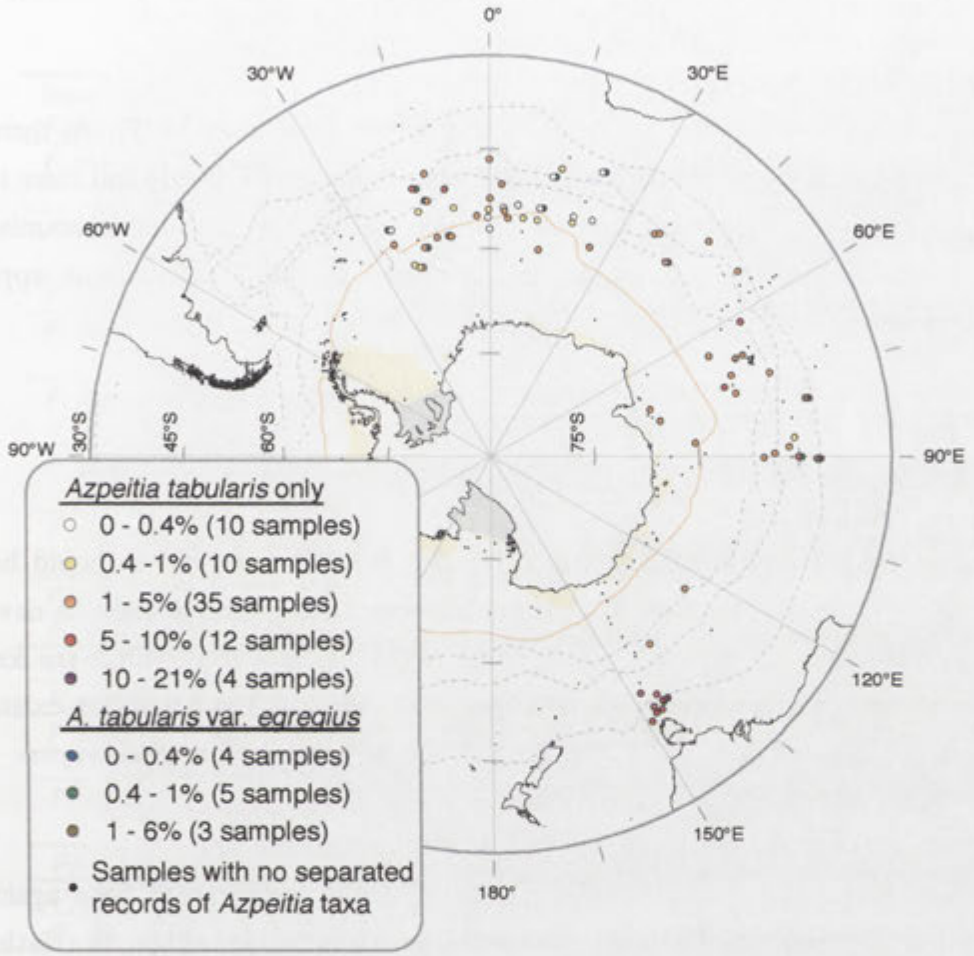

Figure 2.2. Relative abundance distributions of *Azpeitia tabularis* and *A. tabularis* var. *egregius* from data originally distinguishing between the two species. Relative abundances determined from original data sets.

The data for each species in this genus were grouped. Originally (Pichon *et al.* 1987, table IV) no association was made between the grouped *Cocconeis* spp. and any of the three determined factors, even though abundances were stated as up to 9%. In the second paper *Cocconeis* spp. is associated with the ice-zone factor with the same relative abundance (Pichon *et al.* 1992). In this work the grouped *Cocconeis* spp. has a maximum relative abundance of 5.9%.

2.2.7. *COSCINODISCUS DECRESCENS* GRUNOW

This species is known from samples of Eocene to Oligocene age (Fenner 1977). As there is only one record of this species in the 166DB of Pichon (samples RC15-91) and there is a lack of any other re-worked species, it seems probable that the specimen has been mis-identified. For this reason the occurrence is transferred to the *Coscinodiscus* spp. category in this work.

2.2.8. *FRAGILARIA STRIATULA*

"*SYNEDRA KERGUELENSIS* "HEIDEN

FRAGILARIA STRIATULA LYNGBYE

Hasle (1965b) and Simonsen (1992) note that *Synedra kerguelensis* Heiden should be transferred to *Fragilaria striatula* Lyngbye and this has been done in this database. A new marine genus *Synedropsis* described by Hasle *et al.* (1994) is associated with a sea ice environment and is noted to be closely related to *Fragilaria striatula.* The possibility exists that the species initially identified as "*S. kerguelensis*" could belong within *Synedropsis.*

2.2.9. GENERA *FRAGILARIOPSIS* - *NITZSCHIA* - *PSEUDONITZSCHIA*

The two sections *Fragilariopsis* and *Pseudonitzschia* of the *Nitzschia* genus have again been reinstated to the genus level to reflect advances in taxonomic investigation (Hasle 1993). The changes are listed in Table 2.2. *Pseudoeunotia doliolus* was also transferred to *Fragilariopsis* by Medlin and Sims (1993).

Although the species of two sections have been returned to generic status (Medlin and Priddle 1990, Chapters 22 & 24) there are other sections and species occurring in this thesis that have not been formally dealt with in this fashion. These are the species that were recognised belonging to the groups/sections *Nitzschiella* and *Lanceolatae* (Hasle 1964, Hasle and Medlin 1990a). Brief comments were made on the taxonomic position of species of *Nitzschia* that did not fall into *Fragilariopsis, Nitzschiella* and *Pseudonitzshia* sections (Medlin and Hasle 1990). However, this provided no clear indication on the generic status of these remaining "*Nitzschia*" species.

The generic position of several fossil species also remain under the genus *Nitzschia*, when they are obviously aligned to *Fragilariopsis*. Thus, the species listed in Table 2.3 remain within the *Nitzschia* genus. The taxonomic reform required for these groups/sections was not undertaken in this work. Comments on certain *Nitzschia*, *Fragilariopsis* and *Pseudonitzschia* species identifications within the 166DB and this study, follow.

New name	**Previous name/s(Synonyms)**
Fragilariopsis	
F. curta (Van Heurck) Hustedt	*N. curta* (Van Heurck) Hasle, *Fragilaria curta* Van Heurck
F. cylindrus (Grunow) Krieger	*N. cylindrus* (Grunow) Hasle, *Fragilaria cylindrus* Grunow
F. doliolus (Wallich) Medlin et Sims	*Pseudoeunotia doliolus* (Wallich) Grunow
F. kerguelensis (O'Meara) Hustedt	*N. kerguelensis* (O'Meara) Hasle, *Fragilaria antarctica* Castracane,
F. linearis (Castracane) Frenguelli	*N. castracanei* Hasle, *Fragilaria linearis* Castracane
F. obliquecostata (Van Heurck) Heiden	*N. obliquecostata* (Van Heurck) Hasle, *Fragilaria obliquecostata* Van Heurck
F. oceanica (P.T. Cleve) Hasle	*N. grunowii* Hasle, *Fragilaria oceanica* P.T. Cleve
F. pseudonana (Hasle) Hasle	*N. pseudonana* Hasle
F. rhombica (O'Meara) Hustedt	*N. angulata* Hasle, *Diatoma rhombica* O'Meara
F. ritscheri Hustedt	*N. ritscheri* (Hustedt) Hasle
F. separanda Hustedt	*N. separanda* (Hustedt) Hasle
F. sublinearis (Van Heurck)Heiden	*N. sublineata* Hasle, *Fragilaria sublinearis* Van Heurck
F. vanheurckii (M. Pergallo) Hustedt	*N. vanheurckii* (M. Pergallo) Hasle, *Fragilaria vanheurckii* M. Pergallo
Pseudonitzschia	
P. australis Frenguelli	*Nitzschia pseudoseriata* Hasle
P. delicatissima (P.T. Cleve) Heiden	*N. delicatissima* P.T. Cleve, *N. actydrophila* Hasle
P. granii (Hasle) Hasle	*N. granii* Hasle
P. fraudulenta (P.T. Cleve)Hasle	*N. fraudulenta* P.T. Cleve
P. heimii Manguin	*N. heimii* (Manguin) Hasle
P. lineola (P.T. Cleve) Hasle	*N. lineola* P.T. Cleve, *N. barkleyi* Hustedt
P. pseudodelicatissima (Hasle) Hasle	*N. pseudodelicatissima* Hasle, *N. delicatula* Hasle
P. pungens (Grunow) Hasle	*N. pungens* Grunow, *Homoeocladia pungens* Grunow
P. pungens forma *multiseries* (Hasle) Hasle	*N. pungens* forma *multiseries* Hasle
P. seriata (P.T. Cleve) H. Pergallo	*N. seriata* P.T. Cleve
P. seriata forma *obtusa* (Hasle) Hasle	*N. seriata* forma *obtusa* Hasle
P. subpacifica (Hasle) Hasle	*N. subpacifica* Hasle
P. turgidula (Hustedt) Hasle	*N. turgidula* Hustedt
Pseudo-nitzschia turgiduloides Hasle	*N. turgiduloides* Hasle, *P. barkleyi* var. *obtusa* Manguin, *Pseudonitzschia turgiduloides* (Hasle) Hasle

Table 2.2. List of extant *Fragilariopsis* and *Pseudonitzschia* living species relevant to this work recently returned or transferred to generic status. Synonyms are listed. Source Medlin and Sims (1993), Hasle (1993) and Hasle (1995).

Present taxonomic name	Notes
Nitzschia bicapitata Cleve	*Lanceolatae*, see refs 1 -4. *
Nitzschia barberii (M. Pergallo)	*Fragilariopsis*, see ref. 5.
Nitzschia braarudii Hasle	*Lanceolatae*, see ref. 3 & 4. *
Nitzschia closterium (Ehrenberg) W. Smith	*Nitzschiella*
Nitzschia denticuloides Schrader	see refs 6 &7
Nitzschia dietrichii Simonsen	?*Lanceolatae*, see ref. 3. *
Nitzschia interfrigidaria McCollum	see ref. 6
Nitzschia interruptestriata Simonsen	see ref. 3.
Nitzschia kolaczekii Grunow	? *Fragilariopsis*, see ref. 3,5,8
Nitzschia lecointei Heurck	*Nitzschiella*
Nitzschia maleinterpretaria Schrader	see ref. 6
Nitzschia paundriformis Gregory	? *Fragilariopsis*, see ref. 3.
Nitzschia peragalli Hasle	*Fragilariopsis*
Nitzschia sicula (Castracane) Hustedt	*Lanceolatae*
Nitzschia sicula var. *bicuneata* (Grunow) Hasle	*Lanceolatae*
Nitzschia sicula var. *rostrata* Hustedt	*Lanceolatae*
Nitzschia stellata	see ref 9.

Table 2.3. Species remaining in *Nitzschia* genus, which require generic reform. Earlier groups/sections *Lanceolatae* and *Nitzschiella* identified by Hasle (1964) are given. Further references related to the species are noted. 1= Kaczmarska and Fryxell 1984; 2= Tanimura 1992; 3= Simonsen 1974; 4= Hasle 1965b; 5= Hasle 1960; 6= Schrader 1976; 7= Harwood and Mauyama 1992, 8= Hasle 1969; 9= Medlin and Hasle 1990. * = These species are highly related along with other species (*N. longicollum* Hasle, *N. capuluspalae* Simonsen, *N. bifurcata* Kaczmarska et Licea) which have cuspidate poles and lanceolate shape. Taxonomic review is required to separate the forms and reduce the number of species which surely have many synonymies.

2.2.10. *FRAGILARIOPSIS OCEANICA*

"NITZSCHIA GRUNOWI" HASLE

FRAGILARIOPSIS OCEANICA (P.T. CLEVE) HASLE

There are a few records of *Nitzschia grunowi* noted in the early 166DB. These are likely to be mis-identifications of another *Fragilariopsis* species since *N. grunowi* (now *F. oceanica*) is only known from the Arctic (Hasle 1965b, Hasle and Medlin 1990). Hasle (1965b) suggests that the species may be confused with *F. ritscheri* or *F. kerguelensis*. It is assumed that the identification of *N. grunowi* in the Pichon 166DB was based on illustrations provided in Fenner *et al.* (1976, pl. 2 figs 1-5). Since the identity of *F. oceanica* in the database samples is not illustrated or described in Pichon's thesis or subsequent works and the occurrences are rare (less than 1% in samples 1277-2, RC13-273, RC13-268, KR8817, KR8820, KR21, MD73-026) the species counts are preserved independently, but considered mis-identified.

2.2.11. *FRAGILARIOPSIS RITSCHERI* HUSTEDT

Confusion regarding the identification of *F. ritscheri* became apparent when distribution plots and maximum abundances against temperature plots were compared with work of Zielinski and Gersonde (1997, and Bremerhaven workshop 1996). The compiled

databases available for this thesis when mapped geographically for *F. ritscheri* indicated that *F. ritscheri* was contained in the subantarctic to open ocean regions (Figure 2.3). This was in complete disagreement with the data compiled by Zielinski and Gersonde (1997, fig. 17.23) where *F. ritscheri* abundances were located predominantly in waters <1°C.

Previous records of *F. ritscheri* have been made by many workers and almost all of them find *F. ritscheri* located predominantly in the Antarctic zone (Table 2.4). The habitat of this particular species appears to be related with the marginal ice zone, where the species is commonly present but is never found in any great abundance (<3%) in the water column, sea-ice or the sediments. There also appears to be a seasonal increase of the species in the Summer period (Kang and Fryxell 1992, Leventer and Dunbar 1996).

Seven studies (Jousé *et al.* 1962a, Hasle 1965b, Donahue 1970a, Abbott 1973, Fenner *at al.* 1976, DeFelice and Wise 1981, and Pichon 1985) have noted *F. ritscheri* in the subantarctic or open ocean zone, but in all cases with exception to Pichon (l.c.) and Fenner *et al.* (l.c.), these occurrences are rare. There are several plausible explanations for these occurrences such as ice rafting, bottom water movement, neritic habitat associated with islands (eg Kerguelen Island, Jousé *et al.* 1962a), opportunistic blooms associated with a melt water layer or iceberg, and mis-identification. Jousé *et al.* (1962a), Hasle (1965b), Donahue (1971), Abbott (1973) and Fenner *et al.* (1976) all illustrate variations of the species *F. ritscheri* as identified by Hustedt (1958, pl. 11 figs 133-136). Some of the variation illustrated by Fenner *et al.* (l.c., pl. 3) could be referred to *F. kerguelensis*, and this is noted in their floral descriptions. The location of the sampling study (between 100° and 80°W west of Drake Passage) may also prove to be an important consideration for the distribution of the species into the subantarctic region. This is referred to indirectly with the mention of *F. kerguelensis* and other "endemic Antarctic floral elements" being transported northward by bottom currents (Fenner *et al.* 1976 p. 762). The same could be true for Abbott's data where both *F. obliquecostata* and *F. ritscheri*, noted by Abbott as easily confounded, are concentrated south of and within the Australian-Antarctic Discordance (120-125°E).

In deciphering reasons for the large presence of *F. ritscheri* (*sensu* Pichon) in the subantarctic and open ocean zones of the south Atlantic and south west Indian sectors and the lack of presence around Antarctica (Figure 2.3), there is little to go by. In his thesis (Pichon 1985) *F. ritscheri* (*N. ritscherii*) is noted to be very similar to *F. kerguelensis*, and the two species are discriminated by the number of costae in 10µm. This definition is presumably derived from Fenner *et al.* (1976) although Hasle (1965b) is quoted as the source description. There are no illustrations provided for confirmation of the species

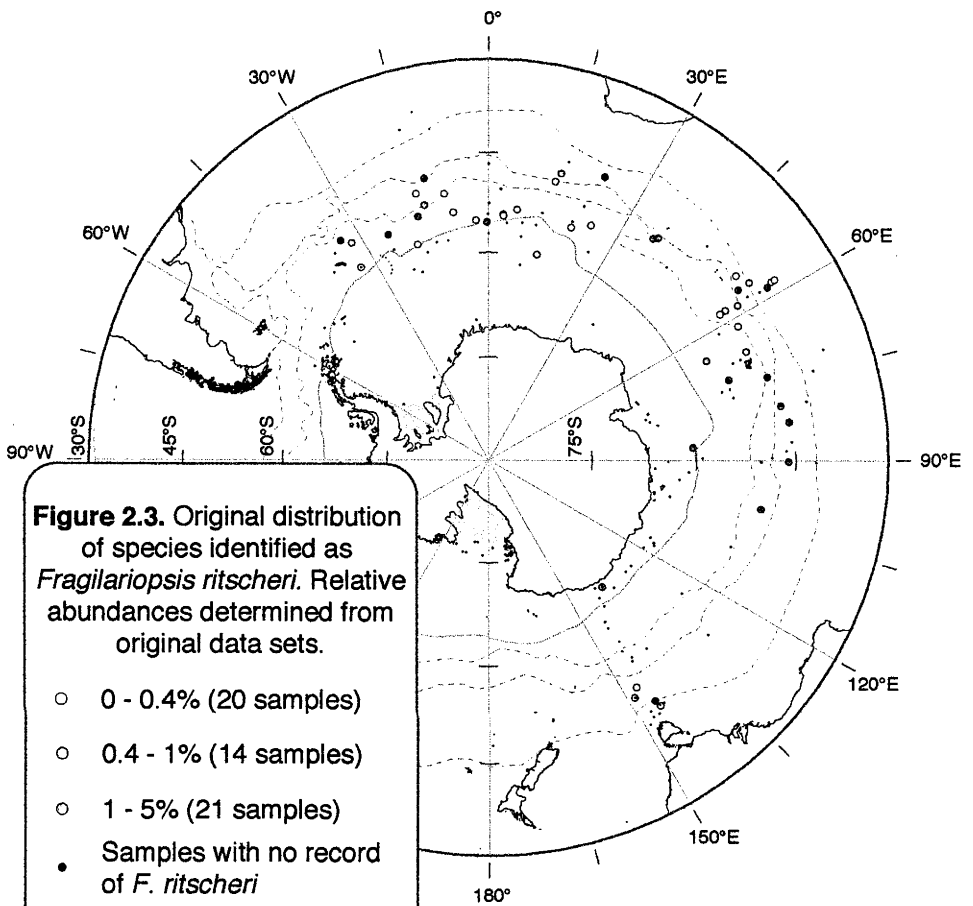

Figure 2.3. Original distribution of species identified as *Fragilariopsis ritscheri.* Relative abundances determined from original data sets.

- ○ 0 - 0.4% (20 samples)
- ○ 0.4 - 1% (14 samples)
- ○ 1 - 5% (21 samples)
- • Samples with no record of *F. ritscheri*

Reference	Region	Sample type	Dominance
Hustedt 1958 (cited in Hasle 1965b)	South Atlantic & South Indian sectors	ws	Abundant Antarctic, S. Atlantic max @ 69°36'S, N limit 51-49° in *Salpa*
Jousé *et al.* 1962a	South Indian sector	sws, sed	Near shore Antarctic & Kerguelen Island.
Kozlova 1962	South Indian	sws	Coastal Antarctic
Kozlova 1966	South Indian, Pacific & Atlantic	sws, sed	Coastal Antarctic 8-33%, N of Ant. Div. 0.1-2%, N limit PF. S. Atlantic abundance 61-69°S
Hasle 1965b	South Pacific	sws	Common Antarctic, rare subantarctic
Donahue 1971	South Pacific	sws, sed	Rare in subantarctic
Abbott 1973	southeast Indian	ct	Rare subantarctic, increased abund. >58°S. Coastal Antarctic
Fenner *et al.* 1976	southeast Pacific	sws	Subantarctic 11%
Truesdale & Kellogg 1979a	Ross Sea	c, sed	Highest relationship to epontic conditions
DeFelice & Wise 1981	southeast Atlantic	sed	More common in diatom ooze belt
Akiba1982	Bellingshausen Sea	sed, c	Antarctic
McConville & Wetherbee 1983	inshore East Antarctic	si	Antarctic, ice and surface melt pool
Gersonde 1984	South Weddell Sea	si, sed	Commonly occurring in both, 3% max. in sediments
Pichon 1985	South Atlantic and south west Indian	sed	Small no. in all regions, statistically abund in subantarctic zone
Prasad & Nienow 1986	Croft Bay	sed	Present in samples
Kellogg & Kellogg, 1987	Amundsen Sea	sed, si, ws	Rare in sediments, not in water/ice samples
Garrison *et al.* 1987	Weddell Sea	si, ws	Average abundance $1.3x10^3$ in water column near ice
Garrison & Buck 1989	Weddell Sea, Antarctic Peninsula	pi	Present, not common
Kang & Fryxell 1991	Kerguelen-Prydz Bay	ws	Greatest abundances in water column at inner Bay sites
Stockwell *et al.* 1991	Prydz Bay - inner and outer	sed	Increases to outer Prydz Bay, max. abund. 3.7%
Leventer 1992	George V Coast	sed	0.3 to 2.7% of samples
Kang & Fryxell 1992	Bellingshausen & Weddell Sea, Prydz Bay	ws, si	Seasonal abundances, peak in Summer
Tanimura 1992	Lützow-Holm Bay, Antarctica	sed	0.8 to 3% of samples
Zielinski 1993	South Atlantic	sed	Statistically heavy in Antarctic ice factor
Scharek *et al.* 1994	Eastern Weddell Sea	ws	Present throughout all study region
Leventer & Dunbar 1996	Ross Sea	trap, sed	Common. Seasonal flux increase, greater numbers in Central Ross Sea
Zielinski & Gersonde 1997	South Atlantic	sed	Max. abundance 2.6%. Temp range -2 to 5°C, max abund between -2 to 1°C

Table 2.4. Occurrences of the species *Fragilariopsis ritscheri* in the literature, noting study region, samples observed and dominance of the species. Abbreviations: c = core sample; ct = core top sample; pi = pack ice sample; si = sea ice sample; sed = surface sediment sample; trap = sediment trap sample; sws = surface water sample; ws = water sample or water column sample.

identified. Since Hasle (1965b) notes that *F. ritscheri* is most closely related to *F. obliquecostata* and *F. kerguelensis*, and as the distributions provided by Fenner *et al.* (1976) provide an indication that *F. ritscheri* is more a subantarctic species, it can only be presumed that mis-identification of a *F. kerguelensis* (presumably highly lanceolate in shape) is the species *F. ritscheri* identified by Pichon (1985) and included in the databases of Pichon *et al.* (1987, 1992). Under this assumption the data identified as *F. ritscheri* in the databases presented here are transferred to *F. kerguelensis*. Although this is not the most satisfactory situation since trace occurrences of the real *F. ritscheri* in the open ocean are lost, it is currently the only approach available in achieving a consistent database.

Independent of isolating the identify of the *F. ritscheri* sensu Pichon, is the question of what the real *F. ritscheri* was identified as. From analysis of samples available at the Bremerhaven workshop (1996) it would appear that *F. ritscheri* was either counted as *F. obliquecostata* or *F. sublinearis*. The following section deals with possibilities.

2.2.12. FRAGILARIOPSIS COOL TAXA

FRAGILARIOPSIS OBLIQUECOSTATA (VAN HEURCK) HEIDEN

FRAGILARIOPSIS SUBLINEARIS (VAN HEURCK) HEIDEN

Zielinski and Gersonde (1997) suggest that the maximum occurrence of *F. obliquecostata* and *F. sublinearis* in the sediments of the south Atlantic are 16.9% and 13.0 % respectively. Kozlova (1966) provided 5-10% abundance of *F. sublinearis* in the surface sediments of the Pacific and Indian Ocean sectors. Maximum abundances for the databases available to this study provide 6.06% for *F. obliquecostata* and 39.22% for *F. sublinearis*. These both appear grossly imbalanced in contrast to previously documented results. Taking into consideration the loss of information of the real *F. ritscheri* and the similar distributions of *F. ritscheri*, *F. sublinearis* and *F. obliquecostata* in the Antarctic Zone (Kozlova 1966, Hasle 1965b, Hasle 1976, Tanimura 1992, and Zielinski and Gersonde 1997) it seems highly probable that all three species have been confounded in the database used here. Tanimura (1992) noted that transitional forms between *F. ritscheri* (*N. ritscheri*) and *F. obliquecostata* (*N. obliquecostata*) were observed in his samples from Lützow-Holm Bay.

By combining the maximum abundances of *F. ritscheri*, *F. obliquecostata* and *F. sublinearis* provided by Zielinski and Gersonde (1997) the product is a comparable value to the combined *F. sublinearis* and *F. obliquecostata* maximum abundances in this database (ie. 33% against 45% respectively). In addition to discrepancies of the relative abundances of these species, slides from the South Atlantic were observed and discussed while visiting Bremerhaven (1996) and a conclusion was reached regarding the likely confusion that may have occurred between the these species. This is also evident from the

figures illustrating *F. sublinearis* in Pichon's thesis (1985, pl.5, figs 9-10, pl. 6, fig. 3). *F. obliquecostata* is shown in figure 9 and 3, and *F. ritscheri* in figure 10.

As a result of likely confusion between the three species *F. ritscheri*, *F. sublinearis*, and *F. obliquecostata* within the database available to this work, all data compiled under *F. sublinearis* and *F. obliquecostata* will be combined and re-named "*Fragilariopsis* Cool Taxa" and is to represent the combination of the three species. The combined floral signal produced by the group, in terms of further statistical analysis for proxy estimation, will be combined. Analysing this effect for temperature estimation and loss of sensitivity we can use the result provided by Zielinski and Gersonde (1997) where temperature signatures have been identified with highest abundances in the sediments (Table 2.5). The *Fragilariopsis* Cool Taxa, will thus, be expected to cover temperature ranges from -2° to 5°C and lose all sensitivity to interspecific differences, more notably between *F. ritscheri* and the other two species.

Species	Summer SST Range	Temp. at maximum observed abundance
F. ritscheri	-2 to 5°C	-2 to 1°C
F. obliquecostata	-2 to 0.5°C	-2 to -1.5°C
F. sublinearis	-2 to 1 °C	-2 to -1°C

Table 2.5. Observations of *Fragilariopsis* species to corresponding summer sea-surface temperatures (SST) in the South Atlantic sector of the Southern Ocean. Data from Zielinski and Gersonde (1997, table 2).

2.2.13. *FRAGILARIOPSIS* CYLINDRIFORM GROUP

FRAGILARIOPSIS CYLINDRUS (GRUNOW)KRIEGER

FRAGILARIOPSIS VANHEURCKII (M. PERGALLO) HUSTEDT

FRAGILARIOPSIS LINEARIS (CASTRACANE) FRENGUELLI

The differentiation between *F. cylindrus* and *F. vanheurckii* in the 166DB was never made, and *F. vanheurckii* has only been identified in one sample in newer material (GC5). It appears that the two species are combined under counts entitled *F. cylindrus*.

F. vanheurckii is thought to have a sea-ice related habitat as it is recorded from sea-ice and its surrounding waters (Jousé *et al.* 1962a, Fenner *et al.* 1976, Gersonde 1984, Garrison *et al.* 1987, Garrison and Buck 1989, Tanimura *et al.* 1990, Gleitz *et al.* 1996) although their concentrations are considerably lower in comparison with *Fragilariopsis curta* and *F. cylindrus* (Garrison *et al.* 1983a, Garrison *et al.* 1987, Tanimura *et al.* 1990, Kang and Fryxell 1993). *F. vanheurckii* is nevertheless preserved in the seafloor sediments (Jousé *et al.* 1962a, Kellogg and Truesdale 1979a, Gersonde 1984, Kellogg and Kellogg 1987, Tanimura 1992), and in the southeast Indian and south Atlantic

sectors this was never greater than 1% of the total specimens observed (Leventer 1992, Zielinski 1993).

F. cylindrus has been intensely investigated and shown to be the dominant marginal sea-ice edge species with increased seasonal abundance during the summer (Kang and Fryxell 1992, Kang *et al.* 1993, Kang and Fryxell 1993). It is also preserved in the sediments (Jousé *et al.* 1962a, Gersonde 1984, Tanimura *et al.* 1990, Tanimura 1992, Leventer 1992, Zielinski 1993, Zielinski and Gersonde 1997)

Hasle (1965b) notes that similarity, predominantly in the valve shape, exists between *F. cylindrus*, *F. vanheurckii* , and *F. linearis*. Yet *F. cylindrus* is considerably smaller and finer than the other three species. Difficulty in separating *F. cylindrus* from *F. curta* has been mentioned by DeFelice and Wise (1981) and Tanimura (1992). From Antarctic sediment samples available to the author at Bremerhaven (1996), *F. vanheurckii* was considered to have most likely been confused with *F. cylindrus*, especially in cases where elongated *F. cylindrus* valves were also encountered in the samples. The location of an enlarged "aperture" in the middle of the keel puncta, typical of *F. vanheurckii*, was in these cases an important guide in differentiating between the two species, as was the constant 5μm width of *F. vanheurckii* (Hasle 1965b).

Specimens typifying *F. linearis* were not encountered and it is difficult to advance any comment on whether this species has been correctly identified in the databases (only one sample DFBC 83-5 II, relative abundance 10%) or confounded with *F. cylindrus* and *F. vanheurckii*. Very few workers have discovered *F. linearis* in the sediments (Jousé *et al.* 1962a Abbott 1973, Prasad and Nienow 1986, Tanimura 1992, Zielinski 1993) where only traces have been noted, the largest maximum relative abundance recorded being 1.7% (Tanimura 1992). Thus, data referring to *F. cylindrus* will henceforth be addressed as the *F.* Cylindriform Group. It contains the data from all records of *F. cylindrus* and *F. vanheurckii*. The sole occurrence of *F. linearis* in the database is included in this *F.* Cylindriform Group. This is a similar step taken by Zielinski (1993) where he combined counts of *F. curta*, *F. cylindrus and F. vanheurckii* under a sea-ice group for statistical analysis.

2.2.14. *NITZSCHIA SICULA*

NITZSCHIA SICULA VAR. *BICUNEATA* (GRUNOW) HASLE

NITZSCHIA SICULA VAR. *ROSTRATA* HUSTEDT

Nitzschia sicula has been identified to two varieties in this study. Hasle (1964) presents data on the two varieties suggesting that apart from the distinct size differences and the differing poles the species are very similar. Biogeographically Hasle (1964) suggests that

the variation *rostrata* is located in warmer waters of the subantarctic, whereas variation *bicuneata* has been recognised in both Antarctic and subantarctic waters to just below the Polar Front. In the databases presented here only very rare occurrences of either species are recorded, and for all but two samples these are referred to as *N. sicula* var. *rostrata.* Since the other two occurrences (one var. *bicuneata* and the other *N. sicula*) are also low in number they are combined with the *N. sicula* var *rostrata* data to produce a *N. sicula* Group.

2.2.15. *NAVICULA GELIDA VAR. PARVULA*

"NAVICULA GLACEI" VAN HEURCK

NAVICULA GELIDA VAR. PARVULA HEIDEN

The species *Navicula glacei* is a benthic diatom species (Whitehead and McMinn 1997) and this is represented by the lack of the species in the database and its occurrence in samples along the Antarctic coast. Simonsen (1992) indicates the species *Navicula glacei* is a synonym of *Navicula gelida* var. *parvula* Heiden, and so the species encountered in the databases used here have been transferred to reflect this change.

2.2.16. GENERA *PARALIA* AND *MELOSIRA*

MELOSIRA ADELIAE

MELOSIRA SOL ("*PARALIA SOL*") (EHRENBERG) KÜTZING

PARALIA SULCATA (EHRENBERG) CLEVE

The taxonomic distinction between the three species has not been pursued in any great detail and it is considered very likely that each species is confounded with the other. Preliminary research in distinguishing each of the species has revealed a need for taxonomic reform for the position of *Melosira sol* to *Paralia sol.* Only the work of Pichon (count sheets of 166DB) distinguished *Melosira adeliae.* Since it is acknowledged that the species placed under *Melosira* or *Paralia* are uncertain, they are grouped under *Paralia* species. This again means that the data is incorporated over the whole study region and should only enhance noise in statistical evaluation.

2.2.17. POROSIRA GROUP

POROSIRA GLACIALIS (GRUNOW) JØRGENSEN

POROSIRA PSEUDODENTICULATA (HUSTEDT) JOUSÉ

Porosira glacialis and *Porosira pseudodenticulata* were provided emended descriptions by Hasle (1973) and classified as neritic Antarctic species.

Initially (as of 1983) neither of the two *Porosira* species were listed in the 166DB count data. *Porosira glacialis* appears to have been incorporated in counts around 1985. The first record of *P. pseudodelicatula* is noted in samples dated 1988. Observations of *P.*

pseudodenticulata have been very rare. Pichon does not make mention of *P. pseudodenticulata* in any of his publications (*et al.* 1987, 1992) or in his thesis (1985). Yet in statistical work counts of *P. pseudodenticulata* were combined with *P. glacialis* data (samples KR8818, KR8817, and DFBC83-40II).

Thus, it appears highly likely that the two species have been confounded in the 166DB. This is supported by the illustrations provided for *P. glacialis* in Pichon's thesis (1985) where plate 5 figure 14, shows *P. glacialis* and figure 13 illustrates *P. pseudodenticulata.* It is not known if current records of either species in the Pichon new dataset (Appendix 2.3) have been consistently separated.

Identifications of *Porosira* species made by this author are all linked to *Porosira glacialis* which appear to have been transported eastward by the West wind drift from the neritic environment provided by Kerguelen Islands (Appendix 2.4). But just as plausibly they could have been displaced via a bottom water route from Antarctica. The counts presented in the appendices (2.2, 2.3, 2.4) preserved the original identifications of each *Porosira* species where they were noted.

Work presented by Zielinski and Gersonde (1997) contains both species separately identified, with *P. pseudodenticulata* representing the very cold waters (-2°C) and *P. glacialis* somewhat less cold waters (-1° to 1.5°C). Such a distribution was acknowledged by Hasle (1973) where *P. pseudodenticulata* was abundant within sea-ice, and *P. glacialis* found in waters adjacent to sea-ice or the coast. Since both species represent cold Antarctic waters, the lack of differentiation in the databases available here can be temporarily overlooked, although obviously could provide more detailed information concerning sea-ice presence. All data assigned to *Porosira glacialis* and *Porosira pseudodenticulata* are combined for further statistical analysis in this thesis and the data are henceforth referred to as the *Porosira* Group.

2.2.18. GENERA *RHIZOSOLENIA* AND *PROBOSCIA*.

Of all the taxa investigated, the largest inter-species confusion is located within the genus *Rhizosolenia*. The genus remains problematical to current workers in the Southern Ocean transfer function field, a product of changes currently only recognised in a couple of publications and one thesis. There is considerable work to be done in coming to terms with the species currently and previously identified within the genus.

Taxa under the genus *Rhizosolenia* was revised by Sundström (1986, thesis unavailable for this work). Since Sundström's work, which has engendered its own controversy as to validity of newly described genera and species, there have been other works which

have endeavoured to clarify and bring status to his revisions (Priddle *et al.* 1990, Jordan *et al.* 1991a, Jordan and Priddle 1991, Takahashi *et al.* 1994). A literature survey of Southern Ocean phytoplankton studies available to the author encountered over 60 identified living and fossil species forms and varieties (See Appendix 2.6). Of these 60 plus species, 16 living species (11 *Rhizosolenia*, 3 *Proboscia*, and 2 species transferred to other genera) are considered valid in the Antarctic (Priddle *et al.* 1990, Jordan *et al.* 1991a). These species are listed below:

Section *Rhizosolenia*

R. antennnata f. *antennata* (Ehrenberg) Brown
R. antennata f. *semispina* Sundström
R. crassa Schimper in Karsten
R. curvata Zacharias
R. polydactyla f. *polydactyla* Castracane
R. polydactyla f. *squamosa* Sundström
R. sima f. *silicea* Sundström
R. sima f. *sima* Castracane
R. simplex Karsten
R. styliformis Brightwell

Section *Imbricatae*

R. chunii Karsten

Proboscia

Proboscia alata (Brightwell) Sundström
P. inermis (Castracane) Jordan & Ligowski
P. truncata (Karsten) Nöthig & Ligowski

Guinardia

G. cylindrus (Cleve) Hasle

Other species that require transfer to new genera.

R. rhombus Karsten

(Source Priddle *et al.* 1990, Round *et al.* 1990, Jordan *et al.* 1991a, Hernandez-Becerril, 1995)

These species are provided with descriptions in Priddle *et al.* (1990) which include characteristics observable under the light microscope to allow identification, but no synonyms are provided so that previous identifications can be revised. This has presumably occurred in Sundström's thesis. As most *Rhizosolenia* species are broken in sediment assemblages and in permanent mounts, criteria distinguishing the *Rhizosolenia* species must deal with the parts that are most commonly remaining: the valve apex, otaria and the basal section of the process (Figure 2.4A). As the illustrations in Priddle *et al.*

(1990) are aimed towards complete valve identifications a diagrammatic figure with some LM and SEM examples are provided (Figure 2.4). All these species were observed in samples taken from the Southern Ocean.

The most reliable reports dealing with these Antarctic species occurrences indicate that their differentiation geographically would be of tremendous value to temperature transfer functions.

- *R. antennata* f. *antennata*: Evidence from reports in the Weddell and Bellingshausen Sea sectors indicate the species is primarily linked to the open ocean water column and not observed in ice conditions (Hart 1934, Hendey 1937, Ligowski 1993).
- *R. antennata* f. *semispina*: If earlier records of *R. hebetata* f. *semispina* are considered to represent *R. antennata* f. *semispina* as suggested in Priddle *et al.* (1990) then *R. antennata* f. *semispina* is the most common *Rhizosolenia* species in the Southern Ocean. Hendey (1937) indicated that the species is in all water types but that thinner forms were noted in the southern reaches of the Weddell and Bellingshausen Seas. More recent work by Ligowski (1993) confirms the adaptability of the species finding it in open ocean stations to sublittoral habitats in sea ice. This is also reflected in the large temperature range of occurrence (-1 to 12°C) referred to by Zielinski and Gersonde (1997). Ligowski (l.c.) found that *R. antennata* f. *semispina* was abundant in hydrological regimes with an average surface salinity of 34.2±0.5‰ and temperature of 0.5±0.5°C. This is reflected extremely well in the surface sediment study of Zielinski and Gersonde (1997) where their plot of relative abundance against Summer temperature indicates the species is more common in waters close to freezing point (-1 to 2°C).
- *R. crassa*: This species appears to be linked to the region near the boundary of the Winter sea-ice edge in the Weddell Sea region or conditions of the marginal sea-ice zone (Hart 1934, Hendey 1937, Ligowski 1993). In the Australian sector the species was reported at 62°S, 135°E and 64°S, 115°E along Wilkes Land (Wood 1960, Crooks 1960) and Hasle (1969) noted it in the southern section of the subantarctic zone in the Pacific.
- *R. curvata*: Quite possibly one of the most important species of the Subantarctic zone. In almost all cases *R. curvata* has been associated with the Polar Front, and it is considered endemic to the Subantarctic, rarely observed in the Antarctic (Hart 1934, Hart 1937, Hendey 1937, Hasle 1969, Cassie 1963, Semina 1979).
- *R. polydactyla* f. *polydactyla*: Castracane (1886) originally described the species as observed in the Antarctic Zone. Hart (1934) subsequently typified the species as a dominant subantarctic species associated with the Polar Front and rarely observed

further south than the Bellingshausen Sea. Hendey's (1937) work appears to have located it throughout the Drake Passage and the Bellingshausen Sea. To the east in the Pacific region, Hasle (1969), noted a neritic, benthic or tychopelagic (removed from its habitat but in plankton) species confined south of 65°S which she identified as *R. styliformis* f. *polydactyla*. It would seem from these few observations *R. polydactyla* f. *polydactyla* is related to the marginal sea ice zone and is distributed near coastal conditions located in the subantarctic zone (ie. Falkland Islands, Hart 1934) where it is able to survive. No reports of the resting spore, *R. polydactyla* f. *squamosa* have been recorded in the literature.

- *R. simplex*: Hasle (1969) reviewed all previous literature regarding the distribution of *R. simplex* and concluded the species was an oceanic form dominant in the northern subantarctic region and restricted to the south between the Polar Front and the ice edge. Semina (1979) reviewing further distributional data, noted *R. simplex* widely in the Antarctic, but also south of the Antarctic Divergence. More recently Ligowski (1993) observed the species only in open ocean conditions of the Bellingshausen and Weddell Seas.
- *R. sima* f. *sima*: Only two references to the distribution of this species were located. Castracane (1886) originally described the species from the Antarctic Ocean and fast ice. Ligowski (1993) observed the species in the Weddell and Bellingshausen Sea open ocean regions, however, the form was most abundant (maximum 12 %) in the ice and open ocean of the Admiralty Bay.
- *R. sima f. silicea*: As above only Castracane (1886) and Ligowski (1993) have noted the resting spore of *R. sima* f. *sima*. Ligowski (l.c.) noted the resting spore to be in high abundance (32%) within Admiralty Bay in both open ocean and ice covered conditions. Two recent publications (Harwood and Maruyama 1992, Mahood and Barron 1996) have noted and illustrated exceptionally well a highly silicified, otaria lacking, *Rhizosolenia* species within and north of Prydz Bay. The species, identified as *Rhizosolenia* sp D. (of Harwood and Maruyama 1992) was found in modern sediments through to lower Pliocene sediments between 54-58°S (Harwood and Maruyama l.c.) and in Upper Pliocene sediments of the outer Prydz Bay region (Mahood and Barron l.c.). The presence of this species from the Antarctic coast to the marginal sea-ice zone thus provides further evidence to the likelihood of this species representing *R. sima* f. *silicea*.
- *R. styliformis*: Cited early on as an abundant oceanic species of the Antarctic (Hart 1934, Hendey 1937), the difficulties in separating *R. styliformis* and *R. hebetata* f. *semispina* by many workers (eg. Hart 1934, Hasle 1969, Fenner *et al.* 1976) made interpretation of such occurrences difficult to define geographically. Simonsen (1974), who believed *R. hebetata* f. *semispina* should be transferred to *R. styliformis*, did not find *R. styliformis* to be oceanic but more frequent in coastal regions of the Indian

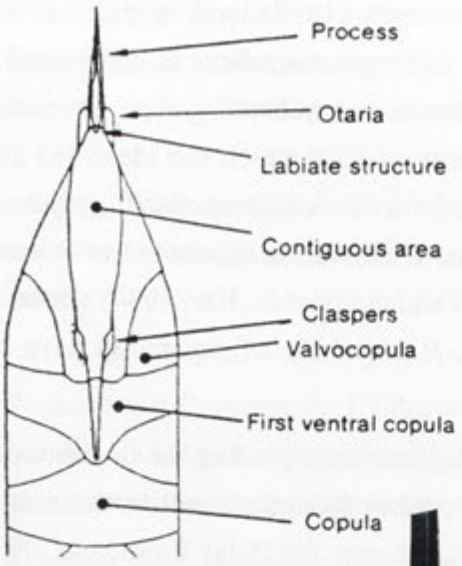

A.

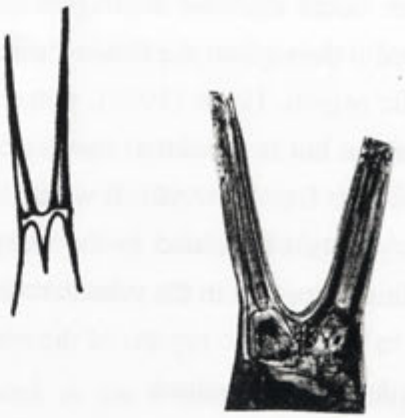

B. ***R. antennata* f. *antennata***
Otaria: None
Process: paired

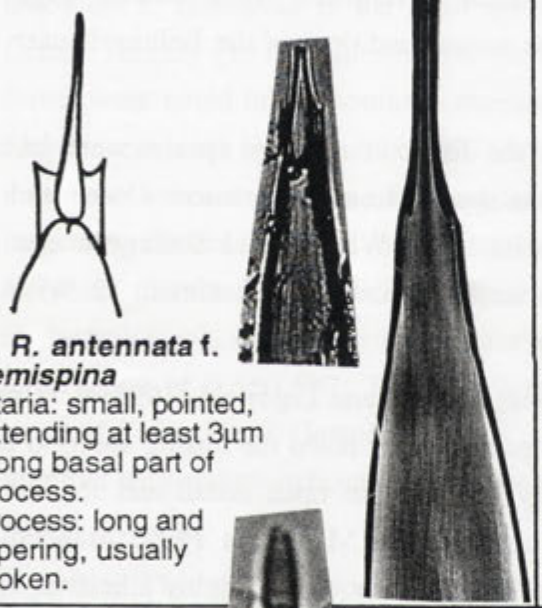

C. ***R. antennata* f. *semispina***
Otaria: small, pointed, extending at least 3µm along basal part of process.
Process: long and tapering, usually broken.

D. ***R. styliformis***
Otaria: small, rounded, usually terminating below the base of the process or extending 1-2µm onto process.
Process: long and tapering, usually broken.

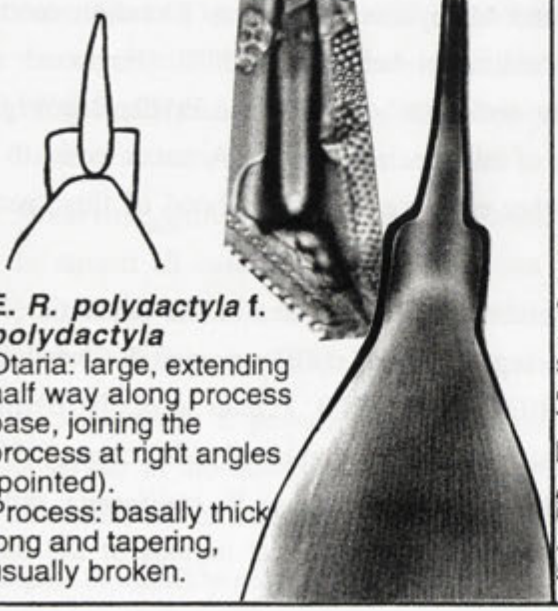

E. ***R. polydactyla* f. *polydactyla***
Otaria: large, extending half way along process base, joining the process at right angles (pointed).
Process: basally thick long and tapering, usually broken.

F. ***R. polydactyla* f. *squamosa***
Otaria: None.
Process: short, heavily silicified, ridging may extend onto process. Transitional forms between the *two R. polydactyla* forma are illustrated in *Priddle et al.* (1990, pl. 15.2 figs 5+6)

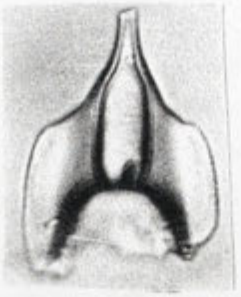

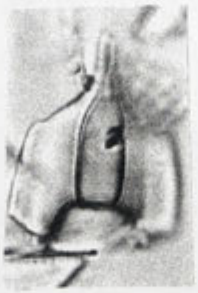

G. *R. crassa*
Otaria: large with distinct convex lateral margins extending to a slight point distally.
Process: long, but usually broken.

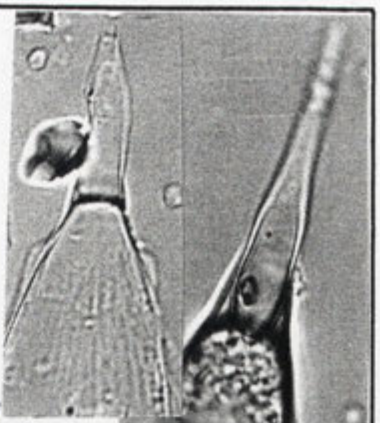

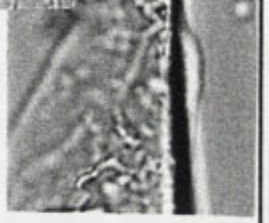

H. *R. curvata*
Otaria: small and rounded, arising on distal part of valve and ending below the valve apex.
Process: tapers uniformly

I. *R. sima* f. *sima*
Otaria: rounded and large, extending as long laterally as in length from valve, arise on valve apex and end after bulbous part of process.
Process: bulbous, tapering distally.

J. *R. sima* f. *silicea*
Otaria: None.
Process: robust arising from thickened valve apex. Whole valve heavily silicified.

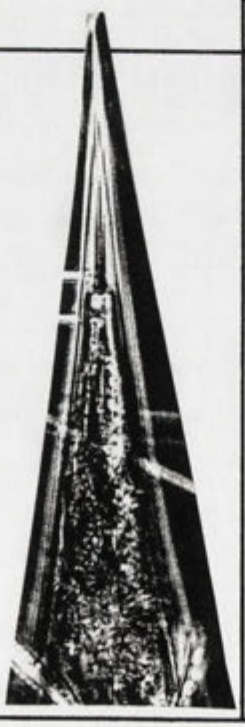

K. *R. simplex*
Otaria: None.
Process: long, weakly silicified, and tapers so it appears as an extension of the valve.

Figure 2.4. Diagrammatic and illustrated variation of *Rhizosolenia* species in the Southern Ocean.

A. Schematic diagram of valve structures. Modified from Medlin and Priddle (1990, fig 12, taken from Sundström 1985).

B-K. Diagrammatic and photographic representation of valve apex, otaria and basal process characteristics for identification of *Rhizosolenia* species. Notes and diagrams modified from Priddle et al. (1990, plates 15.1-15.3). Light micrograph and SEM images taken by Author at the ANU, Canberra, and the Alfred-Wegner-Institüt, Germany. Diagrammatic sketches not to scale.

Ocean. In Antarctic studies, Ligowski (1993), indicates that the species is in very low concentrations (maximum 6.7%) in the open ocean regions of the Bellingshausen and Weddell Seas, and with varying abundances in Admiralty Bay (2-20%), including the sea ice environment (maximum 5%). These lower numbers are reflected in the poor recovery of *R. styliformis* in the sediments (<2%) as indicated by Zielinski and Gersonde (1997).

Reassessment of the *Rhizosolenia* species identified in the databases available to this study is not necessarily an easy task in light of the new revisions. Species that have been recorded previously in the three databases used here are listed in Table 2.6 with their corresponding revised classification. Although most of these changes do not affect the species and their position, there are two very relevant changes which once delved into will reveal lumping and misrepresentation of species has occurred.

Previous identification	Revised classification
R. alata	*Proboscia alata*
R. barboi	*Proboscia barboi*
R. bergonii	*R. bergonii*
R. hebetata f. *bidens*	*R. antennata* f. *antennata*
R. hebetata f. *semispina*	*R. antennata* f. *semispina* *
R. styliformis	*R. styliformis* *

Table 2.6. List of *Rhizosolenia* species in the databases available to this study and their revised classification. Classification based on Priddle *et al.* 1990. * = although this is a revised classification for each of the species, direct transfer of data previously related to these "species" are shown in the text to relate to several species.

2.2.19. *RHIZOSOLENIA HEBETATA* FORMA *SEMISPINA*

Until recently the species *R. hebetata* f. *semispina* or simply *R. hebetata* has been identified in the 166DB by a characteristic lack of otaria. This is predominantly the result of illustrations by Hustedt (1930, fig. 338) and Fenner *et al.* (1976, pl. 13 figs 6-7), which are the two principal works cited by Pichon (1985) and most workers.

Hustedt (1930, fig. 338) illustrates for *R. hebetata* f. *semispina* a specimen lacking otaria but with claspers and a contiguous area. His illustrated *R. hebetata* f. *hemialis* (fig. 337) lacks all three characteristics and is noted to be heavily silicified. As a result of these illustrations, particularly the lack of otaria on *R. hebetata* f. *semispina*, subsequent studies have either noted *R. hebetata* f. *semispina* as specimens with or without otaria. This problem was compounded with the description provided by Hasle (1975) which indicated that *R. hebetata* f. *semispina* carried hook-like otaria and was previously confused with

R. styliformis. This confusion was carried through the work of Fenner *et al.* (1976) where they illustrate specimens with and without otaria and make mention of the difficulties of separating *R. styliformis* from *R. hebetata* f. *semispina*. Hendey (1937), in contrast to the comments made by Fenner *et al.* (1976), does not mention difficulties in separating the two species in question, but does state that there is considerable variation in the dimensions and silicification of *R. hebetata* f. *semispina*. His description does not mention the presence of otaria and is not illustrated.

The figures presented by Fenner *et al.* (1976) provide two specimens one with otaria (pl. 13 fig. 6) and the other without (pl. 13 fig. 7). The specimen with otaria is similar to *R. antennata* f. *semispina* as illustrated in Figure 2.4. The specimen without otaria also shows the presence of a contiguous area and possible claspers. Such features excludes all three *Rhizosolenia* species which lack otaria as defined by Priddle *et al.* (1990, ie. *R. simplex*, *R. sima* f. *silicea*, *R. polydactyla* f. *squamosa*). This leaves us with a specimen that is not currently described by the criteria of Priddle *et al.* (l.c.), but still falls under the illustration and description of *R. hebetata* f. *semispina sensu* Hustedt (1930). Other studies which illustrate "*R. hebetata* f. *semispina*" were re-examined and found to present either *R. antennata* f. *semispina* (Tanimura 1992 fig. 15) or a species lacking otaria (Abbott 1973 pl. 11 fig. g). Furthermore *R. hebetata* f. *hemialis* as presented by Fenner *et al.* (1976) illustrates what appears to be *R. curvata* (pl. 13, figs 11-12) and a specimen lacking otaria but with heavy silicification.

Zielinski (1993) and Zielinski and Gersonde (1997) have noted from Sundström's work that *R. hebetata* f. *semispina* is no longer a valid Southern Ocean diatom and is also defined by pointed otaria, as is acknowledged in Priddle *et al.* (1990). As Zielinski (1993) also finds a form lacking otaria and slightly less silicified but otherwise similar to the revised description of *R. antennata* f. *semispina* he defines a Southern Ocean *R. hebetata* f. *semispina* based on the descriptions of Gran (1904) and Hustedt (1930) (see Zielinski 1993, pl. 7 fig. 3). Although the name is invalid by the review and new descriptions of Sundström, the relationship of this species description sensu Gran (1904) and Hustedt (1930) is not discussed by Zielinski (1993) and Zielinski and Gersonde (1997). In the latter paper they mis-leadingly refer their species as a bi-polar species.

If the species *R. hebetata* f. *semispina* sensu Zielinski and Gersonde is considered to be a spore type, then several possibilities can be entered into. Firstly, the species should alternatively be related to *R. hebetata* form *hiemalis* (or a new species) rather than *R. hebetata* f. *semispina*, since the latter species under Hustedt's description and illustration has claspers and contiguous area which precludes it from spore status. If the species is considered the spore of *R. antennata* f. *semispina*, then it should be transferred to *R.*

antennata f. *antennata* and the description emended to include both single and double processed valves. However, if the species sensu Gran (1904) and Hustedt (1930) is shown to be a form species (ie. because it has a contiguous area and claspers etc. as appears in Fenner *et al.* 1976) then a new species should be erected. Contrary to this the *R. hebetata* f. *semispina* species identified by Zielinski and Gersonde (1997) is shown to occur in exactly the same distribution and highest abundance-temperature range as their identified *R. antennata* f. *semispina* species. This observation lends support to the idea that the two species are in fact the same. One being the form species and the other the resting spore.

Concerning the databases under assessment here, the status of species considered *R. hebetata* f. *semispina*, are likely to be somewhat confused. However, under the authors own additions to the database all species considered *R. hebetata* f. *semispina* have lacked otaria. It is likely that the majority of other data under this title do so as well. In effect this group must be considered to contain the five species: *R. sima* f. *silicea*, *R. polydactyla* f. *squamosa*, *R. simplex* , *R. curvata* (which has very reduced otaria on the valve rather than the process) and *R. hebetata* f. *semispina* (*sensu* Zielinski 1993). For this reason this species category will now be identified as the *Rhizosolenia* otaria absent group.

As detailed previously each of the species within the otaria absent group species have their own distribution pattern. Thus, these discriminating geographic zones are combined and would, under further statistical analysis, simply create noise. The distribution of the current data (Figure 2.5a-b) shows that there is only a very weak trend in the species currently identified as *R. hebetata* f. *semispina* in relation to geographic distribution or to temperature. Abundances between 0° and 2°C are thought to be associated with *R. sima silicea*, which possibly overlap with the distribution of *R. polydactyla* f. *squamosa* from 1°C to 4.5°C. The northern abundance at 15.5°C is most likely *R. curvata* but the presence could be *R. simplex* or a misidentified *R. bergonii* specimen.

Complete revision of the *Rhizosolenia* genus in Southern Ocean sediment samples is required, and all new counts must endeavour to separate the many forms which until now have been lumped on the basis of absent or present otaria. This definition is poorly constructed and is not sufficient or satisfactory in terms of the literature available to help distinguish these species.

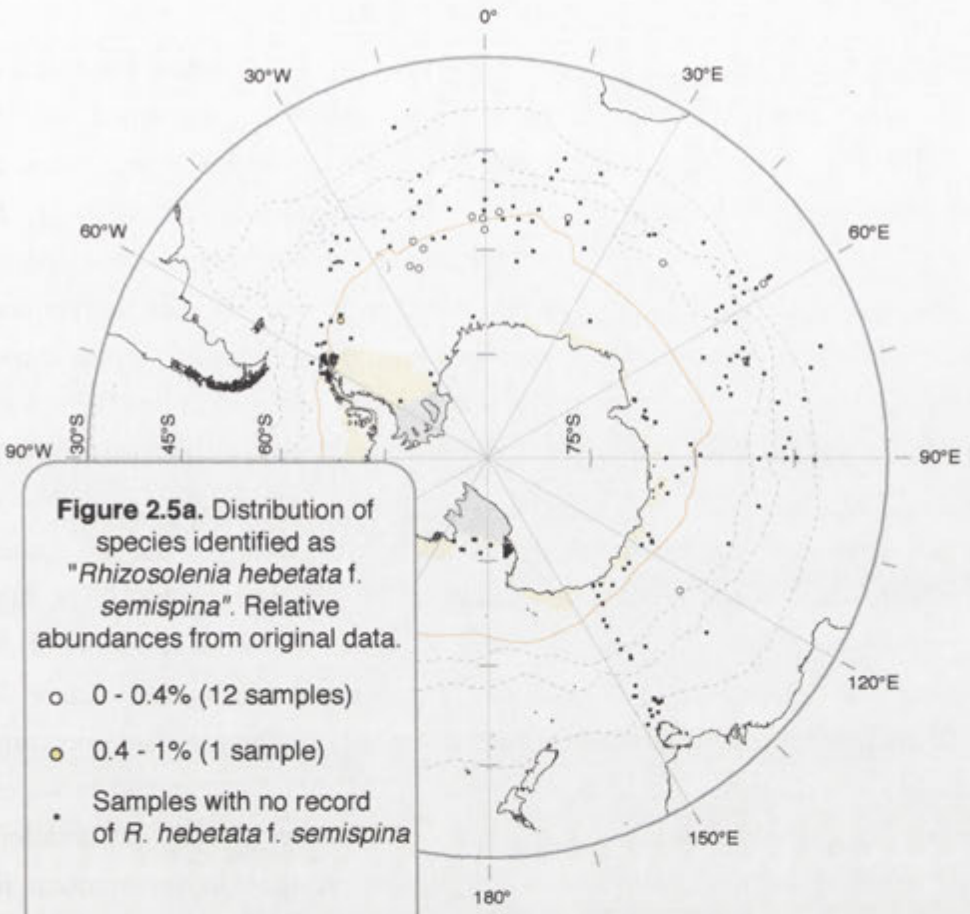

Figure 2.5a. Distribution of species identified as "*Rhizosolenia hebetata* f. *semispina*". Relative abundances from original data.

- o 0 - 0.4% (12 samples)
- o 0.4 - 1% (1 sample)
- . Samples with no record of *R. hebetata* f. *semispina*

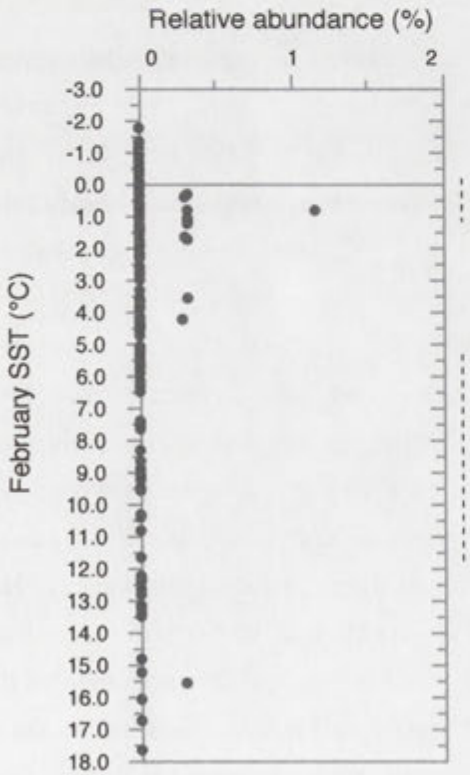

Figure 2.5b. Plot of "*Rhizosolenia hebetata* f. *semispina*" relative abundances against February SST from WOA (1994). Suggested species distributions (to the right) against temperature based on previous records.

R. sima f. *silicea*

R. polydactyla f. *squamosa*

R. simplex

R. curvata or *R. bergonii*

2.2.20. *RHIZOSOLENIA STYLIFORMIS.*

The second main group of *Rhizosolenia* species identified in the combined databases of this thesis, is one distinguished by the presence of otaria and identified as "*R. styliformis*". This definition is very poorly constrained and thus includes six species as identified by Priddle *et al.* (1990); *R. antennata* f. *semispina, R. styliformis*, *R. polydactyla* f. *polydactyla*, *R. crassa*, *R. curvata*, *R. sima* f. *sima*. Most of these species have been observed in sediment samples as illustrated in Figure 2.4, and furthermore each has distinctive otaria. The distribution of the current "*R. styliformis*" group shows no particular trend in geographic distribution in that they are widely distributed from the polar regions to the subantarctic (Figure 2.6a) perhaps with increased abundances near coastal regions. The abundance plot against temperature (Figure 2.6b) provides an exceptional bell peak which misleadingly gives an impression of a single species distribution pattern which is not necessarily evident in the geographical plot. The high abundance peak between 0.5-2°C is highly likely to represent the distribution of *R. antennata* f. *semispina* (Ligowski 1993, Zielinski and Gersonde 1997) and include *R. crassa* and *R. styliformis* occurrences in the warmer end of this temperature spectrum. *Rhizosolenia sima* f. *sima* is thought to be expressed in the abundances noted in waters with temperatures less than 0.5°C. The bulk of warmer water observations (approximately 3°-10°C) of this *Rhizosolenia* distribution are thought to represent *R. polydactyla* f. *polydactyla* , whereas specimens located in water warmer than 10°C could be *R. curvata* .

Initially the distribution of the "*R. styliformis* group" against temperature was expressed in early factor analysis under the subantarctic factor (Pichon *et al.* 1987, table IV, note the negative relation to the sea-ice zone factor). The distribution abundance peak illustrated in Figure 2.6b was then later expressed when the "*R. styliformis* group" was highly related to the dissolution and ice zone factors (Pichon *et al.* 1992, table 4) on the expansion of the dataset to the south.

Pichon cites Hustedt (1930) as his reference source, as does Fenner *et al.* (1976). Hustedt (l.c.) identified three forms of *R. styliformis*, the nominate with right-angled otaria passing and joining onto the process, and two variations, *longispina* where right-angled otaria end at the transition from valve to process, and finally variation *latissima* where the otaria are more rounded and less prominent than the *longispina* variety. Hasle (1975) redefined *R. styliformis* into two forms *R. styliformis* var. *styliformis* (otaria attaching to the process) and var. *oceanica* (otaria attaching below the process) but these were not used subsequently in the literature and appear to be subsumed under the one species description presented by Priddle *et al.* (1990) which appears to follow the *R. styliformis* var. *longispina* described and illustrated in Hustedt (1930, fig. 334).

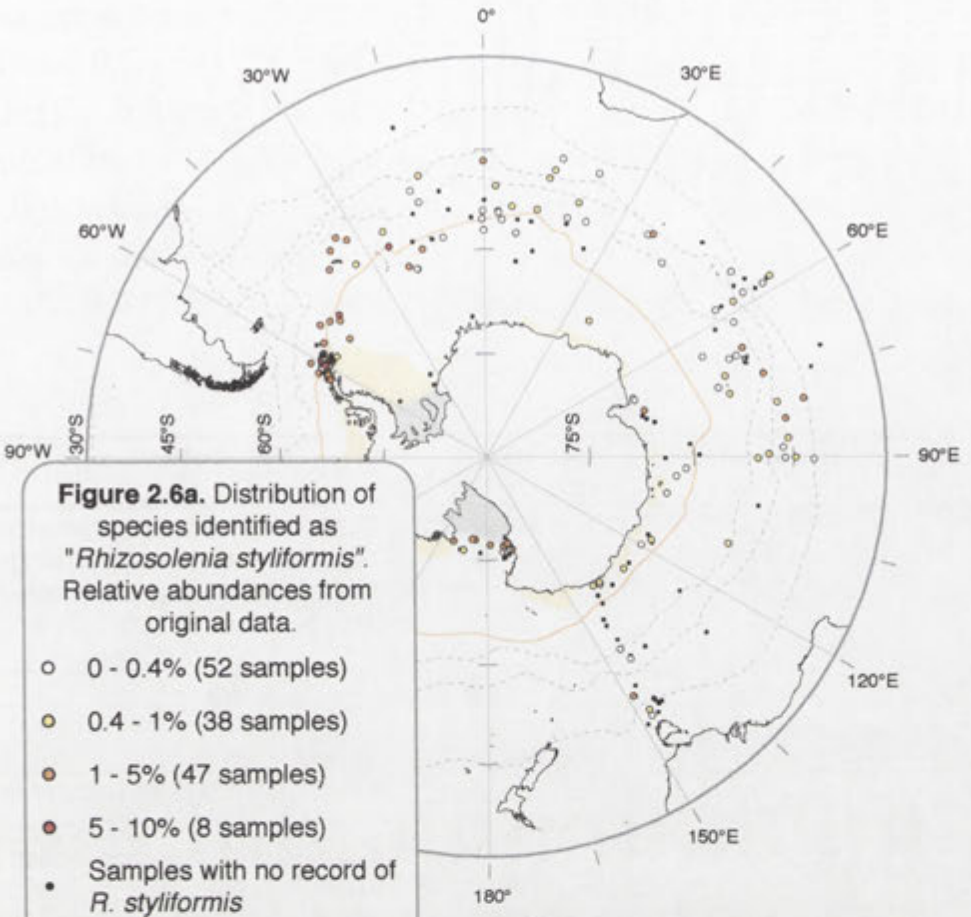

Figure 2.6a. Distribution of species identified as "*Rhizosolenia styliformis*". Relative abundances from original data.

- 0 - 0.4% (52 samples)
- 0.4 - 1% (38 samples)
- 1 - 5% (47 samples)
- 5 - 10% (8 samples)
- Samples with no record of *R. styliformis*

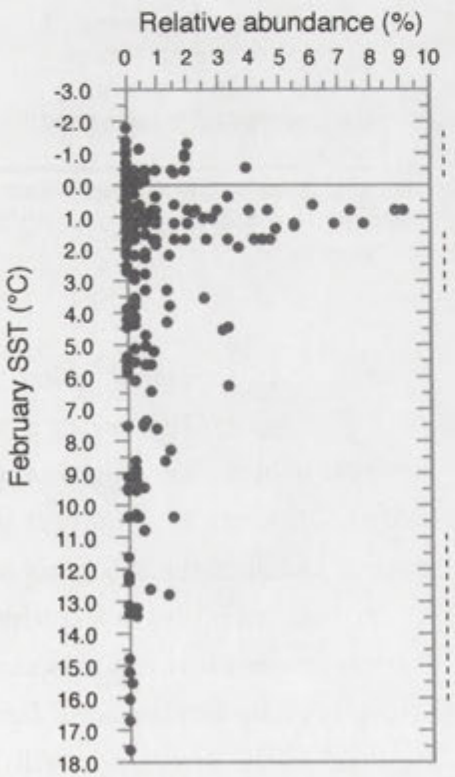

Figure 2.6b. Plot of "*Rhizosolenia styliformis*" relative abundances against February SST from WOA (1994). Suggested species distributions (to the right) against temperature based on previous records.

R. sima f. *sima*

R. antennata f. *semispina*

R. crassa, *R. styliformis*

R. polydactlya f. *polydactyla*

R. curvata ?

The illustrations presented by Fenner *et al.* (1976) can be identified based on the new descriptions and it appears that a mixture of *R. styliformis* (pl. 13 fig. 3) and *R. polydactyla* f. *polydactyla* (pl. 13. fig. 4, 5, and 9) were identified. Pichon (1985) illustrates three different forms; *R. antennnata* f. *semispina* (pl. 4 fig. 3), a form missing otaria (pl. 4 fig. 2) and another which appears to be *R. polydactyla* f. *polydactyla* (pl. 8 fig. 4). Other studies where identifications of *R. styliformis* are illustrated are listed below with the corresponding likely species based on Priddle *et al.* (1990) (Table 2.7).

Study	Illustration	Most likely represents	Notes.
Hendey 1937	pl. XI fig. 15-17	*R. polydactyla* f. *polydactyla*	Otaria are very large ~10μm, description mentions only wing-like projections at process base. Also describes *R. polydactyla* with rounded basal wings.
Jousé *et al.* 1962a	pl. 2 fig. 18	*R. styliformis*	No description
Abbott 1973	pl. 11 fig. h	*R. polydactyla* f. *polydactyla*	Subtropical and subantarctic assemblages
DeFelice and Wise 1981	pl. 2 fig. 13	? *R. polydactyla* f. *polydactyla*	Common throughout study area
Akiba 1982	pl. 7 figs 3-4	*R. styliformis* or *R. polydactyla* (fig. 3), *R. curvata* (fig. 4)	Cites Hustedt 1930 and Abbott 1973
Gersonde and Wefer 1987	pl. IV fig. 3	*R. polydactyla f. polydactyla*	Surface water and trap sites, Bransfield Strait and Drake Passage
Harwood and Maruyama 1992	pl. 18 fig. 20	*R. antennata f. semispina*	Observed in Pleistocene - L. Oligocene Leg 120 cores.
Mahood and Barron 1996	pl. 7 figs 4 & 6	*R. styliformis* ? (fig. 4) *R. antennata f. semispina* (fig. 6)	Found in Late Pliocene sediments (1.6% rel. abund.)

Table 2.7. Additional studies to those presented in the text, which provide illustrations of *Rhizosolenia styliformis*. The potential revision of each illustrated form is provided using the criteria presented in Priddle *et al.* (1990) and in Figure 2.4 of this work.

Zielinski (1993) identified *R. styliformis* and *R. antennata* f. *semispina*, with the illustration for the latter species as correct (Zielinski 1993, pl. 7 fig. 1). The former is not illustrated and thus, it is impossible to tell what his species is akin to. Yet judged on the information presented in their more recent paper with Gersonde, where *R. styliformis* is a rarer species in their data, the likelihood of having correctly identified the species is met but not conclusively proved (Zielinski and Gersonde 1997). In terms of the data currently associated with *R. styliformis* in this thesis, the group is confounded between all species that carry otaria. This makes using the data under this species group another noise factor for future statistical analysis. The data previously identified as *R. styliformis* will be assigned the name *Rhizosolenia* otaria present group.

2.2.21. GENUS *STELLARIMA*

"*COSCINODISCUS STELLARIS* VAR. *SYMBOLOPHORUS*" (GRUNOW)JØRGENSEN

"*COSCINODISCUS FURCATUS*" KARSTEN

"*COSCINODISCUS SYMBOLOPHORUS*" GRUNOW

STELLARIMA MICROTRIAS (EHRENBERG) HASLE ET SIMS

STELLARIMA STELLARIS (ROPER) HASLE ET SIMS

There is much confusion concerning the diatoms listed under any of the five species concepts above. Pichon in his 166DB observations began with (in 1983) *C. stellaris* var. *symbolophorus* and this is reflected in the floral descriptions given in his thesis (Pichon 1985). He noted the species distribution as located in the subantarctic region or south of the Polar Front. Later identification (circa 1988) has *C. stellaris* var. *symbolophorus* replaced with *C. symbolophorus* or *C. furcatus*, but also with *Stellarima microtrias* as a separately identified species. More recent identifications (since 1994) have *Coscinodiscus furcatus* replaced by *Stellarima microtrias*. In both transfer function publications (Pichon *et al* . 1987, 1992a) the species category used has been *C. furcatus*. It is important to note that *C. furcatus* was initially associated under factor analysis as a subantarctic species (Pichon *et al.* 1987, table IV) and in later factor analysis as a ice zone species (Pichon *et al.* 1992a, table 4). No discussion was made as to the change of association or the influence of "*C. furcatus*" geographic distribution or temperature range. All early work compiled by this author in this thesis had identified only *Stellarima microtrias*. The evolution of this species through one name change to the other would not be such a problem had the species in question been just a single species.

Syvertsen (1985) and Hasle *et al.* (1988) have established the differences between the species through geographical distribution, resting stage formation, biology and habitat. *Stellarima microtrias* is an Antarctic cool water species, that forms resting cells and is associated with shelf ice and the surrounding shelf waters (Hasle *et al.* 1988). Generally, previous identifications under the name *C. stellaris* var. *symbolophorus* are considered the resting stage of the species, whereas the vegetative stage was more commonly identified as *C. furcatus* (Syvertsen, 1985). Zielinski and Gersonde (1997) identified the highest abundance of *Stellarima microtrias* where SST was <1°C and with one occurrence at 3°C.

Stellarima stellaris was initially identified as *Coscinodiscus stellaris* Roper (Hasle *et al.* 1988). The species has no resting stage and is found in temperate conditions. Hasle *et al* (loc. cite) suggest that because *S. stellaris* has a form similar to the resting stage of *S.*

microtrias, past identifications of this temperate species would have been made under *C. stellaris* var. *symbolophorus*, as was done in Fenner *et al.* (1976, pl. 7, fig. 14).

The conclusion we are left with regarding the current databases is that the two *Stellarima* species are completely confounded. All data from "*C. stellaris* var. *symbolophorus*", "*C. furcatus*", "*C. symbolophorus*", and *Stellarima microtrias* are plotted on Figure 2.7. The relationship to temperature as a combined group shows no defining relationship. The previous jump after factor analysis of *C. furcatus* from subantarctic to sea-ice zone (Pichon *et al.* 1987, 1992a) simply illustrates the confounding of the species and the bias of samples towards the sea-ice region. The eventual SST estimate may have been likewise influenced by a cold signal when in fact the species identified were the temperate *S. stellaris.*

Hasle *et al.* (1988) caution the splitting of the two species from past records, however, as a strictly temporary means for this thesis and using the temperature range observations provided by Zielinski and Gersonde (1997), a division has been made. The samples containing any of the confounded species have been divided by corresponding February SST attributes greater and less than 3°C. These changes are listed in Table 2.8. The split by temperature distinction indicates that most of the samples are categorised in what is now regarded as *S. microtrias.* Further analysis in this thesis will use the data provided by the division, since without the split the data becomes ineffectual for the transfer function technique. Future work requires that all current database samples be re-counted to determine the real identification of the two species, and that all new surface samples to be used for transfer function work correctly identifies both species of *Stellarima.*

2.2.22. *THALASSIONEMA NITZSCHIOIDES*

THALASSIONEMA NITZSCHIOIDES VAR *PARVA* HEIDEN

THALASSIONEMA NITZSCHIOIDES VAR. *LANCEOLATA* GRUNOW

THALASSIONEMA FORMA 1.SENSU ZIELINSKI AND GERSONDE (1997)

Recent taxonomic studies by Moreno-Ruiz and Licea (1994) indicate that most previously described species of *Thalassionema nitzschioides* should remain at variation level. Within the Southern Ocean several varieties have been described. These include: *Thalassionema nitzschioides,* a species with cosmopolitan distribution (Hasle and De Mendiola 1967, Simonsen 1974, Hallegraeff 1986, Moreno-Ruiz and Licea 1994); *Thalassionema nitzschioides* var. *parva,* a warm water taxa excluded from the Antarctic waters at the STC (Zielinski and Gersonde 1997); *Thalassionema nitzschioides* var. *lanceolata,* an Antarctic species with noted decreasing presence south of the Polar Front (Zielinski and Gersonde 1997); and *Thalassionema nitzschioides* var. *capitulata,* noted as an Antarctic water species (Hustedt 1958, Moreno-Ruiz and Licea 1994).

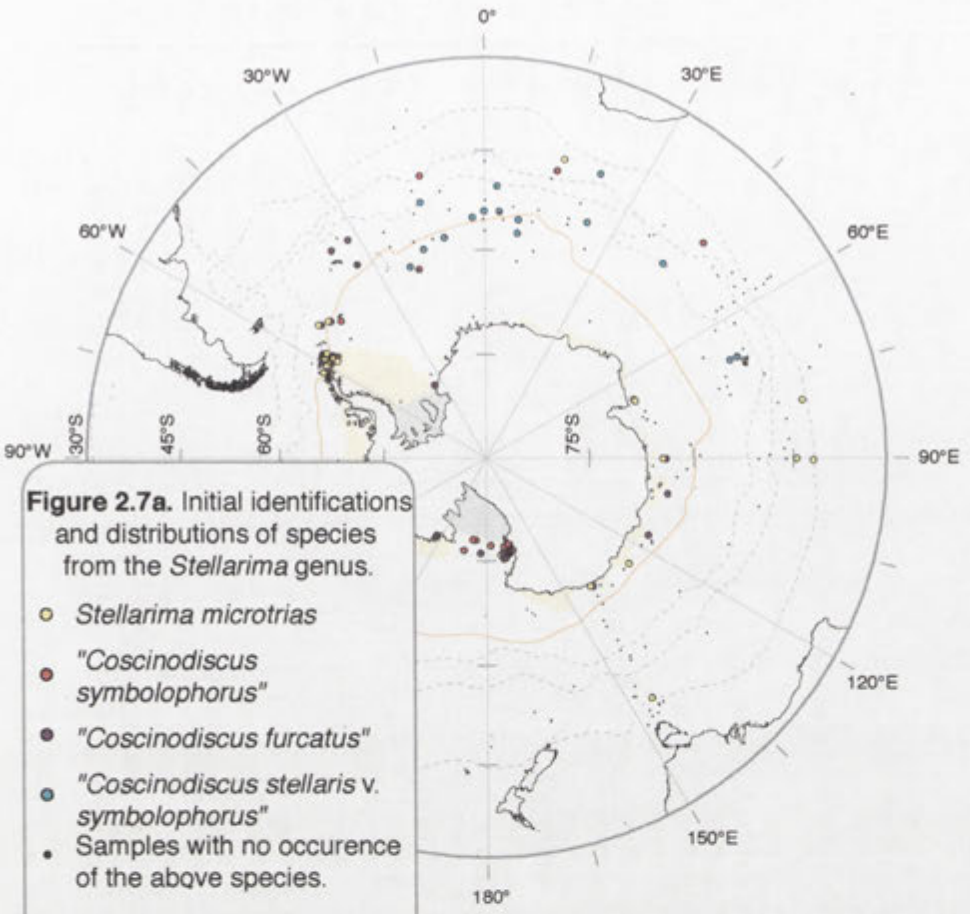

Figure 2.7a. Initial identifications and distributions of species from the *Stellarima* genus.

- *Stellarima microtrias*
- *"Coscinodiscus symbolophorus"*
- *"Coscinodiscus furcatus"*
- *"Coscinodiscus stellaris* v. *symbolophorus"*
- Samples with no occurence of the above species.

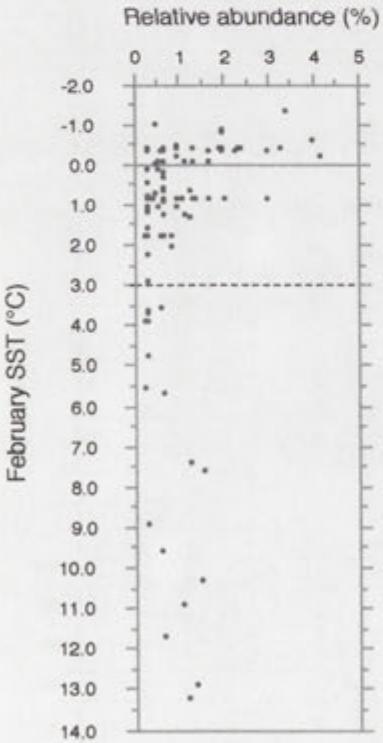

Figure 2.7b. Plot of combined "*Stellarima*" spp. relative abundances against February SST from WOA (1994). Dashed line indicates the delineation made bewteen *S. microtrias* to the south (<3°C) and *S. stellaris* to the north (>3°C) for this thesis.

LKA Code	Core	Lat °S	Long.	February SST (°C)	*S. microtrias*	*"C. furcatus"*	*"C. symbolophorus"*	*"C. s. var. symbolophorus"*	***S. stellaris***	***S. microtrias***
1	V16-65	45°00'	45°46'E	**7.5885**				5	5	
3	1176-91	44°56.7'	15°02.9'E	**10.3343**	5				5	
4	1176-88	46°57.8'	14°18.2'E	**7.443**				4	4	
5	1277-2	45°02.1'	22°28.2'E	**8.9467**				1	1	
9	RC13-255	50°34'	02°53.7'E	**4.7665**				1	1	
13	MD24-KK63	51°56'	42°53'E	**3.6354**				1	1	
16	MD82 424	54°05.8'	00°20.7'W	1.6109				1		1
21	1178-4P	61°24.4'	46°58.9'W	0.8994				7		7
22	1010W	77°20'	35°00'W	-1.3159		4				4
28	MD82 436	61°13.6'	19°28.8'W	0.3489				2		2
30	1176-65	57°12.5'	08°12.4'E	0.7947				1		1
35	1678-80	47°57'	13°01.4'W	**5.7149**				2	2	
36	1678-84	51°57.5'	14°25.2'W	**2.9135**				1	1	
38	1678-96	60°27.9'	21°37.1'W	0.4946				1		1
43	RC13-257	55°02.2'	03°00.1'W	1.2195				1		1
47	RC13-272	55°05.1'	08°00'E	1.1607				1		1
51	MD24 KK02	54°13'	03°31'E	1.8311				1		1
54	MD24 KK37	52°58.4'	23°46.3'E	2.2886				1		1
56	MD82 430	57°52.3'	10°40.3'W	1.1613				1		1
57	MD82 434	58°51.8'	16°39'W	1.0975				1		1
65	MD84 562	51°55.1'	68°13.6'E	**3.9006**				1	1	
66	MD84 563	50°42.7'	68°09.1'E	**3.7004**				1	1	
68	83-11C III	78°15'	172°17'W	-0.7592			1			1
69	83-12 III	78°16'	170°08'W	-0.8354			2			2
72	83-42 III	76°38'	166°03'W	-1.0075			1			1
74	PC82-71	62°38.4'	59°32'W	1.2757	1	1				2
76	PC82-140	64°49.6'	62°37.8'E	0.9467		2				2
77	KR8701	52°50'	32°30'W	**3.5954**		2			2	
78	KR8702	56°27.6'	33°58.5'W	1.8292		1				1
79	KR8703	60°13.3'	48°56.9'W	1.3134	1	3				4
82	KR8707	62°21.2'	57°58.3'W	0.897		1				1
84	KR8710	59°39.6'	51°16.6'W	2.0651	1	2				3
86	KR8713	52°42.8'	36°59.3'W	**3.9009**		1			1	
101	KR8817	66°12.1'	140°30.2'E	0.0301	1	1				2
105	KR8821	64°49.3'	126°43.5'E	1.0572	1					1
109	KR8825	64°17.9'	115°42.1'E	0.605		2				2
110	KR8827	63°39.1'	101°08.9'E	0.7584		2				2
111	KR8828	64°09.5'	98°09.5'E	-0.1942	2	1				3
115	8702-DISS-5'	56°27.6'	33°58.5'W	1.8292	1	1				2
116	8702-DISS10'	56°27.6'	33°58.5'W	1.8292		1				1
119	8702-DISS60'	56°27.6'	33°58.5'W	1.8292	1	1				2
120	8702DISS120'	56°27.6'	33°58.5'W	1.8292	1					1
121	8702DISS180'	56°27.6'	33°58.5'W	1.8292	1					1
122	8702-DISS24H	56°27.6'	33°58.5'W	1.8292	1					1
123	8707-DISS10'	62°21.2'	57°58.3'W	0.897	2	1				3
124	8707-DISS20'	62°21.2'	57°58.3'W	0.897	3					3
125	8707-DISS35'	62°21.2'	57°58.3'W	0.897	3	1				4
126	8707-DISS60'	62°21.2'	57°58.3'W	0.897	3	2				5
127	8707DISS120'	62°21.2'	57°58.3'W	0.897		1				1
133	8810DISS0-20	54°11.2'	144°47.9'E	**5.5964**		1			1	
139	8818-DISS20'	65°45'	138°12'E	-0.0723	1	1				2
140	8818DISS120'	65°45'	138°12'E	-0.0723	5					5
141	8818DISS180'	65°45'	138°12'E	-0.0723	2					2
142	8818DISS240'	65°45'	138°12'E	-0.0723	3					3
145	MDBX 94-01	42°30'	79°25'E	**12.9001**	5				5	
150	MDBX94-06	44°34'	90°04'E	**10.9054**	4				4	

LKA Code	Core	Lat °S	Long.	February SST (°C)	*S. microtrias*	*"C. furcatus"*	*"C. symbolophorus"*	*"C. s.* var. *symbolophorus"*	***S. stellaris***	***S. microtrias***
151	MDBX94-07	41°43'	90°16'E	**13.2718**	4				**4**	
152	93-7/GC33	67°11'	68°30'E	0.1214	1					1
153	93-7/GC5	67°03'	69°05'E	0.1427	2					2
193	PCDF 82-34	62°17.7'	57°37.4'W	0.897		1				1
194	PCDF 82-47	62°55.3'	58°23.7'W	1.0795	2					2
196	PCDF 82-61	63°17'	59°20.2'W	0.6789	2					2
197	PCDF 82-60	63°23.4'	59°34.2'W	0.6789	1	3				4
198	PCDF 82-51	63°43.4'	60°02.9'W	0.8942	3					3
200	PCDF 82-1	63°57.2'	56°21.6'W	0.2168	1	1				2
201	PCDF 82-93	64°04.1'	61°19.6'W	1.0969		1				1
202	PCDF 82-174	64°10'	56°48.5'W	-0.1694	1					1
203	PCDF 82-20	64°14.1'	55°54.4'W	-0.315		1				1
206	PCDF 82-112	64°36.5'	61°38'W	1.0969	1					1
208	PCDF 82-142	63°53.1'	62°26.4'W	1.2902	1					1
210	DFBC 83-27 II	75°42'	170°39'E	-0.3435			2			2
211	DFBC 83-28 II	75°51'	169°18'E	-0.3473		9				9
212	DFBC 83-29 II	76°01'	167°12'E	-0.3336			2			2
213	DFBC 83-30 II	76°05'	166°42'E	-0.378		4				4
214	DFBC 83-1 II	76°10'	168°58'E	-0.3141	4	3				7
215	DFBC 83-40 II	76°21'	167°12'E	-0.3336			5			5
216	DFBC 83-5 II	76°30'	166°00'E	-0.3549		2				2
217	DFBC 83-23 II	76°31'	170°05'E	-0.2881		6				6
218	DFBC 83-2 II	76°37'	164°21'E	-0.4001			1			1
219	DFBC 83-21 II	76°41'	167°49'E	-0.3336		9				9
220	DFBC 83-43 III	76°43'	176°19'W	-0.585		4				4
221	DFBC 83-20 II	76°57'	166°41'E	-0.3549		10				10
222	DFBC 83-10 II	76°57'	166°20'E	-0.3549		6				6
223	DFBC 83-9 II	77°05'	166°31'E	-0.3549		1				1
224	DFBC 83-1 III	77°10'S	169°07'E	-0.2993			9			9
225	DFBC 83-8 II	77°10'	165°48'E	-0.378			7			7
226	DFBC 83-7 II	77°21'	165°53'E	-0.378			2			2
227	DFBC 83-6 II	77°30'	165°48'E	-0.378		3				3
228	DFBC 83-44 II	77°37'	166°15'E	-0.3549			1			1
229	DFBC 83-6 III	77°47'	177°53'E	-0.4631			1			1
235	MD73-026	44°59.0'	53°17.0'E	**9.6361**				2	**2**	
237	PC82-35	62°21.7'	57°22.0'W	0.897	2	2				4
246	8702-DISS-240	56°27.6'	33°58.5'W	1.8292		1				1
247	8707-DISS5'	62°21.2'	57°58.3'W	0.897	1	1				2
248	8707-DISS180	62°21.2'	57°58.3'W	0.897	1	3				4
257	8818DISS035	65°45'	138°12'E	-0.0723		4				4
260	147GC017	47°45.04'	145°49.01'E	**11.7046**	1				**1**	

Table 2.8. Incidences of species considered under the *Stellarima* genus. Species are divided into the two currently valid species *S. microtrias* and *S. stellaris* by February SST of 3°C (refer to text for discussion). Samples in bold are referred to *S. stellaris* .

In addition a cold-water form which appears geographically separated and strongly associated with sea-surface temperatures between 0-3°C, *Thalassionmea nitzschioides* forma 1, has been identified by Zielinski (1993) and Zielinski and Gersonde (1997).

Currently, the combined databases include all variations under the nominate species name. This includes all varieties mentioned above and quite possibly the species *T. n.* var. *claviformis* and *T. incurvata* (*sensu* Moreno-Ruiz and Licea 1994). Zielinski and Gersonde (1997) argue that grouping the variations is of little use to the reconstruction of environmental parameters and this is evident in their respective temperature versus abundance plots. Such statements have been made and upheld for subtropical analysis of *Thalassionema nitzschioides* variations, especially for the variation *parva*, which ecologically identifies waters of lower salinity (Schuette and Schrader 1981, Pokras and Molfino 1986, van Iperen *et al.* 1987).

As there was no consistent separation of the *Thalassionema nitzschioides* variations from data set to data set, all data even where separated (eg. Appendix 2.4), are combined in this thesis. This united data is henceforth identified as the *Thalassionema* taxa group, and thus combines the ecological signatures that each variation is thought to carry. It should also be noted that the illustrations of *T. n.* var *capitulata* in Zielinski (1993, Pl. 6 fig. 1-2) are referable to *T. n.* var *lanceolata* of Moreno-Ruiz and Licea (1994), for this reason species identified previously by this author as former species should be considered as forms of *T. n.* var. *lanceolata.*

2.2.23. *THALASSIOSIRA ANTARCTICA/SCOTIA* GROUP

THALASSIOSIRA ANTARCTICA COMBER

THALASSIOSIRA SCOTIA FRYXELL AND HOBAN

It was Johansen *et al.* (1985) who first reported the close affinity of *Thalassiosira scotia* vegetative cells with those of *T. antarctica* resting cells. Both valves are heavily silicified with coarse striation, and are differentiated by the number of areolae in 10µm, marginal striae and degree of silicification (Johansen *et al.* 1985). Since this time several workers have combined the two species as differentiation has proven difficult (Zielinski 1993, Zielinski and Gersonde 1997). Furthermore, both species have been linked to neritic environments associated with ice conditions of the Antarctic (Hasle and Heimdal 1968, Johansen *et al.* 1985). Fryxell *et al* (1981a) considered the ability to form resting stages within the species as an evolutionary trait of such habitats.

Thalassiosira scotia has only been reported from the South Atlantic. Zielinski and Gersonde (1997) attributed part of their *T. antarctica/scotia* taxon as referable to *T. scotia*

in the Scotia Sea and the adjacent Argentine Basin, and Ligowski (1993) observed *T. scotia* in the South Atlantic but with highest abundances (12.4%) in littoral habitats. The observation of *T. scotia* exterior to the South Atlantic was not located in the literature. The conclusion reached by Johansen *et al.* (1985) did not necessarily deem the two species as separate entities; in fact, they commented that *T. scotia* may be shown to be a form or variety of *T. antarctica.*

The author has only come across the species which appear to refer to *T. antarctica* in core material in the southeast Indian Ocean. In the combined databases available to the thesis *T. scotia* has only once been identified (sample KR8702). It is not unreasonable then to conclude that the two species are confounded particularly in South Atlantic samples. Following previous examples the data identified as *T. antarctica* and *T. scotia* are combined and re-named the *T. antarctica/scotia* Group.

2.2.24. *THALASSIOSIRA* ECCENTRIC GROUP

"*COSCINODISCUS ECCENTRICA*" EHRENBERG

THALASSIOSIRA ECCENTRICA (EHRENBERG) CLEVE

THALASSIOSIRA ECCENTRICA VAR. *JOUSEI* KANAYA

"*THALASSIOSIRA TRIFULTA*" FRYXELL (SYNONYM TO*THALASSIOSIRA LATIMARGINATA* MARKOVA)

Both *Thalassiosira eccentrica* and *T. trifulta* have been confounded throughout the 166DB. *Thalassiosira eccentrica* and its variation *jousei* were the initial species identified in the 166DB using the descriptions of Hustedt (1930 as *Coscinodiscus eccentricus*) and Fenner *et al.* (1976). Only one sample had "*Coscinodiscus eccentrica*" identified (RC11-118) and this was incorporated under *Thalassiosira.* Fryxell and Hasle (1972) confirmed the placement of *Coscinodiscus eccentricus* to *Thalassiosira eccentrica* and re-described the species along with a new description of a closely related species *Thalassiosira symmetrica.* Simonsen (1974) expanded both descriptions and determined two further species *T. punctifera* and *T. spinosa* and suggested that any previous works relating to *Coscinodiscus eccentricus* (*Thalassiosira*) are undoubtedly confounded with the several morphologically similar species. This problem still occurs today even though good descriptions exist with the differentiation of *T. eccentrica, T. symmetrica, T. spinosa, T. punctifera,* and *Planktoniella sol,* and this has been recognised in Fenner *et al.* (1976), Hallegraeff (1984) and Pokras and Molfino (1986). Although the abundance of the specimens identified as *T. eccentrica* in the 166DB are low (between 0.1 and 2% of the total), they must be considered confounded amongst the species that have "the same type of areolation grouped around a heptagonal central areola" (Simonsen 1974, p 11). For this reason this group will be referred to henceforth as the *Thalassiosira* Eccentric Group.

The main problem for the *T.* Eccentric Group arises in the 166DB is through the introduction of *T. trifulta* (Fryxell and Hasle 1979b and Johansen and Fryxell 1985, although T. *latimarginata* Markova has priority, Barron pers. comm. 1998) to the counting lists of Pichon (circa 1988). At this time *T. eccentrica* var. *jousei* was no longer separated from *T. eccentrica*, and *T. trifulta* was listed as a separate species. Only five samples had joint occurrences of *T. trifulta* and *T. eccentrica* noted (KR8806, KR8819, KR8822, KR8824, KR8825). More recent counts (since 1994) have seen the loss of *T. eccentrica* from the group of statistically used species and in its place the counts of *T. trifulta* recorded. The author has, however, endeavoured to count *T. eccentrica* (and related species mentioned previously) as a separate species in her work. The problem arises from the combination and additional confounding of *T. trifulta* with the *T.* Eccentric Group in the database used for statistical analysis. This is best exemplified by the fact that both published works (Pichon *et al.* 1987 and 1992a) cite *T. eccentrica* in data analysis, yet work by the author during the course of the thesis had used the data as *T. trifulta* occurrences.

The distribution of the *T.* Eccentric Group, including data from *T. trifulta*, are dominantly located in the northern subantarctic waters. Observations close to Antarctica are likely to be associated with *T. trifulta* (Figure 2.8). Distribution of *T. eccentrica* was not reported south of the Subtropical Convergence (Johansen and Fryxell 1985), whereas *T. trifulta* was observed in the Pacific and Atlantic sectors of the Southern Ocean, and in subantarctic waters of the Indian Ocean (Fryxell and Hasle 1979b, Johansen and Fryxell 1985). Cultures of *T. eccentrica* between 10° and 25°C suggest the species is not distributed by temperature in temperate regions, yet the extreme limits had not been tested (Fryxell and Hasle 1972, Fryxell pers. comm. 1997). Zielinski and Gersonde (1997) found trace occurrences of *T. eccentrica* in warmer water samples, and do not report *T. trifulta* in the Atlantic sector, as is also observed in this thesis data set near the Antarctic Peninsula region (Figure 2.8). Occurrences of *T. eccentrica* (*C. eccentricus*) close to the Antarctic coast (Akiba 1982, Bellingshausen Sea, Andreoli *et al.* 1995, Ross Sea) have been made but in each case identification of *T. trifulta.* was not made nor the work in which this species is described referenced (Johansen and Fryxell 1985). *Thalassiosira eccentrica* has been observed in shelf waters surrounding Australia, and has been linked to the East Australian Current and the cooler waters of the Great Australian Bight along with the closely related species *Planktoniella sol* and *T. punctifera.* The latter species having only been observed in the warm core eddies pinching off the East Australian Current. *Thalassiosira spinosa* was only located off the North West Shelf of Australia (Hallegraeff 1984). Occurrences attributed to *T. trifulta,* but probably representing members of the *T.* Eccentric Group or *Thalassiosira poroseriata*, have in this study been

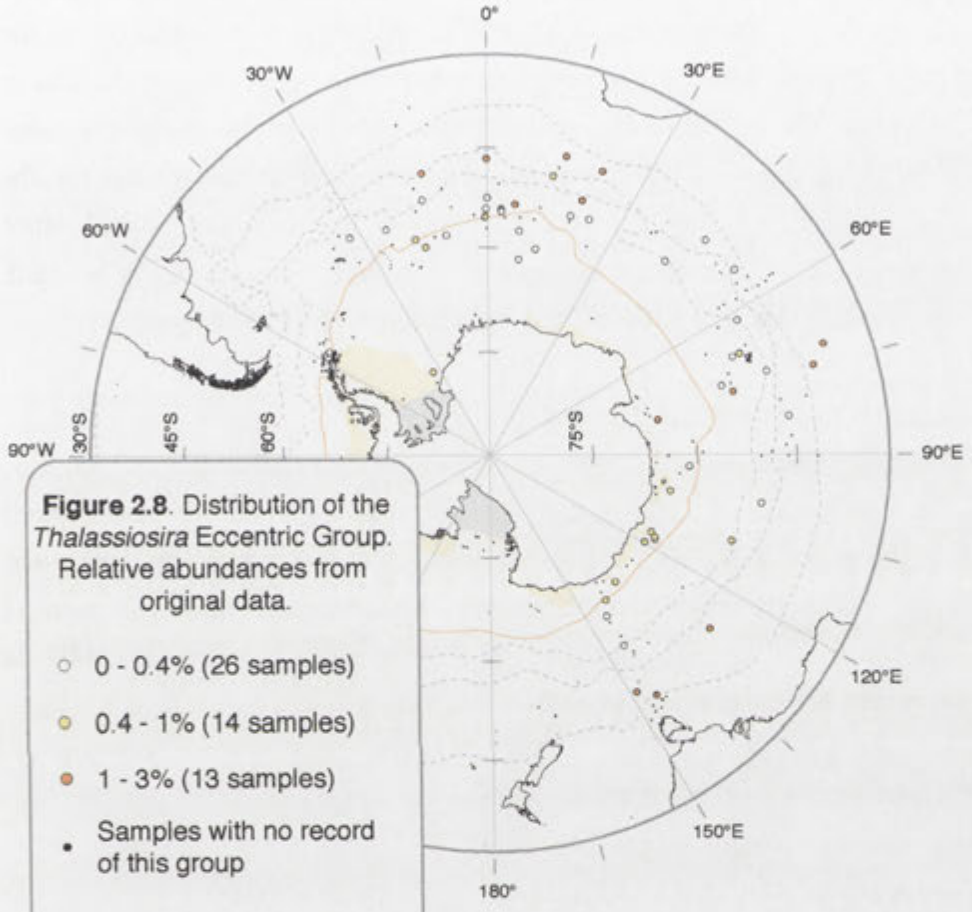

Figure 2.8. Distribution of the *Thalassiosira* Eccentric Group. Relative abundances from original data.

- 0 - 0.4% (26 samples)
- 0.4 - 1% (14 samples)
- 1 - 3% (13 samples)
- Samples with no record of this group

located in surface samples on the South Tasman Rise and in the south Indian sector of the Southern Ocean (Appendix 2.4). The result of the lumping *T. trifulta* data with *T.* Eccentric Group data, plus the likelihood of confounding of all species through time means the counts are unreliable for any of the species concerned. A complete re-count of the samples is required to separate the effects, which as presented in the literature suggest there is a temperate warm water *T.* Eccentric group and a cooler Antarctic component provided by *T. trifulta.* As there is not a great deal of information available on the distribution of these species from the Southern Ocean it is impossible to split them as in the *Stellarima* situation. The *T.* Eccentric Group identified above is regrettably expanded to contain *T. trifulta* for the work in this thesis. The use then of this group for the derivation of SST estimates would only increase the noise of the temperature signal, since equal representation of the *T.* Eccentric Group occurs over the whole region studied. Thus, the data assigned to this group is removed from future statistical analysis.

2.2.25. *THALASSIOSIRA FRENGUELLII*

This species was identified in the original 166DB at site KR8807 (47°06.9'S, 145°47.8'E). The distribution of *T. frenguellii* as described by Johansen and Fryxell (1985) is considerably south of this samples position. Since six other diatoms were attributed to *T. oestrupii* in the sample concerned, and this occurrence of *T. frenguelli* is observed too far north, the species identified as *T. freguellii* in sample KR8807 is considered to represent *T. oestrupii* var *venrickae.*

2.2.26. THALASSIOSIRA GRACILIS TAXA

"*THALASSIOSIRA DELICATULA (DELICATULATA)*" HUSTEDT

THALASSIOSIRA GRACILIS VAR. *EXPECTA* (VAN LANDINGHAM) FRYXELL AND HASLE

THALASSIOSIRA GRACILIS KARSTEN (HUSTEDT)

In the original diatom database *Thalassiosira delicatula /delicatulata* was identified as a separate taxa. It is, however, the synonym of *Thalassiosira gracilis* var. *expectata* (Fryxell and Hasle 1979a). All previous data allocated under *T. gracilis* var *expectata* has been combined with the *Thalassiosira gracilis* data to form the *T. gracilis* taxa because the gradational nature of the two species continues to make rigorous differentiation impossible to implement. Fryxell (1994) comments that the taxonomic distinctions between the two varieties may soon become invalid since they are growth stages of the one species. Zielinski and Gersonde (1997) consider the grouped *Thalassiosira gracilis* taxa as lacking clear relationships to surface water temperature regimes which supports this comment.

2.2.27. *THALASSIOSIRA* LINEATI GROUP

"*COSCINODISCUS LINEATUS*"(EHRENBERG)

THALASSIOSIRA LEPTOPUS (GRUN.) HASLE ET FRYXELL

THALASSIOSIRA LINEATA JOUSÉ

Hasle and Fryxell (1977) discriminated between the many *Coscinodiscus* Lineati species (those with a linear areola array) which had been identified in the past. They found *C. lineatus* to be synonymous with *C. leptopus* (Grun) and that the species in question reflected morphological characteristics of the Thalassiosiraceae family. Since the name *Thalassiosira lineata* was already occupied by a species described by Jousé, the species was re-named as *T. leptopus*. The major difference between these two species under the light microscope is the presence of scattered tubuli over the valve face of *T. lineata* and their absence on *T. leptopus*. Both species are recorded in warm waters and are quoted as absent from colder waters (Simonsen 1974, Hasle and Fryxell 1977, Hasle and Syvertsen 1982, Hallegraeff 1984, Johansen and Fryxell 1985). Sournia *et al.* (1979) located *T. leptopus* in surface waters north of the Polar Front Zone. This is contrary to finds made by Fenner *et al.* (1976) where *T. lineata* is observed south of 52°S and *T. leptopus* (*C. lineatus*) throughout all thermal sectors of the Pacific. Akiba (1982) also identified a species that compares with *T. lineata* from core material of the Bellingshausen Sea.

The only other species with linear areolae patterns that is mentioned with occurrences in southern waters is *Thalassiosira ferelineata* Hasle et Fryxell (1977). This species is differentiated under light microscope by its more irregular linear areola pattern at the centre of the valve (Hasle and Fryxell 1977). All other species falling within this Lineati group are found in much warmer water masses (Hasle and Fryxell 1977). The specimen of *Coscinodiscus anguste-lineatus* identified by Hustedt (1930) from Antarctic waters was reassigned to *Thalassiosira tumida* by Simonsen (1974). The more heavily silicified form of *T. tumida* has a "lineatus" areolae pattern (Hasle *et al.* 1971, Fryxell *et al.* 1984) This pattern was related to silica deposition at SST's less than 0°C (Fryxell 1986, Fryxell 1991). *Thalassiosira ritscheri* is also noted to increase its linear appearance with decreases in temperature and the formation of winter valves (Fryxell 1991).

Both *Thalassiosira leptopus* (*C. lineatus*) and *Thalassiosira lineata* have been identified from the beginning of the 166DB, however, more recent work has seen the loss of *T. leptopus* from the observations even though several samples are in the subtropical/antarctic regions. Uncertainty also exists as to whether previously identified *C. lineatus* counts were transferred to *T. lineata* or kept separate. There is no indication that *T. leptopus* was ever identified. All previous *C. lineatus* counts should be transferred to *T. leptopus* where it can be shown that they are identifiable from other Lineati species. It is not certain if the species identified as *T. lineata* truely represent that species or a mixture of Lineati species. Since the more recent surface samples (both those of Pichon

and the author, although the later has attempted to identify each species) have lumped most Lineati species under *T. lineata*, and as it is impossible to separate the counts on any other biological, geographical or other information within the warmer ocean regions, they will remain grouped. In doing this the data is re-named the *Thalassiosira* Lineati Group.

The identification of Lineati specimens (*T. lineata* and *"C. lineatus"*) south of 60°S (samples 1178-4P, MD84-531, MD84-530, MD84-540, KR8706, 8707Diss10', most 8818Diss samples, 8808Diss20', PCDF82-69, PCDF82-142, DFBC83-28) are very likely to be the heavily silicified lineate forms of *T. tumida*. (Hasle *et al.* 1971, Fryxell 1994) or the heavily silicified sublinear to linear patterned winter stages of *T. ritscheri* (Fryxell 1994) as illustrated in Hustedt (1958). It is difficult make a decision on these samples species affiliations when neither samples or plates are unavailable to check for *T. tumida* or *T. ritscheri* mis-representation. Only five of the 16 samples cited above have both *Thalassiosira* Lineati species and *T. tumida* identified (1178-4P, KR8706, PCDF82-64, PCDF82-142, DFBC83-28). As the literature as a whole suggests that *T. lineata* is not a cold water species, they will be transferred to *T. tumida* for the work in this thesis. This is a temporary measure since the only solution is to re-count the samples.

2.2.28. *THALASSIOSIRA MACULATA*

"*COSCINODISCUS BULLATUS*" JANISCH CIRCA 1888

THALASSIOSIRA MACULATA FRYXELL AND JOHANSEN

Coscinodiscus bullatus is invalid according to Van Landingham (1968, part 2, p. 872) who cites *C. planiusculus* Rattray (1890) as the valid name. Fenner *et al.* (1976) identified specimens as *C. bullatus* based on the description in Hustedt (1958). More recent work by Johansen and Fryxell (1985) indicate that the species identified as *C. bullatus* by Hustedt is not the same species originally identified by Janisch. For this reason *C. bullatus* sensu Hustedt was renamed *Thalassiosira maculata* by Johansen and Fryxell (1985, p 170), a change later reconfirmed by Simonsen (1992, p 9-10).

C. bullatus	*T.* cf. *maculata*
P1160 (1)	RC12-292(1)
MD82 436 (1)	KR8806(1)
MD24KK32 (1)	KR8807 (3)
MD24KK02 (2)	PC82-35 (2)
MD24KK35 (2)	PCDF82-60 (1)
MD82 425 (1)	PCDF83-28II (1)
KTB 20 (1)	DFBC 82-23II (3)
KTB 29 (1)	DFBC 83-8II (1)

Table 2.9. Samples containing species identified as either "*Coscinodiscus bullatus*" or *Thalassiosira* cf. *maculata*. Values in brackets refer to the number of specimens observed.

In the Pichon data sets there are nine samples identified as containing *C. bullatus* and a further nine with *T.* cf. *maculata* (Table 2.9). Although the number of specimens are very low (<1%) they should probably all be referred to as *T. maculata*, and are henceforth done so. Refer also to comments in section 2.2.30 *Thalassiosira oliverana.*

2.2.29. *THALASSIOSIRA OESTRUPII*

Fryxell and Hasle (1980) documented two variations of *Thalassiosira oestrupii* which appeared to have a warm (*T. oestrupii* var. *venrickae*) and cold water (*T. oestrupii* var. *oestrupii*) distribution. These observations have not been used in a positive sense for this work as both variations are currently lumped together in the combined databases. Zielinski and Gersonde (1997) also neglect to make mention that the two varieties are combined in their distribution of the species in the South Atlantic sector (Zielinski pers. comm. 1996).

It is not certain if *T. oestrupii* var. *venrickae* was counted correctly, or at all, in the 166DB. There are no indications from the original publications if both varieties were observed. Only Hustedt 1930, p. 318, fig. 155 is mentioned. Yet in the floral descriptions of Pichon's thesis (1985) two forms were observed, a larger variety with areolae having a consistent regular pattern from valve centre to margin, and a second smaller variety with large areolae in the centre decreasing rapidly to smaller areolae at the margin. Unfortunately, illustrations of the variations for this species appear to be variations of *Thalassiosira antarctica* resting cells (pl. 4 figs 14 - 15), thus it is unclear whether this group has been consistently identified or not. For this work, the species group is assumed to be correctly counted, but again earlier work must be re-examined.

2.2.30. *THALASSIOSIRA OLIVERANA*

"*SCHIMPERIELLA ANTARCTICA*" KARSTEN

THALASSIOSIRA OLIVERANA (O'MEARA) MAKAROVA ET NIKOLAEV

The species *Schimperiella antarctica* was transferred to *Thalassiosira oliverana* during the evolution of the databases and is acknowledged here formally. The transfer was documented in Russian (Makarova and Nikolaev 1983) and first reported in English by Priddle and Fryxell (1985). Fryxell (1994) reports that *T. maculata* is the summer stage form of *T. oliverana*. In this thesis the two species have been conserved separately and as such the low relative abundance of *T. maculata* in the combined databases (<1%) does not make a large difference to the current work.

2.3. REMOVAL OF SPECIES/TAXA FROM ANALYSIS.

As mentioned in the introduction to the taxonomic reform of the databases there has been an evolution over time as to the species incorporated and the advances of taxonomy to be implemented. In some circumstances there are several species which were not integrated throughout the life of the database, or their inclusion has been inconsistent. Four of such groups have been completely removed from the counts of the databases and one from statistical analysis. The reasons behind each of these removals are discussed below.

2.3.1. *CHAETOCEROS* VEGETATIVE AND RESTING CELLS

In the original diatom dataset *Chaetoceros* vegetative cells were counted. These were generally referable to *Chaetoceros bulbosum* complex (*sensu* Priddle and Fryxell 1985) or *Chaetoceros dichaeta*. The distribution of vegetative cells in the sediments of the combined databases is presented in Figure 2.9. Their distribution can be noted to be confined to either neritic Antarctic habitats, or located between the maximum winter sea-ice edge and the Polar Front. In essence, *Chaetoceros* vegetative cells are rarely preserved in the sediments. A survey of the literature reflects the geographical distribution presented in Figure 2.9. Surface samples studied from the Filschner Ice Shelf, Lützow-Holm Bay, Prydz Bay and along George V Coast indicate *Chaetoceros* vegetative cells are rarely preserved and almost always at less than 1% abundance (Gersonde 1984, Tanimura 1992, Stockwell *et al.* 1991, Leventer 1992). Open-ocean surface sediment records are very few and localised to the South Atlantic sector where records are simply stated as rarely encountered (DeFelice and Wise 1981 50-51°S, 11-12°E and 58°S, 19°E, and Zielinski 1993). The geographic abundance distribution presented in Figure 2.9 contains the highest noted distributions in the sediments thus far recorded, and allows a more conclusive relationship to neritic conditions produced by the coast and winter sea-ice to be viewed. Yet, the miserable record of *Chaetoceros* vegetative cells preserved in the sediments and generally undifferentiated species counts make them unusable for statistical work. *Chaetoceros* resting spores were never noted in the original 166DB. Crosta *et al.* (1997) re-analysed most of the original 166DB samples for *Chaetoceros* "spores". The use of these counts, taken as the number of spores against all other diatoms regardless of species, for combination with the original count and subsequent statistical analysis, is not supported nor employed in this thesis. Their data alone suffices to indicate the predominance of *Chaetoceros* resting spores surrounding the Antarctic continent (Crosta *et al.* 1997).

For comparison the distribution of *Chaetoceros* spore relative abundances from all new samples (both Armand and Pichon) have been plotted on the reference data presented by Crosta *et al.* (1997, their samples exceeding 270 total count used only) (Figure 2.10). The new data presents distributional information north of the Polar Front (exception

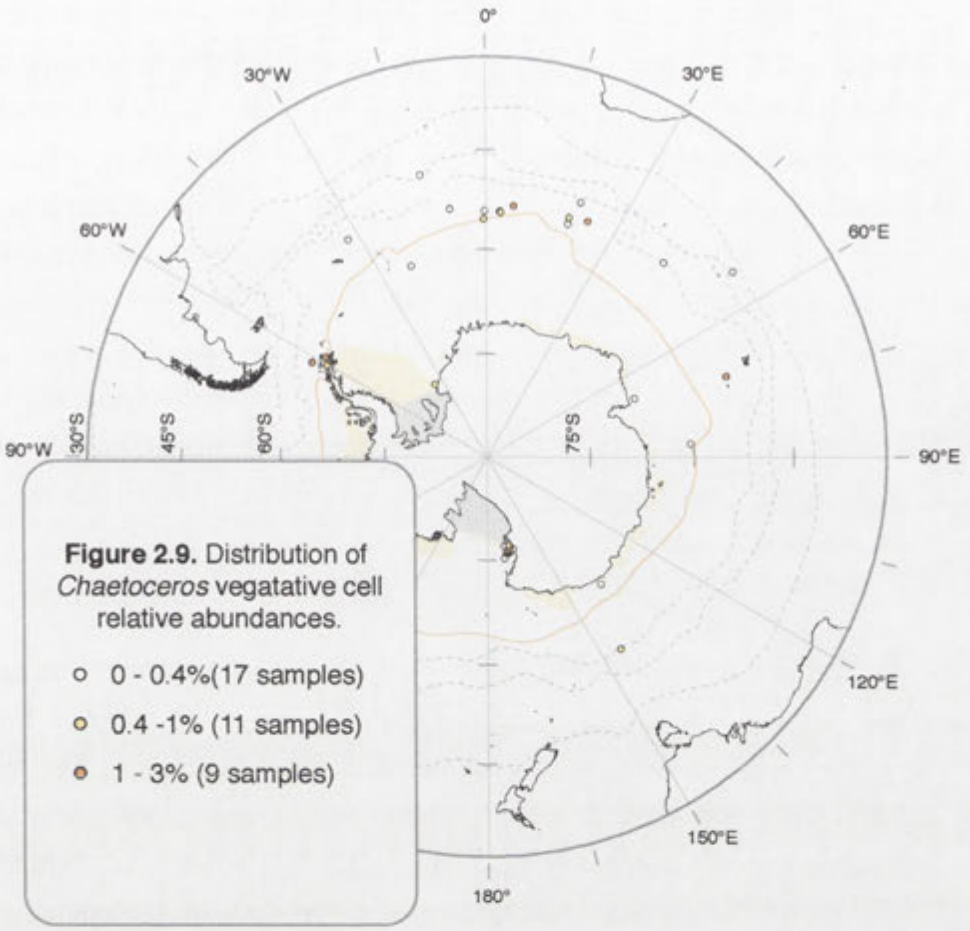

Figure 2.9. Distribution of *Chaetoceros* vegatative cell relative abundances.

- 0 - 0.4%(17 samples)
- 0.4 -1% (11 samples)
- 1 - 3% (9 samples)

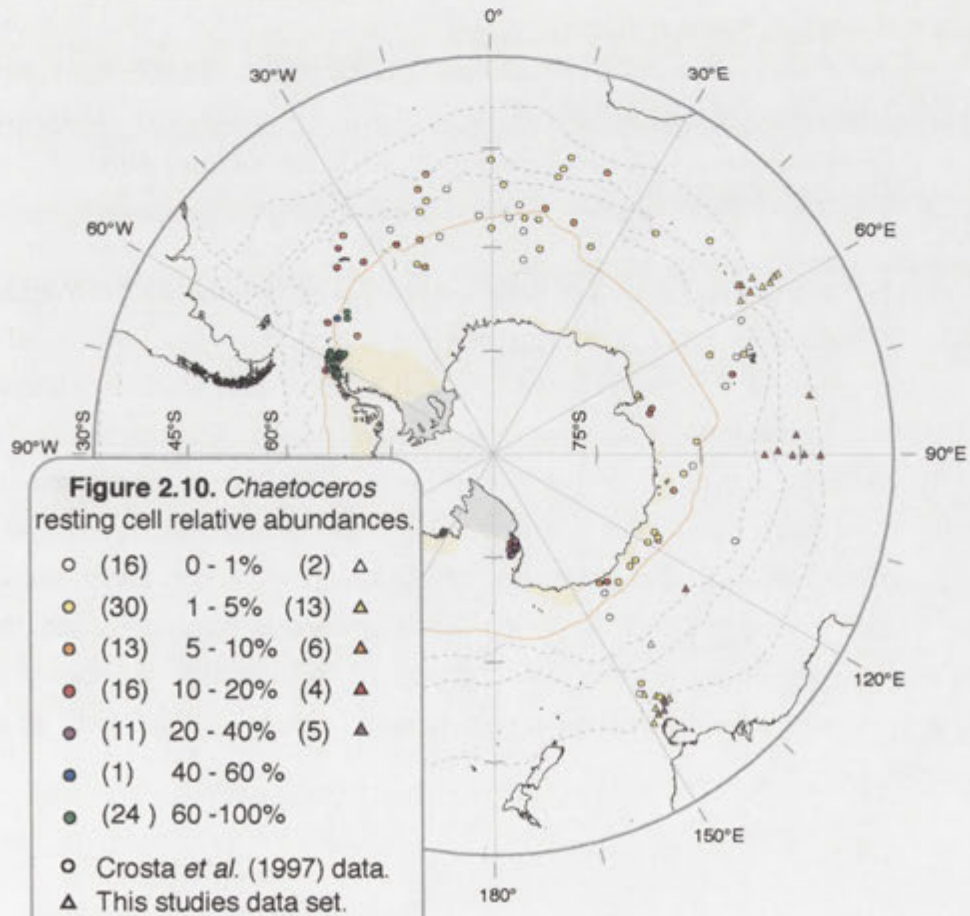

Figure 2.10. *Chaetoceros* resting cell relative abundances.

- (16) 0 - 1% (2) △
- (30) 1 - 5% (13) △
- (13) 5 - 10% (6) △
- (16) 10 - 20% (4) △
- (11) 20 - 40% (5) △
- (1) 40 - 60 %
- (24) 60 -100%

Crosta *et al.* (1997) data.
△ This studies data set.
Total observations noted in brackets

Prydz Bay) which highlights two interesting points. Firstly, samples directly south of Tasmania have increased abundances which reach the 20-40% category, indicating the neritic influence of Tasmania and presumably warm water eddies off East Australian Current. Secondly, a large increase in abundance (between 10 and 40%) is noted along the 90°E meridian. This is in stark contrast to samples along the 60°E meridian and in general north of the Polar Front which are observed with less than 10% (as also reported by Zielinski 1993 for the South Atlantic, Gersonde and Wefer 1987 for Drake Passage, and van Iperen *et al.* 1987 for the southeast Atlantic). There are two possibilities for the presence of such high concentrations of this species; bottom water entrainment and the eastward displacement by the ACC from the neritic influence of Kerguelen Isle and Plateau. Based on the bottom water pathway which makes an easterly turn in this region of the South Indian Basin (Chapter 1) the former of the two hypotheses is favoured.

As the counts from the first 166DB (Crosta *et al.* 1997) cannot be used with the new count data available, all counts related to *Chaetoceros* resting spores are removed from statistical analysis. As such, the removal of *Chaetoceros* resting spores is in line with similar statistical treatments performed by others (Karpuz and Schrader 1990, Schrader and Karpuz 1990, Schrader and Sorknes 1991, Zielinski 1993). Furthermore, Schrader and Karpuz (1990) argue that grouping resting spores, to the loss of taxonomic and biogeographic information, serves little purpose for ecological and thus, statistical work. Linking the spores to vegetative cells is still in its infancy even though many have identified relationships via SEM work or indicate such work is under way (Hargraves 1979, Stockwell and Hargraves 1984, Leventer *et al.* 1993, Riaux-Gobin 1996)

Several Q-mode factor analyses of surface sediment diatom samples from the Weddell Sea integrating *Chaetoceros* taxa (both vegetative and predominantly resting cells) illustrated the dominance of the raw grouped taxa and a heavy bias towards Antarctic Peninsula samples (Zielinski 1993). Ranking of the species reduced this dominance but only to evenly distribute the effect of the *Chaetoceros* taxa, thus in effect provide statistical noise. Even the role of sea-ice in their habitat is poorly understood, and this is supported by the continual negative correlation of *Chaetoceros* taxa to other sea-ice diatom types in factor analysis (Zielinski 1993). Several workers have suggested that *Chaetoceros* resting spores may, once their ecological relationship to sea-ice is understood, prove important to estimating sea-ice cover (Zielinski 1993, Crosta *et al.* 1997, Leventer *et al.* 1996).

A relationship between the grouped *Chaetoceros* taxa abundance distribution and sea-surface temperature was not detected in the work of Zielinski and Gersonde (1997). Alternatively, the influence of high productivity waters is thought to be of primary importance to *Chaetoceros* distribution (Donegan and Schrader 1982, Leventer 1991, Sancetta *et al.* 1992, Karpuz and Jansen 1992, Zielinski and Gersonde 1997). More recently, surface water stratification produced by sea-ice melt water has been suggested as the main significant factor in *Chaetoceros* spp resting spore and *Corethron criophilum* dominance's in the sediment record (Leventer *et al.* 1993, Leventer *et al.* 1996).

In line with the decisions and arguments presented by Schrader and Karpuz (1990), Zielinski (1993) and Zielinski and Gersonde (1997), and the fact that irregular records are available in the combined data sets used here, *Chaetoceros* taxa (both vegetative and resting spores) are removed from further statistical analysis.

2.3.2. *THALASSIOTHRIX LONGISSIMA, THALASSIOTHRIX ANTARCTICA AND TRICHOTOXON REINBOLDII.*

Although there has been considerable discussion on the distribution of *Thalassiothrix antarctica* and *T. longissima*, in particularly the latter species appearance in Antarctic waters (Semina 1981, Hustedt 1958, Hallegraeff 1986, Hasle and Semina 1987), the two species remain difficult to separate under the LM and are generally almost always counted as a combined group. The species group have been recorded in sediments of the South Atlantic (DeFelice and Wise 1981, van Iperen *et al.* 1987, Zielinski 1993.) where the distribution of the group was noted in maximum abundance (9%) within the Polar Front Zone (PFZ) at summer sea-surface temperatures between 2.5-6°C (Zielinski and Gersonde 1997). A northern expression of the group (3-5%) in the permanent open ocean zone (POOZ) was attributed to presence of *T. longissima* (Zielinski and Gersonde l.c.).

Trichotoxon reinboldii, on the other hand, is a considerably larger species with differing pole morphology which can be separated from *Thalassiothrix* species (see Plate 16 figures 9-12) (Hasle and Semina 1987). Stockwell *et al.* (1991) note *Trichotoxon reinboldii* in the sediments of the Prydz Bay region with relative abundances of 0.44 - 0.60%. Other records of this species in the sediments were not encountered and this is expected because of their resemblance to *Thalassiothrix* taxa. Round *et al.* (1990) describe the species as abundant around Antarctica.

The distinction between these three species has never been recognised in the combined databases. Thus, for the databases presented here the *Thalassiothrix* species group includes *Thalassiothrix antarctica*, *Thalassiothrix longissima* and *Trichotoxon reinboldii.*

The data compiled under *Thalassiothrix* species has been inconsistently counted in the combined databases. This counting discrepancy varies from guess-estimates to actual counts on pole ends, in some instances only ranked data was recorded. The methodology proposed by Schrader and Gersonde (1978) for counting occurrences of genera similar and including *Thalassiothrix* suggests counting all pole ends and dividing the number by half to provide the number of cells. Jordan and Pudsey (1992) used a guess-estimated version when working on this data citing the Schrader and Gersonde (1978) methodology was not useful for their particular samples. This was strictly related to the fact that the slides prepared were unprocessed smear slides which happened to contain an over-abundance of *Thalassiothrix* and *Trichotoxon* specimens which could not be dealt with in the normal manner (Jordan pers. comm. 1997). As the opportunity to recount all the slides and re-assess the real proportions of this species was not possible, all respective counts were removed from the data used in this study.

2.3.3. *DACTYLIOSOLEN ANTARCTICUS*

The presence of *Dactyliosolen antarcticus* in the sediments has been noted during the routine counts of the author, but was previously not noted in other databases (Pichon 166DB and Abbott 1973). For this reason the total counts for each sample does not include *D. antarcticus* specimens.

Castracane (1886) first described the species in Antarctic waters (53°55'S, 108°35'E). Since then the species has been frequently recorded throughout the open ocean region of the Antarctic (Hendey 1937, Mann 1937, Hart 1942, Crosby and Wood 1958, Wood 1960, Hasle 1960, Kozlova and Mukhina 1967, El-Sayed 1971, Fenner *et al.* 1976, Sournia *et al.* 1979, Garrison *et al.* 1982, El-Sayed *et al.* 1983, Kang and Fryxell 1993, Ligowski 1993). In particular, *D. antarcticus* has been located between the Antarctic Divergence and the Polar Front (Kozlova 1961, 1962, 1966, Zernova 1970) where it is observed in greatest abundance just south of the Polar Front (Hart 1934, Cassie 1963, Kozlova 1966, Semina and Rat'kova 1988, Froneman *et al.* 1995.). Several authors have also noted *D. antarcticus* present in sea ice samples (Garrison and Buck 1989, Tanimura *et al.* 1990, Bianchi *et al.* 1992, Ligowski 1993), yet such occurrences could be misinterpretations of the cold water species *D. tenuijunctus* (Hasle 1975). *Dactyliosolen tenuijunctus* has been reported from the sea ice and within the surrounding water column (Garrison *et al.* 1987, Kang and Fryxell 1991). A secondary maximum of *D. antarcticus* at the sea surface has been observed by several workers (Hart 1934, Semina and Rat'kova 1958, Kozlova 1966, Hasle 1969), and could be related to species variation which is otherwise near impossible to differentiate aside from possible degree of silicification (Hart 1934, Hasle 1969, 1975).

In the literature, sedimentary records of *D. antarcticus* are lacking, which is in contrast to the heavily silicified nature of the intercalary bands. Kozlova (1966) stated the species as rare and fragmented in Indian Ocean sediments (0.04 -0.1% of the living number preserved in sediments) and absent altogether in Pacific Ocean sediments. Based on Kozlova's (1966) vertical distribution observations, *D. antarcticus*, was most heavily corroded (the valve separated into intercalary bands ?) between 100 and 300m water depth from the surface. The only modern reference to *D. antarcticus* presence in the sediments comes from Stockwell *et al.* (1991) who recorded the species in all surface samples of Prydz Bay (maximum abundance 0.85%) with increasing presence from the inner to outer Prydz Bay region.

From the sediment samples personally observed by the author, *D. antarcticus* is a prominent species of the thanatocoenose. Intercalary bands of the species were counted for all samples including cores, however, the data accumulated under this species was removed from analysis and from total specimen counts. The distribution of the species in the sediments based on 33 samples upon which observations were performed (Figure 2.11a) indicates *D. antarcticus* is present throughout the Southern Ocean. A dominant zone of abundance cannot be necessarily defined with the current distribution of samples. However, superficially they appear higher in abundance in the open ocean zone between the STC and the PF. South of Tasmania and north of the STC, they are generally not observed in the sediments and in the Prydz Bay Region they are in similarly low presence as noted by Stockwell *et al.* (1991). The increased abundance in samples along the 90°E meridian is thought to be associated with bottom water movement. Plotting relative abundance against February SST (Figure 2.11b) indicates an broad increase in abundance between 4 and 13°C, over a range that covers 0 to 17°C. Kozlova (1966) recorded their highest surface water abundances in sea-surface temperatures ranging between 1 and 6°C.

Therefore, as mentioned in the surface-water distribution of the species in the Pacific (Hasle 1969), *D. antarcticus* can be generally referred to as an open ocean species. This relation appears to be recorded in the sediments but, due to its broad distribution range, may not be useful for temperature transfer-function analysis at this point in time. One further issue must be taken into account: how many intercalary bands in the sediments should be considered to represent a single specimen ?

2.3.4. *SILICOFLAGELLATE SPECIES*

The use of silicoflagellates, specifically those of the genera *Dictyocha* and *Distephanus*, in palaeotemperature estimation has a brief history. Gemeinhardt in 1934 noticed distributions of the two genera on a temperature preference. A ratio was proposed by several workers (see Martini 1977 and McCartney 1987 for reviews) and applied to

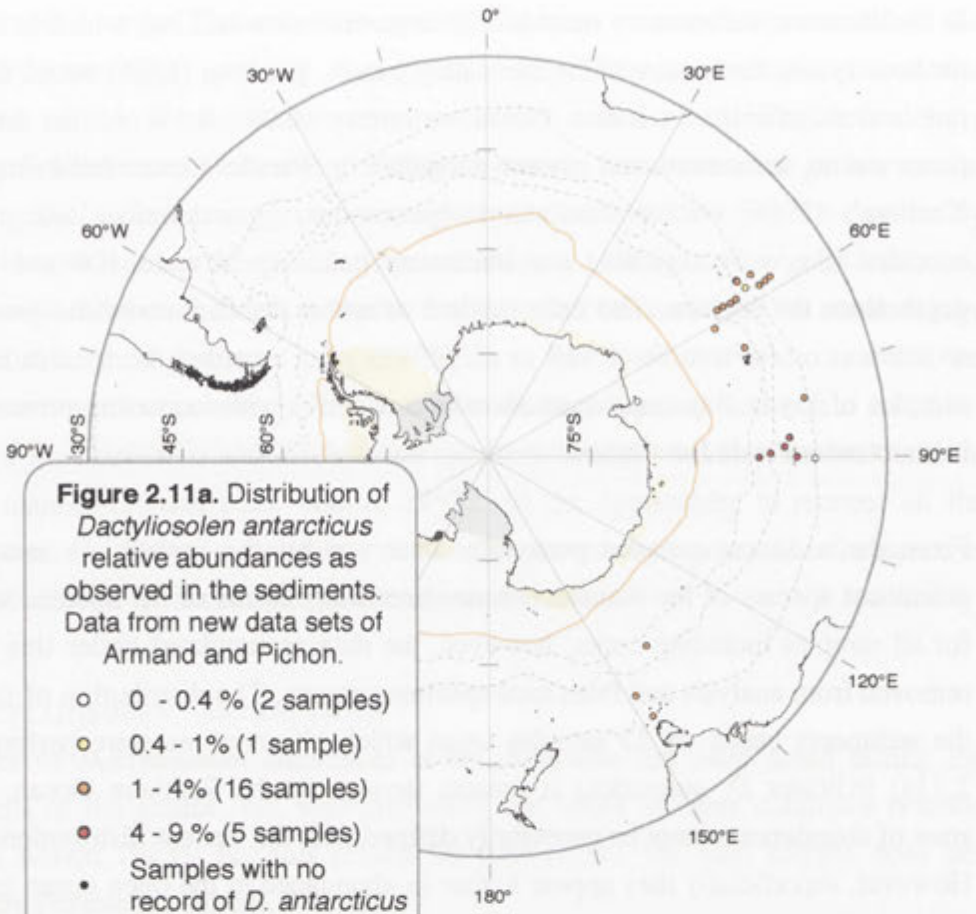

Figure 2.11a. Distribution of *Dactyliosolen antarcticus* relative abundances as observed in the sediments. Data from new data sets of Armand and Pichon.

- 0 - 0.4 % (2 samples)
- 0.4 - 1% (1 sample)
- 1 - 4% (16 samples)
- 4 - 9 % (5 samples)
- Samples with no record of *D. antarcticus*

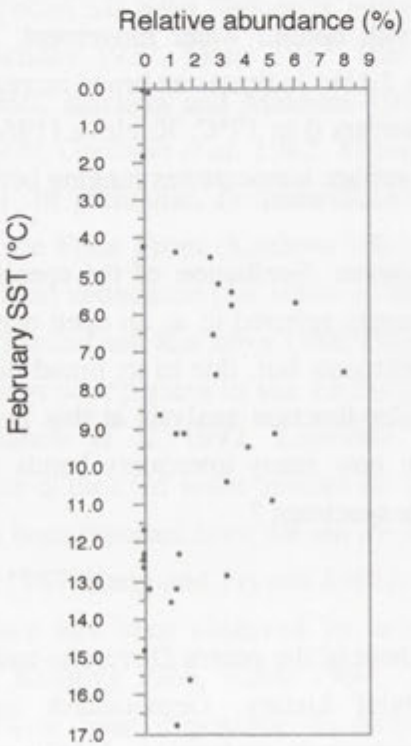

Figure 2.11b. Plot of *Dactyliosolen antarcticus* relative abundances against February SST from WOA (1994).

palaeotemperature estimation in the Pliocene and Eocene (Ciesielski and Weaver 1973, 1974, Weaver and Ciesielski 1974, Mandra *et al.* 1973,1974). The Pliocene estimates were considered erroneously too warm in the high latitudes and a second ratio was derived (Ciesielski 1975 in DeFelice and Wise 1981), although further implementation of silicoflagellate ratios has rested with the original Mandra method (DeFelice and Wise 1981).

Silicoflagellates are noted to have highest abundances in the same waters as diatoms but their total numbers are considerably lower than those of diatoms. Silicoflagellates were shown by DeFelice and Wise (1981) to have very similar distribution patterns in the sediments as diatom species. This was especially true for *Dictyocha* species which are reported as restricted north of the Polar Front. The two silicoflagellate genera were first incorporated into the temperature transfer function by Pichon (1985).

Factor analysis of the South Atlantic distribution of diatoms, silicoflagellates and chrysophite cysts (Zielinski 1993) revealed a lack of affinity in any factor group (or assemblage) for *Distephanus* spp. and chrysophy**te cysts. A minor, but still important contribution in terms of factor loadings, was made by *Dictyocha* spp. to their fourth factor (warm water assemblage). Zielinski (1993) argued that as there was no association for *Distephanus* spp. and chrysophyst cyst distributions with temperature they should be eliminated from analysis. As *Dictyocha* spp. was observed "irregularly" in the northern section of his study region (13 of 48 samples), he decided on eliminating their contribution also.

The inclusion of silicoflagellates has now become an issue of preference. However, several arguments for the removal of the silicoflagellate information in a diatom transfer function can be advanced. Firstly, the number of samples recovered in regions just to the north of the STC are slowly increasing, thus bringing with it an increase in the number of diatom taxa that reflect the warm water temperature signal (Zielinski and Gersonde 1997). In the past, no focus on warm water taxa has been applied and this is reflected in the mix up of several taxa under one species category reported earlier in this chapter. The loss of attention on speciation has affected the warm water assemblage more than any other assemblage. Consequently, the previous use of *Dictyocha* spp. has aided in making the warm water assemblage observable. Secondly, DeFelice and Wise (1981) ably illustrated that the distribution of the two silicoflagellate taxa alone approximated the position of the Polar Front. Quite separately, they also illustrated that this same delineation focus was obtained with the southern extent of their warm-water diatom assemblage. The same can be said for the temperature estimation work of Zielinski (1993). The need to include silicoflagellates in a diatom transfer function, when a more diversified distribution of

diatoms competently reflects the same primary response, becomes questionable. As such, the biology and ecological responses of the silicoflagellates are even less well understood than that of diatoms, with the exception of a known association with upwelling regions (McCartney 1987).

The distribution with temperature of the relative abundances for both *Distephanus* and *Dictyocha* species in the combined databases are presented in Figures 2.12 and 2.13. The plot geographically, and against February SST, of *Distephanus* spp.(Figure 2.12a-b) relative abundances from the untreated data sets, concurs with the conclusion drawn by Zielinski (1993) that there is little reason to include this group in transfer function analysis. Even an association with the winter sea-ice edge is not noted contrary to observations by Fryxell (1989) where *D. speculum* was at highest abundance under the northern edge of the sea-ice. The data compiled under this category will not be used to determine total specimen numbers and will not be used in the transfer function analysis presented in this work.

The distribution of relative abundances of *Dictyocha* spp., geographically draws attention to the limitation of the taxa south, more particularly, bounded by the Subantarctic Front (SAF) (Figure 2.13a). In the plot of relative abundances against February SST (Figure 2.13b), the species abundances can be noted to increase from 7°C and generally "plateau" between 4-6% with a SST of >9°C. This would indicate a southern boundary associated with the SAF rather than the Polar Front. There is obviously some merit in using the distribution of this genus in a transfer function with its obvious relation to temperature. As such the signal derived from *Dictyocha* spp. in previous factor analyses (Pichon *et al.* 1992, table 4) is equivalent to that of the diatom *Roperia tesselata* in terms of weight. There was not sufficient time to test the effect of removing or retaining *Dictyocha* spp. in the transfer function developed in this thesis. Since previous work had suggested that the effect of *Dictyocha* spp. could be provided by warm-water diatom species it was not used in further statistical analysis.

2.3.5. *EUCAMPIA ANTARCTICA*

Zielinski (1993) reviewed the use of *Eucampia antarctica* for palaeo-estimation in transfer functions and concluded, on the basis of a lack of analogues between modern distributions (at generally less than 10% abundance) and that in Late Quaternary cores (up to 40%), that the species should be removed from statistical use. Reference to sediments in the Ross Sea, which showed enrichment of *E. antarctica* and other previously higher modern abundance reports - which made analogue comparisons possible (Burckle 1984b, Pichon *et al.* 1992) - were shown to be either from regions of known bottom winnowing or vertical transport (Truesdale and Kellogg 1979a,b, Leventer and Dunbar 1987) or from

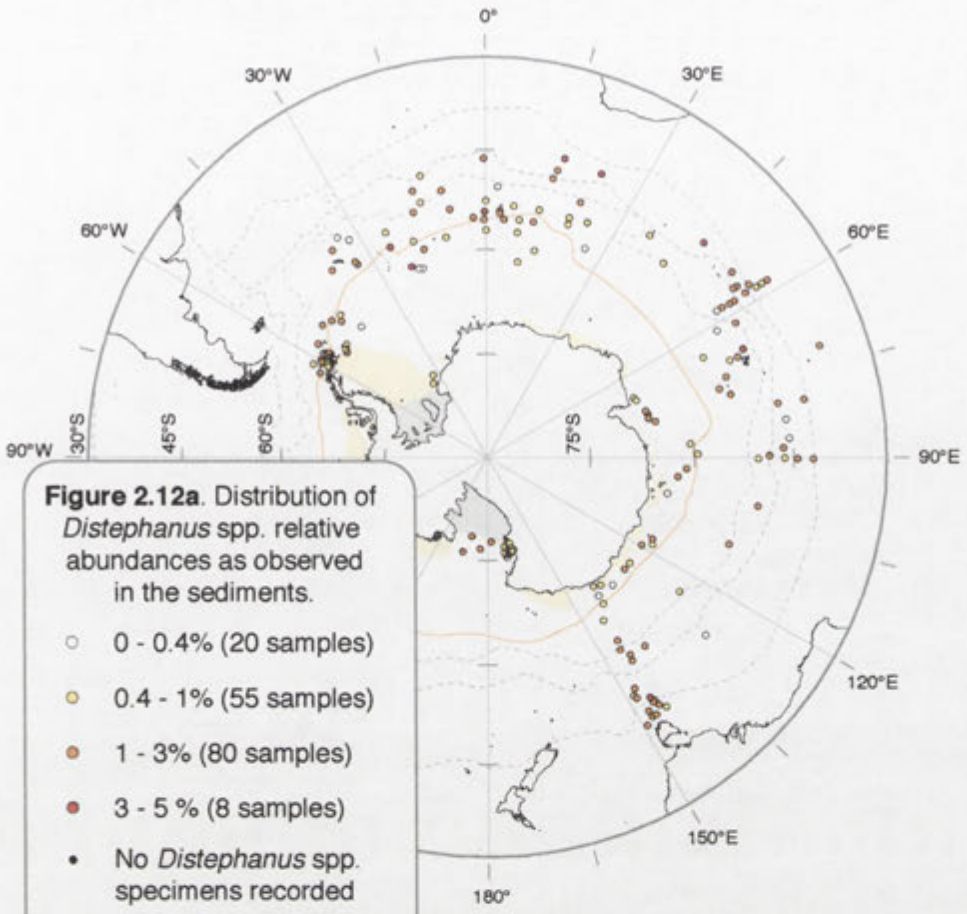

Figure 2.12a. Distribution of *Distephanus* spp. relative abundances as observed in the sediments.

- 0 - 0.4% (20 samples)
- 0.4 - 1% (55 samples)
- 1 - 3% (80 samples)
- 3 - 5 % (8 samples)
- No *Distephanus* spp. specimens recorded

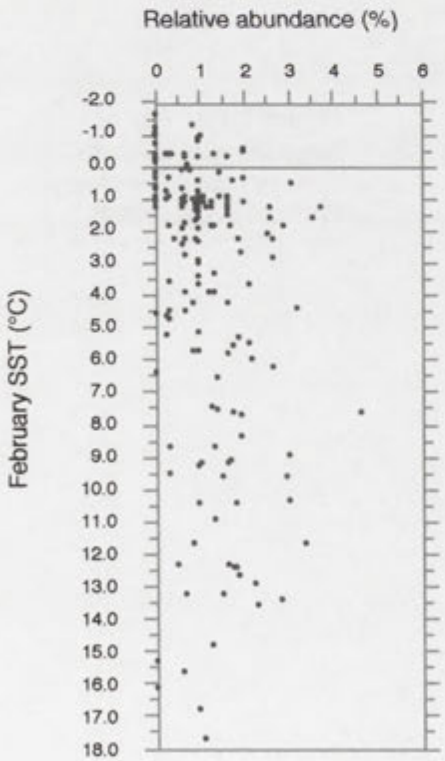

Figure 2.12b. Plot of *Distephanus* spp. relative abundances against February SST from WOA (1994).

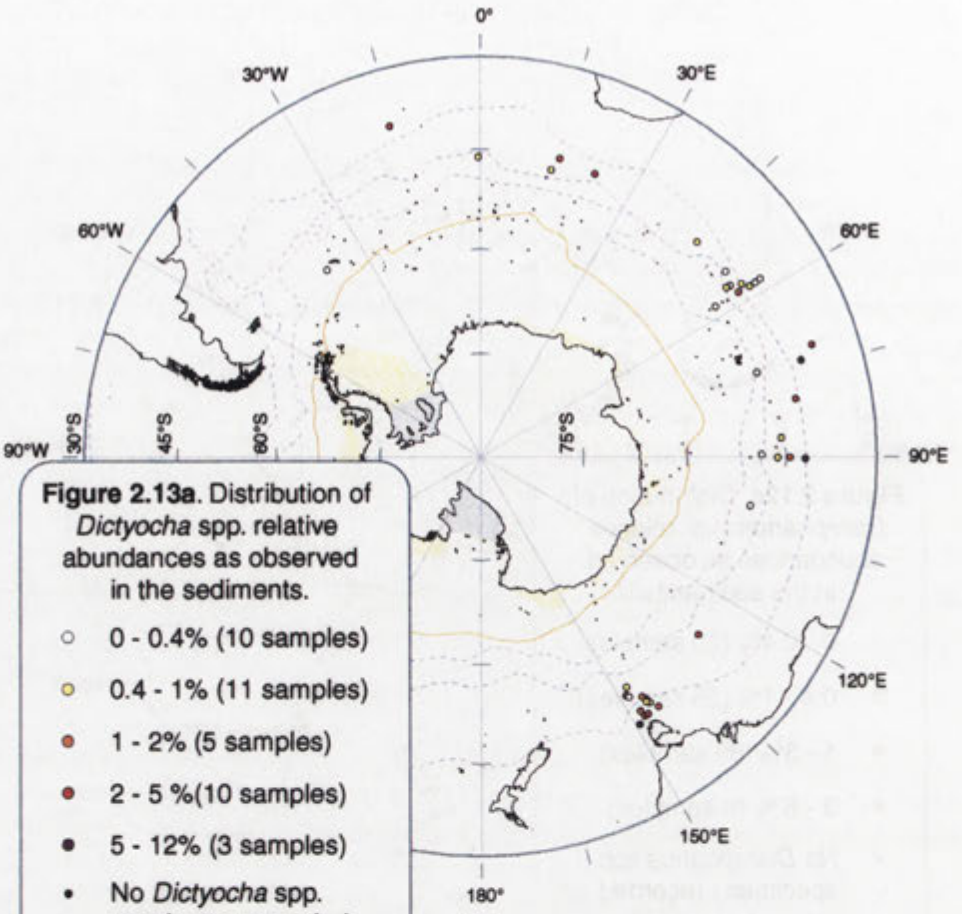

Figure 2.13a. Distribution of *Dictyocha* spp. relative abundances as observed in the sediments.

- 0 - 0.4% (10 samples)
- 0.4 - 1% (11 samples)
- 1 - 2% (5 samples)
- 2 - 5 %(10 samples)
- 5 - 12% (3 samples)
- No *Dictyocha* spp. specimens recorded

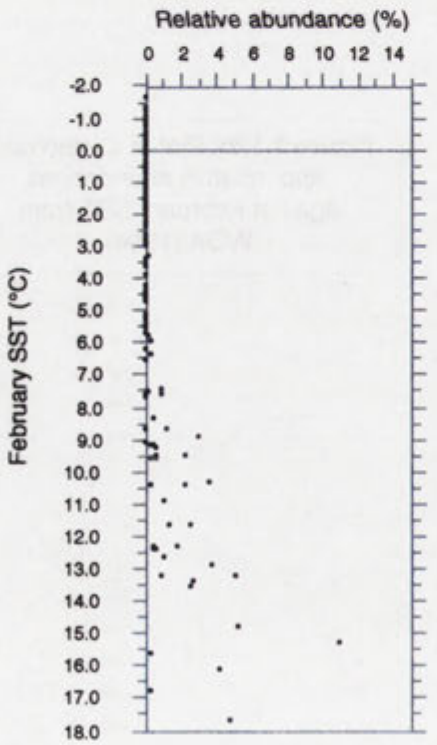

Figure 2.13b. Plot of *Dictyocha* spp. relative abundances against February SST from WOA (1994).

samples which lacked complete species analysis which resulted in elevated abundances (Zielinski and Gersonde 1997).

Zielinski and Gersonde (1997) suggest that the distribution of *E. antarctica* in the sediments is not related to temperature or sea-ice expression, and illustrate a patchy distribution in the South Atlantic which has bimodal maximum abundances in both sea-ice affected regions and the Polar Front. They also advocate the removal of *E. antarctica* from transfer function data sets.

The double distribution of *E. antarctica* noted by Zielinski and Gersonde (1997) provides evidence to the interpretation that two varieties of *E. antarctica* exist as proposed by Fryxell and Prasad (1990). The latter authors described *E. antarctica* var. *recta* as the polar Antarctic form and *E. antarctica* var. *antarctica* as the subpolar type. However, Fryxell and Prasad (l.c.) could not, using the work of Fenner *et al.* (1976), determine the bimodal distribution which Zielinski and Gersonde (l.c.) have since presented.

The stratigraphic use of *E. antarctica* abundances instigated by Burckle and Cooke (1983) must, therefore be considered to combine the signal of both varieties of *E. antarctica* . This should not be used to indicate the position of the sea-ice edge. Burckle and Abrams (1986) acknowledged problems with the use of the *E. antarctica* abundance curves on cores south of the Polar Front. They observed increased abundances of *E. antarctica* in interglacials rather than the expected glacial periods. In contrast to this method, Fryxell and Prasad (1990) and Fryxell (1991) suggest the use of terminal and intercalary ratios of the winter valves to assist in determining sea-ice cover. This method was tested by Kasmarska *et al.* (1993) but has not been employed in this thesis.

Following the results presented by Zielinski (1993) and Zielinski and Gersonde (1997) this study also removes *E. antarctica* from statistical analysis. In contrast to the four previously presented taxa, specimens counted under *E. antarctica* are preserved in the preparation of relative abundances for each sample.

2.4. SUMMARY

Analysis of the several diatom sediment distribution data sets available to the thesis was covered in this chapter. Since each of the data sets were developed over periods of years or were subject to differences in processing and taxonomy, the primary analysis covered in this chapter was concerned with aligning current taxonomic advances and knowledge against the record of species identified in each data. This effort provides a final listing of species which correlate across the years and data sets.

Four data sets were initially analysed. With exception only to the Abbott southeast Indian Ocean data set (section 2.1.4), which could no longer be located for verification, the remaining data sets were combined and subjected to taxonomic reform.

Taxonomic reform and discussion was undertaken on 29 diatom species or taxa. The results of this analysis are compiled in Table 2.10. Here, the thesis defined diatom species or taxa are listed with the previously identified species or taxa found in any of the three data sets compiled. The species definitions used were carried through to the core diatom analyses.

In addition to the major taxonomic revisions, five specific discussions on diatom and silicoflagellate species/taxa were made. These discussions centred on species/taxa where counting methods differentiated between data sets making intercomparison and use in future statistical analysis difficult (ie. *Chaetoceros* vegetative and resting cells, *Thalassiothrix/Trichotoxon* spp. and *Dactyliosolen antarcticus*), or where the inclusion of species/taxa was deemed inappropriate for statistical analysis in this thesis (eg. *Eucampia antarctica* and the silicoflagellates *Dictyocha* and *Distephanus* spp.). Of these five groups, only count data from *E. antarctica* was conserved in determining total diatom abundances for surface sediment and down core samples (refer to Chapters 3 and 6).

Having completed taxonomic revision of the available data sets the following chapter analyses each species in terms of distribution and reference to the two environmental parameters under study in this thesis (ie. sea-surface temperature and sea-ice cover). It is from this taxonomically aligned background that the database for statistical analysis will be selected.

New Species identification (section reference)	Previous species counts found under new species identification
1. *Achnanthes brevipes* (2.2.1)	includes all counts previously listed as *A. brevipes* and *A. brevipes* var. *angustata*
2. *Actinocyclus actinochilus* (2.2.2)	includes counts previously listed as *A. actinochilus* and *Charcotia actinochilus*
3. *Actinocyclus curvatulus* (2.2.3)	includes all species previously listed as *A. curvatulus* and *Coscinodiscus curvatulus*
4. *Asteromphalus hookeri* (2.2.4)	one single count from MDBX94-03 is transferred from *A. heptactis to A. hookeri*
5. *Asteromphalus parvulus* (2.2.4)	includes counts previously listed in all Pichon data (166DB and New data, Appendices 2.3 and 2.2) as *A. heptactis* and *A. parvulus*
6. *Azpeitia tabularis* (2.2.5)	includes counts previously listed as *A. tabularis*, *A. tabularis* var. *egregius*, *Coscinodiscus tabularis*, *C. tabularis* var. *egregius*
7. *Coscinodiscus* spp. (2.2.7)	a single occurrence of *C. decrescens* in sample RC15-91 is transferred to this *Coscinodiscus* species group
8. *Fragilaria striatula* (2.2.8)	includes counts previously listed as *Synedra kerguelensis*
9. *Fragilariopsis* Cylindriform Group (2.2.13)	includes counts previously listed as species of *Fragilariopsis* or *Nitzschia cylindrus*, *linearis*, and *vanheurckii*
10. *Fragilariopsis kerguelensis* (2.2.11)	includes counts previously listed as species of *Fragilariopsis* or *Nitzschia kerguelensis* and *ritscheri*
11. *Fragilariopsis* Cool Taxa (2.2.12)	includes counts previously listed *as Fragilariopsis sublinearis*, *Fragilariopsis obliquecostata*, *Nitzschia obliquecostata* and *Nitzschia sublineata*
12. *Fragilariopsis oceanica* (2.2.10)	includes counts previously listed as *Nitzschia grunowii*
13. *Fragilariopsis rhombica* (2.2.9)	includes counts previously listed as *Nitzschia angulata*
14. *Navicula gelida* var. *parvula* (2.2.15)	includes counts previously listed as *Navicula glacei*
15. *Nitzschia sicula* Group (2.2.14)	includes counts previously listed as *Nitzschia sicula*, *N. sicula* var. *rostrata*, and *N. sicula* var. *bicuneata*
16. *Paralia* Taxa (2.2.16)	includes counts previously listed as *Paralia sol*, *Melosira sol*, *Paralia sulcata*, *Paralia* sp. and *Melosira adeliae*
17. *Porosira* Group (2.2.17)	includes counts previously listed as *Porosira pseudodenticulata* and *Porosira glacialis*
18. *Rhizosolenia antennata* f. *antennata* (2.2.18)	includes counts previously listed as *R. bidens* or *R. hebetata* f. *bidens*

table continues overleaf

New Species identification (refer to section)	Previous species counts found under new species identification
19. *Rhizosolenia* otaria absent Group (2.2.19)	includes counts previously listed as *R. hebetata*, *R. hebetata* f. *semispina*
20. *Rhizosolenia* otaria present Group (2.2.20)	includes counts previously listed as *R. styliformis*
21. *Stellarima microtrias* (2.2.21)	see Table 2.8 for previously listed species and splitting of counts between *S. microtrias* and *S. stellaris*
22. *Stellarima stellaris* (2.2.21)	see Table 2.8 for previously listed species and splitting of counts between *S. microtrias* and *S. stellaris*
23. *Thalassionema* Taxa (2.2.22)	includes counts previously listed as *Thalassionema nitzschioides* and *T. nitzschioides* var. *parva*
24. *Thalassiosira antarctica/ scotia* Group (2.2.23)	includes counts previously listed *as T. antarctica* and *T. scotia*
25. *Thalassiosira* Eccentric Group (2.2.24)	includes counts previously listed as *T. eccentrica*, *T. trifulta*, *T. eccentrica* var. *jousei*, *T. punctifera*, *T. symmetrica*, and *Coscinodiscus eccentrica*
26. *Thalassiosira gracilis* Group (2.2.26)	includes counts previously listed as *T. gracilis*, *T. gracilis* var. *expecta*, *T. delicatulata*, and *T. delicatula*
27. *Thalassiosira* Lineati Group (2.2.27)	includes counts previously listed as *Coscinodiscus lineatus*, *Thalassiosira lineata*, *and T. leptopus*. Counts of *T. lineata* from >60° S are inferred to represent *T. tumida* and so are transferred to this group
28. *Thalassiosira maculata* (2.2.28)	includes counts previously listed as *Coscinodiscus bullatus* and *Thalassiosira maculata*
29. *Thalassiosira oestrupii* Group (2.2.29, 2.2. 25)	includes both variations of the species (var. *oestrupii* and var. *venrickae*) and one species identified as *T. frenguelli.*
30. *Thalassiosira oliverana* (2.2.30)	includes counts previously listed *as Schimperiella antarctica* and *Thalassiosira oliverana*
31. *Thalassiosira ritscheri*	includes counts previously listed as *Coscinodiscus ritscherii* and *Thalassiosira ritscheri*
32. *Thalassiosira tumida* (2.2.31)	includes counts previously listed as *T. tumida* and occurrences of *Thalassiosira lineata* >60°S

Table 2.10. Summary of taxonomic revisions made through the three data sets available to the thesis (Original 166 DB, New Pichon data set, Armand data set). List numbers refer to numbers appearing in Appendices 3.1 and 3.2. Reference to sections where taxonomic changes were discussed in this chapter are indicated.

Chapter 3

Natural and dissolution data sets

CHAPTER 3. SECTION A. NATURAL DATABASE.

3A.0. INTRODUCTION

Choosing the correct selection criteria is an important part of working with statistical methods used to perform ecological predictions (Howe and Webb 1983). Selection criteria assist in reducing statistical noise, eliminating outliers, identifying errors, and increasing the robustness of a data set used such that one can minimise the inaccuracies emanating from the data set. Previous Antarctic diatom transfer function studies have not covered this aspect in great detail with exception to a cut-off criterion for rare species. As part of the revision of the combined databases, several selection criteria were established for both the samples used and also the species selected.

The Natural Database constitutes the selection of surface samples that have until this point been identified by their respective data sets (ie 166DB, new samples of the author etc.), but which are now combined as one set. This database reference set does not include the experimental dissolution database of Pichon *et al.* (1992a,b), formerly associated with the 166DB. The dissolution database will be analysed in Section B of this chapter.

The distribution of each major species in relation to geography, sea-surface temperature and sea-ice cover, along with the species selected for analysis follows the selection criteria section. In response to the species information, regional sample exclusion is applied and discussed. Finally, a brief examination and discussion on the dissolution data set is provided prior to the application of the transfer function for SST and sea-ice in the ensuing chapters.

3A.1. SAMPLE SELECTION CRITERIA.

After finalising the taxonomic reform of the databases, sample selection for statistical analysis was required. Rigorous sample selection criteria were established to aid in eliminating poorly preserved or under-counted samples. A four-step approach was devised and applied to the Natural Database.

3A.1.1 TOTAL NUMBER OF SPECIMENS COUNTED.

On reassessment of the diatom database it was discovered that many samples were not counted to a minimum of 300 specimens, even when considering the removal of *Thalassiothrix* spp., *Chaetoceros* spp. and silicoflagellate data from the total specimen counts. In some instances, this can be associated with heavy dissolution in some regions,

or with artificially dissolved samples at the extreme end of the sample dissolution. Keeping in mind sample totals affected by the removal of certain taxa, a cut-off at 270 minimum specimen count total was enforced. Natural samples removed in this manner number 48 (Table 3.1.) Most of the natural samples appear to fall in the most northern or southern locations (Figure 3.0). All natural samples listed in Table 3.1 are removed from further analysis.

3A.1.2. OLD SPECIES.

It is acknowledged that some re-suspension and movement of sediments can occur and which introduces much older-aged diatoms. Because of the reduced specimen count used in the compilation of this Natural Database, a 1% limit to the relative abundance of old species was used as a cut-off point to determine whether a sample was representative of the modern surface sediment. Generally, it is assumed that published transfer functions are free from reworked samples. It is rare to determine the criteria by which such samples were deemed ineligible. Pichon *et al.*(1987) removed all samples with reworked species in his first transfer function, and all samples in the 166DB (Pichon *et al.* 1992a) were considered to represent Holocene sediments. Burckle (1984) first practiced removing samples which contained greater than 2% reworking. A 3% cut-off was suggested, but ignored by Jordan and Pudsey (1992), and presumably a 1% cut-off was employed by Schuette and Schrader (1979). In contrast, DeFelice and Wise (1981) and Kellogg and Kellogg (1987) noted and used reworked species in their factor analyses.

Species used in determining the 1% cut-off criteria applied in this work include *Actinocyclus ingens*, *Hemidiscus karstenii*, *Rouxia* spp., *Denticulopsis* spp., *Stephanopyxis* spp. and *Rocella gelida.* In 13 samples, these combined species were found to occur at greater than 1% (Table 3.2). It follows that these samples were then removed from further analysis. (Specimens attributed to *Nitzschia denticuloides* a Miocene diatom (Schrader 1976, Harwood and Maruyama 1992) were inadvertently overlooked during the use of this criterion. Two further samples should have been removed RC8-46 (1% reworked, 55°20'S 65°28'E) and 1277-28 (1.7% reworked, 61°28'S, 9°11'E), but due to the delayed nature of this discovery they have been included in all following analyses in making up the diatom total of each sample).

LKA Code	Core	Latitude °S	Longitude	Total minus certain taxa	Original count Total
68	83-11C III	78°15'	172°17'W	50	50
228	DFBC 83-44 II	77°37'	166°15'E	51	51
24	1212W	75°31.1'	56°53.8'W	54	54
111	KR8828	64°09.5'	98°09.5'E	72	72
258	147GC007	45°09.53'	146°17.51'E	73	106
23	1192W	54°30.0'	03°48.4'E	79	81
208	PCDF 82-142	63°53.1'	62°26.4'W	88	88
19	1147-4P	61°36.1'	54°51.6'W	91	91
60	MD84 532	66°06.9'	76°45.6'E	94	99
61	MD84 533	65°09.1'	78°21.2'E	97	100
220	DFBC 83-43 III	76°43'	176°19'W	97	99
207	PCDF 82-127 B	64°39.5'	62°07.4'W	98	98
209	PCDF 82-155	65°01.1'	63°15.6'W	98	100
229	DFBC 83-6 III	77°47'	177°53'E	98	100
69	83-12 III	78°16'	170°08'W	99	100
70	83-19 III	77°18'	158°43'W	99	99
202	PCDF 82-174	64°10'	56°48.5'W	99	99
206	PCDF 82-112	64°36.5'	61°38'W	99	99
73	PC82-197	63°43'	57°13.6'W	100	100
205	PCDF 82-134	64°34.5'	62°39'W	100	101
41	RC11-77	53°03'	16°27'W	102	106
49	V14-53	56°43'	24°31'W	102	107
20	P1160	60°46.6'	45°47.9'W	105	107
58	MD84 531	66°57.7'	75°24.6'E	108	112
18	1184-6P	62°17'	57°20.5'W	110	112
48	RC12-292	39°40.6'	15°28.5'W	110	118
22	1010W	77°20'	35°00'W	115	117
260	147GC017	47°45.04'	145°49.01'E	131	148
261	147GC031	44°32.80'	149°03.81'E	134	152
185	RC11-118	37°48.0'	71°32.0'E	168	182
40	RC11-71	49°08'	37°25'E	178	179
259	147GC013	46°10.01'	144°15.99'E	186	207
72	83-42 III	76°38'	166°03'W	194	196
59	MD84 530	66°06.6	73°59.1'E	195	200
6	RC11-80	46°45'	00°03'W	199	207
25	1223W	75°58.9'	33°32.9'W	201	206
186	RC11-119	40°18.0	74°34.0'E	204	235
146	MDBX94-02	45°35'	86°31'E	207	333
17	1141-2P	61°31.8'	61°47.4'W	209	213
114	KR8831	59°	89°24.3'E	210	212
27	RC17-56	65°24'	37°43'E	212	217
149	MDBX94-05	48°48'	89°32'E	237	360
244	147GC030	46°10.04'	147°27.98'E	239	268
150	MDBX94-06	44°34'	90°04'E	248	368
151	MDBX94-07	41°43'	90°16'E	252	332
80	KR8705	64°03.3'	48°56.9'W	260	264
147	MDBX94-03	46°28'	88°03'E	263	356
83	KR8708	60°55.2'	56°26.3'W	266	270

Table 3.1. Samples with less than 270 specimens counted (modified total). Both the original and modified total (with certain taxa removed) specimen counts are given. The modified total is minus contributions from the following taxa = *Chaetoceros* spp and spores, *Dactyliosolen antarcticus*, silicoflagellates and *Thalassiothrix* Group. All samples listed are removed from further analysis.

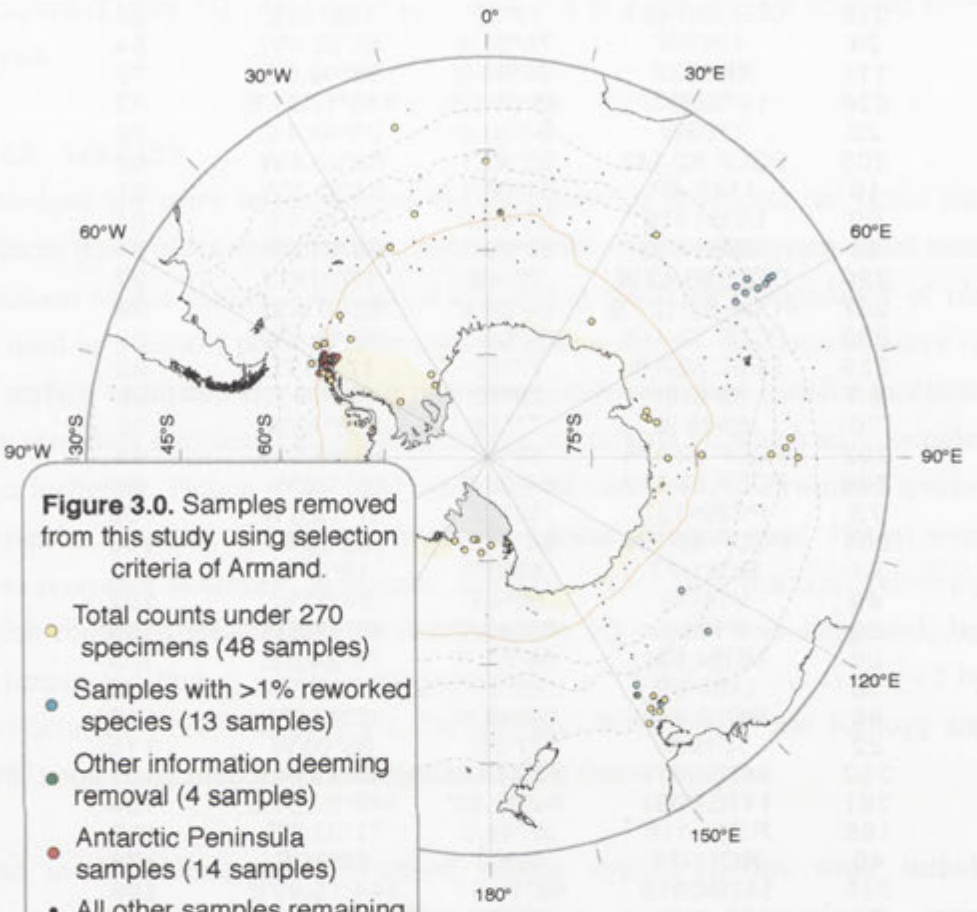

Figure 3.0. Samples removed from this study using selection criteria of Armand.

- Total counts under 270 specimens (48 samples)
- Samples with >1% reworked species (13 samples)
- Other information deeming removal (4 samples)
- Antarctic Peninsula samples (14 samples)
- All other samples remaining

LKA Code	Core	Latitude °S	Longitude	Total minus certain taxa	% reworked species
90	KR8806	49°01.3'	128°46.3'E	295	2.0
93	KR8809	50°35.6'	147°09.3'E	290	2.4
157	KTB20	47°00'	58°01'E	319	1.3
158	KTB21	45°58'	55°59'E	271	1.1
159	KTB22	45°59'	55°59'E	339	2.1
160	KTB25	45°01'	57°57'E	271	1.5
187	KTB 31	40°59'	57°59'E	284	1.1
188	KTB 34	41°59'	58°01'E	601	1.5
189	KTB 29	43°00'	58°01'E	282	1.1
190	KTB 26	43°58'	55°58'E	396	3.0
191	KTB 18	48°00'	57°59'E	326	1.5
241	TC37-19	56°03.5'	124°56'E	292	1.4
242	147GC016	77°37'	166°15'E	290	1.7

Table 3.2. Samples with greater than 1% reworked species. All samples listed are removed from the Natural Database. Total minus certain taxa = minus previous contributions from *Chaetoceros* spp and spores, *Dactyliosolen antarcticus*, silicoflagellates and *Thalassiothrix* Group.

3A.1.3. OTHER INFORMATION.

Although not as rigorous as the previous two criteria, this selection step allows additional information regarding a sample to be taken into consideration before the sample is included in the database. In such cases, sedimentological or continued analysis of a sample may indicate that its removal is warranted. Surface sample E53-10 is such an example. Both silica/zinc ratio studies (Michael Ellwood pers. comm. 1996) and corresponding diatom species analysis, implied that at least the first 2 metres of the core was reworked. Yet, the surface sample appeared to pass the first two criteria (0.7% reworking). With this knowledge, the surface sample was removed from further analysis. Other samples removed were those identified as bag samples (PCDF 82-61, 82-102, 82-167). In this case, the assumption of upper surface sediment representation is not assured.

These first three steps have reduced the Natural Database to 129 samples from an initial 194 samples.

3A.1.4. COMMUNALITY LEVELS.

On a separate level, samples could be assessed after factor analysis for their communalities. Communality is an index describing the amount of compositional information from the original sample that is accounted for in a factor model (Imbrie and Kipp 1971). Values range from 0 (all information lost, poor model fit) to 1 (all information retained). Samples >0.7 are deemed to indicate good compositional information and those below do not. Imbrie and Kipp (1971) did not use communality values to outcast samples and included samples in their transfer function, which fell to a

communality value of 0.5. Both diatom transfer functions constructed by Pichon *et al.* (1987, 1992a) retained samples with communality values down to 0.6. However, Zielinski (1993) applied the communality value as a criteria for removing samples from his data set when samples, which otherwise indicated poor model fit, had communality values less than 0.75. The communality value is affected by the number of factors chosen and is likewise increased when the number of factors resolved are (Imbrie and Kipp 1971, Reyment and Jöreskog 1993). Since this criterion for removing data is linked with the statistical analysis and the number of factors resolved, it will be commented on it is respective section. (Chapter 4.3).

3A.2. RARE SPECIES.

Contrary to the findings of Imbrie and Kipp (1971) and Le (1992), which deemed that rare species did not affect the results of transfer functions, the removal of rare species from data sets continues to be applied. In general, the reasons for removing rare species are to reduce the often large list of species encountered and to reduce the degree of counting error related to mis-identifications. Although there is variation in the tact taken by researchers in applying a criteria for removing rare species, the principal method is to remove or group data associated with species with less than 1 or 2% relative abundance (for examples on variations see Maynard 1976, Schuette and Schrader 1981, Burckle 1989, Karpuz and Schrader 1990, Schrader and Sorknes 1991, Jordan and Pudsey 1992, Zielinski and Gersonde 1997). In contrast, weighting of certain rare species, considered important to ecological features under investigation, was used by Schrader and Sorknes (1991).

In this work, rare species are those encountered with less than 0.4% relative percentage. This value corresponds to 1 valve in 270 specimens counted. There are 26 species/taxa groups found in the Natural Database with less than 0.4% of the total relative abundance. They are listed in Table 3.3. All counts that were associated with these species at less than 0.4% will be relegated under the "Other unidentified species" category, to preserve relative abundance information. The counts of *Thalassiosira* spp. and *Coscinodiscus* spp. are also relegated to the other unidentified species category. Preserving the data is in contrast to the complete removal strategy employed by Schrader and Karpuz (1990) and Zielinski and Gersonde (1997). They were more fortunate in dealing with at least 30 to 100 more specimens in each of their samples so the loss of further specimens was not a concern to them.

Executing the removal of these species leaves the Natural Database with 59 species/taxa group categories. Here 44 species contain more than 1% of the total assemblages, and 15 species remain between 0.4 and 1%.(Table 3.4)

Species under 0.4% relative abundance.
Actinocyclus elongatus, Actinocyclus spp., *Amphora ovalis, Asteromphalus hyalinus, Asteromphalus* spp., *Azpeitia africanus, Coscinodiscus oculus-iridus, Nitzschia baaurdii, Nitzschia bicapitata, Nitzschia closterium, Nitzschia interruptestriata, Nitzschia kolaczekii, Nitzschia sicula* Group, *Odontella litigiosa, Pleurosigma directum, Pleurosigma* spp., *Proboscia barboi*, Pseudonitzschia heimii, Pseudonitzschia lineola, Rhaphoneis suriella, Rhizosolenia ant.* f. *antennata* , *Rhizosolenia* spp., *Rouxia* spp., *Thalassiosira ambigua, Thalassiosira frenguelliopsis, Thalassiosira ritscheri.*

Table 3.3. List of species encountered in the Natural Database with relative abundances under 0.4%. * = reworked species.

Species/Taxa groups	Maximum abundance (%)	Species/Taxa groups	Maximum abundance (%)
Achnanthes brevipes	1.3	*Nitzschia lecointei*	1.0
Actinocyclus actinochilus	11.9	*Nitzschia paundriformis*	1.0
Actinocyclus curvatulus	2.2	*Odontella weissflogii*	11.6
Actinocyclus ingens	0.7	*Paralia* Taxa	1.4
Asteromphalus hookeri	1.4	*Porosira* Group	7.2
Asteromphalus parvulus	3.1	*Proboscia alata*	2.0
Asteromphalus robustus	0.7	*Pseudonitzschia seriata*	0.6
Azpeitia tabularis	24.2	*Rhizosolenia bergonii*	1.1
Cocconeis spp.	5.9	*Rhizosolenia* otaria absent	1.4
Coscinodiscus asteromphalus	1.0	*Rhizosolenia* otaria present	9.4
Coscinodiscus marginatus	2.0	*Roperia tesselata*	7.7
Coscinodiscus radiatus	0.7	*Stellarima microtrias*	3.3
Eucampia antarctica	23.2	*Stellarima stellaris*	1.8
Fragilaria striatula	1.0	*Thalassionema* Taxa	6.5
Fragilariopsis Cool Taxa	27.8	*Th. antarctica/scotia* Group	65.1
Fragilariopsis curta	67.4	*Thalassiosira australis*	0.8
Fragilariopsis Cylindriform Group	17.0	*Thalassiosira decipiens*	2.4
Fragilariopsis doliolus	13.0	*Thalassiosira* Eccentric Group	3.2
Fragilariopsis kerguelensis	82.4	*Thalassiosira gracilis* Group	14.5
Fragilariopsis oceanica	0.8	*Thalassiosira gravida*	0.6
Fragilariopsis pseudonana	2.4	*Thalassiosira lentiginosa*	40.6
Fragilariopsis rhombica	10.7	*Thalassiosira* Lineati Group	1.9
Fragilariopsis separanda	7.8	*Thalassiosira maculata*	1.0
Gomphonema intricatum	0.7	*Thalassiosira oestrupii* Group	7.3
Grammatophora arcuata	3.4	*Thalassiosira oliverana*	4.8
Hemidiscus cuneformis	5.3	*Thalassiosira perpusilla*	1.4
Licmophora "decora"	0.7	*Thalassiosira poroseriata*	2.7
Navicula directa	1.7	*Thalassiosira tumida*	4.7
Navicula gelida var. *parvula*	0.7	Other unidentified species	3.6

Table 3.4. Maximum abundances of diatoms >0.4% in the 129 natural sample database.

In the subsequent section, the spatial distribution of the species with greater than 1% relative abundance in the Natural Database will be presented. The relevance of mapping these distributions is important since one of the basic assumptions of transfer function work is that the species located in the sediments reflects the distribution of physical parameters at the surface of the ocean.

3A.3. SPECIES DISTRIBUTIONS.

There are 43 species/taxa groups which are present in greater than 1% relative abundance in the sediment samples, excluding the other unidentified species category. This section explores these distributions and abundance relationships to two parameters (sea-ice and sea-surface temperature) which are of interest to the transfer functions developed in this work. The SST data has been taken from WOA (1994) and the sea-ice data from Schweitzer (1995). The SST data covers February and August maximum and minimum temperature expressions respectively. The sea-ice data is in percentage of sea-ice cover for February (summer minimum extent) and September (winter maximum extent), and also in number of months with sea-ice cover. It should be noted that where sea-ice cover is observed between 0 to 15% it is interpreted as open ocean conditions, between 15 and 40% unconsolidated pack-ice, and beyond 40% fast-ice. Further descriptions and discussion on sea-ice interpretation is covered in Chapter 5, terms used in the description of zones and ecological habitats were outlined in Chapter 1.

Previous studies on the sedimentary distribution of diatom species are numerous and widely distributed. Yet, relative abundance data is more rarely published. Figure 3.1 schematically portrays such previous work, which is also used in discussion of each of the species covered in this section. Studies, which document sea-ice habitats or associations for certain species, are noted in the respective species descriptions. As this section concentrates on previous recorded species distributions in the sediments and reports of association in sea-ice environments, more generalised reports on species distributions in the sediments were not employed, nor was the phytoplankton distribution at the water surface covered with exception to some rarer species. It is acknowledged that sediment trap data from the Southern Ocean have shown that the major diatom flux from the surface waters to the sediments occurs over summer and that the presence of sea-ice provides a barrier to production and sedimentation (Ablemann and Gersone 1991). Thus, making relationships, and furthermore deriving predictions, between diatom sedimentary distributions and that of various seasonal parameters should be made in reference to summer conditions. Here, I examine such summer relationships, but also incorporate comparisons with the winter parameters on the basis that summer/winter relationships occur among the parameters. Such relationships are tied to the latitudinal position of a sample. The winter parameters simply provide the contrasting environmental extreme expected at a particular sample site. The role of the total habitat seasonality should be expected to play a role in the surface distribution of particular species or taxa, this includes the variation in winter parameters, and in some cases it is expected to be linked to specific species distributions (eg. such as *Fragilariopsis cylindrus* and *Fragilariopsis curta* , Garrison 1991, Leventer and Dunbar 1996).

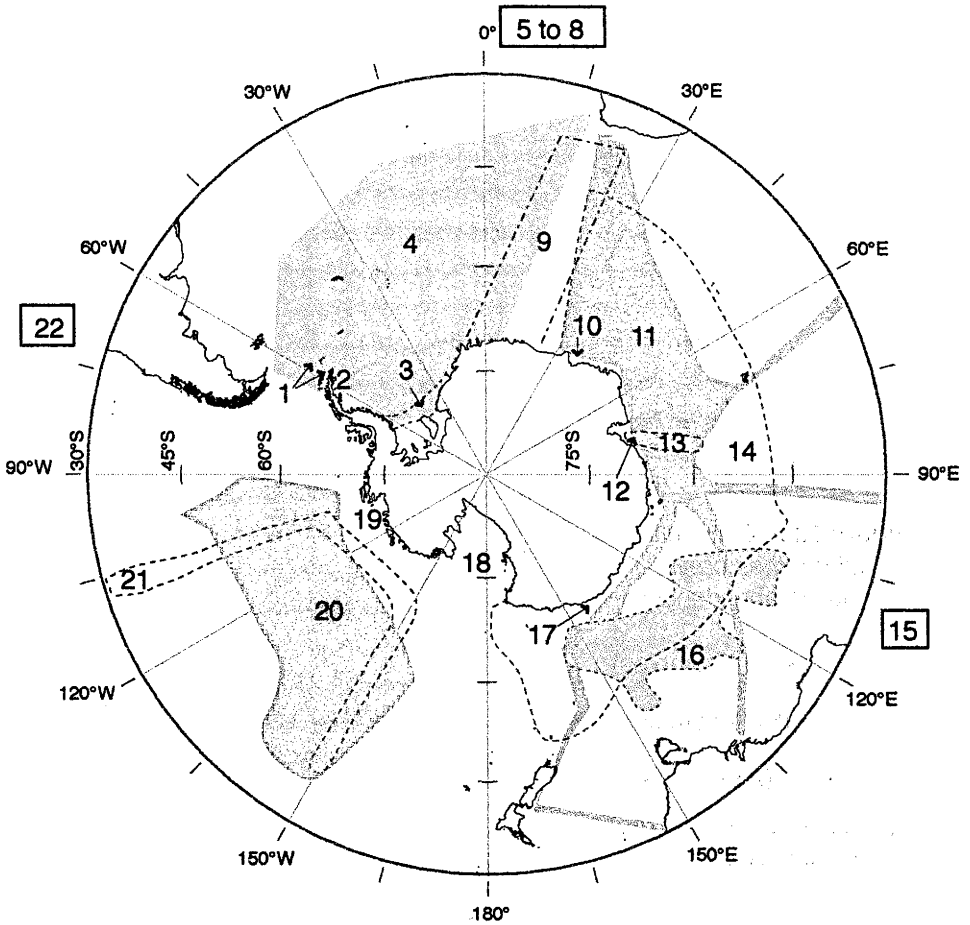

Figure 3.1. Schematic map of previous studies detailing diatom distribution in the surface sediments used in the following section. Studies listed principally include those which documented count or relative abundance data. Such information provided comparison for the species distribution greater than 1% in the database of this thesis. Numbers refer to the publications below. Six publications refer to diatom distributions north of 30°S. These are indicated exterior to the map and in the abbreviation list below.

1	Gersonde & Wefer (1987)	13	Fryxell (1991)
2	Prasad & Nienow (1986)	14	Kozlova (1966) Indian sector only.
3	Gersonde (1984)	15	van Iperen *et al.* (1993) - Indonesian Archipelago.
4	Zielinski & Gersonde (1997)	16	Abbott (1973)
5	Pokras & Molfino (1986) SE Atlantic	17	Leventer (1992)
6	van Iperen *et al.* (1987) SE Atlantic	18	Truesdale & Kellogg (1979)
7	Treppke *et al.* (1996) SE Atlantic	19	Kellogg & Kellogg (1987)
8	Schuette and Schrader (1981) SE Atlantic	20	Donahue (1973)
9	DeFelice & Wise (1981)	21	Kozlova & Mukina (1967)
10	Tanimura (1992)	22	Schuette & Schrader (1979a,b) SE Pacific
11	Jouse *et al.* (1962 a, b)		
12	Stockwell *et al.* (1991)		

N.b. Areas drawn on map are approximate representations.

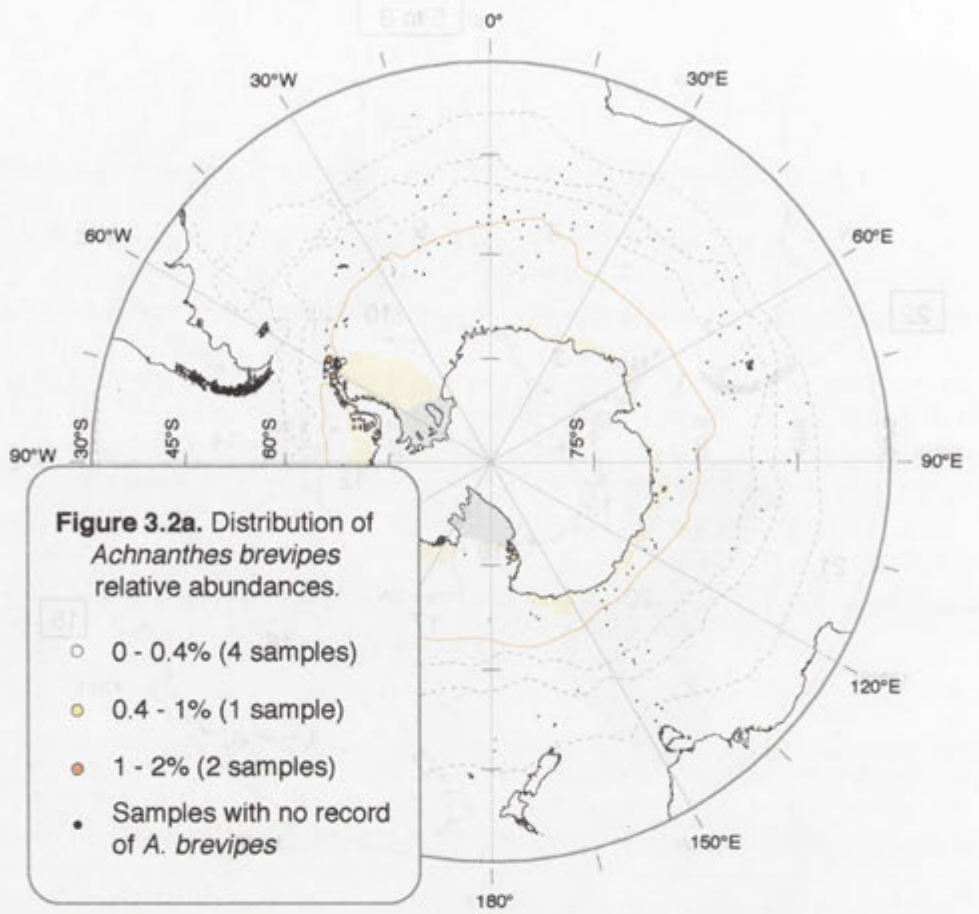

Figure 3.2a. Distribution of *Achnanthes brevipes* relative abundances.

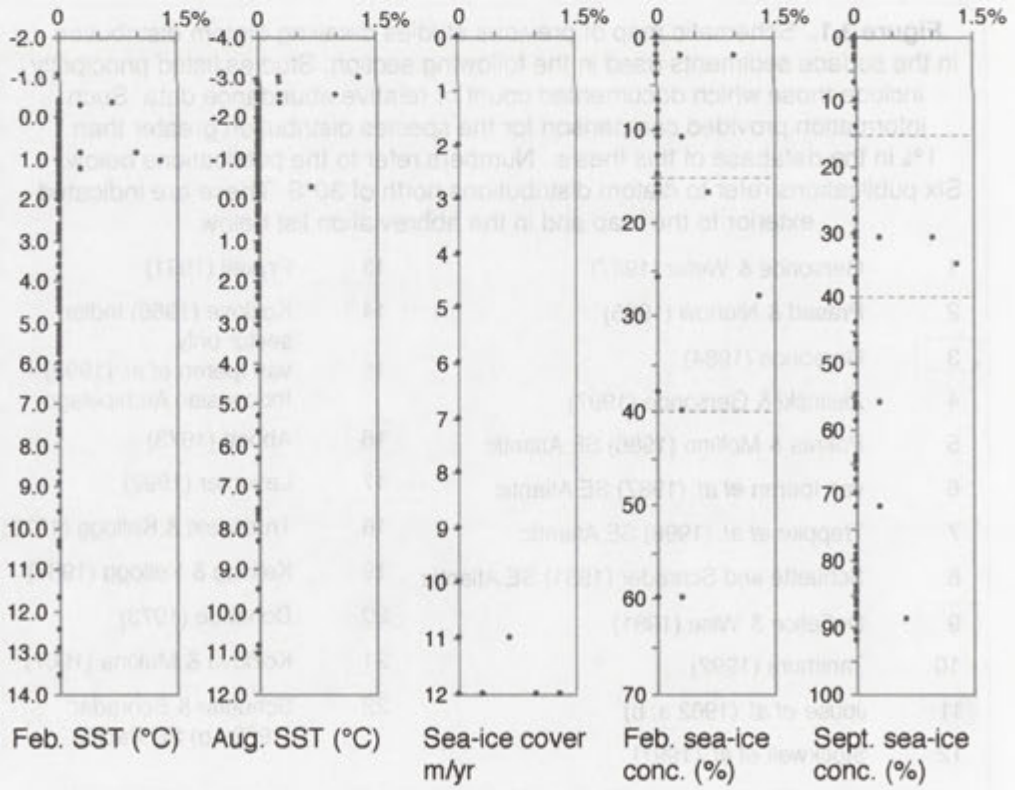

Figure 3.2b. Relative abundances (x-axis) against February and August SST, sea-ice cover in months per year and sea-ice concentration (%) in February and September (annual minimum and maximum sea-ice extents respectively). Sea-ice boundaries between open ocean and pack ice, and pack ice and consolidated fast ice are indicated at 15% and 40% respectively (Gloersen *et al.* 1992). SST data WOA (1994), Sea-ice data Schweitzer (1995), Oceanic Fronts (Orsi *et al.* 1995).

3A.3.1. *ACHNANTHES BREVIPES*

A benthic diatom species with a maximum of 1.3% relative abundance in the Natural Database. The species is noted only in the Antarctic Peninsula region and in the Ross Sea (Fig. 3.2.a). Its maximum distribution is noted within February SST of -0.5 to 1°C, August SST -0.3°C, whereas in relation to sea-ice cover highest abundances are related to year round ice cover with a minimum of 30% ice cover in September and a maximum of 60% in February (Fig. 3.2.b).

Only two previous accounts note the recovery of this species in the sediments. Prasad and Nienow (1986) found *Achnanthes brevipes* v. *angustata* in Croft Bay, Antarctic Peninsula. Tanimura (1992) encountered the species at less than 1% in Lützow-Holm Bay. Garrison (1991) categorised all *Achnanthes* species as associated with land fast-ice. Two reports support this placement, one from Arthur Harbor, Antarctic Peninsula (Krebs *et al.* 1987) and the other from Terra Nova Bay in the Ross Sea (Andreoli *et al.* 1995). These combined analyses show that *A. brevipes* is observed rarely in the sediments and is only found in near shore Antarctic environments with approaching year round ice cover.

3A.3.2 *ACTINOCYCLUS ACTINOCHILUS*

Actinochilus actinochilus has a maximum relative abundance of 11.9% in the Natural Database which is associated with February SST between -1 to 2° C and August SST <0°C. In relation to sea-ice cover *A. actinochilus* is found with increasing abundance in regions with >6 to 12% month per year cover. This converts to a February minimum ice extent with less than 40% ice cover and September maximum extent between 30 and 80% (Fig. 3.3.b). Geographically (Fig. 3.3.a), this can be interpreted as a distribution of northward decreasing abundance from Antarctica, and generally associated with the September maximum sea-ice edge. Observations north of the September sea-ice edge could be linked to bottom-water transport or iceberg pathways.

This species is well recorded in the sediments. Zielinski and Gersonde (1997) report *A. actinochilus* with a maximum abundance of 4.7% in the South Atlantic sector which is associated with summer SST range of -2 to 2°C. Along the Antarctic coast it has been observed in commonly low to medium abundances (eg. <3% off Filschner-Ronne ice shelf (Gersonde 1984), <1% Lützow-Holm Bay (Tanimura 1992), outer Prydz Bay maximum 0.68% (Stockwell *et al.* 1991), between 0.6 to 4% along the Indian Ocean section (Kozlova 1966), George V Coast 2.1% maximum (Leventer 1992), maximum 15.2% Amundsen Sea (Kellogg and Kellogg 1987) <1% in Bransfield Strait and Drake Passage (Gersonde and Wefer 1987).) Further southward only notation on this species recovery has been mentioned (Abbott 1973, Donahue 1973, Jousé *et al.* 1962a, DeFelice and Wise 1981). *Actinocyclus actinochilus* distribution in the sediments has been reported

as confined to the Antarctic Divergence (Kozlova 1966), or more commonly south of the Polar Front (Donahue 1973, DeFelice and Wise 1981, Zielinski and Gersonde 1997).

Actinocyclus actinochilus has been reported in newly formed sea-ice (Gersonde 1984, Tanimura *et al.* 1990, Garrison and Close 1993), and from both fast and pack-ice (Horner 1985, Krebs *et al.* 1987, Garrison and Buck 1989, Garrison 1991). The species appears to have higher presence in sea-ice than in the adjacent water column (Garrison *et al.* 1983a, 1987).

The observations from both previous studies and data in the Natural Database indicate that *A. actinochilus* is a cool water Antarctic species limited to the north by the Polar Front and quite possibly the maximum winter sea-ice edge. The species is most commonly linked with other sea-ice taxa both in the sediments and the sea-ice.

3A.3.3 *ACTINOCYCLUS CURVATULUS*

The Natural Database data of *Actinocyclus curvatulus* in the sediments indicates a scattering of trace occurrences throughout the study region north of the September sea-ice maximum extent (Fig. 3.4a). The maximum abundance of 2.2% is located north of the STC off Tasmania, however, the range of trace occurrences is extremely broad with a February temperature signature of 0.5°C to 14°C (Fig. 3.4b). Most of the data attributed to *A. curvatulus* is not associated with sea-ice presence. Samples found within sea-ice conditions and in colder waters are considered mis-identifications.

Actinocyclus curvatulus and its synonym *Coscinodiscus curvatulus* have been noted as extremely rare in the South Atlantic sector by Zielinski and Gersonde (1997, ie <0.3%) and DeFelice and Wise (1981). The species is also rare in the southeast Indian sector (Abbott 1973, 0.7% one sample only). No other workers report either species in Southern Ocean sediments. Exterior to the Southern Ocean this species is found in greater numbers in the sediments. In the South Atlantic, south west of Africa, *A. curvatulus* and *C. curvatulus* were observed at 4.04% and 14.71 % relative abundances respectively (Schuette and Schrader 1981). In the Indonesian Archipelago the grouped *A. curvatulus, C. curvatulus* and *Actinocyclus vestigulus* taxa were noted in a maximum relative abundance of 2% (van Iperen *et al.* 1993).

Horner (1985) originally noted *Coscinodiscus curvatulus* as observed only in Arctic sea-ice. Androli *et al.* (1995) report *A. curvatulus* in the water column with other sea-ice taxa during the two summer ice free months of Terra Nova Bay in the Ross Sea.

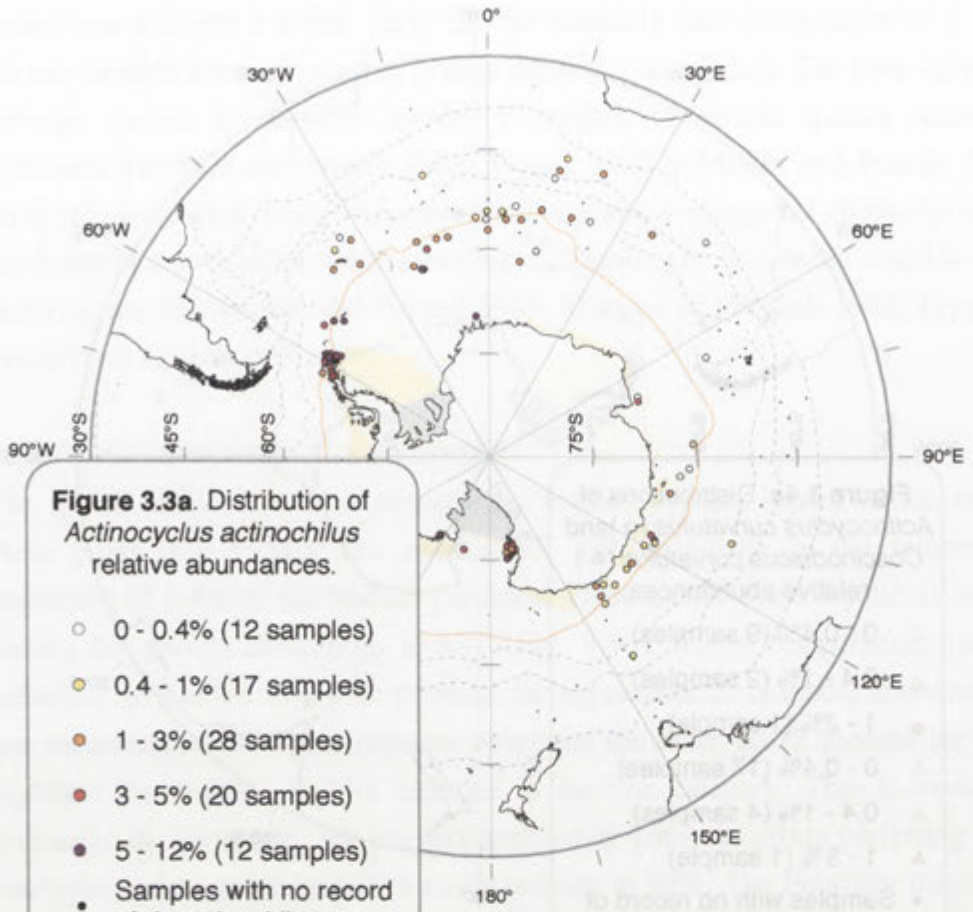

Figure 3.3a. Distribution of *Actinocyclus actinochilus* relative abundances.

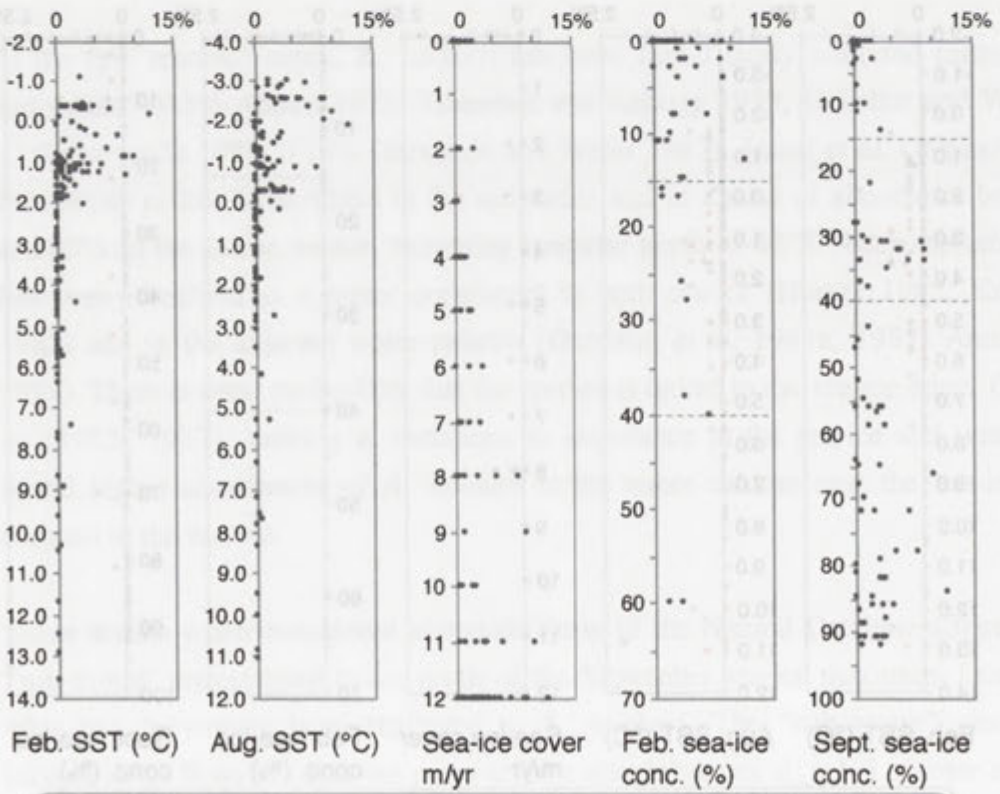

Figure 3.3b. Relative abundances against February and August SST, sea-ice cover in months per year and sea-ice concentration (%) in February and September (annual minimum and maximum sea-ice extents respectively). Other details as in Figure 3.2b.

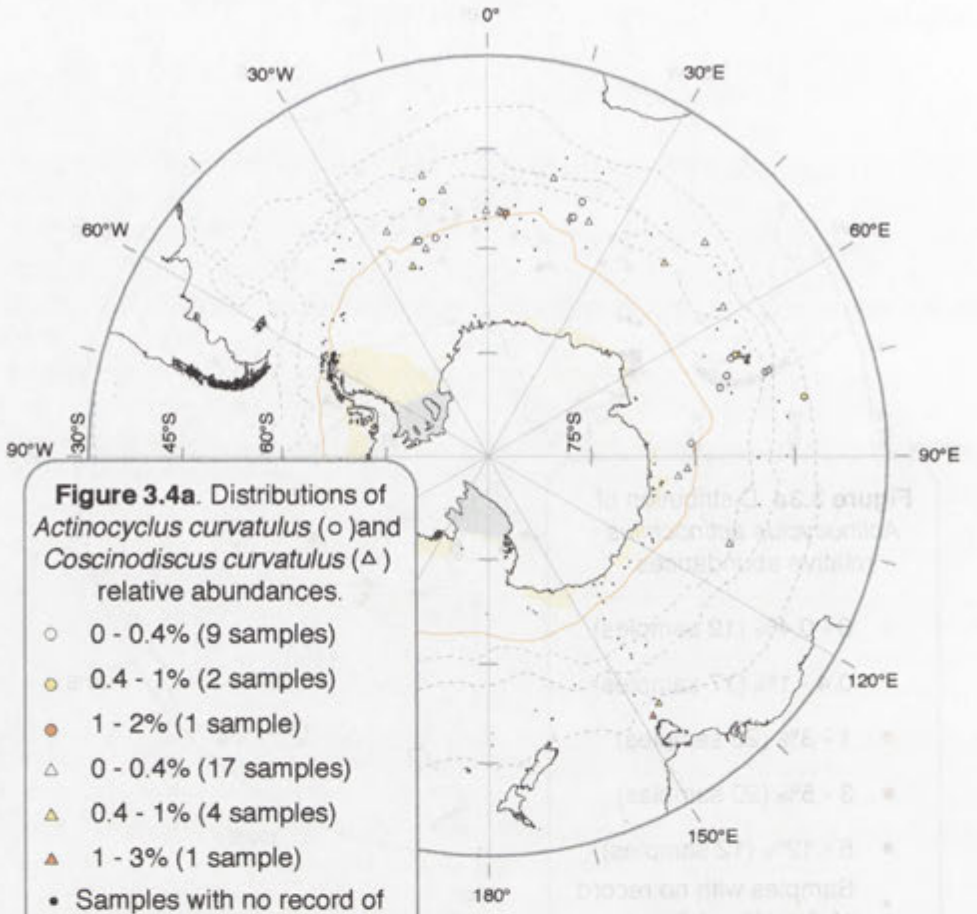

Figure 3.4a. Distributions of *Actinocyclus curvatulus* (○)and *Coscinodiscus curvatulus* (△) relative abundances.

- ○ 0 - 0.4% (9 samples)
- ○ 0.4 - 1% (2 samples)
- ○ 1 - 2% (1 sample)
- △ 0 - 0.4% (17 samples)
- △ 0.4 - 1% (4 samples)
- △ 1 - 3% (1 sample)
- • Samples with no record of *A. curvatulus* or *C. curvatulus*

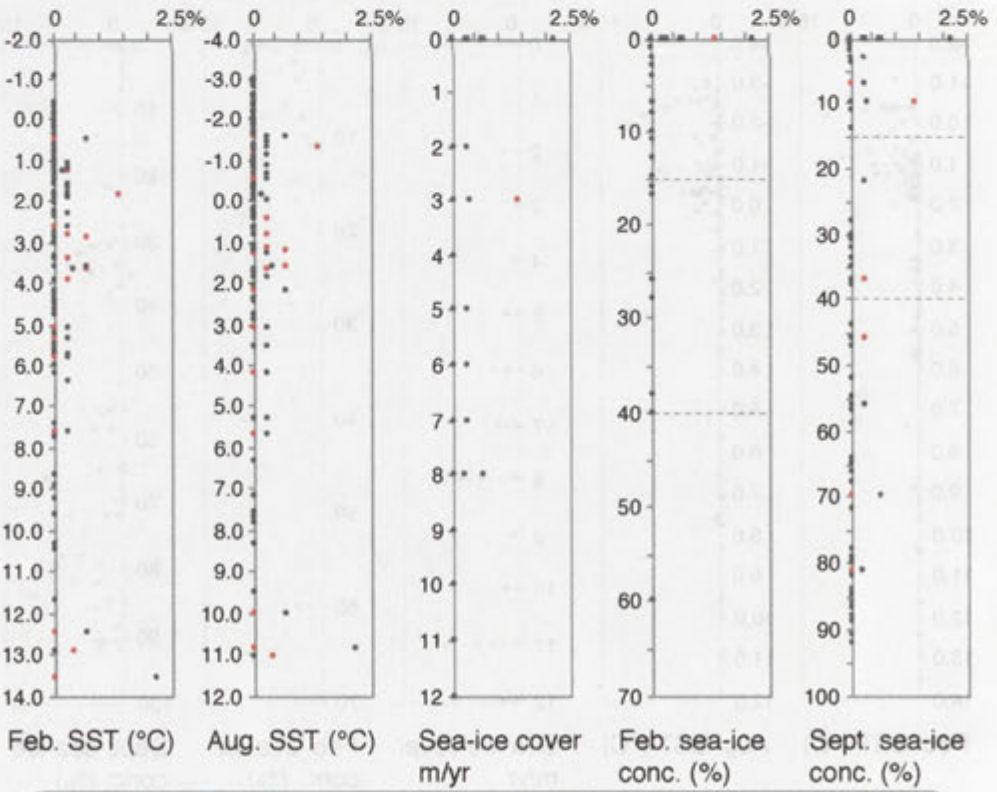

Figure 3.4b. Relative abundances against February and August SST, sea-ice cover in months per year and sea-ice concentration (%) in February and September (annual minimum and maximum sea-ice extents respectively). (●) = *A. curvatulus*, (●) = *C. curvatulus*. Other details as in Figure 3.2b.

From these accounts it seems likely that the southerly trace occurrences of *A. curvatulus* are mis-identifications of another similar *Actinocyclus* species. The very lightly silicified ice-edge species *Actinocyclus spiritus* is unlikely to be this species recorded in the sediments (Watkins and Fryxell 1986, Fryxell 1990 in Medlin and Priddle 1990). This leaves the somewhat poorly described and illustrated *Actinocyclus cholnokyi* as the likely candidate as it has similar fasciculated valve patterning to *A. curvatulus* and is noted as an Antarctic species (Priddle and Fryxell 1985, Watkins and Fryxell 1986, Fryxell 1990 in Medlin and Priddle 1990).

3A.3.4 *ASTEROMPHALUS HOOKERI*

The spatial distribution of *Asteromphalus hookeri* appears limited to the north by the Polar Front (Fig. 3.5a). The species has low abundance in the sediments with a maximum of 1.4% in the Natural Database. There are no evident patterns in dispersion linking this species distribution to SST (Fig. 3.5b). Cooler temperatures indicate some influence. In relation to sea-ice presence the appearance of bi-modal abundance maxima, one increasing to the 0-2 months ice cover and the other 10-12 months ice cover, may highlight the multiple species included in the one category. This bi-modality is also evident in the September sea-ice maximum cover with one group preferring open ocean condition and the other from 30% cover peaking at 90%. The February minimum sea-ice cover indicates both "sub-groups" experience open water conditions.

In the few reported cases, *A. hookeri* has been found rarely scattered throughout the sediments (<0.5% Abbott 1973, Truesdale and Kellogg 1979, DeFelice and Wise 1981, <1% Gersonde 1984, 0.16% Gersonde and Wefer 1987). Jousé *et al.* (1962a) described the species as low in numbers in the sediments and in a zone of abundance between 45° and 65°S in the Indian sector, becoming irregular north of 45°S. *Asteromphalus hookeri* has been identified as a minor constituent in both sea-ice (Horner 1985, Krebs *et al.* 1987) and in the adjacent water column (Garrison *et al.* 1983a, 1987, Andreoli *et al.* 1995). There is some probability that the species is linked to the sea-ice edge. Garrison *et al.* (1983a 1987), looking at variations in abundance in the sea-ice and water column found higher abundances of *A. hookeri* in the water column near the sea-ice edge in contrast to the sea-ice.

These results when considered alongside those of the Natural Database suggest that the "sub-group" encountered to the north of the September sea-ice maximum best represent what has previously been attributed to *A. hookeri.* The "sub-group" predominantly located in the Ross Sea may yet prove to be a allochthonous signal (Leventer and Dunbar 1987, Andreoli *et al.* 1995) or another closely related species within the genera.

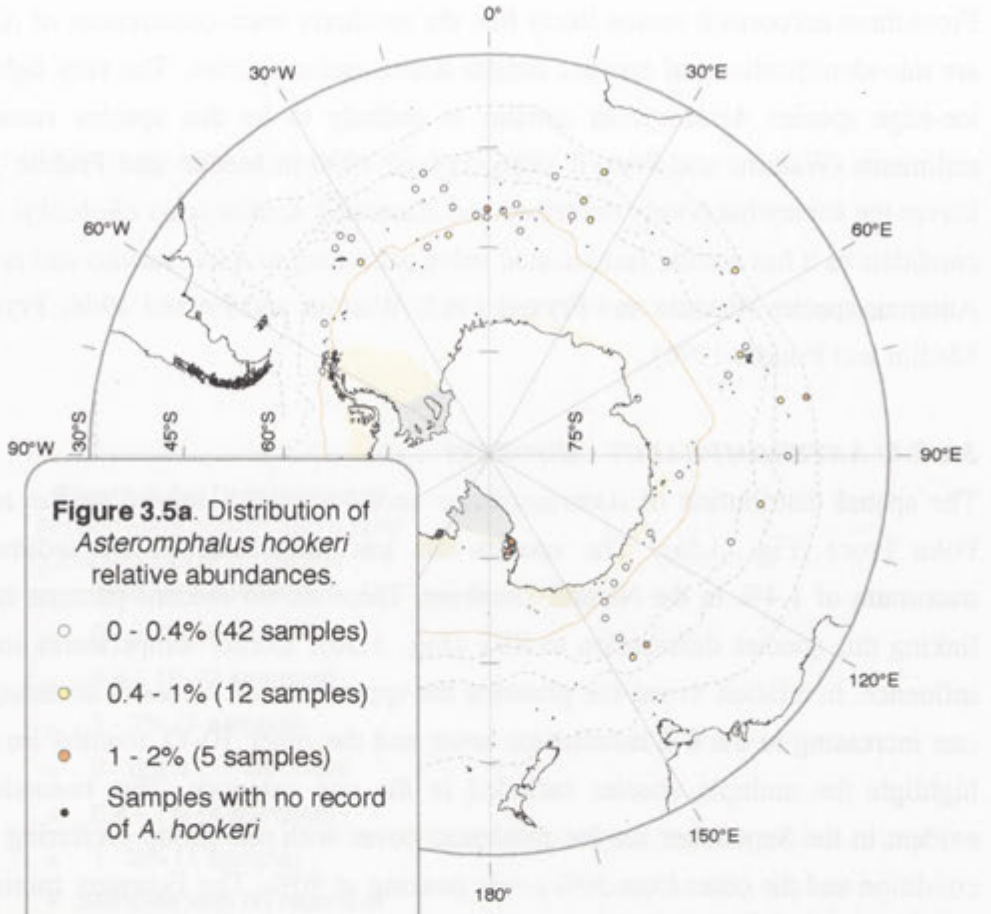

Figure 3.5a. Distribution of *Asteromphalus hookeri* relative abundances.

- 0 - 0.4% (42 samples)
- 0.4 - 1% (12 samples)
- 1 - 2% (5 samples)
- Samples with no record of *A. hookeri*

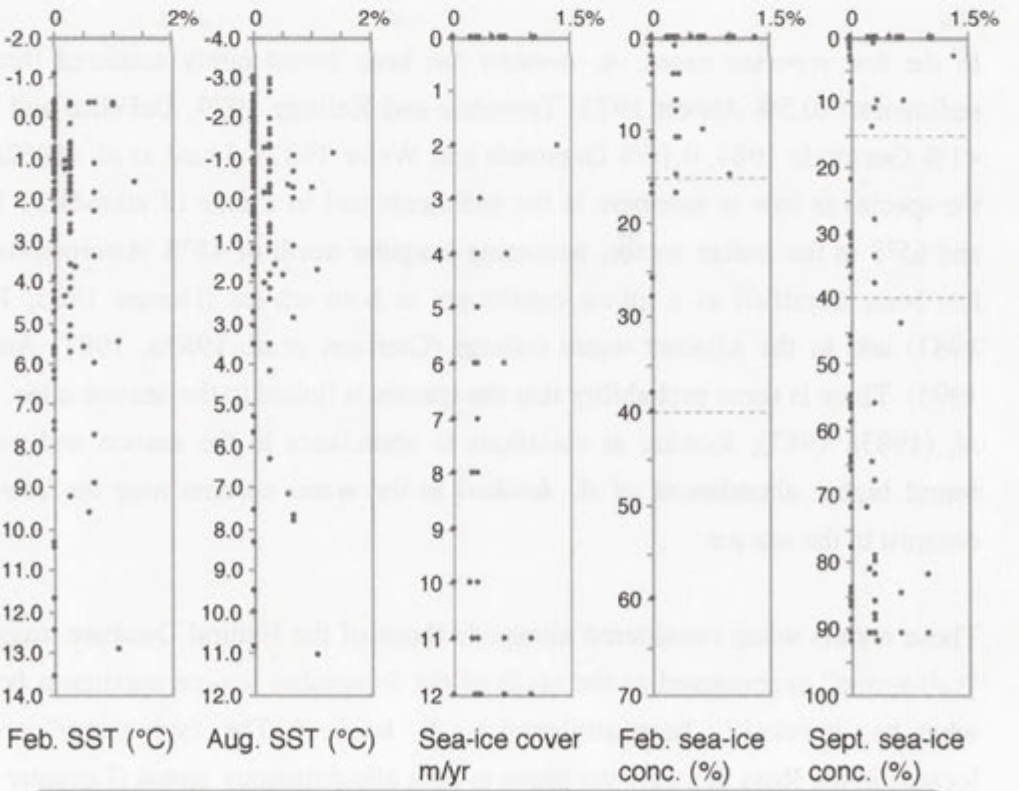

Figure 3.5b. Relative abundances against February and August SST, sea-ice cover in months per year and sea-ice concentration (%) in February and September (annual minimum and maximum sea-ice extents respectively). Other details as in Figure 3.2b.

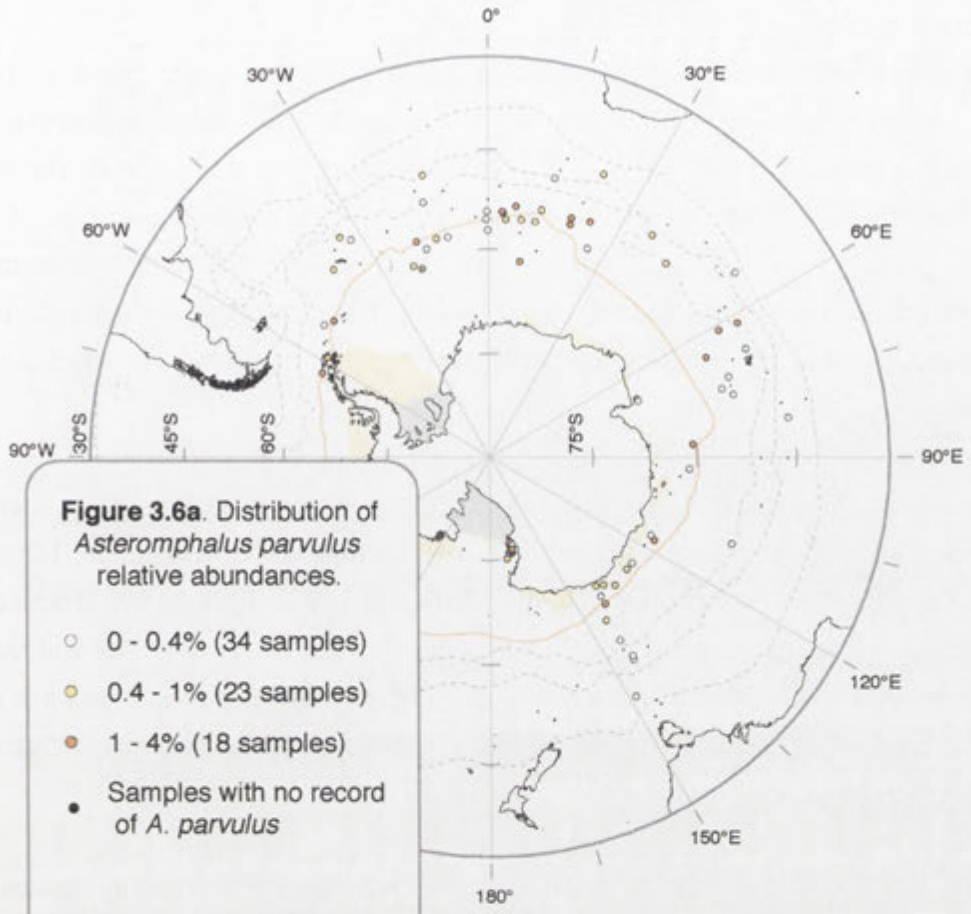

Figure 3.6a. Distribution of *Asteromphalus parvulus* relative abundances.

- 0 - 0.4% (34 samples)
- 0.4 - 1% (23 samples)
- 1 - 4% (18 samples)
- Samples with no record of *A. parvulus*

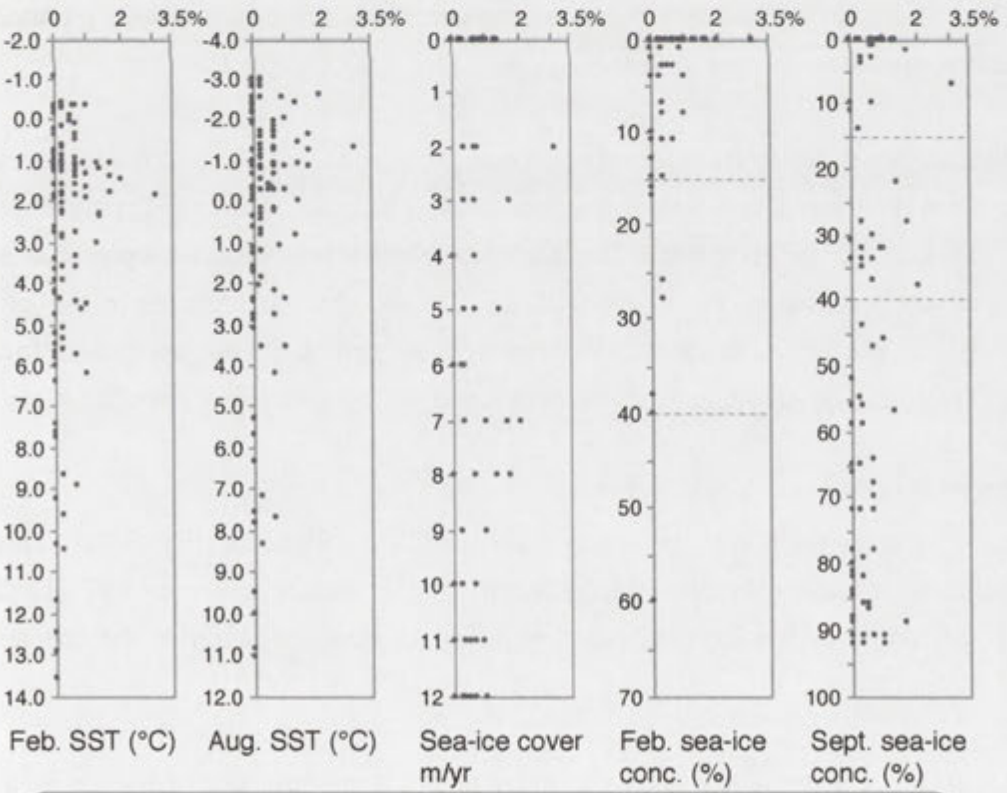

Figure 3.6b. Relative abundances against February and August SST, sea-ice cover in months per year and sea-ice concentration (%) in February and September (annual minimum and maximum sea-ice extents respectively). Other details as in Figure 3.2b.

3A.3.5 *ASTEROMPHALUS PARVULUS*

The distribution of *Asteromphalus parvulus* in the Southern Ocean is maximised in the POOZ, abundances falling off both to the north and south, with some regionalised increases near the Antarctic coast (Fig. 3.6a). Distribution against temperature shows maximum abundances are observed under February SST of 2°C, but within a range of -0.5° to 6°C. August SST show a similar abundance relationship with maximum abundances noted from -3° to -1 °C. Very poor relationships are noted with sea-ice in September and in months per year. The latter indicates some bi-modality. The species is affiliated with open ocean conditions during February (Fig. 3.6b).

Previous investigations suggest *A. parvulus* is not dominant near the Antarctic coast although present in <1% abundances (Truesdale and Kellogg 1979, Gersonde 1984, Kellogg and Kellogg 1987, Stockwell *et al.* 1991, Tanimura 1992). Abbott (1973) found the species commonly in his samples of the POOZ region but most were at <0.4% and the maximum abundance was at 1%. DeFelice and Wise (1981) found *A. parvulus* to have a distinct northern boundary at the Polar Front, with increased numbers between 50° and 60°S in the South Atlantic.

Horner (1985) and Krebs *et al.* (1987) report *A. parvulus* as a species found in sea-ice. Garrison *et al.* (1987) found no presence of the species in spring sea-ice samples of the Weddell Sea, but in abundance in the neighbouring water column. Cassie (1963) reported scarce occurrences of the species in water samples under sea-ice in the Ross Sea.

These results are not different from the other reports presented. Yet, the distribution does continue beyond the Polar Front in trace occurrences. Open ocean conditions appear to be linked with the presence of the species. The lack of differentiation with sea-ice presence is difficult to advance comment, especially with the few reported occurrences in sea-ice. There may be no relation whatsoever or there may be speciation not accounted for. Difficulties under this latter topic have been mentioned for this genus in section 2.2.4.

3A.3.6 *AZPEITIA TABULARIS*

Azpeitia tabularis has a northward increasing presence in the sediments (Fig. 3.7a). This is observed with maximum abundances (maximum 24.2%) located in warm SST (13°C February, 11°C August). Sea-ice does not play a role in the distribution of the species (Fig. 3.7b).

Trace occurrences of *A. tabularis* along the Antarctic coast, as observed in Figure 3.7a, have been reported by others (Truesdale and Kellogg 1979, <0.15% Stockwell *et al.* 1991, <0.1% Tanimura 1992, av. <0.5% Leventer 1992). Zielinski and Gersonde (1997)

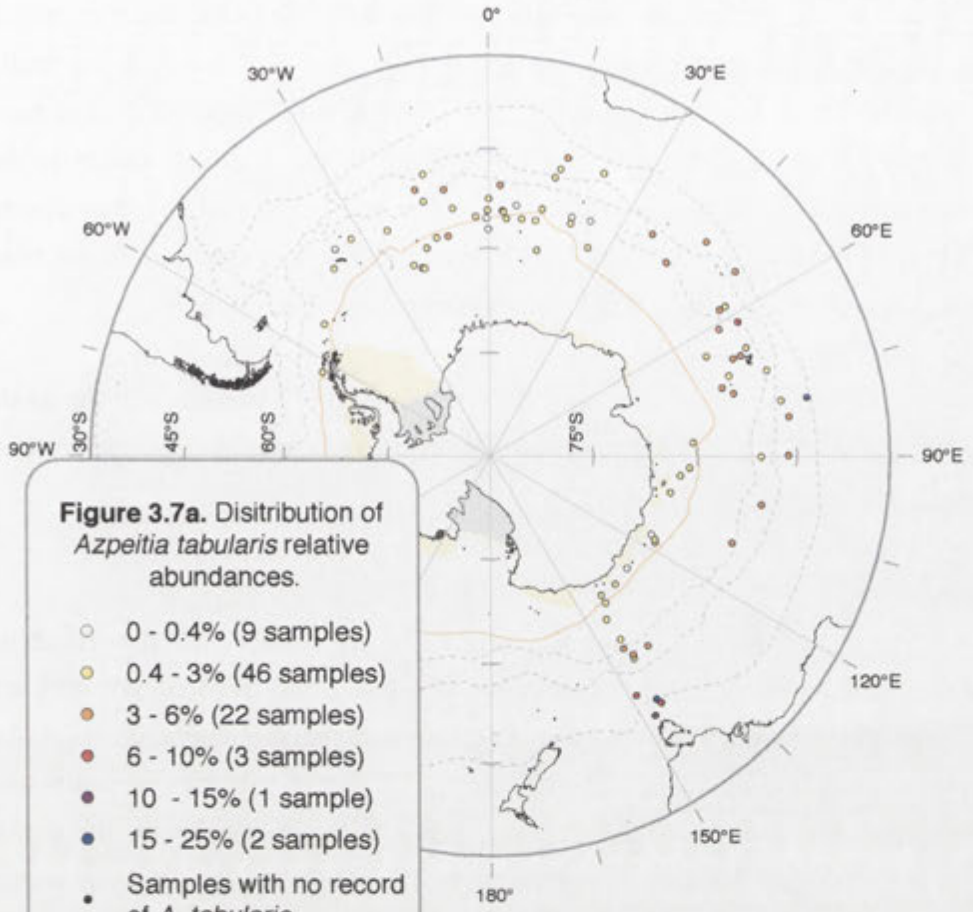

Figure 3.7a. Disitribution of *Azpeitia tabularis* relative abundances.

- 0 - 0.4% (9 samples)
- 0.4 - 3% (46 samples)
- 3 - 6% (22 samples)
- 6 - 10% (3 samples)
- 10 - 15% (1 sample)
- 15 - 25% (2 samples)
- Samples with no record of *A. tabularis*

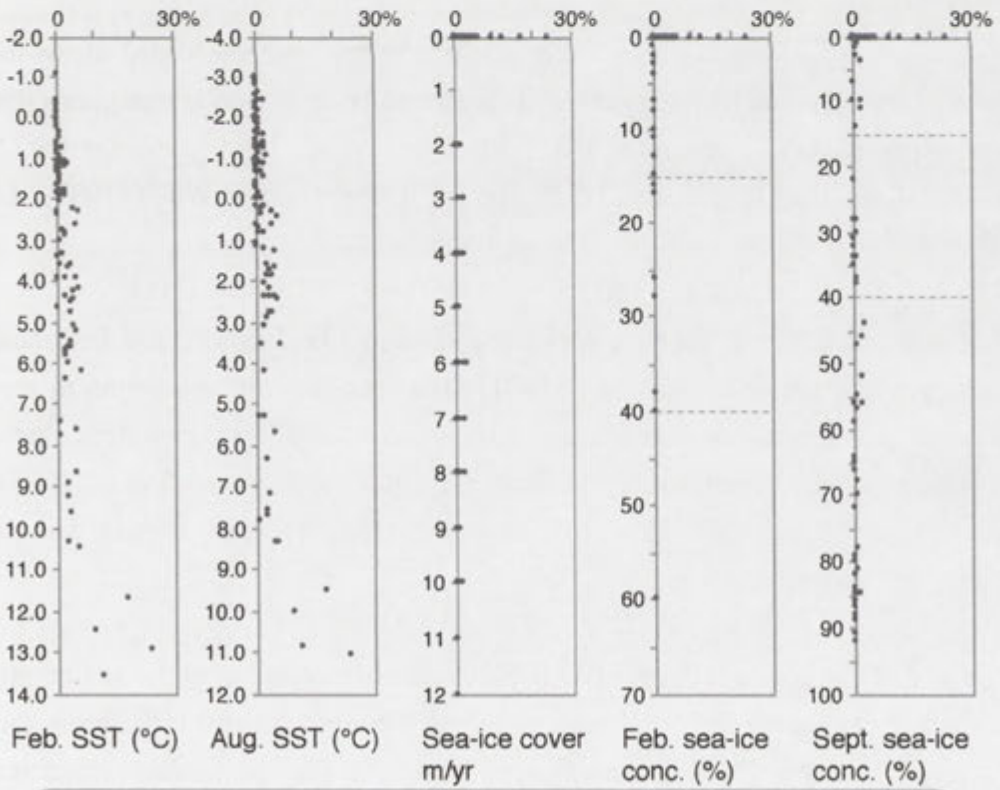

Figure 3.7b. Relative abundances against February and August SST, sea-ice cover in months per year and sea-ice concentration (%) in February and September (annual minimum and maximum sea-ice extents respectively). Other details as in Figure 3.2b.

suggest the species is restricted to the south by the maximum winter sea-ice edge which generally appears to be the case. Increased abundances to the north were originally described as patchy (Jousé *et al.* 1962a, Abbott 1973, DeFelice and Wise 1981), but have been recounted by others to occur from the Polar Front in the Southern Ocean to the Indonesian Archipelago and southeast Atlantic (Schuette and Schrader 1981, van Iperen *et al.* 1993, Treppke *et al.* 1996, Zielinski and Gersonde 1997). The species has not been reported since the work of Horner (1985) as being present in sea-ice samples.

The observations made here are in line with those presented by Zielinski and Gersonde (1997) with the addition of increased maximum abundances at a higher temperature, a result of the inclusion of southeast Indian Ocean samples.

3A.3.7 *COCCONEIS* SPP.

The *Cocconeis* spp. distribution is almost completely regionalised to the Antarctic Peninsula region (Fig. 3.8a) with abundances up to 5.9%. Rare trace occurrences are noted along the maximum winter sea-ice edge. Distribution against temperature show the localised response with the maximum abundance at 0.5°C and -3°C in February and August respectively (Fig. 3.8b). The relationship with sea-ice cover indicates the genus has a preference for >11 months cover with a range of 30-60% sea-ice cover in winter and generally open water conditions in summer.

All sedimentary records of the various *Cocconeis* species have been recorded along the Antarctic coast (Truesdale and Kellogg 1979, Prasad and Nienow 1986, maximum 4% Kellogg and Kellogg 1987, maximum 0.8% Stockwell *et al.* 1991, Leventer 1992, maximum 4% Tanimura 1992) with exception to DeFelice and Wise (1981, *C. scutellum*).

Cocconeis costata and *C. fasciolata* have been categorised as a land fast-ice and both land fast and pack species respectively (Garrison 1991). The species have been found in sea-ice studies in Arthur Harbor, Antarctic Peninsula (Krebs *et al.* 1987) and in water column samples of summer ice free months of Terra Nova Bay, Ross sea (Andreoli *et al.* 1995). Scott *et al.* (1994) characterised *Cocconeis* taxa as related to high salinity fast-ice consisting of ~90% congelation ice.

The observations of *Cocconeis* are similar to those previously recorded in the sediments. Maximum abundances are the same and rare coastal contributions are also reflected in this Natural Database (eg Prydz Bay and near George V Coast). The species are considered benthic and associated with land fast-ice and this is reflected in their distribution.

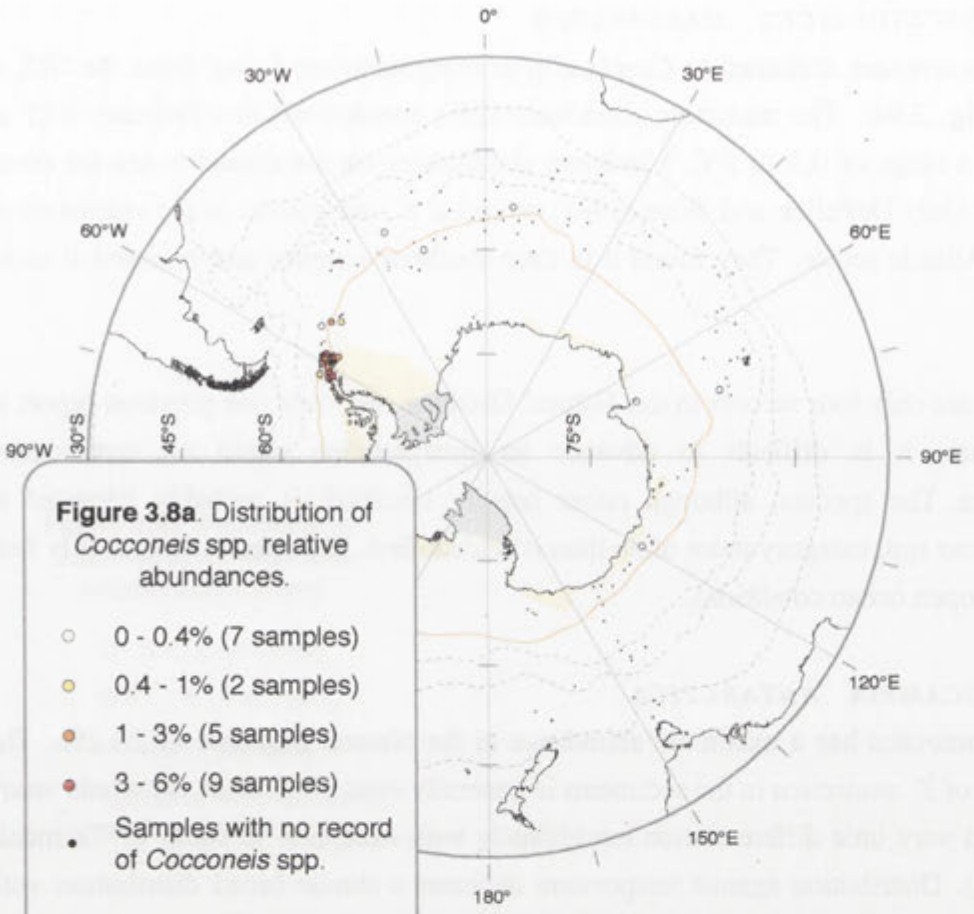

Figure 3.8a. Distribution of *Cocconeis* spp. relative abundances.

- 0 - 0.4% (7 samples)
- 0.4 - 1% (2 samples)
- 1 - 3% (5 samples)
- 3 - 6% (9 samples)
- Samples with no record of *Cocconeis* spp.

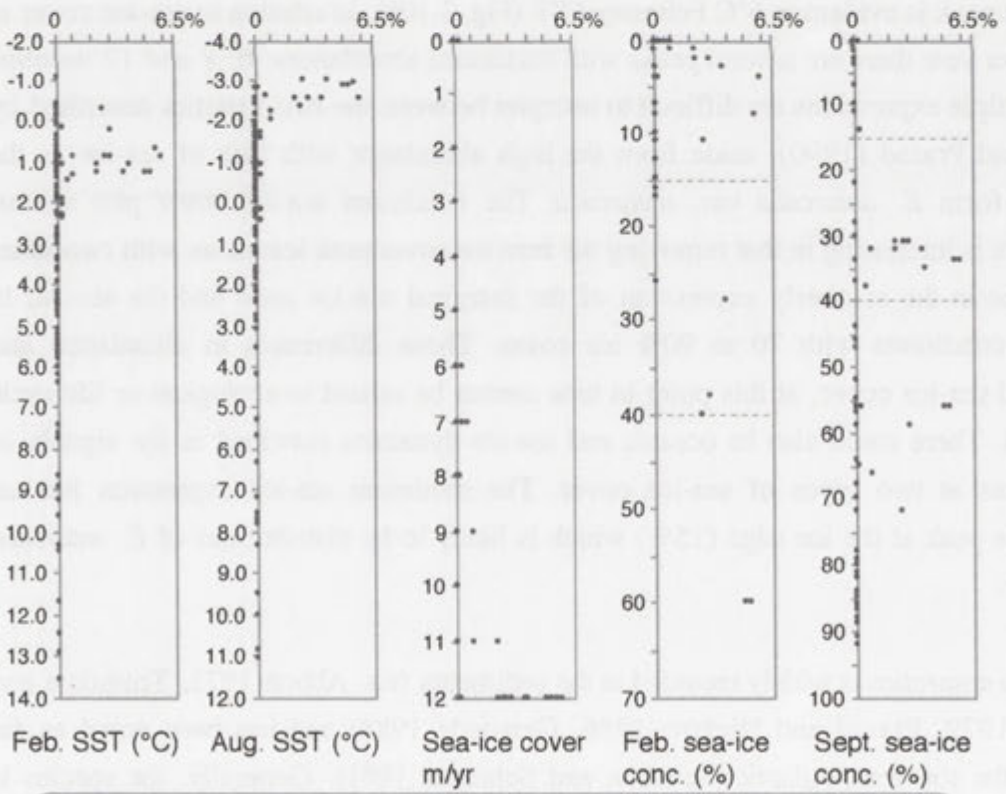

Figure 3.8b. Relative abundances against February and August SST, sea-ice cover in months per year and sea-ice concentration (%) in February and September (annual minimum and maximum sea-ice extents respectively). Other details as in Figure 3.2b.

3A.3.8 *COSCINODISCUS MARGINATUS*

The few occurrences attributed to *Coscinodiscus marginatus* are found from the SIZ to the PFZ (Fig. 3.9a). The maximum abundance (2%) corresponds to a February SST of 2°C within a range of 0.5 to 5°C. Maximum abundances are not related to sea-ice cover (Fig. 3.9b). Only DeFelice and Wise (1981) recorded *C. marginatus* in the sediments of the South Atlantic sector. They found it in their southern samples and believed it to be reworked.

Since there are only four records in the Natural Database and only one previous report in the literature, it is difficult to advance an interpretation based on sedimentary distributions. The species, although rather heavily silicified, is probably relegated to *Coscinodiscus* spp. category more often than it is identified. The species is probably best ascribed to open ocean conditions.

3A.3.9 *EUCAMPIA ANTARCTICA*

Eucampia antarctica has a maximum abundance in the Natural Database of 23.2%. The distribution of *E. antarctica* in the sediments is generally even throughout the whole study region, with very little differentiation meridionally with exception to south of Tasmania (Fig. 3.10a). Distribution against temperature indicates a similar broad distribution with abundance peaking at 0°C February SST and -0.5°C August SST. A second, less dominant peak is evident at 6°C February SST (Fig. 3.10b). In relation to sea-ice cover in months per year there are several peaks with maximum abundances: 0, 8 and 12 months. Such multiple expressions are difficult to interpret between the two varieties described by Fryxell and Prasad (1990), aside from the high abundance with lack of sea-ice as the subpolar form *E. antarctica* var. *antarctica.* The maximum sea-ice cover plot against abundance is interesting in that removing the zero ice cover peak leaves us with two other peaks, one in the southerly expression of the marginal sea-ice zone and the second in pack-ice conditions with 70 to 90% ice cover. These differences in abundance and associated sea-ice cover, at this point in time cannot be related to ecological or life cycle dynamics. There could also be oceanic and sea-ice dynamics entwined in the signals of abundances at two types of sea-ice cover. The minimum sea-ice expression has an abundance peak at the ice edge (15%) which is likely to be distributions of *E. antarctica* var. *recta.*

Eucampia antarctica is widely recorded in the sediments (eg. Abbott 1973, Truesdale and Kellogg 1979, Prasad and Nienow 1986, Gersonde 1984) and has been noted as far north as the southeast Atlantic (Schuette and Schrader 1981). Generally, the species is noted in low abundance near the Antarctic coast (Donahue 1973, Tanimura 1992, Gersonde and Wefer 1987, Stockwell *et al.* 1991, Fryxell 1991, Leventer 1992) although

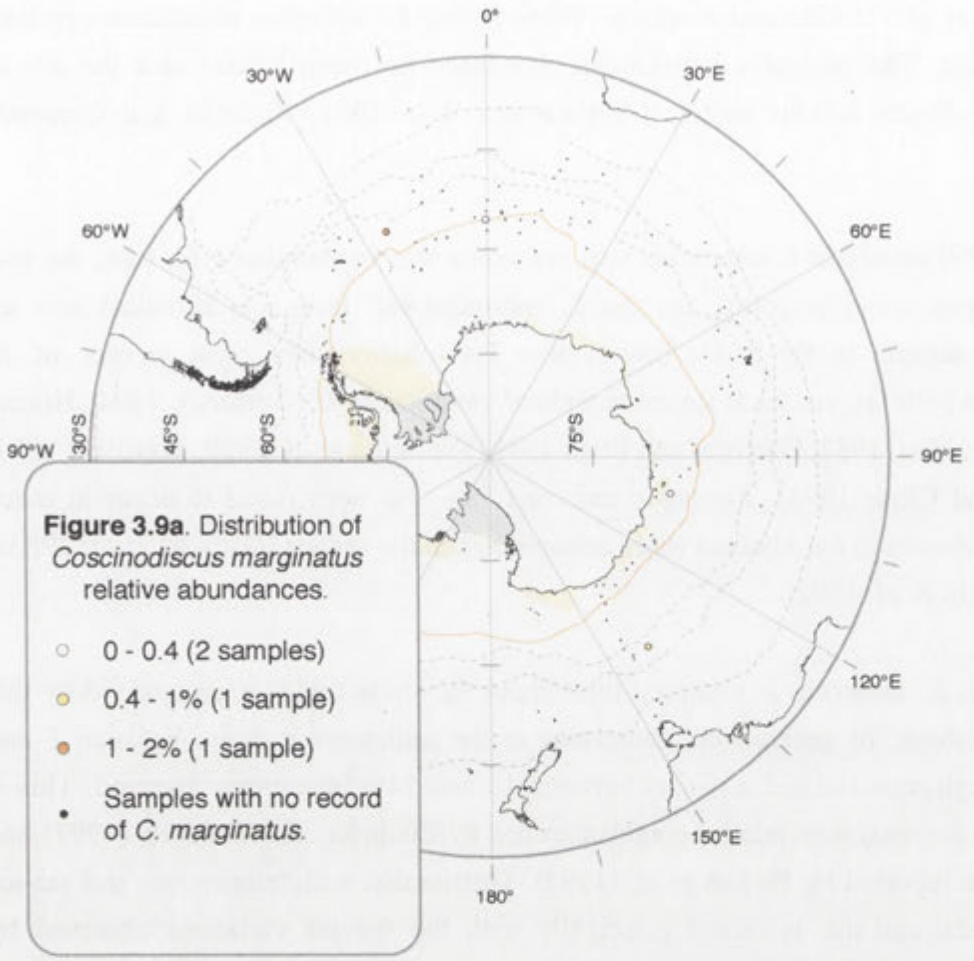

Figure 3.9a. Distribution of *Coscinodiscus marginatus* relative abundances.

- 0 - 0.4 (2 samples)
- 0.4 - 1% (1 sample)
- 1 - 2% (1 sample)
- Samples with no record of *C. marginatus*.

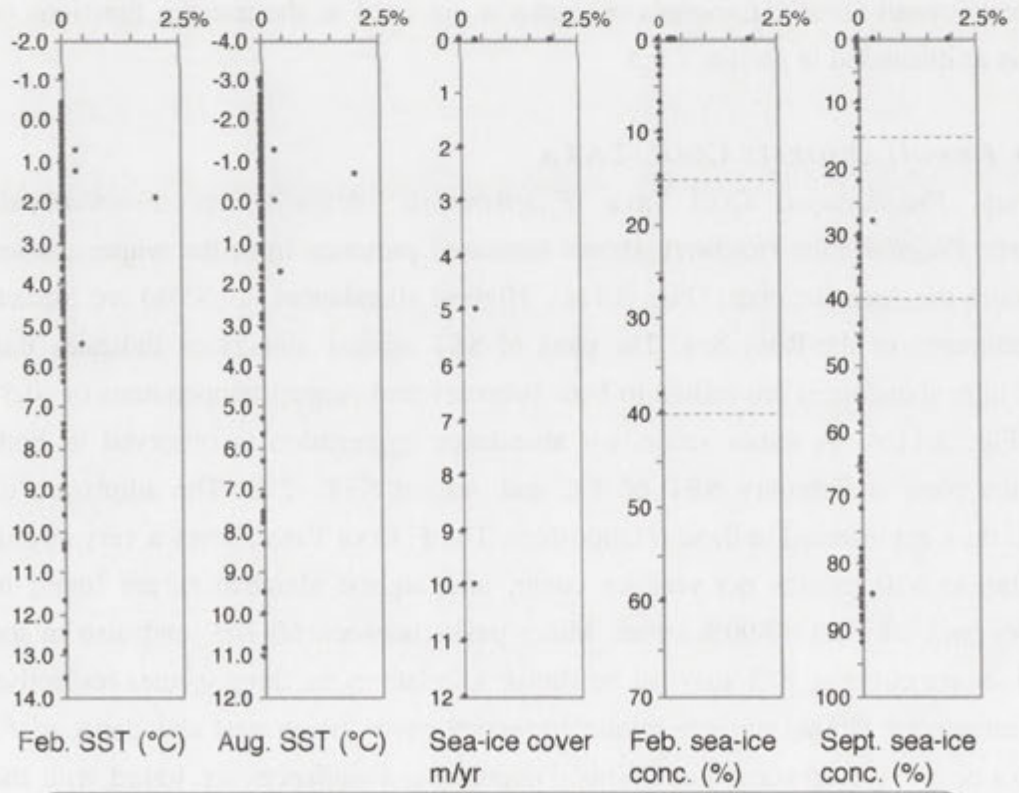

Figure 3.9b. Relative abundances against February and August SST, sea-ice cover in months per year and sea-ice concentration (%) in February and September (annual minimum and maximum sea-ice extents respectively). Other details as in Figure 3.2b.

both Jousé *et al.* (1962a) and Kozlova (1966) found *E. antarctica* abundances greatest near the coast. The generalised maximum abundance has been located near the sea-ice edge in the South Atlantic sector (DeFelice and Wise 1981, Zielinski and Gersonde 1997).

Fryxell (1989) noted that *E. antarctica* var. *antarctica* was in abundance far from the sea-ice in the open ocean in spring, and that *E. antarctica* var. *recta* was abundant near ice during the autumn in the Prydz Bay region. Presumably, then most records of *E. antarctica* in both fast and pack-ice are records of variation *recta* (Gersonde 1984, Horner 1985, Krebs *et al.* 1987, Garrison and Buck 1989, Tanimura *et al.* 1990, Garrison 1991, Garrison and Close 1993). *Eucampia antarctica* has also been noted to occur in much higher abundances in the adjacent water column than in the sea-ice (Garrison *et al.* 1983a, 1987, Bianchi *et al.* 1992).

In summary, *E. antarctica* is observed throughout the study region encompassed by this Natural Database. In general, the abundance in the sediments is noted between 1 and 15%, although rarer isolated instances between 15 and 24% have been observed. This is greater than the maximum relative abundance cited by Zielinski and Gersonde (1997) and less than that reported by Pichon *et al.* (1992). Distribution with temperature and sea-ice is multi-modal and this is related principally with the species variations observed by Prasad and Fryxell (1990). *Eucampia antarctica* is not used in the transfer functions of this thesis as discussed in section 2.3.5

3A.3.10 *FRAGILARIOPSIS* COOL TAXA

The group, *Fragilariopsis* Cool Taxa (*Fragilariopsis obliquecostata, Fragilariopsis sublinearis, Fragilariopsis ritscheri*), shows increased presence from the winter sea-ice maximum to the Antarctic coast (Fig. 3.11a). Highest abundances (27.85%) are located in the sediments of the Ross Sea. The plots of SST against abundance indicates that localised high abundances are related to both February and August temperatures of -0.5° to 0°C (Fig. 3.11b). A minor secondary abundance aggregation is observed in both temperature plots at February SST of 1°C and August SST -2°C. The admixture of species is thus, represented in these relationships. The *F.* Cool Taxa shows a very strong relationship to >10 months per year ice cover, and highest abundances are found in September pack-ice with 80-90% cover. Minor peaks between 60-70% and also in the marginal sea-ice cover at 30% may yet be shown to relate to the three species respective habitat preferences. During summer minimum sea-ice cover the greatest abundance of *F.* Cool Taxa occur in open ocean conditions. Diminishing abundances are found with the presence of more consolidated sea-ice cover.

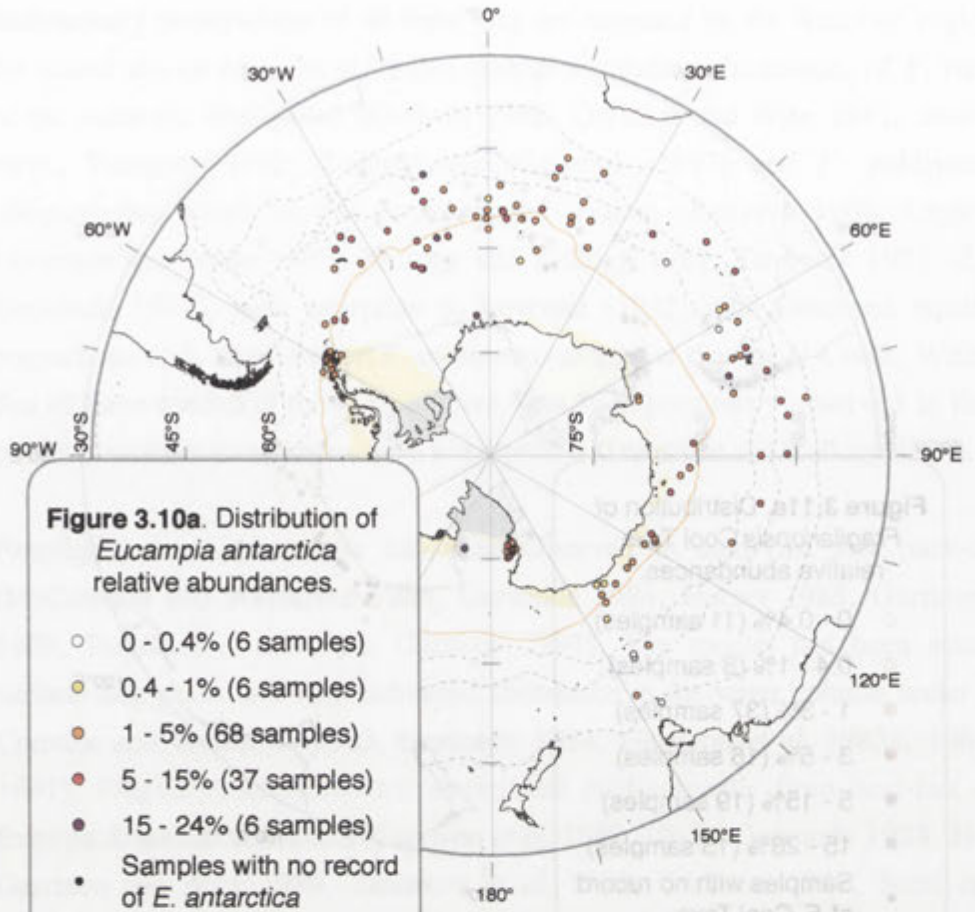

Figure 3.10a. Distribution of *Eucampia antarctica* relative abundances.

- 0 - 0.4% (6 samples)
- 0.4 - 1% (6 samples)
- 1 - 5% (68 samples)
- 5 - 15% (37 samples)
- 15 - 24% (6 samples)
- Samples with no record of *E. antarctica*

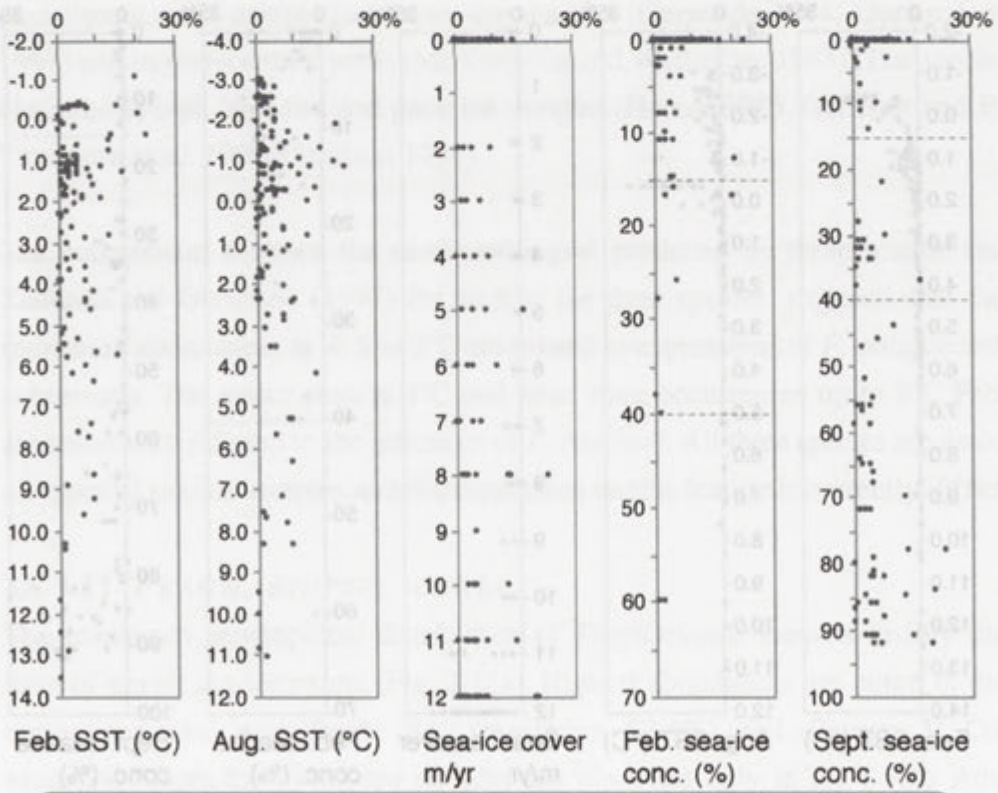

Figure 3.10b. Relative abundances against February and August SST, sea-ice cover in months per year and sea-ice concentration (%) in February and September (annual minimum and maximum sea-ice extents respectively). Other details as in Figure 3.2b.

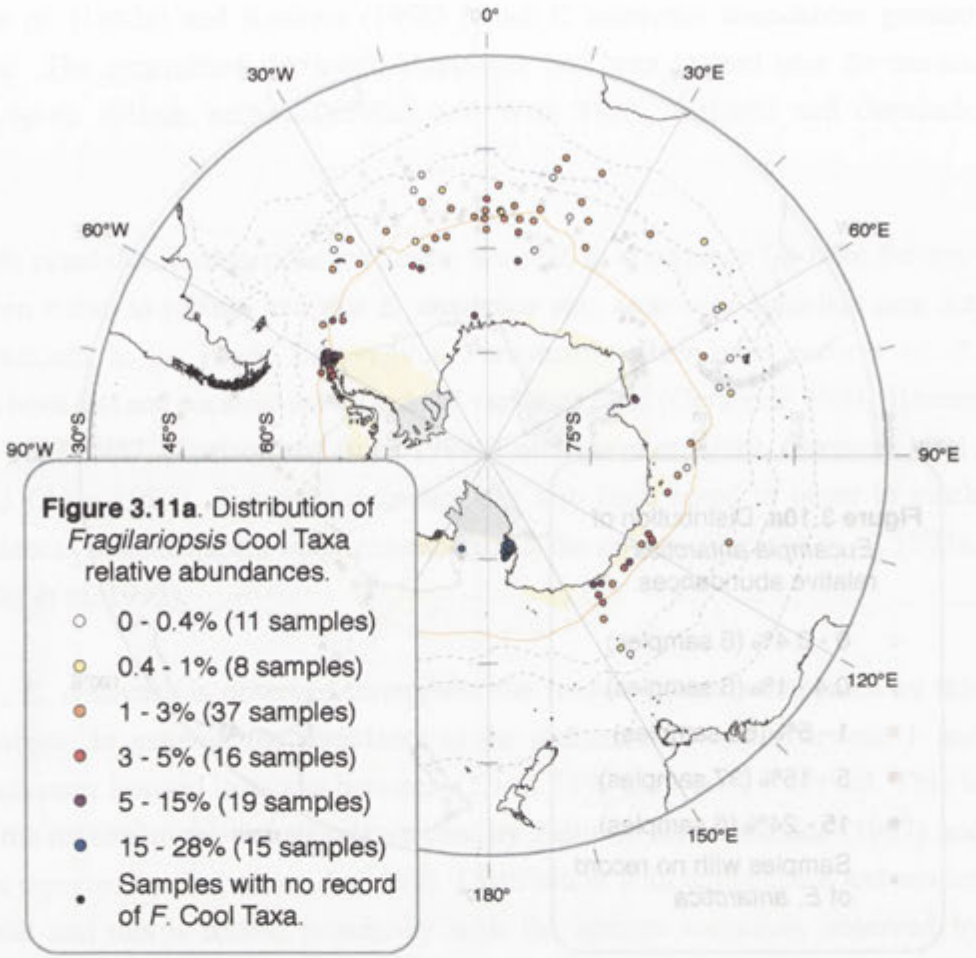

Figure 3.11a. Distribution of *Fragilariopsis* Cool Taxa relative abundances.

- 0 - 0.4% (11 samples)
- 0.4 - 1% (8 samples)
- 1 - 3% (37 samples)
- 3 - 5% (16 samples)
- 5 - 15% (19 samples)
- 15 - 28% (15 samples)
- Samples with no record of *F.* Cool Taxa.

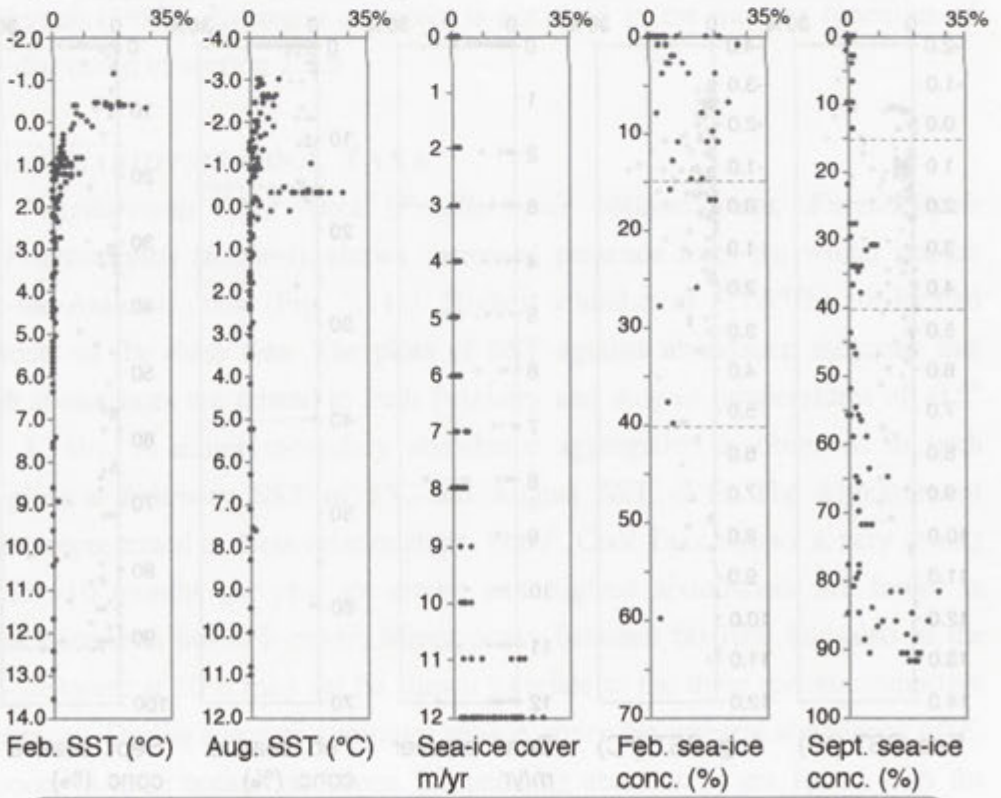

Figure 3.11b. Relative abundances against February and August SST, sea-ice cover in months per year and sea-ice concentration (%) in February and September (annual minimum and maximum sea-ice extents respectively). Other details as in Figure 3.2b.

Sedimentary preservation of all three taxa are focussed on the Antarctic region south of the winter sea-ice edge. Most studies indicate increasing abundances of *F. ritscheri* north of the Antarctic divergence (Kozlova 1966, DeFelice and Wise 1981, Stockwell *et al.* 1991, Tanimura 1992, Zielinski and Gersonde 1997) and *F. sublinearis* and *F. obliquecostata* south of this oceanographic feature (Kozlova 1966, Gersonde 1984, Gersonde and Wefer 1987, Kellogg and Kellogg 1987, Tanimura 1992, Zielinski and Gersonde 1997), with exception to Leventer (1992) who observed equal maximum proportions of *F. ritscheri* and *F. sublinearis* along the George V Coast. Within the Ross Sea all three species of the *F.* Cool Taxa have been previously observed in the sediments but their relative abundances were not reported (Truesdale and Kellogg 1979).

Fragilariopsis obliquecostata has been observed in land fast and pack-ice samples (McConville and Wetherbee 1983, Gersonde 1984, Horner 1985, Garrison and Buck 1989, Tanimura *et al.* 1990, Garrison 1991). The species has been associated with surface melt pools and with increased abundance in the water column under sea-ice (Mc Conville and Wetherbee 1983, Gersonde 1984, Garrison *et al.* 1983a, 1987, Garrison 1991). *Fragilariopsis sublinearis* is reported predominantly from land-fast and less so from pack-ice environments (Garrison *et al.* 1982, 1983a, Gersonde 1984, Horner 1985, Garrison and Buck 1989, Tanimura *et al.* 1990, Garrison 1991, Scott *et al.* 1994). *Fragilariopsis ritscheri*, alike *F. obliquecostata*, has been found in higher abundances in the adjacent water column than in sea-ice samples (Gersonde 1984, Garrison *et al.* 1982, 1987) and in surface melt pools (Mc Conville and Wetherbee 1983). The species has been observed in both land-fast and pack-ice samples (Horner 1985, Garrison and Buck 1989, Tanimura *et al.* 1990, Garrison 1991).

The comparison between the combined signal produced by these results and those of Zielinski and Gersonde (1997) for each of the three species, suggests that the observed maximum abundances at -0.5 to 0°C are related to expressions of *F. obliquecostata* and *F. sublinearis*. The minor peak at 1°C and other trace occurrences up to 9°C February SST are tentatively referred to the influence of *F. ritscheri*. All three species are associated with all types of sea-ice samples and discrimination on this feature is currently difficult.

3A.3.11 *FRAGILARIOPSIS CURTA*

The maximum geographical distribution of *Fragilariopsis curta* is visibly linked to the limit of winter sea-ice extent (Fig. 3.12a). Highest abundances are noted in the Ross Sea region and also near Prydz Bay (maximum 67.4%) and George V Coast. Trace excursions from the winter sea-ice edge are observed only in the South Atlantic Ocean and are most likely linked to iceberg pathways. The relation to sea-ice cover is observed

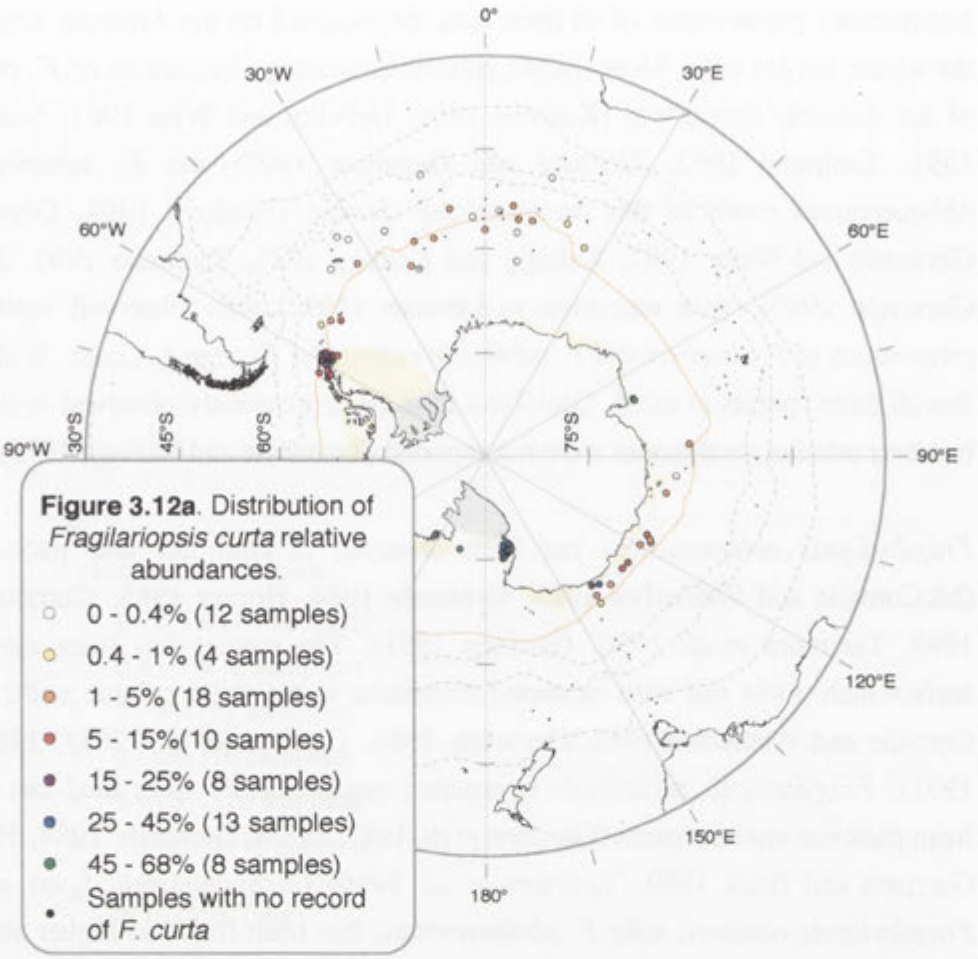

Figure 3.12a. Distribution of *Fragilariopsis curta* relative abundances.

- 0 - 0.4% (12 samples)
- 0.4 - 1% (4 samples)
- 1 - 5% (18 samples)
- 5 - 15%(10 samples)
- 15 - 25% (8 samples)
- 25 - 45% (13 samples)
- 45 - 68% (8 samples)
- Samples with no record of *F. curta*

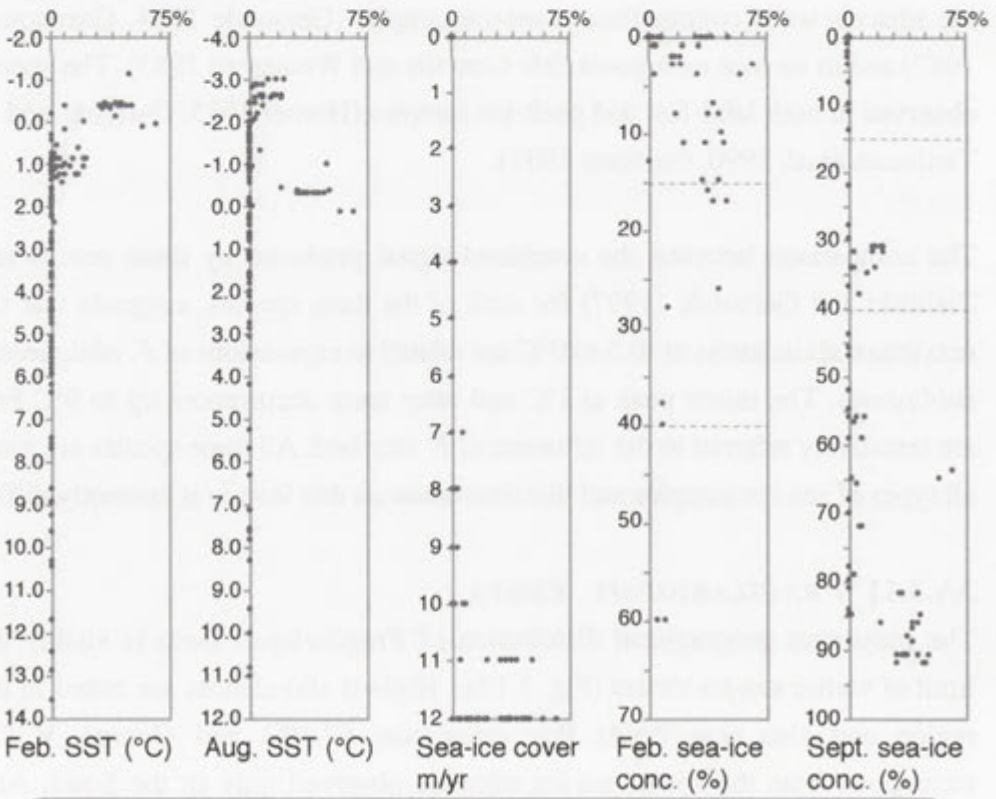

Figure 3.12b. Relative abundances against February and August SST, sea-ice cover in months per year and sea-ice concentration (%) in February and September (annual minimum and maximum sea-ice extents respectively). Other details as in Figure 3.2b.

in the sea-ice plots against abundance (Fig. 3.12b). Highest abundances are linked with 11-12 months ice cover, where highly consolidated ice conditions exist during winter (65-90%) and open ocean conditions exist in summer. Species abundance drops dramatically when summer sea-ice cover increases. The temperature plots exhibit major abundances in February and August water temperatures of 0 to -1°C which are in accord with the sea-ice influence. Only one occurrence of this species was observed in SST over 1.7°C.

Most reference to *F. curta* in sediment samples indicate highest abundances near the Antarctic coast (Kozlova 1966, Truesdale and Kellogg 1979, DeFelice and Wise 1981, Gersonde 1984, Gersonde and Wefer 1987, Kellogg and Kellogg 1987, Stockwell *et al.* 1991, Leventer 1992, Tanimura 1992, Zielinski and Gersonde 1997). Maximum abundances around the Antarctic continent are reported as 42% off the Filschner-Ronne ice shelf (Gersonde 1984), 57% in the coastal Weddell Sea (Zielinski and Gersonde 1997), 50% in Lützow-Holm Bay (Tanimura 1992), 68% Prydz Bay (Stockwell *et al.* 1991), 20-90% between Enderby Land and Prydz Bay (Kozlova 1966), 38% George V Coast (Leventer 1992), and 60% Amundsen Sea (Kellogg and Kellogg 1987). The northward scattered dispersion of *F. curta* in the South Atlantic beyond the winter maximum sea-ice edge was noted by DeFelice and Wise (1981) and Zielinski and Gersonde (1997). Abbott (1973) also mentions the presence of *F. curta* (maximum 3.6%) in his sediment samples of the southeast Indian Ocean but, this is not noted in the samples of this study.

Garrison (1991) ascribed *F. curta* as a species most common in both pack and fast-ice as on previous reports (eg. Gersonde 1984, Horner 1985, Krebs *et al.* 1987, Garrison *et al.* 1983a, 1987, Garrison and Buck 1989, Tanimura *et al.* 1990). The species is also noted in very high abundance in the water column near the sea-ice edge (Garrison *et al.* 1982, Fryxell 1989, Tanimura 1990, Kang and Fryxell 1992, 1993, Andreoli *et al.* 1995, Leventer and Dunbar 1996). Leventer and Dunbar (1996) suggest that in the western Ross Sea region the presence of congelation sea-ice, the predominant ice type of fast sea-ice, is associated with increased relative abundance of *F. curta* .

The distributions of *F. curta* against temperature, sea-ice and within the Southern Ocean confirm previous work in regard to the confined and specified habitat in which *F. curta* is observed. Past sea-ice interpretation will benefit from the retrieval of this species in core sediments. The species distribution in the sediments may be slightly affected by the distribution of icebergs in the South Atlantic.

3A.3.12 *FRAGILARIOPSIS* CYLINDRIFORM GROUP

Fragilariopsis Cylindriform Group (*Fragilariopsis cylindrus, Fragilariopsis vanheurckii, Fragilariopsis linearis*) is also clearly linked to regions with sea-ice cover with maximum abundances associated with maximum sea-ice cover (Fig. 3.13a,b). A bi-modal abundance plot against temperature is noted for this group, more strikingly with August SST at -3°C and 0°C. All abundances are linked with temperatures less than February SST <2°C and August SST <0.5°C. Sea-ice cover during summer is minimal although the maximum abundance is located at the sea-ice edge. Bi-modality in September maximum sea-ice cover is also evident with one peak at 30% and the other at 90%. Most occurrences are located in pack-ice conditions (ie >40% cover).

It has been well established that *F. cylindrus*, although in lesser numbers than *F. curta* (Abbott 1973, Zielinski and Gersonde 1997), occupies sea-ice covered environments and is in highest abundance near the Antarctic coast (>3% Gersonde 1984, <1.1 % Kellogg and Kellogg 1987, max. 1.61% Gersonde and Wefer 1987, max. 8.9% Stockwell *et al.* 1991, 11.7% Leventer 1992, maximum 12% Tanimura 1992, max 29% Zielinski and Gersonde 1997). *Fragilariopsis vanheurckii,* as discussed earlier (section 2.2.13), is believed to be associated with sea-ice cover and is increasingly diminished numbers than *F. cylindrus*. Leventer (1992) suggested that *F. vanheurckii* was linked to the maximum summer sea-ice edge in along the George V Coast. *Fragilariopsis linearis* likewise, is poorly represented in the sediments (Abbott 1973, Gersonde 1984, Prasad and Nienow 1986, Tanimura 1992).

For sea-ice distribution, *F. cylindrus* is the most dominant species recorded by most workers (eg. Gersonde 1984, Horner 1985, Krebs *et al* .1987, Garrison and Buck 1989, Tanimura *et al.* 1990, Garrison and Close 1993, Scott *et al.* 1994). The species is associated with both land fast and pack sea-ice (Garrison 1991), and has been found in extreme high abundance in the water column particularly at the melting sea-ice edge (Fryxell 1989, Kang and Fryxell 1992, 1993, Andreoli *et al.* 1995, Leventer and Dunbar 1996). *Fragilariopsis cylindrus* has been lined with sea-ice formation (Clarke and Ackley 1983, Garrison and Buck 1989, Garrison 1991). *Fragilariopsis vanheurckii* appears to be associated with the sea-ice edge and is in higher abundances in the adjacent water column than in sea-ice samples (Garrison *et al.* 1983a 1987, Tanimura *et al.* 1990). This species is considered only to be located in pack-ice samples (Garrison and Buck 1989, Garrison 1991). *Fragilariopsis linearis* has been found in both fast and pack-ice samples (Mc Conville and Wetherbee 1983, Gersonde 1984, Krebs *et al.* 1987, Garrison and Buck 1989, Garrison 1991).

In relating the bi-modal peaks observed in the winter expressions of SST and sea-ice cover, the maximum abundances must be assumed to be the signal of *F. cylindrus* since it

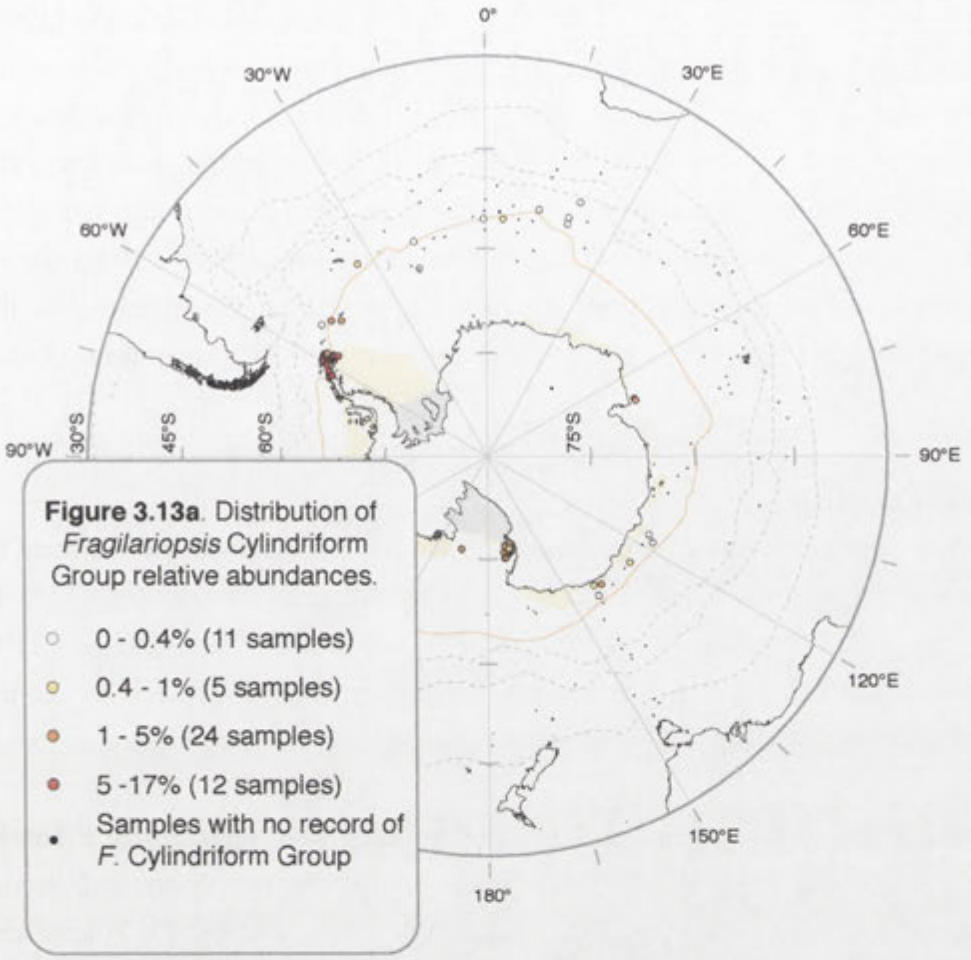

Figure 3.13a. Distribution of *Fragilariopsis* Cylindriform Group relative abundances.

- 0 - 0.4% (11 samples)
- 0.4 - 1% (5 samples)
- 1 - 5% (24 samples)
- 5 -17% (12 samples)
- Samples with no record of *F.* Cylindriform Group

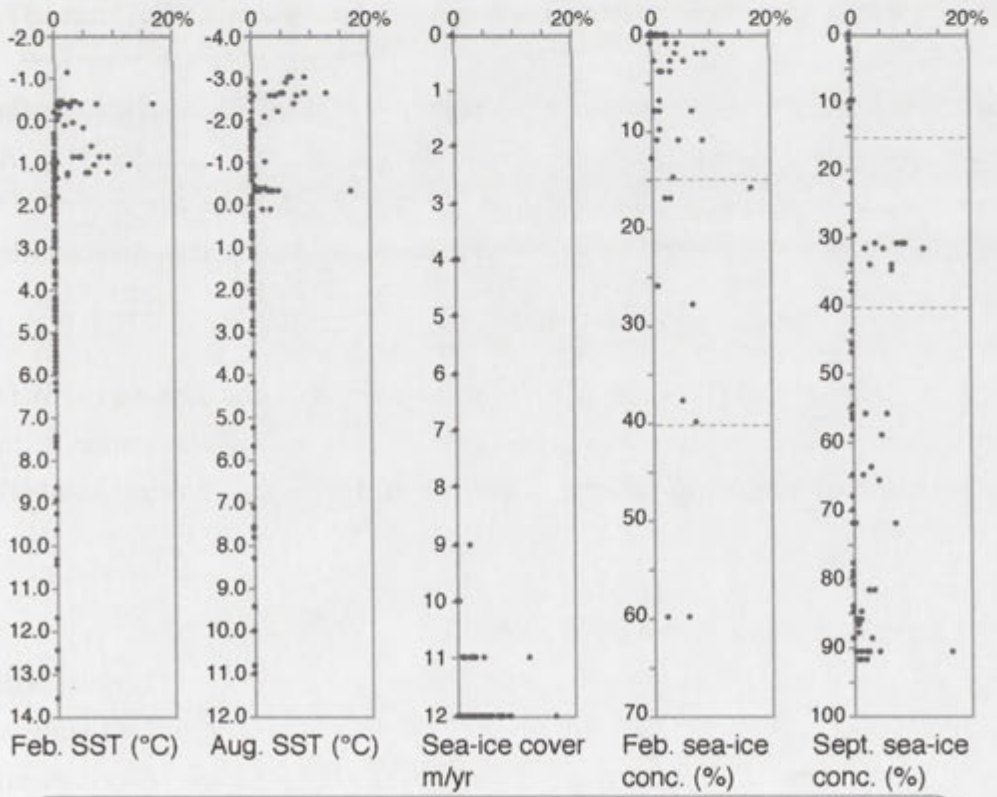

Figure 3.13b. Relative abundances against February and August SST, sea-ice cover in months per year and sea-ice concentration (%) in February and September (annual minimum and maximum sea-ice extents respectively). Other details as in Figure 3.2b.

is the more highly preserved species of the three. Yet, Zielinski and Gersonde (1997) report their highest abundance peak of *F. cylindrus* covering the two peaks noted in the February SST plot (ie -1 to 1°C) reported here. This later observation is most likely a response to the reduced sea-ice cover and summer conditions in the Antarctic. The differentiation of at least two of the species may become apparent in future biological studies directed at winter populations. Differentiation of sea-ice habitats at least for *F. vanheurckii* may also be of importance in assisting separation the species, as the September pack-ice dominance (sea-ice concentration between 30-40%) may be attributed in part to this species.

3A.3.13 *FRAGILARIOPSIS DOLIOLUS*

The seven observations of *Fragilariopsis doliolus* in the Natural Database are confined to the north by the Subantarctic Front (Fig. 3.14a). The maximum abundances (13% at 75°E) are found in SST expressions warmer than 7°C, and at maximum 13°C and 11°C February and August respectively. The species distribution has no relation to sea-ice cover (Fig. 3.14b).

Maximum abundances of this species in the Southern Ocean were reported by Zielinski and Gersonde (1997) as 29% at >15°C. Sediment studies further northward in the southeast Atlantic and Pacific have observed similar high abundances (~20% Pokras and Molfino 1986, >30% as a combined "southern group" van Iperen *et al.* 1987, max. 37% Schuette and Schrader 1981, max 3.2% Treppke *et al.* 1996, max. 14.4% coastal Peru Schuette and Schrader 1979a,b). Exterior to this region Abbott (1973, southeast Indian Ocean) records samples with occurrences of *F. doliolus* (maximum abundance 2%). All three samples occur in his most northerly sites. Further north, low average relative abundances from surface sediments (1.8%) in the Indonesian Archipelago are recorded (van Iperen *et al.* 1993).

As surmised by Zielinski and Gersonde (1997) for the sediments and Hasle (1976) for the surface waters, *F. doliolus* is a low to mid-latitude species. Its abundance in the sediments increases to the north of the SAF which limits the species southerly expression.

3A.3.14 *FRAGILARIOPSIS KERGUELENSIS*

The primary species preserved in the surface sediments is *Fragilariopsis kerguelensis*. Maximum abundances between 70-83% are noted to fall in a zone constrained between the maximum winter sea-ice edge and the Polar Front (Fig. 3.15a). *Fragilariopsis kerguelensis* presence in the sediments is more strongly reduced to the south under ice cover, than to the north. This latter feature however, is a function of the smaller number

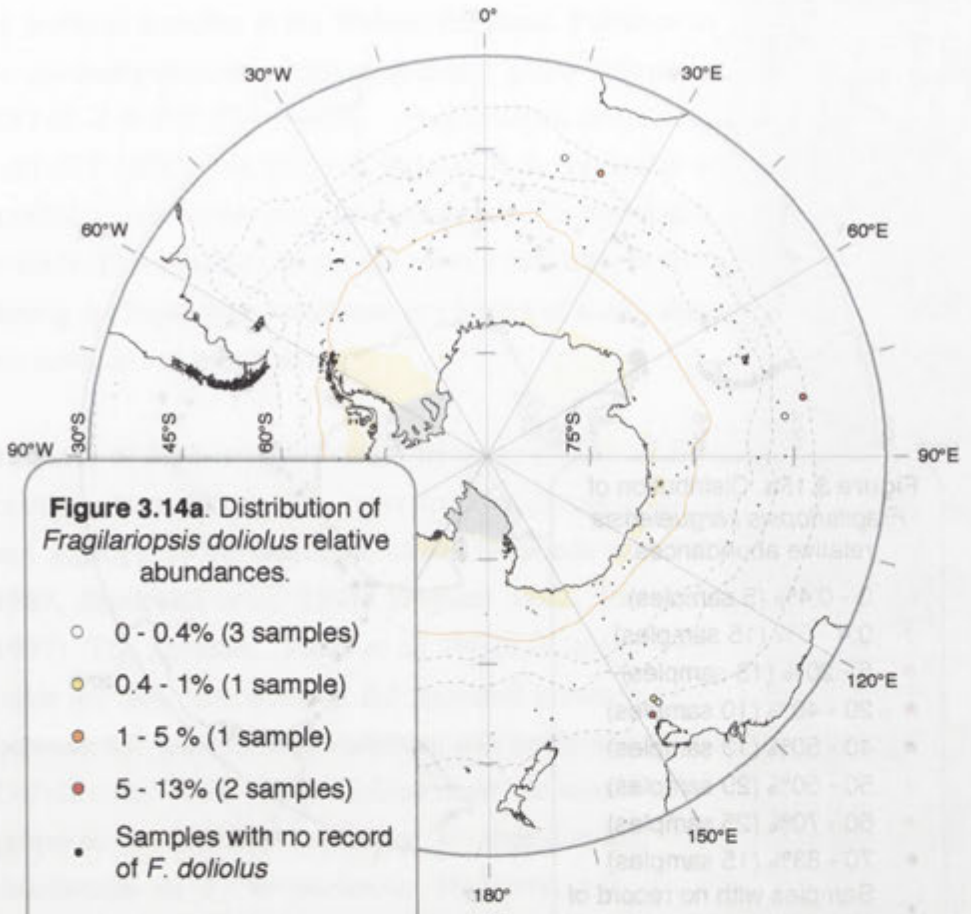

Figure 3.14a. Distribution of *Fragilariopsis doliolus* relative abundances.

- 0 - 0.4% (3 samples)
- 0.4 - 1% (1 sample)
- 1 - 5 % (1 sample)
- 5 - 13% (2 samples)
- Samples with no record of *F. doliolus*

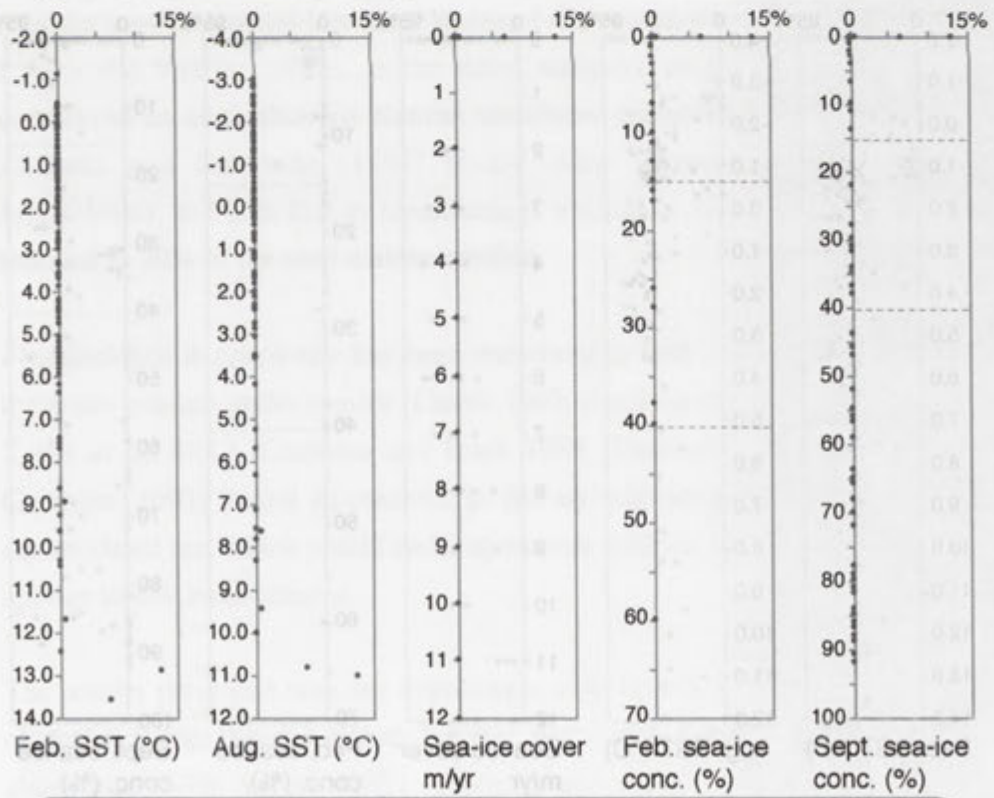

Figure 3.14b. Relative abundances against February and August SST, sea-ice cover in months per year and sea-ice concentration (%) in February and September (annual minimum and maximum sea-ice extents respectively). Other details as in Figure 3.2b.

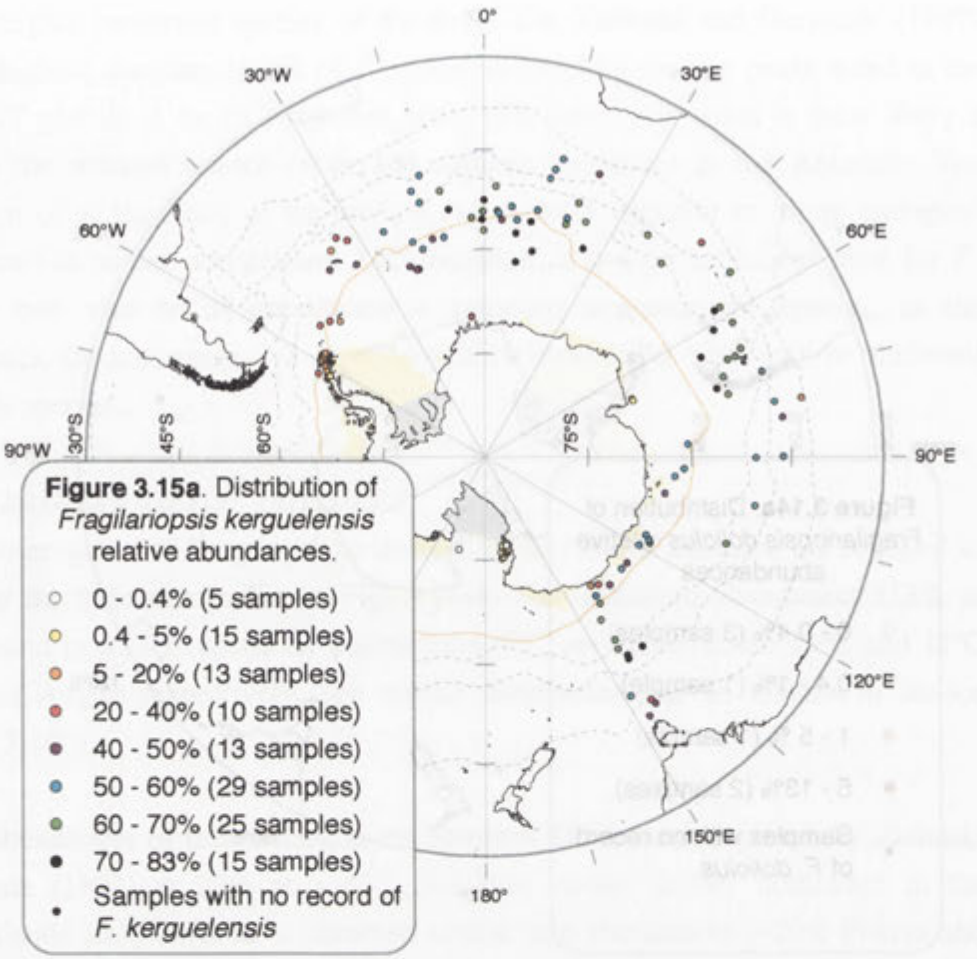

Figure 3.15a. Distribution of *Fragilariopsis kerguelensis* relative abundances.

- 0 - 0.4% (5 samples)
- 0.4 - 5% (15 samples)
- 5 - 20% (13 samples)
- 20 - 40% (10 samples)
- 40 - 50% (13 samples)
- 50 - 60% (29 samples)
- 60 - 70% (25 samples)
- 70 - 83% (15 samples)
- Samples with no record of *F. kerguelensis*

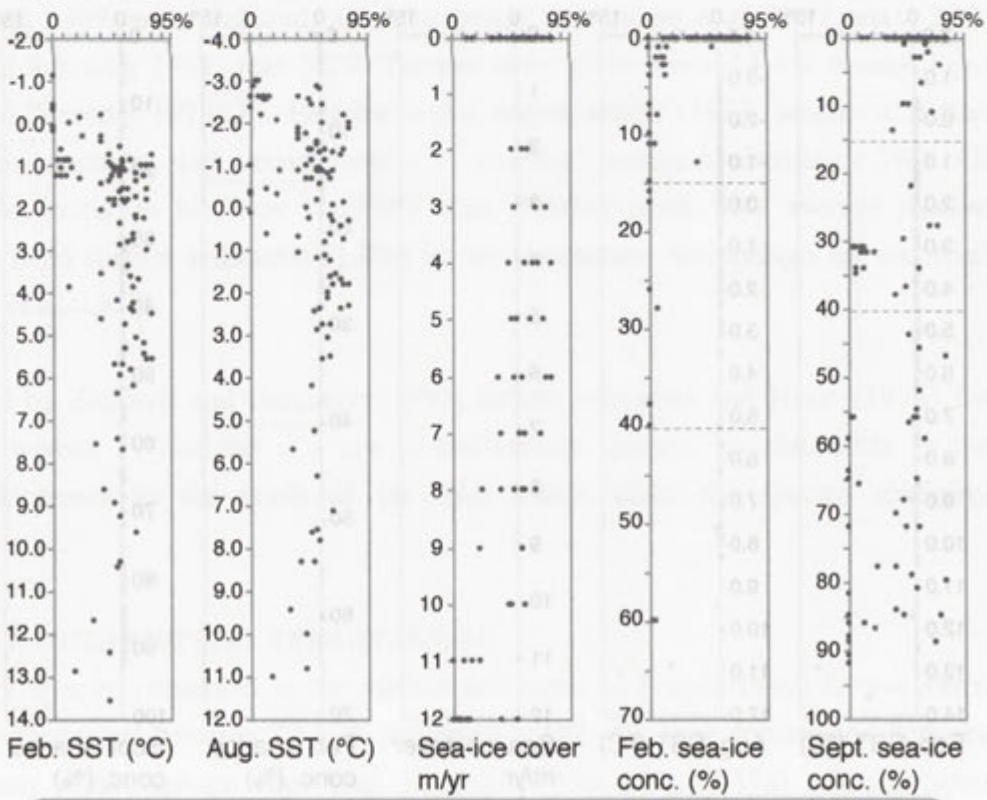

Figure 3.15b. Relative abundances against February and August SST, sea-ice cover in months per year and sea-ice concentration (%) in February and September (annual minimum and maximum sea-ice extents respectively). Other details as in Figure 3.2b.

of northern samples in the Natural Database. Presence in relation to SST reveals that *F. kerguelensis* occurs in high abundances under February SST of 1 to 10°C and August SST of -2 to 2°C (Fig. 3.15b) . *Fragilariopsis kerguelensis* is poorly represented in very cold SST <0°C (Feb. SST). It appears *F. kerguelensis* will support habitats with several months sea-ice cover, yet a decreasing trend in abundance with increasing sea-ice cover is evident. This tolerance to sea-ice cover is reflected in the generally equivalent distribution during the September maximum sea-ice cover across the range. In contrast, February sea-ice cover is not supported.

The lack of high numbers (from traces to <40%) of *F. kerguelensis* along the Antarctic coast has been observed by most workers (Jousé *et al.* 1962a, Kozlova 1966, Truesdale and Kellogg 1979, Gersonde 1984, Gersonde and Wefer 1987, Kellogg and Kellogg 1987, Stockwell *et al.* 1991, Leventer 1992, Tanimura 1992, Zielinski and Gersonde 1997). The Russians (Jousé *et al.* 1962a, Kozlova 1966, Kozlova and Mukhina 1967) made the first comments on the increased presence of *F. kerguelensis* in the sediments between 45° to 69°S. This statement still holds true in more recent studies (Abbott 1973, DeFelice and Wise 1981, Zielinski and Gersonde 1997, and this work). Hasle (1976) proposed a northern boundary at approximately the STC for the phytoplankton distribution of *F. kerguelensis*. However, van der Spoel *et al.* (1973) found *F. kerguelensis* up to 30°N in the phytoplankton, while sediment studies in the southeast Atlantic have also noted low abundances of *F. kerguelensis* (Schuette and Schrader 1981, Pokras and Molfino 1986). In the latter, sediment observations of *F. kerguelensis* are considered an allochthonous element introduced by northward bottom water movement. Zielinski and Gersonde (1997) review other elements in the distribution of *F. kerguelensis*, and note that its abundance in sediments, close to and north of the STC, are reduced to 20% of the total diatom number.

Fragilariopsis kerguelensis has been recovered in both fast and pack-ice samples and in the water column under sea-ice (Cassie 1963, Garrison *et al.* 1982, 1983a, Horner 1985, Krebs *et al.* 1987, Garrison and Buck 1989, Tanimura *et al.* 1990, Garrison 1991). Garrison (1991) linked its presence in fast-ice with ice platelet accumulation beneath the consolidated ice, which would be in agreement with an allochthonous introduction of the species to this environment.

The results presented here for distribution with February SST provide a mirror to those observed in the South Atlantic sector, with only a slightly less observed maximum abundance (83% versus 92%) (Zielinski and Gersonde 1997). In relation to sea-ice cover, *F. kerguelensis* appears to be similarly at home in consolidated sea-ice conditions as in open ocean conditions during the maximum winter sea-ice extent. The species,

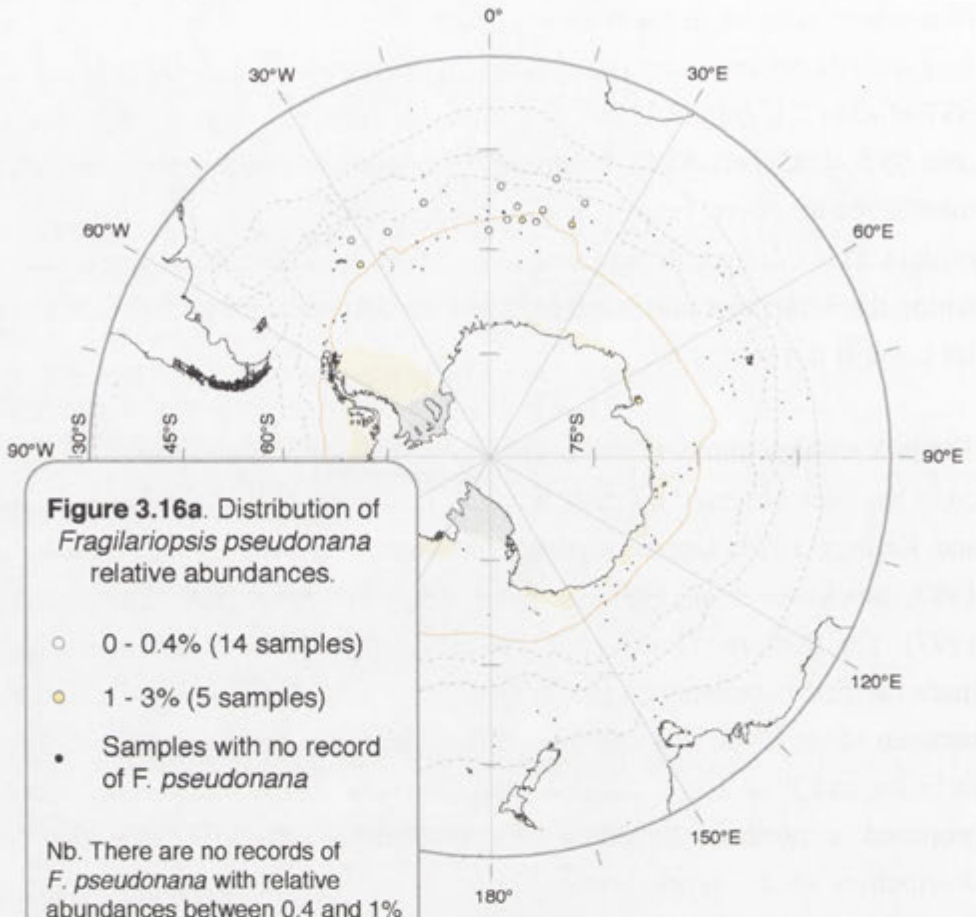

Figure 3.16a. Distribution of *Fragilariopsis pseudonana* relative abundances.

- 0 - 0.4% (14 samples)
- 1 - 3% (5 samples)
- Samples with no record of F. *pseudonana*

Nb. There are no records of *F. pseudonana* with relative abundances between 0.4 and 1%

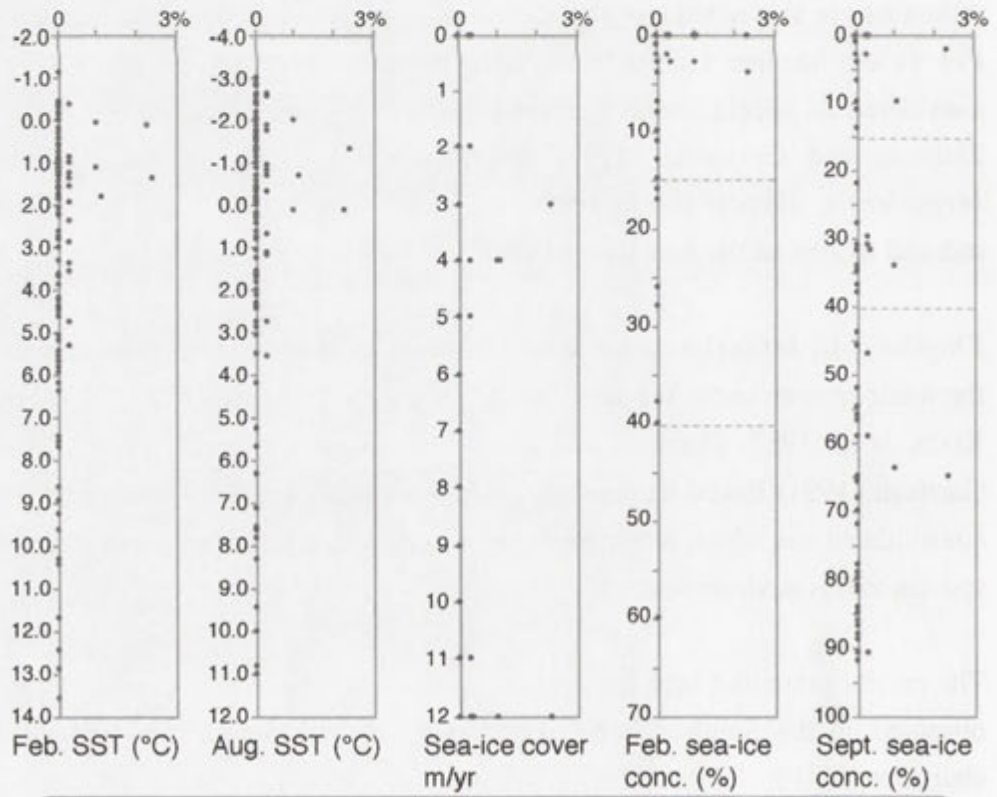

Figure 3.16b. Relative abundances against February and August SST, sea-ice cover in months per year and sea-ice concentration (%) in February and September (annual minimum and maximum sea-ice extents respectively). Other details as in Figure 3.2b.

however, prefers the open ocean in summer and does not show a tendency for residing near the summer sea-ice edge. Presumably this species makes advantage of melting sea-ice to bloom in the northward spreading spring Antarctic surface water layer and can be incorporated in fast-ice after being transported in from the north.

3A.3.15 *FRAGILARIOPSIS PSEUDONANA*

A double geographical distribution of *Fragilariopsis pseudonana* is shown in Figure 3.16a. One region is along the Antarctic coast (Prydz Bay region, Ross Sea, Antarctic Peninsula) and the second region is noted along the maximum winter sea-ice edge in the South Atlantic sector. South Georgia Island, in the western part of this second distribution, may provide an coastal environment for part of this distribution. The bulk of this second distribution may be related to iceberg transport rather than directly with the winter maximum sea-ice edge. Retrieval from the surface samples is low with a maximum abundance of 3%. These maximum abundances are found in February SST between 0° to 2°C and August SST of -1.5° to 0°C (Fig.3.16b). The double geographical distribution is evident in the months of sea-ice cover per year plot. Here, one abundance peak is associated with 12 months cover and the other with 3 months cover. Minimum sea-ice cover is referable to open ocean conditions, while during the September sea-ice maximum, the greatest species abundance is linked with around 65% consolidated ice cover or no ice cover.

Tanimura (1992) and Gersonde (1984) recovered *F. pseudonana* from sediments of Lützow-Holm Bay and along the Filschner-Ronne Ice shelf. The species was rare; it occurs less than 0.1% in the former location and was considered common in the latter. Hasle (1976) described the surface water distribution of *F. pseudonana* as cosmopolitan (69°N to 72°S). The bulk of Southern Hemisphere samples she recorded were from samples located south of 60°S. Within sea-ice samples the species has been reported most often from new sea-ice or sea-ice edge situations (Garrison *et al.* 1983a, 1987, Gersonde 1984). The species is categorised as confined to pack-ice environments (Garrison and Buck 1989, Garrison 1991).

As a result of both the phytoplankton and sea-ice studies we can have some faith in the distributions observed in the physical parameters in contrast to those of the geographic knowing that the signal of the species is not well recorded in the sediments of the open ocean zone. Double signatures in the sea-ice records (with exception to February maximum concentration) allow some further explanation to be made in light of previous sea-ice studies, rather than singly explaining displacement by iceberg transport to regions of less or no sea-ice cover. The use of this species in statistical analysis may require

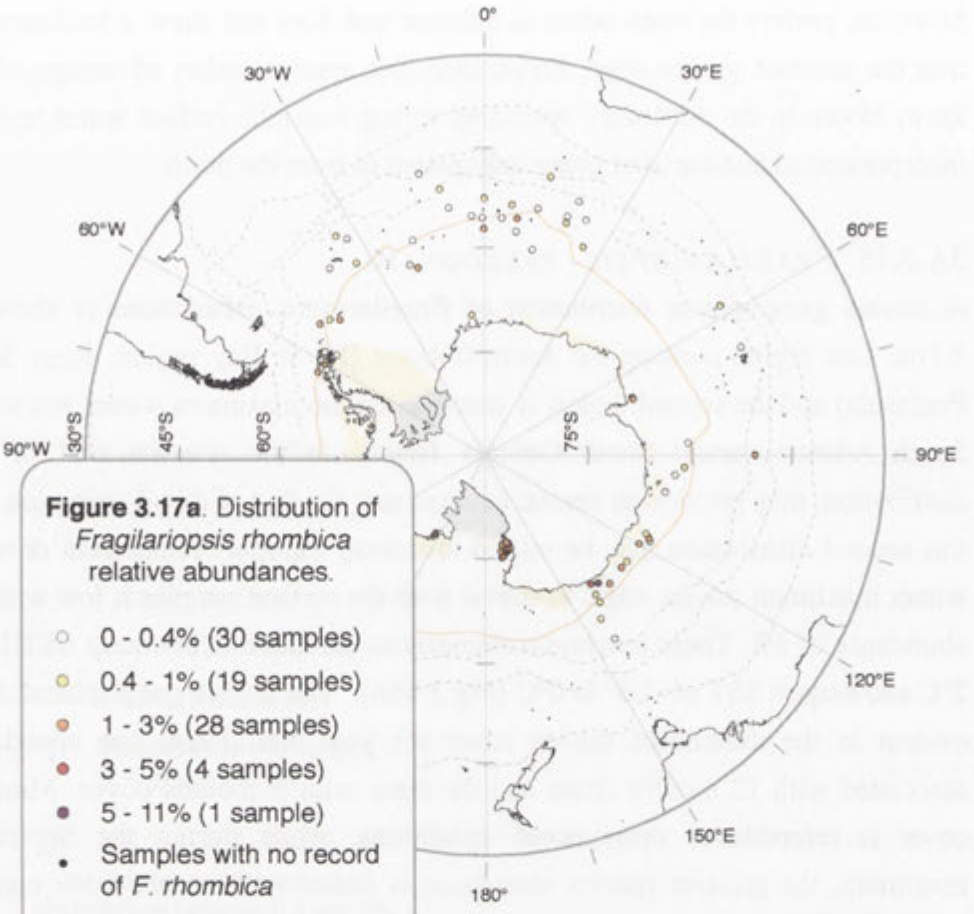

Figure 3.17a. Distribution of *Fragilariopsis rhombica* relative abundances.

- 0 - 0.4% (30 samples)
- 0.4 - 1% (19 samples)
- 1 - 3% (28 samples)
- 3 - 5% (4 samples)
- 5 - 11% (1 sample)
- Samples with no record of *F. rhombica*

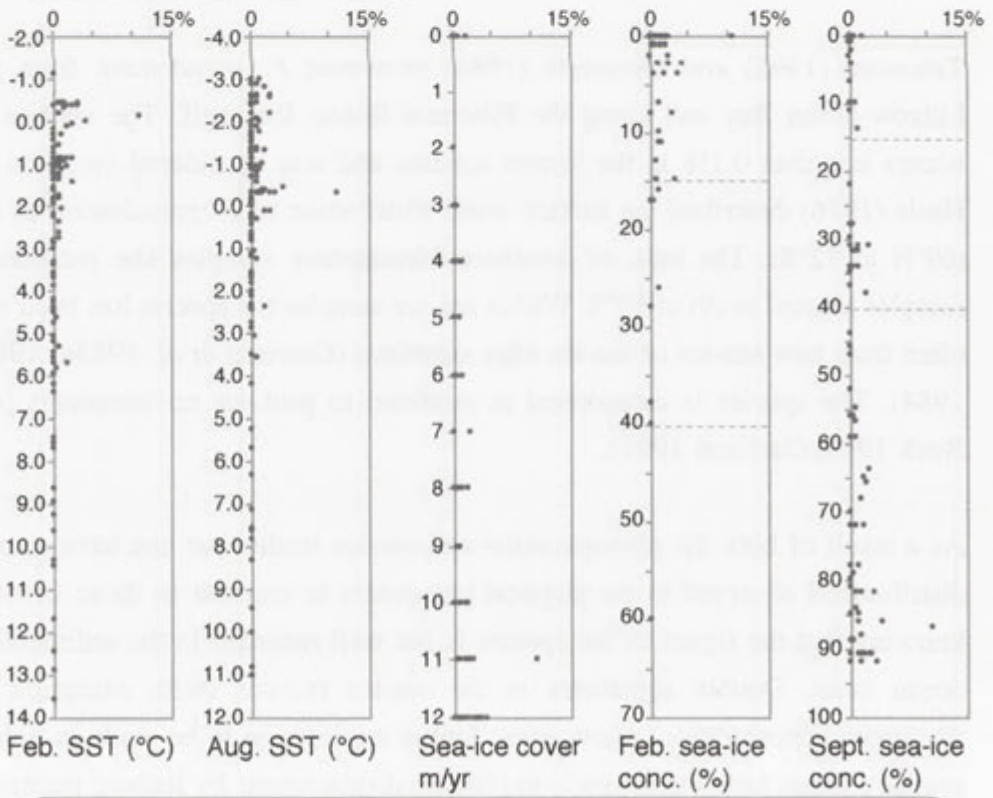

Figure 3.17b. Relative abundances against February and August SST, sea-ice cover in months per year and sea-ice concentration (%) in February and September (annual minimum and maximum sea-ice extents respectively). Other details as in Figure 3.2b.

caution because of the loss of signal in the sediments, but due to it low abundances are not a large concern at this point in time.

3A.3.16 *FRAGILARIOPSIS RHOMBICA*

Fragilariopsis rhombica was mostly encountered in abundances between 1-3% in sediments close to the Antarctic coast (Fig. 3.17a). The maximum abundance (10.7%) was observed along the Adélie coast. The northern limit of the species is at the Polar Front. February temperatures of -0.5 to 1°C and August SST of 0°C reflected the zone where the species achieved highest abundances (Fig. 3.17b). Highest abundances were also related to February sea-ice free conditions and generally highly consolidated sea-ice conditions in September (85%). Eleven to twelve months per year sea-ice cover reflects the sedimentary distribution of the species.

Previous sedimentary accounts of *F. rhombica* are reported near the coast or ice shelves (Kozlova 1966, Abbott 1973, Truesdale and Kellogg 1979, Gersonde 1984, Prasad and Nienow 1986, Gersonde and Wefer 1987, Stockwell *et al.* 1991, Leventer 1992, Tanimura 1992, Zielinski and Gersonde 1997). DeFelice and Wise (1981) noted the species sporadically through their study area and this is also the case for the observations made with this Natural Database. The highest abundance reported for this species in the sediments was 16% by Kozlova (1966) and 15% by Leventer (1992). All other studies report abundances less than 5%. *Fragilariopsis rhombica* is noted in both fast- and pack-ice samples (Garrison *et al.* 1982, 1983a, Gersonde 1984, Horner 1985, Krebs *et al.* 1987, Garrison and Buck 1989, Garrison 1991).

The February SST distribution observed in this work again is directly comparable to that summarised by Zielinski and Gersonde (1997). A strong relationship to the presence of sea-ice is an important observation for this species for transfer function work.

3A.3.17 *FRAGILARIOPSIS SEPARANDA*

More widely distributed than *Fragilariopsis rhombica*, *Fragilariopsis separanda* is also more often observed in relative abundances between 1-3% of the total diatom assemblage. The most dominant presence being positioned near the Antarctic coast, in particularly the Ross Sea (maximum 7.8%) (Fig. 3.18a). The distribution of this species throughout the Southern Ocean north of the winter sea-ice extent may indicate this species ability to be more easily transported in bottom water currents. Highest abundances, are thus, associated with Ross Sea SST signature, specifically -0.5°C for both February and August. The species is noted to have highest abundances when 11-12 months sea-ice cover is present. During February this relationship includes a link with the minimum

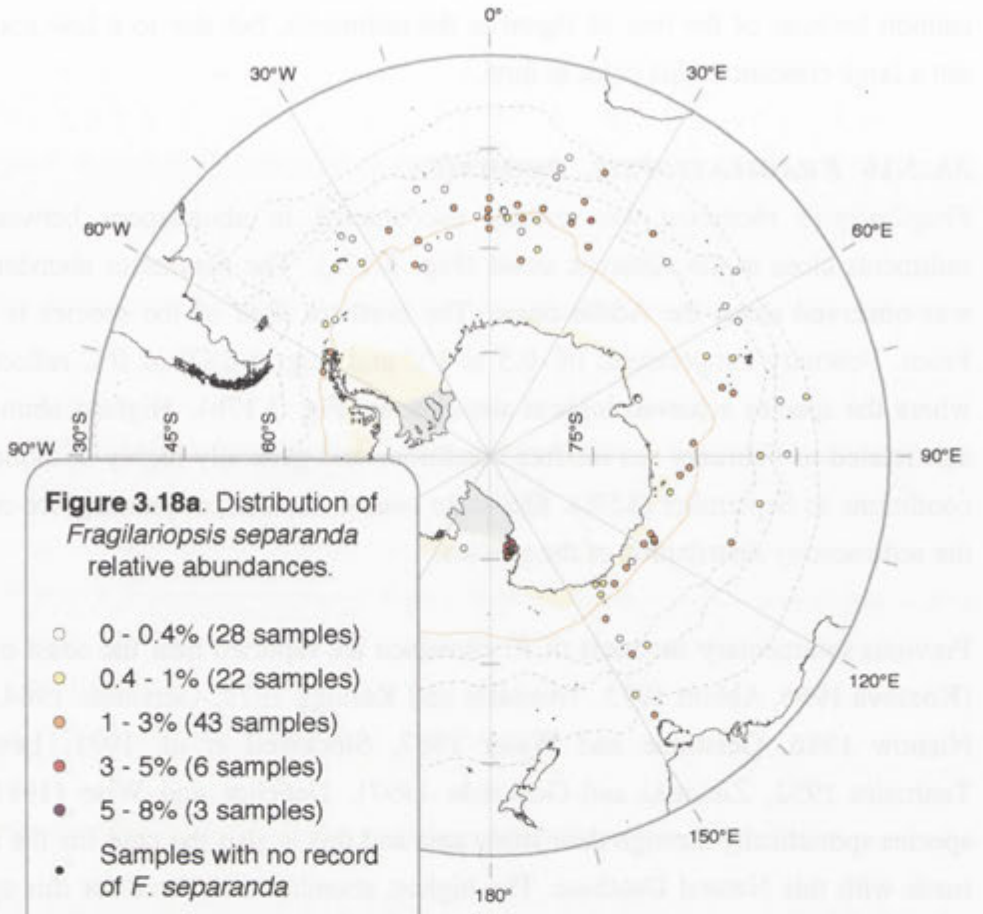

Figure 3.18a. Distribution of *Fragilariopsis separanda* relative abundances.

- 0 - 0.4% (28 samples)
- 0.4 - 1% (22 samples)
- 1 - 3% (43 samples)
- 3 - 5% (6 samples)
- 5 - 8% (3 samples)
- Samples with no record of *F. separanda*

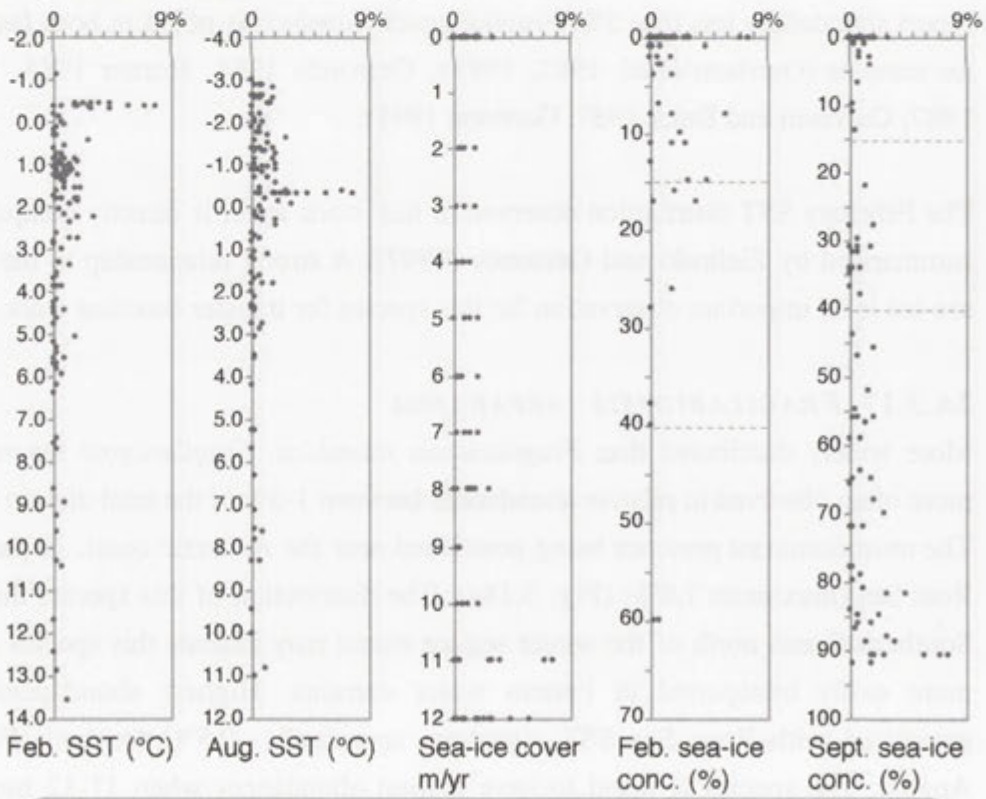

Figure 3.18b. Relative abundances against February and August SST, sea-ice cover in months per year and sea-ice concentration (%) in February and September (annual minimum and maximum sea-ice extents respectively). Other details as in Figure 3.2b.

sea- ice edge, and in maximum sea-ice conditions it includes highly consolidated sea-ice (90%).

Highest maximum abundances of *F. separanda* are observed as slightly increased to off-shore conditions rather than in-shore coastal environments (Kozlova 1966, DeFelice and Wise 1981, Gersonde and Wefer 1987, Stockwell *et al.* 1991, Leventer 1992). The exception being sediment samples from Lützow-Holm Bay which has the highest recorded abundance in the sediments (10%, Tanimura 1992). Both, Zielinski and Gersonde (1997) and DeFelice and Wise (1981), indicate that *F. separanda* is confined to the south by the Polar Front in the South Atlantic sector. This is not the case for the Indian Ocean sector as shown in this work and noted previously by Kozlova (1966) and Abbott (1973).

Fragilariopsis separanda has rather strangely not been reported in any studies of sea-ice samples. One possibility exists that the distinction between *F. rhombica* and *F. separanda* has not been made by investigators of phytoplankton in sea-ice and thus all occurrences are embraced under the *F. rhombica* category.

The SST affinity of *F. separanda* covers a February range of -1 to 14 °C with maximum abundances at -0.5°C, as similarly reported by Zielinski and Gersonde (1997). The relation of this species to environments further off-shore Antarctica leads to the more likely possibility that the species is entrained during bottom-water formation. Since the species is very heavily silicified, it would survive displacement and burial in more northerly regions which is quite likely the case in the Indian and southeast Indian sectors. The distribution in the South Atlantic sector could be attributed to this factor and iceberg transport. Thus, the species may in fact prove to be an allochthonous species that is unreliable for transfer function work in northern positioned cores. The lack of corresponding sea-ice study data unfortunately does not lend support to this hypothesis.

3A.3.18 *GRAMMATOPHORA ARCUATA*

A benthic species observed very rarely in the samples of the Natural Database. The few samples in which it occurs are coastal (Antarctic, South Georgia and South Orkney Islands) or within the winter maximum sea-ice edge (Fig. 3.19a). Abundances are generally less than 1% with a maximum of 3.4% near South Orkney Island. Its distribution in the sediments is associated with SST at 1°C and -2°C for February and August respectively (Fig. 3.19b). Sea-ice cover between 6-10 months per year appear to be the preference with September conditions of marginal sea-ice (30%) but up to 90% concentration possible.

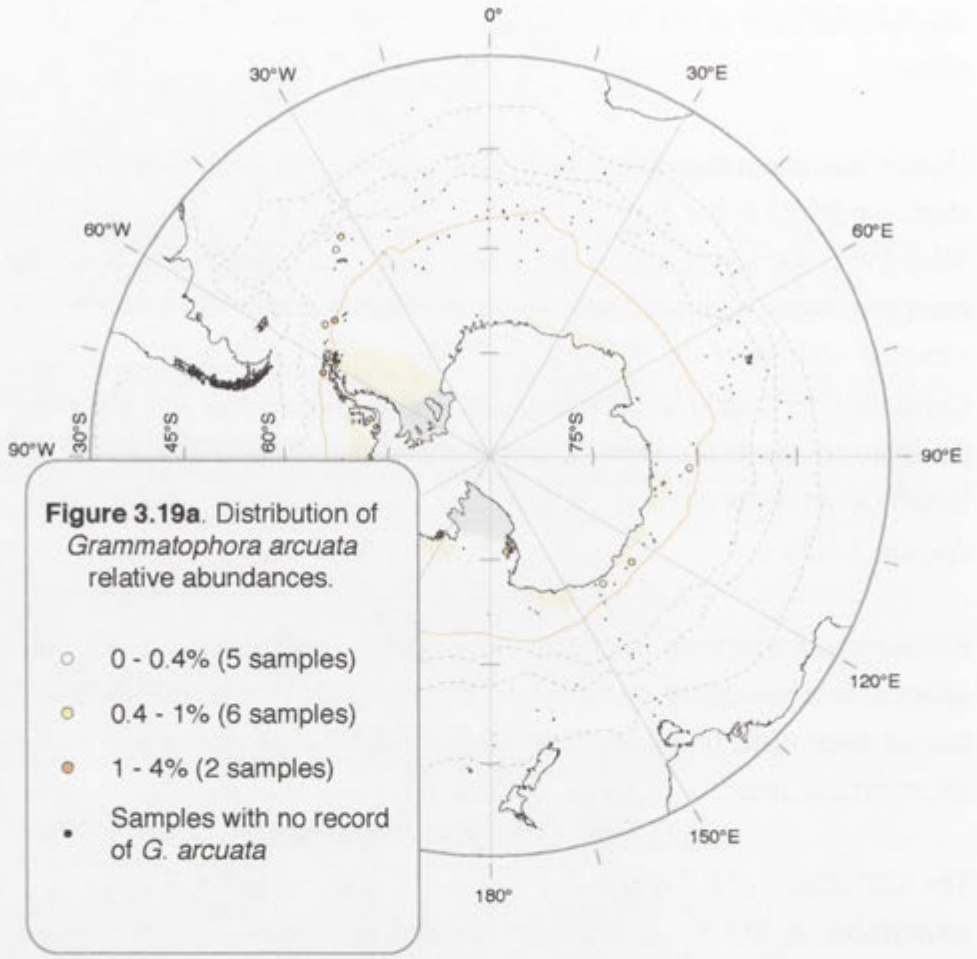

Figure 3.19a. Distribution of *Grammatophora arcuata* relative abundances.

- 0 - 0.4% (5 samples)
- 0.4 - 1% (6 samples)
- 1 - 4% (2 samples)
- Samples with no record of *G. arcuata*

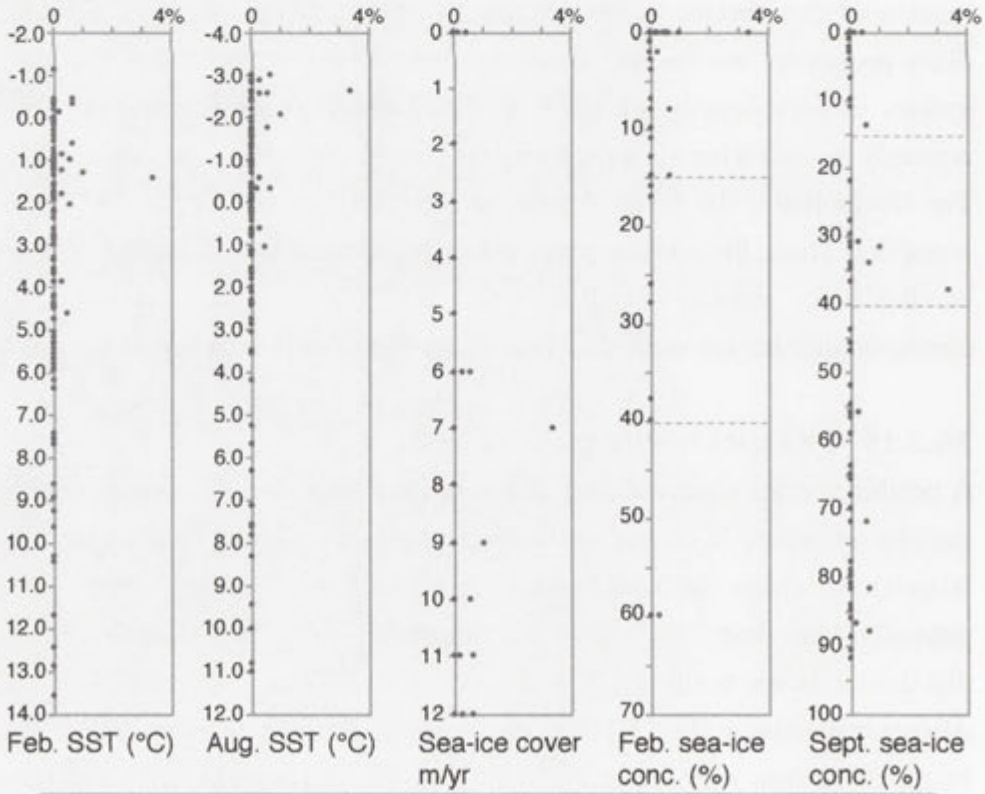

Figure 3.19b. Relative abundances against February and August SST, sea-ice cover in months per year and sea-ice concentration (%) in February and September (annual minimum and maximum sea-ice extents respectively). Other details as in Figure 3.2b.

Grammatophora arcuata has been reported from three samples at less than 2% abundance in sediments of Lützow-Holm Bay (Tanimura 1992) and in one site from the Amundsen Sea at 0.3% (Kellogg and Kellogg 1987). There are no reports of *Grammatophora* taxa in sea-ice samples.

This work expands the regions of preservation and continues to define the species as a coastally influenced species.

3A.3.19 *HEMIDISCUS CUNEIFORMIS*

A warm water species observed in increasing abundance north of the SAF (Fig. 3.20a). This is reflected in the relationship observed with both February and August SST with greatest abundances associated with SST >11°C (Fig. 3.20b). The maximum abundance encountered was 5.3%. *Hemidiscus cuneiformis* abundances are not associated with sea-ice cover.

Zielinski and Gersonde (1997) list *H. cuneiformis* as having its maximum abundance (6.8%) in summer temperatures at >15°C, but otherwise, observe the species in a temperature range between 7.5° to 20°C in the South Atlantic. Other South Atlantic studies confirm the presence of *H. cuneiformis* in sediments of warm water influence (DeFelice and Wise 1981, Schuette and Schrader 1981). In the Pacific sector, Donahue (1973) found the species sporadically north of the Polar Front with a maximum abundance of 7% (from a count of 100 specimens).Along the Peru coast maximum abundances were 1.52% (Schuette and Schrader 1979a,b). In the southeast Indian Ocean the maximum abundance observed by Abbott (1973) was 2.3% and only in samples north of the southeast Indian Ridge.

This work confirms previous accounts of *H. cuneiformis* in the sediments, but notes that the species is not observed south of the SAF, as similarly illustrated by Zielinski and Gersonde (fig. 17.4, 1997).

3A.3.20 *NAVICULA DIRECTA*

Navicula directa , a benthic species, has a disparate and rare sedimentary distribution in the Southern Ocean. Highest abundances and more frequent observations (1.7%) were found in the Antarctic Peninsula region, although other sites between the winter maximum sea-ice edge and the STC show either a slight tendency for coastal (island) habitats or likely displacement (Fig. 3.21a). Highest abundances are found at a February SST of 1°C and August SST of -3°C (Fig. 3.21b). Association with sea-ice characteristics are interesting in that the species is observed in high yearly cover (11-12 months) but where winter sea-ice cover is preferably unconsolidated (30%). The species is also

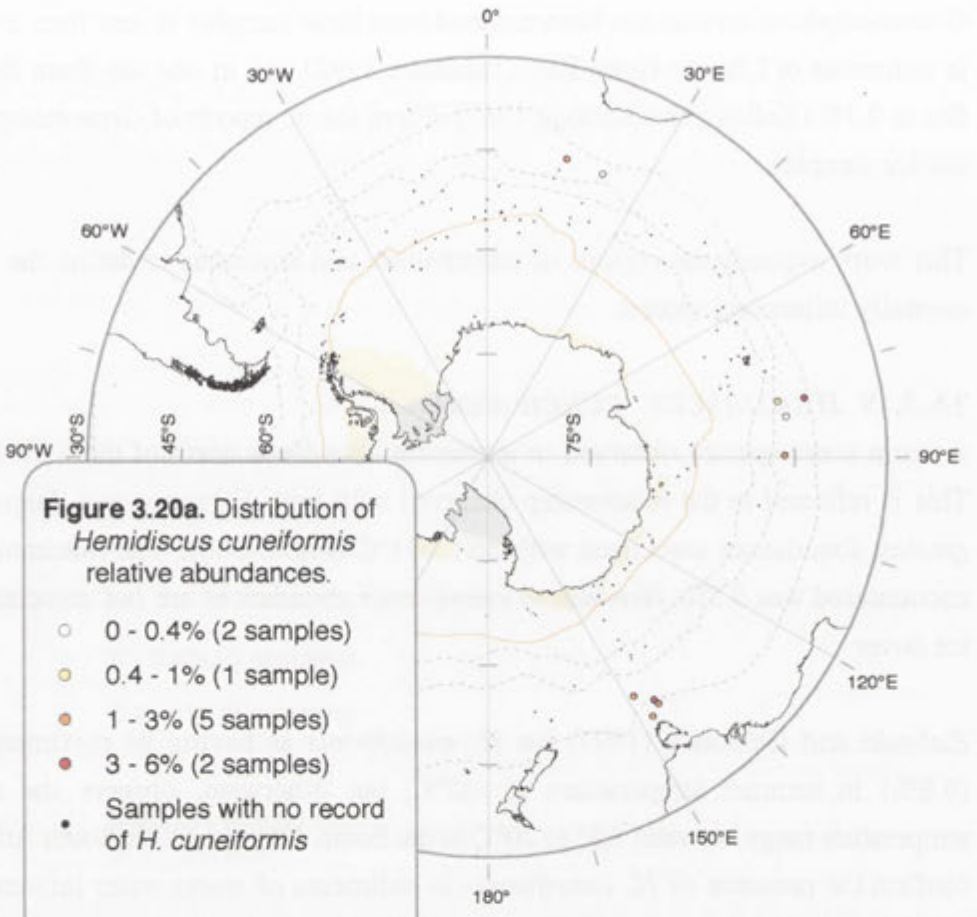

Figure 3.20a. Distribution of *Hemidiscus cuneiformis* relative abundances.

- 0 - 0.4% (2 samples)
- 0.4 - 1% (1 sample)
- 1 - 3% (5 samples)
- 3 - 6% (2 samples)
- Samples with no record of *H. cuneiformis*

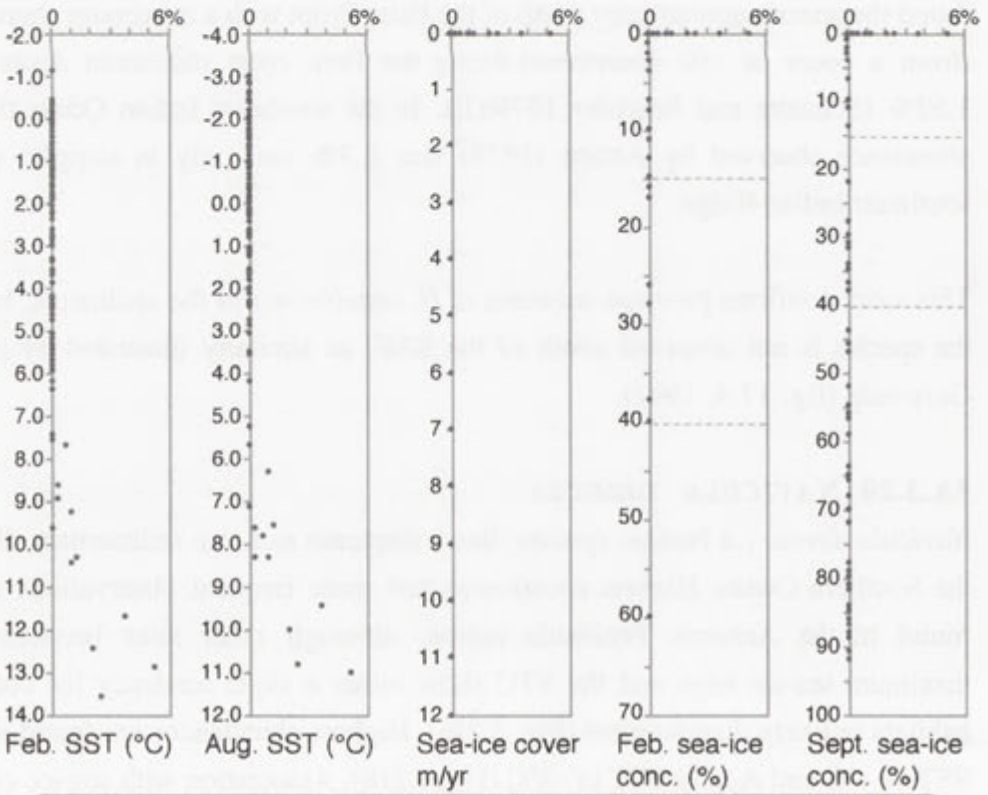

Figure 3.20b. Relative abundances against February and August SST, sea-ice cover in months per year and sea-ice concentration (%) in February and September (annual minimum and maximum sea-ice extents respectively). Other details as in Figure 3.2b.

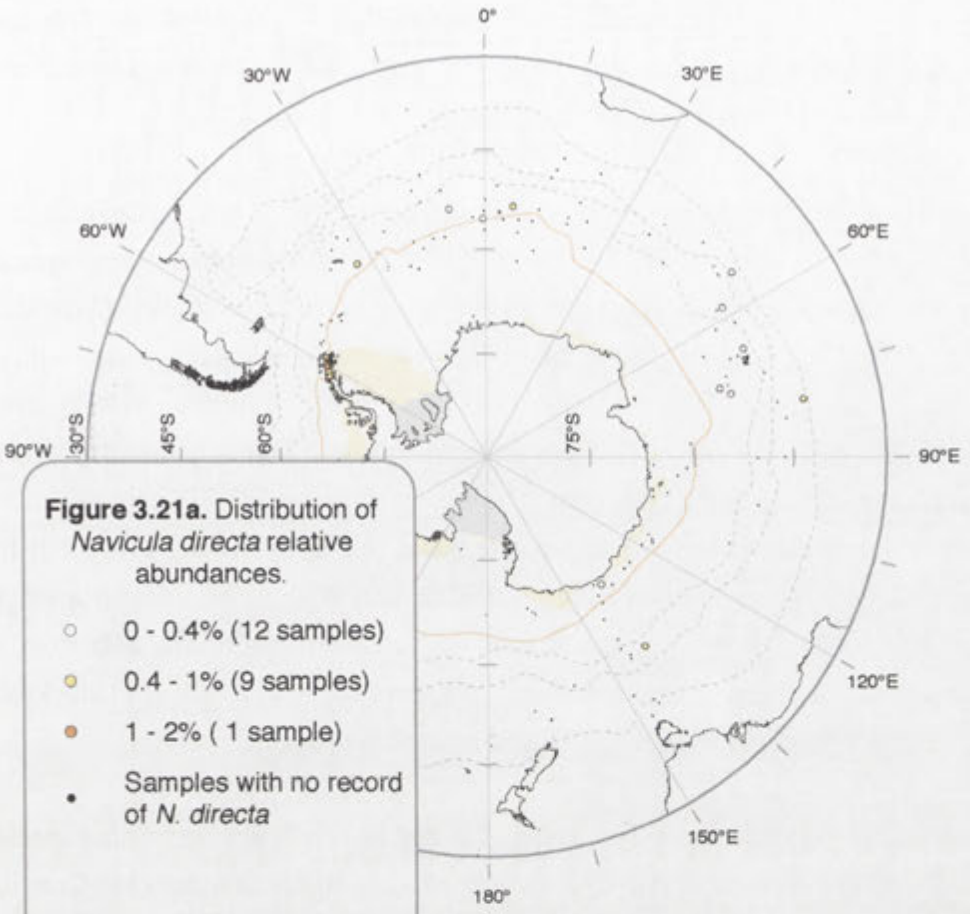

Figure 3.21a. Distribution of *Navicula directa* relative abundances.

- 0 - 0.4% (12 samples)
- 0.4 - 1% (9 samples)
- 1 - 2% (1 sample)
- Samples with no record of *N. directa*

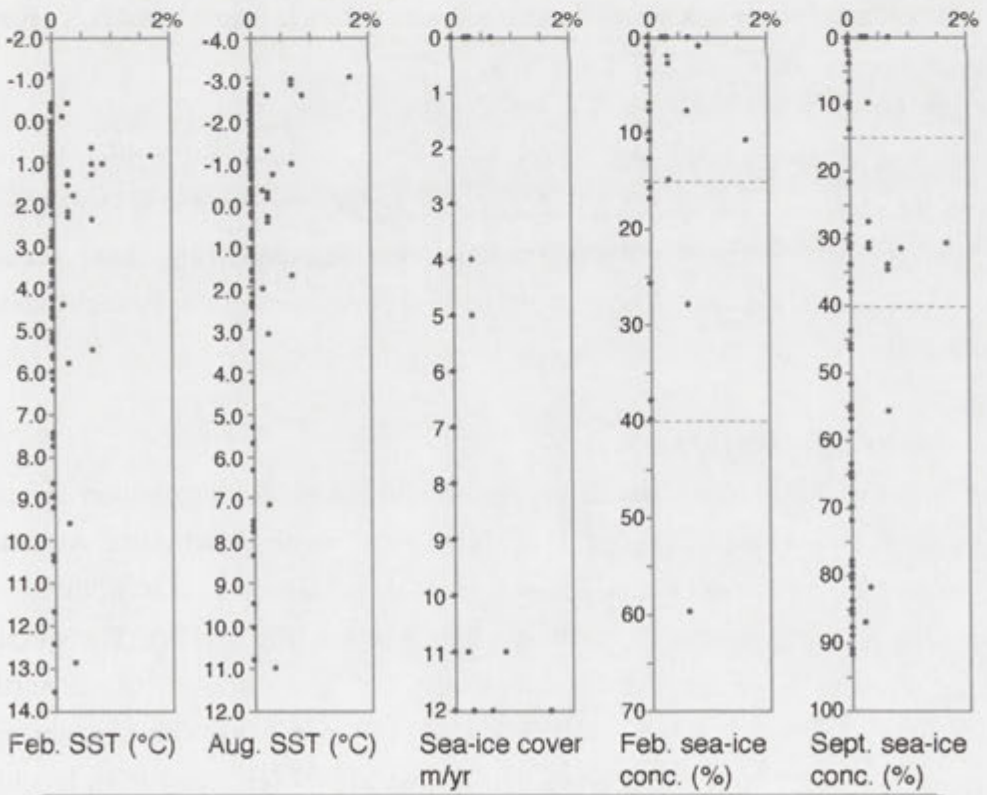

Figure 3.21b. Relative abundances against February and August SST, sea-ice cover in months per year and sea-ice concentration (%) in February and September (annual minimum and maximum sea-ice extents respectively). Other details as in Figure 3.2b.

located in highest abundances near the minimum sea-ice edge during February. This later fact may help in explaining its entrainment in bottom water and displacement to northern regions that are removed from coastal habitats.

The records of *Navicula directa* in the sediments are poor (Abbott 1973, DeFelice and Wise 1981, Prasad and Nienow 1986, Stockwell *et al.* 1991). Most authors lump species of the *Navicula* genus when observing them in the sediments. Such studies (Truesdale and Kellogg 1979, Schuette and Schrader 1981) recount low abundances with a maximum of 0.2% along the George V Coast (Leventer 1992). Tanimura (1992) listed four species of *Navicula*, but not *N. directa* in sediments of Lützow-Holm Bay which attained a maximum of 10% of the specimens observed. Of the studies which recorded *N. directa*, the maximum relative abundance observed was 1.3% by Abbott (1973) in his samples south of the southeast Indian Ridge. DeFelice and Wise (1981) found a single specimen between 50-60°S which is in line with the observations made here. Likewise, in inner Prydz Bay, only a single sample recovered contained 0.3% of *N. directa* (Stockwell *et al.* 1991).

Although Garrison (1991) lists *Navicula directa* as a land fast and pack-ice related species almost all studies find *N. directa* or *Navicula* taxa in coastal fast-ice samples (Mc Conville and Wetherbee 1983, Krebs *et al.* 1987, Tanimura *et al.* 1990). Andreoli *et al.* (1995) report the species in the water column with other sea-ice species in Terra Nova Bay, Ross Sea, during the two months of ice free conditions.

The distribution of *N. directa* in the sediments is not well understood at this time. Its low abundance in the sediments and broad distribution throughout the Southern Ocean, can only be hypothetically defined as an Antarctic benthic, preferring low sea-ice consolidation and is easily entrained and displaced by bottom water flow brought about be sea-ice formation.

3A.3.21 *ODONTELLA WEISSFLOGII*

Considered a neritic species, *Odontella weissflogii* has a wide distribution in the sediments of the Southern Ocean. Predominant abundances are observed in the Antarctic Peninsula region and near South Orkney Island. Lower abundances are noted in the Ross Sea and along the Antarctic coast in the southeast Indian sector (Fig. 3.22a). The species is strongly believed to be entrained by bottom water flow and displaced to the north, particularly in samples found along the 90°E and 145°E meridians. Other northward distributions are associated with ACC eastward drift from islands (eg. Kerguelen Island). The highest abundances are noted in cool waters of 1°C (Feb. SST) and -2.5°C (August SST) (Fig. 3.22b). As with *Navicula directa, O. weissflogii* is found with near year

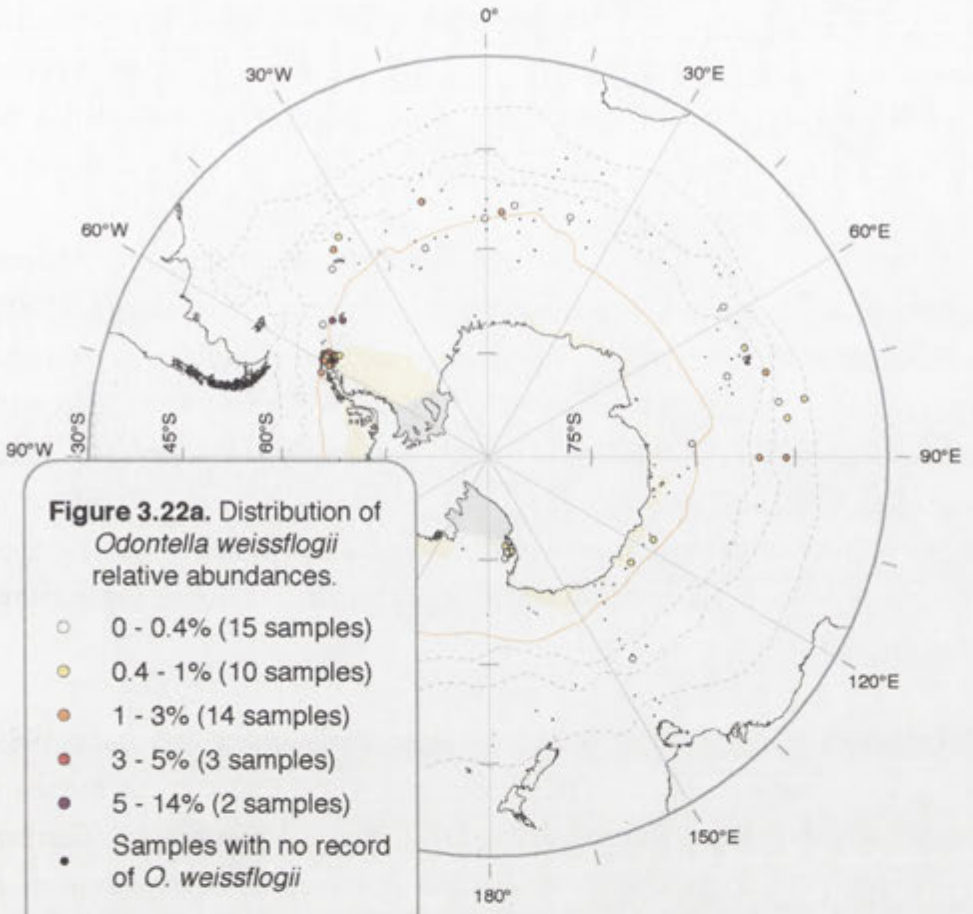

Figure 3.22a. Distribution of *Odontella weissflogii* relative abundances.

- 0 - 0.4% (15 samples)
- 0.4 - 1% (10 samples)
- 1 - 3% (14 samples)
- 3 - 5% (3 samples)
- 5 - 14% (2 samples)
- Samples with no record of *O. weissflogii*

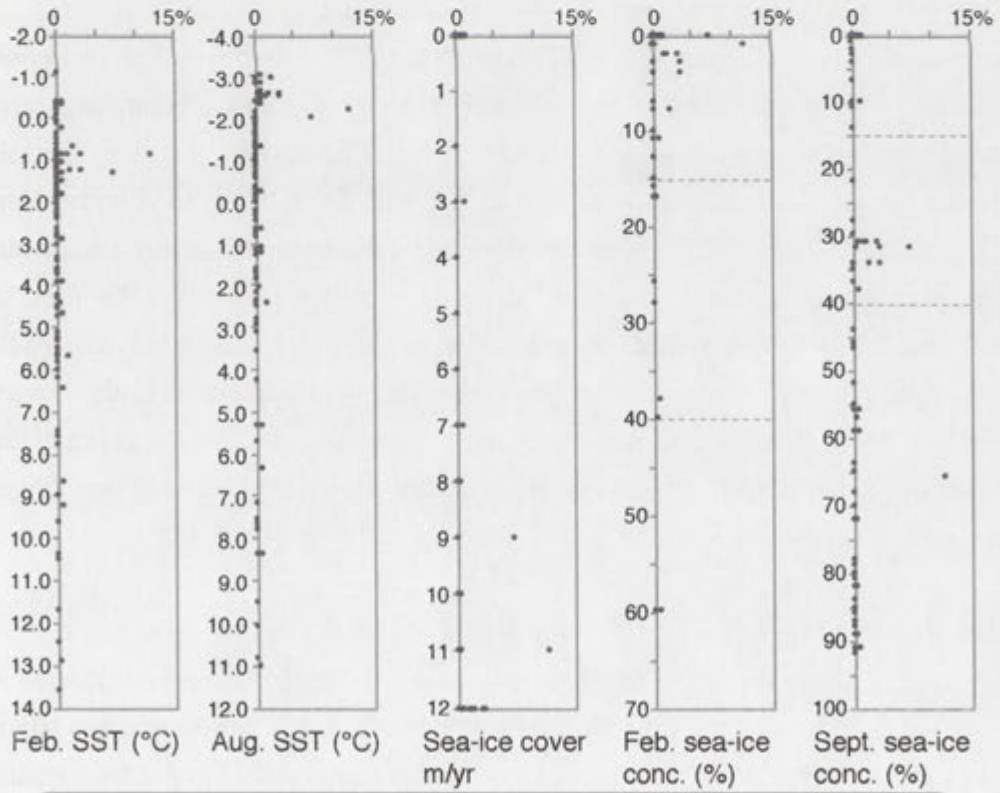

Figure 3.22b. Relative abundances against February and August SST, sea-ice cover in months per year and sea-ice concentration (%) in February and September (annual minimum and maximum sea-ice extents respectively). Other details as in Figure 3.2b.

round ice cover (10-11 months) with September maximum sea-ice concentration low (30%) and no ice cover in summer. Again, this may yet prove to be an important consideration in its displacement northward from regions of bottom water formation that have low ice cover (ie. polynyas).

Jousé *et al.* (1962a,b) suggested the species had high abundances along the Antarctic coast, a patchy distribution around Kerguelen, and an abundance plume along 95-100°E up to 45°S. The high abundances areas along the Antarctic coast have been given rather low abundance values by more recent workers (0.03 to 0.07% Kozlova 1966, max >1% Gersonde 1984, max. 0.32% Gersonde and Wefer 1987, max. 0.2% Leventer 1992) with exception to Zielinski and Gersonde (1997) who recorded a maximum abundance of 4.2% at summer SST of -1.5°C to 1°C predominantly in the Scotia Sea sector. Leventer (1992) noted that one of the two samples in which *O. weissflogii* was observed occurred in a region that experienced 11 months of sea-ice cover.

Odontella weissflogii is categorised as a pack-ice species (Garrison and Buck 1989, Garrison 1991). Most studies agree with this interpretation and find that the species is also located in the adjacent water column sometimes with increasing abundance (Garrison *et al.* 1982, 1983a, 1987, Gersonde 1984, Bianchi *et al.* 1992) with exception to Tanimura *et al.* (1990) who observed it in fast-ice samples in Lützow-Holm Bay.

This work records just over 2.5 times greater abundance of *O. weissflogii* than that noted by Zielinski and Gersonde (1997) for the same region so there is counting error unaccounted for in the Natural Database for this region (eg *Chaetoceros* spp. see Zielinski and Gersonde 1997). Although there is this difference, the relation to summer and February temperature remains equivalent, as does the excursions from this cool water signature to other northern and warm water sites. The species should not be used in transfer functions for its evident bottom water transportation which would bias otherwise warm-water samples (eg. 90°E meridian) with a cold water signal. In contrast, the reports of *O. weissflogii* from pack-ice and adjacent water column samples would indicate that the species was not necessarily confined to the Antarctic coastal regions, but was linked with the environmental dynamics of the sea-ice zone.

3A.3.22 *PARALIA* TAXA

The distribution of *Paralia* species in the Natural Database sediment samples are located in neritic influenced regions of the Antarctic Peninsula, Ross Sea, near Kerguelen Island and south of Tasmania (Fig.3.23a). These various locations are evident in the temperature versus abundance plots with three peaks of abundance noted at February SST of 12-14°C, 6°C, and 1°C (Fig. 3.23b). In terms of sea- ice cover the two extremes, no sea-ice

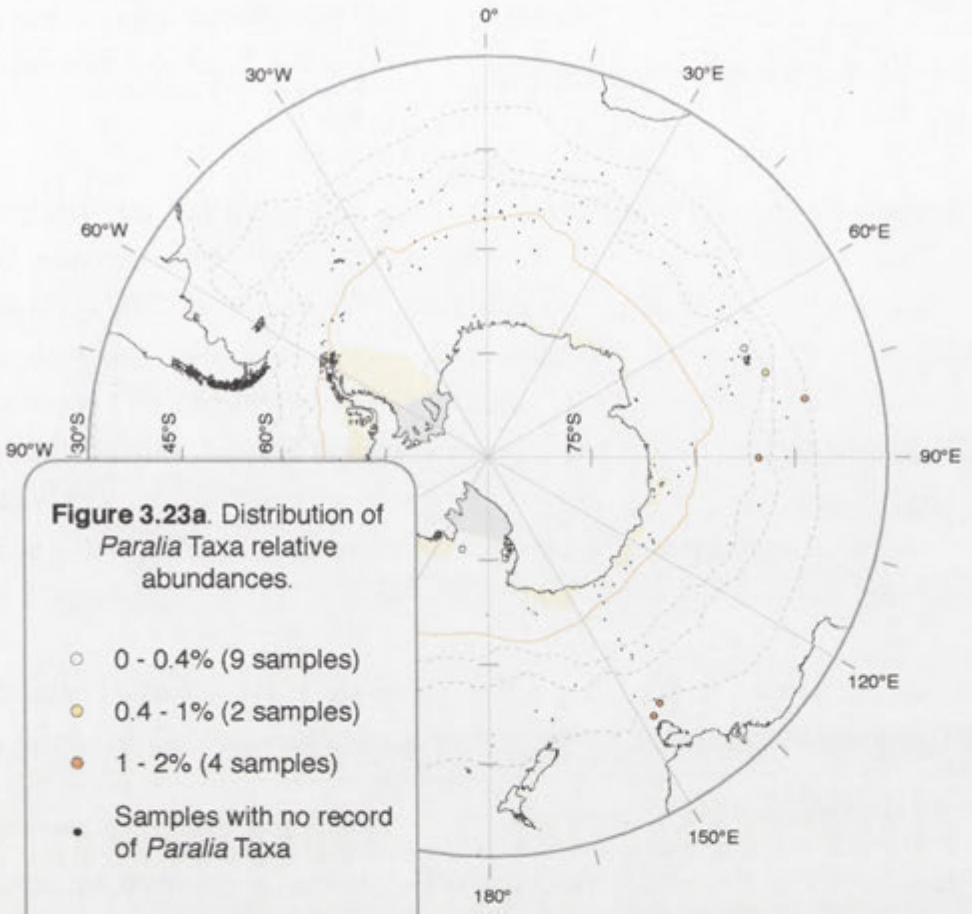

Figure 3.23a. Distribution of *Paralia* Taxa relative abundances.

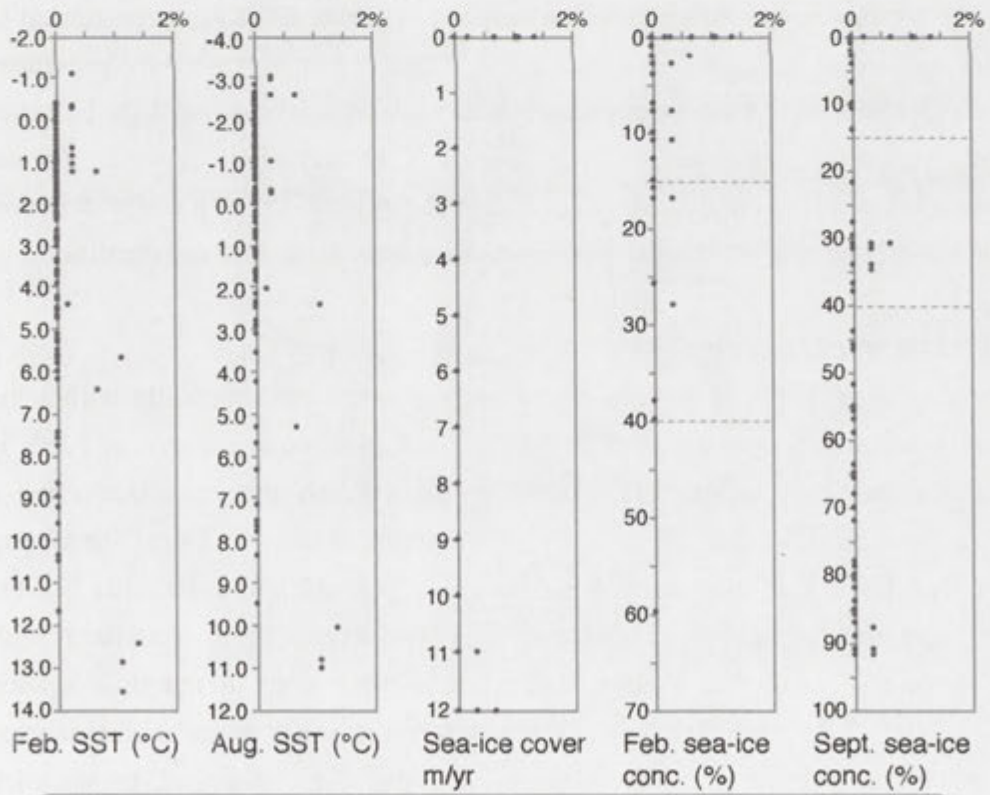

Figure 3.23b. Relative abundances against February and August SST, sea-ice cover in months per year and sea-ice concentration (%) in February and September (annual minimum and maximum sea-ice extents respectively). Other details as in Figure 3.2b.

cover to 11-12 months of sea-ice cover, is observed. These extremes are also evident in the annual maximum and minimum expressions of sea-ice cover in relation to relative abundances.

In previous studies, *Melosira sol* ("*Paralia sol*") has been observed either very rarely at less than 1% (Truesdale and Kellogg 1979, Tanimura 1992) or at higher abundances by Kellogg and Kellogg (1987, average 15%) and Abbott (1973, maximum 2.7%). *Paralia sulcata* ("*Melosira sulcata*") has been identified along the Antarctic coast also with an average abundance of 3% (Gersonde 1984, Leventer 1992). Leventer (1992) observed three of the five samples which contained *P. sulcata* were in regions with 11 months annual ice cover. Northern records of *P. sulcata* by Schuette and Schrader (1979a,b, 1981) report maximum abundances of 2.14% off-shore southwest Africa and 7.82% along the Peru coast.

Only *Melosira* species have been recorded as present in sea-ice in the Antarctic Peninsula (Krebs *et al.* 1987) and also under the sea-ice in the Ross Sea (Cassie 1963, Andreoli *et al.* 1995).

Records of *Paralia* taxa in this study indicate that the species is observed in neritic environments. There has been no previous mention of *Paralia* taxa near Kerguelen Island nor Tasmania. The increase of *Paralia* species east of Kerguelen (90°E) may be related to enhancement by bottom water movement, and this although not supported by presences in this Natural Database, are otherwise made possible with abundances noted by Leventer (1992) which are within source and pathway regions of Antarctic bottom water. *Paralia* taxa require substantial taxonomic work and should be avoided in transfer function analysis because of their very wide relationships to various oceanographical conditions.

3A.3.23 *POROSIRA* GROUP

The geographical distribution of the *Porosira* Group is noted predominantly within the winter annual maximum sea-ice extent (Fig. 3.24a). The maximum abundance of 7.2% is related to a February and August SST of 0°C, with maximum abundances covering a range from -0.5° to 2°C (February SST, 0° to -3°C August SST)(Fig. 3.24b). The Group increases in abundance with >10 months sea-ice cover per year. In September highest abundances are found in pack-ice at 65% concentration, decreasing in abundance with increasing concentration. A minor abundance peak is also noted in marginal sea-ice concentration of 30%. In summer, there is a bi-modal peak in the group's abundances. One peak perceived in open ocean conditions and the other marginal to pack-ice conditions.

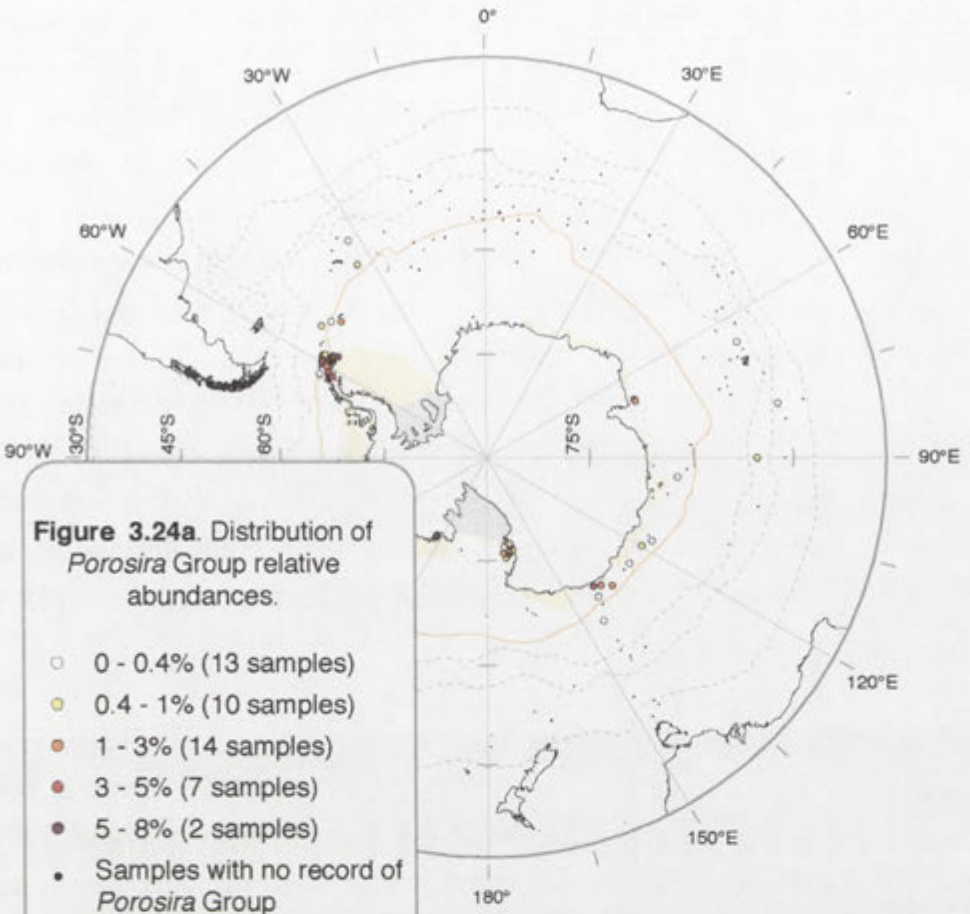

Figure 3.24a. Distribution of *Porosira* Group relative abundances.

- 0 - 0.4% (13 samples)
- 0.4 - 1% (10 samples)
- 1 - 3% (14 samples)
- 3 - 5% (7 samples)
- 5 - 8% (2 samples)
- Samples with no record of *Porosira* Group

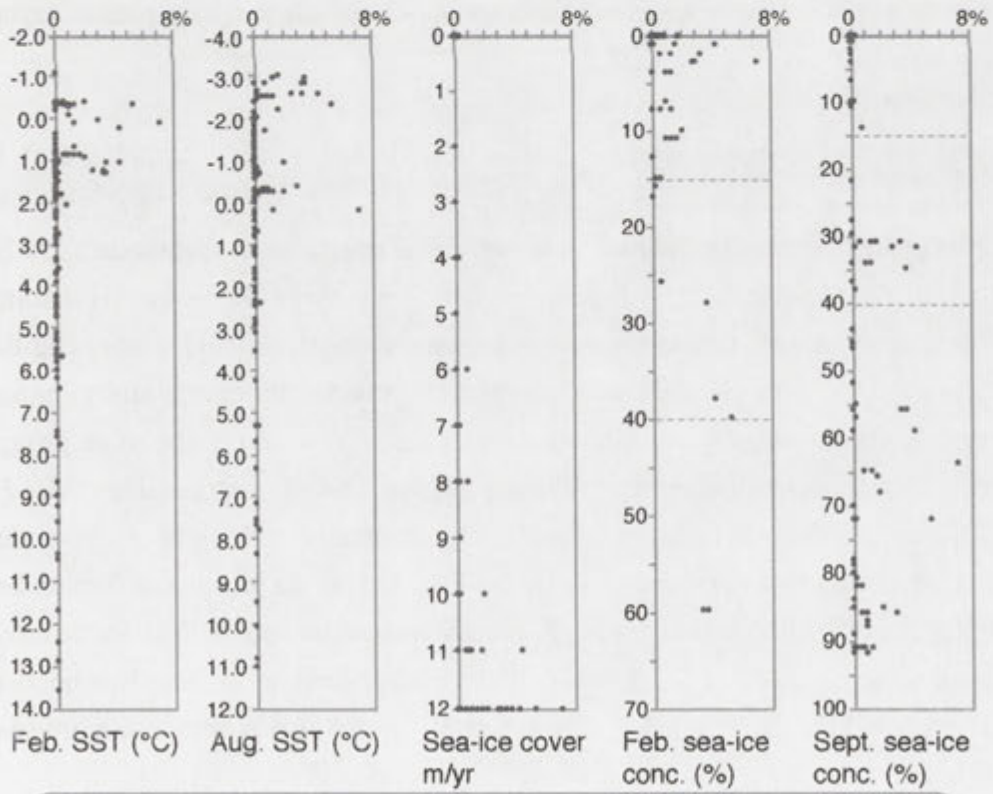

Figure 3.24b. Relative abundances against February and August SST, sea-ice cover in months per year and sea-ice concentration (%) in February and September (annual minimum and maximum sea-ice extents respectively). Other details as in Figure 3.2b.

As mentioned in section 3.2.17 the two species of *Porosira* are lumped in the Natural database. *Porosira glacialis* has been noted in waters adjacent the coast or sea-ice while *Porosira pseudodenticulata* is noted as abundant in sea-ice (Hasle 1973). Zielinski and Gersonde (1997) reported on the temperature signals of the two species in the South Atlantic sector. They found *P. pseudodenticulata* at -2°C and *P. glacialis* at -1 to 1.5°C summer SST. Along the Antarctic coast both species have been recorded in the sediments at less than 1% and a maximum of 3% along the George V Coast (Prasad and Nienow 1986, Kellogg and Kellogg 1987, Stockwell *et al.* 1991, Leventer 1992). Only rare occurrences (<1%) of *P. pseudodenticulata* were observed in Lützow-Holm Bay (Tanimura 1992) which is in contrast to the observations of <5% found along the Filschner-Ronne ice shelf by Gersonde (1984). Transgressions north of the *Porosira* Group sedimentary record, particularly *P. glacialis*, have only been observed in the Bransfield Strait (Gersonde and Wefer 1987) and are inferred from the abundance plot of the species by Zielinski and Gersonde (1997, fig. 17.27).

Porosira glacialis has been reported rarely as a sea-ice species (Horner 1985, Krebs *et al.* 1987, Garrison 1991). In contrast most workers observe *P. pseudodenticulata* in both fast and pack-ice samples (eg. Garrison *et al.* 1983a, Gersonde 1984, Krebs *et al.* 1987) This species has been noted to be in increased numbers in the water column than in sea-ice (Garrison *et al.* 1987, Tanimura *et al.* 1990) and also to be the dominant species in fast-ice (Watanabe 1982) which may be a function of accumulation by ice platelet layers under the consolidated ice (Garrison 1991).

From the relationship observed against February SST and relative abundance it is possible to infer that all occurrences in the Natural database are referable to *P. glacialis* when employing the temperature signal observed by Zielinski and Gersonde (1997). When regarding the August SST relationship there appears to be some dichotomy between the group with one section showing a preference for super cold waters and the other remaining at 0°C. With the additional information provided by the February sea-ice plot it becomes easier to suggest that the two species are represented in the same group. Thus, those abundances observed within sea-ice being attributable to *P. pseudodenticulata* and those abundances found in open ocean condition as *P. glacialis*. These same two variations in distribution may be reflected in the maximum September sea-ice plot with consolidated ice containing *P. pseudodenticulata* and the less ice covered region indicating the presence of *P. glacialis*. With greater attention to the differentiation between the two species, they could become extremely useful species in identifying sea-ice distribution.

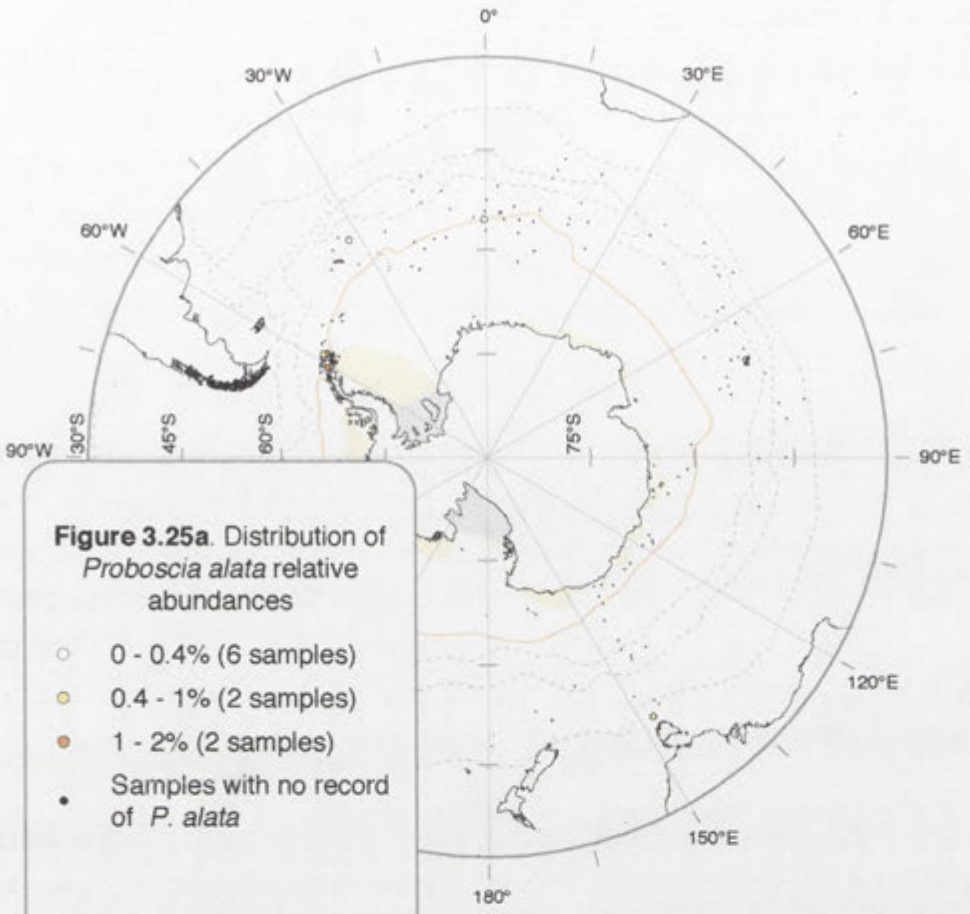

Figure 3.25a. Distribution of *Proboscia alata* relative abundances

- 0 - 0.4% (6 samples)
- 0.4 - 1% (2 samples)
- 1 - 2% (2 samples)
- Samples with no record of *P. alata*

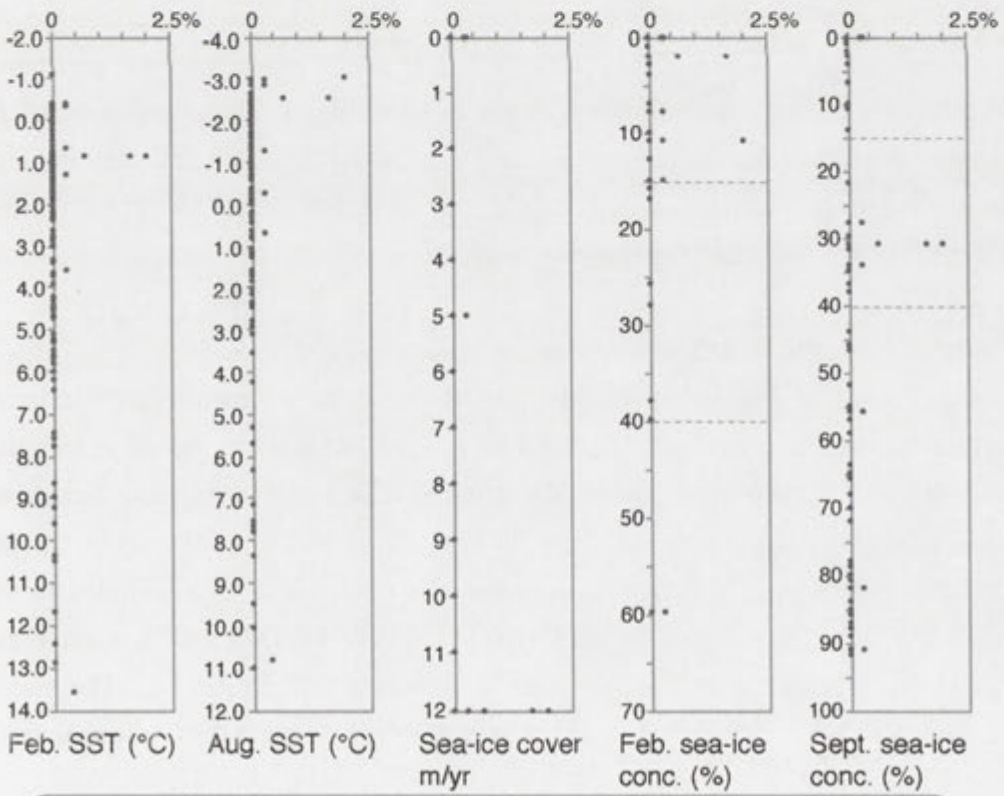

Figure 3.25b. Relative abundances against February and August SST, sea-ice cover in months per year and sea-ice concentration (%) in February and September (annual minimum and maximum sea-ice extents respectively). Other details as in Figure 3.2b.

3A.3.24 *PROBOSCIA ALATA*

Proboscia alata is uncommonly found in the sediments of the Natural Database. Highest abundances (2%) are observed in the Antarctic Peninsula region, and very rare occurrences are noted north of 60°S (Fig. 3.25a). A February SST of 1°C and August SST of -3°C are noted as the temperature signatures for the highest abundances (Fig. 3.25b). This is related to 12 months ice cover but at marginal ice concentration conditions for both maximum and minimum expressions, tending to open ocean conditions in the summer.

All previous identifications of this species (as *Simonseniella alata* or *Rhizosolenia alata*) in the Southern Ocean are located along the Antarctic coast and in the Bransfield Strait (Gersonde 1984, Gersonde and Wefer 1987, Stockwell *et al.* 1991, Tanimura 1992) with relative abundances generally less than 1%. A maximum of 2% was noted in the South Atlantic sector by Zielinski and Gersonde (1997). Northward of the STC and along the Peru coast in the south east Pacific, *P. alata* was observed at a maximum abundance of 2.34% (Schuette and Schrader 1979a.b).

Within the sea-ice, three coastal studies including the Antarctic Peninsula, the Filschner-Ronne Ice shelf and Lützow-Holm Bay have recorded *P. alata* as observed in sea-ice samples (Gersonde 1984, Krebs *et al.* 1987, Tanimura *et al.* 1990).

The results presented here are in accord with those previously made from the sediments but not wholly with the sea-ice records which are fast-ice biased. The observation of *P. alata* in sediments south of Tasmania are considered correctly identified and may indicate a neritic influence from Tasmania which would not seem out of character with other neritic elements already identified (eg. *Paralia* taxa).

3A.3.25 *RHIZOSOLENIA BERGONII*

A single sample, south of Tasmania, records this species in the sediments (1.1% relative abundance, no illustration provided). It should be pointed out that several other samples in the same region, but ineligible under the sample selection criteria, also contained *Rhizosolenia bergonii* occurrences (samples 147GC -007, -017, -030, -031). In the original 166DB (Pichon *et al.* 1992a), *R. bergonii* was observed in two samples in the Indian Ocean (RC11-118 37°48'S 71°32'E, RC11-119 40°18'S 74°34'E), both these samples were also rejected under sample selection criteria in section 3A.1.1. The single occurrence observed here is found in warm waters with greater than 13°C summer SST and no sea-ice influence.

Aside from what is a likely mis-identification of the species in the Ross Sea sediments (Truesdale and Kellogg 1979), *R. bergonii* is a species observed in sediments of the mid and low latitudes (Schuette and Schrader 1979a,b 1981, van Iperen *et al.* 1987, van Iperen *et al.* 1993, Treppke *et al.* 1996, Zielinski and Gersonde 1997). van Iperen *et al.* (1987) consider the species indicative of oceanic, warm saline waters with low to moderate nutrient levels. Highest maximum abundances recorded in the sediments were noted in the southeast Atlantic as 10.8% and in the Indonesian Archipelago at 6.7% (Treppke *et al.* 1996, van Iperen *et al.* 1993 respectively). Within the South Atlantic to 30°S Zielinski and Gersonde (1997) find relative abundances up to 4.2% in sediments with overlying waters of 11-20°C.

The species is poorly represented in the surface samples of the Natural Database due to the removal of a significant number of warm water region samples that were not counted to a minimum of 270 specimens. The species obviously will provide a significant warm water signal to SST transfer function studies if it is observed in further warm region sediment samples, north of the STC.

3A.3.26 *RHIZOSOLENIA* OTARIA ABSENT GROUP

Plotting the remaining 129 samples for the *Rhizosolenia* otaria absent group results in a geographical distribution focused on sediments of the open ocean region and bordering the winter sea-ice edge (Fig.3.26a). A 1.4% maximum abundance is reached at a temperature of ~13°C. A bi-modal distribution is, however, present in the relative abundances plots against temperature and sea-ice cover and September concentration (Fig. 3.26b). As discussed in section 2.2.19 the group combines several species and this is reflected in these plots. *Rhizosolenia sima* f. *silicea* or *Rhizosolenia polydactyla* f. *squamosa* are most likely the cold water species linked with sea-ice presence, while abundances in open ocean and warm waters could be *Rhizosolenia simplex* or *Rhizosolenia curvata.*

This group is not used in the transfer function analysis work presented in this thesis. As previous studies observing *Rhizosolenia* species spore types are rare and have been described in section 2.2.18, further discussion on distributions is not pursued here.

3A.3.27 *RHIZOSOLENIA* OTARIA PRESENT GROUP

This combined group is observed in almost every sample of the Natural Database. Highest distributions are located in the Antarctic Peninsula region (9.4%)(Fig. 3.27a). Relative abundances plotted against February and August Temperature convey this cold water dominance in the sediments, whereas a minor abundance agglomeration is noted in slightly warmer temperatures around 3-5°C February SST (Fig. 3.27b). Relative

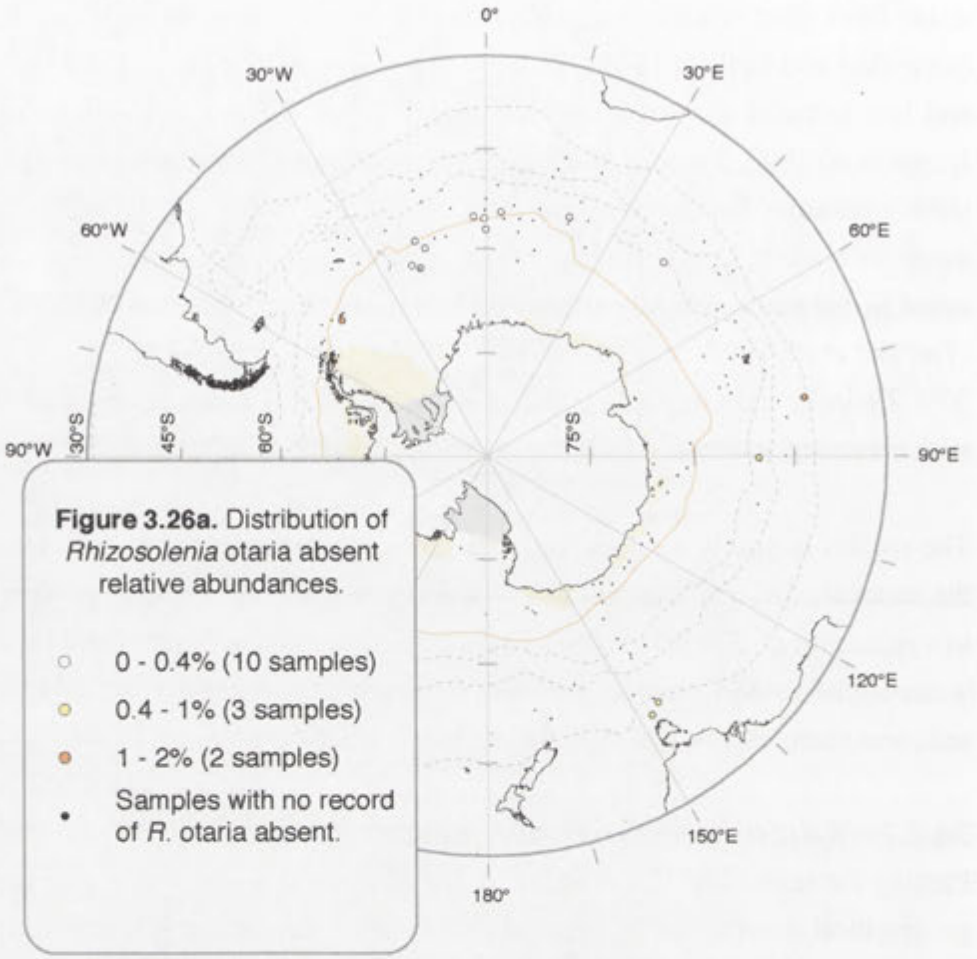

Figure 3.26a. Distribution of *Rhizosolenia* otaria absent relative abundances.

- 0 - 0.4% (10 samples)
- 0.4 - 1% (3 samples)
- 1 - 2% (2 samples)
- Samples with no record of *R.* otaria absent.

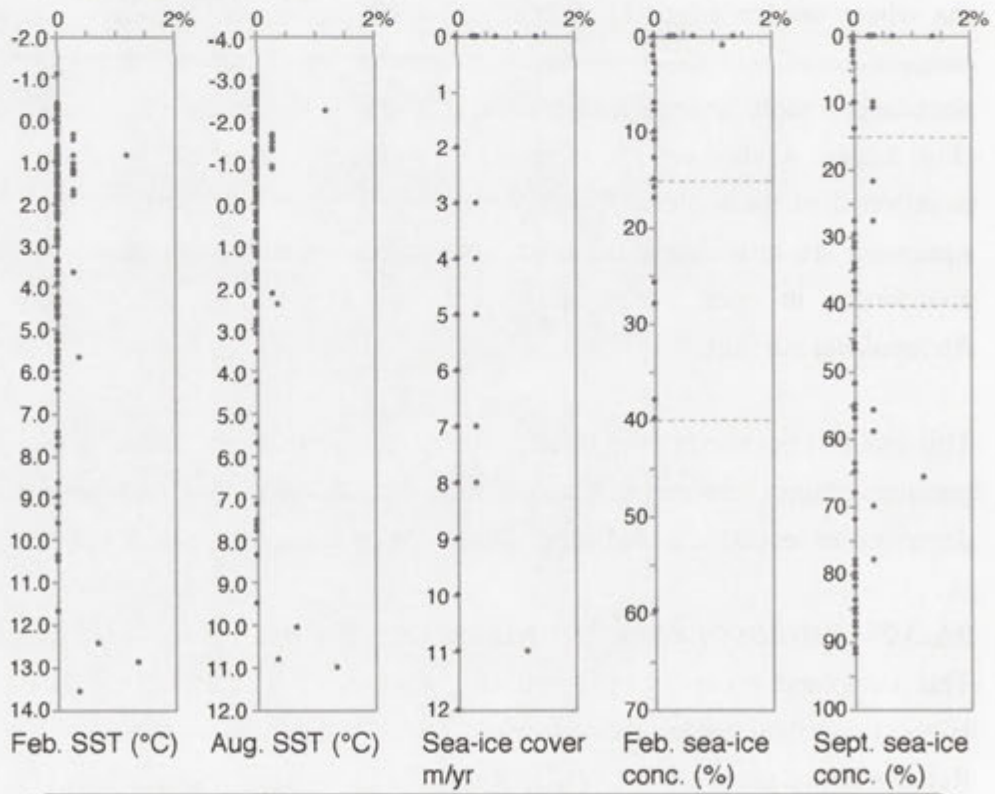

Figure 3.26b. Relative abundances against February and August SST, sea-ice cover in months per year and sea-ice concentration (%) in February and September (annual minimum and maximum sea-ice extents respectively). Other details as in Figure 3.2b.

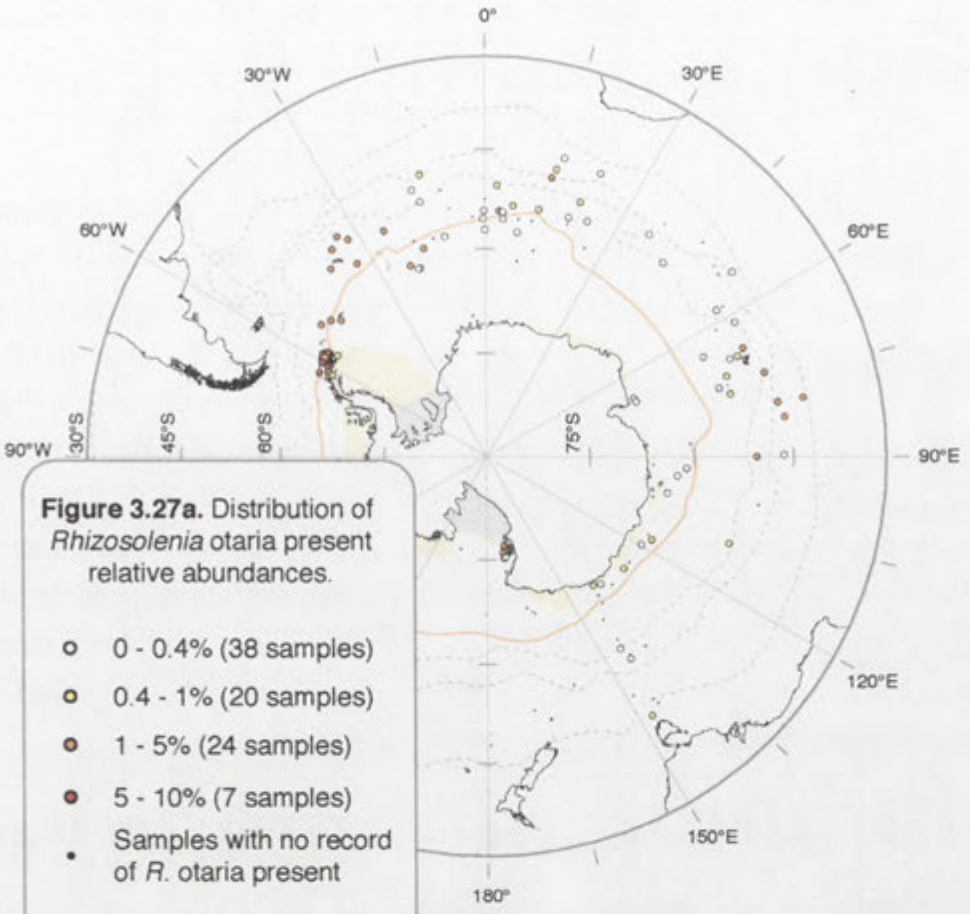

Figure 3.27a. Distribution of *Rhizosolenia* otaria present relative abundances.

- 0 - 0.4% (38 samples)
- 0.4 - 1% (20 samples)
- 1 - 5% (24 samples)
- 5 - 10% (7 samples)
- Samples with no record of *R.* otaria present

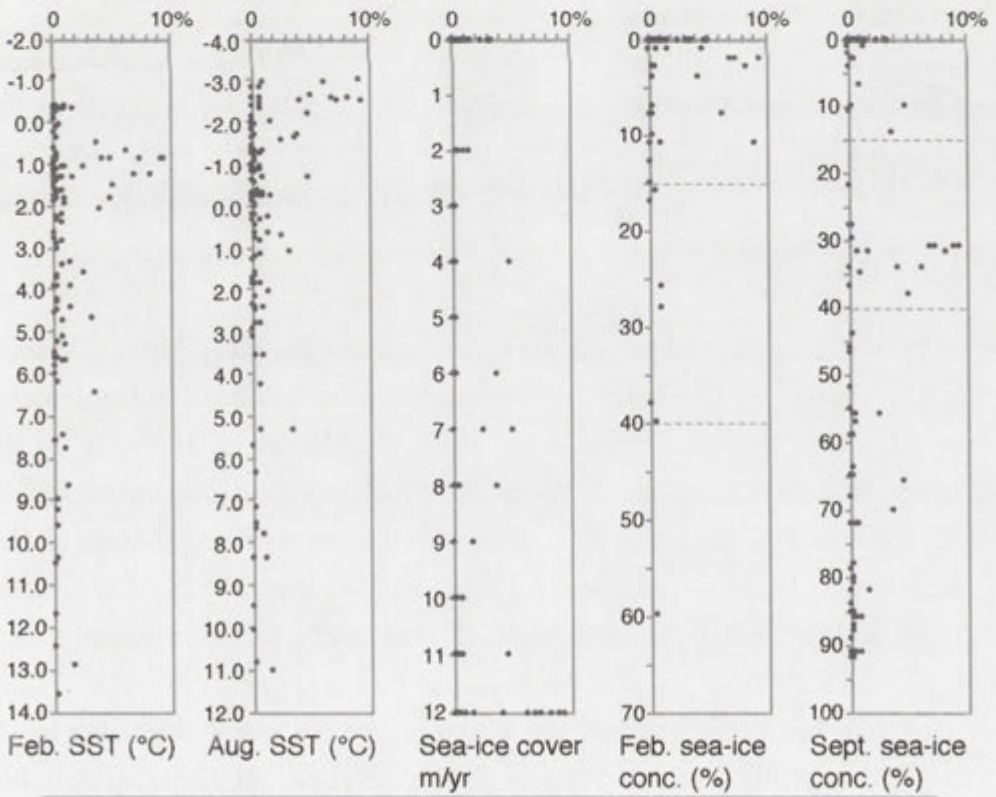

Figure 3.27b. Relative abundances against February and August SST, sea-ice cover in months per year and sea-ice concentration (%) in February and September (annual minimum and maximum sea-ice extents respectively). Other details as in Figure 3.2b.

abundance distribution against degree of annual sea-ice cover indicates increased abundances at 4, 7 and 12 months cover. Ice-free conditions in February and varying degrees of sea-ice concentration during September are observed for this group.

As highlighted in section 2.2.20, several species are incorporated under this *Rhizosolenia* otaria present group. The high abundance data observed in this group is believed to be representative of *Rhizosolenia antennata* f. *semispina*, and this fits well with temperature and abundance data presented by Zielinski and Gersonde (1997). To augment this association, the finding of highest abundances with marginal sea-ice conditions (30-40%) and almost year-round sea-ice cover links in well with the phytoplankton studies of this species made by Ligowski (1993). Although the possibility of including the signal of *Rhizosolenia sima* f. *sima*, which is also associated with sea-ice and cold waters, cannot be denied in these hypotheses, the observation of a small abundance peak in the September sea-ice concentration between 60-70% is more likely to represent this species. Minor species abundances located to the north of the winter sea-ice zone are linked to other *Rhizosolenia* otaria bearing species.

As for *R.* otaria absent group, the *R.* otaria present group is not used in transfer function work in this thesis.

3A.3.28 *ROPERIA TESSELATA*

Roperia tesselata is restricted northward of the SAF (Fig. 3.28a). Maximum abundances are observed in sediments which overlie waters in the range of 7-14°C (Feb. SST) (Fig.3.28b). The highest abundance, 7.7%, is observed at ~11.5°C February SST and 9.5°C August SST. There is no relationship between sea-ice cover and relative abundances.

This species has been observed in the Atlantic sector north of the Polar Front (DeFelice and Wise 1981, Zielinski and Gersonde 1997) throughout the southeast Atlantic sector (Schuette and Schrader 1981, van Iperen *et al.* 1987, Treppke *et al.* 1996) up to the equator (Schuette and Schrader 1979a,b, Pokras and Molfino 1986). Elsewhere, rare or common occurrences of this species in the sediments has been observed. Abbott (1973) found the species south of the southeast Indian Ridge, and van Iperen *et al.* (1993) noted it in the Indonesian Archipelago. Highest reported abundances in the sediments were made by Schuette and Schrader (1981) in off-shore samples southwest Africa (17.28%). The species was considered the second most abundant species in van Iperen *et al.* 's (1987) southern group of the southeast Atlantic, which included *Fragilariopsis doliolus*, *Thalassiosira leptopus*, and *Thalassiosira lineata.* Maximum abundances south of 30°S were reported by Zielinski and Gersonde (1997, fig. 17.7) at 5% between 9 to 10°C.

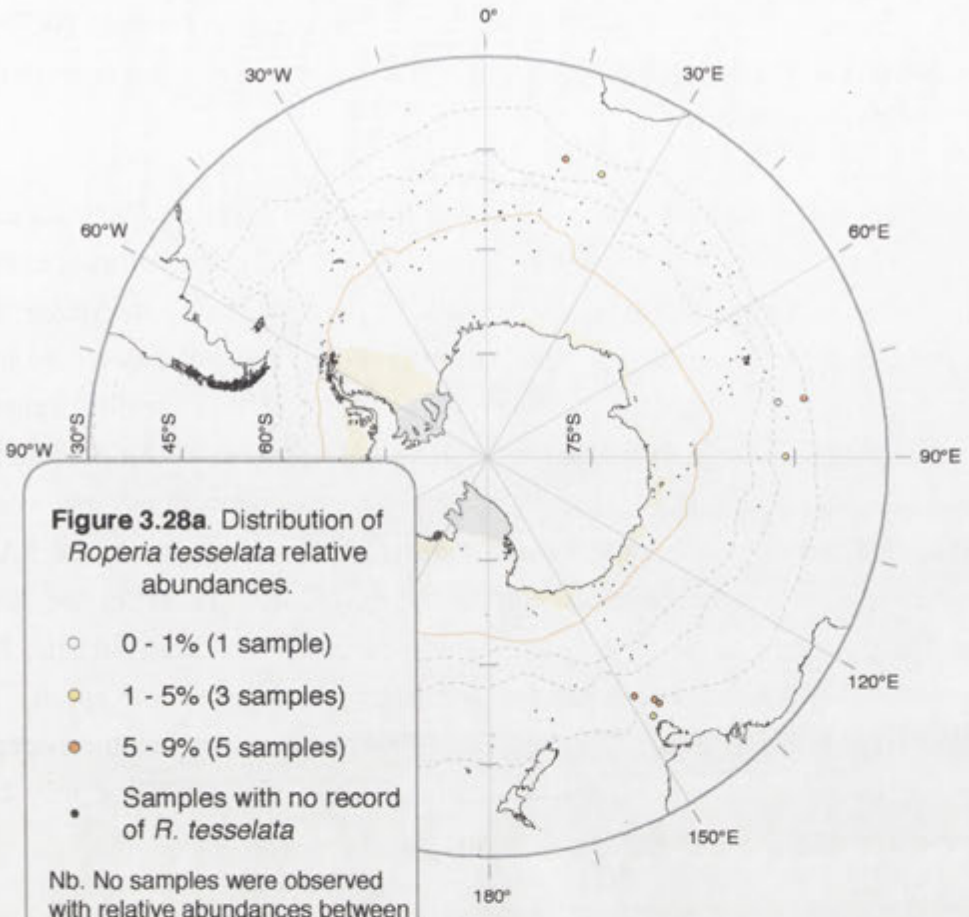

Figure 3.28a. Distribution of *Roperia tesselata* relative abundances.

- 0 - 1% (1 sample)
- 1 - 5% (3 samples)
- 5 - 9% (5 samples)
- Samples with no record of *R. tesselata*

Nb. No samples were observed with relative abundances between 0.1 and 0.6%.

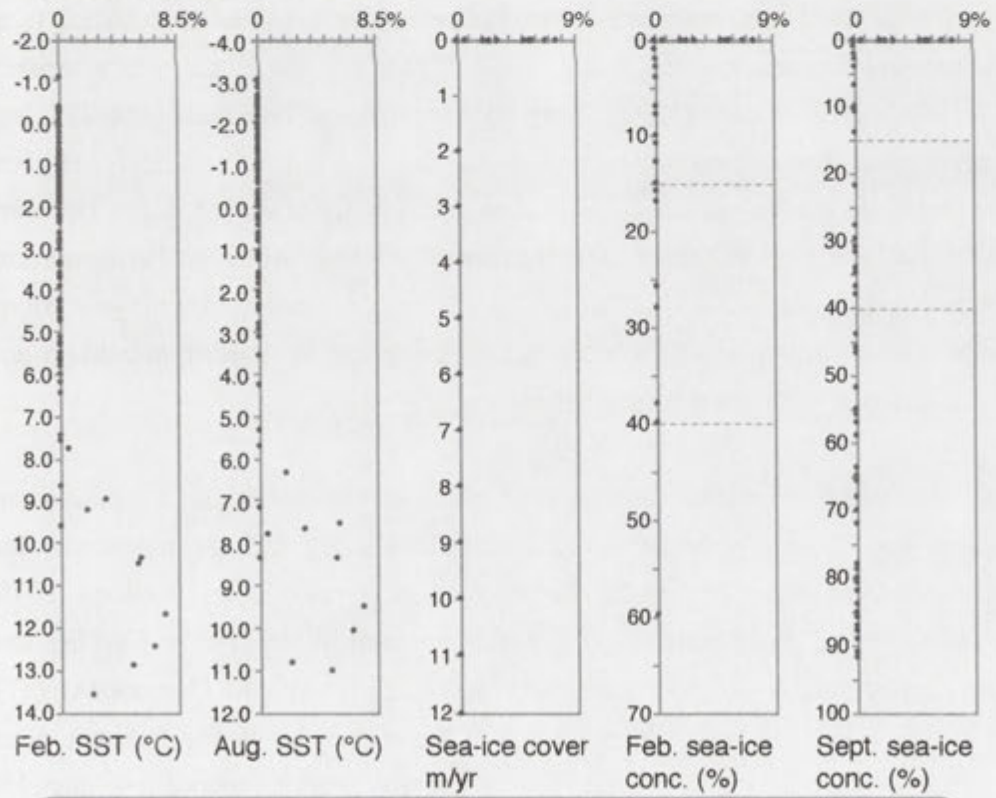

Figure 3.28b. Relative abundances against February and August SST, sea-ice cover in months per year and sea-ice concentration (%) in February and September (annual minimum and maximum sea-ice extents respectively). Other details as in Figure 3.2b.

Hasle (1976) attributed surface water distributions in the Pacific region between 60-70°S as related to current transport and the ability of the species to survive but not necessarily reproduce in a colder environment.

Relative abundances in the Natural Database are higher than those found by Zielinski and Gersonde (1997) and although few in number provide a good bell curve for associating SST. The species was not observed to pass southward of the SAF, unlike the studies in the South Atlantic sector which observe occurrences to the Polar Front but may record the southerly distribution as mentioned by Hasle (1976). Obviously, increased sample number in the warmer water regions will aid in defining this observation. An interesting point to make is that the species appears to have two zones of abundance. Both this work and that of Zielinski and Gersonde (1997) indicate that a maximum occurs in the SAZ with relative abundance numbers dropping off to the north. In contrast in the low latitudes, and based entirely on the distributions observed in the southeast Atlantic, *R. tesselata* is found to reach its maximum known sedimentary abundance. The species is known to have variation in valve shape (Lee and Lee 1990) and this may become evident when comparing the two abundance regions. It seems likely that upwelling may be another factor important to the distribution of the species.

3A.3.29 *STELLARIMA MICROTRIAS*

The distribution of *Stellarima microtrias* and *Stellarima stellaris* (section 3A.3.30) as noted in the previous chapter (section 2.2.21) were divided by temperature characteristics noted by Zielinski and Gersonde (1997). Thus, those specimens observed with SST less than 3°C are attributed to *S. microtrias* and those above 3°C to *S. stellaris*. Highest abundances (3.3% maximum) of the *S. microtrias* division are observed under February SST of -0.5°C and are predominantly located in the Ross Sea, Antarctic Peninsula and west of South Orkney Island (Fig. 3.29a,b). This division is associated with year round sea-ice conditions, with high sea-ice concentration during the September maximum and open ocean to ice edge conditions during February.

All reports of *Stellarima microtrias* (under *Coscinodiscus furcatus*, *Coscinodiscus symbolophorus* and *S. microtrias*) are noted in sediments along the Antarctic coast and various ice shelves (Jousé *et al.* 1962a, Kozlova 1966, Truesdale and Kellogg 1979, Gersonde 1984, Prasad and Nienow 1986, Gersonde and Wefer 1987, Kellogg and Kellogg 1987, Stockwell *et al.* 1991, Leventer 1992, Zielinski and Gersonde 1997). Kozlova (1966) recorded the highest abundances of the species along the Antarctic coast in the Indian sector (maximum 8.7%) but most recent observations record less than 1% with exception to samples along the Filschner-Ronne Ice Shelf which are noted up to 3% (Gersonde 1984, Zielinski and Gersonde 1997). Kozlova (1966) stated the northern limit

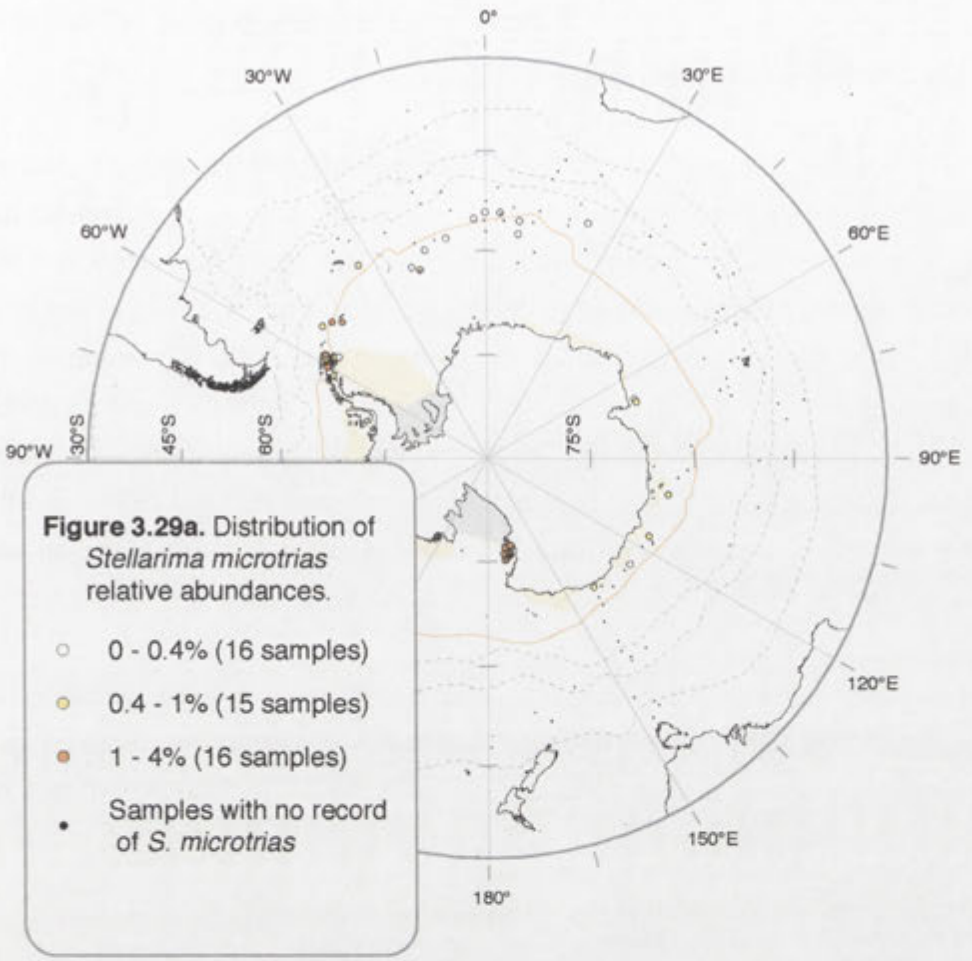

Figure 3.29a. Distribution of *Stellarima microtrias* relative abundances.

- 0 - 0.4% (16 samples)
- 0.4 - 1% (15 samples)
- 1 - 4% (16 samples)
- Samples with no record of *S. microtrias*

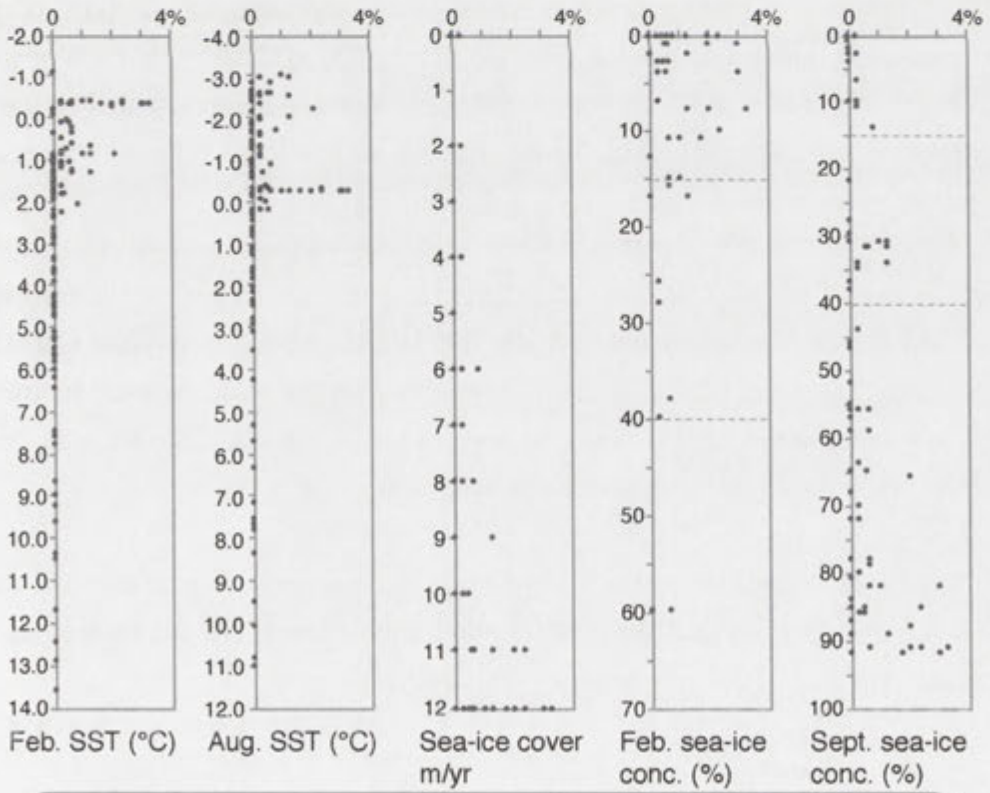

Figure 3.29b. Relative abundances against February and August SST, sea-ice cover in months per year and sea-ice concentration (%) in February and September (annual minimum and maximum sea-ice extents respectively). Other details as in Figure 3.2b.

of the species in the sediments was to 60°S, and only single observations of "*C. furcatus*" were noted this far south in the South Atlantic sector by DeFelice and Wise (1981).

Stellarima microtrias has been reported in both land fast and pack-ice samples (Horner 1985, Garrison and Buck 1989, Garrison 1991). Through the seasons, *S. microtrias* has been located in several sea-ice associated situations. Over spring the vegetative cell has been found in abundance at depth away from the sea-ice edge (Fryxell 1989), whereas in the sea-ice the species is noted in high abundance (Garrison *et al.* 1987). In summer, the species has been noted in very high abundance in fast sea-ice samples (Watanabe 1982, Krebs *et al.* 1987, Tanimura *et al.* 1990). During autumn, the resting spore is found in high abundance under sea-ice and is not present in the open ocean (Fryxell 1989), and the species was commonly found in newly forming sea-ice (Gersonde 1984, Garrison and Close 1993).

The divided data here representing *S. microtrias,* have similar maximum abundances as previously reported. The distribution is linked to sea-ice cover. Due to the emplaced split in the data from *S. stellaris* further comment on the natural distribution will not be advanced.

3A.3.30 *STELLARIMA STELLARIS*

The artificial distribution of this species is north of the PF and south of the STC (Fig. 3.30a). The maximum relative abundance observed in the Natural Database is 1.8% of the total. Distribution in terms of SST signatures link increased abundances with February SST >7°C and August SST >3.5°C (Fig. 3.30b). There is no relationship found with sea-ice cover.

Unqualified accounts of *Coscinodiscus stellaris* and *Coscinodiscus stellaris* var. *symbolophorus* have been made by both Abbott (1973) and DeFelice and Wise (1981). The latter authors, however, do not mention where the species was observed in their study region, whereas Abbott (1973) notes the species as common in siliceous ooze belt which suggests under the PF of the southeast Indian sector.

As the distribution is derived from the split data of *S. microtrias*, comments on the distribution sadly remain as unqualified as those previously reported, but can be used as a base interpretation to check future sedimentary distribution patterns.

3A.3.31 *THALASSIONEMA* TAXA

The grouped *Thalassionema* taxa are principally observed in increasing numbers north of the maximum winter sea-ice edge (Fig. 3.31a). A zone of maximum appears in the

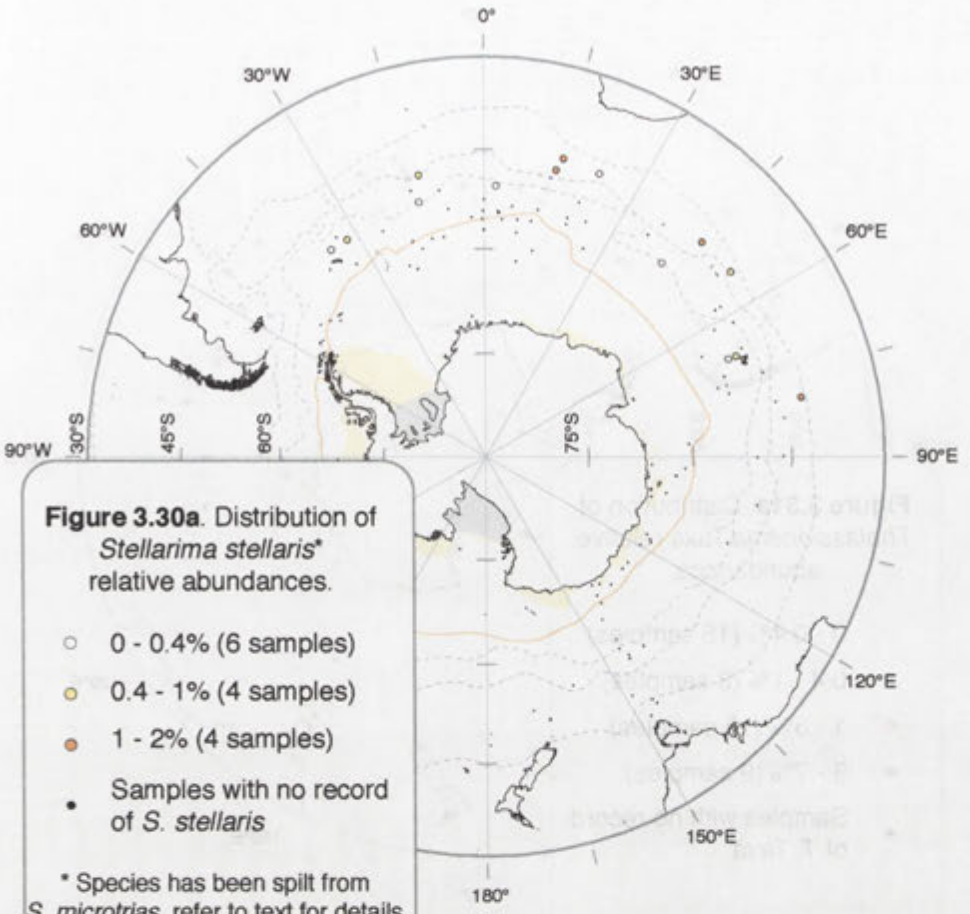

Figure 3.30a. Distribution of *Stellarima stellaris** relative abundances.

- 0 - 0.4% (6 samples)
- 0.4 - 1% (4 samples)
- 1 - 2% (4 samples)
- Samples with no record of *S. stellaris*

* Species has been spilt from *S. microtrias*, refer to text for details.

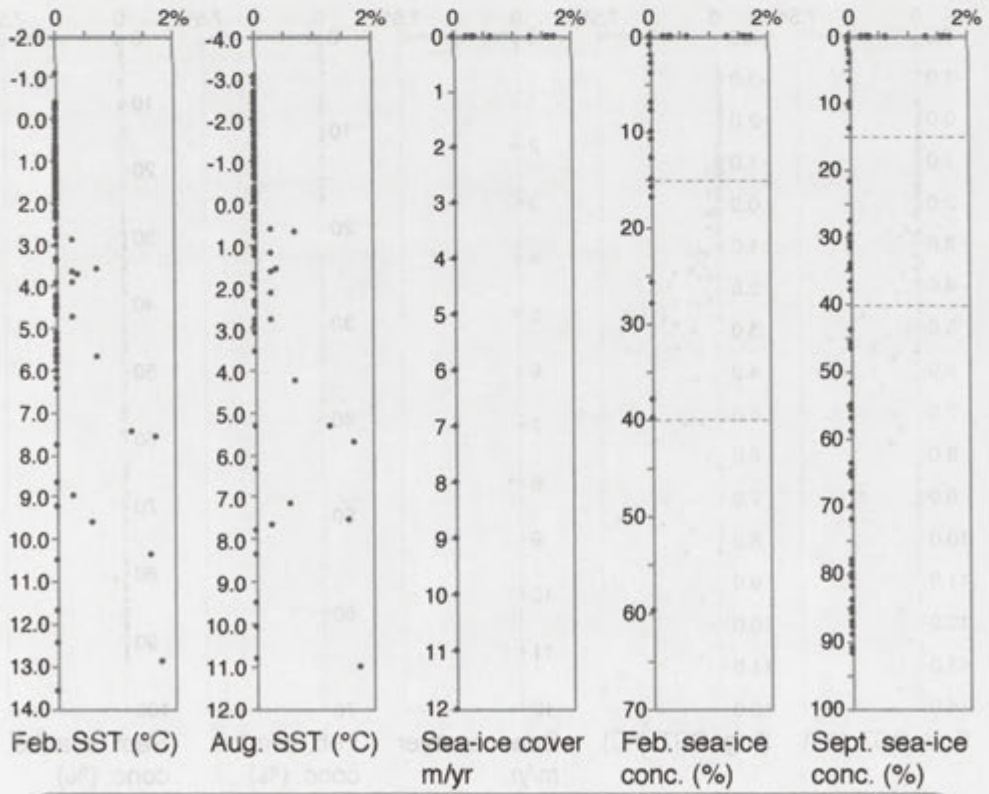

Figure 3.30b. Relative abundances against February and August SST, sea-ice cover in months per year and sea-ice concentration (%) in February and September (annual minimum and maximum sea-ice extents respectively). Other details as in Figure 3.2b.

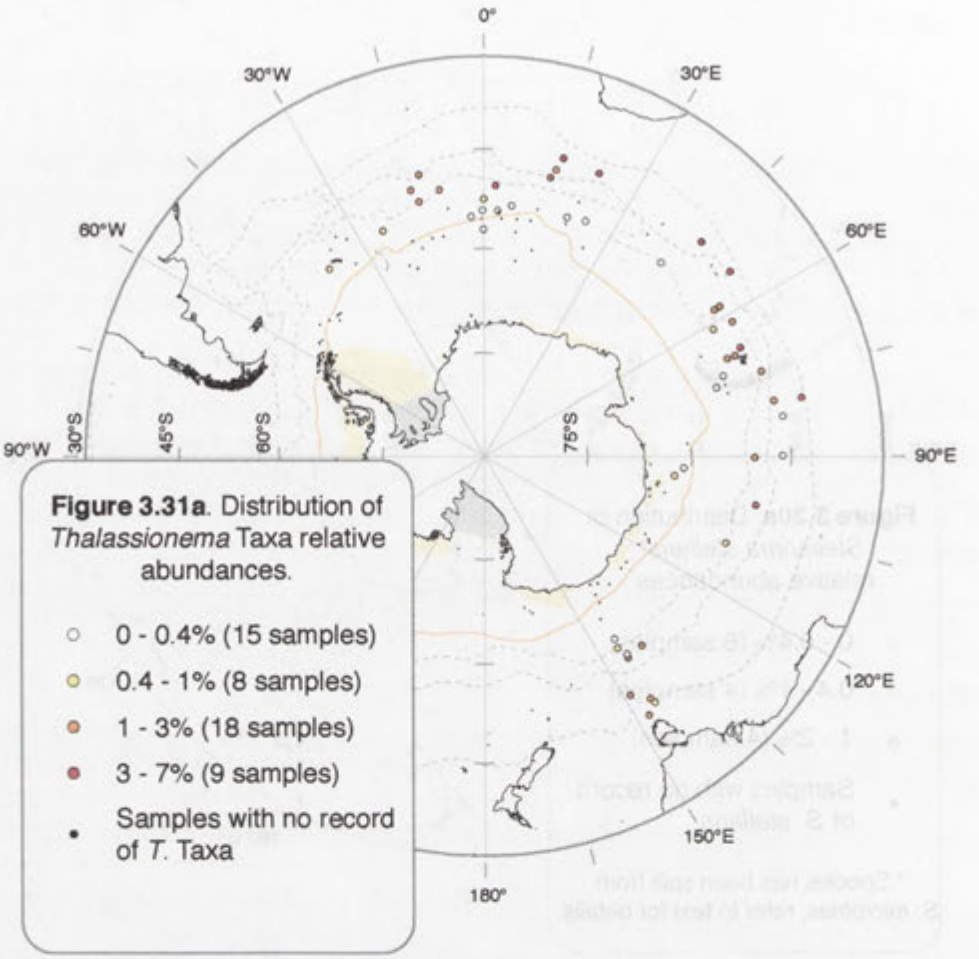

Figure 3.31a. Distribution of *Thalassionema* Taxa relative abundances.

- 0 - 0.4% (15 samples)
- 0.4 - 1% (8 samples)
- 1 - 3% (18 samples)
- 3 - 7% (9 samples)
- Samples with no record of *T.* Taxa

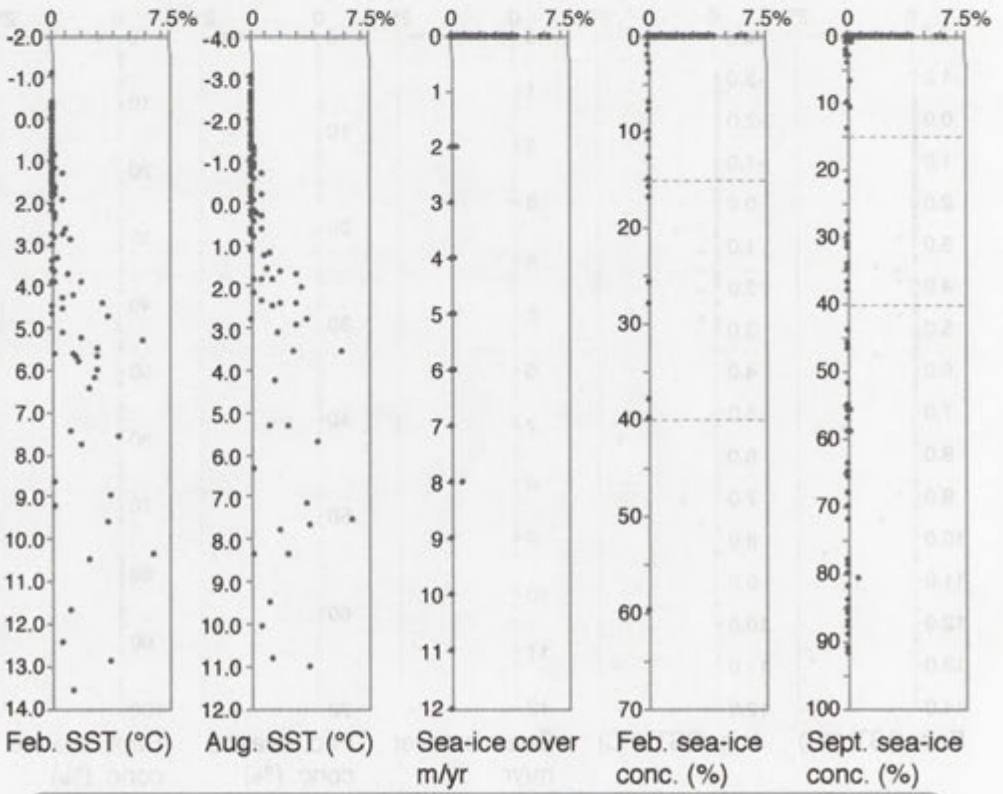

Figure 3.31b. Relative abundances against February and August SST, sea-ice cover in months per year and sea-ice concentration (%) in February and September (annual minimum and maximum sea-ice extents respectively). Other details as in Figure 3.2b.

Subantarctic Zone between the STC and the SAF. The maximum abundance encountered of the taxa is 6.5%. The zone of maximum abundances is translated into February SST between 5° and 10°C, and August SST of 3.5° to 7.5°C (Fig. 3.31b). Aside from trace occurrences in sea-ice covered regions the group is not associated with sea-ice cover.

As acknowledged in the previous chapter (section 3.2.22) several characteristic species have been lumped under the one category in this Natural Database. Of importance to the distributions noted here are *Thalassionema nitzschioides* var. *parva*, *Thalassionema nitzschioides* var. *lanceolata*, *Thalassionema nitzschioides*, and *Thalassionema nitzschioides* forma 1 (*sensu* Zielinski 1993, Zielinski and Gersonde 1997). *Thalassionema n.* var. *parva* is a warm water species noted only in sediments north of the STC (Schuette and Schrader 1979a,b, 1981, Pokras and Molfino 1986, van Iperen *et al.* 1987, van Iperen *et al.* 1993, Treppke *et al.* 1996, Zielinski and Gersonde 1997) and linked to warm waters high salinity and with moderate to low nutrients (van Iperen *et al.* 1987). Highest abundances of the variety in the sediments, 17.9%, is reported by Schuette and Schrader (1979a,b). Some of the abundance data in the Natural Database south of Tasmania can be attributed to *T. n.* var. *parva* and is probably derived from warm water eddies pinched off the East Australian Current.

Thalassionema nitzschioides is also often reported in the warm water regions alongside *T. n.* var *parva*, but has just as equally been observed in Antarctic sediments (Abbott 1973, Truesdale and Kellogg 1979, Stockwell *et al.* 1991, Tanimura 1992). Zielinski and Gersonde (1997) combined *T. nitzschioides*, *T. n.* var *lanceolata* and *T. n.* var. *capitulata* under the one group for the South Atlantic sediments. This group's greatest Southern Ocean abundance of ~5% was observed under summer SST between 5° and 15°C, similar to the main abundance peak found in the Natural Database. The cold water form *T. n.* forma 1 does not appear to have been observed in the same abundances or cold water signature as indicated by Zielinski and Gersonde (1997). The differences between the two databases for this forma species is not understood, and can be considered overlooked, attributed to another diatom species or sample coverage has not been adequate enough in the cooler regions to pick up this forma's presence.

Use of this combined group still has application for SST transfer function work, since a broad abundance curve is associated with the mid-temperature range. The influence of *T. n.* var. *parva* and the cold water *T. n.* forma 1 appear to be missing from the bulk of the data associated with the *Thalassionema* Taxa and so the signal is interpreted as the combination of the Antarctic species *T. nitzschioides*, *T. n.* var *lanceolata* and *T. n.* var. *capitulata*.

3A.3.32 *THALASSIOSIRA ANTARCTICA/SCOTIA* GROUP

An Antarctic coastal distribution of the *Thalassiosira antarctica/scotia* group is noted in the Antarctic Peninsula region, northeast of South Georgia Island and the Ross Sea (Fig. 3.32a). Abundances in the sediments up to 40-66% are observed in the first two of these regions, whereas the Ross Sea has abundances of up to 40%. Relative abundance relationships against SST and sea-ice exhibit regional signatures. These are less easy to interpret under the February SST and annual sea-ice cover for the Ross Sea and the Antarctic Peninsula, but under winter conditions of sea-ice concentration and SST the variation is evident (Fig. 3.32b). Samples from the Antarctic Peninsula are identified by the coldest SST values (-3.5° to -2°C), and year round consolidated pack-ice distribution (~60%). The sample northeast of South Georgia has high abundances at SST of 4°C and 0.5°C during February and August respectively, and is free of sea-ice cover. This lone high abundance may be associated with the presence of *Thalassiosira scotia.*

Thalassiosira antarctica abundances reported in sediments surrounding Antarctica are disparately reported as either rare (Kozlova 1966, Abbott 1973, Tanimura 1992) in medium maximum abundances between 5 -15% (Gersonde 1984, Gersonde and Wefer 1987, Stockwell *et al.* 1991, Leventer 1992) or with maximum abundances of 32% in the coastal sections of the Weddell Sea (Zielinski and Gersonde 1997). Furthermore, observations north of the SAF have been interpreted as surface water transport by the ACC (Zielinski and Gersonde 1997). The increase in abundance northeast of South Georgia Island, as observed in this work, was also reported by Zielinski and Gersonde (1997).

Garrison (1991) notes *Thalassiosira antarctica* as present in both fast and pack-ice. Fast-ice accumulation of the species (Krebs *et al.* 1987) has been speculated to be resultant of ice platelet accumulation under the consolidated sea-ice (Garrison 1991). The species has also been noted under sea-ice or in the adjacent water column (Cassie 1963, Garrison *et al.* 1987). There are no records of *T. scotia* observed in sea-ice.

Maximum relative abundances in the Natural Database are double those reported in the same study region by Zielinski and Gersonde (1997). As mentioned under the distribution of *Odontella weissflogii*, the lack of *Chaetoceros* species data has influenced this Natural Database in relation to the samples of the Antarctic Peninsula region, thus here it is manifest by an increase of *T. antarctica/scotia* Group abundance. The *T. antarctica/scotia* group appears to be related to sea-ice distribution, in particularly with near year round cover that changes from ice-edge to pack-ice conditions in the summer and near consolidated fast-ice conditions (30-60%) during the winter maximum. The exception being the abundance attributed to *T. scotia* in the Argentine Basin.

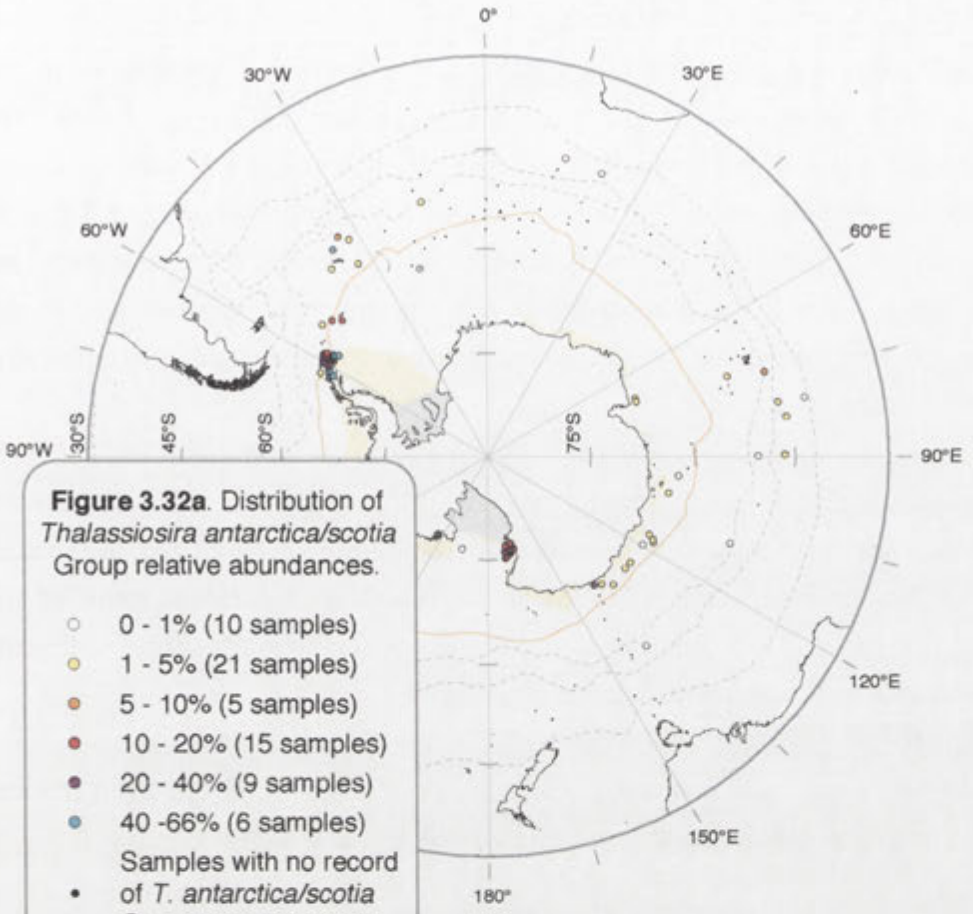

Figure 3.32a. Distribution of *Thalassiosira antarctica/scotia* Group relative abundances.

- 0 - 1% (10 samples)
- 1 - 5% (21 samples)
- 5 - 10% (5 samples)
- 10 - 20% (15 samples)
- 20 - 40% (9 samples)
- 40 -66% (6 samples)
- Samples with no record of *T. antarctica/scotia* Group

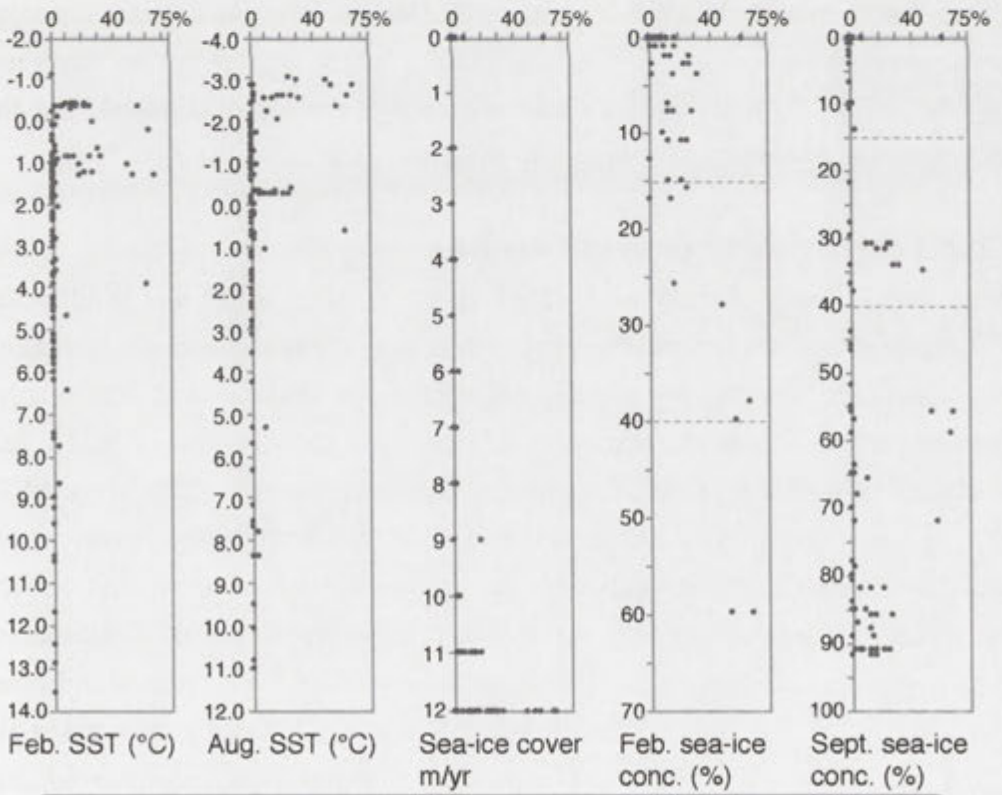

Figure 3.32b. Relative abundances against February and August SST, sea-ice cover in months per year and sea-ice concentration (%) in February and September (annual minimum and maximum sea-ice extents respectively). Other details as in Figure 3.2b.

3A.3.33 *THALASSIOSIRA DECIPIENS*

Thalassiosira decipiens is recorded commonly, but in very low abundance, in the sediments between the maximum winter sea-ice edge and the STC (Fig. 3.33a). The species abundance has a very broad alliance to SST. Ranging from 1°C with increasing abundance to 10.5°C February SST, and -2°C to 7.5°C August SST (Fig. 3.33b). In general the species is not associated with sea-ice cover although trace specimens are found in regions of up to 10 months sea-ice cover. The species is not associated to any particular sea-ice type during the September maximum extent although, geographically, this is observed as the sea-ice edge.

Just as diffuse as the SST response, previous records of *T. decipiens* in the sediments are found in various unrelated regions. Truesdale and Kellogg (1979) reported the species near the Ross Sea-ice Shelf, Abbott (1973) noted it as rare in samples south of the southeast Indian Ridge, and Schuette and Schrader (1981) in off-shore sediments southwest of Africa with maximum abundances of 5.4%.

Only Horner (1985) surmised from early works the presence of *T. decipiens* in sea-ice. Cassie (1963) noted the species under sea-ice in the Ross Sea.

It seems probable that *T. decipiens* is poorly identified in the sediments because of its very small size and similarity to small specimens of *Thalassiosira gracilis* var. *expecta*.. This would account for its broadly reported distribution. As the species has no direct use in transfer function work because of its low recovery it can be overlooked, but the identification and distribution still is a long way from being correctly distinguished.

3A.3.34 *THALASSIOSIRA* ECCENTRIC GROUP

The *Thalassiosira* Eccentric Group is a mixed group of both warm and cold water species. Geographical coverage of the group indicates a slight trend in increasing abundances to the north over a very broad distribution range (Fig. 3.34a). The relative abundances interpreted in terms of February and August SST show two major peaks, one in warm waters (~13°C Feb. SST) and the other in very cold waters (~-0.5°C Feb. SST) (Fig. 3.34b). This double peak is also represented in relation with sea-ice cover, where highest abundances are either with maximum annual sea-ice cover or without sea-ice cover. The variation noted can roughly be attributed to representation of *Thalassiosira trifulta*(a synomyn to *T. latimarginata*) in the south and *Thalassiosira eccentrica* and other warm-water species of the group in the north. These two distributions assist in explaining the wide dispersal pattern observed in the sediments. *Thalassiosira trifulta*has only been reported by Stockwell *et al.* (1991, as *T. trifulta*) as rarely present in sediment samples of inner Prydz Bay. Zielinski and Gersonde (1997) do not

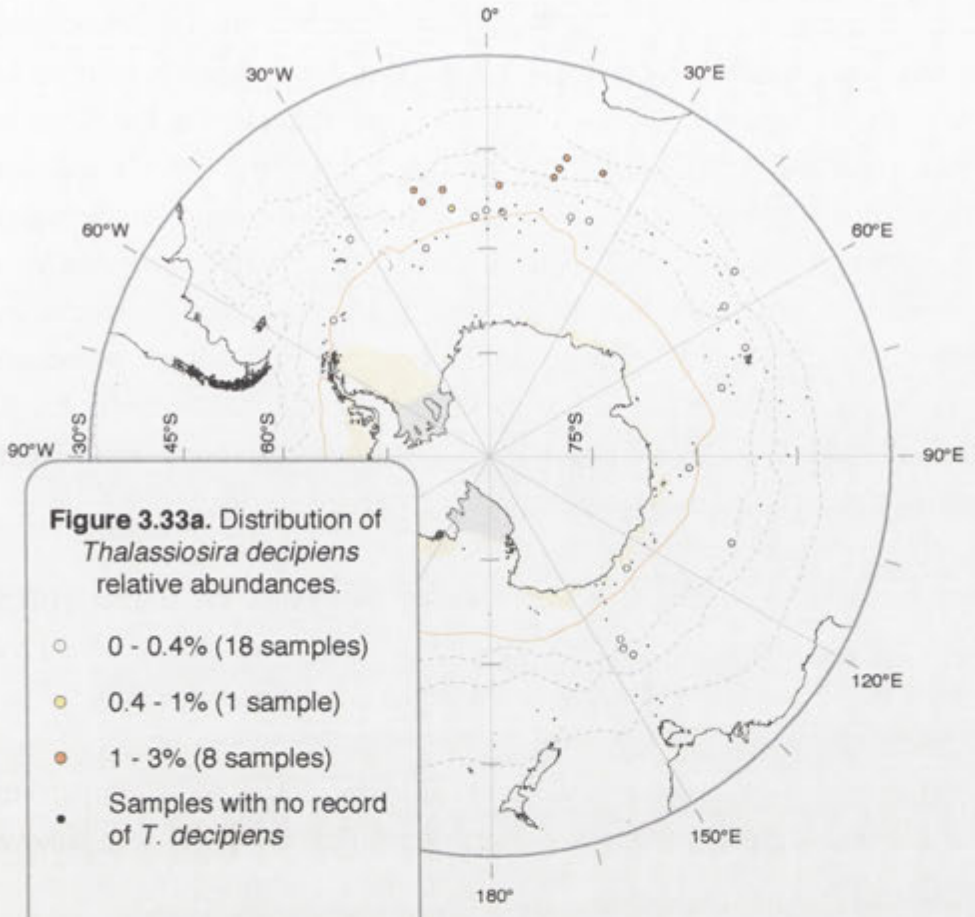

Figure 3.33a. Distribution of *Thalassiosira decipiens* relative abundances.

- 0 - 0.4% (18 samples)
- 0.4 - 1% (1 sample)
- 1 - 3% (8 samples)
- Samples with no record of *T. decipiens*

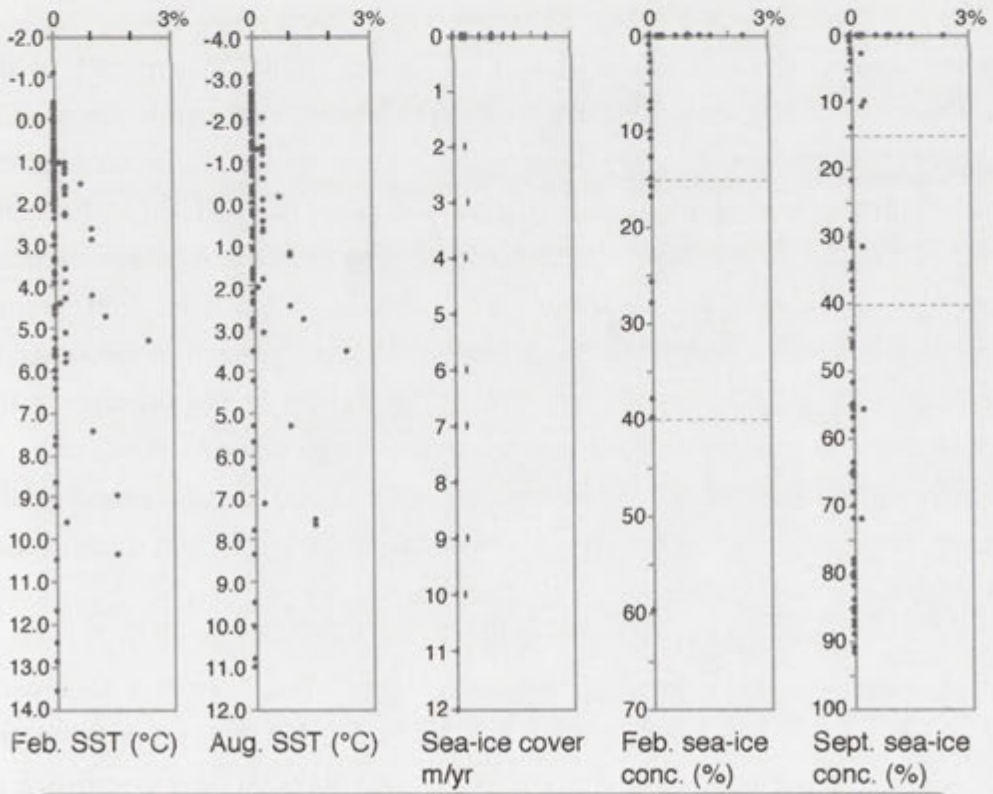

Figure 3.33b. Relative abundances against February and August SST, sea-ice cover in months per year and sea-ice concentration (%) in February and September (annual minimum and maximum sea-ice extents respectively). Other details as in Figure 4.2b.

report having come across *T. trifulta* in the South Atlantic sector. *Thalassiosira eccentrica* or grouped categories (including *Thalassiosira symmetrica, Thalassiosira punctifera, and Thalassiosira spinosa*) have been reported from sediment samples from the Ross and Amundsen Seas (Truesdale and Kellogg 1979, Kellogg and Kellogg 1987) to sediments of the ACC (Abbott 1973, DeFelice and Wise 1981), and in low to mid latitude regions (Schuette and Schrader 1979a,b, 1981, Pokras and Molfino 1986, van Iperen *et al.* 1993). The cold-water occurrences may be attributed to *T. trifulta* since the species was not described at the time of these species identifications. Highest relative abundances (26.5%) were observed by Schuette and Schrader (1979a,b) in the southeast Pacific. Hasle (1976) describes *T. eccentrica* in surface water distributions as a cosmopolitan coastal species that is not found in the Subantarctic and Antarctic regions.

Previous accounts of *T. eccentrica* in sea-ice samples were made by Horner (1985), Krebs *et al.* (1987) and Garrison (1991). In spring sea-ice edge samples *T. trifulta* was noted in adjacent water samples but not in sea-ice samples (Garrison *et al.* 1987).

As a product of the mixed signals within this group, differentiation is not worth pursuing at this point in time and with the need to recount samples. This group has been removed from transfer function analysis.

3A.3.35 *THALASSIOSIRA GRACILIS* GROUP

Increasing abundances of *Thalassiosira gracilis* Group are found on approach to the maximum winter sea-ice extent and Antarctic coast, with highest abundances observed in the Antarctic Peninsula region (14.5%) (Fig. 3.35a). There appears to be no northern boundary to the distribution of the group. Highest abundances are related to February SST between 0-2°C and August SST of -1.5 to-2.5°C (Fig. 3.35b). A steady decrease from these high abundance peaks are noted to ~9°C. Distribution with sea-ice concentration and cover is interesting in that a bi-modal peak is noted in the cover in months per year at 7 and 12 months respectively. This feature is not detected in the specific maximum and minimum concentrations plots. Here, highest abundances are associated with 30-40% September concentration sea-ice, and during February the species group appears associated with an environment varying from open ocean conditions to the sea-ice edge.

As noted in the geographical distribution presented in Figure 3.35a, *T. gracilis* has a wide distribution and is reported in the sediments by most workers. The most northerly record appears to be made by Schuette and Schrader (1981) who found a trace occurrence in their samples off southwest Africa. Jousé *et al.* (1962a), Kozlova (1966), Abbott (1973), Donahue (1973) and DeFelice and Wise (1981) all report it in patchy or low numbers in

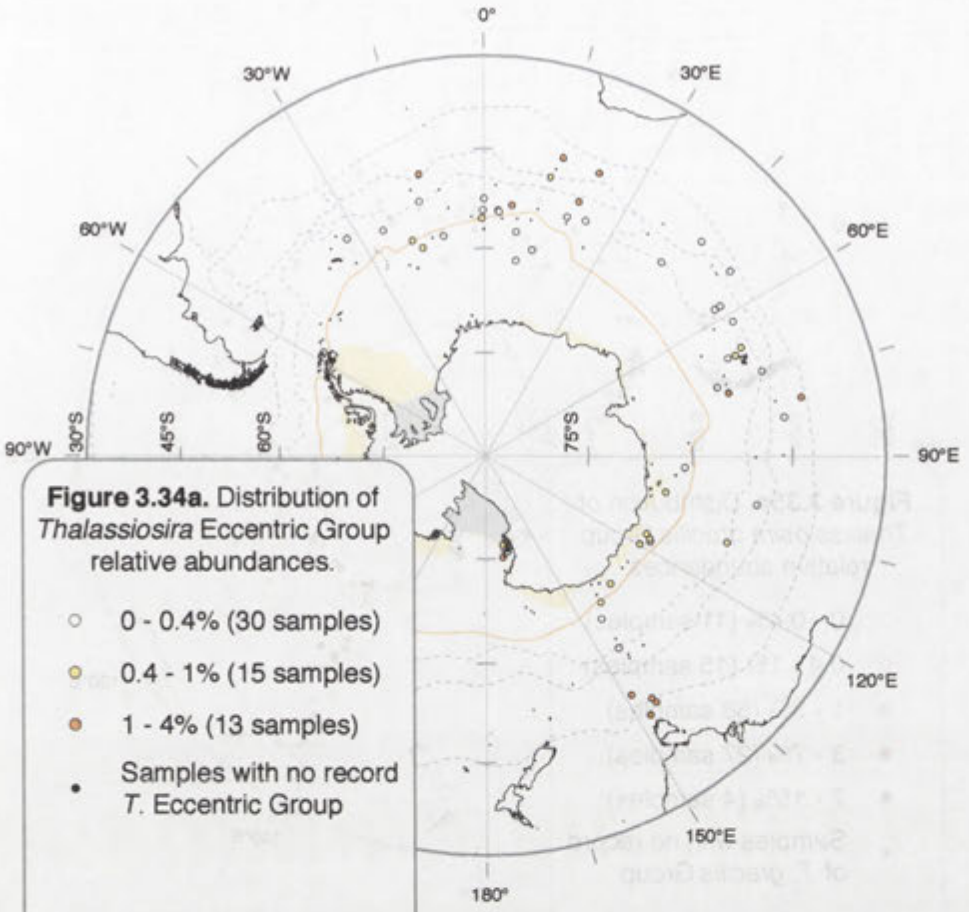

Figure 3.34a. Distribution of *Thalassiosira* Eccentric Group relative abundances.

- 0 - 0.4% (30 samples)
- 0.4 - 1% (15 samples)
- 1 - 4% (13 samples)
- Samples with no record *T.* Eccentric Group

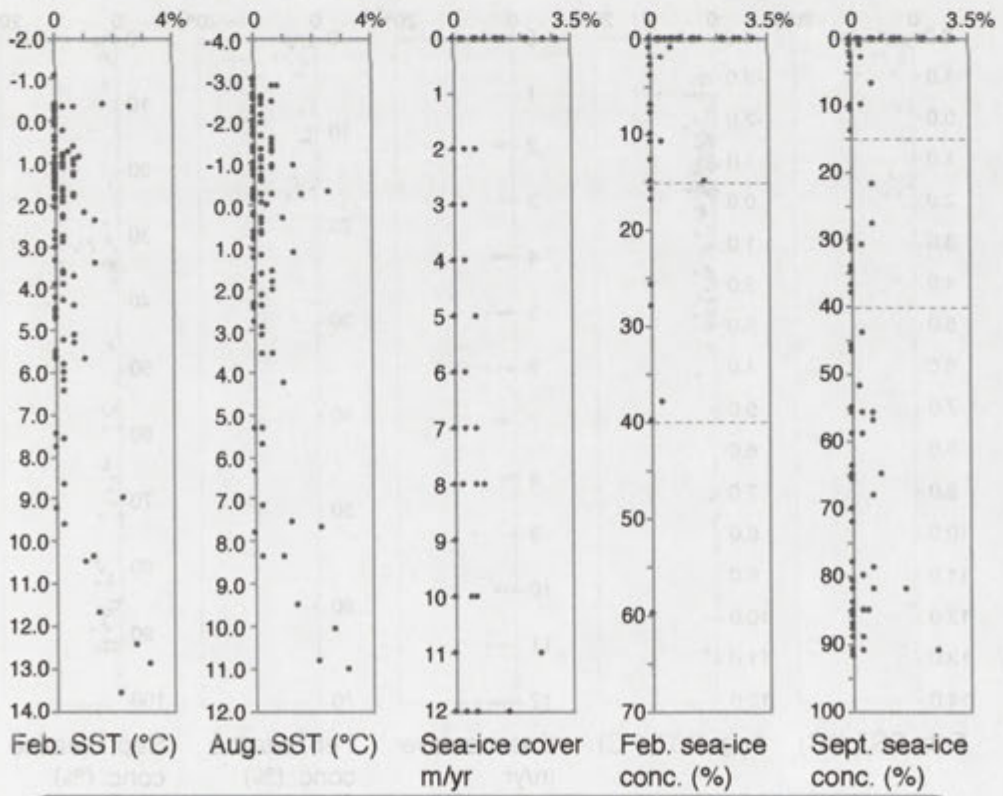

Figure 3.34b. Relative abundances against February and August SST, sea-ice cover in months per year and sea-ice concentration (%) in February and September (annual minimum and maximum sea-ice extents respectively). Other details as in Figure 3.2b.

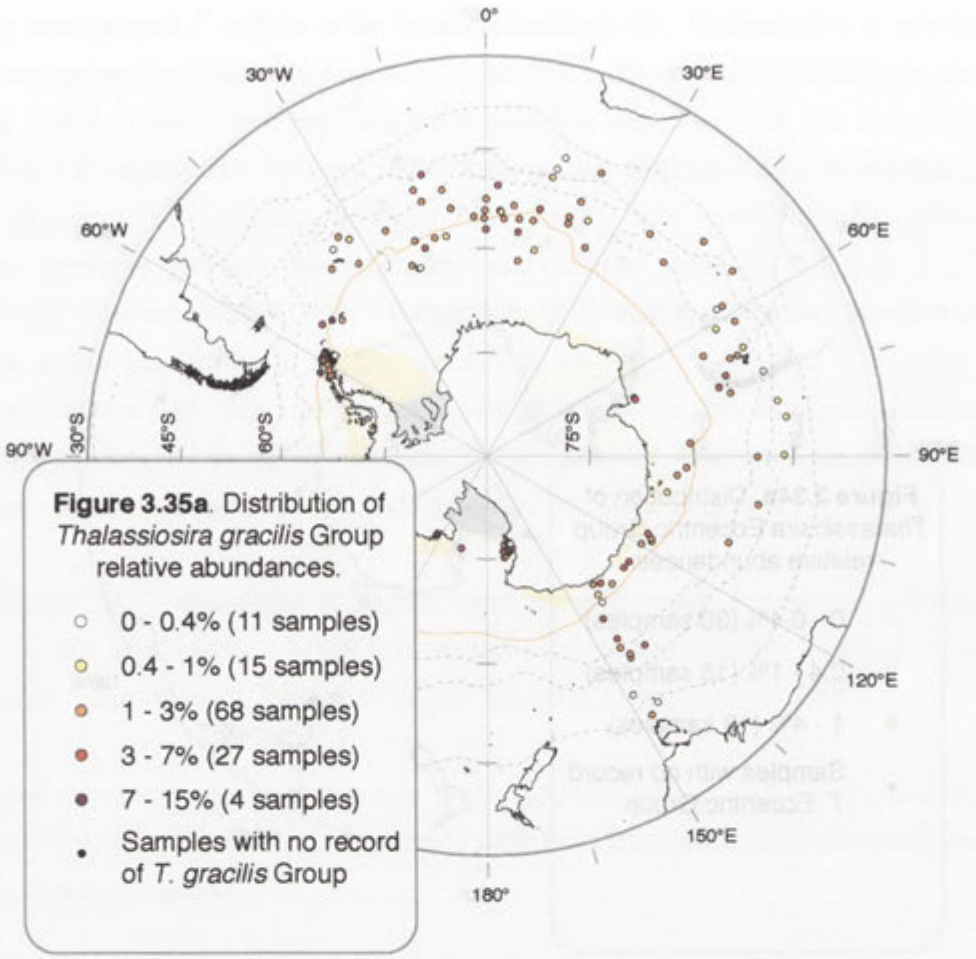

Figure 3.35a. Distribution of *Thalassiosira gracilis* Group relative abundances.

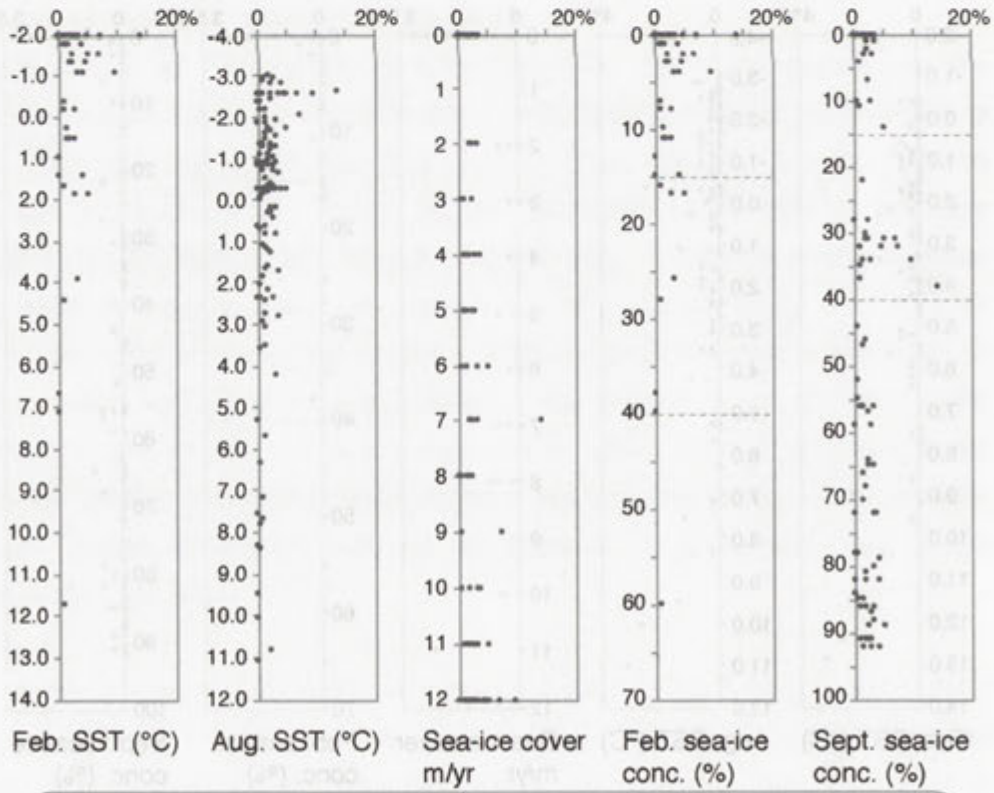

Figure 3.35b. Relative abundances against February and August SST, sea-ice cover in months per year and sea-ice concentration (%) in February and September (annual minimum and maximum sea-ice extents respectively). Other details as in Figure 3.2b.

sediments of the open ocean region of the ACC, and on average with a maximum of 3%. Along the Antarctic coast several reports have been made (Truesdale and Kellogg 1979, Prasad and Nienow 1986, Gersonde 1984, Gersonde and Wefer 1987, Kellogg and Kellogg 1987, Stockwell *et al.* 1991, Tanimura 1992, Leventer 1992). In almost all cases the abundances have been reported at less than 2%. Distribution of the two varieties *expecta* and *gracilis* in Prydz Bay and along the George V Coast was noted with higher abundances of the latter species further from the coast, in contrast to a ubiquitous low distribution of the former variety in the study region (Stockwell *et al.* 1991, Leventer 1992). Zielinski and Gersonde (1997) report the grouped species as uniformly distributed through the South Atlantic but with highest abundances found in the SIZ and POOZ. As in this study, they had similar highest abundances in the Drake Passage/Antarctic Peninsula region.

Thalassiosira gracilis has been reported in sea-ice samples (Gersonde 1984, Horner 1985, Krebs et *al.* 1987, Garrison *et al.* 1983a). Garrison (1991) further described the species as particular to surface layer infiltration and flood ponds on sea-ice which is relevant to observations of *T. gracilis* in abundance near the sea-ice edge but not in sea-ice samples (Garrison *et al.* 1987)

Zielinski and Gersonde (1997) believe the *T. gracilis* group has no relation to environmental parameters. This is not supported in this work since increased abundances do appear to have increase in relation to sea-ice cover and cooler SST. On the whole these occurrences are related to the heavily silicified form *Thalassiosira gracilis* var. *gracilis* which is considered the winter form of the species (Fryxell 1990). The increasing abundance of *T. g.* var. *gracilis* in sediments away from the coast corresponds well with the hypothesis that the species is the winter form of the species and the data which associates it with sea-ice cover. The low and ubiquitous signal previously encountered by others for the distribution of *Thalassiosira gracilis* var. *expecta* along predominantly coastal regions (references as above and Fryxell and Hasle 1979a) provide a possible answer to the lack of relation to sea-ice cover and concentration in this study. Thus, the two variations combined mean the signal is also combined but can be generally attributed to the winter signal produced from the distribution of *T.* g. var *gracilis*.

3A.3.36 *THALASSIOSIRA LENTIGINOSA*

Akin to the sedimentary distribution of *Fragilariopsis kerguelensis*, *Thalassiosira lentiginosa* is found in almost all samples observed in the Natural Database. Lowest abundances are observed in the Ross Sea and Antarctic Peninsula regions, and an ubiquitous distribution in sediments to the north is noted (Fig. 3.36a). Highest abundances are found just within the maximum winter sea-ice edge in the South Atlantic

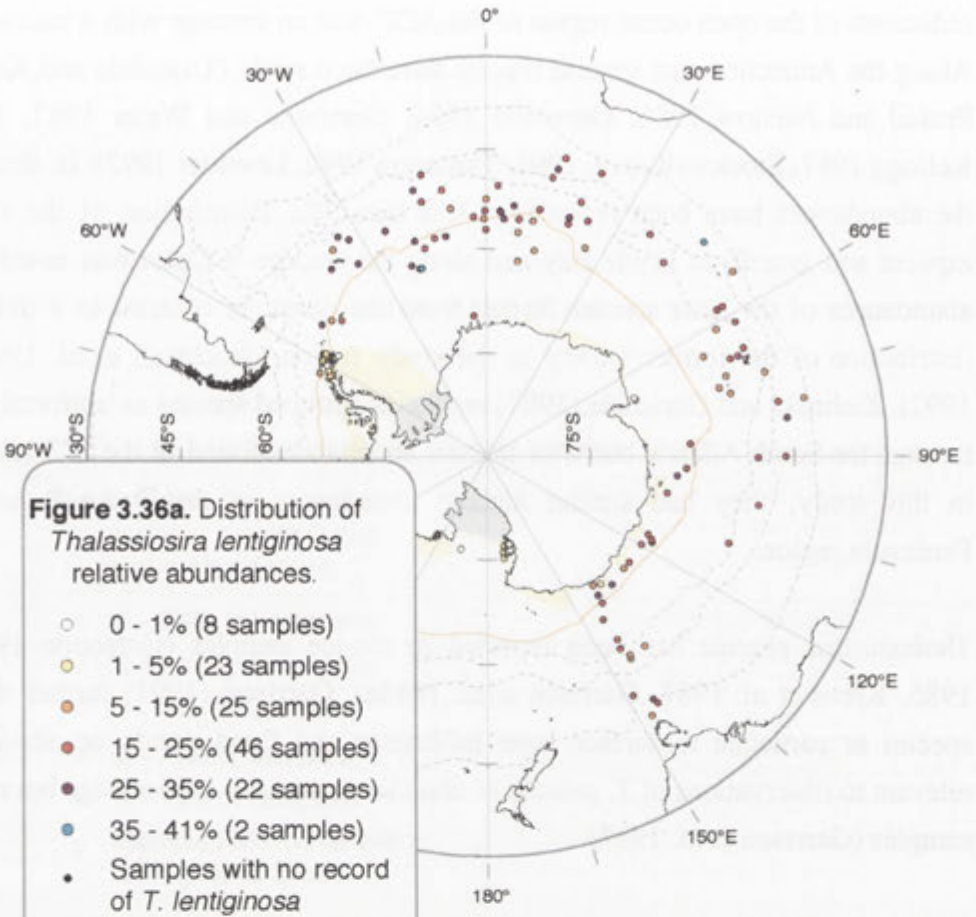

Figure 3.36a. Distribution of *Thalassiosira lentiginosa* relative abundances.

- 0 - 1% (8 samples)
- 1 - 5% (23 samples)
- 5 - 15% (25 samples)
- 15 - 25% (46 samples)
- 25 - 35% (22 samples)
- 35 - 41% (2 samples)
- Samples with no record of *T. lentiginosa*

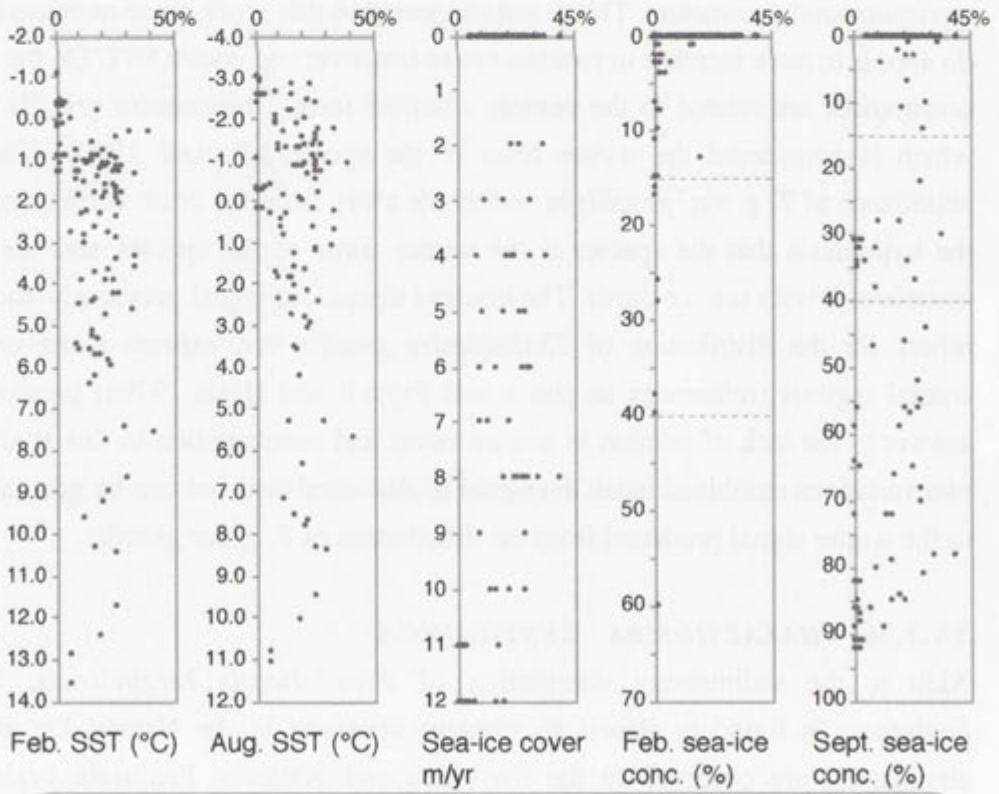

Figure 3.36b. Relative abundances against February and August SST, sea-ice cover in months per year and sea-ice concentration (%) in February and September (annual minimum and maximum sea-ice extents respectively). Other details as in Figure 3.2b.

and also in the SAZ of the Indian sector. There is no discerning relationship between the relative abundances of *T. lentiginosa* and SST (February and August) with exception to lower abundance at highest and lowest temperatures. In addition there is no relation perceived with annual sea-ice cover and maximum sea-ice concentration in September (Fig. 3.36b). *Thalassiosira lentiginosa* is, however, associated only with open ocean conditions during February.

Low Antarctic coastal abundance records of *T. lentiginosa* have been commented on or noted by several workers (Kozlova 1966, Donahue 1973, Gersonde and Wefer 1987, Kellogg and Kellogg 1987, Stockwell *et al.* 1991, Tanimura 1992, Zielinski and Gersonde 1997). The highest coastal abundance is reported by Leventer (1992) in sediments along the George V Coast at 12.4%. The species is most often reported in highest abundances from sediments under the POOZ to the PFZ (Jousé *et al.* 1962a, Kozlova 1966, Kozlova and Muhina 1967, Abbott 1973, Donahue 1973, DeFelice and Wise 1981, Zielinski and Gersonde 1997). In the Indian Ocean sector Kozlova (1966) reports between 10-41% as maximum abundances, whereas in the South Atlantic it is recorded as 26% (Zielinski and Gersonde 1997) and in the Pacific sector 20% (Donahue 1973). Northward of the PFZ lower abundances are reported (Jousé *et al.*1962a, Kozlova 1966, Abbott 1973, Schuette and Schrader 1981) averaging between 10 and 17% of the species total.

Early reports summarised by Horner (1985) observed "*Coscinodiscus lentiginosa*" in sea-ice samples. A more recent reference to the species detects no association with sea-ice but rather abundances located only in the water column (Garrison *et al.* 1987).

The species is an important contributor to the thanatocoenose in the sediments of the Southern Ocean. However, in addition to the species' resistance to dissolution (Kozlova 1966, Shemesh *et al.* 1989, Pichon *et al.* 1992b) and thus, increased presence in the sediments, its true primary signal of distribution remains obscured. The species is apparently not influenced greatly by sea-ice or SST, with exception the extremes of the later parameter in the Southern Ocean where its abundances are reduced and only occasionally absent. The species is in this sense a true pelagic (oceanic-inhabiting) species. The influence of this species in statistical analysis should be further tested because of its lacking signal to the current parameters. This will not be undertaken in this work and the species remains in all further work. Other physical parameters, as yet untested with the various updated physical parameter data sets now available, may be found to influence the distribution of this abundant species.

3A.3.37 *THALASSIOSIRA* LINEATI GROUP

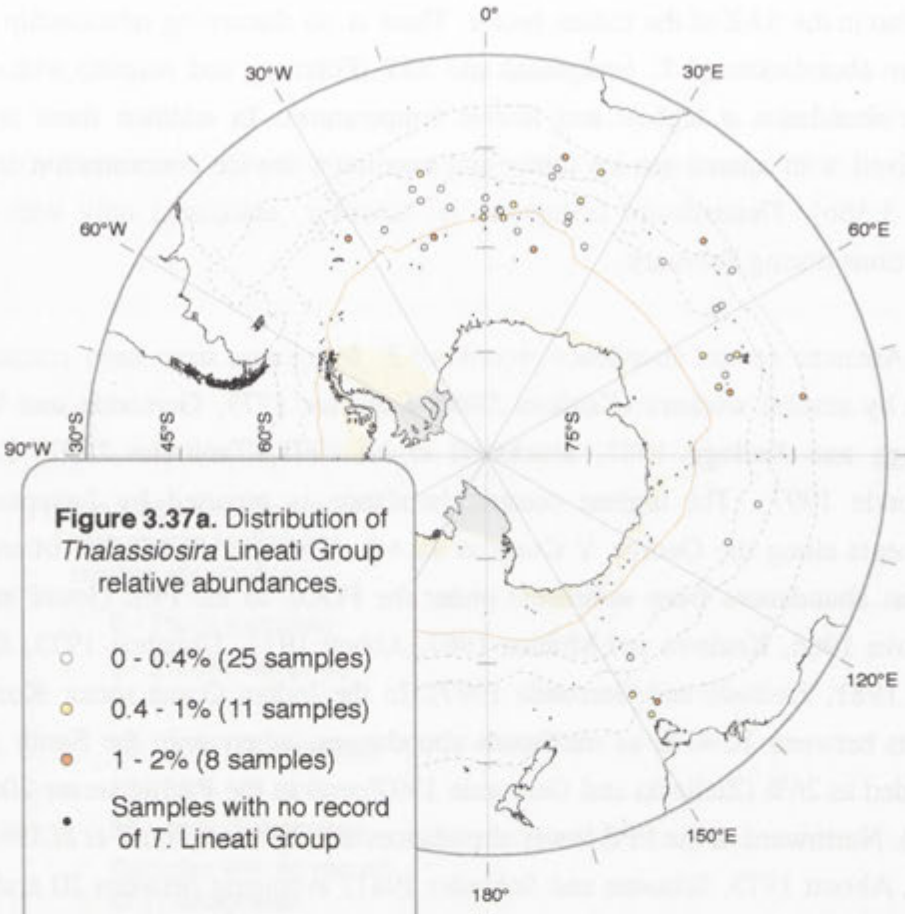

Figure 3.37a. Distribution of *Thalassiosira* Lineati Group relative abundances.

- 0 - 0.4% (25 samples)
- 0.4 - 1% (11 samples)
- 1 - 2% (8 samples)
- Samples with no record of *T.* Lineati Group

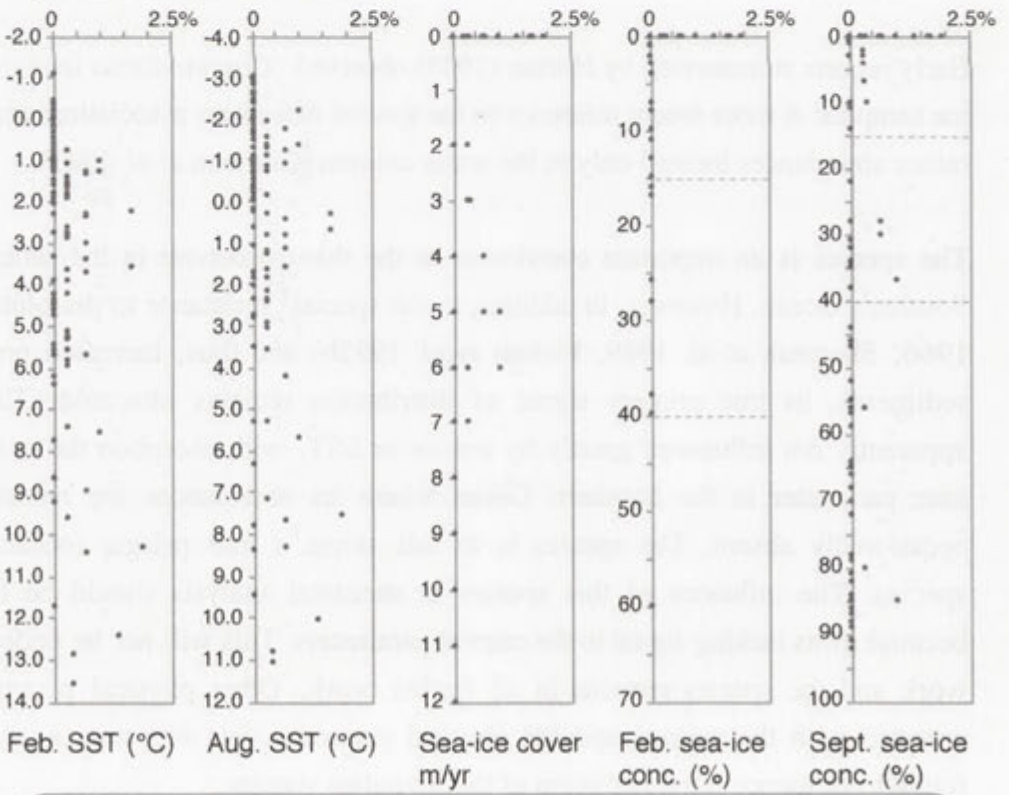

Figure 3.37b. Relative abundances against February and August SST, sea-ice cover in months per year and sea-ice concentration (%) in February and September (annual minimum and maximum sea-ice extents respectively). Other details as in Figure 3.2b.

The geographical distribution of the *Thalassiosira* Lineati group is most concentrated in the region north of the SAF in the southeast Indian Ocean and between the STC and the maximum winter sea-ice edge in the South Atlantic and Indian sectors (Fig. 3.37a). These increased abundances are never greater than 2%. February and August SST show bi-modal abundance peaks in warm (10-12°C Feb SST) and cool waters (2-4°C Feb SST). This bi-modality may be related to the identification of the cool water species *Thalassiosira ferelineata* which is the only Lineati species recorded in cooler waters (Hasle and Fryxell 1977). The relative abundances of the *T.* Lineati group when compared against annual sea-ice cover indicates most occurrences and the highest abundances are found under no sea-ice cover, a small group at percentages less than 1% are found to be related to sea-ice cover between 2-7 months per year. These occurrences are likely to be mis-identifications of either *Thalassiosira tumida* or *Thalassiosira ritscheri* which have similar areolation patterns (especially when only a half valve is observed) to the *T.* Lineati group. It is just as feasible that *Thalassioisra ferelineata* may be related to low sea-ice cover but it has not been reported to date in sea-ice samples.

Most previous accounts of *Thalassiosira lineata* and *Thalassiosira leptopus* are noted in sediments north of the STC (Schuette and Schrader 1981, Pokras and Molfino 1986, van Iperen *et al.* 1987), where abundances are maximised at 5% (Pokras and Molfino 1986). Both DeFelice and Wise (1981, single specimen) and Abbott (1973, max 1%) noted very rare occurrences in their respective study areas. Garrison (1991) list *T. lineata* as a pack-ice species, whereas Krebs *et al.* (1987) found it in the fast-ice of Arthur Harbor, Antarctic Peninsula. The identifications of these "*T. lineata*" species require confirmation under the present discussion of distributions.

In general, the group is useful for warm water occurrences of the species. A problem regarding cool and very cold water expressions of the species group exists. In this work the colder signal was transferred to the *Thalassiosira tumida* category (refer section 2.2.27), however, the cool water signal would appear to be unrelated to the *T.* Lineati group *senso stricto*. As there is not much known on the distribution and ecology of *T. ferelineata*, the only known cool water expression of this Lineati group, it remains impossible to have confidence in the species identified as "*T. lineata*" in this dataset at cooler SST.

3A.3.38 *THALASSIOSIRA OESTRUPII* GROUP

The *Thalassiosira oestrupii* Group is preserved in the sediments with an increasing northward abundance from the maximum winter sea-ice edge to the mid-latitudes (Fig. 3.38a). The maximum abundance for this group is recorded (7.3% at ~55°S, 22°E) in the South Atlantic, but appears to be an outlier from the rest of the Natural Database. Plots of

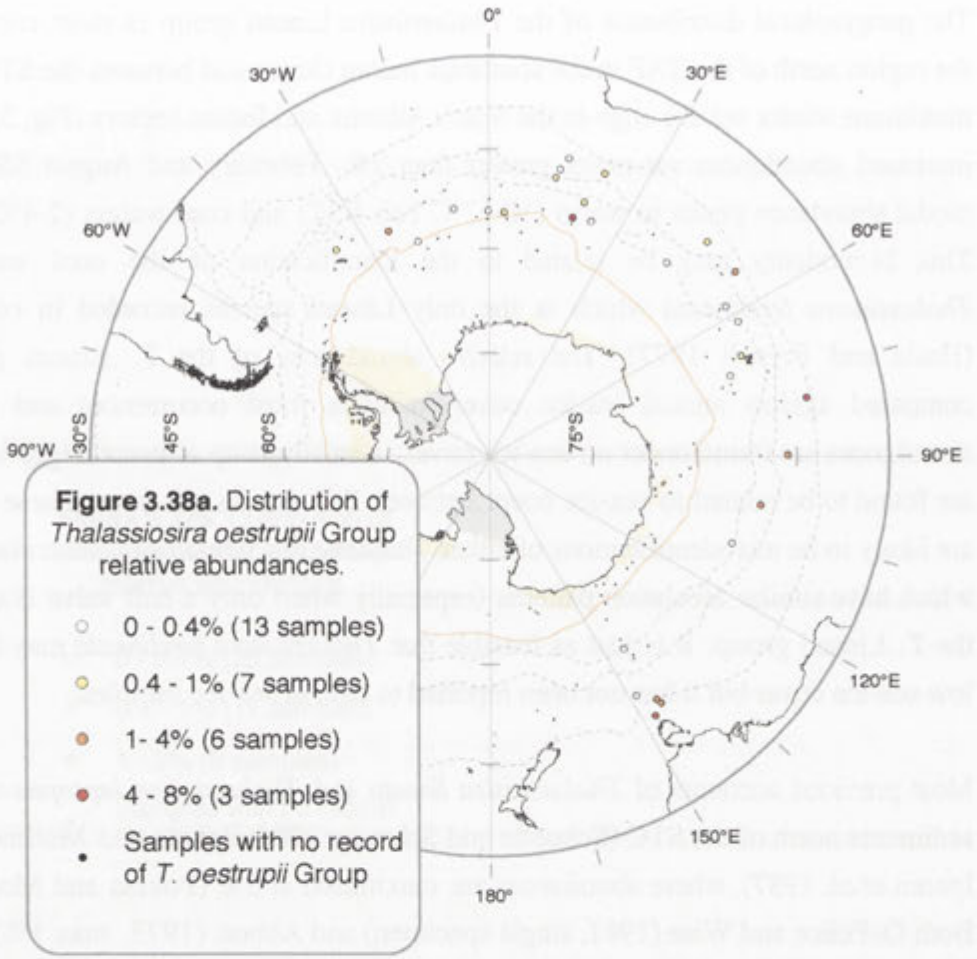

Figure 3.38a. Distribution of *Thalassiosira oestrupii* Group relative abundances.

- 0 - 0.4% (13 samples)
- 0.4 - 1% (7 samples)
- 1- 4% (6 samples)
- 4 - 8% (3 samples)
- Samples with no record of *T. oestrupii* Group

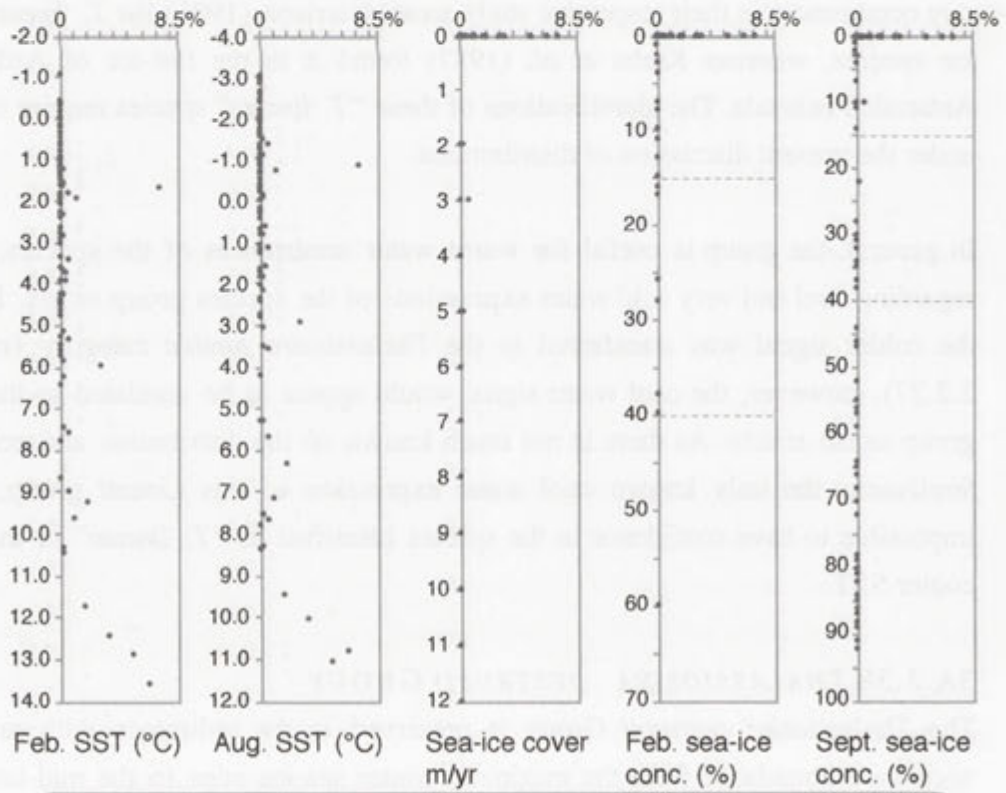

Figure 3.38b. Relative abundances against February and August SST, sea-ice cover in months per year and sea-ice concentration (%) in February and September (annual minimum and maximum sea-ice extents respectively). Other details as in Figure 3.2b.

the relative abundances versus SST attest the outlier feature of this high abundance sample, with the remaining samples illustrating an increase in abundance with increasing February and August SST (Fig. 3.38b). In particular, abundances are increased under February SST >12°C. The species is not found associated with sea-ice occurrence.

Fryxell and Hasle (1980) described the two varieties of *T. oestrupii* as separated into an cosmopolitan oceanic species and an subtropical/tropical continental shelf species. They recorded the former of these two varieties as noted from phytoplankton of the Weddell Sea through to the Artic. Records in the sediments of *T. oestrupii* south of the maximum winter sea-ice edge have been made (Truesdale and Kellogg 1979, Gersonde and Wefer 1987, Kellogg and Kellogg 1987, Leventer 1992) but in all cases the species is rare and recorded at less than 1%. Within the open ocean the species is recorded in the sediments from 1 to 10% of the total specimens recovered, and always in increasing abundance to the north (Abbott 1973, DeFelice and Wise 1981, Zielinski and Gersonde 1997). North of the Southern Ocean accounts of *T. oestrupii* in the sediments are noted in the southeast Atlantic at a maximum of 5.31% (Schuette and Schrader 1981) and with the warmer water species (var. *venrickae*) predominating (van Iperen *et al.*1987). In the Indonesian Archipelago variation *venrickae* was found in lower abundance than var. *oestrupii* (1% to 6.7% respectively, van Iperen *et al.* 1993). Thus it would appear from sedimentary records that maximum abundances of the two species combined are at maximum in the mid latitudes at temperatures ~12°C.

Early reports of *T. oestrupii* in sea-ice (Horner 1985) have not been confirmed in more recent studies, where the species has only been located in the water column adjacent the sea-ice edge in the Weddell Sea (Garrison *et al.* 1987).

The outlier in the Natural Database is currently unexplainable and should be removed from analysis since other previous records in the South Atlantic do not show such elevated recovery in the same region (DeFelice and Wise 1981, Zielinski and Gersonde 1997). Since the French database is to be recounted (Crosta, pers. comm. 1997), the sample is preserved in this dataset and is acknowledged as being a possible cooling factor in the analysis of core material.

3A.3.39 *THALASSIOSIRA OLIVERANA*

The species *Thalassiosira oliverana* has what appears to be an ubiquitous distribution in sediments of the Southern Ocean with exception to the Antarctic coast where abundances are reduced and occasionally rare (Fig. 3.39a). The concentration of highest abundances are noted generally between the Polar Front and just within the maximum winter sea-ice

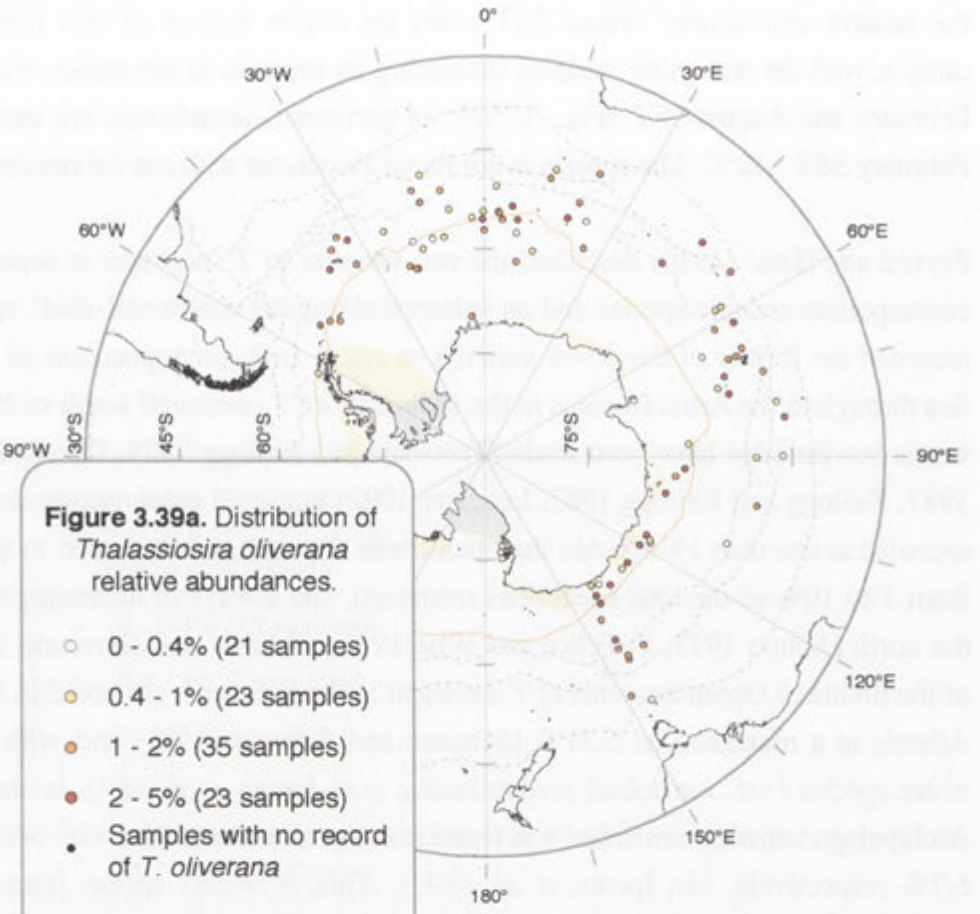

Figure 3.39a. Distribution of *Thalassiosira oliverana* relative abundances.

- 0 - 0.4% (21 samples)
- 0.4 - 1% (23 samples)
- 1 - 2% (35 samples)
- 2 - 5% (23 samples)
- Samples with no record of *T. oliverana*

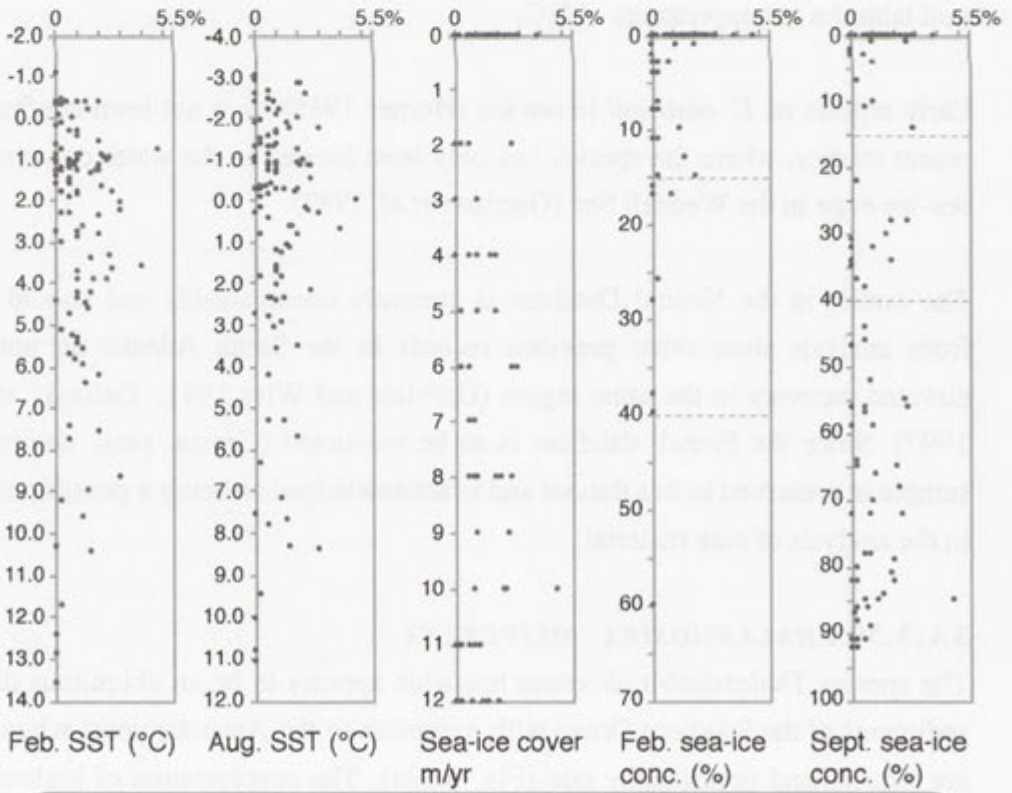

Figure 3.39b. Relative abundances against February and August SST, sea-ice cover in months per year and sea-ice concentration (%) in February and September (annual minimum and maximum sea-ice extents respectively). Other details as in Figure 3.2b.

edge. This generalised geographic distribution is expressed in the wide SST range that high abundances are related, with highest abundances (4-5%) associated with February SST between 0 and 4°C and August SST between -1.5 and 2°C. Some high abundances in warmer waters >8°C (SST Feb.) are probably associated with bottom water transport. Increased abundances are also associated with increasing sea-ice cover up to 10 months per year. In respect to sea-ice concentrations in September *T. oliverana* is equally observed in high and low concentrations of sea-ice, although there is a certain trend for decreasing abundances in concentrations greater than 85%. In the February minimum sea-ice month, the species is found in open ocean conditions but also at the sea-ice edge.

Several workers have tabulated rare occurrences less than 1.5% of *T. oliverana* in the sediments surrounding the Antarctic coast (Kozlova 1966, Truesdale and Kellogg 1979, Kellogg and Kellogg 1987, Stockwell *et al.* 1991, Leventer 1992, Tanimura 1992). Greatest abundance in the sediments has always been record in the open ocean region but with decreased abundance or absent in sediments north of the STC (Jousé *et al.* 1962a, Kozlova 1966, Abbott 1973, Donahue 1973, DeFelice and Wise 1981, Zielinski and Gersonde 1997). Maximum abundance of the species (9%) is noted by Zielinski and Gersonde (1997) in the South Atlantic sector at temperatures between -1.5 to 1°C. Only Schuette and Schrader (1981) report *T. oliverana* to the north in one of their samples off-shore Southwest Africa.

Although Garrison (1991) and Garrison and Buck (1989) list "*Schimperiella antarctica*" (*T. oliverana*) as a pack-ice species, no other reference to this species in sea-ice samples was located in the literature.

From the distribution within the sediments, against SST and sea-ice of this study and the previous documentation of the species elsewhere in the Southern Ocean, *T. oliverana* appears linked to winter sea-ice distribution. Zielinski and Gersonde (1997) noted from their distribution data that the species displayed strong links to the region between the Antarctic Zone and the PFZ with a temperature range of -2 to 5°C. The results of the database support this description and suggest that this circumpolar relationship is furthermore linked to winter sea-ice formation even though there are few studies which report the species occurrence. The species is able to survive bottom water transport and as reported by Kozlova (1966) is a dissolution resistant diatom species.

3A.3.40 *THALASSIOSIRA PERPUSILLA*

Four rare coastal occurrences of *Thalassiosira perpusilla* are recorded in the Natural Database (Fig. 3.40a). Two samples in the Antarctic Peninsula region, one along Wilkes

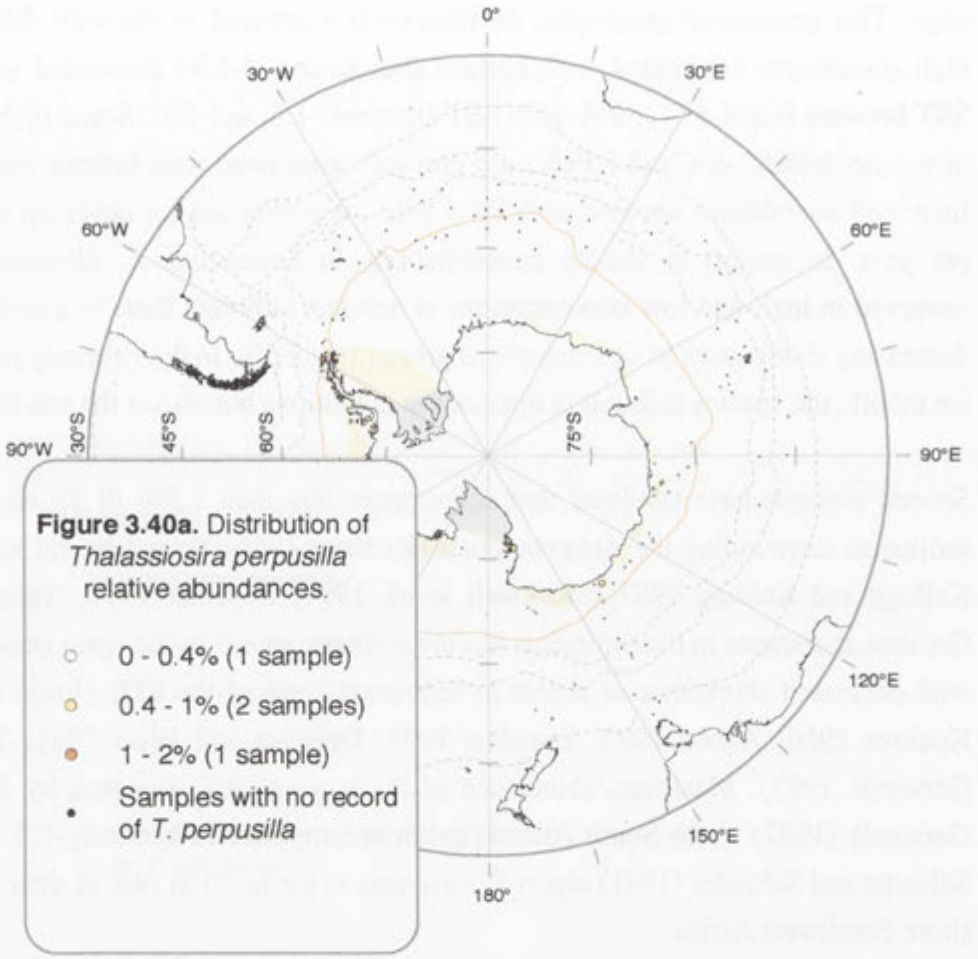

Figure 3.40a. Distribution of *Thalassiosira perpusilla* relative abundances.

- 0 - 0.4% (1 sample)
- 0.4 - 1% (2 samples)
- 1 - 2% (1 sample)
- Samples with no record of *T. perpusilla*

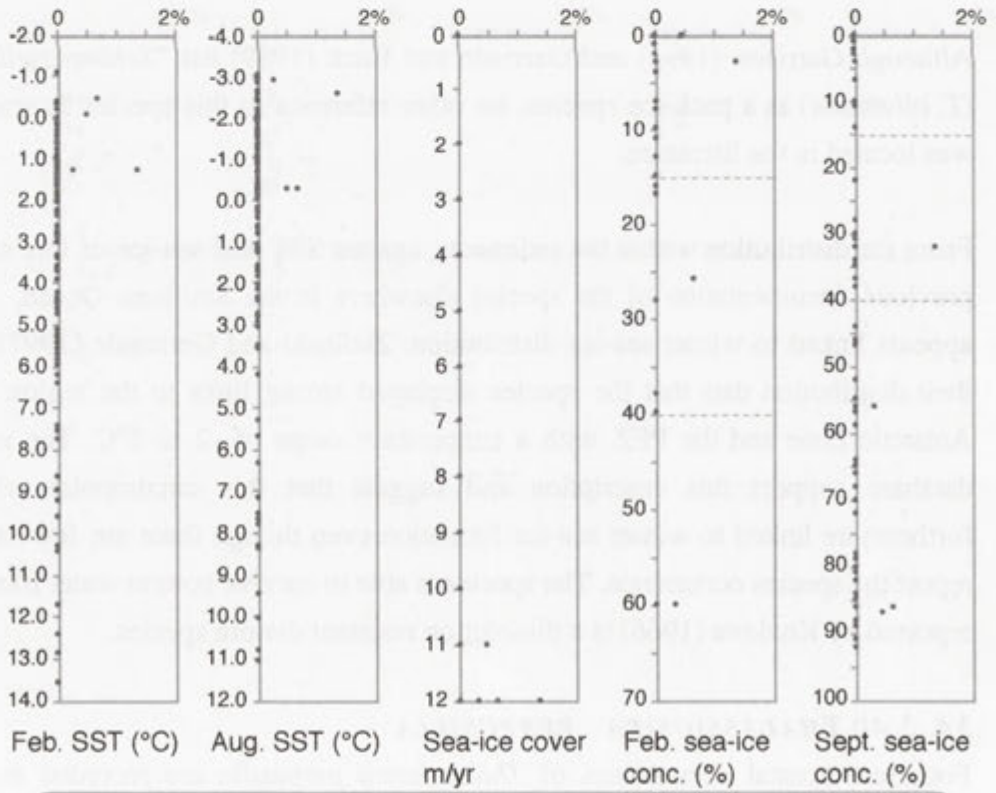

Figure 3.40b. Relative abundances against February and August SST, sea-ice cover in months per year and sea-ice concentration (%) in February and September (annual minimum and maximum sea-ice extents respectively). Other details as in Figure 3.2b.

Land and the other in the Ross Sea. February SST range is between -0.5 to 1.5°C and August SST range is -3 to -0.5°C (Fig. 3.40b). All occurrences are associated with high annual sea-ice cover, generally consolidated fast-ice conditions in September and decreasing abundances with increasing sea-ice concentration in February.

Stockwell *et al.* (1991) observed *T. perpusilla* in one sample of inner Prydz Bay (0.15%). Kozlova (1966) only found the species down to 75m when examining the preservation of species in the water column down to the sea-floor. Likewise, sediment trap data by Gersonde and Wefer (1987) found *T. perpusilla* in samples down to 1835m in the Bransfield Strait and at depth in the North Powell Basin, but did not recover the species from the corresponding sea-floor samples. *Thalassiosira perpusilla* is found, however, frequently in Antarctic waters and less often in subantarctic waters (Fryxell and Hasle 1979a). The latter authors believe the species has been largely overlooked in light microscope studies.

There are no reports of *T. perpusilla* in sea-ice samples, although the species was found in the adjacent water column near the ice edge in the Weddell Sea during spring (Garrison *et al.* 1987).

From this small data compilation, *T. perpusilla* appears linked to the Antarctic coast and with near annual sea-ice cover. Its preservation in the sediments of this region, in contrast to its wider known planktonic occurrence, is probably enhanced by the decrease in water depth around the Antarctic coast.

3A.3.41 *THALASSIOSIRA POROSERIATA*

The distribution of species attributed to *Thalassiosira poroseriata* highlights mis-identifications of this species in ice covered regions (Fig. 3.41a). The sole reliable identification of the species was made from sediments south of Tasmania (0.4%, one specimen only). The other occurrences of this species in the Ross Sea and Antarctic Peninsula region are attributed to *Thalassiosira trifulta*or another similar *Thalassiosira* species. In terms of distribution with SST, the sole specimen was found in waters of 13.6°C February SST, 10.8°C August SST and with no relation to sea-ice cover (Fig. 3.41b).

No previous identifications of this species in the sediments or the sea-ice has been located in the literature. Within the phytoplankton the species has been reported from the Norwegian Sea and "fairly north" in the Antarctic (Hasle and Heimdal 1970), within Antarctic zone near Queen Maud Land and the South Orkney Islands (Fryxell and Hasle 1979b), in abundance at 65°S, 164°44'E (Semina and Rat'kova 1988), between 42° and

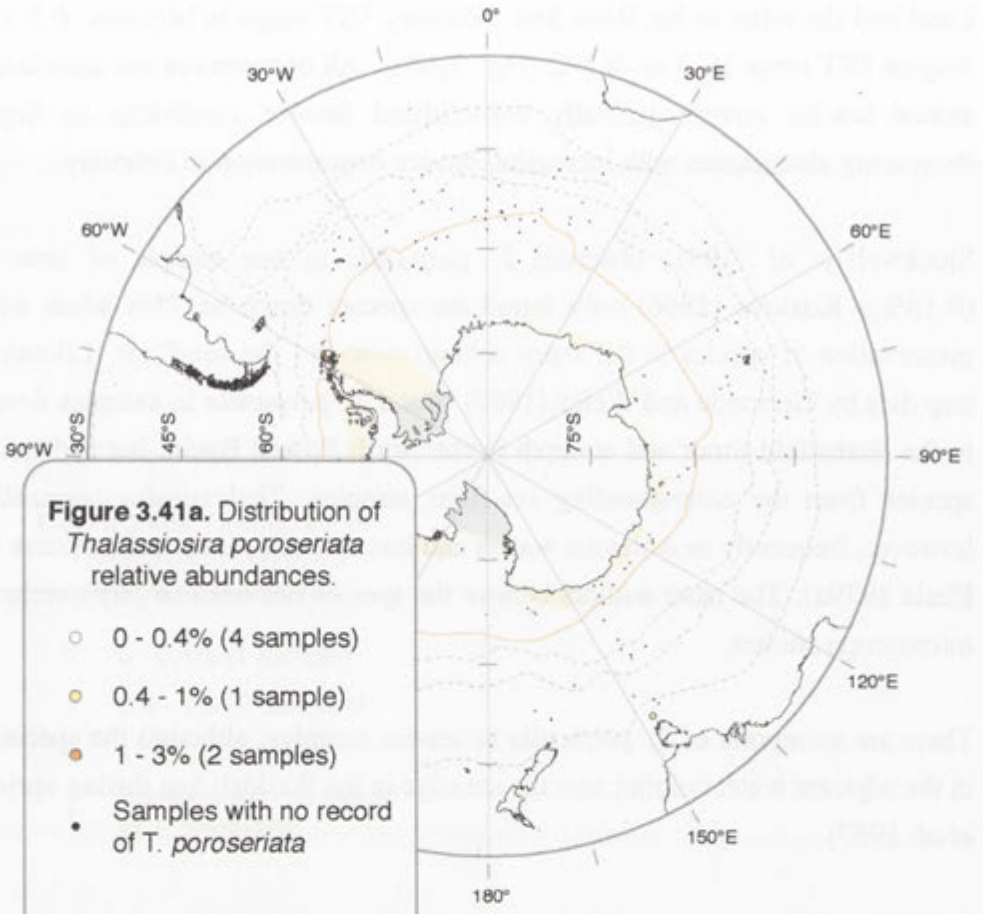

Figure 3.41a. Distribution of *Thalassiosira poroseriata* relative abundances.

- 0 - 0.4% (4 samples)
- 0.4 - 1% (1 sample)
- 1 - 3% (2 samples)
- Samples with no record of T. *poroseriata*

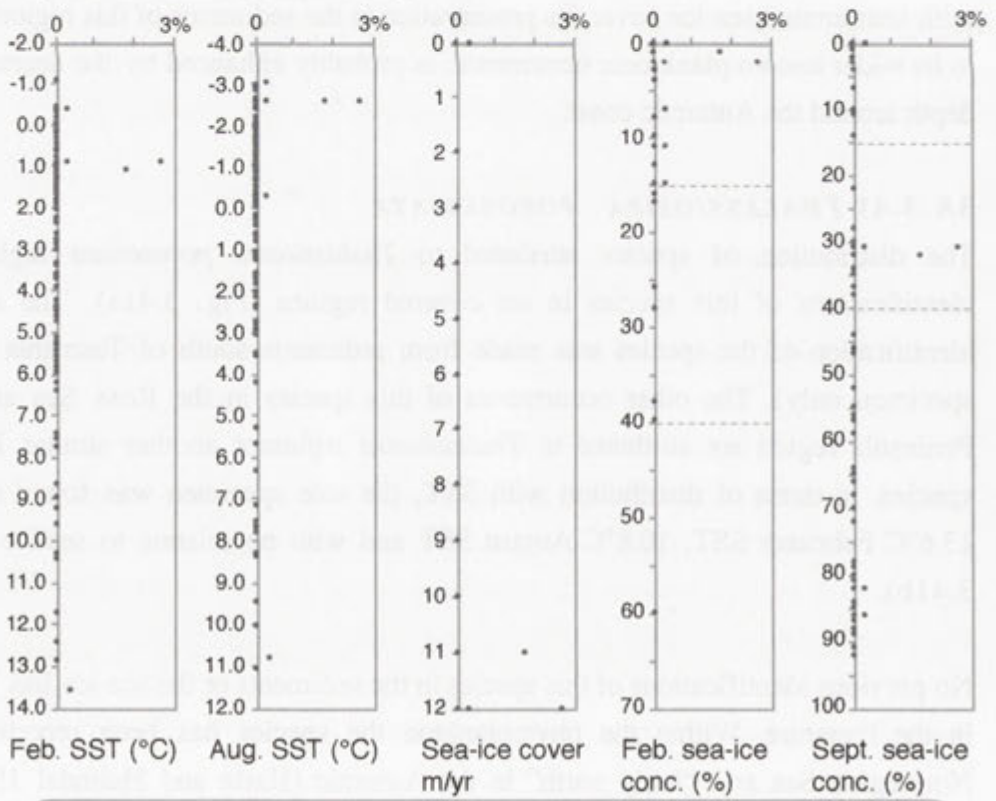

Figure 3.41b. Relative abundances against February and August SST, sea-ice cover in months per year and sea-ice concentration (%) in February and September (annual minimum and maximum sea-ice extents respectively). Other details as in Figure 3.2b.

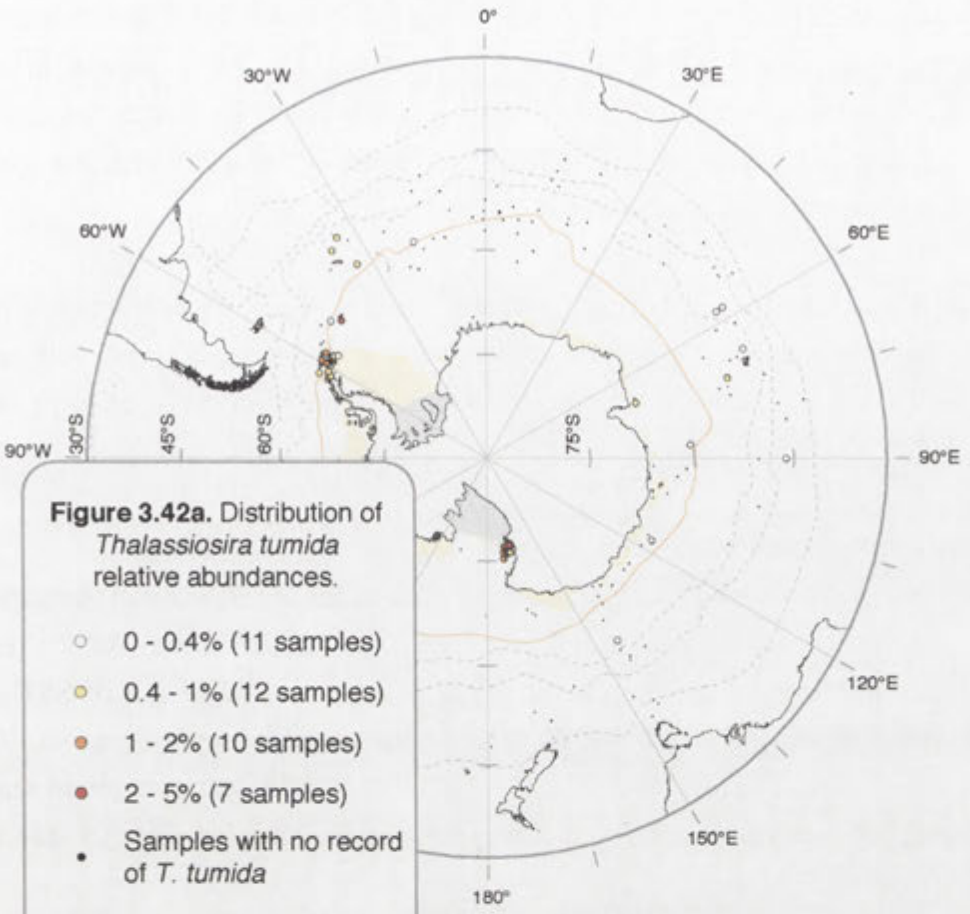

Figure 3.42a. Distribution of *Thalassiosira tumida* relative abundances.

- 0 - 0.4% (11 samples)
- 0.4 - 1% (12 samples)
- 1 - 2% (10 samples)
- 2 - 5% (7 samples)
- Samples with no record of *T. tumida*

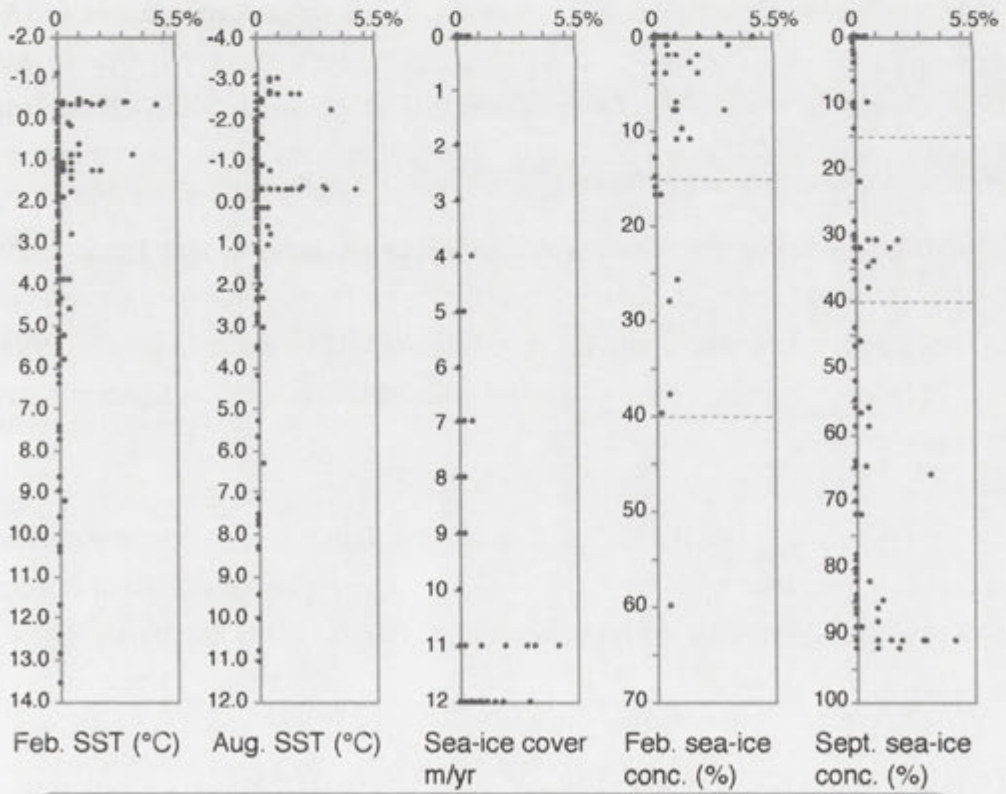

Figure 3.42b. Relative abundances against February and August SST, sea-ice cover in months per year and sea-ice concentration (%) in February and September (annual minimum and maximum sea-ice extents respectively). Other details as in Figure 3.2b.

52°S in the southeastern Pacific (Fenner *et al.* 1976) and along the Chilean coast (Ramirez 1981). Johansen and Fryxell (1985) surmised *T. poroseriata* as being present in all sectors of the Antarctic, although from the literature listed above the greatest presence appears to be associated to the north of the STC in the Pacific region and within the open ocean zone of the South Atlantic and southeast Indian Ocean.

The distribution provided by the Natural Database requires thorough confirmation of occurrences along the Antarctic coast (oral communication Pichon 1997), and with re-analysis of the French database should reveal a better geography of the species in the Southern Ocean.

3A.3.42 *THALASSIOSIRA TUMIDA*

Thalassiosira tumida is observed in highest abundances in the Ross Sea and Antarctic Peninsula regions. Minor abundances also appear linked to Southern Ocean islands (eg South Orkney, South Georgia, and Kerguelen) (Fig. 3.42a). A discreet range of SST is related to highest abundances (4.7%): -0.5° to 2°C February SST and -3° to -0.5°C August SST (Fig. 3.42b). The high abundances are associated with near year round sea-ice cover, around 90% sea-ice concentration during September and open ocean to sea-ice edge conditions during February.

Previous sediment investigations revealed *T. tumida* in low to rare abundances (<3%) around the Antarctic coast (Truesdale and Kellogg 1979, Gersonde 1984, Prasad and Nienow 1986, Stockwell *et al.* 1991, Leventer 1992). Further north, both DeFelice and Wise (1981) and Abbott (1973) noted the species as very rare in open ocean sediments.

Thalassiosira tumida is categorised as a pack-ice species (Garrison and Buck 1989, Garrison 1991). However, it has been recovered from both fast and pack-ice samples of the Weddell Sea and Antarctic Peninsula region (Garrison *et al.* 1983a, Gersonde 1984, Krebs *et al.* 1987). In spring the species is also found in abundance in the adjacent water column at the sea-ice edge (Garrison *et al.* 1987).

The data from this study indicates the species is in highest abundances along the Antarctic coast and under near year round ice cover, more often that of highly consolidated fast-ice during winter. The abundances are the highest recorded, thus far in the literature.

3A.4. SPECIES WITH KNOWN BENTHIC-NERITIC HABITATS.

Since the emphasis of transfer function analysis is on constructing relationships between the planktonic diatoms and their sea-surface environments, species which are known to

reside in benthic environments (be that in the sediments or under permanent sea-ice) represent signals which do not necessarily respond to the same environmental stresses as those considered truely planktonic. In the database being constructed the following species are considered benthic and/or neritic and so their removal from further statistical analysis is warranted (Table 3.5). These species have generally low abundance presence in the sediment samples.

Benthic/neritic species	Maximum abundance in the Natural Database
Achnanthes brevipes	1.3%
Amphora ovalis	<0.4%
Cocconeis spp.	5.9%
Gomphonema intricatum	0.7%
Grammatophora arcuata	3.4%
Fragilaria striatula	1.0%
Licmophora "decora"	0.7%
Navicula directa	1.7%
Navicula gelida var. *parvula*	0.7%
Nitzschia lecointei	1.0%
Odontella litigiosa	<0.4%
Odontella weissflogii	11.6%
Paralia spp.	1.4%
Pleurosigma spp.	<0.4%

Table 3.5. Species considered unrepresentative of planktonic conditions (ie benthic or neritic) which are removed from consideration in the construction of transfer functions. Maximum abundances observed in the sediment samples of the Natural Database are listed.

Although the data is not used in constructing planktonic species based transfer functions their presence in open ocean sediment samples may prove to be very useful in indicating possible bottom water paths from Antarctica. In particularly that of *Odontella weissflogii*, and possibly *Navicula directa* and certain *Paralia* species. The data from these benthic species will still be used when determining the relative abundances from the remaining planktonic species.

3A.5. REGIONAL SAMPLE CONSIDERATIONS - ANTARCTIC PENISULA AND ROSS SEA SAMPLES.

3A.5.1 ANTARCTIC PENINSULA SAMPLES

Samples from around the Antarctic Peninsula region have been noted with very high abundances of *Chaetoceros* taxa (eg. Leventer 1991, Crosta *et al.* 1997, Zielinski and Gersonde 1997). The region is further differentiated from the Open Ocean regions in terms of the oceanography, annual flux, and distribution of diatoms to the sediments (Bodungen *et al.* 1986, Gersonde and Wefer 1987, Wefer *et al.* 1988, Wefer *et al.* 1990, Leventer 1991, Abelmann and Gersonde 1993, Zielinski and Gersonde 1997).

From the previous distribution maps it is apparent that the majority of samples from the Antarctic Peninsula region have the highest records of benthic species and *Chaetoceros* resting spores (refer to section 2.3.1). In the case of benthic species, 11 of them (*Achnanthes brevipes*, *Amphora ovalis*, *Cocconeis* spp., *Fragilaria striatula*, *Gomphonema intricatum*, *Grammatophora arcuata*, *Licmophora "decora"*, *Navicula directa*, *Navicula gelida* var. *parvula*, *Nitzschia lecointei*, *Odontella litigiosa*) have their greatest and/or sole occurrences in this region alone. Only *Odontella weissflogii* and the grouped *Paralia* Taxa are found in lower than their maximum abundances in this region.

There are 14 samples remaining in the 129 Natural Database that are located in the Antarctic Peninsula region. The benthic species on average represent 7% of the total diatom counts (Table 3.6). This is a reasonable contribution to the sediments, however, real proportions are over-estimated as the samples are missing an important component to their biothanatosis; the *Chaetoceros* species.

Crosta *et al.* (1997) provides information on the *Chaetoceros* resting spore content of the same samples for the Antarctic Peninsula region. In all, but one sample, the *Chaetoceros* resting spore abundances are greater than 60% (average 79.4%, Table 3.6). Unfortunately, the two sets of information derived from the very same samples can not be used in unison because of the counting methodology employed by each study. However, the importance of a reasonable benthic/neritic component is important, as is the observation of extreme dominance by *Chaetoceros* resting spores.

It seems reasonable, knowing that the Antarctic Peninsula region has unique environmental stresses, productivity, diatom composition and flux, that the samples should not be used in transfer function work that deals with interpreting cores located generally in open ocean regions. This was also stated by Le (1992). He found no advantage gained by including in transfer function regression core top samples that were ecologically very different from the down-core samples. Zielinski (1993) also removed samples from the Bransfield Strait region of the Antarctic Peninsula in his analysis citing a lack of correlation with hydrological parameters. For this reason the 14 Antarctic Peninsula samples will not be used in further work in this thesis database (refer Fig. 3.0). As such the inclusion of the data as an incomplete diatom assemblage with elevated species composition (eg. *Odontella weissflogii*, *Thalassiosira antarctica*) will serve as a distinct outlier to the remaining samples and provide erroneous estimations under situations that would otherwise be incomparable.

Core	Lat °S	Longitude	Depth (m)	This study (No *Chaetoceros* spp.) Total specimen count	This study (No *Chaetoceros* spp.) Benthic /neritic %	Crosta *et al.* (1997) Total specimen count	Crosta *et al.* (1997) Relative *Chaetoceros* RS (%)
PC82-71	62°38.4'	59°32'W	1350	293	7.8	333	82.9
PC82-136	64°45.4'	62°45.5'W	425	302	8.6	326	83.7
KR8706	63°03.6'	63°03.7'W	630	297	5.1	310	11.9
KR8707	62°21.2'	57°58.3'W	2810	290	9.3	309	60.2
PC82-35	62°21.7'	57°22.0'W	1484	297	6.4	-	-
PCDF 82-34	62°17.7'	57°37.4'W	1979	296	7.4	344	85.8
PCDF 82-47	62°55.3'	58°23.7'W	723	341	4.1	342	88.9
PCDF 82-69	62°59.9'	59°38.1'W	916	299	6.4	340	88.5
PCDF 82-60	63°23.4'	59°34.2'W	673	307	12.1	355	90.4
PCDF 82-51	63°43.4'	60°02.9'W	560	298	7.0	359	92.5
PCDF 82-1	63°57.2'	56°21.6'W	430	298	5.7	343	88.3
PCDF 82-93	64°04.1'	61°19.6'W	690	302	7.0	329	89.1
PCDF82-140	64°49.6'	62°37.8'W	392	301	5.0	328	88.1
PCDF 82-20	64°14.1'	55°54.4'W	381	302	3.6	325	90.5

Table 3.6. Antarctic Peninsula region samples. In this study, where *Chaetoceros* species have not been included or counts made, samples have high benthic/neritic components. In the corresponding Crosta *et al.* (1997) study of the same samples, the dominant component was found to be *Chaetoceros* resting spores with the exception of sample KR8706. *Chaetoceros* data from Crosta *et al.* (1997 table 1 and pers. comm. 1996).

3A.5.2 Ross Sea Samples

The other region which concerns this study in terms of its regionality but has varying conditions to those encountered in the Antarctic Peninsula, is the Ross Sea (eg. Dunbar *et al.* 1985, Ledford-Hoffman *et al.* 1986, Leventer and Dunbar 1996). These samples have a different diatom composition to those of the Antarctic Peninsula region as observed in the distributions provided earlier and previous studies (Leventer and Dunbar 1987, 1988, 1996). This is evidenced in the reduced numbers of benthic species encountered in the sediments in this study (Table 3.7).

In terms of *Chaetoceros* abundances, Crosta *et al.* (1997) report southeastern (~175°W-150°W) and southwestern (160°E-180°E) sedimentary signatures in the Ross Sea varying from 60 to 20% relative abundance respectively. Although these results are not in conflict with the overall interpretation provided by silica flux studies on the same material by Ledford-Hoffman *et al.* (1986) and in part by the species distribution study of Leventer and Dunbar (1996), they are misleading since the samples were not rigorously counted to

300 specimens as stated (average total count for the southeastern and transitional samples 118, average total count for southwestern samples 275). Ambiguity in the comparison of

				This study (No *Chaetoceros* spp.)		Crosta *et al.* (1997)	
Core	Lat °S	Long.	Depth (m)	Total counted	Total benthic/neritic %	Total counted	Relative *Chaetoceros* RS %
DFBC83-41 III	76°40'	164°01'W	516	300	0.3	199	34.7
DFBC 83-27 II	75°42'	170°39'E	322	308	0.7	298	17.4
DFBC 83-28 II	75°51'	169°18'E	485	370	0.0	324	21.3
DFBC 83-29 II	76°01'	167°12'E	622	294	1.0	314	10.8
DFBC 83-30 II	76°05'	166°42'E	668	306	1.3	326	19.3
DFBC 83-1 II	76°10'	168°58'E	540	296	0.7	331	22.7
DFBC 83-40 II	76°21'	167°12'E	732	289	0.0	332	20.2
DFBC 83-5 II	76°30'	166°00'E	640	294	0.0	313	22.0
DFBC 83-23 II	76°31'	170°05'E	860	298	1.0	319	23.8
DFBC 83-2 II	76°37'	164°21'E	540	299	0.0	251	24.3
DFBC 83-21 II	76°41'	167°49'E	768	293	0.0	317	15.5
DFBC 83-20 II	76°57'	166°41'E	750	299	0.0	319	18.8
DFBC 83-10 II	76°57'	166°20'E	878	294	0.0	310	22.3
DFBC 83-9 II	77°05'	166°31'E	915	294	0.0	323	20.4
DFBC 83-1 III	77°10'S	169°07'E	930	299	0.7	291	19.6
DFBC 83-8 II	77°10'	165°48'E	871	295	0.0	317	28.1
DFBC 83-7 II	77°21'	165°53'E	880	300	1.0	314	10.8
DFBC 83-6 II	77°30'	165°48'E	823	300	0.3	284	22.5

Table 3.7. Ross Sea region samples. In this study, where *Chaetoceros* species have not been included or counts made, samples have low benthic/neritic components. In the corresponding Crosta *et al.* (1997) study of the same samples, a sub-dominant component was found to be *Chaetoceros* resting spores. Data from Crosta *et al.* (1997 table 1, and pers. comm. 1996).

the samples over the region ensues because of the variable same sample sizes. Despite this problem the southwestern and southeastern samples are considered here to show difference in preservation, flux and dissolution in reference to previous studies. The samples that remain in the 129 Natural Database from the Ross Sea region are all from the southwestern section with exception to one sample in the transitional region between these sections (DFBC83-41 III). As can be seen in Table 3.7 most of these samples have relative abundances of *Chaetoceros* resting spores in the 20% range. This value is in agreement with the results of Leventer and Dunbar for the same region (1996, maximum relative abundance of ~22%).

As the Ross Sea and Weddell Sea samples provide the extreme end environment and boundary to the open ocean, they are maintained for further use in the statistical work. Overall the Ross Sea samples do not contain an over-dominant signal of *Chaetoceros* resting spores or benthic species in the sediments as noted in the Antarctic Peninsula region. For some of the other cold water species (ie. *Thalassiosira tumida*, *Stellarima microtrias*, *Fragilariopsis separanda*, *Fragilariopsis* Cool taxa, *Fragilariopsis* Cylindriform Group) the Ross Sea region is where the maximum relative abundances are observed. This is important for estimating past sea-ice and SST. More detailed work in both the Weddell and Ross Sea embayments may yet show that both these regions should be kept separate from Open Ocean analysis, but for now both regional sample sets are preserved in the analysis.

CHAPTER 3. SECTION B. DISSOLUTION DATABASE

3B.1. DISSOLUTION DATA SET - INTRODUCTION

Differential dissolution of preserved diatoms is a feature recognised to occur in marine sediments to the north and south of the silica ooze belt in the Southern Ocean (Lisitzin 1971, Shemesh *et al.* 1989, Pichon *et al.* (1987). A preservation index for the Southern Ocean was devised to estimate the degree of dissolution in Holocene aged sediments using only three dominant species *Fragilariopsis kerguelensis*, *Thalassiosira lentiginosa*, and *Eucampia antarctica* (Shemesh *et al.* 1989). This index highlighted the need for careful interpretation of samples occurring in the regions exterior to the silica ooze belt for transfer function analysis. To meet this challenge an experimental dissolution dataset was introduced to the diatom database by Pichon *et al.* (1992a,b).

Five surface samples in two latitudinal transects (Fig. 3.43) were step-wise dissolved over two days. Species composition and corresponding dissolved opal content were calculated in the 48 samples produced. On addition of these samples to the surface sample database (Pichon *et al.* 1992b), a fourth factor was resolved from factor analysis which was related to the dissolution. The fourth factor increased the total variance resolved through factor analysis by 2%.

The dominant species noted for their resistance in the dissolved samples were those previously identified by Jousé *et al.* (1962a), Kozlova (1966) and Shemesh *et al.* (1989). However, Pichon *et al.* (1992b) provided evidence of the need to consider all species in the dissolution signal since differences in sub-dominances were regionally specific. Pichon *et al.* (1992b) used this background work to propose a relationship capable of estimating the amount of opal dissolved by employing the factor loading of the fourth factor (dissolution).

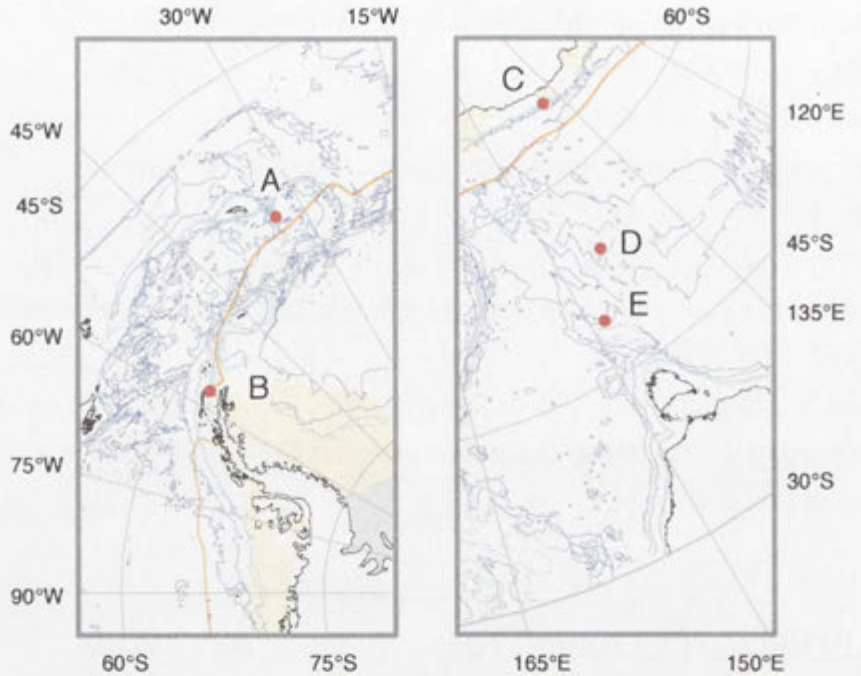

Figure 3.43. Location of the 5 dissolved samples (Pichon *et al.* 1992a,b) with bathymetry (GEBCO, 1992) and maximum sea-ice extents (Schweitzer 1995). Samples identified by the following codes: A= KR8702; B= KR8707; C= KR8818; D= KR8810; E= KR8808. The use of certain samples is discussed in the text.

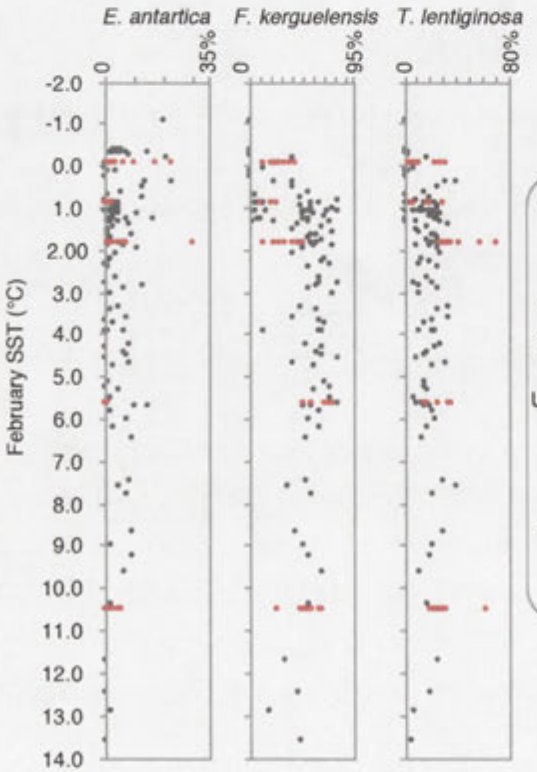

Figure 3.44. Comparison of Natural and Dissolution data set relative abundances of the three most dissolution resistant diatom species against February SST (WOA 1994). The Dissolution data set appears to under-estimate the natural distibution of *F. kerguelensis* in cold waters, under-estimate *E. antartcica* abundances in the mid- to warmer waters, and over-estimates the effect of dissolution of *T. lentiginosa* in most regions.

Although this is an unique data set which seems to decrease the significance of dissolution in further statistical analysis, the nature of the data is of concern to the formation and use in the reformed database being constructed in this thesis. Two foci of discussion are presented below concerning the degree of dissolution and the sample locations.

3B.2. DEGREE OF DISSOLUTION.

Increasing the degree of dissolution, as expected, reduces the number of diatoms for counting. The five samples in the dissolution dataset which were dissolved beyond 240 minutes had on average 74 specimens counted (range 8-144 specimens, Appendix 3.1) and decreased the number of species identified. Pichon *et al.* (1992b) mention rejection of some of these samples due to monospecific assemblages (ie. samples dissolved for times longer than 240 minutes in KR8702, KR8808 and KR8818), but continued to use them in their analyses. Unlike this work (Section 3A.1) they did not restrict the inclusion of samples below 300 specimens because of the increasing dissolution.

Using the three species which generally are of most concern to diatom workers in assessing the role of dissolution prior to burial, *Fragilariopsis kerguelensis*, *Thalassiosira lentiginosa*, and *Eucampia antarctica*, it is possible to analyse the role of the Dissolution data set in comparison to the natural distribution of each of these species in the sediments (Figure 3.44). These distributions are assessed in terms of SST from which estimations are typically derived. From the plots of relative abundances of the Dissolution data set versus that of the Natural Database the following points can be made. The Dissolution data set generally covers the range of natural distribution of *F. kerguelensis* in the sediments of mid- to warm-water regions. In regions cooler than 2°C the Dissolution data set under-estimates the natural distribution response which, under transfer function analysis, would bias warmer temperature estimations. For *E. antarctica* the Dissolution data set covers the natural distribution exceedingly well with exception to the mid-temperature range where again there is under-estimation. Finally, the Dissolution data set significantly over-estimates the natural distribution of *T. lentiginosa*. The response being large in both warm and cold water extremes. Such data lends itself to providing cooler estimations in transfer function estimation (personal observations).

To provide fair comparison with other major, but less resistant diatom species, contrast between other species of the Natural Database distribution and that of the Dissolution data set is illustrated in Figure 3.45. In general, the response of the Dissolution data set occasionally provides adequate coverage of the natural dissolution patterns particular to warm water species (eg *Hemidiscus cuneiformis*, *Roperia tesselata*), but in other cases it considerably over-estimates the natural distribution (eg *Thalassiosira oestrupii,*

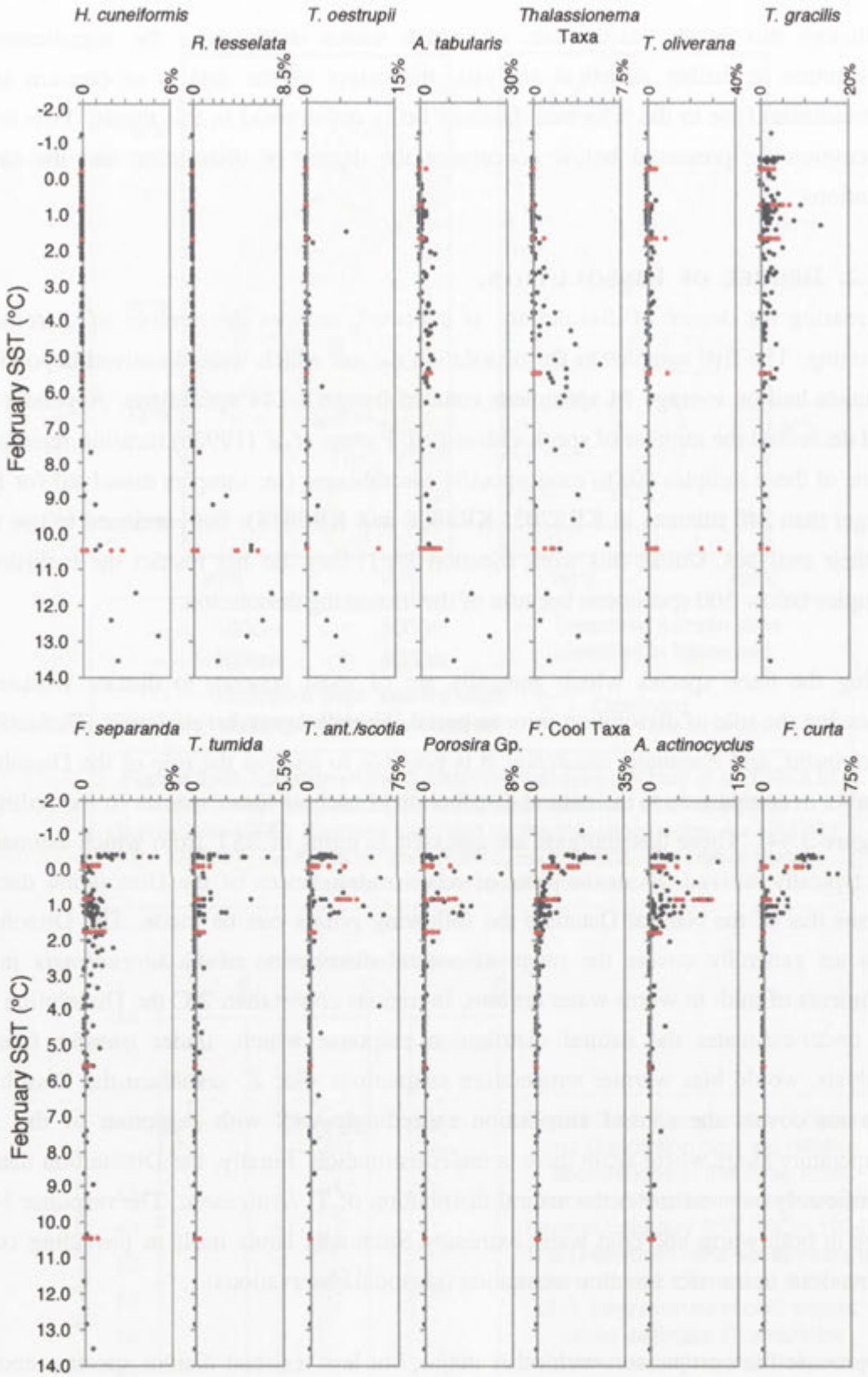

Figure 3.45. Relative abundance distributions of major species against February SST (WOA 1994). Comparative plots between the Natural Database data and the experimentally-dissolved dataset of Pichon *et al.* (1992a,b). The dissolution data generally under-estimates the variabilty observed in cold water species, and does not adequately account for warm water species distributions. (•) Natural Database relative abundances, (•) Dissolution data set relative abundances.

Thalassiosira oliverana). Cold water species, in general, have greater abundances in the sediments than that of the Dissolution data set in their regions of greatest abundance (eg *Thalassiosira tumida*, *Thalassisosira antarctica/scotia* group, *Porosira* group, *Fragilariopsis curta*).

The Dissolution data set is admittedly very small in sample size and concentrated in two dramatically different regions, the Antarctic Peninsula/Weddell Sea confluence region and the southeast Indian Ocean (Fig. 3.43). This fact alone aids understanding the limitations in the application of the Dissolution data set. Increasing the Dissolution data set to other regions will enhance the capabilities and serve to verify certain trends. This obvious feature aside, there are other considerations to be drawn from this Dissolution data set.

Of importance are certain types of counting/identification errors. Increasing dissolution implies increasing fragments and loss of diatom valve definition. Both these processes increase the likelihood of counting valves that may not necessarily be applicable under good counting criteria. Furthermore, reduction of the valve silicification increases the probability of mis-identification, this is already in addition to the errors in taxonomy mentioned in Chapter 2. The problem with discrimination between *Thalassiosira lineata*, *Thalassiosira tumida* and *Thalassiosira ritscheri*, is relevant and enhanced by the increasing dissolution for this data set, as already discussed for the Natural Database.

3B.3 Location of samples

A point that arises from the range of samples is the biogeographical realms covered. Most studies on phytoplankton have shown, or discriminated, three major biogeographical zones for the Southern Ocean (Ice-influenced Zone; Open Ocean Zone; Subantarctic or Subtropical Zone) (eg. Hart 1934, Hasle 1969). These same three zones were identified in subsequent statistical analyses (Burckle 1984a, Pichon 1985, Pichon *et al.* 1987, 1992a, Zielinski 1992). In accounting for the variation in these zones the Dissolution data set covers the ice influenced zone with three samples and the remaining two zones with one sample each. In the case of the subantarctic sample (KR8808, Appendix 3.1), the species identified do not necessarily cover the range of warm water species consistent with its placement in this zone. This lack of warm water coverage is also apparent in the plots of maximum abundances of the warm water species of the Natural Database (Fig. 3.45). The role then of the Dissolution data set under a biogeographical sense compensates for dissolution in the Ice influenced Zone and to a certain degree in the Open Ocean Zone, but is ineffective in assessing Subantarctic Zone dissolution patterns. Translating this into a transfer function application for the estimation of SST, cooler estimates of down-core samples with warm water species would be produced (as I observed personally in transfer function LKA151/23/4, Fig. 3.46).

Two of the samples also require further discussion. The warm water sample (KR8808, E in Figure 3.43) was re-examined (June 1997) in an effort to check certain species abundances and mis-identifications. The series of dissolution samples in question characteristically have very high carbonate content as the samples were not processed in

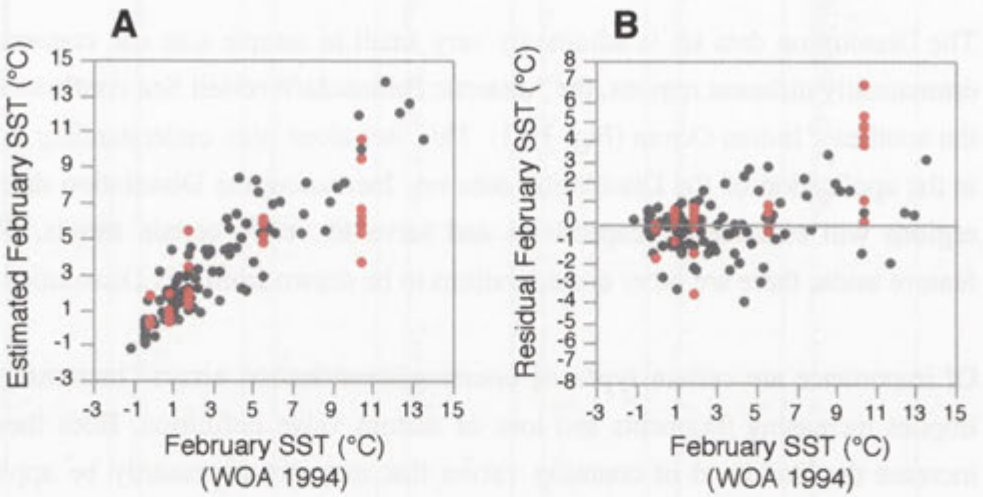

Figure 3.46. Preliminary diagnostic features of SST transfer function LKA151/23/4 which includes the samples from the Natural Database and Dissolution data set of Pichon *et al.* (1992, samples <240min. dissolution). Plot A illustrates the observed versus estimated February SST values, with dissolved samples coloured red. Plot B provides the residual values of the estimation (ie. observed values minus the estimated values). From both plots, but more clearly from Plot B, the effect on estimation from the warm water dissolution sample series is to provide cooler SST estimates by up to 7°C. Warmer estimates from cold water samples are also possible with the expansion of the dissolution data set to samples with >240min. dissolution (not illustrated, but the trend is evident in both plots).

the same manner as the Natural Database (Pichon *et al.* 1992b). This feature obscures the counting of specimens at higher dissolution levels, and can lead to observational biases towards larger species. The original data indicated the sample may not be representative of Holocene sedimentation because of high abundances of younger species such as *Actinocyclus ingens*, *Hemidiscus karstenii* and *Rocella gelida*. Upon reassessing several dissolution levels of this sample, the presence *of A. ingens*, *H. karstenii* and *Denticulopsis* spp., but not *R. gelida,* were confirmed. The sample contains significant reworked species that the samples' use is cautioned. When assessing the sample's location on the sea-floor, it appears the input of sediment from or along the face of the South Tasman Rise is the likely source for the reworked material (refer to Fig. 3.43). Finally, several warm water species were noted as present or in much greater abundance than observed in the original data analysis (eg. *Rhizosolenia bergonii*, *Fragilariopsis doliolus, Thalassionema nitzschioides* taxa, *Thalassiosira oestrupii*, personal

observations). Overall, this warm water sample requires removal from the Dissolution data set for the multiple reasons highlighted above. The sample also advances questions on how to count dissolution data samples, the method of pre-treatment, and the need to carefully examine samples subjected to higher levels of dissolution.

Sample KR8707 in the Antarctic Peninsula region also requires re-analysis for inclusion in future use of the Dissolution data set (Site A in Figure 3.43). In an earlier section (Section 3.5.1), surface samples of the Antarctic Peninsula region were removed from further analysis due to their lacking *Chaetoceros* spp. information and relatively moderate abundances of benthic specimens. Crosta *et al.* (1997) in analysing the *Chaetoceros* content of the Southern Ocean also inspected this dissolution sample. They reported that the sample series commenced with an 83% content of *Chaetoceros* spores which increased to a maximum abundance of 88% before increasing dissolution times began to take affect on their presence. A 83% relative abundance of this single missing species confirms a seriously large component of the thanatocoenose that deserves acknowledgment in any future use of the Dissolution data set. As the Natural database did not include *Chaetoceros* spp. in the derivation of relative abundances, the plots of dissolution data are representative of the remaining species abundances. However, as remarked earlier all species data in this Antarctic Peninsula region are grossly over-estimated due to the lack of *Chaetoceros* spp. information. The other two samples in the Ice influenced Zone (KR8818, KR8702) were also reported with reasonable *Chaetoceros* spore content (range 13-25%, Crosta *et al.* 1997) which requires reassessment. These samples require re-counting if future assessment and use are to be continued.

Since the number of samples considered useful in the Dissolution data set are reduced to three, the continued use of the Dissolution data set was abandoned. This is not to say that such a data set is invaluable to the derivation of SST estimates, quite contrary, the few samples of the dissolution database illustrated here and previously reported by Pichon *et al.* (1992b), make it quite clear that such a dissolution data set is valuable as a correction factor in SST estimation work. The current situation simply suggests that several more experimental samples are required throughout the region of study within the various zones of biogeographical contrast. Pre-treatment and counting methodologies need to be examined, and finally all species have to be included in the identification list. In terms of application, attention needs to be paid to the natural variation of the database and the data which are provided by a dissolution data set. Introducing Dissolution data set information which grossly exceeds or under-estimates the natural signals will introduce errors in the derivation of SST. In particular, over-estimations of relative abundances from dissolution data will affect the ranking procedures employed because of their current reliance on maximum relative abundances. Such a situation allows non-analogue conditions down-

core to be recognised and provided SST estimations, which is probably the case in the transfer function of Pichon *et al.* (1992a). Further studies could address these problems and identify means of interpreting or handling such dissolution data.

CHAPTER 3. SECTION C. THE MINIMISED DATABASE AND APPLIED RANKING METHODOLOGY.

The previous parts and sections of this chapter have discussed in detail the attributes and the samples or species which are relevant in future application of the Natural Database. The multiple reductions in samples or species utilised means the Natural Database is minimised to a new level of use. This new minimised database will henceforth be identified as the Antarctic Diatom Database (ADB). A total of 115 surface samples make up the ADB (Appendix 3.2). Total specimens counted range from 273 to 455 (average 312). Twenty-four species are observed with over 2% maximum abundance within these samples. It is these 24 species that are to be used in statistical analyses. Over each of the 115 samples the 24 species contain a range of 73.8 - 99.7% (average 92.07%) of the samples original count data. Maximum abundances of the 24 species are presented in Table 3.8.

Species used in transfer function analyses	115 ADB Max. relative abundance (%)	Pichon *et al.* (1992a) 166DB. Max. relative abundance (%)	Comments (difference between abundances of 115 ADB & 166DB)
A. actinochilus	11.9	13	- 1.1%
A. curvatulus	2.2	-	new species
A. parvulus	3.1	3	+ 0.1%
A. tabularis	24.2	5	+19.2%
F. curta	67.4	64	+ 3.4%
F. Cylindriform Group	17.0	16	+ 1%
F. doliolus	13.0	39	- 26%
F. kerguelensis	82.4	81	+ 1.4%
F. Cool Taxa	27.8	32	- 4.2%
F. pseudonana	2.4	-	new species
F. rhombica	10.7	11	- 0.3%
F. separanda	7.8	3 (8)*	+ 4.8%
H. cuneiformis	5.3	13	- 7.7%
Porosira Group	7.2	8	- 0.8%
R. tesselata	7.7	12	- 4.3%
S. microtrias	3.3	9	- 5.7%
Thalassionema Taxa	6.5	9	- 2.5%
T. ant./scotia Group	60.6	62	- 1.4%
T. decipiens	2.4	1	+ 1.4%
T. gracilis Group	7.7	15 #	- 7.3%
T. lentiginosa	40.6	41	- 0.4%
T. oestrupii Group	7.3	17	- 9.7%
T. oliverana	4.8	5	- 0.2%
T. tumida	4.7	5	- 0.3%

Table 3.8. Maximum relative abundances of species >2% in the Antarctic Diatom Database (ADB), and comparison with previous maximum abundances reported by Pichon *et al.* (1992a) used in their DTF166/34/4. * = Although published as a 8% maximum the greatest relative abundance of *F. separanda* in the 166 database of Pichon *et al.* (1992a) is 3% (Appendix 2.2, section 6.4.1). # = combined maximum relative abundances of *T. gracilis* and *T. delicatulata.*

In comparison to the Pichon *et al.* (1992a) transfer function DTF166/34/4, eleven species have been removed from the thesis developed transfer function (*Cocconeis* spp., *Eucampia antarctica*, *"Fragilariopsis ritscheri"*, *Odontella weissflogii*, *"Rhizosolenia styliformis"*, *"Thalassiosira delicatulata"*, *"Thalassiosira lineata"*, *"Thalassiosira eccentrica/T. trifulta"*, *Thalassiothrix* spp., *Dictyocha* spp., *Distephanus* spp.) and two new species have been included (*Actinocyclus curvatulus* and *Fragilariopsis pseudonana*). The warm water influence of several of these removed species listed above will be lost to the future transfer functions proposed in the ensuing chapter. A new ranking system is therefore, required for the ADB.

The current ranking method, as given by Pichon (1985) and modified in Pichon *et al.* (1992a), assigns rank values to the derived percentage data taken from raw counts so that all species data are transformed into more representative data of the sample. Thus, species with elevated occurrences and concomitantly high percentages are given equal weighting as a less abundant species. This ranking method instructs users to apply the following ranks to relative abundance data:

Rank 0 = 0% to 1%
Rank 1 = 1% to 2 %
Rank 2 = 2% to 1/2 maximum relative abundance (%) of a particular species.
Rank 3 = > 1/2 maximum relative abundance (%) of a particular species.

A loss of information from species with very low abundances was found to occur with the implementation of this ranking method. This is most pronounced with total specimen counts being less than 300 such that species which generally are not observed over a count of 3, will not be represented in the subsequent analysis (Table 3.9).

% of Total	Total Specimens Counted								
	250	290	300	310	320	330	340	350	400
0.98%	2.4	2.8	2.9	3.0	3.1	3.2	3.3	3.4	3.9
1%	2.5	2.9	**3.0**	3.1	3.2	3.3	3.4	3.5	4.0
2%	5	5.8	6	6.2	6.4	6.6	6.8	7	8

Table 3.9 shows the number of specimens per species required to be counted to reach required ranking values. In the case of the Pichon *et al.* (1992a), ranking method for a normal sample count of 300 specimens, a total of 3 specimens per species must be counted for the species to be included in further statistical work. Increased total specimen counts will increase this value required for inclusion.

Recent work by Zielinski (1993) tackled this problem and changed the ranking method used by Pichon *et al.* (1992) by including all occurrences of species in the ranking method. Therefore the resulting method has the following controls:

Rank 0 = 0%
Rank 1 = 0.1% to 2%
Rank 2 and 3 as in Pichon *et al.* (1992a).

In this thesis, as rare species are those considered less than 0.4%, the Rank 1 category is changed to 0.4% - 2%. The ranking method is completed automatically by the program *PalaeoToolBox* (Sieger 1996), using constructs provided by the user. An important addition to this program is the use of a Rank 4 category which is implemented during ranking of down-core data which exceeds the maximum relative abundances found in the ADB, thus, tagging non-analogue conditions. The ranking of the 24 species used for statistical analysis are given in Table 3.10. Both the ADB and all cores have been ranked using this ranking method.

Species	Rank 1	Rank 2	Rank 3
A. actinochilus	0.4 - 1.9%	2 - 5.95%	5.96 - 11.9%
A. curvatulus	0.4 - 1.9%	2 - 2.2%	-
A. parvulus	0.4 - 1.9%	2 - 3.1%	-
A. tabularis	0.4 - 1.9%	2 - 12.1%	12.2 - 24.2%
F. curta	0.4 - 1.9%	2 - 33.7%	33.8 - 67.4%
F. Cylindriform Group	0.4 - 1.9%	2 - 8.5%	8.6 - 17.0%
F. doliolus	0.4 - 1.9%	2 - 6.5%	6.6 - 13.0%
F. kerguelensis	0.4 - 1.9%	2 - 41.2%	41.3 - 82.4%
F. Cool Taxa	0.4 - 1.9%	2 - 13.9%	14.0 - 27.8%
F. pseudonana	0.4 - 1.9%	2 - 2.4%	-
F. rhombica	0.4 - 1.9%	2 - 5.35%	5.36 - 10.7%
F. separanda	0.4 - 1.9%	2 - 3.9%	4.0 - 7.8%
H. cuneiformis	0.4 - 1.9%	2 - 2.65%	2.66 - 5.3%
Porosira Group	0.4 - 1.9%	2 - 3.6%	3.7 - 7.2%
R. tesselata	0.4 - 1.9%	2 - 3.85%	3.86 - 7.7%
S. microtrias	0.4 - 1.9%	2 - 3.3%	-
Thalassionema Taxa	0.4 - 1.9%	2 - 3.25%	3.26 - 6.5%
T. ant./scotia	0.4 - 1.9%	2 -30.3%	30.4 - 60.6%
T. decipiens	0.4 - 1.9%	2 - 2.4%	-
T. gracilis Group	0.4 - 1.9%	2 - 3.85%	3.86 -7.7%
T. lentiginosa	0.4 - 1.9%	2 - 20.3%	20.4 - 40.6%
T. oestrupii Group	0.4 - 1.9%	2 - 3.65%	3.66 - 7.3%
T. oliverana	0.4 - 1.9%	2 - 2.4%	2.5 - 4.8%
T. tumida	0.4 - 1.9%	2 - 2.35%	2.36 - 4.7%

Table 3.10. Ranking categories employed for each species used in the ADB. Rank 0 is equivalent to all observation between 0 and 0.39%, all other ranks are shown with their respective relative abundances per rank. Use of Rank 4 is reserved for non-analogue situations that arise in down-core work where relative abundances exceed the maximum relative abundances given in this table.

CHAPTER 3. SECTION D. SUMMARY.

This chapter has taken the various surface samples data sets so far available and prepared them for later transfer function analyses. A sample selection criteria was constructed and applied to remove samples that were under-counted, represented high levels of reworking, or indicated their surface qualities did not represent Holocene accumulation. Use of the criteria reduced the available samples from 194 to 129. Communality cut-off criteria were discussed but await factor analysis before their implementation.

The remaining 129 samples were identified as the Natural Database. Species distributions and levels of confidence in species identification were covered in the following section. Species identified in samples at levels less than 0.4% were considered rare and placed in the other unidentified species category along with *Thalassiosira* and *Coscinodiscus* spp. Removing rare species left 59 species/taxa identified, 44 of these species contained abundances greater than 1%. Maximum abundances were presented in Table 3.4. The 44 taxa were then individually discussed in terms of their relative abundance distributions geographically, against February and August SST and also in contrast to annual sea-ice cover and February and September sea-ice concentrations. Comparisons were drawn with current distributions in the sediments and the sea-ice as found in the literature. Certain species departing from current known distributions were encountered (eg. *Thalassiosira antarctica/scotia* Group, *Odontella weissflogii*). These departures are related to *Chaetoceros* taxa obmissions in the species assemblages, which consequently elevated the abundances of all other species encountered.

Species identified as possibly influenced by bottom water or iceberg transport from the south include *Actinocyclus actinochilus, Fragilariopsis curta, Fragilariopsis separanda, Navicula directa, Odontella weissflogii,* and *Thalassiosira oliverana.* Mis-identifications of warm water species in the south were observed under the following species/groups: *Thalassiosira poroseriata, Thalassiosira* Lineati Group, *Thalassiosira* Eccentrica Group, and *Actinocyclus curvatulus.* New records of rarely reported *Thalassiosira perpusilla, Coscinodiscus marginatus, Grammatophora* spp., *Fragilariopsis pseudonana* and *Achnanthes brevipes* were made from the sediments, while new sea-ice relationships were proposed for *Fragilariopsis separanda* and *Grammatophora* spp. New observations in the north for both *Paralia* spp. and *Proboscia alata* are reported. Geographical association and identification of *Thalassiosira decipiens* and *Stellarima stellaris* still require considerable attention. Furthermore, in terms of extracting strong signals from sea-ice related species for elucidating past sea-ice record, identification to species level of *Porosira pseudodenticulata, Stellarima microtrias*, species under *Fragilariopsis* Cool and Cylindriform Groups, and possibly *Thalassioisra gracilis* var. *gracilis* need to be made and will greatly reduce the combined signals that currently exist in this database.

As a result of arguments referring to species responding to sea-surface conditions, benthic and neritic species were removed from further analysis, although their data was conserved in the preparation of relative abundances of the database. Discussion on special regions of the Southern Ocean where diatom communities are largely different from that of the open ocean and Antarctic coast, revealed the need to remove Antarctic Peninsula samples from consideration. Ross Sea samples and a few samples from the Weddell Sea were considered appropriate in their species communities for inclusion in the Natural Database.

The Dissolution data set of Pichon *et al.* (1992a,b) was found to be inappropriate for use in this thesis as a result of the degree of dissolution and the associated comparison to the Natural Database. This was evident in the over-estimation of natural dissolution in the northern sediments and underestimation in the southern sediments, which have repercussions on SST estimation. The level of sample coverage was also considered lacking in terms of biogeographical realms and regional coverage. Two samples of the dissolution database would have required rejection if they were pursued and the remaining three were considered to small a sample group to be employed. The Dissolution data set needs update and expansion for its benefits to be used more successfully.

Having assessed the Natural and Dissolution databases the minimised database that emanates from the previous work contains 115 surface samples and is called the Antarctic Diatom Database (ADB). Twenty-four species with greater than 2% are used for statistical analysis and are ranked using a modified ranking methodology based in part by that of Pichon *et al.* (1992a), and Zielinski (1993). The ranked ADB is the database used in the following chapters dedicated to the SST transfer function and the sea-ice estimation applications.

Chapter 4
Sea-surface temperature transfer function.

4.1. Introduction, methodology, assumptions

A transfer function is a mathematical method that allows quantitative estimations of environmental parameters from past biogenic sedimentation. A transfer function estimating sea-surface temperature was initially designed by Imbrie and Kipp (1971) for foraminifera, and a modified version has since been applied by several workers for marine diatoms (eg. Pichon 1985, Pichon *et al.* 1987, 1992a; Burckle 1989; Zielinski 1993). In broader terms, transfer functions produce equations relating the observed biological species to selected environmental parameter of the ocean. These equations are then employed on observed fossil species from core samples to provide quantitative estimates on one or several selected environmental parameters (Imbrie and Kipp, 1971; Sachs *et al.*, 1977; Reyment *et al.*, 1993). The major assumptions of the diatom transfer function are :

- the estimated parameter(s) (SST) have control on the abundance of the species present,

- the range of present conditions represents the variation of conditions in the past,

- species do not evolve over time frame examined and thus, change their relationship to the parameter being estimated.

Three sources of data are procured to perform the Diatom Transfer Function (DTF). The first data set taken is the ranked diatom species data from core tops (ie. ADB). Here the sediments, in which the core tops are sampled, are representative of the water-sediment surface interface. This interface is assumed to be undisturbed and representative of the modern diatom assemblage for the overlying water mass.

The second data set is taken from the modern environmental variable/s to be related, such as temperature, salinity, nutrients etc... In this study, the present-day reference for SST, the World Ocean Atlas (WOA, 1994) is used. This SST data set for the ADB is presented in Appendix 4.1 along with the sea-ice data set which is to be used in Chapter 5.

Finally, the third data set comprises the down-core data which contains the ranked data derived from the same diatom species used in the modern database. The results of this third step will be presented in Chapter 6.

A flow-chart of the processes followed in the diatom transfer function is shown in Figure 4.1. Detailed descriptions of the statistical methodology are not repeated here. The reader is referred to the original description in Imbrie and Kipp (1971) and to a more recent overview by Reyment and Jöreskog (1993).

Use of Alfred-Wegener-Institüt computer programs *PalaeoToolBox* and *MacTransfer* (Sieger, Nov. 1996) which incorporate the Imbrie and Kipp (1971) subroutines (*Cabfac*, *Regress* and *Thread*) have been used in the work produced here. These programs modernise and simplify the original Factor Analysis Package for PC's (Schrader 1989). Aside from speed and easy data handling, other enhancements include a list of no-analogue occurrences for core material that exceeds the maximum species range in the surface sample database and the lack of communality values for such occurrences.

The aim of this chapter is to construct a new diatom transfer function (DTF) for temperature based on the ADB constructed in the previous chapters. Comparison to the currently employed Pichon *et al.* (1992a) DTF 166/34/4 will be made to facilitate assessment of the differences between the two DTF's. The Pichon *et al.* (1992a) DTF factor analysis and regression steps will be examined first and are followed by the same analyses derived from the ADB.

There are many ways of checking the integrity of statistical output. Simple plots of output data are just one way of understanding the workings and reliability of the model; these are known as diagnostic plots. Diagnostics check for model errors or failure, and can include checks for symmetry, normality, outliers, independence of model errors, geographic auto-correlation, and residual analysis (Molfino *et al.* 1982, Howe and Webb 1983, ANU graduate statistics course notes 1996). In assessing the work presented by transfer functions in this thesis, the following basic diagnostic plots are used.

- Scatter plot of observed values versus estimated values,
- Fitted value plot of observed values versus residuals (residuals = estimated minus observed values) which checks for constant variance and linearity in the model,
- Normality or Quantile-Quantile plots of the sorted residual against expected normal quantiles which checks for deviations from an expected normal distribution,
- Scatter plot of observed values versus communality values for assessing unbiased distribution of compositional information in samples,

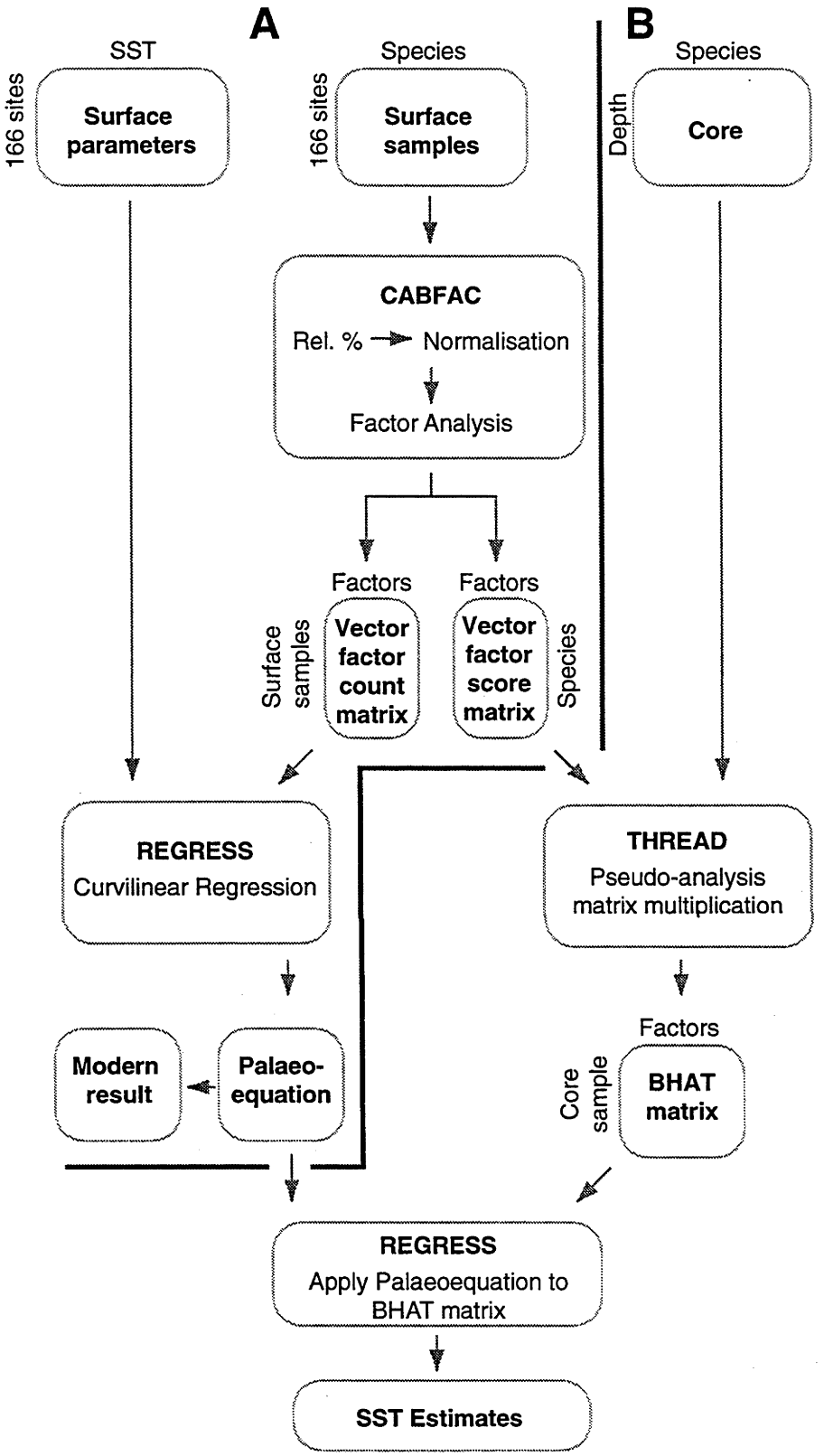

Figure 4.1. Flow-chart of the diatom transfer function used in this thesis. The Diatom Transfer Function is split into two parts the Modern Model (**A**) and the Fossil Model (**B**). Under the Modern Model *Cabfac* transforms the modern diatom assemblages into two matricies, one for regression with corresponding physical parameters for palaeo-equations under *Regress*, and the other matrix for use in converting ranked fossil diatom data in terms of the factors in the modern core top assemblage through the program *Thread*. This resulting varimax factor matrix (BHAT)of *Thread* is entered into the palaeo-equations via *Regress* thus, providing the physical estimates sought.

- Scatter plot of estimated values versus communality values for assessing unbiased communality results from palaeo-equation,
- Scatter plot of communality values versus residuals for assessing possible outliers to the model.

The relationship of each factor, via factor loadings, to the observed SST is provided. This is contrasted to the estimated SST values provided by the palaeo-equation where the original data is re-used to gain SST estimation. This comparison serves to highlight where the palaeo-equation replicates the original SST values in estimation or where over- or under-estimation is occurring. Additionally the geographical distribution of factors, high residual and low communality values are also plotted. This plot highlights the regions of high factor loading and thus, the biogeographic realms held by each factor. Low communality values and high residual values can be assessed geographically which may be important in certain biogeographical zones, and worth taking into account when applied to cores of such a region.

4.2 THE CURRENT PICHON *ET AL.*(1992) DTF166/34/4

This diatom transfer function model is designed for summer SST estimation and has been employed on South Indian Ocean cores in the following publications (Pichon *et al.* 1992a, Sowers *et al.* 1993, Labeyrie *et al.* 1996). The features of this transfer function were described as employing 166 surface sample database, 32 diatom species and 2 silicoflagellate genera, and resolved 4 factors (three biogeographic and one dissolution). The DTF provided estimates of summer SST within a standard error of ±1.0°C over a summer temperature range of -1 to 10°C, where the multiple correlation coefficient of the regression was 0.966. Additionally, the transfer function took into account the role of dissolution because of the inclusion of the Dissolution data set. Other diagnostic data discussion of the transfer function was not entered into and is done so in the subsequent sub-section. The treatment applied to the DTF166/34/4 of Pichon *et al.* (1992a) in this work departs from the original work in that only the ranked data are used as the 166 surface sample database, and the regression is made with February SST (WOA 1994) rather than Summer SST from Levitus (1982).

4.2.1 DIAGNOSTICS OF DTF166/34/4.

Results from the factor analysis of the DTF166/34/4 (Appendix 4.2) are illustrated geographically in Figure 4.2a. Here the dominant factor loading for each surface sample, arbitrarily defined as the factor loading value greater than 0.6, are identified. The first three factors clearly display geographical trends that can be defined oceanographically. Factor 1 is dominant in the zone south of the SAF and north of the southern limit of the ACC (Orsi *et al.* 1995) with exception to the southeast Atlantic. Its southern boundary

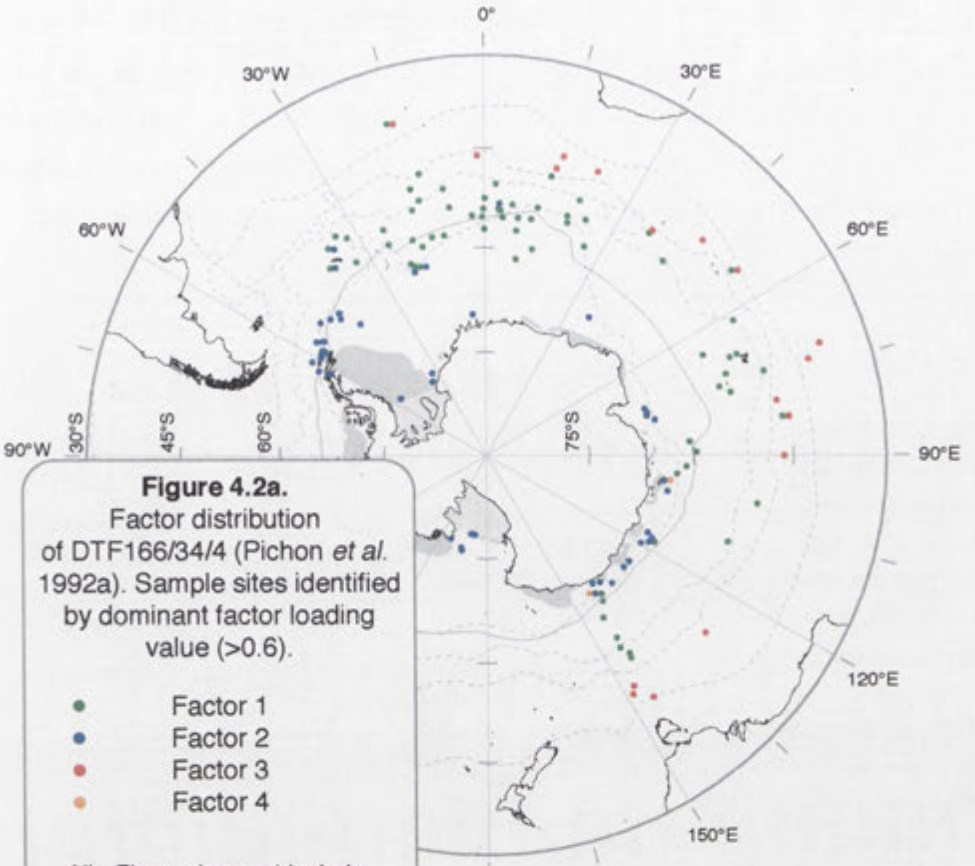

Figure 4.2a.
Factor distribution of DTF166/34/4 (Pichon *et al.* 1992a). Sample sites identified by dominant factor loading value (>0.6).

- Factor 1
- Factor 2
- Factor 3
- Factor 4

Nb. Figure does not include overlapping dissolution data results

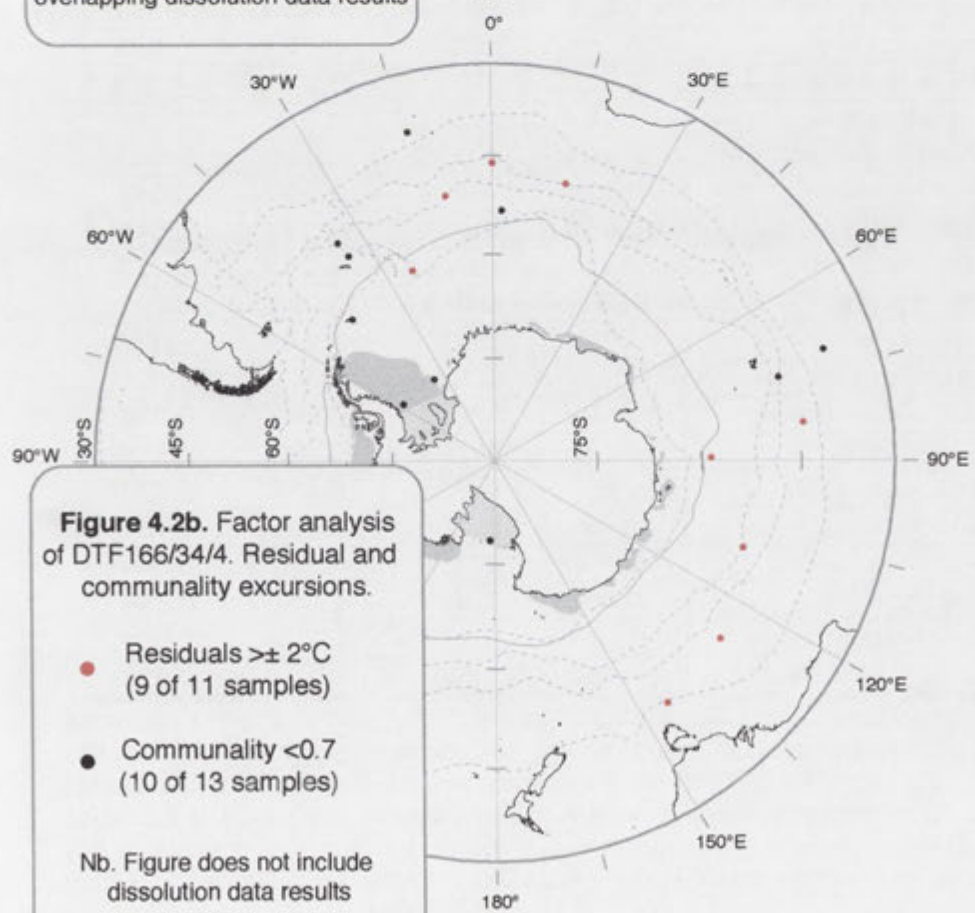

Figure 4.2b. Factor analysis of DTF166/34/4. Residual and communality excursions.

- Residuals >± 2°C (9 of 11 samples)
- Communality <0.7 (10 of 13 samples)

Nb. Figure does not include dissolution data results

does not appear to be controlled by the maximum and minimum positions of sea-ice cover. Factor 2 is dominant from the Antarctic coast to the southern limit of the ACC. Two samples in the South Atlantic near South Georgia reflect high dominance of Factors 1 and 2. This feature is related to the influence of *Thalassiosira antarctica/scotia* abundances that are referable to Factor 2, where the remaining diatom assemblage are

Species	Factor 1	Factor 2	Factor 3	Factor 4
Asteromphalus parvulus	**0.176**	0.022	-0.044	0.075
Chaetoceros veg. spp.	**0.077**	-0.001	-0.045	0.039
Actinocyclus actinochilus	-0.086	**0.379**	-0.051	-0.134
Stellarima microtrias	0.011	**0.073**	0.050	**0.081**
Azpeitia tabularis	0.226	-0.140	**0.411**	-0.055
Eucampia antarctica	0.119	**0.242**	0.059	*-0.247*
Hemidiscus cuneiformis	-0.103	0.005	**0.284**	0.036
Fragilariopsis curta	-0.075	**0.381**	-0.082	-0.055
Fragilariopsis kerguelensis	**0.427**	0.075	0.132	-0.336
Fragilariopsis ritscheri	0.023	-0.019	**0.169**	0.070
Fragilariopsis separanda	**0.227**	0.045	-0.086	0.055
Fragilariopsis sublinearis	0.040	**0.334**	-0.163	-0.206
Rhizosolenia styliformis	0.102	0.203	0.112	**0.318**
Roperia tesselata	-0.116	0.007	**0.345**	0.057
Thalassiosira oliverana	**0.197**	0.033	0.053	-0.174
Thalassionema nitzschioides	0.005	-0.055	**0.411**	0.083
Thalassiosira decipiens	0.030	-0.009	**0.055**	0.033
Thalassiosira delicatulata	0.015	0.007	**0.019**	-0.012
Thalassiosira trifulta	**0.060**	-0.002	0.035	0.028
Thalassiosira gracilis	**0.239**	**0.236**	0.011	**0.236**
Thalassiosira lineata	0.044	-0.004	**0.092**	0.047
Thalassiothrix spp.	**0.566**	0.014	-0.128	0.346
Dictyocha spp.	-0.110	0.009	**0.344**	0.073
Distephanus spp.	**0.269**	0.063	0.083	0.229
Thalassiosira lentiginosa	0.212	0.111	**0.254**	*-0.520*
Fragilariopsis cylindrus	-0.105	**0.242**	0.021	0.031
Fragilariopsis rhombica	0.044	**0.215**	-0.067	0.076
Porosira glacialis	-0.087	**0.231**	0.082	0.125
Odontella weissflogii	-0.036	**0.182**	0.105	0.176
Cocconeis spp.	-0.081	**0.203**	0.100	0.159
Thalassiosira antarctica	-0.167	**0.393**	0.130	0.044
Thalassiosira tumida	-0.002	**0.057**	0.016	0.053
Thalassiosira oestrupii	-0.051	-0.007	**0.246**	0.052
Pseudoeunotia doliolus	-0.054	0.006	**0.134**	0.027

Table 4.1. Vector Score Matrix (VFSM) for the DTF166/34/4. Species are those used by Pichon *et al.* (1992) and follow their definitions not those used in this thesis. Factor scores in bold indicate a species positive dominance under certain factors. Factor scores in italics indicate a greater negative dominance of a species within a factor. Factor 4 scores underlined indicate dominance of species in this factor. Factor 1 = Open-ocean, Factor 2 = Ice Zone, Factor 3 = Subantarctic, Factor 4 = Dissolution.

related to Factor 1 (Table 4.1, Appendix 4.2). Factor 3 has dominance northward of the SAF. Factor 4 is not identified as a dominant geographical feature of the factor distributions. Only two samples show high factor loadings for Factor 4. Both samples are found near the southern limit of the ACC in the southeast Indian Ocean sector. Their significance in this region is not fully understood. Samples with residuals significantly larger than the standard error of the estimate (SEE, arbitrarily set at >±2°C) are identified geographically (Figure 4.2b). With exception to two samples south of the PF, cases of over- or under-estimation by 2°C occurred between the PF and the STC, and more often between the SAF and the STC. This suggests that the DTF166/34/4 is inadequately estimating SST in these regions. The communality values provided by the factor analysis revealed thirteen samples with low values (<0.7) indicating poor utilisation of assemblage data. Their distribution was not located within any one geographic zone or oceanographic sector, and so can be considered random and related to counting discrepancies or preservational differences.

The geographical distribution of factors is reflected in the vector score matrix of species (Table 4.1). Here the first three geographical factors (factors 1-3) can be identified in terms of circumpolar species distributions and thus, the factors can be termed biogeographical. Interpretations of the species associations are provided in Pichon *et al.* (1992a), and can be summarised by the following factor alliances from Table 4.1.

Species in order of highest factor score to lowest with greatest preference for Factor 1 are: *Thalassiothrix* spp., *F. kerguelensis*, *Distephanus* spp., *T. gracilis*, *F. separanda*, *T. oliverana*, *A. parvulus*, *Chaetoceros* veg. spp., and *T. trifulta*. Under Factor 2 the following species have their greatest factor score affinity: *T. antarctica*, *F. curta*, *A. actinochilus*, *F. sublinearis*, *E. antarctica*, *F. cylindrus*, *T. gracilis*, *P. glacialis*, *F. rhombica*, *Cocconeis* spp., *O. weissflogii*, *S. microtrias*, and *T. tumida*

Factor 3 culminates the expressions of the following species in order of highest to lowest factor score: *A. tabularis*, *T. nitzschioides*, *R. tesselata*, *Dictyocha* spp., *H. cuneiformis*, *T. lentiginosa*, *T. oestrupii*, *F. ritscheri*, *P(F.). doliolus*, *T. lineata*, *T. decipiens*, and *T. delicatulata*. Factor 4, the dissolution factor, contains high negative factor scores attributed to *T. lentiginosa*, *F. kerguelensis*, *E. antarctica* and *F. sublinearis*. There are also high positive expressions of some species in this factor which are referable to *R. styliformis*, *T. gracilis*, *Distephanus* spp. and *S. microtrias* which may also need to be considered in the application of this factor.

As the species used in this transfer function were never provided with geographical distribution interpretations and many of the species are no longer used or follow the same species definitions, further comment of the distributions and factor relations are not

advanced and the reader is referred to the analysis of individual species identification in Chapter 2.

The summary diagnostic plots of the DTF166/34/4 are presented in Figure 4.3. All dissolved data, although combined in the analyses, are highlighted from the natural samples of the database. The typical observed versus estimated plot (Fig. 4.3A) illustrates the general ability of the model in estimating the observed data. Natural data estimates are mostly within the SEE (±1.12°C). Dissolved data is estimated less effectively in increasing temperature regimes. The fitted plot (Fig. 4.3B) emphasises the discrepancies between the observed and estimated values using the residual values. The natural data residuals are randomly distributed over the observed temperature range but have values that are considerably larger than the SEE. The dissolved data over-estimate SST in the colder temperatures (1 and 6°C) and largely under-estimate SST at 10°C by up to 3°C. The dissolved data set is not randomly distributed and may require transformation to provide constant variance.

The normality plot (Fig. 4.3C) provides evidence that the original 166 sample database does not always follow true normality (ie. a 45° line is expected). Both the natural and dissolution data sets are have slight skew and stepping at the base indicating over-estimation. The dissolution data set dips in the centre and shows evidence of under-estimation at the top. The natural data set shows greater normality and stronger linearity than the dissolution data set, and departures between the two sets are evident. This feature is important for discerning the value of the dissolution data set against that of the natural variation, and also the natural tendency for the model to provide under-estimated values.

As mentioned in the geographical distribution of factors, thirteen samples with low communality appeared to occur randomly through the study region. Distribution of all communality values against the observed SST indicate that communality decreases with decreasing SST both in the natural and dissolution data sets (Fig. 4.3D). The dissolution data otherwise shows random distribution of communality over the SST range, whereas the natural data indicates a trend for increasing communality with decreasing temperature. The extreme warm temperature samples show similar boarder-line communality values suggesting other influences on the preservation of diatom assemblages. When communality values are plotted against estimated SST (Fig. 4.3E), a left opening megaphone-like trend is further highlighted showing maximum and minimum communality values with decreased temperature estimation.

Finally, the scatter plot of communality values versus residuals in Figure 4.3F is constructed for assessing possible outliers to the model. Here the box delineated by the >0.7 communality values and the region between the ±1.12°C SEE values theoretically

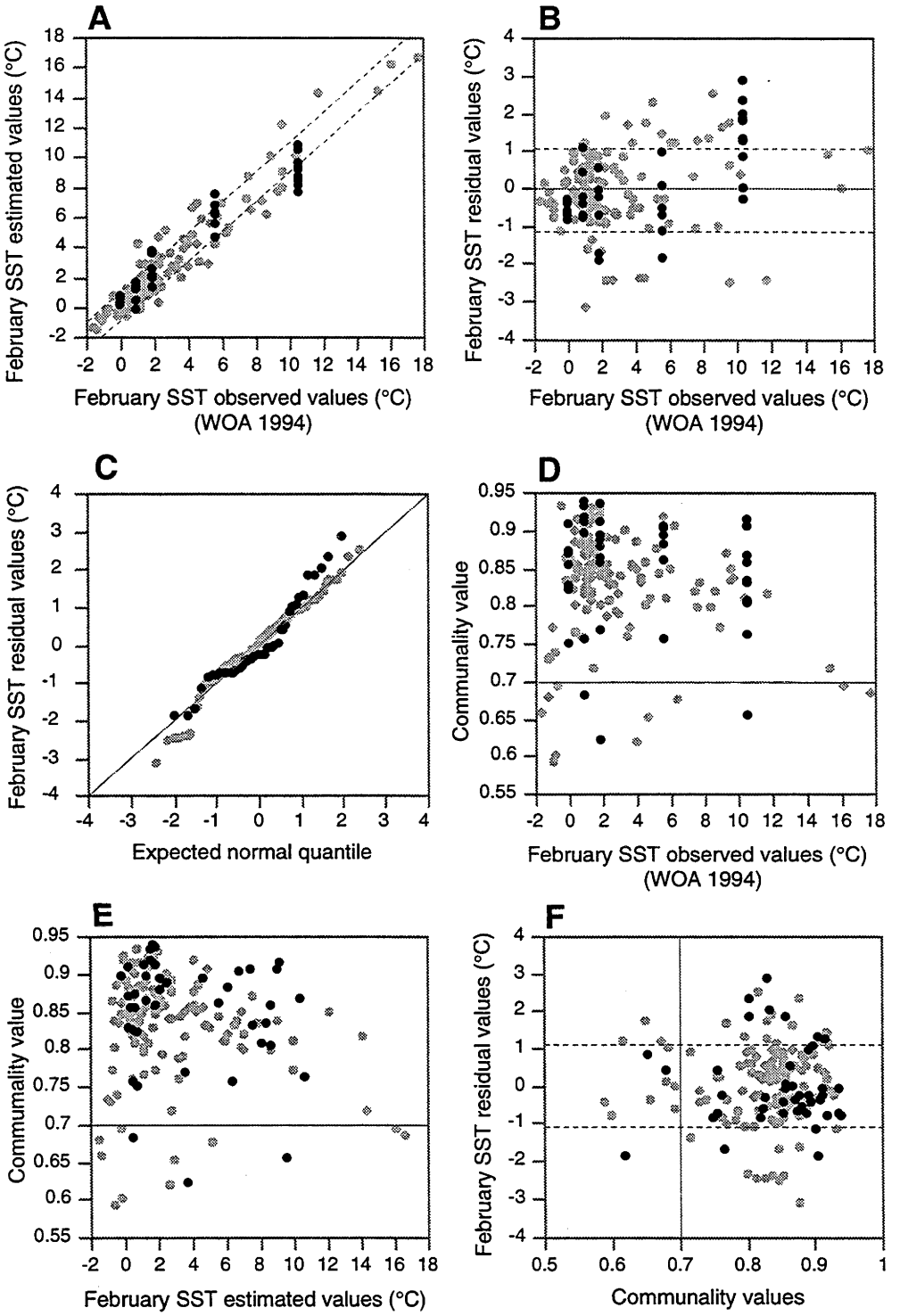

Figure 4.3. Summary diagnostic plots for February SST analysis of DTF166/34/4 (ranked dataset). DTF has a multiple correlation coefficient of 0.957 and standard error of the estimate (SEE) of ±1.128°C. There are 13 samples under communality value 0.7. Diagnostic plots are discussed in the text. **A**= scatter plot of observed versus estimated values; **B**= fitted value plot (observed versus residuals); **C**= Normality or Q-Q plot (expected normal quantiles versus sorted residuals); **D**= Observed SST versus communiality values; **E**= Estimated SST versus communality values; **F**=Communality values versus residuals plot. Dissolved samples identified by black circles, natural samples by grey circles. Dotted lines =SEE, full lines = communality value 0.7, except in figure B where it is the zero residual value, and figure C where it is the 45° line.

define the data of the model which produce the results sought. The points exterior to this region of high accuracy indicate data that decrease the accuracy of the model either from the point of view of information used (communality) or over- and under-estimation by the model. Although the SEE value is restrictive as a boundary to the estimation accuracy, in general the preference is for a SST model that predicts within ±2°C. For this reason, the arbitrary value of ±2°C was represented in Figure 4.2 and could be also considered in Figure 4.3F as a reasonable value by which to further restrict the DTF166/34/4 proposed by Pichon *et al.* (1992a) to increase estimate accuracy. This plot also stresses that high communality does not necessarily mean a sample will provide information for accurate SST estimation, which is often currently implied.

The diagnostic plots presented in Figure 4.3 indicate that the DTF166/34/4 has some problems in handling the dissolution data set for the model, the residuals may have non-constant variance which results in over- and under-estimation of SST, and also exhibit a degree of non-normality. Communality values in contrast show high data retention. The natural samples on the whole show random distribution thus indicating equal variance. However, the lower sample numbers in warmer temperature regions can lead to other interpretations on variance homogeneity (ie. an outward bow requiring transformation). Normality of the natural data is achieved, whereas a trend for increasing low and high communalities with decreasing temperature is evident. The data set and resulting model as a whole provides estimates of SST with increasing departures from the SEE with increases in the communality of a sample (Fig. 4.3F). The dissolution data tends to under-estimate SST with communality values in the 0.8 to 0.9 range whereas the natural data set over-estimates SST in this same communality range. The dissolution data set as a whole has a bias towards over-estimating SST but within the SEE. The natural data is more evenly distributed over the SEE range in its estimations.

To understand the predictive capabilities of the DTF166/34/4 model, analysis of the factor loadings of each factor are presented against the observed WOA SST (Fig. 4.4A-D) and alongside the concomitant estimated SST values (Fig.4.4E-H). Concentrating of the responses of the four resolved factors to February SST it can be seen that the first three factors have response to SST, whereas the fourth factor (Fig. 4.4D) does not. Factors 1 to 3 as noted in the geographical distribution plot of Figure 4.2a, indicate that certain zones of relation are found. Factor 1 was located in the open-ocean region and is observed in Figure 4.4A to have highest factor loadings attributable to February SST of ~1°to 6°C. Factor 2 surrounding the Antarctic and bounded to the north by Factor 1 is here related to SST of ~ -2° to 2°C. Factor 3, the subantarctic distributed factor, shows highest factor loading values where February SST are greater than 9°C. Factor 4 attributed to dissolution shows little response to SST and is dominated by negative factor loadings, in particularly by the dissolved data set.

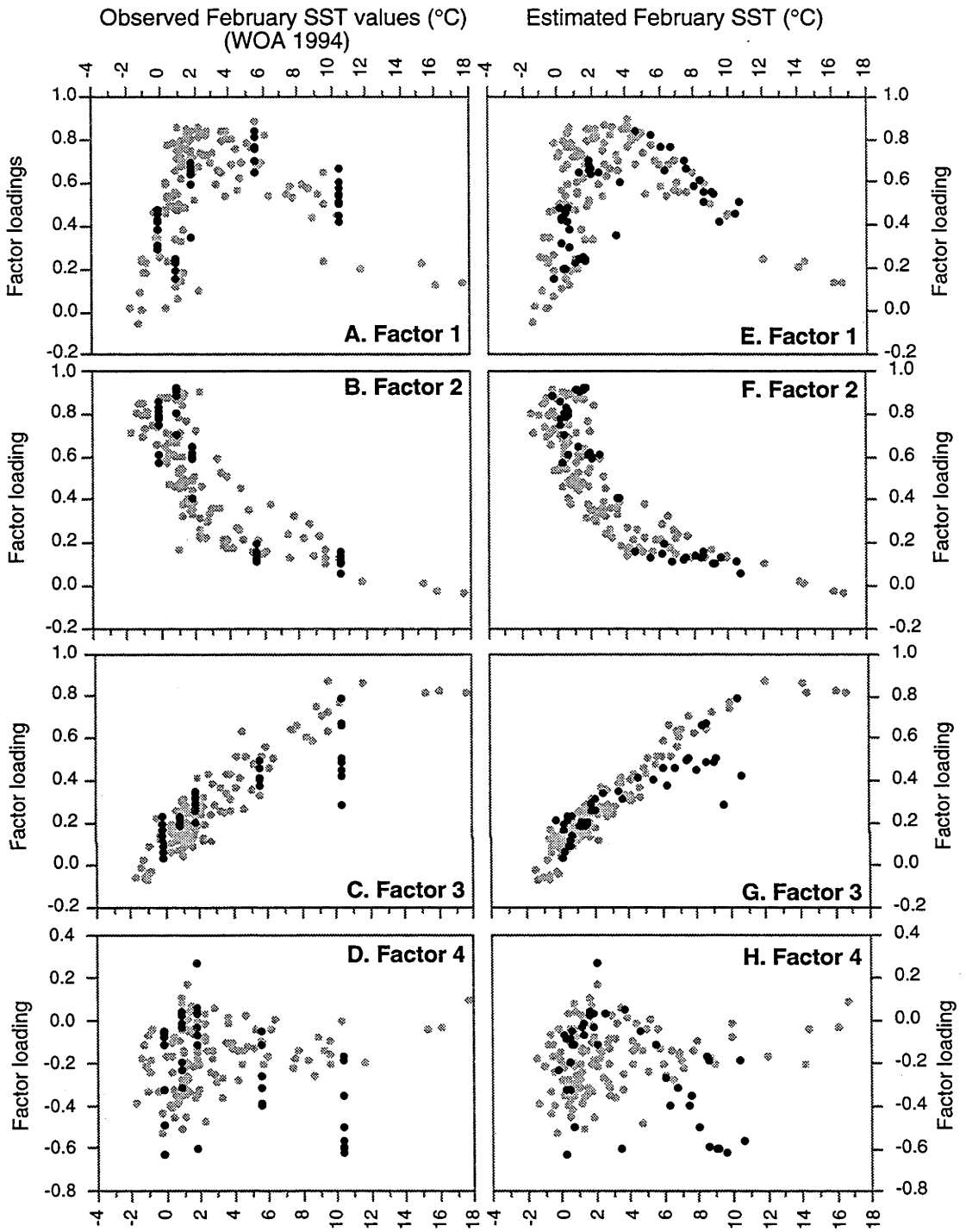

Figure 4.4. Factor loading plots of the four resolved factors against the original observed SST data from WOA(1994) (plots **A-D**) and against the estimated SST values provided by the palaeoequation (plots **E-H**). Factor 1= Open Ocean, Factor 2 = Ice Zone, Factor 3= Subantarctic, Factor 4= Dissolution. The lack of a SST relationship to Factor 4 loadings provides evidence of an independent influence on the distribution of the diatoms. The differences between the relationships formed by the observed SST and each respective factor and that of those formed by the estimated SST and the factors, can provide insight in the effectiveness of the palaeotemperature equation. These differences are discussed in the text. Black circles indicate dissolved data and grey circles the natural data.

The role of the dissolution data set to each of the three temperature related factors has varying relations. Dissolution samples cover the variability of temperature relations in Factor 1 reasonably well, with exception to the warm-water sample at ~10.5°C and that of the sample at 1.5°C. In Factor 2 variation is covered effectively in the cold water regions but is lacking in SST of ~5.5°C. In Factor 3 the warm-water response for dissolution is poorly represented and appears to have more in common with the response provided by the open-ocean sample at ~5.5°C. The other responses are in tune with the variability elicited by the natural samples.

To see how the DTF166/34/4 model reflects the data of its derivation the original diatom assemblage data is re-used to provide the SST estimates (Fig.4.4.E-H). Looking at this data it is possible to assess by each factor the success of mirroring the effects originally observed. Factor 1 provides a good replicate of the original data with a smoothed inverted u-shaped curve. A feature of the curve is the dispersion of most of the warm-water dissolution data over the 4°-11°C range. This feature is evident in all the factor plots of this estimated SST series and has implications that are discussed below. Highest factor values still correspond to February SST between ~1° and 6°C. The response under Factor 2 remains sharp although SST estimation is just slightly warmer at the highest factor loading values (ie. between -1°C to 2°C). Factor 3 can be divided into two signals one from the natural samples which emulates the original distribution, and the second from the dissolved data which trends away from the natural response. This trend as mentioned in the response of the observed SST and factor loading plot (Fig. 4.4D) provides responses that are attributable to the open-ocean response under this factor (eg. factor loading values are at ~0.4). Factor 4 continues to lack a relationship with temperature, although a possible inverted u-shaped trend is formed with the dissolution data.

In general, the DTF166/34/4 model provides good representation of the original data although considerable streamlining is apparent which provides for over-accurate estimation. The dissolution data for the cool water samples is mostly well mirrored by the estimation and serves as a useful tool here. On the other hand, the extreme warm-water sample appears to provide responses in tune with that of the open-ocean dissolution sample. Estimations at the upper end of the 4-11°C range, where these two dissolution samples fall under, obviously experience under-estimation in SST. This feature is related to the >±2°C residuals observed predominantly in the zone between the PF and the STC in the geographic distribution figure (Fig. 4.2b) and also in the diagnostic plots (Fig. 4.3). As previously mentioned in section 3B.2 and 3, this warm-water sample is inappropriate for transfer function work on grounds of its location and diatom assemblage characteristics, the results of choosing this sample for transfer function analysis are thus evident and as hypothesised leads to erroneous SST estimation.

To focus further on the dissolution characteristics of the DTF166/34/4 model, the distribution of the factor loadings of factor 4 for the dissolved samples alone against that of the degree of dissolved opal was reproduced following the results published in Pichon *et al.* (1992b). The response of each of the dissolved samples plus that of the original undissolved samples are plotted against the percentage of dissolved opal in Figure 4.5A. It is evident that the samples have a relationship to the degree of dissolution and thus the fourth factor can be assumed to represent a dissolution factor. The important feature of note in this plot are the two outlier points of KR8702 which are located away from the main downward trending line of points. When trying to emulate the curvilinear response of Factor 4 loadings to opal dissolution (Fig. 4.5B), the curve reproduced varies from that published by Pichon *et al.* (1992b).

Both outlier points were investigated and found displaced from the results provided by the factor analysis of Pichon *et al.* (1992b, fig. 3.c). This is remarkable since the independent factor analysis performed in this work provided factor loading values within 0.02 of those reported by Pichon *et al.* (l.c.) for all other samples and points (compare Appendix 4.2 of this work and table 5 Pichon *et al.* 1992b). In an attempt to discover if removing these two points would resolve the published solution for opal dissolution Figure 4.5C was constructed. Although the response is greatly enhanced and the r value increased the response failed to meet the published version. Finally, the two factor loading values of these questioned points were replaced with those provided by Pichon *et al.* (l.c, table 5). The curvilinear response, plotted in Figure 4.5D, once again enhanced the relationship but did not reflect the published version. The lack of coherency of two points between the factor loading results of this work and that of Pichon *et al.* (1992b) when using the same database, species and factor analysis is not understood. As it was not possible to recheck the original ranked data set for possible errors or changes from the original published version, and the steps of this factor analysis were performed multiple times with the same result, the use of the prediction of dissolved opal from Factor 4 loadings was abandoned and the results of opal dissolution in Pichon *et al.* (1992b) challenged.

4.3. TF WITH NEW DATABASE WITHOUT DISSOLVED SAMPLES

4.3.1 CHOOSING THE APPROPRIATE NUMBER OF FACTORS TO RESOLVE AND A COMMUNALITY CUT-OFF VALUE.

Choosing the number of factors to resolve under Q-mode factor analysis is often an intuitive step made by the researcher. Le (1992) suggested that rather than just taking the known ecological realms noted to occur for the microfauna under study as proposed by Imbrie and Kipp (1977), increasing the number of factors to take into account other unknown relationships to the environment is worth taking into consideration. Statistical

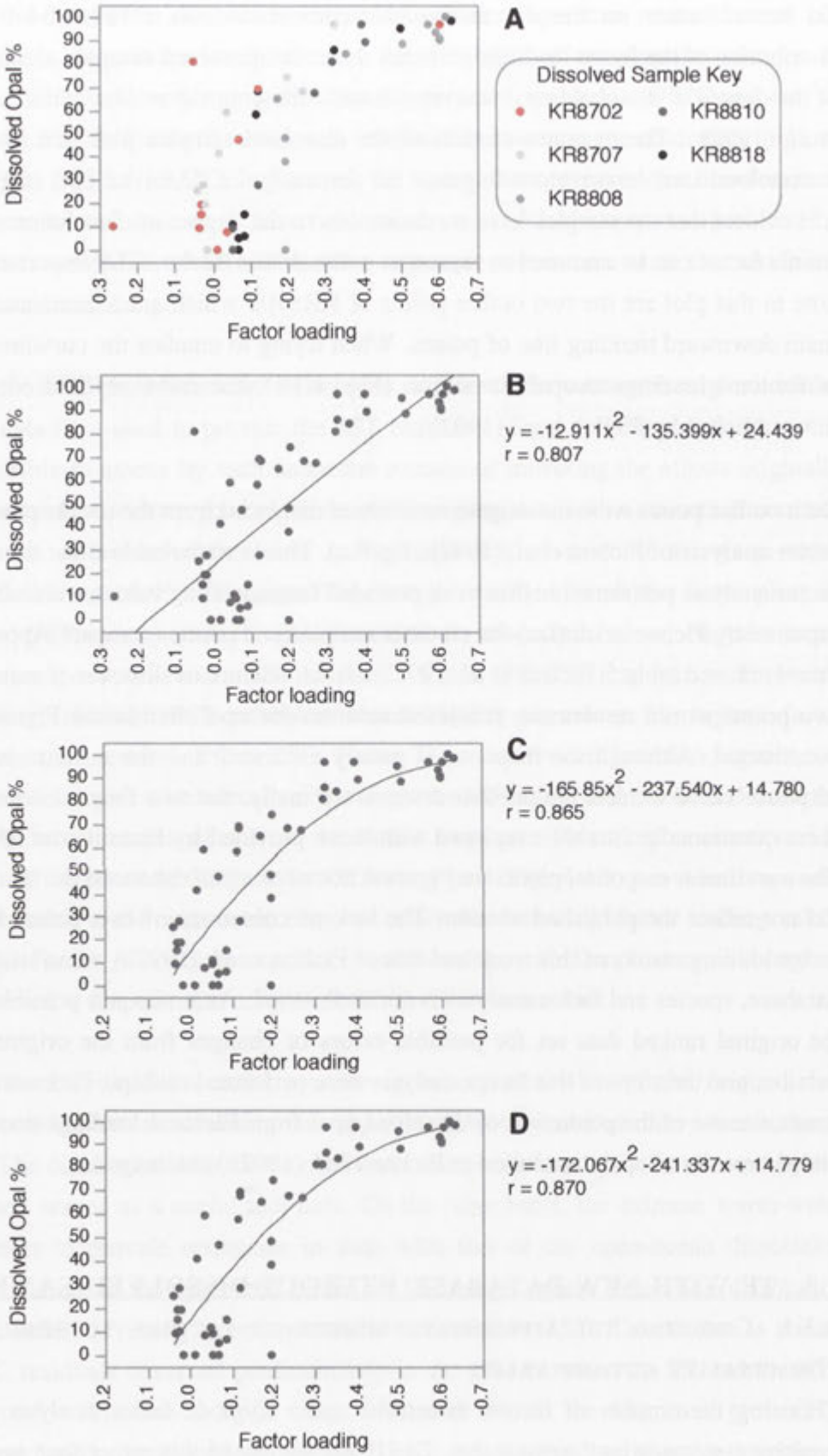

Figure 4.5. Opal dissoluton relationship of Factor 4. **A.** Individual dissolution sample relations to percentage of opal dissolved. Note two outliers from curve in sample KR8702. **B**. Curvilinear response to opal dissolution. **C**. Curvilinear response to opal dissolution removing two outliers. **D**. Curvilinear response to opal dissolution replacing two outlier values with those reported in Pichon *et al.* (1992b)

methods are also proposed by statisticians in deriving the number of relevant factors to resolve (Reyment and Jöreskog 1993), although this approach was not undertaken here since a more logical analysis of the factors resolved was considered appropriate.

Under the constraints of the *MacTransfer* program eight factor analyses were performed on the 115 ADB with variations in the number of factors resolved made from 3 to 10. A primary response of increasing the number of factors resolved is to increase the amount of variance that is accounted for in each of the factor models (Fig. 4.6). Under a 3 factor model 83.8% of the data is used, and this increases to 90.1% with 6 factors and 94. 7% under a 10 factor model.

Entwined in the number of factors resolved is the number of samples which are considered poorly representative of the data set employed, these are identified by the communality value. By increasing the number of factors resolved the number of samples which fall under a communality value chosen for employment (generally and arbitrarily chosen at 0.7) will decrease (Fig.4.7). The need to consider which level of communality to employ as a cut-off level is obviously linked to the number of factors resolved and needs to be adjusted by the researcher depending on the factor model chosen. Continuing with the arbitrary employment of 0.7 as the cut-off value for any factor model without having analysed several models may include or exclude data that should or should not be in the model. Samples with low communalities are considered to provide poor estimates (Le 1992).

As mentioned in section 3-1.1.4, communality values are affected by the number of factors resolved. A plot of the communality values provided for the 115 ADB samples under each factor model is shown in Figure 4.8. The current communality cut-off value of 0.7 is employable under the 3 and 4 factor models but is not good for a selection criteria under any of the greater number of resolved factor models. If choosing a 7 factor model as the appropriate model for describing the distribution of the 115 data then possibly an 0.8 communality value may be more appropriate if a cut-off criteria was pursued.

4.3.2. Species relations to the number of factors resolved.

Such a preliminary understanding of the number of factors required to cover the ecological responses of the data requires further examination from the point of view of geographical factor distribution, as with the individual species response to the number of factors resolved. Le (1992) commented that often a species response under a reduced or over simplistic factor model is forced within another factor to which it does not belong or that altogether misses the appropriate environmental response. This he concluded would lead to misleading results from a transfer function.

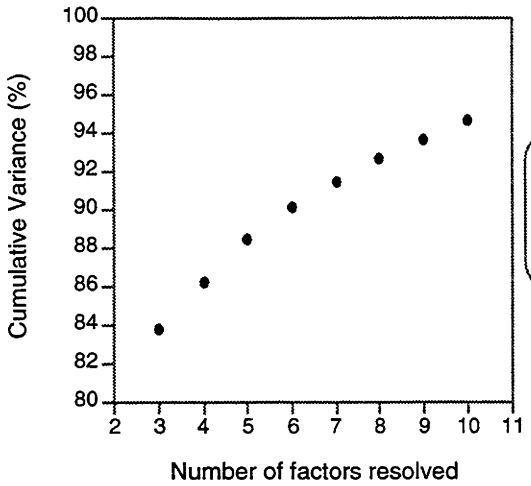

Figure 4.6. Response of increasing cumulative variance of the 115 ADB with step-wise increases in the number of resolved factors.

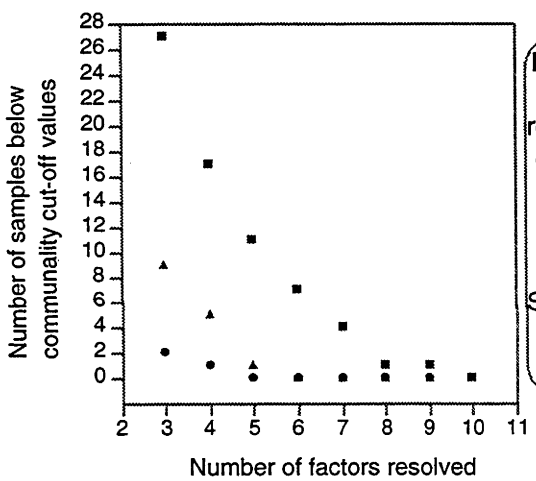

Figure 4.7. A comparative plot of the number of samples in the 115 ADB requiring removal under communality cut-off values of <0.6, <0.7 and <0.8 when the number of resolved factors are increased or decreased.

Samples with
< 0.6 communality •
< 0.7 communality ▲
< 0.8 communality ■

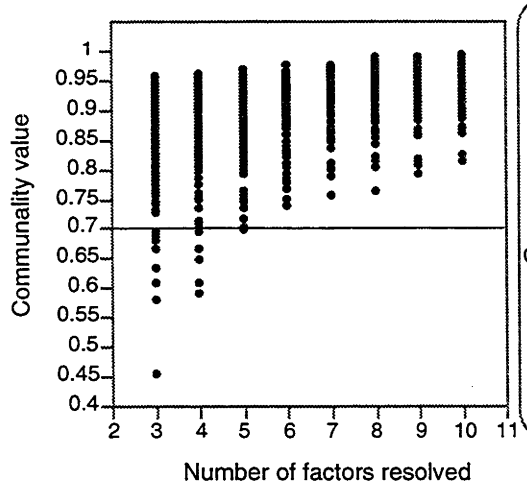

Figure 4.8. Plot of communality values of the 115 samples of the ADB as a function of increasing number of resolved factors. The straight line indicates the 0.7 cut-off point used for excluding samples. It is evident that a 9 factor model will describe the 115 database more than adequately, in comparison to a 3 or 4 factor model. The communality cut-off point requires an increase with the increasing number of factors resolved.

Species are given a weighting measurement for each factor which are known as factor scores. The larger the absolute value of the factor score the greater importance of the species in the factor. The relation of each species to certain factors when increasing the number of factors resolved are summarised in Table 4.2 from Appendix 4.3 (in this example factor models 3, 4, 6, 8, and 10 are used). There are several trends and relationships among factors and species that require comment when subject to increasing resolved factor number. All warm-water species (*Fragilariopsis doliolus, Hemidiscus cuneiformis, Roperia tesselata, Thalassiosira oestrupii* Group) are always found with highest factor scores under Factor 3. This factor score dominance is always increased with increases in the number of factors resolved. All species show steady increases in factor scores over the range of factors resolved except for *Roperia tesselata* which markedly rises in dominance under a 6 factor model. The *Thalassiosira antarctica/scotia* Group also shows the same trend of increasing factor scores with increases in the number of factors resolved, however, in contrast to the warm-water species it is forced into Factor 2 from Factor 4 when the factor model is reduced to 3 factors.

Three cold-water species/groups (*Fragilariopsis curta, Fragilariopsis* Cylindriform Group, *Fragilariopsis* Cool Group) exhibit continuous Factor 2 expression regardless of the number of factors resolved. In each species' case the maximum factor score is observed under the 6 factor model, after which increases in factor number produce a plateau effect (*Fragilariopsis curta* and *Fragilariopsis* Cylindriform Group) or a slight decrease in factor score (*Fragilariopsis* Cool Taxa). Other consistent factor associations, regardless of number of factors resolved, are noted with Factor 1 for *Fragilariopsis kerguelensis* and *Thalassiosira lentiginosa*. For both species, factor score maximums are found under a 4 factor model. Increasing the number of factors resolved introduces another factor which decreases the dominance of Factor 1 factors scores for each species (eg. Factor 5 for *Thalassiosira lentiginosa*). This decrease does not change the overlying dominance of Factor 1 to which each species is associated.

A further four cold-water species (*Thalassiosira tumida, Stellarima microtrias, Porosira* Group, *Fragilariopsis rhombica*) have continuous Factor 2 associations over increases in factor numbers resolved up to the 8 factor model. Both *Stellarima microtrias* and the *Porosira* Group have almost constant factor scores over the 3 to 8 factor models, while *Thalassiosira tumida* and *Fragilariopsis rhombica* exhibit very slight variations in factor scores over the same model range that can otherwise be considered constant. The 10 factor model introduces in each case a dominant negative factor association under Factors 9 or 10. For *Stellarima microtrias*, *Fragilariopsis rhombica* and the *Porosira* Group the dominant positive factor association under the 10 factor model remain with Factor 2, whereas Factor 4 assumes the dominant and maximum observed positive factor score for the expression of *Thalassiosira tumida*.

Species	3 factor model	4 factor model	6 factor model	8 factor model	10 factor model
Actinocyclus actinochilus	F2, 0.301	F2, 0.299	F5, 0.735	F5, 0.762	**F5, 0.767**
A. curvatulus	F1, 0.015	F1, 0.013	F1, 0.028	**F7, -0.076** F8, 0.048	F8, 0.054
Asteromphalus parvulus	F1, 0.127	F1, 0.164	F6, 0.222	**F6, 0.311**	F6, 0.259
Azpeitia tabularis	F3, 0.465	**F3, 0.471**	F1, 0.407	F1, 0.423	F1, 0.465
Fragilariopsis curta	F2, 0.496	F2, 0.498	**F2, 0.501**	**F2, 0.501**	**F2, 0.501**
F. Cylindriform Gp.	F2, 0.258	F2, 0.261	F2, 0.264	**F2, 0.265**	F2, 0.264
F. doliolus	F3, 0.127	F3, 0.128	F3, 0.190	F3, 0.207	**F3, 0.239**
F. kerguelensis	F1, 0.604	**F1, 0.607**	F1, 0.561	F1, 0.571	F1, 0.578
F. Cool Taxa	F2, 0.229	F2, 0.455	**F2, 0.458**	F3, 0.454	F2, 0.448
F. pseudonana	F2, 0.021	F2,0.021 F4, -0.021	F5, -0.025 F2,0.024	F7, -0.096 F6, 0.062	**F10, -0.242** F8, 0.024
F. rhombica	F2, 0.229	F2, 0.229	F2, 0.234	F2, 0.225	**F10, -0.360** F2, 0.226
F. separanda	F2, 0.236	F4, -0.349 F2, 0.242	F6, 0.564	**F7, 0.618**	F10, 0.513 (F7, 0.505)
Hemidiscus cuneiformis	F3, 0.231	F3, 0.231	F3, 0.365	F3, 0.383	**F3, 0.427**
Porosira Group	F2, 0.139	F2, 0.139	F2, 0.141	F2, 0.140	**F10, -0.161** F2, 0.139
Roperia tesselata	F3, 0.350	F3, 0.352	F3, 0.534	F3, 0.543	**F3, 0.600**
Stellarima microtrias	F2, 0.190	F2, 0.191	F2, 0.186	F2, 0.190	**F10, 0.201** (F2, 0.196)
Thalassionema Taxa	F3, 0.590	F3, 0.580	F6, -0.527 F1, 0.368	F8, -0.734 F1, 0.273	**F8, -0.754** F1, 0.296
Thalassiosira ant./scotia	F2, 0.357	F4, 0.490	F4, 0.546	F4, 0.630	**F4, 0.694**
T. decipiens	F3, 0.071	F3, 0.071	F4, -0.085 (F6, -0.083) F1, 0.062	**F8, -0.128** F1, 0.044	F8, -0.192 F1, 0.043
T. gracilis Group	F1, 0.271 F2, 0.222	F1, 0.280 F2, 0.218	F1, 0.372 (F2, 0.271)	F7, -0.552 F1, 0.343	**F7, -0.675** F1, 0.315
T. lentiginosa	**F1, 0.486**	F1, 0.454	F1, 0.357 (F5, 0.343)	F1, 0.375 (F5, 0.307)	F1, 0.363 (F5, 0.304)
T. oestrupii Group	F3, 0.238	F3, 0.236	F3, 0.386	F3, 0.381	**F3, 0.447**
T. oliverana	F1, 0.333	**F4, 0.707**	F4, 0.624	F7,0.464 (F4, 0.404)	F9, 0.650 (F10, 0.352 F1, 0.289 F4, 0.289)
T. tumida	F2, 0.173	F2, 0.173	F2, 0.166	F2, 0.164	**F9, -0.293** F4, 0.196

Table 4.2. Summary table of highest factor scores per species under each of the following factor models (3, 4, 6, 8, and 10). Highest observed factor scores for a species is highlighted in bold. Where the highest factor score for a species under a certain factor model is negative the corresponding highest positive factor score is also provided. Similarly if the overall highest factor score is negative, the highest overall positive factor score is underlined. Factor scores in brackets refer to close or equivalent high factor scores for a species under a certain factor model. Discussion of individual species responses and noted trends are given in the text. Data are summarised from varimax factor score matrices provided in Appendix 4.3.

Three species change factor alliances at the introduction of the 6 factor model. *Actinocyclus actinochilus* dramatically increases its factor score response under Factor 5 from previous associations with Factor 2. This Factor 5 alliance continues to increase in dominance with increases in the number of factors resolved. Similarly *Asteromphalus*

parvulus changes factor association from Factor 1 to Factor 6 with the resolution of a 6 factor model. A change in factor association from Factor 3 to Factor 1 is observed for *Azpeitia tabularis* after the introduction of 6 factor model. As observed with *Actinocyclus actinochilus,* the factor scores of the dominant factor continue to increase with increasing factor numbers resolved. However, on the contrary, *Azpeitia tabularis* has a maximum dominant factor score for the original Factor 3 alliance in the 4 factor model.

Somewhat related to these change-over effects observed under the factor 6 model introduction are also the transitional relations noted under the 6 factor model and subsequent change to new factor associations with the 8 factor model. Both *Thalassiosira decipiens* and the *Thalassionema* Taxa fall under this category and show equivalent associations. Both taxa are aligned under Factor 3 in the 3 and 4 factor models. The transitional factor associations under a 6 factor model are dominated by negative factor associations with Factors 4 and 6, whereas the greatest, albeit small, positive factor scores are located in Factor 1. Increasing the factor models to 8 and 10 factors resolved introduces maximum negative dominances under Factor 8 and diminishes the minor positive factor scores for Factor 1. It may be the case for these two taxa that a 4 factor model adequately describes the associations of these taxa and that increases in factors resolved serves to complicate the signal. Alternatively the increases in factors resolved may serve to align speciation in the *Thalassionema* Taxa and taxonomic errors in the *Thalassiosira decipiens* category.

Two species are noted for their very minor contributions to the factor models employed. *Actinocyclus curvatulus* is always poorly represented in terms of factor scores, although between the 3 and 6 factor models factor alliance is always with Factor 1. Increasing the factors resolved to 8 introduces a negative factor relation, and a new positive factor relation to Factor 8, which is increased and dominant under the 10 factor model. *Fragilariopsis pseudonana* has non-constant alliance to any particular factor over the increasing factor model series. Negative relationships become apparent from the introduction of a 6 factor model. Positive factor scores generally remain constantly low. It is highly likely that neither of these two species have been adequately entrained in the factor models proposed and may show too much variability in their distributions and relationships to environmental features which brings about their low and non-constant factor alliances. Their current lack of association can provide arguments for their removal from continued SST modelling.

Three species remain individual in their responses to variation in number of factors resolved. *Fragilariopsis separanda* changes its factor alliance with every increase in factor number resolved, and can be considered at best related to Factor 2 under 3 and 4 factor models, and Factor 7 under 8 and 10 factor models. *Thalassiosira oliverana* finds

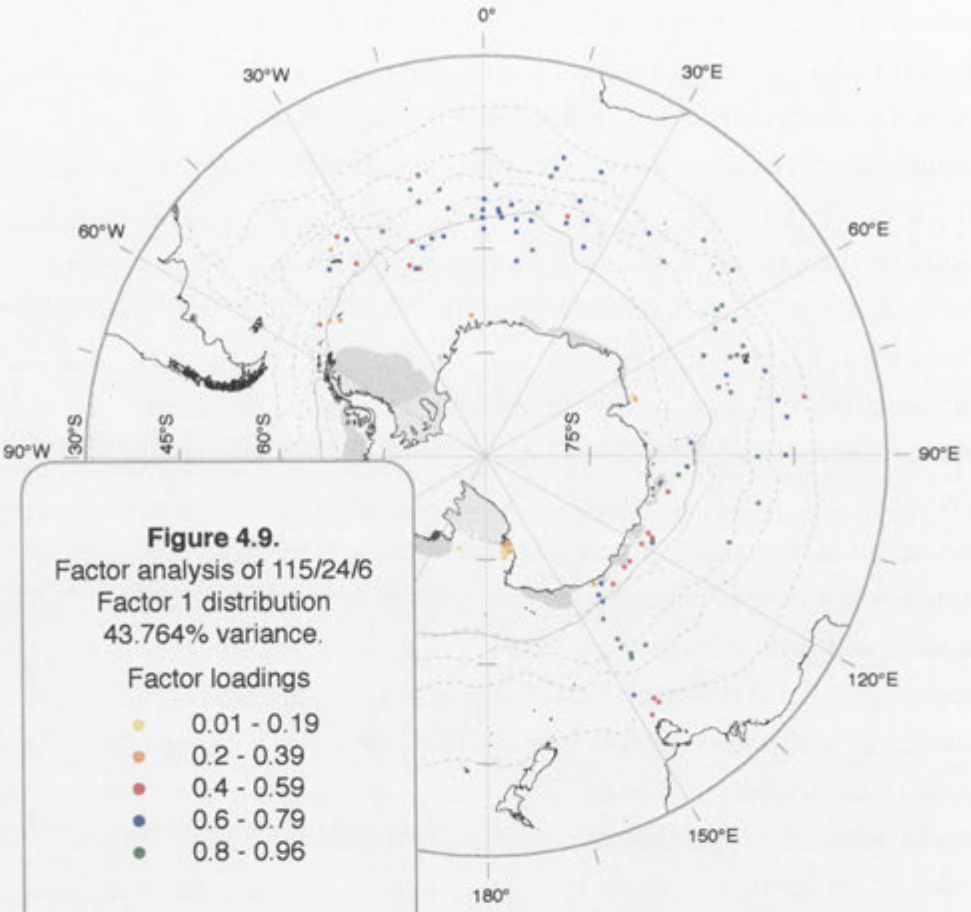

Figure 4.9.
Factor analysis of 115/24/6
Factor 1 distribution
43.764% variance.

Factor loadings

- 0.01 - 0.19
- 0.2 - 0.39
- 0.4 - 0.59
- 0.6 - 0.79
- 0.8 - 0.96

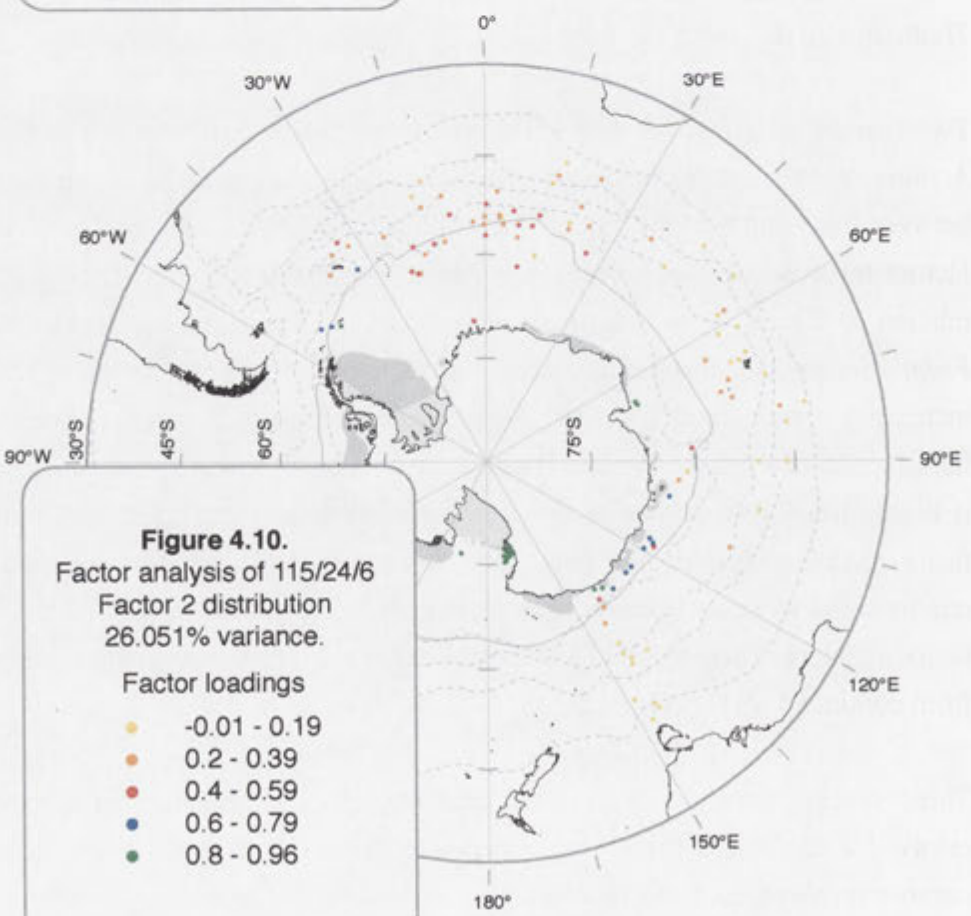

Figure 4.10.
Factor analysis of 115/24/6
Factor 2 distribution
26.051% variance.

Factor loadings

- -0.01 - 0.19
- 0.2 - 0.39
- 0.4 - 0.59
- 0.6 - 0.79
- 0.8 - 0.96

equi-dominance with certain factors with increases in the number of factors resolved. Overall the species is related to Factor 1 in the minimised 3 factor model, then dominated by Factor 4 under the 4 and 6 factor models where it exhibits the maximum factor score observed. Further increases in factor number introduce other relations to Factors 7 and 9 with equi-dominant but considerably reduced factor scores to both Factors 1 and 4. Finally, the *Thalassiosira gracilis* Group is unique in that it appears to respond directly to the bi-modality of the two life stages incorporated in the Group category. From factor models 3 to 6 both Factors 1 and 2 indicate almost equivalent factor scores, with Factor 1 remaining dominant over Factor 2 in each model resolved. Increasing the number of factors resolved to 8 and 10 introduces a dominant negative relation to Factor 7, yet at the same time Factors 1 and 2 remain among the most highly positive associated factors. The Factor 1 association is hypothesised to be representative of the winter stage (*Thalassiosira gracilis* var. *gracilis*) and the Factor 2 association that of the summer stage (*Thalassiosira gracilis* var. *expecta*).

In summary, it would appear from the multiple associations that a 6 factor model adequately takes into account the variation and distinct distributions of the majority of the species used in the factor analysis. A 4 factor model may also be adequate in treating the basic responses of the species chosen, however, reducing the factors resolved down to 3 would miss many of the species associations that would require forcing into three dominant factors. Alternatively, increasing the factor model to resolve more than 6 factors would introduce complicating splits that may not necessarily be resolvable to identifying causes or real ecological differences. The culminative variance explained by a 6 factor model is at 90% and 84% for a four factor model. The communality cut-off value would require increasing to approximately 0.75 or 0.8 to discriminate "poorly" contributing samples from the ADB, whereas under a 4 factor model the 0.7 communality value is adequate as a cut-off value. Lower communality values in the reduced models also reflect the inability of the simplified factor models to account for the alternative ecological distributions of certain species. Increasing the factor number to account for the natural distribution patterns thus decreases the communality value and will provide greater opportunity to assess down-core variations (Le 1992). To further discriminate the best factor solution for the DTF constructed for the 115 ADB, the 4 and 6 factor models are geographically identified and discussed in the subsequent sub-section.

4.3.3. GEOGRAPHICAL DISTRIBUTION VERSUS THE NUMBER OF FACTORS RESOLVED.

The 6 factor model.

The factor loadings of the 6 factor model applied to the 115 ADB are, individually by factor, geographically presented in Figures 4.9 to 4.15. A summary diagram of the 6 dominant factor regions are presented in Figure 4.16.

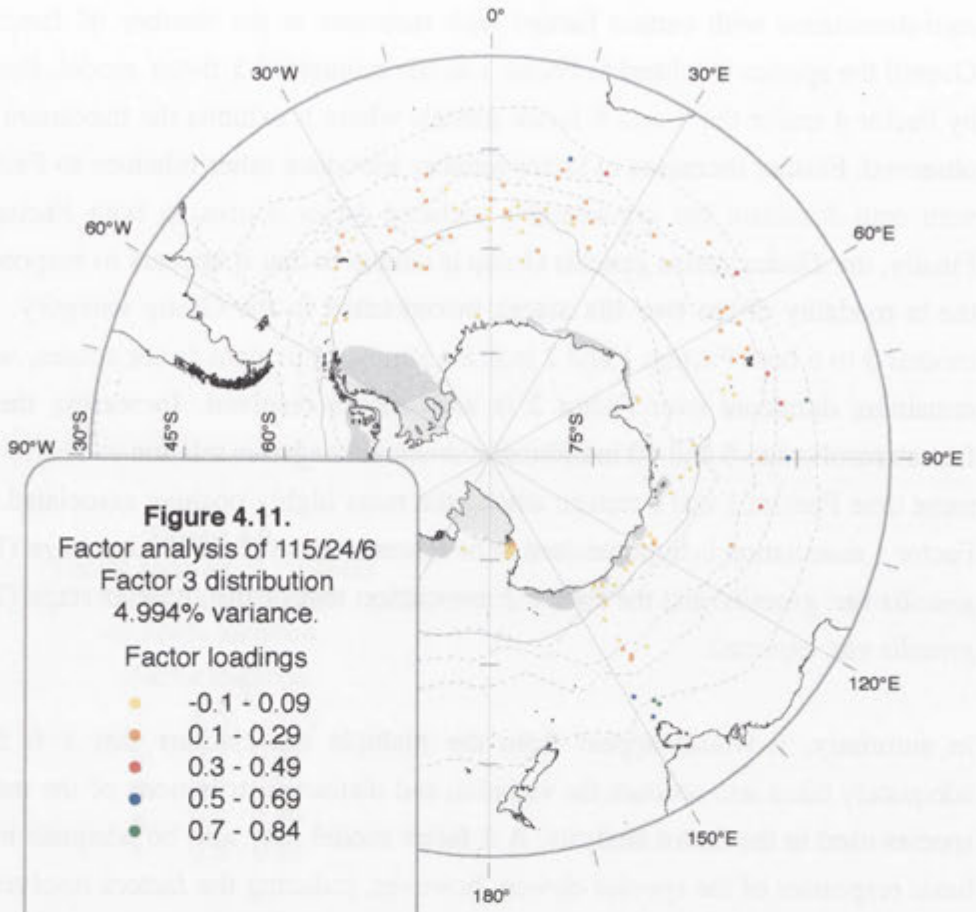

Figure 4.11.
Factor analysis of 115/24/6
Factor 3 distribution
4.994% variance.

Factor loadings

- -0.1 - 0.09
- 0.1 - 0.29
- 0.3 - 0.49
- 0.5 - 0.69
- 0.7 - 0.84

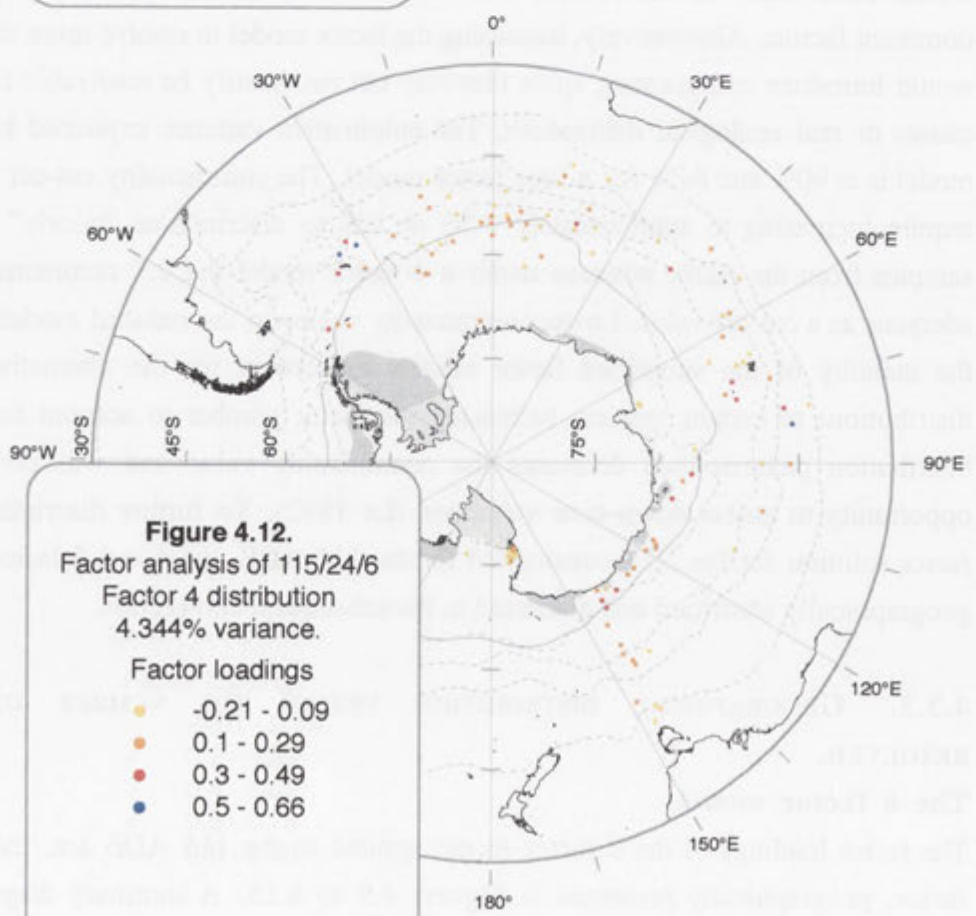

Figure 4.12.
Factor analysis of 115/24/6
Factor 4 distribution
4.344% variance.

Factor loadings

- -0.21 - 0.09
- 0.1 - 0.29
- 0.3 - 0.49
- 0.5 - 0.66

Factor loadings ascribed to Factor 1 are presented in Figure 4.9. This primary factor contains 43.8% of the variance resolved which is almost half of the total variance described by the 6 factor model (total 90%). Factor 1 is dominant (factor loadings greater than 0.8) in the region between the SAF and the southern ACC front (Orsi *et al.* 1995). A zone of sub-dominance (factor loadings between 0.6 to 0.79) surrounds this primary zone of dominance to the STC in the north and what appears to be mid-way between the maximum and minimum sea-ice edge extents. Species associated with this factor in order of factor score dominance are *Fragilariopsis kerguelensis*, *Azpeitia tabularis*, *Thalassiosira gracilis* Group, *Thalassiosira lentiginosa*, *Thalassionema* Taxa, *Thalassiosira decipiens*, and *Actinocyclus curvatulus* (Table 4.2). Each of these species are associated with open-ocean conditions (Chapter 3).

The second resolved dominant factor, Factor 2 (Figure 4.10) have large factor loading values (>0.6) in the Ross Sea, along the East Antarctic coast, east of Prydz Bay and near the South Orkney and South Georgia Islands. Most of the dominance regions occur roughly exterior to the maximum February sea-ice extent, whereas sample sites approaching the maximum September sea-ice extent demonstrate considerably reduced factor loading values. The second factor explains 26.1% of the total variance resolved. The species with high factor scores under this factor are *Fragilariopsis curta*, *Fragilariopsis Cool* taxa, *Fragilariopsis* Cylindriform Group, *Fragilariopsis rhombica*, *Stellarima microtrias*, *Thalassiosira tumida*, *Porosira* Group and *Fragilariopsis pseudonana* (Table 4.2). Each of these species are associated with cold SST and sea-ice cover (Chapter 3).

Factor 3 describes only 5% of the total resolved variance and is the dominant factor in the north of the study region (Figure 4.11). Greatest factor loading values (>0.5) are found in only 7 samples and thus justifies the lower variance resolved. These seven samples are located north of the SAF and just south or north of the STC. Very minor sub-dominances (0.3-0.49) are observed north of the PF in the Indian Ocean sector or north of the SAF in the Southwest Atlantic sector. In order of decreasing factor scores the following warm-water species are aligned with Factor 3: *Roperia tesselata*, *Thalassiosira oestrupii* Group, *Hemidiscus cuneiformis*, and *Fragilariopsis doliolus* (Table 4.2, Chapter 3).

The fourth factor is also a low-describing variance factor (4.4%) that is associated with several samples surrounding South Georgia, samples to the east of Kerguelen and minor dominances along the East Antarctic coast (Figure 4.12). As previously mentioned, this factor is heavily associated with presence of *Thalassiosira antarctica/scotia* and *Thalassiosira oliverana* (Table 4.2). It is hypothesised that aside from the influence *Thalassiosira antarctica/scotia* in the South Georgia Island region, other dominances are related to highly dissolved samples or those that are under the influence of bottom water

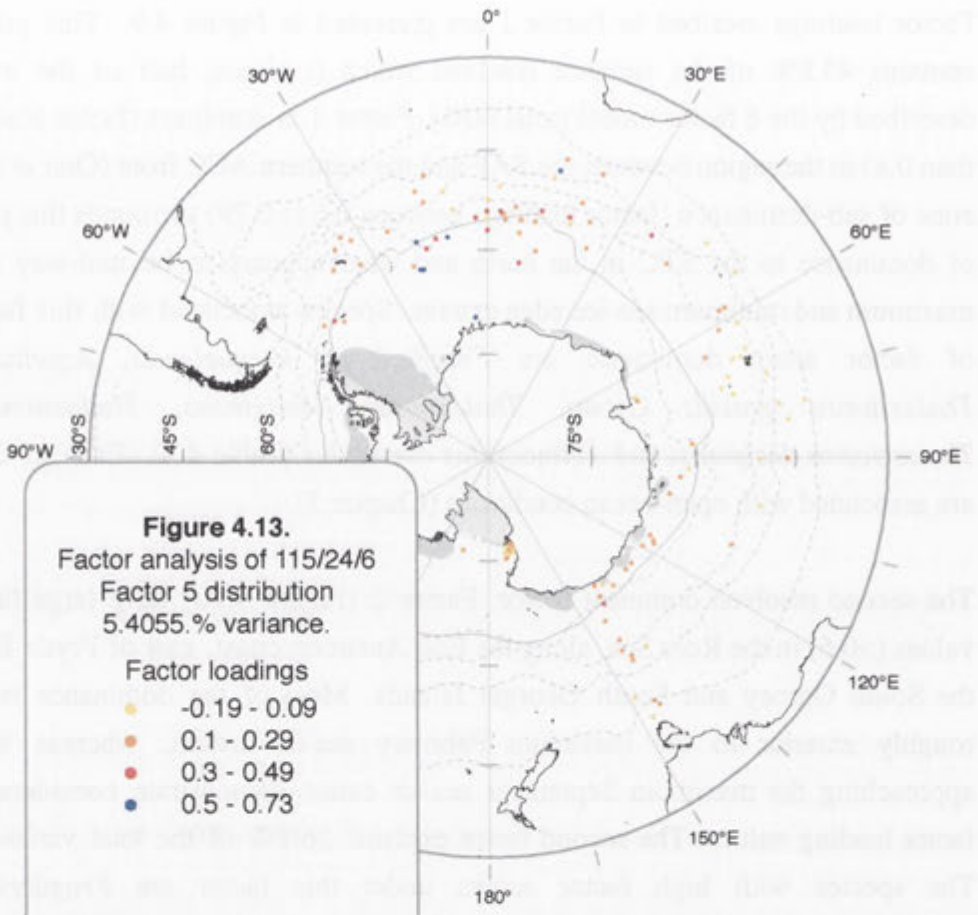

Figure 4.13.
Factor analysis of 115/24/6
Factor 5 distribution
5.4055.% variance.

Factor loadings
-0.19 - 0.09
0.1 - 0.29
0.3 - 0.49
0.5 - 0.73

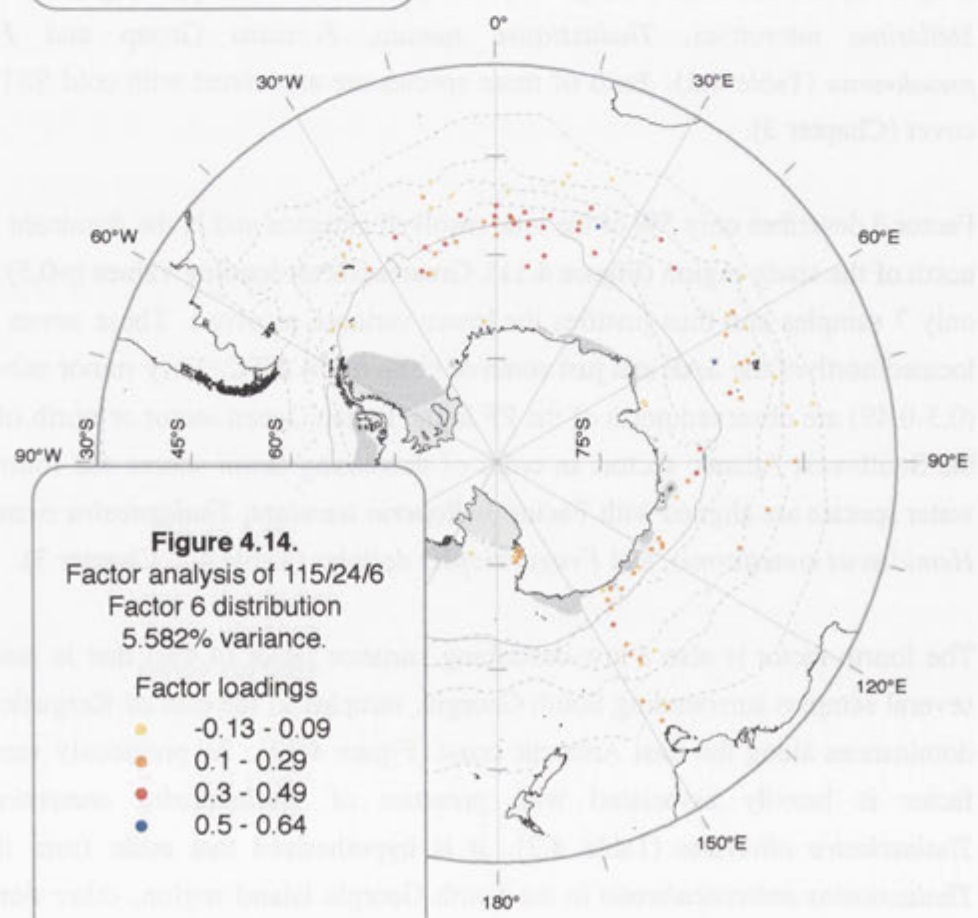

Figure 4.14.
Factor analysis of 115/24/6
Factor 6 distribution
5.582% variance.

Factor loadings
-0.13 - 0.09
0.1 - 0.29
0.3 - 0.49
0.5 - 0.64

currents in which abundances of both *T. antarctica* and *T. oliverana* would be enhanced. Checking the response of this factor to temperature and ice presence is not expected to show an overwhelming relationship, while quantifying a response to dissolution and bottom water currents is obviously increasingly difficult to determine.

Factor 5 factor loadings are found dominant (>0.5) and sub-dominant (>0.3) predominantly in the South Atlantic sector at or just north of the September sea-ice extent maximum (Figure 4.13). This factor is highly affected by the presence of *Actinocyclus actinochilus* and *Thalassiosira lentiginosa* in the sediment samples and is negatively associated with abundances of *Fragilariopsis pseudonana* (Table 4.2). In Chapter 3 each of these species had abundance responses that were observed linked to the September maximum sea-ice edge particularly in the South Atlantic sector. The high abundance of *Thalassiosira lentiginosa* in a northern sample of the SAZ in the South Atlantic has provided the sample with a high factor loading for this factor. External to the South Atlantic sector only one sample is expressed as a sub-dominant member of Factor 5 on the maximum sea-ice edge in the South Indian sector. The variance resolved for the factor is 5.4%. The factor is likely to best represent the maximum September sea-ice edge.

Finally, Factor 6 is also found to be predominant in the South Atlantic sector with other expressions in the South Indian sector (Figure 4.14). The zone of dominance and sub-dominance (>0.3 factor loading) is generally located between the PF and the September sea-ice maximum (ie. the POOZ), the exceptions being south of the maximum sea-ice edge in the South Atlantic sector. Factor 6 is affected positively by the abundances of *Asteromphalus parvulus*, *Fragilariopsis separanda*, and negatively by the abundances of *Thalassionema* Taxa and *Thalassiosira decipiens* (Table 4.2). From descriptions in Chapter 3 we observed that *Asteromphalus parvulus* and *Thalassiosira decipiens* were found to be in highest abundance in the POOZ, *Thalassionema* Taxa were bounded to the north from the September sea-ice edge, and *Fragilariopsis separanda* was considered entrained and deposited in the region of the September sea-ice edge by either bottom water or iceberg transport. The factor resolves 5.6% of the total variance and appears to represent the POOZ particularly in the South Atlantic sector.

Condensing these geographic factor dominances leads us to understand that the model is split predominantly by oceanic boundaries (Figure 4.15) . From the north Factor 3 describes the influence of warm-water and is bounded to the south by the SAF. Factor 1 is then dominant from the SAF to the PF or the south ACC boundary. Sitting right on and occasionally within the southern boundary of Factor 1 is Factor 6, the POOZ factor. The maximum winter sea-ice edge appears to be captured by Factor 5 while along the Antarctic coast Factor 2 reigns and is associated with sea-ice cover. The only factor that does not appear to follow a oceanographic surface division is that of Factor 4 which appears

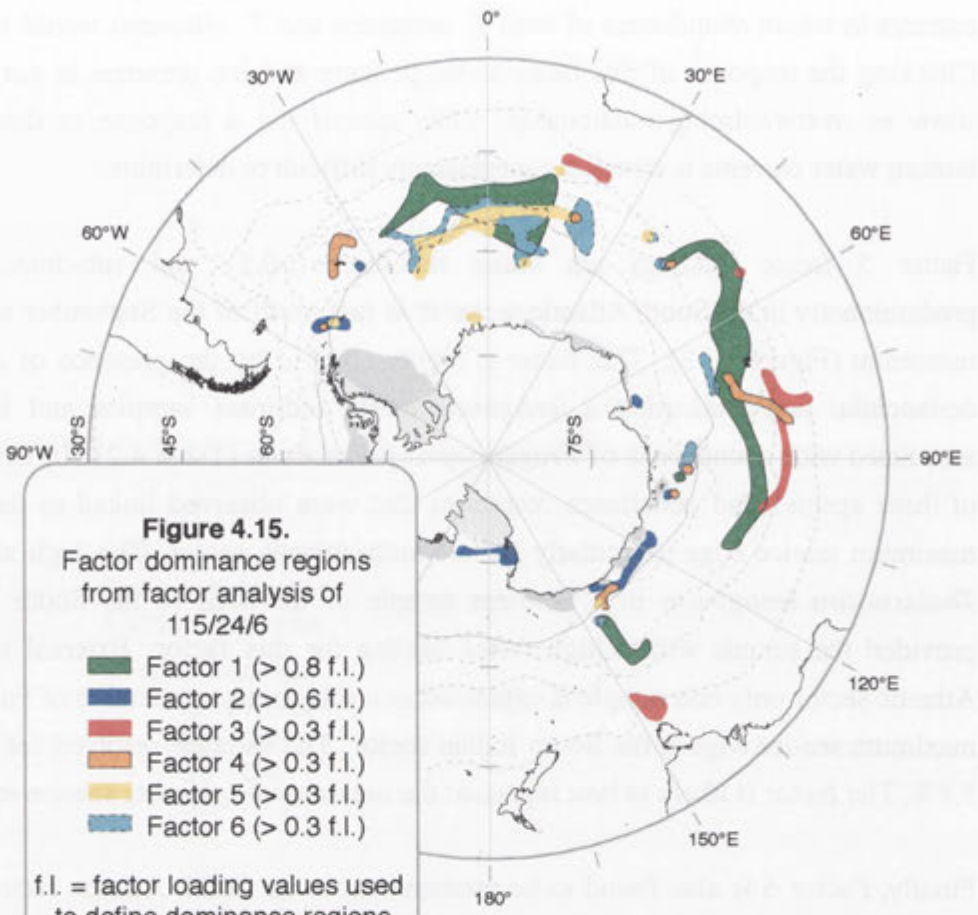

Figure 4.15.
Factor dominance regions from factor analysis of 115/24/6

- Factor 1 (> 0.8 f.l.)
- Factor 2 (> 0.6 f.l.)
- Factor 3 (> 0.3 f.l.)
- Factor 4 (> 0.3 f.l.)
- Factor 5 (> 0.3 f.l.)
- Factor 6 (> 0.3 f.l.)

f.l. = factor loading values used to define dominance regions

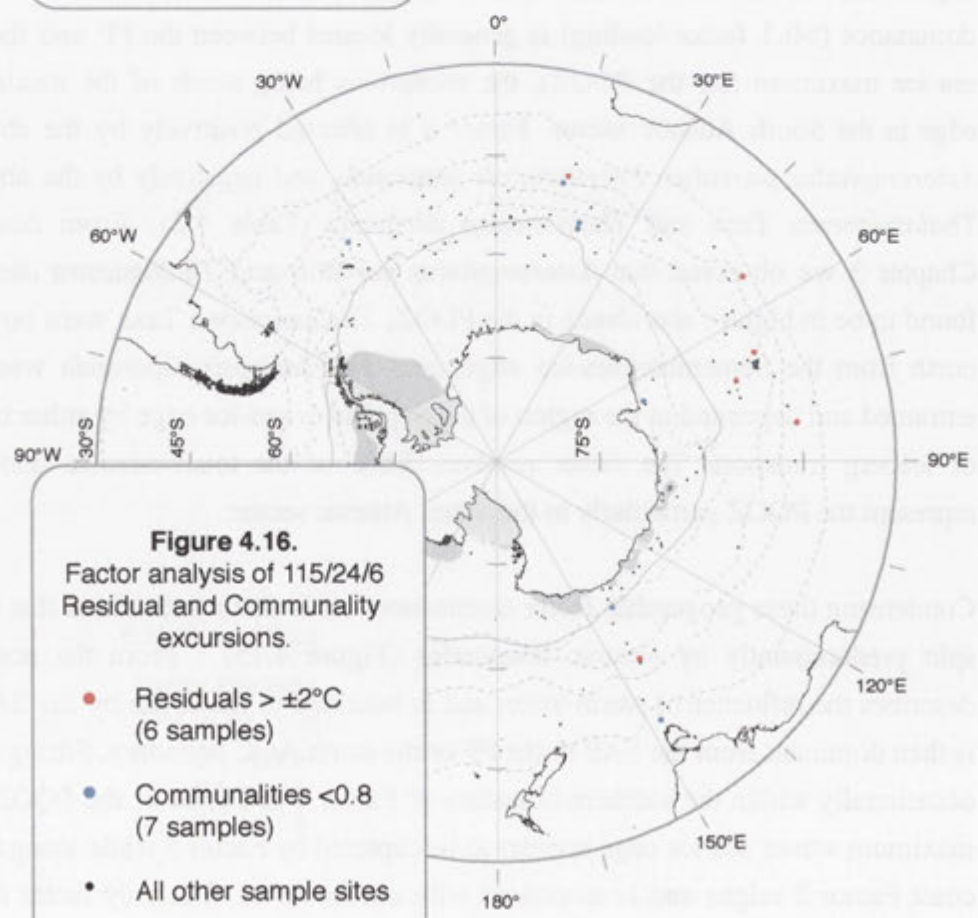

Figure 4.16.
Factor analysis of 115/24/6 Residual and Communality excursions.

- Residuals > ±2°C (6 samples)
- Communalities <0.8 (7 samples)
- All other sample sites

influenced by both islands and bottom water entrainment - for the purpose of this work the factor will be entitled the island/transport factor.

The regions of residual and communality diversions for the 6 factor model are also plotted (Figure 4.16). Communality discrepancies are geographically widely placed and appear random. Residual values on the other hand, are great between the STC and the southern ACC boundary, with exception to one sample in the Ross Sea. Regionally, there is a grouping of large residual values in the South Indian Ocean. The 6 factor model appears to describe the information of the 115 ADB into explainable factor regions by geography, oceanography and species content. A small number of samples are found to contain low communalities and excessive residuals.

The 4 factor model

Decreasing the number of resolved factors down to 4 enlarges predominantly the region covered by Factor 1 when viewed in contrast to the 6 factor model factor distributions. The differentiation described by Factors 5 and 6 of the 6 factor model have been incorporated under the Factor 1 regional distribution in the 4 factor model (compare Figures 4.9 and 4.17). Under the 4 factor model the distribution of high factor loadings is distributed to the south of the PF rather than the SAF in the 6 factor model. This southward movement of the factor territory is also evident along the East Antarctic coastline where the southern boundary for the factor is considerably southward than that observed under the 6 factor model. Species associations for Factor 1 are, in order of highest factor score, *Fragilariopsis kerguelensis*, *Thalassiosira lentiginosa*, *Thalassiosira gracilis* Group, *Asteromphalus parvulus*, and *Actinocyclus curvatulus* (Table 4.2). In comparison to the 6 factor model *Azpeitia tabularis* , *Thalassiosira decipiens* and *Thalassionema* Taxa have been removed from this factor association which explains the southward shift of the northern boundary of Factor 1. *Asteromphalus parvulus*, previously dominant in Factor 6, has been incorporated into the Factor 1 associations and, in part with the increased response of *Thalassiosira lentiginosa* under a sole factor, has contributed to the southward movement of the Factor 1 southern boundary in the 4 factor model. Factor 1 resolves 37.5% of the total model variance of 84%.

Factor 2 generally holds its dominance in exactly the same sample sites described under the 6 factor model, with exception to two sites along the East Antarctic coastline (Figure 4.18 compare with Figure 4.10). Factor 2 embraces species that were previously associated with Factors 5 and 6 in the 6 factor model, however, these inclusions do not expand the region of dominance held by the factor. The species in order of decreasing factor scores are; *Fragilariopsis curta*, *Fragilariopsis* Cool Taxa, *Actinocyclus actinochilus*, *Fragilariopsis rhombica*, *Fragilariopsis* Cylindriform Group, *Fragilariopsis*

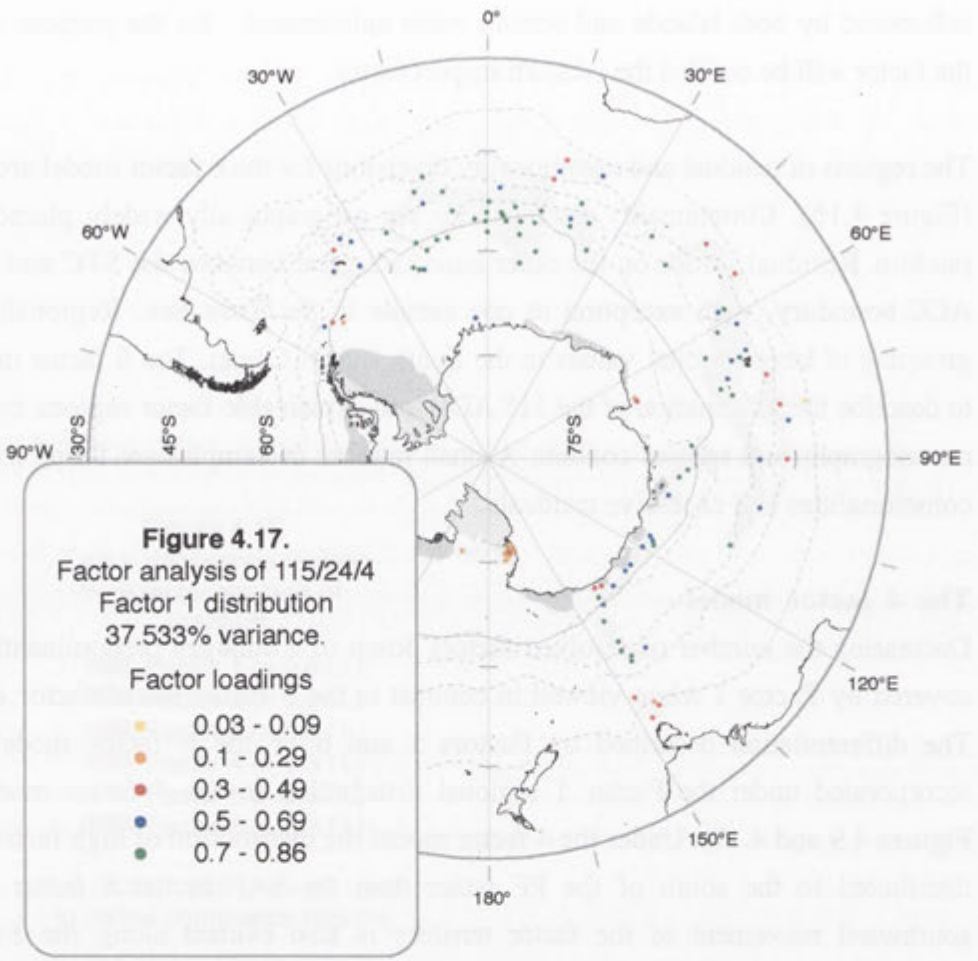

Figure 4.17.
Factor analysis of 115/24/4
Factor 1 distribution
37.533% variance.

Factor loadings

- 0.03 - 0.09
- 0.1 - 0.29
- 0.3 - 0.49
- 0.5 - 0.69
- 0.7 - 0.86

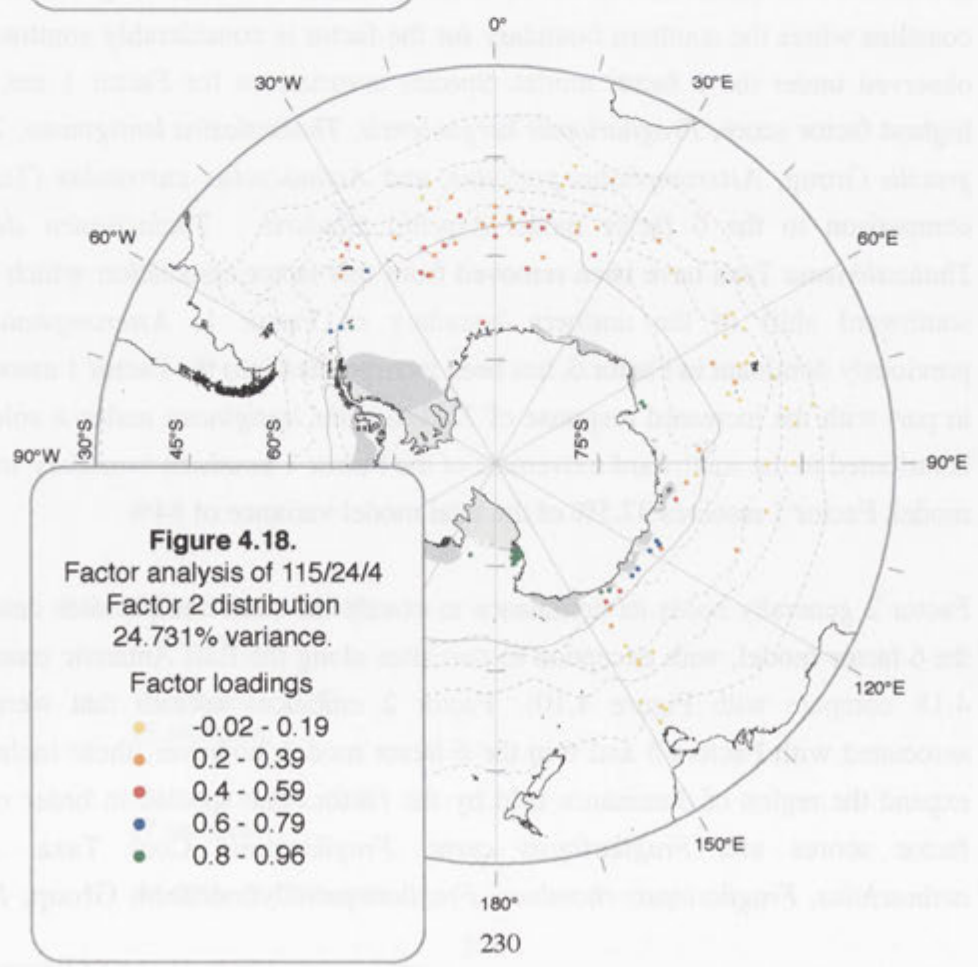

Figure 4.18.
Factor analysis of 115/24/4
Factor 2 distribution
24.731% variance.

Factor loadings

- -0.02 - 0.19
- 0.2 - 0.39
- 0.4 - 0.59
- 0.6 - 0.79
- 0.8 - 0.96

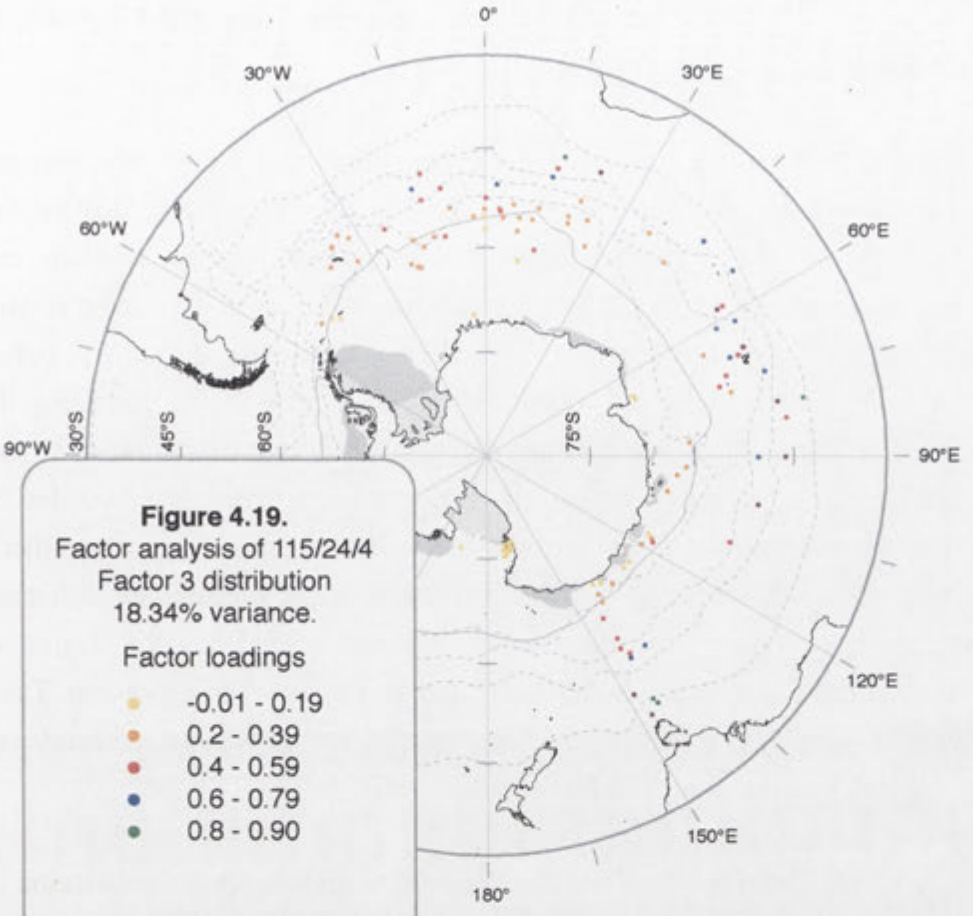

Figure 4.19.
Factor analysis of 115/24/4
Factor 3 distribution
18.34% variance.

Factor loadings

- -0.01 - 0.19
- 0.2 - 0.39
- 0.4 - 0.59
- 0.6 - 0.79
- 0.8 - 0.90

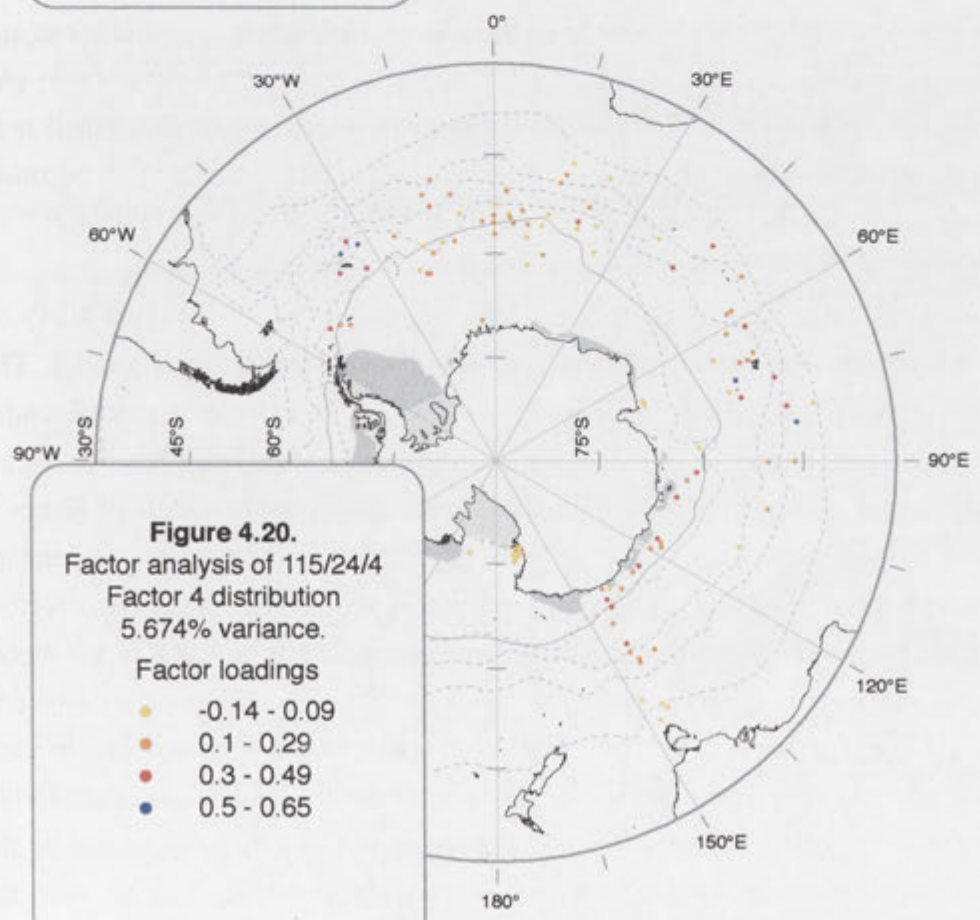

Figure 4.20.
Factor analysis of 115/24/4
Factor 4 distribution
5.674% variance.

Factor loadings

- -0.14 - 0.09
- 0.1 - 0.29
- 0.3 - 0.49
- 0.5 - 0.65

separanda, *Stellarima microtrias*, *Thalassiosira tumida*, *Porosira* Group and *Fragilariopsis pseudonana* (Table 4.2). The variance resolved under Factor 2 is 24.7%.

The strength of Factor 3 under a 4 factor model is considerably increased. The variance resolved increases from 18.3% from that of 5% under a 6 factor model. Most of this change in dominance can be attributed to the re-alignment of *Azpeitia tabularis* and *Thalassionema* Taxa under this factor. The geographic distribution of the factor is now found to have increased presence down to, and occasionally south of, the PF (when taking the 0.6 factor loading value as a boundary edge, Figure 4.19). Reducing the dominance to a 0.7 factor loading value in fact decreases the range of the factor to that north of the SAF in most sectors except the Indian Ocean sector where it is bounded by the PF. On the whole the highest factor loadings are found in the same most northerly sample sites of the study database as that found in the 6 factor model. The difference between the two models being the distribution of species and thus the degree of weighting. The species in order of factor score dominance are: *Thalassionema* Taxa, *Azpeitia tabularis*, *Roperia tesselata*, *Thalassiosira oestrupii* Group, *Hemidiscus cuneiformis*, *Fragilariopsis doliolus* and *Thalassiosira decipiens* (Table 4.2).

Finally, the fourth factor continues to be attributable to a "island/transport" distribution as resolved under the 6 factor model. The variance of the factor is increased to 5.7% and has the additional negative relationship input from the species *Fragilariopsis pseudonana* and *Fragilariopsis separanda*, which at least for the latter species was considered to be in part distributed by bottom water transport and the former species is in part distributed near South Georgia Island (Chapter 3). Positive relations for the factor continue to be made with the *Thalassiosira antarctica/scotia* Group and *Thalassiosira oliverana* (Table 4.2).

The summary distribution diagram of the four factor dominance regions (Figure 4.21) on the whole follow the previous distributions as noted under the 6 factor model. The departure of the two extra factors resolved in the 6 factor model are coalesced under Factor 1 in the 4 factor model. The final remaining difference between the two factor models is the greater resolution of Factor 3 in the 4 factor model due to a shift of Factor 1 to mid to cold water expression and Factor 3 to mid and warm-water temperature expressions with the shift of alliance in two key species that boarder these two factors (*Thalassionema* Taxa and *Azpeitia tabularis*). An interesting feature of the 4 factor model is the presence of several samples with very low dominance associations to any one factor. These 9 samples are indicated by small black spots on the Figure 4.21. In each case these samples have dominant factor loadings lower than 0.7 and are associated with the distribution of Factor 1 and Factor 3. Four samples are in fact jointly dominated by the two factors. Such a feature was not observed in the 6 factor model and as such the

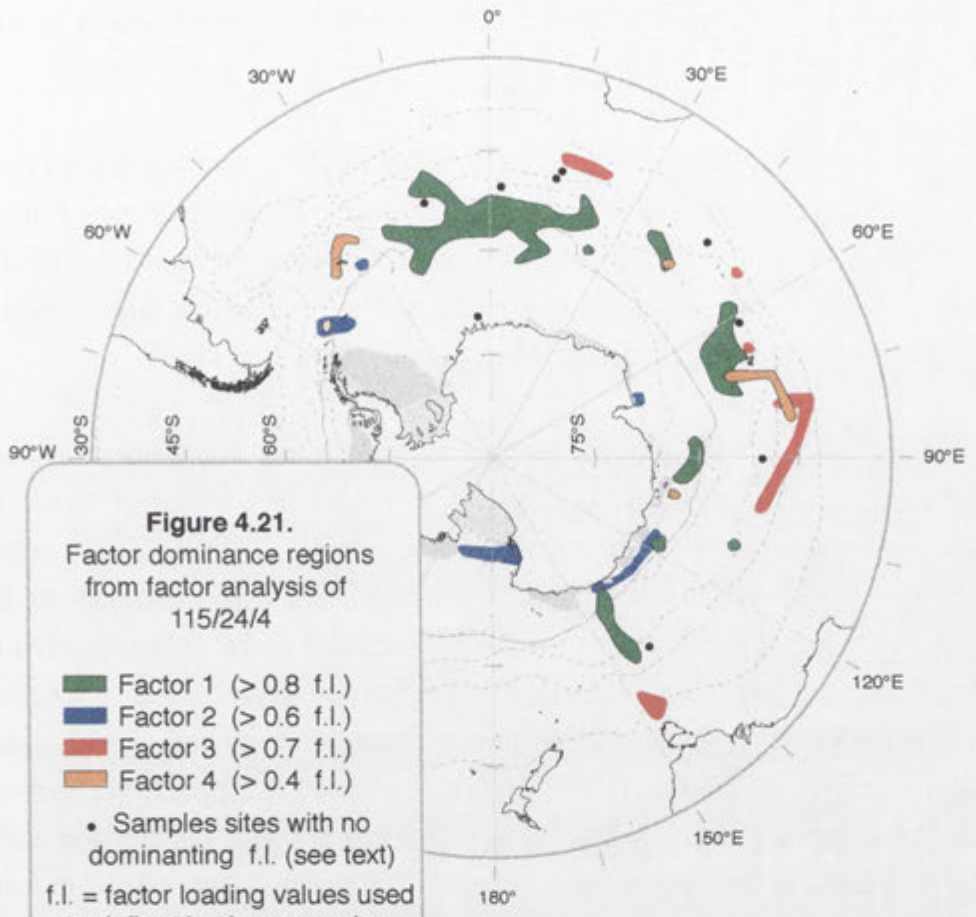

Figure 4.21.
Factor dominance regions from factor analysis of 115/24/4

- Factor 1 (> 0.8 f.l.)
- Factor 2 (> 0.6 f.l.)
- Factor 3 (> 0.7 f.l.)
- Factor 4 (> 0.4 f.l.)
- • Samples sites with no dominanting f.l. (see text)

f.l. = factor loading values used to define dominance regions

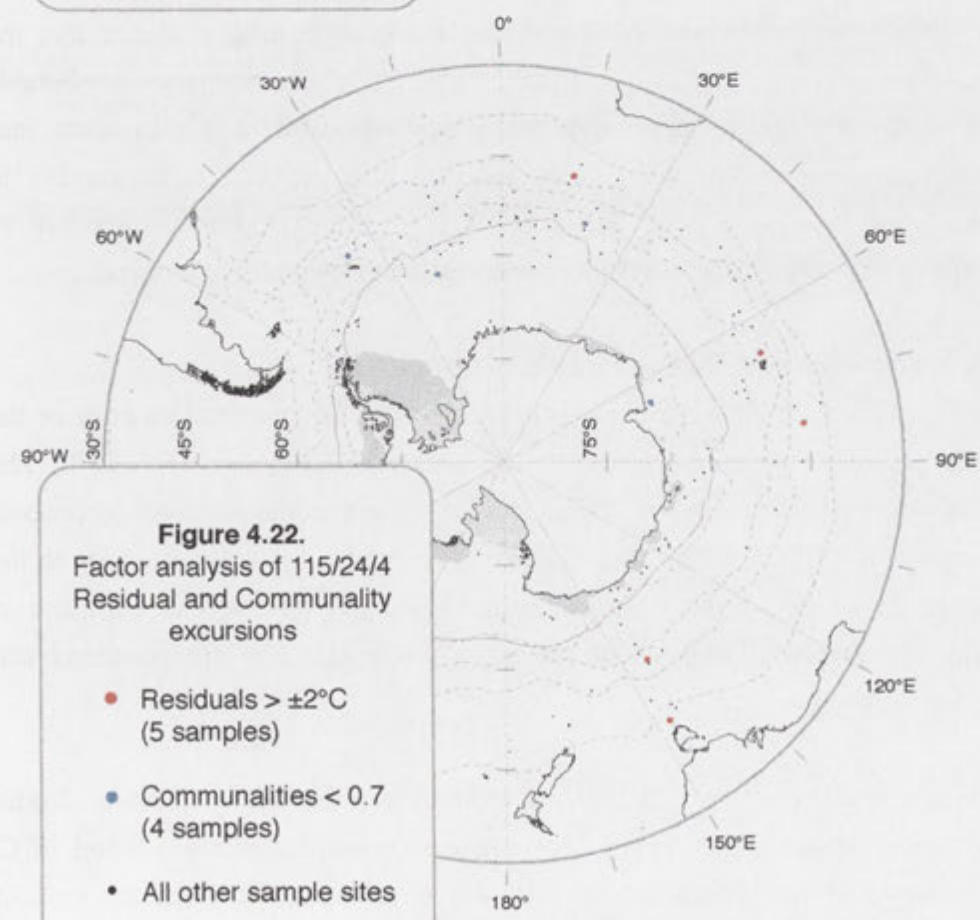

Figure 4.22.
Factor analysis of 115/24/4 Residual and Communality excursions

- • Residuals > ±2°C (5 samples)
- • Communalities < 0.7 (4 samples)
- • All other sample sites

decrease in total resolved variance between the two models is probably related to this feature.

The number of samples with residuals greater than ± 2°C and communalities greater than 0.7 are presented in Figure 4.22. The number of both excursions are decreased from those under a 6 factor model but reflect for the most part the same sample sites with the same problems. At no sample site is a low communality related to a large residual temperature, however, high residuals continue to be observed north of the PF.

Determining which of the two models is better in extracting the dispersion and differentiation of the system under study, simply comes down to a matter of choice in how one interprets the geographical distributions and species alliances. The 4 factor model is a simple model which allows the three major biogeographic zones to be recognised, and attributes a fourth factor to unique data included in the database which is linked to islands and transport. Should this simple approach be taken, it would practically be better to employ a 3 factor model that would then eliminate, through coalescence under the three major factors, the fourth factor. Yet, the analyses performed on species associations and geographical analysis indicate that a 6 factor model takes into account a better natural distribution of the species and one hope's the environmental effects in their distribution. The 6 factor model results when viewed in terms of the natural observed sedimentary distributions discussed in Chapter 3 provide supporting evidence that the model is able to decipher the variations in distribution. Five of the factors are attributable at face level to oceanographic zones, while a transport/island effect is also taken into account. Since all previous Antarctic diatom analyses have reduced factor models to decipher SST (Pichon *et al.* 1992a, Zielinski 1993), it was considered important to explore the just as relevant 6 factor model as an alternative to a simplified analysis.

4.3.4. Diagnostics of the DTF 115/24/6 model

The DTF 115/24/6 has a multiple correlation coefficient of 0.936 and standard error of the estimate (SEE) of 1.306 that is applicable over a February SST range of -1 to 14°C. The DTF does not correct for dissolution effects on the observed diatom thanatocoenose. Statistical output of the DTF115/24/6 are presented in Appendix 4.4 with exception to the vector score matrix which can be found in summarised in Table 4.2 or complete in Appendix 4.3. Geographical analysis of the factor loading results are presented and discussed in the previous section.

The summary diagnostic plots of DTF115/24/6 are presented in Figure 4.23A-F. Under the observed verses estimated plot (Fig. 4.23A) it can be noted that between 6 and 10°C, observed February SST predictions are considerably underestimated, while the bulk of the remaining estimates remain within the SEE of the DTF. The fitted plot (Fig. 4.23B) of

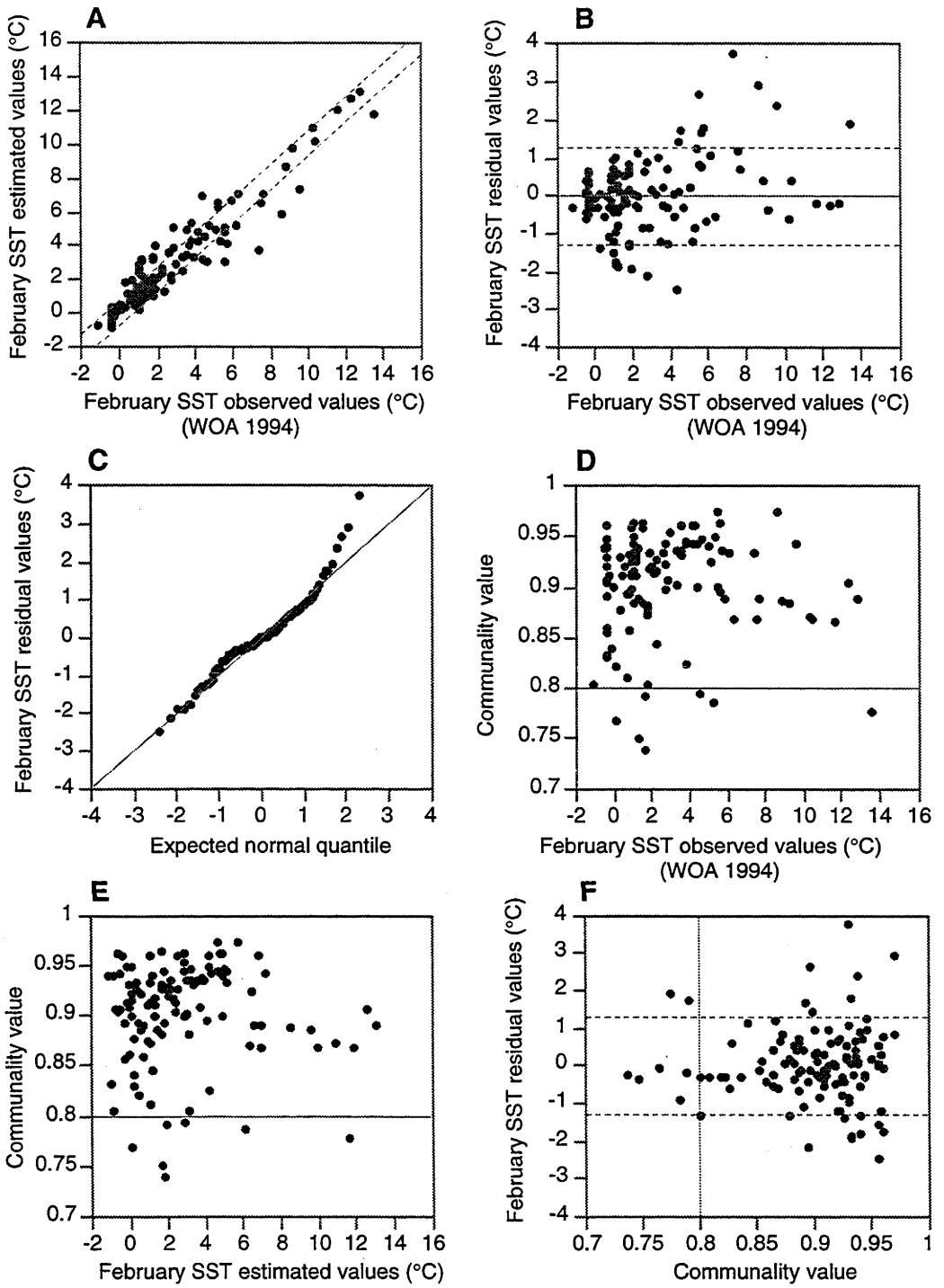

Figure 4.23. Summary diagnostic plots for February SST analysis of DTF 115/24/6. DTF has multiple correlation coefficient of 0.936 and standard error of the estimate (SEE) of ±1.306°C. Seven samples have communality values lower than 0.8. Diagnostic plots are discussed in the text. **A**= scatter plot of observed versus estimated values; **B**= fitted value plot (observed versus residuals); **C**= Normality plot (expected normal quantiles versus sorted residuals); **D**= observed SST versus communality values; **E**= estimated SST versus communality values; **F**= communality values versus residuals plot. Dashed line = SEE, full lines = communality value 0.8, except in figure B where it is the zero residual value, and in figure C where it is the 45°angle.

observed versus residuals highlights the large SST estimation departures not only in the 6-10°C range but also in the 0 to 4°C range. Within the 6-10°C range there are under-estimations and in the 0-4°C range over-estimations are evident. Constant variance is not achieved in the distribution of the residuals, suggesting transformation of the observed data by square roots is required. This was not undertaken in this work due to the need of more complex statistical analysis beyond the authors ability. However, the removal of samples with very large residual results is to be applied as a means of decreasing inaccuracy of estimation (implemented in the following section). The normality plot (Fig. 4.23C) indicates that reasonably good normality is found in the residuals of 115 data set. The under-estimation problem is evident as a departure from the 45° line through the positive residual range.

Distribution of communality values against observed February SST values indicates that a bias towards low communality occurs in samples between -1 and 6 °C, with lowest communality observed at 2°C (Fig.4.23D). One outlier low communality point is also evident at ~14°C. Generally, the communality values remain high and evenly distributed over the observed SST range, although this tendency weakens at the cooler SST range where preservational influences must be considered different. Comparison of communality values with the estimated February SST values indicate a slight decrease in communality values between 8 and 14°C, whereas higher communality values are reached in cooler SST estimates (Fig. 4.23E). Cooler SST estimates, however, continue to vary in range of communality. It is expected then from the results of this plot, that a core applied to this transfer function that was found to have low communality value assessment would in all probability have a cool SST estimation.

The final plot of communality values against residuals (Fig. 4.23F) illustrates the possible outliers of the model which fall exterior to the values contained by the >0.8 communality value and the SEE value. Here, as in the Pichon DTF analysis, the commonly accepted view and reliance on high residual values as an indicator of accurate SST estimation does not necessarily hold true. In fact the largest residual values are found with increasing communality values. Furthermore, the lower a communality value is the greater the chance that the residual is closer to zero, although it is obvious in this model that a certain bias towards over-estimation by less than 1°C is likely at the lower communality value (as also discussed for Figures 4.23D-E).

From these results it would appear that keeping samples with low communality would not change the estimation capabilities of the DTF whereas eliminating samples with excessive residuals would assist in improving the accuracy. For this reason samples with residuals greater than ±2°C are removed from the database, whereas those with low communalities

are withheld and the DTF is re-run. Table 4.3 lists the samples removed under this residual criteria.

4.3.5. Modified DTF109/24/6 and response

The diatom species data contained within the 109 samples continue to reflect the same maximum abundances as observed in the 115 database. Thus, no changes were required on the ranking formula of the data for use in the modified DTF (Table 3.10). The multiple correlation coefficient and SEE determined by the DTF109/24/6 are 0.961 and ±1.008

LKA code	Sample name	Latitude (°S)	Longitude	Depth (m)	Feb. SST Residual (°C)	Communality
4	1176-88	46°57.8'	14°18.2'E	5106	3.73863	0.933
95	KR8811	54°55'	144°04'E	2880	2.62559	0.899
154	KTB01	49°06'	67°01'E	1235	-2.49137	0.959
231	KR8802	45°45.2'	82°56.0'E	3480	2.88822	0.973
234	MD84-561	53°05.3'	71°36.4'E	1754	-2.16706	0.897
235	MD73-026	44°59.0'	53°17.0'E	3429	2.33648	0.941

Table 4.3. Samples with residual SST values >±2°C removed from further DTF analysis.

respectively. At face value these statistics are taken to indicate an improved model in contrast to the DTF115/24/6. Results of the DTF 109/24/6 are contained in Appendix 4.5.

Decreasing the database sample number also means the relationships observed under the DTF115/24/6 are not necessarily carried through to the same 6 factor and 24 species model. On inspection of the summary geographical factors distribution map (Figure 4.24a) it can be observed that zones of factor influence are modified when compared to the DTF 115/24/6 map (Figure 4.15). The differences amount to a shift in cover of Factor 3 slightly to the south, and reduction in cover for Factors 4, 5 and 6. Factor 1 replacing most of the cover of these latter factors. Factor 2 does not change its distribution dominance. The variances resolved for each of the factors are as follows; Factor 1 = 45.8%, Factor 2 = 27.3%, Factor 3 = 7.2%, Factor 4 = 3.4%, Factor 5 = 4.0% and Factor 6 = 2.2%. The reduction of the last three factors are evident. Factor 3 increases by just over a third its resolved variance from that of the DTF115/24/6 model. In part this is taken from the southward move and also from the loss of Factor 4 signal in the Indian sector.

Assessing the species alignment under factor analysis (Table 4.4) reveals that Factor 3 is weighted by the influence of *Azpeitia tabularis* and *Thalassionema* Taxa which were previously identified with Factor 1 in DTF115/24/6. This also reflects the trend observed under the 4 factor model for this particular Factor 3. The inclusion of these two species boosts the variance resolved and the region of dominance observed.

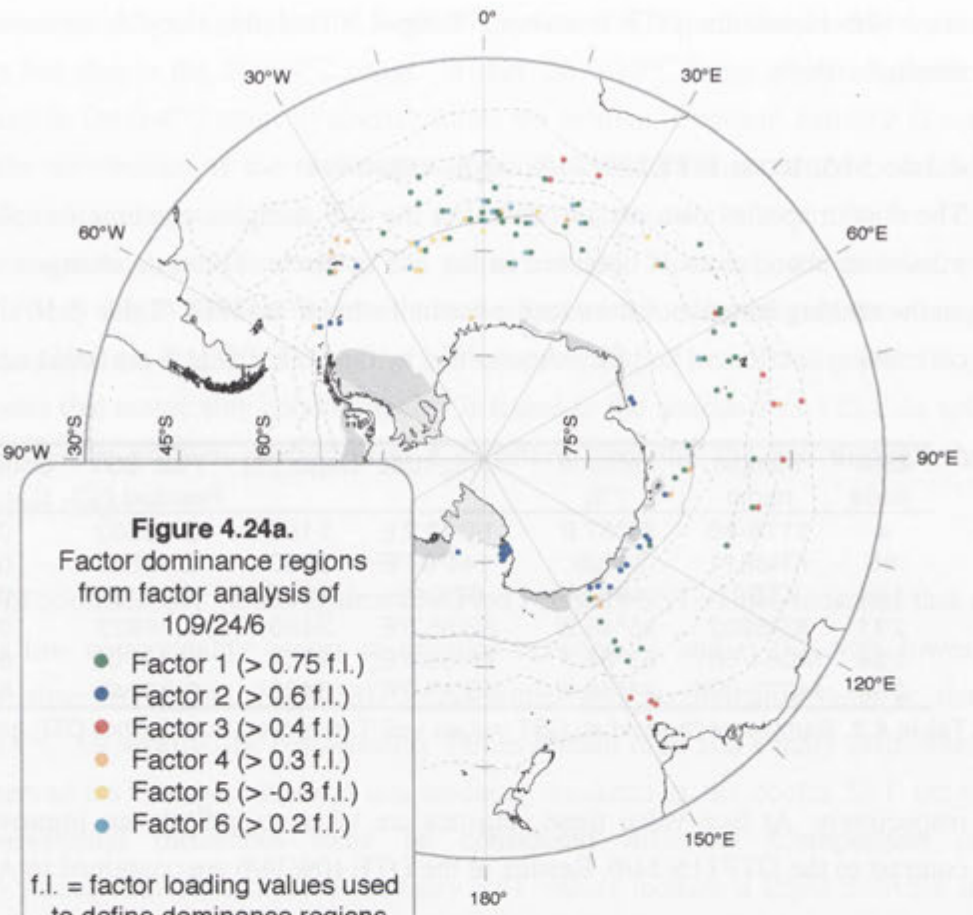

Figure 4.24a.
Factor dominance regions from factor analysis of 109/24/6

- Factor 1 (> 0.75 f.l.)
- Factor 2 (> 0.6 f.l.)
- Factor 3 (> 0.4 f.l.)
- Factor 4 (> 0.3 f.l.)
- Factor 5 (> -0.3 f.l.)
- Factor 6 (> 0.2 f.l.)

f.l. = factor loading values used to define dominance regions

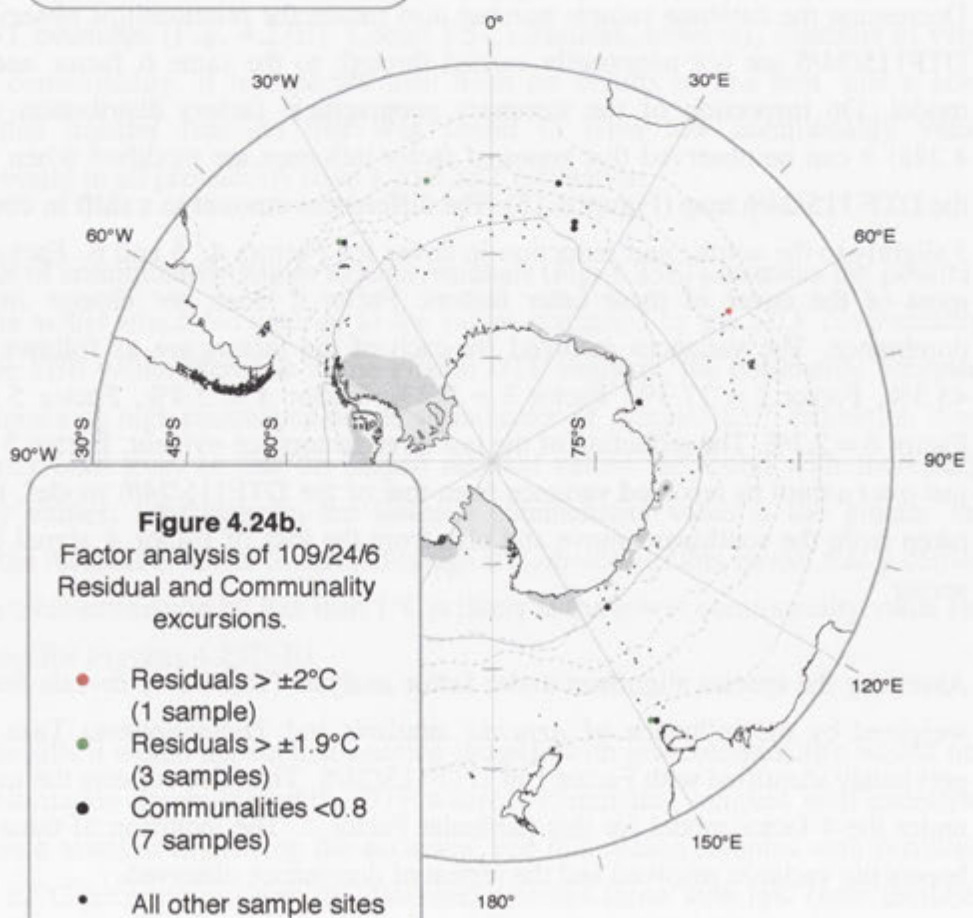

Figure 4.24b.
Factor analysis of 109/24/6 Residual and Communality excursions.

- Residuals > ±2°C (1 sample)
- Residuals > ±1.9°C (3 samples)
- Communalities <0.8 (7 samples)
- All other sample sites

Species	Factor 1	Factor 2	Factor 3	Factor 4	Factor 5	Factor 6
Actinocyclus actinochilus	-0.105	0.264	0.011	0.046	**-0.733**	-0.193
Actinocyclus curvatulus	0.027	-0.008	-0.009	-0.025	-0.005	**-0.043**
Asteromphalus parvulus	0.061	0.032	-0.041	-0.033	-0.126	**0.202**
Azpeitia tabularis	0.312	-0.080	**0.332**	-0.191	0.049	-0.252
Fragilariopsis curta	-0.089	**0.501**	0.033	-0.063	0.134	-0.035
Fragilariopsis Cylindriform Group	-0.066	**0.262**	0.051	-0.102	0.082	-0.115
Fragilariopsis doliolus	-0.039	0.005	**0.177**	-0.012	0.015	0.046
Fragilariopsis kerguelensis	**0.622**	0.016	0.133	0.024	-0.125	0.196
Fragilariopsis Cool Taxa	0.062	**0.453**	-0.082	-0.197	-0.185	0.085
Fragilariopsis pseudonana	0.015	0.024	-0.012	**-0.037**	0.018	-0.005
Fragilariopsis rhombica	-0.004	**0.232**	-0.008	0.036	0.087	-0.069
Fragilariopsis separanda	0.091	0.256	0.022	-0.076	0.339	**0.621**
Hemidiscus cuneiformis	-0.082	0.001	**0.337**	0.019	-0.006	0.096
Porosira Group	-0.032	**0.141**	0.020	0.018	0.097	-0.060
Roperia tesselata	-0.115	0.000	**0.503**	0.004	-0.028	0.123
Stellarima microtrias	-0.078	**0.185**	0.065	0.015	0.003	-0.052
Thalassionema Taxa	0.141	-0.016	0.382	-0.169	0.235	**-0.469**
Th. antarctica/scotia Group	-0.143	0.345	0.165	**0.494**	0.186	-0.136
Thalassiosira decipiens	0.037	0.002	0.037	-0.067	0.040	**-0.092**
Thalassiosira gracilis Group	**0.389**	0.263	-0.251	-0.279	0.161	-0.210
Thalassiosira lentiginosa	**0.413**	0.083	0.205	0.256	*-0.301*	0.141
Thalassiosira oestrupii Group	-0.072	-0.018	**0.344**	0.153	0.010	0.165
Thalassiosira oliverana	0.266	0.001	-0.226	**0.671**	0.171	-0.181
Thalassiosira tumida	-0.089	**0.166**	0.089	0.050	-0.005	-0.050

Table 4.4. Vector Factor Scores Matrix (VFSM) for the DTF109/24/6. Factor scores in bold indicate a species dominance under certain factors. Factor scores underlined indicate the greatest positive dominance of a species within a factor where a negative dominance is observed. High negative response under Factor 5 is italicised and commented in the text.

Species associated with Factor 1 in order of decreasing dominance are *Fragilariopsis kerguelensis*, *Thalassiosira lentiginosa*, and *Thalassiosira gracilis* Group, and *Actinocyclus curvatulus*. As just mentioned, the loss of *Azpeitia tabularis* and *Thalassionema* Taxa to Factor 3 has reduced the species number associated primarily with the factor. It should be pointed out that *Azpeitia tabularis* still contributes significant information to Factor 1 (Table 4.4, compare factor scores between factor 1 and 3 for the species), as does *Thalassiosira oliverana*.

Factor 2 is primarily associated with the same cold water species in the same order of dominance as under the DTF115/24/6 model. The exception to this being the inclusion of the secondary dominance of *Actinocyclus actinochilus* to the group. The Thalassiosira gracilis Group, the Thalassiosira antarctica/scotia Group, and Fragilariopsis separanda provide other sub-dominant but important contributions to this factor.

Species now associated with Factor 3 are, in order of decreasing factor score: *Roperia tesselata*, *Thalassionema* Taxa, *Thalassiosira oestrupii* Group, *Hemidiscus cuneformis*, and *Azpeitia tabularis*. *Thalassiosira lentiginosa* also plays a sub-dominant part in the resolution of this factor.

Factor 4 decreased variance by 1% but continues to represent samples surrounding South Georgia Island, samples along the East Antarctic coast and more discrepant samples in the open-ocean regions of the South Atlantic and Indian Oceans (Fig. 4.24a). The bottom water association east of Kerguelen Islands has been considerably reduced and in part this is due to the removal of three samples in this region (Table 4.3) and the re-organisation of the factor boundaries to compensate for this removal. Both *Thalassiosira oliverana* and *Thalassiosira antarctica/scotia* continue to dominate the species associations reflected by this factor.

A reduction of 1.4% resolved variance differs between this and the DTF115/24/6 model for Factor 5. Of greater change is the factor score and factor loading values which have become negatively dominated from positive associations in the DTF115/24/6 model (Table 4.4, Appendix 4.5). This feature aside, both *Actinocyclus actinochilus* and *Thalassiosira lentiginosa* remain dominant species components to the derivation of the factor, although the response from the latter species is reduced from that under the DTF115/24/6 model. *Fragilariopsis pseudonana* also remains related to this factor but in a positive rather than negative role. The range of geographical dominance is only slightly decreased in the South Atlantic sector of where it is best observed and associated with maximum winter sea-ice extent.

Factor 6 showed the largest decrease in resolved variance (3.4%) and geographical coverage from that of the DTF115/24/6 model. The species contributing to the signal of the factor continue to be the positive factor scores of *Asteromphalus parvulus* and *Fragilariopsis separanda* and the negative factor scores of *Thalassionema* Taxa and *Thalassiosira decipiens* (Table 4.4). The geographical dominance of the factor is lost from the South Indian sector and remains confined to the South Atlantic sector where the relation to the POOZ is better defined. This is in contrary to the factor loadings provided to samples (Appendix 4.5) that are very weakly expressed and generally over-ridden by Factor 1 signals.

The DTF109/24/6 continues to emulate the 6 factor model described by the complete ADB as described in section 4.3 3. However, the strength of the last three resolved factors is diminished in preference of the three major factors upon removal of 6 samples with large departures of SST estimation. Removing the samples with poor estimation capabilities from the ADB has not decreased the number of samples with poor communality value

associations but has decreased the number of samples which continue to estimate SST beyond an acceptable, but arbitrary, value of ±2°C (Figure 4.24b). Under the DTF109/24/6 only one sample in the SAZ of the Indian Ocean was found with a residual value greater than 2°C (KTB12 at 2.041°C, Appendix 4.5). Three other samples were noted with residuals greater than ±1.9°C, two of which are associated with low communality values (Fig. 4.24b).

Diagnostic plots of the model are presented in Figure 4.25A-F. The standard observed versus expected plot indicates the tighter fit of the data which generally remains within the standard error of the estimate (SEE= ±1.008°C) (Figure 4.25A). The fitted plot of residuals against observed SST shows better random distribution of the residuals, and thus a more constant variance (Fig. 4.25B). However, the trend for under-estimated SST in the 4-6°C temperature range continues to exist as does the over-estimation of SST in cooler temperatures (0-4°C). A single outlier to accurate warm-water estimation exists being derived from the sample south of Tasmania (Figure 4.24b) and at the extreme end of the temperature spectrum.

Normality in the residuals provided by the DTF109/24/6 are observed to follow the 45° angle reasonably well as in all other previous plots (Fig. 4.25C). Having eliminated the samples with large over- or under-estimations in the earlier model to that of this model has resulted in a more balanced sorted residual plot that still indicates tendencies for under-estimation in warm-waters and over-estimation in cooler waters. The latter feature being more pronounced in this model than in the previous one where under-estimation was a considerable problem (compare Fig.4.23C) in respect to all other estimations.

The distribution of communality values against both observed and estimated February SST values (Figures 4.25D and E) show no differences in relation than those provided under the DTF115/246 model. Poor communality (<0.8) remains linked to cold SST with exception to the extreme warm sample situated south of Tasmania. Highest communality is also achieved in samples experiencing temperatures less than 6°C.

The plot of communality values versus residuals in Figure 4.25F indicates a good spread of the data between the SEE of the model with smaller excursions exterior to these accuracy values. A greater proportion of residuals greater than the SEE are located in the positive residual range indicating greater under-estimation is more likely proposed in this model than that of over-estimation. Under-estimation does not show a trend for high or low communality values, yet over-estimation increases with increasing communality. Low communality values on the whole are associated with slight over-estimation between 0 and 1°C, with exception to the two samples noted in Figure 4.24b that had high residuals and low communality.

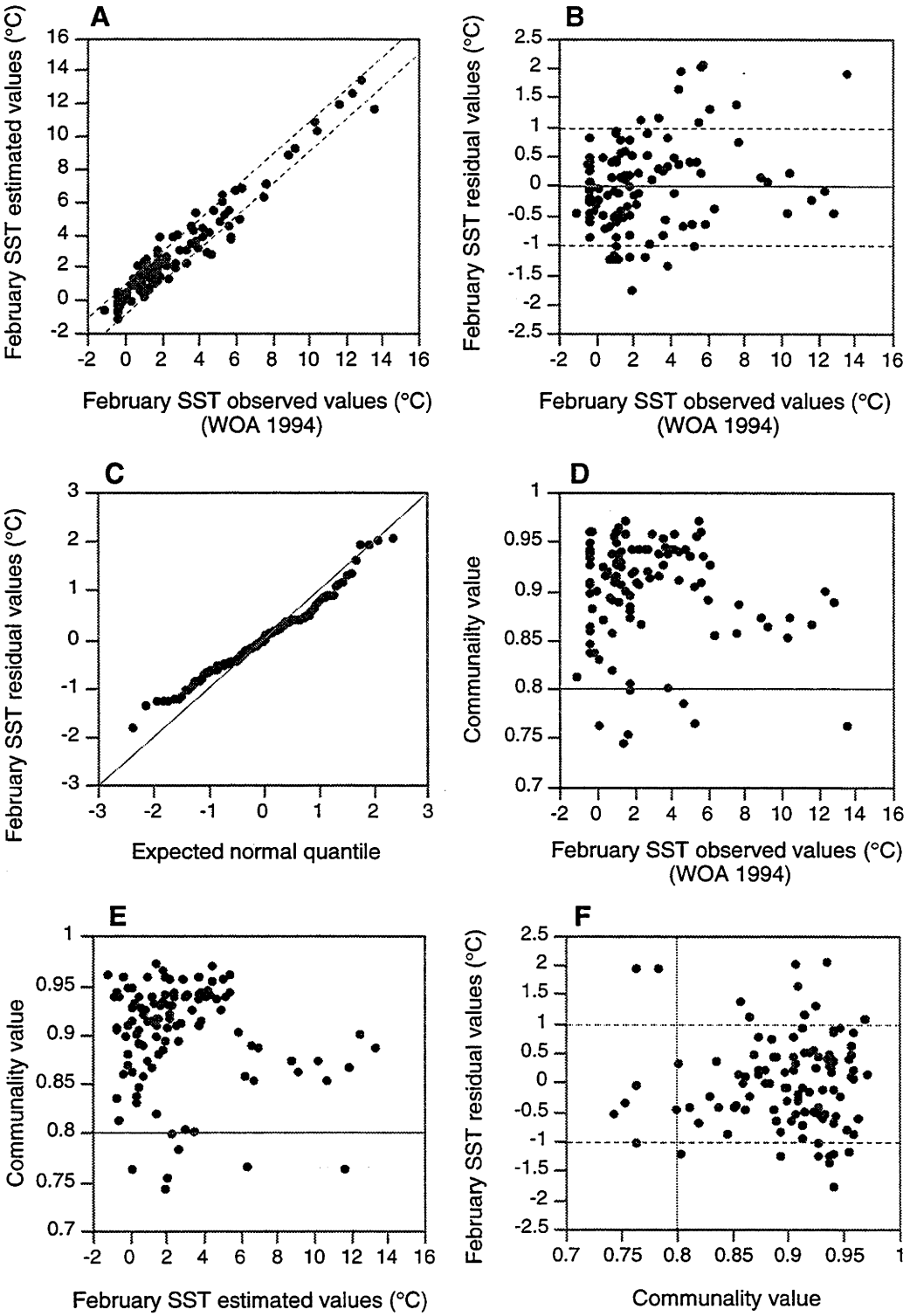

Figure 4.25. Summary diagnostic plots for February SST analysis of DTF 109/24/6. DTF has multiple correlation coefficient of 0.961 and standard error of the estimate (SEE) of ±1.008°C. Six samples have communality values lower than 0.8. Diagnostic plots are discussed in the text. **A**= scatter plot of observed versus estimated values; **B**= fitted value plot (observed versus residuals); **C**= Normality plot (expected normal quantiles versus sorted residuals); **D**= observed SST versus communality values; **E**= estimated SST versus communality values; **F**= communality values versus residuals plot. Dashed line = SEE, full lines = communality value 0.8, except in figure B where it is the zero residual value, and in figure C where it is the 45°angle.

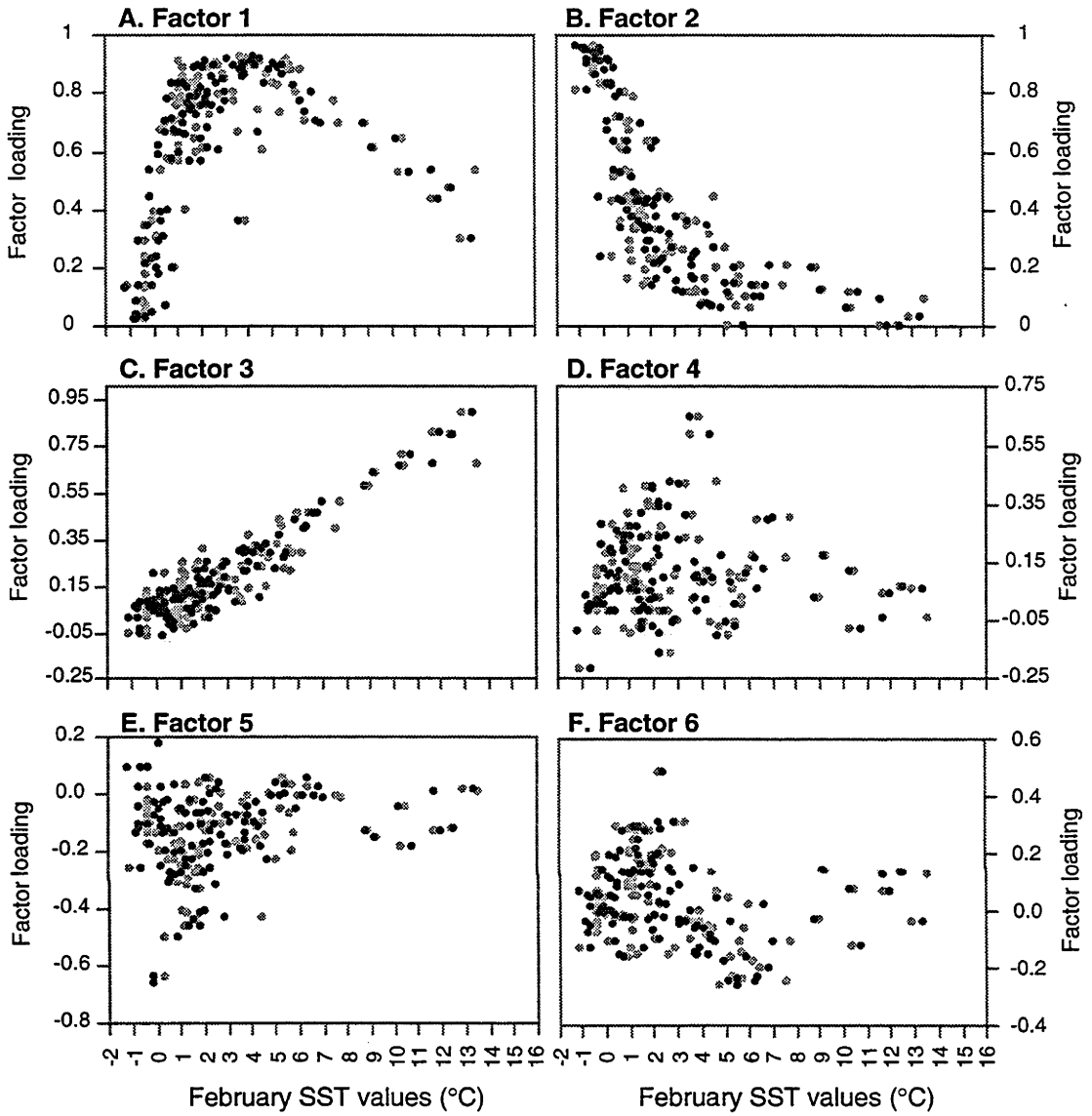

Figure 4.26. Factor loading plots of the six resloved factors against February SST (plots A-F). Light grey circles represent the relationship observed between the observed Feb. SST of WOA (1994), while dark grey circles represent the estimated Feb. SST values provided by the DTF109/24/6. Plots **A-C** show strong relations between factors 1 - 3 with Feb. SST. Factors 4-6 show poor relations with Feb. SST (plots **D-F**). The DTF 109/24/6 model appears to provide mirror-image estimations for Feb. SST with minor evidence of refining the the original responses as observed with the closeness of fit between observed and estimated SST and factor loading relations.

The diagnostic plots indicate that the model proposed by the DTF109/24/6 is effective within the following expectations. Primarily the model is able to provide estimations of February SST to within an accuracy of ±2°C. Slight over-estimation by 1.5°C being possible at cooler SST that are normally observed between 0° and 4°C, whereas greater under-estimation of SST estimates up to 2°C is possible in samples normally observed between 4° and 8°C and also at 14°C. Thus SST estimates which are provided between the range of 1°C and 6°C are likely to be subject to the greatest degree of inaccuracy of ±2°C. External to this range other SST estimates should be within the SEE of ±1°C. Normality and variance of the residuals reasonably follow normal expectations and constant variance respectively, however, latter feature requires further investigation. Communality values are a poor indicator of whether a sample will provide good or poor estimates, there is no reason why communality cut-off criteria should be employed in this model to reduce errors in estimation.

Finally, to establish the response of the 6 resolved factors to SST, the factor loading plots against observed and estimated February SST are presented in Figure 4.26A-F. Factors 1 to 3 are evidently related to SST (Figs. 4.26A-C). Factors 4 to 6 show much poorer relationships (Figs. 4.26D-F). For Factor 4, this was expected since the relationship between the geographical distribution and the factor dominance (Figures 4.12, 4.15, 4.20, 4.21, 4.24a) was considered related to islands and bottom water transport affects (Section 4.3.3.). Factor 5 now has in inverse relationship to that originally observed. The distribution of factor loadings remains randomly distributed with exception to a small peak in the -0.5° to 3°C range (using factor loading values greater than -0.3 as presented in Figure 4.24a). Since the geographical distribution is confined to a fine band in the South Atlantic sector which is best explained by the position of the maximum extent of the sea-ice edge, it is not surprising to find a relationship to SST albeit February. Highest factor loading values are referable to negative February SST values. If the SST values are converted to August SST the SST signature is that of freezing water and thus interpreted as the sea-ice edge (Figure 4.27).

Factor 6 also shows a very weak relationship to February SST (Figure 4.26F). Using the factor loading value of 0.2 as the defining value of dominance (Figure 4.24a) the range of February SST occurs between -0.5 and 3°C as observed in Factor 5. Contrary to Factor 5, Factor 6 by a single sample alone provides the signature of 2°C for the highest factor loading value. Other controls on the factor aside from SST are possible but have not been investigated in this work. The geographic distribution and species composition of the factor alone suggests that the factor is related at best to near sea-ice conditions during winter maximum in the South Atlantic sector.

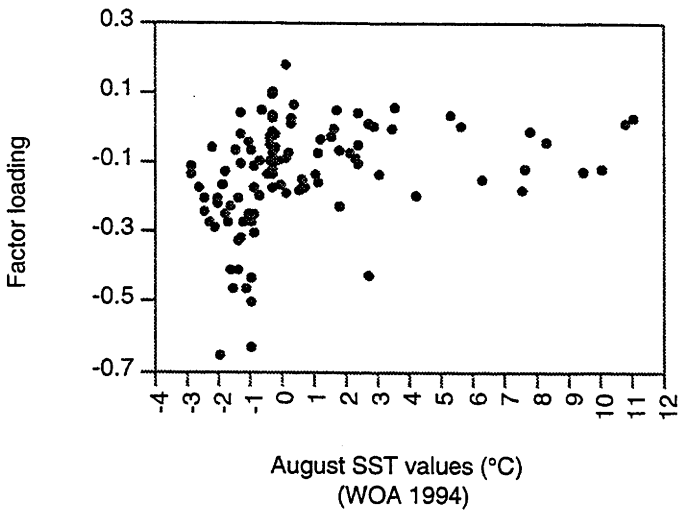

Figure 4.27. Distribution of Factor 5 factor loadings against August SST values from WOA (1994). Highest factor loadings are found to be associated with samples at super cooled temperatures representative of sea-ice edge SST's. Refer to introduction for summary on sea-ice for references.

In each of the factor loading plots presented in Figure 4.26A-F, the observed data (grey spots) relations have been overlain by the estimated SST values (black spots). The DTF model is able to emulate the observed data relations such that the original relationships observed between the WOA February SST values and the factor loadings are held. This feature indicates that little redefining of the relations observed have taken place to provide the desired estimations.

The DTF109/24/6 is the transfer function for February SST that will be used to determine SST using the ADB of this thesis. To compare the differences between this model and that of the currently used Pichon *et al.* (1992a) DTF166/34/6 the following section discusses the differences in the models and their expectations.

4.3.6 Comparison with original 166/34/4 DTF

There are both considerable differences and similarities between the re-run Pichon *et al.* (1992a) DTF166/34/4 model and that proposed from analysis of the same database in this work, DTF109/24/6 for estimating February SST.

The similarities that exist between the two models are generated from the major three factors that are determined from factor analysis of the respective databases. As mentioned in the determination of factor numbers to be resolved (section 4.3.1) a three factor model will derive the primary overlying divisions in species distribution in the Southern Ocean. The distribution of the major species in each of these factors are essentially the same in both models. Both models have similar multiple correlation coefficients (DTF166 = 0.966, DTF109 = 0.961) and standard errors of the estimate (DTF166 = ±1.083°C, DTF109 = ±1.008°C), although total variances resolved vary because of the number of factors resolved (DTF166 = 83.4%, DTF109 = 90.0%).

The differences in the models, therefore, are in part a process of increased factor number, but also referable to inclusion of dissolution data in one model and not the other, and the differences in defining species.

Differences in species and factor associations.

At the base of the differences are the changes in species identification definitions, and thus, respective ranking protocols. These differences have been discussed in detail in Chapters 2 and 3. Looking at the product of these discriminations after factor analysis is interesting in terms of the associations found with particular factors. A summary of the two models and their factor-species relations are presented in Table 4.5. Thirteen species are found to relate to the same main factors in both models (*Azpeitia tabularis, Hemidiscus cuneiformis, Fragilariopsis* Cylindriform Group, *Fragilariopsis curta, Fragilariopsis doliolus, Fragilariopsis kerguelensis, Fragilariopsis rhombica, Porosira* Group, *Roperia tesselata, Stellarima microtrias, Thalassiosira gracilis* Group, *Thalassiosira oestrupii* Group and *Thalassiosira tumida*). Several of these species underwent species redefinition and either include other similar species or restrict the species from a previously broadly applied definition (Chapter 2).

Ten taxa have been deleted from use in the DTF109/24/6 because of poor species definition, non-planktonic species, or relationships deemed inappropriate for analysis (Chapters 2 and 3) These taxa are *Chaetoceros* vegetative spp., *Cocconeis* spp., *Eucampia antarctica, Rhizosolenia styliformis, Odontella weissflogii, Thalassiosira trifulta, Thalassiosira lineata, Thalassiothrix* spp. *Dictyocha* and *Distephanus* spp.

The major discriminations between the two models for species factor associations are found with on two levels. Firstly there is the difference between the number of factors resolved. Increasing the factor number, as explored earlier, allows species to align to express themselves in more natural groupings. The DTF166/34/4 model thus, represents the minimal model identified as the 3 factor model. It allows for the major alliances to be

Species	DTF 166/34/4	DTF 109/24/4	Comments
Actinocyclus actinochilus	F2, 0.379	F5, -0.733	
A. curvatulus	-	F6, -0.043	new species included
Asteromphalus parvulus	F1, 0.176	F6, 0.202	species redefined
Azpeitia tabularis	F3, 0.411	F3, 0.332	
Chaetoceros veg. spp.	F1, 0.077	-	removed from analysis
Cocconeis spp.	F2, 0.203	-	removed from analysis
Dictyocha spp. ¥	F3, 0.344	-	removed from analysis
Distephanus spp. ¥	F1, 0.269	-	removed from analysis
Eucampia antarctica	F2, 0.242	-	removed from analysis
Fragilariopsis Cool Taxa	-	F2, 0.453	new species definition
F. curta	F2, 0.381	F2, 0.501	
F. cylindrus/ F. Cylindriform Gp.	F2, 0.242	F2, 0.262	species redefined
F. doliolus	F3, 0.134	F3, 0.177	
F. kerguelensis	F1, 0.427	F1, 0.622	
F. pseudonana	-	F4, -0.037	new species included
F. rhombica	F2, 0.215	F2, 0.232	
F. ritscheri	F3, 0.169	-	species redefined
F. separanda	F1, 0.227	F6, 0.621	
F. sublinearis	F2, 0.334	-	species redefined
Hemidiscus cuneiformis	F3, 0.284	F3, 0.337	
Odontella weissflogii	F2, 0.182	-	removed from analysis
P. glacialis / Porosira Gp.	F2, 0.231	F2, 0.141	species redefined
Rhizosolenia styliformis	F4, 0.318	-	species redefined
Roperia tesselata	F3, 0.345	F3, 0.503	
Stellarima microtrias	F2, 0.073	F2, 0.185	species redefined
T. nitzschioides/ Thalassionema Taxa	F3, 0.411	F6, -0.469 (F3, 0.382)	species redefined
T. antarctica (/scotia Gp.)	F2, 0.393	F4, 0.494	species redefined
Thalassiosira decipiens	F3, 0.055	F6, 0.092	
T. delicatulata	F3, 0.019	-	species redefined
T. gracilis (Gp.)	F1, 0.239, F2 & F4 0.236	F1, 0.389, F2, 0.263	species redefined
T. lentiginosa	F4, -0.520 (F3, 0.254)	F1, 0.413, (F5, -0.301)	
T. lineata	F3, 0.092	-	species redefined and removed from analysis
T. oestrupii (Gp.)	F3, 0.246	F3, 0.344	species redefined
T. oliverana	F1, 0.197	F4, 0.671	
T. trifulta	F1, 0.060	-	species redefined and removed from analysis
T. tumida	F2, 0.057	F2, 0.166	species redefined
Thalassiothrix spp.	F1, 0.566	-	species redefined and removed from analysis

Table 4.5. Species and dominant factor alliances between the two Diatom Transfer Function models. Changes that occurred between the original DTF166/34/4 and that of the DTF109/24/6 are listed under the comments column. F= factor, 1 to 6 = factor number. All other values are the corresponding factor score. ¥ = silicoflagellates. Discussion on differences and similarities are in the text. Supplementary close negative and positive factor scores are included where of interest. Data derived from tables 4.1 and 4.4. Discussion on individual species definitions given in Chapter 2.

identified but also "pushes" several species into factor associations that are not necessarily the optimum expression. There are five species that under the DTF109/24/6 model are found in much stronger association with increased factor number. These species are *Asteromphalus parvulus, Actinocyclus actinochilus, Thalassiosira oliverana, Thalassionema* Taxa, *Thalassiosira decipiens* and the *Thalassiosira antarctica/scotia* Group. Each of these species also do have some minor relation to one of the primary three factors under which they are aligned in the 3-factor model (see Table 4.4), but are expressed through greater factor scores in the additional three factors resolved in the 6 factor model.

On a second level, a few species are found to have factor associations to factors in complete contrast between the two models. Of interest here is the primary associations found in *Thalassiosira lentiginosa* and *Fragilariopsis separanda.* Under the DTF166/34/4 model *Thalassiosira lentiginosa* has the highest factor score association with the fourth resolved factor of dissolution, followed by Factor 3 representing the warm Subantarctic zone and then Factor 1 (Open-ocean) (Table 4.1). In the DTF109/24/6 *Thalassiosira lentiginosa* is found, under all tested variations in resolved factor number, to be primarily associated with Factor 1, and secondarily with Factor 5 at higher factor number resolution (section 4.3.2, Table 4.2). The variation between the two models for this diatom species is believed linked to the treatment afforded by the dissolution factor inclusion which introduces a bias through the increasing number of *Thalassiosira lentiginosa* specimens in the dissolved sample series. As mentioned in section 3B.2 both warm and cold water samples the dissolution data set over-estimated the presence of *Thalassiosira lentiginosa* when compared against the natural distribution of the species in the sediments. For this reason the difference between the factor associations of this species in the two models is not equivalent.

For *Fragilariopsis separanda* the difference between the two models is, at surface level, lacking relation. The DTF109/24/6 proposed here defines Factor 6 with the dominant representation of the species. In section 4.3.2, *Fragilariopsis separanda* was noted to have an unstable relationship to any one factor when factor number was increased. However, at no time did this species dominate in Factor 1 Open-ocean as is proposed by the DTF166/34/6 (Appendix 4.3, Table 4.1). The species distribution in the sediments indicates that the highest abundance of *Fragilariopsis separanda* is located around the Antarctic coast with a secondary distribution pattern found north of the maximum winter sea-ice extent (Chapter 3). The introduction of the dissolution data set had little effect on this species distribution in terms of providing a bias (Figure 3.45) which would have pushed the dominance to Factor 1 over Factor 2 (ice zone) in the DTF166/34/4 model. The hypothesis we are left with is that the secondary distribution pattern north of the maximum winter sea-ice edge contained the dominating association in the DTF166/34/4

for which the Factor 1 association is directed. The result then determined under the 6-factor model which proposes *Fragilariopsis separanda* dominance with Factor 6 (identified as the weak POOZ factor) also reflects this northerly distribution pattern. Other minor relationships with Factor 2 and 5 in the six factor model can thus be related to the primary distribution of the species around Antarctica and the possible role of transport by sea-ice rather than bottom water. *Fragilariopsis separanda* must be considered a species with a complex distribution in the sediments that is yet to be investigated thoroughly. The sedimentary distribution around Antarctica with lack of supporting evidence from sea-ice community analysis may also yet to prove that there is a winter and summer form of the species which provides a double distribution as already noted for *Thalassiosira gracilis.*

Differences in model output.

Results from the diagnostic analyses indicate that both models can provide adequate estimations from the palaeo-equations formed. In the DTF166/34/4 model there are several problems associated with the inclusion of the dissolution data set which include lack of constant variance, lack of normality in the residuals and a tendency for providing over-estimates of SST even though most estimates remain within the SEE. The incorporation of the warm-water dissolution series (sample KR8808) provides the main departure from natural expectations which biases the dissolution output in this case by under-estimating SST. Considerable streamlining by the palaeo-equation is made to incorporate the departures of the dissolution data in providing estimates. The natural data component of the DTF166/34/4 shows constant variance and strong normality. Under- and over-estimation of SST is equally possible through the SST range of 0° to 10°C. Communality values decrease with decreasing SST values, however, low communality does not imply poor estimation capabilities. It is more likely that a sample with high communality will have a large residual value than that of a low communality sample. There are many sample estimates that fall exterior to the SEE accuracy boundary. SST estimates can be in error by up to ±4°C throughout the 0° to 12°C SST range.

The DTF109/24/6 compiled in this thesis has considerably reduced sample numbers particularly in the northern and southern extremes of the study region, and dissolution data is not included, nor taken into account. A less convincing constant variance is found in the residuals than that of the DTF166/34/4 natural samples and transformation of data may be required, although there is a normal distribution of the residuals. The palaeo-model has a tendency for SST under-estimation particularly in the 4° to 8°C range and minor over-estimation between 0° to 4°C. Residuals are confined to ±2°C and are not overwhelmingly related to high or low communality values. Yet, the same trend of decreasing communality with decreasing SST is also observed in this model as in the DTF166/34/4. There are considerably fewer sample estimates which fall exterior to the SEE boundary in the DTF109/24/6 model. The palaeo-equation thus, reflects the

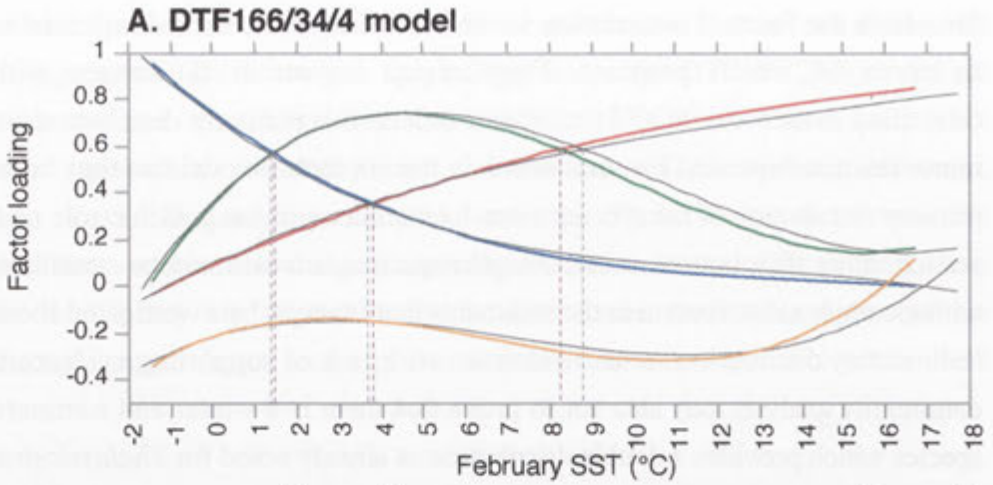

Factor 1observed: $y=0.001x^3 - 0.024x^2 + 0.180x + 0.364$, r = 0.695. expected: $y = 0.001x^3 - 0.027x^2 + 0.191x + 0.354$, r=0.709. Factor 2 obs.: $y = -0.000x^3 + 0.010x^2 - 0.134x + 0.731$, r = 0.835. exp.: $y = -0.000x^3 + 0.009x^2 - 0.132x + 0.744$, r = 0.865. Factor 3 obs.: $y = 0.000x^3 - 0.004x^2 + 0.083x + 0.095$, r = 0.908. exp.: $y = 0.000x^3 - 0.002x^2 + 0.079x + 0.088$, r=0.940. Factor 4 obs.: $y = 0.001x^3 - 0.012x^2 + 0.056x - 0.217$, r = 0.325. exp.: $y= 0.001x^3 - 0.014x^2 + 0.062x - 0.216$, r= 0.348.

Figure 4.28. Summary curves of factor loading influences provided by the two DTF models. **A** = DTF166/34/4 model, **B**= DTF 109/24/6. 3rd order polynomial curves are used to summarise the distribution of factor loadings in each factor (refer figures 4.4 and 4.26). Gray curves refer to the relationships formed with the observed WOA SST data while coloured curves show the relationships to estimated SST values provided by each model for each factor. Factors 1 to 3 are comparable between the two models whereas factors 4 to 6 are not. Interception points between the curves of factors 1 to 3 can be used as basic indicator boundaries between the various factors (dashed lines). Variations in the observed and estimated curves of each factor provide an indication of the adjustments made by the palaeo-equations and thus the biases in estimating SST. The greatest departure is observed under the DTF166/34/4 model for warm SST estimates which are up to 1°C less than the observed data. Refer to text for further discussion. Factor 1 = green, Factor 2 = dark blue, Factor 3 = red, Factor 4 = orange, Factor 5 = yellow, Factor 6 = light blue, estimated intercepts = violet. Curvilinear equations are listed below each figure.

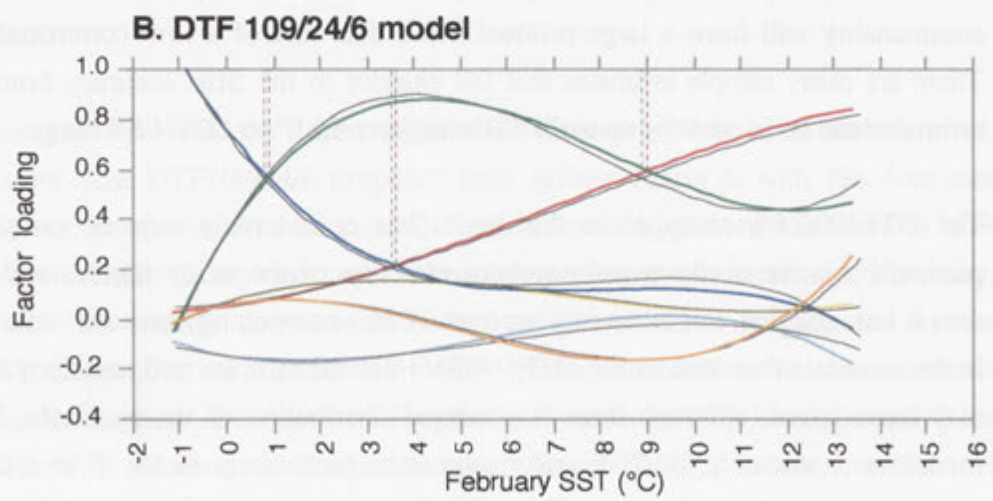

Factor 1 observed: $y = 0.002x^3 - 0.052x^2 + 0.310x + 0.349$, r = 0.865. expected: $y =0.002x^3 - 0.045x^2 + 0.283x + 0.348$, r = 0.863. Factor 2 obs.: $y = -0.002x^3 + 0.035x^2 - 0.261x + 0.751$, r= 0.884. exp.: $-0.001x^3 + 0.031x^2 - 0.248x + 0.761$, r = 0.902. Factor 3 obs. $y = -0.000x^3 + 0.0007x^2 + 0.019x + 0.063$, r = 0.927. exp.: $y = -0.000x^3 + 0.007x^2 + 0.026x + 0.053$, r = 0.953. Factor 4 obs.: $y = 0.000x^3 - 0.011x^2 + 0.060x + 0.068$, r = 0.302. exp.: $y = 0.001x^3 - 0.012x^2 + 0.059x + 0.069$, r = 0.303. Factor 5 obs.: $- 0.000x^3 - 0.009x^2 - 0.023x -0.146$, r = 0.248. exp.: $y = -0.001x^3 = 0.013x^2 - 0.035x - 0.145$, r = 0.305. Factor 6 obs.: $y = 0.001x^3 - 0.017x^2 + 0.041x + 0.055$, r= 0.453. exp.: $y = 0.001x^3 - 0.018x^2 + 0.038x + 0.061$, r = 0.454.

observed data relationships better with little streamlining or over-correction of the data as seen in the DTF166/34/4 model.

Summary plots of the models are presented in Figure 4.28, and indicate regions of factor influence and February SST representation. Differences between the models are best assessed by Factors 1 to 3 which the two models have in common. Comparisons of the curvilinear relationships of the observed and estimated data for each factor show the adjustments made by the palaeo-equation predictions. For the DTF166/34/4 model, there is a shift in the estimations of warm-water samples to around 5°C (ie. under-estimation). Less than 5°C estimations are only marginally over-estimated. These departures are best observed as fore-shortenings of the curvilinear response of the estimated values of each factor against that of the observed responses. Intersections of the three main factors, which are the boundaries to each factors influence, also provide some indication of the lagging or correction made by the palaeo-equation from the original relationships. The greatest departure from the original relationships are found between the intercept of factor 1 and 3, where a 0.5°C difference is observed.

The DTF109/24/6 model provides a good fit between the observed and estimated curvilinear responses of each factor. Slight fore-shortening of the estimated factor curves are observed and intersection points of the three major factors show little displacement. At each intersection, the displacement of estimates are directed towards over-estimation. The major estimation departures are observed under the warmer SST values. At face level, the DTF109/24/6 should provide more appropriate analogue SST estimates than that of the DTF166/34/4. Each model has it own weaknesses, and differences in the results provided by each model assist us in understanding the regions of higher or lower accuracy in estimation which may become crucial to interpretation of core data. Both models will be used to determine the SST records of the cores studied and presented in Chapter 6. The results from each model can then be assessed in terms of variation over time.

4.4. SUMMARY.

Constructing a new Diatom Transfer Function (DTF) for SST based on the Antarctic Diatom Database (ADB) derived from earlier chapters was pursued through the analysis of the number of factors resolved, species distributions in relation to the number of factors resolved, and the geographical distribution of two possible factor models. These two models, considered simplistic and advanced models (4 and 6 factors resolved respectively), indicated the dominance of 3 major biogeographic factors that had previously been identified in diatom transfer function work (Pichon 1985, Pichon *et al.* 1987, 1992a). Additional factors demonstrated that other regions of subdominance existed within the species distributions, two of these are related to, or near, the maximum

sea-ice edge in the South Atlantic sector, and the third to unique distributions in the study area considered as a transport/island component. Species versus factor number analyses indicated, that the over simplistic model could lead to mis-representations of the range of relationships acting on the natural diatom distributions. For this reason along with the suggestion by Le (1992) to increase the factor model size to obtain better results, the 6 factor model was decided over the 4 factor model for determination of February SST for the ADB.

The 6 factor model was tested through diagnostic analyses and plots. Samples with residuals greater than ±2°C were removed from the dataset to decrease error in estimation and the factor model was then re-run. Samples with low communality were not removed due to their lack of departures from the original observed SST value.

The concept that poor communality provides spurious estimates (Le 1992) is not supported in the models tested in this thesis. Low or poor communality is referable to the number of factors resolved by the model and thus, is also related to the ability of the model in covering the natural distribution of the species in the study region. As Le (1992) points out, a species with large factor score in a model with a large number of resolved factors will account for high abundances of that particular species in core-top or down-core assessment. In contrast, should the species not be accounted for in a simplified factor model because it no longer has its appropriate factor expression and is provided a lesser factor loading in another factor, it will not account for this species contribution in either core-top data sets or in down-core samples. This later scenario sets the scene for a non-analogue condition. Thus, down-core samples with high species representation run through a simplified model limiting a species most appropriate factor association will provide a low communality value to the sample in question. Such a scenario can be linked to less accurate estimation. In this case the lack of accuracy is derived from the simplicity of the model itself and provides the need for care and cut-off criteria for low communality values. Since the 6 factor model is expected to take into account the greater variation of the natural distribution, use of communality values as exclusion criteria to the model is not considered appropriate here and was not pursued.

As a comparison to the model derived from the ADB of this thesis, the original Pichon *et al.* (1992a) DTF166/34/4 was re-run and updated replacing the dated Levitus Summer SST data originally applied with the February SST of WOA (1994). Diagnostics revealed that the inclusion of the Dissolution data set was not continuous with the Natural data set. The Dissolution data set was observed to poorly emulate relationships found in the warm-waters. Estimates were noted to be tuned to open-ocean responses between the 4 and 11°C range, and tied into the observations of high residuals between the PF and STC. The inappropriate inclusion in the DTF166/34/4 of the warm-water dissolution sample

KR8808, previously identified on the grounds of location and diatom assemblage characteristics, was thus found to lead to erroneous SST estimation. Consequently forcing the model into a more streamlined palaeo-equation to take into account the dissolution sample departures. A large number of samples were observed to have low communalities and large residuals. None of these samples were removed from the analyses in line with the original construction of the model, although the model could have been improved with criteria used to eliminate major outliers.

The main differences between the DTF166/34/4 and the DTF 109/24/6 of this thesis are related to the number of factors resolved, the inclusion of dissolution data and the differences in the species identified. The latter feature was discussed in detail in Chapters 2 and 3. In terms of the models output, the DTF166/34/4 will provide estimates that can be in error by up to ±4°C though the 0 to 12°C range, most of the abnormalities being referable to the inclusion of the warm-water dissolution samples. The DTF109/24/6 under-estimates in the 4 to 8°C range and over-estimates in the 0 to 4°C range, but in each case the residuals are confined to within ±2°C. The model does not take into account dissolution of the diatoms in the samples, but does increase the number of factors to account for wider distributional patterns.

The trend of decreasing communality values with decreasing SST observed in both models assessed here may indicate other agents at play than just the number of factors resolved and environmental realms covered. The relationship of communality to perhaps the degree of dissolution of a thanatocoenose may be a relationship worth considering in future research.

At face level, the DTF109/24/6 should provide more appropriate analogue SST estimates than that of the DTF166/34/4. The determination of opal dissolution of samples derived from Factor 4 loadings (Pichon *et al.* 1992b) could not be reproduced entirely and thus was abandoned for the time being.

This page left intentionally blank.

Chapter 5

Sea-ice model.

5.1 INTRODUCTION

Increasing emphasis is being placed on the predictive capabilities diatoms may bear in estimating Antarctic sea-ice, one of the most important modulators of Southern Hemisphere climate. Modern sea-ice and marginal ice-edge diatom communities have received increased attention, and have revealed that certain diatoms are more closely related to these environments than other species (eg. Garrison *et al.* 1987, Garrison and Buck 1989, Fryxell 1989, Kang and Fryxell 1991, 1992, Scott *et al.* 1994). Satellite sensing has assisted in assigning the importance of the marginal sea-ice edge to elevated regions of phytoplankton and diatom productivity (Comiso *et al.* 1990, Sullivan *et al.* 1988), which in turn appears referable to the thinness and stability of the mixed surface layer among other factors (Priddle *et al.* 1992, Tréguer and Jacques 1992).

Advances in modern sea-ice observations from satellites, and in understanding the role sea-ice plays in diatom ecology, provide the opportunity to use fossil diatoms to make quantitative and systematic palaeo-sea-ice estimates in much the same way as that currently employed for SST estimates.

Past sea-ice estimation in the Southern Ocean has largely been extrapolated from lithological boundaries, ice rafted-debris records, and faunal changes from deep-sea cores (CLIMAP 1976, 1981, 1984; Hays *et al.* 1976; DeFelice 1979; Cooke *et al.* 1977; Hays 1978; DeFelice and Wise 1981; Cooke and Hays 1982; Burckle *et al.* 1982; Burckle 1984; Burckle and Cirilli 1987). These studies eventuated the view that the southern boundary of the diatomaceous ooze was related to the Spring limit of sea-ice-cover (Burckle *et al.* 1982; Burckle 1984; Burckle and Cirilli 1987), which was later defined as the region of ocean with greater than 65% sea-ice cover in November (Crowley and Parkinson 1988a).

Occasionally studies directed towards diatom distributions at the water surface or in the sediments, identified possible northern or southern most extents of the modern sea-ice (eg Burckle *et al.* 1987; Leventer and Dunbar 1988; Leventer 1992, Jordan and Pudsey 1992). However, little use of diatom species in the sediments have been applied to assess the position of the sea-ice. The exception being the application of relative abundance information of *Eucampia antarctica* (Burckle and Burak 1988) which was later noted to have contrasting records north and south of the PF (Burckle and Abrams 1986). Fryxell and Prasad (1990) solved the answer to this problem with the identification of two

variations in the species (refer to section 2.3.5). The ratio of the polar and subpolar variations of the species was then used to define the northern limit of winter sea-ice (Kaczmarska *et al.* 1993).

Pichon (1985) first indicated that the transfer function may be a tool useful for monthly sea-ice estimation. Zielinski (1993) argued that an annual sea-ice signal could not be drawn from cores because the signal from sea-ice diatoms can only be formed after the melting of the sea-ice in summer. Thus, he concluded that cores can only indicate the frequency of cover in an area rather than degree of yearly extension.

This thesis explores the sea-ice estimation concept further in order to bring the estimation possibilities and capabilities in line with modern advances in sea-ice monitoring and slightly better understood diatom relationships to sea-ice cover.

5.1.1. Satellite sea-ice monitoring.

Sea-ice on the world's polar oceans has only, in the last 25 years, truly been observed and studied in detail through the advance of satellite sensors targeted to record the radiation emitted from the ocean and sea-ice. Prior to satellite derived knowledge, historical records were at best taken from ship travel encountering sea-ice boundaries (Jacka 1983), or by high latitude island studies of the seasonal sea-ice (eg. Budd 1975). Such disparate records made large assumptions on the characteristics of Antarctic sea-ice and its relationship to the physical environment (Ackley, 1981). The first real records of sea-ice extent, character and seasonality came from the Electrically Scanning Microwave Radiometer (ESMR) which functioned between 1972 and 1976. This instrument was then replaced by the Scanning Multichannel Microwave Radiometer (SMMR) from 1978 to 1987, after which the Special Sensor Microwave/Imager (SSM/I) (1987-) was emplaced to receive reflected radiation from the Earth's surface. Results compiled over 13 years from the later two instruments are used as the sea-ice data set in this thesis (Schweitzer 1995). The use of sea-ice concentration, the percentage of sea-ice cover versus open-ocean cover in a certain area, and the amount of sea-ice cover in months per year are the data used for relation with diatom distribution in the sediments in this thesis. The data extracted from the Schweitzer (1995) sea-ice compilation for each sample of the ADB are found in Appendix 4.1.

A brief summary of the data used and the assumptions behind the use of the sea-ice data are detailed below.

5.1.2. Analysis of extent and concentration.

Introduction and Primary Derivations:

Sea-ice concentration is determined from the contrasting brightness temperatures used to define polarisation and spectral gradient ratios emitted from sea-ice and the open-ocean. There is a strong contrast between the sea-ice and the open-ocean in their emissivities, and it was from this discovery that the role of passive satellite microwave imagery was realised. Extensive examinations of sea-ice algorithms and filters can be found in Gloersen and Cavalieri (1986), Gloersen *et al.* (1992), and Steffen *et al.* (1992). Comiso *et al.* (1992) reviews the methods, progress and future work for Southern Ocean microwave remote sensing, and the edited book by Carsey (1992) provides a recent analysis of information pertaining to the remote sensing of sea-ice and its associated problems. Detailed analysis of the NASA algorithm, the interpretation of incoming emissions and corrections for weather affects are not dealt with in this work and can be found in the works listed above. Use of the accumulated sea-ice concentration data, assumptions pertaining to its utilisation and definitions of sea-ice extent are, however, covered in the subsequent sub-sections.

CONCENTRATION:

Sea-ice concentration is the percentage of a given area of ocean that is covered by sea-ice; it represents the amount of sea-ice versus open water (Zwally *et al.* 1983b; Gloersen *et al.* 1992). Sea-ice concentration is increased either from convergence of the ice pack or through the growth of more ice, whereas decreases in concentration are produced by divergences in the ice field by leads and polynyas, or the decay of ice (Zwally *et al.* 1983b).

The zone of partial sea-ice cover is defined as the marginal ice zone (Comiso and Zwally 1984b) or outer zone (Comiso *et al.* 1992) and also in this work as the pack-ice zone. It defines the region of new and young ice floes separated by nilas, frazil or open water that is subject to the effects of waves, winds and currents. Whereas the inner zone (or fast-ice zone in this work) consists of thicker consolidated sea-ice that is interrupted in its extent by leads and polynyas, and is frequently covered by snow. The more stable inner zone thus provides more consistent radiation and emissivity signal.

EXTENT:

Workers generally define a minimum sea-ice concentration for the sea-ice boundary/extent. This can vary from 8% (Comiso and Sullivan 1986) through 12-15% (Zwally *et al.* 1983a; Zwally *et al.* 1983b; Comiso and Zwally 1984b; Gloersen and Campbell 1991; Cavalieri *et al.* 1995] to 30% (Parkinson 1992) depending on the data sets used (ESMR, SMMR, SSM/I), the use of various filters (weather filter Gloersen and Cavalieri 1986; Gloersen *et al.* 1992), weather and atmospheric water filters (Cavalieri *et al.* 1995) and the correlation to in situ measurements. These will be addressed in Section

5.1.3. Use of the SMMR data with in situ studies suggests that the outer ice edge can be located using the 30% isopleth and the compact ice edge at 40-50%, whereas using the SSM/I this is achieved at the 15% isopleth and 40% respectively (Gloersen *et al.* 1992).

VALIDATION STUDIES:

Validation of the sea-ice edge and also the degree of sea-ice concentration derived from satellite instruments to those made by researchers at the sea-ice edge or within sea-ice vary. The initial sea-ice edge validation in the Weddell Sea sector suggested that the information received by the 18 GHz sensor provided the best estimate of the sea-ice edge even though the satellite resolution was large (Comiso *et al.* 1984a). Further attempts at in situ sea-ice edge validation by Comiso and Sullivan (1986), lacked the appropriate comparative in situ data to support their argument of an ice edge defined by the 8% concentration boundary. The only other documented error estimation for calculated sea-ice extent from the SMMR, was extracted from variations of a model seasonal extent and that of the calculated daily observed extent. This work provided a standard deviation of 0.13×10^6 km^2 for the Antarctic, translating to an error of 0.7% during the maximum ice extent and 3.5% during the minimum ice extent (Gloersen *et al.* 1992). But this does not explain possible errors in estimating the real sea-ice edge.

In general, the ice extent is limited by a concentration intercept (Comiso and Sullivan 1986), but confidence in this intercept is decreased during spring melt back conditions. Further validation studies are required, but the biggest problem in assessing such correspondence in the real and satellite sea-ice edges are due to the large resolution of the 18 and 37 GHz frequencies which require large regions of the sea-ice edge to be assessed by ship or helicopter in producing meaningful correlations. Therefore, it will be difficult to place importance on the position of the real sea-ice edge in work conducted in this thesis.

In contrast to sea-ice extent, sea-ice concentration validation studies are greater in number. In the Weddell Sea, the comparisons between SMMR and in situ ice concentrations, revealed in situ measurements with greater concentrations than that of the SMMR (Comiso and Sullivan 1986). The standard error between the estimates was 13%. Part of this discrepancy (up to 10%) was attributed to human errors in estimating sea-ice concentration.

Elementary work in the Prydz Bay region over spring 1982-83 (Streten and Pike 1984) suggested that satellite estimates overestimated concentrations both at high and low level, and more importantly, however, that estimates at the lower concentrations (0-20%) were not distinguished correctly by satellite means.

Comparative measurements of in situ and SSM/I sea-ice concentration during October-December 1988 along East Antarctica (Allison *et al.* 1993), concluded that under high concentrations (>75%), the SSM/I instrument under-estimated the in situ sea-ice concentration by up to 20%. In contrast, at lower concentrations (< 30 %) the SSM/I estimates of sea-ice concentration were higher than those of the in situ measurements. Between these maxima and minima, the two results were in closer agreement and, overall, there is a mean difference of 3.3% ±14.2%. This value is similar to those observed in the Weddell Sea reported above. The reason provided for the under-estimated higher concentrations by the SSM/I and NASA TEAM algorithm relates to the loss of information from very thin ice which resembles the open-ocean in its signature.

Most studies indicate that sea-ice concentration is more accurate in regions of consolidated sea-ice such as the inner zone, but in the outer or marginal sea-ice zone there is much less corroboration with an under-estimation of up to 20% (Allison *et al.* 1993; Sullivan *et al.* 1988). Such an error in determining the sea-ice concentration in this region where sea-ice concentration is believed to range between the concentration intercept sea-ice edge at 15% and the consolidated ice of the inner zone at approximately 40% concentration, requires some caution for interpretation of past estimates of the sea-ice that fall within this range.

5.1.3. Other problems associated with determining sea-ice concentration and the sea-ice edge.

Specific errors in the various instruments and the determination of the emissivity and brightness temperatures are addressed in detail elsewhere (Zwally *et al.* 1983b; Cavalieri *et al.* 1984; Gloersen *et al.* 1992). Here we concentrate on problems in reference to errors which are likely to bias the estimations determined in the work presented in the reconstruction of past sea-ice concentrations. More detail of such features can be found in Tucker *et al.* (1992).

Sea-ice concentrations derived during spring (when there is rapid decay of the sea-ice) and autumn (when ice is advancing) are liable to errors from the monthly averaging as a result of the variability of the ice extent in these periods. Thus, the concentration gradients are not as sharp as in winter and summer. Furthermore, in spring, increases in sea-ice emissivity as a response to the melting sea-ice and snow, make it difficult to determine the true ice concentration (Comiso and Sullivan 1986; Gloersen *et al.* 1992). Errors of up to 20% in sea-ice concentration are estimated as result of this increasing emissivity (Zwally *et al.* 1983b; Comiso *et al.* 1984a). It is for this reason that the modelling of the sea-ice in these transitional periods was not pursued.

The sea-ice edge itself is also prone to difficulties in definition. Thin, new and young ice types are difficult to determine from the open-ocean signal (Zwally *et al.* 1983b, Gloersen *et al.* 1992, Allison *et al.* 1993), but also physical effects such as flooding of the ice, roughness, and varying thickness will alter the signal recorded (Zwally *et al.* 1983b; Comiso *et al.* 1984a; Cavalieri 1992, Eppler *et al.* 1992). New satellite instruments such as RADARSAT-SAR, however, are attempting to define these thinner ice types between 5 and 20 cm thickness (Zabel *et al.* 1996). In addition, there are also problems in determining the ice-concentrations from the coasts due to satellite footprints of the two sensors at different resolutions, and the dynamic variation of the coastline especially in summer in comparison to the land mask used (Jacobs and Comiso 1989; Parkinson 1992; Gloersen *et al.* 1992). This particular problem should not hinder the study in this work as most of the data retrieved in correlation to the sea cores are removed from the coastline.

Other more significant errors in deriving sea-ice concentrations have come from the inclusion of weather effects within the algorithms. The most important of these are the surface winds and water vapour of cloud cover (Cavalieri *et al.* 1984; Gloersen and Cavalieri 1986). The wind was found to affect the signal received by the 18 GHz sensor, because of the roughening of the ocean surface. Thus, an ice concentration error of 16% was produced for a wind change of 6 ms^{-1}. Water vapour in the atmosphere increases the emissivity received in particularly by the 37 GHz sensor such that an increase of 8% ice concentration is provided for each increase of 0.04 cm in cloud water vapour. To counter these and other weather effects, Gloersen and Cavalieri (1986) constructed a weather filter which eliminates conditions produced by weather effects which affect the gradient ratios recorded by the sensors. The filter set at the spectral gradient ration value of 0.08, or alternatively sea-ice concentrations less than 12%, is employed to select NASA algorithm derived sea-ice concentrations that are indeterminable from weather effects thus, defaulting these values to the open-ocean condition. Later work (Gloersen and Cavalieri 1986) suggested that the 12% concentration should be increased to 15% for the definition of the sea-ice edge. The weather filters designed for the SSM/I instrument also use the 15% ice concentration as the sea-ice edge location (Cavalieri *et al.* 1995). In reference to work presented in this thesis, the sea-ice concentration of 15% is used to demarcate the ice edge, values less than 15% are not considered to represent sea-ice.

5.1.4. SEA-ICE DATA USED IN THIS STUDY.

Data from SMMR and SSM/I instruments exclusively, are used in this study because of the difference between the accuracies of sea-ice concentration produced by the multi-spectral, dual-polarisation instruments rather than the single wavelength measurements of the ESMR. These differences result in the various ice types (first-year and multiyear ice) being identified and compared with the open-ocean whereas the ESMR data could only

provide a linear extrapolation between fully consolidated sea-ice and open-ocean (Cavalieri *et al.* 1984). Ambiguity also exists between the ESMR data set and the newer SMMR and SSM/I data sets because no overlap period was obtained from which a calibration could be determined (Parkinson 1992).

A 13.25 year series (1978-1991) of monthly sea-ice concentration averages (Schweitzer 1995) is employed as the data set of sea-ice concentrations, as well as to determine annual duration of sea-ice at the specified locations for all the core top samples. The monthly averaged sea-ice data set contains information derived from the SMMR and SSM/I instruments and allows the user to specify the locations of retrieval. The data for the Antarctic region uses the 'Total sea-ice NASA TEAM algorithm' to compile the information of the CD data set (pers. comm P. Schweitzer, 1996). This algorithm calculates the concentration of two sea-ice types, firstly those which conform to the first year ice (Type A), and subsequently ice which conforms to sea-ice with deeper snow or possible multiyear ice (Type B). However, these results of the two ice type concentrations are summed to produce the a single sea-ice concentration for the Antarctic because of the difficulties in assessing the Type B ice origins which do not appear to resolve purely multiyear ice as in the Arctic (Gloersen *et al.* 1992). The data set here represents the time-averaged probability of finding sea-ice at a given location and its corresponding typical monthly averaged sea-ice concentration.

There are several arguments related to the interpretation of monthly sea-ice concentration maps (Zwally *et al.* 1983b; Gloersen *et al.* 1992) such as;

- monthly averages show slightly greater sea-ice extent than the true minimum (especially in Summer - February),
- a loss of sharpness of transition from open water to high concentrated ice due to the averaging of zero occurrences with positive ice cover, and
- biases towards greatest ice extents,

are equally relevant to the use of the extracted concentrations for the sea-ice estimation method used in this thesis.

The use of the estimated sea-ice concentration can not be used satisfactorily to estimate heat and salinity fluxes because of the large satellite resolutions (55 km) which prevent accurate resolution of the amount of actual open water and new ice. Such estimates are to be developed in the future and await new satellite instruments at much smaller resolutions such as the SAR (Comiso *et al.* 1992).

In summary, the use of satellite derived sea-ice data has improved the understanding and distribution of sea-ice around the Antarctic which, until the early 1970's, was poorly

quantified. The use, however, of satellite derived concentrations and estimates of the sea-ice edge are not without their own errors or biases in estimations. Some of the problems that affect the use of the sea-ice concentration data used in this work have been commented on briefly above. The NASA algorithm with provides the concentrations works on the differences known between emissivities of sea-ice and the open-ocean. Weather effects provide one of the largest errors in determining the concentrations particularly at the sea-ice edge and for this reason sea-ice concentrations less than 15% are considered to represent the open-ocean. Thin and new ice and the degree of snow cover among other physical sea-ice characteristics also are poorly discriminated by the satellite sensors such that the sea-ice edge is difficult to pin-point, as observed in several validation studies. Again, for this reason, the sea-ice edge is defined by a 15% sea-ice concentration level or concentration intercept. More consolidated sea-ice of the inner zone or fast-ice otherwise are better validated and the boundary between the fast and unconsolidated pack-ice are considered located at the 40% sea-ice concentration isocline. Thus, the use of sea-ice concentration data in this work follow the demarcation of the pack-ice edge at 15%, and fast sea-ice edge at 40%. Sea-ice cover in months per year was determined by the author by counting the number of months provided with a value of sea-ice concentration greater than 0%.

Selected distribution characteristics of the data covered by the samples in the database are illustrated in Figure 5.1. The relation observed between the total number of months sea-ice cover versus February sea-ice concentration indicates at least 10.5 months of sea-ice cover before concentrations greater than 0% (or 15% when using the implied sea-ice edge) are observed (Fig. 5.1A). September sea-ice concentrations between 0-15% (open-ocean) are observed in locations where 1.5 to 6.5 months per year sea-ice cover are found (Fig. 5.1B). Pack-ice conditions (15-40%) are found where there is a seasonal 4 to 9 months sea-ice cover. The greatest monthly sea-ice cover variation (4-12 months) occurs in samples subject to fast-ice conditions (ie >40% September sea-ice concentration). The relation between September and February sea-ice concentrations appears exponential (Fig. 5.1C). Samples within the database imply that locations are found with at least 65% September sea-ice concentration prior to February sea-ice concentrations greater than 0% occur. For these locations to be considered sea-ice covered during February (ie. >15%), September sea-ice concentrations are at least at an 80% concentration, which is equivalent to at least 10 months sea-ice cover.

5.2 METHODOLOGY AND ASSUMPTIONS

Sea-ice estimation was originally tested using the DTF model replacing SST with the sea-ice concentration data on the 4-factor model of Pichon *et al.* (1992a) modified with the inclusion and exclusion of several species (Armand *et al.* 1996). The first three factors

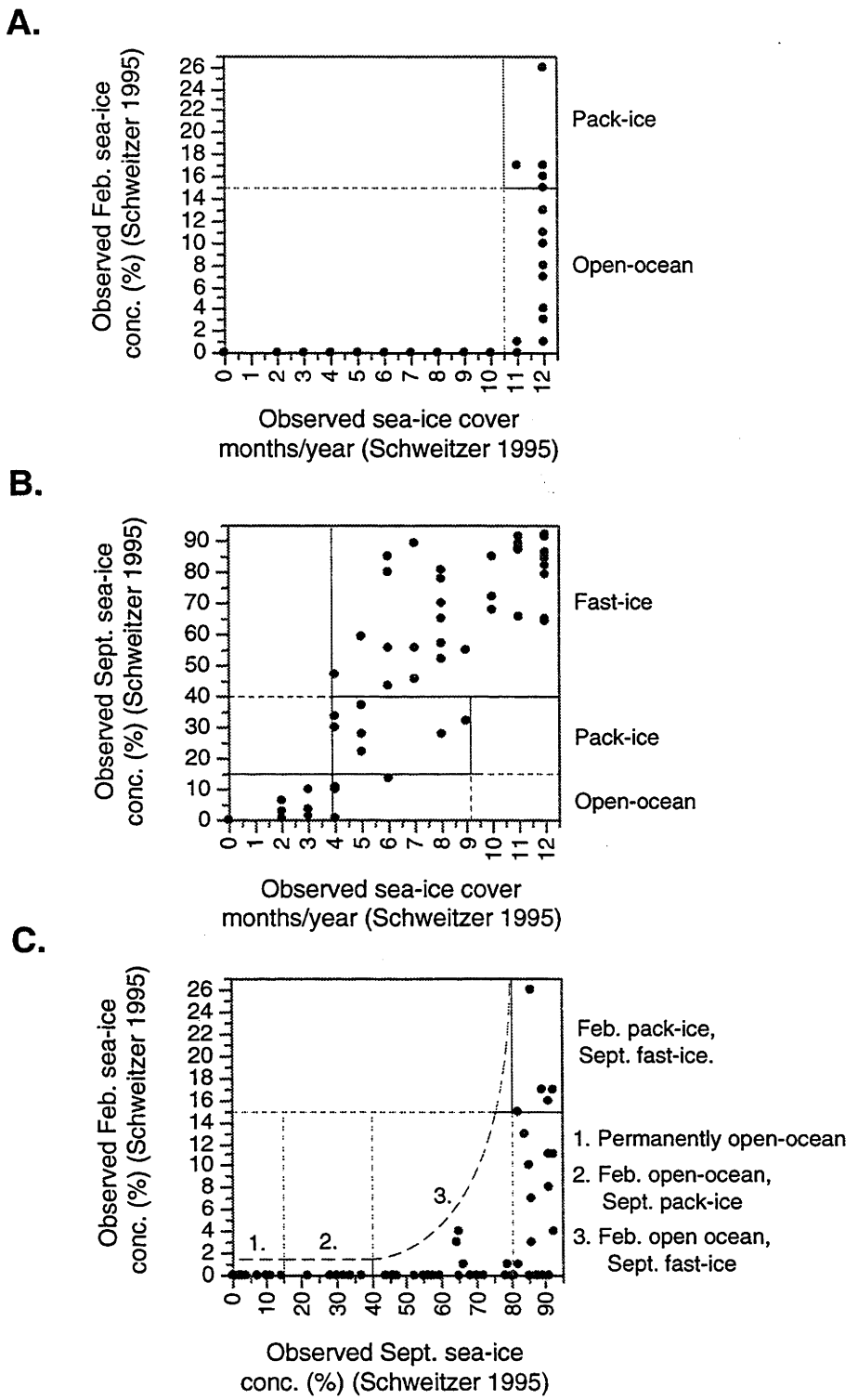

Figure 5.1. Relations between the three sea-ice parameters at each site used in each model. **A**) February sea-ice concentration versus monthly sea-ice cover. **B**) September sea-ice concentration versus monthly sea-ice cover. **C**) February versus September sea-ice concentration. Interpreted exponential effect shown by long broken line. Solid line boxes (and dark sections of long broken line in C) indicate regions of interpreted physical relations identified right of each plot. Refer to text for discussion. Sea-ice data from Schweitzer (1995). Data listed in Appendix 4.1.

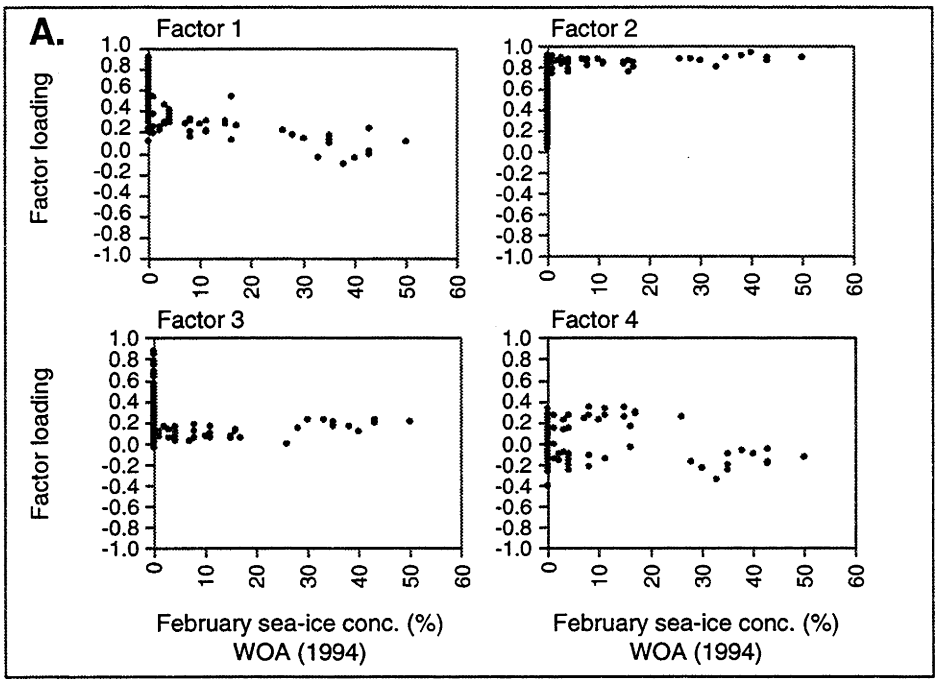
A.
Factor 1
Factor 2
Factor 3
Factor 4
Factor loading
Factor loading
February sea-ice conc. (%)
WOA (1994)
February sea-ice conc. (%)
WOA (1994)

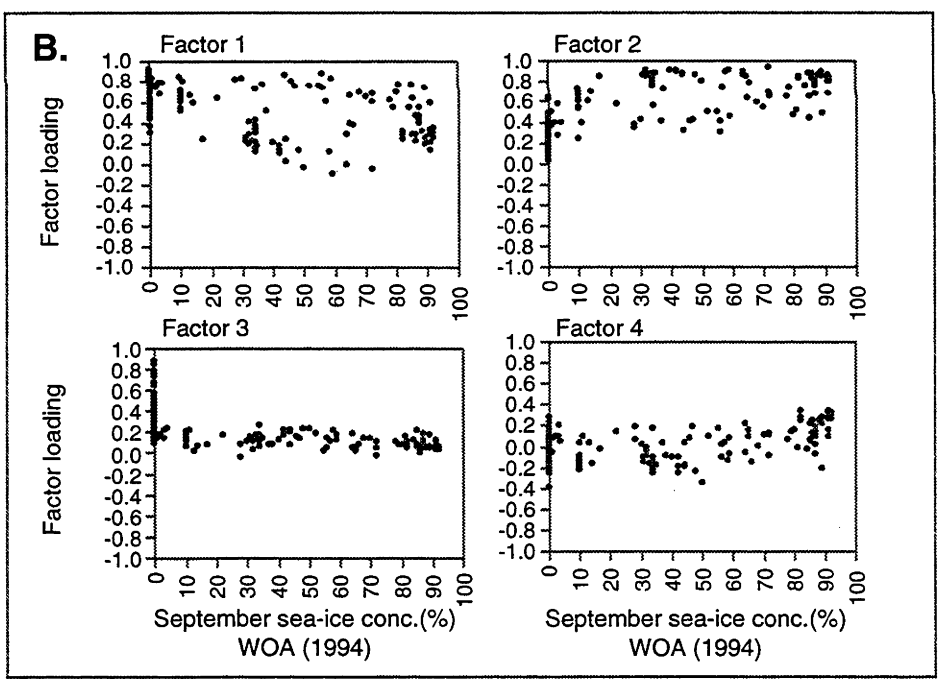
B.
Factor 1
Factor 2
Factor 3
Factor 4
Factor loading
Factor loading
September sea-ice conc.(%)
WOA (1994)
September sea-ice conc.(%)
WOA (1994)

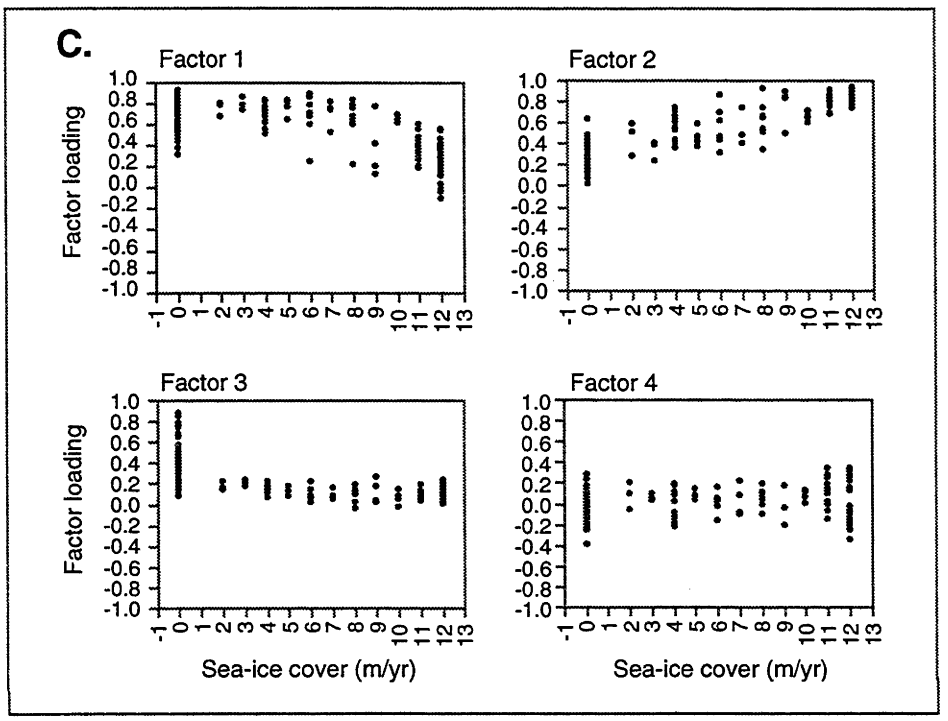

Figure 5.2. Factor loading relations to sea-ice concentrations and sea-ice cover. **A**= February sea-ice concentration, **B**= September sea-ice concentration and **C**=sea-ice cover in months per year. **A** and **B** on preceeding page. A test 176 database (early modified version of the Pichon *et al.* 1992a dataset) used to define the original relations and includes dissolution data. The four-factor model resolved refers to the three main biogeographic distributions under the first three factors and the fouth to dissolution.

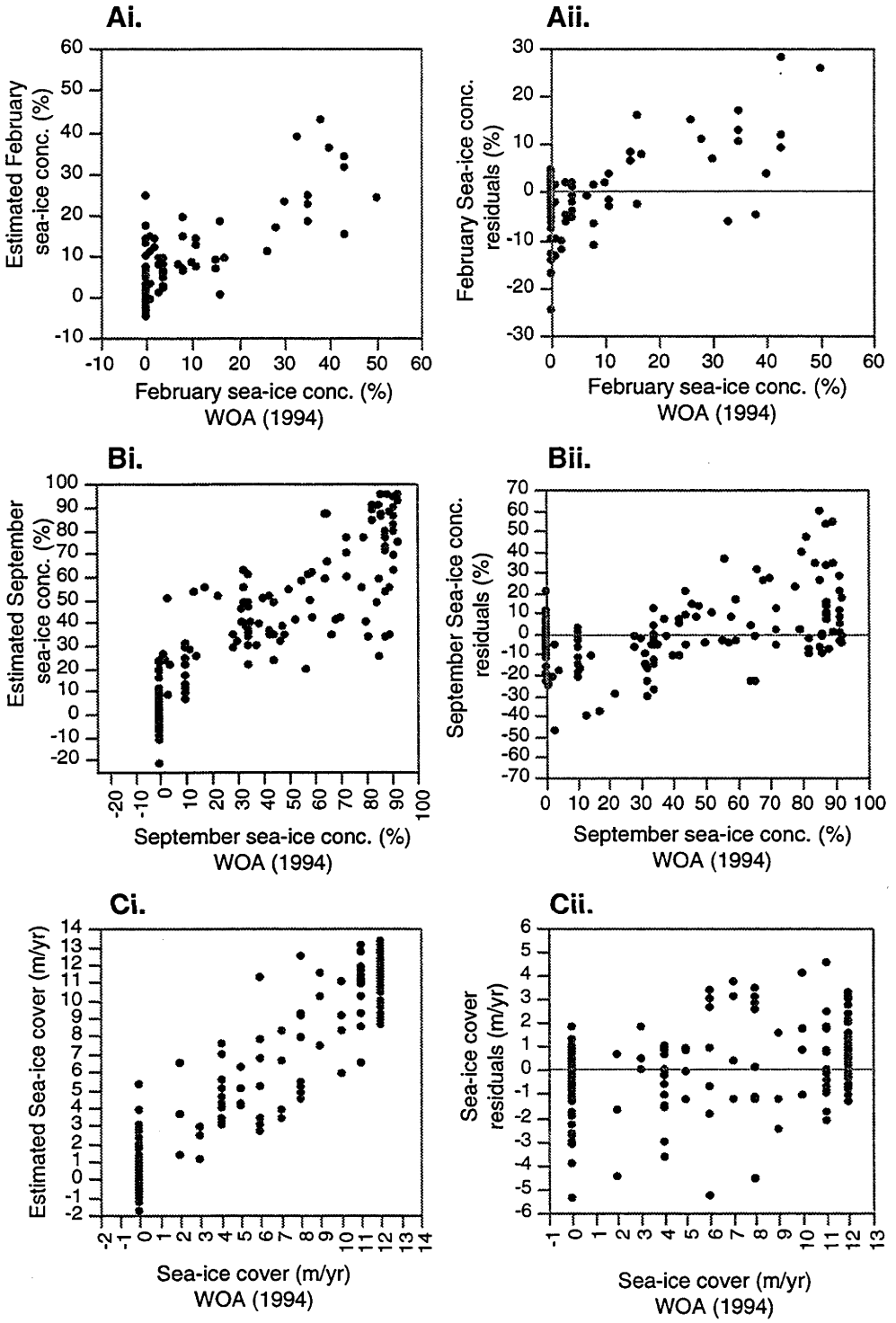

Figure 5.3. Preliminary diagnostic plots for estimation of maximum and minimum sea-ice concentrations and degree of monthly cover. **A**= February sea-ice concentration (minimum extent), **B**= September sea-ice concentration (maximum extent), **C**= sea-ice cover in months per year. All figures (i)= estimated versus observed scatter plot, (ii)= fitted values plot (ie. residuals versus observed data). Although trends for estimation are evident the non-constant variance of the DTF means other statistical approaches are necessary.

indicated reasonable relationships to the sea-ice concentrations (Figure 5.2), while the dissolution factor was not found to respond to maximum and minimum sea-ice concentration nor monthly cover. Of the three sea-ice variables tested for relation the strongest relationship was noted with months per year cover then, minimum and finally maximum sea-ice cover. Although the multiple correlation coefficients appeared high (eg Feb. sea-ice conc. model MCC= 0.799, Sept sea-ice conc. MCC = 0.856, m/yr cover MCC = 0.886) the methodology proved to be unsuitable since the large SEE's would ensue due to the linear projection of the sea-ice estimations onto values that were zero (ie. the no sea-ice cover condition). The residual plots of such an operation on the 176 test database samples (Armand *et al.* 1996) illustrate the non-constant variance of the models (Figure 5.3).

To eliminate some of the problems of the DTF model, the statistical consulting unit of the graduate school were consulted in search of another statistical model that would take into account the large number of zero conditions and the non constant variance of the sea-ice data. The solution to this problem was to consider the data first in a binary format (sea ice presence/absence) and then explicitly model the sea-ice concentration, when present, by a model that took into account the non-constant variance. This was performed as follows.

For each sea-ice variable the estimation took a two-stage approach. First, presence and abundance of sea-ice was modelled via logistic regression. Second, for those samples with non-zero sea-ice concentration, a quasi-likelihood approach was used (Mc Cullage and Nelder 1989). Due to pseudo-binomial nature of the data, the mean was modelled by the logistic link:

$$\log\left[\frac{\mu_i}{1-\mu_i}\right] = \beta_0 + \beta_1 F_1 + \beta_2 F_2 + \beta_3 F_3 + \beta_4 F_4 + \beta_5 (F_1)^2 + \beta_6 (F_2)^2 + \beta_7 (F_3)^2 + \beta_8 (F_4)^2$$

and the variance by,

$$\mathrm{var}(y_i) = \theta \mu_i (1-\mu_i)$$

where θ is a scale parameter, and μ_i is the mean sea-ice concentration for the ith sample.

A backwards elimination procedure was used to select variables (ie. factors and quadratic terms) based on the usual change in deviance tests (Mc Cullage and Nelder 1989). The two resulting models were then combined to produce marginal mean predictions of sea-ice through the usual identities:

E[sea-ice] = E [E(sea-ice/ice present)]

and variance,

var [sea-ice] = E[var(sea-ice/ice present)] = var[E(sea-ice/ice present)]

where *E* and *var* are the expectation and variance operators respectively. This is analogous to the approach used in Welsh *et al.* 1996. These formulas were used to derive the predictions and the standard errors of predictions for the cores in Chapter 6. Each model is presented in Appendix 5.1. Standard residual diagnostics were used on the second model and no problems were observed (Dr S. Barry, pers comm. 1996).

As a result of the required diatom database re-counting, the sea-ice estimation models presented here were not developed or revised further, including adapting the model using the thesis-derived 6 factor distribution of diatom species. However, the models are extremely promising, as evident in Chapter 6, even when considering the database problems already discussed. Continued investigation and presentation of revised sea-ice estimates for the Southern Ocean using the models presented here, is a future research focus for the author.

5.3. SUMMARY

Sea-ice concentration and cover estimation from CABFAC derived factor analysis was developed during the thesis. Previous estimations of sea-ice have relied on other avenues of deriving limits to the maximum sea-ice edge, while the model presented here made use of modern sea-ice satellite observations combined with diatom distributions that are considered more closely linked to the sea-ice cover.

Use of the Imbrie and Kipp (1971) transfer function model was found to be inappropriate for modelling sea-ice cover due to the non-constant variance and large number of zero values in the sea-ice concentration data. A new two-stage model is presented here which takes these features of the data into consideration, and selects appropriate factors from the CABFAC analysis in deriving both sea-ice concentration and sea-ice cover in months per year. Standard errors for each estimate are also derived. Such a feature could not be acquired when applying the transfer function method. A preliminary model was only pursued using a modified 166 database and a four factor analysis keeping in line with earlier work of Pichon *et al.* (1992a). The six factor model, as found appropriate for SST estimation, was not used to derive sea-ice estimates because such estimates would still require re-determination once the diatom database had been recounted on a sounder taxonomic background. For this reason the model remains in its preliminary status awaiting future up-date and analysis on availability of the recounted diatom database.

Chapter 6
Southeast Indian Ocean core records.

6.1 INTRODUCTION AND LOCATION

One of the original aims of this thesis was to reconstruct a late Quaternary history of the southeast Indian Ocean along a roughly north-south transect from Australia to Antarctica. To reach this aim, four cores were chosen on which to study the diatom record and to apply the diatom transfer function. The four cores are located between the PF and the STC approximately along the 146°E meridian (Figure 6.1). The location details of each core are presented in Table 6.1.

Core	Lat.(°S)	Long.(°E)	Water depth (m)	Gear	Core length (m)	Sample interval (cm)
MD88-787	56°22.72'	145°17.56'	3020	Kullenberg	10.40	10
MD88-784	54°11.48'	144°47.65'	2800	Kullenberg	5.00	10
MD88-779	47°50.69'	146°32.75'	2260	Kullenberg	6.70	10
E53-10	49°00.0'	148°06.7'	4026.6	Piston	11.75	5 & 10

Table 6.1. Core location details. MD cores taken by the French in 1988 aboard *the Marion DuFresne*. An additional *Eltanin* core was included to supplement the transect selected (E53-10).

All cores were processed using the silica-selective method described in Chapter 1 and Appendix 1.1. Diatom counts, taxonomy, and ranking criteria followed methods presented in previous chapters.

An overview of the diatom biostratigraphy and oxygen-isotopic stratigraphies of the cores are presented below. This is followed by a discussion of various results from the *Marion DuFresne* cores including SST and sea-ice estimations. A comparison of the SST and sea-ice records is later discussed, as are the relationships to other palaeoceanographic and climatic records.

6.2. CORE STRATIGRAPHY.

Several methods of determining the stratigraphy of the cores under study have been implemented. In particular to the French *MD* cores, magnetostratigraphy, isotope records and biostratigraphy have been involved.

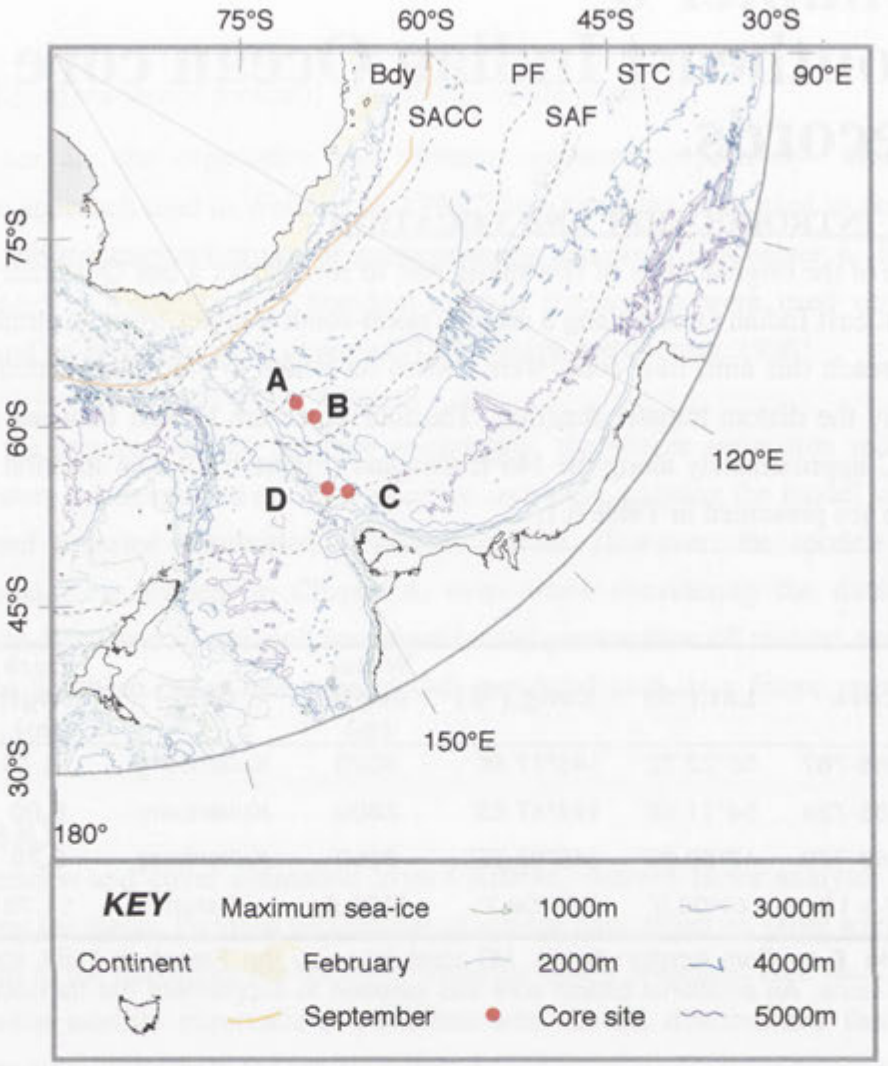

Figure 6.1. Location of the four cores analysed in this thesis. Cores identified by the following codes: A= MD88-787, B= MD88-784, C= MD88-779, D= E53-10. All cores are discussed in the text. Bathymetry from GEBCO (1992), maximum sea-ice extents from Schweitzer (1995) and oceanographic boundaries from Orsi *et al.* (1995). Bdy= the southern limit of the Upper Circumpolar Deep Water (UCDW), SACC= Southern ACC front, PF = Polar Front, SAF= Subantarctic Front, STC= Subtropical Convergence/Front.

6.2.1. CORE E53-10

Eltanin core, E53-10 situated on the edge of the South Tasman rise (Figure 6.1, Table 6.1), was an extra core sampled for this thesis work. The initial core descriptions (Cassidy *et al.* 1977) suggested siliceous material was present in the otherwise dominantly calcareous sedimentary core, which covered the Brunhes normal polarity (Osborn *et al.* 1983). Connolly (1972) indicated that the core was situated in the Tasman manganese pavement zone where bottom-water currents had removed recent sediments. However, indications from the work by Pichon *et al.* (1992b) on surface-samples in this region suggested that a core might be worth examining. Further stratigraphic control was then to be made via comparison with the nearby French core MD88-779.

Core E53-10 was sampled at 5 cm intervals for the first 80 cm and then every 10 cm for the remainder of the core. All material was processed as outlined in Appendix 1.1. On average, 3 gm wet weight samples were processed. A further sub-sample of the remaining material was sent for silica-zinc ratio analysis (M. Ellwood, University of Otago, NZ). Preliminary diatom analysis of the prepared slides indicated the core contained reworked species (Appendix 6.1). The presence of *Actinocyclus ingens*, *Hemidiscus karstenii*, *Stephanopyxis* spp, *Denticulopsis* spp and other non-Holocene/late Quaternary species were encountered throughout all the samples examined in the first two metres of the core. Upon this observation, the core was abandoned for further study. Independent results of the zinc-silica ratio analysis performed on the sub-samples also indicated an anomalous response (M. Ellwood pers. comm. 1996), which is interpreted to be resultant of the reworked material incorporated in the core.

In hindsight from the knowledge acquired regarding the dissolved sample KR8808 (section 3B.2 and 3) which is also situated in the same location, the region appears to be under a sedimentary reworked environment imposed by the drop off to the south of the South Tasman Rise. Bareille (1991, p. 137) found that box-core samples from the region of the South Tasman Plateau and south to the southeast Indian Rise (KR-8807, -8808, and -8809) were impossible to derive isotopic chronologies due to perturbations in the sediments. Unfortunately, this recent investigation was overlooked during the core selection. Future micropalaeontological and palaeoceanographic studies should be conscious of this problem and be cautious when sampling in this region.

Further stratigraphic discussion centres on results previously determined or recovered during this thesis for the French *Marion DuFresne* cores only.

6.2.2. DIATOM BIOSTRATIGRAPHY

Diatom biostratigraphy follows that of Harwood and Maruyama (1992) and Burckle *et al.* (1978) for the placement of biostratigraphic markers. An important marker during the late

Quaternary is the last abundant appearance datum (LAAD) of *Hemidiscus karstenii* in the upper part of Oxygen-isotope-stage 7 (190,000 years, Burckle *et al.* 1978, and Burckle pers. comm. 1997). The most recent and nearest Antarctic diatom biostratigraphy applied in this work is derived from the Kerguelen Plateau region (Harwood and Maruyama 1992).

All three French cores fall within the *Thalassiosira lentiginosa* Partial Range Zone which covers the upper Pleistocene to Holocene from 0 to 620 ka (Figure 6.2) (Harwood and Maruyama 1992). The base of this zone is defined by the last occurrence of *Actinocyclus ingens* while the last occurrence of *T. lentiginosa* signifies the current depositional scenario (ie. the Holocene). The sporadic presence of *A. ingens* in two of the cores at very low abundances is interpreted as reworking rather than indicating the transition into the *Actinocyclus ingens* Partial Range Zone. Further evidence of stratigraphic age is retrieved from the presence of the LAAD of *Hemidiscus karstenii* in two cores (MD88-787 and -779). Thus, an approximate age for each of these cores can be considered as 190 ka at the depth of 1020cm for core MD88-787 and ~249 cm for MD88-779, where the LAAD's are indicated (Fig.6.2). There is room for error in the positioning of the LAAD in core MD88-787 since the core ends just where the signal of *H. karstenii* begins to increase. Consequently, the age of the bottom of the core could be slightly older at the interpreted LAAD identified here.

Further detailed biostratigraphy performed on other micro-fossils in the three French cores have not been produced, with exception to the work currently under preparation for core MD88-779 by Dr S. Nees (benthic foraminifera, GEOMAR, Germany), and the abundance of the radiolarian *Cycladophora davisiana* in core MD88-787 (Bareille 1991).

6.2.3. Isotope Stratigraphy and Preliminary Age model.

The oxygen-isotope records of cores MD88-787 and -784 were produced by the staff at the Centre des Faibles Radioactivités mixte CNRS CEA, France and made available by Dr L. Labeyrie. Both cores have planktonic and benthic foraminiferal-derived isotopic records, although only the planktonic records (*N. pachyderma* 200-250μm) were made over the length of the whole core and are used here. The oxygen-isotope record for the remaining core, MD88-779, was produced by the Mountain Mass Spectrometry Laboratory in Colorado and made available by Dr P. Deckker (ANU, Canberra). The isotopic record is currently derived only from benthic foraminifera (*C. wuellerstorfi* >150μm).

The isotopic record of each core (Figures 6.3 to 6.5) illustrates the various oxygen-isotopic stages through the depth of the cores. Preliminary isotopic stage alignment for each core is presented in section A of each figure. Two climatic cycles are covered

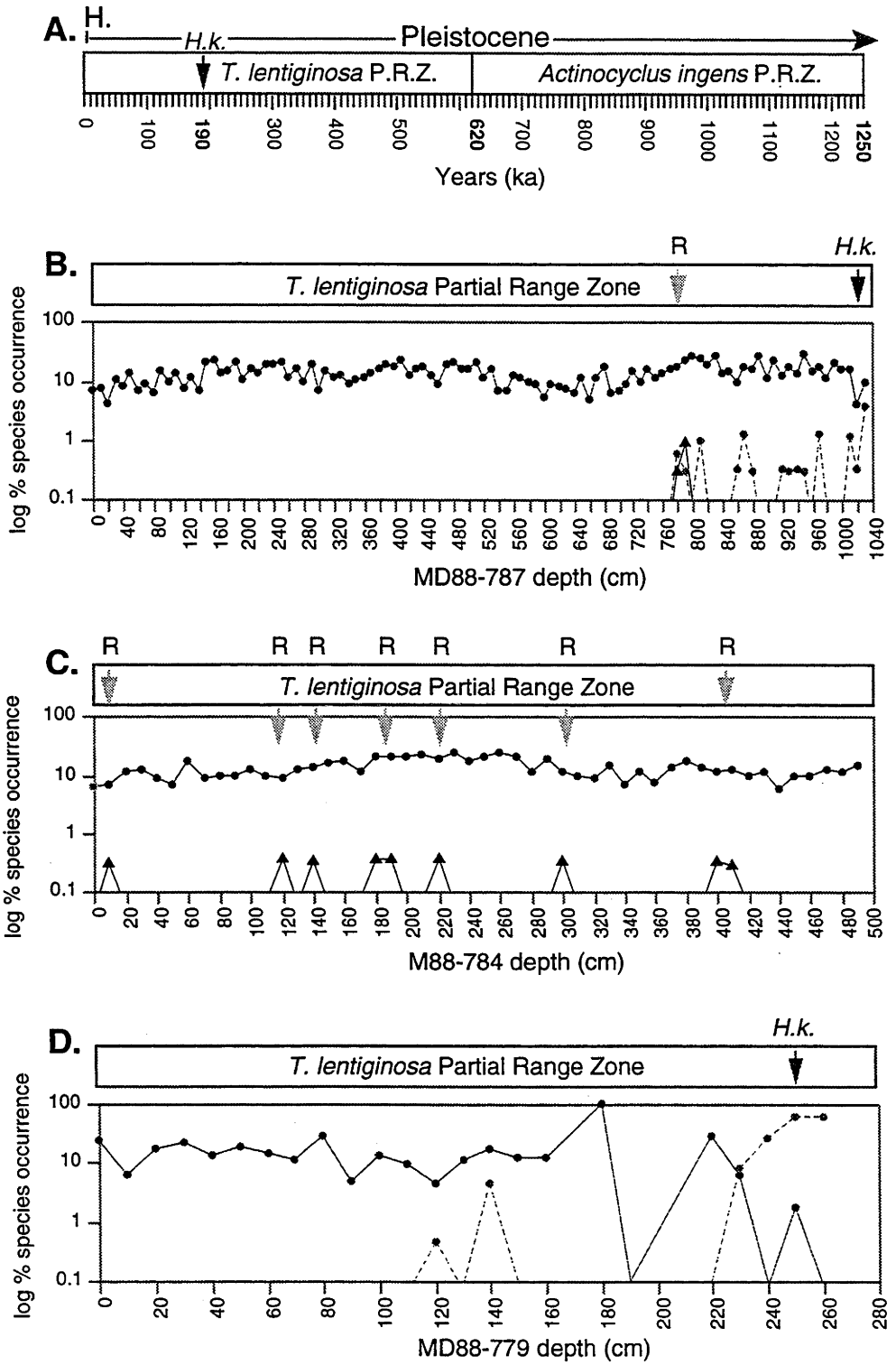

Figure 6.2. Diatom biostratigraphy of the three French *MD*88 cores of this study against the Harwood and Maruyama (1992) biostratigraphic scheme and the Burckle *et al.* (1976) Last Abundant Appearance Datum of *H. karstenii (H.k.).*
A= Published biostratigraphic schema against age, applicable to this study. The last occurrence of *Actinocyclus ingens* divides the two partial range zones.
B to D= Logarithmic plot of *T. lentiginosa*, *A. ingens* and *H. karestenii* relative abundances against depth, with interpreted biostratigraphic relations for each core. *T. lentiginosa* = —●—, *H. karstenii* = ---●---, *A. ingens* = —▲—
H= Holocene; P.R.Z. = Partial Range Zone; *H.k.* = *Hemidiscus karestenii* LAAD; R = reworked occurrences of *A. ingens.*

through the depth of the core MD88-787. The base of the core found to represent the end of isotope-stage 7, as suggested by the LAAD occurrence of *H. karstenii*. Core MD88-784, north of the preceding core, contains isotopic stages 1 to 3, while the most northerly core MD88-779 also contains two climatic cycles that reach into isotope-stage 7. This later feature is also indicated by the LAAD of *H. karstenii*. The benthic isotope curve of core MD88-779, however, shows a melding of isotopic stages 3-5, which are difficult to separate with depth.

To facilitate comparison between the three cores and also with other palaeoceanographic work, a preliminary age model for each core was derived using the program *Analyseries 1.1* (Paillard *et al.* 1996, Paillard 1997). The simple LinAge model was employed to linearly link the planktonic or benthic oxygen-isotope SPECMAP stack age models (Imbrie *et al.* 1984, Martinson *et al.* 1987) to the oxygen-isotope records of the three cores. The derivation of the age models for each of the cores is illustrated in sections B and C of Figures 6.3 to 6.5. The data are located in Appendices 6.2 to 6.4. Each core age model must be considered provisional since additional independent tie-points to age have not been made for the cores, such as AMS ^{14}C dating of the foraminifera in the surface sediments, nor was the oxygen-isotopic data of the cores at high resolution. Confidence on each tie point between peaks and troughs of the SPECMAP and cores are thus, limited. The exception to the latter point being core MD88-779.

The age model of core MD88-787 (Figure 6.3) did not incorporate the suggested LAAD of *H. karstenii* as an age control tie-point between the core and the planktonic SPECMAP stack age model. Since, as mentioned previously, the existence of an error in its placement at the end of the core was possible. However, the proposed age model provided by the correlation to the SPECMAP stack indicates that the LAAD placement is correctly assigned within a 5 kyr error. This is equivalent to the maximum range of error indicated by the Imbrie *et al.* (1984) for their SPECMAP stack age model. The core contains 195 kyr of sedimentation within its 1030 cm length. The linear sedimentation rate for the core is plotted in Figure 6.6A and discussed in section 6.2.4.

Core MD88-784 is considered to have lost the uppermost section of the core that converts to the last 3 kyr against the SPECMAP stack (Figure 6.4). The end of the core is found to reach the oxygen-isotopic stage 3/4 boundary. The linear sedimentation rate for the core is plotted in Figure 6.6B.

In contrast to the previous two cores, core MD88-779 has its age model derived through comparison with the benthic SPECMAP stack of Martinson *et al.* (1987) (Figure 6.5). The age model determined includes the LAAD of *H. karstenii* as an age control point (190 kyr) between the two benthic oxygen-isotopic curves and was provided jointly by the

author and Dr S. Nees (GEOMAR, Germany). The core covers 200 kyr over 260 cm, and thus has a low sedimentation rate (Figure 6.6C).

The oxygen-isotopic changes over the two termination interglacial-glacial boundaries show similar findings. Over Termination I (oxygen-isotope-stage 1/2), a difference in the planktonic records indicates a shift of 1.87 per mil and 1.60 per mil at 56° and 54°S for cores MD88-787 and MD88-784 respectively. The benthic record documents a shift of 1.19 per mil in core MD88-779 (47°S). These amplitudes in the planktonic and benthic $\delta^{18}O$ signals vary to those noted by Charles and Fairbanks (1990) at DSDP site 704 in the subantarctic South Atlantic (1.3 per mil planktonic, 1.6 - 1.7 per mil benthic). However, similarity to planktonic isotopic signals of the South Indian Ocean core MD84-551 at 55°S (Pichon *et al.* 1992a, 1.63 per mil), are met.

Across Termination II (oxygen-isotope-stage 5/6 boundary), the planktonic record from core MD88-787 provides a shift of 1.16 per mil, whereas the benthic record of core MD88-779 observes a shift of 1.36 per mil. The shift in the southern core MD88-787 is larger than that observed in the South Indian Ocean core MD84-551 of 0.83 per mil (Pichon *et al.* 1992a).

6.2.4. Sedimentation rate.

Recent work derived from French box-core material suggest that Holocene sedimentation rates in the transect from Tasmania to Antarctica are in the order of 2 to 7.5 cm/kyr in the Subantarctic Zone and between 10-20 cm/kyr in the Polar Front Zone (Bareille 1991). Cores MD88-787 and MD88-784 are located within the Polar Front Zone. Their Holocene linear sedimentation rates (Figures 6.6A and B) derived from the *Analyseries* produced age model are well within the Bareille (1991) observations of the area. Core MD88-784, the more northern of these two cores, has the greater sedimentation rate, even though the top of the core is presumed missing. Core MD88-779 is located just within northern limit of the Subantarctic Zone. Its Holocene sedimentation rate is considerably reduced and falls just under the minimum predicted range cited by Bareille (1991) (Figure 6.6C). A recent study by Connell and Sikes (1997) suggest low Holocene sedimentation rates on the southern portion of the South Tasman Rise of between 2-5 cm/kyr which are similar to those observed in core MD88-779.

In terms of variation of sedimentation rate over time, the three cores equally have similarities and differences. All three cores show a reduction of sedimentation from the Holocene rates to that of the last glacial (oxygen-isotope stage 2). Bareille (1991) noted that cores within the Subantarctic Zone of the Indian Ocean show an increase in sedimentation rate during this and all glacial periods, while cores in the Polar Front Zone

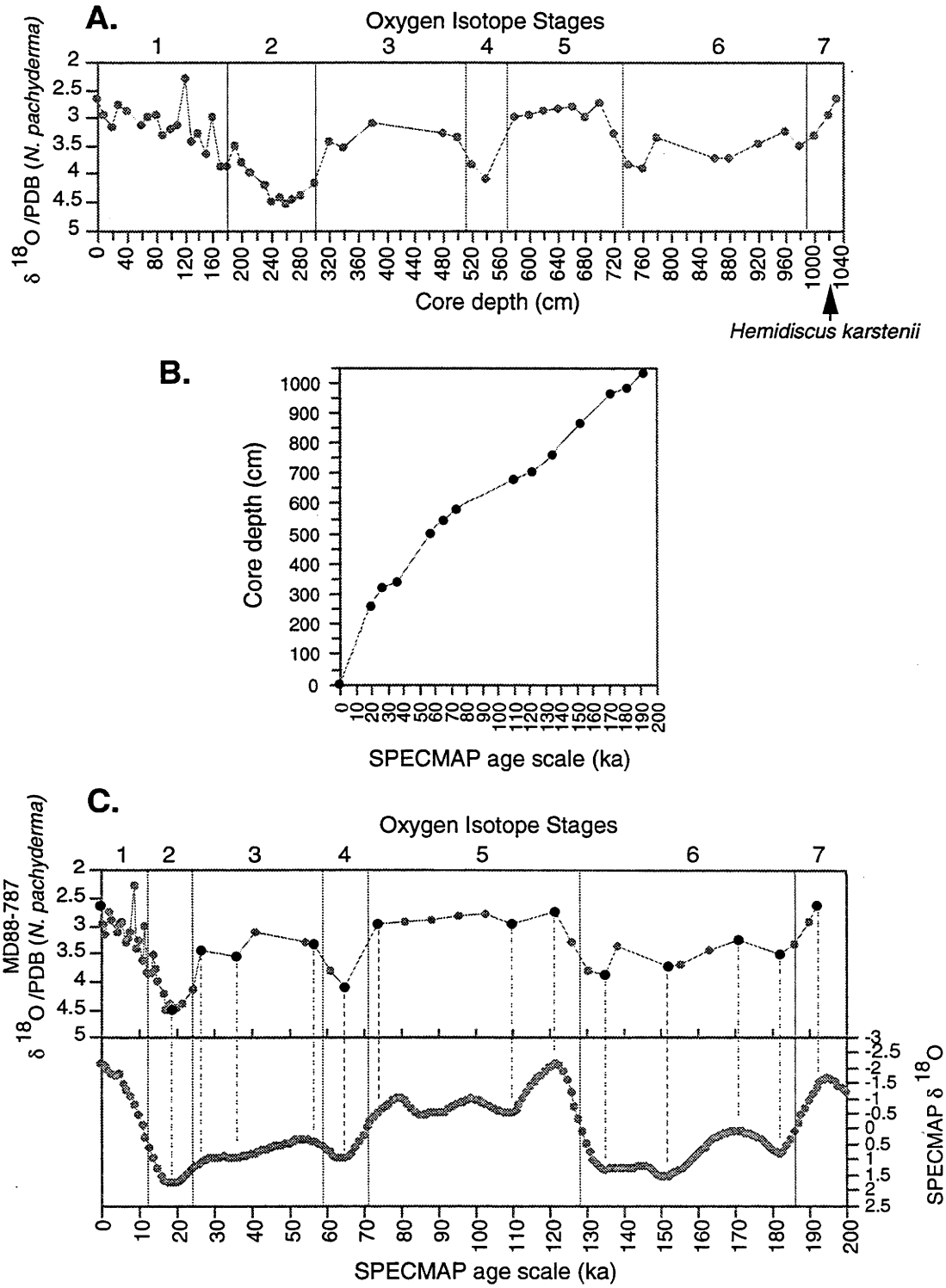

Figure 6.3. Derivation of preliminary age/depth model for core MD88-787. **A**) The planktonic $\delta^{18}O$ record against core depth with inferred oxygen isotope stages indicated. The $\delta^{18}O$ record from *N. pachyderma* (200-250μm) provided by Dr. L. Labeyrie (GIF, France). **B**) Linear age model from *Analyseries 1.1* (Paillard *et. al.* 1996/7). Grey line represents correlation between SPECMAP stack age scale (Imbrie *et al.* 1984) and core depth of MD88-787 determined from black tie points taken from planktonic isotopic curve comparisons indicated in **C**. **C**) Presentation of the oxygen isotopic record of core MD88-787 against the SPECMAP age scale and corresponding SPECMAP stack oxygen isotope record with oxygen isotope stages from Imbrie *et al.* (1984). Dashed lines indicate tie points used to derive age model for core MD88-787. *Analyseries* provided a correlation coefficient of 0.826 for the match between the two isotope curves.

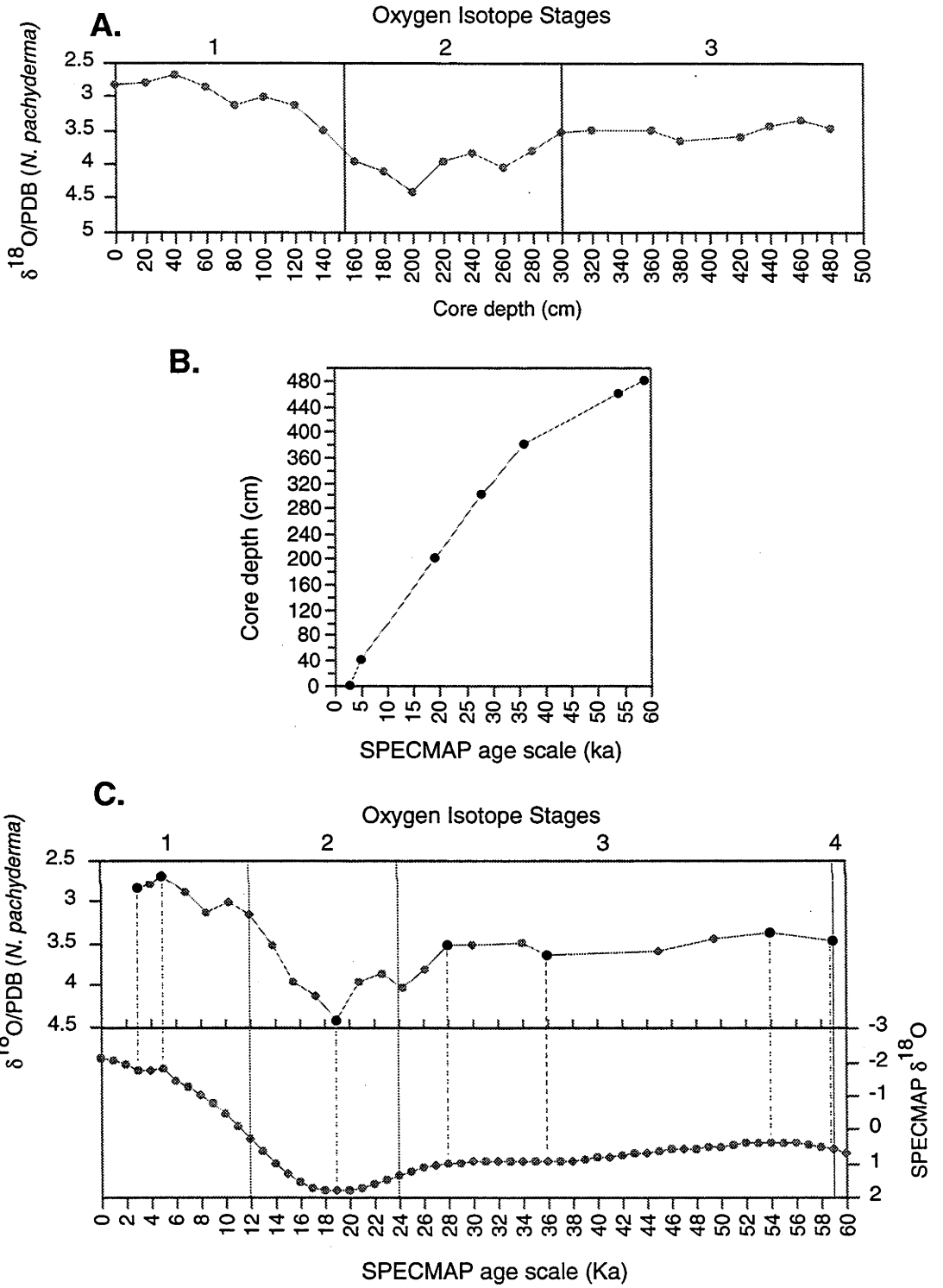

Figure 6.4. Derivation of preliminary age/depth model for core MD88-784. **A**). The planktonic $\delta^{18}O$ record against core depth with inferred oxygen isotope stages indicated. The $\delta^{18}O$ record from *N. pachyderma* (200-250μm) provided by Dr. L. Labeyrie (GIF, France). **B**) Linear age model from *Analyseries 1.1* (Paillard *et al.* 1996/7). Grey line represents correlation between SPECMAP stack age scale (Imbrie *et al.* 1984) and core depth of MD 88-784 determined from black tie points taken from the planktonic isotopic curve comparisons indicated in **C**. **C**) Presentation of the oxygen isotopic record of core MD88-784 against the SPECMAP age scale and corresponding SPECMAP stack oxygen isotope record with oxygen isotope stages from Imbrie *et al.* (1984). Dashed lines indicate tie points used to derive age model for core MD88-784. *Analyseries* provided a correlation coefficient of 0.932 for the match between the two isotope curves.

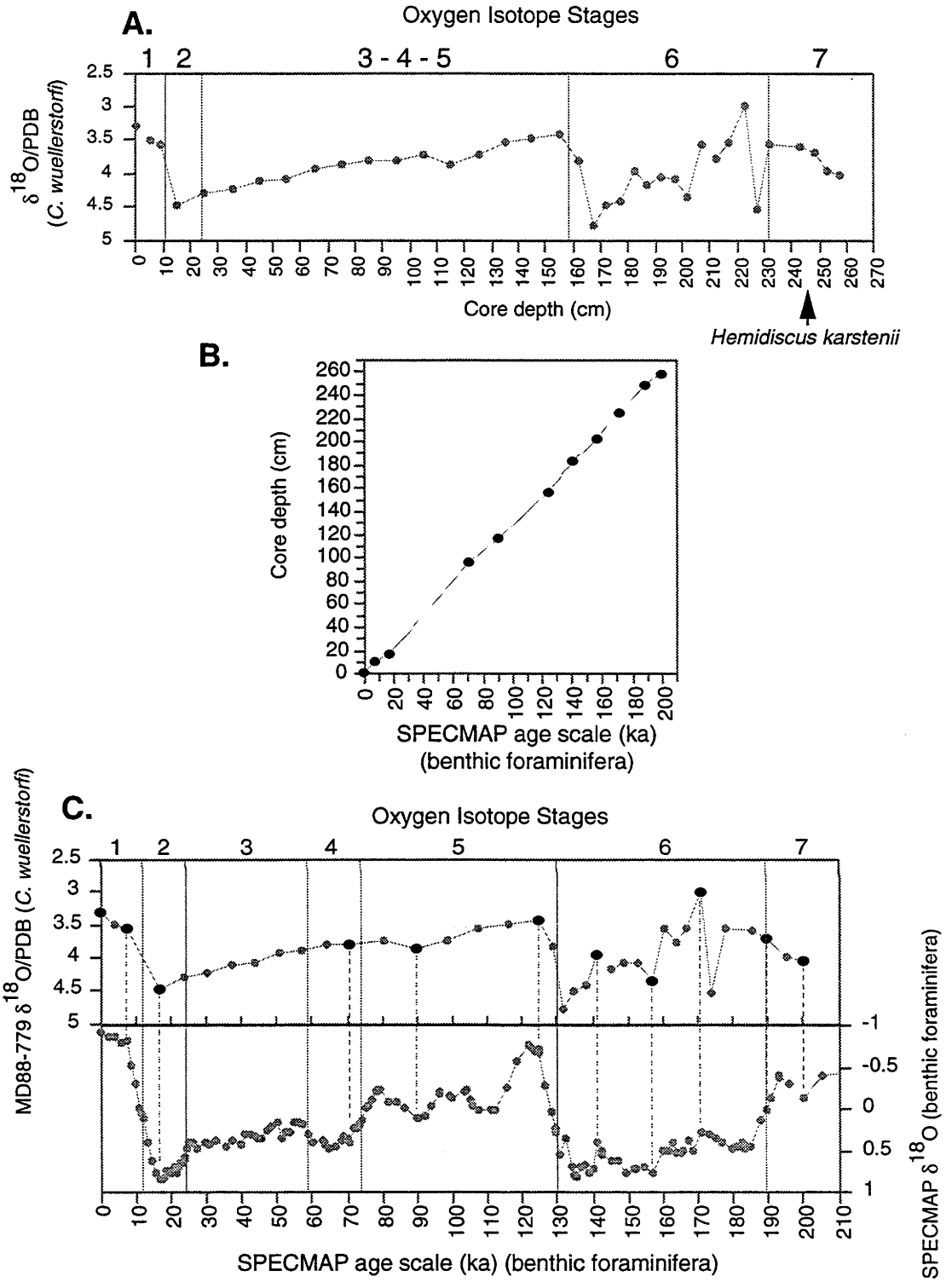

Figure 6.5. Derivation of preliminary age/depth model for core MD88-779. **A**). The benthic $\delta^{18}O$ record against core depth with inferred oxygen isotope stages indicated. The $\delta^{18}O$ record from *C. wuellerstorfi* (>150μm) provided by Dr P. DeDekker (ANU, Australia). **B**) Linear age model from *Analyseries 1.1* (Paillard *et al.* 1996/7). Grey line represents correlation between Martinson *et al.*(1987) benthic age scale and core depth of MD 88-779 determined from black tie points taken from the benthic isotopic curve comparisons indicated in **C**. **C**) Presentation of the oxygen isotopic record of core MD88-779 against the Martinson *et al.* (1987) age scale and corresponding oxygen isotope record with oxygen isotope stages from Martinson *et al.* (1987). Dashed lines indicate tie points used by the author and Dr S. Nees (GEOMAR, Germany) to derive age model for core MD88-779. *Analyseries* provided a correlation coefficient of 0.614 for the match between the two isotope curves.

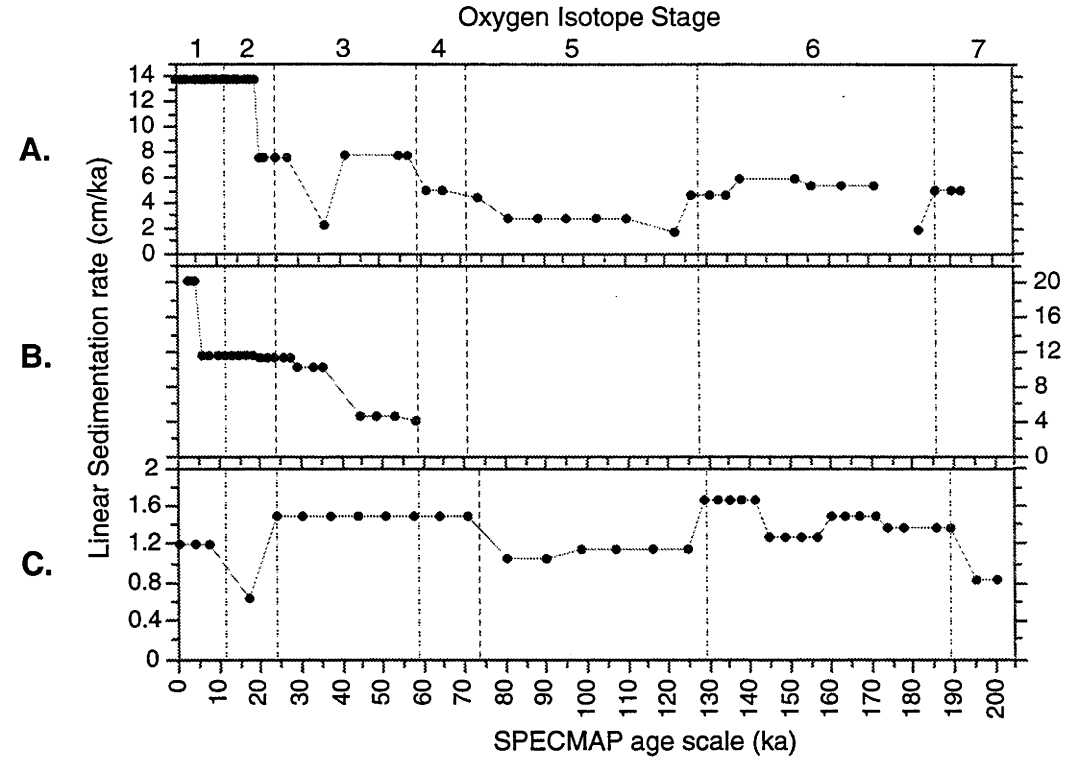

Figure 6.6. Presentation of the linear sedimentation rates of the three French cores against the SPECMAP age scale. Oxygen isotope stages are also provided. **A)** Core MD88-787; **B)** Core MD88-784; **C)** Core MD88-779. Note that each core varies in the degree of sedimentation relative to the other.

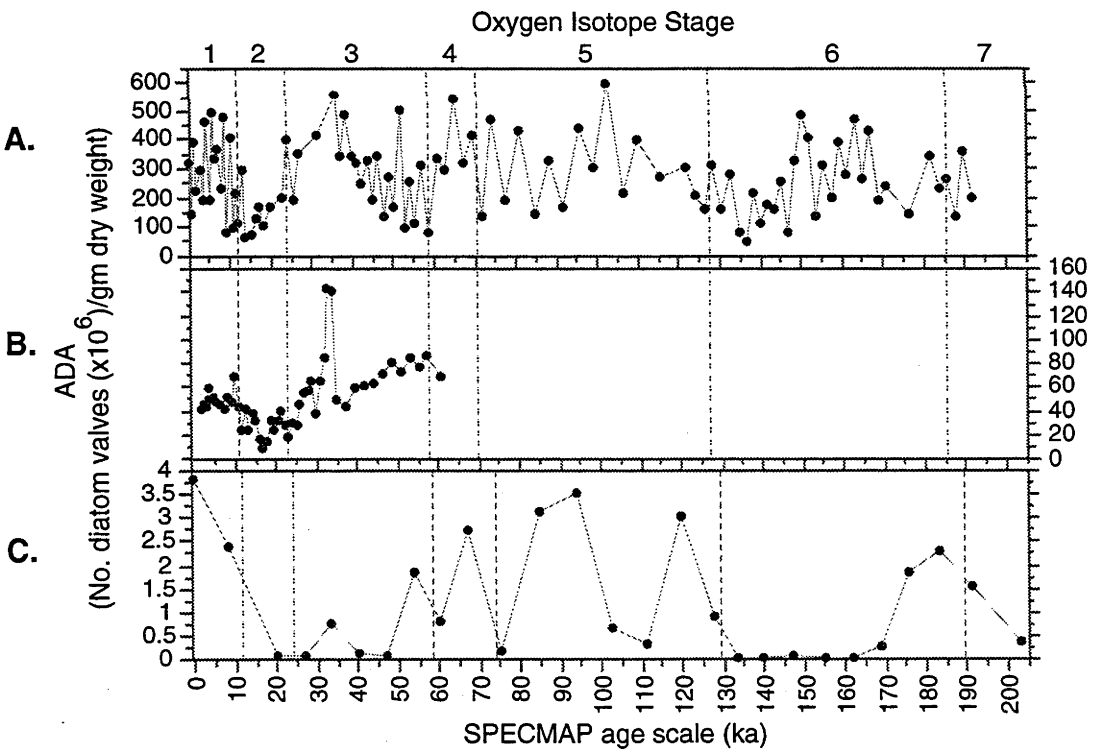

Figure 6.7. The absolute diatom abundance (ADA) in millions of valves per gram dry weight for each core against the SPECMAP age scale. Oxygen isotope stages are also indicated. **A)** Core MD88-787; **B)** Core MD88-784; **C)** Core MD88-779. The decreasing content of diatom occurrence in the sediments to the north of the transects is evident in the decreasing ADA observed over the cores. The see-sawing effect most evident in isotope stage 5 of core MD88-787 can be related to an artefact of counting which is discussed further in the text.

were variable in response; some showing comparable rates to the Holocene and others showing decreases in their rates. The two cores studied in the Polar Front Zone region show this variation in sedimentation rate, but overall are noted with reduced rates in comparison to the Holocene. The Subantarctic Zone core shows from a single point only a reduction in the sedimentation rate and this is believed referable to increased bottom-water movement through this particular region during this time and decreased productivity, and for these reasons discussed later, did not show the predicted sedimentation rate.

Overall, the trend observed from the two Polar Front Zone cores of this study indicate that the Holocene period has the highest rates of sedimentation observed through time in each core. Further variations excluding isotope-stage 1 appear to indicate that a reduction of the sedimentation rate occurred during the interglacial periods, in contrast to that of the glacials. Lowest sedimentation rates were observed in both isotope-stages 3 and 5, which are in line with results plotted by Bareille (1991). The Subantarctic core, in contrast, did not record the highest sedimentation rate during the Holocene but rather in the glacial period of isotope-stage 6, and through isotope-stages 3 and 4. However, in a generalised manner, the core did not largely vary in the rate of sedimentation through the duration of the core and could be interpreted as having a near constant rate of sedimentation of 1.3 cm/kyr for the last 200 kyr. Such a steady rate may indicate other forces at play controlling the fine variations in sedimentation rate. This sedimentation rate is slightly greater than that observed in DSDP site 281 of 0.7 cm/kyr on the South Tasman Rise (The Shipboard Scientific Party 1975).

6.2.5. Absolute Diatom Abundance.

The variation in diatom content throughout the length of the cores was investigated by the Absolute Diatom Abundance of each sample. Absolute diatom abundances (ADA) as millions of valves per gram dry weight (v/gdw) was determined using the following equation.

$$ADA = \frac{\text{total diatom count} \times \text{area of petri dish}(mm^2)}{(\text{area FOV}(mm^2) \times \text{no. FOV}) \times (\text{no. drops} \times 0.15ml)} \times \frac{100ml}{\text{dry weight}(gm)}$$

where the area of the petri dish used as the settling chamber is 2640 mm^2 (5.79 cm diameter) and the area of the field of view (FOV) at 100X magnification is 0.028 mm^2 (189 μm diameter). Only in core MD88-779 was this equation modified to taken into account a 50ml dilution rather than 100ml dilution used for all other cores.

Figure 6.7 A-C presents the ADA in millions of diatom valves per gram of dry weight sediment for each of the three cores against time. A problem particular to core MD88-787 is the see-saw effect of the ADA estimates that are considered an artefact of counting.

Samples of this core were counted over a two year period originally at a 20 cm sampling interval. A 10 cm interval was later achieved, but must be considered to have affected the results of the core for this and other results. Four samples from this core were not used due to being counted at low magnification (Appendix 6.2).

A differential degree of diatom content within the sediments can be observed when comparing the three cores. The greatest abundance of diatoms, as expected, being located to the south and reducing in number to the north. The Russians made early estimates on the diatom content of the sediments. Kozlova (1966) originally reported less than 6.25 ($x10^6$) valves per gram in surface sediments between 40° and 45°S, whereas the main siliceous ooze belt varied from 15 to 102 ($x10^6$) valves per gram. Jousé *et al.* (1971) later redefined the abundance in the Pacific region and proposed 0.04 to 5 ($x10^6$) valves per gram from the south-eastern Tasman Sea down to 55°S. More recent work by Crosta *et al.* (1997) suggest 10-50 ($x10^6$) valves per gram dry weight (v/gdw) in the surface sediments directly south of Tasmania, although this should be limited to the south of the Subtropical Convergence. Whereas, in the Polar Front Zone of this study region, results from box-cores indicate ADA's varying between 100 and 300 $x10^6$ v/gdw (Crosta *et al.* 1997). Within the South Atlantic Ocean sector, Zielinski and Gersonde (1997) report comparable ADA's for the Polar Front Zone varying from 50 to 200 $x10^6$ v/gdw, decreasing to less than $1x10^6$ v/gdw to the north.

Core MD88-787, located just north of the PF, has a high surface ADA (316 $x10^6$ v/gdw). The surface ADA value of core MD88-784, two degrees further north, is not recorded. However, it is presumed well under 70 $x10^6$ v/gdw based on the rather consistent record otherwise indicated by the record in isotope-stage 1. Both these results are in disagreement with the nearest box-core results reported by Crosta *et al.* (1997). They indicate around half the ADA from a box-core KR88-12 (157.2 $x10^6$ v/gdw) near MD88-787, and just under 5 times the value from box-cores KR88-11 and -10 (106 and 280 $x10^6$ v/gdw respectively) near core MD88-784. Discrepancies in the mode of counting and calculation, or real differences in the sediments, may yet indicate why these results are not concurrent, even though the surface samples are situated closely.

For core MD88-779, the diatom recovery is considerably low when compared to samples from the Southern Ocean. Again, the calculated surface value of 4 $x10^6$ v/gdw is considerably diminished in comparison to those reported by Crosta *et al.* (1997) for the same region (KR88-06 12.4 $x10^6$ v/gdw; KR88-07 31.7 $x10^6$ v/gdw), but which are within those suggested by Jousé *et al.* (1971, 0.04 to 5 $x10^6$ v/gm). Low ADA values ($\geq$ 5 $x10^6$ v/gdw) towards the southwest of Africa (Zielinski and Gersonde 1997) are similar to those observed at the surface of core MD88-779.

Over time, all three cores indicate a reduction in the number of diatom valves in the sediments for the last glacial. This trend is not observed during the previous "glacial" period in isotope-stage 4, but is again noted in isotope-stage 6. Interglacial isotope-stages 3 and 5 of the two cores in the Polar Front Zone indicate higher- or equivalent-diatom content comparable to isotope-stage 1. This is only the case in isotope-stage 5 for core MD88-779 in the Subantarctic Zone.

The reduced diatom signal during the glacials appears odd since the expectation - especially in the northern cores - was for an enhanced diatom signal produced by the northward shifting fronts (Cooke and Hays 1982, Burckle and Cirilli 1987). The decrease in signal in core MD88-787 could be interpreted as being affected by sea-ice cover and the resulting change towards more lightly silicified diatom species. The complete loss of a diatom record in glacial isotope-stages 2 and 6 in core MD88-779 is extremely unusual. Under expectations of productivity and frontal shifts to the north, an increase to around $5x10^6$ v/gdw in the core record was anticipated. The diatom signal is almost completely missing. Other reports of missing diatoms signals in glacial intervals have been reported by Mikkelsen (1979) in the equatorial regions, and Fenner *et al.* (1992) north of Chatham Rise. Fenner *et al.* (1992) attributed the loss of expected subantarctic diatom species to a dilution by other allochthonous species that were in greater abundance and the hindered movement of the STC north of the Chatham Rise. An absence of biogenic silica during the last glacial maximum in cores studied in the southern region of the South Tasman Rise has recently been reported and are interpreted to have been affected by northward shifts in the Subantarctic Front, winnowing and post-depositional dissolution (Connell and Sikes 1997). In the case observed for MD88-779, the glacial diatom signal is currently interpreted as having been removed by increased water mass velocity, extreme post-depositional silica dissolution or decreased productivity. There is no other sedimentological evidence from the core, at this point in time, which provides further interpretation to this observed feature.

6.2.6. THE RELATIVE ABUNDANCE RECORD OF *CYCLADOPHORA DAVISIANA*.

The variation in the relative abundance of *Cycladophora davisiana* as a stratigraphic tool was introduced by Hays *et al.* (1976) when it was observed that abundances of this deep-water dwelling radiolarian coincided with the oxygen-isotope record. Within this correlation, the greatest peak in abundance within the last 130 ka was found to correspond to the isotope maximum attributed to the last glacial maximum dated by ^{14}C analysis (Hays *et al.* 1976). Although the peaks and troughs in *C. davisiana* abundance are consistent in Southern Ocean cores (Hays *et al.* 1976), Mélières *et al.* (1996) have determined the implication of high abundances of *C. davisiana* reflecting glacial stages alone is not supported. They contend that cores south of the PF in the Atlantic sector

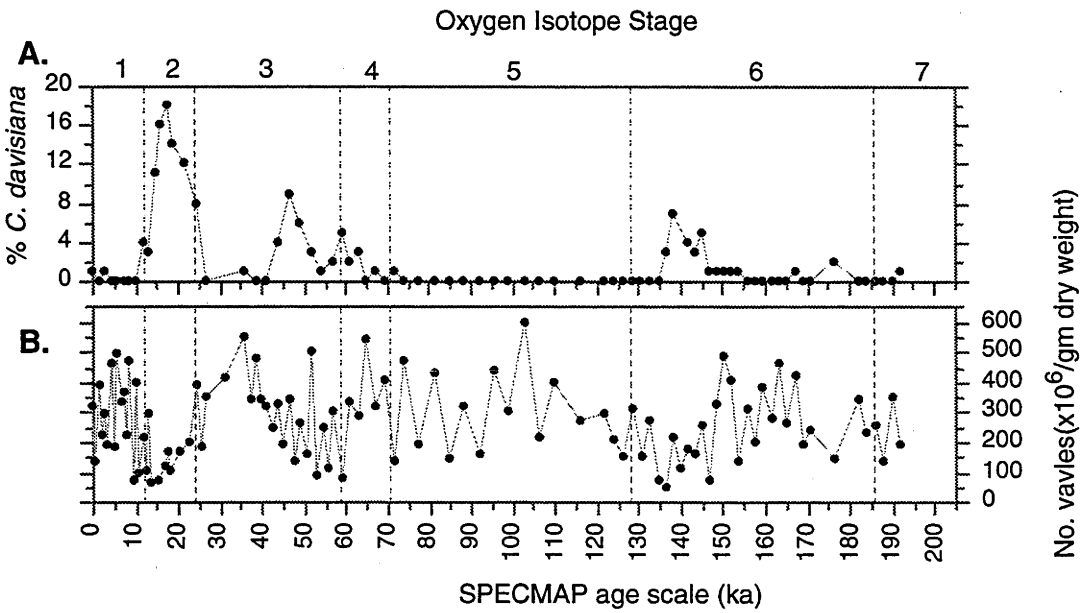

Figure 6.8. Relative abundance of the radiolarian *Cycladophora davisiana* against the SPECMAP age scale (**A**), and in comparison with the ADA curve (**B**) in French core MD88-787. High abundances of the radiolarian in the sediments are observed when diatom numbers in the sediments are reduced. *C. davisiana* data from Bareille (1991).

show high abundances of *C. davisiana* from isotope-stage 2 to 4 and low abundances in glacial isotope-stages 6, 8 and 10. Originally, Hays *et al.* (1976) suggested the abundance curves could be matched through the cores. Low abundance peaks (<5%) occurred at the surface and during isotope stage 3, contrasting with high abundances peaks in isotope stage 2 (>20%) and isotope stage 4 (10-15%) in cores of the South Atlantic and the western Indian Ocean. Abundances of *C. davisiana* were not found to be influenced by changes in SST (Hays *et al.* 1976, Williams and Keany 1978).

The plot of *Cycladophora davisiana* relative abundance in core MD88-787 (Bareille 1991 and pers. comm. 1997) against time and isotopic stages (Figure 6.8), exhibits the large peak in abundance approaching 20% as observed by Hays *et al.* (1976). The second increase peak in abundance (~10%), generally attributed to isotope-stage 4 (Hays *et al.* 1976, Mélières *et al.* 1996), is observed in the early-mid part of isotope-stage 3 (~45 ka). A smaller peak (5%) is observed at the transition between isotope-stage 3 and 4. There are no recorded abundances of *C. davisiana* through isotope-stage 5. The third obvious peak in abundance (8%) is observed in late isotope-stage 6, with a last minor abundance peak noted just after the start of isotope-stage 6.

Comparing the *Cycladophora davisiana* relative abundance to the determined absolute diatom abundance (ADA) curve, an inverse correlation is discernible at least in stages 1 to 4 (Figure 6.8). Increased abundances in the sediments of *C. davisiana* are noted when ADA's are decreased. Hypotheses related to the oceanographic conditions under which high abundances of *C. davisiana* occur were put forward by Morley and Hays (1983) based on modern conditions in the Okhostk Sea where *C. davisiana* has been observed in large abundances. They suggest the ocean was extensively ice covered during winter and early spring. The summer melt-back of the ice resulted in low surface salinity waters that capped an otherwise stable water mass below a strong sub-surface temperature minimum. The period of melt-back was brief allowing biological productivity but retarding the mixing of the low salinity surface waters with those underlying them. The increase of ice cover would have increased the dispersion of polar winds to the north (Morley and Hays 1983). Other workers have since associated past high abundance peaks of *C. davisiana* with changes in the circumpolar deep water characteristics (including North Atlantic deep water abatement) and the increase of melt water from icebergs or sea-ice (Corliss 1983, Labeyrie *et al.* 1986, Burckle and Cirilli 1987, Shemesh *et al.* 1994). Such oceanographical changes recorded from other proxies (IRD, oxygen isotope anomalies, faunal changes) are inferred to exhibit past conditions representative of the modern environmental regime in which *C. davisiana* is observed.

These hypotheses, along with other evidence for decreased productivity in the last glacial maximum and other periods, will be considered later in the chapter. Nevertheless, such

conditions as linked positively with the increased abundance of *Cycladophora davisiana* in the sediments are quite plausible in explaining the decreased response of diatom abundances in the sediments during the same periods.

6.3. CORE MD88-779

6.3.1 DIATOM RECOVERY

MD88-779 was taken during the 1988 French ASPARA IV cruise in the southeast Indian Ocean. The core is situated on the South Tasman Rise (47°50.69'S, 146°32.75'E) at a depth of 2260m and has a recovery of 6.70m (Figure 6.1). Indications from initial micropalaeontological summaries of the core (pers. comm. Dr J. Duprat, and Dr J.-J. Pichon 1994) suggest the first two glacial cycles were covered in the first two metres of the core. The core was chosen for study as it was considered to contain the most northerly record of diatoms that could be used in SST estimation. The core is dominated by calcareous material.

Samples of 2.54 to 3.07 gm dry weight were silica-selective processed as outlined in Chapter 1. As a result of the wide preservational differences throughout the core, 600 to 850 fields of view were observed in an effort to obtain the 'normal' 300 maximum number of specimens. A second set of slides at a lower dilution (ie. sub-sampled 150µl from 50ml dilution instead of 100ml dilution), did not alleviate this problem.

Qualitative counts of the samples indicate the preservation of the diatom silica-frustules down-core was extremely variable and poor. Total specimen counts in most samples did not advance beyond a maximum of 50 specimens, and several samples were found to be barren (Appendix 6.5). The maximum number of specimens (221) were recovered at a depth of 120 cm. The ADA (Figure 6.7C) provides an indication of the sporadic recovery of diatoms from the samples down-core.

A total of 37 diatom species and taxa were observed in the core samples (Appendix 6.5). As such the core displayed no major reworking from diatom observations. The species encountered were predominantly warm-water fauna (*Fragilariopsis doliolus*, *Roperia tesselata*, *Hemidiscus cuneiformis*, *Azpeitia tabularis*, *Thalassiosira lineata*, *Thalassionema nitzschioides*) which included neritic species (*Delphineis* spp. *Trachyneis aspera*, *Cyclotella* spp, *Diploneis* spp, *Paralia* spp, *Chaetoceros* resting spores). Open-ocean species were also encountered (*Fragilariopsis kerguelensis*, *Eucampia antarctica*, *Thalassiosira lentiginosa*, *Thalassiosira gracilis*). The majority of samples were poorly preserved and showed high levels of dissolution making identification to species level often difficult (eg *Rhizosolenia* spp.). The relative abundances of species encountered down-core are presented in Figure 6.9. Here, species with >5% relative abundance are

plotted in section A of the figure whereas those with <5% are plotted separately in section B.

In general, the delicate, warm-water and neritic forms were in lower abundances than the open-ocean species. Distribution of warm-water and benthic/neritic species in the Tasman Sea was reported by Harper (1974). Her study also had poor diatom recovery in down core analysis. The diatom taxa described in core MD88-779 fall broadly in line with the description of tropical taxa of Jousé *et al.* (1971) and the subtropical/temperate assemblage of Abbott (1973). Most species, however, have been observed in sediments of the Indonesian Archipelago (van Iperen *et al.* 1993) and indicate the generally warmer water signal that is most likely linked to the Tasmanian coast, the East Australian Current and the latter's eddies.

Species with greatest abundances were those more heavily silicified, in particular *Fragilariopsis kerguelensis, Thalassiosira lentiginosa, Azpeitia tabularis* and pole ends of the combined *Thalassiothrix /Trichotoxon* group, and to a lesser extent the warm-water forms *Fragilariopsis doliolus, Hemidiscus cuneiformis* and *Thalassionema nitzschioides*. Generally, through each isotopic stage, variations in the diatom species assemblage could be observed.

The diatom species record begins with robust, dissolution-resistant species indicative of warm-water flora in the latter phase of isotope-stage 7 (Fig. 6.9). Diatom assemblages tend towards more transitional and more resistant species at the start of isotope-stage 6, which prior to the loss of the diatom signal for the remainder of this isotopic stage indicate a possible cooling of the waters with the increase and presence of *Eucampia antarctica*. Only very rare *Thalassiosira lentiginosa* and *Cyclotella* spp. were noted in the remainder of isotope-stage 6. No other diatom record was preserved in the sediments. The presence of *Cyclotella* spp. in oxygen-isotope-stage 6 is not well understood, as the species is considered to have a neritic affinity (Foged 1978). Its presence could record a localised bloom event from warm-water eddies.

The transition to isotope-stage 5 re-instates the abundance of diatoms in that interval with robust, dissolution-resistant forms reflecting the open-ocean, but with minor input from warmer species (ie. *Hemidiscus cuneiformis* and *Roperia tesselata*). Through the duration of isotope-stage 5 increased warm-water flora are preserved in the sediments along with the open-ocean species. This record is rather abruptly dissected at the isotope-stage 4/5 boundary by a few robust species, but continues with increased warm-water flora through isotope-stage 4. Isotope-stage 3 shows decreasing variation in the warm-water flora. Just prior to the isotope 2/3 transition, cooler open-ocean taxa are observed (eg.

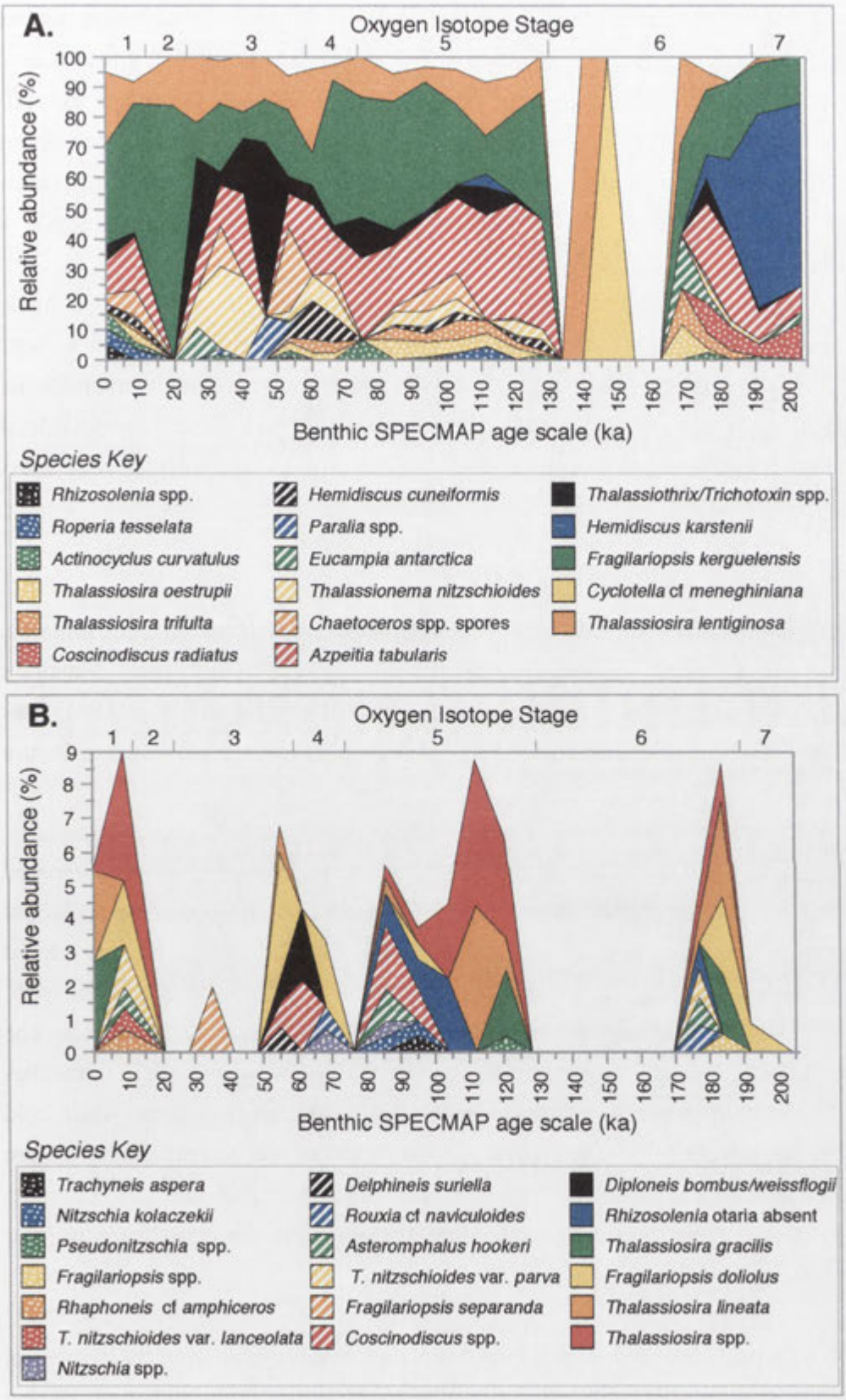

Figure 6.9. Diatom relative abundance over SPECMAP time in core MD88-779. **A**). Species with relative abundances greater than 5%; **B**) Species with relative abundances less than 5%.

Fragilariopsis separanda and *Eucampia antarctica*). Isotopic stage 2 as noted earlier contained very few diatoms in the sediments. Only a few specimens of *Thalassiosira lentiginosa* and *Fragilariopsis kerguelensis* were observed. Following the end of isotope-stage 2 the re-introduction of possibly the greatest diversity of warm-water to open-ocean species observed occurs in isotope-stage 1. Neritic species, probably indicative of warm-water eddies were also observed (eg *Chaetoceros* resting spores and *Rhaphoneis* spp.).

The advanced degree of dissolution and poor diatom recovery in core MD88-779 made SST and sea-ice estimation unachievable. Although the diatom abundance was considerably reduced other siliceous microfossils were present. Such microfossils included silicoflagellates (*Dictyocha* and *Distephanus* taxa), radiolarians, endoskeletal dinoflagellates, sponge spicules and phytoliths. Of these taxa, sponge spicules were most commonly encountered.

6.3.2. SILICOFLAGELLATE RECOVERY

Recovery of silicoflagellate material allowed another opportunity from siliceous remains, to indicate relative past sea-surface temperature at this core site. Mandra's *Dictyocha/Distephanus* ratio (Mandra 1969, Martini 1977, DeFelice and Wise 1981) was employed. The counts, ratio and estimated SST range for this core are presented in Figure 6.10A-C.

Estimates of general SST derived from the Mandra ratio are interesting when compared alongside the variation in diatom assemblages. Cold SST in isotope-stage 7 is not reflected in the warm-water diatom assemblage observed. The results are considered inaccurate in the cold temperature range (<5°C) due to the lack of *Dictyocha* spp. observations which justify the resolution of the ratio (refer to Fig. 6.10 A and C). The decreasing SST trend to colder temperatures in the early stage of isotope-stage 6 matches the diatom flora shift from warm to cool species records during the same time. Again cold SST estimates are inaccurate both from the point of view of the corresponding diatom flora records and the lack of *Dictyocha* in the ratio used to derive the SST estimate. However, the diatom flora observed in the core also supports the trend for a warmer water flora between 90-95 ka.

A very warm SST provided for isotope-stage 4 is not as strongly supported by the warm, yet robust, dissolution resistant diatom species that are observed in the sediments during this stage. Both cold SST estimates during isotope-stage 3 are not considered highly accurate due to the loss of *Dictyocha* spp., however, the later of the two estimates is in coincidence with the cooler flora elements observed prior to the following glacial where no record is provided. Finally the very warm SST estimates are in tune with the warm-water flora observed during isotope-stage 1.

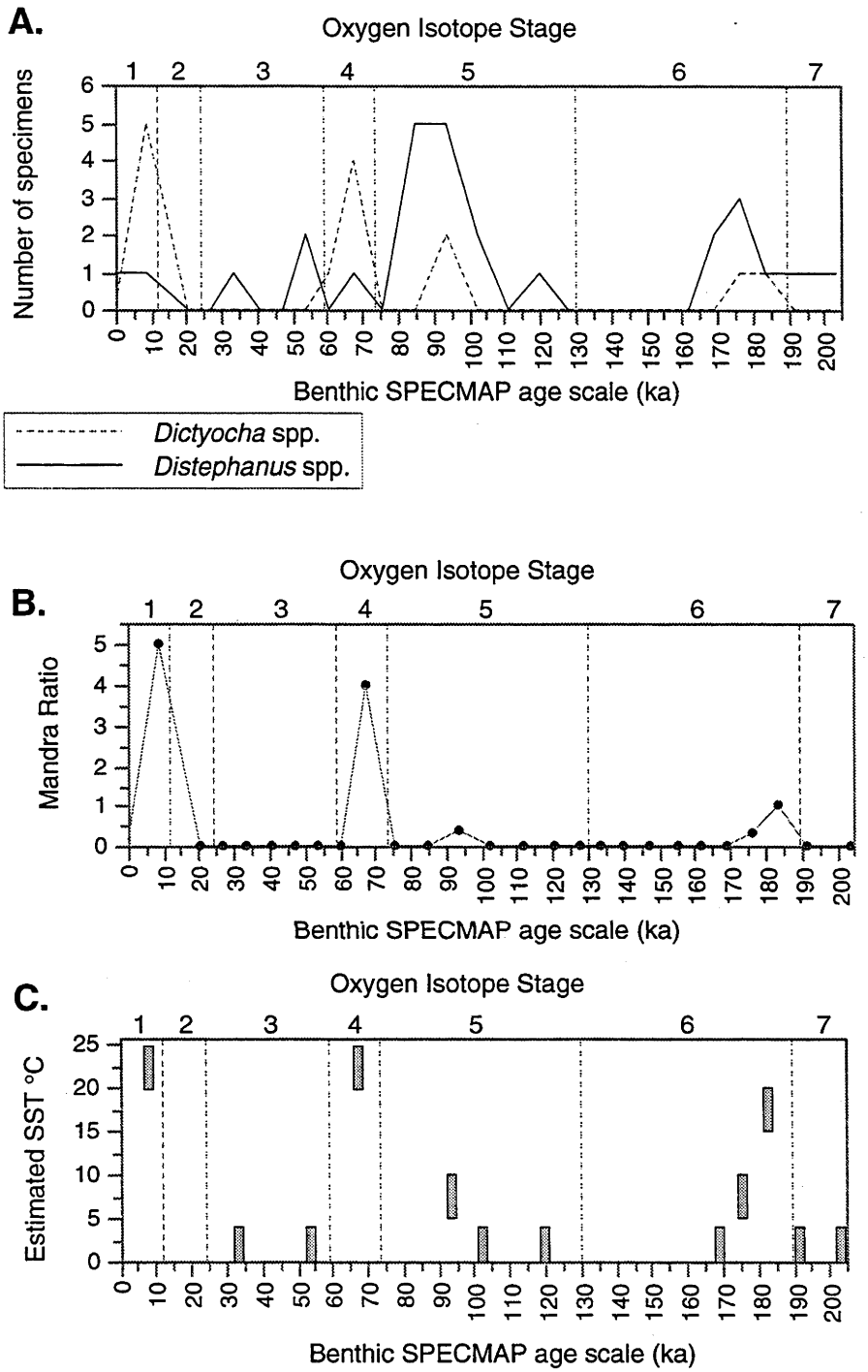

Figure 6.10. **A**) Number of *Dictyocha* & *Distephanus* silicoflagellate specimens encountered in core MD88-779. **B**) Mandra's ratio of *Dictyocha* to *Distephanus* (D/D) species. **C**) Temperature estimates from the Mandra ratio are provided in 5°C ranges. The reliability of the cold water estimates are low because the D/D ratio can not be formed with the lack of *Dictyocha* species, see distribution in **A** above. All plots against SPECMAP age and oxygen isotope stages.

The SST estimates are not considered highly reliable because the dissolution and lack of occurrence of silicoflagellates in the sediments makes their use questionable for the small insight they provide, albeit that most estimates are coincident with changes in the diatom floral record. Dow (1978) who compared radiolarian-derived SST records with that of the *Dictyocha/Distephanus* ratio reached the same conclusion.

6.3.3. PHYTOLITH RECOVERY

Phytolith material (Appendix A2, pl. 17 Figs 1-9) was observed sporadically down-core at the following levels; 0, 130, 140, 220 and 230 cm (approximately falling within the Holocene, 100-110 ka, and 170 ka respectively). Previous core studies indicate that phytoliths are common in the Tasman Sea region, (~31°S, 153°E, Harper 1974, and DSDP Leg 90, Locker and Martini 1986) and southeast of New Zealand (site 594, Locker and Martini 1986). The phytolith casts most readily identifiable were those comprising the grasses, although larger plate-like casts of trees and shrubs were observed. Locker and Martini (1986) attributed the distribution of phytoliths in the Tasman Sea sediments to arid conditions in central Australia during glacial periods, and their subsequent entrainment in intensified westerly winds. This is the first known report of phytoliths in core material this south of Australia. The two occasions of Phytolith occurrence prior to the Holocene occur just prior to the end of the diatom signal in isotope-stage 6 and within isotope-stage 5d, when an increase in robust, dissolution resistant diatoms is evident.

6.3.4. SUMMARY

Core MD88-779 contains a generally poor record of diatom preservation. Greatest diatom abundances are found when surface waters appear to be warmer based on silicoflagellate SST estimations. Diatom floral assemblages generally follow this interpretation, although cold water diatoms or more open-ocean assemblages are missing during isotopic stages 2 and 6. Isotope-stage 4 does not appear to have experienced cool conditions as suggested by the diatom flora. Sedimentation rates do not appear to follow warm/cold phases or the degree of diatoms preserved. Sea-surface temperature and sea-ice estimates could not be determined from the diatoms preserved.

The most distinguishing feature of the diatom record from core MD88-779 is its lack of diatoms during glacial stages. Increases in open-ocean flora and presence in the sediments had been expected as a contrast to the warm-water flora observed. As a result of the "missing" records the following discussion centres on other regional investigations during these isotopic stages.

Recent palaeoceanographic studies located northeast of core MD88-779 and north of the current Subtropical Convergence (STC) were performed by Martinez (1994), Barrows (1995), Passlow *et al.* (1997), and Nees (1997) (Figure 6.11). Benthic ostracod records

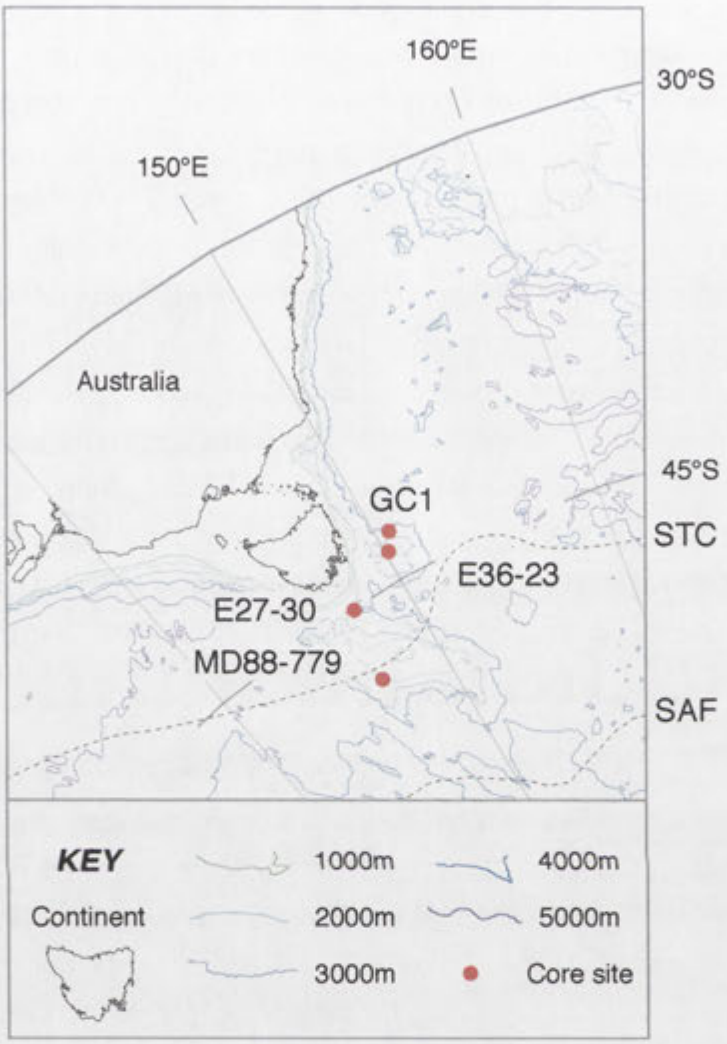

Figure 6.11. Location of recently studied cores discussed in the text adjacent to MD88-779, and in relation to the Subtropical Convergence (STC, Orsi *et al.* 1995). Bathymetry from GEBCO (1992). SAF = Subantarctic Front.

from E27-30 (45°04'S, 147°13'E; Passlow *et al.* 1997) were used to indicate the STC was northward of its current position, with concurrent increases in productivity during isotope-stages 6, 4, and 3 through to the 2/1 boundary. Core MD88-779 is currently situated at the current STC boundary interpreted by Orsi *et al.* (1995). Preliminary unpublished benthic foraminifera results from this core (Dr Nees pers. comm. 1997) indicate the high productivity related *Epistominella exigua* is in low abundances through the length of the core. The exception being in isotope-stage 6 where very large abundances, considerably greater than those reported in core E27-30, suggest the STC is not as far north as previously presumed and probably still in the vicinity of core MD88-779. This is contradictory to the isotope-stage 6 results of Martinez (1994) and Passlow *et al.* (1997). Their results suggest the STC considerably further north (~43°S). Nees (1997) who worked on the same core as Martinez (1994) (E36-23; 43°53'S, 150°03'E) suggested that caution should be applied to an interpreted northward movement of the STC in isotope-stage 6. Since the integration of an enhanced southward flowing East Australian Current during this stage may have stabilised any northward movement of the STC. However, evidence from core FR1-94-GC3 (44°15.38'S, 149°59.47'E) taken from the East Tasman Plateau also suggests a northward shift of the STC (Barrows 1995, and manuscript in prep.).

Oceanographically, should the Indonesian Archipelago throughflow be reduced due to sea-level fall in glacials periods, then an increased western boundary current would be perceived in the Tasman Sea region and possibly further south due to the closure of Bass Strait and its eastward-flowing water mass (Tomczak and Godfrey 1994). Should increases in the East Australia Current be enhanced and eddy formation pushed somewhat further south, it would assist in explaining the presence of the neritic diatom *Cyclotella* spp. in the sediments of core MD88-779 during isotope-stage 6.

A northward movement of the STC in Stage 6 is not currently reflected in the diatom observations, where a lack of diatom preservation obscures any attempt at discerning a northward movement of cold surface waters. The presence of the epifaunal benthic foraminifera *Cibicides wuellerstorfi* in core MD88-779, however, has been related to lateral advection which is present during isotope-stage 6 (Nees, pers. comm. 1997). This species is also observed in higher abundances in isotope-stage 2 where the diatom signal is once again removed from the sediment record. The two interpretations combined add support to the idea that increased bottom-water transport along the base of the south Tasman Rise into the Tasman Basin has winnowed away some of the sedimentary record, in particular to that of the diatoms, during isotopic stages 2 and 6. It does not necessarily explain the increased abundances of the *Epistominella exigua* which is otherwise taken as a productivity indicator species known to profit with increases of phytoplankton detritus to the sea-floor (Smart *et al.* 1994). A discussion on the role of bottom-water will be

made in section 6.7.

Southward movement of the STC was suggested from core E27-30 (Passlow *et al.* 1997) in isotopic-stage 5e and during the Holocene. Evidence for such a movement from the diatom records can not support or deny such a hypothesis, yet during both periods warm-water floras are present.

Core MD88-779 is undergoing continued study (Nees et al., in prep.) in order to elucidate from other microfossil elements, the palaeoceanographic history along the southwestern flank of the South Tasman Rise.

6.4 CORES MD88-784 AND MD88-787

Cores MD88-784 and MD88-787 were also recovered during the French ASPARA IV cruise in 1988. The two cores are separated from the other by approximately 2°S latitude and are located along the north-southward trending Tasman Fracture Zone of the Mid-Ocean Ridge (Figure 6.1, Table 6.1). Sediment samples from the two cores were taken at 10cm intervals and processed as described in Chapter 1 (Appendix 1.1).

Both cores are comparatively discussed in this section which covers aspects of their diatom recovery and subsequent analysis yielding both SST and sea-ice estimates over time.

6.4.1 Diatom recovery and factor analysis

Diatoms were found in abundance throughout both cores (Appendices 6.6 and 6.7). This permitted quantitative assessment of the species and their abundances via factor analysis. A total of 69 diatom species and taxa were recorded in core MD88-787 and a total of 57 diatom species and taxa in core MD88-784. The silicoflagellate taxa, *Dictyocha* spp. and *Distephanus* spp., were also recorded in both cores although no *Dictyocha* spp. were observed in core MD88-787.

Due to the variation in the number of species considered suitable for factor analysis within the Pichon *et al.* (1992a) DTF model (henceforth referred to as the DTF 166/34/3 model) and that of the thesis DTF model (hereafter referred to as the DTF 109/24/6 model), the raw count data was ordered into a format with additive subtotals (refer Appendices 6.6 and 6.7). As described through Chapters 2 and 3, many diatom species or taxa groupings were considered ineligible for analysis and production of SST estimates. To reflect this feature all diatom data considered in the DTF 109/24/6 model were listed and defined by *Diatom subtotal 1* (Appendices 6.6 and 6.7). Additional diatom species and silicoflagellate taxa were included in the DTF 166/34/4 model. To account for this

addition, the raw count data of each core was accordingly supplemented by the species originally included in the Pichon *et al.* (1992a) analysis. The result in terms of data total is provided under the *Silica subtotal 3* (Appendices 6.6 and 6.7).

The two diatom count totals were used in all SST derivations for both cores under each respective DTF model. The percentage of information used by the 24 species in DTF 109/24/6 model (Diatom subtotal 1) and the 34 species/taxa in DTF 166/34/4 (Silica subtotal 3) are plotted over time for each core in Figure 6.12A and B. Overall, the data used as a percentage of the diatom subtotal is greater than 84% for DTF 109/24/6 and greater than 89% for DTF 166/34/4.

Two other diatom taxa were not included in either of the diatom or silica subtotals, which are otherwise used in the two DTF models, since neither taxon were previously identified in diatom databases. The two taxa are *Dactyliosolen antarcticus* and *Chaetoceros* spp. resting cells. These two taxa make up *Silica subtotal 4* which can be considered the grand total of observed siliceous taxa recorded in the core samples (ie. diatoms and silicoflagellates, Appendices 6.6 and 6.7).

Comparison of the data used through the history of the two cores for both DTF models indicates a more stable inclusion of data in the DTF 166/34/4 model over that of the DTF 109/24/6 model. Distinct data decreases are apparent in the DTF 109/24/6 model during cool phases, especially in isotope-stages 2 and 6. The difference between the two models is accounted by the inclusion of the silicoflagellate *Distephanus* spp. during these intervals, and an increase in the number of *Thalassiothrix/Trichotoxon* spp. pole-ends. Both these species were considered invalid for use in the DTF109/24/6 model as a result of poor counting methodology and restriction to diatom analysis, yet both species do indicate in down-core quantitative analysis that their inclusion can be important in cool-event interpretation. Alternatively, the data percentage decrease for the DTF 109/24/6 model also indicates that several rarer species (ie. those species with relative abundances in the database <2%) are important in providing information for cool periods that are not necessarily picked up by the more robust and abundant species recorded.

During warmer intervals, departures in the degree of data inclusion remain considerably similar and high between the two models (>95%, Figures 6.12A-B). This suggests estimates should not vary considerably between the two models assuming that the differences in species included, and their abundances, are equivalent. The higher abundances of data under the DTF 166/34/4 model are mainly attributable to the inclusion of the two silicoflagellate taxa.

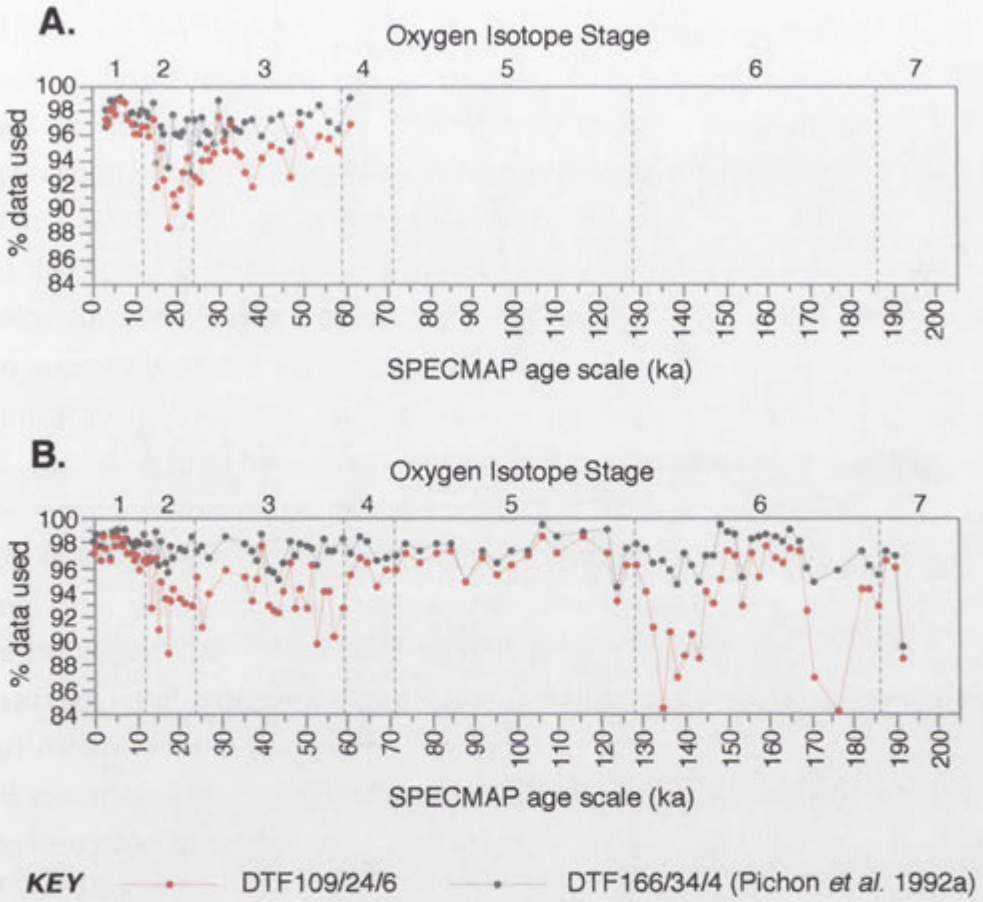

Figure 6.12. Summary of diatom data used in the two diatom transfer functions used to derive SST estimates. **A**) Core MD88-784. **B**) Core MD88-787. In both cores a reduction of the percentage of the diatom information used in the thesis-developed DTF 109/24/6 occurs during cool phases. This is particularly evident in isotopic stages 2 and 6. The DTF 109/24/6, otherwise contains similar high percentages of diatom information as noted in the DTF of Pichon *et al.* (1992a). It should be noted that differences exist between the diatom totals used in each DTF (refer Appendices 6.6 and 6.7).

Factor analysis on the core data using the two DTF models are presented separately for each core in Figures 6.13 and 6.14. Here discussion of each core is treated separately.

Core MD88-784.

DTF 109/24/6 Model

Factor analysis under the DTF 109/24/6 model is illustrated by individual factors in Figure 6.13A. Dominance of Factor 1 (Open-ocean) through the length of the core is apparent, although a slight increasing trend in the degree of dominance is evident from isotope-stage 3 to isotope-stage 1. An interplay between Factor 2 (sea-ice cover) and Factor 6 (POOZ) is surprising given the nature of their geographic distance (Chapter 4). In contrast to Factor 1, the weight carried by these two factors is steadily decreased from subdominance in isotope-stage 3 that lasts partly through isotope-stage 2. Important to note in isotope-stage 1 is the intertwining with Factor 3 (subantarctic) by the two cooler factors. This means increased warm-water features in the region and a marked decrease of cool water input. Factor 3 has generally very low factor loadings that indicate poor warm-water diatom input over time. As mentioned above, this factor is noted to increase only in isotope-stage 1. Factor 4 (transport/island) is here more heavily interpreted as a transport indicator. Increases in this particular factor are noted within isotope-stage 2 and at the transition between isotope-stage 2 and isotope-stage 3. High loadings of the factor are also evident in isotope-stage 3, and are in contrast to the low loadings and thus, effect in isotope-stage 1. Factor 5 (maximum winter sea-ice edge), a negative factor (section 5.3.5), expectedly shows increases in factor loadings that are opposite to those shown by Factor 6 and Factor 2. Consequently, increases in Factor 5 are met with decreases in Factors 2 and 6. The lowest factor loadings observed for Factor 5 occur in isotope-stage 3, particularly close to the isotope transition between isotope-stage 2 and isotope-stage 3 (~27 ka). Low values diminish in prominence through isotope-stage 2 and isotope-stage 1, thus suggesting that the sea-ice boundary, and its influence, was retreating southwards from the core region.

Communality values of each core sample determined from the factor analysis performed are illustrated in Figure 6.13B by red points. High communality values are observed (>0.8), along the length of the core with exception to two samples with values at ~0.7. Only one value was noted to contain a no-analogue event (at 27 ka). This no-analogue event occurs because of an abundance of *Thalassiosira gracilis* (8.1%) which exceeds the 109 Natural database's total relative abundance of 7.7% for that species (Table 3.10).

DTF 166/34/4 Model

Results of factor analysis employing the DTF 166/34/4 model are also plotted for comparison in Figure 6.13C. Similar to the DTF 109/24/6 model, factor dominance is maintained throughout the core by the open-ocean related Factor 1, which also shows an

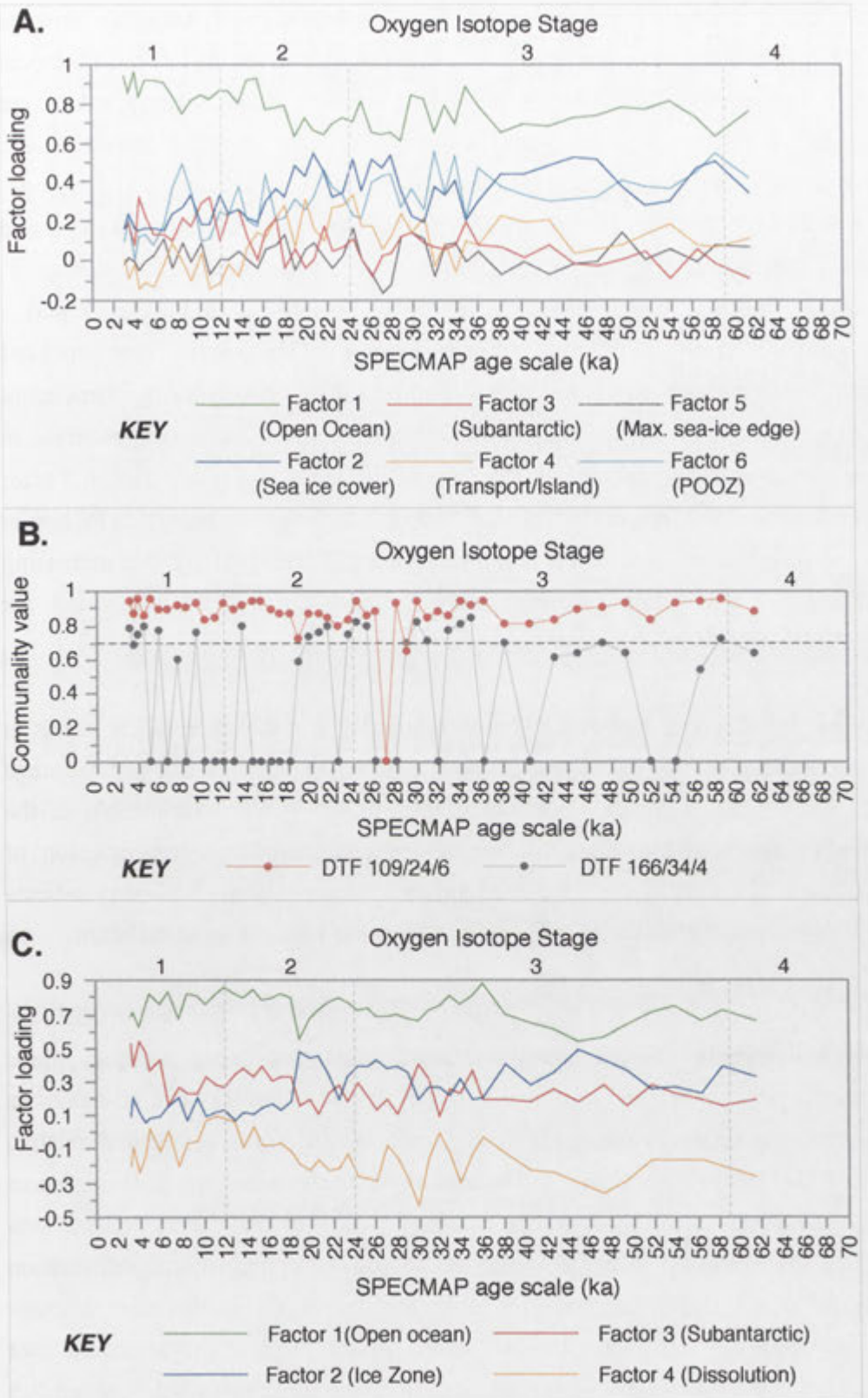

Figure 6.13. Factor analysis results of core MD88-784 using DTF109/24/6 (**A**), and the DTF166/34/4 (**C**, Pichon *et al.* 1992a). Respective communality values for each sample under the two DTF's are jointly displayed in **B**. Refer to text for discussion. Dashed horizontal line in **B** refers to the 0.7 communality cut-off value. All zero communality values indicate non-analogue conditions thus, SST estimates are to be treated with caution.

increasing trend in dominance from isotope-stage 3 to isotope-stage 1. Interplay between Factors 2 (Ice zone influenced) and Factor 3 (subantarctic) are evident in this DTF model and in terms of the degree of influence held by Factor 3, factor loading values are considerably increased in reference to the DTF 109/24/6 model. Factor 3 shows a very gradual increase in influence, becoming increasingly dominant in the later part of isotope-stage 1. Factor 2 has generally high factor loading values throughout isotope-stage 3 and isotope-stage 2 which later decrease in late isotope-stage 2 and through isotope-stage 1. Highest loadings (influence) of Factor 2 are noted in periods when Factors 1 and 3 decrease, particularly in isotope-stage 2 and isotope-stage 3. The fourth factor attributed to dissolution, is a negatively dominated factor (section 5.2.1). This factor is independent of the other three factors in that no direct association between a heightened decrease in Factor 4 is related entirely to increases or decreases of influence in any one factor. Factor 4 acts independently of the temperature related factors 1 to 3 as was intended (Pichon *et al.* 1992 a, b). Over time, dissolution has diminished as suggested by the increasing positive influence of the factor. However, one question remains: *What controls the dissolution* ?

Factor analyses performed by the two DTF models indicate that the same major trends in warming have occurred from what appears to be a cool isotope-stage 3 and isotope-stage 2. The finer differences provided by the models through time are attributable to the differentiation of extended biogeographic regions in one model and the inclusion of dissolution in the other. Results from the communality value analyses, however, indicate that further analysis and derivation of SST by the two models will be quite different.

Communality values for core samples derived from the DTF 16/34/4 model are considerably low (Figure 6.13B, grey points). Most analogous samples have communalities greater than 0.5 and less than 0.9. Twenty-one samples have no-analogue events. These no-analogue situations (Table 6.2) are derived from augmented relative abundances of the following species : *Thalassiothrix/Trichotoxon* spp., *Distephanus* spp., *Azpeitia tabularis*, and *Fragilariopsis separanda*. As previously detailed (sections 3A.1.4, 4.3.1), communality values describe the amount of compositional information from the original sample that is accounted for in the factor analysis. In this case although the DTF 166/34/4 model included between 93-99% of the original diatom count data (Figure 6.12A), under factor analysis the data used from the samples varied between 0.5 (50%) and 0.9 (90%) of this 93-99% total. Should the 0.7 cut-off criteria for communality be enforced in adjunct to the no-analogue events, a total of 31 samples should not be used with any confidence in defining SST estimates on the core using the DTF 166/34/4 model. This is in striking comparison to the removal of only one SST estimate under the DTF 109/24/6 model (three samples would be removed if a 0.8 communality value cut-off criterion was imposed - section 4.3.1).

Depth (cm) (SPECMAP age (ka))	Species	Relative abundance in sample (%)	Max. rel. abundance in 109 or 166 DB (%)
DTF 109/24/6 model no-analogue samples			
290 (27.10)	*Thalassiosira gracilis* Group	8.065	7.7
DTF 166/34/4 model no-analogue samples			
40 (5.05)	*Thalassiothrix/Trichotoxon* spp.	4.467	3
60 (6.75)	*Thalassiothrix/Trichotoxon* spp.	3.401	3
80 (8.5)	*Thalassiothrix/Trichotoxon* spp.	3.311	3
100 (10.25)	*Thalassiothrix/Trichotoxon* spp.	8.146	3
100 (10.25)	*Distephanus* spp.	5.199	5
110 (11.13)	*Thalassiothrix/Trichotoxon* spp.	5.476	3
110 (11.13)	*Distephanus* spp.	5.187	5
120 (12)	*Thalassiothrix/Trichotoxon* spp.	3.553	3
130 (12.88)	*Thalassiothrix/Trichotoxon* spp.	4.097	3
150 (14.63)	*Thalassiothrix/Trichotoxon* spp.	4.078	3
160 (15.5)	*Distephanus* spp.	5.546	5
170 (16.38)	*Distephanus* spp.	6.219	5
180 (17.25)	*Azpeitia tabularis*	6.609	5
180 (17.25)	*Thalassiothrix/Trichotoxon* spp.	7.826	3
190 (18.13)	*Azpeitia tabularis*	5.017	5
190 (18.13)	*Thalassiothrix/Trichotoxon* spp	5.017	3
240 (22.6)	*Fragilariopsis separanda*	3.98	3.9
280 (26.2)	*Fragilariopsis separanda*	4.207	3.9
290 (27.1)	*Fragilariopsis separanda*	4.355	3.9
300 (28.01)	*Fragilariopsis separanda*	3.994	3.9
340 (32)	*Fragilariopsis separanda*	4.628	3.9
380 (36.16)	*Thalassiothrix/Trichotoxon* spp.	3.161	3
400 (40.5)	*Fragilariopsis separanda*	4.069	3.9
450 (51.75)	*Distephanus* spp.	7.063	5
460 (54.03)	*Distephanus* spp.	5.079	5

Table 6.2. No analogue samples in core MD88-784 under both DTF models. *Distephanus* spp. = silicoflagellate. DB = database.

MD88-787.

DTF 109/24/6 Model

Factor analysis of core MD88-787, the more southerly-located core, under the DTF 109/24/6 model is presented by each of the six factors in Figure 6.14A. The most heavily represented factor loadings are observed under Factor 1 (Open-ocean) through most of the core's history. Digressions in dominance are observed during isotope-stages 6, 3 and

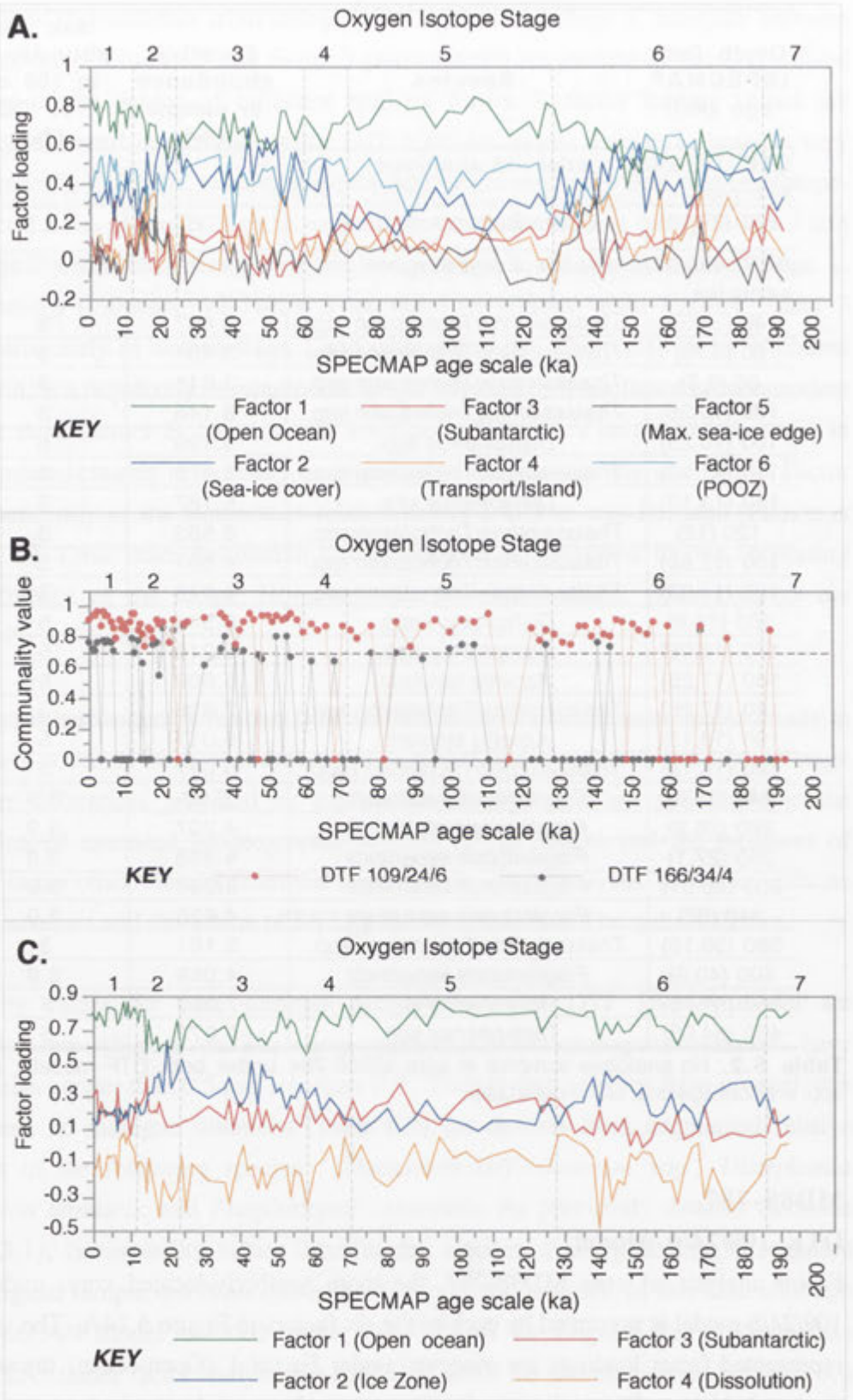

Figure 6.14. Factor analysis of core MD88-787 using DTF 109/24/6 (**A**) and DTF166/34/4 (**C**, Pichon *et al.* 1992a). Respective communality values for each sample under the two DTF's are jointly displayed in **B**. Refer to text for discussion. Dashed horizontal line in **B** refers to the 0.7 communality cut-off value. All zero communality values indicate non-analogue situations thus, SST estimates are to be treated with caution.

2 where the influence of Factors 6 (POOZ) and 2 (sea-ice cover) are dominant. During isotope-stage 7 and until the later part of isotope-stage 6, Factor 6 has its highest expression. This is contrary to all other stages where the factor oscillates between factor loading values of 0.2 and 0.5, in a near mirror image to the fluctuations made by Factor 1. Factor 1 expression is greatest during isotope-stage 5 and isotope-stage 1. Factor 2 (sea-ice cover) influence remains low during these two interglacial periods, but indicates cool conditions in isotope-stage 3 as noted in core MD88-784. The subantarctic factor (Factor 3) has a signal indicative of changes through cool and warm phases albeit that the factor loading values are low in this core. Increased signals from this factor are observed approximately at 165 ka (isotope-stage 6), 130 ka (isotope-stage 5/6), 100 ka (isotope-stage 5), 75 ka (isotope-stage 5), ~13 ka (isotope-stage 2), ~7 ka (isotope-stage 1), and occur where increases in Factor 1 are observed. Factor 4, the transport/island factor, is noted lagging in its response to increases in Factor 2, mostly negatively in tune with decreases in Factor 6, and also associated with the decreased ice-edge influence of Factor 5 (remembering that Factor 5 is a negative factor). This suggests increases in the transport/island factor are recorded in the sediments when the POOZ influence of Factor 6 is decreased along with that of the maximum winter sea-ice edge, but always after increased sea-ice cover around Antarctica. The transport factor is observed with higher loadings in this core than MD88-784.

Communality values from the DTF 109/24/6 model remain for the most part above 0.8 and approach unity during warm phases (Figure 6.14B). Non-analogue situations are more frequent in this core and are common in isotope-stages 6 and 7. The species, which are noted in greater relative abundances in the core than in the 109 Natural database, include *Thalassiosira gracilis, Fragilariopsis kerguelensis*, and *Fragilariopsis separanda.* A total of 17 samples are found to have no-analogue situations between the core and the database (Table 6.3).

DTF 166/34/4 Model

Comparative factor analysis using the DTF 166/34/4 model illustrates less deviation in the first and dominant Factor 1 (Open-ocean), than that observed in the DTF 109/24/6 model, particularly in isotope-stage 6 (Figure 6.14C). A mirror image response is displayed by Factor 2 (ice zone) and only during isotope-stage 2 does Factor 2 cross Factor 1, suggesting a major change in sea-surface environment. The interplay between Factors 2 and 3 continues to be observed in this core as in core MD88-784. Warm phases indicated by the dominance of Factor 3 over Factor 2 and cool phases by the reverse condition. Factor 4 (dissolution, negative relation) is elevated during isotope-stage 6 and increasingly through isotope-stage 3 to peak within early isotope-stage 2.

Depth (cm) (SPECMAP age (ka))	Species	Relative abundance in sample(%)	Max. rel. abund. in 109 or 166 DB (%)
DTF 109/24/6 model no-analogue samples			
300 (24.33)	*Thalassiosira gracilis* Group	10.131	7.7
420 (46.5)	*Thalassiosira gracilis* Group	8.0	7.7
550 (67.25)	*Fragilariopsis kerguelensis*	83.056	82.4
600 (81.2)	*Fragilariopsis kerguelensis*	84.566	82.4
690 (116)	*Fragilariopsis separanda*	8.17	7.8
840 (148.6)	*Fragilariopsis separanda*	11.552	7.2
890 (157.7)	*Fragilariopsis separanda*	11.714	7.2
910 (161.5)	*Fragilariopsis separanda*	7.975	7.2
920 (163.4)	*Fragilariopsis separanda*	12.0	7.2
930 (165.3)	*Fragilariopsis separanda*	12.258	7.2
940 (167.2)	*Fragilariopsis separanda*	12.847	7.2
960 (171)	*Fragilariopsis separanda*	12.057	7.2
980 (182)	*Fragilariopsis separanda*	12.15	7.2
990 (184)	*Fragilariopsis separanda*	8.359	7.2
1000 (186)	*Fragilariopsis separanda*	8.17	7.2
1020 (190)	*Fragilariopsis separanda*	14.87	7.2
1030 (192)	*Fragilariopsis separanda*	10.788	7.2
DTF 166/34/4 model no-analogue samples			
40 (2.92)	*Fragilariopsis separanda*	4.382	3.9
100 (7.31)	*Fragilariopsis separanda*	5.405	3.9
100 (7.31)	*Distephanus* spp.	5.087	5
110 (8.04)	*Thalassiothrix/Trichotoxon* spp.	3.724	3
120 (8.77)	*Fragilariopsis separanda*	4.255	3.9
130 (9.5)	*Fragilariopsis separanda*	4.532	3.9
130 (9.5)	*Thalassiothrix/Trichotoxon* spp.	3.323	3
140 (10.23)	*Fragilariopsis separanda*	4.248	3.9
150 (10.96)	*Thalassiothrix/Trichotoxon* spp.	3.636	3
190 (13.88)	*Azpeitia tabularis*	5.031	5
190 (13.88)	*Thalassiothrix/Trichotoxon* spp.	3.459	3
210 (15.35)	*Thalassiothrix/Trichotoxon* spp.	4.928	3
210 (15.35)	*Distephanus* spp.	7.949	5
220 (16.08)	*Distephanus* spp.	8.215	5
230 (16.81)	*Distephanus* spp.	5.255	5
280 (21.67)	*Fragilariopsis separanda*	6.728	3.9
300 (24.33)	*Fragilariopsis separanda*	7.099	3.9
320 (27)	*Fragilariopsis separanda*	6.259	3.9
360 (38.63)	*Fragilariopsis separanda*	5.17	3.9
380 (41.25)	*Fragilariopsis separanda*	4.37	3.9
380 (41.25)	*Thalassiothrix/Trichotoxon* spp.	3.529	3
400 (43.88)	*Fragilariopsis separanda*	4.831	3.9
410 (45.19)	*Distephanus* spp.	5.152	5
440 (49.13)	*Fragilariopsis separanda*	4.977	3.9
450 (50.44)	*Fragilariopsis separanda*	6.354	3.9
470 (53.06)	*Thalassiosira trifulta*	2.651	1.9
500 (57)	*Thalassiosira trifulta*	1.955	1.9
510 (59)	*Thalassiosira trifulta*	1.977	1.9
530 (63)	*Distephanus* spp.	5.008	5
540 (65)	*Distephanus* spp.	7.895	5
560 (69.5)	*Thalassiothrix/Trichotoxon* spp.	4.407	3
570 (71.75)	*Distephanus* spp.	5.846	5

Depth (cm) (SPECMAP age (ka))	Species	Relative abundance in sample(%)	Max. rel. abund. in 109 or 166 DB(%)
580 (74)	*Thalassiothrix/Trichotoxon* spp.	4.427	3
600 (81.2)	*Fragilariopsis kerguelensis*	82.059	81
640 (95.6)	*Thalassiothrix/Trichotoxon* spp.	5.298	3
680 (110)	*Distephanus* spp.	5.183	5
690 (116)	*Fragilariopsis separanda*	7.74	3.9
700 (122)	*Fragilariopsis separanda*	4.539	3.9
710 (124.17)	*Fragilariopsis separanda*	4.585	3.9
730 (128.5)	*Thalassiothrix/Trichotoxon* spp.	4.427	3
740 (130.67)	*Thalassiothrix/Trichotoxon* spp.	8.946	3
740 (130.67)	*Distephanus* spp.	10.543	5
750 (132.83)	*Thalassiothrix/Trichotoxon* spp.	8.225	3
750 (132.83)	*Distephanus* spp.	6.349	5
760 (135)	*Thalassiothrix/Trichotoxon* spp.	12.333	3
770 (136.7)	*Thalassiothrix/Trichotoxon* spp.	5.625	3
770 (136.7)	*Distephanus* spp.	7.188	5
780 (138.4)	*Thalassiothrix/Trichotoxon* spp.	3.148	3
800 (141.8)	*Thalassiothrix/Trichotoxon* spp.	4.119	3
820 (145.2)	*Fragilariopsis separanda*	4.769	3.9
830 (146.9)	*Fragilariopsis separanda*	5.055	3.9
840 (148.6)	*Fragilariopsis separanda*	10.24	3.9
840 (148.6)	*Thalassiothrix/Trichotoxon* spp.	4.0	3
840 (148.6)	*Distephanus* spp.	7.04	5
850 (150.3)	*Fragilariopsis separanda*	5.436	3.9
860 (152)	*Fragilariopsis separanda*	5.055	3.9
860 (152)	*Thalassiothrix/Trichotoxon* spp.	3.949	3
870 (153.9)	*Fragilariopsis separanda*	4.18	3.9
870 (153.9)	*Thalassiothrix/Trichotoxon* spp.	4.18	3
880 (155.8)	*Fragilariopsis separanda*	6.49	3.9
890 (157.7)	*Fragilariopsis separanda*	11.081	3.9
900 (159.6)	*Fragilariopsis separanda*	6.359	3.9
910 (161.5)	*Fragilariopsis separanda*	7.625	3.9
920 (163.4)	*Fragilariopsis separanda*	11.25	3.9
930 (165.3)	*Fragilariopsis separanda*	11.533	3.9
930 (165.3)	*Thalassiothrix/Trichotoxon* spp.	3.794	3
940 (167.2)	*Fragilariopsis separanda*	11.878	3.9
940 ()167.2	*Thalassiothrix/Trichotoxon* spp.	5.297	5
960 (171)	*Fragilariopsis separanda*	11.296	3.9
960 (171)	*Thalassiothrix/Trichotoxon* spp.	4.983	3
970 (176.5)	*Fragilariopsis separanda*	7.442	3.9
980 (182)	*Fragilariopsis separanda*	11.927	3.9
990 (184)	*Fragilariopsis separanda*	8.0	3.9
990 (184)	*Thalassiothrix/Trichotoxon* spp.	3.7043	3
1000 (186)	*Fragilariopsis separanda*	7.788	3.9
1000 (186)	*Thalassiothrix/Trichotoxon* spp.	3.427	3
1010 (188)	*Thalassiothrix/Trichotoxon* spp.	5.655	3
1020 (190)	*Fragilariopsis separanda*	13.652	3.9
1020 (190)	*Thalassiothrix/Trichotoxon* spp.	7.167	3
1030 (192)	*Fragilariopsis separanda*	9.738	3.9
1030 (192)	*Thalassiothrix/Trichotoxon* spp.	6.742	3

Table 6.3. No analogue samples in core MD88-787 under both DTF models. *Distephanus* spp. = silicoflagellate. DB = database.

Communality values provided by the DTF 166/34/4 model are repeatedly low (Figure 6.14B). A total of 62 samples record non-analogue events that are related to ranked differences between the core and the 166 database concerning the species *Thalassiothrix/Trichotoxon* spp., *Distephanus* spp., *Fragilariopsis separanda*, *Azpeitia tabularis*, *Thalassiosira trifulta*, and *Fragilariopsis kerguelensis* (Table 6.3). A further nine samples are under the 0.7 communality cut-off value. Should all these samples be removed from SST estimation a sole 32 of the original 103 samples are considered useful for SST in core MD88-787 using the DTF 166/34/4 model.

In short, poor communality levels expressed by the DTF 166/34/4 model indicate that the 4 factor model does not take into account the variation contained within the core data. As commented in section 4.3.1 and 4.4, and by Le (1992), a simplified, reduced factor-number factor-model does not take into account each species most appropriate factor association. Consequently, providing a low communality value. In this respect the DTF 166/34/4 does not provide appropriate environmental analogues for the down-core data to which it is applied.

Considering the number of samples with no analogues and the generally poor communality values produced by the DTF 166/34/4, a bias towards the DTF109/24/6 model is reflected at the surface level. The species making up the no-analogue situations under the DTF 166/34/4 model require comment.

***Thalassiothrix / Trichotoxon* spp.**

- removed from the thesis-developed model due to poor counting practices and incongruous distributions (section 2.3.2). It is hardly surprising that including this taxa group in the DTF 166/34/4 model produces non-analogue events, especially when applied to correctly counted pole-ends of the taxa observed in the down-core record, against the largely extrapolated rankings in the original 166 database (Pichon *et al.* 1992a). The result therefore, is a loss of modern analogue situations. *Thalassiothrix* mats have recently been recovered from South Atlantic sediments (ODP site 1091, Barron pers. comm. 1998) and may provide further non-analoguous events that require consideration.

***Distephanus* spp.**

- removed from the thesis-developed model due to a lack of relation with SST and a lack of abundance differentiation south of the PF (section 2.3.4). The non-analogue situations are found with taxa abundances near or two times greater than previously described in the 166 database of Pichon *et al.* (1992a). A lack of database analogues for the taxon is obvious, but may simply be referable to a real non-analogue situation, which occurs either in the study region or over time.

Azpeitia tabularis

- an increased maximum abundance of this species was for the first time observed after including southeast Indian Ocean samples (section 3A.3.6) which were consequently incorporated in the 109 database. Thus, the no-analogue events observed for *Azpeitia tabularis* when applying the 166 database is a reflection on the confined northern distribution of this particular database. Non-analogues of this species, hence, indicate a loss of warm-water signal between the core and the database.

Thalassiosira trifulta

- this group, as the *Thalassiosira* Eccentric group, was removed from the DTF 109/24/6 model due to the mixing of several similar warm and cool water *Thalassiosira* species with eccentric areolation patterns (section 2.2.24 and 3A.3.34). As *Thalassiosira trifulta* was customarily separated from other eccentric patterned species during the counting of the cores, its use in the DTF 166/34/4 model was combined with species previously incorporated under the *Thalassiosira* Eccentric group (eg *Thalassiosira trifulta* and *Thalassiosira eccentrica*). This was done to remain faithful to the original species categories used by Pichon *et al.* (1992a). However, high abundances exceeding the maximum relative abundances of the database in core MD88-787 are minor and probably relate to increases in abundances regionally that were not covered by the samples in the 166 database.

Fragilariopsis kerguelensis

- only in core MD88-787 do *Fragilariopsis kerguelensis* abundances increase just above that of the maximum abundance in the 166 database. The no-analogue situation is thus, referable to a regional difference that has not been previously incorporated into the 166 database.

Fragilariopsis separanda

-as summarised previously *Fragilariopsis separanda* is a difficult species from which to associate an understanding of sedimentary distributional patterns (section 4.3.5). This distribution problem is now further complicated by large increases in past abundances of the species, particularly in isotope-stage 6, compared to modern distributional abundances which are associated with the POOZ and Antarctic coast. *Fragilariopsis separanda* poses a problem for both DTF models and is linked to cool SST estimation, which can not be considered correctly estimated when the species is in high abundance. Pichon *et al.* (1992a) had listed this species as occurring up to 8% in the surface samples of the 166 database which accommodated a rank 3 category for the species. However, a rank 3 category was never made for *Fragilariopsis separanda* (Appendix 2.1) and relative abundances derived from the raw data (Appendix 2.2) indicate that a maximum of 3% was the greatest abundance ever observed. The *Mac Transfer* application, therefore, lists

all ranked 3 and 4 occurrences of *Fragilariopsis separanda* down-core as non-analogue events.

In general, half of the non-analogue events are related to lack of coverage, and hence, diminished maximum relative abundance levels applicable to a certain species, as appears to be the case for *Fragilariopsis kerguelensis*, *Thalassiosira trifulta*, and *Azpeitia tabularis*. The result of their non-analogue condition is a minimised temperature estimate. The same feature may also be said for the non-analogue situation that arises with the *Thalassiosira gracilis* Group in the DTF109/24/6 model. The remaining species may indicate problems akin to that observed with *Eucampia antarctica* (section 2.3.5), where modern analogue situations do not exist for this species record in the past. For both *Distephanus* spp. and *Fragilariopsis separanda* this may be the case. *Fragilariopsis separanda*, however, may also be accumulated in greater numbers in past sediments as a function of bottom-water movement, which can not be dismissed in their currently observed distribution pattern in the sediments. Finally, non-analogue events with *Thalassiothrix/Trichotoxon* spp. reflect the need to re-count the 166 database to redefine relative abundance distributions that are then compatible with pole-end derived counts in cores.

Understanding the reasons behind non-analogue events and low communality values assists the interpretation of SST estimates provided by a model. From the analysis above greater confidence can be placed on the estimates derived from the DTF109/24/6 model over that of the DTF166/34/4 model.

6.4.2 SST ESTIMATION

Sea-surface temperature estimates are provided automatically by *Mac Transfer* regardless of non-analogue events or other discriminating criteria (eg communality cut-off values). For each core, SST estimates are illustrated both in their indiscriminate and selected format (ie. minus non-analogue events). Differences in the SST estimates provided by the two DTF models applied are also presented and discussed.

MD88-784

The SST record from DTF 109/24/6

A plot of all SST estimates including non-analogue events is presented in Figure 6.15A. Estimates of SST in core MD88-784 commence at near 0°C in late isotope-stage 4. Sea-surface temperature increases in warmth to 1.5°C before dropping down to 0°C again in isotope-stage 3. The remainder of isotope-stage 3 illustrates increasing warm SST between 2° and 4°C before decreasing near the isotope-stage 2/3 boundary. Further cool conditions persist early into isotope-stage 2. An oscillating yet mounting, SST signature is then observed from early isotope-stage 2 into isotope-stage 1. The warmest SST

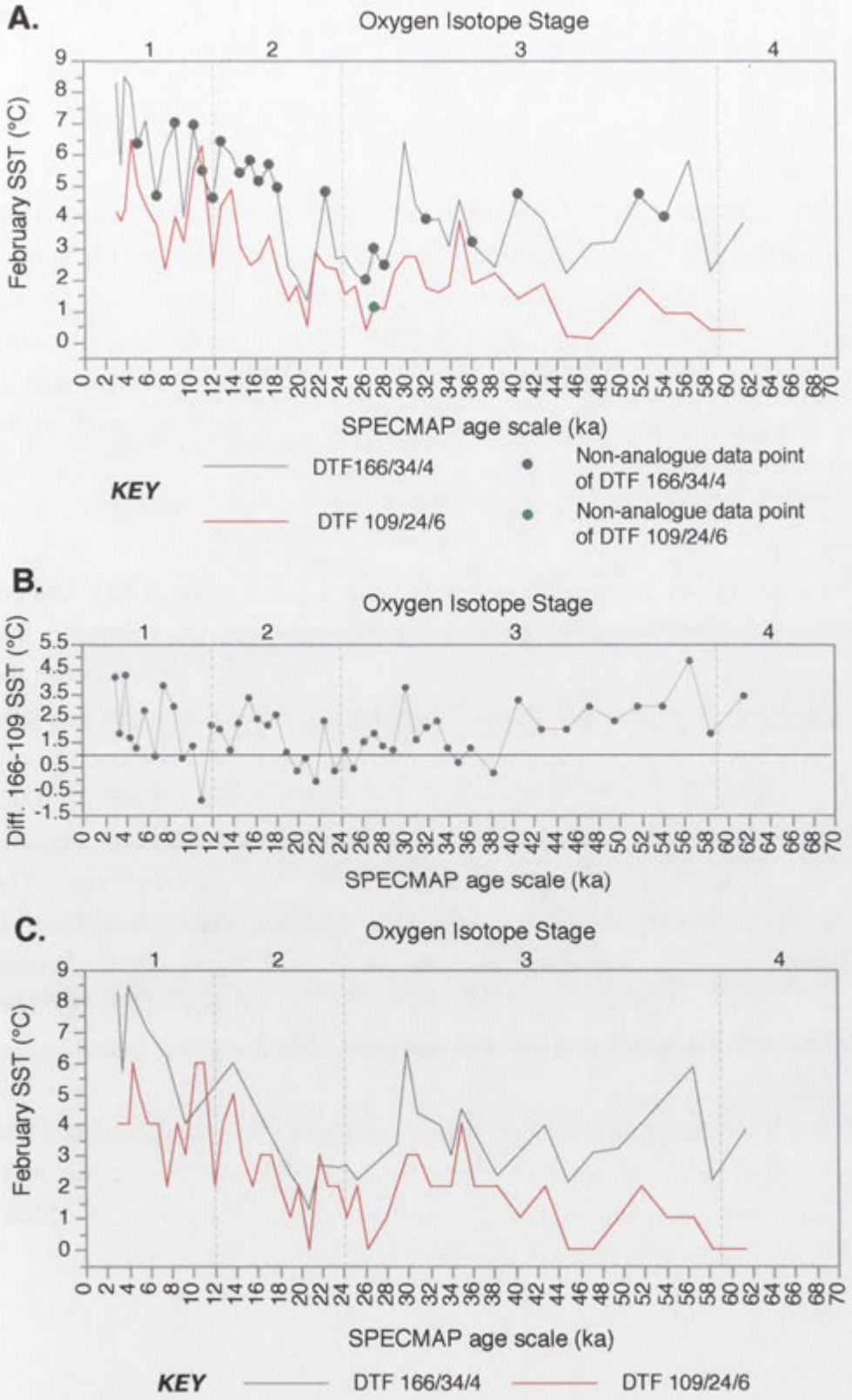

Figure 6.15. SST estimates for core MD88-784. **A**) Preliminary SST estimates including non-analogue samples and their SST estimates derived from both DTF models. **B**) Differences between the two model SST estimates over time using preliminary data in **A**. Zero difference line drawn. **C**) Final SST estimates derived from the two DTF models ie. non-analogue samples removed.

estimates are noted in this isotopic-stage between 6° and 6.5°C at ~11 and ~5 ka respectively. The last SST record at ~3 ka indicates SST at 4°C. Current February SST at the core site is 4.8°C (WOA 1994).

The SST record from DTF 166/34/4

A plot of all SST estimates including non-analogue events is presented in Figure 6.15A. Considerably warmer SST estimates are provided by the DTF 166/34/4 model. Surface waters at their coolest were ~1.5°C in isotope-stage 2. Similar surface water cooling during isotope-stage 3 is also observed, as in the DTF 109/24/6 model. The increasing warm surface water trend is also evident from isotope-stage 2 through isotope-stage 1. However, maximum SST estimates approach 8.5°C around ~5 ka and subsequently as the last SST record estimated.

Model Differences

Differences between the two DTF model estimates along the core using all SST data are illustrated in Figure 6.15B. The zero difference line is shown and indicates generally that during cool phases (eg. isotope-stage 2) SST estimates are reasonably close between the two models. During warmer phases, such as isotope-stage 1, differences in the estimates range from 0° to 4.5°C. The greatest difference between the two models is found in early isotope-stage 3 where up to +5°C is observed between the estimate from the DTF 109/24/6 model and that of the DTF 166/34/4 model. Here the DTF 109/24/6 suggests cool conditions, whereas the DTF 166/34/4 model estimates warm surface waters. The final SST estimates of MD88-784 are considered valid based on analogous arguments, and not communality values, with each model are presented in Figure 6.15C. Further reference to the SST record of this core will refer to the thesis derived DTF 109/24/6 model results, which are considered a better representative of the likely SST signal.

How to place confidence within either of the model estimates now becomes an important question. It requires drawing upon all aspects of the DTF model's capabilities. Discussion dealing with this problem is dealt with following the SST results of MD88-787.

MD88-787

The SST record from DTF 109/24/6

All SST estimates from the DTF 109/24/6 model on core MD88-787 are presented in Figure 6.16A. SST estimates at the base of the core, in isotope-stage 7, are almost all non-analogue estimates as a result of high abundances of *Fragilariopsis separanda*. The sole analogous point at the isotope-stage 6/7 boundary indicates SST at 4.8°C, which decreased to 1.4°C at 176 ka. A warm-spike (7°C) is then estimated at 167 ka, which continues the non-analogues situation derived from elevated abundances of *Fragilariopsis*

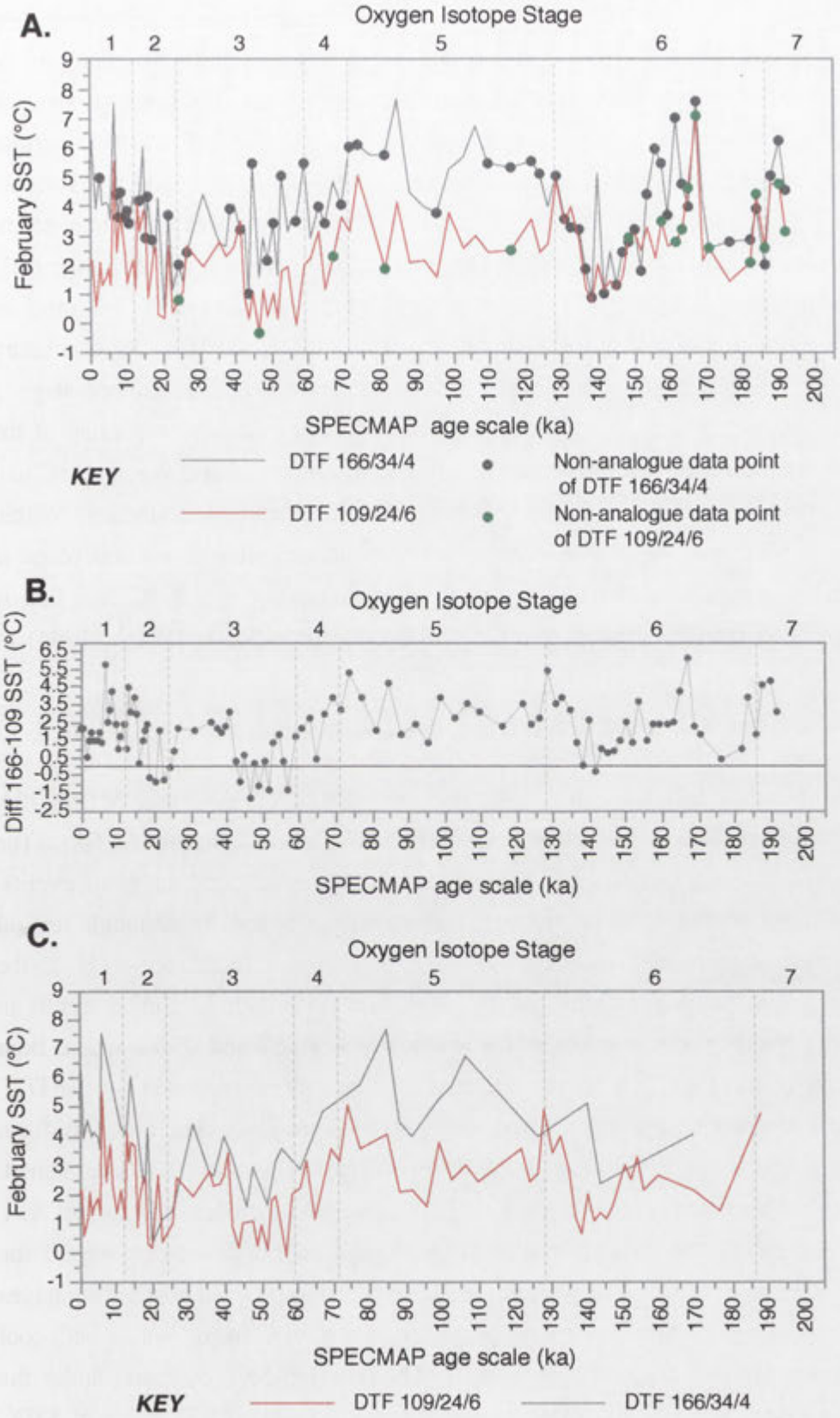

Figure 6.16. SST estimates for core MD88-787. **A**) Preliminary SST estimates including non-analogue samples and their SST estimates derived from both DTF models. **B**) Differences between the two model SST estimates over time using preliminary data in **A**. Zero difference line drawn. **C**) Final SST estimates derived from the two DTF models ie. non-analogue samples removed.

separanda that occur throughout isotope-stage 6. SST estimates remain, otherwise, less than 3°C and greater than 0.5°C through the remainder of isotope-stage 6. Warming of the surface waters to 5°C occurs at the Termination II boundary. Throughout isotope-stage 5, SST oscillates between cooler phases expressed by 2°-3°C, and warmer surface temperatures between 3.7°C to 5°C approaching the isotope-stage 4/5 boundary. Isotope-stage 4 shows a trend for decreasing SST expression, but the estimates are similar to the cooler phases of the previous interglacial. Very cool SST estimates are seen in the early part of isotope-stage 3. Here, SST varies generally between 0° and 1.7°C, and as mentioned earlier, is affected by the counting methodology in part for the oscillatory nature. Slightly warmer SST signals are perceived in the later half of isotope-stage 3 where values between 2° and 3°C are common before further evidence of cooling at the isotope-stage 2/3 transition. The coolest SST estimates in isotope-stage 2 reach 0.1°C and gradually increase in warmth to 3° or 4°C near the Termination I boundary. Within isotope-stage 1, SST remains at cool levels of 1.5°C, with exception to a warm phase at ~6 ka which reaches 4°C. The SST estimate at the core top is 1.97°C and this is considerably cooler than the current observed SST value provided by WOA (1994) of 3.9°C.

The SST record from DTF 166/34/4

SST estimates from the DTF 166/34/4 model on core MD88-787, as in core MD88-784, are warmer than those provided by the DTF 109/24/6 model (Figure 6.16A). The estimates, as already mentioned, are subject to a large number of non-analogous events. SST estimates are relatively similar through isotope-stages 6 and 7, although several warmer episodes are estimated under the DTF 166/34/4 model. In isotope-stage 5, the two models provide estimates which are disjointed and do not show similar trends in warm and cool phases with exception of the interval between 87 and 95 ka where both models indicate a strong cooling phase. Warmest SST estimates, produced by the DTF 16/34/4 model, are 6.7°C at 106 kyr, and 7.6°C at 85 kyr. Over the transition from isotope-stage 5, and through to isotope-stage 3, a cooling SST trend is also established. SST estimates remain warmer than those of the DTF 109/24/6 do model. The coolest SST estimate under the DTF 166/34/4 model, in isotope-stage 3, is 1°C. In isotope-stage 2 the coolest SST estimate is 0.3°C. The warming trend into isotope-stage 1 again disengages the superficial similarities between the two models. However, major warm and cool trends are observed concurrent in both models. The core-top SST estimate, under the DTF 166/34/4 model, is 5.2°C in comparison to the current observed SST value of 3.9°C (WOA 1994).

Model Differences

The SST estimate differences in core MD88-787, between the two models, are plotted in Figure 6.16B. Lowest discrepancies between the two models occur through parts of

isotope-stages 6 and 2, and at a lesser degree in sections of isotope-stage 3 and 1. As noted in the previous core study, smallest differences are evident during cooler phases and largest during warmer phases. The greatest contrasts in estimates between the two models occur in isotope-stage 6 (+6°C), throughout most of isotope-stage 5 (varying between +1 and +5.5°C) and in isotope-stage 1 (+5°C). Both models are incapable of providing similar modern SST estimates for the core top. This in part may be related to the fact that the core top is possibly missing, however presently, there are no stratigraphic arguments to suggest this is so. The DTF 109/24/6 model under-estimates the modern core top SST value by 1.9°C, whereas the DTF 166/34/4 model over-estimates the same surface temperature by 1.3°C. Over-estimation of the surface summer SST by up to 2.5°C by the DTF166/34/4 model was observed previously (*Pichon et al.* 1992a) in the polar core MD84-551 (55°S, 73°E). The discrepancy was attributed to coring disturbance at the core top, which was believed to have elevated the abundance of Thalassionema nitzschioides, and in turn providing an elevated SST estimate. Further over-estimation by 1°C of the surface SST was also observed in the subtropical core MD88-770 (Labeyrie *et al.* 1996). As investigated earlier in this thesis (Chapters 2, 3 and 4), other features of the DTF model and the database itself, are more likely to be the cause of the over-estimation problem in this model.

Previously, in the chapter dealing with the DTF models, the level of SST estimation error was assessed through database re-analysis (Chapter 4). Both models had standard errors of the estimate at ±1°C (±1.083°C DTF 166/34/4, and ±1.008°C DTF 109/24/6). Taking these values into account along with the apparent trend for warmer estimates provided by the DTF model 166/34/4 model against cooler estimates provided by the DTF 109/24/6 model, suggests that neither model accurately estimates SST.

To constrain such a hypothesis, we also have the evidence derived from the models themselves, which can be used to assess their capabilities (Chapter 4). Error associated with SST estimation in DTF 166/34/4 was noted as being up to ±4°C for estimates between 0° and 12°C (section 4.4), and with a higher degree of under-estimation of SST in the warmer temperature range. This suggests that all warmer estimates are actually cooler than what they should be. However, such under-estimation assumptions require a large influence by the dissolution factor (sections 4.4.3 and 4.2.1) to be brought into contention. In the case of core MD88-787, warmest estimates of DTF 166/34/4, when considering analogues to the modern data set, are observed in isotope-stages 1 and 5 (Figure 6.16C). The response of the dissolution factor in these three warm stages is not observed as very elevated in isotope-stage 5 and only slightly responsive in isotope-stage 1 (Figure 6.14C). This suggests the estimates are not under-estimated to any great degree, although the chances for such an occurrence is greater in isotope-stage 1. Although this under-estimation feature can be largely discounted at this stage, the ±4°C

estimation errors still remain within the model and cannot be as easily identified or discussed. The fact that criteria removing samples with large departures from the estimates was not undertaken in the original 166 database (section 4.2.1, Fig. 4.3F) means that confidence in all estimates must remain with this error shadow. This error, as observed earlier, covers all SST estimates from 0 to 12°C.

In the DTF 109/24/6 model, SST estimates can be in error of up to ±2°C between 1° and 6°C. Over-estimation by 1.5°C was common between 0° and 4°C, while under-estimation by up to 2°C was more likely between 4 and 8°C (section 4.3.6). Most warm SST estimates of MD88-787 from the DTF 109/24/6 model fall between 4°C to 5.5°C (Figure 6.16C). The estimates appear to be considerably cooler than those provided by the DTF 166/34/4 model, it seems likely the under-estimation by up to 2°C noted to occur in the initial model self-analysis, is manifested in the core estimates. It is difficult to pin-point the factor or species that may influence this particular under-estimation. Yet, two poignant features of the 109 Natural database are certain to contribute to such a feature: the limited number of warm-water samples, and the low number of species used to define the warm-water region. The latter point possibly indicates the need to include data of the silicoflagellate *Dictyocha* spp in the current DTF109/24/6 to strengthen the warm-water response (section 2.3.4). However, with the expected imminent release of the re-counted 166 database (Crosta pers. comm. 1997), this silicoflagellate addition may not be required.

Cooler SST estimates provided by the DTF 109/24/6 model (ie. between -0.5° and 4 °C) have been shown in the reference 109 database to be possibly over-estimated by up to 1.5°C (section 4.3.6). Again, no particular factor or species can be associated to this problem at this point in time. Cool water estimates are of course influenced by the cool water factors and most dominantly by the interplay of the POOZ and sea-ice cover factors. Yet, the loss of the subantarctic factor quite possibly plays a more dominant role in influencing the SST equation towards cooler estimates than the latter two factors (Figure 6.14A). The answer may simply lie in the fact that the 109 database is too small and restrictive.

It is most probable that the "real" SST signal lies between the two model estimates. The model diagnostics and lower number of non-analogue events from DTF 109/24/6 over that of results produced by DTF 166/34/4 suggest that SST estimates are closer to those provided by the former model. Results for both cores studied, therefore, will be referred to those obtained from the thesis derived DTF 109/24/6 model, acknowledging the fact that warmer estimates are probably too cool by up to 2°C.

Comparison of SST estimates between the two cores

Using the results from DTF 109/24/6, the results of both core MD88-787 and MD88-784 are presented in Figure 6.17 (Appendices 6.8, 6.9). Although the possibility for incorrectly aligned SPECMAP age scales are possible in either core, the two cores show very similar responses and temperature signals where they overlap in time (Figure 6.17B). It was anticipated that SST estimates would be slightly warmer in core MD88-784 than that in core MD88-787 since current modern SST variation between the two sites in February is 0.9°C. Scanning the overlapping SST records between the individual core sites, a division amid the estimates is only clear during isotope-stage 1. Through most of isotope-stages 3 and 2 the records contain identical SST signatures. In some instances (ie. isotope-stage 3), warmer SST estimates are noted in the more southern core MD88-787. The SPECMAP age scale may require re-alignment in isotope-stage 1, yet appears to be closely matched in isotope-stages 2 and 3 between the cores.

6.4.3 Sea-ice estimation

Sea-ice estimation is presented only on core MD88-787 here since the core represents the last two glacial cycles and the method requires amendment with the revision of the diatom database (Chapter 5). A similar, but reduced, sea-ice incidence record was observed in the shorter and northern core MD88-784 (personal observations).

Sea-ice concentration curves for February and September are presented in Figure 6.18A and B. These two curves represent the maximum sea-ice concentration conditions estimated to have been recorded at MD88-787's core location (56°S, 145°E). As surmised earlier (section 5.1.4), sea-ice concentration less than 15% is considered to represent open-ocean conditions due to the nature of the satellite interpretation of the reflected signal against weather effects and the interpretation of the sea-ice edge. For this reason, sea-ice concentration estimates in February at the core site are considered to have always encountered open-ocean conditions. This feature persists even though in the early part of isotope-stage 6 sea-ice concentrations up to 9% were estimated (Fig. 6.18A).

In contrast to February, September sea-ice concentration estimates suggested sediments preserved at the core site were influenced by sea-ice cover during isotope-stages 6, 3-4 and 2 (Fig. 6.18B). Standard errors for each of the sea-ice concentration estimates are indicated, the largest being ±36% for a concentration of 38% concentration (at ~163 kyr). Discussion on the standard errors of each estimate ensues below. For the greater part of isotope-stage 6, sea-ice concentration is between 40% and 76%, indicating fast-ice cover. A decrease in sea-ice cover to pack-ice, and most-likely sea-ice edge, conditions prevails between ~154-170 ka. Prior to the end of isotope-stage 6 (~137 kyr), the record of sea-ice dramatically disappears. This lack of sea-ice influence is carried through isotope-stage 5 and into the start of isotope-stage 4. The record of sea-ice concentration returns during

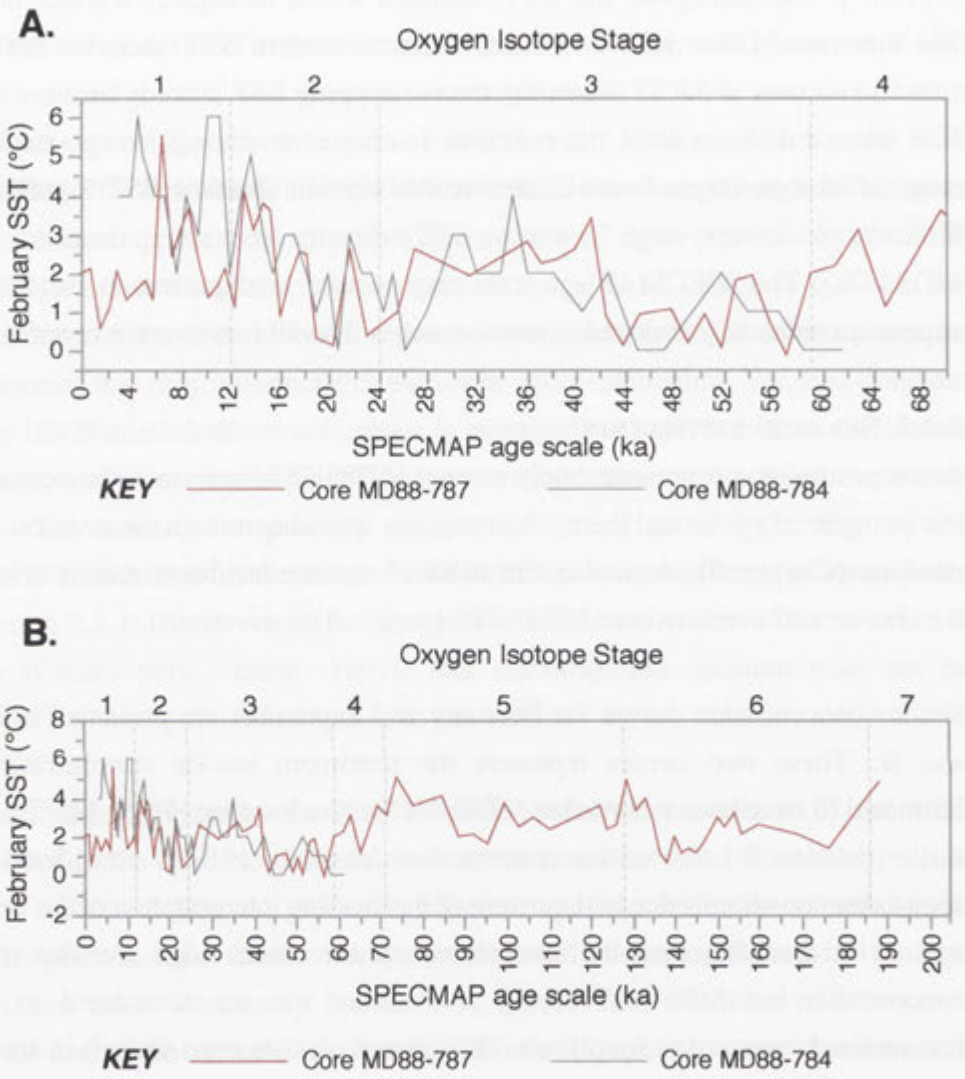

Figure 6.17. Comparison of SST estimates from the DTF 109/24/6 model for cores MD88-787 and MD88-784 over time. **A**) Comparison of SST estimates over the last 70 Ka where estimates overlap in time. **B**) Complete SST records.

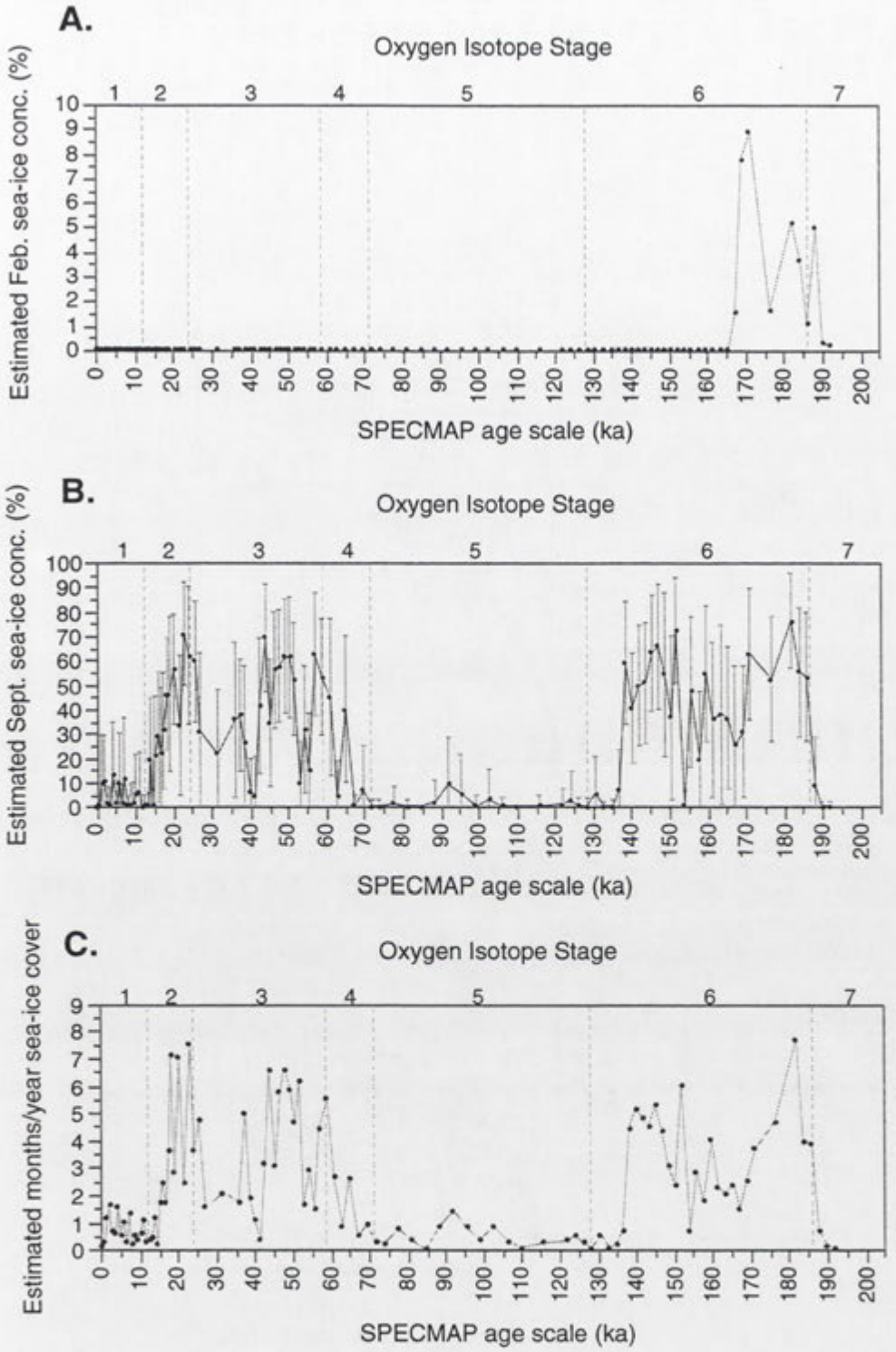

Figure 6.18. Estimated sea-ice over time at site MD88-787 (56°S, 145°E) for maximum sea-ice extent in February (**A**), maximum sea-ice extent in September (**B**), and maximum annual cover in months per year (**C**). Estimates derived from the model presented in this thesis sea-ice concentration refers to the degree of sea-ice versus open-ocean. Sea-ice concentration under 15% should be interpreted as open-ocean conditions, while concentrations between 15-40% are considered pack-ice, and those greater than 40% as fast-ice (refer section 5.2). Standard errors for each estimate are shown but are evident only in B, where they are greater than 0.5 (refer Appendix 6.8).

A.

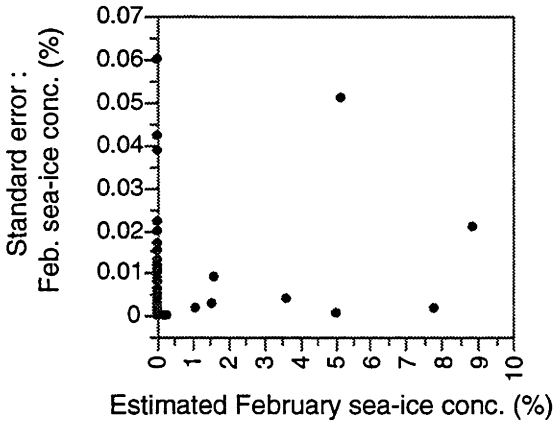

B.

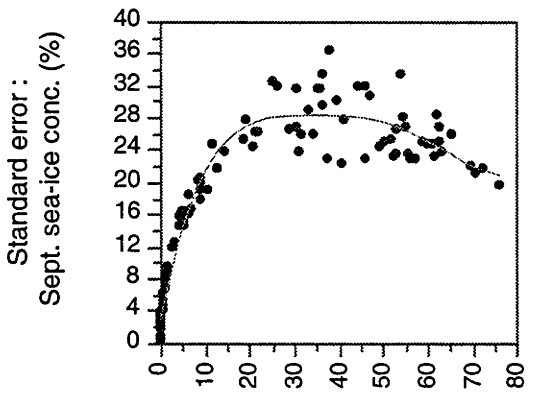

$y = 1.56E\text{-}07x^5 - 3.5E\text{-}05x^4 + 3.02E\text{-}03x^3 - 1.30E\text{-}01x^2 + 2.86x + 2.99$

$r = 0.972$

C.

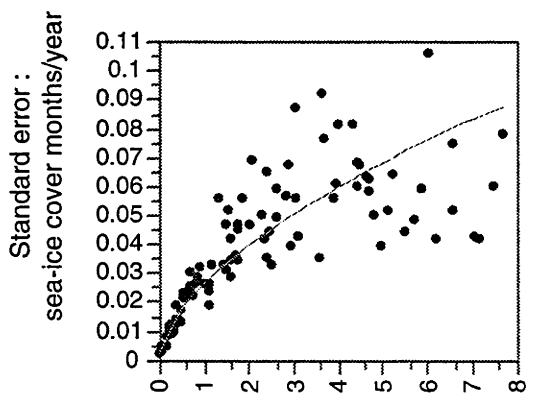

$y = 0.026x^{0.602}$ $r = 0.944$

Figure 6.19. Standard error estimates provided by the thesis sea-ice models. **A**: February sea-ice model. Very small and random standard errors are provided by this model for each of the estimated concentrations. **B**: September sea-ice model. Standard errors for each estimated concentration are best explained by a 5th order polynomial. **C**: Annual sea-ice cover model. Increasing standard errors are observed with increases in the monthly cover. The primary trend is best approximated by a power equation.

Stage 3 and increases to fast-ice conditions until ~43 ka. A minimised, but continued, sea-ice presence varying between open-ocean and pack-ice conditions predominates until isotope-stage 2. Pack-ice cover dominates conditions in the early phase of isotope-stage 2 and gradually diminishes prior to Termination I to open-ocean conditions. The open-ocean conditions are recorded through to the present day.

In terms of the maximum annual sea-ice cover of the core over time, intervals implying sea-ice cover during September are observed with greater than 2 months per year annual sea-ice cover at the core location. Periods with fast-ice conditions are estimated to have between 4 to 7.5 months cover. This latter range is within the modern observations of September and monthly sea-ice cover observed in the database parameters used to construct the sea-ice models (section 5.1.4, Figure 5.1B). In terms of equating open-ocean conditions to that of the annual sea-ice cover estimates, intervals with less than 3.5 months cover are considered. This is in part a consequence of not previously adjusting the number of months with sea-ice cover based on the concentration level of each month, as was done for the September and February data. That is, a month was still counted even when the monthly average sea-ice concentration was between 0 and 15%. This is unlike the February and September sea-ice concentration data set where values less than 15% were given a zero concentration value. In addition, from the plots describing relations between September concentration and monthly cover, samples with less than 15% September sea-ice concentration and unlikely to represent other monthly situations, falls under 4 months annual cover (Fig.5.1B). Each model has standard errors for every estimate particular to that model. Under the February sea-ice concentration model, standard errors are very small and show a random pattern (Fig. 6.19A). Greatest variation on an error occurred at the zero estimate, which is not used by the model since the first step was to determine the zero situation. Standard errors provided for estimates in the September sea-ice concentration model are best explained by a 5th order polynomial relationship (Fig. 6.19B). Greatest standard error variation occurs when estimates are between 25% and 55%, where the variation covers a range of 16% (ie. standard errors can vary from 22-38%). Finally, under the annual sea-ice cover model, increasing variation in the range of standard errors is observed concurrently with increases in monthly cover. This trend is best approximated by a power equation (Fig. 6.19C). These standard errors are unique to the sea-ice model estimates applied to this core data.

Interpreting the sea-ice estimate records to those observed via other methods, and the question of relation between the sea-ice and SST models is considered in the ensuing section.

6.5. A CLIMATIC HISTORY FOR CORE MD88-787.

Core MD88-787, in the modern ocean environment, is overlain by surface waters characteristic of the Polar Front (PF) (Figures 1.6 and 6.1). Here the sub-surface oceanographic signature of 2°C (temperature minimum) defines the boundary between the southern Antarctic surface waters and the northern subantarctic surface and intermediate waters in summer. An approximated surface water signature is often implied at 4°C for the PF (eg. northern boundary of PF, Howard and Prell 1992). This 4°C value is coincident with the modern February SST provided by WOA (1994) for core MD88-787 (ie. 3.9°C).

The oceanographic history acquired from the core includes changes in the surface water environment as interpreted by the diatom fossil assemblages that accumulated on the seafloor. For this part, the movement of the PF over time can be assessed through the inferred 4°C surface-water signature derived from SST estimates. The role of sea-ice cover through time at the core site has also been assessed using the diatom record. These two records, linked with the abundance of the radiolarian *Cycladophora davisiana*, can be used to tie into other Southern Ocean oceanographic and atmospheric conditions thought to have occurred throughout the late Quaternary.

6.5.1. SST AND SEA-ICE HISTORIES VERSUS THE OXYGEN-ISOTOPE RECORD.

Derivation of a SST record from the planktonic foraminifera oxygen-isotope record for comparison with the DTF derived SST was not attempted, due to the uncertainties of isotope-derived SST records in higher latitudes (Pichon *et al.* 1992a). On a very generalised level, the change in isotope signal from isotope-stage 2 to 1, calculated as 1.87 per mil, suggests a change in SST of around 2.7°C. This is after removing the 1.20 per mil considered indicative of sea-level change (Chappell *et al.* 1996) and assuming a change in 1 per mil is equivalent to 4°C (Shackleton 1982). This value is similar to the difference provided by the DTF SST estimates between isotope-stage 1 and 2, of approximately 3°C.

The response between the planktonic foraminifera oxygen-isotope signal and that of the diatom SST estimates are not synchronous. Both leads and lags are observed between the two curves. For example, SST warming leads isotope decreases at the 5/6 boundary, SST cooling lags isotope increase in isotope-stage 4, neither lags nor leads are observed at the cooling over isotope-stage 2/3 between the two cores (Fig. 6.20 A, B). This is in contrast to a Subantarctic Zone core studied by Labeyrie *et al.* (1996, MD88-770, Figure 6.21), where they observed diatom and foraminiferal SST estimates having a 1 to 2 kyr lead on the planktonic foraminifera oxygen-isotope record. Leads in diatom SST (Labeyrie *et al.* 1986, Labeyrie *et al.* 1996) and radiolarian SST (Howard and Prell 1984) over benthic foraminifera oxygen-isotope signatures in the last deglacial have been

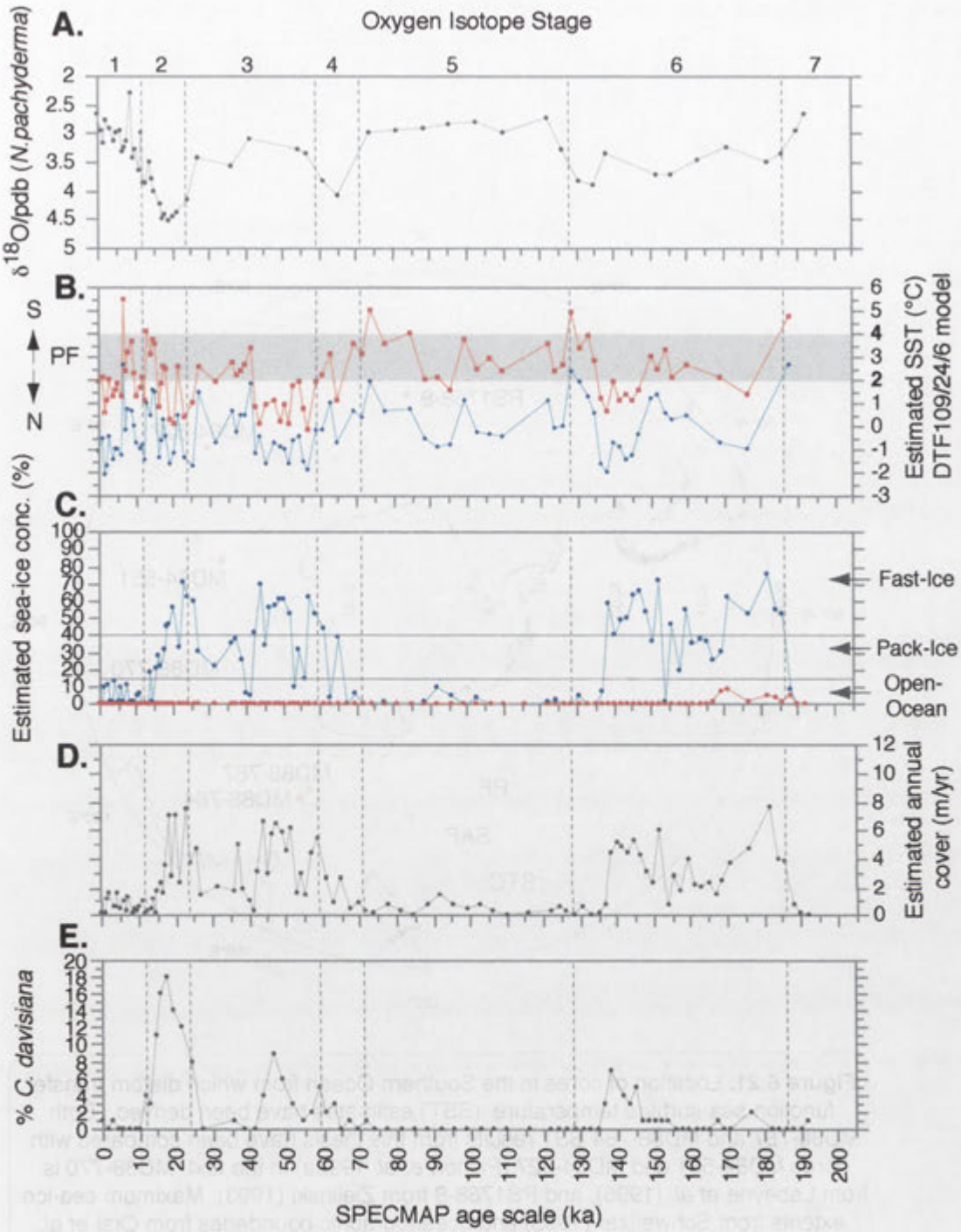

Figure 6.20. Climatic proxies for core MD88-787 over time. **A**: Planktonic foraminifera oxygen-isotope record. **B**: February and August SST estimates from DTFmodel 109/24/6. **C**: February and September maximum sea-ice concentration estimates from thesis model. **D**: Maximum annual sea-ice cover from thesis model. **E**: Percentage of *C. davisiana* observed down-core (Bareille, 1991). February estimates identified in red, September and August estimates in blue. Sea-ice concentrations converted to sea-ice types are identified in **C**. Polar Front (PF) movement north or south of 2° and 4°C SST proxy signatures for the front, are highlighted by shaded region in **B**. Refer to text for discussion.

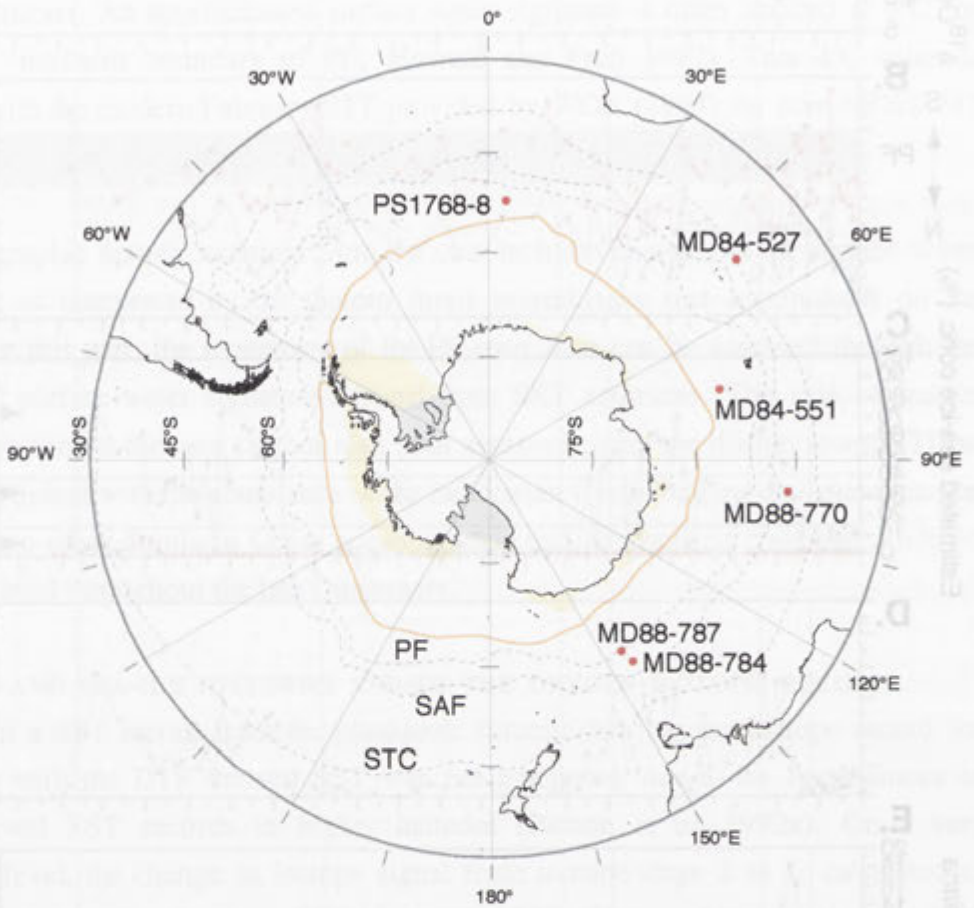

Figure 6.21. Location of cores in the Southern Ocean from which diatom transfer function sea-surface temperature (SST) estimates have been derived . Both MD88-787 and MD88-784 SST results from this thesis have been compared with cores MD84-551 and MD84-527 (Pichon *et al.* 1992a) in the text. MD88-770 is from Labeyrie *et al.* (1996), and PS1768-8 from Zielinski (1993). Maximum sea-ice extents from Schweitzer (1995) and oceanographic boundaries from Orsi *et al.* (1995). PF = Polar Front, SAF = Subantarctic Front, STC = Subtropical Convergence/Front.

observed. They were not assessed in this work due to the incomplete and short records of benthic oxygen-isotope completed on both MD88 cores.

In reference to the sea-ice record, planktonic foraminifera derived isotope changes appear to lag the September sea-ice concentration and annual sea-ice cover estimates by up to 5 kyr, especially with the onset of warmer conditions. Increases in sea-ice cover appear to be recorded concomitantly with the decrease in planktonic $\delta^{18}O$ ratio. Such a double response seems appropriate, as melting of sea-ice, ice shelves and continental ice would influence the isotopic signal after warming events had begun and were mixed into the ocean. Whereas, the somewhat immediate response to cooling and reduction of $\delta^{16}O$ in the system occurs as sea-ice information indicates increased glaciation over Antarctica. Increases in sea-ice coverage are not responsible for the large changes in oxygen isotopic ratios, which is otherwise affected by continental ice over Antarctica and the Northern Hemisphere (Labeyrie *et al.* 1986, Shemesh *et al.* 1994). Yet, another component, snow cover on sea-ice, may be a small but important consideration to the isotopic ratios during glacial periods, especially where long-term build up on multi-year ice occurs. Present studies along East Antarctica observed multi-year ice floes comprising 10% incorporated snow layers (Worby *et al.* in press). Snow can be incorporated into the sea-ice structure when the snow/ice interface is submerged under sea level, flooded and refrozen to the sea-ice surface (Eiken *et al.* 1995). This process results in reducing the $\delta^{18}O$ signal within the newly formed snow sea-ice to values less than the sea-ice oxygen-isotope signal of 0.0 per mil (Worby *et al.* in press). Predictions of extensive and increased multi-year presence have been suggested for glacial periods around Antarctica (CLIMAP Project Members 1976, Grobe and Mackensen 1992). The increased sea-ice signal during isotope-stages 2, 3, and 6 infer the presence of multi-year ice and an extended ice-shelf around Antarctica than occurs at present.

6.5.2. Computability between sea-ice and SST records

The relationship between the SST estimates and the sea-ice estimates for MD88-787 are an important check on the coherency of signals produced. For sea-ice to form, the upper surface layers of the water need to be super cooled to -1.8°C to form frazil ice (Ackley 1991, Tucker *et al.* 1992). The February SST estimates from DTF 109/24/6 are all greater than -0.5°C which is in agreement with the lack of sea-ice cover estimated for February at the core site (Fig. 6.20B and C). To address whether September sea-ice concentration estimates observed over time are relevant to SST, the DTF 109/24/6 was also run using August SST parameters to reflect the traditionally interpreted maximum winter SST signal (eg CLIMAP project members 1976, 1981). This winter SST estimation is in conflict with the understanding of major diatom flux during the summer months (Abelmann and

Gersonde 1991). However, the relationship between summer and winter SST is considered constant under this approach and thus, reflects the variation of the physical environment and consequent influence on the diatom distribution. The resulting DTF has the following basic characteristics; multiple correlation coefficient = 0.909 ; standard error of the estimate ±1.47°C; and has the same communalities as produced by the February SST version of the model. August SST estimates are illustrated in contrast to the February SST estimates in Figure 6.20B. The data is listed in Appendix 6.10.

Almost all August SST estimates below -1°C are linked to conditions where September sea-ice concentrations show sea-ice cover (compare Figures 6.20B and C). The SST signal is less than convincing in isotope-stage 2, as a result of the double interval sampling methodology (section 6.2.5). However, the SST estimates are noted at values less than -1°C. Using the standard error of the estimate alone as a guide to possible errors in estimation, these SST estimates indicate sea-ice formation at the core location was indeed possible. A stronger link is observed between the annual sea-ice cover estimates with the coolest August SST estimates (Fig. 6.20B and D). All warming trends in the SST record are met with loss of the sea-ice record. There are simultaneous changes in August (and February SST) with those observed in the sea-ice cover estimates for September and annually. Based on analysis of diatom SST records in the spectral domain Labeyrie *et al.* (1996) hypothesised that sea-ice would react without any lags to changes in insolation. Spectral analysis of the climatic proxies derived from core MD88-787 is to be examined in later work. However, the observations made here between the SST and sea-ice estimates suggest that sea-ice changes will also show no lag in the obliquity band as observed against diatom-derived SST (Labeyrie *et al.* 1996), and sea-ice extents inferred from *Eucampia antarctica* subspecies abundances in the Brunhes epoch (Kaczmarska *et al.* 1993).

Although both sea-ice and SST methods of estimation are derived by independent means from the diatom data after factor analysis, their coherency in climatic signal suggests the sea-ice model will be a useful application to core data at least in the Polar Front Zone. Further tests are required to validate the sea-ice model south of the current Polar Front Zone.

6.5.3. SEA-ICE AND *CYCLADOPHORA DAVISIANA* RECORDS

Harmony between the sea-ice results and those of the *Cycladophora davisiana* abundances are linked in glacial intervals (Figure 6.20 C to E). Yet, the amplitude of *Cycladophora davisiana* abundance does not appear related to increases in sea-ice cover annually or to September sea-ice concentrations. Such lack of direct correlation to the degree of *Cycladophora davisiana* abundance accumulated in the sediments suggests that other environmental factors play a more important role in abundances or productivity,

even though the presence of sea-ice cover is a part of this environmental characteristic. Additionally, the greatest abundance of *Cycladophora davisiana* occurs during the later part of isotope-stage 2, when maximum September sea-ice concentrations were reducing along with the annual monthly cover, concomitantly with increases in SST. It would appear from the record preserved in core MD88-787, that increased sea-ice cover beyond that of pack-ice or sea-ice edge conditions is not advantageous to the productivity of *Cycladophora davisiana.*

The role of sea-ice cover has been inferred from the modern habitat of *Cycladophora davisiana* (Morley and Hays 1983), and through IRD accumulations (Labeyrie *et al.* 1986), even though the latter are derived from icebergs. The comparison presented here indicates that this hypothesis is valid, and has important kickbacks to other hypotheses on sea-ice melt directed by NADW input, atmospheric conditions, and the surface water structure. In fact, the latter is an important condition to the distribution and abundances of diatoms. As previously indicated in section 6.2.6 and Figure 6.8, absolute diatom abundances are inversely correlated to the abundances of *Cycladophora davisiana* in the sediments. Thus, it appears, at face level, conditions such as a melt water lid and restricted mixing between the low salinity surface waters and the stable, more saline Antarctic waters below them, were not conducive to diatom productivity during such phases. It is also quite feasible that diatom dissolution below the surface waters was enhanced during such phases, although there is no direct evidence at this stage to indicate this was so.

6.5.4. Movement of the Polar Front

Tracing the movement of the Polar Front (PF) through time from core MD88-787 can be assessed in two ways: via the proxy surface 4°C summer signature and via the comparison of factor loadings. The modern SST provided by WOA (1994) is 3.9°C for that site, thus indicating that the PF has influence at that location, although Rintoul *et al.* (1997) recently observed the PF 3° latitude north of core MD88-787.

Under sea-surface temperature evaluation, a simple interpretation of movement north or south of the site is hindered because both DTF models were shown to be incapable of estimating the modern surface water signature of the core. Both model estimates were out by approximately ±1.6°C (section 6.4.2). Consequently, trying to establish a proxy sea-surface temperature signal for the PF becomes construed between the 4°C proxy and the estimated core top SST (~2°C DTF 109/24/6). Data from vertical sections between Tasmania and Antarctica suggest the PF surface temperature expression varies from 3° to 6°C, but in general is noted as 4° or 5°C (Rintoul *et al.* 1997). The change in surface expression is related to the seasonal surface-water changes and the movement of the Subantarctic Front northward from winter to summer (Rintoul *et al.* 1997). In fact, the 3-

5°C surface signature is currently interpreted as the southern expression of the Subantarctic Front (Rintoul *et al.* 1997).

As the oceanographic definition of the PF is a 2°C subsurface minimum it is important to clarify that the DTF 109/24/6 does not reflect this subsurface signature. Rintoul *et al.* (1997) indicate from the February vertical sections that the 2°C subsurface minimum at 56°S occurs at a depth between 100 to 200 metres below sea-level and the overlying surface waters approach 3°C. Thus, the core top February SST estimate of ~2°C may be influenced by the upper expression of the subsurface minimum waters. However, because studies indicate that diatom productivity is confined to the upper 100m of the ocean (El-Sayed 1970, 50m depth between Tasmania and the Ross Sea, Holm-Hansen *et al.* 1977, El-Sayed 1984, Round *et al.* 1990), it is assumed that the derived SST signature represents the upper surface waters.

Since the core-top SST estimate from DTF 109/24/6 is considered to be under-estimated, PF movement is interpreted cautiously herewith. The use of the "4°C proxy", as an indicator of the PF position irrespective of the SST core top estimate, suggests the PF remained north of the core site throughout most of the last 200 kyr (Figure 6.20B, 6.22A). The exceptions being southward incursions in mid isotope-stage 1, late isotope-stage 2, most of isotope-stage 5, and during the transitions between isotope-stages 5/6, and 6/7. In contrast, applying the core top estimated SST (~2°C) as the "proxy PF SST signal" for this core, PF movement north of the core site occurred in isotope-stage 2, early isotope-stage 3, and late isotope-stage 6. In contrast the PF remained stationary or may have shifted slightly northward during early isotope-stage 6, mid isotope-stage 5, isotope-stage 4 and early-isotope-stage 1. Displacement of the PF south of the core MD88-787 under this 2°C SST surface proxy is interpreted to have occurred in isotope-stage 1, late isotope-stage 2, late isotope-stage 3, most of isotope 4 and 5, and mid isotope-stage 6 and very late isotope-stages 6 and 7.

The "2°C proxy" simply exaggerates the primary interpretation of the "4°C proxy" which both provide northward and southward shifts relative to the core site. The true answer probably lies between the two interpretations but nevertheless, it indicates that surface water structure did change relative to glacial and interglacial ages. The pursuit for an interpretation of PF movement is probably better derived from microfossil studies in tune with the subsurface interpretation of PF (eg. radiolarians or foraminifera) rather than diatoms which are considered to reflect conditions in the top 50 to 100 m of the ocean. Should further evidence point towards a continuous circum-polar sea-surface expression of the southern limit of the Subantarctic Front, as identified by Rintoul *et al.* (1997) in the southeast Indian Ocean, then diatom-derived SST results will be more appropriately implemented.

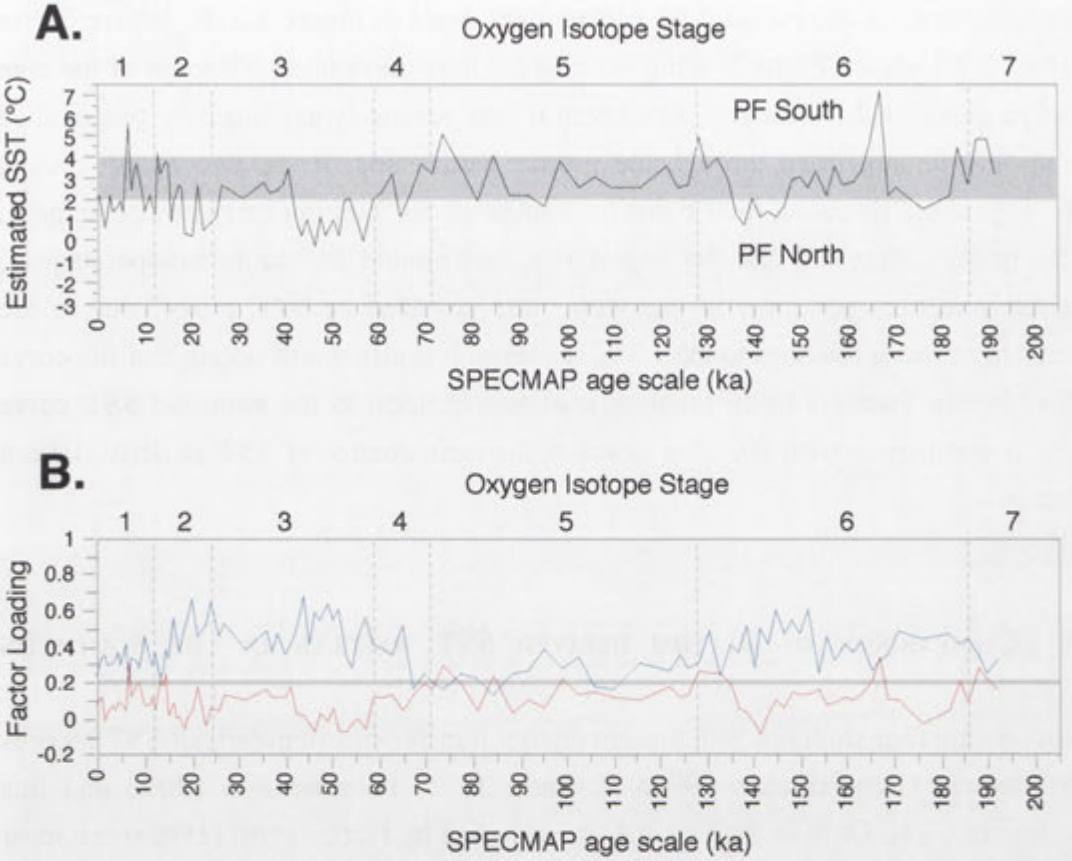

Figure 6.22. Polar Front movement analysis from sea-surface temperature estimates and factor loadings of core MD88-787. **A**. February SST estimates from DTF model 109/24/6. North- or south-ward Polar Front movement is assessed from the 2°C (core top SST) and 4°C (modern PF SST) proxy signatures, indicated by the shaded region. **B**. Factor loadings curves from Factor 2 (blue curve, sea-ice cover) and Factor 3 (red curve, Subantarctic). Where the two curves cross at a factor loading value of 0.2 (grey line) the SST is 3.5°C (Figure 4.28) and can be used to indicate movement of the 3.5°C isotherm as a proxy for the PF. Where the Factor 3 factor loading curve passes the 0.2 loading value the Polar Front is believed to have moved south. Refer to text for discussion.

The relationship between certain factor loadings can identify movement of isotherms. In figure 4.28B it was pointed out that where Factor 3 crosses Factor 2 (at a factor loading value of 0.2) a SST value is identified. In this particular case, the junction of the two factors refers to a SST of ~3.5 °C, which can be used as a tracer of PF movement. The two factors, Factor 3 and Factor 2 are plotted over depth in Figure 6.22B. Where Factor 3 and factor 2 cross the Factor loading value of 0.2 movement of the PF south of the core site can be interpreted. Northward movement is less accurately explained by this method and can only be suggested through the greater partitioning of the two factor loading curves. Figure 6.22B shows the PF did pass south of 56°S during early isotope stage 2, over the isotope stage 4/5 and 5/6 boundaries, and around 165 ka in isotope stage 6. These interpretations are more in line with those provided by "4°C proxy" due to the relationship of factor loadings to the 3.5°C isotherm. It is also worth noting that the curve produced by the Factor 3 factor loadings is almost identical to the estimated SST curve (Fig. 6.22 compare A with B). This indicates the main control of SST is derived from this factor.

6.5.5. Comparison of Diatom derived SST results in the Southern Ocean.

So far, there are four studies which present diatom-transfer-function-derived SST records in the Southern Ocean (Pichon 1992a, Zielinski 1993, Labeyrie *et al.* 1996 and this study)(Figure 6.21). Of these studies, the cores studied by Pichon *et al.* (1992a) are most appropriate for comparison with the two cores presented in this work. The other two studies are of limited use due to their lack of age assignment and on-going assessment (Zielinski 1993), as well as their more northerly placement (Labeyrie *et al.* 1996). This makes comparison complex.

The two cores used for comparison are found in the South Indian Ocean. The first is located in subantarctic waters, MD84-527 (43°49'S, 51°19'E), and the second in the PFZ, MD84-551 (55°00'S, 73°16'E). Sea-surface temperature estimates were determined using the DTF 166/34/4 model of Pichon *et al.* (1992a) and predicted Summer SST, rather than February SST pursued in this work. Comparison of the two cores of this thesis are more latitudinally in line with core MD84-551, since MD84-527 is 11° latitude further south of MD88-784. However, on contrasting the core estimates over time (Figure 6.23A and B), it was considered that the two most southern cores (MD88-784, MD84-527) share more commonality than the two southern cores (MD88-787, MD84-551). However, this is debatable, since cores MD88-787 and -784 have similar SST records except for isotope-stage 1.

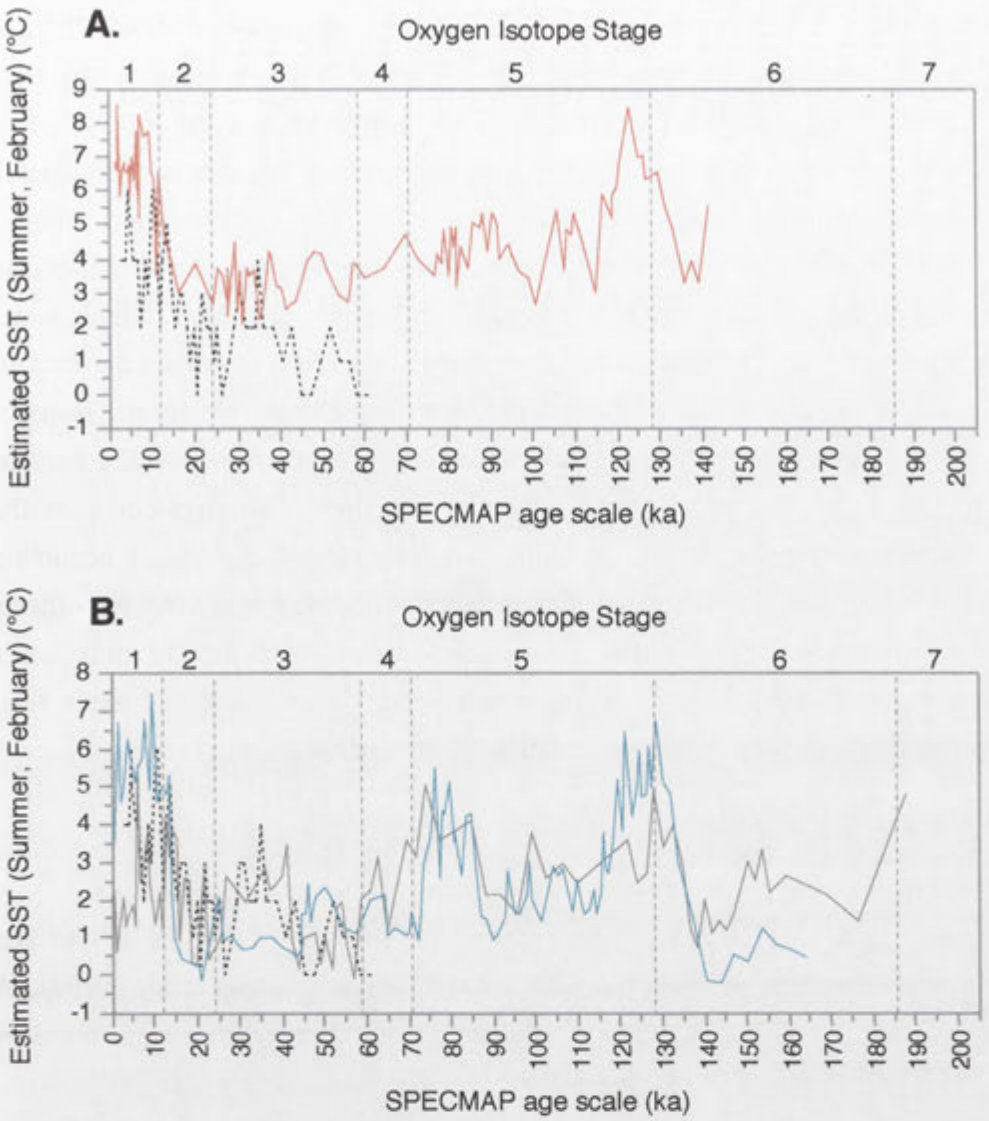

Figure 6.23. Comparative SST estimates between cores MD88-784, -787 (this work) and MD84-551, -527 (Pichon *et al.* 1992a, and Pichon pers. comm. 1996). **A**) Comparison between MD84-527 (red line) against MD88-784 (dashed grey line). MD84-527 occurs in South Indian subantarctic waters 11°latitude south of MD88-784. The latter core shows closer SST affinities to the former core, than the southern located core MD84-551 (B, blue line). **B**) Comparison between the two cores of this study with similarly situated MD84-551 (55°S, 73°E) in the South Indian Ocean. Principal trends and SST estimates between MD88-787 (grey line) and MD84-551 are similar, with exception to isotope-stages 1 and 3. MD84-551 shows greater SST variability than MD88-787 possibly in relation to the lack of a limiting continental mass to the north of the core.

Trends in warm and cold SST estimations are remarkably similar between MD88-787 and MD84-551, with exception to isotope-stages 1 and 3, where divergences in the SST record are obvious (Fig. 6.23B). The range of SST estimation in core MD84-551 is considerably broader than in either of the two cores presented in this thesis. This feature is attributed mainly to the geographical positioning of the cores, since water masses overlying core MD84-551 are not limited to the north by the Tasmanian and Australian landmasses, as is the case for MD88-787 and -784. The increased warm water expressions in isotope-stage 1 and in late isotope-stage 2 are likely to reflect the lack of geographic boundaries. The difference in the cold water expression during late isotope-stage 3 may also be connected to this geographical boundary. As core MD84-551 may be influenced by a greater volume of warm waters to the north, whereas cores in the southeast Indian Ocean are not. In addition, increasing dry, glacial conditions occurring on the Australian landmass would influence these latter cores. However, this hypothesis does not find support during the other cold isotope-stages 2 and 6. The only other reasoning for deviating SST records in late isotope-stage 3 are regional rather than circum-Antarctic ones, or extreme differences in the DTF models.

6.5.6. A COMPARISON OF PAST SEA-ICE REPORTS IN THE SOUTHERN OCEAN.

Most references to past sea-ice cover have reported the position of sea-ice in the last glacial maximum, the exception being the recent study by Kaczmarska *et al.* (1993). A summary of previous early studies, and the resultant sea-ice interpretations, is found in section 5.1.

The current maximum sea-ice extent in the southeast Indian Ocean sector is approximately 61°S (Schweitzer 1995). The continuous results of core MD88-787 indicate that during the last 195 kyr, sea-ice in certain glacial periods has reached and passed beyond 56°S (Fig. 6.18). The CLIMAP (1981) last glacial maximum reconstruction in the study region projected sea-ice at 145°E during August to around 50°S and to 52°S during February. The results obtained from core MD88-787 in the last glacial maximum agree in principle with the CLIMAP (1981) proposed sea-ice extent during August, but not with their February estimates. The observations from MD88-787 do not indicate sea-ice cover in February during the last 195 kyr over the core site.

The last glacial maximum period does not show the greatest or longest sea-ice record for the southeast Indian Ocean. This record is found in isotope-stage 6 (Fig. 6.18B and C). Sea-ice cover records similar to those recorded in isotope-stage 2 are also observed in early isotope-stage 3. The core on Kerguelen Plateau studied by Kaczmarska *et al.* (1993, ODP site 745, 59°S, 85°E), although not studied in high resolution, exposed the link of past sea-ice extent from diatom signals modulated by the earth's obliquity especially in the

Pleistocene. A future test will be to analyse the continuous sea-ice results of this thesis in the spectral domain.

As noted in previous sections, sea-surface temperatures in the region also support the placement of sea-ice as far north during glacial periods. Change in oceanic structure during glacial periods is observed from this work and other sea-surface temperature data (eg Labeyrie *et al.* 1996) and the reduction of conversion of North Atlantic Deep Water (NADW) to the Circumpolar Deep Water of the Southern Ocean (eg. Charles and Fairbanks 1992). These changes should result in an alteration of the temperature structure of the ocean and would reduce the ocean heat flux, allowing more sea-ice to grow. Furthermore, reduction of the "warm" NADW input would result in decreased melting of the ice since most of the sea-ice retreat occurs through direct warming of the ocean rather than by melting of the ice by solar radiation (Crowley and Parkinson 1988a,b). This reduction in summer melt could lead to the presence of multi-year ice as already suggested by others (CLIMAP Project Members 1976, Grobe and Mackensen 1992). Ice production rates may have reached a different balance during glacial periods with a thicker, less variable multi-year ice cover, which could reduce the amount of salt rejection and deep thermohaline convection in the ocean.

In addition to the change in ocean structure and likely movement of frontal positions, the atmospheric pressure systems would be expected to also move north with associated movement of the sea-ice. Air temperature and pressure systems are intricately linked to the presence of sea-ice, as is the sea-ice affected by forcing of atmospheric events. General circulation models dealing with some of these aspects are only beginning to reveal the roles of each field (Watkins and Simmonds 1995, Godfred-Spenning and Simmonds in press) although the use of short-term to long-term records should be treated with caution. It is hypothesised that increased sea-ice and more permanent sea-ice would depress air temperature variability seasonally, influence the pressure systems, and consequently decrease the genesis of storms (Watkins and Simmonds 1995). A reduction of evaporation, and consequently precipitation, has already been noted in glacial periods from the Vostok ^{10}Be record (Yiou *et al.* 1985). An increase in wind strength, associated with the glacial periods, can affect heat fluxes (Crowley and Parkinson 1988a), but the overall effect on the Southern Ocean climate remains to be investigated.

6.6. PALAEOCEANOGRAPHIC TIME SLICES AND HYPOTHESES.

In summarising the results of the three cores studied in this thesis, isotopic-time slices are discussed individually and compared with current hypotheses and studies from the Southern Ocean and Hemisphere. A map of today's surface currents is presented in

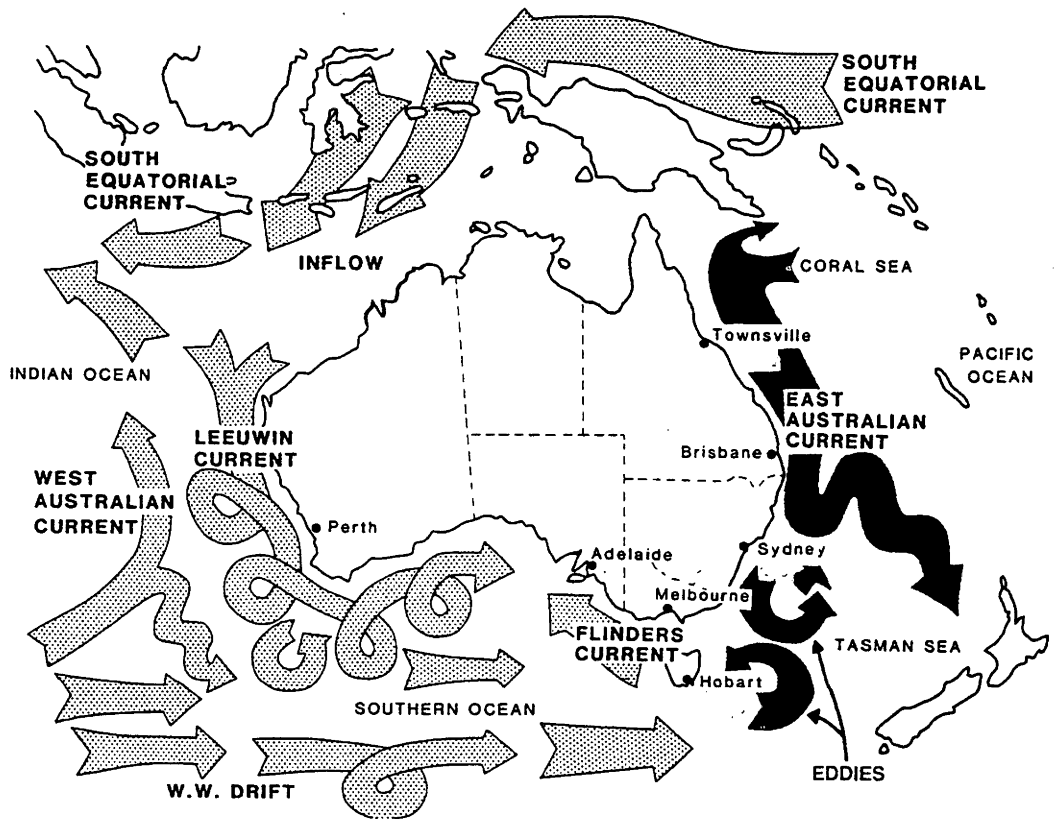

Figure 6.24. The major surface currents surrounding Australia (after Cresswell 1987). Black shading on arrows highlight the East Australian Current and its eddies which pinch off and continue to drift southward past Tasmania to mix with the Antarctic Circumpolar Current (identified here as the West Wind Drift).

Figure 6.24 as documentation for the isotopic stage discussions to follow. A modern/interglacial oceanographic scenario of the region is presented in Figure 6.25. The contrasting maximal glacial conditions that are suggested from isotope stages 6 and 2 are presented in Figure 6.26.

6.6.1. ISOTOPE-STAGE 7.

Latitudinal core studies by Morley (1989a) and Prell *et al.* (1979) in the South Indian Ocean southwest of Australia, both suggested southward shifts in the Subtropical Convergence (STC) particularly in the later part of isotope-stage 7. Morley's (1989a) estimates suggested a 2° latitude movement south of the current STC position and further concluded that the Polar Front (PF) also moved southward from its current position in the South Indian Ocean by up to 9° latitude. Cores MD88-787 and MD88-779 both record the final part of isotope-stage 7. Warm-water flora diminishing in response to open-water fauna at the transition between isotope-stage 6 and 7 indicate that warmer waters were present at 47°S, 146°E. Core MD88-787's SST record indicates that warmer surface waters of around 5°C were also present in the region prior to the glacial conditions of isotope-stage 6. The position of the PF in respect to this warm surface water signal is interpreted to be overlying, or perhaps no more than 1-2° latitude north of the core site. Thus, in effect ~3° latitude south of its current position. This is not to say the PF could have been further south earlier in isotope-stage 7. It would appear that both the STC and PF, and presumably the Subantarctic Front (SAF), were all south of their current positions in late isotope-stage 7.

6.6.2. ISOTOPE-STAGE 6

Core MD88-787 contains the only complete diatom record of the three cores studied in this thesis. Core MD88-779 indicated in the early stage of isotope-stage 6, a replacement of warm-warm water flora by transitional and dissolution-resistant species, before the diatom record disappears for the remainder of isotope-stage 6. Throughout most of isotope-stage 6, SST estimates indicate cooler conditions than present over site MD88-787. The greatest displacement northward of the PF appears most likely around 175 and 140-145 ka whereas, throughout the remainder of isotope-stage 6, the PF was near or just north of 56°S. The northern latitudinal shift cannot be determined from this core alone, but would be confined by the intervening water masses and the Australian landmass. A Tasmanian speleothem records a 2-3°C warming on land between 100-97 ka (Desmarchelier and Goede 1996). However, this warm event is separated by 50 kyr from the warming peak around 155-150 ka in the core SST record.

Studies predominantly located in the South Indian Ocean also concur with cooler surface waters (Williams 1976) and the concomitant northward shifts in the PF, STC (Morley 1989b, Howard and Prell 1992) and SAF (Vella *et al.* 1975) during isotope stage 6. The

suggested northward shift of the PF in the South Indian sector is a maximum of 4° latitude to around 45°S (Morley 1989b, Howard and Prell 1992); while the STC is believed to have moved equatorward by up to 7° latitude (Morley 1989b). The Leeuwin Current, occurring along the western Australian coastline, is considered to have weakened whereas the Western Australian Boundary Current increased in strength. Along the southwest coast of Australia increased offshore upwelling is also inferred with weakened Leeuwin Current (Wells *et al.* 1994, Okada and Wells 1997). Okada and Wells (1997) suggest that these oceanographical changes be linked in part to the northward movement of the STC to the extent that it impinged on the Western Australian Coast during glacial periods (Howard and Prell 1992). The idea that STC was cut by the Australian landmass in the west and therefore did not exist south of Australia during glacials remains to be proven. At this stage, only minor evidence and inferences of the weakened and perhaps missing Leeuwin Current influence is known south of Australia during such periods (Wells and Wells 1994, Wells and Okada 1994).

As discussed previously, records of oceanographic change from the southeast Tasman Sea region also suggest northward movement of the STC (Martinez 1994, 1997, Barrows 1995, Passlow *et al.* 1997, Nees 1997) possibly as far north as 43°S. A potentially more important feature linked with this northward movement in the Tasman Sea region is the observation of Subantarctic Mode Water (SAMW) thermostads located considerably further northward (~20°S) beyond the Tasman Front (Martinez 1994, 1997). Martinez (1997) attributes the northward expansion of SAMW to vigorous mixing of the ocean south of the STC, or a weakened Tasman Front. SAMW is formed north of the SAF as a winter overturning process of the subantarctic waters (Mc Cartney 1977), and is considered a locally derived watermass of the Southern Ocean since it does not pass through the Drake Passage (Peterson and Stramma, 1991). In the southeast Indian Ocean, SAMW has been observed as a separate entity to Antarctic Intermediate Water (AAIW) (Sloyan 1993) but, importantly, was found to still incorporate Antarctic Surface Water (AASW) (Rintoul and Church 1993).

This latter observation has significant implications for the oceanography of the southeast Indian sector during glacial periods. The evidence presented here of northward shifts in oceanographic surface features (ie sea-ice at 56°S, PF at least at 50°S, STC maximum 43°S) suggest the influence of more proximal melt water and a likely southward extension of AASW. This may link in with the northward SAMW presence in the northern Tasman Sea as reported by Martinez (1997). Reports of inferred increases in surface productivity at core E27-30 (45°S, Passlow *et al.* 1997) and also in core MD88-779 (47°S, Dr S. Nees pers. comm. 1997) would suggest that SAMW formation was present at these latitudes. Thus, the SAF would have been present just south of these cores.

The lack of diatom abundance in core MD88-779 still remains a dilemma. If SAMW was formed in this region and high surface productivity is suggested by other micropalaeontological sources, then one must assume that the surface mixing was too vigorous and too short for diatoms to profitably bloom. The enhanced productivity must be attributed to other microflora and fauna, and this seems appropriate with the high sedimentation rate observed in isotope-stage 6 in core MD88-779 (section 6.2.4). Short and vigorous seasonal mixing events may have been the case in isotope-stage 6, since sea-ice cover between 5 to 8 months of the year is estimated during the coolest phases of this stage. Such a seasonal overturning event of the surface waters has already been suggested in the southeast Indian Ocean domain by Nelson *et al.* (1993) and Martinez (1997). The concept of a stratified melt-water lid in the region between the PF and the SAF would not be out of place under this scenario with associated dampening effects on diatom productivity. This feature is further discussed in section 6.8. Other factors such as bottom-water or surface-water dissolution removing diatoms from core MD88-779 before they reach the sea-floor, are equally fair alternatives to explain the diatom record "loss" in this northern core during this glacial interval.

6.6.3. ISOTOPE-STAGE 5

Throughout the interglacial record of isotope-stage 5 in core MD88-787 the SST variation does not allow identification of the various substages. Concentrating on the last interglacial climax, the SST record indicates a southward movement of SST isotherms beyond 56°S and thus, a likely displacement of the PF just south of the site also. Core MD88-779 records increasing warm-water flora along with species considered of open-ocean origin during isotope stage 5.5. A STC movement southwards in the study region during isotope stage 5.5 was concluded by Passlow *et al.* (1997), whereas a slight northwards shift was postulated by Nees (1997) and analogous modern conditions by Martinez (1994). Along the Chatham Rise, SST values 1 °C warmer than today for isotope stage 5.5 were proposed by Nelson *et al.* (1993), and yet, no movement southward of the STC was suggested. In the South Indian Ocean sector, original interpretations suggested a lack of STC movement (Williams 1976, Prell *et al.* 1979, CLIMAP Project Members 1984), but later studies implied southward movement of the STC had occurred at least to 40°S (Morley 1989b, Howard and Prell 1992). Both studies also pointed to a movement of the PF southward of 48°S. The Leeuwin Current was considered reanimated or strengthened during that time (Okada and Wells 1997).

The remaining substages of isotope-stage 5 are not commented on in such detail as substage 5.5. Howard and Prell (1992) illustrate variation in the PF as returning to its modern placement and shifting by around 1-2° latitude south, presumably during isotope substage 5.1. Movement of the STC southwards, again though isotope-stage 5, is not observed in Howard and Prell's (1992) or Morley's (1989b) records, nor in SST records

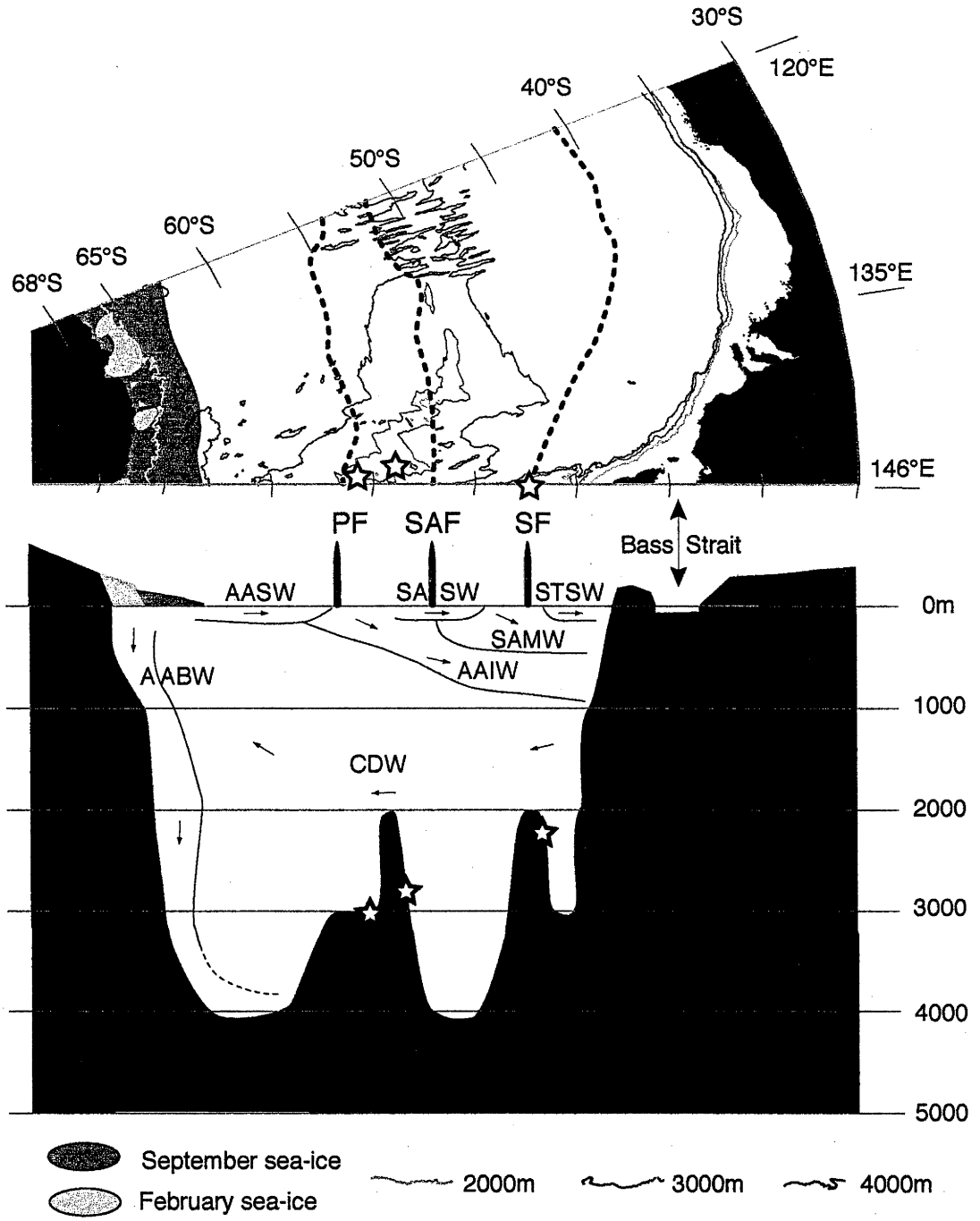

Figure 6.25. Schematic present-day oceanographic setting of study region. Core locations identified by stars (from left to right, MD88-787,-784,-779). Current maximum February and September sea-ice extents are south of 61°S (Schweitzer 1995). Oceanographic fronts from Orsi *et al.* (1995). PF = Polar Front, SAF = Subantarctic Front, SF Subtropical Front/Convergence. Watermasses from Gordon and Molinelli (1986) and Sloyan (1993). AABW = Antarctic Bottom Water, AASW = Antarctic Surface Water, AAIW = Antarctic Intermediate Water, CDW = Central Deep Water, SAMW = Subantarctic Mode Water, SASW = Subantarctic Surface Water, STSW = Subtropical Surface Water.

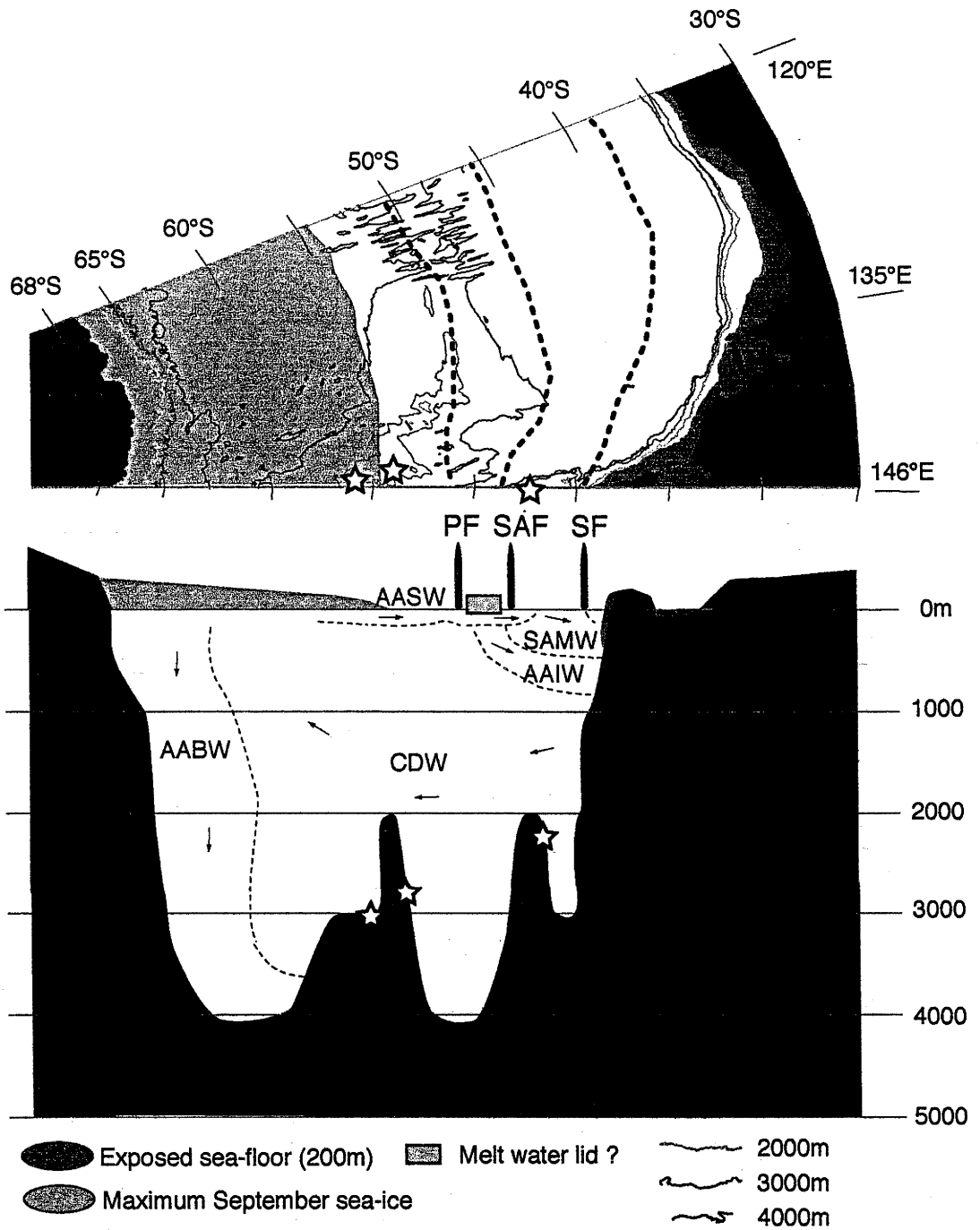

Figure 6.26. Schematic glacial oceanographic setting of study region interpreted from diatom sea-surface temperature and sea-ice estimates. Oceanographic fronts and the maximum september sea-ice moved north. February sea-ice cover is also assumed to have moved north and covered greater an area than present, but it did not reach 55°S. A melt-water lid may have covered the region between the PF and the SAF after spring melt back. SAMW may have included AASW. Core locations identified by red circles (from left to right, MD88-787,-784,-779). PF = Polar Front, SAF = Subantarctic Front, SF = SubtropicalFront/Convergence. AABW = Antarctic Bottom Water, AASW = Antarctic Surface Water, AAIW = Antarctic Intermediate Water, CDW = Central Deep Water, SAMW = Subantarctic Mode Water.

core from subantarctic core MD84-527 (Pichon *et al.* 1992a). From the SST record of core MD88-787 there does not appear to be any major change in the surface structure over the site, except for what is interpreted as substage 5.1 (~72 ka). Here, the probability of a PF southward drift similar to that observed during isotope substage 5.5 occurred. This is consistent with the observations of Howard and Prell (1992) and of the SST record from South Indian core MD84-551 (Pichon *et al.* 1992a).

6.6.4. ISOTOPE-STAGE 4

Recent studies identifying and recording changes during isotope-stage 4 are few. The expected glacial cool signals do not make an appearance in the sedimentary record of the Southern Ocean, and SST estimates remain generally undifferentiated from the transition of isotope-stage 3 to 5 (Howard and Prell 1992, Pichon *et al.* 1992a, Labeyrie *et al.* 1996). The few investigations that advance interpretations for isotope-stage 4, in fact, suggest northward movements of the STC (Morley 1989b, Passlow *et al.* 1997) and PF (Morley 1989b). Increases in surface productivity in the southwest Tasman Sea region are also observed in cores studied by Passlow *et al.* (1997) and Nees (1997), although the former author noted increased dissolution of the carbonate record. Continental records from Tasmanian speleothem temperature histories indicate two cool phases between 60 and 70 ka (Goede 1994). From the SST record of MD88-787 a single cool spike, amongst otherwise modern warm oceanic conditions present in isotope-stages 5 and 3, is observed (Fig.6.20). A similar decrease in SST is observed in the South Indian sector core MD84-551 (Pichon *et al.* 1992a). The cool spike in MD88-787 also reflects the reappearance of minor sea-ice cover at 65 ka over the core site.

6.6.5. ISOTOPE-STAGE 3

Isotope-stage 3 in the southeast Indian Ocean records substantially different sea-surface conditions to the South Indian Ocean, with an early cool phase lasting until 40 ka, followed by warmer conditions to isotope-stage 2/3 boundary. Previous SST records in the South Indian Ocean cores MD84-551 and -527 (Pichon *et al.* 1992a) did not record this double phase (Figure 6.23). Nor was such a two-phase trend evident in the subantarctic core MD88-770 (Labeyrie *et al.* 1996). Howard and Prell (1992) suggested that a cooler phase, possibly cooler than the last glacial maximum, occurred in the South Indian Ocean in late isotope-stage 3. Other studies in the South Indian sector propose generalised northward digressions of the PF, STC (Morley 1989b) and SAF (Vella *et al.* 1975) through isotope-stage 3.

The late cool phase observed in both MD88-787 and -784 in the southeast Indian Ocean may in fact prove to be a product of misaligned isotope/SPECMAP age chronology covering the transition from isotope-stage 4/5 to 2/3. The difficulty in associating oxygen-isotope-stages 2-4 in Southern Ocean cores is not new (Williams and Keany 1978, core

MD88-779 this study). Here, isotope-stage 4 was considered well aligned to the SPECMAP isotope stack, yet room for error due to low oxygen-isotope resolution in this section of the core is possible. Assuming that this is not the problem, isotope-stage 3 in the southeast Indian Ocean records an early cool phase followed by warmer phase. A northward movement of the STC was already suggested by Passlow *et al.* (1997) along with increases in palaeoproductivity signals from benthic ostracods from *Eltanin* core E27-30 and E36-23 during isotope-stage 3 (Passlow *et al.* 1997, Nees 1997). In contrast, benthic foraminifera from core MD88-779 do not infer high surface productivity (Dr S. Nees, pers. comm. 1997); this concurs with the lowering of diatom abundances in the sediments. The case for partial, repeat of isotope-stage 6 conditions, along with a surface melt-water lid south of the SAF, may be the explanation for the varying signals recorded in cores between Tasmania and Antarctica. The results of Martinez (1997) are too coarse between isotope 2 to 4 for interpretation of the SAMW to support this repeated scenario. However, François *et al.* (1993) observe varying palaeofluxes in isotope-stage 3 in core MD84-527 that are not reflected in the stable SST estimates, and these authors refer them to possible northward advances of the PF.

6.6.6. ISOTOPE-STAGE 2

An abundance of studies are charged with information regarding sea-surface change in the last glacial maximum (LGM), most originally generated from individual programs within the CLIMAP project. Reported shifts in the major fronts in the Southern Ocean have essentially remained unchanged from these early observations, although many estimates are based on South Indian Ocean studies.

Southward movement of the STC in the Tasman Sea region was interpreted by Passlow *et al.* (1997) through isotope-stage 2 from an otherwise stable or slightly northward STC at 45°S, while the Tasman Front moved southward to ~26°S (Martinez 1994, Hesse 1994). Recent reconstructions of sea-surface temperatures in the Australian region during the LGM reveal only slight cooling (up to 3°C) in the southern Tasman Sea region (Ayress and Barrows 1996, Barrows *et al.* 1996). Studies east of New Zealand have the STC locked to the Chatham Rise (Fenner *et al.* 1992, Nelson *et al.* 1993). In contrast, primary microfossil assemblage data from the South Pacific argue for a northward movement of Antarctic water masses (Moore 1978, Moore *et al.* 1980). In the South Indian Ocean sector, the STC was considered to have shifted 5° latitude north, introducing the concept of an intensified West Australian Current and a STC, which intersected the Australian Coast (Prell *et al.* 1979, Prell *et al.* 1980). Morley (1989b) also identified a 5° northward shift of the STC in the South Indian Ocean. These results are contrary to those expounded by Hays *et al.* (1976) and CLIMAP (1981), who both considered that no movement of the STC had taken place during the LGM.

The Polar Front location during the LGM was originally believed to have moved 4° latitude northwards in the Southwest Indian Ocean (Hays *et al.* 1976). Labeyrie *et al.* (1986), however, advanced a theory of a melt-water lid based on micropalaeontological, sedimentological and isotopic analyses, which conclude that the PF remained stationary between 17 and 60 ka in the Southwest Indian Ocean sector. Williams (1976) proposed an 8° latitude shift north of the PF in the South Indian Ocean sector. Dow (1978) later refined this northward movement. She suggested the displacement was on the order of 5° latitude in the South Indian sector during the LGM. Further work by Morley (1989b) and Howard and Prell (1992) suggested similar northerly PF movement in the South Indian Ocean in the LGM (equatorwards to 45°S). A 4° northward shift was predicted for the Pacific Ocean (CLIMAP Project Members 1981). An undefined northward advance of the PF at the LGM was observed from diatom assemblage data around the Southern Ocean (Burckle 1984).

Results from cores MD88-787 and -784 both suggest initial cold-water conditions in isotope-stage 2 which show strong deglaciation signals through to Termination I, as also observed by Passlow *et al.* (1997). Displacement of the PF northward appears likely over both sites (56-54°S). However, the loss of diatom frustules again occured in MD88-779 (20-30 cm depth) suggest that an isotope-stage 6 scenario was again taking place. With the evidence for a small northward shift in the STC to 45°S (Passlow *et al.* 1997), the space remaining for the PF and SAF becomes restricted. The development of SAMW in the region would incur strong overturning processes as predicted by Martinez (1997), while productivity at the surface may have been limited. A combined AAIW and SAMW intermediate water mass may have existed in the south Tasman Sea sector as a result of the confined frontal system during this and isotope-stage 6.

Reduced productivity in the LGM has been reported; earlier interpretations considered low isotope-stage 2 sedimentation rates to be a feature of increased dissolution (Bard *et al.* 1989, Pichon *et al.* 1992b). However, increasing biogeochemical studies, predominantly in the South Indian Ocean sector (François and Altabet 1992, François *et al.* 1991, Mortlock *et al.* 1991), have evolved theories on reduced surface productivity in the Southern Ocean. In some instances reduced productivity and opal accumulation are attributable to regionalised iceberg-derived melt-water lids (Labeyrie *et al.* 1986, Shemesh *et al.* 1994) whereas, elsewhere, reduced accumulation rates are yet to be related to other factors (eg. this study). The role of increased bottom-water during the LGM is another factor considered to have decreased opal accumulation in the sediments through winnowing (François *et al.* 1993).

François *et al.* (1993) suggested that low biogenic fluxes in the LGM might be due to stratification of the surface waters by a meltwater lid as revealed by an increase of $\delta^{15}N$ in the sediments. Their hypothesis is linked with the observation of increased *Cycladophora davisiana* abundances, which Morley and Hays (1983) discussed as a low surface-salinity indicator. The distribution of *Cycladophora davisiana* in the sediments is plotted in Figure 6.8 for core MD88-787, and illustrates high abundances during isotope-stage 2 alongside the decrease of absolute diatom abundance. South of Western Australia, nutrient depletion of the subantarctic waters was shown to occur with the northward advance of frontal systems in the LGM (François and Altabet 1992). There are no $\delta^{15}N$ data are available for the cores of this study. Yet, the limited interpretations provided by the SST estimates, *Cycladophora davisiana* and diatom abundances in core MD88-787, imply that stratification of the surface waters and reduced surface productivity did occur in the LGM between 56° and 47°S south of Tasmania.

6.6.7. ISOTOPE-STAGE 1

Variations between cool and warm stages are observed during isotope stage 1 in both MD88 cores of this study. Increasing warm-water floras are evident northwards in core MD88-779, as were the warm water factor of cores MD88-787 and -784 (Figures 6.13, 6.14). On mainland southeastern Australia, speleothem temperature estimates reveal cool conditions (at least 2.3°C lower than present) between 12.3 and 11.4 ka and also around 3ka (Goede *et al.* 1996). Within the surrounding ocean such high resolution variation has not been commented on. In a more general sense, the STC was considered south of 45°S (Passlow *et al.* 1997) and the influence of the Leeuwin Current detectable in cores southeast of Victoria (Wells and Okada, 1996). In the South Indian Ocean sector, Morley (1989b) considered the STC and the PF to have beenpoleward by ~2° and ~4.5° latitude respectively, for the preceeding cooler conditions. Howard and Prell (1992) also observed the southward movement of the STC. These southward shifts are in accord with diatom SST estimates in the South Indian Ocean (Pichon *et al.* 1992a, Labeyrie *et al.* 1996).

Fluctuations of SST estimates in cores MD88-787 and -784, may be in line with those suggested by mainland Australian cooling events. Nevertheless, the need for a better chronological control of the sediments in isotope-stage 1 is required before further relationships are formulated or SST estimates considered representative of specific ages. Obviously, the equivalent of the Younger Dryas should be observable in the cores studied in this thesis as it has been observed within ice cores of the Antarctic (Jouzel *et al.* 1991). The Younger Dryas was identified in the MD84 cores of the South Indian Ocean (Labracherie *et al.* 1989, Bard *et al.* 1990). Preliminary research on high resolution cores from the Tasman Sea and New Zealand have been found to include the Younger Dryas

event although at synchronous times to those observed in Northern Hemisphere records (Ms C. Samson, pers. comm. 1996).

The loss of the core top in MD88-784 combined with the abnormally low SST estimates from the core top of MD88-787 do not allow comparison to modern conditions, and suggest caution in the age determinations of this isotope-stage.

6.7. THE ROLE OF BOTTOM-WATER.

Several references regarding the role of bottom-water have been taken up during the course of the thesis. In the first instance, several diatom species were identified as displaced by bottom-water currents as deduced from the database sediment distributions and relationships between abundances and surface parameters (Chapter 3). The species identified (*Fragilariopsis separanda, Navicula directa, Odontella weissflogii, Paralia* spp., *Thalassiosira oliverana*, and possibly *Actinoyclus actinochilus*) were not those previously considered and used as bottom-water pathway (AABW) indicators (ie. *Eucampia antarctica, Fragilariopsis kerguelensis*, and *Thalassiosira lentiginosa*: eg. Burckle and Stanton 1975, Burckle 1981, Jones and Johnson 1984). The rationale behind following such latter endemic Antarctic diatom species was that they were considered entrained at the site of AABW formation and deposited in the sediments along the northward flowing pathway. For the three species previously considered AABW indicators (*Eucampia antarctica, Fragilariopsis kerguelensis*, and *Thalassiosira lentiginosa*:), it is now apparent that they are not entrained at the place of AABW formation along the Antarctic coast since they are considered generally as oceanic species (Chapter 3). This feature was also raised by Fryxell (1991) who questioned the use of the *Eucampia antarctica* as a bottom-water diatom marker due to the evidence of polar and subpolar subspecies partitioning in the Antarctic Circumpolar Current. Nevertheless, heavily silicified diatoms, endemic to the Southern Ocean, are displaced by AABW and occur at least from the mid high-latitudes to the north (eg. Van der Spoel *et al.* 1973, Abbott 1973, Burckle and Stanton 1975, Booth and Burckle 1976, Burckle 1981, Jones and Johnson 1984, Treppke *et al.* 1996). We now need to elucidate where open-ocean diatoms are entrained along the AABW pathways, and how far the other newly reported species, more in tune with formation pathways of AABW, are transported.

The second instance of inferred influence of bottom-water examined in this thesis was the concept of a factor assemblage that could be determined from the few non-neritic species remaining in the Natural database. This factor contained species interpreted as referable to both island and transport signal previously commented on in Chapter 2. In particular to the distribution associated with the transport feature of this factor were the abundances of *Fragilariopsis separanda* and *Thalassiosira oliverana*. Although the inference requires

concrete evidence, it would appear, in the southeast Indian Ocean at least, that *Fragilariopsis separanda* has been entrained at the site of bottom-water formation in the Ross Sea where the highest relative abundances are recorded in the sediments and displaced northwards. The same cannot be implied for *Thalassiosira oliverana*, at least from the Ross Sea, although there is some evidence with higher abundances along the East Antarctic coastline that the species is potentially entrained in bottom-water formation under less saline conditions. An increase in the sample coverage, both in terms of surface phytoplankton and sediment records along the Antarctic coast, would assist in determining the natural abundance of these two species and their association with AABW formation. Already, there is an implication that *Fragilariopsis separanda* and *Thalassiosira oliverana* occur within regions of AABW formation. However, it is hypothetically possible that their habitats are partitioned as a result of the variation in the upwelled Central Deep Waters to the southeast Indian Ocean and the Ross Sea. It was considered difficult to directly associate the transport/island factor in this analysis (see Chapter 4). Future studies may improve this analysis by applying bottom potential temperatures to a factor analysis concerned with all species suspected of bottom-water movement (ie. neritic/benthic species outcast in this thesis and other planktonic species previously associated with such movement). It should also be noted that this is not the first time factor analysis of Southern Ocean sediments has resolved a transport or bottom-water factor. Dow (1978), in her study of Radiolaria in the south Indian Ocean, found a bottom-water factor that was linked positively with increases in the Antarctic factor suggesting increases in Antarctic water influence were also with periods of concomitant bottom-water flow.

Finally, the reference to bottom-water effects in the core records was examined. One explanation proffered here, linked the decreased or absent diatom record in core MD88-779 to increases in bottom-water movement over the site. However, other features of the surface water structure are discussed in this chapter as contributing to the loss of diatom signal in this region (ie. productivity). It is likely that diatom abundances were reduced in the sediments, in part due to winnowing, dissolution and productivity decreases during the last and penultimate glacial. Core MD88-779 is, as mentioned previously, at a depth of 2260mbsl. The characteristics of the bottom-water at the site (dissolved oxygen 4.2m/ml, temperature ~2.25°C, salinity 34.7 ppm; WOA 1994) identify the water covering the site is of Central Deep Water (CDW) origin, and concomitant with CDW reported in the South Australian Basin (Braatz and Corliss 1984). The sediment record thus, was influenced by CDW changes in line with increased atmospheric circulation and variation in its sources (Ledbetter *et al.* 1983). Braatz and Corliss (1984) interpreted a change in CDW characteristics (ie. colder and fresher) from the increase in *Epistominella exigua* abundances. Ledbetter *et al.* (1983) suggested that CDW activity could have been enhanced during glacials, which could produce shallow water hiatuses. Connell and

Sikes (1997) reported preferential removal of the fine fraction from sediments on the South Tasman Rise which they attributed to winnowing, a result of increased current velocities, both over shallow regions and the southern section of the rise. It is likely that current intensification and winnowing would have affected the sedimentation of diatoms (sizes with less than 60μm) during glacial periods in this region.

The observations of non-analogue events in cores MD88-787 and -784 are both interestingly dominated in isotope stage 6 by occurrences of *Fragilariopsis separanda* over-abundances (Tables 6.2, 6.3). As several workers have pointed out (Connolly and Payne 1972, Rodman and Gordon 1982, section 1.5.3), Antarctic Bottom Water (AABW) from the Ross Sea region passes northwards through the Tasman Fracture Zone. As indicated throughout the thesis, *Fragilariopsis separanda* is highly likely to be associated with bottom-water transport. It is in the study from the southeast Indian Ocean that we may find the first evidence of this phenomenon. *Fragilariopsis separanda* was observed to have the highest relative abundances in the sediments of the Ross Sea (section 3A.3.17) and secondary abundances near the winter sea-ice edge. It would appear that the increased abundances of this species removed from the Ross Sea, in fact, represent an allochthonous element indicating increased northward displacement in the nepholoid layer attributed to pass from the Ross Sea into the south Tasman Basin. The situation presented by the records of the two polar cores used in this study indicate that very strong AABW currents between the Ross Sea region and the Tasman Basin were present at least during isotope stage 6. Increased attention to the record presented by *Fragilariopsis separanda* in these two cores, and quite possibly the removal of the species from SST transfer function analysis, will eventually allow a better history of bottom-water change in the region to be presented and evaluated.

6.8. THE ROLE OF SEA-ICE, MIXING DEPTH AND A MELT WATER LID.

It is likely that in the past melt-water lids existed during the spring month of sea-ice meltback. Today, melt-water derived from spring sea-ice retreat provides regions of high diatom productivity due to the overturn of water column and increased nutrient availability (eg. Garrison *et al.* 1987, Nelson *et al.* 1987, Fryxell and Kendrick 1988, Fryxell 1989, Lancelot *et al.* 1993, Holm-Hansen and Vernet 1990).

Conditions conducive for enhanced *Cycladophora davisiana* productivity and decreased diatom accumulation in the past are likely to reflect surface conditions. These were surmisedby Morley and Hays (1983) as surface waters characterised by a low-salinity, stable surface-layer indicative of a melt water lid. Reduced mixing between this surface melt-water layer and the underlying saline, cool subsurface water is inferred to impede diatom productivity dramatically through reduction of a primary requirement of diatom reproduction - silica. It is the mixing of the silica-rich subsurface waters with the low-

salinity, stable surface waters which allow diatom blooms to occur (Holm-Hansen *et al.* 1977, Mitchell and Holm-Hansen 1991, Round *et al.* 1990, Dugdale *et al.* 1995). Reports of low diatom productivity in sea-ice melt water have been recorded today, and have been associated with the lack of subsurface water mixing in the surface layers (Sakshaug and Holm-Hansen 1984, Mitchell and Holm Hansen 1991, Scharek *et al.* 1994). These modern diatom productivity examples, abridged by the *Cycladophora davisiana* habitat preference and abundances of the past, would point to conditions in isotope-stages 2 and 6 as low diatom productivity events being a product of inefficient or lacking subsurface mixing. The lack of diatom records in core MD88-779, during the same periods of high *Cycladophora davisiana* abundance and minimised diatom abundances in core MD88-787, may indicate that surface waters in the southeast Indian Ocean were stagnant and stratified. This affected diatom productivity throughout much of these phases and is believed to have covered a distance at least from 56°S to the South Tasman Rise. Any production either due to upwelling or shallowing of the subsurface waters to within the euphotic zone, were probably removed by through winnowing along the South Tasman Rise. Alternatively, a melt-water lid may have been a short-lived event due to overturning of the surface waters but still have occurred during the annual bloom phase which reduced diatom production.

Current observations of diatom distributions in the sediments under the Subantarctic Zone are lower than distributions in the Polar Front Zone to the south (ie. $1x10^6$ to $50x10^6$ valves/gram dry sediment in the SAZ, Zielinski and Gersonde 1997). The lower distributions have been attributed to surface depletion of nutrients and increasing temperature, along with reduced flux. The flux of diatoms in this zone is currently unrecorded.

The implication for an unmixed subsurface water mass is that the PF would have been further north than present. Thus, the melt-water cover may have been evident as far north as core site MD88-779. Reports of reduced diatom productivity along the PF have also been referred to low vertical stability of the water column should the Front assume convergence rather than divergence characteristics (El-Sayed 1984, 1988). This has implications for the whole surface structure of the ACC in the southeast Indian Ocean during these phases.

In addition, diatom productivity belts, currently associated with the sea-ice edge, are assumed to have moved northwards with the extension of sea-ice or meltwater influence. Reduced diatom productivity to the south would be restricted by an extended ice shelf and/or multi-year sea-ice boundary around Antarctica (Burckle and Cirilli 1987). The results of this thesis do not necessarily support the former hypothesis of enhanced diatom productivity with the extension of sea-ice to the north. Priddle *et al.* (1992) reached the

same conclusion, but, believed that increased productivity to the north would have occurred because of the more stable surface waters.

6.9. SUMMARY.

Four cores located between the PF and the STC and between Tasmania and Antarctica were chosen for study (MD88-787, -784, -779, E53-10, Figure 6.1, Table 6.1). Core *E*53-10, on the edge of the South Tasman Rise, was abandoned from further study as diatom and silica/zinc ratio analyses demonstrated the extensive re-worked nature of the core. Biostratigraphic analysis on the remaining three MD88 cores was performed. Two cores, MD88-787 and -779, contained the biostratigraphic marker, *Hemidiscus karstenii*, which indicated the cores crossed the isotope-stage 6/7 transition. All three cores fall within the *Thalassiosira lentiginosa* Partial Range Zone.

Oxygen-isotope records were available for each of the three cores. The planktonic foraminifera derived ratios were used in core MD88-787 and -784, whereas the benthic foraminifera derived ratio was used for MD88-779. Preliminary age models for each core were determined using *Analyseries* 1.1 (Paillard 1997). The simple LinAge model was employed to linearly link the respective oxygen-isotope SPECMAP stack age models to the oxygen-isotope records of the three cores. Core MD-88-787 contains 195 kyr of continuous sedimentation. Core MD88-784 appears to be missing the very top and covers isotope-stages 1 to the 3/4 boundary. MD88-779 is found to cover 200 kyr over its 260 cm length. Linear sedimentation rates are within predicted rates for the region. Holocene sedimentation rates are the greatest when compared through the history of the two polar cores (MD88-787, -784). Previous interglacial and glacial periods register lower sedimentation rates. The subantarctic core has the highest rate of sedimentation in isotope-stage 6, in an otherwise near-constant sedimentation record.

Absolute diatom abundances (ADA) in the core-tops of MD88-787 and -779 are in disagreement with values reported from nearby box-cores (Crosta *et al.* 1997). In general, interglacial periods are found to contain similar levels of ADA to those observed in the Holocene, while glacial periods indicate a reduction of ADA in the sediments. Comparison of the ADA values with abundances of the radiolarian *Cycladophora davisiana* reveals an inverse correlation. This relationship is crucial to deciphering the oceanographic conditions leading to decreases in the diatom record in the region. Inferences of oceanographic conditions during periods of low ADA are referred to modern conditions under which *Cycladophora davisiana* currently occur in high abundance. This includes extensive ice cover in winter and spring, low surface salinity waters capping cooler, saline subsurface water, which underwent very low mixing at the surface.

In the subantarctic core, MD88-779, the majority of samples were poorly preserved and showed high levels of dissolution. In some cases, samples were barren of diatoms. However, for each isotopic stage, variations in the diatom species assemblages could be determined. Sea-surface temperature and sea-ice estimation could not be performed on the diatom record preserved in the core. Other siliceous material was present in the core samples. Application of the Mandra silicoflagellate *Distephanus/ Dictyocha* ratio as a proxy for SST was not considered reliable or accurate from this core because of the low number of silicoflagellates recovered

Core MD88-779 has a sedimentation rate independent of climatic conditions and diatom preservation. Diatoms are lacking in isotope-stages 2 and 6. Northward movement of the Subtropical Convergence during glacial phases was therefore obscured. Furthermore, the presence of warm-water flora in the Holocene and isotope-stage 5.5 could not substantiate a southward movement of the Polar Front either. Other micropalaeontological investigations (benthic foraminifera and ostracods) in progress are attempting to elucidate oceanographic change which the diatom record can only provide a part.

The polar cores, MD88-787, -784, contained a sufficient diatom record to permit a quantitative assessment of the species and abundances via factor analysis. Both the Pichon *et al.* (1992a) Diatom Transfer Function (DTF) 166/34/4 model and the thesis-developed SST model (109/24/6) were applied to the cores to derive past SST estimates. Although the percentage of diatom information used in each model remained high in warm phases between both the DTF 166/3/4 and DTF 109/24/6 model (Figure 6.12), it was during glacials that the two models provided closer SST estimates (Fig. 6.15, 6.16). These major differences are considered attributable to the inclusion of silicoflagellate and *Thalassiothrix/Trichotoxon* spp. in the Pichon *et al.* (1992a) model, which had otherwise been rejected for use in the DTF 109/24/6 model.

Factor analysis under the DTF 109/24/6 model indicated the dominance of the open-ocean assemblage (Factor 1) through the entire history of core MD88-784, but showed distinct sub-dominance variation in sea-ice boundary and warm-water influences (Fig. 6.13). A decreasing transport (Factor 4) influence was also noted in the Holocene. A similar picture was observed in factor analysis under the DTF 166/34/4 model, along with a decreasing dissolution signal in the Holocene. Almost no non-analogue events were observed in DTF 109/24/6. This is in substantial contrast to the DTF 166/34/4 model which had 21 non-analogue events and considerably lower communalities, the latter feature being a function of the reduced factor numbers resolved (Table 6.2, Fig. 6.13B).

Factor analysis in core MD88-787, using DTF 109/24/6, was dominated by the open-ocean signal, with exception to isotope-stages 6, 3 and 2. The variations in the cooler

phases are observed with increases in the POOZ and sea-ice cover factors. The transport/island factor has a greater influence in this core than MD88-784. This transport/island factor appears elevated when the sea-ice edge and POOZ factors retreat and just prior to a maximum of sea-ice cover is observed (sea-ice cover factor) (Fig. 6.14A). Less variation in open-ocean and cool conditions are noted from factor analysis in the DTF 166/34/4 model. Only in isotope-stage 2 do the two factors cross (ie. Factors 1 and 2). The dissolution factor is elevated in isotope-stages 6, 3 and 2. Temperature relationships are considered heavily reliant on the interplay between Factors 2 (subantarctic) and 3 (dissolution) rather than with the open-ocean factor (factor 1).

Communality values for each DTF model over the length of the core again indicate major differences in the two models. Seventeen samples are noted with non-analogue conditions in the DTF 109/24/6 model, whereas in contrast 62 samples under the DTF 166/34/4 model are encountered (Fig. 6.14B, Table 6.3). Very low communality values were also characteristic of the DTF 166/34/4 model. It was stressed that the low communality values occurred due to the simplified nature of the model, and consequently reduced relation to appropriate species variation in the down-core data. Only 32 samples of the original 103 samples of the core were useable if a communality cut-off value had been employed under this DTF 166/34/4 model. Species attributed to no-analogue conditions were discussed. Greater confidence was placed in the DTF 109/24/6 model due to the problems encountered with no-analogue events and low communalities in DTF 166/34/4.

Sea-surface temperature estimation was presented from both models for each core and then subsequently compared and discussed (Figs. 6.15, 6.16). Here, it was observed that SST estimates are generally similar during glacial phases in contrast to warmer phases where estimates differed by up to 5°C in core MD88-784, and up to 6°C in core MD88-787 (Figs. 6.15B, 6.16B). Neither model was capable of estimating the modern core-top SST value of 3.9°C. DTF 109/24/6 under-estimated this value by 1.9°C, and DTF 166/34/4 over-estimated by 1.3°C. Over-estimation appears to be a recurrent feature of core-top estimates by the DTF 166/34/4 model. Evidence from model characteristics suggests that the DTF109/26/4 model under-estimates by up to 2°C in the warm temperature range. This is attributed to a very limited number of warm-water samples in the 109 database and likewise the small number of warm-water species identified and used in this region. Addition of the silicoflagellate group *Dictyocha* spp. could alleviate the latter point but is considered unnecessary with the soon-to-be released recounted 166 diatom database (Crosta and Pichon, Bordeaux University, France, pers. comm. 1997). The real SST signature recorded in the cores probably lies between the two model estimates. However, as a result of model diagnostic evaluation indicating significantly lower non-analogue events and high communalities, the DTF 109/24/6 model estimates

are preferred to those of the DTF 166/34/4 model. It is acknowledged that warmer estimates of the DTF 109/24/6 model are probably too cool by up to 2°C.

Sea-surface temperature estimates between the cores MD88-787 and -784 were found closely linked through time and contrary to expected variation in SST. Only, in isotope-stage 1, do the two SST records divide into warmer and colder signals (Fig. 6. 17).

Sea-ice estimates were only presented from the long core record of MD88-787 (Fig. 6.18). February sea-ice concentration estimates are under 15% concentration and are, therefore, considered to reflect open-ocean conditions. September sea-ice concentration estimates record sea-ice cover in isotope-stage 6, 3-4 and 2. These estimates are linked with the annual sea-ice cover estimates (Figs. 6.18, 6.19). Periods of fast- and pack ice are within predicted relationships between the two parameters (Fig. 5.1B). Standard errors are discussed within each model.

A climatic interpretation for core MD88-787 was presented in section 6.5 (Figure 6.20). The planktonic foraminifera isotope record did not indicate a 1 kyr lead on SST results as observed in other studies. Variation in the SST estimates and isotopic ratio difference over Termination I were comparative (3°C versus 2.7°C respectively). Sea-ice cover leads isotope changes by up to 5 kyr in warmer periods, but were concomitant with sea-ice cover increases. This is considered an appropriate paired response to changes occurring in warm and cold phases and the mixing time of the ocean in response to glacial advance and deterioration. Increased snow cover and incorporation into the expected multi-year sea-ice presence around Antarctica were highlighted as another potential, but minor factor, requiring consideration in glacial isotope budgets.

Sea-ice and SST records were demonstrated to be in line with known physical expectations in the freezing temperature of the surface waters to produce sea-ice. This provided an independent check on the appropriateness of the sea-ice model for estimating the extreme sea-ice conditions. Further tests on the model are still required.

This study linked for the first time a relationship between sea-ice cover and the silicoflagellate *Cycladophora davisiana* presence. Distributions were linked to glacial intervals, however the amplitude in abundance is not. Other factors, presumably low salinity, appear to play more important roles in the productivity and diatom abundances preserved. The relation between *Cycladophora davisiana* and sea-ice cover (Figs. 6.20C and E) hints that conditions with more than pack-ice or sea-ice edge conditions are not advantageous to *Cycladophora davisiana* abundance/productivity. A reflection on the observations between *Cycladophora davisiana* and sea-ice, in reference to diatom abundances suggests a melt water lid and restricted mixing between the surface melt water

and subsurface water of the Antarctic region, were not conducive to diatom productivity during such phases (ie. isotope-stages 2 and 6).

Polar Front movement analysis proved difficult due to the lack of core-top SST estimation reflecting observed SST values and the true relationship between the 2°C subsurface minimum and proxy 4°C SST used to indicate Polar Front movement. The conclusion reached by using both a 2°C and 4°C proxy for Polar Front change inferred definite changes in surface water structure relative to interglacial/glacial intervals. Other subsurface dominant microfossil proxies would provide a better guide to the frontal movement. However, the expression of the southern limit of the Subantarctic Front (Rintoul *et al.* 1997) would be a very suitable surface feature worth studying in future diatom research.

Similar SST records are observed between the cores MD88-787 and -784 with those summer SST estimates of core MD84-551 in the South Indian Ocean. Variations between SST during certain isotopic-stages are in part referable to landmass or oceanic boundaries modulating SST in the two regions. Model differences of the diatom transfer functions many have also produced such variations.

The results from the sea-ice model are the first continuous results presented for the region in high resolution. Sea-ice cover was shown to increase during glacial episodes 2, 3/4 and 6 in the southeast Indian Ocean over core site MD88-787 (Fig. 6.20). The results from the last glacial maximum level was found to be comparable to the August sea-ice estimation proposed by CLIMAP (1981), but not for their February sea-ice cover to 52°S. Suggested changes in oceanographic structure and atmospheric circulation were briefly discussed linking increased sea-ice cover.

Combined past studies and the results of this study were used to advance palaeoceanographic interpretation of the region through the isotopic-stage time slices. The product of this section was the development of a specific glacial scenario, which affected diatom productivity and consequently abundance in isotope-stages 2 and 6. Implications of development of SAMW, extensive sea-ice cover, reduced, vigorous surface mixing, and stratified surface waters between the Polar Front and the Subantarctic Front are related to dampening effects on diatom productivity, and subsequent decrease in recorded abundances in the sediment. It is implied that stratified surface waters and reduced surface productivity occurred between 56° and 47°S south of Tasmania during the last glacial maximum.

Possible error in the SPECMAP age alignment in both MD88-787, and -784 over isotope-stages 2 - 4 were identified through non-compliance with other records in the

Tasman Sea or South Indian Ocean. Higher resolution isotope stratigraphy would aid in the amelioration of this problem. Better chronological control was also considered appropriate for isotope-stage 1 interpretations.

The roles of bottom-water, sea-ice, mixing depth and a melt water lid are all considered important elements of the Southern Ocean expression in cores of the southeast Indian Ocean.

It would appear from core MD88-779 that the role of Central Deep Water on the sediment record of the site provides an explanation for increased abundances of benthic foraminifera *Epistominella exigua* and the removal of diatoms from the sediments. In contrast, Antarctic Bottom Water movement to the north through the Tasman Fracture Zone of Mid-Ocean Ridge (~155°E) appears to have had some influence on the sedimentary records of polar cores MD88-787 and -784. This is interpreted from the increased abundances of *Fragilariopsis separanda* leading to non-analogue events in down-core analysis, inferring a direct link with the production of Antarctic Bottom Water from the Ross Sea where *Fragilariopsis separanda* is observed today with greatest abundances.

This page left intentionally blank.

Chapter 7
Conclusions.

7.1. Diatom database analysis results.

The primary conclusion brought about by the taxonomic analysis of species contained within the original database constructed for transfer function application is for the urgent recounting of all samples (Chapter 2). This need arises from several aspects. Firstly, taxonomic advances have taken place over time while the database has been in continuous growth. Some inferred species concepts originally used, and considered updated in the interim, have been shown to be erroneously applied and cause further confusion for species identification (eg. *Coscinodiscus eccentrica* to *Thalassiosira trifulta, Stellarima* genus). Secondly, some species concepts are lumped or confounded between many taxa of the same genus, specific examples being the *Rhizosolenia* genus, and the *Fragilariopsis* Cool Taxa. Application of such mixed species concepts thus, confuses the surface water signals of several species as one single species; consequently leading to errors in sensitivity when included in transfer function analysis. Finally, simple cases of misapplied identifications have also been noted (eg *Fragilariopsis ritscheri*). Such examples are proposed to lead to erroneous transfer function estimations in down-core analyses, since the database reflects a distribution of what is considered a warm water species, but in down-core samples may be correctly identified among species with cold water characteristics.

The original database and the resultant database compiled in this work should be considered lacking in sensitivity to warm-water species that are in general lumped within taxa or similar species groupings (eg. *Thalassionema* Taxa, *Thalassiosira* Lineati Group, *Thalassiosira* Eccentric Group) or missing certain species altogether (eg. *Rhizosolenia bergonii*). The original database should also be considered to be missing a large component of the diatom thanatocoenose along the Antarctic continental shelf regions, such as the Antarctic Peninsula region, in that *Chaetoceros* resting cells have not been included in routine counts. The latter point was shown to elevate relative abundances of the species in this region beyond other previous studies throughout the Southern Ocean. This has lead to the lack of control of non-analogue events associated with *Eucampia antarctica* abundances and over-elevated abundances of other species within the database (eg. *Cocconeis* spp.)

Although the diatom database has taxonomic problems identified throughout, it is possible to use the majority of the available database with limiting criteria, as has been illustrated in

this work. Several taxa were removed for reasons of inappropriate application to open-ocean analysis, lack of consistent counting methodology, known non-analogue situations, and to restrain the diatom response apart from silicoflagellate signal. Further criteria were imposed to assure the database used for analysis contained similarly counted, uncontaminated and core-top representative samples (Chapter 3).

Analysis of the samples derived from such stringent re-alignment of the original databases available, revealed through geographic distribution of the major species (>1%), that taxonomic reform was successful. Relationships previously inferred or documented by previous workers concurred with most of the geographic and relative abundances of species observed in sediments of the Southern Ocean. Relative abundances of each species or taxa were shown to have strong affinities to SST and the presence/absence of sea-ice cover; this placed confidence in the use of the derived database for statistical analysis of these sea-surface parameters. Several species (ie. *Actinocyclus actinochilus, Fragilariopsis curta, Fragilariopsis separanda, Navicula directa, Odontella weissflogii,* and *Thalassiosira oliverana*) are considered linked to AABW formation and transport northward from the Antarctic continental shelf, although sea-ice and icebergs are still possible modes of transport northwards worth considering. Species, which should reveal much better associations to sea-ice cover, are generally in combined or grouped taxa (eg. *Porosira pseudodenticulata, Stellarima microtrias*, species under *Fragilariopsis* Cool and Cylindriform Groups, and possibly *Thalassiosira gracilis* var. *gracilis*) and thus, will benefit the models derived should they be identified on sounder taxonomic foundations.

7.2. Model construction.

The construction of a new SST transfer function appropriate for the newly derived diatom database illustrated some interesting points regarding model applicability. By analysing factor analysis results with increasing factor number resolution it was observed that although the dominating factor groups were consistently observed, subdominant factors did bring attention to other distribution patterns preserved in the diatom thanatocoenose. Species versus the factor number resolved indicated that choosing an over simplistic model (ie. one that contained only the dominant signals) could lead to mis-representations of the range of relationships acting on the natural diatom distributions. This forced some species within un-natural groupings. In essence, expanding the factor number to incorporate other subdominant diatom partionings increases the sensitivity of the model pursued. For this reason, a 6 factor model was decided over the 4 factor model for determination of February SST for the Antarctic Diatom Database. Therefore, it is necessary to consider diatom species and biogeographies in respect to factor analysis or any other statistical grouping methodology, to assess the wider variety of signals preserved within sediment distributions.

With respect to the SST transfer function (Chapter 4), model diagnostics should be applied more widely than just the common observed versus estimated parameter response and the degree of correlation and standard error. Model robustness must be considered at higher levels to assure random distribution of residuals, constant variance, and normality as basic levels of confidence in the derived models ability to provide estimates. Use of communality levels to restrict data inclusion also requires analysis for appropriateness at the factor level resolved, and may be found unwarranted in high factor number models as in this work. Removal of samples from the database that estimates parameters well beyond appropriate expectations is advocated. Since the inclusion of such samples will only serve to generalise the model by bringing noise and error into estimates obtained.

7.3. Limitations and applicability of the Pichon et al. (1992a) diatom transfer function.

Analysis of the natural component of the original database was found to be in need of urgent update as discussed above (section 7.1). Analysis of the dissolution component of the database, undertaken in Chapter 3, also arrived at a similar conclusion based on other features. The degree of dissolution of the samples, in contrast to the natural database, demonstrated over-estimation of natural dissolution in the northern sediments and under-estimation in the southern sediments. Such a feature was later shown to have repercussions on SST estimation (Chapter 4). In addition, over-estimations of relative abundances from dissolution data will affect the ranking procedures employed because of their current reliance on maximum relative abundances. Such a situation allows non-analogue conditions down-core to be recognised and provided SST estimations.

Pre-treatment and counting methodologies of dissolution samples need to be examined, and as with the natural component of the database, all species must be included in the identification list. The level of sample coverage was also considered lacking in terms of biogeographical realms and regional coverage. Two samples of the dissolution database would have required rejection if they were pursued (one an Antarctic Peninsula sample and the other containing a high level of reworked elements). The remaining three dissolution samples were considered too small a sample group to be employed. However, it is clear that such a dissolution data set is valuable as a correction factor in SST estimation work.

The problems identified in both the natural and dissolution database were found manifest in the SST transfer function model of Pichon *et al.* (1992a), DTF 166/34/4. In particular, diagnostics revealed that the inclusion of the dissolution component was not continuous with the natural data set. The dissolution data set was observed to poorly emulate relationships found in the warm-waters. Estimates were noted tuned to open-ocean responses between the 4 and 11°C range, and tied into the observations of high residuals

between the PF and STC. The inappropriate inclusion of the warm-water dissolution sample KR8808 in the DTF166/34/4 was found to lead to erroneous SST estimation. The transfer function was found to compensate for departures in the dissolution data set by streamlining the palaeo-equation of the model. This also resulted in a large number of samples with low communalities and large residuals. Although the Pichon *et al.* (1992a) original model did not identify or remove such large outliers, it was evident that the model could have been improved with criteria used to eliminate them. The model must be considered capable of producing estimates that may be in error by up to ±4°C though the 0° to 12°C range, as a product of including outliers and dissolution samples.

Application of the Pichon *et al.* (1992a) DTF 166/34/4 model to cores confirmed the model diagnostics for a poor model response. The confirmation was observed predominantly in the enormous number of low communality values provided for the core samples and non-analogue events observed. There is one possible alternative explanation for such a poor response of the model when applied to the cores of the southeast Indian Ocean - the database. It could be interpreted that the database has been constructed predominantly from samples derived from the South Atlantic and South Indian Ocean sectors thus, when applied to cores removed from, or at the limit of the database coverage provides inadequate estimates to the regional variation recorded in externally placed cores. Although there is some room for this hypothesis, the circumpolar nature of diatom distributions and as such, generalised taxonomic cover provided by the original database, should not produce the poor response provided by their model. I propose that the DTF 166/34/4 model does poorly as a result of the simplified nature of the model which is incapable of appropriately assessing species variation in the down-core data. It is for this reason low communality values are produced (Le 1992). The large number of non-analogue events are referrable to differences in the counting and taxonomic methods carried out between the core data and the database, and to a very small degree the regional variation preserved in the sediments of this region to that of the database coverage. The DTF model of Pichon *et al.* (1992a) was therefore considered less appropriate, less sensitive and liable to greater estimate error than the transfer function derived in the thesis (DTF 109/24/6).

7.4. Development of the sea-ice estimation model.

A sea-ice model is an appropriate parameter worth pursuing from diatom records, in light of diatoms ability to be restricted by, exist within, or under and in melt waters of sea-ice. Presentation of relationships between three parameters of sea-ice (viz. September concentration, February concentration and months per year sea-ice cover) and the relative abundances of diatoms in the sediments (Chapter 2) provided impetus to continue this research theme. The Imbrie and Kipp methodology was found unsuitable for modelling sea-ice because of non-constant variance and the high number of zeros in the data. A

second model was developed which took into account these features using a logistic regression technique combined with an estimation model (Chapter 5).

Estimates of the three sea-ice parameters provided from the data of core MD88-787 were compared with SST estimates and illustrated the validity of the estimates in terms of sea-surface freezing potential.

The sea-ice estimates provided the first continuous high resolution sea-ice records for the Southern Ocean during the late Quaternary, and also confirmed the association speculated by Morley and Hays (1983) that abundances of the radiolarian *Cycladophora davisiana* indicated the ocean was extensively ice covered during winter and early spring. The sea-ice record was not found linked to the magnitude of *Cycladophora davisiana* abundances in the sediments, but most conclusively to their presence.

In terms of palaeoceanography and palaeoclimatology as a whole, there are many more questions provoked by the first results of the sea-ice estimates. Atmospheric circulation and oceanographic structure changes are the foremost domains where effects previously interpreted from other sources can be related. Full interpretation remains to be compiled from this introductory step in estimations. However, comparisons against Vostok records remain a promising extension of investigation (partially addressed in section 6.5.6.). Perhaps, a more relevant question in considering the expanding sea-ice cover, and presumably the ice shelfs around Antarctica during glacial episodes 2, 3/4 and 6, is the source and "functioning" of AABW formation. Was there such an increase in sea-ice that multi year ice was definitely in place? If so, did such an increased in sea-ice cover block, retard or displace regions of AABW formation? From the polar core records prepared in this thesis, the presence and intensity of the AABW northward flow from the Ross Sea region indicates AABW formation was still possible during these glacial intervals, particularly in isotope stage 6 (section 6.7). Continued study in this topic will ensue, but with an updated database and redefined sea-ice model.

7.5. History of oceanic change in the southeast Indian Ocean.

Analysis of the three French cores along a transect from Tasmania to 56°S has revealed a continuous glacial/interglacial history covering the last 200 kyr (Chapter 6). These changes are observed in sea-surface estimates of SST and sea-ice derived from the diatom record of the three cores, in adjunct to oxygen isotope data, current micropalaeontological studies on core MD88-779 and previous data prepared from MD88-787 (section 6.5 and 6.6).

The major changes in the records occur during the maximum glacial conditions observed in isotope stages 2, 3/4 and 6.

It is hypothesised that, during the coldest glacial events, shifts in the Polar Front, Subantarctic Front, Subtropical Convergence and the sea-ice maximum winter extent occur within what appears to be a small latitudinal spread (ie. sea-ice at 56°S, PF at least at 50°S, STC maximum 43°S). The influence of more proximal meltwater and a likely southward extension of Antarctic Surface Water are believed responsible for strong seasonal overturning producing Subantarctic Mode Water. The lack of diatoms in the subantarctic core MD88-779 suggests that this overturning may have been a short, vigorous event during which the diatoms could not bloom profitably. Alternatively, it is an event that occurred too early in the diatom growth cycle (Barron pers. comm. 1998). Evidence of reduced diatom abundances from the southern cores (MD88-787, -784), together with the enhanced *Cycladophora davisiana* abundances during these phases, lend support to stratification of the surface waters by a meltwater lid. This lid is assumed to have dampened diatom productivity through suppression of silica input from the subsurface waters.

Polar Front movements north and south of core MD88-787 were suggested (section 6.5.4.) but are considered likely trends only due the problems inherent in defining a subsurface feature and the lack of coherency between core top SST estimates and the modern SST signatures. This aside movement both north and south of the core site, occurred throughout changes in interglacial and glacial stages.

The final hypothesis presented, and requiring further inquiry, is the role of bottom-water effects on the cores' sedimentary records (section 6.7.). Cores MD88-787 and -784 are considered to include in their records the influence of AABW from the Ross Sea to the Tasman Basin during maximum glacial events. This feature is highly implicative with the increased non-analogue abundances of *Fragilariopsis separanda* in sediments of isotope stage 6. For core MD88-779, situated on the western flank of the South Tasman Rise, the influence of AABW flow was found to be erroneously conceived as the core is located within CDW representative of the South Australian Basin. The loss of diatoms from the core during the same maximum glacial events, along with interpretations of high primary productivity, fresher water benthic foraminifera presence may be reflected in greater CDW velocity and a varying source during these cold maximum episodes. Diatom hiatuses produced by enhanced activity of the CDW in glacial stages in the southeast Indian and southwest Pacific has also been reported by Ledbetter *et al.* (1983a). Both hypotheses provide new interpretations to bottom and central water pathways in this region of the Southern Ocean, which need further verification.

7.6. Future Research.

The culmination of this thesis brings together many suggestions in applying diatom transfer functions in the Southern Ocean. Behind these suggestions is a continued need for database development. In the case presented here this means three priorities; the first is a drastic revision of the current diatom database of Pichon *et al.* (1992a). This has already taken place and is awaiting discussion within the scientific domain. Secondly, the various diatom databases available (Pichon *et al.* 1992a, and Zielinski and Gersonde 1997) need to be amalgamated where possible to benefit from better coverage. And finally, the Pacific sector of the Southern Ocean requires inclusion. Including the Pacific sector within the diatom surface sample database is a future goal of the author.

All models (SST and sea-ice) require revision and reapplication in light of the advancing databases. It may yet be found important to subdivide a Southern Ocean diatom database to sectors for core application if the noise of the various regional differences becomes increasingly scattered. Should this be the case, one would expect that other statistical modelling efforts, such as the application of the Modern Analogue Technique, might better serve large, noisy databases.

The sea-ice model, aside from requiring an updated data diatom database, calls for further core analyses throughout the Southern Ocean, to assess its range of application. Spectral analysis of the estimates produced are expected to fall in with obliquity isolation periodicities as observed from diatoms on a long scale record by Kaczmarska *et al.* (1993) and inferred by Labeyrie *et al.* (1996). Once a more taxonomically sound model is derived, analysis of the sea-ice estimates demands greater detailed comparison with modelling attempts and past records concerned with linked oceanic and atmospheric circulation changes, to which sea-ice plays an important boundary condition.

Although only preliminary in interpretation, diatom workers may be able to elucidate bottom-water pathways and sources in the past as a result of relationships between diatoms observed in high relative abundance along continental shelf and polynya environments where AABW is formed. One particular diatom to direct attention in this search is *Fragilariopsis separanda.* A bottom-water transfer function may be possible using all diatoms observed and bottom-water potential temperatures. However, a simplified time-slice approach looking for particular Antarctic Bottom Water pathway related diatoms may provide enough evidence to assess such pathways.

This page left intentionally blank.

References

Abbott, W.H., 1971. Diatom investigations of Southern Ocean deep-sea cores. *Antarctic Journal of the United States* **6**(5) : 171-172.

Abbott, W.H., Jr., 1973. Vertical and lateral patterns of diatomaceous ooze found between Australia and Antarctica. Ph. D.; Department of Geology, University of South Carolina.

Abbott, W.H., 1974. Temporal and spatial distribution of Pleistocene diatoms from the southeast Indian Ocean. *Nova Hedwigia* **25** : 291-347.

Abelmann, A. & Gersonde, R., 1991. Biosiliceous particle flux in the Southern Ocean. *Marine Chemistry* **35** : 503-536.

Ackley, S.F., 1981. A review of sea-ice weather relationships in the Southern Hemisphere. In *Sea level, Ice, and Climate change*, Allison, I. eds, IAHS publication, 131. pp 127-159.

Ackley, S.F., 1991. The growth, structure and properties of Antarctic sea ice. In *Glaciers-Ocean-Atmosphere Interactions*, Kotlyakov, V.M., Ushakov, A. & Glazovsky, A. eds, *IAHS publication*, 208. pp 105-117.

Ackley, S.F., 1996. Sea ice. *Encyclopedia of Applied Physics* **17** : 81-103.

Ackley, S.F., Fritsen, C.H., Lytle, V.I. & Sullivan, C.W., 1996. Freezing driven upwelling in Antarctic sea-ice biological systems. *Proceedings of NIPR Symposium on Polar Biology* **9** : 45-59.

Ackley, S.F. & Sullivan, C.W., 1994. Physical controls on the development and characteristics of Antarctic sea ice biological communities- a review and synthesis. *Deep-Sea Research* **41**(10) : 1583-1604.

Akiba, F., 1982. Late Quaternary diatom biostratigraphy of the Bellingshausen Sea, Antarctic Ocean. *Report of the Technology Research Centre, J.N.O.C.* **16** : 31-74.

Aletsee, L. & Jahnke, J., 1992. Growth and productivity of the psychrophilic diatoms *Thalassiosira antarctica* Comber and *Nitzschia frigida* Grunow in batch cultures at temperatures below the freezing point of sea water. *Polar Biology* **11** : 634-647.

Allison, I., 1981. Antarctic sea ice growth and oceanic heat flux. In *Sea Level, Ice, and Climatic Change*, Allison, I. eds, *IAHS Publication*, 131. pp 161-170.

Allison, I. & Akerman, G., 1980. Sea ice and ocean energy balance studies at Mawson, Antarctica. In *Sea Ice Processes and Models*, Pritchard, R. eds, IAHS Publication, 124. pp 347-359.

Allison, I., Brandt, R.E. & Warren, S.G., 1993. East Antarctic sea ice: albedo, thickness distribution, and snow cover. *Journal of Geophysical Research* **98**(C7) : 12,417-12,429.

Allison, I. & Worby, A., 1994. Seasonal changes of sea-ice characteristics off East Antarctica. *Annals of Glaciology* **20** : 195-201.

Amsler, C.D. & Raymond, J.A., 1995. Production of an ice-active substance by Antarctic sea ice diatoms in culture. *Journal of Phycology* **31 (suppl.)** : 10.

Andreoli, C., Tolomio, C., Moror, I., Radice, M., Moschin, E. & Bellato, S., 1995. Diatoms and dinoflagellates in Terra Nova Bay (Ross Sea-Antarctica) during austral summer 1990. *Polar Biology* **15** : 465-475.

Andrews, G.W., 1975. Taxonomy and stratigraphic occurrence of the marine diatom genus *Rhaphoneis*. *Nova Hedwigia Beiheft* **53** : 193-227.

Armand, L.K., 1995 (Nov.). Diatom results. top and bottom core samples. Rig Seismic Cruise 147. *Geology Department, Australian National University unpublished* 31pp.

Armand, L.K., Barry, S., Donnelly, C., Pichon , J.-J. & Labeyrie, L., 1996. A late Quaternary history of sea-ice concentration and extent, south of Tasmania, from diatom assemblage data. *Abstracts of the 14th International Diatom Symposium Tokyo, Japan* Tokyo Diatom Institute p. 4.

Arrhenius, G., 1988. Rate of production, dissolution and accumulation of biogenic solids in the ocean. *Palaeogeography, Palaeoclimatology, Palaeoecology* **67** : 119-146.

Ayress, M.A. & Barrows, T.T., 1996. A reconstruction of Last Glacial Maximum sea-surface temperatures in the Australasian region. *Climate Change Newsletter* **8**(2) : 2-4.

Baines, P.G., Edwards, R.J. & Fandry, C.B., 1983. Observations of a new baroclinic current along the western continental slope of Bass Strait. **34**(1) : 155-157.

Bard, E., Labeyrie, L., Arnold, M., Labracherie, M., Pichon, J.-J., Duprat, J. & Duplessy, J.-C., 1989. AMS-^{14}C ages measured in deep sea cores from the Southern Ocean : implications for sedimentation rates during isotope stage 2. *Quaternary Research* **31** : 309-317.

Bard, E., Labeyrie, L.D., Pichon, J.-J., Labracherie, M., Arnold, M., Duprat, J., Moyes, J. & Duplessy, J.-C., 1990. The last deglaciation in the Southern and Northern Hemispheres : a comparison based on oxygen isotope, sea surface temperature estimates, and accelerator ^{14}C dating from deep sea-sediments. In *Geological History of the Polar Oceans : Arctic versus Antarctic*, Bleil, U. & Thiede, J. eds, *Nato ASI Series*, Kluwer Academic Publishers, Dordrecht, Series C : Mathematical and Physical Sciences - Vol. 308. pp 405-415.

Barde-Labayle-Bounés, M.-F., 1980. Les diatomées du Quaternaire terminal de l'Atlantique nord-oriental, apport à la connaissance des phénomènes hydrologiques. PhD; L'Université de Bordeaux I.

Bareille, G., 1991. Flux sédimentaires : Paleoproductivité et paleocirculation de l'océan Austral au cours des 150,000 dernières années. Ph. D; L'Université de Bordeaux I.

Barron, J.A., 1985. Miocene to Holocene planktic diatoms. In *Plankton Stratigraphy*, Bolli, H.M., Saunders, J.B. & Perch-Nielsen, K. eds, *Cambridge Earth Science Series*, Cambridge University Press, Cambridge, vol. 2. pp 763-809.

Barron, J.A., 1996. Diatom constraints on the position of the Antarctic Polar Front in the middle part of the Pliocene. *Marine Micropaleontology* **27** : 195-213.

Barrows, T., 1995. Three aspects of late Quaternary palaeoclimatic reconstruction in eastern Australia. Honours; Australian National University.

Barrows, T.T., Ayress, M.A. & Hunt, G.R., 1996. A reconstruction of Last Glacial Maximum sea-surface temperatures in the Australasian region. *Quaternary Australasia* **14**(1) : 27-31.

Beklemishev, K.V., 1964. Latitudinal zoning of Antarctic phytoplankton. In *Soviet Antarctic Expedition Information Bulletin*, Elsevier Publishing Co., Amsterdam, 1. pp 113-114.

Belkin, I.M. & Gordon, A.L., 1996. Southern Ocean fronts from the Greenwich meridian to Tasmania. *Journal of Geophysical Research* **101**(C2) : 3675-3696.

Bianchi, F., Boldrin, A., Cioce, F., Dieckmann, G., Kuosa, H., Larsson, A.-M., N_thig, E.-M., Sehlstedt, P.-I., Socal, G. & Syvertsen, E.E., 1992. Phytoplankton distribution in relation to sea ice, hydrography and nutrients in the northwestern Weddell Sea in early spring 1988 during EPOS. *Polar Biology* **12** : 225-235.

Bodungen, B.V., Smetacek, V.S., Tilzer, M.M. & Zeitzschel, B., 1986. Primary production and sedimentation during spring in the Antarctic Penisula region. *Deep-Sea Research* **33**(2) : 177-194.

Booth, J.D. & Burckle, L.H., 1976. Displaced Antarctic diatoms in the southwestern and central Pacific. *Pacific Geology* **11** : 99-108.

Braatz, B.V. & Corliss, B.H., 1984. Bottom water circulation in the South Australian Basin during the last 3.2 million years. *Antarctic Journal of the United States* **20** : 84-88.

Budd, W.F., 1975. Antarctic sea-ice variations from satellite sensing in relation to climate. *Journal of Glaciology* **15**(73) : 417-427.

Bunt, J.S. & Wood, E.J.F., 1963. Microalgae and Antarctic sea ice. *Nature* **199** : 1254-1255.

Burckle, L.H., 1972. Diatom evidence bearing on the Holocene in the South Atlantic. *Quaternary Research* **2** : 323-326.

Burckle, L.H., 1981. Displaced Antarctic diatoms in the Amirante Passage. *Marine Geology* **39** : M39-M43.

Burckle, L.H., 1984a. Diatom distribution and paleoceanographic reconstruction in the Southern Ocean - present and last glacial maximum. *Marine Micropaleontology* **9** : 241-261.

Burckle, L.H., 1984b. Ecology and paleoecology of the marine diatom *Eucampia antarctica* (Castr.) Manguin. *Marine Micropaleontology* **9** : 77-86.

Burckle, L.H., 1987. Diatom distribution in the Weddell Gyre region during late Winter. *Micropaleontology* **33**(2) : 177-184.

Burckle, L.H., 1989. Distribution of diatoms in the sediments of the Northern Indian Ocean : relationship to physical oceanography. *Marine Micropaleontology* **15** : 53-65.

Burckle, L.H. & Abrams, N., 1986. Diatom species diachrony in late Neogene sediments of the Southern Ocean. *South African Journal of Science* **82** : 505-506.

Burckle, L.H. & Abrams, N., 1987. Regional late Pliocene-early Pleistocene hiatuses of the Southern Ocean - diatom evidence. *Marine Geology* **77** : 207-218.

Burckle, L.H. & Burak, R.W., 1988. Fluctuations in late Quaternary diatom abundances : stratigraphic and paleoclimatic implications from subantarctic deep sea cores. *Palaeogeography, Palaeoclimatology, Palaeoecology* **67** : 147-156.

Burckle, L.H. & Cirilli, J., 1987. Origin of diatom ooze belt in the Southern Ocean : Implications for late Quaternary Paleoceanography. *Micropaleontology* **33**(1) : 82-86.

Burckle, L.H., Clarke, D.B. & Shackleton, N.J., 1978. Isochronous last-abundant-appearance datum (LAAD) of the diatom *Hemidiscus karstenii* in the sub-Antarctic. *Geology* **6** : 243-246.

Burckle, L.H. & Cooke, D.W., 1983. Late Pleistocene *Eucampia antarctica* abundance stratigraphy in the Atlantic sector of the Southern Ocean. *Micropaleontology* **29**(1) : 6-10.

Burckle, L.H., Jacobs, S.S. & McLaughlin, R.B., 1987. Late austral spring diatom distribution between New Zealand and the Ross Sea Ice Shelf, Antarctica : Hydrographic and sediment correlations. *Micropaleontology* **33**(1) : 74-81.

Burckle, L.H., Robinson, D. & Cooke, D., 1982. Reappraisal of sea-ice distribution in the Atlantic and Pacific sectors of the Southern Ocean at 18,000 yr BP. *Nature* **299** : 435-437.

Burckle, L.H. & Stanton, D., 1975. Distribution of displaced Antarctic diatoms in the Argentine Basin. In *Third symposium on Recent and Fossil marine diatoms*, Kiel, Germany, pp 283-292.

Bucky, D., 1974. Silicoflagellate and coccolith stratigraphy, Deep Sea Drilling Project, Leg 29. In *Initial Reports of the Deep Sea Drilling Project*, Kennett, J.P., Houtz, R.E. & et al. eds, United States Government Printing Office, Washington, vol. 29. pp 845-872.

Burkholder, P.R. & Mandelli, E.F., 1965. Productivity of microalgae in Antarctic sea ice. *Science* **149** : 872-874.

Burling, R.W., 1961. Hydrology of circumpolar waters south of New Zealand. *New Zealand Department of Science and industrial Resaerch Bulletin* **143** : 66 pp.

Burns, D.A., 1977. Major features of the oceanographic development of the southeast Indian and southwest Pacific Oceans interpreted from microfossil evidence. *Marine Geology* **25** : 35-59.

Bye, J.A.T., 1968. The hydrology of the Southern Ocean. 1. The Australian section - North. *Horace Lamb Centre for Oceanographical Research. The Flinders University of S.A. Research Paper* **26**.

Carsey, F.D., 1992. *Microwave Remote Sensing of Sea Ice*. American Geophysical Union, Washington. vol. 68. 462 pp.

Casey, R.E., 1977. The ecology and distribution of Recent radiolaria. In *Oceanic Micropalaeontology*, Ramsay, A.T.S. ed., Academic Press, London, vol. 2. pp 809-845.

Cassidy, D.S., Kaharoeddin, F.A., Zemmels, I. & Knapp, M.B., 1977. *USNS ELTANIN. An inventory of core location data with core location maps and cruise 55 core descriptions.* Sedimentology Research Laboratory, Florida State University Antarctic Research Facility, vol. 44. Tallahassee. 90 pp.

Cassie, V., 1961. Marine phytoplankton in New Zealand waters. *Botanica Marina* **2** (suppl.) : 1-54, pl. I-VIII.

Cassie, V., 1963. Distribution of surface phytoplankton between New Zealand and Antarctica December 1957. *Trans-Antarctic Expedition 1955-1958, Scientific Reports* 7.

Castracane, A.F.D., 1886. Report on the Diatomaceae collected by H.M.S. *Challenger* during the years 1873-76. *Rept. Challenger Exp. Botany* **2** : i-iii, 1-178, pl. I-XXX.

Cavalieri, D.J., Gloersen, P. & Campbell, W.J., 1984. Determination of sea ice parameters with the NIMBUS 7 SIMMR. *Journal of Geophysical Research* **89**(D4) : 5355-5369.

Cavalieri, D.J. & Martin, S., 1985. A passive microwave study of polynyas along the Antarctic Wilkes Land coast. In *Oceanology of the Antarctic Continental Shelf*, Jacobs, S.S. eds, *Antarctic Research Series*, American Geophysical Union, Washington, vol. 43. pp 227-252.

Cavalieri, D.J. & Parkinson, C.L., 1981. Large-scale variations in observed Antarctic sea ice extent and associated atmospheric circulation. *Monthly Weather Reviews* **109** : 2323-2336.

Cavalieri, D.J., St. Germain, K.M. & Swift, C.T., 1995. Reduction of weather effects in the calculation of sea ice concentration with the DMSP SSM/I. *Journal of Glaciology* **41**(139) : 455-464.

Chappell, J., Omura, A., Esat, T., McCulloch, M., Pandolfi, J., Ota, Y. & Pillans, B., 1996. Reconciliation of late Quaternary sea levels derived from coral terraces at Huon Peninsula with deep sea oxygen isotope records. *Earth and Planetary Science Letters* **141** : 227-236.

Charles, C.D. & Fairbanks, R.G., 1990. Glacial to interglacial changes in the isotopic gradients of the Southern Ocean surface water. *In Geological History of the Polar oceans : Arctic versus Antarctic.* Bleil, U. and Thiede, J. eds. Kluwer Academic Publishers: Dordrect. vol. 308. pp 519-538.

Charles, C.D. & Fairbanks, R.G., 1992. Evidence from Southern Ocean sediments for the effect of North Atlantic deep-water flux on climate. *Nature* **355** : 416-419.

Ciesielski, P.F., 1986. Middle Miocene to Quaternary diatom biostratigraphy of Deep Sea Drilling Project Site 594, Chatham Rise, southwest Pacific. In *Initial Reports of the Deep Sea Drilling Project*, Kennett, J.P., von der Borch, C.C. & *et al.* eds, U.S. Government Printing Office, Washington, vol. 90. pp 863-885.

Ciesielski, P.F., 1991. Relative abundances and ranges of select diatoms and silicoflagellates from sites 699 and 704, subantarctic South Atlantic. In *Proceedings of the Ocean Drilling Program, Scientific Results*, Ciesielski, P.F., Kristoffersen, Y. & *et al.* eds, Ocean Drilling Program, College Station, TX, vol. 114. pp 753-778.

Ciesielski, P.F. & Weaver, F.M., 1973. Southern Ocean Pliocene paleotemperatures based on silicoflagellates from deep sea cores. *Antarctic Journal of the United States* **8** : 295-297.

Ciesielski, P.F. & Weaver, F.M., 1974. Early Pliocene temperature changes in the Antarctic Seas. *Geology* **2** : 511-515.

Clarke, D.B. & Ackley, S.F., 1983. Relative abundance of diatoms in Weddell Sea pack ice. *Antarctic Journal of the United States* **18** : 181-182.

Clarke, D.B. & Ackley, S.F., 1984. Sea ice structure and biological activity in the Antarctic marginal ice zone. *Journal of Geophysical Research* **89**(C2) : 2087-2095.

CLIMAP Project Members, 1976. The surface of the Ice-Age Earth. *Science* **191** : 1131-1137.

CLIMAP Project Members, 1981. *Seasonal reconstructions of the Earth's surface at the last glacial maximum.* Geological Society of America: *Map and Chart Series* **MC-36.**

CLIMAP Project Members, 1984. The Last Interglacial Ocean. *Quaternary Research* **21** : 123-224.

Comiso, J.C., Ackley, S.F. & Gordon, A.L., 1984. Antarctic sea ice microwave signatures and their correlation with *in situ* ice observations. *Journal of Geophysical Research* **89** : 662-672.

Comiso, J.C., Grenfell, T.C., Lange, M., Lohanick, A.W., Moore, R.K. & Wadhams, P., 1992. Microwave remote sensing of the Southern Ocean ice cover. In *Microwave Remote Sensing of Sea Ice*, Carsey, F.D. ed., *Geophysical Monograph*, American Geophysical Union, Washington, vol. 68. pp 243-259.

Comiso, J.C., Maynard, N.G., Smith, W.O., Jr. & Sullivan, C.W., 1990. Satellite ocean colour studies of Antarctic ice edges in Summer and Autumn. *Journal of Geophysical Research* **95** : 9481-9496.

Comiso, J.C., McClain, C., R., Sullivan, C.W., Ryan, J.P. & Leonard, C.L., 1993. Coastal zone colour scanner pigment concentrations in the Southern Ocean and relationships to geophysical surface features. *Journal of Geophysical Research* **98**(C2) : 2419-2451.

Comiso, J.C. & Sullivan, C.W., 1986. Satellite microwave and in situ observations of the Weddell Sea ice cover and its marginal ice zone. *Journal of Geophysical Research* **91**(C8) : 9663-9681.

Comiso, J.C. & Zwally, H.J., 1984. Concentration gradients and growth/decay characteristics of the seasonal sea ice cover. *Journal of Geophysical Research* **89**(C5) : 8081-8103.

Connell, R.D. & Sikes, E.L., 1997. Controls on Late Quaternary sedimentation of the South Tasman Rise. *Australian Journal of Earth Sciences* **44** : 667-675.

Conolly, J.R., 1972. Introduction : Marine sediments of the southeastern Indian Ocean. In *Antarctic Oceanography II. The Australian - New Zealand Sector*, Hayes, D.E. eds, *Antarctic Research Series*, American Geophysical Union, vol. 19. pp 269-272.

Conolly, J.R. & Payne, R.R., 1972. Sedimentary patterns within a continent- mid-oceanic ridge - continent profile: Indian Ocean south of Australia. In *Antarctic Oceanology II. The Australian - New Zealand Sector*, Hayes, D.E. eds, *Antarctic Research Series*, American Geophysical Union, 19. pp 295-315.

Cooke, D.W., Burckle, L.H. & Hays, J.D., 1977. Winter sea-ice cover during the late Pleistocene in the Antarctic Ocean. *EOS Transactions* **58** : 416.

Cooke, D.W. & Hays, J.D., 1982. Estimates of Antarctic Ocean seasonal sea-ice cover during Glacial intervals. In *Antarctic Geoscience*, Craddock, C. eds, *International Union of Geological Sciences*, The University of Wisconsin Press, Wisconsin, Series B, No. 4. pp 1017-1025.

Corliss, B.H., 1983. Quaternary circulation of the Antarctic Circumpolar Current. *Deep-Sea Research* **30**(1) : 47-61.

Corliss, B.H., Martinson, D.G. & Kefer, T., 1986. Late Quaternary deep-ocean circulation. *Geological Society of America Bulletin* **97** : 1106-1121.

Cox, E.J., 1983a. Observations on the Diatom Genus *Donkinia* Ralfs in Pritchard. III. Taxonomy. *Botanica Marina* **26** : 567-580.

Cox, E.J., 1983b. Observations on the diatom Genus *Donkinia* Ralfs in Pritchard. *Botanica Marina* **26** : 553-566.

Cresswell, G.R. 1987. The East Australian Current. *CSIRO Marine Laboratories Info Sheet* **No. 3**. June. pp 4.

Cresswell, G.R., Golding, T.J. & Boland, F.M., 1978. Buoy and ship examination of the Subtropical Convergence south of the Western Australia. *Journal of Physical Oceanography* **8**(3) : 315-320.

Crooks, A.D., 1960. Oceanic observations in Antarctic Waters, *M.V. Magga Dan*, 1959. *CSIRO Oceanographical Station List* **44** : 3-78.

Crosby, L.H. & Wood, E.J.F., 1958. Studies on Australian and New Zealand Diatoms I.- planktonic and allied species. *Transactions of the Royal Society of New Zealand* **85**(4) : 483-530.

Crosta, X., Pichon, J.-J. & Labracherie, M., 1997. Distribution of *Chaetoceros* resting spores in modern peri-Antarctic sediments. *Marine Micropaleontology* **29** : 283-299.

Crowley, T.J. & Parkinson, C.L., 1988a. Late Pleistocene variations in Antarctic sea ice I: effect of orbital insolation changes. *Climate Dynamics* **3** : 85-91.

Crowley, T.J. & Parkinson, C.L., 1988b. Late Pleistocene variations in Antarctic sea ice II: effect of interhemispheric deep-ocean heat exchange. *Climate Dynamics* **3** : 93-103.

Dansie, L.K., 1994. Holocene to Pliocene diatom distribution in the South Indian Ocean, Mission PACIMA MD79 (27 March- 3 May, 1994). *Australian National University for University Of Bordeaux I, Talence, France. Cruise Report* 49 pp. unpublished.

Davidson, I.R., 1991. Environmental effects on algal phytosynthesis: Temperature. *Journal of Phycology* **27** : 2-8.

De Deckker, P., 1997. The significance of the oceans in the Australasian region with respect to global palaeoclimates: future directions. *Palaeogeography, Palaeoclimatology, Palaeoecology* **131**(3/4) : 511-516.

De Vries, T.J. & Schrader, H., 1981. Variation of upwelling/oceanic conditions during the latest Pleistocene through Holocene off the central Peruvian coast : A diatom record. *Marine Micropaleontology* **6** : 157-167.

Deacon, G.E.R., 1937. *The Hydrology of the Southern Ocean.* Discovery Reports Cambridge University Press, Cambridge. vol. 15. pp 1-124, pl. I-XLIV

Deacon, G.E.R., 1982. Physical and biological zonation in the Southern Ocean. *Deep-Sea Research* **29**(1A) : 1-15.

DeFelice, D.R., 1979. Relative diatom abundance as tool for monitoring winter sea ice fluctuations in southeast Atlantic. *Antarctic Journal of the United States* **14** : 105-106.

DeFelice, D.R. & Wise, S.W.J., 1981. Surface lithofacies, biofacies and diatom diversity patterns as models for delineation of climatic change in the southeast Atlantic Ocean. *Marine Micropaleontology* **6** : 29-70.

Desmarchelier, J.M. & Goede, A., 1996. High resolution stable isotope analysis of a Tasmanian speleothem. *Papers and Proceedings of the Royal Society of Tasmania* **130**(1) : 7-13.

Donahue, J.G., 1970a. Diatoms as Quaternary biostratigraphic and paleoclimatic indicators in the high latitudes of the Pacific Ocean. PhD, Columbia University.

Donahue, J.G., 1973. Distribution of planktonic diatoms in surface sediments of the Southern South Pacific. In *Marine sediments of the Southern Ocean.*, Goodell, H.G. & *et al.* eds, American Geophysical Society, Antarctic Map Folio Series 17. p. 18 pl. 9.

Donegan, D. & Schrader, H., 1982. Biogenic and abiogenic components of laminated hemipelagic sediments in the central Gulf of California. *Marine Geology* **48** : 215-237.

Dow, R.L., 1978. Radiolarian distribution and late Pleistocene history of the Southeastern Indian Ocean. *Marine Micropaleontology* **3** : 203-227.

Dugdale, R.C., Wilkerson, F.P. & Minas, H.J., 1995. The role of a silicate pump in driving new production. *Deep-Sea Research* **42**(5) : 697-719.

Dunbar, R.B., MacPherson, A.J. & Wefer, G., 1985. Water-column particulate flux and seafloor deposits in the Bransfield Strait and southern Ross Sea, Antarctica. *Antarctic Journal of the United States* **20** : 98-100.

Edmond, J.M., Jacobs, S.S., Gordon, A.L., Mantyla, A.W. & Weiss, R.F., 1979. Water column anomalies in dissolved silica over opaline pelagic sediments and the origin of deep silica maximum. *Journal of Geophysical Research* **84**(C12) : 7809-7826.

Edwards, R.J. & Emery, W.J., 1982. Australasian Southern Ocean frontal structure during Summer 1976-77. *Australian Journal of Marine and Freshwater Research* **33**(1) : 3-22.

Eicken, H., 1992. The role of sea ice in structuring Antarctic ecosystems. *Polar Biology* **12** : 3-13.

Eicken, H., Fischer, H. & Lemke, P., 1995. Effects of the snow cover on Antarctic sea ice and potential modulation of its response to climatic change. *Annals of Glaciology* **21** : 369-376.

Eittreim, S., Bruchhausen, P.M. & Ewing, M., 1972. Vertical distribution of turbidity in the South Indian and South Australian Basins. In *Antarctic Oceanology II. The Australian - New Zealand Sector.*, Hayes, D.E. eds, *Antarctic Research Series*, American Geophysical Union, vol. 19. pp 51-58.

El-Sayed, S., 1984. Productivity of the Antarctic waters - a reappraisal. In *Marine phytoplankton and productivity*, Holm-Hansen, O. & *et al.* eds, Springer-Verlag, New York, pp 19-34.

El-Sayed, S.Z., 1970. On the productivity of the Southern Ocean. In *Antarctic Ecology*, Holdgate, M.W. eds, Academic Press, London, vol. 1. pp 119-135.

El-Sayed, S.Z., 1971. Observations on phytoplankton bloom in the Weddell Sea. In *Biology of the Antarctic Seas IV*, Llano, G.A. & Wallen, I.E. eds, *Antarctic Research Series*, American Geophysical Union, Washington, 17. pp 301-312.

El-Sayed, S.Z., 1988. Seasonal and interannual variabilities in Antarctic phytoplankton with reference to krill distribution. In *Antarctic Ocean and Resources Variability*, Sahrhage, D. eds, Springer-Verlag, Berlin, pp 101-119.

El-Sayed, S.Z., Weber, L.H. & Kopczynska, E.E., 1983. Phytoplankton studies in the sector between Africa and Antarctica. *Antarctic Journal of the United States* **18** : 188-190.

England, M.H., Godfrey, J.S., Tomczak, M. & Hirst, A.C., 1993. The mechanism for Antarctic Intermediate Water renewal in a world ocean model. *Fourth International Conference on Southern Hemisphere Meteorology and Oceanography March 29-April 2, Hobart, Australia Preprint Volume* American Meteorological Society pp 324-325.

Enomoto, H. & Ohmura, A., 1990. The influences of Atmospheric half-yearly cycle on the sea ice extent in the Antarctic. *Journal of Geophysical Research* **95** : 9497-9511.

Eppler, D.T., Farmer, D., Lohanick, A.W., Anderson, M.R., Cavalieri, D.J., Comiso, J., Gloersen, P., Garrity, C., Grenfell, T.C., Hallikainen, M., Maslanik, J.A., Mätzler, C., Melloh, R.A., Rubinstein, I. & Swift, C.T., 1992. Passive microwave signatures of sea ice. In *Microwave Sensing of Sea Ice*, Carsey, F.D. eds, American Geophysical Union, Washington, Geophysical Monograph 68. pp 47-71.

Estrada, M. & Delgado, M., 1990. Summer phytoplankton distributions in the Weddell Sea. *Polar Biology* **10** : 441-449.

Exon, N.F., Marshall, J., McCorkle, D.C., Alcock, M., Chaproniere, G.C.H., Connell, R.D., Dutton, S.J., Elmes, M., Findlay, C., Robertson, L.G., Rollet, N., Samson, C., Shafik, S. & Whitmore, G.P., 1995. AGSO Cruise 147 - Tasman Rise geological sampling cruise of the Rig Seismic: stratigraphy, tectonic history and paleoclimate of the offshore Tasmanian region. *AGSO Record* **1995/56** : 159.

Fenner, J., 1977. Cenozoic diatom biostratigraphy of the Equatorial and Southern Atlantic Ocean. In *Initial reports of the Deep Sea Drilling Project, Supplement*, Supko, P.R., Perch-Nielsen, K. & *et al.* eds, U.S. Government Printing Office, Washington, vol. 39. pp 491-624.

Fenner, J., 1991. Rare and unknown noncalcareous microfossils recovered from Leg 114 sites. In *Proceedings of the Ocean Drilling Program. Scientific Results*, Ciesielski, P.F., Kristofferson, Y. & *et al.* eds, Ocean Drilling Program, College Station, vol. 114. pp 303-310.

Fenner, J., Carter, L. & Stewart, R., 1992. Late Quaternary paleoclimatic and paleoceanographic change over northern Chatham Rise, New Zealand. *Marine Geology* **108** : 383-404.

Fenner, J., Schrader, H.-J. & Wienigk, H., 1976. Diatom phytoplankton studies in the Southern Pacific Ocean, composition and correlation to the Antarctic Convergence and its paleoecological significance. In *Initial Reports of the Deep Sea Drilling Project*, Hollister, C.D., Craddock, C. & *et al.* eds, U.S. Government Printing Office, Washington, vol. XXXV. pp 757-813.

Fiala, M. & Oriol, L., 1990. Light-temperature interactions on the growth of Antarctic diatoms. *Polar Biology* **10** : 629-636.

Fisher, A.E., Berges, J.A. & Harrison, P.J., 1996. Does light quality affect the sinking rates of marine diatoms ? *Journal of Phycology* **32** : 353-360.

Fisher, A.E. & Harrison, P.J., 1996. Does carbohydrate content affect the sinking rates of marine diatoms ? *Journal of Phycology* **32** : 360-365.

Foged, N., 1978. Diatoms in Eastern Australia. *Bibliotheca Phycologica* **41** : 1-243.

Francois, R., Altabet, M.A. & Burckle, L.H., 1992. Glacial to interglacial changes in surface nitrate utilisation in the Indian sector of the Southern Ocean as recorded by sediment $\delta^{15}N$. *Paleoceanography* **7**(5) : 589-606.

Francois, R., Bacon, M.P. & Altabet, M.A., 1993. Glacial/interglacial changes in sediment rain rate in the SW Indian sector of subantarctic waters as recorded by ^{230}Th, ^{231}Pa, U, and $\delta^{15}N$. *Paleoceanography* **8**(5) : 611-629.

Frankes, L.A., 1975. Oceanographic and biological influences on sediment distribution in the Southern ocean. *Search* **6**(8) : 339-341.

Froneman, P.W., Perissinotto, R., McQuaid, C.D. & Laubscher, R.K., 1995. Summer distribution of netphytoplankton in the Atlantic sector of the Southern Ocean. *Polar Biology* **15** : 77-84.

Fryxell, G.A., 1983. New evolutionary patterns in diatoms. *Bioscience* **33**(2) : 92-98.

Fryxell, G.A., 1986. Polymorphism in relation to environmental conditions as exemplified by clonal cultures of *Thalassiosira tumida* (Janisch) Hasle. *9th Diatom- Symposium* pp 61-73.

Fryxell, G.A., 1989. Marine phytoplankton at the Weddell Sea ice edge: seasonal changes at the specific level. *Polar Biology* **10** : 1-18.

Fryxell, G.A., 1990. Planktonic marine diatom winter stages: Antarctic alternatives to resting spores. *Proceedings of the 11th International Diatom Symposium .Memoirs of the Californian Academy of Sciences.* **17** : 437-448.

Fryxell, G.A., 1991. Comparison of winter and summer growth stages of the diatom *Eucampia antarctica* from the Kerguelen Plateau and south of the Antarctic Convergence Zone. In *Proceedings of the Ocean Drilling Program, Scientific Results*, Barron, J., Larsen, B. & *et al.* eds, Ocean Drilling Program, College Station, Texas, vol. 119. pp 675-685.

Fryxell, G.A., 1994. Planktonic marine diatom winter stages: Antarctic alternatives to resting spores. *Memoirs of the California Academy of Sciences* **17** : 437-448.

Fryxell, G.A., Buck, K.R. & Theriot, E.C., 1983. Phytoplankton from the southwestern Atlantic and Indian Oceans. *Antarctic Journal of the United States* **18** : 186-188.

Fryxell, G.A., Doucette, G.J. & Hubbard, G.F., 1981a. The genus *Thalassiosira*: the bipolar diatom *T. antarctica* Comber. *Botanica Marina* **24** : 321-335.

Fryxell, G.A. & Hasle, G.R., 1971. *Corethron criophilum* Castracane: Its distribution and structure. In *Biology of the Antarctic Seas IV*, Llano, G.A. & Wallen, I.E. eds, *Antarctic Research Series*, American Geophysical Union, Washington, vol. 17. pp 335-346.

Fryxell, G.A. & Hasle, G.R., 1972. *Thalassiosira eccentrica* (Ehrenb.) Cleve, *T. symmetrica* sp. nov., and some related centric diatoms. *Journal of Phycology* **8**(4) : 297-317.

Fryxell, G.A. & Hasle, G.R., 1979a. The genus *Thalassiosira* : species with internal extensions of the strutted processes. *Phycologia* **18**(4) : 378-393.

Fryxell, G.A. & Hasle, G.R., 1980. The marine diatom *Thalassiosira oestrupii* : structure, taxonomy and distribution. *American Journal of Botany* **67**(5) : 804-814.

Fryxell, G.A., Hasle, G.R. & Carty, S.V., 1984. *Thalassiosira tumida* (Janisch) Hasle : Observations from field and clonal cultures. *8th International Diatom Symposium* pp 11-21.

Fryxell, G.A. & Kendrick, G.A., 1988. Austral spring microalgae across the Weddell Sea ice edge; spatial relationships found along a northward transect during AMERIEZ 83. *Deep-Sea Research* **35** : 1-20.

Fryxell, G.A. & Prasad, A.K.S.K., 1990. *Eucampia antarctica* var. *recta* (Manguin) stat. nov. (Biddulphiaceae, Bacillariophyceae): life stages at the Weddell Sea ice edge. *Phycologia* **29**(1) : 27-38.

Fryxell, G.A., Sims, P.A. & Watkins, T.P., 1986. *Azpeitia* (Bacillariophyceae): related genera and promorphology. *Systematic Botany Monographs* **13** : 1-74.

Garrison, D.L., 1991. Antarctic sea ice biota. *American Zoologist* **31** : 17-33.

Garrison, D.L., Ackley, S.F. & Buck, K.R., 1983b. A physical mechanism for establishing algal populations in frazil ice. *Nature* **306** : 363-365.

Garrison, D.L. & Buck, K.R., 1989. The biota of Antarctic pack ice in the Weddell Sea and Antarctic Peninsula regions. *Polar Biology* **10** : 211-219.

Garrison, D.L. & Buck, K.R., 1991. Surface-layer sea ice assemblages in Antarctic pack ice during the austral spring: environmental conditions, primary production and community structure. *Marine Ecology Progress Series* **75** : 161-172.

Garrison, D.L., Buck, K.R. & Fryxell, G.A., 1987. Algal assemblages in Antarctic pack ice and in ice-edge plankton. *Journal of Phycology* **25** : 564-572.

Garrison, D.L., Buck, K.R. & Silver, M.W., 1982. Ice algal communities in the Weddell Sea. *Antarctic Journal of the United States* **17** : 157-159.

Garrison, D.L., Buck, K.R. & Silver, M.W., 1983a. Studies of ice-algal communities in the Weddell Sea. *Antarctic Journal of the United States* **18** : 179-181.

Garrison, D.L. & Close, A.R., 1993. Winter ecology of the sea ice biota in Weddell Sea pack ice. *Marine Ecology Progress Series* **96** : 17-31.

Garrison, D.L., Close, A.R. & Reimnitz, E., 1989. Algae concentrated by frazil ice: evidence from laboratory experiments and field measurements. *Antarctic Science* **1**(4) : 313-316.

Garrison, D.L., Sullivan, C.W. & Ackley, S.F., 1986. Sea ice microbial communities in Antarctica. *Bioscience* **36** : 243-250.

Gersonde, R., 1984. Siliceous microorganisms in sea ice and their record in sediments in the southern Weddell Sea (Antarctica). *Proceedings 8th Diatom Symposium Paris* Koeltz, Koenigstein pp 549-566.

Gersonde, R., 1986. Biogenic siliceous particle flux in Antarctic waters and its palaeoecological significance. *South African Journal of Science* **82** : 500-501.

Gersonde, R., 1990a. Taxonomy and morphostructure of the Neogene diatoms from the Southern Ocean, ODP Leg 113. In *Proceedings of the Ocean Drilling Program. Scientific Results*, Barker, P.F., Kennett, J.P. & *et al.* eds, Ocean Drilling Program, College Station, TX, 113. pp 791-802.

Gersonde, R., 1990b. The paleontological significance of fossil diatoms from the high-latitude oceans. In *Polar Marine Diatoms*, Medlin, L.K. & Priddle, J. eds, British Antarctic Survey, Cambridge, pp 57-63.

Gersonde, R. & Wefer, G., 1987. Sedimentation of biogenic siliceous particles in Antarctic waters from the Atlantic sector. *Marine Micropaleontology* **11** : 311-322.

Gleitz, M., Grossmann, S., Scharek, R. & Smetacek, V., 1996. Ecology of diatom and bacterial assemblages in water associated with melting summer sea ice in the Weddell Sea, Antarctica. *Antarctic Science* **8** : 135-146.

Gloersen, P. & Campbell, W.J., 1991. Recent variations in Arctic and Antarctic sea-ice covers. *Nature* **352** : 33-36.

Gloersen, P., Campbell, W.J., Cavalieri, D.J., Comiso, J.C., Parkinson, C.L. & Zwally, H.J., 1992. *Arctic and Antarctic Sea Ice, 1978-1987: Satellite Passive-microwave Observations and Analysis.* NASA Scientific and Technical Information Program, NASA SP-511. Washington. 290 pp.

Gloersen, P. & Cavalieri, D.J., 1986. Reduction of weather effects in the calculation of sea ice concentration from microwave radiances. *Journal of Geophysical Research* **91**(C3) : 3913-3919.

Godfred-Spenning, C.R. & Simmonds, I., in press. An analysis of Antarctic sea ice and extratropical cyclone associations. *International Journal of Climatology* :

Goede, A., 1994. Continuous early last glacial palaeoenvironmental record from a Tasmanian speleothem based on stable isotope and minor element variations. *Quaternary Science Reviews* **13** : 283-291.

Goede, A., McDermott, F., Hawkesworth, C., Webb, J. & Findlayson, B., 1996. Evidence of Younger Dryas and Neoglacial cooling in a Late Quaternary palaeotemperature record from a speleothem in eastern Victoria, Australia. *Journal of Quaternary Science* **11**(1) : 1-7.

Gonzàlez, H.E., 1992. The distribution and abundance of krill faecal material and oval pellets in the Scotia and Weddell Seas (Antarctica) and their role in particle flux. *Polar Biology* **12** : 81-91.

Goodell, H.G., eds, 1973. *Marine sediments of the Southern Ocean.* 17. pp. 1-18, pl.1-9.

Gordon, A.L., 1971a. Oceanography of Antarctic waters. In *Antarctic Oceanology I*, Reid, J.L. eds, *Antarctic Research Series*, American Geophysical Union, 15. pp 169-203.

Gordon, A.L., 1972. Circulation of Antarctic bottom waters South of Australia and New Zealand. In *Antarctic Geology and Geophysics*, Adie, R.J. eds, *International Union of Geological Sciences*, Universitetsforlaget, Oslo, Series B, No. 1. p. 1.

Gordon, A.L., 1972. Introduction : Physical Oceanography of the Southeast Indian Ocean. In *Antarctic Oceanology II. The Australian - New Zealand Sector*, Hayes, D.E. eds, *Antarctic Research Series*, American Geophysical Union, vol. 19. pp 3-9.

Gordon, A.L., 1972. On the interaction of the Antarctic Circumpolar Current and the Macquarie Ridge. In *Antarctic Oceanology II. The Australian - New Zealand Sector*, Hayes, D.E. eds, *Antarctic Research Series*, American Geophysical Union, Washington, vol. 19. pp 71-78.

Gordon, A.L., 1988. Spatial and temporal variability within the Southern Ocean. In *Antarctic Ocean and Resources Variability*, Sahrhage, D. ed., Springer-Verlag, Berlin, pp 41-56.

Gordon, A.L., 1991. Two stable modes of Southern Ocean winter stratification. In *Deep Convection and Deep Water Formation in the Oceans*, Chu, P.C. & Gascard, J.C. eds, Elsevier Science Publishers, pp 17-35.

Gordon, A.L. & Molinelli, E.J., 1986. Thermohaline and chemical distributions and the atlas data set. In *Southern Ocean Atlas*, Gordon, A.L. & *et al.* eds, A.A. Balkema, Rotterdam, 34 pp

Gordon, A.L. & Tchernia, P., 1972. Waters of the Continental Margin off Adélie Coast, Antarctica. In *Antarctic Oceanology II. The Australian - New Zealand Sector*, Hayes, D.E. eds, *Antarctic Research Series*, American Geophysical Union, Washington, vol. 19. pp 59-69.

Granata, T., Wiggert, J. & Dickey, T., 1995. Trapped, near-inertial waves and enhanced chlorophyll distributions. *Journal of Geophysical Research* **100**(C10) : 20,793 - 20,804.

Grieg, M.A., 1982. Satellite-tracked buoy data report VI. Bureau of Meteorology buoys tracked in the Southern, Indian and Pacific Oceans March to June 1979. *CSIRO Marine Laboratories Report* **137** : 1-40.

Grobe, H. & Mackensen, A., 1992. Late Quaternary climatic cycles as recorded in sediments from the Antarctic continental margin. In *The Antarctic Paleoenvironment: A Perspective on Global Change. Part 1.*, Kennett, J.P. & Warnke, D.A. eds, *Antarctic Research Series*, American Geophysical Union, Washington, vol. 56. pp 349-376.

Hajós, M. & Stradner, H., 1974. Late Cretaceous Archaeomonadaceae, Diatomaceae, and Silicoflagellatae from the south Pacific Ocean, Deep Sea Drilling Project, Leg 29, Site 275. In *Initial Reports of the Deep Sea Drilling Project*, Kennett, J.P., Houtz, R.E. & *et al.* eds, U.S. Government Printing Office, Washington, vol. 29. pp 913-1009.

Hallegraeff, G.M., 1984. Species of the diatom genus *Thalassiosira* in Australian waters. *Botanica Marina* **27** : 495-513.

Hallegraeff, G.M., 1986. Taxonomy and morphology of the marine plankton diatoms *Thalassionema* and *Thalassiothrix*. *Diatom Research* **1**(1) : 57-80.

Hallegraeff, G.M., 1994. Species of the diatom genus *Pseudonitzschia* in Australian waters. *Botanica Marina* **37** : 397-411.

Haq, B.U. & Riley, A., 1976. Antarctic silicoflagellates from the southeast Pacific, Deep Sea Drilling Project Leg 35. In *Initial Reports of the Deep Sea Drilling Project*, Hollister, C.D., Craddock, C. & *et al.* eds, U.S. Government Printing Office, Washington, vol. XXXV. pp 673-691.

Hargraves, P.E., 1968. Species composition and distribution of net plankton diatoms in the Pacific sector of the Antarctic Ocean. PhD thesis; Columbia University.

Hargraves, P.E., 1979. Studies on marine plankton diatoms IV. Morphology of *Chaetoceros* resting spores. *Beiheft zur Nova Hedwigia* **64** : 99-120.

Hargraves, P.E. & French, F., 1975. Observations on the survival of diatom resting spores. *Nova Hedwigia* **Beiheft 53** : 229-239.

Hargraves, P.E. & French, F.W., 1983. Diatom resting spores: significance and strategies. In *Survival Strategies of the Algae*, Fryxell, G. ed., Cambridge University Press, Cambridge, pp 49-68.

Harper, M.A., 1974. Diatoms in two sediment cores from the Tasman Sea. *Records of the New Zealand Oceanographic Institute* **2**(2) : 17-24.

Hart, T.J., 1934. On the Phytoplankton of the south-west Atlantic and the Bellingshausen Sea, 1929-31. *Discovery Reports* **VIII** : 1-268.

Hart, T.J., 1937. *Rhizosolenia curvata* Zacharias, an indicator species in the Southern Ocean. *Discovery Reports* **XVI** : 413-446, pl. XIV.

Hart, T.J., 1942. Phytoplankton periodicity in Antarctic surface waters. *Discovery Reports* **XXI** : 261-356.

Harwood, D.M. & Maruyama, T., 1992. Middle Eocene to Pleistocene diatom biostratigraphy of Southern Ocean sediments from the Kerguelen Plateau, Leg 120. In *Proceedings of the Ocean Drilling Program. Scientific Results*, Wise, S.W., Jr., Schlich, R. & *et al.* eds, College Station, TX, vol. 120. pp 683-733.

Hasle, G.R., 1960. Phytoplankton and ciliate species from the Tropical Pacific. *Skrifter Utgitt av det Norske Videnskaps- Akademi I Oslo I. Mat. - Naturv. Klasse* **2** : 1-50, pl. i-viii.

Hasle, G.R., 1964. *Nitzschia* and *Fragilariopsis* species studied in the light and electron microscopes. I. Some marine species of the groups *Nitzschiella* and *Lanceolatae*. *Skrifter utgitt av det Norske Videnskaps - Akademi I Oslo. I. Mat.-Naturv. Klasse. NY Serie* **16** : 1-48, pl. 1-16.

Hasle, G.R., 1965a. *Nitzschia* and *Fragilariopsis* species studied in the light and electron microscopes. II. The group *Pseudonitzschia*. *Skrifter utgitt av det Norske Videnskaps - Akademi I. Matematisk- Naturvidenskaplig Klasse* **18** : 1-45, pl. 1-17.

Hasle, G.R., 1965b. *Nitzschia* and *Fragilariopsis* species studied in the light and electron microscopes. III. The genus *Fragilariopsis*. *Skrifter utgitt av det Norske Videnskaps - Akademi. I. Matematisk - Naturvidenskaplig Klasse* **21** : 1-49, pl. 1-17.

Hasle, G.R., 1969. *An analysis of the phytoplankton of the Pacific Southern Ocean : abundance, composition and distribution during the Brategg expedition, 1947-1948. Hvalradets Skrifter. Det norske videnskaps - akademi i Oslo. Scientific results of marine biological research* **52**. 169 pp.

Hasle, G.R., 1972. *Thalassiosira subtilis* (Bacillariophyceae) and two allied species. *Norwegian Journal of Botany* **19**(2) : 111-137.

Hasle, G.R., 1973. Some marine plankton genera of the diatom family *Thalassiosiraceae*. Second symposium on recent and fossil marine diatoms London, Sept. 4-9, 1972. *Beihefte zur Nova Hedwigia* **45**: 1-49, pl. 1-18.

Hasle, G.R., 1975. Some living marine species of the diatom family Rhizosoleniaceae. *Beiheft zur Nova Hedwigia* **53** : 99-140, 1-13 pl.

Hasle, G.R., 1976. The biogeography of some marine planktonic diatoms. *Deep-Sea Research* **23** : 319-338.

Hasle, G.R., 1990. The planktonic marine diatom *Thalassiosira mediterranea* (synonym *Thalassiosira stellaris*). *Diatom Research* **5**(2) : 415-418.

Hasle, G.R., 1993. Nomenclatural notes on marine planktonic diatoms. The family Bacillariaceae. *Nova Hedwigia, Beiheft* **106** : 315-321.

Hasle, G.R., 1995. Nomenclatural notes on *Palmerina* nom. nov.: *Pseudo-nitzschia turgiduloides* sp. nov. *Diatom Research* **10**(2) : 375-378.

Hasle, G.R. & Booth, B.C., 1984. *Nitzschia cylindriformis* sp. nov., a common and abundant nanoplankton diatom of the eastern subartic Pacific. *Journal of Plankton Research* **6**(3) : 493-503.

Hasle, G.R. & De Mendiola, B.R.E., 1967. The fine structure of some *Thalassionema* and *Thalassiothrix* species. *Phycologia* **61**(2/3) : 107-125.

Hasle, G.R. & Fryxell, G.A., 1977. *Thalassiosira conferta* and *T. binata*, two new diatom species. *Norwegian Journal of Botany* **24** : 239-248.

Hasle, G.R. & Heimdal, B.R., 1968. Morphology and distribution of the marine centric diatom *Thalassiosira antarctica* Comber. *Journal of the Royal Microscopical Society* **88**(3) : 357-369.

Hasle, G.R. & Heimdal, B.R., 1970. Some species of the centric diatom genus *Thalassiosira* studied in the light and electron microscopes. *Beihefte zur Nova Hedwigia* **31** : 543-581.

Hasle, G.R., Heimdal, B.R. & Fryxell, G.A., 1971. Morphologic variability in fasciculated diatoms as exemplified by *Thalassiosira tumida* (Janisch) Hasle, comb. nov. In *Biology of the Antarctic Seas IV*, Llano, G.A. & Wallen, I.E. eds, *Antarctic Research Series*, American Geophysical Union, Washington, vol. 17. pp 313-333.

Hasle, G.R. & Lange, C.B., 1992. Morphology and distribution of *Coscinodiscus* species from the Oslofjord, Norway, and the Skagerrak, North Atlantic. *Diatom Research* **7**(1) : 37-68.

Hasle, G.R. & Medlin, L.K., 1990a. Family Bacillariaceae Genus *Nitzschia* Section *Pseudonitzschia*. In *Polar Marine Diatoms*, Medlin, L.K. & Priddle, J. eds, British Antarctic Survey, Natural Environment Research Council, Cambridge, pp 169-176.

Hasle, G.R., Medlin, L.K. & Syvertsen, E.E., 1994. *Synedropsis* gen. nov., a genus of araphid diatoms associated with sea ice. *Phycologia* **33**(4) : 248-270.

Hasle, G.R. & Semina, H.J., 1987. The marine planktonic diatoms *Thalassiothrix longissima* and *Thalassiothrix antarctica* with comments on *Thalassionema* spp. and *Synedra reinboldii*. *Diatom Research* **2**(2) : 175-192.

Hasle, G.R. & Sims, P.A., 1986. The diatom genus *Coscinodiscus* Ehrenb.: *C. argus* Ehrenb. and *C. radiatus* Ehrenb. *Botanica Marina* **24** : 305-318.

Hasle, G.R., Sims, P.A. & Syvertsen, E.E., 1988. Two recent *Stellarima* species: *S. microtrias, S. stellaris* (Bacillariophyceae). *Botanica Marina* **31** : 195-206.

Hasle, G.R. & Syvertsen, E.E., 1982. *Coscinodiscus pseudolineatus* Pant. and *Coscinodiscus praelineatus* Jousé as synonyms of *Thalassiosira leptopus* (Grun.) Hasle & G. Fryx. *7th Diatom-Symposium* pp 145-155.

Hayes, D.E. & Conolly, J.R., 1972. Morphology of the Southeast Indian Ocean. In *Antarctic Oceanology II. The Australian - New Zealand Sector*, Hayes, D.E. eds, *Antarctic Research Series*, American Geophysical Union, vol. 19. pp 125-145.

Hays, J.D., 1978. A review of the Late Quaternary climatic history of Antarctic Seas. In *Antarctic Glacial History and World Palaeoenvironments Proceedings of the 10th INQUA*, Zinderen, B.V. eds, Balkema, Rotterdam, pp 57-71.

Hays, J.D., Lozano, J.A., Shackleton, N. & Irving, G., 1976. Reconstruction of the Atlantic and western Indian Ocean sectors of the 18,000 B.P. Antarctic Ocean. *Geological Society of America, Memoir* **145** : 337-372.

Heath, R.A., 1985. A review of the physical oceanography of the seas around New Zealand -1982. *New Zealand Journal of Marine and Freshwater Research* **19** : 79-124.

Hendey, N., 1937. The plankton diatoms of the Southern Seas. *Discovery Reports* **16** : 151-364.

Hernàndez-Becerril, D.U., 1995. Planktonic diatoms from the Gulf of California and coasts off Baja California: the genera *Rhizosolenia, Proboscia, Pseudosolenia*, and former *Rhizosolenia* species. *Diatom Research* **10**(2) : 251-267.

Hesse, P., 1994. The record of continental dust from Australia in Tasman Sea sediments. *Quaternary Science Reviews* **13** : 257-272.

Hibler, W.D., III. & Zhang, J., 1995. On the effect of sea-ice dynamics on oceanic thermohaline circulation. *Annals of Glaciology* **21** : 361-368.

Hoban, M.A., Fryxell, G.A. & Buck, K., 1980. Biddulphoid diatoms: resting spores in Antarctic *Eucampia* and *Odontella*. *Journal of Phycology* **16** : 591-602.

Hollibaugh, J.T., Seibert, D.L.R. & Thomas, W.H., 1981. Observations on the survival and germination of resting spores of three *Chaetoceros* (Bacillariophyceae) species. *Journal of Phycology* **17** : 1-9.

Holm-Hansen, O., El-Sayed, S.Z., Franceschini, G.A. & Cuhel, R.L., 1977. Primary production and the factors controlling Phytoplankton growth in the Southern Ocean. In *Adaptations within Antarctic Ecosystems*, Llano, G.A. eds, *Proceedings of the third SCAR symposium on Antarctic Biology*, Smithsonian Institution, pp 11-50.

Holm-Hansen, O. & Mitchell, B.G., 1991. Spatial and temporal distribution of phytoplankton and primary production in the western Bransfield Strait region. *Deep-Sea Research* **38**(8/9) : 961-980.

Holm-Hansen, O. & Vernet, M., 1990. RACER: Phytoplankton distribution and rates of primary production during the austral spring bloom. *Antarctic Journal of the United States* **25**(5) : 141-144.

Horner, R., 1985. *Sea Ice Biota.* CRC Press, Boca Ranton.

Howard, W.R. & Prell, W.L., 1984. A comparison of Radiolarian and Foraminiferal paleoecology in the Southern Indian Ocean: New evidence for the interhemispheric timing of climatic change. *Quaternary Research* **21** : 244-263.

Howard, W.R. & Prell, W.L., 1992. Late Quaternary surface circulation of the Southern Indian Ocean and its relationship to orbital variations. *Paleoceanography* **7**(1) : 79-117.

Howe, S. & Webb III, T., 1983. Calibrating pollen data in climatic terms: improving the methods. *Quaternary Science Reviews* **2** : 17-51.

Hustedt, F., 1930. Die Kieselalgen Deutschlands, ...sterreichs und der Schweiz. In *Kryptogamen-Flora Deutschlands, ...sterreichs und der Schweiz*, Rabenhorst, L. eds, Reprint 1977. Otto Koeltz Science Publishers, West Germany, 1. pp 1-920.

Hustedt, F., 1958. *Diatomeen aus der Antarktis und dem sŸdatlantik. Reprinted from "Deutsche Antarktishe Expedition 1938/1939" Band II, Geographisch - kartographische Anstalt "Mundus".* Hamburg. 191 pp, pl. 3-13.

Hustedt, F., 1959. Die Kieselalgen Deutschlands, ...sterreichs und der Schweiz. In *Kryptogamen-Flora Deutschlands, ...sterreichs und der Schweiz*, Rabenhorst, L. eds, Reprint 1977. Otto Koeltz Science Publishers, West Germany, vol. 2. pp 1-45.

Hutson, W.H. & Prell, W.L., 1980. A paleoecological transfer function, FI-2, for Indian Ocean planktonic Foraminifera. *Journal of Paleontology* **54**(2) : 381-399.

Imbrie, J., Hays, J.D., Martinson, D.G., McIntyre, A., Mix, A.C., Morley, J.J., Pisias, N.G., Prell, W.L. & Shackleton, N.J., 1984. The orbital theory of Pleistocene climate : support from a revised chronology of the marine $\delta^{18}O$ record. In *Milankovitch and Climate*, Berger, A., Imbrie, J., Hays, J., Kukla, G. & Saltzman, B. eds, D. Riedel Publishing Co., Dordrecht, NATO ASI Series C: Mathematical and Physical Sciences vol. 126. pp 269-305.

Imbrie, J. & Kipp, N.G., 1971. A new micropaleontological method for quantitative paleoclimatology : application to a late Pleistocene Carribbean core. In *Late Cenozoic Glacial Ages*, Turekian, K.K. eds, Yale University Press, New Haven, pp 71-181.

Jacka, T.H., 1983. A computer data base for Antarctic Sea Ice Extent. *ANARE Research Notes* **13** : 1-54.

Jacobs, S.S. & Comiso, J.C., 1989. Satellite microwave sea-ice observations and oceanic processes on the Antarctic continental shelf. *Antarctic Journal of the United States* **24** : 135-136.

Jacques, G., 1983. Some ecophysiological aspects of the Antarctic Phytoplankton. *Polar Biology* **2** : 27-33.

Jacques, G. & Fukuchi, M., 1994. Phytoplankton of the Indian Antarctic Ocean. In *Southern Ocean ecology: the BIOMASS perspective*, El-Sayed, S.Z. eds, Cambridge University Press, Cambridge, pp 63-78.

Johansen, J.R., Doucette, G.J. & Fryxell, G.A., 1985. The genus *Thalassiosira* (Bacillariophyceae) : morphology of heterovalvate resting spores of *T. scotia*. *American Journal of Botany* **72**(12) : 1861-1870.

Johansen, J.R. & Fryxell, G.A., 1985. The genus *Thalassiosira* (Bacillariophyceae) : studies on species occurring south of the Antarctic Convergence Zone. *Phycologia* **24**(2) : 155-179.

Jones, G.A. & Johnson, D.A., 1984. Displaced Antarctic diatoms in Vema Channel sediments : Late Pleistocene/Holocene fluctuations in AABW flow. *Marine Geology* **58** : 165-186.

Jordan, R.W., Ligowski, R., Nöthing, E.-M. & Priddle, J., 1991a. The diatom genus *Proboscia* in Antarctic waters. *Diatom Research* **6**(1) : 63-78.

Jordan, R.W. & Priddle, J., 1991. Fossil members of the diatom Genus *Proboscia*. *Diatom Research* **6**(1) : 55-61.

Jordan, R.W., Priddle, J., Pudsey, C.J., Barker, P.F. & Whitehouse, M.J., 1991b. Unusual diatom layers in Upper Pleistocene sediments from the northern Weddell Sea. *Deep-Sea Research* **38**(7) : 829-843.

Jordan, R.W. & Pudsey, C.J., 1992. High-resolution diatom stratigraphy of Quaternary sediments from the Scotia Sea. *Marine Micropaleontology* **19** : 201-237.

Jousé, A.P., Koroleva, G. & Nagaeva, G.A., 1962b. Stratigraphic and paleographic investigations in the Indian sector of the Southern Ocean. *Akademiia NAUK SSSR, Moscow* **8** : 137-161.

Jousé, A.P., Koroleva, G.S. & Nagaeva, G.A., 1962a. Diatoms in the surface layer of sediment in the Indian sector of the Antarctic. *Trudy Instituta Okeanologii Akademiya Nauk SSSR* **61** : 20-91.

Jousé, A.P., Kozlova, O.G. & Muhina, V.V., 1971. Distribution of diatoms in the surface layer of sediment from the Pacific Ocean. In *The Micropalaeontology of the Oceans*, Funnell, B.M. & Riedel, W.R. eds, Cambridge University Press, Cambridge, pp 263-269.

Jouzel, J., Petit, J.R., Chapellaz, J., Barnola, J.M., Barkov, N.I. & Petrov, V.N., 1991. The last deglaciation in Antarctica; evidence of a "Younger Dryas" type climatic event. In *Glaciers-Ocean-Atmosphere Interactions*, Kotlyakov, V.M., Ushakov, A. & Glazovsky, A. eds, *IAHS Publication*, vol. 208. pp 269-446.

Kaczmarska, I., Barbrick, N.E., Ehrman, J.M. & Cant, G.P., 1993. *Eucampia* Index as an indicator of the Late Pleistocene oscillations of the winter sea-ice extent at the ODP Leg 119 Site 745B at the Kerguelen Plateau. *Hydrobiologia* **269/270** : 103-112.

Kaczmarska, I. & Fryxell, G.A., 1984. The diatom Genus *Nitzschia*. *Proceedings of the Eighth International Diatom Symposium Paris* Koenigstein pp 237-252.

Kaczmarska, I. & Fryxell, G.A., 1996. *Alveus*, gen. nov. (Bacillariaceae, Bacillariophyta), a heavily silicified diatom found in warm water oceans. *Microscopy Research and Technique* **33** : 2-11.

Kaczmarska, I. & Kilarski, W., 1979. The structure of *Melosira sulcata* (Ehr.) Kütz. var. *sulcata* frustules from lower Oligocene diatomites from Futoma (Carpathians, Poland). *Annales de la Société Géologique de Pologne (Rocznik Polskiego Towarzystwa Geologicznego)* **XLIX**(1) : 185-194.

Kamatani, A., Ejiri, N. & Tréguer, P., 1988. The dissolution kinetics of diatom ooze from the Antarctic area. *Deep Sea Research* **35**(7) : 1195-1203.

Kang, S.-H. & Fryxell, G.A., 1992. *Fragilariopsis cylindrus* (Grunow) Krieger: The most abundant diatom in water column assemblages of Antarctic marginal ice-edge zones. *Polar Biology* **12** : 609-627.

Kang, S.-H. & Fryxell, G.A., 1993. Phytoplankton in the Weddell Sea, Antarctica: composition, abundance and distribution in water-column assemblages of the marginal ice-edge zone during austral autumn. *Marine Biology* **116** : 335-348.

Kang, S.-H., Fryxell, G.A. & Roelke, D.L., 1993. *Fragilariopsis cylindrus* compared with other species of the diatom family Bacillariaceae in antarctic marginal ice-edge zones. *Nova Hedwigia* **Heft 106** : 335-352.

Karpuz, N.K. & Jansen, E., 1992. A high-resolution diatom record of the last deglaciation from the SE Norwegian Sea: documentation of rapid climatic changes. *Paleoceanography* **7**(4) : 499-520.

Karpuz, N.K. & Schrader, H., 1990. Surface sediment diatom distribution and Holocene paleotemperature variations in the Greenland, Iceland and Norwegian Sea. *Paleoceanography* **5**(4) : 557-580.

Karsten, G., 1905. *Das Phytoplankton des Antarktischen Meeres nach dem Material der deutschen Tiefsee-Expedition 1898-1899.* 1978. Otto Koeltz Science Publishers, W-Germany. 136 pp, pl. I-XIX

Kellogg, D.A. & Kellogg, T.B., 1987. Microfossil distributions in modern Amundsen Sea sediments. *Marine Micropaleontology* **12** : 203-222.

Kellogg, T.B. & Truesdale, R.S., 1979a. Late Quaternary paleoecology and paleoclimatology of the Ross Sea : the diatom record. *Marine Micropaleontology* **4** : 137-158.

Kennett, J.P., Houtz, R.E. & *et al.*, 1974. *Initial reports of the Deep Sea Drilling Project.* U.S. Government Printing Office, vol. 29. Washington. pp 17-445.

Kirst, G.O., Thiel, C., Nothnagel, J., Wanzek, M. & Ulmke, R., 1991. Dimethylsulphoniopropionate (DMSP) in ice-algae and its possible biological role. *Marine Chemistry* **35** : 381-388.

Kirst, G.O. & Wiencke, C., 1995. Ecophysiology of Polar Algae. *Journal of Phycology* **31** : 181-199.

Knaack, J.-J., Pflaumann, U. & Sarnthein, M., 1995. Palaeoproductivity estimates from the Subtropical and Tropical Atlantic based on diatom assemblages. *ICP V Program and Abstracts* p. 131.

Kolla, V., Henderson, L., Sullivan, L. & Bicaye, P.E., 1978. Recent sedimentation in the Southeast Indian Ocean with special reference to the effects of Antarctic bottom water circulation. *Marine Geology* **27** : 1-17.

Kolla, V., Sullivan, L., Streeter, S.S. & Langseth, M.G., 1976. Spreading of the Antarctic bottom water and its effects on the floor of the Indian Ocean inferred

from bottom water potential temperature, turbidity, and sea-floor photography. *Marine Geology* **21** : 171-189.

Kozlova, O.G., 1961. Quantitative content of diatoms in the Indian Ocean sector of the Antarctic (Kolichestvennoe soderzhanie diatomey b bodakh indiyskogo sektora antarktiki). *Doklady Akademii Nauk SSSR. Translated and produced by Scripta Technica Inc. for the American Geophysical Union* **138**(1) : 25-28. (Russian 38 : 207-210).

Kozlova, O.G., 1962. Specific composition of diatoms in the waters of the Indian sector of the Antarctic. *Trudy Instituta Okeonologii. Akademiya Nauk SSSR* **61** : 3-18.

Kozlova, O.G., 1966. *Diatoms of the Indian and Pacific sectors of the Antarctic.* National Science Foundation, Israel Program for Scientific Translations, Washington, D.C. 185 pp, pl. I-VI.

Kozlova, O.G., 1970. Diatoms in suspension and in the bottom sediments in the Southern Indian and Pacific Oceans. In *Antarctic Ecology*, Holdgate, M.W. eds, Academic Press, London, 1. pp 148-153.

Kozlova, O.G., 1971. The main features of diatom and silicoflagellate distribution in the Indian Ocean. In *The Micropalaeontology of the Oceans*, Funnell, B.M. & Riedel, W.R. eds, Cambridge University Press, Cambridge, pp 271-275.

Kozlova, O.G. & Muchina, V.V., 1967. Diatoms and silicoflagellates in suspension and floor sediments of the Pacific Ocean. *International Geology Review (Translated from Geokhimiya Kremnezema, N.K. 65-12(51), 192-218, 1966)* **9**(1) : 1322-1342.

Krause, M., 1981. Vertical distribution of faecal pellets during FLEX '76. *Helgoländer Meeresuntersuchungen* **34** : 313-327.

Krebs, W.N., 1983. Ecology of neritic marine diatoms, Arthur Harbor, Antarctica. *Micropaleontology* **29**(3) : 267-297.

Krebs, W.N., Lipps, J.H. & Burckle, L.H., 1987. Ice diatom floras, Arthur Harbour, Antarctica. *Polar Biology* **7** : 163-171.

Labeyrie, L.D., Labracherie, M., Gorfti, N., Pichon, J.-J., Vautravers, M., Arnold, M., Duplessy, J.-C., Paterne, M., Michel, E., Duprat, J., Caralp, M. & Turon, J.-J., 1996. Hydrographic changes of the Southern Ocean (southeast Indian sector) over the last 230 kyr. *Paleoceanography* **11**(1) : 57-76.

Labeyrie, L.D., Pichon, J.J., Labracherie, M., Ippolito, P., Duprat, J. & Duplessy, J.C., 1986. Melting history of Antarctica during the past 60,000 years. *Nature* **322** : 701-706.

Labracherie, M., Labeyrie, L.D., Duprat, J., Bard, E., Arnold, M., Pichon, J.-J. & Duplessy, J.-C., 1989. The last deglaciation in the Southern Ocean. *Paleoceanography* **4**(6) : 629-638.

Lancelot, C., Mathot, S., Veth, C. & de Baar, H., 1993. On the factors controlling phytoplankton ice edge blooms in the marginal ice zone of the northwestern Weddell Sea during sea ice retreat 1988. In *Weddell Sea Ecology.*, Hempel, G. eds, Springer-Verlag, Berlin, vol. 12. pp 333.

Lapointe, M., 1995. Postglacial palaeoceanography of the Gulf of St. Lawerence (CANADA) based on the diatom assemblage analysis. *ICP V Program and Abstracts* pp 49.

Laws, R.A., 1983. Preparing strewn slides for quantitative microscopical analysis : A test using calibrated microspheres. *Micropaleontology* **29**(1) : 60-65.

Le, J., 1992. Palaeotemperature estimation methods: sensitivity test on two western equatorial Pacific cores. *Quaternary Science Reviews* **11** : 801-829.

Ledbetter, M.T. & Ciesielski, P.F., 1981. Bottom-current erosion in the South Atlantic sector of the Southern Ocean. *Antarctic Journal of the United States* **16** : 110-112.

Ledbetter, M.T., Ciesielski, P.F., Osborn, N.I. & Allison, E.T., 1983a. Bottom-current erosion in the southeast Indian and southwest Pacific oceans during the last 5.4 million years. *Antarctic Earth Science*. Australian Academy of Science, Canberra. pp 379-383.

Ledford-Hoffman, P.A., DeMaster, D.J. & Nittrouer, C.A., 1986. Biogenic-silica accumulation in the Ross Sea and the importance of Antarctic continental-shelf deposits in the marine silica budget. *Geochimica et Cosmochimica Acta* **50** : 2099-2110.

Lee, J.H. & Lee, J.Y., 1990. A light and scanning electron microscopic study on the marine diatom *Roperia tesselata* (Roper) Grunow. *Diatom Research* **5**(2) : 325-335.

Legrand, M., Feniet-Saigne, C., Saltzman, E.S., Germain, C., Barkov, N.I. & Petrov, V.N., 1991. Ice-core record of oceanic emissions of dimethylsulphide during the last climate cycle. *Nature* **350**(144-146) :

Lemke, P., Trinkl, E.W. & Hasselmann, K., 1981. Stochastic dynamic analysis of Polar sea ice variability. *Journal of Physical Oceanography* **10** : 2100-2120.

Levasseur, M., Gosselin, M. & Michaud, S., 1994. A new source of dimethylsulfide (DMS) for the artic atmosphere: ice diatoms. *Marine Biology* **121** : 381-387.

Leventer, A., 1991. Sediment trap diatom assemblages from the northern Antarctic Peninsula region. *Deep-Sea Research* **38**(8/9) : 1127-1143.

Leventer, A., 1992. Modern distribution of diatoms in sediments from the George V Coast, Antarctica. *Marine Micropaleontology* **19** : 315-332.

Leventer, A., Dunbar, R. & DeMaster, D.J., 1993. Diatom evidence for late Holocene climatic events in Granite Harbor, Antarctica. *Paleoceanography* **8**(3) : 373-386.

Leventer, A. & Dunbar, R.B., 1987. Surface sediment diatom assemblages, McMurdo Sound, Antarctica. *Antarctic Journal of the United States* **22** : 194-196.

Leventer, A. & Dunbar, R.B., 1988. Recent diatom record of McMurdo Sound, Antarctica : implications for history of sea ice extent. *Paleoceanography* **3**(3) : 259-274.

Leventer, A. & Dunbar, R.B., 1996. Factors influencing the distribution of diatoms and other algae in the Ross Sea. *Journal of Geophysical Research* **101**(C8) : 18,489-18,500.

Levitus, S., 1982. *Climatological Atlas of the World Ocean.* U.S. Gov. Printing Office, NOAA Professional Paper 13. Washington D.C. 173 pp.

Ligowski, R., 1993. *Marine diatoms (Bacillariophyceae) in the Antarctic ecosystem and their importance as an indicator of food source of krill (Euphasia superba Dana).* Wydanwnictwo Uniwersytetu Lódzkiego, Lódz, Poland. 242 pp. In Polish with English summary.

Lisitzin, A.P., 1971. Distribution of siliceous microfossils in suspension and in bottom sediments. In *The Micropalaeontology of Oceans*, Funnell, B.M. & Riedel, W.R. eds, Cambridge University Press, Cambridge, pp 173-195.

Lisitzin, A.P., 1972. *Sedimentation in the World Ocean.* Society of Economic Paleontologists and Mineralogists, vol. 17. 218 pp.

Locker, S. & Martini, E., 1986. Phytoliths from the southwest Pacific, Site 591. In *Initial Reports of the Deep Sea Drilling Project*, Kennett, J.P., von der Borch, C.C. & *et al.* eds, U.S. Government Printing Office, Washington, vol. 90. pp 1079-1084.

Lozano, J.A. & Hays, J.D., 1976. Relationship of radiolarian assemblages to sediment types and physical oceanography in the Atlantic and western Indian Ocean sectors of the Antarctic Ocean. *Geological Society of America, Memoir* **145** : 303-336.

Mahood, A. & Barron, J.A., 1996. Late Pliocene diatoms in a diatomite from Prydz Bay, East Antarctica. *Micropaleontology* **42**(3) : 285-302.

Makarova, I.V., 1993. Morphology of some species of the genus *Cosinodiscus* Ehrenberg. *Nova Hedwigia, Beiheft* **106** : 185-196.

Mandra, Y.T., 1969. Silicoflagellates: A new tool for the study of Antarctic Tertiary climates. *Antarctic Journal of the United States* **4** : 172-174.

Mandra, Y.T. & Brigger, A.L., 1973. Temperature fluctuations during the Late Eocene in southern ocean waters near South Island, New Zealand. *Antarctic Journal of the United States* **8** : 282-284.

Mandra, Y.T. & Brigger, A.L., 1974. Late Eocene temperatures indicated by silicoflagellates from the Oamaru diatomite, New Zealand. *Antarctic Journal of the United States* **9** : 265-268.

Mann, A., 1937. Diatoms. *Australasian Antarctic Expedition 1911-1914, Scientific Reports. Series C. Zoology and Botany* **1**(1) : 5-82, pl. I-VI.

Marret, F. & de Vernal, A., in press. Dinoflagellate cyst distribution in surface sediments of the southern Indian Ocean. *Marine Micropaleontology* .

Martinez, J.I., 1994. Late Pleistocene palaeoceanography of the Tasman Sea: Implications for the dynamics of the warm pool in the western Pacific. *Palaeogeography, Palaeoclimatology, Palaeoecology* **112** : 19-62.

Martinez, J.I., 1997. Decreasing influence of Subantarctic Mode Water north of the Tasman Front over the past 150 kyr. *Palaeogeography, Palaeoclimatology, Palaeoecology* **131**(3/4) : 355-364.

Martini, E., 1977. Systematics, distribution and stratigraphical application of silicoflagellates. In *Oceanic Micropalaeontology*, Ramsay, A.T.S. eds, Academic Press, London, vol. 2. pp 1327-1343.

Martinson, D.G., Pisias, N.G., Hays, J.D., Imbrie, J., Moore, T.C., Jr. & Shackleton, N.J., 1987. Age dating and the orbital theory of the ice ages : development of a high-resolution 0 to 300, 000 - year chronostratigraphy. *Quaternary Research* **27** : 1-29.

Maynard, N.G., 1976. Relationship between diatoms in the surface sediments of the Atlantic Ocean and the biological and physical oceanography of overlying waters. *Paleobiology* **2** : 99-121.

Mc Cartney, M.S., 1977. Subantarctic Mode Water. In *A Voyage of Discovery*, Angel, M. eds, Pergamon Press, Oxford, pp 103-119.

McCartney, K., 1987. Silicoflagellates, Ebridians, and Archaeomonads. In *Fossil Prokaryotes and Protists - Notes for a short course*, Broadhead, T.W. eds, *Studies in Geology*, Department of Geological Sciences, University of Tennessee, Tennessee, vol. 18. pp 146-168.

McCollum, D.W., 1975. Diatom stratigraphy of the Southern Ocean. In *Initial Reports of the Deep Sea Drilling Project*, Hayes, D.E., Frakes, L.A. & *et al.* eds, U.S. Govt. Printing Office, Washington, vol. XXVIII. pp 515-571.

McConville, M. & Wetherbee, R., 1983. The bottom-ice microalgal community from annual ice in the inshore waters of East Antarctica. *Journal of Phycology* **19** : 431-439.

McCullagh, P. & Nelder, J.A., 1989. *Generalized linear models.* 2nd Edition. Chapman and Hall, New York.

Medlin, L.K. & Hasle, G.R., 1990. Some *Nitzschia* and related diatom species from fast ice samples in the Artic and Antarctic. *Polar Biology* **10** : 451-479.

Medlin, L.K. & Priddle, J., 1990. *Polar Marine Diatoms.* British Antarctic Survey, Natural Environment Research Council, Cambridge. 214 pp.

Medlin, L.K. & Sims, P.A., 1993. The transfer of *Pseudoeunotia doliolus* to *Fragilariopsis. Nova Hedwigia, Beiheft* **106** : 323-334.

Mélières, M.-A., Burckle, L. & Petit, J.-R., 1996. Diatom *E. antarctica* and radiolaria *C. davisiana* as proxy in sediment records in high southern latitudes. *OPALEO: On the use of opal as a paleo-productivity proxy Brest, France* Institut Universitaire Européen de la Mer, Université de Bretagne Occidentale pp 155-156.

Mikkelsen, N., 1979. Diatoms in Equatorial deep-sea sediments: sedimentation and dissolution over the last 20,000 years. *Beiheft zur Nova Hedwigia* **64** : 489-502.

Mitchell, B.G. & Holm-Hansen, O., 1991. Observations and modelling of the Antarctic phytoplankton crop in relation to mixing depth. *Deep-Sea Research* **38**(8/9) : 981-1007.

Molfino, B., Kipp, N.G. & Morley, J.J., 1982. Comparison of foraminiferal, coccolithophorid, and radiolarian paleotemperature equations: assemblage coherency and estimate concordancy. *Quaternary Research* **17** : 279-313.

Moore, T.C., Jr., 1973. Method of randomly distributing grains for microscopic examination. *Journal of Sedimentary Petrology* **43**(3) : 904-906.

Moore, T.C., Jr., 1978. The distribution of radiolarian assemblages in the modern and ice-age Pacific. *Marine Micropaleontology* **3** : 229-266.

Moore, T.C., Jr., Burckle, L.H., Geitzenauer, K., Luz, B., Molina-Cruz, A., Robertson, J.H., Sachs, H., Sancetta, C., Thiede, J., Thompson, P. & Wenkam, C., 1980. The reconstruction of the sea surface temperatures in the Pacific Ocean of 18,000 BP. *Marine Micropaleontology* **5** : 215-247.

Moriarty, K.C., 1977. Clay minerals in southeast Indian Ocean sediments, transport mechanisms and depositional environments. *Marine Geology* **25** : 149-174.

Morley, J.J., 1989a. Radiolarian-based transfer functions for estimating paleooceanographic conditions in the South Indian Ocean. *Marine Micropaleontology* **13** : 293-307.

Morley, J.J., 1989b. Variations in high-latitude oceanographic fronts in the Southern Indian Ocean : an estimation based on faunal changes. *Paleoceanography* **4**(5) : 547-554.

Morley, J.J. & Hays, J.D., 1983. Oceanographic conditions associated with high abundances of the radiolarian *Cycladophora davisiana*. *Earth and Planetary Science Letters* **66** : 63-72.

Morley, J.J. & Stepien, J.C., 1985. Antarctic radiolaria in late winter/early spring Weddell Sea waters. *Micropaleontology* **31**(4) : 365-371.

Morrow, R., Church, J., Coleman, R., Chelton, D. & White, N., 1992. Eddy momentum flux and its contribution to the Southern Ocean momentum balance. *Nature* **357** : 482-484.

Mortlock, R.A., Charles, C.D., Froelich, P.N., Zibello, M.A., Saltzman, J., Hays, J.D. & Burckle, L.H., 1991. Evidence for lower productivity in the Antarctic Ocean during the last glaciation. *Nature* **351** : 220-223.

Nees, S., 1997. Late Quaternary palaeoceanography of the Tasman Sea: the benthic foraminiferal view. *Palaeogeography, Palaeoclimatology, Palaeoecology* **131**(3-4) : 365-390.

Nelson, C.S., Cooke, P.J., Hendy, C.H. & Cuthbertson, A.M., 1993. Oceanographic and climatic changes over the past 160,000 years at deep sea drilling project site 594 off southeastern New Zealand, Southwest Pacific Ocean. *Paleoceanography* **8**(4) : 435-458.

Nelson, D.M. & Gordon, L.I., 1982. Production and pelagic dissolution of biogenic silica in the Southern Ocean. *Geochimica et Cosmochimica Acta* **46** : 491-501.

Nelson, D.M., Smith, W.O., Jr., Gordon, L.I. & Huber, B.A., 1987. Spring distributions of density, nutrients, and phytoplankton biomass in the ice edge zone of the Weddell-Scotia Sea. *Journal of Geophysical Research* **92**(C7) : 7181-7190.

Neori, A. & Holm-Hansen, O., 1982. Effect of temperature on rate of photosynthesis in Antarctic phytoplankton. *Polar Biology* **1** : 33-38.

Okada, H. & Wells, P., 1997. Late Quaternary nannofossil indicators of climatic change in two deep-sea cores associated with the Leeuwin Current off Western Australia. *Palaeogeography, Palaeoclimatology, Palaeoecology* **131**(3/4) : 413-432.

Orr, W.N., 1972. Pacific Northwest siliceous phytoplankton. *Palaeogeography, Palaeoclimatology, Palaeoecology* **12** : 95-114.

Orsi, A.H., Whitworth, T., III & Nowlin, W.D., 1995. On the meridonal extent and fronts of the Antarctic Circumpolar Current. *Deep-Sea Research* **42**(5) : 641-673.

Osborn, N.I., Ciesielski, P.F. & Ledbetter, M.T., 1983. Disconformities and paleoceanography in the southeast Indian Ocean during the past 5.4 million years. *Bulletin of the Geological Society of America* **94** : 1345-1358.

Paillard, D., Labeyrie, L. & Yiou, P., 1996. Macintosh program performs time series analysis. *EOS Transactions, American Geophysical Union* **77** : 379.

Palmisano, A.C., SooHoo, J.B. & Sullivan, C.W., 1987. Effects of four environmental variables on photosynthesis-irradiance relationships in Antarctic sea-ice microalgae. *Marine Biology* **94** : 299-306.

Palmisano, A.C. & Sullivan, C.W., 1982. Physiology of sea ice diatoms. I. Response of three polar diatoms to a simulated summer-winter transition. *Journal of Phycology* **18** : 489-498.

Palmisano, A.C. & Sullivan, C.W., 1983. Sea ice microbial communities (SIMCO). 1. Distribution, abundance, and primary production of ice microalgae in McMurdo Sound, Antarctica in 1980. *Polar Biology* **2** : 171-177.

Park, Y.-H., Gambéroni, L. & Charriaud, E., 1993. Frontal structure, water masses, and circulation in the Crozet Basin. *Journal of Geophysical Research* **98**(7) : 12,361- 12,385.

Parkinson, C.L., 1992. Interannual variability of monthly Southern Ocean sea ice distributions. *Journal of Geophysical Research* **97** : 5349-5363.

Parkinson, C.L. & Cavalieri, D.J., 1982. Interannual sea-ice variations and sea-ice/atmosphere interactions in the Southern Ocean, 1973-1975. *Annals of Glaciology* **3** : 249-254.

Passlow, V., Pinxian, W. & Chivas, A.R., 1997. Late Quaternary palaeoceanography near Tasmania, southern Australia. *Palaeogeography, Palaeoclimatology, Palaeoecology* **131**(3-4) : 433-464.

Peltier, W.R., eds, 1993. *Ice in the Climate System.* Springer-Verlag, Berlin. 12. 673 pp.

Peterson, R.G. & Stramma, L., 1991. Upper-level circulation in the South Atlantic Ocean. *Progress in Oceanography* **26** : 1-73.

Pichon, J.-J., 1985. Les diatomées traceurs de l'évolution climatique et hydrologique de L'Océan Austral au cours du dernier cycle climatique. Ph D thesis; L'Université de Bordeaux I.

Pichon, J.-J., Bareille, G., Labracherie, M., Labeyrie, L.D., Baudrimont, A. & Turon, J.-L., 1992b. Quantification of the biogenic silica dissolution in Southern Ocean sediments. *Quaternary Research* **37** : 361-378.

Pichon, J.-J., Labeyrie, L.D., Bareille, G., Labracherie, M., Duprat, J. & Jouzel, J., 1992a. Surface water temperature changes in the high latitudes of the Southern Hemisphere over the last glacial-interglacial cycle. *Paleoceanography* **7**(3) : 289-318.

Pichon, J.-J., Labracherie, M., Labeyrie, L.D. & Duprat, J., 1987. Transfer functions between diatom assemblages and surface hydrology in the Southern Ocean. *Palaeogeography, Palaeoclimatology, Palaeoecology* **61** : 79-95.

Pisias, N.G., Prell, W., Phral, F., Delaney, M., Lea, D., Jasper, J., Popp, B., Rau, G., Murray, R., McCorckle, D., Rea, D., Derry, L. & Participants, W., 1995. *Marine aspects of Earth system history (MESH) proxy development workshop.* Oregon State University, Corvallis Oregon. 75 pp.

Plancke, J., 1977. Phytoplankton biomass and productivity in the Subtropical Convergence Area and shelves of the Western Indian Subantarctic Islands. *Adaptations within Antarctic Ecosystems. Proceedings of the Third SCAR Symposium on Antarctic Biology Washington D.C.* Smithsonian Institution pp 51-73.

Pokras, E.M. & Molfino, B., 1986. Oceanographic control of diatom abundances and species distributions in surface sediments of the tropical and southeast Atlantic. *Marine Micropaleontology* **10** : 165-188.

Prasad, A.K.S.K. & Nienow, J.A., 1986. Marine diatoms of sediments from Croft Bay, Antarctica. *Antarctic Journal of the United States* **21** : 157-159.

Prell, W.L., Hutson, W.H. & Williams, D.F., 1979. The subtropical convergence and late Quaternary circulation in the Southern Indian Ocean. *Marine Micropaleontology* **4** : 225-234.

Prell, W.L., W.H., H., Williams, D.F., Bé, A.W.H., Geitzenauer, K. & Molfino, B., 1980. Surface circulation of the Indian Ocean during the last glacial maximum, approximately 18,000 yr B.P. *Quaternary Research* **14** : 309-336.

Priddle, J. & Fryxell, G., 1985. *Handbook of Common Plankton Diatoms. (Centrales except the Genus Thalassiosira).* British Antarctic Survey: Natural Environment Research Council, Cambridge. 159 pp.

Priddle, J., Heywood, R.B. & Theriot, E., 1986. Some environmental factors influencing phytoplankton in the Southern Ocean around South Georgia. *Polar Biology* **5** : 65-79.

Priddle, J., Jordan, R.W. & Medlin, L.K., 1990. Family Rhizosoleniaceae. In *Polar marine diatoms*, Medlin, L.K. & Priddle, J. eds, British Antarctic Survey, Cambridge, pp 115-127.

Priddle, J., Smetacek, V. & Bathmann, U., 1992. Antarctic marine primary production, biogeochemical carbon cycles and climatic change. *Phil. Trans. R. Soc. Lond. B* **338** : 289-297.

Ramirez, P.R., 1981. Beiträge zur Taxonomie und Verbreitung der Gattung *Thalassiosira* Cleve. *Bibliotheca Phycologica* **Band 56** : 220, maps 1-9, pl.1-71.

Raymond, J.A., Sullivan, C.W. & DeVries, A.L., 1994. Release of an ice-active substance by Antarctic sea ice diatoms. *Polar Biology* **14** : 71-75.

Reyment, R., Jöreskog, K.G. & Marcus, L., 1993. *Applied Factor Analysis in the Natural Sciences.* Cambridge University Press, Cambridge. 371 pp.

Riaux-Gobin, C., 1996. Deep subantarctic sediments: revival tests and comparison of diatom spores from cultures and sediment samples. *14th International Diatom Symposium Tokyo 1996* Tokyo Diatom Institute p. 99.

Riaux-Gobin, C. & Descolas-Gros, C., 1992. Assemblage de microphytes enkystés à la surface de sédiments profonds, sur le talus continental du golfe du Lion. *C.R. Acad. Sci. Paris* **314**(Série III) : 545-552.

Rintoul, S.R. & Church, J.A., 1993. A late winter section between Tasmania and Antarctica : circulation, transport and water mass formation. *Fourth International Conference on Southern Hemisphere Meteorology and Oceanography March 29-April 2, 1993, Hobart, Australia Preprint Volume* American Meteorological Society pp 21-22.

Rintoul, S.R., Donguy, J.-R. & Roemmich, D.H., 1997. Seasonal evolution of upper ocean thermal structure between Tasmania and Antarctica. *Deep-Sea Research* **44** : 1185-1202.

Rochford, D.J., 1961. Hydrology of the Indian Ocean. I The water masses in intermediate depths of the South-East Indian Ocean. *Australian Journal of Marine and Freshwater Research* **12**(2) : 129-149.

Rochford, D.J., 1962. Hydrology of the Indian Ocean. II The surface waters of the South-East Indian Ocean and the Arafura Sea in the Spring and Summer. *Australian Journal of Marine Freshwater Research* **13** : 226-251.

Rochford, D.J., 1963. Mixing trajectories of intermediate depth waters of the South-East Indian Ocean as determined by a salinity frequency method. *Australian Journal of Marine Freshwater Research* **14** : 1-23.

Rochford, D.J., 1965. Rapid changes in the characteristics of the deep salinity maximum of the South-East Indian Ocean. *Australian Journal of Marine and Freshwater Research* **16**(4) : 129-149.

Rochford, D.J., 1981. Anomalously warm sea surface temperatures in the Western Tasman Sea, their causes and effects upon the Southern Bluefin Tuna catch, 1966-1977. *CSIRO Division of Fisheries and Oceanography Report* **114** : 1-19.

Rochford, D.J., 1986. Seasonal changes in the distribution of Leeuwin Current waters off southern Australia. *Australian Journal of Marine and Freshwater Research* **37**(1) : 1-10.

Rodman, M.R. & Gordon, A.L., 1982. Southern Ocean bottom water of the Australian-New Zealand sector. *Journal of Geophysical Research* **87**(C8) : 5771-5778.

Romero, O.E., 1996. Ultrastructure of four species of the diatom genus *Cocconeis* with the description of *C. pseudocostata* spec. nov. *Nova Hedwigia* **63**(3-4) : 361-396.

Round, F.E., Crawford, R.M. & Mann, D.G., 1990. *The Diatoms. Biology & Morphology of the Genera.* Cambridge University Press, Cambridge. 747 pp.

Sachs, H.M., Webb, T., III & Clark, D.R., 1977. Paleoecological transfer functions. *Ann. Rev. Earth Planet. Sci.* **5** : 159-178.

Sakshaug, E. & Holm-Hansen, O., 1984. Factors governing pelagic production in Polar Oceans. In *Marine Phytoplankton and Productivity*, Holm-Hansen, O., Bolis, L. & Gilles, R. eds, Springer-Verlag, New York, pp 1-18.

Sancetta, C., 1981. Diatoms as hydrographic tracers : example from Bering Sea sediments. **211** : 279-281.

Sancetta, C., Heusser, L. & Hall, M.A., 1992. Late Pliocene climate in the Southeast Atlantic : preliminary results from a multi-disciplinary study of DSDP Site 532. *Marine Micropaleontology* **20** : 59-75.

Sarthein, M., Winn, K., Jung, S.J.A., Duplessy, J.-C., Labeyrie, L., Erlenkeusser, H. & Ganssen, G., 1994. Changes in east Atlantic deepwater circulation over the last 30,000 years : Eight time slice reconstructions. *Paleoceanography* **9**(2) : 209-267.

Scharek, R., Smetacek, V., Fahrbach, E., Gordon, L.I., Rohardt, G. & Moore, S., 1994. The transition from winter to early spring in the eastern Weddell Sea, Antarctica: plankton biomass and composition in relation to hydrography and nutrients. *Deep-Sea Research* **41**(8) : 1231-1250.

Schloss, I. & Estrada, M., 1994. Phytoplankton composition in the Weddell-Scotia confluence area during austral spring in relation to hydrography. *Polar Biology* **14** : 77-90.

Schrader, H. & Karpuz, N.K., 1990. Norwegian-Iceland Seas : Transfer functions between marine planktic diatoms and surface water temperature. In *Geological History of the Polar Oceans : Arctic versus Antarctic*, Bleil, U. & Thiede, J. eds, *NATO ASI Series C: Mathematical and Physical Sciences*, Kluwer Academic Publishers, Netherlands, vol. 308. pp 337-361.

Schrader, H. & Sorknes, R., 1991. Peruvian coastal upwelling : Late Quaternary productivity changes revealed by diatoms. *Marine Geology* **97** : 233-249.

Schrader, H., Swanberg, N., Lycke, A.K., Paetzel, M., Schrader, T. & Schrader, T., 1993. Diatom-inferred productivity changes in the eastern equatorial Pacific: the Quaternary record of ODP Leg 111, Site 677. *Hydrobiologia* **269/270** : 137-151.

Schrader, H.J., 1976. Cenozoic planktonic diatom biostratigraphy of the Southern Pacific Ocean. In *Initial Reports of the Deep Sea Drilling Project*, Hollister, C.D.,

Craddock, C. & *et al.* eds, U.S. Government Printing Office, Washington, vol. 35. pp 605-671.

Schrader, H.J. & Gersonde, R., 1978. Diatoms and Silicoflagellates. In *Micropaleontological counting methods and techniques - an exercise on an eight metres section of the Lower Pliocene of Capo Rossello, Sicily*, Zachariasse, W.J., Riedel, W.R., Sanfilippo, A., Schmidt, R.R., Brolsma, M.J., Schrader, H.J., Gersonde, R., Drooger, M.M. & Broekman, J.A. eds, Utrecht Micropaleontological Bulletin, vol. 17. pp 129-176.

Schrader, T., 1989. *Factor Analysis Package*. University of Bergen: Bergen.

Schuette, G. & Schrader, H., 1979a. Diatom taphocoenoses in the coastal upwelling area off western South America. *Nova Hedwigia* **64** : 359-378.

Schuette, G. & Schrader, H., 1979b. Diatom taphocoenoses in the coastal upwelling areas off western South America. *Oregon State University, School of Oceanography Data Report 73* Reference number 79-8.

Schuette, G. & Schrader, H., 1981. Diatom taphocoenoses in the coastal upwelling area off south west Africa. *Marine Micropalaeontology* **6** : 131-155.

Schweitzer, P.N., 1995. *Monthly averaged polar sea-ice concentration.* U.S. Geological Survey Digital Data Series: Virginia. CD, **Ed 1. DDS-27**.

Semina, H.J., 1979. The geography of plankton diatoms of the Southern Ocean. *Beiheft zur Nova Hedwigia* **64** : 341-358.

Semina, H.J., 1981. A morphological examination of the diatom *Thalassiothrix longissima* Cleve et Grunow. *Bacillaria* **4** : 147-160.

Semina, H.J. & Rat'kova, T., 1988. Occurrence of some diatom species in the Southern ocean southward of New Zealand. In *10th Diatom Symposium*, eds, pp 275-284.

Shackleton, N.J., 1982. The deep-sea sediment record of climate variability. *Progress in Oceanography* **11** : 199-218.

Shemesh, A., Burckle, L.H. & Froelich, P.N., 1989. Dissolution and preservation of Antarctic diatoms and the effect on sediment thanatocoenoses. *Quaternary Research* **31** : 288-308.

Shemesh, A., Burckle, L.H. & Hays, J.D., 1994. Meltwater input to the Southern Ocean during the Last Glacial Maximum. *Science* **266** : 1542-1544.

Sieger, R., 1996. *PalaeoTool Box and MacTransfer.* Alfred-Wegener-Institut für Polar- und Meeresforschung: Bremerhaven.

Simmonds, I., 1981. The effect of sea ice on a general circulation model of the Southern Hemisphere. In *Sea Level, Ice, and Climatic Change*, Allison, I. eds, *IAHS Publication*, 131. pp 193-206.

Simmonds, I., in press. Climatic role of the Southern Hemisphere extratropical cyclones and their relationship with sea ice. *Papers and proceedings of the Royal Society of Tasmania.*

Simmonds, I. & Budd, W.F., 1990. A simple parametrization of ice leads in a general circulation model, and the sensitivity of climate to change in Antarctic ice concentration. *Annals of Glaciology* **14** : 266-269.

Simmonds, I. & Wu, X., 1993. Cyclone response to changes in winter southern hemisphere sea-ice concentration. *Quaternary Journal of the Royal Meteorological Society* **119** : 1121-1148.

Simonsen, R., 1974. The diatom plankton of the Indian Ocean Expedition of R/V *Meteor* 1964-1965. *"Meteor" Forsch.-Ergebnisse* **Reihe D No.19** : 1-107.

Simonsen, R., 1982. Note on the diatom genus *Charcotia* M. Pergallo. *Bacillaria* **5** : 101-116.

Simonsen, R., 1992. The diatom types of Heinrich Heiden in Heiden & Kolbe 1928. *Bibliotheca Diatomologica* **Band 24** : 100 pp, pl. 1- 86.

Sloyan, B., 1993. Upper ocean structure in the subantarctic and polar frontal zone Southeast of Australia. *Fourth International Conference on Southern Hemisphere Meterology and Oceanography March 29-April 2, 1993, Hobart, Australia Preprint Volume* American Meterological Society pp 308-309.

Smart, C.W., King, S.C., Gooday, A.J., Murray, J.W. & Thomas, E., 1994. A benthic foraminiferal proxy of pulsed organic matter paleofluxes. *Marine Micropaleontology* **23** : 89-99.

Smetacek, V., Scharek, R., Gordon, L.I., Eicken, H., Fahrbach, E., Rohardt, G. & Moore, S., 1992. Early spring phytoplankton blooms in ice platelet layers of the southern Weddell Sea, Antarctica. *Deep-Sea Research* **39**(2) : 153-168.

Smetacek, V.S., 1985. Role of sinking diatom life-history cycles : ecological, evolutionary and geological significance. *Marine Biology* **84** : 239-251.

Smith, R.E.H., Stapleford, L.C. & Ridings, R., 1994. The acclimated response of growth, photosynthesis, composition, and carbon balance to temperature in the psychrophilic ice diatom *Nitzschia seriata. Journal of Phycology* **30** : 8-16.

Smith, W.O., Jr, 1987. Phytoplankton dynamics in marginal ice zones. *Oceanography and Marine Biology Annual Review* **25** : 11-38.

Smith, W.O. & Nelson, D.M., 1985. Phytoplankton bloom produced by a receding ice edge in the Ross Sea : Spatial coherence with the density field. *Science* **227** : 163-166.

Smith, W.O., Jr. & Nelson, D.M., 1986. Importance of ice edge phytoplankton production in the Southern Ocean. *Bioscience* **36**(251-257) :

Smith, W.O., Jr. & Sakshaug, E., 1990. Polar Phytoplankton. In *Polar Oceanography*, Smith, W.O., Jr. eds, Academic Press Inc., San Diego, Part B. pp 477-525.

Sournia, A., Grall, J.-R. & Jacques, G., 1979. Diatomées et Dinoflagelles planctoniques d'une coupe méridienne dans le sud de l'océan Indien (campagne Antipode I du Marion-DuFresne, mars 1977) (Plankton diatoms and dinoflagellates along a Meridian transect in the Southern Indian Ocean (Cruise Antipod I of the R/V "Marion DuFresne", March 1977). *Botanica Marina* **XXII** : 183-198.

Sowers, T., Bender, M., Labeyrie, L., Martinson, D., Jouzel, J., Raynaud, D., Pichon, J.-J. & Korotkevich, Y.S., 1993. A 135,000-year Vostok-SPECMAP common temporal framework. *Paleoceanography* **8**(6) : 737-766.

Steffen, K., Key, J., Cavalieri, D.J., Comiso, J., Gloersen, P., St. Germain, K. & Rubinstein, I., 1992. The estimation of geophysical parameters using passive microwave algorithms. In *Microwave Remote Sensing of Sea Ice*, Carsey, F.D. eds, American Geophysical Union, Washington, Geophysical Monograph 68. pp 201-231.

Sterrenburg, F.A.S., 1995. Studies on the genera *Gyrosigma* and *Pleurosigma* (Bacillariophyceae) *Gyrosigma balticum* (Ehrenberg) Rabenhorst, *G. pensacole* sp. n. and simulacrum species. *Botanica Marina* **38** : 401-408.

Stidolph, S.R., 1988. Observations and remarks on morphology and taxonomy of the diatom genera *Gyrosigma* Hassall and *Pleurosigma* W. Smith. *Nova Hedwigia* **47**(3-4) : 377-388.

Stockwell, D.A. & Hargraves, P.E., 1984. Morphological variability within resting spores of the marine diatom genus *Chaetoceros* Ehrenberg. *Proceedings of the Eighth International Diatom Symposium Paris* Koenigstein pp 81-95.

Stockwell, D.A., Kang, S.-H. & Fryxell, G.A., 1991. Comparisons of diatom biocoenoses with Holocene sediment assemblages in Prydz Bay, Antarctica. In *Proceedings of the Ocean Drilling Program. Scientific Results*, Barron, J., Larsen, B. & *et al.* eds, Ocean Drilling Program, College Station, TX, vol. 119. pp 667-673.

Streten, N.A. & Pike, D.J., 1984. Some observations of the sea-ice in the southwest Indian Ocean. *Australian Meteorology Magazine* **32** : 195-206.

Sullivan, C.W., Arrigo, K.R., McClain, C.R., Comiso, J.C. & Firestone, J., 1993. Distributions of Phytoplankton blooms in the Southern Ocean. *Science* **262** : 1832-1837.

Sullivan, C.W., McClain, C.R., Comiso, J.C. & Smith, W.O., Jr., 1988. Phytoplankton standing crops within an Antarctic ice edge assessed by satellite remote sensing. *Journal of Geophysical Research* **93** : 12,487-12,498.

Sundström, B.G., 1986. The marine diatom genus *Rhizosolenia*. A new approach to taxonomy. PhD; Lund University.

Suzuki, Y. & Takahashi, M., 1995. Growth responses of several diatom species isolated from various environments to temperature. *Journal of Phycology* **31** : 880-888.

Syvertsen, E.E., 1977. *Thalassiosira rotula* and *T. gravida*: Ecology and morphology. *Beiheft zur Nova Hedwigia* **54** : 99-112.

Syvertsen, E.E., 1985. Resting spore formation in the Antarctic diatoms *Coscinodiscus furcatus* Karsten and *Thalassiosira australis* Pergallo. *Polar Biology* **4** : 113-119.

Takahashi, K., 1994. From modern flux to paleoflux : Assessment from sinking assemblages to thanatocoenosis. In *Carbon cycling in the glacial ocean : Constraints on the ocean's role in global change.*, Zahn, R. & *et al.* eds, Springer-Verlag, Berlin Heidelberg, NATO ASI Series Vol. 117. pp 413-424.

Takahashi, K., Jordan, R. & Priddle, J., 1994. The diatom genus *Proboscia* in Subartic waters. *Diatom Research* **9**(2) :

Tanimura, Y., 1992. Distribution of diatom species in the surface sediments of Lützow-Holm Bay, Antarctica. In *Centenary of Japanese Micropaleontology*, Ishizaki, K. & Saito, T. eds, Terra Scientific Publishing Company, Tokyo, pp 399-411.

Tanimura, Y., Fukuchi, M., Watanabe, K. & Moriwaki, K., 1990. Diatoms in water column and sea-ice in Lützow-Holm Bay, Antarctica, and their preservation in preservation in the underlying sediments. *Bulletin of the National Science Museum, Tokyo, Series C* **18**(1) : 15-39.

Tchernia, P., 1980. *Descriptive Regional Oceanography.* Pergamon Marine Series Pergamon Press, 3. Oxford. pp 43-84, pl.1-3, 10-19.

The Shipboard Scientific Party, 1975. Site 281. In *Initial Reports of the Deep Sea Drilling Project, LEG 29*, Kennett, J.P., Houtz, R.E. & *et al.* eds, US Government Printing Office, Washington, vol. 29. pp 271-316.

Thompson, R.O.R.Y. & Veronis, G., 1983. Poleward boundary current off Western Australia. *Australian Journal of marine and Freshwater Research* **34**(1) : 173-185.

Tilzer, M.M. & Dubinsky, Z., 1987. Effects of temperature and day length on the mass balance of Antarctic phytoplankton. *Polar Biology* **7** : 35-42.

Tilzer, M.M., Elbrächter, M., Gieskes, W.W. & Beese, B., 1986. Light-temperature interactions in the control of photosynthesis in Antarctic phytoplankton. *Polar Biology* **5** : 105-111.

Tomas, C.R., 1996. *Identifying marine diatoms and dinoflagellates.* Academic Press, 598 pp.

Tomczak, M. & Godfrey, J.S., 1994. *Regional Oceanography : An Introduction.* Pergamon Press, Oxford. 422 pp.

Tréguer, P. & Jacques, G., 1992. Dynamics of nutrients and phytoplankton, and fluxes of carbon, nitrogen and silicon in the Antarctic Ocean. *Polar Biology* **12** : 149-162.

Tréguer, P., Kamatani, A., Gueneley, S. & Quéguiner, B., 1989. Kinetics of dissolution of Antarctic diatom frustules and the biogeochemical cycle of silicon in the Southern Ocean. *Polar Biology* **9** : 397-403.

Treppke, U.F., Lange, C.B. & Wefer, G., 1996. Vertical fluxes of diatoms and silicoflagellates in the eastern equatorial Atlantic, and their contribution to the sedimentary record. *Marine Micropaleontology* **28** : 73-96.

Truesdale, R.S. & Kellogg, T., 1979. Ross Sea diatoms : modern assemblage distributions and their relationship to ecologic, oceanographic, and sedimentary conditions. *Marine Micropaleontology* **4** : 13-31.

Tucker, W.B., III, Perovich, D.K., Gow, A.J., Weeks, W.F. & Drinkwater, M.R., 1992. Physical properties of sea ice relevant to remote sensing. In *Microwave Sensing of Sea Ice*, Carsey, F.D. eds, American Geophysical Union, Washington, Geophysical Monograph 68. pp 9-28.

Van der Spoel, S., Hallegraeff, G.M. & Van Soest, R.W.M., 1973. Notes on variation of diatoms and silicoflagellates in the South Atlantic Ocean. *Netherlands Journal of Sea Research* **6**(4) : 518-541.

van Iperen, J.M., van Bennekom, A.J. & van Weering, T.C.E., 1993. Diatoms in surface sediments of the Indonesian Archipelago and their relation to hydrography. *Hydrobiologia* **269/270** : 113-128.

van Iperen, J.M., van Weering, T.C.E., Jansen, J.H.F. & van Bennekom, A.J., 1987. Diatoms in surface sediments of the Zaire deep-sea fan (SE Atlantic Ocean) and their relation to overlying water masses. *Netherlands Journal of Sea Research* **21**(3) : 203-217.

Van Landingham, S.L., 1967-1979. *Catalogue of the fossil and recent Genera and species of the diatoms and their synonyms.* J. Cramer, parts I-VIII. Vaduz, Germany.

Vella, P., Ellwood, B.B. & Watkins, N.D., 1975. Surface-water temperature changes in the Southern Ocean southwest of Australia during the last one million years. In *Quaternary Studies*, Suggate, R.P. & Cresswell, M.M. eds, The Royal Society of New Zealand, Wellington, Bulletin 13. pp 297-309.

Villareal, T.A. & Fryxell, G.A., 1983. Temperature effects on the value structure of the bipolar diatoms *Thalassiosira antarctica* and *Porosira glacialis*. *Polar Biology* **2** : 163-169.

Wadhams, P., Lange, M.A. & Ackley, S.F., 1987. The ice thickness distribution across the Atlantic sector of the Antarctic Ocean in midwinter. *Journal of Geophysical Research* **92** : 14,535-14,552.

Watanabe, K., 1982. Centric diatom communities found in the Antarctic sea ice. *Antarctic Record, National Institute of Polar Research* **74** : 119-126.

Watkins, A.B. & Simmonds, I., 1995. Sensitivity of numerical prognoses to Antarctic sea ice distribution. *Journal of Geophysical Research* **100**(C11) : 22,681-22,696.

Watkins, N.D. & Kennett, J.P., 1971. Antarctic bottom water : major change in velocity during the late Cenozoic between Australia and Antarctica. *Science* **173** : 813-818.

Watkins, N.D. & Kennett, J.P., 1972. Regional sedimentary disconformities and upper Cenozoic changes in bottom water velocities between Australia and Antarctica. In *Antarctic Oceanology II. The Australia - New Zealand Sector*, Hayes, D.E. eds, *Antarctic Research Series*, American Geophysical Union, 19. pp 273-293.

Weaver, F.M. & Ciesielski, P.F., 1974. Pliocene paleotemperatures and regional correlations, Southern Ocean. *Antarctic Journal of the United States* **9** : 251-253.

Wefer, G., Fischer, G., Fütterer, D. & Gersonde, R., 1988. Seasonal particle flux in the Bransfield Strait, Antarctica. *Deep-Sea Research* **35**(6) : 891-898.

Wefer, G., Fischer, G., Fütterer, D.K., Gersonde, R., Honjo, S. & Ostermann, D., 1990. Particle sedimentation and productivity in Antarctic waters of the Atlantic sector. In *Geological History of the Polar Oceans : Arctic versus Antarctic*, Bleil, U. & Thiede, J. eds, Kluwer Academic Publishers, Dordrecht, Series C :Mathematical and Physical Sciences - 308. pp 363-379.

Wells, P. & Okada, H., 1996. Holocene and Pleistocene glacial palaeoceanography off southeastern Australia, based on foraminifers and nannofossils in Vema cored hole V18-222. *Australian Journal of Earth Sciences* **43** : 509-523.

Wells, P., Wells, G., Cali, J. & Chivas, A., 1994. Response of deep-sea benthic foraminifera to Late Quaternary climate changes, southeast Indian Ocean, offshore Western Australia. *Marine Micropaleontology* **23** : 185-229.

Wells, P.E. & Wells, G.M., 1994. Large scale reorganisation of ocean currents offshore Western Australia during the Late Quaternary. *Marine Micropaleontology* **24** : 157-186.

Welsh, A.H., Cunningham, R.B., Donnelly, C.F. & Lindenmayer, D.B., 1996. Modelling the abundance of rare species: statistical models for counts with extra zeros. *Ecological Modelling* **88** : 297-308.

Westall, F. & Fenner, J., 1990. Polar Front fluctuations and the upper Gauss to Brunhes Paleo-oceanographic record in the Southeast Atlantic Ocean. In *Geological History of the Polar oceans : Antarctic versus Antarctic*, Bleil, U. & Theiede, J. eds, *NATO ASI Series C : Mathematical and Physical Sciences*, Kluwer Academic Publishers, Dordrecht, 308. pp 761-782.

Whitehead, J.M. & McMinn, A., 1997. Paleodepth determination from Antarctic benthic diatom assemblages. *Marine Micropaleontology* **29** : 301-318.

Whiting, M.C. & Schrader, H., 1985. *Actinocyclus ingens* Rattray: Reinvestigation of a polymorphic species. *Micropaleontology* **31** : 68-75.

Whitworth, T., III, 1988. The Antarctic Circumpolar Current. *Oceanus* **31** : 53-58.

Williams, D.F., 1976. Late Quaternary fluctuations of the Polar Front and Subtropical Convergence in the southeast Indian Ocean. *Marine Micropaleontology* **1** : 363-375.

Williams, D.F. & Keany, J., 1978. Comparison of radiolarian/planktonic foraminiferal paleoceanography of the Subantarctic Indian Ocean. *Quaternary Research* **9** : 71-86.

Wilson, D.L., Smith, W.O., Jr. & Nelson, D.M., 1986. Phytoplankton bloom dynamics of the western Ross Sea ice edge - I. Primary productivity and species-specific production. *Deep-Sea Research I* **33**(10) : 1375-1387.

Winsborough, B. & Abbott, W.H., 1985. Cenozoic diatom biostratigraphy of the Middle America Trench and slope, Deep Sea Drilling Project Leg 84. In *Initial Reports of the Deep sea Drilling Project*, von Huene, R., Aubouin, J. & *et al.* eds, U.S. Govt. Printing Office, Washington, 84. pp 515-526.

Wood, E.J.F., 1960. Antarctic phytoplankton studies. *Proceedings of the Linnean Society of New South Wales.* **LXXXV**(2) : 215-229.

Worby, A.P., Massom, R.A., Allison, I., Lytle, V.I. & Heil, P., in press. East Antarctic sea ice : a review of its structure, properties and drift. In *Antarctic sea ice properties, structure and processes*, eds, *Antarctic Research Series*, American Geophysical Union.

Wyrtki, K., 1962a. Geopotential topographies and associated circulation in the south-eastern Indian Ocean. *Australian Journal of Marine Freshwater Research* **13**(1) : 1-17.

Wyrtki, K., 1962b. The subsurface water masses in the western south Pacific Ocean. *Australian Journal of Marine Freshwater Research* **13**(1) : 18-49.

Yanagisawa, Y. & Akiba, F., 1990. Taxonomy and phylogeny of the three marine diatom genera, *Crucidenticula, Denticulopsis*, and *Neodenticula. Bulletin of the Geological Survey of Japan* **41**(5) : 197-301.

Yiou, F., Raisbeck, G.M., Bourles, D., Lorius, C. & Barkov, N.I., 1985. ^{10}Be in ice at Vostok Antarctica during the last climatic cycle. *Nature* **316** : 616-617.

Yoder, J.A., Ackleson, S.G., Barber, R.T., Flaments, P. & Balch, W.M., 1994. A line in the sea. *Nature* **371** : 689-692.

Zabel, I.H.H., Jezek, K.C., Gogineni, S.P. & Kanagaratnam, P., 1996. Search for proxy indicators of young sea ice thickness. *Journal of Geophysical Research* **101**(C3) : 6697-6709.

Zernova, V.V., 1970. Phytoplankton of the Southern Ocean. In *Antarctic Ecology*, Holdgate, M.W. eds, Academic Press, London, 1. pp 136-142.

Zernova, V.V., 1990. Seasonal variations of the Antarctic pelagic diatoms. *Proceedings of the 10th International Diatom Symposium Joensuu, Finland, Aug. 28 -Sept. 2, 1988* Koenigstein pp 267-275.

Zielinski, U., 1993. Quantitative estimation of palaeoenvironmental parameters of the Antarctic surface water in the Late Quaternary using transfer functions with diatoms. *Berichte zur Polarforschung* **126** : 1-148.

Zielinski, U. & Gersonde, R., 1997. Diatom distribution in Southern Ocean surface sediments (Atlantic sector): Implications for paleoenvironmental reconstructions. *Palaeogeography, Palaeoclimatology, Palaeoecology* **129** : 213-250.

Zwally, H.J., Comiso, J.C. & Gordon, A.L., 1985. Antarctic offshore leads and polynyas and oceanographic effects. In *Oceanology of the Antarctic Continental Shelf*, Jacobs, S.S. eds, *Antarctic Research Series*, American Geophysical Union, Washington, 43. pp 203-226.

Zwally, H.J., Comiso, J.C., Parkinson, C.L., Campbell, W.J., Carsey, F.D. & Gloersen, P., 1983b. *Antarctic Sea Ice, 1973-1976 satellite passive-microwave observations.* NASA Scientific and Technical Information Branch, NASA SP-459. Washington. 206 pp.

Zwally, H.J., Parkinson, C.L. & Comiso, J.C., 1983a. Variability of Antarctic sea ice and changes in carbon dioxide. *Science* **220** : 1005-1012.

This page left intentionally blank.

Appendix A.1
Floral List and Plates.

The siliceous flora observed in core and surface samples in this study are listed.
The flora are listed alphabetically and follows the taxonomy of Van Landingham (1967-1979), Hustedt (1930-1958), Round *et al.* (1990), Johansen and Fryxell (1985), Hasle (1993, 1995) and other more recent specific works as listed.

Included in the notes of each species is the core and or new surface sample in which the species occured. The reader can cross reference to the species distribution tables in the Appendicies, to locate a particular species occurrence.

Plates illustrating most of the flora described follows this section.

DIATOMS

- GENUS ***ACTINOCYCLUS*** EHRENBERG (1837).

ACTINOCYCLUS ACTINOCHILUS (EHRENBERG) SIMONSEN (1982).

SYNONYMS: *Charcotia actinochilus* (Ehrenberg) Hustedt
in Abbott 1973, Fenner *et al.* 1976, Akiba 1982, Krebs 1983.

ILLUSTRATION: Plate 1, figures 1and 2.

REFERENCES USED: Abbott 1973 Pl. 2 fig. C; Fenner *et al.* 1976 Pl. 5 fig. 5; Pichon 1985 Pl. 5 figs 11-12; Akiba 1982 Pl. 3 figs 7-10; Krebs 1983 Pl. 1 fig. 6; Villareal and Fryxell 1993 figs 21-24; Zielinski, 1993 Pl. 1 figs 1,3.

NOTES: - Occurs in cores MD88-784, MD88-, E53-10; and in new surface samples MDBX94-03, -04, TC53-10, TC37-19.

ACTINOCYCLUS CURVATULUS JANISCH IN SCHMIDT (1878)

SYNONYMS: *Coscinodiscus divisus* Grunow
in Hustedt 1930; Barde-Labayle-Bounès 1980.
Coscinodiscus curvatulus Grunow in Schmidt (1878)
in Hustedt 1930, Fenner *et al.* 1976, Pichon 1985.

ILLUSTRATION: Plate 1, figures 3 and 4 as *A. curvatulus*, and Plate 4 figures 7 to 9 as *Coscinodiscus curvatulus*.

REFERENCES USED: Hustedt 1930 figs 307 (as *A. curvatulus*), 214 (as *C. curvatulus*) and 217 (as *C. curvatulus* var. *minor*); Hustedt 1958 Pl. 8 figs 82-83, Simonsen 1974 -text p. 20; Fenner *et al.* 1976 Pl. 6 figs 1-2 (as *A. curvatulus*) and 3-10 (as *C. curvatulus*); Barde-Labayle-Bounès 1980 Pl. IV fig. 3; Akiba 1982 Pl. 5 figs 5-6; Pichon 1985 Pl. 1 figs 1-2 (as *A. curvatulus*) and fig. 3 (as *C. curvatulus*).

NOTES: - Occurs in cores MD88-779, MD88-784, MD88-787, E53-10 and new surface samples MDBX94-01, -02, -07, TC53-10, GC007, GC013, GC014, GC016, GC017, GC031, GC034
- E53-10 (as both *A. diviscus* and *A. curvatulus).*
- Simonsen (1974) suggests that *Actinocyclus diviscus* Hustedt 1930 and *Coscinodicsus diviscus* Hustedt are synonyms of *A. curvatulus.* Whereas Fryxell (in Meddlin and Priddle 1990) suggests *A. diviscus* Hustedt 1930 is a synonymn of*Actinocyclus cholnokyi.*

ACTINOCYCLUS cf. ***EXIGUUS*** FRYXELL ET SEMINA (1981)

REFERENCES USED: Fryxell in Medlin and Priddle 1990.

NOTES: - Occurs in new surface sample GC016.

ACTINOCYCLUS INGENS RATTRAY(1890)

ILLUSTRATION: Plate 1, figure 5.

REFERENCES USED: Abbott 1973 Pl. 1 figs A-C; Akiba 1982 Pl. 5 figs 7-14; Barron 1985 Fig. 9 2-4, Pichon 1985 Pl. 2 fig. 9.,Whiting and Schrader 1985, Ciesielski 1986 Pl. 1 figs 8-10, Gersonde 1990, pl. 1 figs 1, 3-7.

NOTES: - Occurs in cores MD88-784,MD88-787; and in new surface samples MDBX94-01,-02,-03, TC53-10, TC37-19, E53-10.

ACTINOCYCLUS OCTONARIUS EHRENBERG (1838)1861

SYNONYMS: *Actinocyclus ehrenbergii* Ralfs
in Hustedt 1930.

REFERENCES USED: Hustedt 1930 fig. 298; Foged 1978 Pl. IV fig. 5; Fenner *et al.* 1976 Pl. 5 figs 1-2, 10; Barde-Labayle-Bounès 1980 Pl. I figs 1-2.

NOTES: - Occurs in core MD88-787.

***ACTINOCYCLUS* SPP.**

NOTES: - Occurs in cores MD88-784, MD88-787, E53-10.

- GENUS ***ALVEUS*** (GRUNOW) KACZMARSKA ET G. FRYXELL (1996)

ALVEUS MARINUS KACZMARSKA ET G. FRYXELL (1996)

SYNONYMS: *Nitzschia marina Grunow*
in Barron 1985 fig. 13 no. 1.
ILLUSTRATION: Plate 1, figure 6.
REFERENCES USED: Kaczmarska and Fryxell (1996).
NOTES: - Occurs in surface sample MDBX94-11 (33°34.71'S, 110°35.09E)
- sample not included in statistical treatment in this thesis.

- GENUS ***ASTEROMPHALUS*** EHRENBERG (1844).

ASTEROMPHALUS HOOKERI EHRENBERG (1844)

ILLUSTRATION: Plate 2, figures 1-2.
REFERENCES USED: Fenner *et al.* 1976 Pl. 4 fig. 24; Akiba 1982 Pl. 1 fig.1; Pichon 1985 Pl. 1 fig. 7; Zielinski 1993 Pl. 1 fig. 4.
NOTES: - Occurs in cores MD88-779, MD88-784, MD88-787, E53-10; and in new surface samples MDBX-01,-02,-03,-04,-05,-07, TC53-10, E36-6, GC013.

ASTEROMPHALUS HYALINUS KARSTEN (1905)

ILLUSTRATION: Plate 2, figure 3.
REFERENCES USED: Abbott 1973 Pl. 2 fig. B; Fenner *et al.* 1976 Pl. 4 figs 17-19; Schrader 1976 Pl. 8 figs 5,7; Akiba 1982 Pl. 1 fig. 4; Pichon 1985 Pl. 1 fig. 8; Zielinski 1993 Pl. 1 fig. 5.
NOTES: - Occurs in cores MD88-784, MD88-787, E53-10.

ASTEROMPHALUS PARVULUS KARSTEN (1905)

SYNONYMS: *Asteromphalus heptacis* (BRÉBISSON) RALPHS
in Hustedt 1930 fig. 277; Fenner *et al.* 1976 Pl. 4 figs 22-23; Pichon 1985 Pl. 1 fig. 6 (as *A. heptactis*)
ILLUSTRATION: Plate 2, figure 4.
REFERENCES USED:Abbott 1973 Pl. 2 fig. A; Fenner *et al.* 1976 Pl. 4 figs 20-21; Schrader 1976 Pl. 8 figs 3, 7; Pichon 1985 Pl. 1 fig. 9; Zielinski 1993 Pl. 1 fig. 2.
NOTES: - Occurs in cores MD88-784, MD88-78, E53-10; and in new surface sample MDBX94-03.

***ASTEROMPHALUS* SPP.**

NOTES: - Occurs in core MD88-787; and in new surface sample GC014.

- GENUS ***AZPEITIA*** PERGALLO IN TEMPÉRE ET PERGALLO (1912).

AZPEITIA AFRICANUS (JANISCH EX SCHMIDT) FRYXELL ET WATKINS 1986.

SYNONYMS: *Coscinodiscus africanus* Janisch ex Schmidt (1878)
in Hustedt 1930, Simonsen 1974, Barde-Labayle-Bounés 1980.
ILLUSTRATION: Plate 4, figure 4. (Idenitified as *Coscinodiscus africanus*).
REFERENCES USED: Hustedt 1930 fig. 231,Simonsen 1974 pl. 9 fig. 1, Barde-Labayle-Bounés 1980 pl. III figs 1-2.
NOTES: - Occurs in new surface sample MDBX94-01.

AZPEITIA TABULARIS (GRUNOW) FRYXELL ET SIMS (1986)

SYNONYMS: *Coscinodiscus tabularis*
in Hustedt 1930, Abbott 1973, Fenner *et al.* 1976, Schrader 1976, Akiba 1982, Pichon 1985.
T. antarctica , in Pichon 1985 Pl. 4 fig. 4.
ILLUSTRATION: Plate 2, figures 5-7.
REFERENCES USED: Hustedt 1930 fig. 230a; Abbott 1973 Pl. 3 figs A-C; Fenner *et al.* 1976 Pl. 7 figs 10-13; Akiba 1982 Pl. 2 figs 6-9; Pichon 1985 Pl. 2 figs 11-14; Fryxell *et al.* 1986 Pl. XXX fig. 1; Zielinski 1993 Pl. 2 figs 1,4.
NOTES: - Occurs in cores MD88-779, MD88-784, MD88-787, E53-10; and in new surface samples MDBX94-01, -02, -03, -04, -05, -05, -06, -07, TC53-10, TC37-19, E36-6, GC007, GC013, GC014, GC 016. GC017, GC030, GC031, GC034.

AZPEITIA TABULARIS VAR. EGREGIUS (RATTRAY) HUSTEDT (1930)

SYNONYMS: *Coscinodiscus tabularis* var. *egregius*
in Hustedt 1930; Fenner *et al.* 1976.
ILLUSTRATION: Plate 2, figures 8-10.
REFERENCES USED: Hustedt 1930 fig. 230b; Fenner *et al.*1976 Pl. 7 figs 8-9; Zielinski 1993 Pl. .2 fig. 3.
NOTES: - Occurs in new surface samples MDBX94-01,-06,-07.

- GENUS ***CESTODISCUS*** GREVILLE (1865)

CESTODISCUS SPP.

REFERENCE USED: Schrader 1976 Pl. 12 fig. 3 (*Cestodiscus* sp. 5).
NOTES: - Occurs in core E53-10.

- GENUS ***CHAETOCEROS*** EHRENBERG (1844).

***CHAETOCEROS* VEGETATIVE CELLS**

ILLUSTRATION: Plate 3, figures 1-8.
NOTES: - Occurs in cores MD88-784, MD88-787; and in new surface samples MDBX-01, -04.
- Specimens considered and identified as *Chaetoceros* vegetative cells are listed below:

CHAETOCEROS BULBOSUM COMPLEX(EHRENBERG) HEIDEN

SYNONYMS: *Chaetoceros schimperianum* Karsten.
Chaetoceros atlanticum Clève.
Chaetoceros atlanticus Clève - in Hustedt 1930.
Chaetoceros atalnticum var. *bulbosum* - in Abbott 1973.
Chaetoceros bulbosum - in Akiba 1982.
Chaetoceros atalnticum forme *bulbosum* Hargraves- in Pichon 1985.
ILLUSTRATION: Plate 3, figures 1-3.
REFERENCES USED: Hustedt 1930 figs 363-366; Abbott 1973 Pl. 10 fig. E; Akiba 1982 Pl. 7 fig. 9; Pichon 1985 Pl. 2 fig. 5.

CHAETOCEROS CRIOPHILUM CASTRACANE 1886

ILLUSTRATION: Plate 3, figure 4.
REFERENCES USED: Castracane, p. 78, Priddle and Fryxell 1985 pp 30-31.

CHAETOCEROS DICHAETA EHRENBERG

ILLUSTRATION: Plate 3, figure 5.
REFERENCES USED: Hustedt 1930 fig. 367; Abbott 1973 Pl. 10 fig. F. Priddle and Fryxell 1985 pp 32-33.

CHAETOCEROS DICLADIA CASTRACANE 1886

ILLUSTRATION: Plate 3, figures 6-8.
SYNONYMS: *Dicladia capreolus* Ehrenberg - in Orr 1972
Dicladia sp. cf *Dipylea* Hanna and Grant - in Burky 1974.
Chaetoceros (Dicaldia) lorenzianus resting spore - in Harwood and Maruyama 1992.
REFERENCES USED: Castracane 1886 Pl. XIX figs 7-8; Orr 1972 Pl. III fig. 1; Burcky 1974 Pl. 2 figs 3-4, Harwood and Maruyama 1992 Pl. 18 figs 1,18-19.

***CHAETOCEROS* RESTING SPORES/CELLS.**

ILLUSTRATION: Plate 3, figures 9-27.
REFERENCES USED: Castracane 1886 Pl. XIX figs 7-8; Hustedt 1930 figs 384b, 385e-f, 386, 387, 396, 397, 400d, 404, 405b-d, 406a-b, 407c-e, 411a, 417d, 423, 430b, 432b, 436, 437, 439, 442, 440; Barde-Labayle-Bounès 1980 Pl. II figs 8-18, Pl. VX fig. 1-3; Riaux-Gobin and Descolas-Gros 1992 figs 1.1, Pl. I fig. 5-6, Pl. II figs 1-4; Zielinski 1993 Pl. 7 figs 6-12.
NOTES: - Occurs in cores MD88-779, MD88-784, MD88-787, E53-10; and in new surface samples MDBX94-01, -02, -03, -04, -05, -05, -06, -07, TC53-10, TC37-19, E36-6, GC007, GC013, GC014, GC 016, GC017, GC030, GC031, GC034.
- Specimens considered and identified in a very simplistic manner sa *Chaetoceros* resting cells are listed below:

C. DIADEMA SPORES (EHRENBERG) GRAN

REFERENCES USED: Hargraves and French 1975 fig. 2; Hargraves and French 1983 fig. 2d; Hollibaugh *et al.* 1981 fig. 4a-g.

C. RADICANS SPORES SCHUTTE

ILLUSTRATION: Plate 3 figures 14-16.
REFERNCES USED: Hustedt 1930 fig. 432b; Stockwell and Hargraves 1984 Text fig. 1a-c, Pl. 4 figs 22-27. Fryxell *et al.* 1981 figs 1-2.
NOTES: -Both *C. radians* and *C. cinctus* are very similar. Stockwell and Hargraves (1984) describe the differences between the two species. Further synonomy with either of these two species is made with Castracane's *C. incurvum* Bail., var. *umbonatum* (1886 Pl. XXIX figs 10 and 16).

C. CINCTUS SPORES

REFERENCES USED: Hustedt 1930 fig. 432b; Stockwell and Hargraves 1984 Text fig. 1a-c, Pl. 3 figs 16-21.

CHAETOCEROS SPORE TYPE A.

ILLUSTRATION: Plate 3 figures 17-20.

Notes: Oval spores with no major descriptive trait.

CHAETOCEROS SPORE TYPE B.
ILLUSTRATION: Plate 3 figures 21-23.
Notes: Stretched oval spores some with no descriptive traits, others with central raised area and two apical spines.

CHAETOCEROS SPORE TYPE C.
ILLUSTRATION: Plate 3 figure 24.
Notes: Large stretched oval spores.

CHAETOCEROS SPORE TYPE D.
ILLUSTRATION: Plate 3 figures 25-27.
Notes: Oval to circular spores with spines covering valve face.

- GENUS ***COCCONEIS*** (EHRENBERG (1837).

***COCCONEIS* SPP.**
ILLUSTRATION: Plate 4 figure 1.
REFERENCES USED: Hustedt 1959 fig. 785 (*C. costata*), Krebs 1983 Pl. 1 figs 8-9 (*C. costata*, and var. *kerguelensis*), Akiba 1982 Pl.7 fig. 12 (*C. costata*), Romero 1996, Romero and Rivera 1996.
NOTES: - Occurs in surface sample MDBX94-03.
Includes *Cocconeis costata, C. fasciolata, C. california* in the original Pichon data.

- GENUS ***CORETHRON*** CASTRACANE (1886).

CORETHRON CRIOPHILUM CASTRACANE (1886)
ILLUSTRATION: Plate 4, figure 2-3.
REFERENCES USED: Fryxell and Hasle 1971 figs 2-4,6.Harwood and Mauyama 1992 Pl. 19 figs 13-14.
NOTES: - Occurs in core MD88-787; and in possibly in new surface sample TC53-10.

- GENUS ***COSCINODISCUS*** EHRENBERG (1838).

"COSCINODISCUS AFRICANUS" JANISCH IN SCHMIDT (1878)
NOW KNOWN AS *AZPEITIA AFRICANUS* JANISCH EX SCHMIDT) FRYXELL ET WATKINS (1986). REFERENCE: FRYXELL, G.A., SIMS, P.A. AND WATKINS, T.P.1986.
ILLUSTRATION: Plate 4, figure 4.
REFERENCES USED: Hustedt 1930 fig. 231,Simonsen 1974 pl. 9 fig. 1, Barde-Labayle-Bounés 1980 pl. III figs 1-2.
NOTES: - Occurs in new surface sample MDBX94-01.

COSCINODISCUS ASTEROMPHALUS EHRENBERG (1844)
ILLUSTRATION: Plate 4, figure 5-6.
REFERENCES USED: Hustedt 1930 fig. 250, Barde-Labayle-Bounés 1980 pl. III figs 3-8, Hasle and Lange 1992 fig.10, Makarova 1993 fig. 5.
NOTES: - Occurs in core MD88-787; and in new surface sample MDBX94-07.

COSCINODISCUS MARGINATUS EHRENBERG
ILLUSTRATION: Plate 4, figures 10-11b.
REFERENCES USED: Hustedt 1930 fig. 223, Abbott 1973 Pl. 6 fig. A, Schrader 1976 Pl. 10 fig. 3, Barde-Labayle-Bounés 1980 Pl. IV figs 8-10, Makarova 1993 fig.2.
NOTES: - Occurs in core MD88-784, MD88-787, E53-10; and in new surface sample E36-6.

COSCINODISCUS RADIATUS EHRENBERG (1840)
ILLUSTRATION: Plate 5, figures 1-2.
REFERENCES USED: Hustedt 1930 fig. 225, Fenner *et al.* 1976 Pl. 7 fig. 1, Barde-Labayle-Bounés 1980 Pl. IV figs 8-9, Hasle and Sims 1986 figs 35-39, Makarova 1993 fig. 1.
NOTES: - Occurs in core MD88-779, E53-10; and in new surface samples GC007, GC014, GC016, GC017, GC030, GC034.

***COSCINODISCUS* SPP.**
ILLUSTRATION: Plate 5, figures 3-4.
NOTES: - Occurs in core MD88-779, MD88-784, MD88-787, E53-10; and in new surface samples MDBX94-01,-07,TC53-10, GC007, GC013, GC014, GC017, GC030, GC031, GC034.

COSCINODISCUS cf. *OCCULOIDES*
ILLUSTRATION: Plate 5 figure 3.
REFERENCES USED: Karsten 1905, Abbott 1973, Priddle and Fryxell 1985, Zielinski 1993.

COSCINODISCUS cf *ARGUS*
ILLUSTRATION: Plate 5 figure 4.
REFERENCES USED: Hustedt 1930, Hasle and Sims 1986.

- GENUS ***CYCLOTELLA*** KÜTZING EX DE BREBISSON (1838)

***CYCLOTELLA* SPP.**
ILLUSTRATION: Plate 5, figures 5-6.
REFERENCES USED: Foged 1978.
NOTES: - Occurs in core MD88-779.

- GENUS ***DACTYLIOSOLEN*** CASTRACANE (1886)

DACTYLIOSOLEN ANTARCTICA CASTRACANE (1886)
ILLUSTRATION: Plate 5, figures 7-8.
REFERENCES USED: Castracane 1886 Pl. IX fig. 7, Hasle 1975 Pl. 80 figs 90-100, Fenner *et al.* 1976 Pl. 11 fig. 11, Harwood and Maruyama 1992 Pl. 18 fig. 12.
NOTES: - Occurs in cores MD88-784, MD88-787, E53-10; and in surface samples MDBX94-01, -02, -03, -04, -05, -06, -07, TC53-10, GC034.

- GENUS **DELPHINEIS** ANDREWS 1977

DELPHINEIS SURIELLA (EHRENBERG) ANDREWS
ILLUSTRATION : Plate 5 figures 9-11.
SYNONYMS: *Rhaphoneis suriella* (Ehrenberg) Grunow 1881
REFERENCES USED: Andrews 1975 Pl. 13 figs 35-37, Barde-Labayle-Bounés 1980 Pl. XII fig. 19, Round *et al.* 1990.
NOTES: - Occurs in core MD88-779, and in new surface samples GC031, GC034.

- GENUS ***DENTICULOPSIS*** (SIMONSEN) AKIBA ET YANAGISAWA (1990)

***DENTICULOPSIS* SPP.**
REFERENCES USED: Akiba 1982 pl. 10 figs 12-26b, Pl. 11 figs 1-32. Yanagisawa and Akiba 1990.
NOTES: - Occurs in core E53-10; and new surface sample TC37-19.

DENTICULOPSIS DIMORPHA (SCHRADER) AKIBA ET YANAGISAWA (1990)
SYNONYMS: *Denticuloides dimorpha* (Schrader) Simonsen
REFERENCES USED: Barron 1985 fig. 13 no. 22-23, Yanagisawa and Akiba 1990.
NOTES: - Occurs in core E53-10.

- GENUS ***DIPLONEIS*** EHRENBERG EX P.T. CLEVE (1894).

DIPLONEIS WEISSFLOGII CLEVE (1894)
DIPLONEIS BOMBUS EHRENBERG (1854)
ILLUSTRATION: Plate 5, figures 12-13.
REFERENCES USED: Hustedt 1959 fig. 1085 (*D.weissfogii*), fig. 1086 (*D. bombus*), Barde-Labayle-Bounés 1980 Pl. XI figs 14-15 (*D. bombus*).
NOTES: - Occurs in core MD88-779.
- Differetiation betwen the two species *D. weissflogii* and *D. bombus* was not achieved as the two have overlapping features. *D. bombus* has length 30-150µm, greatest valve width 15-47µm, mid-valve width 6-25 µm and 6-8 sometimes 9 rows in 10 µm. *D. weissflogii* has length 27-110 µm, greatest valve width 11-35 µm, mid-valve width 7-25 µm and 7-8 rows in 10 µm (Hustedt 1959).

- GENUS ***EUCAMPIA*** EHRENBERG (1839).

EUCAMPIA ANTARCTICA (CASTRACANE) MANGUIN
SYNONYMS: *E. balaustium* Castracane
in Castracane 1886, Abbott 1973, Fenner *et al.* 1976, Schrader 1976, Akiba 1982
ILLUSTRATION: Plate 6, figures 1-2.
REFERENCES USED: Castracane 1886 Pl. XVIII figs 5-6, Fenner *et al.* 1976 Pl. 5 figs 8-9, Akiba 1982 figs 1-9, Krebs 1983 Pl. 3 figs 3a-b, Burckle 1984 figs 1-7, Fryxell and Prasad 1990 figs 2-18.
NOTES: - Occurs in cores MD88-779, MD88-784, MD88-787, E53-10; and in new surface samples MDBX94-01, -02, -03, -04, -05, -06, TC53-10, TC37-19, E36-6, GC014.

- GENUS ***FRAGILARIOPSIS*** HUSTEDT (1913)

FRAGILARIOPSIS CURTA (VAN HEURCK) HUSTEDT (1958)
SYNONYMS: *Nitzschia curta* (Van Heurck) Hasle, *Fragilaria curta* Van Heurk
ILLUSTRATION: Plate 6 figures 3-4.

REFERENCES USED: Hustedt 1958 Pl. 11 figs 140-144, Hasle 1965b Pl. 12 figs 2-5, Pl. 13 fig. 1-6. Fenner *et al.* 1976 Pl. 4 figs 5-9, Akiba 1982 Pl. 10 figs 1-2b, Zielinski 1993 Pl. 5 figs 11-13

NOTES: - Occurs in cores MD88-784, MD88-787; and in new surface samples MDBX94-02, -05, TC37-19.

FRAGILARIOPSIS CYLINDRUS (GRUNOW) KRIEGER (1954)

SYNONYMS: *Nitzschia cylindrus* (Grunow) Hasle, *Fragilaria cylindrus* Grunow, *Nitzschia cylindra* (Grunow) Hasle in Krebs 1983.

ILLUSTRATION: Plate 6, figures 5-7.

REFERENCES USED: Hustedt 1958 Pl. 11 figs 145-146, Hasle 1965b Pl. 12 figs 6-12, Pl. 14 figs 1-10, Fenner *et al.* 1976 Pl. 4 figs 10-15, Krebs 1983 Pl. 4 fig. 5, Hasle and Booth 1984 figs 23,25-26, 37-39.

NOTES: - Occurs in cores MD88-784, MD88-787; and in new surface sample TC37-19.

FRAGILARIOPSIS DOLIOLUS (WALLICH) MEDLIN ET SIMS (1993)

SYNONYMS: *Psuedoeunotia doliolus* (Wallich) Grunow

ILLUSTRATION: Plate 6, figures 8-9.

REFERENCES USED: Hustedt 1958 Pl. 12 figs 147, Hustedt 1959 fig. 737, Fenner *et al.* 1976 Pl. 14 fig. 12, Barde-Labayle-Bounés 1980 Pl. XII figs 3-4, Barron 1985 fig. 13.2, Zielinski 1993 Pl. 6 figs 11-12, Medlin and Sims 1993 figs 6,9.

NOTES: - Occurs in core MD88-779; and in new surface samples MDBX94-01, -02, -03, -05, -06, -07, GC007, GC0013, GC014, GC017, GC030, Gc031, GC034.

FRAGILARIOPSIS KERGUELENSIS (O'MEARA) HUSTEDT (1952)

SYNONYMS: *Nitzschia kerguelensis* (O'Meara) Hasle, *Fragilaria antarctica* Castracane, *Nitzschia lanceolata* in Abbott 1973.

ILLUSTRATION: Plate 6, figures 10-12.

REFERENCES USED: Hustedt 1958 Pl. 10 figs 121-127. Hasle 1965b Pl. 4 figs 11-18, Pl. 5 figs 1-11, Pl. 7 fig. 9, Fenner *et al.* 1976 Pl. 2 figs 19-30, Akiba 1982 Pl.9 figs 1a-4.

NOTES: - Occurs in cores MD88-779, MD88-784, MD88-787, E53-10; and in new surface samples MDBX94-01, -02, -03, -04, -05, -05, -06, -07, TC53-10, TC37-19, E36-6, GC007, GC013, GC014, GC 016. GC017, GC030, GC031, GC034.

- Abberent forms of *F. kerguelensis* were observed often generally with displaced raphe and disrupted areolation patterns.

ILLUSTRATION: Plate 6, figures 13-17.

REFERENCES USED: Hustedt 1958 Pl. 12 fig. 158.

NOTES: - Occurs in core MD88-787; and in new surface sample MDBX94-06.

FRAGILARIOPSIS OBLIQUECOSTATA (VAN HEURCK) HEIDEN IN HEIDEN ET KOLBE (1928)

SYNONYMS: *Nitzschia obliquecostata* (Van Heurck) Hasle, *Fragilaria obliquecostata* Van Heurck.

ILLUSTRATION: Plate 6, figures 18-19.

REFERENCES USED: Hasle 1965b Pl.7 figs 2-7, Fenner *et al.* 1976 Pl.2 figs 15-18, Zielinski 1993 Pl. 5 figs 15-17.

NOTES: - Occurs in core MD88-787.

FRAGILARIOPSIS PSEUDONANA (HASLE) HASLE 1993

SYNONYMS: *Nitzschia pseudonana* Hasle

ILLUSTRATION: Plate 6, figure 20.

REFERENCES USED: Hasle 1965b Pl.1 figs 7-14, Pl. 4 figs 20-21, Fenner *et al.* 1976 Pl. 2 figs 6-11, Hasle and Booth 1984 figs 29-31.

NOTES: - Occurs in cores MD88-784, MD88-787.

FRAGILARIOPSIS RHOMBICA (O'MEARA) HUSTEDT (1952)

SYNONYMS: *Nitzschia angulata* Hasle, *Diatoma rhombica* O'Meara, *Nitzschia rhombica* in Abbott 1973.

ILLUSTRATION: Plate 6, figures 21-23.

REFERENCES USED: Hustedt 1958 Pl. 10 figs 113-120, Hasle 1965b Pl. 10 figs 2-6, Pl. 9 figs 1-6, Pl. 4 fig. 19, Pl. 1 fig. 6, Abbott 1973 Pl. 7 figs D-E, Fenner *et al.* 1976 Pl. 1 figs 17-39, Akiba 1982 Pl. 10 figs 6-8.

NOTES: - Occurs in cores MD88-784, MD88-787, E53-10; and in surface samples MDBX94-02, -03, -04, -06, TC53-10, TC37-19.

FRAGILARIOPSIS RITSCHERI HUSTEDT (1958)

SYNONYMS: *Nitzschia ritscheri* (Hustedt) Hasle

ILLUSTRATION: Plate 7, figures 1-4 .

REFERENCES USED: Hustedt 1958 Pl. 11 figs 133-136, Hasle 1965b Pl. 1 fig. 20, Pl. 4 figs 1-10, Pl. 15 figs 12-13, Pl. 17 fig. 8, Zielinski 1993 Pl. 5 figs 18-19.

NOTES: - Occurs in cores MD88-784, MD88-787, E53-10; and in new surface sample GC016.

FRAGILARIOPSIS SEPARANDA HUSTEDT (1958)

SYNONYMS: *Nitzschia seperanda* (Hustedt) Hasle

ILLUSTRATION: Plate 7, figures 5-9.

REFERENCES USED: Hustedt 1958 Pl. 10 figs 108-112, Hasle 1965b Pl. 9 figs 7-10, Pl. 10 fig. 1, Fenner *et al.* 1976 Pl. 1 figs 1-16, Akiba 1982 Pl.10 figs 3-5b, 9-11, Zielinski 1993 Pl.5 figs 8-10.

NOTES: - Occurs in cores MD88-779, MD88-784, MD88-787,E53-10; and in new surface samples MDBX94-01, -02, -04, -05, -06, TC53-10, TC37-19, E36-6, GC017, GC034.

FRAGILARIOPSIS SUBLINEARIS (VAN HEURCK) HEIDEN (1928)

SYNONYMS: *Nitzschia sublineata* Hasle, *Fragilaria sublinearis* Van Heurck, *Nitzschia sublinearis* (Heiden and Kolbe) Hasle in Pichon 1985, Akiba 1982, Zielinski 1993.

REFERENCES USED: Hasle 1965b Pl. 7 fig.1, Pl. 11 figs 1-10, Pl. 12 fig. 1, Zielinski 1993 Pl. 5 figs 25-26.

NOTES: - Occurs in cores MD88-784, MD88-787, E53-10; and in new surface samples MDBX94-03, -05, TC53-10, TC37-19, GC034.

Abberent forms with displaced raphe (as reported common in *Fragilariopsis* in Hustedt 1958) were observed in Core MD88-787.

***FRAGILARIOPSIS -NITZSCHIA* SPP.**

ILLUSTRATION: Plate 8, figures 1-2.

NOTES: - Occurs in cores MD88-779, MD88-784, MD88-787, E53-10.

- GENUS ***GYROSIGMA*** HASSAL (1845)

aff. ***GYROSIGMA*** SPP.

ILLUSTRATION: Plate 8, figure 3.

REFERENCES USED: Stildolph 1988

NOTES: - Occurs in cores MD88-784, MD88-787.

- In reference to *Gryosigma* and *Pleurosigma,* differentiation based only on valve shape and size is not considered useful (Stidolph 1988, Sterrenburg 1995) whereas rectilinear versus quincunx areolae rows are generally the best source for separation. I have found it difficult to seperate the two taxa and earlier work will have both genera counted under *Pleurosigma.* The species encountered are not of the closely related genus *Donkinia* Ralfs (Cox 1983a,b).

- GENUS ***HEMIDISCUS*** WALLICH (1860).

HEMIDISCUS CUNEIFORMIS WALLICH (1860)

ILLUSTRATION: Plate 8 figures 4-9.

REFERENCES USED: Hustedt 1930 fig. 542, Fenner *et al.* 1976 Pl. 11 fig. 17, Barron 1985 Fig. 9 no. 13.

NOTES: - Occurs in core MD88-779, E53-10; and in new surface samples MDBX94-01, -02, -06, -07, TC53-10, GC007, GC013, GC014, GC016, GC016, GC030, GC031, GC034.

- The variation in forms was noticed in the samples observed by the author (see plates) as previously remarked by Hustedt 1930, Kolbe 1954, Simonsen 1974, Mikkelsen 1979 and Barron (pers comm. 1996).

HEMIDISCUS KARSTENII JOUSÉ (1962)

ILLUSTRATION: Plate 9, figures 1-2.

REFERENCES USED: Abbott 1973 Pl. 1 figs D-F, Schrader 1976 Pl. 15 figs 17-18, Akiba 1982 Pl. 5 figs 1-4, Barron 1985 fig. 14 no. 20.

NOTES: - Occurs in cores MD88-779, MD88-787, E53-10; and in surface sample GC016.

- GENUS ***LICMOPHORA*** AGARDH (1827)

aff. ***LICMOPHORA* SPP.**

ILLUSTRATION: Plate 9, figure 4.

REFERENCES USED: Hustedt 1930, Hargraves 1968 fig.122.

NOTES: - Occurs in new surface sample MDBX94-01.

- GENUS ***MELOSIRA***AGARDH (1832)

MELOSIRA SOL (EHRENBERG)KÜTZING 1849

REFERENCES USED: Hustedt 1930 fig. 115, Kützing 1849 pp 30-31.

NOTES: - Occurs in new surface sample GC014.

- Refer to notes for *Paralia* spp.

- GENUS ***NAVICULA*** BORY DE ST-VINCENT(1822).

NAVICULA DIRECTA (SMITH) RALFS IN PRITCHARD (1861)

ILLUSTRATION: Plate 9, figure 3.

REFERENCES USED: Abbott 1973 Pl. 7 fig. M, Fenner *et al.* 1976 Pl. 14 fig. 7, Akiba 1982 Pl. 8 fig. 14, Krebs 1983 Pl. 3 fig. 7.
NOTES: - Occurs in cores MD88-784, MD88-787; and in new surface samples MDBX-01, -02, -05, -06, E36-6.

- GENUS ***NITZSCHIA*** A. H. HASSALL (1845)

NITZSCHIA BARBIERI M. PERGALLO (1921)
ILLUSTRATION: Plate 7, figures 9a-b.
REFERENCES USED: Hasle 1965b Pl. 15 figs 6-7.
NOTES: - Occurs in core MD88-787.

NITZSCHIA BICAPITATA CLEVE (1900)
ILLUSTRATION: Plate 7, figure 12.
REFERENCES USED: Hasle 1960 text fig. 10a-i, Pl. VI figs 53-57, Hasle 1964 Pl. 15 figs 3-6, Pl. 14 figs 8-12, Simonsen 1974 Pl. 35 figs 3-15, Fenner *et al.* 1976 Pl. 3 figs 27-29, Zielinski 1993 Pl. 6 figs 9-10.
NOTES: - Occurs in new surface samples GC013, GC030, GC031.

NITZSCHIA BRAAURDII HASLE (1960)
ILLUSTRATION: Plate 7, figures 10-11.
REFERENCES USED: Hasle 1960 text fig. 11 a-d, Pl. VII figs 58-63, Hasle 1964 Pl. 15 figs 1-2, Pl. 14 fig. 20, Simonsen 1974 Pl. 35 fig. 2, Pl. 38 figs 8-11.
NOTES: - Occurs in core MD88-787; and in new surface samples GC014, GC030, GC031.

NITZSCHIA DENTICULOIDES SCHRADER (1976)
REFERENCES USED: Schrader 1976 Pl. 3 figs 7-8, 10,12,18-24, Pl. 15 fig. 22.
NOTES: - Occurs in core MD88-787.

NITZSCHIA cf ***DIETRICHII*** SIMONSEN (1974)
REFERENCES USED: Simonsen 1974 Pl.36 figs 1-3.
NOTES: - Occurs in new surface sample GC016.

NITZSCHIA INTERRUPTESTRIATA SIMONSEN (1974)
SYNONYMS: *Nitzschia interrupta* Heiden in Heiden and Kolbe 1928
ILLUSTRATION: Plate 7, figure 13.
REFERENCES USED: Simonsen 1974 Pl. 36 figs 9-11, Pl. 37 figs 1-7, Pl. 38 figs 1-7. Simonsen 1992 Pl. 82 figs 5-9.
NOTES: - Occurs in new surface sample GC034.

NITZSCHIA KOLACZEKII GRUNOW (1877)
ILLUSTRATION: Plate 7, figures 14-16.
REFERENCES USED: Hasle 1960 Pl. V figs 50a-c, Fenner *et al.* 1976 Pl. 3 fig. 16, Barde-Labayle-Bounés 1980 Pl. XII fig. 18
NOTES: - Occurs in core MD88-779; and in new surface samples GC007, GC014.

NITZSCHIA PAUNDRIFORMIS GREGORY
ILLUSTRATION: Plate 7, figures 17-18.
REFERENCES USED: Abbott 1973 Pl. 11 fig. A, Simonsen 1974, Barde-Labayle-Bounés 1980 Pl. XII figs 16-17, Pichon 1985 Pl.3 fig. 78.
NOTES: - Occurs in new surface sample MDBX94-09.

NITZSCHIA PERAGALLI HASLE (1965)
ILLUSTRATION: Plate 7, figure 19a-b.
REFERENCES USED: Hasle 1965b Pl. 9 figs 11-12, Pl. 15 figs 1-5, Fenner *et al.* 1976 Pl. 2 figs 12-14.
NOTES: - Occurs in cores MD88-784, MD88-787.

NITZSCHIA SICULA (CASTRACANE) HUSTEDT
REFERENCES USED: Hasle 1960 text fig. 16 a-b, Pl. VII figs 64-65b.
NOTES: - Occurs in cores MD88-784, MD88-787.

NITZSCHIA SICULATA VAR BICUNEATA (GRUNOW) HASLE (1960)
ILLUSTRATION: Plate 7, figures 21-22.
REFERENCES USED: Hasle 1960 text fig. 16c-d, Hasle 1964 text figs 11-12, Pl. 13 fig. 14, Pl. 16 fig. 1.

NITZSCHIA SICULA VAR. ROSTRATA HUSTEDT (1958)
REFERENCES USED: Hustedt 1958 Pl. 11 figs 128-132, Hasle 1964 text fig. 13, Pl.16, figs 2,4, Fenner *et al.* 1976 Pl. 3 figs 13-14.

NOTES: - Occurs in core MD88-784; and in new surface sample GC017.

- GENERA ***ODONTELLA*** AGARDH (1832).

ODONTELLA WEISSFLOGII (JANISCH) GRUNOW

SYNONYMS: *Biddulphia weissflogii* (Grunow in Van Heurck) 1882
ILLUSTRATION: Plate 9, figures 5-6.
REFERENCES USED: Hoban *et al.* 1980 figs 15-26
NOTES: - Occurs in core MD88-787; and in MDBX94-01, -02, -03, -04, -05.

- GENERA ***PARALIA*** HEIBERG (1863)

PARALIA SULCATA (EHRENBERG) CLEVE 1873

SYNONYMS: *Melosira sulcata* (Ehrenberg) Kützing 1844
REFERENCES USED: Hustedt 1930 fig. 119 (as *M. sulcata*), Kaczmarska and Kilarski 1979 (as *Melosira sulcata*), Barde-Labayle-Bounès 1980 Pl.VII figs 6-7 (as *Melosira sulcata*)
NOTES: - Occurs in surface samples GC013, GC017, GC030, GC031, GC034.
- Refer to comments under *Paralia* spp.

***PARALIA* SPP.**

ILLUSTRATION: Plate 9, figures 7a-10.
NOTES: - Occurs in core MD88-779; and in surface samples MDBX94-01, -02, -03, -04, -05, -06, E36-6, GC014.
- Taxonomic differentiation among the *Paralia* and *Melosira* genera and species was not undertaken due to lack of reference material and need for taxonomic reform. All occurrences of specimens with *Paralia/Melosira* traits were lumped under *Paralia* spp.

- GENUS ***PLEUROSIGMA*** SMITH (1852).

PLEUROSIGMA DIRECTUM GRUNOW IN VAN HEURCK (1880)

ILLUSTRATION: Plate 9, figures 11-12 .
REFERENCES USED: Fenner *et al.* 1976 Pl. 14 fig. 6, Simonsen 1974 Pl.29 figs 2a-b.
NOTES: - Occurs in cores MD88-784, MD88-787.
- Refer to comments under *Gyrosigma* spp.

***PLEUROSIGMA* SPP. (*PLEUROSIGMA/GYROSIGMA* SPP.)**

NOTES: - Occurs in cores MD88-784, MD88-787; and in new surface samples E36-6 and GC030.
- Refer to comments under *Gyrosigma* spp.

- GENUS ***POROSIRA*** JØRGENSEN (1905).

POROSIRA GLACIALIS (GRUNOW) JØRGENSEN (1905)

SYNONYMS: ? *Thalassiosira* sp 9 of Schrader 1976 Pl. 15 figs 11-12, Pl. 13 figs 4a-b.
ILLUSTRATION: Plate 10, figures 1a-b.
REFERENCES USED: Hasle 1972 figs 62-63, Akiba 1982 Pl. 1 fig. 7, Krebs 1983 figs 12a-b, Zielinski 1993 Pl. 3 figs 1-2.
NOTES: - Occurs in cores MD88-784, MD88-787; and in new surface samples MDBX94-02, -03, -04, -06.

POROSIRA PSEUDODENTICULATA (HUSTEDT) JOUSÉ (1962)

REFERENCES USED: Hasle 1972 figs 64-65, Hasle 1973 Pl.5 fig. 30-31, Pl.6 fig. 32, Pl. 7 fig. 38, Krebs 1983, Pl. 4 fig. 13, Zielinski 1993 Pl. fig. 6.
NOTES: - Occurs in cores MD88-784, MD88-787.

- GENUS ***PROBOSCIA*** SUNDSTRÖM (1986).

PROBOSCIA ALATA (BRIGHTWELL) SUNDSTRÖM (1986)

SYNONYMS: *Rhizosolenia alata* (Brightwell)
ILLUSTRATION: Plate 10, figures 2-3.
REFERENCES USED: Priddle *et al.* 1990 (in Medlin and Priddle 1990), Jordan *et al.* 1991 figs 1-9, Takahashi *et al.* 1994 figs 2-7.
NOTES: - Occurs in cores MD88-784, MD88-787; and in new surface samples GC031, GC034.

PROBOSCIA* cf. *CURVIROSTRIS (JOUSÉ)JORDAN ET PRIDDLE (1991)

SYNONYMS: *Rhizosolenia curvirostris* Jousé
REFERENCES USED: Jordan and Priddle 1991 figs 5-7.
NOTES: - Occurs in coresE53-10.

Verification of the species observed in core E53-10 is required since it may also have been *P. barboi.*

- GENUS ***PSEUDONITZSCHIA*** H. PERGALLO IN H. ET M. PERGALLO (1900)

PSEUDONITZSCHIA HEIMII MANGUIN (1957)

SYNONYMS: *Nitzschia heimii* (Manguin) Hasle
REFERENCES USED: Hasle 1965a Pl. 10 figs 9-13, Simonsen 1974 Pl. 36, figs 4-5.
NOTES: - Occurs in cores MD88-784, MD88-787.

PSEUDONITZSCHIA LINEOLA (P.T. CLEVE) HASLE (1993)

SYNONYMS: *Nitzschia lineola* P.T. Cleve, *Nitzschia barkleyi* Hustedt
ILLUSTRATION: Plate 10, figure 4.
REFERENCES USED: Hasle 1965a Pl. 12 figs 15-21, Simonsen 1974 Pl. 39 figs 4-6, Fenner *et al.* 1976 Pl. 13 figs 24-26, Hallegraeff 1994 figs 7a-e.
NOTES: - Occurs in cores MD88-784, MD88-787; and in new surface samples MDBX94-05, TC37-19.

PSEUDONITZSCHIA SERIATA (P.T. CLEVE) H. PERGALLO (1900)

P. SERIATA* COMPLEX *SENSU HASLE (1965a)

SYNONYMS: *Nitzschia seriata* P.T. Cleve
REFERENCES USED: Hustedt 1958 Pl. 13 fig. 191-192, Hasle 1965a Pl. 3 figs 1-11, Pl. 6 fig. 2, Fenner *et al.* 1976 Pl. 3 figs 19-120, Hallegraeff 1994.
NOTES: - Occurs in core MD88-784.
- *Pseudonitzschia seriata senso stricto* has been shown to be restricted to the Northern Hemisphere (see Hasle 19 72, and Hasle and Medlin 1990a in Medlin and Priddle 1990). Species attributed to *P. seriata* in the low and middle latitudes of the Southern Hemisphere belong to various other species akin to *P. seriata-* eg. *P. fraudulenta, P. pungens, P. turgidula, P pseudodelicatissima, P. heimii, P. subpacifica.* Hallegraeff (1994) identified from his study of *Pseudonitzschia* in Australian coastal waters the presence *of N. subpacifica* (previously identified by Hallegraeff as *P. heimii*), *P. pseudodelicatissima, and P. pungens* in their most southern samples of Tasmania. The species thus identified under P. seriata could be attributed to any of the species which fall under the *P. seriata* complex of Hasle (1965a).

PSEUDO-NITZSCHIA TURGIDULOIDES (HASLE) HASLE(1995)

SYNONYMS: *Pseudonitzschia turgiduloides* (Hasle) Hasle (1993), *Nitzschia turgiduloides* Hasle, *Pseudonitzschia barkleyi* var. *obtusa* Manguin.
REFERENCES USED: Hasle 1965a Pl.12 figs 9-14, Fenner *et al.* 1976 Pl. 4 figs 1-3, Zielinski 1993 Pl. 6 fig. 16, Hasle 1995.
NOTES: - Occurs in core MD88-787.

***PSEUDONITZSCHIA* SPP.**

NOTES: - Occurs in cores MD88-779, MD88-787.
- A category which consists of several species belonging to *Pseudonitzschia* but not identified to species level.

- GENUS ***PSEUDOTRICERATIUM*** GRUNOW (1884)

aff. ***PSEUDOTRICERATIUM SP.***

ILLUSTRATION: Plate 10, figure 5a-b.
REFERENCES USED: Hustedt 1930 pp 791-828, Simonsen 1974 pp. 23-24 (*Pseudotriceratium*), 27-28 (*Triceratium*), Akiba 1982 Pl. 6 figs 10-11 (*Triceratium* sp.), Round *et al.* 1990 pp 258-259 (*Pseudotriceratium*), 218-219 (*Triceratium*), 254-255 (*Trigonium*).
NOTES: - Occurs in new surface sample MDBX94-02.
The species illustrated on Plate 10 fig. 5a-b, is thought to be representative of *Pseudotriceratium* but could equally be a species of *Triceratium* (eg *T. reticulum* Ehrenberg) or *Trigonium.*

- GENUS ***RHAPHONEIS*** EHRENBERG (1844)

RHAPHONEIS cf ***AMPHICEROS*** EHRENBERG (EHRENBERG)

SYNONYMS: *Cocconeis amphiceros*
REFERENCES USED: Andrews 1975 Pl.2 figs 9-12, Barde-Labayle-Bounès 1980 Pl. XII fig. 20, 23, Ciesielski 1986 Pl. 6 figs 1-3.
NOTES: - Occurs in core MD88-779.

RHAPHONEIS SPP.

REFERENCES USED: Andrews 1975, Ciesielski 1986 Pl. 6 figs 4-5.
NOTES: - Occurs in new surface sample GC007, GC016.

- GENUS ***RHIZOSOLENIA*** BRIGHTWELL (1858)

RHIZOSOLENIA ANTENNATA* FORMA *ANTENNATA (EHRENBERG) BROWN (1920)

SYNONYMS: *Rhizosolenia hebetata* (Bailey) Gran forma *bidens* Heiden in Heiden and Kolbe (1928)
ILLUSTRATION: Plate 10, figures 6-7.
REFERENCES USED: Priddle *et al.* 1990 (in Medlin and Priddle 1990)
NOTES: - Occurs in cores MD88-784, MD88-787; and in new surface samples MDBX94-01, -02, -04, -06, -07, TC53-10, TC37-19, GC014, GC016, GC030, GC034.

RHIZOSOLENIA BERGONII H. PERGALLO (1892)

ILLUSTRATION: Plate 10, figures 9-12.
REFERENCES USED: Hustedt 1930 fig. 327, Fenner *et al.* 1976 Pl. 13 fig. 13, Zielinski 1993 Pl. 7 fig.4.
NOTES: - Occurs in new surface samples GC007, GC017, GC030, GC031, GC034.

***RHIZOSOLENIA* SPP.**

NOTES: - Occurs in cores MD88-779, MD88-784, MD88-787; and in new surface samples TC53-10, E36-6, GC007, GC017.
A lumped group of predominantly highly dissolved forms still attributable to *Rhizosolenia.*

***RHIZOSOLENIA* OTARIA ABSENT GROUP**

NOTES: - Occurs in cores MD88-779, MD88-784, MD88-787; and in new surface sample TC53-10.
- Contains information originally but erroneously counted as either *Rhizosolenia antennata* or *Rhizosolenia hebetata*- these species are distinguished by a lack of otaria (with exception to *R. curvata*). See Chapter 2 for discussion.
- In reality this category lumps the following species:

RHIZOSOLENIA CURVATA ZACHARIAS(1905)

ILLUSTRATION: See text figure 2.4H.
SYNONYMS: ? *R. hebetata* forma *hiemialis* in Fenner *et al.* 1976 Pl. 13 figs 11-12.
REFERENCE USED: Priddle *et al.* 1990 (in Medlin and Priddle 1990)

RHIZOSOLENIA POLYDACTYLA CASTRACANE (1886) FORMA *SQUAMOSA* SUNDSTRÖM (1986)

ILLUSTRATION: Pl.11. fig.1.
REFERENCE USED: Priddle *et al.* 1990 (in Medlin and Priddle 1990)

RHIZOSOLENIA SIMA CASTRACANE (1886)FORMA *SILICEA* SUNDSTRÖM (1986)

SYNONYMS: ? *Rhizosolenia* sp. D of Harwood and Maruyama 1992 Pl. 18 figs 7-10, Mahood and Barron Pl. 1 figs 4a-5b, Pl. 7 fig. 3.
REFERENCE USED: Priddle *et al.* 1990 (in Medlin and Priddle 1990)

RHIZOSOLENIA SIMPLEX KARSTEN (1905a)

Illustration: Pl. 11 fig. 2.
REFERENCE USED: Priddle *et al.* 1990 (in Medlin and Priddle 1990)

***RHIZOSOLENIA* OTARIA PRESENT GROUP**

NOTES: - Occurs in cores MD88-784, MD88-787; and in new surface samples MDBX94-01, -02, -03, -04, -05, -06, -07, GC030, GC034.
- Contains information originally but erroneously counted as either *Rhizosolenia antennata f. semispina* and *Rhizosolenia styliformis.* See Chapter 2 for discussion.
- In reality this category lumps the following species:

RHIZOSOLENIA ANTENNATA (EHRENBERG) BROWN (1920) FORMA *SEMISPINA* SUNDSTRÖM (1986)

Illustration: Pl. 10 fig. 8.
SYNONYMS: *R. hebetata* f. *semispina* in Fenner *et al.* Pl. 13 fig. 7.
REFERENCE USED: Priddle *et al.* 1990 (in Medlin and Priddle 1990)

RHIZOSOLENIA CRASSA SCHIMPER IN KARSTEN (1905a)

ILLUSTRATION: See text figure 2.4G.
REFERENCE USED: Priddle *et al.* 1990 (in Medlin and Priddle 1990)

RHIZOSOLENIA POLYDACTYLA FORMA *POLYDACTYLA* CASTRACANE (1886)

ILLUSTRATION: See text figure 2.4E.
SYNONYMS: *R. styliformis* in Fenner *et al.* 1976 Pl. 13 figs 4, 5, 9.
REFERENCE USED: Priddle *et al.* 1990 (in Medlin and Priddle 1990)

RHIZOSOLENIA SIMA FORMA *SIMA* CASTRACANE (1886)

REFERENCE USED: Priddle *et al.* 1990 (in Medlin and Priddle 1990)

RHIZOSOLENIA STYLIFORMIS BRIGHTWELL (1858)
REFERENCE USED: Priddle *et al.* 1990 (in Medlin and Priddle 1990)

- GENUS ***ROCELLA*** HANNA (1930)

***ROCELLA* SPP.**
REFERENCES USED: Barron 1985 fig. 12 no. 16 (*R. gelida*), fig. 12 no. 15 (*R. gelida* var. *schraderi*), Ciesielski 1986 Pl. 2 fig. 26 (*R. gelida* var. *schraderi*).
NOTES: - Occurs in core MD88-787.

- GENUS ***ROPERIA*** GRUNOW EX PELLETAN (1889)

ROPERIA TESSELATA (ROPER) GRUNOW (1881)
ILLUSTRATION: Plate 11, figures 3-5.
REFERENCES USED: Hustedt 1930 fig. 297, Abbott 1973 Pl. 6 fig. G, Fenner *et al.* 1976 Pl. 12 figs 1-4, Fryxell *et al.* 1986 fig. XXXII no 4a-b, Lee and Lee 1990 figs 1-19.
NOTES: - Occurs in core MD88-779; and in new surface samples MDBX94-, -02, -05, -06, -07, TC53-10, GC013, GC014, GC016, GC030, GC031, GC034.
- Variations for example *R. tesselata* var. *coscinodiscoide*, were not seperated.

- GENUS ***ROUXIA*** BRUN ET HÉRIBAUD IN HÉRIBAUD (1893).

ROUXIA* cf *NAVICULOIDES SCHRADER (1976)
REFERENCES USED: Schrader 1976 Pl. 5 figs 13,18.
NOTES: - Occurs in cores MD88-779, MD88-784.

***ROUXIA* SPP.**
ILLUSTRATION: Plate 11, figures 6-7.
NOTES: - Occurs in core MD88-787; and in new surface samples MDBX94-06, TC37-19.
Species under this category probably are those of *Rouxia isopolica* or *Rouxia antarctica* as described below.

ROUXIA ANTARCTICA (HEIDEN) HANNA (1930)
SYNONYMS: *Rouxia peragalli* var. *antarctica* Heiden
REFERENCES USED: Schrader 1976, Pl. 5 figs 1-8. Simonsen 1992 Pl. 65 figs 11-15.

ROUXIA ISOPOLICA SCHRADER (1976)
SYNONYMS: *Rouxia peragalli* BRUN ET HÉRIBAUD IN HÉRIBAUD and *R. peragalli* f. *yabei* (Hanna) Sheshukova-Poretskaja as in Abbott 1973.
REFERENCES USED: Schrader 1976 Pl. 5 figs 9, 14, 15, 20, Akiba 1982 Pl. 8 figs 1-7. Refer to taxonomic discussion in Akiba (1982).

- GENUS ***STELLARIMA*** HASLE ET SIMS (1986)

STELLARIMA MICROTRIAS (EHRENBERG) HASLE ET SIMS (1986)
SYNONYMS: *Coscinodiscus stellaris* var *symbolophorus* Grunow 1884, *Coscinodiscus furcatus* Karsten 1905.
REFERENCES USED: Syvertsen 1985, Hasle *et al.* 1988.
NOTES: - Occurs in new surface samples MDBX94-01, -06, -07, GC017.
- See discussion in Chapter 2 section 3.2.21.

STELLARIMA STELLARIS (ROPER) HASLE ET SIMS (1988)
SYNONYMS: *Coscinodiscus stellaris* Roper, *Coscinodiscus stellaris* var *symbolophorus* (Grunow) Jørgensen.
ILLUSTRATION: Plate 11, figures 8-11.
REFERENCES USED: Syvertsen 1985, Hasle *et al.* 1988.
NOTES: - Occurs in new surface samples MDBX94-01, -06, -07, GC017.
- See discussion in Chapter 2 section 2.2.21.

***STELLARIMA* SPP.**
Notes: - Occurs in core E53-10.
- The species observed under this category probably belong *to S. stellaris*, however, the samples of E53-10 require verification for this species.

- GENUS ***STEPHANOPYXIS*** (EHRENBERG) EHRENBERG (1845)

***STEPHANOPYXIS* SPP.**

REFERENCES USED: Hustedt 1930, figs. 140-148,

NOTES: - Occurs in core MD88-787, E53-10; and in new surface samples MDBX94-03, TC53-10, GC030.

- GENUS ***THALASSIONEMA*** GRUNOW IN VAN HEURCK (1881).

THALASSIONEMA NITZSCHIOIDES GRUNOW

REFERENCES USED: Hustedt 1930 fig. 725, Abbott 1973 Pl. 11 fig. C, Fenner *et al.* 1976 Pl. 14 fig. 11, Barde-Labayle-Bounès 1980 Pl. XII fig. 5-7, Akiba 1982 Pl. 8 figs 15-16, Zielinski 1993 Pl. 6 figs 5-6, Moreno-Ruiz and Licea 1994 figs 1-3.

NOTES: - Occurs in cores MD88-779, MD88-784, MD88-787, E53-10; and in new surface samples MDBX94-01, -02, -03, -04, -05, -05, -06, -07, TC53-10, TC37-19, E36-6, GC007, GC013, GC014, GC 016. GC017, GC030, GC031, GC034.

- This species group contains the following 3 species which were generally not differentiated during counting:

THALASSIONEMA NITZSCHIOIDES FORMA 1 (SENSU ZIELINSKI ET GERSONDE 1997)

ILLUSTRATION: Plate 12. figures 3-4.

REFERENCE USED: Zielinski and Gersonde 1997 fig. 3.

NOTES: Counts are most likely included under counts of *Thalassionema nitzschioides.* The difference between this forma species and the nominate species are not fully understood and requires further observation on this authors part.

THALASSIONEMA NITZSCHIOIDES VAR. *CAPITULATA* (CASTRACANE) MORENO-RUIZ(1994)

SYNONYMS: *Synedra capitulata* Castracane, *Spinigera capitata* Heiden in Heiden and Kolbe (see Simonsen 1992)

REFERENCES USED: Simonsen 1992 Pl. 22 figs 7-10, Moreno-Ruiz and Licea 1994 figs 6-7.

NOTES: - The species noted as *T. n.* var *capitualata* in this study should be attributed to *T. n.* var. *lanceolata* under the descriptions and illustrations provided by Moreno-Ruiz and Licea (1994). This problem arose from using the work of Zielinski 1993 to originally define the species. Based on the illustrations in Simonsen (1992) and Moreno-Ruiz and Licea (1994) it is considered that the species *T. n.* var. *capitulata* has only been very rarely observed in the counts made under *T. nitzschioides* in this study.

THALASSIONEMA NITZSCHIOIDES VAR. *LANCEOLATA* (GRUNOW) PERGALLO ET PERGALLO (1897-1908)

SYNONYMS: *Thalassiothrix nitzschioides* var. *lanceolata* Grunow, *Spinigera lanceolata* Heiden, *T. nitzschioides* var *capitulata* in Zielinski 1993

ILLUSTRATION: Plate 12, figure 2, and Plate 12, figure 1 (incorrectly entitled *T. nitzschioides* var. *capitulata*).

REFERENCES USED: Zielinski 1993 Pl. 6 fig. 1-2 (as *T. n.* var. *capitulata*), Simonsen 1992 Pl. 22 figs 16-17, Moreno-Ruiz and Licea 1994 figs 23-24.

NOTES: - Occurs in core MD88-779 (as *T. n.* var *lanceolata*) and MD88-784 (as *T. n.* var. *capitulata*).

THALASSIONEMA NITZSCHIOIDES* VAR. *PARVA HEIDEN (1928)

ILLUSTRATION: Plate 12, figure 5.

REFERENCES USED: Fenner *et al.* 1976 Pl. 14 fig. 10, Akiba 1982 Pl. 8 fig. 17 (? T. *n.* var *parva*) , Zielinski 1993 Pl. 6 figs 7-8.

NOTES: - Occurs in core MD88-779; and in surface samples MDBX94-01, -02, -03, -04, -06, -07, GC013, GC030, GC031.

- The emended taxonomic species *T. n.* var *parva* (Heiden) Moreno-Ruiz 1994 as described by Moreno-Ruiz and Licea (1994), uses a less than 10µm length to define the species. Although reduced size was feature in determining the species in this study it cannot be assured that all the species encountered were under 10µm length.

- GENUS ***THALASSIOSIRA*** CLEVE (1873).

THALASSIOSIRA ANTARCTICA COMBER (1896)

THALASSIOSIRA SCOTIA FRYXELL ET HOBAN (1979)

THALASSIOSIRA ANTARCTICA-SCOTIA GROUP

ILLUSTRATION: Plate 12, figures 6-12.

REFERENCES USED: *T. antarctica* Hasle and Heimdal 1967 figs 7-13, Fryxell *et al.* 1981 figs 1-5, 11-13, 17-20, Akiba 1982 Pl. 4 figs 5a-6b, Krebs 1983, Pl. 5 figs 4a-f, Johansen and Fryxell 1985 figs 37-39. *T. scotia* Johansen *et al.* 1985 figs 5-8, Johansen and Fryxell 1985 figs 40-42.

NOTES: - Occurs in cores MD88-784, MD88-787; and in new surface samples MDBX94-01, -02, -03, -04, -05, E36-6.

- The two species are difficult to separate and thus are deemed a mixed group for the work in this thesis, refer to Chapter 2 section 2.2.23 for discussion.

THALASSIOSIRA* cf *DECIPIENS (GRUNOW) JØRGENSEN (1905)

Synonyms: *Coscinodiscus decipiens* Grunow
Illustration: Plate 12, figures 13-16.
References used: Hustedt 1930 fig. 158, Fenner *et al.* 1976 Pl. 11 figs 4-6, Barde-Labayle-Bounès 1980 Pl. IX, figs 4, 8-9, Ramirez 1981 Pl. 71 figs 438-442.
Notes: - Occurs in new surface sample MDBX94-05.

THALASSIOSIRA ECCENTRICA (EHRENBERG) CLEVE (1904)

SYNONYMS: *Coscinodiscus eccentricus* Ehrenberg, *Coscinodiscus excentricus*
ILLUSTRATION: Plate 12, figure 17-18.
REFERENCES USED: Fryxell and Hasle 1972 figs 1-15, Simonsen 1974 Pl. 2 figs 1-3, Ramirez 1981 Pl. 20-22, figs 129-144, Hallegraeff 1984 figs 15a-d.
NOTES: - Occurs in core MD88-784; and in new surface sample MDBX94-01.
- Refer to Chapter 2 section 2.2.234for discussion.

THALASSIOSIRA FERELINEATA HASLE ET FRYXELL (1977)

ILLUSTRATION: Plate 12, figure 19.
REFERENCES USED: Hasle and Fryxell 1977 Pl. 10 figs 46-49b, Pl. 11 figs 50 -53b, Ramirez 1981 Pl. 25 figs 158-163.
NOTES: - Occurs in core MD88-784; and in new surface sample MDBX94-01.
- Refer to Chapter 2 section 2.2.27 for discussion.

THALASSIOSIRA FRENGUELLIOPSIS FRYXELL ET JOHANSEN (1985)

REFERENCES USED: Johansen and Fryxell 1985 figs 6,67-68, 71, 81.
NOTES: - Occurs in core MD88-787; and in new surface sample GC016.
- The species on Plate 12 figure 20 is thought to be incorrectly identified as *T. frengueliopsis* when it is *T. oestrupii* var. *venrickae.*

THALASSIOSIRA GERLOFFII RIVERA (1981)

REFERENCES USED: Ramirez 1981 Pl. 26-28 figs164-183, Johansen and Fryxell 1985 figs 18, 44-45.
NOTES: - Occurs in core MD88-784.

THALASSIOSIRA GRACILIS VAR. GRACILIS (KARSTEN) HUSTEDT (1958)

ILLUSTRATION: Plate 13, figures 1-3.
REFERENCES USED: Hustedt 1958 Pl. 3 figs 4-7, Fryxell and Hasle 1979 figs 12-16, Ramirez 1981 Pl. 66-67 figs 411-420, Johansen and Fryxell 1985 figs 58-59, Fryxell 1990 Pl. 2 figs 5-9
NOTES: - Occurs in cores MD88-779, MD88-784, MD88-787, E53-10; and in new surface samples MDBX94-02, -03, -04, -05, -06, TC53-10, TC37-19, E36-6, GC007, GC013, GC014, GC016, GC017, GC030, GC031, GC034.
- See Fryxell 1990 Pl. 2 figs 5-13, for photographic illustration of graduation of var. *gracilis* to var. *expecta.*

THALASSIOSIRA GRACILIS* VAR. *EXPECTA (VAN LANDINGHAM) FRYXELL ET HASLE (1979b)

SYNONYMS: *Thalassiosira delicatula* (Hustedt), *Thalassiosira delicatulata*
ILLUSTRATION: Plate 13, figures 4-7.
REFERENCES USED: Hustedt 1958 Pl. 3. figs 8-10, Hasle and Heimdal 1970 fig. 1-4, Fryxell and Hasle 1979 figs 23-28, , Ramirez 1981 Pl. 68 figs 421-424Hallegraeff 1984 fig. 24a-b, Johansen and Fryxell 1985 figs 60-63, Fryxell 1990 Pl. 2 figs 9-13;
NOTES: - This variation was not counted separately from the nominate variety.

THALASSIOSIRA GRAVIDA CLEVE (1896)

ILLUSTRATION: Plate 13, figures 8-9.
REFERENCES USED: Hustedt 1930 fig. 161, Fenner *et al.* 1976 Pl. 8 fig. 5, Barde-Labayle-Bounès 1980 Pl. IX figs10-11, Ramirez 1981 Pl. 70 fig. 437, Zielinski 1993 Pl. 3 figs 10-11.
NOTES: - Occurs in core MD88-784.

THALASSIOSIRA LATIMARGINATA MAKAROVA (1975)

SYNONYMS: *Thalassiosira trifulta* Fryxell (1979).
ILLUSTRATION: Plate 15, figures 2-4b.
REFERENCES USED: Fryxell and Hasle 1979 Pl.1 figs 3,5, Pl. 3 figs 13, 15a, Pl. 5 fig. 20b, Johansen and Fryxell 1985 figs 65-66, Zielinski 1993 Pl. 2 fig. 6.
NOTES: - Occurs in cores MD88-779, MD88-784, MD88-787, E53-10; and in new surface samples MDBX94-01, -02, -06, -07, TC53-10, GC007, GC013, GC014, GC 016. GC017, GC030, GC031, GC034.
- Refer to Chapter 2 section 2.2.24 for discussion. under *T.trifulta.*
- Reference for *T. latimarginata* : Makarova, I.V. 1975. New species of the genus *Thalassiosira* Cleve from the Barents Sea. Novosti Systematiki Nizshih Rastenij, (Leningrad) 12:149-152. (in Russian).

THALASSIOSIRA LENTIGINOSA (JANISCH) FRYXELL (1977)

SYNONYMS: *Coscinodiscus lentiginosus* Janisch in Schmidt 1878, in Abbott 1973, Fenner *et al.* 1976, Akiba 1982.

ILLUSTRATION: Plate 13, figures 10-12.

REFERENCES USED: Hustedt 1958 Pl. 4 figs 22-25, Abbott 1973 Pl.3 figs D-F, Fenner *et al.* 1976 Pl. 7 figs 4-6, Fryxell 1977 figs 13-14, Johansen and Fryxell 1985 figs 49-50.

NOTES: - Occurs in cores MD88-779, MD88-784, MD88-787, E53-10; and in new surface samples MDBX94-01, -02, -03, -04, -05, -05, -06, -07, TC53-10, TC37-19, E36-6, GC007, GC013, GC014, GC 016. GC017, GC030, GC031, GC034.

THALASSIOSIRA LEPTOPUS (GRUNOW) HASLE ET G. FRYXELL (1977)

SYNONYMS: *Coscinodiscus lineatus* - in Hustedt 1930, Fenner *et al.* 1976, Barde-Labayle-Bounès 1980, *"Coscinodiscus" lineatus* (Ehrenberg) - in Simonsen 1974, *Coscinodiscus lineata* - in Pichon 1985.

ILLUSTRATION: Plate 13, figures 13-14.

REFERENCES USED: Simonsen 1974 Pl. 9 figs 3-4, Hasle and Fryxell 1977, Pl. 1-4 figs, 1-14b, Hasle and Syvertsen 1982 Pl. 1-4 figs 22, Hallegraeff 1984 fig. 20a-b.

NOTES: - Occurs in core MD88-784, MD88-787; and in new surface sample GC034.
- Refer to Chapter 2 section 2.2.27 for discussion.

THALASSIOSIRA LINEATA JOUSÉ (1968)

ILLUSTRATION: Plate 13, figures 15-17.

REFERENCES USED: Simonsen 1974 Pl. 1 figs 6-7, Fenner *et al.* 1976 Pl. 11 figs 8-10, , Hasle and Fryxell 1977 Pl. 5-6 figs 15-25, Barde-Labayle-Bounès 1980 Pl. IX figs 14-19, Ramirez 1981 Pl. 29-30 figs 184-196, Hallegraeff 1984 fig. 21a-b,

NOTES: - Occurs in cores MD88-779, MD88-784, MD88-787, E53-10; and in new surface samples MDBX94-01, -06, -07, TC53-10, GC007, GC013, GC014, GC016, GC017, GC030.
- Refer to Chapter 2 section 2.2.27 for discussion.

THALASSIOSIRA MACULATA FRYXELL ET JOHANSEN (1985)

SYNONYMS: *Coscinodiscus bullatus* (Janisch)

REFERENCES USED: Hustedt 1958 Pl. 4 figs 26-28, Fenner *et al.* 1976 Pl. 6 fig. 11-14, Johansen and Fryxell 1985 figs 69-70, 72-74.

NOTES: - Occurs in core MD88-784, ?MD88-787 (or *T. kolbei ?*). Fryxell (1990) suggests that *T. maculata* is the summer stage valve of *T. oliverana.*

THALASSIOSIRA OESTRUPII (OSTENFELD) HASLE (1972)

ILLUSTRATION: Plate 14, figure 1-5 and Plate 12, figure 20 (mis-identified as *T. frenguelliopsis*).

REFERENCES USED: Abbott 1973 Pl. 6 fig. E, Fenner *et al.* 1976 Pl. 9 figs 1-11 (type 1 and 2), Fryxell and Hasle 1980 figs 1-3, 6-7, 12-19 (variations *oestrupii* and *venrickae*), Ramirez 1981 Pl. 42-44, figs 263-280 (variations *oestrupii* and *venrickae*) Hallegraeff 1984 figs 18a-f, Johansen and Fryxell 1985 figs 75-76.

NOTES: - Occurs in cores MD88-779, MD88-784, MD88-787, E53-10; and in new surface samples MDBX94-01, -02, -03, -05, -06, -07, GC007, GC013, GC014, GC016, GC017, GC030, GC031, GC034.
- No separation was made between the two variations var. *oestrupii* and var. *venrickae* (refer Fryxell and Hasle 1980) during this work.

THALASSIOSIRA OLIVERANA (O'MEARA) MAKAROVA ET NIKOLAEV (1983)

SYNONYMS: *Schimperiella antarctica* Karsten - in Abbott 1973, Fenner *et al.* 1976, Akiba 1982, Pichon 1985.

ILLUSTRATION: Plate 14, figures 6a-7b.

REFERENCES USED: Abbott 1973 Pl. 2, figs D-F, Fenner *et al.* 1976 Pl. 14 figs 1-5, Akiba 1982 figs 1-5, Pichon 1985 Pl. 4 fig. 7, Priddle and Fryxell 1985 pp 146-7, Zielinski 1993 Pl. 4 fig. 1.

NOTES: - Occurs in cores MD88-784, MD88-787, E53-10; and in new surface samples MDBX94-02, -04, TC53-10, TC37-19, E36-6.

THALASSIOSIRA POROSERIATA (RAMSFJELL) HASLE 1972

SYNONYMS: *Coscinosira poroseriata* Ramsfjell

ILLUSTRATION: Plate 14, figures 8-10.

REFERENCES USED: Hasle and Hiemdal 1970 figs 65-68, Fenner *et al.* 1976 Pl. 9 fig. 26-33, Fryxell and Hasle 1979 Pl. 7 figs 33-34, Pl. 8 fig. 35a-c, Ramirez 1981 Pl. 55-56, figs 340-352, Johansen and Fryxell 1985 figs 51-52.

NOTES: - Occurs in core MD88-787; and in new surface samples GC030, GC031, GC034.

THALASSIOSIRA cf ***PUNCTIFERA*** (GRUNOW) FRYXELL, SIMONSEN ET HASLE (1974)

SYNONYMS: *Coscinodiscus excentricus* var. *punctifera* Grunow

ILLUSTRATION: Plate 15, figure 1.

REFERENCES USED: Simonsen 1974 Pl. 2 fig. 4, Pl. 3 figs 1-3c, Hallegraeff 1984 fig. 16a-d.
NOTES: - Occurs in new surface samples MDBX94-01,-07.
- Refer to Chapter 2 section 2.2.24 for discussion.

THALASSIOSIRA RITSCHERI (HUSTEDT) HASLE (1968)
SYNONYMS: *Coscinodiscus ritscherii* Hustedt
REFERENCES USED: Hustedt 1958 Pl. 6 figs 44-46, Hasle and Heimdal 1970 figs 39-43, Krebs 1983 Pl. 6 fig. 1, Fryxell 1990 Pl. 1 figs 1-4;
NOTES: - Occurs in core MD88-787, E53-10.
- Due to the similarities between *T. ritscheri* and *T. gerloffii*, possible northern occurrences of *T. ritscheri* may be attributable to *T. gerloffii* in this work.

"THALASSIOSIRA TRIFULTA" FRYXELL IN FRYXELL ET HASLE (1979)
SPECIES IS REFERABLE TO *THALASSIOSIRA LATIMARGINATA* MARKOVA(1975).
ILLUSTRATION: Plate 15, figures 2-4b.
REFERENCES USED: Fryxell and Hasle 1979 Pl.1 figs 3,5, Pl. 3 figs 13, 15a, Pl. 5 fig. 20b, Johansen and Fryxell 1985 figs 65-66, Zielinski 1993 Pl. 2 fig. 6.
NOTES: - Occurs in cores MD88-779, MD88-784, MD88-787, E53-10; and in new surface samples MDBX94-01, -02, -06, -07, TC53-10, GC007, GC013, GC014, GC 016. GC017, GC030, GC031, GC034.
- Refer to Chapter 2 section 2.2.24 for discussion.

THALASSIOSIRA TUMIDA (JANISCH) HASLE (1971)
SYNONYMS: *Coscinodiscus tumidus* Janisch
ILLUSTRATION: Plate 15, figures 5a-6b.
REFERENCES USED: Hasle *et al.* 1971 figs 13-25, Fenner *et al.* 1976 Pl. 10 figs 6-7, Fryxell *et al.* 1984 figs 1, 7, 8, 12-15, Johansen and Fryxell 1985 figs 29-32, Zielinski 1993 Pl. 4 fig. 4.
NOTES: - Occurs in cores MD88-784, MD88-787; and in new surface sample E36-6.

***THALASSIOSIRA* SPP.**
ILLUSTRATION: Plate 16, figures 1-8.
NOTES: - Occurs in cores MD88-779, MD88-784, MD88-787, E53-10; and in new surface samples MDBX94-01, -02, -03, -04, -05, -06, -07, TC53-10, TC37-19, GC007, GC013, GC014, GC016, GC030, GC031, GC034.

- GENUS ***THALASSIOTHRIX*** CLEVE ET GRUNOW (1880).

***THALASSIOTHRIX* SPP.**
THALASSIOTHRIX ANTARCTICA SCHIMPER EX KARSTEN (1905)
THALASSIOTHRIX LONGISSIMA CLEVE ET GRUNOW (1880)
ILLUSTRATION: Plate 16, figures 9-11.
REFERENCES USED: Hasle and Semina 1987 figs 26-59 (*T. antarctica*) 1-25 (*T. longissima*), Hasle 1990 Pl. 17.1 figs 1-3 (*T. longissima*) figs 4-6 (*T. antarctica*).
NOTES: - Occurs in cores MD88-779, MD88-784, MD88-787.
- The two species are co-joined in this study under *Thalassiothrix* spp. and are confounded with *Trichotoxon reinboldii*.

- GENUS ***TRACHYNEIS*** CLEVE (1894)

TRACHYNEIS ASPERA (EHRENBERG) CLEVE (1894)
REFERENCES USED: Simonsen 1974, Fenner *et al.* 1976 Pl. 14 fig. 13, Barde-Labayle-Bounès 1980 Pl. XII fig. 26, Krebs 1983 Pl. 6 figs 2-3.
NOTES: - Occurs in core MD88-779.

- GENUS ***TRICHOTOXON*** REID ET ROUND 1987

TRICHOTOXON REINBOLDII (VAN HEURCK) REID ET ROUND (1987)
SYNONYMS: *Synedra reinboldii* Van Heurck
ILLUSTRATION: Plate 16, figure 12.
REFERENCES USED: Hasle and Semina 1987 figs 67-70, Hasle 1990 (in Medlin and Priddle 1990) Pl. 17.1 figs 7-9,
NOTES: - Occurs in cores MD88-779, MD88-784, MD88-787.
- Refer to notes of *Thalassiothrix* spp.

SILICOFLAGELLATES.

- GENUS **DICTYOCHA** EHRENBERG (1839).

***DICTYOCHA* SPP.**

ILLUSTRATION: Plate 16, figure 14.
REFERENCES USED: Haq and Riley 1976, Pichon 1985 pl. 11 fig. 1, Zielinski 1993 Pl. 7 fig. 5.
NOTES: - Occurs in cores MD88-779, MD88-784, E53-10; and in new surface samples MDBX94-01, -02, -05, -06, -07, TC53-10, GC007, GC013, GC014, GC016, GC017, GC030, GC031, GC034.

- GENUS **DISTEPHANUS** STOEHR (1880).

***DISTEPHANUS* SPP.**

ILLUSTRATION: Plate 16, figure 13.
REFERENCES USED: Krebs 1983 Pl. 6 fig. 5, Pichon 1985 pl. 11 fig. 2, Zielinski 1993 Pl. 7 fig. 13.
NOTES: - Occurs in cores MD88-779, MD88-784, MD88-787, E53-10; and in new surface samples MDBX94-01, -02, -03, -04, -05, -05, -06, -07, TC53-10, TC37-19, E36-6, GC007, GC013, GC014, GC 016. GC017, GC030, GC031, GC034.

OTHER SILICEOUS MICROFOSSILS

CHRYSOPHYCEAE

ILLUSTRATION: Plate 17, figures 14-15.
REFERENCES USED: Krebs 1983 Pl. 6 fig. 6, Zielinski 1993 Pl.7 figs 14-16.
NOTES: - Found rarely.

PHYTOLITHS

ILLUSTRATION: Plate 17, figures 1-9.
REFERENCES USED: Locker and Martini 1986
NOTES: - Occurs in core MD88-779; and in new surface samples MDBX94-07 and possibly in new surface sample GC030.

RADIOLARIANS

NOTES: - Occurs in core E53-10 and sporadically through material observed in this work detailed record not made.

SPONGE SPICULES

ILLUSTRATION: Plate 17, figure 10-11.
NOTES: - Occurs in core E53-10 and more notably in northern samples. Detailed record not made.

ENDOSKELETAL DINOFLAGELLATES

ILLUSTRATION: Plate 17, figure 12.
REFERENCE USED: Fenner 1991.
NOTES: - Occurs in core E53-10 and sporadically in samples of this work. Occurrences of one genera, *Actiniscus,* only noted. Specimens are presumed to be *A. pentaserius.*

SPORE TYPE A

ILLUSTRATION: Plate 17, figures 13, 16a.

SPORE TYPE B

ILLUSTRATION: Plate 17, figure 16b, Plate 18, figures 1-2.
NOTES: Only observed in great number, generally clumped or joined together in core MD88-787 (at depth 1020 and 1030 cm).

PLATES.

- Plates 1 to 16 illustrate light microscope images of diatoms and silicoflagellates observed from samples of surface and core sediments. All photos were taken on a Nikon camera attached to a Nikon microscope using Phase contrast (Phase 4) at 1000X magnification with oil and a GIF filter, unless otherwise stated in the captions. Conversion of eye graticule to μm was made (ratio of 12 intervals to 10μm at 100X, and ratio of 10 intervals to 24 μm at 40X). Early images did not have measurements taken directly from the specimens, however, a 10 μm scale bar is provided in each plate for scale.
- Plate 17 illustrates Phytoliths, sponge spicules, and other cysts or spores of uncertain origin, under the same conditions as Plates 1 to 16.
- Plate 18 illustrates SEM images of unidentified spores and *Chaetoceros* species resting cells. All photos were taken on a Cambridge SEM at the Electron Micrscopy Unit, Research School of Biological Sciences, Australian National University.

PLATE 2.

Figures 1-2. ***Asteromphalus hookeri***

1. MD88-787 180 cm 2/3. Radius 96 µm.
2. MD88-787 660 cm 3/3. Diameter 79.2 µm.

Figure 3. ***Asteromphalus hyalinus***

3. MD88-787 180 cm 2/3. Diameter 40.8 µm.

Figure 4. ***Asteromphalus parvulus***

4. MD88-787 920 cm 3/3. Diameter 60 µm.

Figures 5-7. ***Azpeitia tabularis***

5. MD88-787 180 cm 2/3. Diameter 79.2 µm.
6. MD88-787 150 cm 2/3. Diameter 68.4 µm.
7. MD88-787 620 cm 2/3. Diameter 33.6 µm.

Figures 8-10. ***Azpeitia tabularis* var. *egregius***

8. MDBX94-01 0cm 2/3 2nd set. Diameter 28.8 µm.
9. MDBX94-01 0cm 3/3 2nd set. Diameter 28.8 µm.
10. MDBX94-01 0 cm 1/2 1st set. Diameter not recorded.

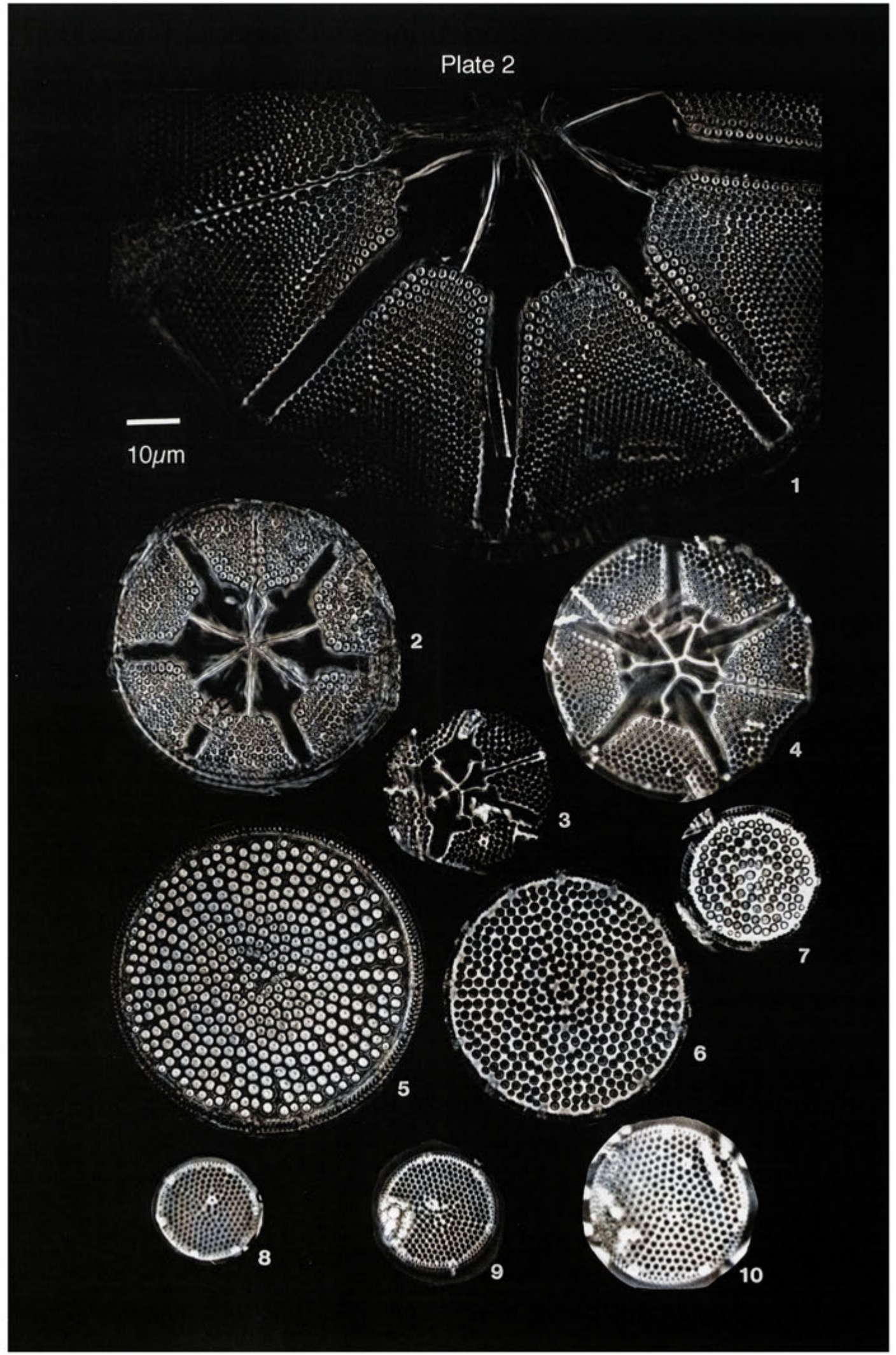
Plate 2
10μm
1
2
3
4
5
6
7
8
9
10

PLATE 3.

Figures 1-9. *Chaetoceros* species.

1. *Chaetoceros bulbosum* complex.MD88-787 500 cm 2/3. 48 µm across base.
2. " " " MD88-787 3/3. 21.6 µm.
3. cf. " " " MD88-787 920 cm 3/3. Diameter 28.8 µm.
4. *Chaetoceros criophilus.* MD88-787 800 cm 1/3. 38.4 µm across base.
5. *Chaetoceros dicheata* MD88-787 200 cm 1/3.
6. *Chaetoceros* cf. *dicladia.* MDBX94-02 0 cm 1/3. 33.6 µm across base.
7. " " MDBX94-03 0 cm 3/3. x40 Brightfield. No measurement recorded.
8. " " MDBX94-04 0 cm 1/3 2nd set. No measurement recorded.

Figures 9-27. *Chaetoceros* spores.

9. *Chaetoceros* cf. *dichaeta* spore. BC003A, 1/3 0cm. Widest length 33.6 µm.
10. " " MDBX94-01 0 cm 1/3 2nd set. Widest length 26.4 µm.
11. " " BC003 0cm 2/3. Widest length 24 µm.
12. " " GR003 0cm 1/3. Widest length 16.8 µm.
13. " " GC031 0cm 1/3. Widest length 14.4 µm.
14. *Chaetoceros* cf. *radians* spore MDBX94-05 0 cm 3/3 2nd set. Widest length of round body 10.8 µm.
15. " " " GC031 0 cm 1/3. Widest length ~19.2 µm.
16. " " " GR034 0 cm 3/3. Widest length 9.6 µm.
17. *Chaetoceros* spore type A. MDBX94-02 0 cm. 11.7 µm wide, 10.8 µm high.
18. " " " GR034 0 cm 2/3. Widest length 18 µm.
19. " " " GR034 0 cm 2/3. Measurement not taken.
20. " " " GC031 0 cm 1/3. Measurement not taken.
21. *Chaetoceros* spore type B. GC030 0 cm 3/3. Widest length 16.8 µm.
22. " " " MDBX94-02 0 cm 1/3. Measurement not taken.
23. " " " MDBX94-02 0 cm 1/3. Measurement for smaller spore is 8.4 µm.
24. *Chaetoceros* spore type C. MDBX94-03 0cm 3/3 2nd set. Widest length48 µm.
25. *Chaetoceros* spore type D. GR034 0 cm 2/3. Widest length 19.2 µm.
26. " " " GC031 0 cm 1/3. Widest length 8.4 µm.
27. " " " MDBX94-02 0 cm 1/3. 15.6 µm wide, 9.6 µm high.


Plate 3
1
2
3
4
5
6
7
8
9
10
11
12
13
14
15
16
17
18
19
20
21
22
23
24
25
26
27
10μm

PLATE 4.

Figure 1. ***Cocconeis*** **cf.** ***costata***

1. MDBX94-03 0cm 3/3 2nd set. Length ~38.4 µm.

Figures 2-3. ***Corethron criophilum***

2. MD88-787 720 cm. Brightfield. Diameter 55.2 µm.
3. MD88-787 660 cm 1/3. Brightfield. Diameter 45.6 µm.

Figure 4. ***Coscinodiscus africanus***

4. MDBX94-01 0cm 2/3 2nd set. Diameter 62.4 µm.

Figures 5-6. ***Coscinodiscus*** **cf.** ***asteromphalus***

5. MD94-109 Top III. Diameter ~72 µm.
6. GC016 0 cm 2/3. Diameter 72 µm.

Figures 7-9. ***Coscinodiscus curvatulus***

7. MDBX94-12 0 cm 1/3. No measurement recorded.
8. GC034 0 cm 3/3. Diameter 60 µm.
9. GR003 0 cm 2/3. Diameter 73.2 µm.

Figures 10-11b. ***Coscinodiscus marginatus***

10. E36-6 0-2cm 2/3. Diameter 31.2 µm.

11a+b. MDBX94-12 0 cm 1/3. No measurement recorded.


Plate 4
1
2
3
4
5
6
7
8
9
10
11a
11b
10μm

PLATE 5.

Figures 1-2. *Coscoinodiscus* cf. *radiatus*

1. MD88-779 230 cm 3/3 2nd set. Diameter 60 µm.
2. MD88-779 230 cm 3/3 2nd set. Diameter 52.8 µm.

Figures 3-4. *Coscinodiscus* species.

3. *Coscinodiscus* cf. *oculoides*. MD88-787 760 cm 1/2. No measurement taken.
4. *Coscinodiscus* cf. *argus*. GC031 0 cm 1/3. Diameter ~132 µm.

Figures 5-6. *Cyclotella* spp.

5. MD88-779 60 cm 1/3 2nd set. Diameter 15.6 µm.
6. GC014 0 cm 1/3. Diameter 10.8 µm.

Figures 7-8. *Dactyliosolen antarctica*

7. E36-6 0-2 cm 1/3. No measurement taken.
8. MD88-787 920 cm 3/3. Width across intercalary band 8.4 µm.

Figures 9-11. *Delphineis* cf *suriella*

9. GC016 0 cm 1/3. Width 15.6 µm.
10. GC016 0 cm 1/3. Width 19.2 µm.
11. MD88-779 230 cm 2/3 2nd set. Width 12 µm.

Figures 12-13. *Diploneis bombus/weissflogii*

12. MDBX94-11 0 cm 3/3. No measurement taken.
13. GC034 0cm 3/3. Length 57.6 µm.

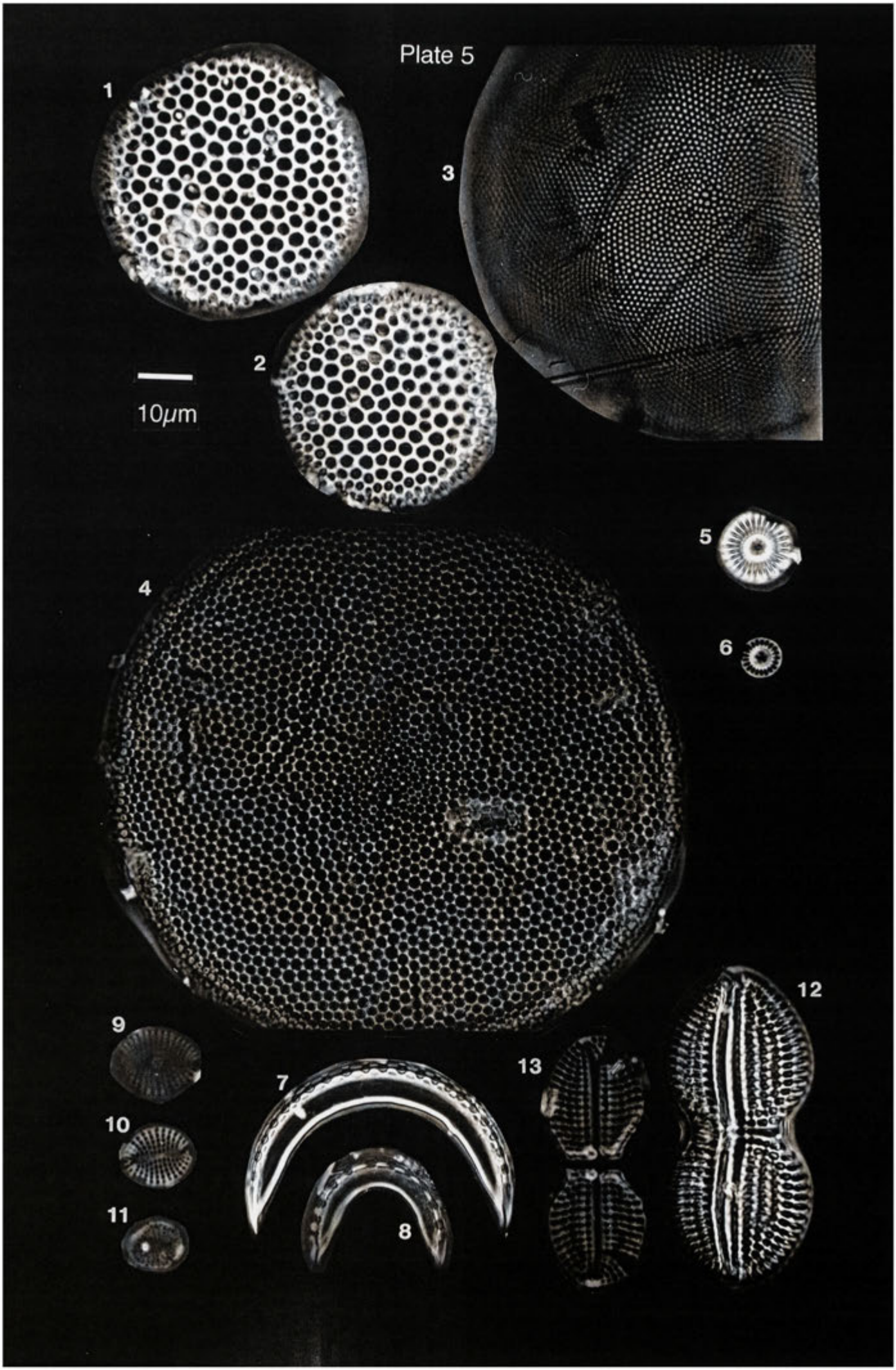
Plate 5
1
2
3
10μm
4
5
6
7
8
9
10
11
12
13

PLATE 6.

Figures 1-2. ***Eucampia antarctica***

1. MD88-784 180 cm 3/3. 84µm along base.
2. MD88-784 250 cm 1/3. 66µm along base.

Figures 3-4. ***Fragilariopsis curta***

3. MD88-787 970 cm. Length 30 µm.
4. MD88-787 460 cm 2/3. Length 34.8 µm, width 9.6 µm.

Figures 5-7. ***Fragilariopsis cylindrus***

5. MD88-784 250 cm 1/3. Length 14.4 µm.
6. MD88-787 520 cm 3/3 Length 30 µm, width 4.8µm.
7. MD88-787 450 cm 1/1. Length 34.8 µm, width 3.6 µm.

Figures 8-9. ***Fragilariopsis doliolus***

8. MDBX94-02 0 cm 1/3. Length 78 µm.
9. MDBX94-02 0 cm 1/3. Length 76.8 µm.

Figures 10-12. ***Fragilariopsis kerguelensis***

10. MD88-787 920 cm 3/3. Length ~132 µm, width 18 µm.
11. MD88-784 330 cm 1/3. No measurement taken.
12. MD88-787 920 cm 3/3. Length 60 µm.

Figures 13-17. Abberent forms of ***Fragilariopsis kerguelensis***

13. MD88-787 380 cm. Length 114 µm, width 20.4 µm.
14. MD88-787 620 cm 2/3. No measurement taken.
15. MD88-787 3/3. Length 66 µm, width 13.2 µm.
16. MD88-787 630 cm. Brightfield. No measurement taken.
17. MD88-787 620 cm 1/3. Brightfield. No measurement taken.

Figures 18-19. ***Fragilariopsis obliquecostata***

18. MD88-787 850 cm. Brightfield. No measurement taken.
19. MD88-787 280 cm. Brightfield 40x. No measurement taken. 10µm scale bar provided bottom right of photo.

Figure 20. ***Fragilariopsis pseudonana***

20. MD88-784 250 cm 1/3. Length 7.2 µm.

Figures 21-23. ***Fragilariopsis rhombica***

21. MD88-787 920 cm 3/3. Width 15.6 µm.
22. MD88-787 920 cm 3/3. Length 48 µm.
23. MD88-787 660 cm. 3/3. Length 61.2 µm, width 18 µm.

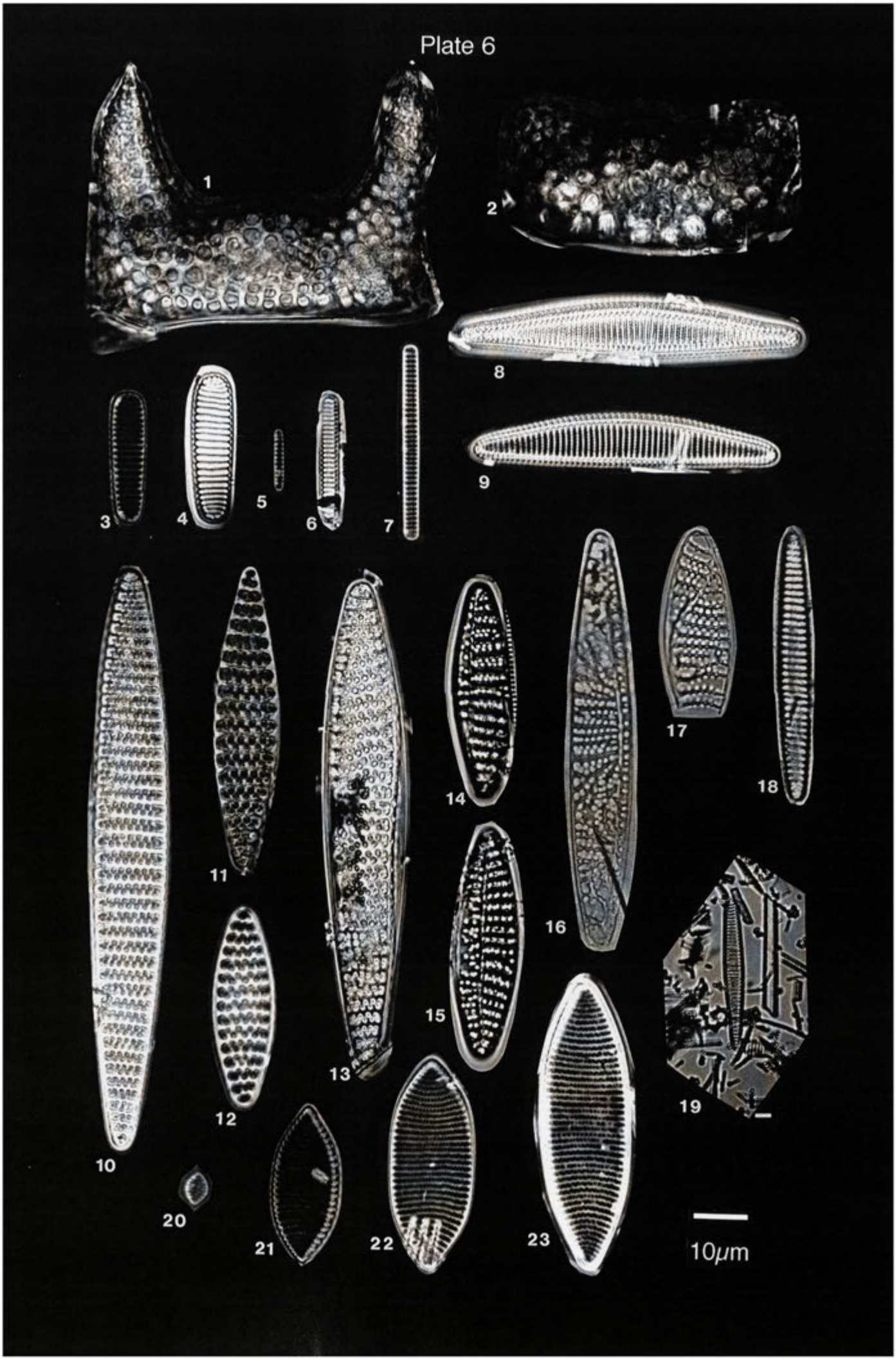
Plate 6
1
2
8
3
4
5
6
7
9
10
11
13
14
16
17
18
12
15
19
20
21
22
23
10μm

PLATE 7.

Figures 1-4. ***Fragilariopsis ritscheri***

1. MD88-787 920 cm 3/3. Length 67.2 µm.
2. MD88-787 180 cm 2/3. Length 67.2 µm.
3. MD88-787 950 cm 1/3. Length 58.8.
4. MD88-787 340 cm 1/3. No measurement taken.

Figures 5-8. ***Fragilariopsis separanda***

5. MD88-787 820 cm 3/3 Length 62.4 µm, width 16.8 µm.
6. MD88-787 920 cm 3/3. Length 42 µm.
7. GC034 0 cm 3/3. Length 20.4 µm.
8. MD88-787 920 cm 3/3. Width 13.2 µm.

Figures 9a+b. ***Nitzschia barberii***

9a+b. MD88-787 820 cm 2/3. Length 91.2 µm, width 10.8 µm.

Figures 10-11. ***Nitzschia* cf. *braarudii***

10. GC031 0 cm 3/3. Length 108 µm, width 7.2 µm.
11. GC030 0 cm 3/3. Length 46.8 µm.

Figure 12. ***Nitzschia* cf. *bicapitata***

12. GC017 0 cm 1/3. Length 45.6 µm.

Figure 13. ***Nitzschia* cf. *interruptestriata***

13. GC034 0 cm 3/3. Length 31.2 µm.

Figures 14-16. ***Nitzschia kolaczekii***

14. Fragment. GC014 0 cm 3/3. Length 54 µm.
15. Fragment. GC007 0 cm 2/3. Length 22 µm.
16. Fragment. GC034 0 cm 3/3. No measurement taken.

Figures 17-18. ***Nitzschia paundriformis***

17. GC031 0 cm 2/3. Length 30 µm.
18. MDBX94-04 0 cm 1/3 2nd se. Length 110.4 µm.

Figures 19-20. ***Nitzschia* cf. *peragalli***

19. MD88-787 490 cm Length 86.4 µm, width 16.8 µm.
20. MD88-787 490 cm. Width 15.6 µm.

Figures 21-22. ***Nitzschia sicula* var. *bicuneata***

21. MD88-784 330 cm 1/3. Length 66 µm.
22. MD88-787 540 cm 2/3. Length 73.2 µm, width 12 µm.

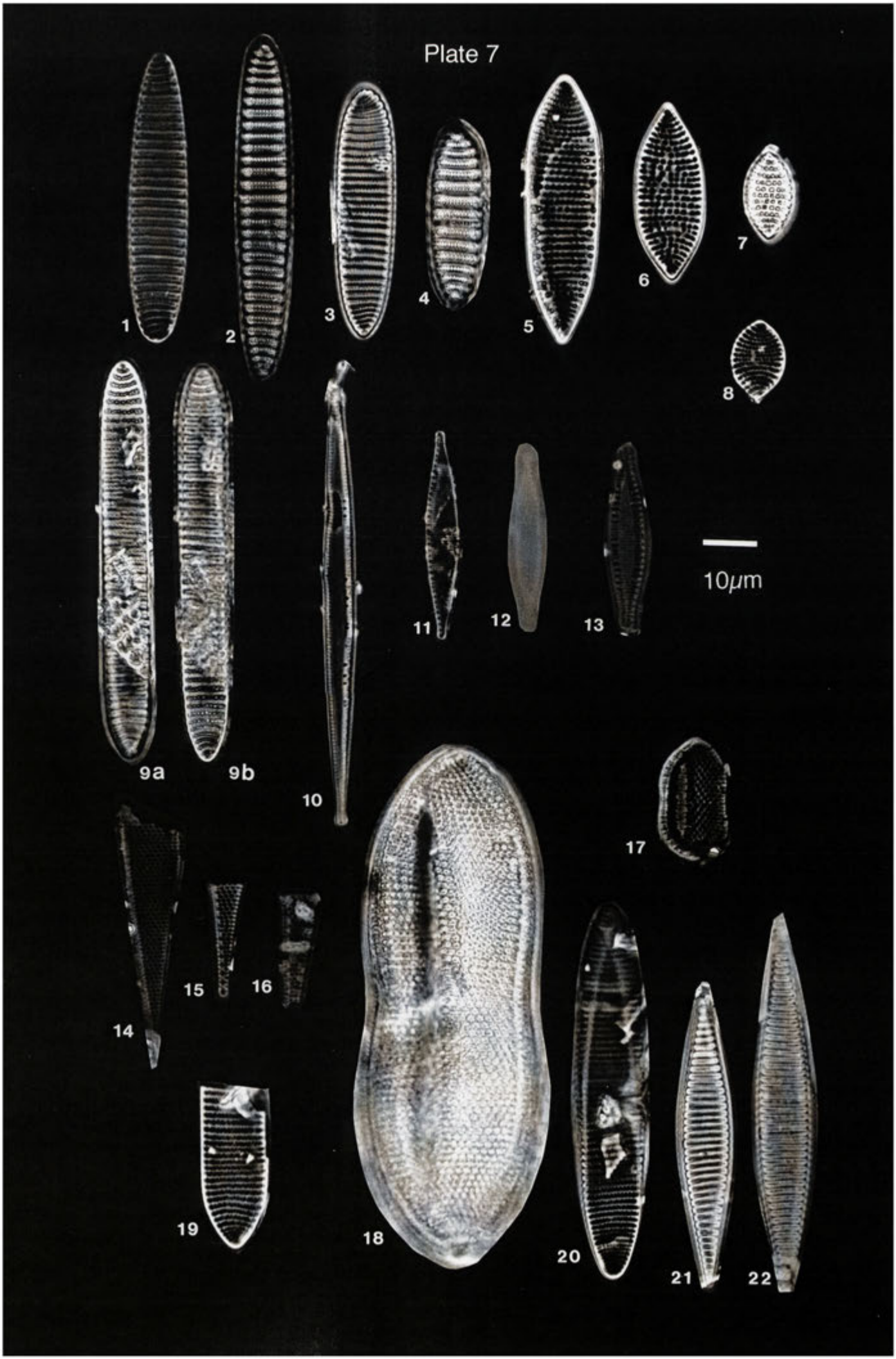
Plate 7
1
2
3
4
5
6
7
8
9a
9b
10
11
12
13
10μm
14
15
16
17
18
19
20
21
22

PLATE 8.

Figures 1-2. *Fragilariopsis/Nitzschia* species.

1. *Nitzschia* cf *reinholdi*. MD94-109 Top XX. Brightfield. No measurement taken.
2. *Nitzschia* sp. MDBX94-05 0 cm 1/3. No measurement taken.

Figure 3. aff. *Gyrosigma* sp.

3. Composite photograph. MD88-787 770 cm 1/2. Length ~181.2 µm.

Figures 4-9. *Hemidiscus cuneformis*

4. MDBX94-07 0 cm 1/3 2nd set. Width 49.2 µm.
5. MDBX94-07 0 cm 1/3 2nd set. No measurement taken.
6. MD88-779 230 cm 2/3 2nd set. Length 81.6 µm.
7. MDBX94-01 0 cm 1/3 1st set. No measurement taken.
8. MDBX94-01 0 cm 3/3 2nd set. Length 74.4 µm.
9. MDBX94-01 0 cm 2/3 2nd set. Length 69.6 µm.


Plate 8
1
2
3
4
5
10μm
6
7
8
9

PLATE 9.

Figures 1-2. *Hemidiscus karstenii*

1. MD88-779 230 cm 2/3 2nd set. Length 92.4 µm.
2. E53-10 130-131 cm 3/3. No measurement taken.

Figure 3. *Navicula directa*

3. MD88-787 620 cm 2/3. No measurement taken.

Figure 4. aff. *Licmophora* sp.

4. MDBX94-01 0 cm 2/3 2nd set. Length 38.4 µm.

Figures 5-6. *Odontella weissflogii*

5. MD88-787 770 cm 2/2. Length across base 52.8 µm.
6. MD88-787 760 cm 1/2. Length across base 45.6 µm.

Figures 7a-10. *Paralia* spp.

7a+b. GC034 505-507 cm Smear slide. Diameter 24 µm.
8. MDBX94-04 0 cm 3/3 2nd set. Diameter 8.4 µm.
9. GC030 0 cm 3/3. Diameter 25.2 µm.
10. MDBX94-01 0 cm 1/3 2nd set. Diameter 39.6 µm.

Figures 11-12. *Pleurosigma* spp.

11. MD88-787 350 cm 1/3. Length from centre to edge 28.8 µm..
12. MD88-787 350 cm 1/3. Brighfield 40X. Length ~ 165.6 µm. 10µm scale bar to left of photo.


Plate 9
1
2
3
4
5
6
7a
7b
10μm
8
9
10
11
12

PLATE 10.

Figure 1a+b. ***Porosira glacialis***

1a+b. MDBX94-03 0 cm 2/3 1st set. High and low focus. No measurement taken.

Figures 2-3. ***Proboscia alata***

2. MD88-784 110 cm 1/3. Length 72 µm.

3. MD88-784 330 cm 1/3. Length 66 µm.

Figure 4. ***Pseudonitzschia lineola***

4. Composite image. MD88-787 380 cm. Length from end to central point 99.6 µm, width 3.6 µm, 16-17 costae in 12µm.

Figure 5a+b. aff ***Pseudotriceratium/Triceratium*** **sp.**

5a+b. MDBX94-12 0 cm 1/3. No measurement taken.

Figures 6-7. ***Rhizosolenia antennata*** **forma** ***antennata***

6.MD88-787 260 cm 1/3. Brightfield 40X. No measurement taken. 10 µm scale provided bottom right of photo.

7. MD88-787 320 cm 3/3. Length from base to end of shortest process 48 µm.

Figure 8. ***Rhizosolenia antennata*** **forma** ***semispina***

8. MD88-787 320 cm 3/3. Brightfield. Length 72 µm.

Figures 9-12. ***Rhizosolenia bergonii***

9. GC007 0 cm 1/3. Length 64.8 µm.

10. GC034 0 cm 3/3. Length 36 µm.

11. MDBX94-07 0 cm 2nd set. No measurement taken.

12. GC030 0 cm 2/3. Brightfield. Length 75.6 µm.

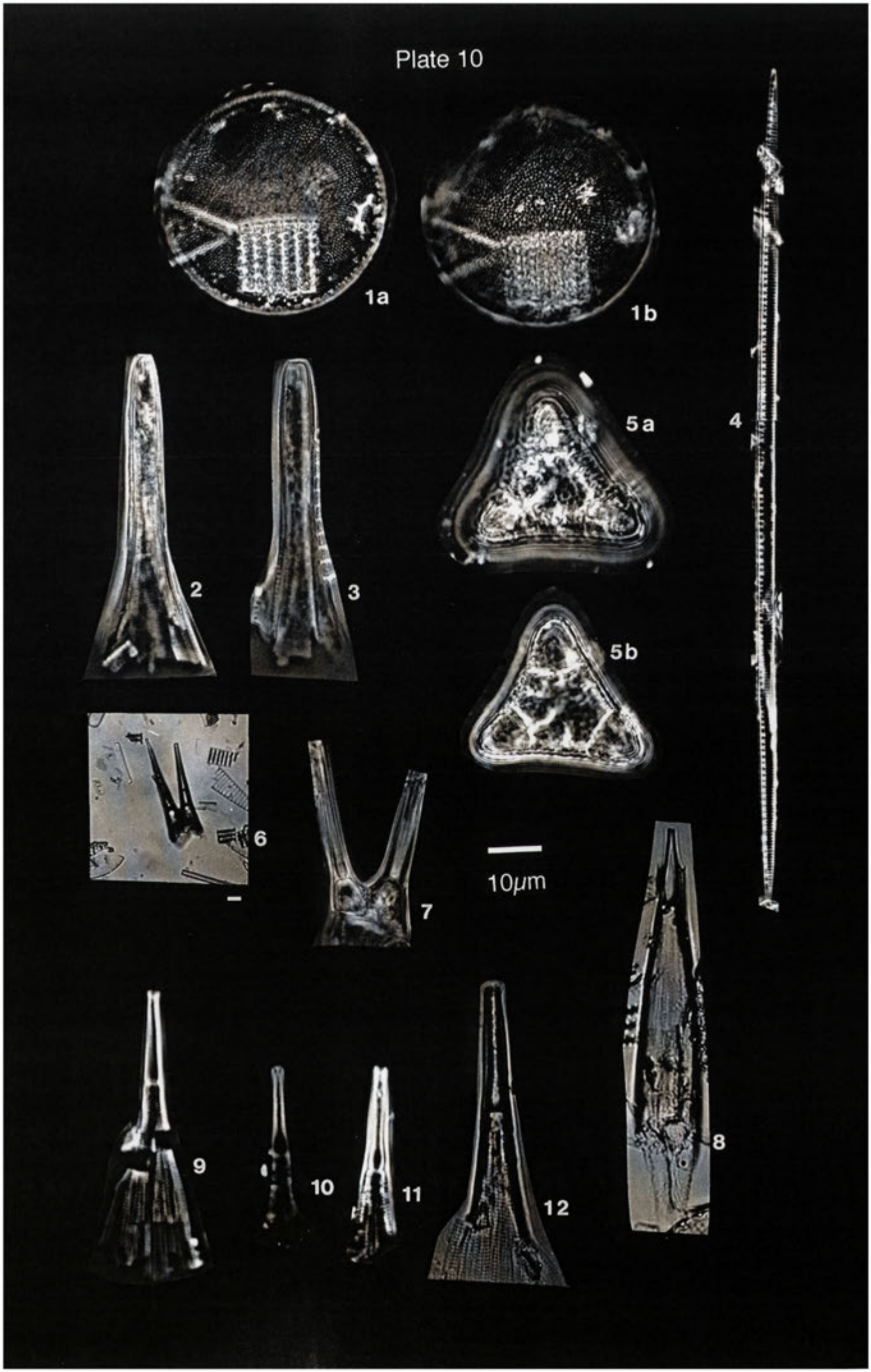
Plate 10
1a
1b
2
3
4
5a
5b
6
7
10μm
8
9
10
11
12

PLATE 11.

Figure 1. ***Rhizosolenia*** **cf.** ***polydactyla*** **forma** ***squamosa***

1. MD88-787 390 cm 3/3. Length 78 µm.

Figure 2. ***Rhizosolenia*** **cf.** ***simplex***

2. MD88-787 620 cm 3/3. No measurement taken.

Figures 3-5. ***Roperia tesselata***

3. MDBX94-01 0 cm 2/3 2nd set. Diameter 61.2 µm.
4. E36-6 0-2 cm 1/3. Diameter 57.6 µm.
5. MDBX94-01 0 cm 1/3 1st set. Measurement not taken.

Figures 6-7. ***Rouxia*** **spp.**

6. MD88-787 970 cm. Length 84 µm.
7. MD88-787 800 cm 1/3. Length 66 µm.

Figures 8-11. ***Stellarima stellaris***

8. GC017 0 cm 1/3. Diameter 63.6 µm.
9. GR003 0cm 1/3. Diameter 68.4 µm

10a+b. High and low focus. MDBX94-01 0cm 1/3 2nd set. Diameter 69.6 µm.

11. MDBX94-01 0 cm 3/3. Diameter 38.4 µm.


Plate 11
1
2
3
4
5
10μm
6
7
8
9
10A
10ß
11

PLATE 12.

Figures 1-5 *Thalassionema nitzschioides* group.

1. *Thalassionema nitzschioides* var. *capitulata*. GR003 0 cm 1/3. Length ~138 µm.
2. *Thalassionema nitzschioides* var. *lanceolata*. Partially dissolved. MD88-779 230 cm 2/3 2nd set. Length 85.2 µm.
3. *Thalassionema nitzschioides* var. forma 1. (sensu Zielinski and Gersonde 1997) MDBX94-01 0 cm 3/3 2nd set. Length 48 µm.
4. " " " MDBX94-01 0 cm 2/3 2nd set. Length 31.2 µm.
5. *Thalassionema nitzschioides* var. *parva*. GC034 0 cm 2/3. Length 20.4 µm.

Figures 6-12. *Thalassiosira antarctica*

6. MD88-787 430 cm 1/3. Diameter 22.8 µm.
7. MD88-787 820 cm 1/3. Diameter 24 µm.
8. E36-6 0-2 cm 1/3. Diameter 27.6 µm.
9. GC028 228-230 cm. Smear slide. Diameter 30 µm.
10. MD94-109 Top VIII. Smear slide. No measurement taken.
11. MDBX94-05 0 cm 1/3 2nd set. Diameter 43.2 µm.
12. MDBX94-01 0 cm 3/3 2nd set. Diameter from broken edge to spine edge 45.6 µm.

Figures 13-16. *Thalassiosira* cf. *decipiens*

13. MD88-787 440 cm 3/3. Diameter 26.4 µm.
14. MD88-787 1010 cm. Diameter 8.4 µm.
15. MD88-787 540 cm 3/3. Diameter 15.6 µm.
16. MD88-787 920 cm 3/3. Diameter 13.2 µm.

Figures 17-18. *Thalassiosira* cf. *eccentrica*

17. MDBX94-01 0 cm 2/3 1st set. No measurement taken.
18. MDBX94-12 0 cm 1/3. No measurement taken.

Figures 19. *Thalassiosira ferelineata*

19. MDBX94-01 0 cm 1/3 2nd set. Diameter 62.4 µm.

Figure 20. *Thalassiosira* cf. *frenguelliopsis*

20. GC016 0 cm 1/3. Diameter 52.8 µm.

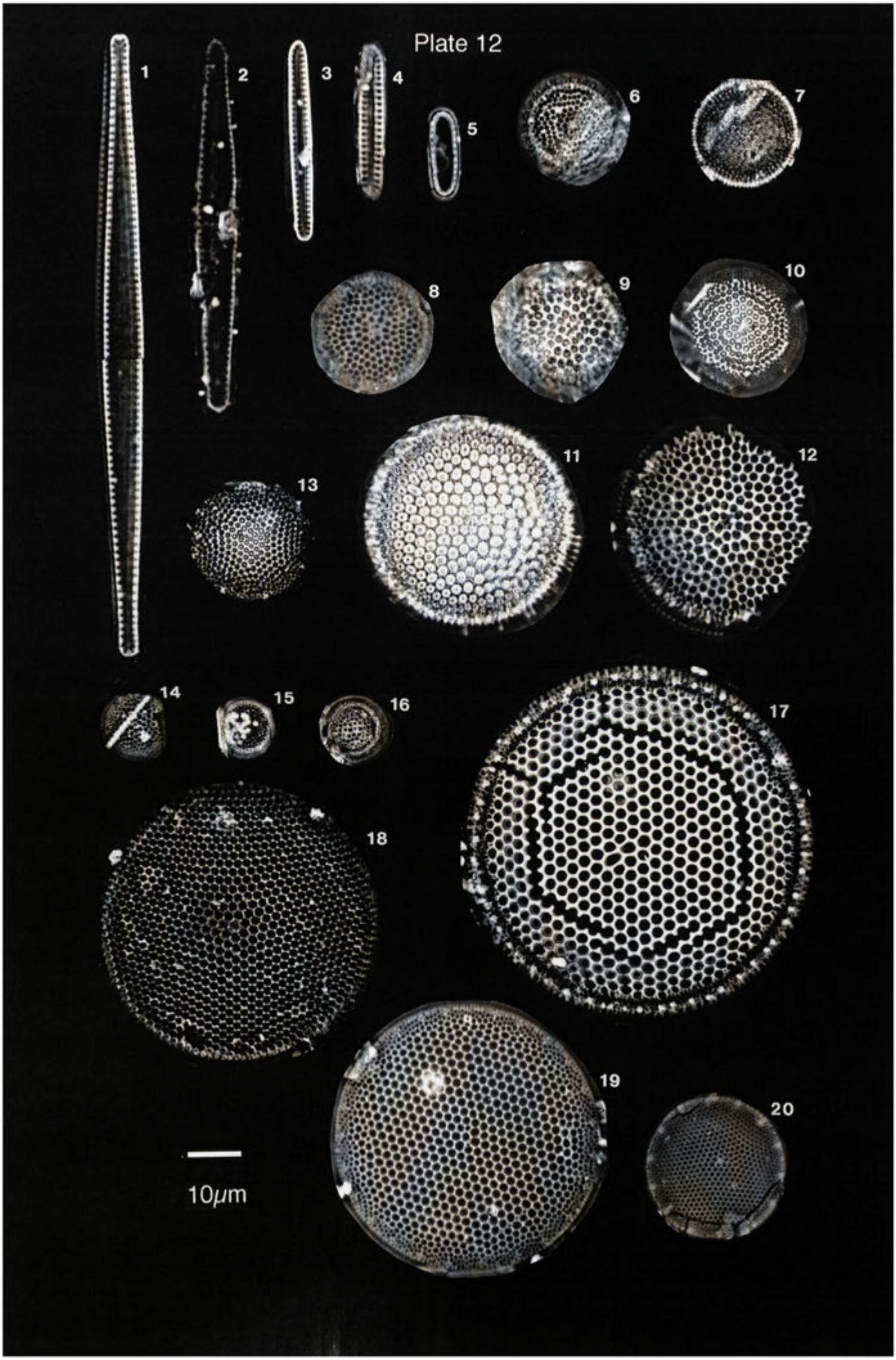
Plate 12
1
2
3
4
5
6
7
8
9
10
11
12
13
14
15
16
17
18
19
20
10μm

PLATE 13.

Figures 1-7. *Thalassiosira gracilis* group.

Thalassiosira gracilis var. *gracilis*

1. MD88-787 630 cm. No measurement taken.
2. MD88-787 110 cm. Diameter 22.8 µm.
3. MD88-787 970 cm. Diameter 16.8 µm.

Thalassiosira gracilis var. *expecta*

4. MD88-787 240 cm 1/2. Diameter 12 µm.
5. MD88-787 460 cm 2/3. Diameter 15.6 µm.
6. MD88-787 620 cm 1/3. Diameter 7.2 µm.
7. MD88-787 2/3. Diameter 10.8 µm.

Figures 8-9. *Thalassiosira gravida*

8. MD88-787 810 cm 1/2. Diameter 42 µm.
9. MD88-784 180 cm 3/3. Diameter 33.6 µm.

Figures 10-12. *Thalassiosira lentiginosa*

10. MD88-787 380 cm 2/3. Diameter 76.8 µm.
11. E53-10 54-55 cm 1/3. Diameter 69.6 µm.
12. MD88-784 180 cm 3/3. Diameter 45.6 µm.

Figures 13-14. *Thalassiosira leptopus*

13. GC034 0 cm 2/3. Diameter 61.2 µm. (*F. doliolus* adjacent)
14. GC016 0 cm 1/3. Diameter 52.8 µm.

Figures 15-17. *Thalassiosira lineata*

15. MDBX94-01 0 cm 2/3.2nd set. Diameter 58.8 µm.
16. MD88-779 220 cm 2/3 2nd set. Diameter 49.2 µm.
17. MDBX94-05 0 cm 2/3 1st set. No measurement taken.

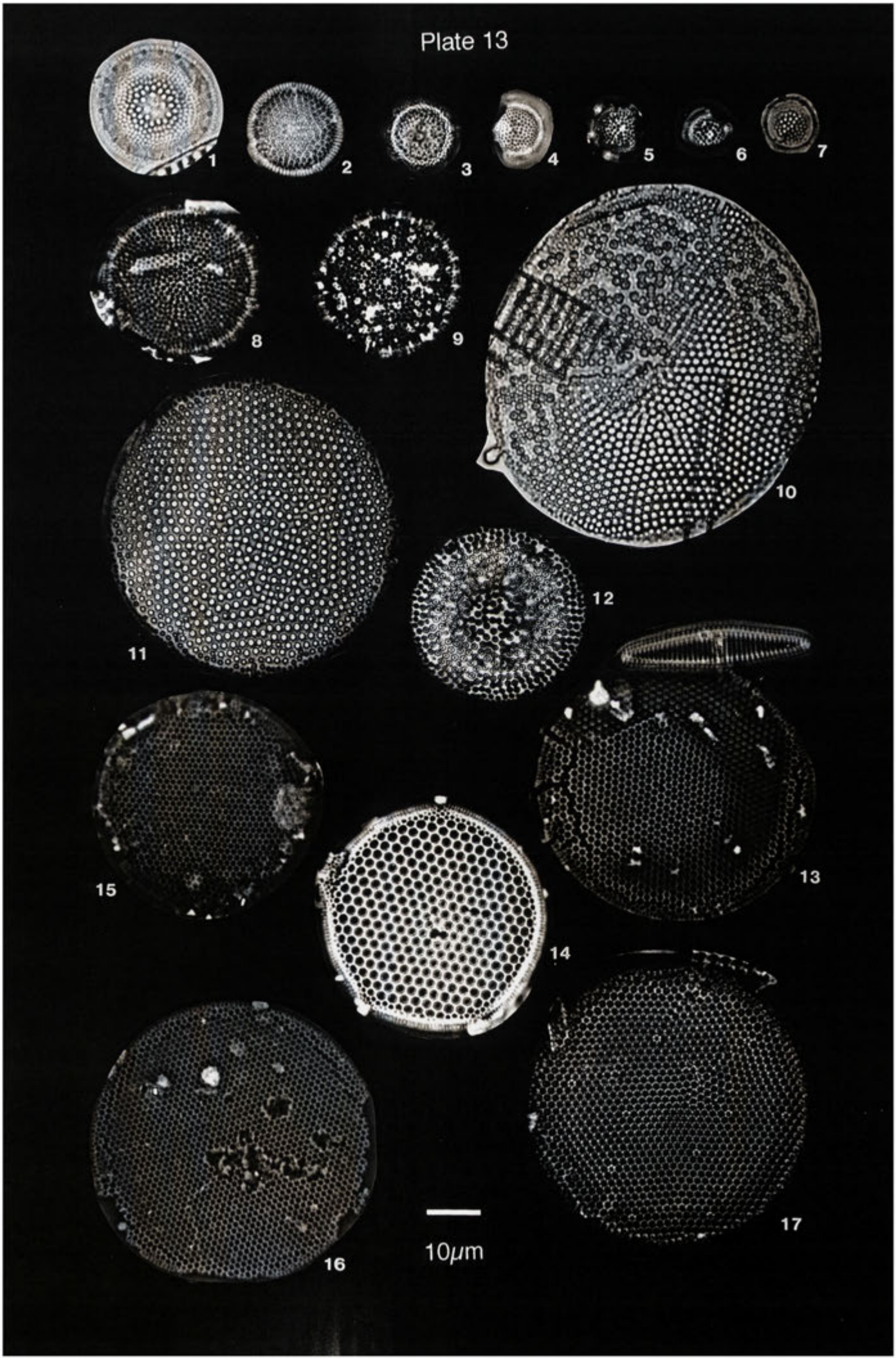
Plate 13
1
2
3
4
5
6
7
8
9
10
11
12
13
14
15
16
17
10μm

PLATE 14.

Figures 1-5. *Thalassiosira oestrupii*

Thalassiosira oestrupii var. *venrickae*

1. MD88-779 130 cm 2/3 2nd set. Diameter 46.8 µm.
2. MDBX94-07 0 cm 1/3. No measurement taken.
3. MDBX94-07 0 cm 2nd set. Diameter ~33.6 µm.

Thalassiosira oestrupii var. *oestrupii*

4. MD88-787 970 cm. Diameter 25.2 µm.
5. MD88-787 460 cm 3/3 Brightfield. Diameter 20µm.

Figures 6a-7b. *Thalassiosira oliverana*

6a+b. MD88-787 920 cm 3/3. Diameter 80.4 µm.

7a+b. E53-10 54-55 cm 1/3. Diameter 52.8 µm.

Figures 8-10. *Thalassiosira poroseriata*

8. Thalassiosira cf. poroseriata. MD88-787 3/3. Diameter 78 µm.
9. GC034 0 cm 2/3. Diameter 36 µm.
10. GC034 0 cm 2/3. Diameter 24 µm.

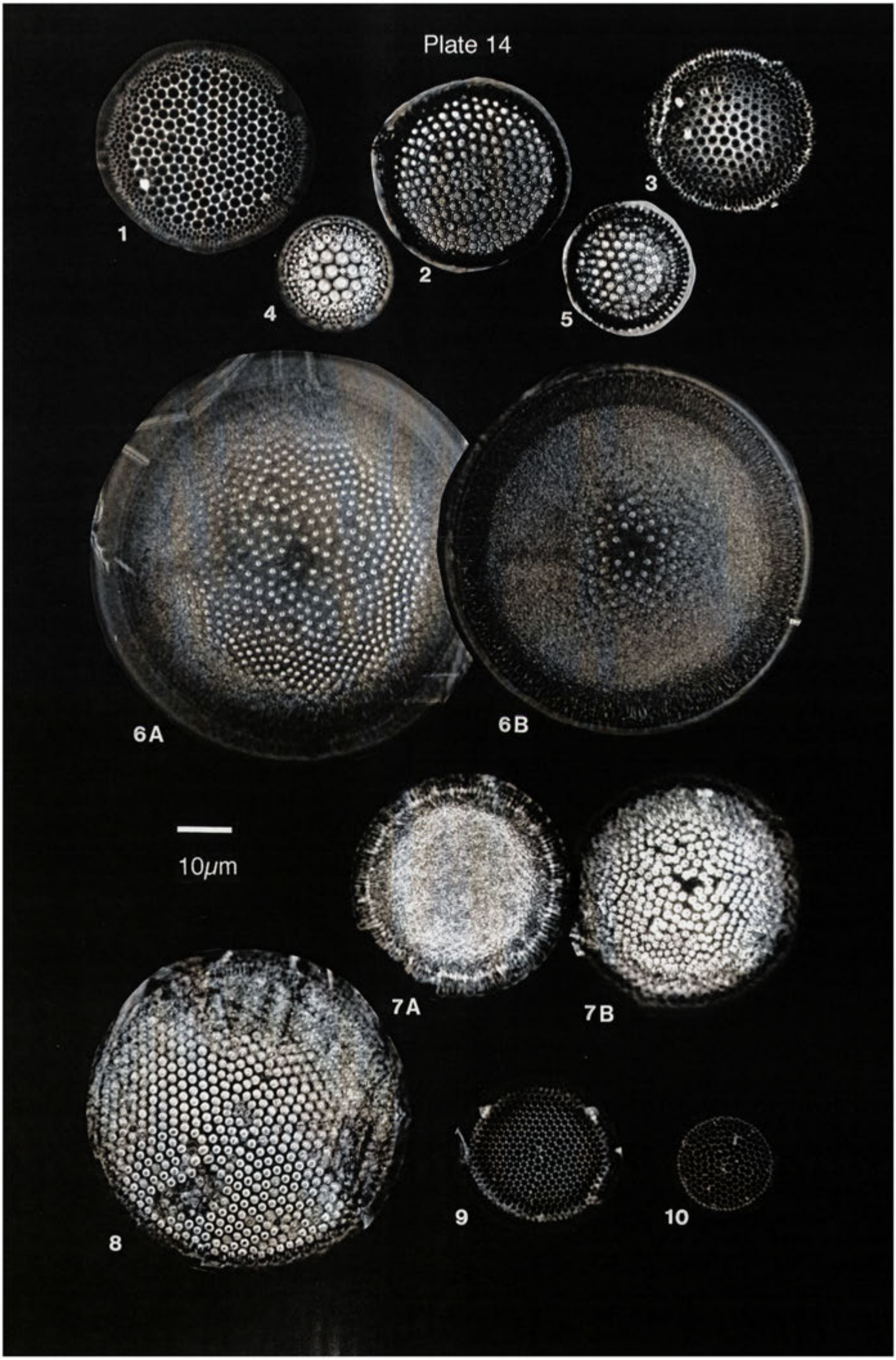
Plate 14
1
2
3
4
5
6A
6B
10μm
7A
7B
8
9
10

PLATE 15.

Figures 1. ***Thalassiosira*** **cf.** ***punctifera***

1. MDBX94-01 0 cm 1/3 2nd set. Diameter 57.6 µm.

Figures 2-4b. ***Thalassiosira trifulta***

2. MDBX94-07 0 cm 3/3 2nd set. Diameter 63.6 µm.

3a+b. MD88-787 640 cm 2/3. Diameter 48 µm.

4a+b. MD787 260 cm 1/3. No measurement taken.

Figures 5-6b. ***Thalassiosira tumida***

5. MD88-787 490 cm. Diameter 84 µm.

6a+b. High and low focus. MD788-787 380 cm 2/3. Diameter 56.4 µm.

Plate 15

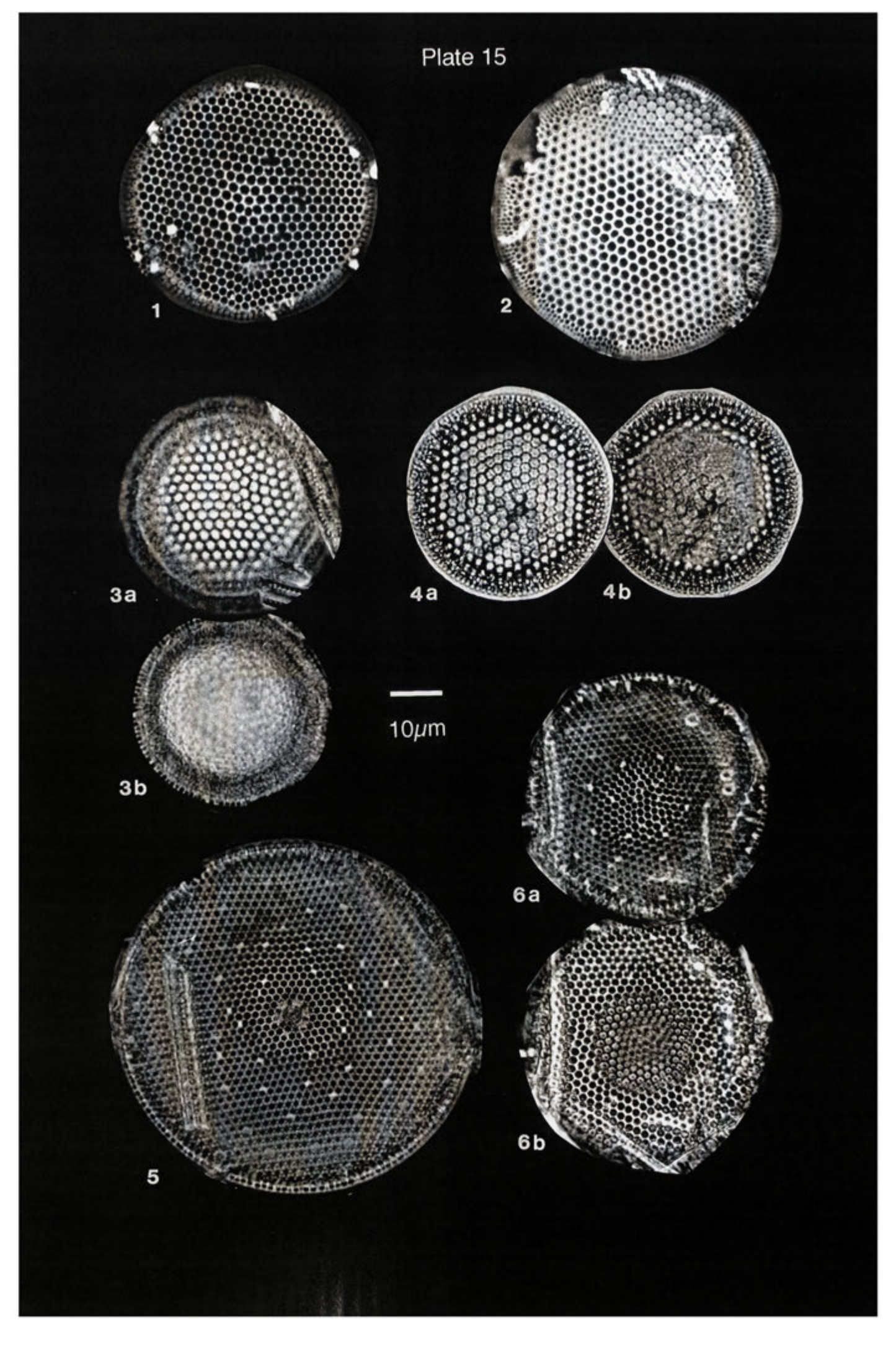

PLATE 16.

Figures 1-8. *Thalassiosira* spp.

1. *Thalassiosira* sp. A. MD88-787 3/3. Diameter 54 µm.
2. " " MDBX94-04 0 cm 2/3. No measurement taken.
3. " " MD88-789 550 cm. Diameter 32.4 µm.
4a+b." " MD88-787 340 cm 3/3. No measurement taken.
5. *Thalassiosira* sp. MD88-787 560 cm 1/3. No measurement taken.
6. " " MD88-787 910 cm. Diameter 27.6 µm.
7. " " MD88-787 600 cm 1/3 Diameter 51.6 µm.
8. " " GC0040 cm 2/3. Diameter 96 µm.

Figures 9-11. *Thalassiothrix* spp.

9. MD88-787 380 cm 2/3. Length 62.4 µm.
10. MD88-787 890 cm 1/2. No measurement taken.
11. MD88-787 380 cm 3/3. Length 60 µm.

Figure 12. *Trichotoxon reinboldii*

12. MD88-787 2/3. Width 9.6 µm.

Figures 13. *Distephanus* sp. (Silicoflagellate)

13. MD88-787 350 cm 1/3. Brightfield 40X. No measurement taken. 10µm scale bar provided between figures 13 and 14.

Figure 14. *Dictyocha* sp. (Silicoflagellate)

14. MDBX94-02 0 cm 1/3. Brightfield 40X.Length from top to bottom spine 57.6 µm. 10µm scale bar provided between figures 13 and 14.


Plate 16
1
2
3
4 A
4B
5
6
7
8
9
10
11
12
10μm
13
14

PLATE 17.

Figures 1-9. Phytoliths

1. MD88-779 220 cm 2/3 2nd set. Length 45.6 μm.
2. MD88-779 0 cm 3/3 2nd set. Length 91.2 μm.
3. MD88-779 130 cm 2/3 2nd set. Length 91.2 μm.
4. MD88-779 140 cm 1/3 2nd set. Length 15.6 μm.
5. MD88-779 0 cm 3/3 2nd set. Length 44.4 μm.
6. MD88-779 230 cm 3/3 2nd set. No measurement taken.
7. MD88-779 0 cm 1/3 2nd set. Length 26.4 μm.
8. MD88-779 140 cm 1/3 2nd set. Length 34.8 μm.
9. MD88-779 130 cm 2/3 2nd set. Length 22.8 μm.

Figures 10-11. Sponge spicules

10. MDBX88-779 130 cm 2/3 2nd set. Length 90 μm.
11. Unidentified siliceous remain, ? sponge spicule. MDBX94-12 0 cm 1/3. No measurement taken.

Figure 12. Endoskeletal dinoflagellate

12. MDBX94-01 0 cm 2/3 2nd set. Length of "spine" 20.4 μm.

Figures 13-16b. Other siliceous cysts/spores.

13. Spore type A. MD88-787 1030 cm 1/2. Width 9.6 μm.
14. ?Chrysophyst cyst. MD88-787 760 cm 1/2. Width 8.4 μm.
15. ? Chrysophyst cyst. MD88-787 970 cm. No measurement taken.
16a. Spore type A. MD88-787 1030 cm 1/2. No measurement taken.
16b. Spore type B (? Arenaceous siliceous). MD88-787 1030 cm 1/2. Width ~3 μm.

Plate 17


1


2

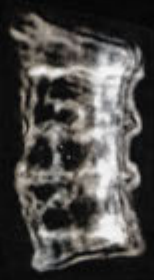
3


4


5


6


7


8

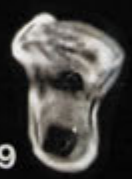
9


10

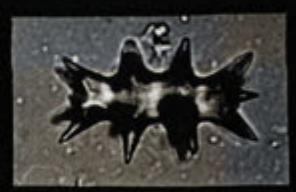
11

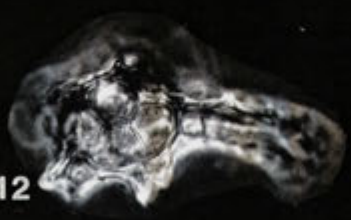
12


13


14

10μm


15

16B

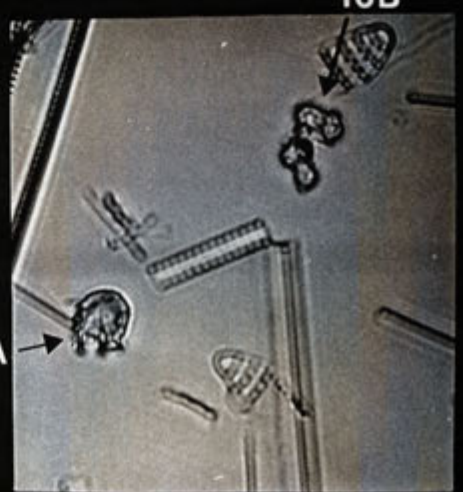
16A

PLATE 18.

Figures 1-2. Spore type B (? Arenaceous siliceous).

1. Group of type B spores. MD88-787 1020 cm. SEM.
2. Single type B spore showing aperture. MD88-787 1020 cm. SEM.

Figures 3-4. *Chaetoceros* spores.

3. *Chaetoceros* cf. *dichaeta* spore. MD88-787 1020 cm. SEM.
4. aff. *Chaetoceros* spore. MD88-787 1020 cm. SEM.

Plate 18

Appendix 1.1. Silica-selective methodology.

The following details the method used in this work to produce diatom slides from sediment samples. The methodology follows that in Pichon *et al.* (1987).

1.Place approximately 1gm of the undried sample in a crucible, obtain the wet weight and then cover with a watchglass and dry in an 60°C oven for 24 hours. Place the dried sample into a 250 ml beaker and obtain the dry weight of the sample.

2. Oxidisation of the organic material. A pre-made solution of 42gm Na_4P_2O7 (anhydrous tetra sodium phosphate) dissolved in 1 litre of distilled H_20 (130cc) and H_2O_2 (870cc), is added to the sample in the beaker so that the sample is just covered (~2 cm). Agitated to disperse the sample. Place the beaker in a warm (~70°C) water bath for a maximum of 30 minutes and agitate every 3 minutes until there is no further reaction with organic matter. Remove beakers from the water bath and allow to cool.

3. Transfer the remaining solution into a 16 cm deep by 3 cm diameter plastic test tube for centrifugation[1]. Centrifuge at ~1200 rev/min for 7 minutes. This speed ensures that the small diatoms are pulled down but that most of the clays are held in suspension. After spinning it may be necessary to re-spin at 1500 rev/min for 3 minutes if the diatoms have not been pulled down. Check by pipetting a small amount of the suspension on to a glass slide and viewing under a microscope. Pour the supernatant off. Add distilled water to the tube to re-suspended the remaining sediment. Centrifuge at 1500 rev/min for 7 minutes. This procedure is repeated until the pH of the supernatant has reached a value characteristic of the distilled water (~6.5). Once the pH level is met the supernatant is poured off and the sediment is transferred with as little distilled water as possible into the beakers initially used for each sample These beakers are covered with watchglasses and heated in the oven at 60°C overnight.

4. Once dry, a small amount of 10% HCl is added to the beaker to cover the dried sample. A solution of 25% HCl is used if a lot of carbonate is contained in the samples (eg. those derived from the subantarctic region). Small amounts of HCl are added until there is no further reaction. The resulting solution is then placed in the same centrifuge tubes topped with distilled water and centrifuged at ~1200 rev/min for 7 minutes. The supernatant is poured off, then the sediment re-suspended with distilled water, the pH checked, with the procedure repeated until the pH of the distilled water is achieved (approximately 3 repeats for pH 6.5). The last supernatant is poured off.

5. While waiting for the centrifugation to complete, the coverslips for the slides are set up for the random settling method (Moore, 1973). The equipment consists of a plastic petri-dish (5.5 cm diameter x 1.5 cm depth) containing one 1 oz 22 x 22 mm square coverslip that is held down to the dish by a drop of distilled water. On top of the slide is placed a 150µl of Calgon™ solution (Calgon™ laundry powder in distilled water), which assists in dispersion of the diatoms. There are three petri-dishes per sample. Cotton knitting yarn (4 ply) is cut into 3 cm lengths and soaked in distilled water until required.

6. Place the siliceous sediment remaining in the test tube to a new clean 200 ml beaker. Add distilled water to 100 ml. Agitate the solution in a non-circular manner. A 150µl drop of the agitated sample is taken from the middle of the solution by a micropipette with a disposable plastic tip, and placed within the drop of Calgon™ solution on the coverslip. Repeat for the remaining coverslips representative of this sample. Add distilled water rapidly to the top of the petri-dishes ensuring that the diatom/Calgon drop is well homogenised. A soaked cotton string is added so that the water is slowly drawn off by capillary action, thus allowing the siliceous material to settle evenly over the coverslip. The remaining solution in the beaker is then dried in the oven at 60°C and the sample is transferred using distilled water to 50 ml clean plastic specimen jars for curation.

7. When the cover-slips are dry they are removed from the petri-dishes and mounted to labelled glass slides with two drops of Naphrax (r.i. 1.74) on a hot plate at 110°C. The slides are then cooled and placed in slide boxes ready for counting.

---

[1] The possibility for error in diatom extraction from the sediments using centrifugation may have occurred as the centrifuge available for this work could not be adjusted for precise revolutions per minute. A calibration was made using a strobe light and proxy samples. This possibility for error was evident in the initial stage of the centrifugal processing, such that the second run was required to ensure that the smaller diatoms were kept and not poured off in the supernatant.

Appendix 2.1. Original Ranked 166 surface sample database .

Core	*A. parvulus*	*Chaetoceros spp.*	*A. actinochilus*	*S. microtrias*	*A. tabularis*	*E. antarctica*	*H. cuneiformis*	*F. curta*	*F. kerguelensis*	*F. ritscheri*	*F. seperanda*	*F. sublinearis*	*R. styliformis*	*R. tesselata*	*T. oliverana*	*T. nitzschioides*	*T. decipiens*	*T. delicatulata*	*T. trifulta*	*T. gracilis*	*T. lineata*	*Thalassiosthrix spp.*	*Dictyocha spp.*	*Distephanus spp.*	*T. lentiginosa*	*F. cylindrus*	*F. rhombica*	*P. glacialis*	*O. weissflogii*	*Cocconeis spp.*	*T. antarctica*	*T. tumida*	*T. oestrupi*	*P. dollolus*
MD73-026	1	1	0	0	3	2	0	0	3	2	1	0	1	0	1	3	1	0	1	1	1	1	2	2	0	0	0	0	0	0	0	1	0
V16-65	0	0	0	1	3	2	0	0	2	1	0	0	0	0	2	3	0	1	1	1	1	1	3	3	0	0	0	0	0	0	0	1	0
V16-60	1	0	1	0	3	2	0	0	3	2	1	1	1	0	1	1	0	0	0	1	0	2	0	1	2	0	0	0	0	0	0	0	0
1176-91	1	0	0	2	3	2	1	0	3	1	1	0	1	3	0	3	1	0	1	1	2	1	3	2	2	0	0	0	0	0	0	1	0
1176-88	0	0	1	2	3	2	0	0	3	1	1	1	1	0	1	3	1	0	0	1	1	1	2	1	3	0	0	0	0	0	0	1	0
1277-2	2	0	0	1	3	1	1	0	2	2	1	1	1	3	2	3	2	0	2	1	1	1	3	1	3	0	0	0	0	0	0	1	0
RC11-80	0	0	1	0	2	2	0	0	3	1	1	0	1	0	0	3	1	1	1	1	1	1	2	3	0	0	0	0	0	0	0	1	0
1176-86	0	0	0	0	2	2	0	0	3	0	1	0	1	0	1	3	1	0	1	1	1	3	0	2	2	0	0	0	0	0	0	1	0
RC15-91	0	0	0	0	3	2	0	0	2	1	1	0	1	0	1	1	1	1	0	1	0	1	0	1	3	0	0	0	0	0	0	0	0
RC11-78	0	0	0	0	3	2	0	0	3	1	1	1	0	0	1	1	1	1	0	2	0	1	0	2	2	0	0	0	0	0	0	0	0
RC13-255	0	0	0	1	3	2	0	0	3	1	0	1	1	0	1	3	1	0	0	2	0	2	0	1	2	0	0	0	0	0	0	0	0
1176-82	0	0	0	0	1	1	0	0	3	1	1	0	0	0	1	1	0	0	0	1	0	3	0	1	2	0	0	0	0	0	0	0	0
RC13-274	1	0	2	0	1	2	0	0	3	0	1	2	1	0	0	0	0	0	0	2	0	3	0	1	3	0	1	0	0	0	0	0	0
RC13-273	1	0	0	0	1	1	0	1	3	0	1	1	0	0	0	0	0	0	0	2	0	2	0	1	2	1	2	0	0	0	0	0	0
MD24-KK63	1	1	0	0	3	1	0	0	3	0	1	0	1	0	0	1	0	0	0	3	0	3	0	1	2	0	0	0	0	0	0	0	0
RC13-263	1	1	0	0	1	1	0	1	3	0	2	2	0	0	1	0	0	0	0	2	0	3	0	3	2	1	1	0	0	0	0	0	0
1277-28	2	0	1	0	0	1	0	1	3	0	1	2	0	0	1	0	0	0	0	2	0	2	0	1	2	1	1	0	0	0	0	0	0
MD82 424	1	1	1	0	1	1	0	0	3	0	2	2	1	0	1	0	0	0	0	2	0	3	0	3	2	0	0	0	0	0	0	0	0
1141-2P	0	0	3	0	0	1	0	3	2	0	0	2	1	0	0	0	1	1	0	3	0	0	0	1	1	3	3	2	3	1	3	0	0	0
1184-6P	0	0	3	0	0	1	0	2	2	0	0	2	1	0	0	0	0	1	0	3	0	1	0	0	1	3	3	2	3	3	3	0	0	0
1147-4P	0	0	3	0	0	2	0	2	2	0	0	2	2	0	0	0	0	1	0	1	0	0	0	0	1	2	3	2	3	1	3	0	0	0
P1160	0	0	3	0	0	1	0	3	2	0	0	2	3	0	1	0	0	1	0	1	0	1	0	1	1	2	1	3	2	1	2	0	0	0
1178-4P	0	0	3	0	0	2	0	2	2	0	0	2	3	0	1	0	0	0	0	2	0	1	0	1	2	2	3	2	3	1	2	3	0	0
1010W	0	0	2	0	0	3	0	3	0	0	0	3	0	0	0	0	0	0	0	0	0	0	0	0	1	0	3	0	1	0	0	2	0	0
1192W	0	1	2	0	0	3	0	3	0	0	0	3	0	0	0	0	0	0	0	0	0	0	0	0	1	3	0	0	0	0	0	0	0	0
1212W	0	0	3	0	0	3	0	3	0	0	0	3	0	0	0	0	0	0	0	0	0	0	0	0	1	1	0	0	0	0	0	0	0	0
1223W	0	0	2	0	0	3	0	2	1	0	0	3	0	0	0	0	0	0	0	0	0	1	0	1	0	2	0	1	1	0	0	0	0	0
1277-41	0	0	3	0	0	2	0	1	3	0	0	2	0	0	1	0	0	0	0	1	0	1	0	0	2	1	0	1	0	0	2	0	0	0
RC17-56	0	0	3	0	0	2	0	0	3	0	2	2	1	0	2	0	0	0	0	1	0	1	0	0	2	0	0	1	0	0	1	1	0	0
MD82 436	1	0	2	0	1	2	0	1	2	0	0	1	1	0	1	0	0	0	0	1	0	1	0	1	1	0	0	0	0	0	0	1	0	0
1176-55	1	2	1	0	1	1	0	1	3	0	1	1	1	0	2	0	0	0	1	1	1	2	0	1	2	0	1	0	1	1	0	0	0	0
1176-65	0	0	0	1	0	1	0	1	3	0	1	2	1	0	1	0	0	0	1	2	0	3	0	1	2	0	1	0	0	0	0	0	0	0
1277-8	0	1	0	0	0	2	0	0	3	0	1	1	1	0	2	0	0	1	1	1	1	1	0	1	3	1	0	0	0	0	0	0	1	0
1277-12	1	1	0	0	1	2	0	1	3	1	1	0	0	0	0	0	0	0	1	0	2	1	1	0	1	2	1	1	0	0	0	0	0	0
1578-49	0	0	2	0	1	2	0	1	2	0	1	2	1	0	1	0	0	0	0	1	0	1	0	1	3	0	1	0	0	0	0	0	0	0
1678-64	0	0	0	0	1	2	0	1	3	1	1	1	1	0	1	1	0	0	1	1	0	1	0	1	3	0	0	0	0	1	0	0	1	0
1678-80	1	0	0	0	3	2	1	0	3	2	0	1	1	0	1	2	0	2	1	1	1	2	0	1	3	0	1	0	0	0	0	0	0	0
1678-84	1	0	0	1	1	2	0	0	3	0	0	1	1	0	1	1	1	0	1	2	1	1	0	1	3	0	0	0	1	0	0	0	0	0
1678-89	1	0	2	0	0	2	0	1	3	0	1	1	0	0	1	0	0	0	0	1	1	0	3	0	1	2	1	1	1	0	0	0	0	1	0
1678-96	1	1	1	0	1	2	0	1	3	0	2	2	3	0	1	0	0	1	0	1	0	3	0	3	3	0	1	0	0	0	0	0	0	0
RC8-46	1	0	1	0	1	1	0	0	3	1	1	1	1	0	1	0	0	1	0	1	1	1	0	1	2	0	0	0	0	0	0	0	0	0
RC11-71	1	0	0	0	2	2	0	0	2	1	0	0	2	2	1	1	1	0	0	1	0	1	1	1	3	0	0	0	1	0	0	0	0	0
RC11-77	0	0	0	0	1	2	0	0	3	1	1	0	0	0	0	0	1	0	0	2	0	3	0	1	2	0	0	0	1	0	0	0	0	0
RC11-90	1	0	0	0	2	2	0	0	3	0	2	2	0	0	1	0	0	0	0	0	1	1	1	0	1	2	0	1	0	0	0	0	0	0
RC13-257	0	0	1	1	2	2	0	0	3	0	1	1	0	0	1	0	1	0	0	1	0	2	0	1	2	0	0	0	0	0	0	0	0	0
RC13-268	1	0	2	0	1	2	0	1	3	0	1	2	1	0	1	0	0	0	0	2	0	1	0	1	2	0	1	0	0	0	0	0	0	0
RC13-269	0	0	0	0	1	1	0	0	3	0	2	2	0	0	0	0	0	1	1	2	0	3	0	1	2	0	0	0	0	0	0	0	0	0
RC13-270	1	0	1	0	1	2	0	0	3	0	1	1	1	0	2	0	0	1	0	2	1	1	0	1	3	1	1	0	0	0	0	0	0	0
RC13-272	1	0	1	1	1	2	0	2	3	0	1	2	0	0	2	0	0	0	0	2	0	3	0	1	2	1	1	0	0	0	0	0	0	0
RC11-118	0	0	0	0	3	0	3	0	2	0	0	0	0	3	0	3	0	0	0	0	0	1	3	1	0	0	0	0	0	0	0	0	3	3
RC11-119	0	0	0	0	3	0	3	0	2	0	0	0	0	2	0	3	1	0	0	1	2	1	3	0	2	0	0	0	0	0	0	0	1	3
RC12-292	0	0	0	0	3	0	3	0	1	0	0	0	0	2	0	2	0	0	0	0	1	1	3	0	2	0	0	0	0	0	0	0	3	3
V14-53	0	0	1	1	1	2	0	1	3	0	1	1	1	0	1	0	0	0	0	1	0	2	0	1	2	0	1	0	0	0	0	0	0	0
V14-58	1	0	1	0	1	2	0	2	3	0	0	2	0	0	1	0	0	1	0	1	1	3	0	1	2	0	0	0	0	0	0	0	0	0
MD24 KK02	3	1	1	1	1	2	0	1	3	0	1	1	1	0	1	0	0	0	1	2	0	2	0	1	2	0	0	0	0	1	1	0	0	
MD24 KK32	1	1	1	0	2	2	0	0	3	0	0	1	1	0	1	0	0	0	0	1	0	3	0	3	3	0	0	0	1	0	0	0	0	0
MD24 KK35	1	1	1	0	1	2	0	0	3	0	1	1	1	0	2	0	1	0	0	1	1	3	0	1	3	0	0	0	1	0	0	0	1	0
MD24 KK37	1	2	1	1	1	1	0	0	3	0	2	1	1	0	1	0	0	0	1	1	0	3	0	1	2	0	0	0	0	0	0	0	0	0
MD82 425	1	1	1	0	1	2	0	0	3	0	2	1	1	0	2	0	0	1	1	1	1	2	0	1	2	0	0	0	1	0	0	0	0	0
MD82 430	1	0	2	1	2	2	0	1	3	0	1	1	1	0	1	0	0	0	0	1	0	2	0	1	3	0	1	0	0	0	0	0	0	0
MD82 434	1	0	1	0	1	2	0	2	3	0	2	2	1	0	1	0	0	0	0	2	0	3	0	1	2	0	1	0	0	0	0	0	0	0
MD84 531	0	0	2	0	0	2	0	3	1	0	0	2	0	0	0	0	0	0	0	2	0	1	0	1	2	1	2	2	0	0	2	0	0	0
MD84 530	1	0	2	0	1	2	0	2	3	0	0	2	1	0	1	0	0	1	0	1	1	1	0	1	2	1	1	1	0	0	0	0	0	0
MD84 532	0	0	2	0	0	2	0	2	3	0	0	2	0	0	1	0	0	1	0	1	0	1	0	1	2	0	1	1	0	0	1	0	0	0
MD84-529	1	0	0	0	3	2	0	0	3	1	1	0	1	0	2	2	0	0	1	1	0	3	0	3	2	0	0	0	0	0	0	0	1	0
MD84 533	1	0	2	0	1	2	0	1	2	0	0	2	0	0	1	0	0	0	0	1	0	1	0	1	3	0	1	0	0	0	1	0	0	0
MD 84 540	1	1	1	0	2	2	0	2	3	1	2	2	0	0	1	0	0	0	0	2	1	2	0	1	2	0	1	0	1	0	0	0	0	0
MD84 552	1	0	0	0	3	0	0	0	3	0	2	1	1	0	1	0	0	0	1	2	1	3	0	1	2	0	0	0	0	1	0	0	0	0

Appendix 2.1. Original Ranked 166 surface sample database .

Core	*A. parvulus*	*Chaetoceros spp.*	*A. actinochilus*	*S. microtrias*	*A. tabularis*	*E. antarctica*	*H. cuneiformis*	*F. curta*	*F. kerguelensis*	*F. ritscherl*	*F. seperanda*	*F. sublinearis*	*R. styliformis*	*R. tesselata*	*T. oliverana*	*T. nitzschioides*	*T. decipiens*	*T. delicatulata*	*T. trifulta*	*T. gracilis*	*T. lineata*	*Thalassiosthrix spp.*	*Dictyocha spp.*	*Distephanus spp.*	*T. lentiginosa*	*F. cylindrus*	*F. rhombica*	*P. glacialis*	*O. weissflogii*	*Cocconeis spp.*	*T. antarctica*	*T. tumida*	*T. oestrupi*	*P. dolioius*
MD84 557	1	0	0	0	3	2	0	0	3	0	1	1	1	0	3	0	0	0	1	2	1	3	0	3	2	0	0	0	0	0	0	0	0	0
MD84-561	1	2	0	0	2	2	0	0	3	2	0	0	1	0	2	1	0	0	0	3	0	3	0	3	2	0	0	0	1	0	2	1	1	0
MD84 562	0	0	0	1	3	1	0	0	3	0	1	1	1	0	1	2	0	0	1	2	1	3	0	1	3	0	0	0	0	0	0	0	0	0
MD84 563	0	0	0	1	2	2	0	0	3	2	0	0	1	0	1	1	0	0	1	2	1	3	0	2	2	0	0	0	0	0	0	0	1	0
MD84 569	0	1	0	0	2	2	0	0	3	2	0	0	3	0	1	2	0	0	1	1	0	2	0	0	2	0	0	1	2	0	2	0	0	0
83-11C III	0	0	2	2	0	3	0	3	0	0	1	3	1	0	2	0	0	0	0	2	0	1	0	0	0	2	2	0	0	0	2	2	0	0
83-12 III	0	0	2	2	0	3	0	3	1	0	0	3	2	0	1	0	0	0	0	0	0	1	0	1	2	2	0	0	0	0	2	0	0	0
83-19 III	0	0	3	0	0	3	0	3	0	0	0	2	2	0	0	0	0	0	0	1	0	1	0	0	1	2	0	0	0	0	2	1	0	0
83-41 III	0	1	2	0	0	2	0	3	1	0	1	3	0	0	0	0	0	0	0	2	0	1	0	0	1	2	0	0	0	0	1	0	0	0
83-42 III	0	0	2	0	0	2	0	3	1	0	1	3	0	0	0	0	0	0	0	2	0	1	0	1	0	2	1	1	0	0	1	0	0	0
PC82-197	0	0	2	0	0	1	0	2	1	0	0	2	0	0	0	0	0	0	0	2	0	0	0	0	2	2	0	3	2	1	3	1	0	0
PC82-35	0	0	3	1	0	1	0	2	2	0	2	2	3	0	0	0	0	0	0	3	0	1	0	2	2	2	1	1	2	2	2	1	0	0
PC82-71	1	0	2	1	0	1	0	2	2	0	1	2	3	0	0	0	0	0	0	3	0	1	0	3	2	2	1	3	2	2	2	2	0	0
PC82-136	0	0	2	0	0	2	0	2	2	0	1	2	1	0	0	0	0	0	0	2	0	1	0	0	2	2	1	3	1	3	3	1	0	0
PC82-140	0	0	2	1	0	1	0	2	2	0	1	2	1	0	0	0	0	0	0	1	0	1	0	0	2	2	1	3	1	3	3	1	0	0
KR8701	1	1	1	1	1	2	0	1	2	1	1	1	2	0	3	0	1	0	0	1	2	3	0	1	3	0	1	1	0	0	2	0	0	0
KR8702	1	0	1	1	1	2	0	1	3	0	2	2	3	0	2	1	0	0	0	2	0	3	0	2	3	0	1	1	1	1	2	1	0	0
KR8703	1	0	3	1	0	2	0	2	2	0	1	2	2	0	1	0	1	0	0	3	0	1	0	2	2	2	1	1	2	1	2	1	0	0
KR8705	0	0	2	0	1	2	0	2	3	0	1	2	1	0	1	0	0	0	0	1	0	1	0	1	3	0	1	1	0	1	2	1	0	0
KR8706	2	0	2	0	1	1	0	2	2	0	1	2	3	0	1	0	0	0	0	3	1	1	0	2	2	0	2	1	1	1	2	1	0	0
KR8707	0	0	3	1	0	2	0	2	2	0	1	2	3	0	0	0	0	0	0	3	0	0	0	1	2	2	1	1	2	3	3	0	0	0
KR8708	1	0	2	0	0	2	0	1	3	0	0	2	0	0	3	0	0	0	0	3	0	0	0	1	3	1	1	0	1	0	1	0	0	0
KR8710	1	0	2	1	1	2	0	1	2	0	1	2	3	0	3	0	0	0	0	2	0	1	0	3	3	1	1	1	1	1	2	0	0	0
KR8712	1	0	1	0	1	2	0	1	3	0	1	1	1	0	2	1	0	0	0	2	0	1	1	1	3	0	1	0	1	0	2	0	0	0
KR8713	0	0	0	0	0	2	0	0	2	0	0	0	1	0	1	0	0	0	0	1	0	2	0	1	2	0	0	0	1	0	3	0	0	0
KR8714	1	0	0	0	0	2	0	0	2	2	0	0	3	0	1	0	0	0	0	1	0	3	0	1	3	0	1	0	1	0	2	0	0	0
KR8801	0	0	0	0	1	2	1	0	3	2	1	0	1	1	1	2	0	1	0	1	0	1	1	2	3	0	0	1	1	0	1	0	1	0
KR8802	1	0	0	0	3	2	1	0	3	1	0	0	1	0	3	1	0	0	1	1	0	1	0	1	3	0	0	0	1	0	2	0	1	1
KR8803	0	0	0	0	3	2	1	0	3	2	1	0	1	2	2	1	0	0	0	1	0	2	2	1	3	0	0	0	1	0	1	1	2	0
KR8804	1	0	0	0	2	2	0	0	3	2	1	0	0	0	1	2	0	0	1	1	1	2	1	2	3	0	0	0	0	0	0	0	2	0
KR8805	1	0	1	0	2	2	0	0	3	0	1	1	1	0	1	1	1	0	1	1	1	3	0	1	2	0	0	0	0	0	1	0	1	0
KR8806	0	0	0	0	3	1	3	0	2	0	0	0	0	3	1	2	0	1	1	1	1	0	3	1	3	0	0	1	0	0	0	0	2	1
KR8807	0	0	0	0	3	0	3	0	2	1	0	0	0	3	1	1	0	0	0	0	0	0	3	1	3	0	0	0	0	0	0	0	2	1
KR8808	1	0	0	0	3	2	2	0	3	2	1	0	0	3	2	2	0	0	1	1	1	1	3	1	3	0	0	0	0	0	0	0	2	0
KR8809	1	0	0	0	3	1	2	0	3	1	0	1	0	3	2	2	0	0	0	1	0	1	1	2	3	0	1	0	0	0	0	0	2	0
KR8810	1	0	0	0	3	1	0	0	3	0	0	0	1	0	2	1	0	0	0	1	1	3	0	2	2	0	0	0	1	0	0	0	0	0
KR8811	1	0	0	0	2	1	0	0	3	0	1	0	0	0	1	1	1	0	0	1	0	3	0	2	2	0	0	0	0	0	0	0	0	0
KR8812	0	1	0	0	2	0	0	0	3	0	0	1	1	0	2	1	1	0	0	1	0	3	0	2	3	0	0	0	0	0	0	0	1	0
KR8813	1	0	0	0	2	0	0	0	3	0	1	0	0	0	2	1	1	0	0	2	0	3	0	1	3	0	1	0	0	0	0	1	0	0
KR8814	1	0	0	0	2	1	0	0	3	0	1	1	0	0	1	0	0	0	1	2	0	3	0	1	3	0	1	1	0	0	0	0	0	0
KR8815	1	0	1	0	1	2	0	1	3	0	0	2	0	0	3	0	0	0	1	1	0	2	0	1	2	0	1	0	0	0	0	0	0	0
KR8816	1	0	1	0	1	2	0	1	3	0	1	2	0	0	3	0	0	0	0	1	0	0	0	1	3	1	1	1	0	0	0	0	0	0
KR8817	1	0	2	0	0	1	0	3	2	0	1	2	1	0	1	0	0	0	0	2	0	0	0	1	2	1	2	2	0	0	3	0	0	0
KR8818	1	1	1	0	0	1	0	3	2	0	1	2	1	0	1	0	0	0	0	2	0	2	0	1	2	1	3	1	0	0	2	0	0	0
KR8819	1	0	1	0	1	2	0	2	3	0	2	2	0	0	2	0	0	0	1	2	0	0	0	1	3	0	2	2	0	0	2	0	0	0
KR8820	1	0	1	0	1	2	0	2	3	0	1	2	1	0	1	0	1	0	0	2	0	0	0	1	2	0	2	0	0	0	2	0	0	0
KR8821	1	0	2	0	0	2	0	2	3	0	1	2	0	0	2	0	0	0	0	2	0	1	0	1	2	1	1	1	1	0	2	0	0	0
KR8822	0	0	1	0	0	2	0	2	3	0	2	2	1	0	2	0	0	0	1	2	0	1	0	1	3	0	2	1	0	1	1	0	0	0
KR8823	0	0	1	0	2	2	0	1	3	0	2	1	0	0	1	0	0	0	0	1	0	0	0	1	3	1	1	0	0	0	2	0	0	0
KR8824	1	0	1	0	1	2	0	2	3	0	1	2	1	0	1	0	0	0	1	2	0	0	0	1	3	0	1	1	1	0	2	1	0	0
KR8825	1	0	2	1	1	2	0	2	3	0	1	2	0	0	2	0	0	0	1	2	0	1	0	0	2	1	1	0	0	0	2	0	0	0
KR8827	0	0	2	1	2	2	0	2	3	0	1	2	1	0	3	0	0	0	1	1	0	1	0	1	3	0	1	0	0	0	2	0	0	0
KR8828	0	0	2	1	0	2	0	2	3	0	0	2	0	0	0	0	0	0	0	0	0	1	0	0	3	0	0	0	0	0	2	0	0	0
KR8829	0	0	1	0	1	2	0	1	3	0	1	2	1	0	2	1	0	0	0	2	0	1	0	1	3	0	1	1	0	0	1	0	0	0
KR8830	1	0	1	0	2	2	0	0	3	0	2	1	1	0	2	1	1	0	1	2	0	3	0	1	3	0	1	0	0	0	0	0	0	0
KR8831	0	0	0	0	2	2	0	0	3	0	2	2	0	0	2	1	0	0	0	0	0	1	0	1	3	0	0	0	0	0	0	1	0	0
8702-DISS-5'	1	0	1	1	2	2	0	1	3	0	2	2	2	0	1	1	0	0	0	2	0	3	0	2	3	0	1	1	1	1	2	1	0	0
8702-DISS10'	1	0	1	1	1	2	0	1	3	0	2	1	3	0	1	1	0	0	0	2	0	3	0	2	3	0	1	1	1	1	2	1	0	0
8702-DISS20'	1	0	1	1	1	2	0	1	3	0	1	1	3	0	2	1	0	0	0	3	0	3	1	3	0	1	1	1	1	2	1	0	0	0
8702-DISS35'	1	0	1	1	1	2	0	1	2	0	2	1	3	0	3	1	0	0	0	3	0	3	0	1	3	0	1	1	1	1	2	1	0	0
8702-DISS60'	1	0	1	1	2	2	0	1	2	0	1	1	3	0	1	1	0	0	0	2	0	3	0	1	3	0	1	1	1	1	2	0	0	0
8702DISS120'	1	0	2	1	1	2	0	1	2	0	2	1	2	0	3	0	0	0	0	2	0	3	0	1	3	0	1	1	1	1	2	0	0	0
8702DISS180'	0	0	1	1	2	2	0	1	2	0	1	1	2	0	1	0	0	0	0	2	0	2	0	1	3	0	1	0	1	1	1	0	0	0
8702-DISS-240	0	0	1	1	2	2	0	0	2	0	1	1	1	0	1	0	0	0	0	1	0	1	1	1	3	0	0	0	1	0	1	0	0	0
8702-DISS24H	0	0	0	0	1	2	0	0	2	0	0	1	0	0	0	0	0	0	0	0	0	0	0	0	3	0	0	0	0	0	2	0	0	0
8707-DISS5'	0	0	3	1	0	2	0	2	2	0	1	2	2	1	0	0	0	0	0	3	0	1	0	1	2	2	1	2	2	2	3	0	0	0
8707-DISS10'	0	0	3	1	0	2	0	2	2	0	0	2	3	0	1	0	0	0	0	3	0	1	0	1	2	2	1	2	2	3	3	0	0	0
8707-DISS20'	0	0	3	1	0	2	0	2	2	0	0	2	3	0	1	0	0	0	0	3	0	1	0	1	2	2	1	2	2	2	3	0	0	0

Appendix 2.1. Original Ranked 166 surface sample database .

Core	*A. parvulus*	*Chaetoceros spp.*	*A. actinochilus*	*S. microtrias*	*A. tabularis*	*E. antarctica*	*H. cuneiformis*	*F. curta*	*F. kerguelensis*	*F. ritscheri*	*F. seperanda*	*F. sublinearis*	*R. styliformis*	*R. tesselata*	*T. oliverana*	*T. nitzschioides*	*T. decipiens*	*T. delicatulata*	*T. trifulta*	*T. gracilis*	*T. lineata*	*Thalassiosthrix spp.*	*Dictyocha spp.*	*Distephanus spp.*	*T. lentiginosa*	*F. cylindrus*	*F. rhombica*	*P. glacialis*	*O. weissflogii*	*Cocconeis spp.*	*T. antarctica*	*T. tumida*	*T. oestrupi*	*P. dolilolus*
8707-DISS35'	0	0	2	1	0	2	0	2	2	0	0	2	1	0	1	0	0	0	0	3	0	1	0	1	2	2	1	2	2	3	3	0	0	0
8707-DISS60'	0	0	3	1	0	2	0	2	2	0	0	2	2	0	1	0	0	0	0	2	0	1	0	1	2	2	1	1	2	3	3	0	0	0
8707DISS120'	0	0	3	1	0	2	0	2	2	0	0	2	1	0	1	0	0	0	0	1	0	0	0	1	3	2	1	1	1	3	3	0	0	0
8707-DISS180	0	0	2	3	0	2	0	2	2	0	0	2	0	0	1	0	0	0	0	2	0	0	0	1	3	0	1	2	1	3	3	0	0	0
8707DISS240'	0	0	2	0	0	2	0	1	2	0	0	1	0	0	0	0	0	0	0	2	0	0	0	0	3	0	0	0	0	3	3	0	0	0
8808-DISS05'	1	0	0	0	3	2	2	0	3	2	1	0	0	3	2	2	0	0	1	1	1	1	3	1	3	0	0	0	0	0	0	0	2	0
8808-DISS10'	1	0	0	0	3	2	3	0	3	0	1	0	1	3	2	2	0	0	0	1	1	1	0	2	3	0	0	0	0	0	0	0	0	0
8808-DISS020	1	0	0	0	3	1	1	0	3	0	1	0	1	3	1	2	0	0	0	1	1	1	0	2	3	0	0	0	0	0	0	0	0	0
8808-DISS035	0	0	0	0	3	1	0	0	3	0	1	0	1	0	3	2	0	0	0	1	0	1	0	0	3	0	0	0	0	0	0	0	0	0
8808-DISS60'	0	0	0	0	2	1	0	0	3	0	1	0	1	0	3	1	0	0	0	0	0	0	0	0	3	0	0	0	0	0	0	0	0	0
8808-DISS0120	0	0	0	0	2	1	0	0	3	0	0	0	0	0	1	1	0	0	0	0	0	0	0	0	3	0	0	0	0	0	0	0	0	0
8808-DISS0180	0	0	0	0	2	1	0	0	3	0	0	0	0	0	2	1	0	0	0	0	0	0	0	0	3	0	0	0	0	0	0	0	0	0
8808-DISS0240	0	0	0	0	2	2	0	0	3	0	0	0	0	0	0	1	0	0	0	0	0	0	0	0	3	0	0	0	0	0	0	0	0	0
8808-DISS24H	0	0	0	0	2	0	0	0	3	0	0	0	0	0	0	0	0	0	0	0	0	0	0	0	3	0	0	0	0	0	0	0	0	0
8808-DISS48H	0	0	0	0	0	0	0	0	2	0	0	0	0	0	0	0	0	0	0	0	0	0	0	0	3	0	0	0	0	0	0	0	0	0
8810DISS0-20	1	0	0	0	3	1	0	0	3	0	0	0	1	0	2	1	0	0	0	1	1	3	0	2	2	0	0	0	1	0	0	0	0	0
8810DISS3560	1	0	0	0	3	1	0	0	3	0	0	0	0	0	1	1	0	0	0	1	1	3	0	1	2	0	0	0	1	0	0	0	0	0
8810DISS120	1	0	0	0	3	1	0	0	3	0	0	0	0	0	1	1	0	0	0	1	0	2	0	1	3	0	0	0	1	0	0	0	0	0
8810DISS180	0	0	0	0	3	1	0	0	3	0	0	0	0	0	1	1	0	0	0	1	0	2	0	1	3	0	0	0	0	0	0	0	0	0
8810DISS240'	0	0	0	0	3	1	0	0	3	0	0	0	0	0	2	1	0	0	0	1	0	1	0	1	3	0	0	0	0	0	0	0	0	0
8810DISS24H	0	0	0	0	2	1	0	0	3	0	0	0	0	0	3	0	0	0	0	2	0	0	0	2	3	0	0	0	0	0	0	0	0	0
8818DISS0-05	1	1	1	0	0	1	0	3	2	0	1	2	1	0	1	0	0	0	0	2	0	2	0	1	2	1	3	1	0	0	2	0	0	0
8818-DISS10'	1	0	2	0	0	2	0	3	2	0	1	3	1	0	1	0	0	0	1	2	1	2	0	1	2	1	3	1	1	1	2	0	0	0
8818-DISS20'	1	0	1	0	0	2	0	3	2	0	1	2	1	0	1	0	0	0	1	2	1	2	0	1	2	0	3	1	1	1	2	0	0	0
8818DISS035	1	0	1	0	0	2	0	3	2	0	1	2	1	0	1	0	0	0	1	1	1	2	0	1	2	0	3	1	1	1	2	0	0	0
8818DISS120'	1	0	2	0	0	2	0	2	2	0	1	2	1	0	1	0	0	0	1	2	1	1	0	1	2	0	3	1	1	1	2	0	0	0
8818DISS180'	1	0	2	0	0	2	0	2	2	0	1	2	1	0	3	0	0	0	1	2	1	1	0	1	2	0	3	2	1	1	3	0	0	0
8818DISS240'	1	0	2	0	0	2	0	1	2	0	1	2	1	0	1	0	0	0	0	1	1	1	0	0	3	0	1	0	1	1	2	0	0	0
8818-DISS24H	0	0	2	0	0	2	0	0	2	0	0	2	1	0	3	0	0	0	0	0	0	0	0	0	3	0	0	0	1	1	2	0	0	0
8818-DISS48H	0	0	2	0	0	2	0	0	2	0	0	2	0	0	1	0	0	0	0	0	0	0	0	0	3	0	0	0	1	0	1	0	0	0

Appendix 2.2. Raw data of 166 database.

LKA Code	1	2	3	4	5	6	7	8	9	10	11	12	13	14	15	16	17	18	19	20	21	22	23	24	25	26	27
Core	V16-65	V16-60	1176-91	1176-88	1277-2	RC11-80	RC15-91	RC11-78	RC13-255	1176-82	RC13-274	RC13-273	MD24-KK63	RC13-263	1277-28	MD82 424	1141-2P	1184-6P	1147-4P	P1160	1178-4P	1010W	1192W	1212W	1223W	1277-41	RC17-56
Lat °S	45°00'	49°59.6'	44°56.7'	46°57.8'	45°02.1'	46°45'	49°55.3'	50°52'	50°34'	59°31.2'	53°09'	55°04.5'	51°56'	53°48.3'	61°20'	54°05.8'	61°31.8'	62°17'	61°36.1'	60°46.6'	61°24.4'	77°20'	54°30.0'	75°31.1'	75°58.9'	69°59.9'	65°24'
Species Long.	45°46'E	36°45.5'E	15°02.9'E	14°18.2'E	22°28.2'E	00°03'W	15°34.1'W	09°52'W	02°53.7'E	13°11.5'E	12°25.6'E	11°34.5'E	42°53'E	08°13'W	09°11'E	00°20.7'W	61°47.4'W	57°20.5'W	54°51.6'W	45°47.9'W	46°58.9'W	35°00'W	03°48.4'E	56°53.8'W	33°32.9'W	05°04.6'W	37°43'E
"Achnanthes brevipes (var. angustata)"																											
Actinocyclus actinochilus ("Charcotia act.")	1	6	2	6	3	1				1	8				3	2	12	9	5	11	34	3	2	5	12	39	16
Actinocyclus curvatulus																											
Actinocyclus ingens		1																									
Actinocyclus spp.																											
Asteromphalus heptactis																											
Asteromphalus hookeri					2		1	1					1	1		4											
Asteromphalus hyalinus																1											
Asteromphalus parvulus		2			2						2	2	2		5	1											
"Asteromphalus robustus"													1	1													
Azpeitia tabularis			10																								
"C. stellaris var symbolophorus"	5			4	1				1				1			1					7						
Chaetoceros spp.													1	1		1	3					1	1				
Cocconeis spp.																	3	12	1	2	3				2		
Coscinodiscus asteromphalus																1											
"Coscinodiscus bullatus"																				1							
Coscinodiscus centralis																											
Coscinodiscus curvatulus	1						1						2			1											
Coscinodiscus decrescens							1																				
"Coscinodiscus eccentrica"																						4					
"Coscinodiscus furcatus"																											
"Coscinodiscus lineatus"							1			3				1							1						
Coscinodiscus marginatus																											
Coscinodiscus nodulifer																											
Coscinodiscus occuloides																											
Coscinodiscus oculus-iridus																											
Coscinodiscus radiatus				1		1															2						
"Coscinodiscus nitscherii"																											
Coscinodiscus spp.																											
"Coscinodiscus symbolophorus"																											
"Coscinodiscus tabularis"	15	12		3	8	8	15	16	11	4	1	3	9	2		3											
"Coscinodiscus tabularis var. egregius"					1		2				1		2														
Dactyliosolen antarctica																											
Dictyocha spp.	3		12	3	10	1																					
Distephanus spp.	15	2	10	4	10	4	5	6	1	3	3	5	3	8	2	11	1			1	5	1			2		
Eucampia antarctica	16	22	6	26	7	13	26	12	9	9	28	7	1	4	2	3	1		3	1	17	19	33	23	110	69	9
Grammatophora arcuata																											
Hemidiscus cuneiformis			4		1																						
Hemidiscus karstenii																											
Melosira adeliae																								1			
Melosira sol ("Paralia sol")																											1
Navicula directa														1				1									
"Nitzschia angulata"								2		1	1			1			5	2	3	1	8				3		
"Nitzschia bicapitata"																											
"Nitzschia closterium"																											
"Nitzschia curta"						1						4		4	1		30	10	4	25	21	48	10	6	19		
"Nitzschia cylindrus"											1						15	14	2	2	16	13	12	1	8		
"Nitzschia denticuloides"															5												
"Nitzschia fraudulenta"																											
"Nitzschia grunowii"					2							1															
"Nitzschia heimii"																											
"Nitzschia karguelensis"	108	190	166	151	146	88	150	193	179	225	176	244	187	221	218	179	27	6	5	7	32				2	128	126
"Nitzschia koloczeckii"																											
Nitzschia lecointei																					1	1		1	1		
"Nitzschia obliquecostata"	1																										
Nitzschia paundriformis																											
"Nitzschia pseudonana"						1			1		1	1															
"Nitzschia reinholdii"		5		3	6		1	1		3				1													
"Nitzschia separanda"		3	1	1	3	1	1	1		2	3	2	1	6	4	5	1										6
"Nitzschia seriata"			2																								
"Nitzschia sicula var. bicuneata"																											
"Nitzschia sicula var. rostrata"	1															1											1

Appendix 2.2. Raw data of 166 database.

LKA Code	1	2	3	4	5	6	7	8	9	10	11	12	13	14	15	16	17	18	19	20	21	22	23	24	25	26	27
Core	V16-65	V16-60	1176-91	1176-88	1277-2	RC11-80	RC15-91	RC11-78	RC13-255	1176-82	RC13-274	RC13-273	MD24-KK63	RC13-263	1277-28	MD82 424	1141-2P	1184-6P	1147-4P	P1160	1178-4P	1010W	1192W	1212W	1223W	1277-41	RC17-56
Lat °S	45°00'	49°59.6'	44°56.7'	46°57.6'	45°02.1'	46°45'	49°55.3'	50°52'	50°34'	59°31.2'	53°00'	55°04.5'	51°56'	53°48.3'	61°28'	54°05.8'	61°31.8'	62°17'	61°36.1'	60°46.6'	61°24.4'	77°20'	54°30.0'	75°31.1'	75°58.9'	69°59.9'	65°24'
Species Long.	45°46'E	36°45.5'E	15°02.9'E	14°18.2'E	22°28.2'E	00°03'W	15°34.1'W	09°52'W	02°53.7'E	13°11.5'E	12°25.6'E	11°34.5'E	42°53'E	08°13'W	09°11'E	00°20.7'W	61°47.4'W	57°20.5'W	54°51.6'W	45°47.9'W	46°58.9'W	35°00'W	03°48.4'E	56°53.8'W	33°32.9'W	05°04.6'W	37°43'E
"Nitzschia sicula"																											
"Nitzschia sublinearis"	1	3	3	4	5		1	2	4	1	8	8		7	16	7	10	12	6	10	12	18	18	16	35	24	12
Odontella litigiosa																											
Odontella weissflogii																	20	7	14	4	39						
Paralia sulcata																						1					
Pleurosigma directum													1			1											
Porosira glacialis																	4	3	5	8	6	1		1			
Porosira pseudodenticulata																											
"Pseudonotia doliolus"			1		3																						
"Rhizosolenia alata"																											
"Rhizosolenia barboi"													1														
Rhizosolenia bergonii																											
Rhizosolenia "hebetata f. bidens"																				1	1						
Rhizosolenia "hebetata f. semispina "													1								4						
Rhizosolenia styliformis		1	1	2	1	3	1		2		2		1			1	3	1	2	6	16						1
"Rocella gelida"																											
Roperia tesselata			18		10																						
Rouxia spp.																											
Stellarima microtrias			5																								
T. oliverana ("Schimperiella antarctica")	6			2	5		3	4	2	2			8	2	3	2				1	4					5	4
Thalassionema nitzschioides	13		20	4	12	12	4	3	11				1			1											
Thalassionema nitzschioides var. parva																											
Thalassiosira ambigua																											
Thalassiosira antarctica			1		1												59	21	39	20	38	6					
Thalassiosira australis																											
Thalassiosira cf. maculata																											
Thalassiosira decipiens			5	3	5	1	3	3	4					2		1	2						1				1
"Thalassiosira delicatulata (delicatula)"	1						1								1	1	1	5		4							
Thalassiosira eccentrica	1				7	2				1			1		1	1			1						1		
Thalassiosira eccentrica var. jousei																											
Thalassiosira fraguellii																											
Thalassiosira fraguelliopsis																											
Thalassiosira gerloffi																											
Thalassiosira gracilis	4	4	1	1	4	3	3	8	12	2	11	5	6	3	6	5	10	7	1		5						2
Thalassiosira gracilis var. expecta																											
Thalassiosira gravida																											
Thalassiosira lentiginosa	123	45	52	85	66	62	78	51	61	43	63	24	65	34	35	70	6			1	52		3			60	33
Thalassiosira lineata	3		6	1	2	1		1					1			1											
Thalassiosira oestrupii	2		1	1	2	1							1	1		1											
Thalassiosira perpusilla																											
Thalassiosira poroseriata																											
Thalassiosira ritscheri																											
Thalassiosira scotia																											
Thalassiosira spp.	1				1																6				11		
Thalassiosira symmetrica																											
Thalassiosira trifulta			4																								
Thalassiosira tumida																					11	1					
Thalassiothrix spp.		1		3	3	3	3	1	3	5		1	8	7	3	3		2		1	2		1		3	3	5
Other unidentified spp.								1							1												
TOTAL	321	299	331	308	329	207	300	307	301	305	309	307	304	308	306	309	213	112	91	107	343	117	81	54	206	331	217

Notes:
Species names with quotations are no longer considered valid. Refer to Chapter 2 for discussion.

Appendix 2.2. Raw data of 166 database.

LKA Code	28	29	30	31	32	33	34	35	36	37	38	39	40	41	42	43	44	45	46	47	48	49	50	51	52	53	54
Core	MD82 436	1176-55	1176-65	1277-8	1277-12	1578-49	1678-64	1678-80	1678-84	1678-89	1678-96	RC8-46	RC11-71	RC11-77	RC11-90	RC13-257	RC13-268	RC13-269	RC13-270	RC13-272	RC12-292	V14-53	V14-58	MD24 KK02	MD24 KK32	MD24 KK35	MD24 KK37
Lat °S	61°13.6'	53°22.9'	57°12.5'	50°32.5'	54°00.6'	61°05.6'	54°00.5'	47°57'	51°57.5'	57°03.6'	60°27.9'	55°20'	49°08'	53°03'	56°38'	55°02.2'	57°02.3'	52°37.6'	55°28.8'	55°05.1'	39°40.6'	56°43'	57°37'	54°13'	54°30'	53°08.3'	52°58.4'
Species Long.	19°28.8'W	06°39.6'E	08°12.4'E	20°53'E	19°47.5'E	19°51.9'W	24°11.7'W	13°01.4'W	14°25.2'W	18°32.4'W	21°37.1'W	65°28'E	37°25'E	16°27'W	25°43'E	03°00.1'W	00°05.6'W	00°07.5'E	04°38.2'E	08°00'E	15°28.5'W	24°31'W	13°36'W	03°31'E	03°48.4'E	19°24.7'E	23°46.3'E
"Achnanthes brevipes (var. angustata)"																											
Actinocyclus actinochilus ("Charcotia act.")	24	1				16		2		7	4	1				2	6		4	3		1	3	2	1	4	1
Actinocyclus curvatulus				1					2	1												1	1		4	1	
Actinocyclus ingens												2															
Actinocyclus spp.																											
Asteromphalus heptactis								1																			
Asteromphalus hookeri		1	1	2				1								1									1	1	2
Asteromphalus hyalinus					1																			1			
Asteromphalus parvulus	2	4			5			1	1	4	2	4	1		1		1		2	2			2	9	2	3	4
"Asteromphalus robustus"																								2	1		
Azpeitia tabularis																					7						
"C. stellaris var symbolophorus"	2		1					2	1		1					1				1			1			1
Chaetoceros spp.		7		1	1			1			1													2	2	2	4
Cocconeis spp.		1					1																				
Coscinodiscus asteromphalus								2			1														3		
"Coscinodiscus bullatus"	1																							2	1	1	
Coscinodiscus centralis																											
Coscinodiscus curvatulus							1	1		1	2													1	1	1	1
Coscinodiscus decrescens																											
"Coscinodiscus eccentrica"																											
"Coscinodiscus furcatus"																											
"Coscinodiscus lineatus"			1	1			1	1				1						1	1		2		2	1			
Coscinodiscus marginatus							6						2														
Coscinodiscus nodulifer																											
Coscinodiscus occuloides																											
Coscinodiscus oculus-indus																											
Coscinodiscus radiatus	1	1					1	2					1			1								1	1		
"Coscinodiscus ritscherii"																											
Coscinodiscus spp.																											
"Coscinodiscus symbolophorus"																											
"Coscinodiscus tabularis"	3	1			2	2	1	7	7		3	4	5	1	8	8	1	5	4	2		2	3	1	8	1	1
"Coscinodiscus tabularis var. egregius"							2		1																		
Dactyliosolen antarctica			1																								
Dictyocha spp.																					5						
Distephanus spp.	1	2	3	3	3	1	2	3	3	2	10	3		2	1	5	3	2	3	3		4		4	9	3	2
Eucampia antarctica	69	3		7	9	42	34	46	21	23	39	7	25	8	5	8	14	2	26	15		8	52	7	19	7	3
Grammatophora arcuata																											
Hemidiscus cuneiformis																					16						
Hemidiscus karstenii																											
Melosira adeliae																											
Melosira sol ("Paralia sol")																											
Navicula directa		2																									
"Nitzschia angulata"		2	1	1	2	4		1		1	1		1		2	1	3	2	1	4		3				1	1
"Nitzschia bicapitata"							1														1						
"Nitzschia closterium"																											
"Nitzschia curta"		6	1		2	1	1	1		3	5				2	1	3			6		1	4	1			
"Nitzschia cylindrus"	1			1	1					1									2							1	
"Nitzschia denticuloides"		1					1					1								2							
"Nitzschia fraudulenta"																											
"Nitzschia grunowii"																	1										
"Nitzschia heimii"																											
"Nitzschia karguelensis"	72	161	242	178	201	121	145	145	159	158	122	228	59	70	231	206	192	244	137	183	2	58	147	180	146	172	195
"Nitzschia koloczeckii"																											
Nitzschia lecointei																											
"Nitzschia obliquecostata"			1						1																		
Nitzschia paundriformis																											
"Nitzschia pseudonana"		1		1	7		1		1								1		1	3							
"Nitzschia ritscherii"		1			1		6	5	2	1		2	8	2		1								2	1		1
"Nitzschia seperanda"		4	1	4	3	1	4			4	8	2		1	5	1	3	6	2	3		1		2	1	1	9
"Nitzschia seriata"																											
"Nitzschia sicula var. bicuneata"																											
"Nitzschia sicula var. rostrata"	1	1																									

Appendix 2.2. Raw data of 166 database.

	LRA Code	28	29	30	31	32	33	34	35	36	37	38	39	40	41	42	43	44	45	46	47	48	49	50	51	52	53	54
	Core	MD82 436	1176-55	1176-65	1277-8	1277-12	1578-49	1678-64	1678-80	1678-84	1678-89	1678-96	RC8-46	RC11-71	RC11-77	RC11-90	RC13-257	RC13-268	RC13-269	RC13-270	RC13-272	RC12-292	V14-53	V14-58	MD24 KK02	MD24 KK32	MD24 KK35	MD24 KK37
	Lat °S	61°13.6'	53°22.9'	57°12.5'	50°32.5'	54°00.6'	61°05.6'	54°00.5'	47°57'	51°57.5'	57°03.6'	60°27.9'	55°20'	49°08'	53°03'	56°38'	55°02.2'	57°02.3'	52°37.6'	55°28.8'	55°05.1'	39°40.6'	56°43'	57°37'	54°13'	54°30'	53°08.3'	52°58.4'
Species	Long.	19°28.6'W	06°30.6'E	08°12.4'E	20°53'E	19°47.5'E	19°51.9'W	24°11.7'W	13°01.4'W	14°25.2'W	18°32.4'W	21°37.1'W	65°28'E	37°25'E	16°27'W	25°43'E	03°00.1'W	00°05.6'W	00°07.5'E	04°38.2'E	08°00'E	15°28.5'W	24°31'W	13°36'W	03°31'E	03°48.4'E	19°24.7'E	23°46.3'E
"Nitzschia sicula"																												
"Nitzschia sublinearis"			5	8	3		11	3	1	2	2	10	3			6	3	5	9	3	7		3	6	5	2	1	4
Odontella litigiosa																												
Odontella weissflogii			1							3					1											3	1	
Paralia sulcata																												
Pleurosigma directum												1														1	1	1
Porosira glacialis																												
Porosira pseudodenticulata																												
"Pseudonotia doliolus"																						49						
"Rhizosolenia alata"																												
"Rhizosolenia barboi"																									1			
Rhizosolenia bergonii																												
Rhizosolenia "hebetata f. bidens"				1		1																			1			
Rhizosolenia "hebetata f. semispina"	1										1	1				1	1									1	1	
Rhizosolenia styliformis	1	2	1	2		1	3	2	1			11	1	6			1		1				6		3	1	1	1
"Rocella gelida"																												
Roperia tesselata														5								4						
Rouxia spp.			1																									
Stellarima microtrias																												
T. oliverana ("Schimperiella antarctica")	2	6	1	5		3	2	2	3	1	3	1	1		3	2	3		5	6		1	1	1	3	7	1
Thalassionema nitzschioides		1					2	5	4				1	1		1	1	2			2			1		1	1
Thalassionema nitzschioides var. parva																					1							
Thalassiosira ambigua																												
Thalassiosira antarctica						1			3																			
Thalassiosira australis																												
Thalassiosira cf. maculata																					1							
Thalassiosira decipiens									3					1	1	1									1	1	1	
"Thalassiosira delicatulata (delicatula)"				1	1			6				1	2						1	1				2				
Thalassiosira eccentrica		3		2			1	2	1	2									1						1	1		1
Thalassiosira eccentrica var. jousei		1	1	2				1																	1		1	
Thalassiosira frenguellii																												
Thalassiosira frenguelliopsis																												
Thalassiosira gerloffi																												
Thalassiosira gracilis	1	4	10	3	6	2	3	4	6	5	4	3	1	3	3	4	9	6	5	5		1	2	7	2	3	2
Thalassiosira gracilis var. expecta																												
Thalassiosira gravida																									1			
Thalassiosira lentiginosa	116	75	26	72	54	95	78	58	74	78	79	36	60	14	31	56	53	19	102	64	8	16	72	61	82	79	56
Thalassiosira lineata		2		1	1			1	1				1		1				1		1		1		1	1		
Thalassiosira oestrupii				2			4			1			1								16				2	23	1
Thalassiosira perpusilla																												
Thalassiosira poroseriata																												
Thalassiosira ritscheri																												
Thalassiosira scotia																												
Thalassiosira spp.															1													
Thalassiosira symmetrica																												
Thalassiosira trifulta																												
Thalassiosira tumida											1																	
Thalassiothrix spp.		2	6	3	4	3	2	4		3	8	14	3	1	2	1	3	3	2			3	1	2	6	5	7	6
Other unidentified spp.							1					2						1										
	TOTAL	300	306	304	298	303	305	308	304	303	305	325	305	179	106	301	307	305	302	301	309	118	107	300	307	307	327	300

Appendix 2.2. Raw data of 166 database.

Species	LKA Code	55	56	57	58	59	60	61	62	63	64	65	66	67	68	69	70	71	72	73	74	75	76	77	78	79	80	81
	Core	MD82 425	MD82 430	MD82 434	MD84 531	MD84 530	MD84 532	MD84 533	MD 84 540	MD84 552	MD84 557	MD84 562	MD84 563	MD84 569	83-11C III	83-12 III	83-19 III	83-41 III	83-42 III	PC82-197	PC82-71	PC82-136	PC82-140	KR8701	KR8702	KR8703	KR8705	KR8706
	Lat °S	55°34.7'	57°52.3'	58°51.8'	66°57.7'	66°06.6	66°06.9'	65°09.1'	60°44.5'	54°55.4'	53°19.6'	51°55.1'	50°42.7'	47°38.6'	78°15'	78°16'	77°18'	76°40'	76°38'	63°43'	62°38.4'	64°45.4'	64°49.6'	52°50'	56°27.6'	60°13.3'	64°03.3'	63°03.6'
	Long.	00°43'W	10°40.3'W	16°39'W	75°24.6'E	73°59.1'E	76°45.6'E	78°21.2'E	86°23.3'E	73°50'E	75°48'E	68°13.6'E	68°09.1'E	73°23.1'E	172°17W	170°08'W	158°43'W	164°01'W	166°03'W	57°13.6'W	59°32'W	62°45.5'W	62°37.8'W	32°30'W	33°58.5'W	48°56.9'W	48°56.9'W	63°03.7'W
"Achnanthes brevipes (var. angustata)"																						1						
Actinocyclus actinochilus ("Charcotia act.")		1	6	10	7	4	7	7	2						1	3	8	10	7	6	16	11	6	3	4	27	6	6
Actinocyclus curvatulus									1	1		1	2	1													
Actinocyclus ingens																												
Actinocyclus spp.																												
Asteromphalus heptactis																												1
Asteromphalus hookeri		1	2	1		1							1						1					1	2		1	1
Asteromphalus hyalinus																												
Asteromphalus parvulus		1	1	1		3		2	3	1	1										1			1		3		5
"Asteromphalus robustus"											1																	
Azpeitia tabularis																								3			2	3
"C. stellaris var symbolophorus"			1	1								1	1															
Chaetoceros spp.		3							1					2										1				
Cocconeis spp.				1						1										1	11	16	15			3	1	2
Coscinodiscus asteromphalus		1																										
"Coscinodiscus bullatus"		1																										
Coscinodiscus centralis																												
Coscinodiscus curvatulus				1									1	1														
Coscinodiscus decrescens																												
"Coscinodiscus eccentrica"																												
"Coscinodiscus furcatus"																					1		2	2	1	3		
"Coscinodiscus lineatus"		1			2	2				2	2																	
Coscinodiscus marginatus		1																										
Coscinodiscus nodulifer																												
Coscinodiscus occuloides																												
Coscinodiscus oculus-iridus																												
Coscinodiscus radiatus				1		1	1																					
"Coscinodiscus ritscherii"																												
Coscinodiscus spp.																												
"Coscinodiscus symbolophorus"															1	2			1									
"Coscinodiscus tabularis"		1	4	7		4		2	8	17	13	15	9	7														
"Coscinodiscus tabularis var. egregius"			5	1																								
Dactyliosolen antarctica																												
Dictyocha spp.														1														
Distephanus spp.		4	2	4	2	2	2	1	3	3	8	2	6			1			2		8			1	5	5	1	5
Eucampia antarctica		5	32	13	4	13	7	7	20		6	3	8	27	14	39	25	60	32	1	3	8	4	22	7	15	18	4
Grammatophora arcuata																						1				3		10
Hemidicus cuneiformis																												
Hemidiscus karstenii																												
Melosira adeliae																		1										
Melosira sol ("Paralia sol")														2	1						1							
Navicula directa		1								1	1									2	1	2	2		1			
"Nitzschia angulata"		1			5	1	1	1	1						1				2		3	1	1	1	2	2	2	7
"Nitzschia bicapitata"																												1
"Nitzschia closterium"																											1	
"Nitzschia curta"					32	17	9	3	5						9	23	41	150	82	4	46	31	20	1	3	14	4	23
"Nitzschia cylindrus"		1			2	1									1	2	6	8	3	2	17	18	7		2	7		
"Nitzschia denticuloides"																												
"Nitzschia fraudulenta"																												
"Nitzschia grunowii"																												
"Nitzschia heimii"																						1						
"Nitzschia kerguelensis"		223	149	165	15	103	40	40	172	217	199	196	190	144		1		1	3	1	36	12	13	118	133	68	109	116
"Nitzschia koloczeckii"																												
Nitzschia lecointei																			1			2	1					
"Nitzschia obliquecostata"		1	1	1	3	1									1			6	1		1	1	2			2		2
Nitzschia paundriformis										1	2			3														
"Nitzschia pseudonana"																					1			1	3			
"Nitzschia ritscherii"		5							4					9										2	2			
"Nitzschia seperanda"		6	1	1					6	6	3	2			1			1	3		2	2	1	1	1	1	1	3
"Nitzschia seriata"																												
"Nitzschia sicula var. bicuneata"																												
"Nitzschia sicula var. rostrata"																												

Appendix 2.2. Raw data of 166 database.

LKA Code	55	56	57	58	59	60	61	62	63	64	65	66	67	68	69	70	71	72	73	74	75	76	77	78	79	80	81
Core	MD82 425	MD82 430	MD82 434	MD84 531	MD84 530	MD84 532	MD84 533	MD 84 540	MD84 552	MD84 557	MD84 562	MD84 563	MD84 569	83-11C III	83-12 III	83-19 III	83-41 III	83-42 III	PC82-197	PC82-71	PC82-136	PC82-140	KR8701	KR8702	KR8703	KR8705	KR8706
Lat °S	55°34.7'	57°52.3'	58°51.8'	66°57.7'	66°06.6	66°06.9'	65°09.1'	60°44.5'	54°55.4'	53°19.6'	51°55.1'	50°42.7'	47°38.6'	78°15'	78°16'	77°18'	76°40'	76°38'	63°43'	62°38.4'	64°45.4'	64°49.6'	52°50'	56°27.6'	60°13.3'	64°03.3'	63°03.6'
Species Long.	00°43'W	10°40.3'W	16°39'W	75°24.6'E	73°59.1'E	76°45.6'E	78°21.2'E	86°23.3'E	73°50'E	75°48'E	68°13.6'E	68°09.1'E	73°23.1'E	172°17'W	170°08'W	158°43'W	164°01'W	166°03'W	57°13.6'W	59°32'W	62°45.5'W	62°37.8'W	32°30'W	33°58.5'W	46°58.9'W	48°56.9'W	63°03.7'W
"Nitzschia sicula"																											
"Nitzschia sublinearis"	3	3	3	13	12	7	5	5	1	2	1			15	21	10	51	47	3	16	11	8	3	6	15	6	11
Odontella litigiosa																					1						
Odontella weissflogii	1		1					1					3						4	10	3	1			22		3
Paralia sulcata																											
Pleurosigma directum	1																										
Porosira glacialis				4	2	3							1					1	5	7	11	10	1	1	1	1	1
Porosira pseudodenticulata																				1							
"Pseudonotia doliolus"																											
"Rhizosolenia alata"	1																					1	1				
"Rhizosolenia barboi"																											
Rhizosolenia bergonii																									1		
Rhizosolenia "hebetata f. bidens"	1		1																								
Rhizosolenia "hebetata f. semispina"	1		1																								
Rhizosolenia styliformis	1	1	8		2				1	2	1	1	10	1	2	2		1		24	2	2	8	14	5	4	15
"Rocella gelida"																											
Roperia tesselata																											
Rouxia spp.																											
Stellarima microtrias																				1					1		
T. oliverana ("Schimperiella antarctica")	6	2	2		2	2	1	2	2	9	3	3	4	2	1								12	3	3	4	2
Thalassionema nitzschioides									1		6	3	7														
Thalassionema nitzschioides var. parva																											
Thalassiosira ambigua																											
Thalassiosira antarctica				9		1	1						27		3	4	1	1	66	65	156	196	9	7	53	25	9
Thalassiosira australis																											
Thalassiosira cf. maculata																											
Thalassiosira decipiens			1						1														1		1		
"Thalassiosira delicatulata (delicatula)"	1	1	1		2	1																					
Thalassiosira eccentrica	2	1	2				1		1																		
Thalassiosira eccentrica var. jousei										3	1	2	1														
Thalassiosira frenguellii																							1				
Thalassiosira frenguelliopsis																											
Thalassiosira gerloffi																											
Thalassiosira gracilis	6	1	9	8	3	4	2	6	9	6	5	6	1	1		1	9	7	2	14	4	3	2	8	23	3	43
Thalassiosira gracilis var. expecta																											
Thalassiosira gravida		1																									
Thalassiosira lentiginosa	31	84	60	4	21	11	25	59	31	37	61	43	39		2	1	2		2	6	4	4	102	80	26	71	26
Thalassiosira lineata	1		1					1		3	1	2											5				1
Thalassiosira oestrupii												1															
Thalassiosira perpusilla																				4	1						
Thalassiosira poroseriata																		1									
Thalassiosira ritscheri																											
Thalassiosira scotia																								1			
Thalassiosira spp.																								2			1
Thalassiosira symmetrica																							1				
Thalassiosira trifulta																											
Thalassiosira tumida														1		1			1	5	2	2		2	1	1	1
Thalassiothrix spp.	3	6	15	2	3	3	2	2	3	3	3	3	2							3	3		3	3	3	3	3
Other unidentified spp.																											
TOTAL	317	304	313	112	200	99	100	302	300	301	302	282	292	50	100	99	300	196	100	304	305	301	308	293	308	264	305

Appendix 2.2. Raw data of 166 database.

LKA Code	82	83	84	85	86	87	88	89	90	91	92	93	94	95	96	97	98	99	100	101	102	103	104	105	106
Core	KR8707	KR8708	KR8710	KR8712	KR8713	KR8714	KR8801	KR8805	KR8806	KR8807	KR8808	KR8809	KR8810	KR8811	KR8812	KR8813	KR8814	KR8815	KR8816	KR8817	KR8818	KR8819	KR8820	KR8821	KR8822
Lat °S	62°21.2'	60°55.2'	59°39.6'	54°55.8'	52°42.8'	51°27.7'	46°40.6'	52°56.7'	49°01.3'	47°08.9'	49°15.7'	50°35.6'	54°11.2'	54°55'	56°23.8'	57°56.9'	61°16.8'	63°18.3'	64°46.2'	66°12.1'	65°45'	64°34.3'	64°56.1'	64°49.3'	64°40.1'
Species Long.	57°58.3'W	56°26.3'W	51°16.6'W	39°47.6'W	36°59.3'W	34°00.5'W	79°29.2'E	109°55.1E	128°46.3'E	145°47.8'E	148°48.2'E	147°09.3'E	144°47.9'E	144°04'E	145°17.2'E	144°35'E	144°26.5'E	141°55.5'E	141°13.4'E	140°30.2'E	138°12'E	135°37.5'E	129°00.3'E	126°43.5'E	119°30.2'E
"Achnanthes brevipes (var. angustata)"																									
Actinocyclus actinochilus ("Charcotia act.")	26	5	12	4	2	1		2						2				2	4	9	2	2	4	8	2
Actinocyclus curvatulus																									
Actinocyclus ingens									6		2	7						1							
Actinocyclus spp.			1																						
Asteromphalus heptactis															1										
Asteromphalus hookeri		1	1		1	1	2	1				1	2			1	1	1				1	1		
Asteromphalus hyalinus																									
Asteromphalus parvulus		2	1	3		3		1			1	1	1	1		1	2	5	1	2	2	2	3	1	
"Asteromphalus robustus"																									
Azpeitia tabularis			3	6	1		3	13	28	57	18	10	11	14	13	8	6	4	4			4	1		
"C. stellaris var symbolophorus"																									
Chaetoceros spp.															2						1				
Cocconeis spp.	17		1																						1
Coscinodiscus asteromphalus																									
"Coscinodiscus bullatus"																									
Coscinodiscus centralis		1																							
Coscinodiscus curvatulus								1																	
Coscinodiscus decrescens																									
"Coscinodiscus eccentrica"																									
"Coscinodiscus furcatus"	1		2		1															1					
"Coscinodiscus lineatus"																									
Coscinodiscus marginatus																									
Coscinodiscus nodulifer																									
Coscinodiscus occuloides									1																
Coscinodiscus oculus-iridus										1							1								
Coscinodiscus radiatus				1				1																	
"Coscinodiscus ritscherii"																									
Coscinodiscus spp.																									
"Coscinodiscus symbolophorus"																									
"Coscinodiscus tabularis"																									
"Coscinodiscus tabularis var. egregius"																									
Dactyliosolen antarctica																									
Dictyocha spp.				1					7	9	7	2													
Distephanus spp.	1	4	9	6	5	1	6	3	1	3	3	9	7	7	5	4	2	2	1	3	3	1	5	3	5
Eucampia antarctica	12	18	14	19	28	34	22	5	2		5	2	1	1			2	6	17	3	2	15	14	15	11
Grammatophora arcuata			2		1	2															1			2	
Hemidiscus cuneiformis							2		9	12	3	3													
Hemidiscus karstenii																									
Melosira adeliae																									
Melosira sol ("Paralia sol")																									
Navicula directa																					1				
"Nitzschia angulata"	1	2	4	1		2						3				1	2	2	3	17	44	5	8	3	8
"Nitzschia bicapitata"																									
"Nitzschia closterium"																									
"Nitzschia curta"	13	1	3	1		1												2	5	85	170	5	34	32	12
"Nitzschia cylindrus"	10	2	1																1	2	5			2	
"Nitzschia denticuloides"																									
"Nitzschia fraudulenta"																									
"Nitzschia grunowii"																				3			1	1	
"Nitzschia heimii"																									
"Nitzschia kerguelensis"	41	142	130	200	57	148	166	205	66	105	149	140	321	302	193	190	193	203	200	56	93	145	266	164	261
"Nitzschia koloczeckii"																									
Nitzschia lecointei																									
"Nitzschia obliquecostata"																				7	1	2	6	2	3
Nitzschia paundriformis																									
"Nitzschia pseudonana"		1																							
"Nitzschia ritscherii"						10	6			4	7	1									2				
"Nitzschia seperanda"	1		2	2		1	1	5			2			4		1	4		2	3	2	6	5	1	8
"Nitzschia seriata"																									
"Nitzschia sicula var. bicuneata"																									
"Nitzschia sicula var. rostrata"																									

Appendix 2.2. Raw data of 166 database.

	LKA Code	82	83	84	85	86	87	88	89	90	91	92	93	94	95	96	97	98	99	100	101	102	103	104	105	106
	Core	KR8707	KR8708	KR8710	KR8712	KR8713	KR8714	KR8801	KR8805	KR8806	KR8807	KR8808	KR8809	KR8810	KR8811	KR8812	KR8813	KR8814	KR8815	KR8816	KR8817	KR8818	KR8819	KR8820	KR8821	KR8822
	Lat °S	62°21.2'	60°55.2'	59°39.6'	54°55.8'	52°42.8'	51°27.7'	46°40.6'	52°56.7'	49°01.3'	47°08.9'	49°15.7'	50°35.6'	54°11.2'	54°55'	56°23.8'	57°56.9'	61°16.8'	63°18.3'	64°46.2'	66°12.1'	65°45'	64°34.3'	64°56.1'	64°49.3'	64°40.1'
Species	Long.	57°58.3'W	56°26.3'W	51°16.6'W	39°47.6'W	36°59.3'W	34°00.5'W	79°29.2'E	109°55.1E	128°46.3'E	145°47.8'E	148°48.2'E	147°09.3'E	144°47.9'E	144°04'E	145°17.2'E	144°35'E	144°26.5'E	141°55.5'E	141°13.4'E	140°30.2'E	138°12'E	135°37.5'E	129°00.3'E	128°43.5'E	119°30.2'E
"Nitzschia sicula"																										
"Nitzschia sublinearis"		13	6	7	4	1	2		3				2		1	2		4	9	11	37	37	6	14	17	10
Odontella litigiosa																										
Odontella weissflogii		10	2	1	1	4	3	1						1											2	
Paralia sulcata																										
Pleurosigma directum																										
Porosira glacialis		3		3				1		1								1		1	1		6		1	4
Porosira pseudodenticulata																					11	4				
"Pseudonotia doliolus"										2	3															
"Rhizosolenia alata"																										
"Rhizosolenia barboi"																										
Rhizosolenia bergonii																										
Rhizosolenia "hebetata f. bidens"																										
Rhizosolenia "hebetata f. semispina "																										
Rhizosolenia styliformis		12		13	6	6	13	3	2					1		1					2	1		4		1
"Rocella gelida"																										
Roperia tesselata								2		35	25	17	8													
Rouxia spp.																										
Stellarima microtrias				1																	1				1	
T. oliverana ("Schimperiella antarctica")			10	10	11	7	6	2	1	2	1	5	5	5	5	5	7	3	8	9	3	1	7	4	8	10
Thalassionema nitzschioides					2			6	2	8	4	7	9	6	1	2	1									
Thalassionema nitzschioides var. parva																										
Thalassiosira ambigua															1											
Thalassiosira antarctica		90	1	16	9	241	39	14	1												107	20	12	13	9	2
Thalassiosira australis																					3					2
Thalassiosira cf. maculata										1	3															
Thalassiosira decipiens									1						1	1	1							1		
"Thalassiosira delicatulata (delicatula)"								1		1																
Thalassiosira eccentrica									2	1		3											1			1
Thalassiosira eccentrica var. jousei																										
Thalassiosira frenguellii										1	5															
Thalassiosira frenguelliopsis										2					1									1		
Thalassiosira gerloffi										2																
Thalassiosira gracilis		28	18	18	11	1	5	1	3	1		1	1	4	5	4	10	11	1	3	9	13	6	15	13	11
Thalassiosira gracilis var. expecta																										
Thalassiosira gravida											2															
Thalassiosira lentiginosa		12	54	91	138	43	127	62	45	118	84	74	95	37	54	69	72	65	52	90	26	9	80	60	50	103
Thalassiosira lineata									1	1		2		1												
Thalassiosira oestrupii					2				1	5	6	1	1			1										
Thalassiosira perpusilla																						2				
Thalassiosira poroseriata																										
Thalassiosira ritscheri																					1					
Thalassiosira scotia																										
Thalassiosira spp.											3		1					1			8					
Thalassiosira symmetrica																										
Thalassiosira trifulta										2	5					1		1	2				1			3
Thalassiosira tumida					2	2											1									
Thalassiothrix spp.				3	13	10		3			3	3	3													
Other unidentified spp.											3															
	TOTAL	291	270	349	438	413	401	304	299	303	338	310	304	398	400	300	298	299	300	352	400	416	307	460	335	458

Appendix 2.2. Raw data of 166 database.

LKA Code	107	108	109	110	111	112	113	114	115	116	117	118	119	120	121	122	123	124	125	126	127
Core	KR8823	KR8824	KR8825	KR8827	KR8828	KR8829	KR8830	KR8831	8702-DISS-5'	8702-DISS10'	8702-DISS20'	8702-DISS35'	8702-DISS60'	8702DISS120'	8702DISS180'	8702-DISS24H	8707-DISS10'	8707-DISS20'	8707-DISS35'	8707-DISS60'	8707DISS120'
Lat °S	63°18'	63°44.8'	64°17.9'	63°39.1'	64°09.5'	62°29.5'	61°00.2'	59°	56°27.6'	56°27.6'	56°27.6'	56°27.6'	56°27.6'	56°27.6'	56°27.6'	56°27.6'	62°21.2'	62°21.2'	62°21.2'	62°21.2'	62°21.2'
Species Long.	117°15.8'E	116°44.9'E	115°42.1'E	101°08.9'E	98°09.5'E	95°53.1'E	93°11.9'E	89°24.3'E	33°58.5'W	33°58.5'W	33°58.5'W	33°58.5'W	33°58.5'W	33°58.5'W	33°58.5'W	33°58.5'W	57°58.3'W	57°58.3'W	57°58.3'W	57°58.3'W	57°58.3'W
"Achnanthes brevipes (var. angustata)"																					
Actinocyclus actinochilus ("Charcotia act.")	2	9	10	8	2	1	1		4	3	3	2	2	6			28	29	14	27	17
Actinocyclus curvatulus																					
Actinocyclus ingens							1	2					1								1
Actinocyclus spp.																					
Asteromphalus heptactis													1								
Asteromphalus hookeri			1			1			2	1	1	1	1	1	1			1			
Asteromphalus hyalinus																					
Asteromphalus parvulus		4	1				1		2	2	1	2	1	1		1					
"Asteromphalus robustus"																					
Azpeitia tabularis	7	4	1	6		5	8	8	3	3	4	2	6	1	8	1		4			
"C. stellaris var symbolophorus"																					
Chaetoceros spp.																					
Cocconeis spp.										1				2	2		17	12	17	20	26
Coscinodiscus asteromphalus																					
"Coscinodiscus bullatus"																					
Coscinodiscus centralis																					
Coscinodiscus curvatulus						1	1														
Coscinodiscus decrescens																					
"Coscinodiscus eccentrica"																					
"Coscinodiscus furcatus"			2	2	1				1	1			1				1		1	2	1
"Coscinodiscus lineatus"																					
Coscinodiscus marginatus				1				1													
Coscinodiscus nodulifer																					
Coscinodiscus occuloides																					
Coscinodiscus oculus-iridus																					
Coscinodiscus radiatus										1											
"Coscinodiscus ritscheri"																					
Coscinodiscus spp.									1												
"Coscinodiscus symbolophorus"																					
"Coscinodiscus tabularis"																					
"Coscinodiscus tabularis var. egregius"																					
Dactyliosolen antarctica																					
Dictyocha spp.																					
Distephanus spp.	3	3		1		5	4	2	6	7	3	4	4	1	1		1			3	
Eucampia antarctica	10	7	16	50	6	20	14	26	8	6	5	6	16	15	120	9	9		7	8	7
Grammatophora arcuata							1		1											1	
Hemidiscus cuneiformis																					
Hemidiscus karstenii																					
Melosira adeliae																					
Melosira sol ("Paralia sol")																					
Navicula directa									1												
"Nitzschia angulata"	1	3	2	1		1	2		1	1		6	2		1		2	1	3	3	1
"Nitzschia bicapitata"																					
"Nitzschia closterium"																					
"Nitzschia curta"	4	12	15	8	7	1			2	1	2	2	1	2	2		11	17	12	12	4
"Nitzschia cylindrus"	1		1											1			9	9	11	11	
"Nitzschia denticuloides"																					
"Nitzschia fraudulenta"																					
"Nitzschia grunowii"																					
"Nitzschia heimii"																					
"Nitzschia kerguelensis"	190	153	160	175	31	233	169	81	130	140	147	117	123	102	91	17	30	28	30	35	45
"Nitzschia koloczeckii"																					
Nitzschia lecointei																					
"Nitzschia obliquecostata"	1	2		1		1											3	1	1		1
Nitzschia paundriformis														1							
"Nitzschia pseudonana"																					
"Nitzschia ritscheri"											1										
"Nitzschia seperanda"	5	4	3	3		5	6	3	5	4	2	7	4	6					1		2
"Nitzschia seriata"																					
"Nitzschia sicula var. bicuneata"																					
"Nitzschia sicula var. rostrata"																					

Appendix 2.2. Raw data of 166 database.

LKA Code	107	108	109	110	111	112	113	114	115	116	117	118	119	120	121	122	123	124	125	126	127
Core	KR8823	KR8824	KR8825	KR8827	KR8828	KR8829	KR8830	KR8831	8702-DISS-5'	8702-DISS10'	8702-DISS20'	8702-DISS35'	8702-DISS60'	8702DISS120'	8702DISS180'	8702-DISS24H	8707-DISS10'	8707-DISS20'	8707-DISS35'	8707-DISS60'	8707DISS120'
Lat °S	63°18'	63°44.8'	64°17.9'	63°39.1'	64°09.5'	62°29.5'	61°00.2'	59°	56°27.6'	56°27.6'	56°27.6'	56°27.6'	56°27.6'	56°27.6'	56°27.6'	56°27.6'	62°21.2'	62°21.2'	62°21.2'	62°21.2'	62°21.2'
Species Long.	117°15.8'E	116°44.9'E	115°42.1'E	101°08.9'E	98°09.5'E	95°53.1'E	93°11.9'E	89°24.3'E	33°58.5'W	33°58.5'W	33°58.5'W	33°58.5'W	33°58.5'W	33°58.5'W	33°58.5'W	33°58.5'W	57°58.3'W	57°58.3'W	57°58.3'W	57°58.3'W	57°58.3'W
"Nitzschia sicula"																					
"Nitzschia sublinearis"	4	10	11	11	3	8	1	3	6	2	4	2	2	3	2	2	13	16	23	10	5
Odontella litigiosa																					
Odontella weissflogii		2							2	3		1	1	2			8	5	6	7	1
Paralia sulcata																					
Pleurosigma directum									1				1								
Porosira glacialis		1				1			2	3		4	1	2			5	8	8	2	3
Porosira pseudodenticulata																					
"Pseudonotia doliolus"																					
"Rhizosolenia alata"																					
"Rhizosolenia barboi"																					
Rhizosolenia bergonii																					
Rhizosolenia "hebetata f. bidens"							1	2		1			1	2							
Rhizosolenia "hebetata f. semispina"																					
Rhizosolenia styliformis		2		1		1	1		10	14	8	13	5	6	8		9	11	3	6	1
"Rocella gelida"																					
Roperia tesselata																					
Rouxia spp.																					
Stellarima microtrias					2				1				1	1	1	1	2	3	3	3	
T. oliverana ("Schimperiella antarctica")	3	2	6	18		8	8	10	8	3	6	3	6	12	10	2			1		1
Thalassionema nitzschioides						3	1	3				3	3								
Thalassionema nitzschioides var. parva																					
Thalassiosira ambigua																					
Thalassiosira antarctica	5	8	9	8	5	1			9	10	7	9	12	5	3	2	102	83	96	105	51
Thalassiosira australis																					
Thalassiosira cf. maculata																					
Thalassiosira decipiens							1			1	1										
"Thalassiosira delicatulata (delicatula)"																					
Thalassiosira eccentrica		1	1	2			1							1						2	
Thalassiosira eccentrica var. jousei																					
Thalassiosira frenguellii																					
Thalassiosira frenguelliopsis								1													
Thalassiosira gerloffi																					
Thalassiosira gracilis	2	7	13	3		9	5			11	13	12	8	5	5		16	14	20	12	1
Thalassiosira gracilis var. expecta																					
Thalassiosira gravida																					
Thalassiosira lentiginosa	80	65	45	75	15	113	74	89	84	87	95	108	104	128	145	82	23	15	19	20	43
Thalassiosira lineata										2							1				
Thalassiosira oestrupii																					
Thalassiosira perpusilla																					
Thalassiosira poroseriata																					
Thalassiosira ritscheri						1				1									1		
Thalassiosira scotia																					
Thalassiosira spp.															1		11	11	10	8	
Thalassiosira symmetrica																					
Thalassiosira trifulta	1	1	1																		
Thalassiosira tumida		1						1	2	1			1		1						
Thalassiothrix spp.																					
Other unidentified spp.																			2		2
TOTAL	319	301	298	374	72	419	301	212	292	310	303	304	309	306	402	117	301	268	289	297	213

Appendix 2.2. Raw data of 166 database.

	LKA Code	128	129	130	131	132	133	134	135	136	137	138	139	140	141	142	143	144	185	186	230
	Core	8707DISS240'	8808-DISS05'	8808-DISS10'	8808-DISS60'	8808-DISS24H	8810DISS0-20	8810DISS3560	8810DISS240'	8810DISS24H	8818DISS0-05	8818-DISS10'	8818-DISS20'	8818DISS120'	8818DISS180'	8818DISS240'	8818-DISS24H	8818-DISS48H	RC11-118	RC11-119	1176-86
	Lat °S	62°21.2'	49°15.7'	49°15.7'	49°15.7'	49°15.7'	54°11.2'	54°11.2'	54°11.2'	54°11.2'	65°45'	65°45'	65°45'	65°45'	65°45'	65°45'	65°45'	65°45'	37°48.0'	40°18.0	48°02.3'
Species	Long.	57°58.3'W	148°48.2'E	148°48.2'E	148°48.2'E	148°48.2'E	144°47.9'E	144°47.9'E	144°47.9'E	144°47.9'E	138°12'E	138°12'E	138°12'E	138°12'E	138°12'E	138°12'E	138°12'E	138°12'E	71°32.0'E	74°34.0'E	13°49.0'E
"Achnanthes brevipes (var. angustata)"																					
Actinocyclus actinochilus ("Charcotia act.")		3									8	7	5	6	5	5	4	4			1
Actinocyclus curvatulus																					
Actinocyclus ingens			4	3	3					4											
Actinocyclus spp.																					
Asteromphalus heptactis																					
Asteromphalus hookeri			1	2	1		3		2					1							1
Asteromphalus hyalinus																					
Asteromphalus parvulus				1			1	1			2	1	1	1	2	1					1
"Asteromphalus robustus"																					
Azpeitia tabularis			18	18	2	1	16	18	11	2						7			6	20	
"C. stellaris var symbolophorus"																					
Chaetoceros spp.																					
Cocconeis spp.		4									1	7		5	3	2	2				
Coscinodiscus asteromphalus																					
"Coscinodiscus bullatus"																			1		
Coscinodiscus centralis																			34	1	1
Coscinodiscus curvatulus																					
Coscinodiscus decrescens																			2		
"Coscinodiscus eccentrica"													1								
"Coscinodiscus furcatus"							1												9	3	
"Coscinodiscus lineatus"																			1	5	
Coscinodiscus marginatus			2	1		1														1	
Coscinodiscus nodulifer																					
Coscinodiscus occuloides																					
Coscinodiscus oculus-iridus													1						5		
Coscinodiscus radiatus																				6	
"Coscinodiscus ritscheri"																					
Coscinodiscus spp.																					
"Coscinodiscus symbolophorus"																					1
"Coscinodiscus tabularis"																					3
"Coscinodiscus tabularis var. egregius"																					
Dactyliosolen antarctica																			9	26	
Dictyocha spp.			5	5															2		6
Distephanus spp.			3	6	2		5	1		2	2	2	3	2	4				2		14
Eucampia antarctica		1	6	6	8		1	4	1	1	13	8	7	3	25	27	25	18	1		
Grammatophora arcuata											2	2	3								
Hemidicus cuneiformis			6	7															7	17	
Hemidiscus karstenii				1																	
Melosira adeliae																					
Melosira sol ("Paralia sol")																					
Navicula directa																					2
"Nitzschia angulata"				2							40	21	24	20	9	1			2		
"Nitzschia bicapitata"																					
"Nitzschia closterium"											105	88	94	14	8	3					1
"Nitzschia curta"												2		1							
"Nitzschia cylindrus"																					
"Nitzschia denticuloides"																				3	
"Nitzschia fraudulenta"																					
"Nitzschia grunowii"																					
"Nitzschia heimii"																					
"Nitzschia kerguelensis"		15	144	115	64	12	300	345	189	40	43	60	65	111	96	112	48	22	24	37	170
"Nitzschia koloczeckii"																				2	
Nitzschia lecointei																					
"Nitzschia obliquecostata"																					
Nitzschia paundriformis																					
"Nitzschia pseudonana"											2		1	4	2						1
"Nitzschia ritscheri"			1																		1
"Nitzschia seperanda"			1		1		1				1	1	1	4	6	1					1
"Nitzschia seriata"																				2	
"Nitzschia sicula var. bicuneata"																					
"Nitzschia sicula var. rostrata"																					

Appendix 2.2. Raw data of 166 database.

	LKA Code	128	129	130	131	132	133	134	135	136	137	138	139	140	141	142	143	144	185	186	230
	Core	B707DISS240'	8808-DISS05'	8808-DISS10'	8808-DISS60'	8808-DISS24H	8810DISS0-20	8810DISS3560	8810DISS240'	8810DISS24H	8818DISS0-05	8818-DISS10'	8818-DISS20'	8818DISS120'	8818DISS180'	8818DISS240'	8818-DISS24H	8818-DISS48H	RC11-118	RC11-119	1176-86
	Lat °S	62°21.2'	49°15.7'	49°15.7'	49°15.7'	49°15.7'	54°11.2'	54°11.2'	54°11.2'	54°11.2'	65°45'	65°45'	65°45'	65°45'	65°45'	65°45'	65°45'	65°45'	37°48.0'	40°18.0	48°02.3'
Species	Long.	57°58.3'W	148°48.2'E	148°48.2'E	148°48.2'E	148°48.2'E	144°47.9'E	144°47.9'E	144°47.9'E	144°47.9'E	138°12'E	138°12'E	138°12'E	138°12'E	138°12'E	138°12'E	138°12'E	138°12'E	71°32.0'E	74°34.0'E	13°49.0'E
"Nitzschia sicula"																					
"Nitzschia sublinearis"			1	1							45	51	42	20	22	17	12	3			1
Odontella litigiosa																					
Odontella weissflogii											1			1	1	1		1		1	
Paralia sulcata																					
Pleurosigma directum																					
Porosira glacialis											2	1	3	2	9						
Porosira pseudodenticulata																					
"Pseudonotia doliolus"																			46	68	
"Rhizosolenia alata"																					
"Rhizosolenia barboi"																					
Rhizosolenia bergonii																			2	5	
Rhizosolenia "hebetata f. bidens"																					
Rhizosolenia "hebetata f. semispina"																					
Rhizosolenia styliformis			1	1	2		1				2	1	1			1	1				3
"Rocella gelida"																					
Roperia tesselata			18	11																8	
Rouxia spp.																					1
Stellarima microtrias													1	5	2	3					
T. oliverana ("Schimperiella antarctica")			3	4	6		9	6	8	4			1	3	8		4	1			3
Thalassionema nitzschioides			5	4	2		2	1	2										7	4	17
Thalassionema nitzschioides var. parva																					
Thalassiosira ambigua																					
Thalassiosira antarctica		16									17	18	23	55	114	12	7	1			
Thalassiosira australis										1											
Thalassiosira cf. maculata																					
Thalassiosira decipiens															1					2	7
"Thalassiosira delicatulata (delicatula)"																					
Thalassiosira eccentrica			2		1						1			2	1					3	2
Thalassiosira eccentrica var. jousei																					
Thalassiosira frenguellii																					
Thalassiosira frenguelliopsis																					
Thalassiosira gerloffi																					
Thalassiosira gracilis		2					4	2	2	2	3	9	5	6	6	2				1	2
Thalassiosira gracilis var. expecta																					
Thalassiosira gravida																			1	1	
Thalassiosira lentiginosa		18	68	67	39	4	67	66	112	27	12	12	17	24	38	62	41	25	1	8	52
Thalassiosira lineata			1	1				2	1			2	3	1	1	1			2	4	1
Thalassiosira oestrupii																			16	1	2
Thalassiosira perpusilla																					
Thalassiosira poroseriata																			1		
Thalassiosira ritscheri																					
Thalassiosira scotia																					
Thalassiosira spp.																					
Thalassiosira symmetrica																				3	
Thalassiosira trifulta																					
Thalassiosira tumida																					
Thalassiothrix spp.																			3	5	18
Other unidentified spp.																		3			
TOTAL		59	290	258	131	18	411	446	328	83	302	293	302	291	363	258	144	78	182	235	313

Appendix 2.2. Raw data of 166 database.

LKA Code	231	232	233	234	235	236	237	246	247	248	249	250	251	252	253	254	255	256	257
Core	KR8802	KR8803	KR8804	MD84-561	MD73-026	MD84-529	PC82-35	8702-DISS-240	8707-DISS5'	8707-DISS180	8808-DISS020	8808-DISS035	8808-DISS0120	8808-DISS0180	8808-DISS0240	8808-DISS48H	8810DISS120	8810DISS180	8818DISS035
Lat °S	45°45.2'	46°04.1'	49°55.3'	53°05.3'	44°59.0'	48°54.3'	62°21.7'	56°27.6'	62°21.2'	62°21.2'	62°21.2'	62°21.2'	62°21.2'	62°21.2'	62°21.2'	62°21.2'	54°11.2'	54°11.2'	65°45'
Species Long.	82°56.0'E	90°06.7'E	100°05.0'E	71°36.4'E	53°17.0'E	61°59.8'E	57°22.0'W	33°58.5'W	57°58.3'W	57°58.3'W	57°58.3'W	57°58.3'W	57°58.3'W	57°58.3'W	57°58.3'W	57°58.3'W	144°47.9'E	144°47.9'E	138°12'E
"Achnanthes brevipes (var. angustata)"																			1
Actinocyclus actinochilus ("Charcotia act.")							26	3	29	8	1	1		1	1				5
Actinocyclus curvatulus				1															
Actinocyclus ingens	2	1									3	8	9	6	7	1			
Actinocyclus spp.																			
Asteromphalus heptactis																			
Asteromphalus hookeri		1	2	1	2								1	1	1			3	2
Asteromphalus hyalinus																			
Asteromphalus parvulus	1			1	1	3					2						1		1
"Asteromphalus robustus"																			
Azpeitia tabularis	16	10	10					7	1		11	7	6	2	2		12	12	
"C. stellaris var symbolophorus"					2														
Chaetoceros spp.				4	1														
Cocconeis spp.							9		10	17									2
Coscinodiscus asteromphalus																			
"Coscinodiscus bullatus"																			
Coscinodiscus centralis																			
Coscinodiscus curvatulus																			
Coscinodiscus decrescens																			
"Coscinodiscus eccentrica"																			
"Coscinodiscus furcatus"							2	1	1	3									4
"Coscinodiscus lineatus"																			
Coscinodiscus marginatus									1		2	1							
Coscinodiscus nodulifer																			
Coscinodiscus occuloides																			
Coscinodiscus oculus-iridus																			
Coscinodiscus radiatus	1	1																	
"Coscinodiscus ritscherii"																			
Coscinodiscus spp.																			
"Coscinodiscus symbolophorus"																			
"Coscinodiscus tabularis"				7	11	19													
"Coscinodiscus tabularis var. egregius"																			
Dactyliosolen antarctica																			
Dictyocha spp.		2	1		1						4	1							
Distephanus spp.	1	3	7	9	5	8	5	1	2	1	1	1	2		2		2	3	3
Eucampia antarctica	26	27	22	36	20	10	5	22	6	3	11		3	3	2		1	1	11
Grammatophora arcuata																			
Hemidiscus cuneiformis	1	3									1								
Hemidiscus karstenii											1		2						
Melosira adeliae																			
Melosira sol ("Paralia sol")																			
Navicula directa					1					1									
"Nitzschia angulata"							1		1	1									23
"Nitzschia bicapitata"																			
"Nitzschia closterium"																			
"Nitzschia curta"							46		15	3									69
"Nitzschia cylindrus"							13		4										
"Nitzschia denticuloides"																			
"Nitzschia fraudulenta"																			
"Nitzschia grunowii"					1														
"Nitzschia heimii"										1									
"Nitzschia kerguelensis"	126	157	162	168	206	186	43	90	33	16	111	102	94	58	44	2	274	172	73
"Nitzschia koloczeckii"																			
Nitzschia lecointei																			
"Nitzschia obliquecostata"										1									2
Nitzschia paundriformis	1	1			1														
"Nitzschia pseudonana"																			
"Nitzschia ritscherii"	4	6	7	7	1	1													
"Nitzschia separanda"		1	2		1	1	5	1	1		1	3					1	2	3
"Nitzschia seriata"																			
"Nitzschia sicula var. bicuneata"																			
"Nitzschia sicula var. rostrata"																			

Appendix 2.2. Raw data of 166 database.

LKA Code	231	232	233	234	235	236	237	246	247	248	249	250	251	252	253	254	255	256	257
Core	KR8802	KR8803	KR8804	MD84-561	MD73-026	MD84-529	PC82-35	8702-DISS-240	8707-DISS5'	8707-DISS180	8808-DISS020	8808-DISS035	8808-DISS0120	8808-DISS0180	8808-DISS0240	8808-DISS48H	8810DISS120	8810DISS180	8818DISS035
Lat °S	45°45.2'	46°04.1'	49°55.3'	53°05.3'	44°59.0'	48°54.3'	62°21.7'	56°27.6'	62°21.2'	62°21.2'	62°21.2'	62°21.2'	62°21.2'	62°21.2'	62°21.2'	62°21.2'	54°11.2'	54°11.2'	65°45'
Species Long.	82°56.0'E	90°08.7'E	100°05.0'E	71°36.4'E	53°17.0'E	61°59.8'E	57°22.0'W	33°58.5'W	57°58.3'W	57°58.3'W	57°58.3'W	57°58.3'W	57°58.3'W	57°58.3'W	57°58.3'W	57°58.3'W	144°47.9'E	144°47.9'E	138°12'E
"Nitzschia sicula"							1												
"Nitzschia sublinearis"							22	1	10	4		2		1					45
Odontella litigiosa																			
Odontella weissflogii	2	3		1			10	1	5	1									1
Paralia sulcata																			
Pleurosigma directum													1						
Porosira glacialis							2		8	3									3
Porosira pseudodenticulata																			
"Pseudonotia doliolus"	1																		
"Rhizosolenia alata"							5												
"Rhizosolenia barboi"					1														
Rhizosolenia bergonii																			4
Rhizosolenia "hebetata f. bidens"																			
Rhizosolenia "hebetata f. semispina"																		1	1
Rhizosolenia styliformis	4	1		2	1	1	28	3	7				1		1				
"Rocella gelida"											10	1							
Roperia tesselata		6																	
Rouxia spp.																			
Stellarima microtrias							2		1	1									
T. oliverana ("Schimperiella antarctica")	9	1	4	6	4	6		4	1	1	3	6	1	4	2		4	2	
Thalassionema nitzschioides	1	1	9	1	11	8						3		1	1		1	1	
Thalassionema nitzschioides var. parva																			
Thalassiosira ambigua																			
Thalassiosira antarctica	12	4		6			42	5	120	41									24
Thalassiosira australis																			
Thalassiosira cf. maculata							2												
Thalassiosira decipiens					1														1
"Thalassiosira delicatulata (delicatula)"																			
Thalassiosira eccentrica	1		1		1							1		1			1		
Thalassiosira eccentrica var. jousei						1													
Thalassiosira frenguelii																			
Thalassiosira frenguelliopsis																			
Thalassiosira gerloffi																			
Thalassiosira gracilis	2	2	3	10	3	4	18	1	18	4		3					1		4
Thalassiosira gracilis var. expecta							3												
Thalassiosira gravida																			
Thalassiosira lentiginosa	93	60	68	35	36	48	7	189	17	24	73	43	28	22	30	5	102	106	20
Thalassiosira lineata			1	1	1						1							1	1
Thalassiosira oestrupii		6	9	1	3	1									1				
Thalassiosira perpusilla																			
Thalassiosira poroseriata							1												
Thalassiosira ritscheri																			
Thalassiosira scotia																			
Thalassiosira spp.																			
Thalassiosira symmetrica							1												
Thalassiosira trifulta																			
Thalassiosira tumida		1		2			3												
Thalassiothrix spp.	3	10	10	3	12	4	3		3		1	3							
Other unidentified spp.									10			5	2	1	2				
TOTAL	309	308	318	303	328	301	305	329	302	134	237	189	150	101	96	8	400	304	303

Appendix 2.3. All new French raw data.

	LKA Code	152	153	154	155	156	157	158	159	160	187	188	189	190	191	192	193	194	195	196	197	198
	JJP Code	6711	6703	4906	4900	5001	4700	4558	4559	4501	4059	4160	4300	4358	4800	5159	6217	6255	6259	6317	6323	6343
	Core	93-7/GC33	93-7/GC5	KTB01	KTB12	KTB14	KTB20	KTB21	KTB22	KTB25	KTB 31	KTB 34	KTB 29	KTB 26	KTB 18	KTB 08	PCDF 82-34	PCDF 82-47	PCDF 82-69	PCDF 82-61	PCDF 82-60	PCDF 82-51
	Lat °S	67°11'	67°03'	49°06'	49°00'	50°00'	47°00'	45°58'	45°59'	45°01'	40°59'	41°59'	43°00'	43°58'	48°00'	51°59'	62°17.7'	62°55.3'	62°59.9'	63°17'	63°23.4'	63°43.4'
Species	Long.	68°30'E	69°05'E	67°01'E	57°59'E	57°59'E	58°01'E	55°59'E	55°59'E	57°57'E	57°59'E	58°01'E	58°01'E	55°58'E	57°59'E	61°07'E	57°37.4'W	58°23.7'W	59°38.1'W	59°20.2'W	59°34.2'W	60°02.9'W
"Achnanthess brevipes (var. angustata)"																	3		1			1
Actinocyclus actinochilus	1	11						1				3	1	1	1		11	20	13	24	21	6
Actinocyclus ingens				1		3	2	6	3	3	8	1	7	4								
Amphora ovalis																	1				1	
Asteromphalus heptactis			1			1	1									3						
Asteromphalus hookeri		1	1				1	1			3										1	
Asteromphalus parvulus	2	1							1		1		1				3				1	
Azpeitia tabularis			11	9	17	12	15	15	5	7	28	15	14	8	11							
Chaetoceros spores	10	15	3			8	19	25	17	4	16	11	13	10								
Chaetoceros spp.	1																	4				2
Cocconeis spp.		1									1						9	8	7	19	17	8
Corathron criophilum							1															
Coscinodiscus asteromphalus											2											
"Coscinodiscus bullatus"						1					3	1										
Coscinodiscus curvatulus				1																		
"Coscinodiscus furcatus"																	1				3	
Coscinodiscus radiatus						2		1				1	1	1								
Coscinodiscus spp.								1				1										
"Coscinodiscus symbolophorus"																						
Dactyliosolen antarctica		1	6	13	11	10	5	5	2	4	12	4	8	10	8							
Dictyocha spp. ¥				1			1	2	4	1	2	3	2									
Distephanus spp. ¥	2	3	14	6	1	6	5	4	4	3	4	2	7	5	1	2		5	2	2	2	
Eucampia antarctica	5	15	29	9	3	24	13	15	16	31	57	28	25	11	1	5	8	9	9	5	5	
Gomphonema intricatum																		2			2	
Grammatophora arcuata																1				1	2	
Hemidiscus cuneiformis									3	1	2	1	1									
Hemidiscus karstenii						1	1	1	1		1	2	5	1								
Licmophora "decora"																2						
Melosira adeliae			1				1		1									2				
Melosira sol ("Paralia sol")																				2	1	1
Navicula directa			1	1													3	1		1	2	5
Navicula glacei																						
"Nitzschia angulata"	8	7	1	2				2	2	1				4			8	3	1	2	1	4
"Nitzschia" bicapitata																						
"Nitzschia closterium"																						
"Nitzschia curta"	207	205															65	78	53	38	54	68
"Nitzschia cylindrus"	10	4															24	43	28	21	21	27
"Nitzschia heimii"																					1	
"Nitzschia kerguelensis"	3	7	260	216	263	178	136	210	136	139	269	103	188	212	239	36	53	18	12	21	16	
Nitzschia lecontei																1	1				2	3
"Nitzschia lineata"																						
"Nitzschia lineola"																						
"Nitzschia obliquecostata"	2	6														2					2	1
Nitzschia paundriformis			1				1		1		4	1	1									
"Nitzschia pseudonana"	3	8				1		1								1						
"Nitzschia ritscheri"			2	2	1	2	1	5		1	10		3	1				6	2			
"Nitzschia seperanda"	3	1		1			2	1	2	1	1	1	2	2		2	1		2			
"Nitzschia sublineata"	18	37		2	1						2	1		3		21	20	25	18	7	26	
"Nitzschia van heurckii"		3																				
Odontella weissflogii			2	1				2			2					5	2	6	21	7	3	
Pleurosigma directum																						
Pleurosigma spp.																				1		
Porosira glacialis	6	5														4	15	9	14	4	5	

Appendix 2.3. All new French raw data.

	LKA Code	152	153	154	155	156	157	158	159	160	187	188	189	190	191	192	193	194	195	196	197	198
	JJP Code	6711	6703	4906	4900	5001	4700	4558	4559	4501	4059	4160	4300	4358	4800	5159	6217	6255	6259	6317	6323	6343
	Core	93-7/GC33	93-7/GC5	KTB01	KTB12	KTB14	KTB20	KTB21	KTB22	KTB25	KTB 31	KTB 34	KTB 29	KTB 26	KTB 18	KTB 08	PCDF 82-34	PCDF 82-47	PCDF 82-69	PCDF 82-61	PCDF 82-60	PCDF 82-51
	Lat °S	67°11'	67°03'	49°06'	49°00'	50°00'	47°00'	45°58'	45°59'	45°01'	40°59'	41°59'	43°00'	43°58'	48°00'	51°59'	62°17.7'	62°55.3'	62°59.9'	63°17'	63°23.4'	63°43.4'
Species	Long.	68°30'E	69°05'E	67°01'E	57°59'E	57°59'E	58°01'E	55°59'E	55°59'E	57°57'E	57°59'E	58°01'E	58°01'E	55°58'E	57°59'E	61°07'E	57°37.4'W	58°23.7'W	59°38.1'W	59°20.2'W	59°34.2'W	60°02.9'W
Porosira pseudodenticulata		18																	1			
Psuedoenotia doliolus									1	1	3	8	1	2								
Rhizosolenia alata																	2			1	1	6
Rhizosolenia hebetata												2										
*Rhizosolenia *hebetata f. bidens**																				1	1	
Rhizosolenia styliformis		1	1	6		1	2			1		1			3		22	3	21	5	19	27
Roperia tesselata							1	2	1	1	4	7	3	5						1		
Stellarima microtrias		1	2															2		2	1	3
Synedra kerguelensis																					3	
Thalassionema nitzschioides				14	6	7	9	6	12	4	9	17	9	13	5	2						
Thalassiosira antarctica		10	6				5	2	2		2	5	4		2		31	62	79	93	88	75
Thalassiosira australis																		1				
Thalassiosira cf. maculata																					1	
Thalassiosira decipiens				1	1																	
Thalassiosira delicatula					1			1						1	1							
Thalassiosira frenguelliopsis																					1	
Thalassiosira gracilis		7	11	3	4	1		2	3			2		3	3	2	15	4	8	4	9	6
Thalassiosira lentiginosa		2	10	72	75	55	71	67	50	85	66	140	86	108	54	28	11	5	3	7	4	1
Thalassiosira lineata					1	1		1	1				3		1				2			
Thalassiosira oestrupii					1			5	1	1	3	4	8	2								
Thalassiosira oliverana		1	1	4	3	3	4	7	4	5	6	10	8	9	4	4						
Thalassiosira perpusilla																						
Thalassiosira poroseriata																	8	6				1
Thalassiosira spp.					1					1	4	1	1				3	2				
Thalassiosira symmetrica																						
Thalassiosira trifulta				3	1	1		1	1			2	1	1	2							
Thalassiosira tumida			2	1	1	1	1	1	2	1	1	4	1		1		2		4	2	3	
Other unidentified species		1					1				2	1		3	2							
	TOTAL	320	364	437	360	367	343	301	375	298	296	635	302	424	351	299	298	345	304	305	309	302

Notes.

All species and their counts are as originally identified.

The total number of species includes all species listed including Silicoflagellates.

Silicoflagellates are marked with "¥".

Species names with quotations are no longer considered valid. Refer to Chapter 2 for discussion.

Appendix 2.3. All new French raw data.

	UKA Code	199	200	201	202	203	204	205	206	207	208	209	210	211	212	213
	JJP Code	6352	6357	6404	6410	6414	6419	6435	6436	6439	6453	6501	7542	7551	7601	7605
	Core	PCDF 82-167	PCDF 82-1	PCDF 82-93	PCDF 82-174	PCDF 82-20	PCDF 82-102 B	PCDF 82-134	PCDF 82-112	PCDF 82-127 B	PCDF 82-142	PCDF 82-155	DFBC 83-27 II	DFBC 83-28 II	DFBC 83-29 II	DFBC 83-30 II
	Lat °S	63°52.5'	63°57.2'	64°04.1'	64°10'	64°14.1'	64°18.6'	64°34.5'	64°36.5'	64°39.5'	63°53.1'	65°01.1'	75°42'	75°51'	76°01'	76°05'
Species	Long.	56°36.6'W	56°21.6'W	61°19.6'W	56°48.5'W	55°54.4'W	61°52.7'W	62°39'W	61°38'W	62°07.4'W	62°26.4'W	63°15.6'W	170°39'E	169°18'E	167°12'E	166°42'E
"Achnanthess brevipes (var. angustata)"				4	4	1	2	1		1						2
Actinocyclus actinochilus		5	12	13	5	21	11	4	3	1	2	5	8	14	2	4
Actinocyclus ingens						1							2		2	
Amphora ovalis																
Asteromphalus heptactis																
Asteromphalus hookeri							1						2	1	1	1
Asteromphalus parvulus				1									2		2	
Azpeita tabularis																
Chaetoceros spores																
Chaetoceros spp.													1		3	
Cocconeis spp.		1	9	12	2	8	8	6	9	10	4	4				
Corethron criophilum																
Coscinodiscus asteromphalus														1		1
"Coscinodiscus bullatus"																
Coscinodiscus curvatulus																
"Coscinodiscus furcatus"			1	1		1								9		4
Coscinodiscus radiatus																
Coscinodiscus spp.																
"Coscinodiscus symbolophorus"													2		2	
Dactyliosolen antarctica																
Didyocha spp. ¥																
Distephanus spp. ¥							2	1				2		1	2	
Eucampia antarctica		6	1	4	1	6	2	3	1	2	1	4	47	16	10	9
Gomphonema intricatum																
Grammatophora arcuata																
Hemidiscus cuneiformis																
Hemidiscus karsteni																
Licmophora "decora"				1												
Melosira adeliae				1												
Melosira sol ("Paralia sol")		1					2		2				1			
Navicula directa				2	1		3	1		1						
Navicula glacei			2													
"Nitzschia angulata"				1		1	4	1		1			6	6	4	2
"Nitzschia" bicapitata			1													
"Nitzschia closterium"													1			
"Nitzschia curta"		1	26	40	21	30	45	15	8	13	5	8	98	193	106	127
"Nitzschia cylindrus"		4	16	21	8	22	16	6	5	3	5	10	8	6	14	10
"Nitzschia heimii"							3									
"Nitzschia kerguelensis"		9		14	1		19	4	2	1	1	3	3	5	3	4
Nitzschia lecontei			3													
"Nitzschia lineata"																
"Nitzschia lineola"																
"Nitzschia obliquecostata"						1							4	8	3	3
Nitzschia paundriformis																
"Nitzschia pseudonana"																
"Nitzschia ritscheri"				7			2									
"Nitzschia seperanda"													22	10	8	11
"Nitzschia subtineata"			17	11	10	23	7	2	2	2	5	7	52	59	50	58
"Nitzschia van heurckii"																
Odontella weissflogii		1	3	1	1	2	7		2	4	2	2	1		3	2
Pleurosigma directum																
Pleurosigma spp.																
Porosira glacialis		14	13	11	5	16	4	2	3	2		2		3	4	

Appendix 2.3. All new French raw data.

	LKA Code	199	200	201	202	203	204	205	206	207	208	209	210	211	212	213
	JJP Code	6352	6357	6404	6410	6414	6419	6435	6436	6439	6453	6501	7542	7551	7601	7605
	Core	PCDF 82-167	PCDF 82-1	PCDF 82-93	PCDF 82-174	PCDF 82-20	PCDF 82-102 B	PCDF 82-134	PCDF 82-112	PCDF 82-127 B	PCDF 82-142	PCDF 82-155	DFBC 83-27 II	DFBC 83-28 II	DFBC 83-29 II	DFBC 83-30 II
	Lat °S	63°52.5'	63°57.2'	64°04.1'	64°10'	64°14.1'	64°18.6'	64°34.5'	64°36.5'	64°39.5'	63°53.1'	65°01.1'	75°42'	75°51'	76°01'	76°05'
Species	Long.	56°36.6'W	56°21.6'W	61°19.6'W	56°48.5'W	55°54.4'W	61°52.7'W	62°39'W	61°36'W	62°07.4'W	62°26.4'W	63°15.6'W	170°39'E	169°18'E	167°12'E	166°42'E
Porosira pseduodenticulata																
Psuedoenotia doliolus															1	
Rhizosolenia alata																
Rhizosolenia hebetata																
*Rhizosolenia *hebetata f. bidens**																
Rhizosolenia styliformis				3		2	8	1		2		1			3	
Roperia tesselata									1		1					
Stellarima microtrias			1		1											
Synedra kerguelensis																
Thalassionema nitzschioides																
Thalassiosira antarctica		255	189	144	39	185	122	52	60	53	59	48	10	22	61	45
Thalassiosira australis														1		
Thalassiosira cf. maculata																
Thalassiosira decipiens																
Thalassiosira delicatula													1			
Thalassiosira frenguelliopsis													9	7	9	16
Thalassiosira gracilis			1	4			8	1	1	1						
Thalassiosira lentiginosa				4		1	1			1	1	1	11			3
Thalassiosira lineata											1			1		
Thalassiosira oestrupii													2	1		3
Thalassiosira oliverana																
Thalassiosira perpusilla																
Thalassiosira poroseriata																
Thalassiosira spp.																
Thalassiosira symmetrica			1										8		1	
Thalassiosira trifulta																
Thalassiosira tumida		1	2	2		1	3	1			1	3	10	7	5	1
Other unidentified species							1									
	TOTAL	298	298	302	99	302	281	101	99	98	88	100	309	371	299	306

Appendix 2.3. All new French raw data.

	UKA Code	214	215	216	217	218	219	220	221	222	223	224	225	226	227	228	229
	JJP Code	7610	7621	7630	7631	7637	7641	7643	7647	7657	7705	7710	7711	7721	7730	7737	7747
	Core	DFBC 83-1 II	DFBC 83-40 II	DFBC 83-5 II	DFBC 83-23 II	DFBC 83-2 II	DFBC 83-21 II	DFBC 83-43 III	DFBC 83-20 II	DFBC 83-10 II	DFBC 83-9 II	DFBC 83-1 III	DFBC 83-8 II	DFBC 83-7 II	DFBC 83-6 II	DFBC 83-44 II	DFBC 83-6 III
	Lat °S	76°10'	76°21'	76°30'	76°31'	76°37'	76°41'	76°43'	76°57'	76°57'	77°05'	77°10'S	77°10'	77°21'	77°30'	77°37'	77°47'
Species	Long.	168°58'E	167°12'E	166°00'E	170°05'E	164°21'E	167°49'E	176°19'W	166°41'E	166°20'E	166°31'E	169°07'E	165°48'E	165°53'E	165°48'E	166°15'E	177°53'E
"Achnanthess brevipes (var. angustata)"																	
Actinocyclus actinochilus		11	2	4	12	11	9		9	8	15	10	7	12	11	3	4
Actinocyclus ingens																	
Amphora ovalis																	
Asteromphalus heptactis																	
Asteromphalus hookeri		3	1		1		1		1	1	1	1	2	1	3	1	
Asteromphalus parvulus		1	1			1	3		3	3	1			1		1	1
Azpeita tabularis																	
Chaetoceros spores																	
Chaetoceros spp.		3	1			1	2			3	2	1					
Cocconeis spp.																	
Corethron criophilum																	
Coscinodiscus asteromphalus																	
"Coscinodiscus bullatus"																	
Coscinodiscus curvatulus																	
"Coscinodiscus furcatus"		3		2	6		9	4	10	6	1				3		
Coscinodiscus radiatus																	
Coscinodiscus spp.																	
"Coscinodiscus symbolophorus"			5			1						9	7	2		1	1
Dactyliosolen antarctica																	
Dictyocha spp. ¥																	
Distephanus spp. ¥		3	2	1	2		5	2	2	1	4	2	4	1	2		2
Eucampia antarctica		9	14	15	24	18	21	17	18	10	14	24	9	15	13	5	13
Gomphonema intricatum																	
Grammatophora arcuata					2									2			
Hemidiscus cuneiformis																	
Hemidiscus karsteni																	
Licmophora "decora"																	
Melosira adeliae		1			1												
Melosira sol ("Paralia sol")																	2
Navicula directa														1	1		
Navicula glacei																	
"Nitzschia angulata"		8	4	4	5	4	10	2	1	9	4	5	4	10	3		
"Nitzschia" bicapitata																	
"Nitzschia closterium"																	
"Nitzschia curta"		103	139	113	114	134	90	18	114	134	125	98	136	135	106	6	25
"Nitzschia cylindrus"		9	3	20	3	4	5	3	2	5	5	9	5	11	11		3
"Nitzschia heimii"																	
"Nitzschia kerguelensis"		1	4		5		6	7	1	2	1	3	1	5	2	2	1
Nitzschia lecontei													1	1	1		2
"Nitzschia lineata"				30													
"Nitzschia lineola"														1			
"Nitzschia obliquecostata"		7	3	16	5	1	7	6	5	3	2	5		8	9		3
Nitzschia paundriformis																	
"Nitzschia pseudonana"		1															
"Nitzschia ritscheri"																	
"Nitzschia seperanda"		23	5	6	9	5	5	3	5	17	2	13	7	13	9	1	
"Nitzschia sublineata"		57	58	3	49	42	53	28	57	44	70	78	58	31	39	20	29
"Nitzschia van heurckii"																	
Odontella weissflogii		1										2					
Pleurosigma directum													1				
Pleurosigma spp.																	
Porosira glacialis		2		1	3	2			2		3	1	6	1	2		

Appendix 2.3. All new French raw data.

	LKA Code	214	215	216	217	218	219	220	221	222	223	224	225	226	227	228	229
	JJP Code	7610	7621	7630	7631	7637	7641	7643	7647	7657	7705	7710	7711	7721	7730	7737	7747
	Core	DFBC 83-1 II	DFBC 83-40 II	DFBC 83-5 II	DFBC 83-23 II	DFBC 83-2 II	DFBC 83-21 II	DFBC 83-43 III	DFBC 83-20 II	DFBC 83-10 II	DFBC 83-9 II	DFBC 83-1 III	DFBC 83-8 II	DFBC 83-7 II	DFBC 83-6 II	DFBC 83-44 II	DFBC 83-6 III
	Lat °S	76°10'	76°21'	76°30'	76°31'	76°37'	76°41'	76°43'	76°57'	76°57'	77°05'	77°10'S	77°10'	77°21'	77°30'	77°37'	77°47'
Species	Long.	166°58'E	167°12'E	166°00'E	170°05'E	164°21'E	167°49'E	176°19'W	166°41'E	166°20'E	166°31'E	169°07'E	165°48'E	165°53'E	165°48'E	166°15'E	177°53'E
Porosira pseudodenticulata			3														
Pseudoenotia doliolus																	
Rhizosolenia alata														1			
Rhizosolenia hebetata																	
*Rhizosolenia *hebetata f. bidens**		1									1		1		1		
Rhizosolenia styliformis		2		2	1	3	1			1	1	5	1			1	4
Roperia tesselata																	
Stellarima microtrias		4															
Synedra kerguelensis																	
Thalassionema nitzschioides																	
Thalassiosira antarctica		23	37	72	36	49	48		46	38	37	19	30	39	63		4
Thalassiosira australis																	
Thalassiosira cf. maculata					1	3							1				
Thalassiosira decipiens																	
Thalassiosira delicatula																	
Thalassiosira trenguelliopsis																	
Thalassiosira gracilis		7	4	4	10	10	12	6	9	3	4	6	5	1	13	3	5
Thalassiosira lentiginosa		4	2	2	7	5	6	3	5	8	2	7	5	2	4	6	1
Thalassiosira lineata																	
Thalassiosira oestrupii																	
Thalassiosira oliverana		1	1		1	1	1		1		1		4	1	6	1	
Thalassiosira perpusilla						2											
Thalassiosira porosenata											1			1			
Thalassiosira spp.																	
Thalassiosira symmetrica																	
Thalassiosira trifulta												2		5			
Thalassiosira tumida		14	3		3	3	6		10	3	3	2	4				
Other unidentified species										1							
TOTAL		302	292	295	300	300	300	99	301	298	300	302	299	301	302	51	100

Appendix 2.4. Authors new surface samples- all species raw data.

	LKA Code No.	145	146	147	148	149	150	151	240	241	184	258	259	243	242	260	244	261	245
	Core	MDBX 94-01	MDBX94-02	MDBX94-03	MDBX94-04	MDBX94-05	MDBX94-06	MDBX94-07	TC53-10	TC37-19	E36-6	147GC007	147GC013	147GC014	147GC016	147GC017	147GC030	147GC031	147GC034
	Depth(m)	2620	3572	3460	4036	3730	3315	2768	4091	4594	3303	3307	4452	750	384	3001	2968	3403	4002
	Latitude °S	42°30'	45°35'	46°28'	50°22'	48°48'	44°34'	41°43'	49°00.05	56°03.5'	54°32.4'	45°09.53'	46°10.01'	46°26.98'	46°47.99'	47°45.04'	46°10.04'	44°32.80'	45°06.00'
Species	Longitude	79°25'E	86°31'E	88°03'E	90°16'E	89°32'E	90°04'E	90°16'E	148°06.7'E	124°56'E	140°03.1'E	146°17.51'E	144°15.99'E	145°14.47'E	145°14.99'E	145°49.01'E	147°27.98'E	149°03.81'E	147°44.5'E
Actinocyclus actinochilus				1	0.1				4	0.1									
Actinocyclus curvatulus		1	1	0	0	0	0	1	1	0	0	2	3	2	9	4	0	7	6
Actinocyclus cf. exiguus															1				
Actinocyclus ingens		1	1	1					1	2									
Asteromphalus hookeri		3	1	4	0.1	1		1	5		3		1						
Asteromphalus spp.														1					
Azpeitia tabularis		50	3	14	7	6	24	36	29	8	10	7	30	28	79	9	25	14	34
Azpeitia tabularis var. egregius		19					3	7											
Chaetoceros resting spores		28	96	58	38	78	77	47	5	35	3	24	7	20	83	5	12	2	34
Chaetoceros spp. (vegetative)		1			2														
Cocconeis spp.				1															
Corethron criophilum									?1										
Coscinodiscus africanus		1																	
Coscinodiscus asteromphalus								1											
Coscinodiscus marginatus											1								
Coscinodsicus radiatus												2		1	2	1	1		1
Coscinodiscus spp.		1						2	1			2	3	1		2	1	4	4
Dactyliosolen antarcticus		12	14	19	22	29	19	1	11		12								4
Delphineis surirella																		1	1
Denticulopsis sp.										2									
Eucampia antarctica		7	18	18	28	12	4		7	3	5			1					
Fragilariopsis curta			1			1				16									
Fragilariopsis cylindrus										3									
Fragilariopsis doliolus		37	1	1		1	14	28				2	7	1		2	5	7	18
Fragilariopsis kerguelensis		53	112	154	159	139	106	58	129	171	209	21	73	132	106	66	123	46	129
(F. kerguelensis (malformed)+)							1												
Fragilariopsis rhombica			1	1	5		2		1	4									
Fragilariopsis ritscheri															1				
Fragilariopsis separanda		1	3		1	7	2		2	15	1					1			3
Fragilariopsis sublinearis				1		1			3	8									0.1
Hemidiscus cuneiformis		15	1				4	17	3			4	13	7	7	1	11	7	7
Hemidiscus karstenii															5				
Licmophora sp.		1																	
Melosira sol														3					
Navicula directa		1	1			2	1				2								
Nitzschia baarudii														1			?1	2	
Nitzschia bicapitata													1				?1	1	
Nitzschia cf. dietrichii															1				
Nitzschia interruptestriata																			1
Nitzschia kolaczekii												1		1					
Nitzschia paundriformis					1														
Nitzscia sicula var. rostrata																1			
Odontella weissflogii		1	4	1	4	5													
Paralia sol													2			1	1	1	3
Paralia sp.		3	1	2	3	1	2							1					
Pleurosigma spp.											1						0.1		
Porosira glacialis			1	2	1		1												

Appendix 2.4. Authors new surface samples- all species raw data.

Species	LKA Code No.	145	146	147	148	149	150	151	240	241	184	258	259	243	242	260	244	261	245
	Core	MDBX 94-01	MDBX94-02	MDBX94-03	MDBX94-04	MDBX94-05	MDBX94-06	MDBX94-07	TC53-10	TC37-19	E36-6	147GC007	147GC013	147GC014	147GC016	147GC017	147GC030	147GC031	147GC034
	Depth(m)	2620	3572	3460	4036	3730	3315	2768	4091	4594	3303	3307	4452	750	384	3001	2968	3403	4002
	Latitude °S	42°30'	45°35'	46°28'	50°22'	48°48'	44°34'	41°43'	49°00.05	56°03.5'	54°32.4'	45°09.53'	46°10.01'	46°26.98'	46°47.99'	47°45.04'	46°10.04'	44°32.80'	45°06.00'
	Longitude	79°25'E	86°31'E	88°03'E	90°16'E	89°32'E	90°04'E	90°16'E	148°06.7'E	124°56'E	140°03.1'E	146°17.51'E	144°15.99'E	145°14.47'E	145°14.99'E	145°49.01'E	147°27.98'E	149°03.81'E	147°44.5'E
Proboscia alata																		1	1
Pseudonitzschia fineola						1				0.1									
Pseudotriceratium sp.			1																
Rhaphoneis spp.												1			4				
Rhizosolenia antennata		4	2		1		6	8	3	3				2	7		2		1
Rhizosolenia cf. *bergonii*												2				2	1	2	3
Rhizosolenia hebetata f. *semispina*										1									
Rhizosolenia spp.											1	2				1			
Rhizosolenia styliformis		5	2	1	3	2	2	1									2		1
Roperia tesselata		15	2			1	11	12	14				10	20	4	5	8	4	7
Rouxia spp.							2			2									
Stellarima microtrias		5					4	4								1			
Stephanopyxis sp.				1					1								1		
Thalassionema nitzschioides+		11	6	7	8	6	11	13	7	3	8	2	5	2	14	4	3	2	4
(*Thalassionema nitz.* var *parva* +)		3	3	1	1		3	4					1				1	1	
Thalassiosira antarctica		2	3	3	1	2					1								
Thalassiosira cf. *decipiens*						1													
Thalassiosira eccentrica		1																	
Thalassiosira freguellopsis															1				
Thalassiosira gracilis			7	5	8	14	8		4	20	11	1	1	1	4	1	3	1	7
Thalassiosira lentiginosa		18	28	41	49	31	27	21	59	29	23	15	22	56	21	20	31	7	16
Thalassiosira leptopus																			1
Thalassiosira lineata		1					1	8	0.1			1	3	4	2	3	1		
Thalassiosira oestrupii		15	1	1		1	7	21				4	4	10	12	1	14	12	18
Thalassiosira oliverana			1		2				2	1	3								
Thalassiosira poroseriata																	1	4	1
Thalassiosira cf. *punctifera*		4						1											
Thalassiosira trifulta		4	2				1	7	2			2	5	8	4	5	2	9	6
Thalassiosira tumida											0.1								
Thalassiosira spp.		5	2	3		2	5	5	2	1		2	3	5	6		3	2	4
Thalassiothrix/ Trichotoxon spp.		12	13	10	17	10	15	10	24	19	30	3	9	12	10	5	9	6	12
Dictyocha spp.¥		14	2			1	4	17	1			3	4	2	2	2	3	8	9
Distephanus spp.¥		8	1	6	3	5	5	5	6	3	7	3	1	6	7	5	5	2	8
TOTAL		358	336	357	358	360	368	332	327	346	331	106	208	328	392	147	269	153	344

Abbreviations and Notes.

Numbers recorded indicate raw counts of a particular species. A '?' means compares with (cf).

Where '0.1' is recorded, it refers to a fragment/presence of a particular species not included in the total counts for the sample.

LKA Code No. = numeric code of identification used by author.

"+" = Sub-species are included in the total given for the normal species (ie. *Thalassionema nitzschoides*).

¥ = denotes silicoflagellates.

Appendix 2.5. Abbott's diatom counts - all data.

Core	E34-17	E34-19	E34-20	E35-3	E35-4	E35-5	E35-6	E35-7	E36-5	E36-6	E36-8	E36-11	E36-14	E34-16	E36-34	E37-19	E37-20	E39-13
Latitude	60°17.1'S	56°40.0'S	54°10.2'S	48°16.0'S	56°52.1'S	56°03.0'S	59°12.1'S	49°58.1'S	53°01.6'S	54°32.4'S	58°05.5'S	60°37.4'S	58°05.6'S	58°08.2'S	60°00.0'S	56°05.6'S	50°53.5'S	45°00.7'S
Longitude	144°58.3'E	135°13.1'E	135°12.7'E	131°51.0'E	129°38.1'E	128°10.8'E	128°05.8'E	128°04.4'E	139°59.2'E	140°03.1'E	139°54.6E	142°04.7'E	150°14.4'E	149°59.6'E	155°02.6'E	124°53.3'E	125°10.3'E	125°58.9'E
slide no.	0-2A	0-2A	0-2A	0-2B	0-2A	0-2A	0-2A	0-2B	0-2A	0-2A	0-2B	0-2B	0-2A	0-2A	0-2A	0-2A	0-2B	0-2A
date(m/d/yr)	4/04/72	4/04/72	3/19/72	3/31/72	3/19/72	3/24/72	3/24/72	3/31/72	4/02/72	4/02/72	4/02/72	3/18/72	4/04/72	4/02/72	4/02/72	3/21/72	3/19/72	4/01/72
Age (Abbott 1973)	U. Bruhnes	Matuyama	M. Brunhes	Bruhnes ?	U. Bruhnes	U. Bruhnes	M-U. Bruhne	?	U. Bruhnes	U. Bruhnes	U. Bruhnes	M. Bruhnes	L. Bruhnes	U. Bruhnes	U. Bruhnes	M. Bruhnes	M. Bruhnes	U. Bruhnes
Depth (fathoms)	2480	2196	2180	2060	2512	2455	2185	2120	1620	1835	2390	2332	1670	2090	1528	2500	2205	2480
Curent Names used in this work	Abbott's Diatom species																	
Actinocyclus ingens	*Actinocyclus ingens*		11		5		present		present					5				5	
Asteromphalus cf. *hyalinus*	*Asteromphalus cf. hyalinus*												1			1			
Asteromphalus cf. *roperianus*	*Asteromphalus cf. roperianus*																		
Asteromphalus hookeri	*Asteromphalus hookeri*			1						1	1				present		present		
Asteromphalus parvulus	*Asteromphalus parvulus*	present	1		1		present					1		1	1	1			
Chaetoceros bulbosum complex	*Chaetoceros bulbosus*																		
Acinocyclus actinochilus	*Charcotia actinochilus*												1			3	present		
Actinocyclus curvulatus	*Coscinodiscus curvulatus*																		
Coscinodiscus decrescens	*Coscinodiscus decrescens*	1			1														
Thalassiosira elliptopora	*Coscinodiscus elliptipora*			1					fragment										
Thalassiosira Eccentric Group	*Coscinodiscus excocentricus*																		
Thalassiosira lentiginosa	*Coscinodiscus lentiginous*	14	10	22	16	22	22	19	21	15	19	21	13	22	25	26	23	37	8
Thalassiosira leptopus	*Coscinodiscus lineatus*															1			
Coscinodiscus marginatus	*Coscinodiscus marginatus*	1				1	1			1	1				present	2			
Coscinodiscus occuloides	*Coscinodiscus occuloides*				present						present				present		present		
Stellarima microtrias	*Coscinodiscus symbolophorus*			present	present														
Azpeitia tabularis	*Coscinodiscus tabularis*	3	2	16	4	5	5	5	5	9	7	5	3	1	2	1	4	8	1
Thalassiosira tumida	*Coscinodiscus tumidus*				present					present					present			1	
Denticula hustedii	*Denticula hustedii*	1	2														1		
Distephanus fibula	*Distephanus fibula*						1											3	
Distephanus speculum	*Distephanus speculum*	2	3	8	3	6	5	12	3	6	9	4	present	1	5	5	2	4	1
Ethmodiscus rex	*Ethmodiscus rex*																		
Eucampia antarctica	*Eucampia balaustium*	2		5	3	6	3	11	8	3	4	1	3	4	1	3	1	9	1
Gyrosigma subsalinum	*Gyrosigma subsalinum*				2								1						
Hemidiscus cuneiformis	*Hemidiscus cuneiformis*								1										
Hemidiscus karstenii	*Hemidiscus karstenii*	1			present	1			1							present	present		
Melosira sol	*Melosira sol*				1	1	1	2	1	1	3		1			1			
Navicula cf. *directa*	*Navicula cf. directa*			1			1	1		1					1				1
Fragilariopsis curta	*Nitzschia curta*				1					1			1	5	1	4			
Fragilariopsis cylindrus	*Nitzschia cylindrus*																		
Pseudonitzschia heimii	*Nitzschia heimii*						1	1											
Fragilariopsis kerguelensis	*Nitzschia kergulensis*	127	67	90	118	116	102	120	123	113	132	158	143	44	155	122	156	76	78
Fragilariopsis kerguelensis	*Nitzschia kergulensis ovalis*	42	21	19	46	16	24	50	40	55	56	28	39	21	33	42	27	27	26
Fragilariopsis kerguelensis	*Nitzschia lanceolata*	12	91	8	16	2	10	8	13	13	14	12	4	14	5	1	3	8	16
Fragilariopsis linearis	*Nitzschia linearis*		1		1									1					
Fragilariopsis obliquecostata	*Nitzschia obliquecostata*			1															
Nitzschia paunduriformis	*Nitzschia paunduriformis*																		
Fragilariopsis rhombica	*Nitzschia rhombica*	2	1	2	1		1	3	1	6	1	1		1	2	4	2		
Fragilariopsis ritscheri	*Nitzschia ritscherii*	1	1		1	6			2		3	4	1	2	3				1
Fragilariopsis separanda	*Nitzschia separanda*	7	7	4	5	4	2		5	2	4		29	3	1	14		4	5

Appendix 2.5. Abbott's diatom counts - all data.

	Core	E34-17	E34-19	E34-20	E35-3	E35-4	E35-5	E35-6	E35-7	E36-5	E36-6	E36-8	E36-11	E36-14	E34-16	E36-34	E37-19	E37-20	E39-13
?	*Nitzschia sp. 200*		5																
Nitzshcia sicula var. *rostrata*	*Nitzshcia sicula var. rostrata*		1	1	1						2						1		
Fragilariopsis doliolus	*Pseudonotia doliolus*																		
Proboscia barboi	*Pyxilla barboi*		3																
Rhizosolenia styliformis	*Rhizosolenia styliformis*				1			1	1			1		1		1	1		3
Roperia tesselata	*Roperia tesselata (coscinodiscoides)*																	1	
Rouxia peragalli f. *yabei*	*Rouxia peragallii f. yabei*		6	3	1								2	1			4	1	
Thalassiosira oliverana	*Shrimperiella antarctica*	2		2	1	2	2		1	present	1	2	1	2	1	present	present	1	
Thalassionema nitzschioides	*Thalassionema nitzschioides*			11	2	1	6	1		4		1	9				2	14	1
Thalassiosira cf. *dubia*	*Thalassiosira cf. dubia*																		
Thalassiosira cf. *oestrupii*	*Thalassiosira cf. oestrupii*				2						1				1				1
Thalassiosira gracilis	*Thalassiosira gracilis*	3	6	1	2	3	1	1	1	4	4		1		4	6	3	1	3
Thalassiothrix/Trichotoxon spp.	*Thalassiothrix spp.*	80	57	113	66	62	115	65	76	68	45	65	43	70	63	67	44	101	53
Tropidoneis belsica	*Tropidoneis belsica*							1											
unknown	unknown	1	7	5	1	2	3	5		3	1		2	1	1		3	6	1
	TOTAL	902	303	314	302	256	306	306	303	306	308	304	297	201	305	305	277	307	200

Appendix 2.5. Abbott's diatom counts - all data.

Core	E39-17	E39-18	E39-23	E39-26	E39-35	E39-38	E39-39	E39-53	E39-55	E44-13	E44-15	E44-16	E44-21	E44-22	E44-23	E44-27	E45-33	E45-35	E45-39	E45-42	E45-60
Latitude	47°01.6'S	48°00.5'S	51°07.3'S	52°58.5'S	57°30.6'S	53°S	52°05.1'S	48°49.0'S	49°56.9'S	58°01.1'S	57°59.6'S	57°59.2'S	58°03.6'S	58°05.3'S	58°06.2'S	53°02.3'S	51°58.7'S	53°29.7'S	56°00.4'S	57°12.7'S	55°03.7'S
Longitude	125°56.8'E	126°05.5'E	126°10.6'E	126°08.2'E	133°58.5'E	133.5°E	133°56.3'E	144°32.4'E	145°55.8'E	142°27.0'E	137°26.6'E	134°58.2'E	130°06.5'E	130°0.8.2'E	130°11.0'E	119°44.1'E	110°28.4'E	111°20.0'E	112°42.9'E	113°20.2'E	114°09.1'E
slide no.	0-2B	0-2A	0-2B	2-4 cm A&B	0-2B	0-2A	0-2B	0-2A	0-2A	0-2B	0-2A	0-2B	0-2B	0-2A	0-2B	0-2A	0-2B	0-2A	0-2A	0-2A	0-2A
date(m/d/yr)	4/01/72	3/31/72	3/17/72		3/21/72	4/01/72	9/08/71	4/02/72	3/22/72	4/02/72	1/19/72	4/01/72	1/11/72	1/13/72	3/17/72	3/27/72	9/22/71	9/16/71	3/23/72	9/13/71	1/10/72
Age (Abbott 1973)	U. Bruhnes	M. Bruhnes	U. Bruhnes	U. Bruhnes	M. Bruhnes	U. Bruhnes	U. Bruhnes	U. Bruhnes	Matuyama	U. Bruhnes	U. Bruhnes	U. Bruhnes	U. Bruhnes	M. Bruhnes	M. Bruhnes	M. Bruhnes	U. Bruhnes	U. Bruhnes	M. Bruhnes	M. Bruhnes	M. Bruhnes
Depth (fathoms)	2185	2522	2570	2555	2530		1855	2140	2570	2074	2361	2419	2512	2512	2514	1917	1872	2100	2390	2368	2246
Abbott's Diatom species																					
Actinocyclus ingens		1	1		present				6					fragments			1		2		
Asteromphalus cf. hyalinus																					
Asteromphalus cf. roperianus					present																
Asteromphalus hookeri	1				2				present	1										1	
Asteromphalus parvulus			present		1	2			present	present	1		2	1			1	1			
Chaetoceros bulbosus			1												1						
Charcotia actinochilus				1													1			1	
Coscinodiscus curvulatus				2																	
Coscinodiscus decrescens														1							
Coscinodiscus elliptipora									1												
Coscinodiscus excentricus														1							
Coscinodiscus lentiginous	7	19	33	18	17	7	10	20	24	10	13	16	9	13	21	16	22	24	24	30	17
Coscinodiscus lineatus								1													
Coscinodiscus marginatus		1			2	2								2					1		
Coscinodiscus oculoides					1														present		
Coscinodiscus symbolophorus			present							present											
Coscinodiscus tabularis	3	8	3		5	4	5	10	8	2	4	6	1	1	3	5	1	6	6	1	2
Coscinodiscus tumidus						1		1		present			present								
Denticula hustedii					1																
Distephanus fibula		2	present			present		3								1					
Distephanus speculum	1		5	9	12	4	8	2	3	5	2	5	8	6	4	6	1	3	present	3	3
Ethmodiscus rex																					
Eucampia balaustium	2	10	7	5	15	1	4	2	3		3	1	3	4	11	5	3	5	3	8	1
Gyrosigma subsalinum																					2
Hemidiscus cuneiformis		1						1													
Hemidiscus karstenii		1			2						present			present					present		
Melosira sol				3			7		2		1	1	1	1	1			1		2	1
Navicula cf. directa			1		2										1	2		2			
Nitzschia curta			4								4	1		1						1	
Nitzschia cylindrus												1						1			
Nitzschia heimii					1	1				2								1			
Nitzschia kerguelensis	88	99	83	167	101	111	101	48	90	171	137	123	155	126	118	103	143	146	177	107	174
Nitzschia kerguelensis ovalis	27	53	51	11	36	30	31	41	21	24	19	28	27	23	27	47	33	19	21	36	42
Nitzschia lanceolata	18	19	5		14	5	26	13	13	4	12	23	8	18	15	5	11	7	2	19	5
Nitzschia linearis																					
Nitzschia obliquecostata							1														
Nitzschia paunduriformis						present															
Nitzschia rhombica	2	1	5	4	1	1	4		1	1	1	3	12	7	2	2		2	2	2	2
Nitzschia ritscheril	1		1							1		1	1	1			1	4	1	1	
Nitzschia separanda	1	2	4		3	1	3		1	3	4	3	8	11	5	2	4	9	7	6	4

Appendix 2.5. Abbott's diatom counts - all data.

Core	E39-17	E39-18	E39-23	E39-26	E39-35	E39-38	E39-39	E39-53	E39-55	E44-13	E44-15	E44-16	E44-21	E44-22	E44-23	E44-27	E45-33	E45-35	E45-39	E45-42	E45-60
Nitzschia sp. 200																	2				
Nitzschia sicula var. rostrata								1													
Pseudonotia doliolus																					
Pyxilla barboi		1																			
Rhizosolenia styliformis	1		1		1							2		1	1					2	
Roperia tesselata (coscinodiscoides)		2						1													
Rouxia peragallii f. yabei		1			2				4		1			1		1			2	1	4
Shrimpsiella antarctica			present	3	3	1	1	1	present	2	1	1			1	1			3	1	1
Thalassionema nitzschioides		2	9	10	1	10		3	2		4		5			12	4	1	1		3
Thalassiosira cf. dubia													2								
Thalassiosira cf. oestrupii			3		1			1			2			1	1						1
Thalassiosira gracilis	1	2	3			2	2			6	3	1	9			5	1	3	1	4	4
Thalassiothrix spp.	48	76	83	55	82	120	48	56	121	69	88	88	56	83	90	86	61	63	42	72	35
Tropidoneis belgica																					
unknown		1	2	2	1	1	7		3	4	2		2	3	1	4	2	5	5	4	2
TOTAL	201	302	305	290	307	304	258	205	303	305	302	304	309	306	303	303	292	303	300	302	303

Appendix 2.5. Abbott's diatom counts - all data.

Core	E45-69	E45-71	E45-77	E45-79	Conrad 8-63	Conrad 8-64	Verna 16-11(	E45-44	E38-4	E36-12	E45-58	E35-16	E44-24	E45-37	E44-26	E45-63	E35-15	E45-64	E39-21	E45-31	E45-29
Latitude	48°50.9'S	48°01.5'S	46°26.9'S	45°03.4'S	51°05.0'S	51°30'S	55°41'S	58°28.5'S	64°13.9'S	61°45.1'S	56°35.0'S	53°11.6'S	56°02.4'S	54°41.8'S	54°01.1'S	53°26.2'S	52°56.4'S	52°29.0'S	48°51.7'S	46°04.2'S	44°52.6'S
Longitude	114°37.0'E	114°29.2'E	114°25.0'E	114°22.0'E	129°58.0'E	135°51'E	141°17'E	114°07.3'E	150°03.8'E	149°33.1'E	114°06.9'E	116°57.5'E	119°54.0'E	111°57.9'E	119°46.4'E	114°15.4'E	116°59.5'E	114°05.4'E	126°01.0'E	107°13.5'E	106°31.1'E
slide no.	0-2A	0-2A	0-2A	0-2A	0-2A	1-5A	top	0-2B	0-2A	0-2A	0-2A	1-3B	0-2A	0-2	0-2A	0-2B	0-2A	0-2A	0-2A	0-2A	0-2A
date(m/d/yr)	3/30/72	3/04/72	3/30/72	3/30/72	9/30/71	4/02/72	3/30/72	9/14/71	3/17/72	4/02/72	12/08/71	9/15/71	1/19/72	9/21/71	3/17/72	1/10/71	3/30/72	1/05/71	4/01/72	9/21/71	9/23/71
Age (Abbott 1973)	M. Bruhnes	L-M. Bruhne	L. Bruhnes	U. Bruhnes	U. Bruhnes	L. Bruhnes	NO Diatoms	U. Bruhnes	U. Bruhnes	U. Bruhnes	U. Bruhnes	U. Bruhnes	U. Bruhnes	U. Bruhnes	U. Bruhnes	U. Bruhnes	U. Bruhnes	U. Bruhnes	U. Bruhnes	U. Bruhnes	U. Bruhnes
Depth (fathoms)	1865	2000	2081	2240	3442m			2428	1905	2218	2416	2350	2405	2270	2328	2142	2058	2090	2230	1818	2088
Abbott's Diatom species																					
Actinocyclus ingens	2	4	1			14											1				
Asteromphalus cf. hyalinus														1							
Asteromphalus cf. roperianus													present								
Asteromphalus hookeri	1						present			present			1		1	1					
Asteromphalus parvulus					1	1	present	1	3	1	4		2	1	1		2			1	
Chaetoceros bulbosus										1											
Charcotia actinochilus									present											1	
Coscinodiscus curvulatus																					
Coscinodiscus decrescens			1											1					1		
Coscinodiscus elliptipora			1																		1
Coscinodiscus excentricus																					
Coscinodiscus lentiginous	60	69	40	33	63	8	15	26	19	20	29	25	9	12	13	17	18	25	19	30	50
Coscinodiscus lineatus				1									1		1					1	3
Coscinodiscus marginatus			1	3											present						
Coscinodiscus oculoides													present								
Coscinodiscus symbolophorus	2																				
Coscinodiscus tabularis	17	5	6	15	28	1	8	4	3		11	11	7	4	5	8	3	3	5		18
Coscinodiscus tumidus														1	present	1	present				
Denticula hustedii																					
Distephanus fibula	3	4	1	5	1										present				1		1
Distephanus speculum	3	2	2	2	6		5	3	3	2	3	8	4	2	6	3	1	1		1	1
Ethmodiscus rex						1															
Eucampia balaustium	6	9	12	4	35		1	3	5	1	5	8	3	1	4	3	3	4	3	20	6
Gyrosigma subsalinum															1						
Hemidiscus cuneiformis		1	3	4															3	1	7
Hemidiscus karstenii			1																		
Melosira sol				2	1	4									2	1				1	
Navicula cf. directa							1		1	1	3	2	2	3	3	2	4				
Nitzschia curta				1				1	11	2				1	1	2				1	
Nitzschia cylindrus									4	3											
Nitzschia heimii									1					3			3				
Nitzschia kerguelensis	36	23	31	54	69	28	180	152	120	165	235	168	173	157	133	161	101	171	72	36	41
Nitzschia kerguelensis ovalis	33	37	33	54	67	69	27	14	19	26	21	34	18	21	49	11	46	8	20	50	41
Nitzschia lanceolata	13	23	19	42	23	13	5	16	5	6	6	21	6	10	5	5	16	3	11	45	34
Nitzschia linearis									2												
Nitzschia obliquecostata					1																
Nitzschia paunduriformis	1																				
Nitzschia rhombica				1	6	2		4	14		2	3	2	1	10	7	2		2	1	
Nitzschia ritscherii								1	6											1	
Nitzschia separanda		2		2	4	2		10	6	12	8	3	1	18	4	7	1	1	3	2	

Appendix 2.5. Abbott's diatom counts - all data.

Core	E45-69	E45-71	E45-77	E45-79	Conrad 8-63	Conrad 8-64	Vema 16-11!	E45-44	E38-4	E36-12	E45-58	E35-16	E44-24	E45-37	E44-26	E45-63	E35-15	E45-64	E39-21	E45-31	E45-29
Nitzschia sp. 200																					
Nitzshoia sicula var. rostrata													1								1
Pseudonotia doliolus				2																	6
Pyxilla barboi																					
Rhizosolenia styliformis		2						1			1						2		1	2	3
Roperia tesselata (cosoinodiscoides)	7	6	6																		
Rouxia peragallii f. yabei	1					2	1		fragments				1								
Shrimperiella antarctica	1	1	2	2	2	8	3			present		1	2		2	2	1	2		2	
Thalassionema nitzschioides	6	2		9	2		2				7	5	10	5	18	6	3	2	4	1	6
Thalassiosira cf. dubia																					
Thalassiosira cf. oestrupii	1	1	2	3														1			
Thalassiosira gracilis					1	1	3	5	10	5	3	5	2	2		4	2	6			
Thalassiothrix spp.	111	110	36	61	96	40	51	60	68	54	62	107	56	55	42	56	90	70	52	97	71
Tropidoneis belsica															1						
unknown	3	5	5	7	1	6	2	2	2	3	3	7	3	3	4	6	2	3		8	13
TOTAL	307	306	203	307	407	200	304	303	302	302	403	408	304	302	306	303	301	300	197	302	303

Appendix 2.6. Citations of Rhizosolenia in the Southern Ocean.

Species	Reported In:
R. acuminata	Hustedt 1930, Crosby and Wood 1958
R. alata (synonym of Proboscia alata)	Van Heurck 1909*, Hustedt 1930, Hart 1934, Hendey 1937, Mann 1937, Crosby and Wood 1958, Hasle 1960, Wood 1960, Cassie 1961, Jouse et al. 1962, Bunt and Wood 1963, Cassie 1963, Kozlova 1966, Hargraves 1968†, Hasle 1968, Hasle 1969, Zernova 1970, Simonsen 1974, Hasle 1975, Fenner et al. 1976, Schrader 1976, Soumia et al. 1979, Gersonde 1984, Priddle and Fryxell 1985, Garrison et al. 1987, Gersonde & Wefer 1987, Garrison and Buck 1989, Estrada and Delgado 1990, Tanimura et al. 1990, Kang and Fryxell 1991, Stockwell et al. 1991, Tanimura 1992, Garrison and Close 1993, Kang and Fryxell 1993, Schloss and Estrada 1994, Scharek et al. 1994, Andreoli et al. 1995.
R. alata* f. *curvirostirus (synonym of ***Proboscia subarctica***)	Hustedt 1930
R. alata* f. *gracillima (synonym of ***P. alata***)	Hustedt 1930, Hart 1934, Hendey 1937, Hart 1942, Crosby and Wood 1958, Cassie 1963, Ligowski 1993.
R. alata* f. *indica (synonym of ***Proboscia indica***)	Hustedt 1930, Hendey 1937, Crosby and Wood 1958, Wood 1960, Cassie 1963, Hargraves 1968†, Simonsen 1974, Soumia et al. 1979, Garrison et al. 1983.
R. alata* f. *inermis (synonyms to ***Proboscia inermis*** and ***P. sumorpha***)	Hustedt 1930, Hendey 1937, Crosby and Wood 1958, Wood 1960, Cassie 1963, Kozlova 1966, Hargraves 1968†, Fenner et al. 1976, Soumia et al. 1979, Akiba 1982, Garrison et al. 1983, Garrison and Buck 1989, Tanimura et al. 1990.
R. annulata	Hendey 1937.
R. antarctica (conspecific with ***R. cylindrus***)	Hart 1934, Hart 1942, Wood 1960, Cassie 1963, Zernova 1970, Soumia et al. 1979.
R. antennata	Hooker 1847*.
R. antennata* f. *antennata	Jordan and Pudsey 1992, Ligowski 1993 (as *R. antennata*) Zielinski 1993, Zielinski and Gersonde 1997.
R. antennata* f. *semispina	Ligowski 1993, Zielinski 1993, Wright et al. 1996Δ, Zielinski and Gersonde 1997.
R. barboi (synonym of ***Proboscia barboi***)	Schrader 1976, DeFelice and Wise 1981, Pichon 1985.
R. bergonii	Hustedt 1930, Hendey 1937, Mann 1937, Hasle 1960, Kozlova and Mukhina 1967, Simonsen 1974, Fenner et al. 1976, Kellogg and Trusedale 1979, Winsborough and Abbott 1985, Pokras and Molfino 1986, Burckle 1989, Zielinski 1993, Hernández-Becerril 1995, Zielinski and Gersonde 1997.
R. bidens (synonym of ***R. antennata* f. *antennata***)	Hart 1934, Hendey 1937, Mann 1937.
R. calcar-avis (synonym of ***Pseudosolenia calar-avis***)	Hustedt 1930, Hendey 1937, Crosby and Wood 1958, Kozolva and Mukhina 1967, Simonsen 1974, Hasle 1975.
R. castracanei	Hustedt 1930, Hart 1934, Hendey 1937, Crosby and Wood 1958, Simonsen 1974, Hasle 1975, Hernández-Becerril 1995.
R. chunii	Hart 1934, Hendey 1937, Hart 1942, Crosby and Wood 1958, Wood 1960, Cassie 1963, Hasle 1968,1969, Zernova 1970, Soumia et al. 1979, Priddle and Fryxell 1985, Garrison et al. 1987, Garrison and Buck 1989, Ligowski 1993, Schloss and Estrada 1994, Wright et al. 1996Δ.
R. cochlea	Simonsen 1974
R. crassa	Hart 1934, Hendey 1937, Wood 1960, Hasle 1969, Priddle and Fryxell 1985, Ligowski 1993.
R. curvata	Hart 1934 (*R. curva*), Hendey 1937, Hart 1937, Crosby and Wood 1958, Wood 1960, Cassie 1963, Hargraves 1968†, Hasle 1968, Hasle 1969, Zernova 1970, Soumia et al. 1979, Semina 1979, Priddle and Fryxell 1985.
R. curvirostris (+ var. ***inermis***) (synonym of ***Proboscia curvirostirus*** or ***P. barboi*** respectively)	Donahue 1970a, Abbott 1973, DeFelice and Wise 1981.
R. cylindrus ((Cleve) synonym of ***Guinardia cylindrus***)	Hustedt 1930, Crosby and Wood 1968, Wood 1960, Hasle 1960, Hasle 1969, Simonsen 1974, Hasle 1975, Priddle and Fryxell 1985, Garrison et al. 1987, Garrison and Buck 1989, Ligowski 1993, Wright et al. 1996Δ.
R. delicatulata ((Cleve) synonym of ***Guinardia delicatulata***)	Hendey 1937, Ligowski 1993.
R. fragilissima	Heiden and Kolbe 1928*, Hustedt 1930, Hendey 1937, Crosby and Wood 1958, Hasle 1975.
R. hebetata	Hustedt 1930, Hendey 1937, Crosby and Wood 1958, Kozlova 1966, Kozlova and Mukhina 1967, Abbott 1973, Booth 1984*, Garrison et al. 1987, Gersonde & Wefer 1987, Tanimura 1992, Schloss and Estrada 1994, Andreoli et al. 1995.
R. hebetata* f. *bidens (synonym of ***R. antennata* f. *antennnata***)	Jouse et al. 1962, Kozlova 1966, Kozolva and Mukhina 1967, Fenner et al. 1976, Semina 1979, Akiba 1982, Pichon 1985, Stockwell et al. 1991, Simonsen 1992.
R. hebetata* f. *hemialis-spinosa	Schrader 1976.
R. hebetata* f. *hiemalis	Hustedt 1930, Crosby and Wood 1958, Wood 1960, Donahue 1970a, Schrader 1976, Fenner et al. 1976, Ciesielski 1991, Harwood and Maruyama 1992.
R. hebetata* f. *semispina	Heiden and Kolbe 1928*, Hustedt 1930, Hart 1942, Crosby and Wood 1958, Wood 1960, Cassie 1961, Jouse et al. 1962, Cassie 1963, Kozlova 1966, Hasle 1969, Zernova 1970, Simonsen 1974, Hasle 1975, Fenner et al. 1976, Kellogg and Trusedale 1979, Soumia et al. 1979, Fryxell et al. 1983, El-Sayed et al. 1983, Pichon 1985, Priddle and Fryxell 1985, Priddle et al. 1986, Ciesielski 1991, Kang and Fryxell 1991, Stockwell et al. 1991, Kang and Fryxell 1993, Zielinski 1993, Froneman et al. 1995, Hernández-Becerril 1995, Zielinski and Gersonde 1997.
R. cf. hyalina	Hasle 1969.
R. imbricata	Castracane 1886, Hustedt 1930, Hendey 1937, Mann 1937, Crosby and Wood 1958, Wood 1960, Simonsen 1974, Hasle 1975, Soumia et al. 1979.
R. imbricata* var. *shrubsolei (synonym of ***R. imbricata***)	Hustedt 1930, Crosby and Wood 1958, Cassie 1961, Cassie 1963, Hasle 1969, Garrison et al. 1983.
R. i.* var. *shrubsolei* f. *tenuissima	Cassie 1963
R. indica (synonym of ***Probosia indica***)	Mann 1937, Froneman et al. 1995
R. inermis (synonym of ***Prboscia inermis***)	Castracane 1886, Van Heurck 1909*, Mann 1937, Wright et al. 1996Δ.
R. inermis* f. *castracane	Simonsen 1974.
R. inermis* f. *rostrata (synonym of ***Proboscia truncata***)	Heiden and Kolbe 1928*, Simonsen 1974.
R. minima sensu Hustedt	Hustedt 1930.
R. minima sensu Schrader	Schrader 1976, Akiba 1982.
R. polydactyla	Castracane 1886, Hart 1934, Hendey 1937, Mann 1937.
R. rhombus	Hart 1934, Hendey 1937, Mann 1937, Wood 1960, Hasle 1969, Priddle and Fryxell 1985.
R. robusta	Castracane 1886, Hustedt 1930, Hendey 1937, Mann 1937, Crosby and Wood 1958, Cassie 1961,Simonsen 1974, Hasle 1975.
R. rostrata (synonym of ***Proboscia truncata***)	Wood 1960, Bunt and Wood 1963.
R. semispina	Mann 1937.
R. setigera	Hustedt 1930, Hendey 1937, Mann 1937, Crosby and Wood 1958, Cassie 1961, Kozlova 1966, Simonsen 1974.
R. shrubsolei	Hendey 1937, Mann 1937, Priddle and Fryxell 1985, Garrison et al. 1987, Garrison and Buck 1989.

Appendix 2.6. Citations of Rhizosolenia in the Southern Ocean.

Species	Reported In:
R. sima	Castracane 1886, Ligowski 1993.
R. sima* var. *sima	Castracane 1886.
R. sima* var. *silicea	Ligowski 1993.
R. simplex	Hart 1934, Hendey 1937, Hart 1942, Wood 1960, Jouse et al. 1962, Cassie 1963, Kozolva 1964, Kozlova and Mukhina 1967, Hasle 1968, Hargraves 1968†, Hasle 1969, Semina 1979, Soumia et al. 1979, Priddle and Fryxell 1985, Ligowski 1993, Froneman et al. 1995.
R. stolterforthii **((Stolterforth) synonym of *Guinardia striata***)	Hustedt 1930, Hendey 1937, Mann 1937, Crosby and Wood 1958, Cassie 1961, Hasle 1975, Soumia et al. 1979
R. styliformis	Hooker 1847*, Castracane 1886, Hustedt 1930, Hart 1934, Hendey 1937, Mann 1937, Crosby and Wood 1958, Hasle 1960, Wood 1960, Cassie 1961, Jouse et al. 1962, Cassie 1963, Kozolva 1964, Hargraves 1968†, Hasle 1969, Donahue 1970, Abbott 1973, Simonsen 1974, Schrader 1976, Fenner et al. 1976, Kellogg and Truesdale 1979, Soumia et al. 1979, DeFelice and Wise 1981, Akiba 1982, Garrison et al. 1983, Burckle 1984, Pichon 1985, Priddle and Fryxell 1985, Pokras and Molfino 1986, Garrison et al. 1987, Kellogg and Kellogg 1987, Gersonde & Wefer 1987, Garrison and Buck 1989, Estrada and Delgado 1990, Ciesielski 1991, Jordan and Pudsey 1992, Tanimura 1992, Ligowski 1993, Zielinski 1993, Andreoli et al. 1995, Zielinski and Gersonde 1997.
R. styliformis* f. *polydactyla	Hasle 1969.
R. styliformis* var. *oceanica	Hasle 1975. (synonym to *R. styliformis* Hustedt1930 fig 333, and Hendey 1937 pl. 11, fig 16-17.)
R. styliformis* var. *latissima	Hooker 1847*, Van Heurck 1909*, Heiden and Kolbe 1928*, Hustedt 1930, Cassie 1963, Crosby and Wood 1958, Hargraves 1968†.
R. styliformis* var. *longispina	Hustedt 1930, Crosby and Wood, 1958.
R. styliformis* var. *styliformis	Hasle 1975. (synonym to *R. styliformis* var *longispina* (Hustedt) 1930).
R. torpedo	Hart 1934, Hasle 1969.
R. truncata **(synonym of *Proboscia truncata***)	Van Heurck 1909*, Hart 1934, Hendey 1937, Wood 1960, Cassie 1963, Burkholder and Mandelli 1965*, Soumia et al. 1979, Krebs 1983, Wright et al. 1996Δ.
R. tubiformis	Hasle 1969, Hasle 1975, Garrison et al. 1987.
Rhizosolenia **spp.**	Akiba 1982, Kellogg and Kellogg 1987, Estrada and Delgado 1990, Bianchi et al. 1992, Jordan and Pudsey 1992, Leventer 1992, Ligowski 1993, Kang and Fryxell 1993, Scharek et al. 1994, Andreoli et al. 1995, Leventer et al. 1996.
Simonseniella barboi **(junior synonym of *Proboscia barboi***)	Fenner 1991
Simonseniella curvirostris **(junior synonym of *Proboscia curvirostris***)	Fenner 1991
Simonseniella praebarboi **(junior synonym of *Proboscia praebarboi***)	Fenner 1991
Proboscia inermis	Jordan and Pudsey 1992
Proboscia **spp.**	Gleitz et al. 1996.

Notes.

All synonyms are referenced from Priddle *et al.* 1990, Jordan & Priddle 1991, Jordan *et al.* 1991, Hernández-Becerril 1995, & Takahashi *et al.* 1994. The reader is responsible for checking these references for their respective synonyms list and new descriptions before applying their own taxonomy. This table is as comprehensive as possible, but is known to have deficiencies. Sundström's thesis, which would have reviewed the synonyms, was not available for this work.

* = refered to in Horner 1985, Appendix "Algal species reported from sea ice". Reference otherwise unsighted.

† = Plates only sighted from Hargarves 1968.

Δ = report taken from the Australian Antarctic Divison Internet site late 1996.

Appendix 3.1 . Dissolved data set - raw data (Pichon et al. (1996b).

	LKA Code	115	116	117	118	119	120	121	246	122	247	123	124	125	126	127	248	128	129
	Core	8702-DISS-5'	8702-DISS10'	8702-DISS20'	8702-DISS35'	8702-DISS60'	8702DISS120'	8702DISS180'	8702-DISS-240	8702-DISS24H	8707-DISS5'	8707-DISS10'	8707-DISS20'	8707-DISS35'	8707-DISS60'	8707DISS120'	8707-DISS180	8707DISS240'	8808-DISS05'
	Lat °S	56°27.6'	56°27.6'	56°27.6'	56°27.6'	56°27.6'	56°27.6'	56°27.6'	56°27.6'	56°27.6'	62°21.2'	62°21.2'	62°21.2'	62°21.2'	62°21.2'	62°21.2'	62°21.2'	62°21.2'	49°15.7'
Species	Long.	33°58.5'W	33°58.5'W	33°58.5'W	33°58.5'W	33°58.5'W	33°58.5'W	33°58.5'W	33°58.5'W	33°58.5'W	57°58.3'W	57°58.3'W	57°58.3'W	57°58.3'W	57°58.3'W	57°58.3'W	57°58.3'W	57°58.3'W	146°48.2'E
Achnanthes brevipes (1)																			
Actinocyclus actinochilus (2)		4	3	3	2	2	6		3		29	28	29	14	27	17	8	3	
Actinocyclus ingens						1										1			4
Asteromphalus hookeri (3)		2	1	1	1	1	1	1					1						1
Asteromphalus parvulus (4)		2	2	1	2	2	1			1									
Azpeitia tabularis (5)		3	3	4	2	6	1	8	7	1	1		4						18
Cocconeis spp.			1				2	2			10	17	12	17	20	26	17	4	
Coscinodiscus marginatus											1								2
Coscinodiscus radiatus			1																
Coscinodiscus spp. (6)		1																	
Eucampia antarctica		8	6	5	6	16	15	120	22	9	8	9		7	8	7	3	1	6
Fragilariopsis curta		2	1	2	2	1	2	2			15	11	17	12	12	4	3		
Fragilariopsis Cylindriform Group (8)							1				4	9	9	11	11				
Fragilariopsis kerguelensis (9)		130	140	148	117	123	102	91	90	17	33	30	28	30	35	45	16	15	145
Fragilariopsis Cool Taxa (10)		6	2	4	2	2	3	2	1	2	10	16	17	24	10	6	5		1
Fragilariopsis pseudonana																			
Fragilariopsis rhombica (12)		1	1		6	2		1			1	2	1	3	3	1	1		
Fragilariopsis separanda		5	4	2	7	4	6		1		1			1		2			1
Grammatophora arcuata		1													1				
Hemidiscus cuneiformis																			6
Hemidiscus karstenii																			
Navicula directa		1															1		
Nitzschia paundriformis							1												
Odontella weissflogii		2	3		1	1	2		1		5	8	5	6	7	1	1		
Pleurosigma directum		1				1													
Porosira Group (16)		2	3		4	1	2				8	5	8	8	2	3	3		
Pseudonitzschia heimii																	1		
Rhizosolenia ant. f. antennata (17)			1			1	2												
Rhizosolenia otaria present (19)		10	14	8	13	5	6	8	3		7	9	11	3	6	1			1
Rocella gelida																			
Roperia tesselata																			18
Stellarima microtrias (20)		2	1			2	1	1	1	1	2	3	3	4	5	1	4		
Stellarima stellaris (21)																			5
Thalassionema Taxa (22)					3	3													
Th. antarctica/scotia Group (23)		9	10	7	9	12	5	3	5	2	120	102	83	96	105	51	41	16	
Thalassiosira australis																			
Thalassiosira decipiens			1	1															
Thalassiosira Eccentric Group (24)						1									2				2
Thalassiosira gracilis Group (25)			11	13	12	8	5	5	1		16	16	14	20	12	1	4	2	
Thalassiosira lentiginosa		84	87	95	108	104	128	145	189	82	17	23	15	19	20	43	24	18	68
Thalassiosira Lineati Group (26)			2																1
Thalassiosira oestrupii Group (28)																			
Thalassiosira oliverana (29)		8	3	6	3	6	12	10	4	2	1			1		1	1		3
Thalassiosira ritscheri (30)			1											1					
Thalassiosira tumida (31)		2	1			1		1				1							
Thalassiosira spp.								1				11	11	10	8				
Other unidentified spp.											10			2		2			
	TOTAL	286	303	300	300	305	305	401	328	117	297	300	268	289	294	213	133	59	282

Notes:
Bracketed numbers in species column refer to species listed in summary table of Chapter 2

Appendix 3.1 . Dissolved data set - raw data (Pichon et al. (1996b).

LKA Code	130	249	250	131	251	252	253	132	254	133	134	255	256	135	136	137	138
Core	8808-DISS10'	8808-DISS020'	8808-DISS035'	8808-DISS60'	8808-DISS0120	8808-DISS0180	8808-DISS0240	8808-DISS24H	8808-DISS48H	8810DISS0-20	8810DISS35-60	8810DISS120	8810DISS180	8810DISS240'	8810DISS24H	8818DISS0-05	8818-DISS10'
Lat °S	49°15.7'	62°21.2'	62°21.2'	49°15.7'	62°21.2'	62°21.2'	62°21.2'	49°15.7'	62°21.2'	54°11.2'	54°11.2'	54°11.2'	54°11.2'	54°11.2'	54°11.2'	65°45'	65°45'
Species Long.	148°48.2'E	57°58.3'W	57°58.3'W	148°48.2'E	57°58.3'W	57°58.3'W	57°58.3'W	148°48.2'E	57°58.3'W	144°47.9'E	144°47.9'E	144°47.9'E	144°47.9'E	144°47.9'E	144°47.9'E	138°12'E	138°12'E
Achnanthes brevipes (1)																8	7
Actinocyclus actinochilus (2)		1	1			1	1								4		
Actinocyclus ingens	3	3	6	3	9	6	7		1								
Asteromphalus hookeri (3)	2			1	1	1	1			3			3	2			
Asteromphalus parvulus (4)	1	2								1	1	1				2	1
Azpeitia tabularis (5)	18	11	7	2	6	2	2	1		16	18	12	12	11	2		
Cocconeis spp.																1	7
Coscinodiscus marginatus	1	2	1					1									
Coscinodiscus radiatus																	
Coscinodiscus spp. (6)																	
Eucampia antarctica	6	11		8	3	3	2			1	4	1	1	1	1	13	8
Fragilariopsis curta																105	88
Fragilariopsis Cylindriform Group (8)																	2
Fragilariopsis kerguelensis (9)	115	111	102	64	94	58	44	12	2	300	345	274	172	189	40	43	60
Fragilariopsis Cool Taxa (10)	1		2			1										45	51
Fragilariopsis pseudonana																2	
Fragilariopsis rhombica (12)	2															40	21
Fragilariopsis separanda		1	3	1						1		1	2			1	1
Grammatophora arcuata																2	2
Hemidiscus cuneiformis	7	1															
Hemidiscus karstenii	1	1			2												
Navicula directa																	
Nitzschia paundriformis																1	
Odontella weissflogii																	
Pleurosigma directum					1											2	1
Porosira Group (16)																	
Pseudonitzschia heimii																	
Rhizosolenia ant. L antennata (17)																	
Rhizosolenia otaria present (19)	1			2						1			1			2	1
Rocella gelida					1		1										
Roperia tesselata	11	10	1														
Stellarima microtrias (20)																	
Stellarima stellaris (21)										1							
Thalassionema Taxa (22)	4		3	2		1	1			2	1	1	1	2			
Th. antarctica/scotia Group (23)																17	18
Thalassiosira australis															1		
Thalassiosira decipiens																	
Thalassiosira Eccentric Group (24)			1	1		1						1					
Thalassiosira gracilis Group (25)			3							4	2	1		2	2	3	9
Thalassiosira lentiginosa	67	73	43	39	28	22	30	4	5	67	66	102	106	112	27	12	12
Thalassiosira Lineati Group (26)	1										2		1	1			
Thalassiosira oestrupii Group (28)							1										
Thalassiosira oliverana (29)	4	3	6	6	1	4	2			9	6	4	2	8	4		
Thalassiosira ritscheri (30)																	2
Thalassiosira tumida (31)		1															
Thalassiosira spp.																	
Other unidentified spp.			5		2	1	2										
TOTAL	245	231	184	129	148	101	94	18	8	406	445	398	301	328	81	300	291

Appendix 3.1 . Dissolved data set - raw data (Pichon et al. (1996b).

	LKA Code	139	257	140	141	142	143	144
	Core	8818-DISS20'	8818DISS035	8818DISS120'	8818DISS180'	8818DISS240'	8818-DISS24H	8818-DISS48H
	Lat °S	65°45'	65°45'	65°45'	65°45'	65°45'	65°45'	65°45'
Species	Long.	138°12'E	138°12'E	138°12'E	138°12'E	138°12'E	138°12'E	138°12'E
Achnanthes brevipes (1)			1					
Actinocyclus actinochilus (2)		5	5	6	5	5	4	4
Actinocyclus ingens								
Asteromphalus hookeri (3)			2	1				
Asteromphalus parvulus (4)		1	1	1	2	1		
Azpeitia tabularis (5)						7		
Cocconeis spp.			2	5	3	2	2	
Coscinodiscus marginatus								
Coscinodiscus radiatus		1						
Coscinodiscus spp. (6)								
Eucampia antarctica		7	11	3	25	27	25	18
Fragilariopsis curta		94	69	14	8	3		
Fragilariopsis Cylindriform Group (8)				1				
Fragilariopsis kerguelensis (9)		65	73	111	96	112	48	22
Fragilariopsis Cool Taxa (10)		42	47	20	22	17	12	3
Fragilariopsis pseudonana		1		4	2			
Fragilariopsis rhombica (12)		24	23	20	9	1		
Fragilariopsis separanda		1	3	4	6	1		
Grammatophora arcuata		3						
Hemidiscus cuneiformis								
Hemidiscus karstenii								
Navicula directa								
Nitzschia paundriformis								
Odontella weissflogii			1	1	1	1		1
Pleurosigma directum								
Porosira Group (16)		3	3	2	9			
Pseudonitzschia heimii								
Rhizosolenia ant. f. antennata (17)			4					
Rhizosolenia otaria present (19)		1	1			1	1	
Rocella gelida								
Roperia tesselata								
Stellarima microtrias (20)		2	4	5	2	3		
Stellarima stellaris (21)								
Thalassionema Taxa (22)								
Th. antarctica/scotia Group (23)		23	24	55	114	12	7	1
Thalassiosira australis								
Thalassiosira decipiens			1		1			
Thalassiosira Eccentric Group (24)				2	1			
Thalassiosira gracilis Group (25)		5	4	6	6	2		
Thalassiosira lentiginosa		17	20	24	38	62	41	25
Thalassiosira Lineati Group (26)			1					
Thalassiosira oestrupii Group (28)								
Thalassiosira oliverana (29)		1		3	8		4	1
Thalassiosira ritscheri (30)								
Thalassiosira tumida (31)		3		1	1	1		
Thalassiosira spp.								
Other unidentified spp.								3
TOTAL		299	300	289	359	258	144	78

Appendix 3.2. Antarctic Diatom Database (ADB) - raw data.

LKA Code	1	2	3	4	5	7	8	9	10	11	12	13	14	15	16	21	26	28	29	30	31	32	33	34	35
Core	V16-65	V16-60	1176-91	1176-88	1277-2	RC15-91	RC11-78	RC13-255	1176-82	RC13-274	RC13-273	MD24-KK63	RC13-263	1277-28	MD82 424	1178-4P	1277-41	MD82 436	1176-55	1176-65	1277-8	1277-12	1578-49	1678-64	1678-80
Lat °S	45°00'	49°59.6'	44°56.7'	46°57.8'	45°02.1'	49°55.3'	50°52'	50°34'	59°31.2'	53°09'	55°04.5'	51°56'	53°48.3'	61°28'	54°05.8'	61°24.4'	69°59.9'	61°13.6'	53°22.9'	57°12.5'	50°32.5'	54°00.6'	61°05.6'	54°00.5'	47°57'
Species Long.	45°46'E	36°45.5'E	15°02.9'E	14°18.2'E	22°28.2'E	15°34.1'W	09°52'W	02°53.7'E	13°11.5'E	12°25.6'E	11°34.5'E	42°53'E	08°13'W	09°11'E	00°20.7'W	46°58.9'W	05°04.6'W	19°28.8'W	06°39.6'E	08°12.4'E	20°53'E	19°47.5'E	19°51.9'W	24°11.7'W	13°01.4'W
Actinocyclus actinochilus	1	8	2	6	3				1	8				3	2	34	39	24	1				16		2
Actinocyclus curvatulus															1						1				2
Actinocyclus Ingens		1																							
Asteromphalus hookeri					2	1	1					1	1		4				1	1	2				1
Asteromphalus parvulus		2			2					2	2	2		5	1			2	4			5			2
Asteromphalus robustus												1	1												
Azpeitia tabularis	15	12	10	3	9	17	16	11	4	2	3	11	2		3			3	1			2	2	3	7
Coscinodiscus asteromphalus															1										2
Coscinodiscus marginatus																								6	
Coscinodiscus radiatus				1												2		1	1					1	2
Eucampia antarctica	16	22	6	28	7	26	12	9	9	28	7	1	4	2	3	17	69	69	3		7	9	42	34	46
Fragilariopsis curta											4		4	1		21			6	1		2	1	1	1
Fragilariopsis Cylindriform Group										1						16		1			1	1			
Fragilariopsis doliolus			1		3																				
Fragilariopsis kerguelensis	108	195	166	154	152	151	194	179	228	176	244	187	222	218	179	32	128	72	162	242	178	202	121	151	150
Fragilariopsis Cool Taxa	2	3	3	4	5	1	2	4	1	8	8		7	16	7	13	24		5	9	3		11	3	1
Fragilariopsis oceanica					2						1														
Fragilariopsis pseudonana								1		1	1								1		1	7		1	
Fragilariopsis rhombica							2		1	1			1			8	3		2	1	1	2	4		1
Fragilariopsis separanda		3	1	1	3	1	1		2	3	2	1	6	4	5				4	1	4	3	1	4	
Hemidiscus cuneiformis			4		1																				
Nitzschia denticuloides														5					1					1	
Nitzschia paundriformis																									
Porosira Group																6									
Proboscia alata																									
Pseudonitzschia seriata			2																						
Rhizosolenia bergonii																									
Rhizosolenia otaria absent												1				4		1							
Rhizosolenia otaria present		1	1	2	1	1		2		2		1			1	16		1	2	1	2		1	3	2
Roperia tesselata			18		10																				
Stellarima microtrias															1	7		2		1					
Stellarima stellaris	5		5	4	1			1				1													2
Thalassionema Taxa	13		20	4	12	4	3	11				1			1				1					2	5
Th. antarctica/scotia Group			1		1											38							1		
Thalassiosira australis																									
Thalassiosira decipiens			5	3	5	3	3	4					2		1										
Thalassiosira Eccentric Group	1		4		7				1			1		1	1				4	1	4			1	3
Thalassiosira frenguellii																									
Thalassiosira gracilis Group	5	4	1	1	4	4	8	12	2	11	5	6	3	7	6	5		1	4	10	4	7	2	3	10
Thalassiosira gravida																									
Thalassiosira lentiginosa	123	45	52	85	66	78	51	61	43	63	24	65	34	35	70	52	60	116	75	26	72	54	95	78	58
Thalassiosira Lineati Group	3		6	1	2	1	1		3			1	1		1				2	1	2	1		1	2
Thalassiosira maculata																		1							
Thalassiosira oestrupii Group	2		1	1	2							1	1		1						2			4	
Thalassiosira oliverana	6			2	5	3	4	2	2			8	2	3	2	4	5	2	6	1	5		3	2	2
Thalassiosira perpusilla																									
Thalassiosira poroseriata																									
Thalassiosira tumida																12									
Other unidentified spp.	2				1	1	1					2	1	1	3	49		1	5	1	1	1	2	2	
TOTAL	303	298	309	298	306	292	300	297	297	306	301	294	292	301	294	336	328	297	291	297	290	296	302	302	300
% old species	0.00	0.34	0.00	0.00	0.00	0.00	0.00	0.00	0.00	0.00	0.00	0.34	0.00	0.00	0.00	0.00	0.00	0.00	0.00	0.34	0.00	0.00	0.00	0.00	0.00
% data used in 24 major species	90.76	91.89	92.23	88.59	92.48	89.73	94.67	95.96	95.62	90.20	97.34	95.92	97.26	97.01	95.24	73.81	78.96	75.08	93.47	98.32	93.79	96.28	85.10	83.44	80.33

Appendix 3.2. Antarctic Diatom Database (ADB) - raw data.

	LKA Code	36	37	38	39	42	43	44	45	46	47	50	51	52	53	54	55	56	57	62	63	64	65	66	67
	Core	1678-84	1678-89	1678-96	RC8-46	RC11-90	RC13-257	RC13-268	RC13-269	RC13-270	RC13-272	V14-58	MD24 KK02	MD24 KK32	MD24 KK35	MD24 KK37	MD82 425	MD82 430	MD82 434	MD 84 540	MD84 552	MD84 557	MD84 562	MD84 563	MD84 569
	Lat°S	51°57.5'	57°03.6'	60°27.9'	55°20'	56°38'	55°02.2'	57°02.3'	52°37.6'	55°28.8'	55°05.1'	57°37'	54°13'	54°30'	53°06.3'	52°58.4'	55°34.7'	57°52.3'	58°51.8'	60°44.5'	54°55.4'	53°19.6'	51°55.1'	50°42.7'	47°38.6'
Species	Long.	14°25.2'W	18°32.4'W	21°37.1'W	65°28'E	25°43'E	03°00.1'W	00°05.6'W	00°07.5'E	04°38.2'E	08°00'E	13°36'W	03°31'E	03°48.4'E	19°24.7'E	23°46.3'E	00°43'W	10°40.3'W	16°39'W	86°23.3'E	73°50'E	75°48'E	68°13.6'E	68°09.1'E	73°23.1'E
Actinocyclus actinochilus			7	4	1		2	6		4	3	3	2	1	4	1	1	6	10	2					
Actinocyclus curvatulus		2	1	1								1		7	1		1			1	1		1	2	1
Actinocyclus ingens					2																				
Asteromphalus hookeri							1							1	1	2	1	2	1					1	
Asteromphalus parvulus		1	4	2	4	1		1		2	2	2	9	2	3	4	1	1	1	3	1	1			
Asteromphalus robustus													2	1								1			
Azpeitia tabularis		8		3	4	8	8	1	5	4	2	3	1	8	1	1	1	9	8	8	17	13	15	9	7
Coscinodiscus asteromphalus				1										3			1								
Coscinodiscus marginatus																	1								
Coscinodiscus radiatus						1							1	1					1						
Eucampia antarctica		21	23	39	7	5	8	14	2	26	15	52	7	19	7	3	5	32	13	20		6	3	8	27
Fragilariopsis curta			3	5		2	1	3			6	4	1							5					
Fragilariopsis Cylindriform Group			1							2					1		1								
Fragilariopsis dollolus																									
Fragilariopsis kerguelensis		161	159	122	230	231	207	192	244	137	183	147	182	147	172	198	228	149	165	176	217	199	196	190	153
Fragilariopsis Cool Taxa		3	2	10	3	6	3	5	9	3	7	6	5	2	1	4	4	4	4	5	1	2	1		
Fragilariopsis oceanica								1																	
Fragilariopsis pseudonana		1						1		1	3														
Fragilariopsis rhombica			1	1		2	1	3	2	1	4				1	1	1			1					
Fragilariopsis separanda			4	8	2	5	1	3	6	2	3		2	1	1	9	6	1	1	6	6	3	2		
Hemidiscus cuneiformis																									
Nitzschia denticuloides					1						2														
Nitzschia paundriformis																					1	2			3
Porosira Group																									1
Proboscia alata																	1								
Pseudonitzschia seriata																									
Rhizosolenia bergonii																									
Rhizosolenia otaria absent			1	1			1	1						1	1		1		1						
Rhizosolenia otaria present		1		11	1			1		1			3	1	1	1	1	1	8		1	2	1	1	10
Roperia tesselata																									
Stellarima microtrias				1			1				1		1			1		1	1						
Stellarima stellaris		1																					1	1	
Thalassionema Taxa		4					1	1	2				1		1	1					1		6	3	7
Th. antarctica/scotia Group		3																							27
Thalassiosira australis																									
Thalassiosira decipiens		3					1							1	1	1			1		1				
Thalassiosira Eccentric Group		1	2						1				2	1	1	1	2	1	2		1	3	1	2	1
Thalassiosira frenguellii																									
Thalassiosira gracilis Group		6	5	5	5	3	4	9	7	6	5	4	7	2	3	2	7	2	10	6	9	6	5	6	1
Thalassiosira gravida														1				1							
Thalassiosira lentiginosa		74	78	79	36	31	56	53	19	102	64	72	61	82	79	56	31	84	60	59	31	37	61	43	39
Thalassiosira Lineati Group		1			2	1			1	2		3	1	1	1		2		1		2	5	1	2	
Thalassiosira maculata													2	1	1		1								
Thalassiosira oestrupii Group			1											2	23	1								1	
Thalassiosira oliverana		3	1	3	1	3	2	3		5	6	1	1	3	7	1	6	2	2	2	2	9	3	3	4
Thalassiosira perpusilla																									
Thalassiosira poroseriata																									
Thalassiosira tumida			1																	1					
Other unidentified spp.		3		3		1		1					3	4	2	1	4		3	1	2	1			5
TOTAL		297	295	300	299	299	299	299	298	298	308	298	295	291	315	288	307	296	294	296	294	290	297	273	287
% old species		0.00	0.00	0.00	0.67	0.00	0.00	0.00	0.00	0.00	0.00	0.00	0.34	0.00	0.00	0.00	0.00	0.00	0.00	0.00	0.00	0.00	0.00	0.00	0.00
% data used in 24 major species		90.57	90.85	81.33	95.65	97.66	96.32	93.98	98.66	90.27	94.44	81.54	92.54	88.66	94.92	96.88	93.81	87.50	89.46	92.91	97.62	93.10	97.64	94.14	83.62

Appendix 3.2. Antarctic Diatom Database (ADB) - raw data.

Species	LKA Code	71	77	78	79	84	85	86	87	88	89	91	92	94	95	96	97	98	99	100	101	102	103	104	105
	Core	83-41 III	KR8701	KR8702	KR8703	KR8710	KR8712	KR8713	KR8714	KR8801	KR8805	KR8807	KR8808	KR8810	KR8811	KR8812	KR8813	KR8814	KR8815	KR8816	KR8817	KR8818	KR8819	KR8820	KR8821
	Lat °S	76°40'	52°50'	56°27.6'	60°13.3'	59°39.6'	54°55.8'	52°42.8'	51°27.7'	46°40.6'	52°56.7'	47°08.9'	49°15.7'	54°11.2'	54°55'	56°23.8'	57°56.9'	61°16.8'	63°18.3'	64°46.2'	66°12.1'	65°45'	64°34.3'	64°56.1'	64°49.3'
	Long.	164°01'W	32°30'W	33°58.5'W	48°56.9'W	51°16.6'W	39°47.6'W	36°59.3'W	34°00.5'W	79°29.2'E	109°55.1E	145°47.8'E	148°48.2'E	144°47.9'E	144°04'E	145°17.2'E	144°35'E	144°26.5'E	141°55.5'E	141°13.4'E	140°30.2'E	139°12'E	135°37.5'E	129°00.3'E	126°43.5'E
Actinocyclus actinochilus		10	3	4	27	12	4	2	1		2				2				2	4	9	2	2	4	8
Actinocyclus curvatulus																									
Actinocyclus ingens													2						1						
Asteromphalus hookeri			1	2		1		1	1	2	1			2			1	1	1				1	1	
Asteromphalus parvulus			1		3	1	3		3		1		1	1	1		1	2	5	1	2	2	2	3	1
Asteromphalus robustus																									
Azpeitia tabularis			3			3	6	1		3	13	57	18	11	14	13	8	6	4	4			4	1	
Coscinodiscus asteromphalus																									
Coscinodiscus marginatus																									
Coscinodiscus radiatus							1				1														
Eucampia antarctica		60	22	7	15	14	19	28	34	22	5		5	1	1			2	6	17	3	2	15	14	15
Fragilariopsis curta		150	1	3	14	3	1		1										2	5	85	170	5	34	32
Fragilariopsis Cylindriform Group		8		2	7	1														1	2	5			2
Fragilariopsis doliolus												3													
Fragilariopsis kerguelensis		1	120	135	68	130	200	57	158	172	205	109	156	321	302	193	190	193	203	200	56	95	145	268	164
Fragilariopsis Cool Taxa		57	3	6	17	7	4	1	2		3				1	2		4	9	11	44	38	8	20	19
Fragilariopsis oceanica																					3			1	1
Fragilariopsis pseudonana			1	3																					
Fragilariopsis rhombica			1	2	2	4	1		2								1	2	2	3	17	44	5	8	3
Fragilariopsis separanda		1	1	1	1	2	2		1	1	5		2		4		1	4		2	3	2	6	5	1
Hemidiscus cuneiformis										2		12	3												
Nitzschia denticuloides																									
Nitzschia paundriformis																									
Porosira Group			1	1	1	3				1								1		1	12	4	6		1
Proboscia alata			1																						
Pseudonitzschia seriata																									
Rhizosolenia bergonii																									
Rhizosolenia otaria absent																									
Rhizosolenia otaria present			8	14	5	13	6	6	13	3	2			1		1					2	1		4	
Roperia tesselata										2		25	17												
Stellarima microtrias				1	4	3															2				1
Stellarima stellaris			2					1																	
Thalassionema Taxa							2			6	2	4	7	6	1	2	1								
Th. antarctica/scotia Group		1	8	8	53	16	8	241	39	14	1										107	20	12	13	9
Thalassiosira australis																					3				
Thalassiosira decipiens			1		1						1				1	1	1							1	
Thalassiosira Eccentric Group			1								2	5	3			1		1	2				2		
Thalassiosira frenguellii												5													
Thalassiosira gracilis Group		9	2	8	23	18	11	1	5	2	3		1	4	5	4	10	11	1	3	9	13	6	15	13
Thalassiosira gravida												2													
Thalassiosira lentiginosa		2	102	80	26	91	138	43	127	62	45	84	74	37	54	69	72	65	52	90	26	9	80	60	50
Thalassiosira Lineati Group			5								1		2	1											
Thalassiosira maculata												3													
Thalassiosira oestrupii Group								2			1	6	1			1									
Thalassiosira oliverana			12	3	3	10	11	7	6	2	1	1	5	5	5	5	7	3	8	9	3	1	7	4	8
Thalassiosira perpusilla																						2			
Thalassiosira poroseriata																									
Thalassiosira tumida				2	1			2	2								1								
Other unidentified spp.		1	1	3	29	5	1	5	5	1		7		1	2			2			9	2		1	4
TOTAL		300	301	285	300	337	418	398	400	295	296	323	297	391	393	292	294	297	298	351	397	412	306	455	332
% old species		0.00	0.00	0.00	0.00	0.00	0.00	0.00	0.00	0.00	0.00	0.00	0.67	0.00	0.00	0.00	0.00	0.00	0.34	0.00	0.00	0.00	0.00	0.00	0.00
% data used in 24 major species		79.67	86.38	90.88	83.67	90.21	93.54	89.70	88.75	90.51	95.61	93.19	95.96	98.47	99.24	99.32	99.66	97.98	96.64	95.16	94.96	98.30	94.12	95.38	93.98

Appendix 3.2. Antarctic Diatom Database (ADB) - raw data.

Species	LKA Code	106	107	108	109	110	112	113	145	148	152	153	154	155	156	184	192	210	211	212	213	214	215	216
	Core	KR8822	KR8823	KR8824	KR8825	KR8827	KR8829	KR8830	MDBX 94-0	MDBX94-0	93-7/GC33	93-7/GC5	KTB01	KTB12	KTB14	E36-6	KTB 08	BC 83-2	BC 83-2	BC 83-2	BC 83-3	DFBC 83-1 II	DFBC 83-40 II	DFBC 83-5 II
	Lat°S	64°40.1'	63°18'	63°44.8'	64°17.9'	63°39.1'	62°29.5'	61°00.2'	42°30'	50°22'	67°11'	67°03'	49°06'	49°00'	50°00'	54°32.4'	51°59'	75°42'	75°51'	76°01'	76°05'	76°10'	76°21'	76°30'
	Long.	119°30.2'E	117°15.8'E	116°44.9'E	115°42.1'E	101°08.9'E	95°53.1'E	93°11.9'E	79°25'E	90°16'E	68°30'E	69°05'E	67°01'E	57°59'E	57°59'E	140°03.1'E	61°07'E	170°39'E	169°18'E	167°12'E	166°42'E	168°58'E	167°12'E	166°00'E
Actinocyclus actinochilus		2	2	9	10	8	1	1			1	11						8	14	2	4	11	2	4
Actinocyclus curvatulus									1										1		1			
Actinocyclus ingens								1	1					1				2		2				
Asteromphalus hookeri					1		1		3			1	1			3		2	1	1	1	3	1	
Asteromphalus parvulus				4	1			1			2	1	1				3	2		2		1	1	
Asteromphalus robustus																								
Azpeitia tabularis			7	4	1	6	5	8	69	7			11	9	17	10	11							
Coscinodiscus asteromphalus																			1		1			
Coscinodiscus marginatus					1											1								
Coscinodiscus radiatus																								
Eucampia antarctica		11	10	7	16	50	20	14	7	28	5	15	29	9	3	5	1	47	16	10	9	9	14	15
Fragilariopsis curta		12	4	12	15	8	1				207	205						96	193	106	127	103	139	113
Fragilariopsis Cylindriform Group			1		1						10	7						8	6	14	10	9	3	50
Fragilariopsis doliolus									37															
Fragilariopsis kerguelensis		261	190	153	160	175	233	169	53	159	3	7	262	218	264	209	239	3	5	3	4	1	4	
Fragilariopsis Cool Taxa		13	5	12	11	12	9	1			20	43		2	1			56	67	53	61	64	61	19
Fragilariopsis oceanica																								
Fragilariopsis pseudonana											3	8										1		
Fragilariopsis rhombica		8	1	3	2	1	1	2		5	8	7	1	2				6	8	4	2	8	4	4
Fragilariopsis separanda		8	5	4	3	3	5	6	1	1	3	1		1		1		22	10	8	11	23	5	6
Hemidiscus cuneiformis									15															
Nitzschia denticuloides																								
Nitzschia paundriformis										1			1											
Porosira Group		4		1			1			1	22	5							3	4		2	3	1
Proboscia alata																				1				
Pseudonitzschia seriata																								
Rhizosolenia bergonii																								
Rhizosolenia otaria absent									4	1														
Rhizosolenia otaria present		1		2		1	1	1	5	3	1	1	6		1					3		2		2
Roperia tesselata									15															
Stellarima microtrias					2	2					1	2						2	9	2	4	7	5	2
Stellarima stellaris									5															
Thalassionema Taxa							3	1	11	8			14	6	7	8	2							
Th. antarctica/scotia Group		2	5	8	9	8	1		2	1	10	6				1		10	22	61	45	23	37	72
Thalassiosira australis		2																						
Thalassiosira decipiens								1					1	1										
Thalassiosira Eccentric Group		4	1	2	2	2		1	9				3	1	1			8		1				
Thalassiosira frenguelliii																								
Thalassiosira gracilis Group		11	2	7	13	3	9	5		8	7	11	3	5	1	11	2	9	7	9	16	7	4	4
Thalassiosira gravida																								
Thalassiosira lentiginosa		103	80	65	45	75	113	74	18	43	2	10	72	75	55	23	28	11			3	4	2	2
Thalassiosira Lineati Group									1					1	1									
Thalassiosira maculata																			1					
Thalassiosira oestrupii Group									15					1										
Thalassiosira oliverana		10	3	2	6	18	8	8		2	1	1	4	3	3	3	4	2	1		3	1	1	
Thalassiosira perpusilla																								
Thalassiosira poroseriata																								
Thalassiosira tumida				1								2	1	1	1			10	8	5	1	14	3	
Other unidentified spp.		1		2			1	2	13	7	1	1	4	3		4		4		3	4	3		
TOTAL		453	316	298	298	373	414	297	285	275	307	345	414	340	355	279	290	308	370	294	306	296	289	294
% old species		0.00	0.00	0.00	0.00	0.00	0.00	0.34	0.35	0.00	0.00	0.00	0.00	0.29	0.00	0.00	0.00	0.65	0.00	0.68	0.00	0.00	0.00	0.00
% data used in 24 major species		95.81	96.52	95.64	93.62	85.52	94.20	93.27	83.16	85.45	97.72	94.78	89.37	95.29	98.31	85.34	99.66	79.55	95.14	92.86	95.42	94.26	94.81	94.22

Appendix 3.2. Antarctic Diatom Database (ADB) - raw data.

LKA Code	217	218	219	221	222	223	224	225	226	227	230	231	232	233	234	235	236	243	245
Core	DFBC 83-23 II	DFBC 83-2 II	DFBC 83-21 II	DFBC 83-20 II	DFBC 83-10 II	DFBC 83-9 II	DFBC 83-1 III	DFBC 83-8 II	DFBC 83-7 II	DFBC 83-6 II	1176-86	KR8802	KR8803	KR8804	MD84-561	MD73-026	MD84-529	147GC014	147GC034
Lat°S	76°31'	76°37'	76°41'	76°57'	76°57'	77°05'	77°10'S	77°10'	77°21'	77°30'	48°02.3'	45°45.2'	46°04.1'	49°55.3'	53°05.3'	44°59.0'	48°54.3'	46°26.98'	45°06.00'
Species Long.	170°05'E	164°21'E	167°49'E	166°41'E	166°20'E	166°31'E	169°07'E	165°48'E	165°53'E	165°48'E	13°49.0'E	82°56.0'E	90°06.7'E	100°05.0'E	71°36.4'E	53°17.0'E	61°59.8'E	145°14.47'E	147°44.5'E
Actinocyclus actinochilus	12	11	9	9	8	15	10	7	12	11	1								
Actinocyclus curvatulus															1				
Actinocyclus ingens												2	1						
Asteromphalus hookeri	1		1	1	1	1	1	2	1	3	1		1	2	1	2			
Asteromphalus parvulus		1	3	3	3	1			1		1	1			1	1	3		
Asteromphalus robustus																			
Azpeitia tabularis											4	16	10	10	7	11	19	28	34
Coscinodiscus asteromphalus																			
Coscinodiscus marginatus																			
Coscinodiscus radiatus												1	1					1	1
Eucampia antarctica	24	18	21	18	10	14	24	9	15	13	14	28	27	22	36	20	10	1	
Fragilariopsis curta	114	134	90	114	134	125	98	136	135	106	1								
Fragilariopsis Cylindriform Group	3	4	5	2	5	5	9	5	11	11									
Fragilariopsis doliolus												1						1	18
Fragilariopsis kerguelensis	5		6	1	2	1	3	1	5	2	171	130	163	169	175	207	187	132	129
Fragilariopsis Cool Taxa	54	43	60	62	47	72	83	58	39	48	1								
Fragilariopsis oceanica																1			
Fragilariopsis pseudonana											1								
Fragilariopsis rhombica	5	4	10	1	9	4	5	4	10	3	2								
Fragilariopsis separanda	9	5	5	5	17	2	13	7	13	9	1		1	2		1	1		3
Hemidiscus cuneiformis												1	3					6	7
Nitzschia denticuloides																			
Nitzschia paundriformis												1	1			1			
Porosira Group	3	2		2		3	1	6	1	2									
Proboscia alata									1										1
Pseudonitzschia seriata																			
Rhizosolenia bergonii																			3
Rhizosolenia otaria absent																		2	1
Rhizosolenia otaria present	1	3	1		1	1	5	1			3	4	1		2	1	1		1
Roperia tesselata													6					20	7
Stellarima microtrias	6	1	9	10	6	1	9	7	2	3									
Stellarima stellaris																2			
Thalassionema Taxa											17	1	1	9	1	11	8	2	4
Th. antarctica/scotia Group	36	49	48	46	36	37	19	30	39	63		12	4		8				
Thalassiosira australis																			
Thalassiosira decipiens											7					1			
Thalassiosira Eccentric Group							2		5		2	1		1		1	1	8	6
Thalassiosira frenguellii																			
Thalassiosira gracilis Group	10	10	12	9	3	4	6	5	1	13	2	2	2	3	10	3	4	1	7
Thalassiosira gravida																			
Thalassiosira lentiginosa	7	5	6	5	8	2	7	5	2	4	52	93	60	68	35	36	48	56	16
Thalassiosira Lineati Group											1			1	1	1		4	1
Thalassiosira maculata	1	3						1											
Thalassiosira oestrupii Group											2		6	9	1	3	1	10	18
Thalassiosira oliverana	1	1	1	1		1		4	1	6	3	9	1	4	6	4	6		
Thalassiosira perpusilla		2																	
Thalassiosira poroseriata						1			1										1
Thalassiosira tumida	3	3	6	10	3	3	2	4					1		2				
Other unidentified spp.	3				1	1	2	3	5	3	1	2	3		1	2		14	13
TOTAL	298	299	293	299	294	294	299	295	300	300	289	305	293	300	288	309	289	288	277
% old species	0.00	0.00	0.00	0.00	0.00	0.00	0.00	0.00	0.00	0.00	0.35	0.66	0.34	0.00	0.00	0.32	0.00	0.00	0.00
% data used in 24 major species	89.93	91.30	92.15	93.65	95.58	93.88	88.63	94.58	90.67	93.67	92.04	87.21	88.05	91.33	85.76	89.97	95.85	88.89	87.73

Appendix 4.1. ADB parameters.

LKA Code	Core sample	Depth (m)	Longitude	Latitude °S	SST Feb. (°C)	% Feb. sea-ice conc.	% Sept. sea-ice conc.	m/yr sea-ice cover
1	V16-65	1618	45°46'E	45°00'	7.5885	0	0	0
2	V16-60	4575	36°45.5'E	49°59.6'	4.4593	0	0	0
3	1176-91	4649	15°02.9'E	44°56.7'	10.3343	0	0	0
4	1176-88	5106	14°18.2'E	46°57.8'	7.443	0	0	0
5	1277-2	4806	22°28.2'E	45°02.1'	8.9467	0	0	0
7	RC15-91	3775	15°34.1'W	49°55.3'	4.2171	0	0	0
8	RC11-78	3115	9°52'W	50°52'	2.634	0	0	0
9	RC13-255	3332	02°53.7'E	50°34'	4.7665	0	0	0
10	1176-82	4100	13°11.5'E	59°31.2'	1.0259	0	85	6
11	RC13-274	3372	12°25.6'E	53°09'	1.6226	0	3	2
12	RC13-273	4970	11°34.5'E	55°04.5'	1.0484	0	47	4
13	MD24-KK63	2550	42°53'E	51°56'	3.6354	0	0	0
14	RC13-263	3389	8°13'W	53°48.3'	1.5809	0	0	0
15	1277-28	5322	09°11'E	61°28'	1.0565	0	89	7
16	MD82 424	2350	00°20.7'W	54°05.8'	1.6109	0	3	2
21	1178-4P	486	46°58.9'W	61°24.4'	0.8994	1	66	11
26	1277-41	1873	5°04.6'W	69°59.9'	-0.1728	13	84	12
28	MD82 436	3620	19°28.8'W	61°13.6'	0.3489	0	78	8
29	1176-55	2926	06°39.6'E	53°22.9'	2.3855	0	0	0
30	1176-65	5483	08°12.4'E	57°12.5'	0.7947	0	80	6
31	1277-8	4492	20°53'E	50°32.5'	3.3873	0	0	0
32	1277-12	3178	19°47.5'E	54°00.6'	1.4217	0	2	3
33	1578-49	4718	19°51.9'W	61°05.6'	0.3489	0	78	8
34	1678-64	4515	24°11.7'W	54°00.5'	1.9477	0	0	0
35	1678-80	3102	13°01.4'W	47°57'	5.7149	0	0	0
36	1678-84	3952	14°25.2'W	51°57.5'	2.9135	0	0	0
37	1678-89	4285	18°32.4'W	57°03.6'	1.2358	0	22	5
38	1678-96	4177	21°37.1'W	60°27.9'	0.4946	0	70	8
39	RC8-46	2761	65°28'E	55°20'	3.036	0	0	0
42	RC11-90	5334	25°43'E	56°38'	1.8598	0	4	3
43	RC13-257	2837	03°00.1'W	55°02.2'	1.2195	0	11	4
44	RC13-268	4005	00°05.6'W	57°02.3'	0.9031	0	59	5
45	RC13-269	2591	00°07.5'E	52°37.6'	2.761	0	0	0
46	RC13-270	3160	04°38.2'E	55°28.8'	1.3854	0	30	4
47	RC13-272	2538	08°00'E	55°05.1'	1.1607	0	34	4
50	V14-58	3543	13°36'W	57°37'	1.2719	0	37	5
51	MD24 KK02	NO DATA	03°31'E	54°13'	1.8311	0	7	2
52	MD24 KK32	2020	03°48.4'E	54°30'	1.8311	0	10	3
53	MD24 KK35	2725	19°24.7'E	53°06.3'	1.6769	0	0	0
54	MD24 KK37	2905	23°46.3'E	52°58.4'	2.2886	0	0	0
55	MD82 425	1940	00°43'W	55°34.7'	1.2917	0	28	5
56	MD82 430	3863	10°40.3'W	57°52.3'	1.1613	0	44	6
57	MD82 434	3640	16°39'W	58°51.8'	1.0975	0	56	7
62	MD 84 540	3964	86°23.3'E	60°44.5'	1.9204	0	46	7
63	MD84 552	1780	73°50'E	54°55.4'	2.3019	0	0	0
64	MD84 557	1080	75°48'E	53°19.6'	2.2306	0	0	0
65	MD84 562	3553	68°13.6'E	51°55.1'	3.9006	0	0	0
66	MD84 563	1720	68°09.1'E	50°42.7'	3.7004	0	0	0
67	MD84 569	1720	73°23.1'E	47°38.6'	6.4127	0	0	0
71	83-41 III	516	164°01'W	76°40'	-1.081	17	92	12
77	KR8701	3510	32°30'W	52°50'	3.5954	0	0	0
78	KR8702	3350	33°58.5'W	56°27.6'	1.8292	0	10	4
79	KR8703	1300	48°56.9'W	60°13.3'	1.3134	0	32	9
84	KR8710	2820	51°16.6'W	59°39.6'	2.0651	0	14	6
85	KR8712	2790	39°47.6'W	54°55.8'	3.3511	0	1	2
86	KR8713	2020	36°59.3'W	52°42.8'	3.9009	0	0	0
87	KR8714	2600	34°00.5'W	51°27.7'	4.6519	0	0	0
88	KR8801	2925	79°29.2'E	46°40.6'	7.7497	0	0	0
89	KR8805	3510	109°55.1E	52°56.7'	5.1163	0	0	0
91	KR8807	2890	145°47.8'E	47°08.9'	11.7046	0	0	0
92	KR8808	3885	148°48.2'E	49°15.7'	10.4595	0	0	0
94	KR8810	2785	144°47.9'E	54°11.2'	5.5964	0	0	0
95	KR8811	2880	144°04'E	54°55'	5.5964	0	0	0
96	KR8812	3020	145°17.2'E	56°23.8'	4.265	0	0	0
97	KR8813	3740	144°35'E	57°56.9'	3.9256	0	0	0
98	KR8814	4200	144°26.5'E	61°16.8'	2.7739	0	1	4
99	KR8815	3880	141°55.5'E	63°18.3'	1.7849	0	28	8
100	KR8816	3320	141°13.4'E	64°46.2'	0.9807	0	55	9
101	KR8817	2700	140°30.2'E	66°21.1'	0.0301	3	86	12
102	KR8818	615	138°12'E	65°45'	-0.0723	0	87	11
103	KR8819	2930	135°37.5'E	64°34.3'	0.9524	0	68	10
104	KR8820	1670	129°00.3'E	64°56.1'	1.08	0	72	10
105	KR8821	2250	126°43.5'E	64°49.3'	1.0572	0	72	10
106	KR8822	3140	119°30.2'E	64°40.1'	0.894	0	65	8
107	KR8823	3292	117°15.8'E	63°18'	1.1571	0	52	8
108	KR8824	2600	116°44.9'E	63°44.8'	1.0914	0	57	8
109	KR8825	2232	115°42.1'E	64°17.9'	0.605	1	79	12
110	KR8827	1210	101°08.9'E	63°39.1'	0.7584	0	85	10
112	KR8829	3790	95°53.1'E	62°29.5'	1.2904	0	81	8
113	KR8830	4300	93°11.9'E	61°00.2'	1.8192	0	56	6
145	MDBX94-01	2920	79°25'E	42°30'	12.9001	0	0	0
148	MDBX94-04	4022	90°16'E	50°22'	5.6976	0	0	0

LKA Code	Core sample	Depth (m)	Longitude	Latitude °S	SST Feb. (°C)	% Feb. sea-ice conc.	% Sept. sea-ice conc.	m/yr sea-ice cover
152	93-7/GC33	320	68°30'E	67°11'	0.1214	3	64	12
153	93-7/GC5	376	69°05'E	67°03'	0.1427	4	65	12
154	KTB01	1235	67°01'E	49°06'	4.3975	0	0	0
155	KTB12	4450	57°59'E	49°00'	5.8148	0	0	0
156	KTB14	4656	57°59'E	50°00'	5.2495	0	0	0
184	E36-6B	3303	140°03.1'E	54°32.4'S	5.4698	0	0	0
192	KTB 08	4710	61°07'E	51°59'	4.515	0	0	0
210	DFBC 83-27 II	322	170°39'E	75°42'	-0.3435	0	91	11
211	DFBC 83-28 II	485	169°18'E	75°51'	-0.3473	0	91	11
212	DFBC 83-29 II	622	167°12'E	76°01'	-0.3336	11	91	12
213	DFBC 83-30 II	668	166°42'E	76°05'	-0.378	17	89	11
214	DFBC 83-1 II	540	168°58'E	76°10'	-0.3141	0	91	11
215	DFBC 83-40 II	732	167°12'E	76°21'	-0.3336	11	92	12
216	DFBC 83-5 II	640	166°00'E	76°30'	-0.3549	16	91	12
217	DFBC 83-23 II	860	170°05'E	76°31'	-0.2881	0	88	11
218	DFBC 83-2 II	540	164°21'E	76°37'	-0.4001	26	86	12
219	DFBC 83-21 II	768	167°49'E	76°41'	-0.3336	4	92	12
221	DFBC 83-20 II	750	166°41'E	76°57'	-0.3549	8	91	12
222	DFBC 83-10 II	878	166°20'E	76°57'	-0.3549	8	91	12
223	DFBC 83-9 II	915	166°31'E	77°05'	-0.3549	7	86	12
224	DFBC 83-1 III	930	169°07'E	77°10'S	-0.2993	1	82	12
225	DFBC 83-8 II	871	165°48'E	77°10'	-0.378	10	85	12
226	DFBC 83-7 II	880	165°53'E	77°21'	-0.378	15	82	12
227	DFBC 83-6 II	823	165°48'E	77°30'	-0.378	15	82	12
230	1176-86	4338	13°49.0'E	48°02.3'	5.3212	0	0	0
231	KR8802	3480	82°56.0'E	45°45.2'	8.6693	0	0	0
232	KR8803	3400	90°06.7'E	46°04.1'	9.2531	0	0	0
233	KR8804	3350	100°05.0'E	49°55.3'	5.9779	0	0	0
234	MD84-561	1754	71°36.4'E	53°05.3'	2.8553	0	0	0
235	MD73-026	3429	53°17.0'E	44°59.0'	9.6361	0	0	0
236	MD84-529	2600	61°59.8'E	48°54.3'	6.1958	0	0	0
243	GC014	3360	145°14.47'E	46°26.98'	12.4471	0	0	0
245	GC034	4002	147°44.5'E	45°06.00'	13.5823	0	0	0

Notes:
LKA Code = numeric code of identification used by author.
February SST extracted from WOA (1994) 1°x1° grid.
Sea-ice concentrations extracted from Schweitzer (1995) 1°x1°grid.
Sea-ice cover in months per year determined from monthly data of Schweitzer (1995). Any evidence of monthly sea-ice concentration no matter what value was counted as 1 month. Zero concentration was counted as ice free.

Appendix 4.2. Results of DTF 166/34/4.

DTF166/34/4 **NB. Varimax Factor Scores Matrix provided in Table 4.1.**

Multiple correlation coefficient	0.96
(adjusted for d.f.)	**0.957**
Standard error of estimate	1.083
(adjusted for d.f.)	**1.128**

		Variance	33.98	30.265	12.601	6.527			
		Cumulative Var.	33.98	64.244	76.845	83.373			
		Communality	Factor loadings (Varimax Factor Matrix)				Observed SST	Estimated SST	Residual SST (°C)
LKA No.	Surface sample	(<0.7 in bold)	Factor 1	Factor 2	Factor 3	Factor 4	SST Feb. (WOA) (°C)	Feb (°C) 166/34/4	(>±2°C in bold)
235	MD73-026	0.833	0.644	0.132	0.625	-0.099	9.636	7.927	1.709
1	V16-65	0.797	0.585	0.126	0.636	-0.183	7.589	8.689	-1.100
2	V16-60	0.857	0.758	0.269	0.406	-0.213	4.459	4.170	0.289
3	1176-91	0.809	0.447	0.133	0.769	-0.013	10.334	10.003	0.331
4	1176-88	0.819	0.549	0.244	0.636	-0.232	7.443	7.135	0.308
5	1277-2	0.773	0.440	0.135	0.744	-0.084	8.947	9.976	-1.030
6	RC11-80	0.799	0.591	0.221	0.605	-0.190	8.343	7.038	1.304
230	1176-86	0.844	0.769	0.161	0.473	-0.044	5.321	5.611	-0.290
7	RC15-91	0.838	0.680	0.178	0.513	-0.285	4.217	6.616	**-2.399**
8	RC11-78	0.829	0.732	0.225	0.428	-0.244	2.634	5.115	**-2.481**
9	RC13-255	0.810	0.696	0.216	0.511	-0.133	4.767	5.830	-1.063
10	1176-82	0.877	0.860	0.164	0.298	-0.148	1.026	4.180	**-3.154**
11	RC13-274	0.869	0.755	0.484	0.128	-0.219	1.623	0.704	0.918
12	RC13-273	0.796	0.745	0.447	0.128	-0.158	1.048	1.192	-0.143
13	MD24-KK63	0.856	0.842	0.189	0.332	0.012	3.635	3.841	-0.206
14	RC13-263	0.854	0.823	0.406	0.084	-0.065	1.581	0.709	0.871
15	1277-28	0.846	0.713	0.536	0.031	-0.224	1.057	0.110	0.946
16	MD82 424	0.883	0.853	0.374	0.112	-0.047	1.611	0.792	0.819
17	1141-2P	0.838	0.096	0.903	0.109	0.027	2.274	0.357	1.917
18	1184-6P	0.825	0.114	0.891	0.109	0.077	0.897	0.741	0.156
19	1147-4P	0.845	0.059	0.907	0.128	-0.048	0.976	-0.162	1.138
20	P1160	0.838	0.181	0.888	0.126	0.034	1.348	0.881	0.467
21	1178-4P	0.816	0.241	0.858	0.145	0.019	0.899	1.160	-0.261
22	1010W	**0.680**	-0.058	0.801	-0.025	-0.186	-1.316	-1.428	0.113
23	1192W	**0.591**	0.008	0.689	-0.060	-0.337	-1.008	-0.565	-0.443
24	1212W	**0.659**	0.016	0.707	-0.071	-0.392	-1.668	-1.294	-0.374
25	1223W	**0.600**	0.183	0.726	-0.044	-0.192	-0.867	-0.095	-0.772
26	1277-41	0.865	0.342	0.737	0.120	-0.437	-0.173	-0.655	0.483
27	RC17-56	0.761	0.492	0.607	0.106	-0.373	0.718	0.511	0.207
28	MD82 436	0.766	0.598	0.565	0.167	-0.248	0.349	1.199	-0.850
29	1176-55	0.808	0.736	0.459	0.186	-0.146	2.386	1.421	0.964
30	1176-65	0.847	0.787	0.462	0.060	-0.102	0.795	0.420	0.374
31	1277-8	0.759	0.654	0.363	0.256	-0.365	3.387	3.186	0.201
32	1277-12	0.717	0.680	0.388	0.241	-0.213	1.422	2.790	-1.368
33	1578-49	0.900	0.588	0.591	0.176	-0.417	0.349	0.653	-0.304
34	1678-64	0.850	0.650	0.389	0.408	-0.330	1.948	3.645	-1.698
35	1678-80	0.810	0.678	0.215	0.510	-0.211	5.715	6.044	-0.329
36	1678-84	0.817	0.692	0.357	0.380	-0.258	2.914	3.605	-0.692
37	1678-89	0.807	0.679	0.544	0.097	-0.201	1.236	0.634	0.602
38	1678-96	0.848	0.777	0.465	0.146	-0.085	0.495	0.860	-0.365
39	RC8-46	0.841	0.743	0.359	0.277	-0.289	3.036	2.682	0.354
40	RC11-71	0.801	0.562	0.254	0.631	-0.150	4.558	6.929	**-2.371**

Appendix 4.2. Results of DTF 166/34/4.

LKA No.	Surface sample	Communality (<0.7 in bold)	Factor loadings (Varimax Factor Matrix) Factor 1	Factor 2	Factor 3	Factor 4	Observed SST SST Feb. (WOA) (°C)	Estimated SST Feb (°C) 166/34/4	Residual SST (°C) (>±2°C in bold)
41	RC11-77	0.786	0.810	0.261	0.233	-0.087	2.249	3.131	-0.883
42	RC11-90	0.839	0.744	0.332	0.225	-0.353	1.860	2.781	-0.921
43	RC13-257	0.878	0.775	0.319	0.268	-0.321	1.220	2.833	-1.613
44	RC13-268	0.906	0.659	0.595	0.141	-0.314	0.903	0.433	0.470
45	RC13-269	0.791	0.817	0.303	0.104	-0.144	2.761	2.219	0.542
46	RC13-270	0.874	0.701	0.457	0.247	-0.335	1.385	1.800	-0.415
47	RC13-272	0.891	0.736	0.543	0.084	-0.218	1.161	0.162	0.999
238	RC11-118	**0.685**	0.130	-0.036	0.812	0.087	17.708	16.687	1.021
239	RC11-119	0.719	0.225	0.011	0.816	-0.043	15.316	14.433	0.882
48	RC12-292	**0.695**	0.125	-0.022	0.823	-0.039	16.126	16.151	-0.025
49	V14-53	0.914	0.755	0.492	0.184	-0.262	1.276	0.901	0.375
50	V14-58	0.820	0.718	0.463	0.111	-0.280	1.272	1.043	0.229
51	MD24 KK02	0.802	0.723	0.484	0.163	-0.136	1.831	1.214	0.617
52	MD24 KK32	0.858	0.807	0.330	0.269	-0.155	1.831	2.392	-0.561
53	MD24 KK35	0.866	0.795	0.354	0.249	-0.218	1.677	2.170	-0.493
54	MD24 KK37	0.829	0.838	0.316	0.127	-0.105	2.289	1.779	0.509
55	MD82 425	0.845	0.789	0.374	0.198	-0.210	1.292	1.804	-0.512
56	MD82 430	0.910	0.723	0.476	0.243	-0.319	1.161	1.511	-0.350
57	MD82 434	0.918	0.776	0.535	0.071	-0.159	1.098	-0.077	1.175
58	MD84 531	0.838	0.232	0.867	0.056	-0.171	0.411	-0.525	0.936
59	MD84 530	0.854	0.529	0.663	0.168	-0.327	0.479	0.610	-0.132
60	MD84 532	0.885	0.456	0.709	0.101	-0.405	0.347	-0.351	0.697
236	MD84-529	0.906	0.821	0.154	0.455	-0.043	6.196	5.000	1.196
61	MD84 533	0.915	0.533	0.619	0.186	-0.461	0.448	0.500	-0.052
62	MD 84 540	0.846	0.721	0.501	0.176	-0.212	1.920	1.084	0.836
63	MD84 552	0.843	0.849	0.217	0.273	-0.017	2.302	3.264	-0.962
64	MD84 557	0.890	0.862	0.241	0.283	-0.090	2.231	2.853	-0.623
234	MD84-561	0.789	0.726	0.335	0.383	0.059	2.855	3.529	-0.674
65	MD84 562	0.886	0.804	0.211	0.424	-0.127	3.901	4.434	-0.534
66	MD84 563	0.851	0.789	0.214	0.427	-0.016	3.700	4.447	-0.746
67	MD84 569	**0.676**	0.535	0.376	0.498	-0.001	6.413	5.215	1.198
68	83-11C III	**0.695**	0.178	0.812	-0.042	-0.048	-0.759	-0.178	-0.582
69	83-12 III	0.740	0.222	0.790	0.083	-0.245	-0.835	-0.443	-0.393
70	83-19 III	0.731	0.091	0.841	0.019	-0.120	-1.202	-0.760	-0.442
71	83-41 III	0.733	0.248	0.787	-0.063	-0.219	-1.081	-0.954	-0.127
72	83-42 III	0.772	0.235	0.840	-0.079	-0.074	-1.008	-0.637	-0.371
73	PC82-197	0.802	0.011	0.874	0.160	-0.114	0.360	-0.528	0.888
237	PC82-35	0.879	0.332	0.859	0.142	0.099	0.897	1.677	-0.780
74	PC82-71	0.856	0.327	0.831	0.174	0.169	1.276	2.156	-0.880
75	PC82-136	0.856	0.178	0.893	0.155	-0.057	1.290	0.607	0.683
76	PC82-140	0.816	0.141	0.877	0.159	-0.047	1.290	0.541	0.749
77	KR8701	0.771	0.651	0.526	0.245	-0.106	3.595	1.901	1.695
78	KR8702	0.920	0.677	0.629	0.256	-0.014	1.829	1.673	0.156
79	KR8703	0.922	0.377	0.871	0.147	0.000	1.313	1.439	-0.125
80	KR8705	0.932	0.468	0.740	0.219	-0.343	-0.405	0.764	-1.169
81	KR8706	0.858	0.484	0.766	0.182	0.062	1.492	1.797	-0.304
82	KR8707	0.890	0.187	0.906	0.184	0.013	0.897	1.272	-0.375
83	KR8708	0.821	0.469	0.644	0.160	-0.402	0.217	0.451	-0.234
84	KR8710	0.846	0.516	0.714	0.250	-0.085	2.065	1.920	0.145
85	KR8712	0.899	0.589	0.586	0.366	-0.273	3.351	2.509	0.842

Appendix 4.2. Results of DTF 166/34/4.

LKA No.	Surface sample	Communality (<0.7 in bold)	Factor loadings (Varimax Factor Matrix) Factor 1	Factor 2	Factor 3	Factor 4	Observed SST SST Feb. (WOA) (°C)	Estimated SST Feb (°C) 166/34/4	Residual SST (°C) (>±2°C in bold)
86	KR8713	**0.618**	0.533	0.508	0.253	-0.109	3.901	2.714	1.187
87	KR8714	**0.651**	0.619	0.446	0.262	0.016	4.652	2.931	1.721
88	KR8801	0.832	0.527	0.323	0.654	-0.147	7.750	6.508	1.242
231	KR8802	0.819	0.573	0.288	0.581	-0.265	8.669	6.159	**2.510**
232	KR8803	0.869	0.548	0.229	0.704	-0.144	9.253	7.665	1.589
233	KR8804	0.849	0.696	0.151	0.559	-0.175	5.978	6.969	-0.991
89	KR8805	0.877	0.781	0.351	0.354	-0.140	5.116	2.813	**2.303**
90	KR8806	0.848	0.233	0.101	0.869	-0.169	9.570	12.085	**-2.516**
91	KR8807	0.815	0.200	0.019	0.856	-0.205	11.705	14.182	**-2.478**
92	KR8808	0.868	0.445	0.110	0.788	-0.194	10.460	10.472	-0.013
93	KR8809	0.837	0.497	0.162	0.720	-0.211	9.638	9.015	0.623
94	KR8810	0.893	0.835	0.161	0.409	-0.056	5.596	4.625	0.972
95	KR8811	0.918	0.886	0.140	0.324	-0.099	5.596	4.169	1.427
96	KR8812	0.832	0.803	0.179	0.368	-0.144	4.265	4.802	-0.537
97	KR8813	0.848	0.839	0.177	0.309	-0.134	3.926	4.250	-0.324
98	KR8814	0.888	0.843	0.298	0.237	-0.182	2.774	2.274	0.500
99	KR8815	0.856	0.710	0.445	0.138	-0.368	1.785	1.275	0.510
100	KR8816	0.868	0.545	0.519	0.207	-0.509	0.981	1.283	-0.303
101	KR8817	0.860	0.252	0.870	0.101	-0.174	0.030	-0.142	0.172
102	KR8818	0.829	0.475	0.773	0.029	-0.068	-0.072	0.227	-0.299
103	KR8819	0.826	0.473	0.664	0.191	-0.354	0.952	0.725	0.228
104	KR8820	0.835	0.484	0.692	0.181	-0.299	1.080	0.730	0.350
105	KR8821	0.923	0.470	0.779	0.112	-0.287	1.057	0.014	1.043
106	KR8822	0.871	0.554	0.682	0.132	-0.284	0.894	0.374	0.520
107	KR8823	0.851	0.501	0.543	0.307	-0.459	1.157	1.916	-0.759
108	KR8824	0.884	0.469	0.710	0.243	-0.319	1.091	1.112	-0.021
109	KR8825	0.881	0.492	0.702	0.144	-0.355	0.605	0.198	0.407
110	KR8827	0.881	0.539	0.610	0.252	-0.394	0.758	1.250	-0.492
111	KR8828	0.835	0.341	0.649	0.137	-0.528	-0.194	-0.307	0.113
112	KR8829	0.930	0.616	0.593	0.282	-0.346	1.290	1.557	-0.267
113	KR8830	0.931	0.838	0.345	0.273	-0.187	1.819	1.934	-0.115
114	KR8831	0.856	0.675	0.257	0.322	-0.480	2.282	4.719	**-2.437**
115	8702-DISS-5'	0.935	0.692	0.607	0.294	-0.038	1.829	1.907	-0.078
116	8702-DISS10'	0.913	0.677	0.612	0.280	0.032	1.829	1.919	-0.090
117	8702-DISS20'	0.893	0.634	0.598	0.251	0.264	1.829	2.086	-0.257
118	8702-DISS35'	0.859	0.647	0.610	0.259	0.030	1.829	1.889	-0.060
119	8702-DISS60'	0.887	0.637	0.607	0.335	0.027	1.829	2.552	-0.723
120	8702DISS120'	0.865	0.637	0.643	0.202	-0.070	1.829	1.305	0.525
121	8702DISS180'	0.880	0.654	0.587	0.306	-0.119	1.829	2.085	-0.255
246	8702-DISS-240	**0.622**	0.596	0.407	0.314	0.051	1.829	3.723	-1.894
122	8702-DISS24H	0.769	0.346	0.406	0.345	-0.605	1.829	3.547	-1.718
247	8707-DISS5'	0.938	0.233	0.919	0.200	0.020	0.897	1.698	-0.801
123	8707-DISS10'	0.918	0.232	0.910	0.189	0.040	0.897	1.659	-0.762
124	8707-DISS20'	0.934	0.248	0.915	0.184	0.023	0.897	1.613	-0.716
125	8707-DISS35'	0.896	0.238	0.897	0.186	-0.017	0.897	1.349	-0.452
126	8707-DISS60'	0.913	0.222	0.911	0.182	-0.038	0.897	1.164	-0.267
127	8707DISS120'	0.897	0.148	0.880	0.208	-0.239	0.897	-0.158	1.055
248	8707-DISS180	0.758	0.188	0.799	0.213	-0.199	0.897	0.507	0.390
128	8707DISS240'	**0.682**	0.187	0.701	0.225	-0.325	0.897	0.490	0.407
129	8808-DISS05'	0.868	0.445	0.110	0.788	-0.194	10.460	10.472	-0.013

Appendix 4.2. Results of DTF 166/34/4.

LKA No.	Surface sample	Communality (<0.7 in bold)	Factor loadings (Varimax Factor Matrix) Factor 1	Factor 2	Factor 3	Factor 4	Observed SST SST Feb. (WOA) (°C)	Estimated SST Feb (°C) 166/34/4	Residual SST (°C) (>±2°C in bold)
130	8808-DISS10'	0.804	0.547	0.154	0.666	-0.195	10.460	8.613	1.846
249	8808-DISS020	0.835	0.599	0.134	0.655	-0.171	10.460	8.461	1.999
250	8808-DISS035	0.831	0.663	0.130	0.498	-0.355	10.460	7.615	**2.844**
131	8808-DISS60'	0.806	0.577	0.138	0.446	-0.506	10.460	8.114	**2.345**
500	8808-DISS0120	0.915	0.538	0.100	0.501	-0.603	10.460	9.226	1.233
501	8808-DISS0180	0.905	0.546	0.101	0.483	-0.603	10.460	9.131	1.328
502	8808-DISS0240	0.859	0.503	0.136	0.483	-0.595	10.460	8.643	1.816
132	8808-DISS24H	0.764	0.505	0.059	0.422	-0.571	10.460	10.737	-0.277
503	8808-DISS48H	**0.654**	0.414	0.134	0.285	-0.619	10.460	9.608	0.852
133	8810DISS0-20	0.893	0.835	0.161	0.409	-0.056	5.596	4.625	0.972
134	8810DISS3560	0.860	0.816	0.127	0.404	-0.120	5.596	5.538	0.058
255	8810DISS120	0.883	0.762	0.145	0.457	-0.270	5.596	6.159	-0.562
256	8810DISS180	0.903	0.760	0.115	0.459	-0.319	5.596	6.760	-1.164
135	8810DISS240'	0.905	0.698	0.118	0.489	-0.406	5.596	7.470	-1.874
136	8810DISS24H	0.757	0.648	0.193	0.377	-0.398	5.596	6.341	-0.744
137	8818DISS0-05	0.829	0.475	0.773	0.029	-0.068	-0.072	0.227	-0.299
138	8818-DISS10'	0.910	0.420	0.850	0.053	-0.087	-0.072	0.282	-0.354
139	8818-DISS20'	0.854	0.472	0.789	0.083	-0.053	-0.072	0.656	-0.729
257	8818DISS035	0.824	0.452	0.778	0.083	-0.087	-0.072	0.559	-0.632
140	8818DISS120'	0.874	0.414	0.823	0.109	-0.115	-0.072	0.619	-0.692
141	8818DISS180'	0.822	0.379	0.804	0.134	-0.122	-0.072	0.761	-0.833
142	8818DISS240'	0.871	0.428	0.745	0.165	-0.326	-0.072	0.310	-0.382
143	8818-DISS24H	0.750	0.294	0.604	0.227	-0.498	-0.072	0.751	-0.823
144	8818-DISS48H	0.856	0.308	0.567	0.190	-0.635	-0.072	0.348	-0.421

Variable Name	Regression Coefficient	Std. error of Reg. Coeff.	Computed T-value
KP 3	-3.98648	3.19818	-1.246
KP 4	23.48006	6.31436	3.719
KP 5	6.41339	6.87274	0.933
KP 6	-1.67219	3.57509	-0.468
KP 7	21.10118	5.91045	3.57
KP 8	9.72475	5.79912	1.677
KP 9	-6.17375	4.53322	-1.362
KP 10	21.40998	12.0499	1.777
KP 11	3.4862	6.30888	0.553
KP 12	-2.10698	8.1024	-0.26
KP 13	-14.71966	6.42525	-2.291
KP 14	-49.07035	12.53845	-3.914
KP 15	-14.83518	12.6217	-1.175
KP 16	3.60058	7.72855	0.466
Intercept	24.31516		

Appendix 4.2. Results of DTF 166/34/4.

Correlation Matrix

	SST feb	SST aug	Factor 1	Factor 2	Factor 3	Factor 4	Factor 1x2	Factor 1x3	Factor 1x4	Factor 2x3	Factor 2x4	Factor 3x4	Factor 1sq	Factor 2sq	Factor 3sq	Factor 4sq
SST feb	1															
SST aug	**0.947**	1														
Factor 1	0.061	-0.006	1													
Factor 2	-0.665	-0.644	-0.666	1												
Factor 3	**0.881**	**0.869**	-0.063	-0.585	1											
Factor 4	0.084	0.150	-0.136	-0.179	-0.062	1										
Factor 1x2	-0.591	-0.594	0.291	0.271	-0.591	-0.127	1									
Factor 1x3	0.661	0.626	0.538	**-0.812**	0.652	-0.019	-0.346	1								
Factor 1x4	-0.120	-0.140	-0.301	0.431	0.018	-0.738	-0.050	-0.238	1							
Factor 2x3	-0.100	-0.190	-0.077	0.191	-0.017	-0.055	0.295	0.162	0.073	1						
Factor 2x4	0.392	0.271	0.213	-0.169	0.317	-0.592	-0.196	0.351	0.528	0.029	1					
Factor 3x4	-0.506	-0.530	-0.051	0.513	-0.424	-0.705	0.367	-0.494	0.755	-0.057	0.216	1				
Factor 1sq	0.097	0.044	**0.971**	-0.681	-0.024	-0.060	0.381	0.578	-0.378	0.020	0.174	-0.142	1			
Factor 2sq	-0.783	-0.750	-0.561	**0.973**	-0.695	-0.148	0.436	**-0.830**	0.365	0.239	-0.266	0.537	-0.565	1		
Factor 3sq	**0.891**	**0.841**	0.107	-0.684	**0.947**	0.005	-0.532	**0.808**	-0.095	0.171	0.347	-0.521	0.161	-0.775	1	
Factor 4sq	-0.040	-0.126	0.029	0.249	0.038	**-0.894**	0.094	-0.040	**0.879**	0.115	0.759	0.747	-0.038	0.195	-0.007	1

Notes.
High positive or negative correlations (ie. >0.8) between factors and/or parameters are highlighted in bold.
sq = squared

Appendix 4.3. *Varimax factor score matricies of factor models 3, 4, 6, 8, and 10.*

Species	Factor model 3			Factor model 4				Factor model 6						Factor model 8				
	Factor 1	2	3	1	2	3	4	1	2	3	4	5	6	1	2	3	4	5
Actinocyclus actinochilus	0.088	0.301	-0.090	0.080	0.299	-0.091	0.080	-0.097	0.272	0.016	-0.021	0.735	-0.212	-0.079	0.280	0.030	-0.063	0.762
Actinocyclus curvatulus	0.015	-0.010	0.009	0.013	-0.010	0.009	0.006	0.028	-0.007	-0.016	-0.014	-0.001	-0.013	0.025	-0.005	-0.001	-0.005	-0.010
Asteromphalus parvulus	0.127	0.036	-0.087	0.164	0.037	-0.072	-0.118	-0.007	0.032	0.000	-0.016	0.095	0.222	-0.005	0.027	-0.015	0.062	0.042
Azpeitia tabularis	0.118	-0.090	0.465	0.097	-0.091	0.471	0.022	0.407	-0.077	0.235	-0.123	-0.067	-0.150	0.423	-0.051	0.326	-0.306	0.001
Fragilariopsis curta	-0.131	0.496	0.027	-0.115	0.498	0.024	-0.046	-0.063	0.501	0.030	-0.070	-0.134	-0.054	-0.068	0.501	0.027	-0.098	-0.110
Fragilariopsis Cylindriform Group	-0.125	0.258	0.065	-0.119	0.261	0.060	-0.030	-0.024	0.264	0.033	-0.090	-0.094	-0.111	-0.041	0.265	0.055	-0.081	-0.090
Fragilariopsis doliolus	-0.068	0.014	0.127	-0.058	0.016	0.128	-0.063	-0.028	0.003	0.190	0.004	-0.035	0.024	-0.027	0.008	0.207	-0.010	-0.027
Fragilariopsis kerguelensis	0.604	0.003	0.259	0.607	-0.005	0.290	0.021	0.561	0.014	0.108	0.059	0.156	0.320	0.571	0.008	0.089	0.115	0.087
Fragilariopsis Cool Taxa	0.109	0.453	-0.104	0.175	0.455	-0.085	-0.198	0.012	0.458	-0.067	-0.216	0.202	0.123	0.023	0.454	-0.107	-0.227	0.201
Fragilariopsis pseudonana	0.004	0.021	-0.002	0.010	0.021	-0.001	-0.021	0.011	0.024	-0.011	-0.024	-0.025	0.017	0.000	0.021	-0.007	0.021	-0.049
Fragilariopsis rhombica	-0.029	0.229	0.016	-0.038	0.229	0.011	0.047	0.011	0.234	-0.021	0.010	-0.068	-0.057	-0.008	0.225	-0.044	0.063	-0.081
Fragilariopsis separanda	0.097	0.236	-0.061	0.194	0.242	-0.033	-0.349	-0.027	0.241	0.104	-0.054	-0.305	0.564	0.050	0.254	0.068	-0.257	-0.241
Hemidicus cuneiformis	-0.118	0.021	0.231	-0.106	0.024	0.231	-0.094	-0.066	-0.003	0.365	0.043	-0.031	0.045	-0.065	0.003	0.383	0.034	-0.018
Porosira Group	-0.064	0.139	0.034	-0.074	0.139	0.028	0.037	-0.011	0.141	0.012	0.017	-0.093	-0.060	-0.023	0.140	0.016	0.033	-0.094
Roperia tesselata	-0.173	0.030	0.350	-0.153	0.035	0.352	-0.154	-0.083	-0.004	0.534	0.022	-0.016	0.041	-0.085	0.001	0.543	0.014	0.007
Stellarima microtrias	-0.088	0.190	0.045	-0.094	0.191	0.039	0.021	-0.049	0.186	0.058	0.003	-0.008	-0.087	-0.046	0.190	0.067	-0.038	0.020
Thalassionema Taxa	-0.169	-0.018	0.590	-0.204	-0.016	0.580	0.028	0.368	0.006	0.237	-0.327	-0.169	-0.527	0.273	-0.020	0.193	-0.210	-0.164
Th. antarctica/scotia Group	-0.130	0.357	0.140	-0.255	0.350	0.101	0.490	-0.078	0.336	0.151	0.546	-0.216	-0.227	-0.105	0.330	0.153	0.630	-0.223
Thalassiosira decipiens	-0.013	-0.002	0.071	-0.013	-0.001	0.071	-0.014	0.062	0.004	0.010	-0.085	0.008	-0.083	0.044	-0.003	-0.007	-0.053	0.003
Thalassiosira gracilis Group	0.271	0.222	-0.018	0.280	0.218	-0.004	0.013	0.372	0.271	-0.316	-0.165	-0.214	0.065	0.343	0.279	-0.213	-0.081	-0.312
Thalassiosira lentiginosa	0.486	0.097	0.221	0.454	0.088	0.236	0.162	0.357	0.080	0.206	0.250	0.343	0.193	0.375	0.074	0.165	0.291	0.307
Thalassiosira oestrupii Group	-0.086	0.006	0.238	-0.088	0.008	0.236	-0.037	-0.060	-0.022	0.386	0.137	-0.041	0.073	-0.066	-0.023	0.381	0.180	-0.047
Thalassiosira oliverana	0.333	-0.014	-0.055	0.168	-0.032	-0.084	0.707	0.268	-0.005	-0.283	0.624	-0.061	-0.147	0.330	0.007	-0.296	0.405	0.036
Thalassiosira tumida	-0.091	0.173	0.061	-0.110	0.173	0.051	0.069	-0.054	0.166	0.081	0.068	-0.025	-0.096	-0.068	0.164	0.086	0.101	-0.028

Notes.

Factor score data for each species derived from factor analysis under increasing numbers of factors resolved.

Data derived from factor analysis of 115 samples of the ADB.

Appendix 4.3. *Varimax factor score matricies of factor models 3, 4, 6, 8, and 10.*

Species	Factor model 8			Factor model 10									
	Factor 6	7	8	1	2	3	4	5	6	7	8	9	10
Actinocyclus actinochilus	-0.199	-0.142	0.096	-0.066	0.287	-0.004	-0.008	0.767	-0.165	-0.065	0.060	-0.219	0.205
Actinocyclus curvatulus	-0.012	-0.076	0.048	0.028	-0.006	-0.004	-0.007	-0.004	-0.022	-0.037	0.054	-0.045	-0.051
Asteromphalus parvulus	0.311	-0.096	-0.019	0.003	0.025	-0.048	0.077	0.062	0.259	0.097	0.034	-0.092	-0.238
Azpeitia tabularis	-0.408	0.004	0.369	0.465	-0.046	0.256	-0.290	0.027	-0.436	0.224	0.445	-0.091	-0.053
Fragilariopsis curta	-0.086	0.085	-0.050	-0.068	0.501	0.062	-0.188	-0.114	-0.159	0.078	0.013	0.260	-0.327
Fragilariopsis Cylindriform Group	-0.111	-0.092	0.014	-0.032	0.264	0.048	-0.077	-0.086	-0.122	-0.024	0.024	-0.089	-0.044
Fragilariopsis doliolus	-0.004	-0.013	0.101	-0.037	0.005	0.239	-0.021	-0.034	0.011	-0.106	0.068	0.019	0.067
Fragilariopsis kerguelensis	0.378	-0.040	-0.079	0.578	0.007	0.049	0.124	0.107	0.341	0.136	-0.019	-0.022	-0.247
Fragilariopsis Cool Taxa	0.153	0.119	-0.174	-0.021	0.448	-0.008	-0.296	0.168	0.195	-0.173	-0.246	0.242	0.070
Fragilariopsis pseudonana	0.062	-0.096	-0.017	0.005	0.019	-0.006	-0.006	-0.038	0.009	0.001	0.024	0.011	-0.242
Fragilariopsis rhombica	0.016	-0.003	-0.187	0.000	0.226	-0.041	0.008	-0.075	-0.064	0.097	-0.113	0.145	-0.360
Fragilariopsis separanda	0.303	0.618	0.181	0.046	0.260	0.005	-0.159	-0.258	0.411	0.505	0.169	0.070	0.513
Hemidicus cuneiformis	0.018	-0.006	0.129	-0.075	-0.001	0.427	0.005	-0.025	0.013	-0.102	0.105	0.070	-0.002
Porosira Group	-0.048	-0.029	-0.026	-0.017	0.139	0.019	0.005	-0.090	-0.085	0.014	0.007	0.050	-0.161
Roperia tesselata	0.026	0.039	0.079	-0.099	-0.003	0.600	-0.017	-0.006	0.024	-0.090	0.046	0.105	0.025
Stellarima microtrias	-0.134	0.041	0.041	-0.026	0.196	0.008	0.035	0.025	-0.101	0.139	0.044	-0.177	0.201
Thalassionema Taxa	-0.323	-0.045	-0.734	0.296	-0.016	0.161	-0.135	-0.174	-0.284	0.085	-0.754	-0.226	0.173
Th. antarctica/scotia Group	-0.160	-0.088	-0.026	-0.065	0.337	0.065	0.694	-0.205	-0.183	0.108	0.032	-0.175	-0.036
Thalassiosira decipiens	-0.024	-0.005	-0.182	0.043	-0.003	-0.002	-0.048	-0.001	-0.017	-0.004	-0.192	-0.014	0.019
Thalassiosira gracilis Group	0.066	-0.552	0.319	0.315	0.261	-0.145	-0.089	-0.306	0.139	-0.675	0.207	-0.340	0.095
Thalassiosira lentiginosa	0.267	0.047	-0.120	0.363	0.074	0.171	0.280	0.304	0.267	0.007	-0.119	0.115	-0.064
Thalassiosira oestrupii Group	0.115	0.000	0.010	-0.091	-0.030	0.447	0.164	-0.067	0.150	-0.211	-0.062	0.068	0.136
Thalassiosira oliverana	-0.413	0.464	0.139	0.289	0.014	-0.205	0.288	-0.019	-0.314	-0.162	0.058	0.650	0.352
Thalassiosira tumida	-0.060	-0.073	-0.020	-0.037	0.169	0.002	0.196	-0.011	-0.049	0.145	0.005	-0.293	0.109

Appendix 4.4. Results of DTF 115/24/6.

DTF115/24/6 **NB. Varimax Factor Scores Matrix provided in Appendix 4.3.**

Multiple correlation coefficient	0.951
(adjusted for d.f.)	**0.936**
Standard error of estimate	1.147
(adjusted for d.f.)	**1.306**

		Variance	43.764	26.051	4.994	4.344	5.405	5.582			
		Cumulative Var.	43.764	69.815	74.809	79.152	84.557	90.139			
		Communality	Factor loadings (Varimax Factor Matrix)						Observed SST	Estimated SST	Residual SST (°C)
LKA No.	Surface sample	(<0.8 in bold)	Factor 1	Factor 2	Factor 3	Factor 4	Factor 5	Factor 6	SST Feb. (WOA) (°C)	Feb (°C) 115/24/4	(>±2°C in bold)
1	V16-65	0.869	0.865	0.144	0.253	0.112	0.092	-0.121	7.589	6.447	1.142
2	V16-60	0.900	0.674	0.319	0.192	-0.012	0.454	0.319	4.459	3.088	1.372
3	1176-91	0.871	0.637	0.125	0.615	-0.122	0.221	-0.086	10.334	10.993	-0.658
4	1176-88	0.933	0.708	0.233	0.213	0.146	0.554	0.064	7.443	3.704	**3.739**
5	1277-2	0.886	0.754	0.21	0.487	-0.007	0.182	0.056	8.947	8.585	0.361
7	RC15-91	0.942	0.91	0.079	0.208	0.143	0.182	0.107	4.217	4.798	-0.581
8	RC11-78	0.932	0.917	0.252	0.088	0.021	0.099	0.095	2.634	3.514	-0.880
9	RC13-255	0.946	0.935	0.216	0.127	-0.072	0.056	-0.039	4.767	5.095	-0.328
10	1176-82	0.958	0.829	0.153	0.115	0.233	0.123	0.407	1.026	2.598	-1.572
11	RC13-274	0.963	0.644	0.432	0.095	-0.012	0.464	0.37	1.623	1.713	-0.090
12	RC13-273	0.924	0.662	0.446	0.14	-0.039	0.199	0.477	1.048	2.266	-1.218
13	MD24-KK63	0.930	0.851	0.114	-0.011	0.368	0.141	0.191	3.635	3.442	0.194
14	RC13-263	0.884	0.669	0.45	0.095	0.062	0.094	0.461	1.581	1.555	0.026
15	1277-28	0.926	0.66	0.44	-0.039	0.09	0.319	0.43	1.057	0.362	0.694
16	MD82 424	0.958	0.743	0.396	0.045	0.108	0.324	0.36	1.611	1.116	0.495
21	1178-4P	0.857	0.224	0.806	0.096	0.22	0.292	-0.119	0.899	0.788	0.112
26	1277-41	0.911	0.385	0.448	0.05	0.158	0.725	0.09	-0.173	-0.041	-0.132
28	MD82 436	0.876	0.495	0.239	0.175	0.254	0.687	0.082	0.349	0.341	0.008
29	1176-55	0.844	0.633	0.451	0.024	0.286	0.147	0.368	2.386	1.274	1.111
30	1176-65	0.810	0.691	0.362	-0.007	-0.018	0.247	0.376	0.795	1.140	-0.345
31	1277-8	0.902	0.692	0.255	0.16	0.261	0.225	0.462	3.387	2.441	0.947
32	1277-12	**0.749**	0.684	0.337	0.084	0.009	0.038	0.399	1.422	1.795	-0.374
33	1578-49	0.929	0.616	0.43	0.07	0.148	0.561	0.15	0.349	1.758	-1.409
34	1678-64	0.934	0.819	0.231	0.248	0.161	0.168	0.308	1.948	3.895	-1.947
35	1678-80	0.894	0.886	0.174	0.104	0.068	0.234	0.098	5.715	4.100	1.615
36	1678-84	0.907	0.879	0.258	0.144	0.155	0.124	0.087	2.914	3.782	-0.869
37	1678-89	0.931	0.548	0.448	0.139	0.07	0.502	0.391	1.236	1.109	0.127
38	1678-96	0.910	0.586	0.512	0.114	0.107	0.287	0.446	0.495	1.055	-0.560
39	RC8-46	0.953	0.744	0.265	0.163	0.024	0.204	0.511	3.036	2.912	0.124
42	RC11-90	0.881	0.745	0.433	0.115	0.068	0.126	0.326	1.860	1.706	0.154
43	RC13-257	0.934	0.822	0.228	0.121	0.143	0.367	0.191	1.220	3.118	-1.899
44	RC13-268	0.892	0.617	0.533	-0.02	0.118	0.359	0.29	0.903	0.501	0.402
45	RC13-269	0.922	0.736	0.435	0.119	-0.119	0.041	0.4	2.761	2.147	0.614
46	RC13-270	0.938	0.748	0.373	0.065	0.13	0.292	0.363	1.385	1.304	0.081
47	RC13-272	0.884	0.634	0.524	0.051	0.199	0.273	0.301	1.161	0.659	0.502
50	V14-58	0.927	0.653	0.423	0.149	0.019	0.446	0.319	1.272	2.108	-0.836
51	MD24 KK02	0.872	0.626	0.345	0.067	0.051	0.351	0.48	1.831	1.184	0.647
52	MD24 KK32	0.803	0.756	0.152	0.198	0.183	0.241	0.278	1.831	3.192	-1.361
53	MD24 KK35	**0.738**	0.58	0.134	0.212	0.409	0.32	0.263	1.677	1.924	-0.247
54	MD24 KK37	0.926	0.808	0.323	0.125	0.039	0.14	0.645	2.289	2.645	-0.356
55	MD82 425	0.910	0.713	0.328	-0.063	0.249	0.038	0.477	1.292	1.048	0.243
56	MD82 430	0.962	0.748	0.259	0.145	0.164	0.513	0.159	1.161	2.934	-1.772
57	MD82 434	0.943	0.778	0.295	0.082	0.127	0.45	0.163	1.098	2.914	-1.816
62	MD 84 540	0.917	0.733	0.425	0.087	0.054	0.149	0.408	1.920	1.374	0.546
63	MD84 552	0.916	0.818	0.209	0.098	0.121	-0.016	0.423	2.302	2.323	-0.021
64	MD84 557	0.912	0.838	0.225	-0.042	0.301	0.054	0.251	2.231	2.491	-0.261
65	MD84 562	0.943	0.913	0.12	0.258	0.08	0.083	0.124	3.901	5.234	-1.333
66	MD84 563	0.936	0.943	0.119	0.105	0.078	0.074	0.1	3.700	3.968	-0.268

Appendix 4.4. Results of DTF 115/24/6.

LKA No.	Surface sample	Communality (<0.8 in bold)	Factor loadings (Varimax Factor Matrix) Factor 1	Factor 2	Factor 3	Factor 4	Factor 5	Factor 6	Observed SST SST Feb. (WOA) (°C)	Estimated SST Feb (°C) 115/24/4	Residual SST (°C) (>±2°C in bold)
67	MD84 569	0.867	0.796	0.142	0.333	0.293	0.037	-0.12	6.413	6.988	-0.576
71	83-41 III	0.803	0.127	0.821	-0.079	-0.208	0.252	-0.021	-1.081	-0.728	-0.353
77	KR8701	0.960	0.645	0.338	0.029	0.604	0.252	0.027	3.595	4.860	-1.264
78	KR8702	0.874	0.562	0.636	0.053	0.289	0.225	0.131	1.829	1.011	0.818
79	KR8703	0.888	0.38	0.793	-0.033	0.151	0.3	-0.003	1.313	0.775	0.538
84	KR8710	0.919	0.579	0.632	-0.049	0.378	0.183	0.071	2.065	2.055	0.010
85	KR8712	0.935	0.75	0.377	0.045	0.438	0.148	0.124	3.351	3.315	0.036
86	KR8713	0.824	0.362	0.351	0.28	0.669	0.209	-0.009	3.901	4.223	-0.322
87	KR8714	**0.793**	0.55	0.437	0.111	0.472	0.175	0.182	4.652	2.933	1.719
88	KR8801	0.889	0.76	0.206	0.405	0.317	0.061	-0.021	7.750	7.058	0.692
89	KR8805	0.939	0.819	0.276	0.252	-0.075	0.271	0.226	5.116	4.939	0.178
91	KR8807	0.866	0.495	0	0.77	0.078	0.115	0.091	11.705	11.954	-0.249
92	KR8808	0.867	0.686	0.058	0.596	0.115	0.094	0.125	10.460	10.071	0.388
94	KR8810	0.973	0.944	0.071	0.189	0.126	0.129	0.098	5.596	4.805	0.792
95	KR8811	0.899	0.813	0.18	0.159	0.178	0.256	0.287	5.596	2.971	**2.626**
96	KR8812	0.959	0.9	0.168	0.193	0.117	0.22	0.148	4.265	4.249	0.016
97	KR8813	0.945	0.885	0.12	0.039	0.292	0.148	0.196	3.926	3.256	0.670
98	KR8814	0.943	0.821	0.293	0.092	0.126	0.143	0.372	2.774	1.914	0.860
99	KR8815	**0.791**	0.624	0.371	0.003	0.341	0.348	0.161	1.785	2.017	-0.232
100	KR8816	0.897	0.688	0.432	0.001	0.32	0.274	0.246	0.981	1.439	-0.458
101	KR8817	0.899	0.358	0.833	0.024	0.201	0.164	0.097	0.030	0.157	-0.127
102	KR8818	0.839	0.324	0.835	0.054	0.092	0.042	0.155	-0.072	0.294	-0.366
103	KR8819	0.912	0.595	0.602	0.059	0.323	0.1	0.28	0.952	1.115	-0.163
104	KR8820	0.914	0.52	0.704	0.026	0.242	0.142	0.262	1.080	0.154	0.926
105	KR8821	0.910	0.54	0.699	-0.076	0.276	0.212	0.051	1.057	1.430	-0.373
106	KR8822	0.931	0.597	0.633	-0.011	0.284	0.182	0.243	0.894	0.385	0.509
107	KR8823	0.933	0.735	0.409	0.195	0.246	0.254	0.251	1.157	2.182	-1.025
108	KR8824	0.948	0.564	0.668	0.093	0.231	0.28	0.207	1.091	0.141	0.951
109	KR8825	0.920	0.526	0.716	-0.056	0.279	0.176	0.138	0.605	0.645	-0.040
110	KR8827	0.892	0.533	0.608	0.036	0.415	0.239	0.086	0.758	1.884	-1.125
112	KR8829	0.924	0.836	0.331	0.033	0.158	0.141	0.262	1.290	1.740	-0.450
113	KR8830	0.880	0.773	0.181	0.071	0.376	0.047	0.318	1.819	3.153	-1.334
145	MDBX94-01	0.889	0.425	0.029	0.834	0.055	-0.037	-0.086	12.900	13.145	-0.245
148	MDBX94-04	0.962	0.956	0.16	0.143	0.016	0.024	-0.016	5.698	4.951	0.747
152	93-7/GC33	**0.767**	0.192	0.83	0.014	0.034	-0.182	0.085	0.121	0.220	-0.099
153	93-7/GC5	0.820	0.302	0.829	0.043	0.005	0.198	0.006	0.143	0.482	-0.339
154	KTB01	0.959	0.936	0.062	0.249	-0.017	0.045	-0.117	4.398	6.889	**-2.491**
155	KTB12	0.935	0.885	0.21	0.185	0.117	0.203	0.134	5.815	4.072	1.743
156	KTB14	0.923	0.899	0.012	0.298	0.086	0.133	-0.033	5.250	6.514	-1.265
184	E36-6B	0.948	0.957	0.156	0.081	-0.017	-0.004	0.007	5.470	4.230	1.240
192	KTB 08	0.941	0.919	0.077	0.184	0.119	0.146	0.144	4.515	4.412	0.103
210	DFBC 83-27 II	0.860	0.198	0.877	0.057	0.128	0.066	0.166	-0.344	0.092	-0.436
211	DFBC 83-28 II	0.904	0.023	0.946	0.08	0.009	0.039	0.038	-0.347	-0.696	0.349
212	DFBC 83-29 II	0.961	0.108	0.96	0.014	-0.041	-0.103	0.128	-0.334	-0.582	0.249
213	DFBC 83-30 II	0.940	0.262	0.917	-0.059	0.056	-0.085	0.129	-0.378	-0.393	0.015
214	DFBC 83-1 II	0.903	0.028	0.945	0.064	0.002	-0.033	0.062	-0.314	-0.593	0.279
215	DFBC 83-40 II	0.947	0.129	0.958	0.084	0.055	0.036	0.048	-0.334	-0.037	-0.296
216	DFBC 83-5 II	0.855	0.025	0.914	0.086	0.025	-0.09	0.055	-0.355	-0.203	-0.152
217	DFBC 83-23 II	0.959	0.188	0.943	0.079	0.047	0.11	0.116	-0.288	-0.272	-0.016
218	DFBC 83-2 II	0.938	0.082	0.96	0.001	0.011	0.096	-0.018	-0.400	-0.758	0.358
219	DFBC 83-21 II	0.891	0.312	0.865	0.034	0.053	0.169	0.11	-0.334	-0.172	-0.161
221	DFBC 83-20 II	0.831	0.039	0.904	0.044	0.026	0.097	-0.028	-0.355	-0.926	0.571
222	DFBC 83-10 II	0.920	0.125	0.91	0.129	0.057	0.108	0.211	-0.355	0.155	-0.510
223	DFBC 83-9 II	0.938	0.021	0.956	0.056	0.04	0.138	-0.03	-0.355	-0.987	0.632
224	DFBC 83-1 III	0.907	0.187	0.904	0.091	0.033	0.083	0.195	-0.299	0.013	-0.312
225	DFBC 83-8 II	0.905	0.038	0.94	0.041	0.124	0.047	0.001	-0.378	-0.435	0.057

LKA No.	Surface sample	Communality (<0.8 in bold)	Factor loadings (Varimax Factor Matrix) Factor 1	Factor 2	Factor 3	Factor 4	Factor 5	Factor 6	Observed SST SST Feb. (WOA) (°C)	Estimated SST Feb (°C) 115/24/4	Residual SST (°C) (>±2°C in bold)
226	DFBC 83-7 II	0.829	0.039	0.88	0.156	0.062	0.046	0.154	-0.378	0.263	-0.641
227	DFBC 83-6 II	0.929	0.266	0.91	-0.09	0.138	0.002	0.062	-0.378	0.082	-0.460
230	1176-86	**0.785**	0.83	0.113	0.264	0.002	0.038	-0.111	5.321	6.230	-0.909
231	KR8802	0.973	0.765	0.176	0.092	0.58	0.089	0.068	8.669	5.781	**2.888**
232	KR8803	0.884	0.611	0.118	0.601	0.248	0.137	0.235	9.253	9.679	-0.425
233	KR8804	0.889	0.835	0.105	0.377	0.123	0.063	0.141	5.978	6.654	-0.676
234	MD84-561	0.897	0.782	0.259	0.072	0.458	0.002	0.06	2.855	5.022	**-2.167**
235	MD73-026	0.941	0.909	0.057	0.317	0.009	0.037	-0.101	9.636	7.300	**2.336**
236	MD84-529	0.932	0.933	0.068	0.154	0.162	0.085	-0.003	6.196	5.182	1.014
243	GC014	0.904	0.521	-0.002	0.769	0.09	0.112	0.148	12.447	12.717	-0.270
245	GC034	**0.776**	0.564	0.094	0.636	0.021	-0.037	0.208	13.582	11.686	1.896

Variable Name	Regression Coefficient	Std. error of Reg. Coeff.	Computed T-value
KP 6	-17.09507	14.19004	-1.205
KP 7	-17.38433	16.33199	-1.064
KP 8	15.64183	13.04221	1.199
KP 9	7.53677	5.8561	1.287
KP 10	0.53396	4.75686	0.112
KP 11	7.97624	5.82188	1.37
KP 12	-34.14221	27.64425	-1.235
KP 13	-8.89691	21.00039	-0.424
KP 14	-9.25595	9.84263	-0.94
KP 15	4.72524	10.35156	0.456
KP 16	-11.23627	11.35577	-0.989
KP 17	-8.15983	25.24515	-0.323
KP 18	-7.23729	11.95685	-0.605
KP 19	-3.82773	13.25611	-0.289
KP 20	-2.85135	12.13033	-0.235
KP 21	-12.8256	9.78942	-1.31
KP 22	-12.9545	12.9324	-1.002
KP 23	14.5361	11.78067	1.234
KP 24	-14.49969	10.33889	-1.402
KP 25	-1.53296	6.96457	-0.22
KP 26	-6.53842	7.25177	-0.902
KP 27	41.42393	31.19375	1.328
KP 28	36.43967	34.21847	1.065
KP 29	13.54394	27.26174	0.497
KP 30	11.02164	12.8507	0.858
KP 31	1.68894	13.40657	0.126
KP 32	1.15556	14.40448	0.08
Intercept	-20.24928		

CORRELATION MATRIX

	SST Feb	SST Aug	Factor 1	Factor 2	Factor 3	Factor 4	Factor 5	Factor 6	Factor 1x2	Factor 1x3	Factor 1x4	Factor 1x5	Factor 1x6	Factor 2x3	Factor 2x4
SST Feb	1														
SST Aug	**0.925**	1													
Factor 1	0.444	0.243	1												
Factor 2	-0.635	-0.403	**-0.834**	1											
Factor 3	0.782	0.788	-0.024	-0.301	1										
Factor 4	0.058	-0.008	-0.009	-0.166	-0.101	1									
Factor 5	-0.175	-0.226	-0.085	-0.151	-0.129	-0.029	1								
Factor 6	-0.170	-0.297	0.103	-0.238	-0.158	-0.151	0.033	1							
Factor 1x2	-0.428	-0.569	-0.022	0.052	-0.448	0.132	0.174	0.338	1						
Factor 1x3	**0.866**	**0.818**	0.054	-0.580	0.790	-0.148	-0.107	-0.136	-0.498	1					
Factor 1x4	0.083	-0.023	0.250	-0.341	-0.132	**0.806**	-0.009	-0.076	0.160	-0.108	1				
Factor 1x5	-0.041	-0.205	0.267	-0.425	-0.150	0.012	0.798	0.182	0.310	0.009	0.142	1			
Factor 1x6	-0.181	-0.356	0.238	-0.340	-0.192	-0.076	0.094	**0.870**	0.417	-0.162	0.105	0.343	1		
Factor 2x3	0.074	0.140	-0.141	0.065	0.105	-0.069	0.040	0.043	-0.216	0.269	-0.211	0.018	-0.034	1	
Factor 2x4	-0.241	-0.322	-0.245	0.179	-0.233	0.635	0.023	-0.136	0.507	-0.390	0.593	0.027	-0.075	-0.110	1
Factor 2x5	-0.367	-0.443	-0.269	0.128	-0.256	0.041	0.666	0.088	0.493	-0.342	-0.007	0.584	0.107	0.009	0.292
Factor 2x6	-0.446	-0.494	-0.195	0.152	-0.307	-0.154	0.065	0.718	0.607	-0.405	-0.123	0.143	0.668	0.100	0.098
Factor 3x4	0.357	0.344	0.048	-0.291	0.347	0.457	-0.007	-0.126	-0.294	0.424	0.422	-0.001	-0.088	0.249	0.123
Factor 3x5	0.350	0.287	0.137	-0.385	0.341	-0.035	0.495	-0.004	-0.193	0.533	-0.065	0.573	0.049	0.375	-0.180
Factor 3x6	0.185	0.101	0.054	-0.239	0.239	-0.126	0.060	0.424	-0.036	0.320	-0.059	0.180	0.545	0.270	-0.206
Factor 4x5	-0.122	-0.245	-0.045	-0.183	-0.168	0.622	0.538	-0.107	0.252	-0.195	0.615	0.515	0.018	-0.046	0.638
Factor 4x6	-0.143	-0.274	0.122	-0.221	-0.157	0.340	0.005	0.338	0.273	-0.220	0.603	0.161	0.503	-0.207	0.390
Factor 5x6	-0.209	-0.353	0.085	-0.263	-0.183	-0.116	0.538	0.635	0.415	-0.141	-0.013	0.724	0.672	0.064	-0.052
Factor 1sq	0.470	0.232	**0.967**	**-0.904**	0.032	0.066	0.006	0.198	0.131	0.412	0.321	0.370	0.336	-0.177	-0.140
Factor 2sq	-0.733	-0.539	**-0.831**	**0.971**	-0.414	-0.105	-0.059	-0.125	0.257	-0.691	-0.289	-0.311	-0.212	0.061	0.278
Factor 3sq	**0.839**	**0.827**	0.159	-0.442	**0.919**	-0.116	-0.092	-0.136	-0.536	**0.940**	-0.141	-0.057	-0.182	0.358	-0.325
Factor 4sq	0.009	-0.090	0.052	-0.199	-0.128	**0.880**	0.033	-0.117	0.217	-0.173	**0.937**	0.108	0.021	-0.128	0.787
Factor 5sq	-0.157	-0.283	0.019	-0.241	-0.159	0.054	**0.894**	0.132	0.317	-0.097	0.089	**0.916**	0.229	0.040	0.115
Factor 6sq	-0.255	-0.393	0.084	-0.206	-0.207	-0.106	0.106	**0.898**	0.448	-0.223	0.036	0.297	**0.963**	0.028	-0.044

	Factor 2x5	Factor 2x6	Factor 3x4	Factor 3x5	Factor 3x6	Factor 4x5	Factor 4x6	Factor 5x6	Factor 1sq	Factor 2sq	Factor 3sq	Factor 4sq	Factor 5sq	Factor 6sq
Factor 2x5	1													
Factor 2x6	0.190	1												
Factor 3x4	-0.125	-0.269	1											
Factor 3x5	0.144	-0.139	0.291	1										
Factor 3x6	-0.018	0.258	0.288	0.374	1									
Factor 4x5	0.426	-0.058	0.338	0.232	-0.019	1								
Factor 4x6	0.045	0.313	0.081	-0.043	0.162	0.387	1							
Factor 5x6	0.507	0.604	-0.062	0.294	0.377	0.208	0.283	1						
Factor 1sq	-0.159	-0.091	0.085	0.201	0.117	0.066	0.208	0.203	1					
Factor 2sq	0.261	0.291	-0.329	-0.395	-0.227	-0.092	-0.147	-0.126	**-0.865**	1				
Factor 3sq	-0.300	-0.348	0.461	0.513	0.336	-0.156	-0.217	-0.142	0.187	-0.558	1			
Factor 4sq	0.086	-0.095	0.476	-0.043	-0.083	0.738	0.549	-0.036	0.144	-0.135	-0.150	1		
Factor 5sq	**0.818**	0.115	0.014	0.535	0.131	0.582	0.115	0.671	0.136	-0.122	-0.108	0.121	1	
Factor 6sq	0.124	**0.817**	-0.112	0.029	0.564	0.006	0.491	0.710	0.193	-0.076	-0.208	-0.013	0.211	1

Notes.
High positive or negative correlations (ie. >0.8) betweenthe factors and/or parameters are highlighted in bold.

Appendix 4.5. Results of DTF 109/24/6.

DTF109/24/6 — **Nb. Varimax Factor Scores Matrix presented in Table 4.4**

Multiple correlation coefficient	0.971
(adjusted for d.f.)	**0.961**
Standard error of estimate	0.878
(adjusted for d.f.)	**1.008**

		Variance	45.83	27.343	7.189	3.425	4.04	2.204			
		Cumulative Var.	45.83	73.173	80.362	83.787	87.826	90.031			
		Communality	Factor loadings (Varimax Factor Matrix)						Observed SST	Estimated SST	Residual SST (°C)
LKA No.	Surface sample	(<0.8 in bold)	Factor 1	Factor 2	Factor 3	Factor 4	Factor 5	Factor 6	SST Feb. (WOA) (°C)	Feb (°C) 115/24/4	(>±2°C in bold)
1	V16-65	0.857	0.773	0.135	0.392	0.165	-0.004	-0.247	7.589	6.241	1.348
2	V16-60	0.910	0.741	0.317	0.228	-0.058	-0.431	0.135	4.459	2.840	1.619
3	1176-91	0.852	0.529	0.116	0.709	-0.079	-0.183	-0.124	10.334	10.788	-0.454
5	1277-2	0.873	0.695	0.203	0.576	0.025	-0.126	-0.032	8.947	8.811	0.136
7	RC15-91	0.941	0.894	0.076	0.318	0.12	-0.112	-0.087	4.217	4.353	-0.136
8	RC11-78	0.942	0.901	0.245	0.21	-0.016	-0.041	-0.153	2.634	3.840	-1.206
9	RC13-255	0.942	0.867	0.203	0.274	-0.073	0.005	-0.262	4.767	5.474	-0.707
10	1176-82	0.955	0.909	0.159	0.166	0.172	-0.062	0.205	1.026	2.223	-1.197
11	RC13-274	0.972	0.741	0.429	0.119	-0.056	-0.44	0.164	1.623	1.511	0.112
12	RC13-273	0.928	0.763	0.446	0.157	-0.097	-0.169	0.291	1.048	2.306	-1.257
13	MD24-KK63	0.925	0.894	0.116	0.076	0.313	-0.078	-0.043	3.635	3.386	0.249
14	RC13-263	0.898	0.767	0.455	0.12	0.021	-0.023	0.296	1.581	1.416	0.165
15	1277-28	0.927	0.781	0.44	-0.018	0.048	-0.275	0.213	1.057	0.618	0.438
16	MD82 424	0.958	0.834	0.396	0.089	0.061	-0.274	0.138	1.611	1.017	0.594
21	1178-4P	0.856	0.202	0.804	0.133	0.223	-0.278	-0.159	0.899	0.775	0.124
26	1277-41	0.880	0.446	0.444	0.065	0.211	-0.659	0.003	-0.173	-0.145	-0.028
28	MD82 436	0.869	0.535	0.238	0.205	0.278	-0.638	-0.01	0.349	-0.127	0.476
29	1176-55	0.865	0.728	0.456	0.048	0.271	-0.07	0.217	2.386	1.289	1.096
30	1176-65	0.819	0.784	0.359	0.031	-0.081	-0.224	0.135	0.795	1.503	-0.708
31	1277-8	0.915	0.8	0.261	0.171	0.232	-0.163	0.311	3.387	2.256	1.131
32	1277-12	**0.743**	0.759	0.339	0.121	-0.074	-0.027	0.178	1.422	1.984	-0.562
33	1578-49	0.924	0.672	0.426	0.117	0.15	-0.504	-0.023	0.349	0.852	-0.503
34	1678-64	0.941	0.858	0.231	0.307	0.15	-0.1	0.154	1.948	3.744	-1.797
35	1678-80	0.908	0.879	0.167	0.213	0.026	-0.199	-0.145	5.715	3.715	2.000
36	1678-84	0.913	0.865	0.254	0.255	0.107	-0.074	-0.133	2.914	3.888	-0.975
37	1678-89	0.931	0.656	0.449	0.138	0.054	-0.466	0.247	1.236	1.366	-0.131
38	1678-96	0.914	0.697	0.516	0.119	0.081	-0.229	0.299	0.495	1.242	-0.748
39	RC8-46	0.957	0.85	0.268	0.186	-0.046	-0.175	0.31	3.036	2.940	0.096
42	RC11-90	0.883	0.802	0.434	0.172	0.019	-0.07	0.129	1.860	1.881	-0.021
43	RC13-257	0.938	0.857	0.226	0.202	0.096	-0.32	-0.029	1.220	2.471	-1.252
44	RC13-268	0.890	0.703	0.532	0.013	0.096	-0.309	0.095	0.903	0.493	0.410
45	RC13-269	0.920	0.798	0.434	0.168	-0.16	0.004	0.202	2.761	2.254	0.507
46	RC13-270	0.939	0.836	0.374	0.107	0.074	-0.252	0.141	1.385	1.239	0.146
47	RC13-272	0.888	0.713	0.526	0.085	0.185	-0.204	0.138	1.161	0.749	0.411
50	V14-58	0.933	0.73	0.42	0.18	-0.015	-0.416	0.133	1.272	1.803	-0.531
51	MD24 KK02	0.879	0.752	0.346	0.071	-0.002	-0.332	0.28	1.831	1.647	0.184
52	MD24 KK32	0.804	0.806	0.153	0.252	0.13	-0.208	0.086	1.831	3.040	-1.209
53	MD24 KK35	**0.754**	0.645	0.138	0.225	0.407	-0.275	0.162	1.677	2.030	-0.353
54	MD24 KK37	0.942	0.757	0.33	0.107	-0.018	-0.101	0.489	2.289	2.419	-0.130
55	MD82 425	0.924	0.832	0.335	-0.036	0.2	0.035	0.277	1.292	0.744	0.548
56	MD82 430	0.964	0.786	0.257	0.212	0.138	-0.464	-0.035	1.161	1.785	-0.623
57	MD82 434	0.959	0.817	0.291	0.157	0.082	-0.413	-0.07	1.098	1.985	-0.887
62	MD 84 540	0.916	0.816	0.428	0.129	-0.015	-0.113	0.194	1.920	1.428	0.492
63	MD84 552	0.906	0.89	0.214	0.154	0.032	0.057	0.197	2.302	2.113	0.189
64	MD84 557	0.909	0.892	0.228	0.041	0.244	0.019	0.019	2.231	2.553	-0.323

Appendix 4.5. Results of DTF 109/24/6.

LKA No.	Surface sample	Communality (<0.8 in bold)	Factor loadings (Varimax Factor Matrix) Factor 1	Factor 2	Factor 3	Factor 4	Factor 5	Factor 6	Observed SST SST Feb. (WOA) (°C)	Estimated SST Feb (°C) 115/24/4	Residual SST (°C) (>±2°C in bold)
65	MD84 562	0.937	0.883	0.116	0.369	0.081	-0.007	-0.037	3.901	5.258	-1.357
66	MD84 563	0.944	0.924	0.114	0.228	0.024	-0.032	-0.153	3.700	4.272	-0.571
67	MD84 569	0.853	0.701	0.14	0.459	0.298	0.026	-0.201	6.413	6.818	-0.405
71	83-41 III	0.812	0.138	0.812	-0.057	-0.214	-0.257	-0.134	-1.081	-0.627	-0.454
77	KR8701	0.954	0.667	0.342	0.1	0.583	-0.178	-0.104	3.595	4.423	-0.828
78	KR8702	0.873	0.599	0.636	0.101	0.242	-0.197	-0.026	1.829	1.052	0.777
79	KR8703	0.905	0.397	0.789	0.012	0.12	-0.295	-0.153	1.313	0.564	0.750
84	KR8710	0.920	0.61	0.633	0.015	0.345	-0.13	-0.1	2.065	2.237	-0.172
85	KR8712	0.938	0.774	0.379	0.123	0.416	-0.077	-0.036	3.351	3.064	0.287
86	KR8713	0.801	0.358	0.359	0.303	0.646	-0.186	0.001	3.901	3.576	0.325
87	KR8714	**0.784**	0.601	0.442	0.145	0.427	-0.141	0.066	4.652	2.716	1.936
88	KR8801	0.886	0.695	0.205	0.504	0.307	-0.016	-0.112	7.750	7.037	0.712
89	KR8805	0.935	0.83	0.272	0.331	-0.101	-0.227	0.042	5.116	4.716	0.401
91	KR8807	0.866	0.435	0.002	0.808	0.043	-0.129	0.07	11.705	11.953	-0.249
92	KR8808	0.873	0.639	0.059	0.662	0.121	-0.047	0.077	10.460	10.259	0.200
94	KR8810	0.970	0.919	0.067	0.308	0.095	-0.07	-0.111	5.596	4.538	1.059
96	KR8812	0.958	0.899	0.164	0.294	0.095	-0.157	-0.053	4.265	3.815	0.450
97	KR8813	0.941	0.92	0.121	0.132	0.226	-0.094	-0.05	3.926	3.103	0.822
98	KR8814	0.941	0.895	0.294	0.151	0.054	-0.103	0.134	2.774	1.901	0.873
99	KR8815	**0.799**	0.68	0.372	0.053	0.359	-0.255	0.026	1.785	2.275	-0.490
100	KR8816	0.908	0.759	0.434	0.051	0.318	-0.18	0.082	0.981	1.520	-0.539
101	KR8817	0.900	0.39	0.833	0.05	0.179	-0.139	-0.014	0.030	0.339	-0.309
102	KR8818	0.837	0.359	0.835	0.073	0.056	-0.031	0.045	-0.072	0.347	-0.419
103	KR8819	0.913	0.663	0.608	0.093	0.276	-0.048	0.131	0.952	1.047	-0.095
104	KR8820	0.913	0.589	0.707	0.051	0.195	-0.111	0.112	1.080	0.184	0.896
105	KR8821	0.915	0.568	0.697	-0.015	0.238	-0.178	-0.131	1.057	1.560	-0.503
106	KR8822	0.937	0.667	0.636	0.028	0.26	-0.118	0.078	0.894	0.507	0.387
107	KR8823	0.928	0.779	0.412	0.251	0.195	-0.206	0.085	1.157	2.185	-1.028
108	KR8824	0.948	0.618	0.67	0.129	0.19	-0.249	0.053	1.091	0.193	0.899
109	KR8825	0.920	0.573	0.716	-0.009	0.242	-0.137	-0.027	0.605	0.792	-0.187
110	KR8827	0.893	0.563	0.612	0.086	0.405	-0.171	-0.02	0.758	2.013	-1.254
112	KR8829	0.928	0.884	0.329	0.11	0.138	-0.063	0.052	1.290	1.736	-0.446
113	KR8830	0.894	0.837	0.189	0.129	0.341	0.043	0.152	1.819	2.668	-0.849
145	MDBX94-01	0.887	0.297	0.028	0.89	0.059	0.02	-0.042	12.900	13.384	-0.484
148	MDBX94-04	0.960	0.892	0.15	0.289	0.002	0.033	-0.239	5.698	5.482	0.216
152	93-7/GC33	**0.763**	0.2	0.831	0.033	-0.015	0.177	-0.003	0.121	0.167	-0.046
153	93-7/GC5	0.830	0.304	0.825	0.079	-0.018	-0.195	-0.111	0.143	0.387	-0.245
155	KTB12	0.935	0.882	0.206	0.287	0.1	-0.137	-0.065	5.815	3.774	**2.041**
156	KTB14	0.903	0.824	0.005	0.429	0.114	-0.051	-0.161	5.250	5.903	-0.654
184	E36-6B	0.955	0.903	0.146	0.226	-0.055	0.044	-0.248	5.470	5.096	0.374
192	KTB 08	0.939	0.91	0.073	0.292	0.085	-0.096	-0.064	4.515	4.143	0.372
210	DFBC 83-27 II	0.862	0.241	0.88	0.056	0.102	-0.052	0.116	-0.344	0.112	-0.455
211	DFBC 83-28 II	0.907	0.027	0.947	0.076	-0.004	-0.041	0.041	-0.347	-0.671	0.323
212	DFBC 83-29 II	0.960	0.13	0.961	0.015	-0.086	0.09	0.069	-0.334	-1.155	0.821
213	DFBC 83-30 II	0.939	0.292	0.918	-0.036	0.009	0.096	0.015	-0.378	-0.619	0.241
214	DFBC 83-1 II	0.905	0.037	0.947	0.06	-0.021	0.027	0.049	-0.314	-0.724	0.410
215	DFBC 83-40 II	0.948	0.136	0.958	0.092	0.035	-0.031	0.015	-0.334	-0.077	-0.257
216	DFBC 83-5 II	0.859	0.028	0.917	0.082	0.004	0.092	0.051	-0.355	-0.313	-0.042
217	DFBC 83-23 II	0.959	0.216	0.944	0.083	0.023	-0.103	0.057	-0.288	-0.355	0.067
218	DFBC 83-2 II	0.942	0.085	0.958	0.014	-0.013	-0.104	-0.077	-0.400	-0.738	0.338
219	DFBC 83-21 II	0.897	0.342	0.863	0.058	0.011	-0.177	-0.009	-0.334	-0.243	-0.090
221	DFBC 83-20 II	0.835	0.035	0.902	0.052	-0.002	-0.122	-0.057	-0.355	-0.690	0.335
222	DFBC 83-10 II	0.927	0.176	0.914	0.107	0.048	-0.092	0.196	-0.355	0.199	-0.554

LKA No.	Surface sample	Communality (<0.8 in bold)	Factor loadings (Varimax Factor Matrix) Factor 1	Factor 2	Factor 3	Factor 4	Factor 5	Factor 6	Observed SST SST Feb. (WOA) (°C)	Estimated SST Feb (°C) 115/24/4	Residual SST (°C) (>±2°C in bold)
223	DFBC 83-9 II	0.937	0.021	0.955	0.058	0.035	-0.137	-0.044	-0.355	-0.804	0.449
224	DFBC 83-1 III	0.909	0.232	0.907	0.085	0.004	-0.074	0.141	-0.299	-0.096	-0.203
225	DFBC 83-8 II	0.909	0.044	0.943	0.042	0.128	-0.026	0.003	-0.378	-0.087	-0.291
226	DFBC 83-7 II	0.845	0.07	0.885	0.131	0.068	-0.02	0.185	-0.378	0.499	-0.877
227	DFBC 83-6 II	0.932	0.29	0.91	-0.061	0.111	0.025	-0.047	-0.378	0.249	-0.627
230	1176-86	**0.764**	0.733	0.102	0.399	0.06	0.052	-0.228	5.321	6.369	-1.048
232	KR8803	0.862	0.612	0.124	0.631	0.175	-0.152	0.145	9.253	9.179	0.074
233	KR8804	0.889	0.803	0.103	0.465	0.129	-0.003	0.022	5.978	6.626	-0.648
236	MD84-529	0.925	0.881	0.061	0.287	0.172	-0.006	-0.181	6.196	4.912	1.284
243	GC014	0.899	0.473	0.001	0.799	0.066	-0.121	0.133	12.447	12.538	-0.091
245	GC034	**0.763**	0.532	0.096	0.673	-0.044	0.01	0.125	13.582	11.674	1.908

Variable Name	Regression Coefficient	Std. error of Reg. Coeff.	Computed T-value
KP 6	-24.59074	10.10001	-2.435
KP 7	-19.67286	14.60195	-1.347
KP 8	21.93499	12.88555	1.702
KP 9	2.33585	5.32945	0.438
KP 10	-0.27917	4.56056	-0.061
KP 11	9.6244	5.35318	1.798
KP 12	-42.84893	22.14913	-1.935
KP 13	-13.82531	19.24545	-0.718
KP 14	-7.00983	7.94773	-0.882
KP 15	13.39293	8.25451	1.622
KP 16	-1.14735	11.16782	-0.103
KP 17	2.45703	24.28326	0.101
KP 18	-10.84423	10.44241	-1.038
KP 19	27.16559	11.57062	2.348
KP 20	5.4648	11.93802	0.458
KP 21	-11.49764	9.68597	-1.187
KP 22	29.28438	11.72683	2.497
KP 23	16.31716	11.65797	1.4
KP 24	22.16671	8.86415	2.501
KP 25	-1.87162	6.53766	-0.286
KP 26	-3.47593	7.04261	-0.494
KP 27	51.44719	25.10761	2.049
KP 28	46.26428	30.47376	1.518
KP 29	12.9215	26.61691	0.485
KP 30	12.46468	11.41685	1.092
KP 31	-22.72708	11.74794	-1.935
KP 32	-8.59838	14.20747	-0.605
Intercept	-27.80946		

Correlation Matrix

	SST Feb.	SST Aug.	Factor 1	Factor 2	Factor 3	Factor 4	Factor 5	Factor 6	Factor 1x2	Factor 1x3	Factor 1x4	Factor 1x5	Factor 1x6	Factor 2x3	Fcator 2x4	Factor 2x5
SST Feb.	1															
SST Aug.	**0.920**	1														
Factor 1	0.268	0.022	1													
Factor 2	-0.629	-0.385	**-0.825**	1												
Factor 3	**0.879**	**0.887**	-0.057	-0.384	1											
Factor 4	0.015	-0.076	-0.040	-0.145	-0.097	1										
Factor 5	-0.210	-0.251	-0.043	-0.121	-0.142	0.010	1									
Factor 6	0.031	-0.042	0.261	-0.229	-0.086	-0.155	-0.089	1								
Factor 1x2	-0.454	-0.602	0.142	0.065	-0.503	0.107	0.156	0.127	1							
Factor 1x3	**0.856**	0.773	0.452	-0.700	0.733	-0.113	-0.135	0.028	-0.486	1						
Factor 1x4	0.034	-0.083	0.206	-0.277	-0.095	0.743	-0.007	-0.200	0.123	-0.019	1					
Factor 1x5	0.142	0.284	-0.223	0.295	0.150	-0.023	**-0.806**	0.035	-0.340	0.045	-0.057	1				
Factor 1x6	-0.234	-0.302	0.027	-0.017	-0.137	-0.068	0.085	0.456	0.386	-0.272	-0.089	-0.227	1			
Factor 2x3	0.067	0.100	-0.099	0.031	0.059	0.042	0.032	0.002	-0.044	0.214	-0.136	-0.071	0.026	1		
Factor 2x4	-0.164	-0.267	-0.144	0.097	-0.204	0.660	0.031	-0.213	0.413	-0.303	0.690	-0.061	-0.060	0.046	1	
Factor 2x5	0.347	0.413	0.183	-0.135	0.271	-0.061	-0.669	0.054	-0.411	0.347	0.003	0.653	-0.125	-0.095	-0.235	1
Factor 2x6	-0.203	-0.211	0.058	0.022	-0.153	-0.155	-0.019	0.455	0.282	-0.186	-0.154	-0.105	0.712	0.227	-0.111	0.107
Factor 3x4	0.320	0.296	0.040	-0.308	0.286	0.602	-0.024	-0.137	-0.274	0.371	0.605	0.040	-0.162	0.166	0.316	0.102
Factor 3x5	-0.274	-0.196	-0.075	0.344	-0.336	-0.030	-0.555	0.119	0.108	-0.375	0.021	0.658	-0.092	-0.271	0.047	0.280
Factor 3x6	-0.086	-0.122	-0.143	0.075	0.042	-0.035	0.085	0.129	0.191	-0.156	-0.087	-0.194	0.764	0.023	-0.027	-0.118
Factor 4x5	0.139	0.236	0.087	0.112	0.138	-0.606	-0.546	0.213	-0.153	0.155	-0.569	0.429	0.062	-0.060	-0.626	0.372
Factor 4x6	-0.146	-0.173	0.020	-0.008	-0.058	-0.037	-0.014	0.098	0.095	-0.139	0.113	-0.021	0.426	-0.086	0.019	0.020
Factor 5x6	0.056	0.136	-0.169	0.180	0.068	0.129	-0.205	-0.466	-0.271	0.036	0.150	0.392	-0.603	-0.088	0.147	0.157
Factor 1sq	0.320	0.050	**0.974**	**-0.874**	0.004	0.032	0.026	0.268	0.252	0.473	0.263	-0.296	0.066	-0.102	-0.049	0.106
Factor 2sq	-0.728	-0.526	-0.771	**0.971**	-0.508	-0.079	-0.037	-0.180	0.272	**-0.801**	-0.233	0.178	0.088	0.061	0.187	-0.251
Factor 3sq	**0.916**	**0.887**	0.150	-0.548	**0.935**	-0.075	-0.123	-0.035	-0.553	**0.906**	-0.064	0.095	-0.209	0.248	-0.240	0.306
Factor 4sq	0.012	-0.099	0.051	-0.183	-0.085	**0.838**	0.041	-0.217	0.148	-0.074	**0.941**	-0.064	-0.097	-0.017	**0.842**	-0.075
Factor 5sq	0.194	0.300	-0.022	0.158	0.147	-0.083	**-0.878**	0.069	-0.292	0.129	-0.050	**0.927**	-0.173	-0.087	-0.128	**0.846**
Factor 6sq	-0.217	-0.265	0.012	0.005	-0.122	-0.096	0.057	0.457	0.343	-0.250	-0.111	-0.201	**0.966**	0.094	-0.071	-0.043

	Factor 2x6	Factor 3x4	Factor 3x5	Factor 3x6	Factor 4x5	Factor 4x6	Factor 5x6	Factor 1sq	Factor 2sq	Factor 3sq	Factor 4sq	Factor 5sq	Factor 6sq
Factor 2x6	1												
Factor 3x4	-0.176	1											
Factor 3x5	0.014	-0.142	1										
Factor 3x6	0.461	-0.083	-0.229	1									
Factor 4x5	0.140	-0.398	0.329	-0.041	1								
Factor 4x6	0.350	-0.063	-0.067	0.368	-0.031	1							
Factor 5x6	-0.655	0.073	0.158	-0.401	-0.102	-0.262	1						
Factor 1sq	0.067	0.088	-0.146	-0.103	-0.003	0.020	-0.211	1					
Factor 2sq	0.088	-0.342	0.337	0.121	0.041	0.019	0.102	-0.798	1				
Factor 3sq	-0.148	0.385	-0.408	-0.047	0.108	-0.109	0.043	0.194	-0.668	1			
Factor 4sq	-0.157	0.660	-0.027	-0.067	-0.695	0.055	0.149	0.130	-0.131	-0.060	1		
Factor 5sq	0.020	0.009	0.643	-0.182	0.522	-0.018	0.275	-0.106	0.048	0.125	-0.102	1	
Factor 6sq	**0.847**	-0.164	-0.092	0.778	0.070	0.451	-0.655	0.045	0.095	-0.178	-0.112	-0.121	1

Notes.

High positive or negative correlations (ie. >0.8) between the factors and/or parameters are highlighted in bold.

APPENDIX 5.1

Sea-ice concentration models output (Statistical package GENSTAT 5). All model output courtesy of Dr S. Barry , Statistical Consulting Unit, Graduate School, Australian National University.

1. February sea-ice estimation

Summary(new.final.feb.01.model)

Call: glm(formula = structure(.Data = cbind(febice, 1 - febice) ~ F2 + F3 + I(F3^2) + I(F4^2), class = "formula"), family = binomial(), data = full.frame)

Deviance Residuals: Min 1Q Median 3Q Max
-2.47725 -0.0482307 -0.0006730624 0.3107655 1.887255

Coefficients:	Value	Std. Error	t value
(Intercept)	-21.93062	4.836432	-4.534463
F2	23.34964	5.369961	4.348196
F3	43.10360	22.856324	1.885850
I(F3^2)	141.28339	84.813492	-1.665813
I(F4^2)	20.16218	11.074929	1.820525

(Dispersion Parameter for Binomial family taken to be 1)
Null Deviance: 204.2649 on 175 degrees of freedom
Residual Deviance: 64.8305 on 171 degrees of freedom
Number of Fisher Scoring Iterations: 9

Correlation of Coefficients:

	(Intercept)	F2	F3	I(F3^2)
F2	-0.9520388			
F3	-0.4631584	0.1971841		
I(F3^2)	0.4532796	-0.2135731	-0.9719296	
I(F4^2)	-0.1625692	-0.0454453	0.4506104	-0.4041095

Summary(new.final.feb.abund.model)

Call: glm(formula = structure(.Data = cbind(SI1feb, 100 - SI1feb) ~ F1 + F2 + I(F1^2) + I(F3^2) + I(F4^2), class = "formula"), family = quasi(link = logit, variance = "mu(1-mu)"), data = full.frame, subset = as.logical(sepice))

Deviance Residuals: Min 1Q Median 3Q Max
-7.048781 -1.078151 -0.3024175 -0.02754867 7.95573

Coefficients:	Value	Std. Error	t value
(Intercept)	-21.292910	5.860167	-3.633499
F1	-5.370159	1.634957	-3.284588
F2	21.384608	6.133435	3.486563
I(F1^2)	9.011708	5.991979	1.503962
I(F3^2)	30.198675	9.242501	3.267370
I(F4^2)	16.212052	5.269704	3.076464

(Dispersion Parameter for Quasi-likelihood family taken to be 6.203161)
Null Deviance: 2037.788 on 110 degrees of freedom
Residual Deviance: 529.8335 on 105 degrees of freedom
Number of Fisher Scoring Iterations: 5

Correlation of Coefficients:

	(Intercept)	F1	F2	I(F1^2)	I(F3^2)
F1	0.1862971				
F2	-0.9983165	-0.2073886			
I(F1^2)	-0.7538776	-0.6875402	0.7534758		
I(F3^2)	-0.6980209	-0.0153004	0.6644775	0.5728261	
I(F4^2)	-0.8133295	-0.2753278	0.8007726	0.6739676	0.5898942

2. September sea-ice estimation

Summary(new.final.sept.01.model)

Call: glm(formula = structure(.Data = cbind(sepice, 1 - sepice) ~ F1 + F2 + F3 + F4 + I(F1^2), class = "formula"), family = binomial(), data = full.frame)

Deviance Residuals:	Min	1Q	Median	3Q	Max
	-2.10026	-0.01590397	0.009120799	0.09094388	2.335466

Coefficients:	Value	Std. Error	t value
(Intercept)	-14.596606	8.469249	-1.723483
F1	-15.040303	14.659377	-1.025985
F2	30.631064	9.027704	3.393007
F3	-13.498186	6.364987	-2.120693
F4	9.670042	4.560406	2.120434
I(F1^2)	27.298168	14.136569	1.931032

(Dispersion Parameter for Binomial family taken to be 1)
Null Deviance: 231.8243 on 175 degrees of freedom
Residual Deviance: 40.93442 on 170 degrees of freedom
Number of Fisher Scoring Iterations: 8

Correlation of Coefficients:

	(Intercept)	F1	F2	F3	F4
F1	-0.3979684				
F2	-0.8025281	-0.1542388			
F3	-0.2073837	0.0200736	0.0556382		
F4	-0.3128128	-0.1246673	0.5598952	-0.0184579	
I(F1^2)	-0.0981919	-0.8649155	0.5670255	0.0275270	0.2265778

Summary(new.final.sept.abund.model)
Call: glm(formula = structure(.Data = cbind(SI1sept, 100 - SI1sept) ~ F2 + F4, class = "formula"), family = quasi(link = logit, variance = "mu(1-mu)"), data = full.frame, subset = as.logical(sepice))

Deviance Residuals:	Min	1Q	Median	3Q	Max
	-10.95836	-2.905341	0.04909682	2.464611	10.63947

Coefficients:	Value	Std. Error	t value
(Intercept)	-2.420095	0.3782734	-6.397740
F2	3.411627	0.5203161	6.556835
F4	5.401017	0.6435645	8.392347

(Dispersion Parameter for Quasi-likelihood family taken to be 19.36646)
Null Deviance: 4437.865 on 110 degrees of freedom
Residual Deviance: 2224.195 on 108 degrees of freedom
Number of Fisher Scoring Iterations: 3

Correlation of Coefficients:

	(Intercept)	F2
F2	-0.9695962	
F4	-0.3262466	0.3246896

3. Months/year sea-ice estimation

Summary(new.final.my.model.red)
Call: glm(formula = structure(.Data = cbind(SI1my, 12 - SI1my) ~ F1 + F2 + F4 + I(F1^2) + I(F3^2), class = "formula"), family = quasi(link = logit, variance = "mu(1-mu)"), data = full.frame, subset = good.my.points)

Deviance Residuals:	Min	1Q	Median	3Q	Max
	-4.929051	-0.7870758	-0.006115381	0.7691001	3.193416

Coefficients:	Value	Std. Error	t value
(Intercept)	-3.625893	1.9736161	-1.837182
F1	-14.418993	3.1329734	-4.602335
F2	11.435477	2.0963380	5.454978
F4	3.258844	0.8988055	3.625750
I(F1^2)	15.512690	3.6724021	4.224126
I(F3^2)	-23.421805	6.6690085	-3.512037

(Dispersion Parameter for Quasi-likelihood family taken to be 2.114862)
Null Deviance: 2044.115 on 174 degrees of freedom
Residual Deviance: 296.5424 on 169 degrees of freedom
Number of Fisher Scoring Iterations: 6

Correlation of Coefficients:

	(Intercept)	F1	F2	F4	I(F1^2)
F1	-0.1348970				
F2	-0.9083262	-0.2690585			
F4	-0.0354536	-0.0207015	0.0750736		
I(F1^2)	-0.3402511	-0.8793688	0.6701187	-0.0161600	
I(F3^2)	-0.3923296	0.1397343	0.2911337	0.2749963	0.0019042

Appendix 6.1. *Core E53-10 - survey data.*

Core E53-10		*Actinocyclus actinocyclus*	*A. curvatulus*	*A. "divisus"*	*A. ingens*	*Actinocyclus* spp.	*Asteromphalus hookeri*	*A. hyalinus*	*A. parvulus*	*Azpeitia tabularis*	*Castodiscus* spp.	*Chaetoceros* resting spores	*Coscinodiscus marginatus*	*C. radiatus*	*Coscinodiscus* spp.	*Dactyliosolen antarcticus*	*Denticulopsis dimorpha*	*Denticulopsis* spp.	*Eucampia antarctica*	*Fragilariopsis kerguelensis*	*F. ritscheri*	*F. separanda*	*F. sublinearis*	*F. rhombica*	*Fragilariopsis* spp.	*Hemidiscus cuneiformis*	*H. karsetenii*	*Proboscia cf. curvirostris*	*Rhizosolenia* otaria absent	*Rhizosolenia* otaria present	*Rhizosolenia* spp.	*Stellarima* spp.	*Stephanopyxis* spp.	*Thalassionema nitzschioides*	*Thalassiosira gracilis*	*T. lentiginosa*	*T. lineata*	*T. oestrupii*	*T. oliverana*	*T. cf. ritscheri*	*T. trifulta*	*Thalassiosira* spp.	*Thalassiothrix/Trichotoxon* spp.	*Xanthiopyxis* spp.	species indet.	*Distephanus* spp.¥	*Dictyocha* spp.¥	Other silicoflagellates	Radiolarians	Sponge spicules	Endoskeletal dinoflagellates
Depth	Total																																															
0-1cm	304 (530 FOV)		1		1		1			12						12			5	182	1	4	3				1			1			5	5	61		1	5			2		1		2					
10-11 cm		x			x					x		x							x	x						x				x			x		x	x								x	x	x
30-31 cm		x			x		x												x	x						x			x		x			x	x			x					x	x	
35-36 cm	312 (356 FOV)		1		9	1	2		1	1	2					7			8	188		10	7	1	1		6		3			1		1	1	43		13	5							5					
50-51 cm		x	x			x	x			x		x		x					x	x		x	x		x	x								x			x			x				x	x		
70-71 cm		x					x			x									x	x					x	x								x			x	x						x	x		
90-91 cm		x			x		x			x						x			x	x		x			x	x								x				x						x	x		x
110-111 cm					x	x	x		x	x		x					x		x	x		x			x	x			x					x			x	x	x					x	x		
130-131 cm		x	x	x	x	x	x		x	x					x	x		x	x	x		x			x	x								x			x	x	x		x			x	x		
150-151 cm		x					x			x		x		x			x		x	x					x	x	x							x	x	x								x	x		
170-171 cm					x		x	x		x					x	x			x	x		x				x								x			x				x			x	x		
190-191 cm					x					x						x			x	x		x				x			x					x			x							x			

Notes.

Quantitative samples viewed under x100 magnification. Samples observed qualitatively under both x40 and x100 magnification.

FOV = fields of view. ¥ = silicoflagellates.

x = observed in sample

Appendix 6.2. Core 787 - Age model and other data.

Core MD88 -787

Core depth (cm)	δ O18 (*N. pachyderma* s. 200-250µm)	Tie points in SPECMAP age scale	Corresponding SPECMAP age scale (Ka)	Linear sedimentation rate (cm/Ka)	*Analyseries* extrapolated age scale (Ka) at 10cm interval	Core sample Dry weights (gm)	Field of views counted	Diatom subtotal 2 count (Δ)	No. diatom frustules (x10E6)/gm dry weight	DTF 109/24/6 Factor 1 loading	DTF 109/24/6 Factor 2 loading	DTF 109/24/6 Factor 3 loading	DTF 109/24/6 Factor 4 loading	DTF 109/24/6 Factor 5 loading	DTF 109/24/6 Factor 6 loading	DTF 166/34/4 Factor 1 loading	DTF 166/34/4 Factor 2 loading	DTF 166/34/4 Factor 3 loading	DTF 166/34/4 Factor 4 loading
0	2.66	0	0.00	13.68	0.00	0.7	87	306.5	316.35	0.8678	0.2376	0.0742	0.0221	-0.0817	0.2996	0.7885	0.162	0.2994	-0.1699
10	2.97	-	0.73	13.68	0.73	1.3	117	336	138.86	0.8313	0.3281	0.1183	0.0124	-0.0035	0.3502	0.7629	0.1288	0.3375	-0.1206
20	3.17	-	1.46	13.68	1.46	0.8	65	321.5	388.63	0.7699	0.3478	-0.0221	0.0667	-0.0045	0.4633	0.8068	0.2128	0.1352	-0.0441
30	2.77	-	2.19	13.68	2.19	1	97	342.5	221.94	0.8089	0.297	0.0198	0.1198	0.1258	0.4452	0.7874	0.1994	0.2684	-0.1892
40	2.9	-	2.92	13.68	2.92	0.7	95	313.5	296.33	0.6956	0.3006	0.0644	0.1292	-0.0715	0.5225	0.7246	0.2202	0.1765	-0.1488
50	-	-	-	-	3.65	0.9	121	327.5	189.03	0.7534	0.3268	0.0394	0.1016	0.057	0.5304	0.8332	0.1865	0.2018	-0.0527
60	3.13	-	4.38	13.68	4.38	0.8	55	321.5	459.29	0.8145	0.3612	0.081	0.0406	-0.0092	0.362	0.8276	0.1868	0.1963	-0.0677
70	2.99	-	5.12	13.68	5.12	0.8	131	311	186.53	0.8046	0.2935	0.0831	0.0772	0.0237	0.4388	0.8332	0.1865	0.2018	-0.0527
80	2.95	-	5.85	13.68	5.85	0.8	50	314	493.43	0.6623	0.4035	0.0424	-0.053	-0.0576	0.54	0.8221	0.2224	0.181	-0.053
90	3.31	-	6.58	13.68	6.58	0.7	83	310	335.38	0.7104	0.2068	0.2986	0.0623	0.0178	0.4603	0.7389	0.0872	0.356	-0.1879
100	3.23	-	7.31	13.68	7.31	0.8	64	298.5	366.46	0.6266	0.3337	0.1094	0.0147	-0.0704	0.5216	0.7542	0.2274	0.143	0.0412
110	3.14	-	8.04	13.68	8.04	1	97	347.5	225.18	0.8216	0.3182	0.1888	0.0403	-0.0283	0.323	0.8687	0.1665	0.1745	0.08
120	2.28	-	8.77	13.68	8.77	0.7	60	316	472.93	0.7518	0.2745	0.1948	-0.0668	-0.099	0.4038	0.7836	0.1992	0.2185	0.0111
130	3.43	-	9.50	13.68	9.50	2	131	321	77.01	0.7661	0.3565	0.13	0.0003	-0.1066	0.3792	0.8733	0.1639	0.1815	0.0685
140	3.27	-	10.23	13.68	10.23	0.8	59	301	400.85	0.6821	0.4562	0.0705	-0.0087	-0.0358	0.4071	0.7718	0.2452	0.0628	0.0122
150	3.65	-	10.96	13.68	10.96	1.1	190	316	95.04	0.7724	0.3307	0.0709	0.1829	0.1	0.3868	0.828	0.2251	0.1867	-0.0355
160	3	-	11.69	13.68	11.69	0.8	126	346.5	216.07	0.7887	0.285	0.1111	0.1105	0.0977	0.4691	0.8079	0.1958	0.2837	-0.1453
170	3.86	-	12.42	13.68	12.42	0.9	196	302	107.61	0.757	0.3672	0.0352	0.1068	0.0244	0.4746	0.7475	0.2552	0.2446	-0.0996
180	3.86	-	13.15	13.68	13.15	0.7	95	313.5	296.33	0.7381	0.2158	0.2246	0.035	0.0267	0.455	0.8141	0.1919	0.2548	-0.0993
190	3.52 *	-	13.88	13.68	13.88	1.5	199	309	65.07	0.7946	0.2637	0.1782	0.1975	0.1118	0.3098	0.8213	0.1968	0.3035	-0.1258
200	3.79	-	14.62	13.68	14.62	0.6	18	308	283.25 ¥	0.7344	0.3792	0.2468	0.0788	0.2254	0.1352	0.5618	0.261	0.412	-0.275
210	4	-	15.35	13.68	15.35	1	251	289.5	72.5	0.6977	0.341	0.0125	0.3328	0.159	0.0393	0.7615	0.3148	0.2198	-0.0682
220	-	-	-	-	16.08	0.9	15	324	238.37 ¥	0.5981	0.5532	0.0822	0.0734	0.1955	0.3849	0.613	0.3216	0.197	-0.2094
230	4.22	-	16.81	13.68	16.81	0.9	163	288.5	123.61	0.7038	0.4459	-0.005	0.3073	0.1322	0.2077	0.6214	0.4074	0.2104	-0.2702
240	4.51	-	17.54	13.68	17.54	0.9	128	304	165.87	0.6932	0.3679	0.0096	0.3461	0.1024	0.2061	0.6561	0.4095	0.1965	-0.3426
250	4.42	-	18.27	13.68	18.27	1.1	163	299	104.82	0.6911	0.4919	-0.0674	0.3359	0.2713	0.0897	0.5705	0.4322	0.2668	-0.4217
260	4.53	-	19.00	13.68	19.00	1.2	12	344	237.27 ¥	0.6065	0.5408	-0.0084	-0.0407	0.1163	0.4508	0.6147	0.3216	0.1787	-0.2051
270	4.47	-	20.33	7.50	20.33	1.5	80	319.5	167.36	0.5828	0.6553	0.0403	0.005	0.0707	0.357	0.6045	0.6333	0.1122	-0.2811
280	4.39	19	21.67	7.50	21.67	1	10	312	309.89 ¥	0.5279	0.4548	0.1801	0.1367	0.1398	0.4607	0.5824	0.3552	0.1207	-0.3281
290	-	-	-	-	23.00	1	99	314	199.37	0.6504	0.515	-0.0395	0.1194	-0.0962	0.4528	0.7545	0.435	0.1322	-0.2552
300	4.15	-	24.33	7.50	24.33	1.1	45	311	394.92	0.5237	0.6374	0.0537	-0.1264	-0.1233	0.3898	0.5709	0.5244	0.1429	-0.0538
310	-	-	-	-	25.67	1.2	92	327	186.18	0.6641	0.4469	0.0482	0.2298	0.1835	0.4001	0.7016	0.4404	0.1586	-0.3951
320	3.44	27	27.00	7.50	27.00	0.9	64	322.5	351.93	0.6019	0.5208	0.1338	0.05	-0.1195	0.4835	0.7579	0.3453	0.1706	-0.1095
330	-	-	-	-	31.50	1	49	323	414.34	0.7179	0.3758	0.0937	-0.0184	0.0374	0.5144	0.6587	0.2928	0.2442	-0.2087
340	3.56	-	30.11	6.43	36.00	0.9	40	317	553.49	0.6291	0.4784	0.1539	-0.0492	0.0693	0.5461	0.7201	0.3516	0.1704	-0.2204
350	-	-	-	-	37.31	1	60	327	342.57	0.7518	0.3712	0.1205	0.2905	0.095	0.3392	0.6688	0.4064	0.271	-0.3426
360	-	-	-	-	38.63	0.77	51	299.5	479.39	0.6033	0.467	0.1181	0.0311	-0.012	0.5369	0.6119	0.3404	0.1028	-0.2187
370	-	-	-	-	39.94	1	56	303	340.1	0.7527	0.3564	0.1185	0.0868	0.0851	0.1844	0.7656	0.2447	0.2668	-0.0644
380	3.11	-	36.33	6.43	41.25	0.68	83	286.5	319.07	0.6525	0.4117	0.1794	0.1729	-0.0612	0.4214	0.7999	0.2602	0.2141	0.0005
390	-	-	-	-	42.56	0.8	96	303.5	248.4	0.6803	0.4752	0.0338	0.0836	0.0027	0.4635	0.7379	0.3086	0.2302	-0.1441
400	-	-	-	-	43.88	0.84	69	300.5	325.89	0.5725	0.6771	0.0175	0.062	-0.1227	0.3825	0.6779	0.5123	0.0922	-0.1201
410	-	-	-	-	45.19	1	103	313	191.01	0.7112	0.4095	-0.0377	0.2692	0.1324	0.3903	0.6348	0.2465	0.2399	-0.2593
420	-	-	-	-	46.50	0.9	62	304.5	343.01	0.6097	0.5882	-0.0807	0.0727	-0.0491	0.4109	0.6489	0.4855	0.1107	-0.1323
430	-	-	-	-	47.81	1.2	125	323.5	135.56	0.6216	0.5354	0.0235	0.215	-0.0127	0.4742	0.6131	0.4102	0.2196	-0.2559
440	-	-	-	-	49.13	1	73	309.5	266.5	0.5645	0.6299	-0.0196	0.0961	-0.0904	0.4558	0.6842	0.4089	0.0933	-0.1668
450	-	-	-	-	50.44	1	123	319.5	163.28	0.6117	0.5395	0.0616	0.0485	0.0719	0.4771	0.6882	0.3271	0.1327	-0.1387

Appendix 6.2. Core 787 - Age model and other data.

Core MD88-787

Core depth (cm)	δ O18 (*N. pachyderma* s. 200-250µm)	Tie points in SPECMAP age scale	Corresponding SPECMAP age scale (Ka)	Linear sedimentation rate (cm/Ka)	*Analyseries* extrapolated age scale (Ka) at 10cm interval	Core sample Dry weights (gm)	Field of views counted	Diatom subtotal 2 count (Δ)	No. diatom frustules (x106)/gm dry weight	DTF 109/24/6 Factor 1 loading	DTF 109/24/6 Factor 2 loading	DTF 109/24/6 Factor 3 loading	DTF 109/24/6 Factor 4 loading	DTF 109/24/6 Factor 5 loading	DTF 109/24/6 Factor 6 loading	DTF 166/34/4 Factor 1 loading	DTF 166/34/4 Factor 2 loading	DTF 166/34/4 Factor 3 loading	DTF 166/34/4 Factor 4 loading
460	-	-	-	-	51.75	0.87	45	311	499.32	0.6178	0.6037	-0.0818	0.2034	-0.0373	0.3833	0.807	0.3504	0.0961	-0.1339
470	-	-	-	-	53.06	1	225	326.5	91.21	0.7664	0.3384	-0.0796	0.3125	0.06	0.3125	0.704	0.2323	0.1614	-0.1176
480	3.3	-	51.89	6.43	54.38	0.82	88	285.5	248.69	0.7673	0.2749	-0.0268	0.3324	0.0676	0.3829	0.7549	0.3048	0.2361	-0.3031
490	-	-	-	-	55.69	1.2	149	319.5	112.32	0.6594	0.4424	-0.0016	0.1122	0.0436	0.5496	0.7373	0.2863	0.1582	-0.142
500	3.36	55	55.00	6.43	57.00	0.95	74	344	307.58	0.6203	0.6519	-0.054	0.0576	-0.034	0.4634	0.606	0.3731	0.1138	-0.1729
510	-	-	-	-	59.00	0.9	304	352	80.87	0.7449	0.4121	0.1138	0.1158	0.0396	0.2928	0.5461	0.2822	0.2803	-0.3503
520	3.83	-	60.00	4.00	61.00	0.99	58	304	332.79	0.7026	0.3848	0.1135	0.0114	-0.0312	0.4783	0.7028	0.3516	0.1346	-0.113
530	-	-	-	-	63.00	0.7	94	303.5	289.93	0.6372	0.3558	0.1334	0.1522	-0.0587	0.5187	0.8011	0.2165	0.1967	-0.0762
540	4.1	65	65.00	4.00	65.00	0.71	46	280	538.89	0.5766	0.5074	0.044	-0.0081	0.027	0.5256	0.7449	0.2891	0.1113	0.0069
550	-	-	-	-	67.25	0.8	75	305	319.52	0.7042	0.1552	0.1347	0.1102	0.1686	0.4893	0.7184	0.23	0.1979	-0.1904
560	-	-	-	-	69.50	0.71	62	287	409.81	0.7006	0.2487	0.1883	0.0651	0.0436	0.5215	0.8555	0.1629	0.1228	0.0581
570	-	-	-	-	71.75	0.8	175	306	137.39	0.7672	0.2046	0.1556	0.1556	0.0132	0.4044	0.7396	0.1551	0.2762	-0.0957
580	2.98	80	80.00	2.67	74.00	0.56	76	318.5	470.39	0.6754	0.1629	0.297	0.071	0.0729	0.4513	0.8268	0.0944	0.1527	0.0036
590	-	-	-	-	77.60	0.7	155	325.5	188.57	0.7006	0.2487	0.1883	0.0651	0.0436	0.5215	0.761	0.1578	0.2433	-0.1945
600	2.94	-	85.80	3.45	81.20	0.72	64	313.5	427.64	0.8242	0.2175	0.0467	0.1631	0.072	0.3791	0.6547	0.2227	0.2662	-0.2475
610	-	-	-	-	84.80	1	138	309	140.75	0.8158	0.1285	0.228	0.0486	0.1149	0.3843	0.7241	0.0876	0.3744	-0.1525
620	2.9	-	91.60	3.45	88.40	0.72	81	298	321.18	0.774	0.2534	0.0316	0.1182	0.0456	0.2302	0.819	0.1683	0.2003	0.0157
630	-	-	-	-	92.00	0.8	162	333.5	161.75	0.7898	0.2554	0.0944	0.0402	0.064	0.4099	0.7177	0.2741	0.1589	-0.1898
640	2.84	-	97.40	3.45	95.60	0.76	56	295	435.69	0.6861	0.3792	0.0511	0.0876	-0.0334	0.5362	0.8741	0.1622	0.1264	0.0495
650	-	-	-	-	99.20	0.7	106	359	304.12	0.7646	0.2826	0.2189	0.0332	0.0652	0.3413	0.8026	0.1466	0.2315	-0.0739
660	2.8	-	103.20	3.45	102.80	0.81	43	331	597.35	0.7552	0.3395	0.1336	-0.041	0.0223	0.4561	0.8012	0.1229	0.3019	-0.0384
670	-	-	-	-	106.40	0.7	134	322.5	216.11	0.8375	0.1772	0.1446	0.01	0.0612	0.371	0.7871	0.0863	0.3378	-0.0893
680	2.99	109	109.00	3.45	110.00	0.6	82	311	397.33	0.8037	0.1565	0.1122	0.2223	0.1419	0.4478	0.7894	0.1481	0.2251	-0.0621
690	-	-	-	-	116.00	0.9	81	314	270.74	0.6384	0.3112	0.1026	0.0816	-0.1273	0.4893	0.7893	0.1523	0.261	-0.0173
700	2.75	122	122.00	1.54	122.00	0.8	84	319.5	298.85	0.7125	0.2646	0.1685	0.1236	-0.0858	0.4765	0.8107	0.1298	0.291	-0.1246
710	-	-	-	-	124.17	1	105	344	205.93	0.6249	0.3464	0.1116	0.0089	-0.1064	0.5001	0.6795	0.2425	0.1965	-0.1178
720	3.3	-	126.67	4.29	126.33	1.2	107	317	155.18	0.8137	0.2825	0.133	0.0088	-0.0977	0.263	0.7668	0.2512	0.2903	-0.125
730	-	-	-	-	128.50	0.7	92	318.5	310.87	0.7721	0.3123	0.2628	-0.1243	-0.0137	0.2144	0.8272	0.1275	0.2659	0.0613
740	3.83	-	131.33	4.29	130.67	0.8	142	280	164.93	0.6607	0.4767	0.2449	0.0928	0.0811	0.1744	0.8085	0.2244	0.2145	0.0659
750	-	-	-	-	132.83	0.5	149	324.5	273.79	0.6789	0.2363	0.2407	0.1074	0.0853	0.3893	0.7903	0.2604	0.0786	0.0321
760	3.91 *	136	136.00	4.29	135.00	0.9	295	323.5	76.59	0.7127	0.4142	0.1857	0.3099	0.1211	0.2121	0.7843	0.2697	0.1204	0.0025
770	-	-	-	-	136.70	1	379	297	49.26	0.6901	0.3599	0.0554	0.1742	0.2678	0.4002	0.8093	0.3329	0.0968	-0.0198
780	3.37	-	139.00	6.67	138.40	0.8	117	321.5	215.9	0.5734	0.5154	0.0279	0.2099	0.2432	0.3337	0.8038	0.4085	0.0618	-0.0746
790	-	-	-	-	140.10	1.1	173	333.5	110.16	0.6857	0.271	-0.0305	0.4208	0.3111	0.2942	0.6487	0.2424	0.2142	-0.4934
800	-	-	-	-	141.80	1.12	95	296.5	175.16	0.6425	0.4974	-0.0933	0.2475	-0.0274	0.3046	0.744	0.4517	0.0722	-0.0686
810	-	-	-	-	143.50	1.2	101	310.5	161.03	0.581	0.4095	0.0326	0.3441	0.224	0.3524	0.6731	0.3901	0.1452	-0.3318
820	-	-	-	-	145.20	1.04	73	304.5	252.11	0.5538	0.5935	0.1012	0.2492	0.1284	0.4049	0.7513	0.4196	0.0922	-0.2071
830	-	-	-	-	146.90	1	251	301.5	75.5	0.618	0.466	0.0548	0.1179	-0.0253	0.6254	0.6864	0.3929	0.1657	-0.234
840	-	-	-	-	148.60	0.86	65	290.5	328.65	0.3779	0.5354	0.1404	0.0946	-0.0172	0.5434	0.7014	0.358	0.0105	-0.0487
850	-	-	-	-	150.30	0.9	48	333.5	485.25	0.5193	0.4685	0.1322	0.0145	0.0049	0.6109	0.7449	0.2999	0.0897	-0.0791
860	3.74	151	151.00	6.67	152.00	0.71	67	306.5	405	0.4514	0.5948	0.1283	0.0721	-0.0099	0.5142	0.7907	0.3464	-0.003	-0.0289
870	-	-	-	-	153.90	0.8	179	306	134.32	0.5605	0.2494	0.1526	0.073	0.0052	0.647	0.8241	0.1841	0.0448	-0.0439
880	3.72	-	155.00	5.00	155.80	0.85	77	324	311.16	0.5497	0.4566	0.0739	0.1289	0.0111	0.6029	0.7194	0.1808	0.1425	-0.1351
890	-	-	-	-	157.70	1	113	359	199.7	0.5412	0.3231	0.0858	0.3639	-0.0529	0.4932	0.7245	0.1984	0.1258	-0.2182
900	-	-	-	-	159.60	0.84	59	303.5	384.93	0.5219	0.4065	0.1151	-0.0158	0.0826	0.6445	0.6808	0.3132	0.0829	-0.2065
910	-	-	-	-	161.50	0.9	82	329	280.22	0.5287	0.358	0.1074	0.1518	0.037	0.6407	0.6036	0.1877	0.2046	-0.3467
920	3.47	-	163.00	5.00	163.40	0.79	53	309	463.88	0.47	0.4205	0.1272	0.1004	0.0079	0.6495	0.693	0.2658	0.0417	-0.1616
930	-	-	-	-	165.30	0.8	96	322.5	263.95	0.5637	0.2687	0.1977	0.1619	-0.0887	0.5807	0.8115	0.2079	0.0702	-0.0059

Core MD88 -787																				
Core depth (cm)	δ O18 (*N. pachyderma* s. 200-250µm)	Tie points in SPECMAP age scale	Corresponding SPECMAP age scale (Ka)	Linear sedimentation rate (cm/Ka)	*Analyseries* extrapolated age scale (Ka) at 10cm interval	Core sample Dry weights (gm)	Field of views counted	Diatom subtotal 2 count (Δ)	No. diatom frustules (x106)/gm dry weight	DTF 109/24/6 Factor 1 loading	DTF 109/24/6 Factor 2 loading	DTF 109/24/6 Factor 3 loading	DTF 109/24/6 Factor 4 loading	DTF 109/24/6 Factor 5 loading	DTF 109/24/6 Factor 6 loading	DTF 166/34/4 Factor 1 loading	DTF 166/34/4 Factor 2 loading	DTF 166/34/4 Factor 3 loading	DTF 166/34/4 Factor 4 loading
940	-	-	-	-	167.20	0.88	51	304.5	426.47	0.3555	0.3239	0.3394	0.18	-0.0274	0.6159	0.7298	0.1092	0.097	0.0162
950	-	-	-	-	169.10	1	113	339	188.57	0.6699	0.3538	0.0962	0.3671	0.1948	0.3405	0.7953	0.2208	0.2378	-0.3195
960	3.26	171	171.00	5.00	171.00	0.74	105	297	240.26	0.5366	0.4876	0.1076	0.0495	-0.0334	0.5686	0.7754	0.3146	0.0348	-0.1318
970	-	-	-	-	176.50	0.9	158	321.5	142.11	0.5592	0.441	-0.0265	0.3208	0.0962	0.4103	0.637	0.3708	0.0781	-0.3956
980	3.52	182	182.00	1.82	182.00	1	60	325	340.48	0.5026	0.4698	0.0436	0.0963	-0.1259	0.5759	0.6204	0.3919	0.0522	-0.244
990	-	-	-	-	184.00	0.8	114	335.5	231.23	0.5533	0.4071	0.204	0.1376	-0.0017	0.5972	0.7792	0.2394	0.0626	-0.1836
1000	3.34	-	186.40	4.55	186.00	0.93	83	317	258.14	0.5981	0.4308	0.0798	0.1724	-0.1117	0.5205	0.8213	0.3125	0.0597	-0.0762
1010	-	-	-	-	188.00	0.9	169	330	136.38	0.652	0.3551	0.2746	0.1372	0.0266	0.444	0.8226	0.1439	0.2263	-0.0708
1020	2.95	-	190.80	4.55	190.00	0.82	63	290	352.86	0.4672	0.2541	0.2195	0.0778	-0.0577	0.6717	0.7699	0.1407	0.056	0.0105
1030	2.66	193	193.00	4.55	192.00	0.9	94	260	193.18	0.6302	0.3169	0.1537	0.0306	-0.0975	0.4749	0.8125	0.1807	0.0875	0.0144

Abbreviations and notes:

- = no data, * = questioned results

δO^{18} data from Dr. L. Labeyrie (GIF, France)

SPECMAP data and *Analyseries 1.1* program from GIF, France (Imbrie *et al* . 1984; Paillard *et al* . 1996, Paillard 1997).

LinAge program of *Analyseries* used in deriving age model.

¥ = counts made at x40 magnification thus number of diatom frustules /gm dry weight accordingly adjusted. Data not used in analysis.

Δ = diatom count total, refer to this cores raw count appendix 7.6 which defines diatom subtotal 2.

Core MD88-784																				
Core depth (cm	δO18 (*N. pachyderma s.* 200-250µm)	Tie points in SPECMAP age scale	Corresponding SPECMAP age scale (Ka)	Linear sedimentation rate (cm/Ka)	*Analyseries* extrapolated age scale (Ka) at 10cm interval	Core sample dry weights (gm)	Field of views counted	Diatom subtotal 2 count (Δ)	no. diatom frustules(x10⁶) gm dry weight	DTF 109/24/6 Factor 1 loading	DTF 109/24/6 Factor 2 loading	DTF 109/24/6 Factor 3 loading	DTF 109/24/6 Factor 4 loading	DTF 109/24/6 Factor 5 loading	DTF 109/24/6 Factor 6 loading	DTF 166/34/4 Factor 1 loading	DTF 166/34/4 Factor 2 loading	DTF 166/34/4 Factor 3 loading	DTF 166/34/4 Factor 4 loading
0	2.84	3	3	20.00	3.13	0.72	95	297.5	41.01	0.9374	0.157	0.1612	0.0006	-0.0214	0.0994	0.6794	0.0869	0.5203	-0.2044
10	-	-	-	-	3.50	0.69	101	338.5	45.8	0.8522	0.2372	0.1792	-0.098	0.0068	0.2002	0.7045	0.1985	0.3796	-0.0984
20	2.8	-	4	20.00	4.00	0.72	100	323.5	42.36	0.9575	0.1559	0.0806	-0.0169	-0.0038	0.0072	0.6233	0.1106	0.5365	-0.241
30	-	5	-	-	4.50	0.78	77	313	49.14	0.8321	0.1471	0.3249	-0.1478	-0.0559	0.1182	0.7416	0.0503	0.4719	-0.1454
40	2.7	-	5	20.00	5.05	0.77	59	287	59.56	0.9147	0.1653	0.2259	-0.119	-0.01	0.1345	0.8129	0.0798	0.3559	0.0134
50	-	-	-	-	5.88	0.8	72	313.5	51.32	0.9081	0.1625	0.1315	-0.1318	0.0242	0.0735	0.7532	0.0928	0.4234	-0.1234
60	2.88	-	6.75	11.43	6.75	0.81	72	289	46.72	0.8984	0.1544	0.1321	-0.0238	0.1124	0.1833	0.8354	0.1518	0.1535	-0.003
70	-	-	-	-	7.63	0.91	72	306	44.03	0.843	0.2347	0.1023	0.0843	-0.0369	0.3633	0.667	0.1951	0.261	-0.2085
80	3.13	-	8.5	11.43	8.50	0.82	85	300	40.58	0.7383	0.2625	0.215	-0.0121	0.083	0.4925	0.8143	0.0624	0.2233	-0.0737
90	-	-	-	-	9.38	0.76	74	302.5	50.71	0.8111	0.3345	0.1759	-0.1021	-0.01	0.3483	0.8115	0.205	0.2251	-0.0845
100	3.02	-	10.25	11.43	10.25	0.55	100	273.5	46.89	0.8378	0.179	0.2892	0.0296	0.085	0.0944	0.7614	0.0864	0.3188	0.0658
110	-	-	-	-	11.13	0.58	78	329	68.57	0.921	0.1881	0.3161	-0.1437	-0.067	0.1062	0.8129	0.118	0.2786	0.095
120	3.15	-	12	11.43	12.00	0.63	100	262.5	42.28	0.8565	0.3288	0.0933	-0.1189	0.0069	0.2454	0.8571	0.1262	0.2613	0.0755
130	-	-	-	-	12.88	0.64	204	318.5	23	0.8589	0.2393	0.2309	-0.0166	-0.0002	0.2194	0.8235	0.0644	0.3404	0.0527
140	3.52	-	13.75	11.43	13.75	0.8	84	298	41.81	0.7979	0.2582	0.2588	-0.0786	0.0467	0.3746	0.793	0.1168	0.3763	-0.1006
150	-	-	-	-	14.63	0.9	135	295.5	22.93	0.915	0.2132	0.1222	0.0706	-0.0022	0.2018	0.8426	0.0992	0.3242	0.0328
160	3.97	-	15.5	11.43	15.50	0.73	102	289.5	36.66	0.9199	0.1941	0.0058	0.142	-0.0385	0.1739	0.7748	0.1431	0.3898	-0.0894
170	-	-	-	-	16.38	0.7	121	286.5	31.89	0.764	0.2976	0.1454	0.1152	0.0539	0.4316	0.7982	0.1586	0.2966	-0.0854
180	4.13	-	17.25	11.43	17.25	0.76	210	273.5	16.16	0.7742	0.3577	0.2153	0.2188	0.0815	0.1997	0.8133	0.1206	0.3179	-0.0737
190	-	-	-	-	18.13	1.05	348	284	7.33	0.7683	0.3242	-0.0401	0.2791	0.1268	0.2128	0.7911	0.1811	0.3282	-0.1201
200	4.44	19	19	11.43	19.00	1.15	169	266	13.87	0.8222	0.475	0.0512	0.0832	-0.0508	0.3091	0.5498	0.4733	0.1465	-0.1974
210	-	-	-	-	19.90	1.02	89	293.5	30.48	0.7257	0.4255	-0.0378	0.3039	0.0561	0.2557	0.8743	0.4386	0.1925	-0.2284
220	3.96	-	20.8	11.11	20.80	0.9	126	279	23.2	0.6606	0.5457	0.004	0.1581	0.0874	0.3224	0.7219	0.4446	0.1	-0.1694
230	-	-	-	-	21.70	0.89	100	268.5	30.56	0.6352	0.4435	0.1685	0.0948	0.0166	0.4552	0.7627	0.3308	0.2278	-0.2328
240	3.86	-	22.6	11.11	22.60	0.89	82	295.5	38.18	0.6894	0.3175	0.0477	0.269	-0.0404	0.371	0.7955	0.1837	0.2735	-0.218
250	-	-	-	-	23.50	0.89	101	269	28.22	0.724	0.3408	0.0632	0.278	0.0206	0.3271	0.7744	0.3184	0.1738	-0.1274
260	4.05	-	24.4	11.11	24.40	1.3	118	292.5	17.98	0.6956	0.5106	0.1033	0.332	0.1621	0.2238	0.7179	0.3832	0.2894	-0.2648
270	-	-	-	-	25.30	1.03	94	310.5	30.24	0.8073	0.3567	-0.0013	0.1755	0.0027	0.2184	0.7255	0.3861	0.1978	-0.2825
280	3.83	-	26.2	11.11	26.20	1.01	101	302	27.91	0.6487	0.5091	-0.084	0.171	-0.0739	0.3971	0.6822	0.4171	0.1278	-0.2956
290	-	-	-	-	27.10	0.98	68	313.5	45.28	0.6346	0.4631	0.0237	0.0535	-0.1654	0.4289	0.6974	0.3674	0.1892	-0.0849
300	3.53	28	28	11.11	28.01	0.9	60	314.5	54.91	0.65	0.5265	0.0327	0.1136	-0.1271	0.4385	0.6892	0.3887	0.1057	-0.1607
310	-	-	-	-	29.00	0.81	66	317	55.91	0.6057	0.3568	0.1134	0.2329	0.1186	0.2669	0.6699	0.3444	0.2372	-0.2768
320	3.52	-	30	10.00	30.00	0.71	64	314	65.15	0.8371	0.2211	0.1405	0.1353	0.1401	0.3603	0.6565	0.1852	0.3957	-0.4384
330	-	-	-	-	31.00	0.75	106	318	37.71	0.822	0.1907	0.0919	0.2171	0.1067	0.2608	0.7232	0.259	0.3092	-0.1575
340	-	-	-	-	32.00	0.75	57	292.5	64.51	0.8464	0.3763	0.0826	-0.0324	-0.0673	0.5575	0.7476	0.2612	0.0915	-0.0138
350	-	-	-	-	33.00	0.7	54	338	83.81	0.7842	0.3313	0.0531	0.0852	0.0719	0.3387	0.804	0.2188	0.2489	-0.1294
360	3.51	-	34	10.00	34.00	0.48	43	313	142.98	0.6899	0.405	0.081	-0.062	0.0888	0.5295	0.7569	0.308	0.2298	-0.3092
370	-	-	-	-	35.00	0.42	51	322	141.74	0.8855	0.2047	0.1955	0.0963	-0.0102	0.2122	0.8114	0.1891	0.3641	-0.1327
380	3.65 *	36	36	10.00	36.16	0.9	62	293.5	49.59	0.7888	0.2942	0.0816	0.0728	0.0412	0.4728	0.8756	0.1993	0.1926	-0.0326
390	-	-	-	-	38.25	0.97	72	314	42.39	0.6432	0.4365	0.0642	0.2275	-0.0705	0.3722	0.6944	0.4034	0.1899	-0.1368
400	-	-	-	-	40.50	1.07	47	309.5	58.03	0.6883	0.4346	0.017	0.198	-0.0074	0.3301	0.6495	0.2796	0.1812	-0.2278
410	-	-	-	-	42.75	1.1	48	344	61.43	0.6791	0.4798	0.0731	0.203	-0.0729	0.2978	0.6102	0.3476	0.2555	-0.2401
420	3.61 ¥	-	45	4.44	45.00	1.08	44	319.5	63.39	0.7226	0.5205	-0.0233	0.0329	-0.0145	0.3075	0.5277	0.4871	0.171	-0.3028
430	-	-	-	-	47.25	0.96	45	320.5	69.95	0.7288	0.5151	-0.033	0.0508	-0.0099	0.3172	0.5532	0.423	0.2792	-0.3714
440	3.45	-	49.5	4.44	49.50	0.99	38	319.5	80.08	0.7783	0.3713	0.0053	0.0739	0.1423	0.408	0.6289	0.3849	0.1523	-0.2902
450	-	-	-	-	51.75	0.81	46	289.5	73.26	0.7692	0.2736	0.0497	0.1247	0.0074	0.3765	0.7093	0.247	0.2707	-0.164
460	3.37	54	54	4.44	54.03	0.9	37	299	84.66	0.8095	0.3029	-0.0924	0.1864	0.0575	0.3662	0.7459	0.2638	0.2276	-0.1658
470	-	-	-	-	56.50	0.91	44	326	76.77	0.7231	0.4642	0.051	0.0714	-0.0075	0.4442	0.6539	0.2211	0.1897	-0.1712
480	3.48	59	59	4.00	58.38	0.91	37	310	86.81	0.6253	0.5046	-0.0142	0.0652	0.0794	0.5426	0.7184	0.3813	0.1464	-0.2068
490	-	-	-	-	61.50	1	41	296.5	68.18	0.7532	0.3418	-0.0916	0.1072	0.0696	0.4162	0.6523	0.3217	0.1895	-0.2667

Abbreviations and notes:

- = No data, * = requires checking, ¥ = 150-200µm sample

δO^{18} data from Dr L. Labeyrie (GIF, France)

SPECMAP data and *Analyseries 1.1* program from GIF, France (Imbrie *et al.* 1984, Paillard *et al.* 1996, Paillard 1997), *LinAge* program of *Analyseries* used in deriving age model.

Δ = total number of diatoms counted, refer to raw data appendix 7.7 of this core for definition of diatom subtotal 2.

Appendix 6.4. Core MD88-779 - Age model and other data.

Core MD88-779										
Oxygen Isotope core depth (cm)	δO^{18} (Benthic 200-250µm)	Tie points in SPECMAP age scale	Corresponding SPECMAP age scale (Ka)	Linear sedimentation rate (cm/Ka)	Diatom core depth (cm)	*Analyseries* extrapolated age scale (Ka) at 10 cm intervals	Core sample dry weights (gm)	Field of views counted	Diatom subtotal 2 count (Δ)	No. diatom frustules (x10⁶)/gm dry weight
0.5	3.31	0.21	0.21	1.18	0	-0.21	0.3	994	37	3.90
5.5	3.52	-	4.43	1.18	10	8.60	2.63	810	156	2.30
9.5	3.58	7.81	7.81	1.18	20	20.34	2.82	858	6	0.08
15.5	4.5	17.31	17.31	0.63	30	27.06	2.61	781	9	0.14
25.5	4.3	-	24.04	1.49	40	33.79	2.76	786	52	0.75
35.5	4.24	-	30.76	1.49	50	40.52	2.59	780	11	0.17
45.5	4.13	-	37.49	1.49	60	47.24	2.69	601	7	0.14
55.5	4.09	-	44.22	1.49	70	53.97	2.89	772	133	1.87
65.5	3.95	-	50.94	1.49	80	60.69	2.71	649	47	0.84
75.5	3.89	-	57.67	1.49	90	67.42	2.77	639	150	2.66
85.5	3.82	-	64.39	1.49	100	75.39	2.89	753	15	0.22
95.5	3.82	71.12	71.12	1.49	110	84.88	2.79	755	213	3.18
105.5	3.74	-	80.61	1.05	120	94.03	3	662	216	3.42
115.5	3.87	90.1	90.10	1.05	130	102.75	2.99	727	45	0.65
125.5	3.74	-	98.83	1.15	140	111.48	2.71	784	23	0.34
135.5	3.56	-	107.55	1.15	150	120.20	3.07	690	205	3.04
145.5	3.5	-	116.28	1.15	160	127.72	2.99	679	58	0.90
155.5	3.44	125	125.00	1.15	170	133.77	2.92	668	0	0.00
162.5	3.83	-	129.23	1.65	180	139.82	2.89	763	1	0.01
167.5	4.8	-	132.26	1.65	190	147.25	2.92	697	3	0.05
172.5	4.51	-	135.28	1.65	200	155.13	2.59	794	0	0.00
177.5	4.42	-	138.31	1.65	210	162.20	2.56	716	0	0.00
182.5	3.96	141.33	141.33	1.65	220	168.99	2.54	831	17	0.25
187.5	4.19	-	145.27	1.27	230	176.12	2.71	760	123	1.88
192.5	4.08	-	149.22	1.27	240	183.41	2.9	844	174	2.23
197.5	4.09	-	153.16	1.27	250	191.44	2.64	881	114	1.54
202.5	4.36	157.1	157.10	1.27	260	203.61	2.84	767	25	0.36
207.5	3.57	-	160.50	1.47						
212.5	3.78	-	163.90	1.47						
217.5	3.56	-	167.29	1.47						
223.5	3.01	171.37	171.37	1.47						
227.5	4.55	-	174.29	1.37						
232.5	3.58	-	177.94	1.37						
243.5	3.6	-	185.96	1.37						
248.5	3.71	189.61	189.61	1.37						
253.5	3.99	-	195.70	0.82						
257.5	4.05	200.57	200.57	0.82						

Abbreviations and notes:

- = No data

δO^{18} data from Dr P. De Deckker (ANU, Australia) and age model from author and Dr S. Nees (GEOMAR, Germany)

SPECMAP data and *Analyseries 1.1* program from GIF, France (Martinson *et al.* 1984, Paillard *et al.* 1996, Paillard 1997).

LinAge program of Analyseries used in deriving age model.

Δ = diatom count total, refer to this cores raw count appendix 6.5 for definition of diatom subtotal 2.

Appendix 6.5. Core MD88-779 - raw data.

Core MD88-779 Depth (cm)	*Actinocyclus curvatulus*	*Asteromphalus hookeri*	*Azpeitia tabularis*	*Chaetoceros* resting spores *	*Coscinodiscus radiatus*	*Coscinodiscus* spp.	*Cyclotella* cf *meneghiniana*	*Delphineis surirella*	*Diploneis bombus/weissflogii*	*Eucampia antarctica*	*Fragilariopsis doliolus*	*Fragilariopsis kerguelensis*	*Fragilariopsis separanda*	*Fragilariopsis* spp.	*Hemidiscus cuneiformis*	*Hemidiscus karstenii*	*Nitzschia kolaczekii*	*Nitzschia* spp.	*Paralia* spp.	*Pseudonitzschia* spp.	*Rhaphoneis* cf *amphiceros*	*Rhizosolenia otaria* absent	*Rhizosolenia* spp.	*Roperia tesselata*	*Rouxia* cf *naviculoides*	*Thalassionema nitzschioides*	*T. nitzschioides* var. *lanceolata*	*T. nitzschioides* var. *parva*	*Thalassiosira gracilis*	*Thalassiosira lentiginosa*	*Thalassiosira lineata*	*Thalassiosira oestrupii*	*Thalassiosira trifulta*	*Thalassiosira* spp.	*Thalassiothrix/Trichotoxon* spp. *	*Trachyneis aspera*	Diatom Subtotal 1	Diatom Subtotal 2	*Dictyocha* spp.¥	*Distephanus* spp.¥	Silica Subtotal 3
0	2		4	1								12			1								2	2					1	9	1				2		37	37		1	38
10	3	1	27	13							3	67			4						1			6		2	1	2		10		6	2	6	2		156	156	5	1	162
20												5			0														1							6	6			6
30			1							1		1														1			2					3		9	9			9
40	1		7	7								12	1						1							14			7					2		52	52		1	53
50			3									1														3			2					2		11	11			11
60												1							1										1					4		7	7			7
70	3		15	37		1		1	1	1	5	29			4				2				1			4			15	1	4	2		7		133	133		2	135
80			11			1			1			5			6											4			13		1	2		3		47	47	1		48
90	1		20	10							3	72			13			1							1	11			7		3	5		3		150	150	4	1	155
100	1		4									6																	2					2		15	15			15
110		2	44	3		4						90			2		1	1				2		1		9			20	1	14	8	1	10		213	213		5	218
120	2		53	14		2					1	92			3	1	1		1			2				12			10		11	6	1	3	1	216	216	2	5	223
130			11	4								12			1							1		1		2			5		2	3	1	2		45	45		2	47
140			8									3				1								1					4	1	1	1	1	2		23	23			23
150			78	1						2		56			3					1						10			25	2	8	4	6	5		205	205		1	206
160	1		21									24			2											2			7			1				58	58			58
170																																				0	0			0
180																													1							1	1			1
190							3																													3	3			3
200																																				0	0			0
210																																				0	0			0
220										3		5																	5		2	2				17	17		2	19
230	3	1	31	1	12					4		26				10						1			1	5		1	8	1	2	6	1	9		123	123	1	3	127
240			46		14						4	44		1		44										4			3		5	1	4	2	2		174	174	1	1	176
250	1		10		5						1	19				72										2			2					2		114	114		1	115
260			2		3					1		4				15																				25	25		1	26

Abbreviations and Notes

¥ = denotes silicoflagellates.

Diatom subtotal 1 = includes all diatoms observed (* = species not normally included, but due to low diatom occurrences included here)

Diatom subtotal 2 = includes all diatoms observed

Silica subtotal 3 = all diatoms plus silicoflagellates

MD88-787

| Depth (cm) | *Actinocyclus actinochilus* | *Actinocyclus curvatulus* | *Actinocyclus octonarius* | *Actinocyclus ingens* | *Actinocyclus* spp. | *Asteromphalus hookeri* | *Asteromphalus hyalinus* | *Asteromphalus parvulus* | *Asteromphalus* spp. | *Azpeitia tabularis* | *Corethron criophilum* | *Coscinodiscus asteromphalus* | *Coscinodiscus marginatus* | *Coscinodiscus* spp. | *Eucampia antarctica* | *Fragilariopsis curta* | *Fragilariopsis cylindrus* | *Fragilariopsis kerguelensis* | *Fragilariopsis obliquecostata* | *Fragilariopsis pseudonana* | *Fragilariopsis rhombica* | *Fragilariopsis ritscheri* | *Fragilariopsis separanda* | *Fragilariopsis subilinearis* | *Gyrosigma* spp. | *Hemidiscus karstenii* | *Navicula directa* | *Nitzschia barbieri* | *Nitzschia braaunii* | *Nitzschia denticuloides* | *Nitzschia* cf. *granulata* | *Nitzschia peragallii* | *Nitzschia sicula* | *Nitzschia* spp. | *Odontella weissflogii* | *Pleurosigma* spp. | *Pleurosigma/Gyrosigma* spp. | *Porosira glacialis* | *Porosira pseudodenticulata* | *Proboscia* cf. *alata* | *Pseudonitzschia heimii* | *Pseudonitzschia lineola* | *Pseudo-nitzschia turgiduloides* | *Pseudonitzschia* spp. | *R. ant.* forma *antennata* | *Rhizosolenia* otarta absent | *Rhizosolenia* otarta present | *Rhizosolenia* spp. | *Rocella* spp. | *Rouxia* spp. | *Stephanopyxis* spp. | *Thalassionema nitzschioides* | *Thalassiosira antarctica* | *Thalassiosira gracilis* | *Thalassiosira lentiginosa* | *Thalassiosira leptopus* | *Thalassiosira lineata* | *Thalassiosira oestrupii* | *Thalassiosira oliverana* | *Thalassiosira porosertata* | *Thalassiosira ritscheri* | *Thalassiosira trifulta* | *Thalassiosira tumida* | *Thalassiosira* spp. | sp. indet. |
|---|---|---

Appendix 6.6. Core MD88-787 - raw data.

| MD88-787 Depth (cm) | *Actinocyclus actinochilus* | *Actinocyclus curvatulus* | *Actinocyclus octonarius* | *Actinocyclus ingens* | *Actinocyclus* spp. | *Asteromphalus hookeri* | *Asteromphalus hyalinus* | *Asteromphalus parvulus* | *Asteromphalus* spp. | *Azpeitia tabularis* | *Corethron criophilum* | *Coscinodiscus asteromphalus* | *Coscinodiscus marginatus* | *Coscinodiscus* spp. | *Eucampia antarctica* | *Fragilariopsis curta* | *Fragilariopsis cylindrus* | *Fragilariopsis kerguelensis* | *Fragilariopsis obliquecostata* | *Fragilariopsis pseudonana* | *Fragilariopsis rhombica* | *Fragilariopsis ritscheri* | *Fragilariopsis separanda* | *Fragilariopsis sublinearis* | *Gyrosigma* spp. | *Hemidiscus karstenii* | *Navicula directa* | *Nitzschia barberi* | *Nitzschia braarudii* | *Nitzschia denticuloides* | *Nitzschia* cf. *granulata* | *Nitzschia peragallii* | *Nitzschia sicula* | *Nitzschia* spp. | *Odontella weissflogii* | *Pleurosigma* spp. | *Pleurosigma/Gyrosigma* spp. | *Porosira glacialis* | *Porosira pseudodenticulata* | *Proboscia* cf. *alata* | *Pseudonitzschia heimii* | *Pseudonitzschia lineola* | *Pseudo-nitzschia turgiduloides* | *Pseudonitzschia* spp. | *R. ant.* forma *antennata* | *Rhizosolenia* otaria absent | *Rhizosolenia* otaria present | *Rhizosolenia* spp. | *Rocella* spp. | *Rouxia* spp. | *Stephanopyxis* spp. | *Thalassionema nitzschioides* | *Thalassiosira antarctica* | *Thalassiosira gracilis* | *Thalassiosira lentiginosa* | *Thalassiosira leptopus* | *Thalassiosira lineata* | *Thalassiosira oestrupii* | *Thalassiosira oliverana* | *Thalassiosira poroseriata* | *Thalassiosira ritscheri* | *Thalassiosira trifulta* | *Thalassiosira tumida* | *Thalassiosira* spp. | sp. indet. |
|---|---|---

| MD88-787 Depth (cm) | *Actinocyclus actinochilus* | *Actinocyclus curvatulus* | *Actinocyclus octonarius* | *Actinocyclus ingens* | *Actinocyclus* spp. | *Asteromphalus hookeri* | *Asteromphalus hyalinus* | *Asteromphalus parvulus* | *Asteromphalus* spp. | *Azpeitia tabularis* | *Corethron criophilum* | *Coscinodiscus asteromphalus* | *Coscinodiscus marginatus* | *Coscinodiscus* spp. | *Eucampia antarctica* | *Fragilariopsis curta* | *Fragilariopsis cylindrus* | *Fragilariopsis kerguelensis* | *Fragilariopsis obliquecostata* | *Fragilariopsis pseudonana* | *Fragilariopsis rhombica* | *Fragilariopsis ritscheri* | *Fragilariopsis separanda* | *Fragilariopsis sublinearis* | *Gyrosigma* spp. | *Hemidiscus karstenii* | *Navicula directa* | *Nitzschia barberi* | *Nitzschia braarudii* | *Nitzschia denticuloides* | *Nitzschia* cf. *granulata* | *Nitzschia peragallii* | *Nitzschia sicula* | *Nitzschia* spp. | *Odontella weissflogii* | *Pleurosigma* spp. | *Pleurosigma/Gyrosigma* spp. | *Porosira glacialis* | *Porosira pseudodenticulata* | *Proboscia* cf. *alata* | *Pseudonitzschia heimii* | *Pseudonitzschia lineola* | *Pseudo-nitzschia turgiduloides* | *Pseudonitzschia* spp. | *R. ant.* forma *antennata* | *Rhizosolenia* otaria absent | *Rhizosolenia* otaria present | *Rhizosolenia* spp. | *Rocella* spp. | *Rouxia* spp. | *Stephanopyxis* spp. | *Thalassionema nitzschioides* | *Thalassiosira antarctica* | *Thalassiosira gracilis* | *Thalassiosira lentiginosa* | *Thalassiosira leptopus* | *Thalassiosira lineata* | *Thalassiosira oestrupii* | *Thalassiosira oliverana* | *Thalassiosira porosentata* | *Thalassiosira ritscheri* | *Thalassiosira trifulta* | *Thalassiosira tumida* | *Thalassiosira* spp. | sp. Indet. |
|---|---|---

Appendix 6.6. Core MD88-787 - raw data.

MD88-7									
Depth (cm)	Diatom Subtotal 1	*Thalassiothrix/Trichotoxon* spp. *	*Chaetoceros* spp. (vegetative)	Diatom Subtotal 2	*Distephanus* spp. *	Silica Subtotal 3	*Dactyliosolen antarcticus*	*Chaetoceros* spp. spores	Silica Subtotal 4
0	302	4.5		306.5	7	313.5	21		334.5
10	330	6		336	10	346	33	1	380
20	315	6.5		321.5	8	329.5	39	1	369.5
30	336	6.5		342.5	7	349.5	10		359.5
40	308	5.5		313.5	6	319.5	59		378.5
50	319	8.5		327.5	9	336.5	46		382.5
60	315	6.5		321.5	7	328.5	65		393.5
70	304	7		311	8	319	40	2	361
80	305	9		314	7	321	51	2	374
90	306	4		310	7	317	18	1	336
100	292	6.5		298.5	16	314.5	18		332.5
110	332	13.5		347.5	15	362.5	11	2	375.5
120	307	9		316	13	329	27		356
130	310	11		321	10	331	10	1	342
140	292	9		301	5	306	13	5	324
150	303	12	1	316	14	330	7	5	342
160	338	8.5		346.5	18	364.5	12	4	380.5
170	298	4		302	15	317	8	2	327
180	303	9.5	1	313.5	15	328.5	5	5	338.5
190	298	11		309	9	318	7	13	338
200	306		2	308	12	320	14	9	343
210	274	15.5		289.5	25	314.5	24	24	362.5
220	322		2	324	29	353	33	51	437
230	286	2.5		288.5	16	304.5	25	9	338.5
240	298	3	3	304	4	308	20	11	339
250	294	2	3	299	5	304	14	3	321
260	344			344	9	353	13	7	373
270	313	4.5	1	319.5	5	324.5	18	4	346.5
280	312			312	15	327	20	21	368
290	305	7	2	314	6	320	23	6	349
300	306	5		311	13	324	16	14	354
310	319	4	3	327	3	330	11	1	342
320	316	6.5		322.5	13	335.5	17	11	363.5
330	321	2		323	11	334	39		373
340	312	5		317	12	329	21	7	357
350	323	4		327	6	333	21	1	355
360	297	2.5		299.5	10	309.5	21	4	334.5
370	294	9		303	11	314	21	3	338

Appendix 6.6. Core MD88-787 - raw data.

MD88-7									
Depth (cm)	Diatom Subtotal 1	*Thalassiothrix/Trichotoxon* spp. *	*Chaetoceros* spp. (vegetative)	Diatom Subtotal 2	*Distephanus* spp. *	Silica Subtotal 3	*Dactyliosolen antarcticus*	*Chaetoceros* spp. spores	Silica Subtotal 4
380	273	10.5		286.5	11	297.5	34	1	332.5
390	299	3.5		303.5	9	312.5	15	1	328.5
400	293	6.5		300.5	10	310.5	10	3	323.5
410	311	1		313	17	330	17		347
420	300	4.5		304.5	12	316.5	7	2	325.5
430	319	2.5	1	323.5	7	330.5	15	1	346.5
440	306	3.5		309.5	12	321.5	11	6	338.5
450	313	4.5	2	319.5	11	330.5	16	1	347.5
460	301	9		311	11	322	11	4	337
470	319	6.5		326.5	13	339.5	8	4	351.5
480	279	5.5	1	285.5	14	299.5	12	3	314.5
490	312	5.5	2	319.5	16	335.5	13	1	349.5
500	337	6	1	344	14	358	6	2	366
510	347	4	1	352	2	354	13	4	371
520	299	5		304	9	313	15	2	330
530	296	6.5	1	303.5	16	319.5	21	3	343.5
540	272	8		280	24	304	12	1	317
550	301	4		305	15	320	19		339
560	273	13		287	8	295	19	2	316
570	303	3		306	19	325	16		341
580	304	14.5		318.5	9	327.5	2		329.5
590	320	5.5		325.5	7	332.5	17		349.5
600	311	2.5		313.5	7	320.5	14	1	335.5
610	303	5	1	309	10	319	8		327
620	288	9	1	298	10	308	14		322
630	329	4.5		333.5	4	337.5	2		339.5
640	278	16	1	295	7	302	4	1	307
650	351	8		359	13	372	5	2	379
660	324	7		331	11	342	2		344
670	315	7.5		322.5	11	333.5			333.5
680	304	7		311	17	328	3		331
690	306	8		314	9	323		1	324
700	312	6.5	1	319.5	11	330.5	4		334.5
710	338	6		344	5	349	2	4	355
720	309	6	2	317	9	326	4	2	332
730	304	14.5		318.5	9	327.5	1	8	336.5
740	246	28	6	280	33	313	4	17	334
750	290	28.5	6	324.5	22	346.5	8	16	370.5

Appendix 6.6. Core MD88-787 - raw data.

MD88-7									
Depth (cm)	Diatom Subtotal 1	*Thalassiothrix/Trichotoxon* spp. *	*Chaetoceros* spp. (vegetative)	Diatom Subtotal 2	*Distephanus* spp. *	Silica Subtotal 3	*Dactyliosolen antarcticus*	*Chaetoceros* spp. spores	Silica Subtotal 4
760	280	41.5	2	323.5	13	336.5	12	23	371.5
770	279	18		297	23	320	11	8	339
780	311	10.5		321.5	12	333.5	22	11	366.5
790	328	5.5		333.5	1	334.5	4		338.5
800	282	12.5	2	296.5	7	303.5	11	3	317.5
810	305	5.5		310.5	9	319.5	7		326.5
820	298	6.5		304.5	10	314.5	9	1	324.5
830	296	5.5		301.5	15	316.5	9	3	328.5
840	277	12.5	1	290.5	22	312.5	6	10	328.5
850	326	7.5		333.5	16	349.5	20	1	370.5
860	294	12.5		306.5	10	316.5	3		319.5
870	291	13		306	5	311	1		312
880	318	6		324	15	339	2	1	342
890	350	8	1	359	11	370	3	1	374
900	299	4.5		303.5	11	314.5	1	2	317.5
910	326	3		329	12	341	1	1	343
920	300	9		309	11	320	3		323
930	310	12.5		322.5	7	329.5	6	1	336.5
940	288	16.5		304.5	7	311.5	4	4	319.5
950	329	10		339	8	347	8	7	362
960	282	15		297	4	301	6	8	315
970	317	4.5		321.5	1	322.5	8	7	337.5
980	321	3	1	325	2	327	5	5	337
990	323	12.5		335.5	2	337.5	2	3	342.5
1000	306	11		317	4	321	1	2	324
1010	311	19		330	6	336	1	1	338
1020	269	21		290	3	293			293
1030	241	18	1	260	7	267	1	9	277

Appendix 6.10. *Core MD88-787 - August SST estimates using DTF109/24/6.*

Analyseries extrapolated age scale (Ka) at 10cm interval	Depth (cm)	DTF 109/24/6 Communality	DTF 109/24/6 SSTAug. (°C)
71.75	570	0.843	0.396
74.00	580	0.785	1.965
77.60	590	0.866	0.694
81.20	600	NA	-0.906
84.80	610	0.897	0.746
88.40	620	0.733	-0.497
92.00	630	0.872	-0.861
95.60	640	0.914	-0.738
99.20	650	0.834	1.087
102.80	660	0.914	-0.275
106.40	670	0.895	-0.358
110.00	680	0.953	-0.417
116.00	690	NA	0.051
122.00	700	0.856	1.157
124.17	710	0.784	-0.050
126.33	720	0.838	0.069
128.50	730	0.824	2.422
130.67	740	0.769	1.951
132.83	750	0.745	1.264
135.00	760	0.870	0.584
136.70	770	0.871	-1.552
138.40	780	0.810	-1.916
140.10	790	0.905	-0.675
141.80	800	0.824	-0.863
143.50	810	0.799	-1.380
145.20	820	0.912	-1.220
146.90	830	0.893	-0.299
148.60	840	NA	1.673
150.30	850	0.880	1.241
152.00	860	0.844	1.412
153.90	870	0.824	0.539
155.80	880	0.896	0.273
157.70	890	NA	1.716
159.60	900	0.873	0.460
161.50	910	NA	0.613
163.40	920	NA	1.346
165.30	930	NA	2.361
167.20	940	NA	5.283
169.10	950	0.872	-0.697
171.00	960	NA	0.884
176.50	970	0.788	-0.918
182.00	980	NA	0.482
184.00	990	NA	2.551
186.00	1000	NA	1.004
188.00	1010	0.843	2.700
190.00	1020	NA	2.137
192.00	1030	NA	0.589

Abbreviations and notes:

Multiple correlation coeff. (adjusted for d.f) = 0.909

Standard error of the estimate (adjusted for d.f) = ±1.469°C

NA = No-analogue event, no communality value provided but SST estimates are derived.